

On Topaz
Editor

Lasers in Cardiovascular Interventions

Lasers in Cardiovascular Interventions

On Topaz
Editor

Lasers in Cardiovascular Interventions

 Springer

Editor

On Topaz, MD, FACC, FACP, FSCAI
Professor of Medicine
Duke University School of Medicine
Director, Interventional Cardiology
Chief, Division of Cardiology
Charles George Veterans Affairs Medical Center
Asheville
NC
USA

ISBN 978-1-4471-5219-4 ISBN 978-1-4471-5220-0 (eBook)
DOI 10.1007/978-1-4471-5220-0

Library of Congress Control Number: 2015953338

Springer London Heidelberg New York Dordrecht
© Springer-Verlag London 2015

This work is subject to copyright. All rights are reserved by the Publisher, whether the whole or part of the material is concerned, specifically the rights of translation, reprinting, reuse of illustrations, recitation, broadcasting, reproduction on microfilms or in any other physical way, and transmission or information storage and retrieval, electronic adaptation, computer software, or by similar or dissimilar methodology now known or hereafter developed.

The use of general descriptive names, registered names, trademarks, service marks, etc. in this publication does not imply, even in the absence of a specific statement, that such names are exempt from the relevant protective laws and regulations and therefore free for general use.

The publisher, the authors and the editors are safe to assume that the advice and information in this book are believed to be true and accurate at the date of publication. Neither the publisher nor the authors or the editors give a warranty, express or implied, with respect to the material contained herein or for any errors or omissions that may have been made.

Printed on acid-free paper

Springer-Verlag London Ltd. is part of Springer Science+Business Media (www.springer.com)

*This book is dedicated to the wonderful laser lights of my life – my children
– Allyne, Guy, Shelli, and Gil.*

Foreword

Dr. On Topaz and I met during my first days of residency in 1985 at Jackson Memorial Hospital in Miami, Florida. He was a hard-driving first year Cardiology fellow, and we became fast friends. Instantly, I recognized that he had an internal fire for pursuing scientific truth and was drawn to his drive in research pursuits in cardiovascular medicine. His deep passion for both cardiology and research stood out as a bright beacon, and I greatly benefited from his mentorship in both areas.

As a House Officer, I learned a great many things from On: how to effectively gain central line access using multiple approaches, how to deal with the heavy work burden of my internship, and how to screen through extensive research data more efficiently, to name just a few. One ever-present constant during my early mentorship by On was that he led by example. He was always the first to do, to act, to volunteer, and even to take over, if necessary. This very relatable aspect of his approach made him an excellent role model. But most importantly, he is an extraordinary teacher. His in-depth knowledge of cardiovascular medicine and research and his didactic ability are what make him so special.

Even after moving on to do my own Cardiology fellowship, I always kept in touch with On. Over the years, I have followed his career and accomplishments with great interest. His keen interest in the application of laser technologies in cardiology has led him, not surprisingly, to publish extensively on the use of lasers in acute coronary syndromes and multiple facets of interventional cardiology.

A review of the contents of *Lasers in Cardiovascular Interventions* shows clearly that he has carefully assembled a comprehensive collection of chapters addressing the various cutting-edge applications of laser in cardiovascular disease. It includes extensive details on laser use in vessels ranging from the coronaries to the peripheral arteries and veins and on laser treatment of thrombotic disease and arrhythmias as well as procedures for laser lead extraction and direct myocardial application. It is clear that lasers have a myriad of clinical and therapeutic applications. In one place, this book brings the diversity of laser applications into focus and makes them accessible and understandable.

Using his skillful ability to convey complex information and his vast practical knowledge of lasers, On Topaz has brought together world-renowned experts to produce a fascinating and authoritative book on an extraordinary subject. This book will be of great interest to a wide readership and provides insight into the multiple therapeutic uses of laser technology in treating complex cardiovascular diseases.

Emerson C. Perin, MD, PhD
Director, Research in CV Medicine, Texas Heart Institute
Medical Director, Baylor/St. Luke's Medical Center Catheterization Laboratory
Clinical Professor of Medicine, Baylor College of Medicine
Houston, Texas, USA

Preface

Celebrating almost 100 years since its original description, *laser* is one of the astounding gifts which Albert Einstein's phenomenal brain contributed to science and humanity. Since the introduction of laser devices to the biomedical sciences five decades ago, this technology has created great interest and found multiple indications for utilization in a variety of medical fields. Specifically, the laser's unique physical properties and precise bio-tissue interactions render this versatile source of unique energy an attractive tool for multiple therapeutic purposes in cardiovascular medicine. Indeed the application of laser for management of various cardiovascular conditions and diseases has expanded dramatically over the last decade and entered the global arena. Currently, cardiovascular lasers are used in the USA, Europe, Japan, Australia, and are entering Asia.

Notably, leading reference books on cardiovascular laser utilization were already published more than 20 years ago, and their content accordingly represents knowledge and data pertaining to the early to the late 1980s. As such, it seems prudent that the considerable body of scientific information on the technological progress and clinical experience with cardiovascular lasers gained over the last 25 years should appear in a new, focused book.

Laser physics, technology, and the clinical applications in cardiovascular medicine always fascinated me. Thus, I am grateful to the publisher Springer for granting me the privilege of editing this book. Special thanks to the editors at Springer's London, UK headquarters, Dr. Victoria Jones, and Mr. Grant Weston. My US-based project coordinator, Mr. Michael Wilt, merits well-earned accolades for his excellent management skills, reliability, and accommodating pleasant personality when dealing with busy clinicians and scientists, each requiring special attention to ensure timely completion of the project.

I am deeply indebted to the contributing authors who eagerly submitted chapters for this book. Each contributor was selected based on recognition for their world-renowned, extensive expertise, and their proven impact on the field of cardiovascular laser medicine. As an editor I faced an intriguing academic dilemma of choosing between two options: to exercise a heavy, controlling hand and modify each chapter to a point of integrating the product into a uniformed structure, or to enable the preservation of the personal styles and perspectives of the contributing authors. I preferred the latter course. In the process, the dialogue between the authors and readers creates a unique personal, teaching atmosphere. Consequently, this book provides a host of views and a scale of technical descriptions true to the reality of cardiovascular laser science and applications. The need to accommodate unique requirements of contemporary editing and focus the book's scope inevitably led to exclusion of traditional topics [such as laser safety] shared with other medical fields and already well published elsewhere.

This book provides a thorough, up-to-date coverage of multiple topics for scientists who invent and explore medical lasers; for health care specialists including cardiologists, electrophysiologists, cardiac and vascular surgeons, interventional radiologists, and interventional cardiologists who are interested in laser utilization and those who already use laser devices for management of complex cardiovascular diseases; for medical students and nurses seeking to learn about laser application for cardiovascular diseases; for fellows in advanced training who

wish to expand on the clinical correlates of the laser technology; and for students and graduates of biomedical engineering in quest of comprehensive scientific data on the basic research aspects and clinical outcomes of various cardiovascular lasers.

The contributing authors and myself trust that our readers will find this book an authoritative, comprehensive, and contemporary reference covering the major aspects of laser application in cardiovascular medicine. We hope that the content will evoke a desire for further research in the field and, finally, our sincere wish is that many patients will benefit from this extraordinary biotechnology.

Asheville, NC, USA

On Topaz

Contents

1 From Laser Physics to Clinical Utilization: Design and Ablative Properties of Cardiovascular Laser Catheters	1
Kevin D. Taylor and Christopher Reiser	
2 Fluid-Dynamic Phenomena in Cardiovascular Ablation with Laser Irradiation	15
Robert Splinter and Christian G. Parigger	
3 Excimer Coronary Laser Atherectomy During Percutaneous Coronary Intervention of Complex Lesions: Balloon Failures, Chronic Total Occlusions and Under-Expanded Stents	31
Omar A. Rana, Suneel Talwar, and Peter O’Kane	
4 Laser in Acute Myocardial Infarction	55
On Topaz and Allyne Topaz	
5 Laser Revascularisation in Saphenous Vein Grafts	69
William R. Davies, Tiffany Patterson, and Simon R. Redwood	
6 Excimer Laser Revascularization of Calcified Lesions	83
Waleed Alharbi and Luc Bilodeau	
7 Laser Atheroablation in Challenging Coronary Lesions	97
Itsik Ben-Dor and Ron Waksman	
8 Optical Coherence Tomography for Assessment of Percutaneous Coronary Intervention with Excimer Laser Coronary Atherectomy	103
John Rawlins, Suneel Talwar, and Peter O’Kane	
9 308 Nanometer Excimer Laser in the Therapy of Peripheral Vascular Disease	125
Craig M. Walker	
10 Laser Revascularization for Critical Limb Ischemia	141
Gagan D. Singh, Ehrin J. Armstrong, and John R. Laird	
11 Treatment of Subacute and Chronic Thrombotic Occlusions of the Lower Extremity Peripheral Arteries: The Role of Excimer Laser	157
Nicolas W. Shammass	
12 Laser for Treatment of Complex Superficial Femoral Artery Disease	167
Robert A. Gallino	
13 Laser Synergism with Drug Eluting Balloon for Treatment of In-Stent Restenosis in the Lower Extremities	171
Jos C. van den Berg	

14 Synergistic Strategy of Laser Atherectomy and Drug Eluting Balloon Angioplasty for Treatment of In-Stent Restenosis in the Superficial Femoral Artery.	181
Roberto Gandini and Costantino Del Giudice	
15 In Situ Laser Fenestration During Thoracic Endovascular Aortic Repair	191
Richard E. Redlinger Jr., Sadaf S. Ahanchi, and Jean M. Panneton	
16 Laser Catheter Ablation of Cardiac Arrhythmias: Experimental and Basic Research and Clinical Results.	199
Robert Splinter	
17 Laser-Based Approach to Cardiac Mapping and Arrhythmia Ablation	221
Helmut P. Weber and Michaela Sagerer-Gerhardt	
18 Laser for Transvenous Lead Extraction	245
Roger Carrillo and Chris Healy	
19 Application of Excimer Laser for Percutaneous Extraction of Pacemaker and Defibrillator Leads: Experience from the Hunter Holmes McGuire Veterans Administration Medical Center and the Virginia Commonwealth University	255
Karoly Kaszala, Alex Tan, Harsimran Saini, Yuhning L. Hu, Jennifer Winfield, Jayanthi Koneru, Richard K. Shepard, Kenneth A. Ellenbogen, and Jose F. Huizar	
20 Transmyocardial Laser Revascularization: Physiology, Pathology, and Basic Research Concepts.	271
Anthony J. Minisi, Deepak D. Banerjee, and Laxmi B. Mohanty	
21 The Impact of Various Wavelength Lasers on Myocardial Function following Transmyocardial Laser Revascularization.	287
Keith A. Horvath and Cristian Militaru	
22 Preconditioning of the Heart Following Transmyocardial Revascularization.	305
Chartchai Kositprapa, On Topaz, Arun Samidurai, Shinji Okubo, Vigneshwar Kasirajan, and Rakesh C. Kukreja	
23 Transmyocardial Revascularization Using CO₂ Lasers in Ischemic Heart Disease	311
Andrew C.W. Baldwin and O.H. Frazier	
24 Laser Treatment of the Venous System	321
Mark W. Moritz, Michael Ombrellino, and Harry Agis	
25 Endovenous Diode Laser Ablation of Varicose Perforating Veins	337
Christof Zerweck and Thomas Schwarz	
26 Excimer Laser Assisted Retrieval of Embedded Vena Cava Filters: Insights from the Preclinical Animal Model	345
Naritatsu Saito and Takeshi Shimamoto	
27 Landmarks Along the Application of Laser Energy for Cardiovascular Therapy	349
Jagadeesh Kumar Kalavakunta, Mohammad Anas Hajjar, Prem Srinivas Subramaniam, and George S. Abela	
Index	361

Contributors

George S. Abela, MD, MSc, MBA, FACC, FAHA, FNLA Division of Cardiology, Michigan State University (CHM), East Lansing, MI, USA

Harry Agis, MD The Vein Institute of New Jersey at the Cardiovascular Care Group, New Jersey Medical School, Rutgers University, Morristown, NJ, USA

Sadaf S. Ahanchi, MD Division of Vascular Surgery, Eastern Virginia Medical School, Norfolk, VA, USA

Waleed Alharbi, MD, FRCPC Libin Cardiovascular Institute of Alberta, Foothills Interventional Cardiology Service, Foothills Medical Center, University of Calgary, Calgary, AB, Canada

Ehrin J. Armstrong, MD, MSc, MAS Division of Cardiovascular Medicine, Department of Internal Medicine, VA Eastern Colorado Healthcare System, Denver, CO, USA

Division of Cardiology, University of Colorado School of Medicine, Denver, CO, USA

Andrew C.W. Baldwin, MD Department of Cardiothoracic Transplantation, Center for Cardiac Support, Texas Heart Institute, Houston, TX, USA

Deepak D. Banerjee, MD, FSCAI Interventional Cardiology, Memorial Hospital of Martinsville and Henry Counties, Martinsville, VA, USA

Division of Cardiology, McGuire VA Medical Center and Medical College of Virginia, Campus of Virginia Commonwealth University, Richmond, VA, USA

Itsik Ben-Dor, MD Division of Cardiology, Department of Interventional Cardiology, Washington Hospital Center, Washington, USA

Luc Bilodeau, MD, FRCPC Cardiac Catheterization Laboratory, Cardiology Department, Royal Victoria Hospital, McGill University, Montreal, QC, Canada

Roger Carrillo, MD Department of Cardiothoracic Surgery, University of Miami Hospital, Miami, FL, USA

William R. Davies, BSc, PhD, MB ChB, MRCP, MRCS Cardiovascular Department, Guy's and St. Thomas' NHS Foundation Trust, London, UK

Costantino Del Giudice, MD Department of Diagnostic and Molecular Imaging, Interventional Radiology and Radiation Therapy, Fondazione IRCCS Policlinico Tor Vergata, Rome, Italy

Kenneth A. Ellenbogen, MD Division of Cardiology, VCU Pauley Heart Center, Medical College of Virginia and VCU School of Medicine, Richmond, VA, USA

O.H. Frazier, MD, FACC, FACS Department of Cardiopulmonary Transplantation, Center for Cardiac Support, Texas Heart Institute, Houston, TX, USA

Robert A. Gallino, MD Department of Cardiology, Medstar Montgomery Medical Center and Washington Hospital Center, Olney, MD, USA

Roberto Gandini, MD Department of Diagnostic and Molecular Imaging, Interventional Radiology and Radiation Therapy, Fondazione IRCCS Policlinico Tor Vergata, Rome, Italy

Mohammad Anas Hajjar, MD Division of Cardiology, Department of Medicine, Sparrow Hospital, East Lansing, MI, USA

Chris Healy, MD Division of Cardiology, University of Miami, Miami, FL, USA

Keith A. Horvath, MD Cardiothoracic Surgery Research Program, National Heart, Lung, and Blood Institute, National Institutes of Health, Bethesda, MD, USA

Yuhning L. Hu, MD Clinical Cardiac Electrophysiology, VCU Pauley Heart Center, Medical College of Virginia and VCU School of Medicine, Richmond, VA, USA

Jose Huizar, MD Arrhythmia and Device Clinic, Medical College of Virginia and VCU School of Medicine, Hunter Holmes McGuire VA Medical Center, Richmond, VA, USA

Jagadeesh Kumar Kalavakunta, MD Division of Cardiology, Department of Cardiology, Michigan State University/Borgess Medical Center, Kalamazoo, MI, USA

Vigneshwar Kasirajan, MD Department of Surgery, Virginia Commonwealth University Medical Center, Richmond, VA, USA

Division of Cardiology, Department of Medicine, Pauley Heart Center, Virginia Commonwealth University, Richmond, VA, USA

Karoly Kaszala, MD, PhD Cardiac Electrophysiology Laboratory, Hunter Holmes McGuire VA Medical Center, Medical College of Virginia and VCU School of Medicine, Richmond, VA, USA

Jayanthi Koneru, MBBS Division of Cardiology, VCU Pauley Heart Center, Medical College of Virginia and VCU School of Medicine, Richmond, VA, USA

Chartchai Kositprapa, MD Department of Internal Medicine, Division of Cardiology, Virginia Commonwealth University Medical Center, Richmond, VA, USA

Department of Medicine, Division of Cardiology, Pauley Heart Center, Virginia Commonwealth University, Richmond, VA, USA

Rakesh C. Kukreja, PhD Department of Internal Medicine, Virginia Commonwealth University Medical Center, Pauley Heart Center, Richmond, VA, USA

Division of Cardiology, Department of Medicine, Pauley Heart Center, Virginia Commonwealth University, Richmond, VA, USA

John R. Laird, MD Division of Cardiovascular Medicine, UC Davis Vascular Center, Sacramento, CA, USA

Cristian Militaru, MD Cardiothoracic Surgery Research Program, National Heart, Lung, and Blood Institute, National Institutes of Health, Bethesda, MD, USA

Department of Surgery, Carol Davila University of Medicine and Pharmacy, Bucharest, Romania

Anthony J. Minisi, MD, FACC Division of Cardiology, McGuire VA Medical Center and Medical College of Virginia, Campus of Virginia Commonwealth University, Richmond, VA, USA

Laxmi B. Mohandy, MD Department of Pathology and Laboratory Medicine, McGuire VA Medical Center, Richmond, VA, USA

Division of Cardiology, McGuire VA Medical Center and Medical College of Virginia, Campus of Virginia Commonwealth University, Richmond, VA, USA

Mark W. Moritz, MD The Vein Institute of New Jersey at the Cardiovascular Care Group, New Jersey Medical School, Rutgers University, Morristown, NJ, USA

Peter O’Kane, BSc, MBBS, FRCP, MD Dorset Heart Centre, Royal Bournemouth Hospital, Castle Lane East, Bournemouth, UK

Shinji Okubo, MD, PhD Division of Cardiology, Department of Medicine, Pauley Heart Center, Virginia Commonwealth University, Richmond, VA, USA

Tokyo Medical University, Ibaraki Medical Center, Ibaraki, Japan

Michael Ombrellino, MD The Vein Institute of New Jersey at the Cardiovascular Care Group, New Jersey Medical School, Rutgers University, Morristown, NJ, USA

Jean M. Panneton, MD, FRCSC, FACS Division of Vascular Surgery, Eastern Virginia Medical School, Norfolk, VA, USA

Christian G. Parigger, PhD Department of Physics, University of Tennessee Space Institute, Tullahoma, TN, USA

Tiffany Patterson, BSc, MBBS, MRCP Cardiovascular Division, King’s College London British Heart Foundation Centre of Research Excellence, Rayne Institute, St Thomas’ Hospital, London, UK

Omar A. Rana, MBBS, MRCP, DM Dorset Heart Centre, Royal Bournemouth Hospital, Castle Lane East, Bournemouth, UK

John Rawlins, BSc, MBBS, MRCP, MD (Res) Dorset Heart Centre, Royal Bournemouth Hospital, Castle Lane East, Bournemouth, UK

Richard E. Redlinger Jr. , MD Division of Vascular Surgery, Eastern Virginia Medical School, Norfolk, VA, USA

Simon R. Redwood, MB, BS, MD, FRCP, FACC, FSCAI Cardiovascular Division, King’s College London British Heart Foundation Centre of Research Excellence, Rayne Institute, St Thomas’ Hospital, London, UK

Cardiovascular Department, Guy’s and St. Thomas’ NHS Foundation Trust, London, UK

Christopher Reiser, BA, PhD Vice President, Quality Assurance, Acutus Medical, Inc. San Diego, CA, USA

Michaela Sagerer-Gerhardt, MD Department of Anesthesiology, Hospital Neuperlach, Teaching Hospital of the LM-University of Munich, München, Germany

Harsimran Saini, MD Clinical Cardiology, VCU Pauley Heart Center, Medical College of Virginia and VCU School of Medicine, Richmond, VA, USA

Naritatsu Saito, MD Department of Cardiovascular Medicine, Graduate School of Medicine, Kyoto University, Kyoto, Japan

Arun Samidurai, PhD Virginia Commonwealth University Medical Center, Pauley Heart Center, Department of Internal Medicine, Richmond, VA, USA

Thomas Schwarz, MD Venous Section, Department of Angiology, Universitaets—Herzzentrum Freiburg Bad Krozingen, Bad Krozingen, Germany

Nicolas W. Shammass, MD, EJD, MS, FACC, FSCAI, FICA President and Research Director, Midwest Cardiovascular Research Foundation, Adjunct Clinical Associate Professor of Medicine, University of Iowa Interventional Cardiologist, Cardiovascular Medicine, PC Davenport, IA, USA

Richard K. Shepard, MD VCU Pauley Heart Center, Medical College of Virginia and VCU School of Medicine, Richmond, VA, USA

Takeshi Shimamoto, MD Department of Cardiovascular Surgery, Kurashiki Central Hospital, Kurashiki, Japan

Gagan D. Singh, MD Department of Internal Medicine, Division of Cardiovascular Medicine, University of California Davis Medical Center, Sacramento, CA, USA

Robert Splinter Department of R&D, Splinter Consultants, Graham, NC, USA

Prem Srinivas Subramaniam, MD Department of Cardiology, Michigan State University, East Lansing, MI, USA

Suneel Talwar, BSc, MBBS, MD Dorset Heart Centre, Royal Bournemouth Hospital, Castle Lane East, Bournemouth, UK

Alex Tan, MD Cardiac Electrophysiology Laboratory, Hunter Holmes McGuire VA Medical Center, Medical College of Virginia and VCU School of Medicine, Richmond, VA, USA

Kevin D. Taylor, BS Director, Engineering, CEA Medical Manufacturing, Colorado Springs, CO, USA

Allyne Topaz, MD Department of Emergency Medicine, Hackensack University Medical Center, Hackensack, NJ, USA

On Topaz, MD, FACC, FACP, FSCAI Professor of Medicine, Duke University School of Medicine, Director, Interventional Cardiology, Chief, Division of Cardiology, Charles George Veterans Affairs Medical Center, Asheville, NC, USA

Jos C. van den Berg, MD, PhD Service of Interventional Radiology, Ospedale Regionale di Lugano, Lugano, Switzerland

Ron Waksman, MD Division of Cardiology, Washington Hospital Center, Washington, DC, USA

Craig M. Walker, MD Cardiovascular Institute of the South, Houman, LA, USA
Tulane University School of Medicine, New Orleans, LA, USA
LSU Medical School, New Orleans, LA, USA

Helmut P. Weber Department of Research—Development and Education, CCEP—Center Taufkirchen, Taufkirchen, Germany
Section for Research and Development, CCEP Center Taufkirchen, Taufkirchen, Germany

Jennifer Winfield, BSN, RN Cardiac Electrophysiology Laboratory, Hunter Holmes McGuire VA Medical Center, Richmond, VA, USA

Christof Zerweck, MD Venous Section, Department of Angiology, Universitaets—Herzzentrum Freiburg Bad Krozingen, Bad Krozingen, Germany

From Laser Physics to Clinical Utilization: Design and Ablative Properties of Cardiovascular Laser Catheters

Kevin D. Taylor and Christopher Reiser

Introduction

Although the notion of excimer laser atherectomy (ELA) first appeared in the early 1980's, almost 10 years passed before the technique became commercially available [1–5].

During this period, several critical elements of workable systems were developed so that the technique could be investigated clinically. Elucidation of the basic science behind the phenomenon became known at the end of this period, when efforts began to focus on optimization of technique, catheter designs, and clinical results. The technology continued to mature after ELA became commercially available in the early 1990's.

As with many new technologies, improvements in the clinical application of ELA relied on the interplay among several technical disciplines. Understanding the biophysics of laser-tissue interaction, designing fiberoptic catheters that leveraged that understanding, and developing clinical technique required to use those catheters successfully, were required to advance the practice of ELA. That interplay created a relentless drive for improvement as challenges and disappointments were addressed with new understanding and updated catheter designs.

This chapter attempts to unravel the historically complex interplay into a rational sequence of concepts. A short review of laser biophysics leads naturally to the clinical technique required to apply the technology. In turn, the clinical implication of tissue photoablation leads to advancements in catheter designs, which will be covered in detail. Lastly, the

possibilities for applying optimized laser catheters to a wider variety of clinical situations will be discussed. More than three decades since excimer laser coronary atherectomy appeared, we find that the hard-won lessons from the past still guide us toward optimization of debulking with ELA and improved patient care.

Background

Excimer Lasers

ELA utilizes a xenon-chloride (XeCl) excimer laser to produce bursts of ultraviolet light pulses at 308 nanometers (nm). This wavelength lies in the UVB range, and is significantly longer in wavelength than the 193 nm excimer lasers used for photorefractive surgery on the cornea. Typical excimer lasers share design features that dictate their general operating parameters; a brief review of these features will be helpful in understanding how to maximize their usefulness in ELA.

Every excimer laser contains a gas mixture with at least three components: a rare gas (such as xenon), a halogen donor (such as HCl) and a diluent (such as neon). The laser is energized by passing a pulsed electric discharge through the gas; this discharge has a peak electrical power of at least 10–500 MW. In the volume of gas excited by the electrical discharge, many exotic molecular species are formed, including the excited dimer that lases, XeCl*. The excited “dimers”, or excimers, are stimulated to release their energy into the laser light field in the form of photons, which comprise the beam emerging from the laser. Each excimer system delivers photons of a different wavelength, depending on which rare gas and halogen comprises the gas mixture (see Table 1.1).

Because the pulsed electrical power necessary for excimer lasers must be extremely intense, it can be delivered only in a short pulse between 5 and 200 nanoseconds (ns) in duration. In turn this dictates that each laser light pulse is also between 5 and 200 ns long. That is, excimer lasers are inher-

K.D. Taylor, BS (✉)
 Director, Engineering, CEA Medical Manufacturing, 1735
 Merchants Court, Colorado Springs, CO 80916, USA
 e-mail: kdt.tmed@gmail.com

C. Reiser, BA, PhD (✉)
 Vice President, Quality Assurance,
 Acutus Medical, Inc. 10840 Thornmint Road, Suite 100
 San Diego, CA 92127, USA
 e-mail: creiserphd@gmail.com

Table 1.1 Excimer laser types and wavelengths

Active medium	Wavelength, nm
ArF	193
KrF	248
KrCl	222
XeCl	308
XeF	353

ently pulsed, like a strobe light. As will be shown below, the pulsed nature of the excimer is used to advantage in ELA. In between laser pulses, the laser system stores up energy and prepares for the next laser pulse. For lasers currently used in ELA, the wait between laser pulses is about 25 milliseconds, making a pulse repetition frequency of 40 Hz. The maximum rate of pulsing is determined by the design and size of the system; rates above 1000 Hz are attained for some industrial applications. For coronary ELA catheters, the laser is typically operated for 5 s (during which 200 individual laser pulses can be delivered), followed by a 10-s rest period, whereas peripheral ELA catheters can be operated continuously without a rest period.

ELA Catheters

To deliver the light to a lesion site inside an artery, a catheter containing optical fibers must be supplied. Very pure fused silica (synthetic quartz) must be used to make these fibers; ordinary glass fiber will not conduct UV light at the necessary power levels [5]. Up to 250 individual fibers are packed into each catheter; the fibers are typically between 50 and 130 micrometers (microns) in diameter [6, 7]. Multiple small fibers, rather than large fibers, are used to maintain the flexibility required to navigate through the arterial tree. At the proximal end of the catheter the catheter plugs into the laser system. In the plug, the fibers are arranged in a bundle shaped to receive the laser beam from the excimer laser efficiently. At the distal end, the fibers are gathered around a guidewire lumen, potted in epoxy, and polished. In actual use, the distal tip is threaded over the guidewire and through the vasculature until the tip contacts the arterial lesion. When the laser is activated, the 3-meter-long fibers conduct the light pulses directly to the tissue, which is vaporized by the light.

Laser-Tissue Interaction

Ultraviolet lasers as a class differ fundamentally from other popular lasers used for various surgical applications, such as the Ho:YAG laser at 2100 nm or the CO₂ laser at 10,600 nm. To understand the difference between the mechanisms of tissue interaction for these lasers, we play a game of “follow the energy.” That is, where do the photons go when they exit the catheter, and what do they do to the tissue?

Table 1.2 Absorption depths of popular laser wavelengths

Laser	Wavelength, nm	Absorption depth, microns
ArF	193	1
XeCl	308	100
Ho:YAG	2100	1000
Er:YAG	2900	1
CO ₂	10,600	10

The first important parameter is absorption depth -- that is, the distance into the tissue that the beam penetrates before absorption diminishes the beam to 37 % of its original fluence (defined here as the energy delivered divided the cross-sectional area of the beam, typically in millijoules per square millimeter, mJ/mm²). Absorption depths reported for popular laser wavelengths are shown in Table 1.2 [5]. For precise tissue interaction, penetration depths should be absolutely minimized. Among the lasers mentioned in Table 1.2, the ArF laser at 193 nm has the smallest depth, and this property makes it uniquely suited for corneal sculpting. The XeCl laser in the ultraviolet and the CO₂ laser in the infrared range also have shallow absorption depths in vascular tissue. However, standard optical fibers cannot conduct ArF and CO₂ laser light, and specialized hollow waveguides for CO₂ lasers are too stiff for intravascular use.

In the early 1990's, two additional properties of ultraviolet light in tissue were quantified. Jacques and Gijsbers [8, 9] pointed out that scattering, and not absorption, dominates the trajectory of ultraviolet photons through tissue. In fact, they showed through Monte-Carlo simulation that the ultraviolet rays follow “drunken sailor” paths under the beam delivery point, effectively trapping the photons at their point of entry. Because the tissue is dominated by scattering, the photons propagate by diffusion from their point of entry through the tissue. And because the absorption coefficient is high for 308 nm light, the photons simply cannot diffuse far before being absorbed. For 308 nm light, the effective penetration depth is not more than 10–50 μm for typical vascular tissue, which is much less than the absorption depth would predict. A shallow absorption depth means less energy is required per laser pulse to create ablation.

The Monte-Carlo simulations also showed that the volume of tissue in which the photons are absorbed is always immediately beneath the point where the beam entered the tissue. For a beam delivered by an optical fiber in contact with the tissue, the photons emitted by the fiber, at the catheter tip, are effectively trapped directly under the fiber. This implies that we should expect ablation to occur only in the tissue in contact with the fibers.

In order to avoid thermal damage to surrounding tissue, the laser energy must be pulsed. Specifically, the laser pulse duration must be less than the time required for heat energy to diffuse out of the volume of tissue directly irradiated by the laser. This can be achieved by operating the laser at a pulse width less than the thermal relaxation time for the tissue [10].

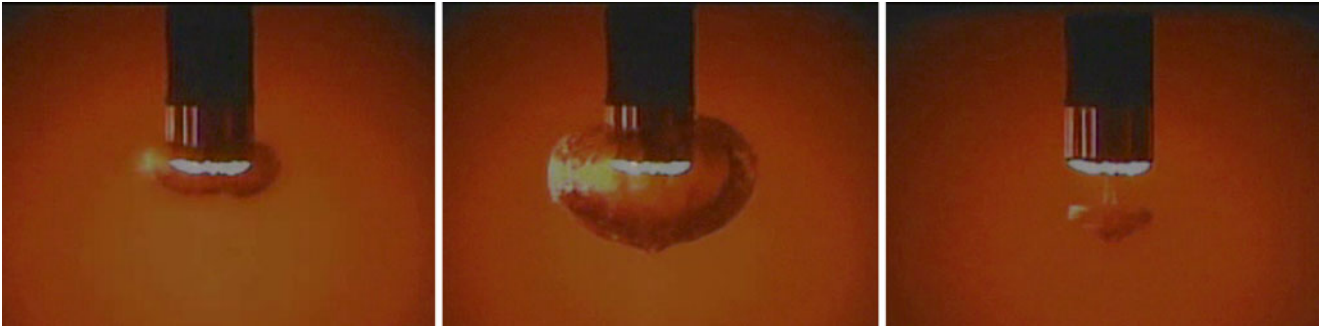


Fig. 1.1 High-speed photographs of the transient vapor bubble from a 2.0 mm diameter catheter 45 mJ/mm² pulse into an UV-absorbing liquid. Time after laser pulse: 20 us (*left*), 220 us (*center*), and 420 us (*right*). Images courtesy of The Spectranetics Corporation

At 308 nm in tissue, the thermal relaxation time has been calculated at 840 μ s [5]. Typical ELA excimer lasers operate at 100–220 ns pulse width, representing a three orders of magnitude margin of safety against thermal damage.

Also, pulse width places a unique constraint on the design of the excimer lasers for ELA. Typical excimer lasers produce ultraviolet light in pulses lasting about 10 ns. Such short pulses degrade optical fibers so quickly that the fibers become opaque and effectively useless before the end of an ELA procedure. When the laser pulse width is stretched to more than 80 ns, the photodegradation effect decreases dramatically. For this reason, ELA excimer lasers must be specifically designed for long-pulse operation.

Energy Pathways

Important to note at this point are exactly which molecules absorb the photons. At 308 nm, most small molecules, such as water, sugar, etc. do not absorb. However, proteins and lipids are strong absorbers; these are the primary chromophores for ELCA photons. These macromolecules, which tend to comprise the walls and enzymes of the cells, receive a large dose of energy by absorbing merely a single photon of UV light. During the laser pulse, the energy absorbed by the chromophores does not have sufficient time to diffuse into nearby tissue. For the first few nanoseconds the energy absorbed by the macromolecules remains in those molecules, inside the cells immediately under the individual fibers that deliver the light pulse.

The second property of ultraviolet light in tissue elucidated in the early 1990s recalled the invocation by the pioneers of the field that photons at 308 nm have the ability to break molecular bonds directly [1, 3, 11–14]. That is, the energy in a 308 nm photon is larger than the binding energy of some molecular bonds, and so some photon absorption events should lead directly to molecular disassociation. This unimolecular pyrolysis was theorized to be a potent reason for the extraordinary efficiency of deep UV ablation, but the extent to which it contributed to tissue effects at 308 nm was not initially known. Using elegant technique, Oraevsky [13]

measured energy pathways in tissue models to determine the fate of the energy represented by the absorbed photons. Oraevsky estimated that 16 % of the incident energy was lost by the tissue, either as fluorescence or by reflectance. The remaining energy remained in the tissue to contribute to the photoablation process. An estimated 2 % of the photons were consumed in bond-breaking events, leaving 82 % to be converted to heat.

To continue the game of “follow the energy” we must ask where the heat goes. Since the large molecules of the cell absorbed the photons, the heat begins its equilibration process by exciting the vibrational modes of the macromolecules. This excitation is rapidly shared with all cellular constituents, including intracellular water. The water molecules become transiently heated to above the vaporization temperature, and explode into the gas phase as steam [8, 15–17]. Thus the cells located under the optical fiber, where the photons were trapped and eventually absorbed, are first weakened by photolysis of macromolecules, then disrupted from the inside by a steam explosion. This largely explains why the particulates detected in ELCA vaporization of tissue tend to be subcellular in size [3, 11, 18, 19].

Using flash photography techniques, the existence of the steam created under each optical fiber was verified [8, 16, 17]. The steam forms a bubble roughly twice the diameter of the fiber, at the fluences typically utilized in ELCA. In a multifiber catheter, where up to 250 individual fibers are used, the individual bubbles coalesce into one orb at the tip of the catheter (see Fig. 1.1). This bubble expands for the first 220 microseconds immediately following the arrival of the laser pulse, as it performs thermodynamic work displacing the surrounding liquid and losing energy by nonadiabatic cooling through the wall of the bubble. After reaching a maximum volume, the bubble rapidly collapses approximately 400 microseconds after the laser pulse. The tissue under the catheter typically has 12 μ s (for a 80 Hz laser system) to equilibrate before the arrival of the next laser pulse.

A secondary effect of the expanding and collapsing vapor bubble is pressure and cavitation effects that act to disrupt the tissue. Vogel et al. [20] calculated the pressures created during bubble expansion and collapse in a liquid environment

at 580 MPa (5800 bar) and 62 MPa (620 bar) respectively. This contrasts to pressures measured by Esenaliev et al. [21] of 100 MPa for excimer laser ablation in air. In a liquid environment the bubble is confined by the liquid medium, resulting in higher pressures, whereas in the air environment the vaporization results in free ejection of debris from the irradiated site. Mechanical confinement can also occur when the catheter tip is pressed or tunneled into the tissue. This effect, dubbed the “Photomechanical Effect” is believed to be the dominant mechanism for tissue removal for ELA [22, 23].

Tissue Removal

Measured ablation rates for ELA catheters in porcine aortic tissue range from 3 to 12 $\mu\text{m}/\text{pulse}$ [6, 24]. Limited experience with highly calcified tissue yielded a penetration rate of less than 1 $\mu\text{m}/\text{pulse}$ with a small, high density catheter operating at 80 fluence, 80 Hz [25]. A tissue penetration rate of 5 $\mu\text{m}/\text{pulse}$ at 40 and 80 Hz calculates to 0.2–0.4 mm/s ablation speed. The ELA ablation rate is tissue dependent and slow in these tissue types. This suggests catheter advancement therefore should be slow, otherwise incomplete ablation can occur. Extensive in-vitro work by Hamburger et al. [26] compared pressure driven catheter advancement (PAD) to speed driven catheter advancement (SDA) with ELA catheters in porcine aortic tissue. In PAD, a constant force, typically tens of grams, is maintained between the catheter tip and the tissue, while SDA advances the catheter through the tissue at a constant velocity. PDA forces of 12, 24, and 36 g and SDC velocities of 0.51, 0.24, 0.12, and 0.06 mm/s using 45 fluence, 25 Hz and 60 fluence, 25 Hz from a 1.7 mm multifiber catheter. The results were remarkable, demonstrating that only the slowest SDA speed, 0.06 mm/s produced clean ablation craters roughly approximating the optical area of the catheter. Ablation quality, assessed by gross microscopic examination of sectioned craters, was also deemed to be superior at the 0.06 advancement speed. Craters produced by PDA and higher SDA speeds were characterized by incomplete tissue ablation and luminal areas much smaller than the optical area of the catheter. Follow-up work investigating the effect of 40 and 80 Hz repetition rates with SDA demonstrated advancement speed could be increased to 0.1 and 0.19 mm/s respectively without impacting ablation efficiency [26]. Further increases in repetition rates should be evaluated to speed up the ablation process to better match advancement speeds possible by hand, estimated to be in the 1–5 mm/s range.

Excimer laser ablation of thrombus has been studied extensively. Pettit et al. [27] performed ex-vivo ablation of thrombosed dog arteries with 351 nm excimer laser and a 800 μm fiber. He reported efficient ablation resulting in complete clot removal, small particulate debris composed of

fragmented and intact red-blood cells, minimal vessel wall damage and suggested a mechanical (photoacoustic) mode of tissue removal. Papaioannou et al. [28], performed in-vitro thrombus ablation experiments and concluded the thrombus removal rate increased with increased fluence, catheter size and repetition rate. Analysis of excimer laser thrombolysis particulate debris by Papaioannou et al. [29] using light obscuration counting equipment revealed less than 9 %, 1 %, and 0.006 % of ablation debris particles were greater than 10, 25, and 100 μm respectively. In the same study, using filtering and weighing techniques measuring the mass of material removed and debris greater than 10 μm , the influence of laser parameters (45 fluence, 25 Hz and 60 fluence, 40 Hz), clot consistency (0.3, 0.7, and 1.0 % fibrin content), and catheter size (0.9, 1.4, 1.7, and 2.0 mm) was measured. Results showed ablation mass increased with catheter size, increased laser parameters, and decreased clot consistency while debris production decreased with increasing laser parameters, lower clot consistency, and the smallest (0.9 mm) catheter size. It was also observed that for all catheter sizes, the measured ablated volumes exceeded those expected based on the diameter of the catheter tip. In the 0.9 mm catheter, a 200 % increase was seen, suggesting the photomechanical effect from the transient vapor bubble can fragment fibrin strands outside the zone of the catheter tip.

At this point the basic features of excimer laser ablation can be summarized as follows:

- Utilization of 308 nm is key – fiber delivery is possible
- Energy confinement under the fibers ensures that only a small layer of tissue is affected- this leads to precise ablation and minimal energy requirements per pulse
- Ablation occurs through a combination of photolysis, photothermal, and photomechanical effects which reduce tissue to microscopic debris
- Ablation cannot occur without the transient steam bubble
- Tissue removal rates and ablation areas achieved are tissue and technique dependent. They increase in softer tissues and decrease with harder tissue. Maximal ablation areas are achieved when the catheter advancement does not exceed the tissue removal rate.

Techniques to Improve Ablation Results

Several researchers have linked the transient bubble to unwanted side-effects of ELA [16, 17, 30–32]. As the bubble expands, the bubble diameter may reach or exceed the inner diameter of the artery. In this case, the transient bubble momentarily dilates the artery wall in which the ELA catheter has been placed. This can cause the dissection or perforation of the arterial wall. Furthermore, confinement

of the vapor bubble can eject vapor, liquid, and ablation debris at high pressures that will follow the path of least resistance. If the path of least resistance occurs in layered tissue, dissection of the layers can occur. Vacuolization, or bubble formation, between tissue layers is a frequent observation on histology sections of porcine aorta ablation craters [26]. However, UV ablation of plaque cannot proceed without the micro-disruptive effect of turning intracellular water to steam, so the transient bubble cannot be altogether eliminated. It was therefore theorized that smaller transient bubbles would be preferable in clinical situations, and a long search for the means to minimize the bubble size began.

Comprehensive theoretical treatises have shown that the size of the transient bubble is proportional to the energy delivered to the tissue [33, 34]. Thus smaller catheters, and lower fluences, imply that smaller transient bubbles will be formed. For most ELA applications, the desired outcome is to provide the occluded artery with as large a lumen as possible after angioplasty. From a treatment perspective, “bigger is better,” and ELA catheters typically create lumens no larger than the catheter tip diameter. Hence simply making ELA catheters smaller was not an acceptable option.

Saline Flush

It was also learned that blood and radiographic contrast absorb 308 nm light rather avidly [30]. Presence of either of these two liquids at the catheter tip exacerbates the transient bubble phenomenon, and prevents the light from reaching the tissue. This effect was not appreciated prior to 1993, when the first registries of ELA cases were enrolled, and may have led to rates of dissection, abrupt closure, spasm, and other complications that were higher than expectations based on balloon angioplasty [35–39]. Despite the largely successful statistics reported for these registries, the stigma of unpredictable dissection was attached to ELA performed in a blood field [40].

Once the deleterious effects of blood and contrast were identified, a straightforward procedure for saline flush through the guide catheter during the laser bursts in an ELA procedure was developed [31, 32, 41]. Saline (or Ringer’s lactated solution) does not appreciably absorb the excimer laser light. By replacing the fluid at the catheter tip with saline, the light emerging from the tip travels through the saline to the lesion tissue, where ablation is desired. In essence, the saline layer at the catheter tip provides the last few microns of beam delivery system for the ultraviolet light pulses. Clinical evidence quickly mounted for a dramatic decrease in complications using the saline infusion protocol, which has become standard technique for ELCA [31, 42–44].

Multiple-Sector Catheters

As this understanding was reached in the early 1990’s, efforts to increase the debulking efficiency of ELA began. It was reasoned that larger catheters would provide greater debulking, but at the concomitant necessity of delivering a correspondingly larger energy per pulse into the artery. In turn this would create a larger transient steam bubble, a side-effect to avoid. Several clever methods to minimize the energy per pulse, and thereby the size of the transient bubble, while maximizing ablation, were investigated.

In a typical ELA catheter, up to 250 individual fibers comprise the total bundle that transmits the excimer pulses from the laser to the distal tip of the catheter. All fibers conduct a tiny portion of the total energy on each laser pulse. It was reasoned that, if the total bundle were divided into six or eight sub-bundles, each sub-bundle subtending a wedge-shaped section of the catheter distal tip, then sequential activation of each sub-bundle would provide ablation over the entire tip of the device while delivering a fraction of the total energy on each pulse. If, at the same time, the pulse repetition frequency of the excimer laser were increased by six or eight times, the net effect should be to achieve the same penetration rate through atheroma, but with a fraction of the side effects.

Systems employing this technique were marketed under the name “SELCA” for Smooth Excimer Laser Coronary Angioplasty (Medolas Lasertechnik, Germany) [45]. Prototype systems were also made by Spectranetics® (Colorado Springs, Colorado). Testing the SELCA technique in rabbit iliac arteries revealed that each wedge-shaped sub-bundle does indeed make a transient bubble that is a fraction of the size one would expect from energizing the entire catheter bundle in one shot [45, 46]. However, the transient bubble under each sub-bundle distended the artery locally by approximately the same amount that would be expected from a full-bundle laser pulse. After six or eight pulses through the respective sub-bundles, the entire artery circumference was effectively transiently distended, one section at a time. The net effect achieved the same collateral damage to the artery wall as a single full-bundle laser pulse. In addition, the tissue penetration rate was reduced, due to the reduction of the size of the vapor bubble and corresponding acoustic pressures [30]. After this realization was reached, SELCA techniques were not actively pursued.

Ablation in Gas

Several researchers theorized if ELA ablation could be performed in a gaseous environment, the high pressures associated with liquid confinement of the vapor bubble could be reduced. Vogel et al. [20] demonstrated a three-fold decrease

in pressures using an innovative double pulse ablation technique to create a gaseous environment for ablation. An initial pre-pulse at 10 mJ energy was delivered to create a small vapor bubble. Approximately 70 microseconds later a larger, 70 mJ laser pulse was delivered into the smaller vapor bubble. Vapor bubble volumes were reduced 15-fold and maximum pressures were reduced to 230 MPa from 732 MPa. Van den Broecke et al. [47] compared excimer laser ablation in CO₂, saline, and blood environments and concluded CO₂ delivered the highest quality ablation result. These unique solutions were not pursued, presumably due to the associated technical and clinical challenges and success of the saline infusion technique.

Catheter Design

Design of fiber optic catheters for laser angioplasty has progressed significantly from the metal tipped probes and intraoperative single fiber devices first evaluated in the 1980s [48, 49]. Second-generation laser introduced in the late 1980s featured flexible, multifiber construction for percutaneous introduction into the coronary vasculature. Most of the clinical data that led to commercial regulatory approval for excimer laser coronary angioplasty was generated with these catheters. In the early 1990s, the performance of third-generation catheters was enhanced by using a larger number of small diameter fibers densely packed into a flexible catheter shaft. Advanced, lubricous coatings were utilized, the first rapid exchange and eccentric designs were developed, and

an array of catheter sizes was offered during this period. Clinical success improved from 87 to 94 % and complications decreased from 8 to 5 % when going from second-generation to third-generation catheters [50], demonstrating the influence catheter performance has on clinical outcomes.

The basic anatomy of a laser catheter is shown in Fig. 1.2. There are four main segments of a catheter: the laser coupler, the extension (tail) section, the working section, and the distal tip.

The laser coupler plugs into the laser system and is adapted to receive the energy from the laser system. The laser fibers are prepared and arranged in a manner to produce efficient and reliable transmission. This means the proximal ends of the fibers must be uniform and polished, the coating of the fiber must be removed, and ablative interactions with mounting components must be avoided as these will produce explosive reactions that destroy the ends of the fibers. This is typically accomplished by mounting the uncoated fibers in a synthetic quartz capillary tube or an aluminum slide.

The tail section runs between the laser coupler and working section of the catheter and provides the length necessary to reach from the laser system to the procedural area. This length is typically 2–3 m and allows for sufficient placement of the non-sterile laser system away from the sterile procedure area. This segment is typically composed of flexible plastic tubing encasing the optical fibers.

The working section is the portion of the catheter which is inserted into the patient. The length of this section is dependent on the type of procedure- coronary laser catheters are typically 130 cm long and peripheral laser catheters are 110–150 cm long. The working section contains an internal

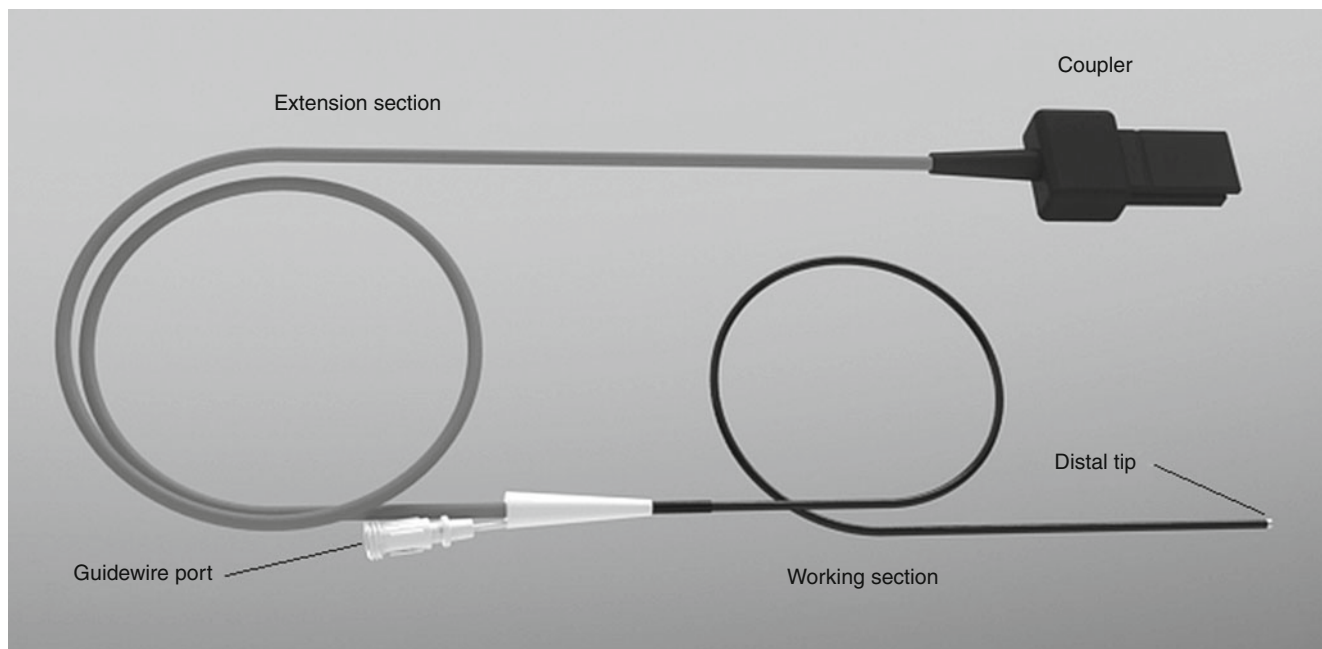


Fig. 1.2 Laser catheter anatomy (not to scale) shows the basic features of an over-the-wire ELA catheter

lumen to accept a guidewire, a shaft consisting of a plastic tubing containing the fibers with a diameter and stiffness profile designed to be introduced into vascular anatomy, and the distal tip.

The distal tip is the energy emitting, treatment end of the catheter. It is typically composed of optical fibers arranged concentrically around the guidewire lumen, encased in epoxy and polished to provide efficient and reliable energy transmission. A radiopaque metal band surrounds the fibers to allow for visualization of tip position under x-ray. The tip is polished at an angle and the leading distal, outer edge is rounded to allow for atraumatic insertion of the catheter. The polish angle of the optical fibers at the tip cannot exceed 24° , otherwise the fibers will fail due to internal reflection. Since the distal tip construction results in a very stiff segment, the tip length is minimized (typically 1.5–3 mm) to eliminate any negative effects to catheter alignment or access performance.

There are two primary types of ELA catheters, Rapid Exchange (RX) and Over-the-Wire (OTW). An OTW catheter is shown in Fig. 1.2 and is characterized by a guidewire lumen which extends the entire length of the catheters working section. A RX type catheter has a shorter guidewire lumen, typical 9–35 cm long, that extends through the most distal portion of the catheter. The RX catheter is preferred by many physicians because it is easier to insert and/or remove over a standard length guidewire. OTW catheters require a longer guidewire or use of a guidewire extension to perform catheter exchanges. Commercially available RX lasers are described in US Patent 5,456,680 [51]. This invention discloses a fiber optic catheter with a short guidewire lumen (less than 10 cm) with a tapered stiffening mandrel for optimum stiffness and flexibility characteristics.

Optical Fibers

The primary component of a laser catheter is the optical fiber required to deliver the laser energy and their properties dictate much of the performance aspects of the catheter. An optical fiber is a cylindrical waveguide that transmits light along its axis by the process of total internal reflection (see Fig. 1.3). The fiber consists of a core surrounded by a cladding layer and then a protective buffer layer. To confine the laser light in the core, the refractive index of the core must be greater than that of the cladding. Total internal reflection occurs along the core/clad interface but only up to a maximum critical angle. If the light is incident at the interface at a steeper angle than the critical angle, light can escape the fiber.

Optical fibers used in medical applications are composed of high grade silica glass for both core and clad and the cladding is doped with fluorine to lower the refractive index.

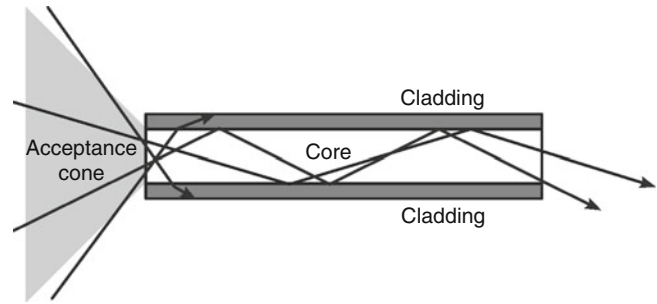


Fig. 1.3 Optical fiber construction and mode of operation (not to scale). Light rays that enters the fiber from an angle within the acceptance cone are trapped by the total internal reflection created at the interface between the core and the cladding

Typical fibers used in ELA have a 1–1.1 or a 1–1.05 core to clad ratio with approximately 3–5 μm of polyimide protective coating. For example a 1:1.1, 50 μm core fiber will have a diameter of 55 μm at the outer edge of the cladding layer and 71 μm total diameter.

Optical fibers for excimer applications low attenuation (<0.2 decibels/meter), and very high energy damage thresholds [52]. One limiting characteristic of optical fibers for UV wavelengths is color center generation, or photodegradation resulting in transmission losses of up to 25 % [53]. Photodegradation increases with lower wavelengths, lower pulse durations, and higher energy densities. Improvements in fiber optic technology have reduced the photodegradation effect by nearly 50 % [53] but it still requires consideration when designing an ELA catheter.

Another key consideration with optical fiber is its inherent stiffness. Synthetic quartz has a modulus of elasticity of 72 GPa, 90 times greater than that of high density polyethylene (HDPE), a common catheter material. Since bending stiffness is related to the fourth power of the diameter, an effective way to obtain more flexibility is to reduce the fiber diameter. For example, going from a 100 μm fiber to a 50 μm fiber will reduce bending stiffness by a factor of 16. However, it requires 4 times more 50 μm fibers to fill the equivalent optical area of 100 μm fibers, but this still results in a four-fold reduction in bending stiffness. Optical fibers over 200 μm diameter are typically too stiff for intravascular catheter construction.

Lastly, small diameter optical fibers are very fragile and require protective jacketing and care during catheter manufacturing to preserve their integrity and energy transmission. Any damage to the polyimide coating will eventually result in a broken fiber. In addition, care must be taken during the bundling and construction processes to ensure the fibers lie substantially parallel to each other. Fiber “crosses” in the bundle, combined with compression, can produce micro-bending that can result in light escaping the core of the fiber.

Design for Performance

The key performance attributes for an intravascular laser catheter are trackability, pushability, wire movement, profile, and optical area. In this section we will define each of these attributes and discuss ways to achieve desirable performance, along with the associated challenges.

Trackability is defined as the catheters ability to navigate vascular anatomy over a guidewire. Success is defined as navigation to the target site with minimal force. Moving the catheter with low force is very important in ELA as it allows the physician to feel the catheter tip as it contacts the plaque and allows for precise, slow advancement of the catheter. Excessive force will mask any tactile feedback “feel” and make it difficult to control the catheter advancement. Friction is the enemy of trackability and can result from excessive catheter stiffness (resulting in high friction against the vascular wall or guidewire), high surface area contact between mating surfaces, rough surfaces, and a high coefficient of friction (COF) between mating surfaces. To combat friction, the lubricious coatings are applied to the catheter shaft, low COF materials such as Teflon or HDPE are used for the guidewire lumen, shaft and lumen materials are designed with sufficient wall thickness to prevent collapse or kinking when exposed to curvature, and the portion of the catheter (usually the distal end) exposed to curves and bends in the vascular anatomy is made flexible to minimize bending forces. Flexibility is accomplished by using small diameter optical fibers combined with low durometer shaft materials. Loosely bundling the optical fibers within the outer jacket (shaft) will also promote flexibility. This allows the individual fibers to move within the bundle during bending and minimize bending resistance.

Pushability is defined as the as the ability to efficiently transfer force from the proximal end of the catheter to the distal tip. The term was popularized by cardiologists that desired balloon catheters that could be “pushed” across tight coronary lesions. Excessive flexibility and friction are the antagonists of pushability. The friction-reducing methods discussed above also apply here. Good pushability is obtained by making the portion of the catheter not subject to bends and curves (usually the most proximal portion) as stiff as possible. With an ELA catheter this is accomplished by jacketing the fibers with a stiff tubing having a thicker wall thickness. Bundling the fibers tight within this jacket will also create a stiffer shaft. For rapid exchange catheters, a tapered stainless steel mandrel is placed within the fiber bundle to provide proximal stiffness. Combining the aspects of both pushability and trackability, Fig. 1.4 shows the optimal stiffness profile for a coronary ELA catheter.

Profile is the diameter of the catheter as it pertains to insertion into the patient and/or the presentation to the target. For a balloon angioplasty catheter, important profiles are the

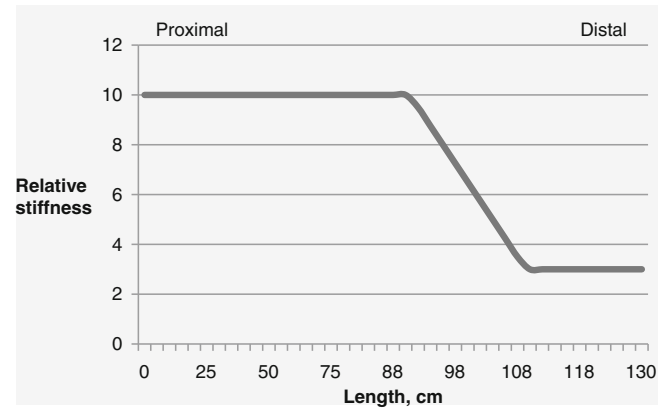


Fig. 1.4 An optimal catheter stiffness profile achieves pushability by being reasonably stiff in its proximal section, where the operator grasps and manipulates the catheter body. Stiffness gradually decreases toward the distal tip, which allows the catheter to navigate through tortuous arteries without buckling

maximum catheter diameter, the crossing profile (deflated balloon diameter), and the inflated balloon diameter. In general, for intravascular procedures, lower profile catheters are preferred as they are less invasive and offer better performance. This creates a dilemma for ELA catheters, as the catheter diameter is determined by the optical area or tip diameter. For maximal debulking a larger catheter is required. For an ELA catheter, the important profiles are maximum catheter diameter, tip diameter, and distal shaft diameter. It is important that the distal shaft closely match the tip diameter as it must follow the catheter tip through the ablation lumen. Reducing the overall catheter diameter to present a less invasive catheter profile is accomplished by using fewer optical fibers, utilizing thin wall thickness jacketing materials, and bundling the optical fibers in a tight configuration. Since all these techniques could negatively affect trackability, pushability, and optical area, the catheter designer must compromise in all areas to deliver acceptable all-around catheter performance.

One technology that enabled the best compromise between trackability, pushability, profile and optical area is described in US Patent 5,415,653 by Wardle and Goldenberg [54] that discloses a fiber optic catheter with stranded fibers. In this invention, the optical fibers are spirally wound around the longitudinal axis of the catheter, similar to cotton fibers in a string or wire in a cable. See Fig. 1.5. Bending a stranded fiber bundle produces a round bundle cross section in contrast to the flat cross section produced with a traditional longitudinal oriented fiber bundle thus reducing friction. A stranded fiber bundle provides flexibility, a lower profile, reduced friction, and improved durability (kink and crush resistance). A stranded bundle can be tightly jacketed thus allowing the construction of high optical density catheters without sacrificing performance or increasing shaft profile.

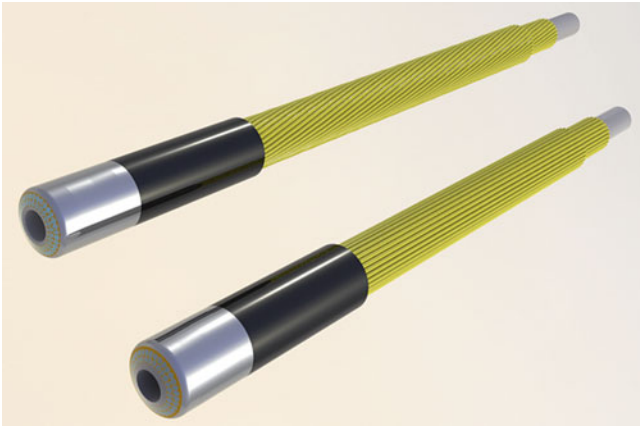


Fig. 1.5 In a stranded optical fiber bundle (*top*), the fibers are spirally wrapped around the catheter core. In a traditional optical fiber bundle (*bottom*), fibers extend straight along the catheter core, resulting in a stiffer device. Drawing not to scale

To obtain a low profile, flexible, stranded bundle, the bundle is tightly coated with a low durometer material by shrinking, necking, extrusion coating or other techniques well known in the catheter art. To obtain a stiffer stranded shaft, a high durometer material is used for the jacketing process.

Wire movement is defined as the force required to move and steer the guidewire through the catheter. This catheter property is actually accounted for in the trackability definition and methods, however, it is very important from a clinical and ease-of-use perspective that it deserves its own explanation. During ELA procedures it is common for the physician to first insert the guidewire into the catheter, then insert the catheter (and guidewire) into the patient, then advance and steer the guidewire across the stenosis. Steering a guidewire through tortuous anatomy, into specific vascular branches, and across the stenosis requires considerable expertise and precise response from the guidewire. If guidewire movement is hindered by the catheter, feel and control of the guidewire is lost making it very difficult to reach and cross the stenosis. This can result in extended procedure times, scraped catheters, angry customers and in rare cases, procedural complications. Current ELA catheters use low COF materials for the guidewire lumen; have adequate clearance between the guidewire outside diameter and the inside diameter of the guidewire lumen; and have sufficient wall thickness of the inner lumen to avoid collapse or kinking when exposed to curvature.

The optical area of the catheter is the sum of the light-emitting surface area at the tip of the catheter. ELA ablation occurs only in close proximity to the light emitting optical fiber surface, and the ablated lumen created in ELA is determined by the diameter of the optical fiber bundle presented at the tip of the catheter. Furthermore, ablation of tough fibrocalcific plaque requires higher energy densities and

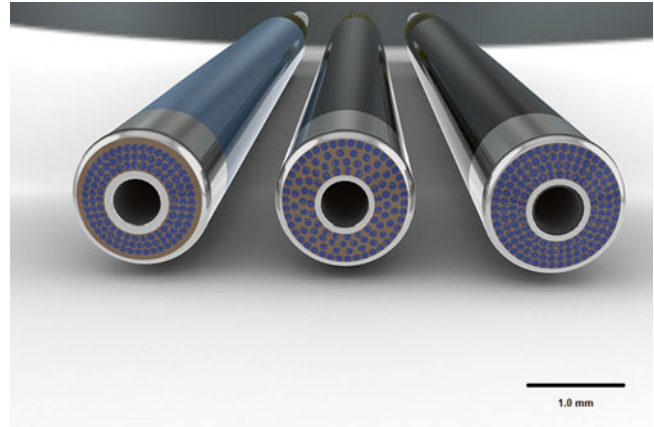


Fig. 1.6 CP (*left*), OS (*center*), HD (*right*) tip configurations use different strategies to present the individual optical fibers at the distal tip of the catheter

minimal “dead space” at the tip of the catheter. We will review the design and merits of three types of ELA tip configurations in use today; Close-Packed (CP), Optimal Spaced (OS), and High-Density (HD). See Fig. 1.6.

Close Packed (CP) Tip Design

Early ELA multi-fiber catheter designs featured a close-packed ring of fibers located central in the catheter tip. Sufficient optical dead space existed in and around the central lumen and the outer edge of the catheter tip to allow for use of larger guidewires, and to present a less traumatic tip profile. This was important as early ELA catheters were constructed of larger diameter fibers and required larger guidewires for introduction into the vasculature. Larger outer peripheral dead space allowed for generous rounding of the catheter tip edge to reduce the possibility of vessel wall damage during catheter introduction. In the quest for better ablation efficiency, it was quickly apparent that the optical fiber area in the tip had to increase. Advances in catheter and guidewire technology enabled use of smaller wires to deliver the catheters safety into the vascular, thus eliminating the need for large guidewire lumens or heavy rounding of the tip. This realization led to the development of the OS and HD catheter designs.

Optimal Space (OS) Tip Design

The desire to increase the diameter of the ablated lumen without increasing the number of fibers, the size of the transient vapor bubble, catheter profile and catheter stiffness, led to the development of the OS tip design. This concept took

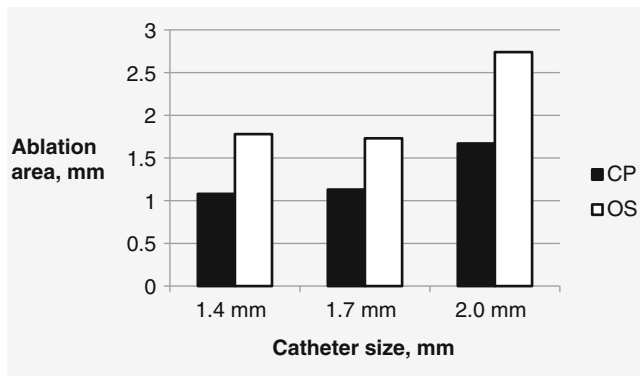


Fig. 1.7 The area ablated in porcine aorta for OS catheters, compared to CP catheters. Laser parameters were 60 fluence, 40 Hz (From Lippincott et al. [24])

the same number of fibers from a CP tip and spread them over a wider area, resulting in a reduction of outer and internal dead space (around the guidewire lumen). Only the outermost fibers were close packed to give a smoother ablation crater edge. Catheters of the OS type have the same number of fibers as the close-packed (CP) fiber bundle design. OS catheters deliver the same energy per pulse as CP, and therefore produce similarly sized transient steam bubbles. OS devices feature the same flexibility as the CP predecessors, because the fiber optic cable is identical. The difference lies only in the catheter tip, and this creates specific differences in the way the devices work.

Bench testing compared the diameter of holes ablated in porcine aorta with OS devices to those created with CP devices [24]. OS devices consistently produced larger ablation areas for all sizes of OS catheters (see Fig. 1.7). Remarkably, OS devices could produce ablation holes at least as large as the tip of the device, a performance feature formerly lacking in ELA catheters. In addition, particulate debris analysis revealed the OS devices produced less, similar sized particulate when compared to the CP devices [24]. This result is surprising considering the honeycomb area between the fibers has increased and may be further evidence that the photomechanical effect is a primary mode of tissue removal in ELA.

Comparison of penetration rates between OS and CP devices revealed the penetration rate of OS devices were approximately one half that of CP devices [24]. This is not surprising since the total tissue area exposed to UV light was increased by 40 % [25] leading to a corresponding drop in energy (light and pressure) density. In-vitro comparison of advancement speeds of 0.2 mm/s, 0.5 mm/s, and 1.0 mm/s with the 2.0 mm OS catheter at 45 fluence, 40 Hz revealed the largest ablation areas (equivalent to 100 % of the tip diameter) were achieved with the slowest advancement speed [25]. See Fig. 1.8. Advancing the catheter slowly is a key to maximal debulking in ELA.

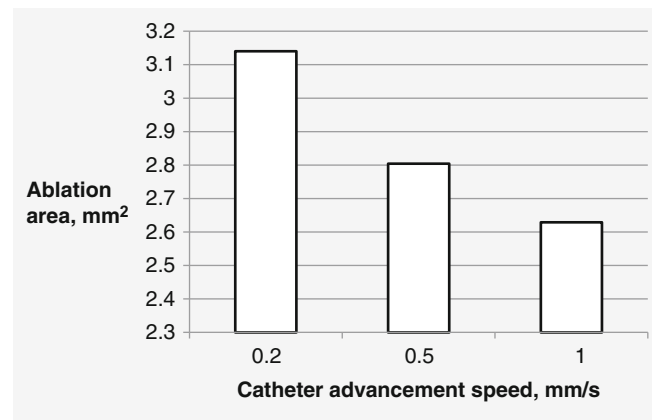


Fig. 1.8 The area ablated with the 2.0 mm OS catheter at 45 fluence, 40 Hz was the greatest at the slowest advancement speed (From Lippincott et al. [24])

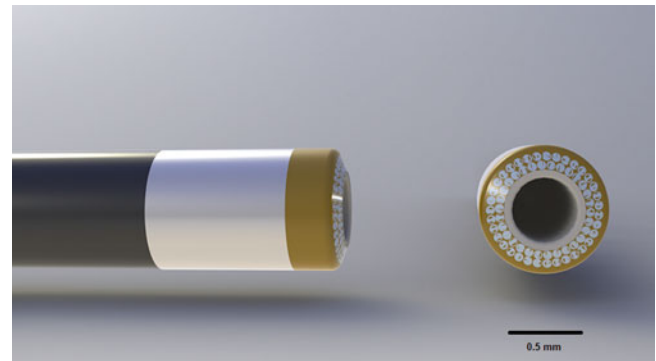


Fig. 1.9 The 0.9 mm catheter (side and front tip views) features two circumferential rows of close-packed fibers, with minimal dead space around the guidewire lumen and around the outside rim of the tip

High Density (HD) Tip Design

While the OS tip design significantly increased the debulking capability of ELA it did not address the issue of hard calcified plaque. Penetrating hard calcified plaque requires a high energy density [55] and minimal dead space. The fiber spacing in OS devices reduces energy density impacting the tissue while dead space around the outer diameter in the CP tip design causes another problem- the hole ablated in a calcified tissue is smaller than the outer diameter of the catheter, blocking the passage of the catheter. An HD tip design, with fibers covering almost the entire catheter tip, is required here.

Figure 1.9 shows an ELA catheter design meeting the requirements for treating very hard tissue. The 0.9 mm device has a closest-packed array of fibers around a 0.014" guidewire lumen; two circular rows of fibers surround the lumen. The radiopaque marker band has been moved back from the tip to allow the fibers to occupy the radial space

nearly out to the edge. Since only 65 fibers were required for this device, it maintains a supple feel and excellent tracking. Increased laser parameters up to 80 fluence and 80 Hz were tested with this catheter.

Testing in ex-vivo tissue compared CP devices with the 0.9 mm catheter in their ability to penetrate calcified human cadaver plaque. As expected, the CP devices ablated a tapered hole and failed to cross the sample despite prolonged (65 s total) lasing. However, the 0.9 mm device at 80 fluence, 80 Hz laser parameters penetrated the sample in less than 35 s [25].

A prospective clinical trial was conducted evaluating the 0.9 mm catheter in 100 calcified and/or balloon-resistant lesions [56]. Successful laser catheter crossing was obtained in 87 lesions (92 %), procedural success was reached in 88 lesions (93 %), and clinical success in 82 lesions (86 %). Increased laser parameters (greater than 60 fluence, 40 Hz) was required for 29 resistant lesions.

Commercial ELA Catheters

Spectranetics offers a full line of ELA catheters for coronary and peripheral vascular indications. The catheters feature many of the advanced features detailed above: stranded fiber bundles; advanced hydrophilic coatings, HD and OS tip designs, and multi-durometer shaft construction. Smaller fibers of 50 and 61 μm core diameter are used with the exception of some of the larger peripheral catheters that use 100–130 μm fibers. The peripheral Turbo-Elite® catheter line offers OTW catheter sizes from 0.9 to 2.5 mm and RX catheters from 0.9 to 2.0 mm, and features 80 Hz and a continuous lasing capability. The ELCA® coronary catheter line contains catheter sizes from 0.9 to 2.0 mm in the RX configuration and OTW catheters are offered in the 0.9 mm size. Laser parameters for the ELCA catheters are 60 fluence, 40 Hz combined with 5 s “on” followed by 10 s “off” lasing sequence. The exception is the 0.9 mm catheter size which is offered in a model configured for 80 fluence, 80 Hz and a 10 s “on” followed by 5 s “off” lasing sequence.

Catheter Designs and Techniques for Greater Debulking

OS and HD devices, combined with slow catheter advancement, appear to deliver on the promise made in the 1980s for ELA, that being to debulk atheroma and to create a lumen the same size as the catheter, predictably and without complications. Ultimately the size of lumen created is limited by the size of the ELA catheter, which in turn is limited by the guide catheter or introducer sheath through which the ELA catheter is deployed. Multiple catheter passes can occasionally

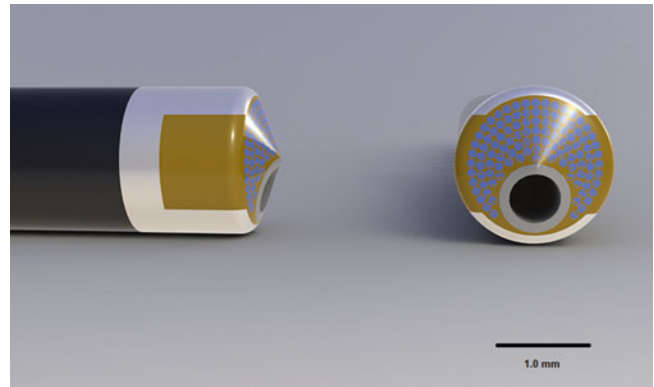


Fig. 1.10 The 1.7 mm Vitesse eccentric catheter (side and front tip views) features an optical fiber array located eccentrically to the guidewire lumen and a slotted radiopaque tip marker for catheter alignment under fluoroscopy

achieve slightly larger lumens, however, catheter designs that can target more of the residual plaque are required.

Eccentric Catheter

The first catheter evaluated for creation of larger lumens in the coronaries was the Vitesse E eccentric catheter produced by Spectranetics. The catheter featured an optical fiber pack located eccentrically to the guidewire lumen at the tip. See Fig. 1.10. Originally designed for eccentric lesions, the catheter featured construction in a rapid exchange catheter that allowed the tip to be rotated and aligned with the bulk of the lesion. It was surmised this featured could also be used to make multiple passes through a lesion, each pass realigning the tip of the catheter to target the remaining tissue. The catheter was available in 1.7 and 2.0 mm sizes.

Clinical study of the eccentric catheter in 53 coronary in-stent restenosis patients was performed by Dahm et al. [57]. Using a slow, multiple pass technique, the mean residual lumen diameter post laser was 2.4 mm. Residual lumens as large as 2.2 mm were obtained with the 1.7 mm catheter and 3.0 mm with the 2.0 mm catheter. Six-month follow-up revealed low restenosis rates rivaling brachytherapy results, the most effective therapy at the time, and demonstrated the benefit of maximal debulking. Interest in laser debulking of coronary in-stent restenosis waned with the success of drug-eluting stents which virtually eliminated the clinical problem of restenosis.

The Bias Sheath

One of problems experienced with the eccentric catheter was the catheter frequently fell back into the channel created by the catheter on the first pass, thus making subsequent passes

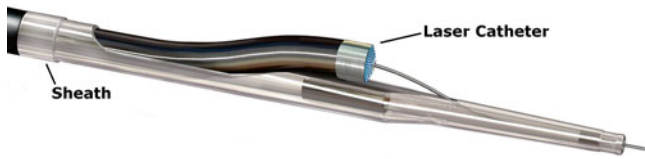


Fig. 1.11 Tip view of the Turbo-Tandem bias sheath. In this view, the laser catheter is biased away from the center of the lumen, so that it can engage and ablate residual plaque between the existing lumen and the artery wall. Image courtesy of The Spectranetics Corporation

ineffective. What was needed was a method to deflect the catheter and prevent this occurrence. US Patent 7,572,254 by Hebert et al. [58] discloses a sheath designed to bias the laser catheter away from its central axis and allow for targeting of plaque outside the initial laser channel. The sheath features a lumen to contain a laser catheter and a nosecone-shaped tip designed to act as a ramp to bias the laser catheter 1-2 mm away from the central axis. See Fig. 1.11. To use, a pilot channel is created in the occlusion using the laser catheter. The laser catheter is withdrawn, inserted into the bias sheath, and reinserted back into the artery over the guidewire. Once positioned proximal the occlusion, the laser catheter is advanced up onto the ramp and locked into position. Positioning of the catheter tip on the ramp is aided by radiopaque markers located on the bias sheath tip. The biased laser catheter is then used to debulk the occlusion using multiple pass technique, repositioning the catheter between passes to target residual plaque. The sheath was commercialized by Spectranetics for peripheral vascular use as the Turbo-Booster® and later a next generation system named the Turbo-Tandem®. The Turbo-Tandem is available in two sizes- a 7 French introducer sheath compatible model designed for use with a 1.7 mm catheter and a 8 French compatible model design for a 2.0 laser catheter.

Clinical evaluation of the 8 French Turbo-Booster sheath was performed in the CELLO study [59]. Sixty-five lesions in the leg with a mean reference diameter of 4.9 mm and an average length of 5.6 cm were treated. The percent diameter stenosis was reduced from 77 to 35 % (1.1 mm to 3.2 mm luminal diameter) after 8 passes (mean) of the Turbo-Booster sheath. Final residual stenosis was 21 % after adjunctive therapy (balloon angioplasty and stenting). Eight patients did not receive adjunctive therapy. Patency rates were 59 % and 54 % at 6 and 12 months, respectively.

Future Opportunities and Challenges

While HD catheter tips combined with increased laser parameters and smaller catheter diameters have improved ELAs ability to penetrate fibrocalcific lesions, there are still

calcified lesions laser cannot recanalize [56]. Dense intravascular calcium is a very hard ceramic-like material called calcium hydroxyapatite. Laser can etch this material but ablation rates are very slow and the resulting lumen diameters are very close to the optical fiber diameter of the catheter. Even if penetration is achieved, the catheter will ultimately become stuck in the lesion due to frictional and clearance issues. Rocky calcium remains an area of challenge for ELA.

ELA catheters have earned a place in the interventionalist toolbox primarily for recanalization of occlusions resistant to conventional therapy. Increased treatment of peripheral vascular disease has fueled ELA utilization due to the extent and complexity of the disease. Peripheral lesions are commonly occluded, longer, and with high plaque burden, requiring more specialized tools and techniques compared to coronary procedures. Conventional angioplasty tools (balloon and stent) have failed to produce a durable result in the periphery and created another problem, in-stent restenosis. Interest in debulking has resurfaced as a means to reduce plaque burden and improve long term results.

In order to compete in the debulking peripheral vascular market, ELA will have to prove it can provide superior long-term results. Removing more plaque burden may be key to obtaining the desired results, representing a lofty goal for ELA catheter design. Past catheter design attempts to accomplish this yielded modest results, only 0.5 and 0.7 mm more luminal gain than what could theoretically be accomplished with a large catheter in one pass [57, 59]. These small gains came at the expense of increased treatment time. To alleviate this issue, steps to increase the cutting rate of ELA should be taken. Advancing the catheter at 1 mm per second or slower is very difficult and results in extended treatment times, particularly in long lesions and when multiple passes are required. Increasing the repetition rate of the laser system to over 400 Hz is technically possible and should be investigated. A 400 Hz repetition rate would allow for a 5 mm/s advancement speed, decrease treatment time five-fold and may also yield some improvements in ablation efficiency. For future ELA systems, advances in both laser parameters and catheter designs will be required to achieve the goal of safely treating a blocked artery, and leaving behind a clear lumen with a diameter larger than the catheter itself.

References

1. Grundfest WS, Litvack F, Forrester J. Laser angioplasty. *Coron Artery Dis.* 1990;1:99–104.
2. Haase KK, Baumbach A, Spyridopoulos I, Oberhoff M, Karsch K. Initial clinical experience with a modified excimer laser for coronary angioplasty. *Lasers Med Sci.* 1994;9:7–15.
3. Isner JM, Clarke RH. Mechanisms. In: Isner J, Clarke R, editors. *Cardiovascular laser therapy.* New York: Raven Press Ltd; 1989. p. 89–104.

4. Izatt JA, Albigli D, Itzkan I, Feld MS. Pulsed laser ablation of calcified tissue: physical mechanisms and fundamental parameters. *Proc SPIE*. 1990;1202:133–40.
5. Golobic RA. Laser selection criteria for coronary laser angioplasty. In: Ginsburg R, Geschwind HJ, editors. *Laser angioplasty*. 2nd ed. Mount Kisco: Futura Publishing Company Inc; 1992. p. 205–15.
6. Taylor K, Reiser C. Large eccentric laser angioplasty catheter. *Proc SPIE*. 1997;2970:35–40.
7. Taylor KD, Papaioannou T, Harlan K, Sorokoumov O, Shehada R, Rentrop P. Small excimer laser angioplasty catheter for fibrocalcific tissue penetration. (abstr). *Lasers Surg Med*. 2000;26:10.
8. Gijssber GHM, Sprangers RLH, van Gemert MJC. Excimer laser coronary angioplasty: laser-tissue interactions at 308 nm. In: Ginsburg R, Geschwind HJ, editors. *Laser angioplasty*. 2nd ed. Mount Kisco: Futura Publishing Company Inc; 1992. p. 217–41.
9. Jacques SL. Role of tissue optics and pulse duration on tissue effects during high- power laser irradiation. *Appl Optics*. 1993; 32:2447–54.
10. Anderson RR, Parrish JA. Microvasculature can be selectively damaged using dye lasers: a basic theory and experimental evidence in human skin. *Lasers Surg Med*. 1981;1:263–76.
11. Abil' siitov GA, Belyaev AA, Bragin MA, et al. Investigation of photoablation of atherosclerotic plaques by laser radiation. *Soy J Quantum Electron*. 1985; 15:13 14–15.
12. Litvack F, Grundfest WS, Goldenberg T, Laudenslager J, Pacala T, Segalowitz J, Forrester JS. Pulsed laser angioplasty: wavelength power and energy dependencies relevant to clinical application. *Lasers Surg Med*. 1988;8:60–5.
13. Oraevsky AA, Jacques SL, Pettit GH, Saidi LS, Tittel FK, Henry PD. XeCl laser ablation of atherosclerotic aorta: optical properties and energy pathways. *Lasers Surg Med*. 1992;12:585–97.
14. Oraevsky AA, Jacques SL, Pettit GH, Tittel FK, Henry PD. XeCl laser ablation of atherosclerotic aorta: luminescence spectroscopy of ablation products. *Lasers Surg Med*. 1993;13:168–78.
15. Gijssbers GHM, Sprangers RLH, van den Broecke DG, van Wieringen N, Brugmans MJP, van Gemert MJC. Temperature increase during in vitro 308 nm excimer laser ablation of porcine aortic tissue. *Proc SPIE*. 1991;1425:80–7.
16. van Leeuwen TG, van Erven L, Meertens JH, Motamedi M, Post MJ, Borst C. Origin of arterial wall dissections induced by pulsed excimer and mid-infrared laser ablation in the pig. *JACC*. 1992;19: 1610–8.
17. van Leeuwen TG, Meertens JH, Velema E, Post MJ, Borst C. Intraluminal vapor bubble induced by excimer laser pulse causes microsecond arterial dilation and invagination leading to extensive wall damage in the rabbit. *Circulation*. 1993;87:1258–63.
18. Clarke RH, Isner JM, Donaldson RF, Jones G. Gas chromatographic-light microscopic correlative analysis of excimer laser photoablation of cardiovascular tissues: evidence for a thermal mechanism. *Circ Res*. 1987;60:429–37.
19. Furzikov NP, Karu TI, Letokhov VS, Beljaev AA, Ragimov SE. Relative efficiency and products of atherosclerotic plaque destruction by pulsed laser radiation. *Lasers Life Sci*. 1987;1:265–74.
20. Vogel A, Engelhardt R, Behule U, Parlitz U. Minimization of cavitation effects in pulse laser ablation illustrated on laser angioplasty. *Appl Phys B*. 1996;62:173–82.
21. Esenaliev RO, Oraevsky AA, Letokhov VS, Karabutov AA, Malinsky TV. Studies of acoustical and shock wave in pulsed laser ablation of biotissue. *Lasers Surg Med*. 1993;13:470.
22. Albagli D. Fundamental mechanisms of pulsed laser ablation of biological tissue, PhD thesis. Cambridge: Massachusetts Institute of Technology; 1994.
23. Verdaasdonk RM, Vos P, van Leeuwen TG, Borst C, van Swol CF. Contribution of photothermal and photomechanical effects during tissue ablation by the XeCl-excimer laser. *Proc SPIE*. 1994;2134A: 333–41.
24. Lippincott RA, Bellendir J, Taylor KD, Reiser C. Optimally spaced fiber catheter for excimer laser coronary angioplasty (ELCA). Anderson RR, Bartels KE, Bass LS, Bornhop DJ, Garrett CG, Gregory KW, Kollias N, Lui H, Malek RS, Perlmutter AP, Reidenbach H-D, Reinisch L, Robinson DS, Tate LP, Trowers EA (eds.). *Proc. SPIE 3590, Lasers in Surgery: Advanced Characterization, Therapeutics, and Systems IX*. San Jose, CA. (June 22, 1999).
25. Taylor KD, Reiser C. Next generation catheters for excimer laser angioplasty. *Lasers Med Sci*. 2001;16:133–40.
26. Hamburger JN. New aspects of excimer laser coronary angioplasty: physical aspects and clinical results. Doctoral thesis. Rotterdam: Erasmus University. 1999.
27. Pettit GH, Saidi IS, Tittel FK, et al. Thrombolysis by excimer laser photoablation. *Lasers Life Sci*. 1993;5(3):185–97.
28. Papaioannou T, Sorocoumov O, Taylor K, Grundfest W. Excimer laser assisted thrombolysis: the effect of fluence, repetition rate and catheter size. In: Bartels KE, et al., editors. *Lasers in surgery: advanced characterization, therapeutics, and systems XII*. Proceedings of SPIE 2002; vol. 4609. p. 413–8.
29. Papaioannou T, Levinsman J, Sorocoumov O, Taylor K, Pitzer S, Grundfest WS. Particulate debris analysis during excimer laser thrombolysis: an in-vitro study. In: Bartels et al., editors. *Lasers in surgery: advanced characterization, therapeutics, and systems XII*. Proceedings of SPIE vol. 4609. 2002. p. 404–12.
30. Baumbach A, Haase KK, Rose C, Oberhoff M, Hanke H, Karsch KR. Formation of pressure waves during in vitro excimer laser irradiation in whole blood and the effect of dilution with contrast media and saline. *Lasers Surg Med*. 1994;14:3–6.
31. Deckelbaum LI, Natarajan MK, Bittl JA, et al. Effect of intracoronary saline infusion on dissection during excimer laser angioplasty: a randomized trial. *JACC*. 1995;26:1264–9.
32. Tchong JE, Phillips HR, Wells LD, Golobic RA, Power JA, Deckelbaum LI. A new technique for reducing pressure pulse phenomena during coronary excimer laser angioplasty. *JACC*. 1993;21:938–74.
33. van Leeuwen TG, Borst C. Fundamental laser-tissue interactions. *Semin Intervent Cardiol*. 1996;1:100–20.
34. Sauerbrey R, Pettit GH. Theory for the etching of organic materials by ultraviolet laser pulses. *Appl Phys Lett*. 1989;55:421–3.
35. Bittl JA. Clinical results with excimer laser coronary angioplasty. *Semin Intervent Cardiol*. 1996;1:53–78.
36. Klein LW, Litvack F, Holmes D, et al. Six month outcome and determinants of adverse clinical events after successful excimer laser coronary angioplasty. *J Invas Cardiol*. 1995;7:191–9.
37. Litvack F, Eigler N, Margolis J, et al. Percutaneous excimer laser coronary angioplasty: results in the first consecutive 3,000 patients. *JACC*. 1994;23:323–9.
38. Reifart N, Vandormael M, Krajcar M, et al. Randomized comparison of angioplasty of complex coronary lesions at a single center. Excimer laser, rotational atherectomy, and balloon angioplasty comparison (ERBAC) study. *Circulation*. 1997;96(1): 91–8.
39. Sanborn TA. Laser angioplasty: historical perspective. *Semin Intervent Cardiol*. 1996;1:161–74.
40. Estella P, Ryan TJ, Landzberg JS, Bittl JA. Excimer laser-assisted coronary angioplasty for lesions containing thrombus. *JACC*. 1993;21:1550–6.
41. van Leeuwen TG, Velema E, Pasterkamp G, Post MJ, Borst C. Saline flush during excimer laser angioplasty: short and long term effects in the rabbit femoral artery. *Lasers Surg Med*. 1998;23:128–40.
42. Ebersole DO. Clinical applications for the excimer laser. *Cardiovasc Rev Rep*. 1999;10:6.
43. Margolis JR. Excimer laser vs. balloon angioplasty: (AMRO study) – what is the relevance? *Eur Heart J*. 1996;17:807–8.

44. Mehran R, Mintz GS, Satler LF, Pichard AD, Kent KM, Bucher TA, Popma JJ, Leon MB. Treatment of in-stent restenosis with excimer laser coronary angioplasty. *Circulation*. 1997;96:2183–8.
45. Oberhoff M, Baumbach A, Herdeg C, et al. Smooth excimer laser coronary angioplasty (SELCA) and conventional excimer laser angioplasty: comparison of vascular injury and smooth muscle cell proliferation. *Lasers Med Sci*. 1997;12:328–35.
46. Gijsbers GHM, Hamburger JN, Serruys PW. Homogeneous light distribution to reduce vessel trauma during excimer laser angioplasty. *Semin Intervent Cardiol*. 1996;1:143–8.
47. van den Broecke DG, Hamburger JN, Gijsbers GHM, Serruys PW. The influence of CO₂ flush on the quality of excimer laser tissue ablation. (abstract) *Proc 1st Int Meet Intervent Cardiol*. 1995;7(Suppl C):21.
48. Abela GS, Norman SL, Cohen DM, et al. Laser recanalization of occluded arteries in vivo and in vitro. *Circulation*. 1985;75:403–11.
49. Isner JM, Donaldson RF, Funai JT, et al. Factors contributing to perforations resulting from laser coronary angioplasty: observations in an intact human postmortem preparation of intraoperative laser coronary angioplasty. *Coron Artery Surg*. 1985;72 Suppl 2:191–9.
50. Bittl JA, Brinker JA, Sandborn TA, Isner JM, Tchong JE. The changing profile of patient selection, procedural techniques, and outcomes in excimer laser coronary angioplasty. *J Intervent Cardiol*. 1995;8:653–60.
51. Taylor KD, Bellendir J, Hamersmark DJ. Fiber optic catheter with shortened guidewire lumen. United States of America Patent 5,456,680, 10 October 1995.
52. Grzesik U, Fabian H, Neu W, Hillrichs G. Reduction of photodegradation in optical fibers for excimer laser applications. *SPIE vol 1649 Optical Fibers in Medicine VII*. 1992. p. 80–90.
53. Fabian H, Grzesik U, Hillrichs G, Neu W. Optical fibers with enhanced performance for excimer laser power transmission at 308 nm. *SPIE vol 1893 Optical Fibers in Medicine VIII*. 1993. p. 24–32.
54. Wardle JL, Goldenberg T. Optical catheter with stranded fibers. United States of America Patent 5,415,653, 16 May 1995.
55. Taylor RS, Higginson AJ, Leopold KE. Dependence of the XeCl laser cut rate of plaque on the degree of calcification, laser fluence, and optical pulse duration. *Lasers Surg Med*. 1990;10:414–9.
56. Bilodeau L, Fretz EB, Taeymans Y, Taylor K, et al. Novel use of a high energy excimer laser catheter for calcified and complex coronary artery lesions. *Cath Cardio Interv*. 2004;62:155–61.
57. Dahm JB, Kuon E, Hummel A, Möx B, Staudt A, Felix SB. Area ablation: a new lasing concept provides significantly enhanced acute and long-term results for treatment of in-stent restenosis. *Lasers Surg Med*. 2002;31(1):1–8.
58. Hebert CJ, Bowe WA, Wood TJ, Tedder S. Apparatus and methods for directional delivery of laser energy US Patent 7,572,254, August 11, 2009.
59. Dave RM, Patlola R, Kollmeyer K, et al. Excimer laser recanalization of femoropopliteal lesions and 1-year patency. *J Endovasc Ther*. 2009;16:665–75.

Fluid-Dynamic Phenomena in Cardiovascular Ablation with Laser Irradiation

2

Robert Splinter and Christian G. Parigger

Introduction

Removal of atherosclerotic plaque is a therapeutic modality in the prevention of heart-attacks as well as pertaining to the preservation of circulation to the extremities. Atherosclerosis in the leg contributes to loss of independence, specifically for the elderly. Poor circulation in the leg is often associated with claudication pain, resulting in reduction in mobility. Obstructive blood flow in the coronaries can result in cell death leading to arrhythmias as well as total cessation of vascular circulation. The physician can resolve vascular occlusion disease using mechanical displacement, mechanical removal or chemical ablation, thermal ablation or laser irradiation. The mechanical process of increasing the lumen of an artery, or vein, can be achieved by balloon inflation [1]. Balloon angioplasty does not remove material; however, it relies on the placement of a stent to ensure a degree of permanency in the preservation of flow [2]. Other mechanical processes include cutting into the plaque for active excision. For mechanical removal one uses either a forward or side-ways directed blade to scrape thin layers of predominantly soft tissue for gradual advancement [3]. Due to the cumulative effect of the mechanical removal, the catheter is frequently discharged from the acquired content, which may also require removal from the vessel. For chemical ablation of plaque, administration of a chemical is needed to initially break-down plaque followed by removal. In addition, chemical treatment is applied for prevention of restenosis as well as for control of endothelial regrowth and proliferation [4].

Laser irradiation in arterial-vascular and cardiovascular applications is used for photo-thermal ablation of diseased tissue, for vaporization and for photo-mechanical removal of vascular plaque, as for instance during Percutaneous Transluminal Coronary Angioplasty (PTCA) in the coronaries [5] or in the peripheral veins (as part of the treatment of peripheral artery disease: PAD).

This chapter discusses the mechanism-of-action associated with the removal of atherosclerotic plaque facilitated by laser energy. In photo-thermal ablation of tissue in a confined biological environment it is important to evaluate the efficiency of removal of target material. Furthermore, formation and eradication of the resulting debris is of interest while preserving the integrity of the surrounding tissue structure. Photo-thermal ablation relies on irradiation with electromagnetic radiation (EM-radiation) to induce destruction of structural integrity.

Laser ablation with near-infrared light may yield a high volume of vaporization due to the deep penetration of the light, but it is substantially limited to the ablation of materials that have low vaporization entropy. Long wavelength (i.e., infrared) laser ablation relies on volumetric heating, yet there are associated risks for inducing thermal damage to healthy tissues in the vicinity of volume to be treated. The same principle holds true when using radiation in most of the visible region. Ultraviolet light on the other hand has shallow tissue penetration, but can induce breaking molecular bonds. This may also apply to a certain range of blue light irradiation, depending on the chemical bonds under consideration [6].

Ultra-Violet excimer laser radiation based ablation of plaque shows direct interaction with calcified hard tissue. Usually a fiber-optic based catheter is used to administer the treatment (Fig. 2.1). The limited penetration depth under ultra-violet light absorption provides a thermally confined process, with associated diminished peripheral thermal range. This thermal confinement restricts tissue removal. The photoablative mechanism-of-action can be classified in two categories: vaporization and Photodisruption [7].

R. Splinter (✉)
Department of R&D, Splinter Consultants,
318 Albright Avenue, Graham, NC 27253, USA
e-mail: rsplinter@gmail.com

C.G. Parigger, PhD
Department of Physics, University of Tennessee Space Institute,
411 B.H. Goethert Parkway, Tullahoma, TN 37388, USA
e-mail: cparigge@tennessee.edu

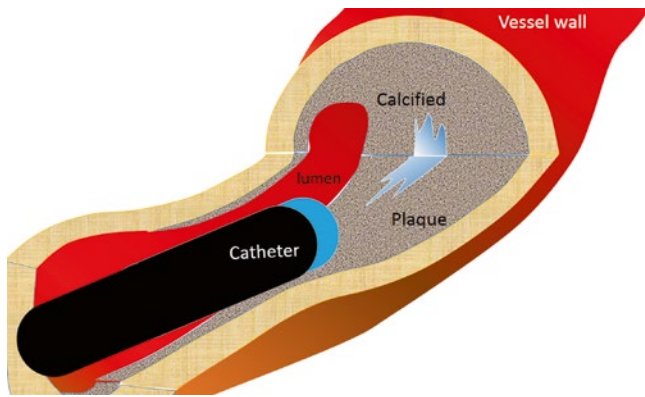


Fig 2.1 Graphical representation of the geometry and composition of plaque in the vessel with imbedded calcified areas. The catheter will not necessarily face the plaque at perpendicular angle, unless it is a total occlusion. The total occlusion may however still be composed with a surface at an angle. Additionally, the inhomogeneous composition of the plaque will force the catheter to follow the path of ablation with respect to the softer tissues that have a lower ablation threshold

Fluid-Dynamic Phenomena in Plaque Ablation

During laser irradiation, the vaporization of biological media (i.e. plaque) and specifically blood (thrombus) generates an expanding bubble followed by cavitation. Additionally, other pulsatile flow conditions directly related to the blood flow itself may cause vortices as well. Both bubble expansion and bubble collapse (i.e., cavitation) create conditions of mechanical and chemical non-equilibrium, hence removing the homeostasis on a local level. The rapid changes in pressure and associated changes in the concentration gradient affect local tissue structure. Tissue exposure that does not result in irreversible damage and cell-death can induce regenerate action (neo-intimal hyperplasia) that does not conform to the established anatomical cell growth. Specifically neo-intimal hyperplasia can be viewed as a type of cell growth that can contribute to the formation of plaque.

Turbulence and cavitation can result in boundary layers with little or no net flow, which instigate conditions for thrombus formation. The localized thrombus formation is one of the first indicators of plaque formation.

The formation of cavitation and required boundary conditions were first described by Osborne Reynolds (1842–1912) in 1894. The classifications of the conditions for turbulence and cavitation are indicated by the Reynolds number

($Re = \frac{v\ell}{\eta}$, the ratio of inertial and viscous forces, with v the

flow velocity, ℓ the characteristic length, η the kinematic velocity) of the local flow circumstances [8]. Full cavitation will occur when the Reynolds number exceeds 3000, not

considering the Cavitation Number of the phenomenon [8]. Other theoretical considerations of nonequilibrium in mechanical and chemical conditions with respect to turbulence includes effects described by the Bernoulli equation, an increase in flow velocity (v_{flow}) corresponds to a decrease in local pressure (as for example realized on an aerofoil [wing], causing a plane to become and remain airborne). Noteworthy is as well, when the locally applied pressure drops below the vapor pressure a liquid will vaporize. This phenomenon is known and recognized as cavitation.

Dissolved constituents, usually encountered in complex chemical media, are subject to Henry's Law [8]. Henry's law asserts that as the pressure drops certain gasses will be freed from solution and form bubbles. The cavitation number (k_d) associated with this Bernoulli pressure gradient:

$$k_d = \frac{P_\infty - P_{vapor}}{\rho \left(\frac{v_{flow}^2}{2} \right)},$$

indicating whether cavitation is likely, as

it is for small cavitation number, where P_∞ is the local pressure, P_{vapor} the fluid vapor pressure, v_{flow} the flow velocity (average), ρ the fluid density [9]. In addition to analysis of flow in cylindrical arteries, this also provides insight in special flow architecture especially in a curved vessel, and can be useful in determining the impact of shape and angular velocity in bifurcations and expansion/constriction at a stenosis.

Generally the formation of bubbles progresses at a slower rate than the collapse, providing a unique mechanism of mechanical interaction. A representative real-time progression of the bubble evolution is illustrated in Fig. 2.2a, with the theoretical outline of the resonance phenomenon for a unobstructed bubble displayed in Fig. 2.2b. Cavitation can be described resulting from thermal ablation processes, specifically from short duration events, such as pulsed laser ablation (i.e., initiated by thermal expansion) [10, 11]. Cavitation can cause mechanical effect as well as chemical changes. The chemical interaction is based on the concentration gradient that is created as a result of the turbulence associated with the bubble flow.

Mechanism-of-Action in Tissue Ablation

The mechanical and chemical mechanisms involved in photo-ablation are based on the following physical actions. Tissue vaporization relies on the conversion of one form of energy mediated by a thermodynamic phase transition based on molecular vibration, resulting in a conversion from solid preferably to gas. Molecular vibration is the fundamental consequence of temperature. The average vibrational kinetic energy

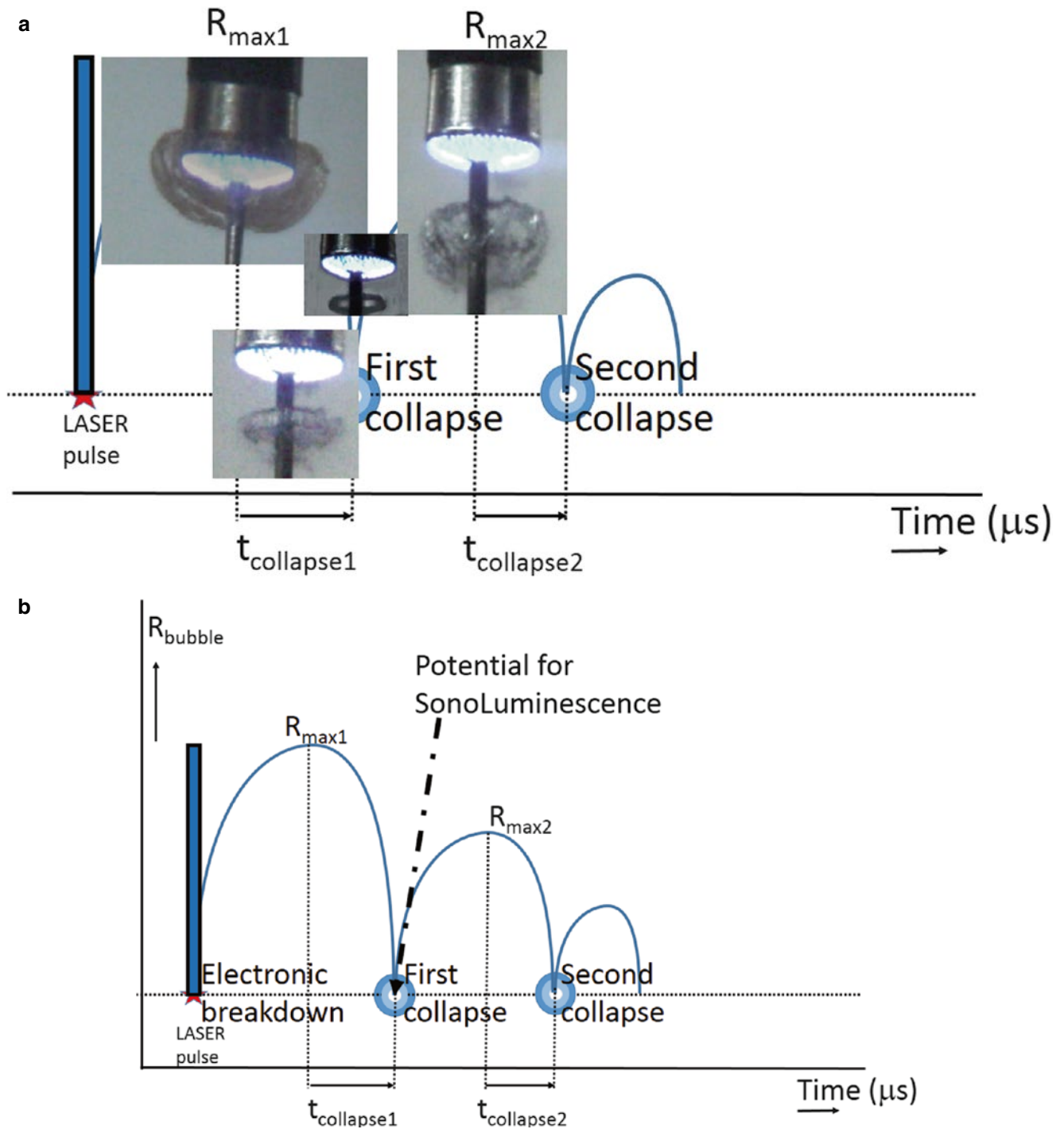


Fig 2.2 Schematic representation of the bubble evolution in an un-obstructed ultraviolet light absorbing liquid field. The same fundamental theoretical principles will apply to the ablation process of plaque, however the bubble will be confined between the catheter tip and the solid plaque surface. The bubble progression illustrated in (a) represents the real-time maximum bubble size formation under 308 nm excimer irradiation in an absorbing liquid using a 2.0 mm

diameter catheter with an inserted guide wire. The cavitation process is of the order of tens of microseconds with respect to the initiating laser pulse-width of 200 ns (not drawn to scale). The time span between the first and second maximum radius is of the order of 300 μs . (b) Graphical illustration of the fluid-dynamic resonance corresponding to the solution to the Rayleigh-Plesset equation for the bubble wall-motion

(E_{kin} , where $\overline{E_{kin}}$ represent the average Kinetic Energy) of molecular motion is directly correlated to the absolute value for temperature in Kelvin as $T = \frac{\overline{E_{kin}}}{k_b} = \frac{1}{k_b} \left\langle \sum \frac{1}{2} m_i \overline{v_i^2} \right\rangle$,

where $\overline{v^2}$ represents the average vibrational and translational velocity of the conglomerate of individual molecules (i) with respective mass m_i , summed over the total volume of molecules in the tissue under irradiation and averaged, and $k_b = 1.381 \times 10^{-23} \text{ m}^2 \text{ kg} / \text{s}^2 \text{ K}$ is the Boltzmann constant [12].

Thermal effects are designated to EM-radiation, ranging from blue to long wavelength infra-red. Photodisruption is a combination of primary chemical bond-breaking, as well as initiating vibrations resulting from thermal heating, which in-turn results in an acoustic effect and/or thermal expansion due to heating of either liquid or solid biological media. Photodisruption has a high likelihood of providing gas-formation (viz. vapor-bubble).

Long wavelength visible and near-infrared light by nature provides sufficient energy to increase molecular vibrations. Long wavelength electromagnetic radiation primarily results in a large-volume temperature increase which may eventually lead to liquefaction or vaporization. Prior to reaching vaporization conditions, the tissue will reach a temperature that will cause protein denaturation, resulting in cell death for living tissue. For calcified plaque, however, infrared light does not deliver the energy to melt or vaporize the solids containing calcium in complex chemical structures with tight atomic and molecular bonds. Hence the attention is drawn to breaking high-energy atomic bonds, mandating the need for high energy photon irradiation, i.e., ultraviolet light. The high energy ($E_{EM} = h\nu = h \frac{c}{\lambda}$ where ν is the EM radiation frequency, λ the wavelength of the light, and c the speed of light) in pulsed ultraviolet light provides potentially the most powerful mechanism available to break-up calcium based solid structures. In most cases, the energy requirements for ultraviolet laser light generation also define the stimulated emission process. The high excitation energy requirements for ultraviolet laser light can primarily be achieved under pulsed conditions, since the intermittent process of energy storage yields the required threshold for excitation of the medium. Fluorescence at short wavelengths may not be maintained for extended periods for excitation in the laser light generation process.

In this chapter the primarily focus will be on pulsed events with a time-resolved mechanism-of-action for ablation, specifically geared to ultraviolet irradiation. The alternating nature of ablation is directly correlated to pulsatile nature of the irradiation used for plaque removal. When the photon energy is high enough to break molecular bonds the net result is formation of microscopic plasma. The physics of the plasma formation has complex fluid-dynamic and engineering implications.

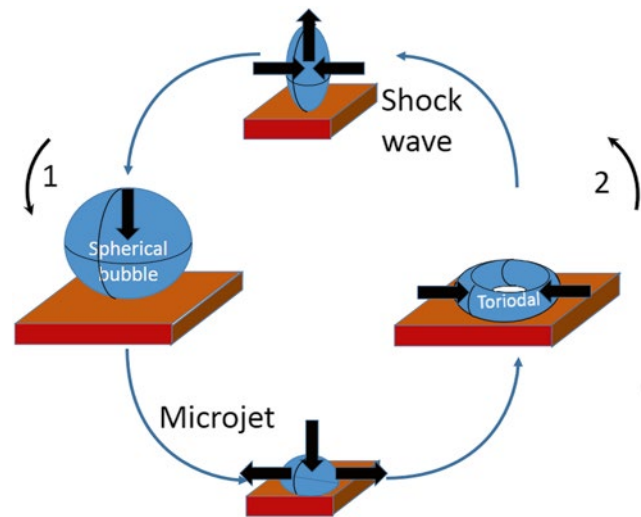


Fig 2.3 Schematic representation of the various phases in the fluid-dynamics aspects of bubble evolution. The stage of micro-jet formation produces a forceful flow of debris that will impact both the catheter tip as well as the remaining plaque, respectively thrombus. The micro-jet formed under the ablation of calcified plaque has a size distribution of microscopic particles that will chip away on the epoxy fixation for the fiber-optics in the distal tip of the catheter. The toriodal bubble is one particular configuration for the cavitation process, as illustrated in Fig. 2.2a, the bubble is wider than long

The exact energy conversion will depend on the photon energy and thus the irradiation wavelength as well as on the biological medium in the direct path of the photon stream. Residual and secondary thermal effects may also be involved due to heat dissipation, convection and conduction. This causes vaporization of the liquid media within the irradiated volume and potential boundary layers, specifically water due to the lower vaporization heat with respect to proteins and fat of the cellular construction. Photodisruption is achieved by pulsed laser ablation, in this case utilizing the short wavelength ultraviolet EM-radiation. Conversely, vaporization can be achieved with both pulsed and steady-state laser irradiation across the full visible and infrared spectrum.

Tissue, thrombus and plaque vaporization creates expanding bubbles that subsequently collapse, creating microjets and shockwaves that cause destructive mechanisms when near a boundary [13]. The bubble phases are outlined in Fig. 2.3. These processes form the mechanical constituents of the cavitation phenomena during plaque ablation.

Laser and Light Propagation

The main aspect of laser ablation is associated with the wavelength of the irradiating light and the physical interaction at the atomic and bulk material scale, respectively. For bulk biological media, the individual tissues in the target volume can be

represented by their respective spectral attenuation profiles, prescribing the primary absorption wavelengths for volumetric thermal effects. However, it is virtually impossible to predict the exact chemical composition within the plaque and the three-dimensional chemical configuration; even when in-situ high-resolution imaging would become available. At the microscopic scale there is molecular binding, yielding the requirements for dissociation energy ($h\nu$, the latent heat of dissociation for the respective tissues l in the tissue volume). The requirement of breaking molecular bonds specifies the upper threshold for the sanctioned wavelength and associated energy that matches or exceeds the energy of the chemical bond: $E = h\nu > E_{bond}$, where ν is the frequency of the light (which may have a band-width: $\Delta\nu$) [14].

The amount of energy that can be deposited in a specific volume of tissue will depend on laser-light spot-size which yields the energy-density of the electromagnetic radiation on the surface of the target medium, as well as a range of tissue conditions and operating parameters (e.g., pulse-width, repetition frequency, and focal area) in addition to the EM wavelength. The spatial light-distribution inside the tissues will provide the location specific probability of light absorption, defined by the local absorption coefficient (μ_a). The volumetric light-distribution is a function of all the tissue optical properties: including the scattering coefficient (μ_s) and scattering angle (θ), represented by the scattering anisotropy factor: $g = \langle \cos\theta \rangle$, that indicates the mean cosine of the bulk scattering angle distribution profile. Various tissues have distinctive and unique optical parameters. The magnitude of the amount of light is a function of both the electric field amplitude and the magnetic field amplitude, expressed as fluence or radiance. In any given location, the locally delivered light-fluence will be absorbed with appropriate thermal and photo-chemical effects as a function of position within the irradiated volume and the local tissue constituents.

Mechanism of Delivery

In laser assisted atherectomy the use of fiber-optics allows for achieving microscopic delivery precision as well as micro-positioning for targeted ablation. Catheters are designed with fiber-optics bundles consisting of groupings of fibers of one or more individual diameters, ranging from several micrometers to several hundred micrometers [15–17]. A representation of the fiber-optic bundle at the catheter tip is illustrated in Fig. 2.4. The fiber-optic diameter will place restrictions on the smallest radius of curvature with increasing diameter. Based on the application the fiber-optic diameter will be selected for tortuosity to maneuver through small curvy blood-vessels, or target high energy density during relatively straight vessel geometry with large diameter and large number of fiber-optics. The catheter will also provide a

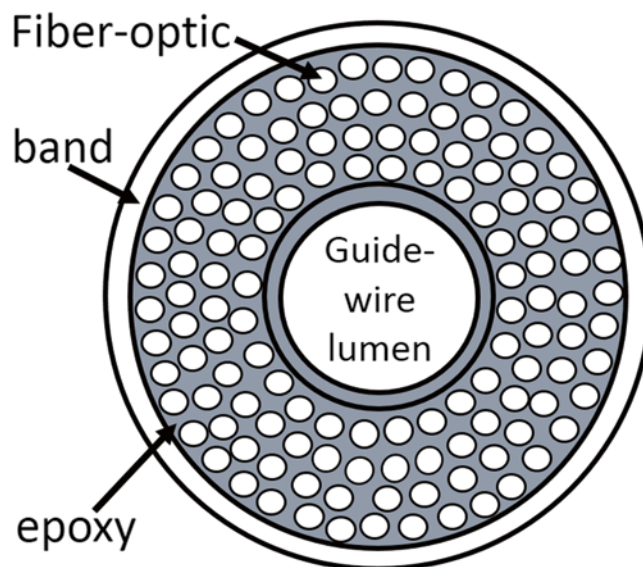


Fig 2.4 Diagram of the distal tip design of the catheter. A multitude of fiber-optic light-guides are held in a fixed location with respect to each other for mechanical stability and predictable optical delivery configuration

core lumen that is void from fiber-optics, designed to advance a guide-wire through the vasculature under fluoroscopic guidance. The specifics of the fiber-optic annulus at the catheter tip will provide special boundary conditions, and in turn, cause inherent limitations to the ablation process that will need to be understood on a structural basis but falls outside the context of this chapter.

Light-Tissue Interaction

The light distribution in a scattering medium can be generally described by the Equation of Radiative Transfer. The Equation of Radiative Transfer is concerned with a three-dimensional energy density distribution as a function of the distribution profile administered to the surface of a tissue volume. The influence of the local optical properties of all the tissues and materials encountered in both plaque and vessel wall and thrombus in this case is outlined in Chap. 16 (R. Splinter). The theoretical analysis in the case of Chap. 16 (R. Splinter) however primarily addresses the scenario where scattering dominates over absorption, primarily in the long wavelength range of red and infra-red radiation. When the absorption dominates scattering, the theoretical evaluation of the light-distribution reduces to a linear decay function with distance, known as the Beer-Lambert law of attenuation [14]. Absorption dominated light-tissue interaction occurs in so-called short wavelength atherectomy, especially in the ultra-violet as well as at specific spectral attenuation peaks associated with relevant molecular signatures.

The absorption dominated interaction of electromagnetic radiation can be explained on a molecular level, based on a partial or specific match between either the molecular kinetics, or on the binding energy with respect to the wavelength specific energy.

Light Propagation Under Dominant Absorption

When absorption is much greater than scattering the light distribution inside a turbid medium is dramatically reduced in complexity. This situation is certainly valid for ultraviolet light irradiation of biological media. In the wavelength range below 400 nm, absorption is much greater than scattering. For instance, for muscle the absorption is at least 1.5 times larger than scattering at 400 nm and 3 times larger at 308 nm [18], further increasing for shorter wavelength. Under these conditions, the light fluence ($\Psi(z)$) can be described by a one dimensional exponential attenuation proportional to the distance (the Beer – Lambert law): $\Psi(z) = \Psi_0 e^{-\mu_a z}$.

The light profile in this case depends on the fiber-optic placement and arrangement in the catheter in question. Generally, the light profile will be considered as uniform across the catheter diameter as a “top-hat”, with equal radiance across the diameter of the face of the catheter in contact with the target area [14].

Laser Light Mediated Atherectomy Mechanisms and Applications

When ultraviolet laser energy is deposited in a tissue, there are four types of effects that contribute to the ablation process:

- Vaporization
- Thermoelastic expansion
- Plasma formation
- Spallation and Cavitation

There is supporting evidence that UV ablation requires “priming” of the treatment area. Ultraviolet irradiation of tissues has been documented to increase the attenuation at the irradiation wavelength more than two-fold [19]. This phenomenon has been confirmed under laboratory conditions using high-speed video [20–22]. During 308 nm excimer laser irradiation, the very first pulse has little or no ablative effect, i.e., relatively small tissue vapor bubble, not much greater in free liquid than the spot-size of the delivery catheter or with bubble totally absent, whereas the subsequent pulses, delivered routinely at a rate of 80 pulses per second, show bubble formation of significant volume, growing to more than twice the diameter of the irradiated area [19], as illustrated in Fig. 2.2a.

Vaporization

As the temperature of a tissue is raised by pulsed laser radiation, the water in the tissue can vaporize. Vaporization processes can occur in three different ways: surface evaporation, subsurface explosive vaporization, and explosive expansion of superheated fluid.

Pulsed Vaporization

The rate of tissue removal as a function of irradiation fluence can be defined as the ablation velocity (v_{abl}) which can be written as: $v_{abl} = \frac{L_0'}{W_{abl}}$ [14]. The vaporization ablation depth

for soft tissue, d per pulse follows from the integral over the portion of the pulse duration (t_p) over which the ablation

process occurs; $d = \int_{t_0=0}^{t_p} \frac{L'(t)}{W_{abl}} dt$. The point in time, t_0 ,

denotes when the ablation threshold energy, E_{th} is reached. The actual pulse duration is longer than t_p , by the “pre-warming time” needed to reach the boiling point of a minimum tissue volume. Combined with the absorbed incident total irradiation power density $\mu_a L_0'$ within first order approximation (i.e., instantaneous removal) of the ablation depth can be

written as: $d = \frac{\mu_a L_0' - E_{th}}{W_{abl}}$. The radiant energy deposited at

depth d follows from Beer-Lambert’s law of attenuation. As discussed above, the theoretical soft-tissue ablation depth is only reached when the deposited energy at depth d exceeds the threshold. Therefore, we find: $L(d) > E_{th} = (1 - R) L_0 e^{-\mu_a d}$, where R denotes the loss-factor that includes the coupling efficiency into the tissue, which actually increases with the proximity of the delivery fiber-optic [14].

Due to the short duration excimer laser pulse of ~ 200 ns, the thermal conduction loss is considered negligible during the exposure. This provides a quasi-steady state situation in first order approximation with soft tissue volume removal per

pulse (V_{PV}): $V_{PV} = \frac{A(\mu_a L_0' - E_{th})}{W_{abl}}$. In this derivation, the sur-

face area (A) is taken to be equal to the area of the distal tip of the catheter. For a thermally confined pulse rate, the ablation processes can be seen as short (continuous and in equilibrium) ablation steps. The expelled volume (V_{abl}) is

computed using: $V_{abl} = \frac{A}{\mu_a} \ln\left(\frac{\mu_a L_0' \tau}{E_{th}}\right)$ [14].

The size of the bubble with respect to the ablated volume is difficult to infer since there are many boundary conditions involved that influence the final volume. In a coarse approximation, the number of molecules in the ablated volume (n) can serve as the indication of the gas volume based on the ideal

Gas Law: $V = \frac{n}{P} R_{gas} T$, where T is the temperature of the

bubble vapor which can be in excess of the vaporization temperature, depending on the processes involved and the superheating effects under confined, ‘pressurized heating’ i.e., pressure-cooker. The number of moles, n , denotes all the constituents in the vapor bubble, P the pressure in the bubble resulting from the surface tension applied by the surrounding solid and liquid media (Laplace Law). The Universal Gas constant is: $R_{\text{gas}} = 8.314 \frac{\text{J}}{\text{Kmol}}$, and the volume of the sphere is $V = \frac{4}{3}\pi(r(t))^3$, with $r(t)$ describing the time-dependent bubble radius [12, 23, 24].

In general, for excimer laser ablation, the pulse delivery sequence (i.e. pulse interval $\tau_{p \rightarrow p}$) is longer than the thermal relaxation time (τ_r) and hence each pulse can be treated as a unique event [12, 25, 26]. This is in particular true for excimer pulsing rates of 80 Hz or less.

Surface Evaporation

Vapor can be formed at the surface, subsequently the liquid evaporates from the surface. Such surface evaporation can dissociate the superficial layers of a tissue. The rate of vaporization is an indicator for the rate of energy deposition in the tissue surface. In the case of ultraviolet laser irradiation the light is strongly absorbed by tissue and facilitates surface evaporation. For an incident laser pulse radiant exposure $L \left[\frac{\text{J}}{\text{m}^2} \right]$, the evaporation, expressed as the escaping mass

of water per unit area of surface $m_{\text{evap}} \left[\frac{\text{kg}}{\text{m}^2} \right]$, is about

$$m_{\text{evap}} = \frac{L}{Q_{\text{vap}}} . \text{ The heat of vaporization of water } (Q_{\text{vap}}) \text{ at } 100^\circ\text{C} \text{ is } 2.259 \times 10^6 \frac{\text{J}}{\text{kg}} .$$

To illustrate desiccation, consider a laser pulse that heats the surface of a tissue from 37 to 100 °C, $\Delta T = (100 - 37) = 63^\circ\text{C}$. In this case, there is no explosive vaporization but there is sufficient heat to drive surface evaporation. However, the temperature does not need to be elevated to the boiling point for vaporization to commence. The temperature rise can be evaluated as follows: Let the optical penetration depth of light be 20 μm ($\mu_a = 300 \text{ cm}^{-1}$; which is a typical value for tissue when using an excimer laser operating at 308 nm). The radiant exposure to

$$\text{achieve this temperature rise amounts to } \frac{\Delta T \rho c_v}{\mu_a} = 527 \frac{\text{mJ}}{\text{cm}^2}$$

.For complete absorption of all the laser energy, the mass of evaporated soft tissue will result in an approximate removal depth of 10 μm . This estimate will apply to thrombus and soft plaque, however calcified plaque has very low water content, and will require the vaporization of fatty and soft tissues next to calcified structures, with much higher energy requirements.

Subsurface Explosive Vaporization

As the light is absorbed below the surface and if surface cooling were to prevent the surface layer to evaporate, then the subsurface vapor pressure builds until it overcomes the surface tension of the tissue. Rapid vapor expansion subsequently disrupts the tissue [27]. Only a small amount of water vapor is needed to cause tissue disruption. A 10–30 °C excess temperature in pure water can evaporate 2–6 % of the water. Just a small fraction of the cellular water is converted to vapor, and this small amount is sufficient to cause disruptive vaporization in the tissue. For example, the threshold temperature for explosive disruption of red blood cells is about 125 °C [28, 29]. When targeting a medium which shows absorption peaks, the energy requirements will become less, as would be the case involving melanin. The threshold temperature for explosive disruption of melanosomes by a pulsed laser is about 112 °C [29]. Melanosomes are an animal cell constituent that host the process for chemical amalgamation, production and storage of melanin. The melanosomes also provide the transport mechanism for melanin.

Thermoelastic Expansion

Energy deposition raises the temperature of the tissue by, $\Delta T = \frac{\mu_a H}{\rho c_v}$ [°C]. This temperature rise causes thermoelastic expansion of the tissue expressed as strain (ϵ_{strain}) which is the change in length ($\Delta \ell$) normalized by the initial length (ℓ), $\epsilon_{\text{strain}} = \frac{\Delta \ell}{\ell}$. The strain is related to the temperature

rise, $\epsilon_{\text{strain}} = \beta \Delta T$ [dimensionless], where β is the thermal expansivity [K^{-1}]. The stress (or pressure) generated by this strain is expressed as $P = M \sigma_{\text{stress}}$, where $\sigma_{\text{stress}} = \frac{dF_n}{dA}$

is the normal stress, and M is the bulk modulus [J/m^3] that specifies the pressure per unit strain. In summary, the pressure exerted by thermoelastic expansion is: $P = \Gamma_{\text{Grün}} \mu_a H$ where, $\Gamma_{\text{Grün}}$ is a dimensionless parameter called the Grüneisen coefficient that specifies the fraction of thermal energy deposition that couples into mechanical energy [14]. The value of $\Gamma_{\text{Grün}}$ varies with the type of material, the temperature, and the rate of heating. The Grüneisen coefficient: $\Gamma_{\text{Grün}}$, of water at room temperature is about 0.12, meaning that about 12 % of thermal energy deposited by a 200-ns-pulse laser in biological tissues couples into mechanical energy. For reference, 1 J/m^3 of pressure equals 1 Pascal [Pa], and 10⁵ Pa equals about 1 bar [bar] or 1 atmosphere. Figure 2.2 illustrates evolution of the expansion and modes of crack propagation.

Based on this model, only a modest temperature rise occurs subsequent to pulsed laser irradiation than can create significant pressures via thermoelastic expansion. Of course, by means of focusing lenses the pressure of the thermoelastic expansion can easily be modified and manipulated.

To achieve the maximum amount of pressure, the laser pulse energy must be deposited in the target tissue volume faster than the speed of sound at which dissipation of mechanical energy occurs from the irradiated volume. Pressure waves propagate away from the volume at the speed of sound in the medium, although higher shock speeds can be measured for smaller time delays from the laser pulse that generates the ablation, the ablation. The concept of depositing energy faster than the speed of sound is referred to as stress confinement. The portion of the laser pulse duration (after accomplishing the initial ‘warm-up’ to reach ablation threshold), t_p [s], required to achieve stress confinement in a tissue volume whose size is characterized by a length d [m] (representative of the laser interaction depth) is: $t_p < \frac{d}{v_s}$,

where v_s [m/s] is the velocity of sound in the tissue. The value of v_s for water is 1480 m/s, and values for soft tissues are similar. In solid media, the speed of sound will be larger. The speed of sound characterizes the propagation of pressure wave, which causes bubble formation. If the laser pulse is significantly longer than $\frac{d}{v_s}$, the pressure dissipates faster than it can accumulate. Also, the maximum pressure is not achieved for significantly longer pulses. For an excimer laser with a pulse-width of 200 ns, the interaction depth will in this case need to be greater than 10 μm . Once a laser pulse has deposited pressure under stress-confined conditions, the pressure will propagate away from the heated volume at the speed of sound as a pressure wave.

Plasma Formation

Plasma is an ionized substance that is not quite a liquid nor a solid and in laser ablation processes a ‘‘cloud’’ of free electrons occurs in a ‘‘cloud’’ of free-electrons in a medium [30, 31]. When either the photon energy exceeds the molecular bounding energy of the target or when the irradiance of a pulsed laser on a tissue exceeds 1000 W/m^2 (or $10^7 \text{ W}/\text{cm}^2$), optical breakdown can occur and a plasma is formed. For an excimer laser with 200 ns pulse width, producing in excess of 200 mJ/pulse , the fiber-optic delivered radiance for a single fiber can be of the order of 80 mJ/mm^2 . In terms of irradiance this would equal $4 \times 10^{10} \text{ W}/\text{cm}^2$. In terms of power density, a bundle of 100 fiber-optic strands can sustain $4 \times 10^7 \text{ W}/\text{cm}^2$. Excimer laser ablation can hence form a micro-plasma at the tip of the catheter with a depth of less than a few micrometers.

This laser ablation process is usually called photodisruption. The photodisruption process is an electromechanical mechanism. Excimer lasers emit photons with energy of the order of covalent bonding energies. The shorter the excimer laser wavelength, the higher the energy per photon and, consequently, stronger molecular bonds can be broken. Additionally, focusing a pulsed laser will achieve high peak irradiances in the focus. One particular mode of pulsed laser delivery includes femtosecond pulse width laser radiation. The pulse width is short enough to confine a larger photonic power, and for a 200 femtosecond pulse-width and 10–100 nJ per pulse, laser irradiation can achieve similar peak power in comparison to a 200 nanosecond laser pulse at 10–100 mJ, such as available from a 308 nm excimer laser device.

The rapid expansion of the plasma induces a rapidly expanding bubble that subsequently collapses to produce extreme pressure fluctuations. The process of plasma formation is significant, but compared to thermal relaxation times, it constitutes a relatively short aspect of excimer photochemical ablation.

Spallation and Cavitation

Cavitation is defined as a sudden expansion (e.g., mechanical deformation or vapor bubble; nucleation) or decrease in volume (collapse) resulting in an exertion of forces on the boundary media and materials.

As tensile pressure develops in a tissue after a laser exposure, there is a limit to the tensile pressure that a tissue can sustain without rupture. When this limit is exceeded, the tissue will ‘‘break’’. This process is in principle similar to a rubber band that has been stretched too far. In solids, such material breakdown involves a process of initial void formation and subsequent void growth usually along a plane of fracture. This process is called spallation [32, 33]. In liquids, such a breakage causes the initiation and growth of a bubble [34].

The combined effects of all four mechanisms effects of all four mechanisms (i.e., vaporization, expansion, plasma formation, spallation and cavitation) cause bubble formation, with associated fluid-dynamic aspect of material dispersion. The bubble process is described in the next section.

Bubble Formation

The aqueous nature of most soft tissues (e.g. thrombus and fatty plaque) makes it likely that cavitation bubbles are forming rather than spallation planes. In contrast, calcified plaque will invoke spallation. The threshold for cavitation bubbles in water is affected by the purity of the water. For not rigorously pure water, the threshold pressure is about 8 bar, or $8 \times 10^5 \text{ Pa}$, which requires an initial temperature jump of $3.2 K (T = \frac{2P}{\Gamma_{Grum} C_v})$ where $\Gamma_{Grum} = 0.12$, $\rho = 1000 \text{ kg}/\text{m}^3$,

$c_v = 4.184 \frac{kJ}{m^3}$ and $P = 8 \times 10^5$ Pa, and the tensile pressure

achieves half of the initial maximum compressive pressure initially. A relatively small temperature jump is required to cavitate water. The threshold tensile pressure for cavitation after a 12 K temperature rise in a 10 % collagen gel is about 8×10^5 Pa [35]. With increasing mechanical strength, the threshold for cavitation in a medium or tissue increases. Cavitation has been observed photographically in the cornea of the eye during LASIC surgery, when a temperature jump of 40 K is induced by a 10-ns pulsed laser [36, 37]. Therefore, it is possible to have cavitation using pulsed laser induced temperature jumps that do not cause the tissue temperature to reach or exceed 373.16 K (the boiling point of water).

Surface tension at the tissue vapor – blood field interface provides a mechanism that will form the bubble configuration; the sphere has the greatest potential for holding energy due to the fact that it has the largest volume with respect to the smallest surface area, adhering to the cohesion forces in the enclosing liquid medium [27]. On an ideal fluid/liquid stress level, in classical description, the material must continually flow or deform, when subjected to any shear stress. A polar fluid, such as blood (or liquefied fat from the plaque), does not behave this way, it can withstand shear stress. Viscoelastic and Bingham plastic fluids, such as blood and lipids, can withstand shear stress to a threshold level. Another good example is liquid cement (a typically Bingham plastic), which will not deform unless a yield stress is reached before it will flow. The polar behavior of the fluid and the liquid both will influence the velocity potential and vorticity of a liquid in motion where polarity during expansion couples to the stress tensor while generating torques that will need to be accounted for in the equation of motion. The Equation of Motion can be used to solve for the development of the vaporization and cavitation bubble, and the inherent time related radial expansion effects

$\left(\frac{\partial r}{\partial t}\right)_{\vec{r}}$, both magnitude and rate of change) as a function of

location (\vec{r}) in the vicinity of the delivered energy. Surface tension in the surface of a bubble will confine a medium by force, hence the vapor pressure inside the bubble will always be greater than the outside partial pressure or liquid/solid medium internal cohesion force. The surface tension for a single surface (bubble) is defined by the Laplace law [27].

For all cases of cavitation, vaporization, plasma formation and spallation, a bubble is often formed which expands to its maximum diameter that subsequently collapses to a point with very high pressure. This collapse process is very disruptive to the material at the surface of the bubble (i.e. cavitation). During the bubble collapse the yield stress is higher due to the greater rate of change. The process of bubble collapse is an important mechanism for tissue disruption.

Flow and Cavitation Processes

Mechanisms Associated with Bubble Expanse and Collapse in Ablation Process

The cavitation process is accompanied by shear waves that are described by the Wave-Equation with associated propagation of effects [11, 13, 38, 39]. The wave-equation will provide a solution for the longitudinal acoustic displacement wave. The interaction of the bubble surface with the tissue surface with which it makes contact will result in shear-stress and strain. Depending on the material properties the wave can be critically damped, but under certain conditions the wave pattern may range to undamped (under the rare condition of super-fluidity). The collapse of a spherical bubble can be associated with a Kinetic Energy (KE) that is a function of the rate of change over time (t) of the bubble radius ($r = \vec{r}(t)$,

which is location specific over the bubble surface) expressed as $\dot{r} = \frac{dr(t)}{dt}$, with respect to the initial radius r_0 (note: this is the bubble surface velocity as a function of location) with associated internal pressure P_1 , defined using the bubble vapor density as a function of time $\rho = \rho(\vec{r}, t)$ expressed as:

$$KE = 2\pi\rho(\vec{r}, t)r^3\dot{r}^2 \xrightarrow{\text{start-finish}} \frac{4}{3}\pi P_1(r_0^3 - r^3). \quad \text{The}$$

rate of change in bubble radius is a source function in the acoustic effects contributing to the fluid-dynamic aspects of the ablation process. The velocity distribution forms the basis of the velocity potential [13, 39]. The velocity potential is a three-dimensional matrix that forms the basis for the location and severity of vortex formation. The formation of vortices in the ablation flow generates additional velocity gradients that contribute to the disruptive forces acting on the plaque. As an indication of the order of magnitude of the bubble surface velocity we can consider a 2 mm radius bubble collapsing within a 10 μs time-frame (note: the bubble formation is a mechanical event that is orders of magnitude greater than the laser pulse duration), yielding a first order approximation of velocity in the 200 $\frac{m}{s}$ range (note that Mach-1 in air equals 334 $\frac{m}{s}$, whereas in water $v_{sound} = 1522 \frac{m}{s}$ at body temperature).

However, it is the rate of change that determines the impact rather than the averaged result. The term KE_{finish} on the right-hand side can be used for an order of magnitude estimation (merely of anecdotal importance). The nature of the bubble collapse is rather complex, specifically when considering the ionized plasma created during an ablation process or when condensation occurs during the size reduction of the bubble, this is referred to as the Stirling effect [12, 24, 40, 41]. During condensation the density of the vapor bubble changes and hence other conservation laws need to be

included in the theoretical evaluation process. After initial expansion resulting from an energy source (i.e. laser irradiation) applied in a Dirac-delta-distribution profile [42, 43], the bubble collapses and rebounds several times. The number of oscillations will depend on the elastic condition and form a critically damped mechanical wave (i.e. acoustic wave) with rapidly decreasing amplitude [44]. The rate of change in bubble diameter can be described as an asymmetric wave-phenomenon. Due to the fact that the bubble collapse progresses faster than the expansion, a Fourier transform [45] of the resonant bubble will reveal a broad acoustic spectrum. The frequency spectrum of the bubble growth will be a function of the local elastic moduli of all materials in the boundary as well as the full three-dimensional geometry of the plaque with respect to the vessel wall, next to the laser pulse duration (i.e. source) and the irradiated area with associated point-spread function [46]. The wave-function for pressure in the bubble with respect to the radius and rate of change in the radius (r) is described by the Rayleigh-Plesset equation

$$r\ddot{r} + \frac{3}{2}\dot{r}^2 = \frac{1}{\rho} \left(P_g - P_0 - P(t) - 4\eta\frac{\dot{r}}{r} - \frac{3\sigma_{stress}}{r} \right) \quad [47], \quad \text{where}$$

$\dot{r} = dr^2/d^2t$ and η the viscosity [48]. The solution to the Rayleigh-Plesset equation for the bubble wall-motion as a function of time is of the form: $r(t) = R_0 \left\{ \frac{t^* - t}{t^*} \right\}^{2/5}$, where t^*

is the time frame of total collapse and R_0 a constant. The sum of viscous stress, proportional to: $\frac{4\eta\dot{r}}{r} \propto \frac{1}{t^* - t}$, and the surface tension, proportional to $\frac{\sigma_{stress}}{r} \propto \frac{1}{(t^* - t)^{2/5}}$, will both

diverge at a slower rate than the inertial (i.e. $P_{inertia} = mv$, the inertia) forces, proportional to $F = \frac{dp}{dt} \propto \frac{1}{(t^* - t)^{2/5}}$, making

the inertial aspect the dominant factor in the cavitation process. The pressure inside the bubble at this point obeys the adiabatic equation of state. In the adiabatic process the pressure diverges as: $P_g \propto r^{-3\gamma_g} \propto (t^* - t)^{-2}$. Here we use the fact that for a mono-atomic ideal gas $\gamma_g = \frac{5}{3}$. Assuming the special case of adiabatic expansion/collapse the rate of change is captured by a surface velocity equivalent (i.e. $v_s' = \sqrt{\left(\frac{P_1}{\rho}\right)}$;

“constant” parameter with the dimensions of velocity) in second order derivative $r\ddot{r} + \frac{3}{2}\dot{r}^2 = v_s'^2 \left(\frac{R_0}{r}\right)^{3\gamma_a}$, where γ_a represents the adiabatic factor. The adiabatic factor is defined

as the ratio of the specific heat (h_{sp}) with respect to the gas in two phases of the rarefaction versus expansion processes: $h_{sp} = \frac{Q}{m\Delta T}$, describing the heat (Q) required for changing

the temperature (T) of a mass (m) by 1 K , all. This provides

for the cavitation inertia:
$$P_{inertia} = m \sqrt{\frac{r\ddot{r} + \frac{3}{2}\dot{r}^2}{\left(\frac{R_0}{r}\right)^{3\gamma_a}}}$$

The pressure (P) and density (ρ) are related as follows:

$$\frac{P}{P_0} = \left(\frac{\rho(\vec{r}, t)}{\rho_0} \right)^{\gamma_a}, \quad \text{assuming a constant “surface velocity”}$$

(“ \vec{r} ”). The velocity at the time approaching total collapse (t^*) approaches a divergent value. During the collapse at one point the thermal diffusion rate is too slow, trapping the heat in the collapsing bubble. This singularity is the main feature that contributes to the cavitation damage during ultra-violet pulsed laser ablation. The collapsing bubble confining the trapped energy causes sound generation and may also cause a flash of light resulting from conversion of energy (luminescence; viz. sonoluminescence) [7, 49]. Note that light is the result of accelerated charges. The electron plasma formed during the tight collapse will reach high acceleration for ions and electrons to produce visible light. The rate of heat exchange of the bubble to the surrounding liquid medium is primarily subject to the Nusselt number ($Nu = \frac{\text{convective heat-transfer}}{\text{conductive heat-transfer}}$) [25, 26] of the system. The net force (F) exerted by the cavitation

process at any specific point in the collapse is directly proportional to the momentary change in kinetic energy ($W = \Delta KE$, i.e. the work) over the distance traveled by the surface of the bubble captured by incremental delta in radius (Δr): $W = F \Delta r$. This yields for the cavitation force (F_{cav}) exerted by the expanding, respectively collapsing bubble on the surrounding media:

$$F_{cav} = \Delta KE / \Delta r = C 2\pi V_{bubble} \frac{\partial}{\partial r} \left(\dot{\rho}(t) \left\{ \frac{3}{2} \dot{r}'^2 + r' \ddot{r}' \right\} \right) \tau_{cav},$$

where V_{bubble} is the bubble volume, with A_{bubble} the bubble surface; τ_{cav} the cavitation time, $C = \left(\frac{R_0}{r}\right)^{-3\gamma_a}$ a constant, and

a rate of change in density $\dot{\rho}(\vec{r}, t) = \frac{\partial \rho}{\partial t}$, which represents a

three-dimensional time dependent density gradient that contributes to the flow pattern [13, 50]. The respective rate of change in bubble radius and gaseous bubble volume is faster during collapse (cavitation) than during expansion (Fig. 2.2).

The rate of change is the dominant factor and illustrates that the forces on the surrounding medium are dominating during cavitation. In order to obtain an order of magnitude approximation for the cavitation force (F_{cav}) the expression for kinetic energy is used:

$$KE \xrightarrow{\text{start finish}} \frac{4}{3} \pi P_1 (R_0^3 - r^3) = \frac{4}{3} \pi R_{max}^3 (P_0 - P_v) \quad \text{and}$$

$F_{cav} \Delta r = \Delta KE$ which technically needs to be written as differential function due to the continuous change in equilibrium

conditions: $\frac{\partial^2 F(t)r(t)}{\partial t \partial r} = \frac{\partial^2 KE}{\partial t \partial r}$, which can be solved for well-defined boundary conditions in discrete steps only [51]. Using the 4 mm diameter (maximum expansion before onset of cavitation, assuming liquid medium. Note: under solid-state ablation the bubble diameter will be significantly smaller) bubble resulting from a laser pulse emitted from a 2.0 mm catheter with a time of collapse in the order of $\tau_{cav} \approx 10 \mu s = 10^{-5} s = \Delta t$ the discrete one step approximation yields a cavitation force in the order of $F_{cavitation} \propto 10^{-3} N$, operating on a microscopic scale.

The bubble cavitation in second order approximation yields a velocity of the bubble surface in the order of $10^3 m/s$ (reaching the Mach velocity), more than five orders greater than the first order approximation, illustrating the magnitude of the momentum during cavitation with its destructive impact on the surrounding media.

Unfortunately (from a theoretical point) during catheter based ablation, the bubble will not be spherical nor symmetric and the process can preferably be approached using finite element simulation, where R_{max} is the first maximum radius, P_0 the minimum pressure and P_v the vapor pressure at temperature T [41, 44].

Energy dissipated during the cavitation bubble collapse close to a solid wall is derived here using the ideal Gas Law: $P = \frac{n}{V} R_{gas} T$, where the volume of the sphere is $V = \frac{4}{3} \pi (r(t))^3$, T is the temperature of the bubble vapor, $r(t)$ the time-dependent bubble radius, n the number of moles of all the constituents in the vapor bubble and the Universal Gas constant: $R_{gas} = 8.3144621 \frac{J}{Kmol}$, which conforms to

the expression $KE = \frac{3}{2} n R_{gas} T$. This provides for the average

force estimation: $\bar{F} = \frac{3}{2} n R_{gas} \frac{T}{r(t)\tau}$, with τ the duration of

the expanse/collapse. The number of moles affected can, in theory, be derived from the absorbed light energy over the duration of the laser pulse using the latent heat of vaporization (h_v) for the composite medium of plaque, where the absorbed fraction is related to the Grüneisen factor (coefficient) for the mixture of tissues. The volumetric rate-of-change time can be measured (rather, inferred from ex-vivo high-speed video imaging under idealized conditions) as is the maximum bubble radius, whereas the maximum temperature in the core of the bubble can be approximated from empirical data depending on the ablation source and boundary conditions (but remains relatively undefined) [24, 52]. The interaction between two molecules is often represented by the Lennard-Jones 6-12 formula [53].

The shear-stress and strain caused by the bubble dynamics on the plaque as well as the vessel wall are described as follows [41, 54]. The normal stress exerted by the bubble on the adjacent tissues of the resident plaque is: $\overline{\sigma}_{norm} = \vec{F} \cdot \vec{A} = |F| * |A| \cos \alpha$,

where A is the contact area in the direction normal to the surface, indicated by the normal vector to the surface; defined as the dot-product. In the dot-product the greatest magnitude is achieved when the vectors line up, where α represents the angle between the normal to the surface and the direction of the local force. The local force has a different direction at every location due to the asymmetry of the bubble and the geometry of the medium. This yields an approximate normal-stress on the surrounding plaque of $\overline{\sigma}_{norm} = 10^{-8} Nm^2$, but it is the rate of change in stress produced by the fluid-dynamics of the cavitation of the bubble that provides the ultimate factor determining the impact of the stress on the surrounding media [55]. The turbulence obtained at the bubble surface creates a mechanism referred to as the Jaumann stress rate, which involves calculation of the rotation of the stress and this falls outside the current topics under discussion [55]. Practical evidence has been provided illustrating the power of demolition of resilient structures, including calcified plaque by means of the stress at the cavitation bubble surface.

The shear-stress in the tissue surrounding the bubble is:

$$\overline{\sigma}_{shear} = \vec{F} \times \vec{A} = \varepsilon_{shear} \frac{E_Y}{2(1 + \nu_{poisson})} = \gamma_{shear} G_{shear}; \text{ where } \vec{F} \times \vec{A}$$

is the cross-product, in direction perpendicular to both vectors, following from the right-hand-rule [42], where ε_{shear} the shear strain, G_{shear} is the shear modulus of the tissue under deformation, E_Y the Young's modulus of the tissue, and $\nu_{poisson}$ the tissue composition specific 'Poisson Ratio', and the shear-strain $\gamma_{shear} = \frac{\Delta x}{x} = \tan \beta$, where β the deformation angle [52].

The deformation strain (ε_{shear}) acting in the plaques surrounding the bubble is defined as the angular change of a boundary with respect to the rest position, e.g. from square to diamond shape. Strain also applies on a molecular scale or molecular matrix rather and can be torsional as well as linear. For the macroscopic contact surface this is the spherical outline of the bubble with initial and final diameter D_i and D_f respectively: $\varepsilon_{shear} = \frac{\pi(D_f - D_i)}{\pi D_i}$ [52].

When the normal-stress applied by the bubble exceeds the shear-stress in the plaque the medium will be demolished, generating crack-propagation.

The ablation process is intended to break molecular bonds next to vaporization, specifically for complex structures. This bond breaking mechanism is inherent to the excimer UV radiation. The molecular cohesion of the tissue (F_{tissue} , force between two molecules) is a direct function of the molecular potential energy (U_{molec}) with distance ($r(t)$):

$$F_{tissue} = \frac{\partial U_{molec}}{\partial r(t)} \quad [24].$$

The interaction between two molecules is often represented by the Lennard-Jones 6-12 formula [44, 53, 56]. The surface tension: $T_{surface}$, and the spallation forces, including the inherent shear-stress

$$(\overline{\sigma}_{shear} = \vec{F} \times \vec{A}_{bubble\ surface} = \varepsilon_{shear} \frac{E_Y}{2(1 + \nu_{poisson})}) \quad \text{interacting}$$

with the molecular binding forces provides the mechanism

of ablation on a microscopic level. The surface tension follows from the Laplace equation (also referenced as Young-Laplace equation): $\Delta P = 4T_{\text{surface}} \left(\frac{1}{r_1} + \frac{1}{r_2} \right)$, where ΔP the pressure gradient over the surface, and r_1 , respectively r_2 the orthogonal primary axis of an ellipsoid [11, 13, 38, 39]. Hence when the applied forces exceed the internal forces the bond-breaking process will take place, which in this case also involve the (polar) covalent bonds in the liquid and solid phases, next to the complex molecular structures, including calcium bonds.

Optimization in Cavitation with Respect to the Ablation Process

The bubble collapse has a much shorter rate of change than the expansion phase, therefore, the cavitation is more likely to break solid material for ablative removal than the laser bubble formation. The pattern of collapse and rebound of a cavitation bubble near a rigid boundary can be modeled in two acoustic cycles. [57].

The ideal cavitation conditions required to obtain maximum depth and volume of material removed under cavitation depend on the correlation between the bubble surface and the surface of the plaque [58]. The ratio between the size of the bubble and the distance to the vessel boundary will have an optimum, where $S_{\text{separation}}$ is the distance from the center of the bubble to the boundary and R_{max} is the maximum radius of the bubble. The optimum is based on the ratio:

$$\gamma_{\text{bubble}} = \frac{S_{\text{separation}}}{R_{\text{max}}}. \text{ Usually one finds that a large bubble in}$$

close proximity to the vessel-wall will have the greatest potential for damage; $\gamma_{\text{bubble}} < 0.3$. In contrast, a small bubble at large distance (i.e. in the center of a large vessel) will have the smallest potential to induce damage, hence for $\gamma_{\text{bubble}} > 2.21$ the impact of the bubble is negligible. Experimentally a resonance effect was found to provide optimal ablation efficiency in the approximate range $1.2 < \gamma_{\text{bubble}} < 1.4$ and $\gamma_{\text{bubble}} \leq 0.3$ [58]. The latter condition would be at a distance of the fiber-optics to the plaque surface much smaller than the bubble radius, but not necessarily in direct contact.

Fluid-Dynamics in Vascular Flow and with Respect to the Ablation Process

Under a perfectly straight uniform vessel configuration the blood-flow will be symmetric according to a Non-Newtonian liquid. Under bifurcation and curvature in the vessel structure the flow will become turbulent under its own boundary conditions. Similarly, a stenosis will introduce asymmetry and induced

turbulence in a specific manner that is unique to the configuration of the vessel structure and the outline of the plaque. Under conditions of a total occlusion there will be no blood flow. The ablation process with excimer laser radiation, and resulting microscopic flow will be much more forceful than the standard flow conditions until the vessel diameter drops below a threshold ratio of catheter diameter to vessel diameter, and the ablation bubble may experience a degree of deformation based on the local flow-velocity. This can partially be attributed to the shorter time-frame of the excimer ablation event. Additionally the ablation bubble process occurs during an at least 3 orders of magnitude shorter time-scale than the periodicity of the flow, which will make the bubble flow phenomena more pronounced than the blood-flow interference. In light of these conditions the bubble flow can be treated separately.

Crack Propagation

A point of (theoretical) importance in the ablation of plaque is the demolition process of the rigid or semi-rigid plaque or thrombus structure after the bubble has formed. The bubble may break, causing formation of crack due to the plaque surface tension. A crack may form under various conditions, specifically in locations where there is a discontinuity in the surface tension that extends over long enough regions, or where the gradient in surface tension has a minimum. A discontinuity will generally involve the joining face of two separate materials, or an impurity with respect to an otherwise relatively homogeneous volume. These material features can be classified as fracture toughness or plasticity [59]. Additional factors involve the material structure directly underneath the “weak-point” where the elastic modulus is lower than the adjacent volume to support the initiation of a crack. The length and depth of the crack is a direct function of the cavitation force. Note that the crack formation and crack-growth is a three-dimensional phenomenon, with three-dimensional boundary conditions, such as the proximity to the vessel wall and the respective locations of calcified structures.

Any crack formed as a result of the cavitation process will allow liquid (i.e. blood) to seep in and provide an environment with lower ablation threshold than the solid structure. Specifically calcified plaque may benefit from crack-propagation, since this will macroscopically break down a structure that is hard to remove in a layer-by-layer fashion and has high energy requirements.

Additionally, soft tissue may naturally be embedded in fissures within the calcified plaque, also requiring a lower energy for ablation. Both blood vaporization and soft tissue disruption will form a bubble that, in turn, facilitates the crack propagation and the disintegration of the solid plaque composite medium. The process of crack formation distinguishes three specific types of crack propagation, also illustrated in Fig. 2.5. The three means are (I) opening mode, (II) sliding mode, and (III) tearing

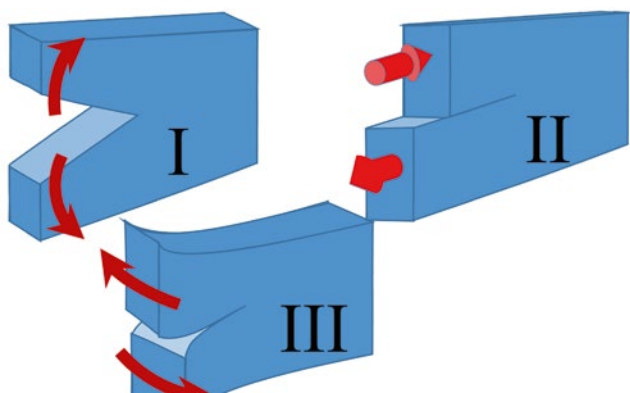


Fig 2.5 Modes of crack propagation that can occur individually or in combination with three degree of freedom. The three modes of tearing are (I) opening mode, where a wedge is formed; (II) sliding mode, making a segment perform a longitudinal translation motion with respect to a more rigid segment; and (III) tearing mode, in this mode the medium tears laterally. All the modes of tissue movement are a function of the bubble shape, the phase of the bubble and the three-dimensional distribution of Yong's modulus within the plaque material

mode [59]. The exact mode of disintegration strongly depends on the tissue structure, including weak points in the matrix of plaque materials as well as the 3-dimensional shear applied by the expanding bubble. In most cases the breakdown of plaque will proceed in a mixed mode of deformation and demolition. The crack forming mode(s) may as well be subject to resonance effects due to the confined space of atherosclerotic plaque and elastic nature of materials and boundaries.

The rate of tear is generally unpredictable, depending on the local distribution of elastic moduli and respective force distribution resulting from cavitation, elastic confinement and inhomogeneity [60]. The details of crack propagation fall outside the specific context of this chapter and may be deferred to a later theoretical treatment.

Fluid-dynamics and Cather Advancement

Catheter ablation utilizes a catheter that is continuously advanced in anticipation of plaque clearing through the ablation process. The forward motion of the catheter requires attempting to move the catheter at a steady forward motion and maintain a constant advancement speed. The forward motion will require the application of a relatively constant force. The forward force will result in a close-contact between the distal tip of the catheter and the uneven and likely slanted face of the plaque.

Recoil

Due to the formation of an ablation bubble while the catheter is in close contact with the plaque, the catheter will experience recoil that is a function of the applied forward motion force,

the energy of the delivered laser pulse, the geometry of the target material as well as the flexibility of the catheter. The size of the catheter and the packing density of fiber-optics will provide the basis for the rigid nature of the catheter. The respective core size of the fiber-optic packing will also contribute to the compliance of the catheter.

All these factors yield a complex (theoretical) platform in defining or predicting the true shape and evolution of the spallation bubble. In general the catheter tip will experience some form of displacement (viz. recoil) resulting from the bubble formation [61]. The catheter tip may move side-ways or backwards and may even gyrate. The ultimate tip movement will be a combination of the three displacement mechanisms. This process repeats itself during each ablation cycle.

Bubble Shape

Due to the compression at the catheter tip the generation of the ablation bubble will most likely not form a perfect sphere, as assumed in the majority of the technical description. The bubble may even take the shape of a torus. All these factors create deviations from the idealized theoretical model discussed in this chapter.

Soft Tissue/Thrombosis

Soft tissue will require the least amount of energy for vaporization and may hence generate a relatively large bubble. The soft tissue and thrombus itself will be compliant and may deform under the bubble expansion itself.

Calcified Plaque

The cavitation forces that are produced during the bubble process have been shown to exert enough force to dissociate complex calcium molecular structures with tight binding forces. The process of calcium break-up is an important factor in the success of laser assisted atherectomy.

One additional factor that comes with the destruction of calcified plaque is deformation of debris. The bubble formation in calcified plaque will include debris containing calcium rich particles. The bubble expansion and cavitation process, with the imbedded solid material debris, will impact the surface of distal catheter tip (Fig. 2.4), in the form of a micro-jet (Fig. 2.3). This debris fluid-dynamic process will result in erosion of the epoxy that is designed to make the fiber-optic placement a rigid pattern while simultaneously protect the fibers from moving with respect to each other laterally. When the fibers are free to move they will move and contact

each-other (chatter) during the acoustic process, and this may eventually lead to fiber breakage. The broken fiber-optics will reduce the total radiance at the tip and will result in an asymmetric irradiation pattern. The resulting disproportionateness of irradiation causes asymmetric bubble shape formation as well as affects the crack-propagation mode of operation.

In general there is a delicate balance between the advancement force and the material that is the target. Soft tissue, and specifically thrombus, will ablate in larger quantities than calcified plaque.

In all cases the use of excessive force on the catheter applied by the operator will change the fluid-dynamic aspects of the ablation process and may have disadvantages in the ablation process. Due to the confinement of the bubble under applied forward force (i.e. continuous advancement), especially in targeting soft plaque and thrombus, the crack-propagation process is modified with addition phenomena that will need to be addressed, such as the increased risk of vessel dissection. Since the plaque is an integral part of the vessel wall the crack propagation will always take the path of least resistance, which can be the media, or the adventitia of the vessel wall, depending on the penetration of the chemical changes in cellular composition associated with the plaque growth process.

Conclusions

The fluid-dynamic aspects of laser assisted atherectomy form a complex engineering aspect in the clinical process of blood-flow restoration. Certain optimal operating conditions can be described based on idealized theoretical conditions that can assist in the design of atherectomy devices as well as providing guidance on the application methods. The formation of a tissue vapor bubble comes with spallation and cavitation that provide a secondary mechanism-of-action to remove and break-up various types of plaque of complex chemical composition. The fluid-dynamics of the cavitation process can be shown to provide sufficient force to break strong molecular bonds, specifically with respect to the clinical challenge of calcified plaque. Excimer laser photo ablation has been shown to be the most effective in clearing calcified plaque compared to all other available techniques of mechanical and chemical ablation.

Acknowledgments The author wants to thank the efforts of the following people: Holly Scott, Katie Hardman, Paola Garcia, Melissa Kromer, Ashley Roberts and Kevin Taylor for the basic research and

practical verification aspects as well as providing in-depth scientific discussion and insight.

Appendix: Ablation Threshold

The ablation threshold for a specific medium will place constraints on the energy requirements which depend both on the irradiation wavelength and magnitude (i.e. fluence: $\Psi(\vec{r}, \vec{s}) = \overline{L(z)}$ $\vec{s} = \int_{4\pi} L(\vec{r}, \vec{s}, t) d\omega'$, where $L(\vec{r}, \vec{s}, t)$ is the time dependent radiance, \vec{s} represent the net direction of propagation, \vec{r} the location in the volume, and ω the solid angle). Considering only vaporization in the ablation process the ablation energy is the sum of the heat requirement to bring the medium to the boiling point ($E_b = mc_v \Delta T$) and the vaporization energy ($E_v = mh_v$); when considering sublimation of solids only the sublimation energy is considered [14]:

$$E_{abl} = m(h_v + c_v \Delta T) = \int_{4\pi} \int_t \mu_a L'(\vec{r}, \vec{s}, t) dt d\omega = \int_t \mu_a \Psi(\vec{r}, t) dt$$

Where $\Delta T = T_b - T_0$ is the temperature rise from steady state (T_0) to vaporization temperature (T_b), h_v equals the latent heat of vaporization for the medium, c_v is the specific heat of the medium, and m is the mass that can be evaporated based on the light absorbed in the volume. This will provide the threshold fluence: Ψ_{th} with respect to the required ablation energy (E_{abl}) in the tissue to achieve vaporization. The ablation energy density then becomes: $w_{abl} = \rho(h_v + c_v \Delta T)$, for tissue density ρ . Note, this does not set the requirements for molecular bond-breaking, specifically for chemical matrices incorporating calcium.

As an indication of the nature of ablation of various materials in plaque the following parameters illustrate the nature of the various processes. The specific heat for water is $c_{v,H_2O} = 75.28 \text{ J/molK}$, where 1 mol of water equals 18 g, while the sublimation heat for unbound calcium is $h_{v,Ca} = 179.3 \text{ kJ/mol}$, compared to the vaporization heat for water of $h_{v,H_2O} = 40.7 \text{ kJ/g} = 2.257 \text{ kJ/mol}$, while for a generalized lipid (butter) the specific heat and vaporization heat are respectively $c_{v,lipid} = 2.4 \text{ J/gK}$ and $h_{v,lipid} = 38 \text{ kJ/g}$ [62]. The nature of calcified plaque initiates different requirements, specifically for braking up calcium, which will need to occur at the molecular level. The bond-dissociation energy for a mol of calcium in chemical connection with various elements (oxygen, fluorine, chlorine, etc.) on a single scale is on average $h_{v,Ca} = 565 \text{ kJ/mol}$ (NSRDS-NBS

31 1970) while the calcium matrix in calcified plaque is much more complex than a calcium connection with a single element.

References

- Dotter CT, Judkins MP. Transluminal treatment of arteriosclerotic obstruction. *Circulation*. 1964;30:654–70.
- Ozdil E, Krajcer Z, Paolo Angelini P. Percutaneous balloon angioplasty with adjunctive stent placement in the mesenteric vessels in a patient with Takayasu's arteritis. *Circulation*. 1996;93:1940–1.
- Buecker A, Minko P, Massmann A, Katoh M. Percutaneous mechanical atherectomy for treatment of peripheral arterial occlusive disease [Article in German]. *Radiologe*. 2010;50(1):29–37. doi:10.1007/s00117-009-1913-0.
- Naftilan AJ. Chemical atherectomy; a novel approach to restenosis. *Circulation*. 1991;84(2):945–7.
- Jang JS, Jin HY, Seo JS, Yang TH, Kim DK, Kim DK, Kim DI, Cho KI, Kim BH, Park YH, Je HG, Kim DS. The transradial versus the transfemoral approach for primary percutaneous coronary intervention in patients with acute myocardial infarction: a systematic review and meta-analysis. *EuroIntervention*. 2012;8(4):501–10.
- Prince M, LaMuraglia G, Teng P, Deutsch T, Anderson R. Preferential ablation of calcified arterial plaque with laser-induced plasmas. *IEEE J Quant Electron*. 1987;23(10):1783–6.
- Autrique D, Wendelen W, Bogaerts A. Laser-induced plasma formation: a better insight by computer simulations. Proceedings of the seventh Euro-Mediterranean symposium on laser induced breakdown. *Spectroscopy*. 2013;96.
- Smits AJ. A physical introduction to fluid mechanics. Hoboken: Wiley; 2000.
- Eisenberg P. Handbook of fluid mechanics, section 12 “cavitation”. New York: McGraw-Hill Book Co. Inc; 1961.
- Boulais É, Lachaine R, Meunier M. Plasma-mediated nanocavitation and photothermal effects in ultrafast laser irradiation of gold nanorods in water. *J Phys Chem C*. 2013;117(18):9386–96.
- Melodelima D, Chapelon JY, Theillère Y, Cathignol D. Combination of thermal and cavitation effects to generate deep lesions with an endocavitary applicator using a plane transducer: ex vivo studies. *Ultrasound Med Biol*. 2004;30(1):103–11.
- Nag PK. Engineering thermodynamics. 3rd ed. New Delhi: Tata McGraw-Hill Publishing Co; 2005.
- Sato K, Sugimoto Y, Ohjimi S. Pressure-wave formation and collapses of cavitation clouds impinging on solid wall in a submerged water jet; Proceedings of the 7th international symposium on cavitation 2009; CAV2009, Paper No. 66; August 17–22, Ann Arbor.
- Splinter R, Hooper B. An introduction to biomedical optics. Boca Raton: Taylor and Francis/CRC Press; 2007.
- Van den Berg JC. Stenting and laser debulking in the SFA. *Envovasc Today*. 2009;62–6.
- Scheinert D, Laird JR, Schröder M, Steinkamp H, Balzer JO, Biamino G. Excimer laser assisted recanalization of long, chronic superficial femoral artery occlusions. *J Endovasc Ther*. 2001;8:156–66.
- Laird Jr JR, Reiser C, Biamino G, Zeller T. Excimer laser assisted angioplasty for the treatment of critical limb ischemia. *J Cardiovasc Surg (Torino)*. 2004;45(3):239–48.
- Tuchin VV. Light scattering study of tissues. *Physics – Uspekhi*. 1997;40(5):495–515.
- Schwarzmaier H-J, Kaufmann R, Wolbarsht ML, Heintzen MP, Mueller W. Optical density of vascular tissue before and after 308-nm Excimer laser irradiation. *Opt Eng*. 1992;31(7):1436–40.
- Palanker D, Turovets I, Lewis A. Dynamics of ArF Excimer laser-induced cavitation bubbles in gel surrounded by a liquid medium. *Lasers Surg Med*. 1997;21(3):294–300.
- Van Leeuwen TGJM, Jansen ED, Motamedi M, Welch AJ, Borst C. Bubble formation during pulsed laser ablation: mechanism and implications. Proc. SPIE 1882, Laser-Tissue Interaction IV, 1993:13. doi:10.1117/12.147658.
- Yang S-H, Jaw S-Y and Yeh K-C. Experimental study on generation of single cavitation bubble collapse behavior by a high speed camera record. 2012 Intech open-source: http://cdn.intechopen.com/pdfs/35274/InTechExperimental_study_on_generation_of_single_cavitation_bubble_collapse_behavior_by_a_high_speed_camera_record.pdf.
- Dabiri S, Sirignano WA, Joseph DD. Interaction between a cavitation bubble and shear flow. *J Fluid Mech*. 2010;651:93–116.
- Brennen CE. Cavitation and bubble dynamics. Oxford: Oxford University Press; 1995.
- Incropera FP, DeWitt DP, Bergman TL, Lavine AS. Fundamentals of heat and mass transfer. 7th ed. Hoboken: Wiley; 2011.
- Kothandaraman CP. Fundamentals of heat and mass transfer. Delhi: New Age International; 2006.
- Aris R. Vectors, tensors and the basic equations of fluid-mechanics. New York: Dover Publications Inc.; 1962.
- Goldman MP. Chapter 2; Laser treatment of cutaneous vascular lesions. In: Roberts and Hedges' clinical procedures in emergency medicine. 6th ed. Philadelphia: Elsevier; 2014.
- Jacques SL, McAuliffe DJ. The melanosome: threshold temperature for explosive vaporization and internal absorption coefficient during pulsed laser irradiation. *Photochem Photobiol*. 1991;53(6):769–75.
- Noach J, Vogel A. Laser-induced plasma formation in water at nanosecond to femtosecond time scales: calculation of thresholds, absorption coefficients, and energy density. *IEEE J Quant Electron*. 1999;35(8):1156–67.
- Bogaerts A, Bultinck E, Eckert M, Georgieva V, Mao M, Neyts E, Schwaederlé L. Computer modeling of plasmas and plasma-surface interactions. *Plasma Proc Polym*. 2009;6(5):295–307.
- Wanga J, Nancy R, Sottosa NR, and Weaver RL. A novel technique for mixed-mode thin film adhesion measurement, MRS proceedings, vol 750, 2003 Symposium Y3.5 – Surface engineering 2002–synthesis, characterization and applications, Cheng Y-T, Doll GL, Kumar A, Meng WJ, Veprek S, Zabinski J, editors.
- De Rességuier T, Cottet F. Spallation of glass materials under laser induced shocks. *J de Physique IV Colloque C8 suppl J de Physique III*. 1994;4(C8):629–34.
- Zein A, Hantke M, Warnecke G. On the modeling and simulation of a laser-induced cavitation bubble. *Int J Numer Meth Fluids*. 2013;73(2):172–203, 20.
- Jacques SL. Comparison of breaking strengths of adhesives and laser welds versus the threshold tensile pressure of pulsed-laser-induced cavitation of water and gels, Conference Volume 4609, SPIE 4609, Lasers in surgery: advanced characterization, therapeutics, and systems XII, 195 (June 14, 2002); In: Bartels KE, Bass LS, de Riese WT, Gregory KW, Katzir A, Kollias N, Lucroy MD, Malek RS, Peavy GM, Reidenbach H-D, Robinson DS, Shah UK, Tate LP, Trowers EA, Wong BJ, Woodward TA, editors, Lasers in surgery: advanced characterization, therapeutics, and systems XII.
- Suthamjariya K, Farinelli WA, Koh W, Anderson R. Mechanisms of microvascular response to laser pulses. *J Investig Dermatol*. 2004;122:518–25.

37. Wilkinson PS, Davis EA, Hardten DR. LASIK. In: Yanoff M, Duker JS, editors. *Ophthalmology*. 3rd ed. St. Louis: Mosby Elsevier; 2008. Chap 3.5.
38. Juhasz T, Kastis GA, Suarez C, Bor Z, Bron WE. Time-resolved observations of shock waves and cavitation bubbles generated by femtosecond laser pulses in cornea tissue and water. *Lasers Surg Med*. 1996;19(1):23–31.
39. Dullemond CP, Kuiper R. Lecture numerical fluid dynamics. Heidelberg: Heidelberg University Press. 2008. Chapter 1. <http://www.mpia.de/homes/dullemon/fluidynamics08/>.
40. Kadkhodae R, Hemmati-Kakhki A. Ultrasonic extraction of active compounds from saffron. *Acta Hort*. 2007;739:417–26.
41. Vinatoru M. An overview of the ultrasonically assisted extraction of bioactive principles from herbs. *Ultrason Sonochem*. 2001;8(3):303–13.
42. Beer F, Johnston Jr ER, Cornwell P. *Vector mechanics for engineers: dynamics*. 10th ed. New York: McGraw-Hill Science/Engineering/Math; 2012.
43. Dirac PAM. *Principles of quantum mechanics*. 4th ed. Oxford: Clarendon Press; 1958.
44. Franc J-P, Michel J-M. *Fundamentals of cavitation FMA 76*. Dordrecht: Kluwer Academic Publishers; 2004.
45. Fourier J. Théorie du mouvement de la chaleur dans les corps solides (suite) p. 1–94 Mémoires de l'Académie royale des sciences de l'Institut de France, Paris, France; 1821 et 1822, t. V, p. 153 à 246; 1826.
46. Najarian K, Splinter R. *Biomedical signal and image processing*. Boca Raton: Taylor and Francis/CRC Press; 2013.
47. Brenner MP, Hilgenfeldt S, Lohse D. Single-bubble sonoluminescence. *Rev Mod Phys*. 2002;74(2):425–84.
48. Plesset M, Prosperetti A. Bubble dynamics and cavitation. *Annu Rev Fluid Mech*. 1977;9:145–85.
49. Vogel A, Linz N, Freidank S, Paltauf G. Energy density, temperature, and pressure upon generation and collapse of spherical cavitation bubbles in water produced by femtosecond optical breakdown. European Conference on Lasers and Electro-Optics 2009 and the European Quantum Electronics Conference. CLEO Europe-EQEC. 2009.
50. Yamaguchi A, Shimizu S. Erosion due to impingement of cavitating jet. *Trans ASME J Fluids Eng*. 1987;109:442–7.
51. Muller M, Zima P and Unger J. Energy Dissipated during the Cavitation Bubble Collapse Close to a Solid Wall. In: Claus-Dieter, Evert Klaseboer, Siew Wan, Shi Wei and Boo Cheong, editord. *Proceedings of the eighth international symposium on cavitation*. Singapore: Research Publishing; 2012. p. 146–52. CAV2012.
52. Prieve D. A course in fluid mechanics with vector field theory. 2001 <http://www.andrew.cmu.edu/course/06-703/Book2001.pdf>.
53. Goin K, Mo KC, Starling KE. Analytical equation of state for isotropic fluid based perturbation theory. *Proc Okla Acad Sci*. 1977;57:119–21.
54. Stavarache C, Vinatoru M, Maeda Y, Bandow H. Ultrasonically driven continuous process for vegetable oil transesterification. *Ultrason Sonochem*. 2007;14(4):413–7.
55. Nair S. *Introduction to continuum mechanics*. Cambridge: Cambridge University Press; 2009.
56. Lennard-Jones JE. On the determination of molecular fields. *Proc R Soc Lond A*. 1924;106(738):463–77.
57. Bai L-X, Xu W-L, Tian Z, Li NW. A high-speed photographic study of ultrasonic cavitation near rigid boundary. *J Hydrodyn Ser B*. 2008;20(5):637–44.
58. Philipp A, Lauterborn W. Cavitation erosion by single laser-produced bubbles. *J Fluid Mech*. 1998;361:75–116.
59. Patricio M, Mattheij RMM. Crack propagation analysis; TU/e workbook. 2009. <http://www.win.tue.nl/analysis/reports/rana07-23.pdf>.
60. Paris P, Erdogan F. A critical analysis of crack propagation laws. *J Basic Eng*. 1963;85(4):528–33.
61. Strikwerda S, van Swijndregt EM, Melkert R, Serruys PW. Quantitative angiographic comparison of elastic recoil after coronary Excimer laser-assisted balloon angioplasty and balloon angioplasty alone. *J Am Coll Cardiol*. 1995;25(2):378–86.
62. Morad NA, Mustafa Kamal AA, Panau F, Yew TW. Liquid specific heat capacity estimation for fatty acids, triacylglycerols, and vegetable oils based on their fatty acid composition. *JAOCS*. 2000; 77(9):1001–5.

Excimer Coronary Laser Atherectomy During Percutaneous Coronary Intervention of Complex Lesions: Balloon Failures, Chronic Total Occlusions and Under-Expanded Stents

Omar A. Rana, Suneel Talwar, and Peter O’Kane

Introduction

Over the last several decades, the average life span of an adult in the western world has increased [1]. In fact, the proportion of the very elderly (≥ 80 years) is expected to rise the fastest [1]. As a consequence, more elderly patients with more complex coronary lesions are being treated with percutaneous coronary intervention (PCI) by interventional cardiologists, particularly in high volume PCI centres [2]. Typically such lesions are calcified and frequently may be either non-crossable or non-dilatable with standard angioplasty balloons and techniques [3]. Often additional adjunctive equipment and skill sets are required for success in this cohort of cases.

Furthermore, the evidence for treatment of chronic total occlusions (CTO) and achieving full revascularization is more robust in the current era with the result that more operators are taking on these challenging cases [4, 5]. CTOs occur more commonly in older patients and in those patients who have been previously treated with coronary artery bypass graft (CABG) surgery [6]. They are usually associated with at least moderate calcification making it more likely that the operator may encounter difficulty in completing the PCI even if successful with wiring of the vessel. Recently, development of the CTO PCI algorithm has seen major advances in techniques to achieve higher overall success rates with utilization of anterograde-dissection re-entry and retrograde approaches (Fig. 3.1) [6–8]. However, even in experienced hands there occasionally remains the frustration of being unable to complete the PCI having spent a significant time to achieve a distal wire position across the occlusion and despite having applied a variety of advanced technical methods and devices.

O.A. Rana, MBBS, MRCP, DM
S. Talwar, BSc, MBBS, MRCP, MD
P. O’Kane, BSc, MBBS, FRCP, MD (✉)
Dorset Heart Centre, Royal Bournemouth Hospital,
Castle Lane East, BH7 7DW, UK
e-mail: omarrana78@gmail.com; Suneel.talwar@rbch.nhs.uk;
peter.o’kane@rbch.nhs.uk

The purpose of this review is to examine the role of excimer laser coronary atherectomy (ELCA) as an adjunctive technique during PCI of balloon failure cases and CTOs. ELCA will be examined in the context of the alternative techniques available and the potential utilization will be demonstrated in a number of clinical cases. The expanding experience of ELCA in the treatment of under expanded stents will also be discussed.

Balloon Failure and Techniques to Achieve PCI Success Including Excimer Laser Coronary Atherectomy

The failure to cross or expand a coronary stenosis with an angioplasty balloon is often associated with immediate technical failure, incomplete revascularization and complications. Failure of a pre-dilatation balloon to either cross (non-crossable) or fully dilate a stenosis with a balloon (non-dilatable) are highest when there is a heavy infiltration of calcium within the lesion, particularly when this is concentric and deep into the intima.

To define balloon failure in the context of complex lesions we describe potentially four cohorts of clinical scenarios (Fig. 3.2). Firstly lesions that can be crossed with a guide wire and where there is TIMI 3 flow in the distal vessel in contrast to the second group where there is TIMI 0 flow i.e. there is a CTO. Similarly, group 3 consist of lesions occurring in vessels with TIMI 3 flow where a balloon can be advanced across but subsequently fails to fully expand with group 4 represented by failed balloon expansion in CTOs.

Adequate lesion preparation and debulking are considered mandatory in the drug eluting stent (DES) era to ensure procedural success, target lesion revascularization (TVR) and facilitate stent expansion with sufficient wall apposition to reduce the incidence of late stent thrombosis (ST) [9]. The most commonly used device for heavily calcified coronary lesions and non-dilatable lesions is rotational atherectomy (RA) [10]. Perhaps it is not surprising that this device has seen a surge in uptake over the last few years [11–16].

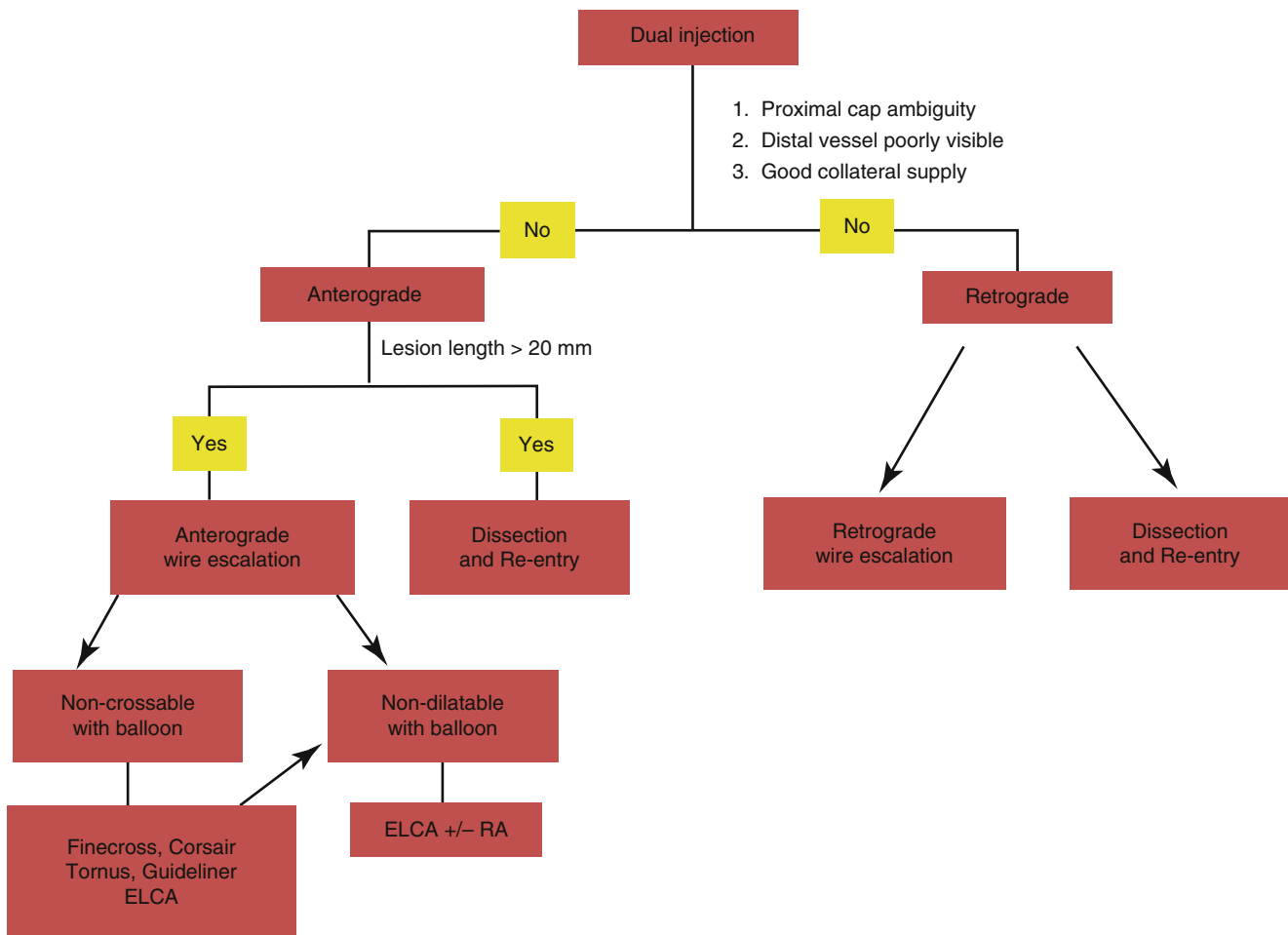


Fig. 3.1 Algorithm to schematically depict various approaches to treat a chronic total occlusion. *ELCA* excimer laser coronary atherectomy, *RA* rotational atherectomy

Other alternatives include upsizing the guide catheter for more rigidity and selection of a catheter shaped to provide more support from the contra-lateral wall of the aortic root or a deep-seated positioning of the guide catheter into the vessel. Another option is the utilization of the GuideLiner™ catheter (Vascular Solutions, Minneapolis, USA) which can be advanced right up to the lesion as necessary to facilitate lesion balloon crossing and then onto the distal vessel for subsequent stent delivery [17].

The anchor balloon technique can be useful to assist passage of balloon or micro-catheter across the lesion, but success is variable and traditionally dependent on a suitably sized (>1.5 mm diameter) branch to position the anchor balloon. When the primary problem is failure of balloon expansion, Cutting balloons and double-coated balloons (Schwager, Medica AG, Winterthur, Switzerland) are other devices which can successfully dilate lesions where conventional semi- and non-compliant balloons have failed although these devices are often difficult to deliver owing to the crossing profile [18–20].

Finally, the use of microcatheters for example, Corsair™ microcatheter (Asahi Intecc Co. Ltd, Aichi, Japan) or Tornus™ (Asahi Intecc, Aichi, Japan) is also a viable option [21].

As an alternative to the aforementioned techniques in dealing with balloon failure cases including CTOs, ELCA has a long established history when balloon failure occurs due to mild-moderate calcification [22–25]. As will be set out in greater detail within this Chapter, a major advantage of ELCA is that the catheter is deliverable using the standard 0.014' guidewire and therefore, unlike RA, it can be utilized more readily when a CTO has been crossed with whichever 0.014' guidewire selected by the operator. Furthermore, the technique itself is relatively simple to master and more easily adoptable by most PCI operators when compared to RA (Table 3.1) [26, 27]. From a cost perspective, use of upstream ELCA when confronted with balloon failure cases may be advantageous compared to the aforementioned strategies of multiple balloons, guidewires, microcatheters and specialist devices such as Tornus.

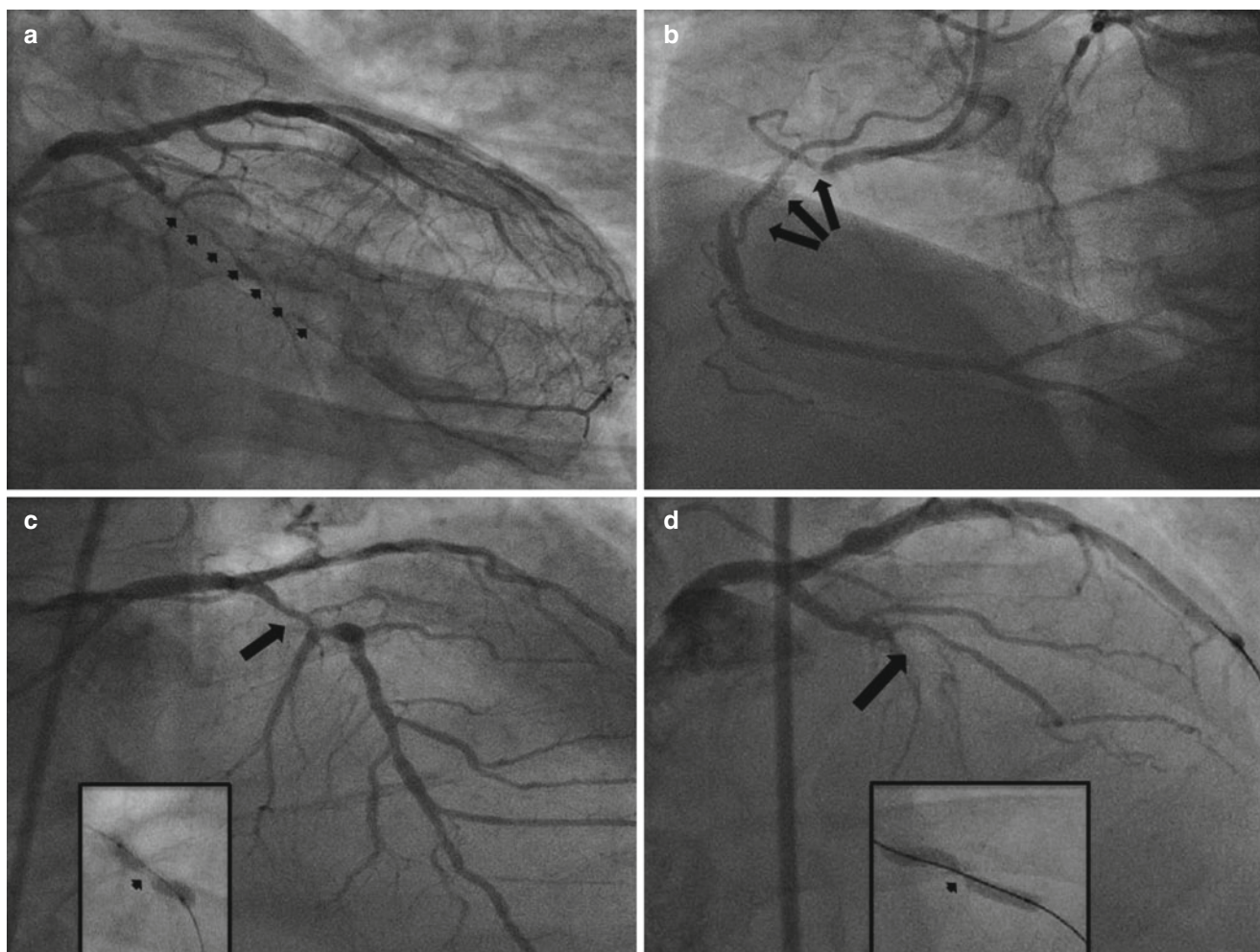


Fig. 3.2 Cohort of lesions where excimer laser coronary atherectomy would be appropriate. (a) Non-crossable lesion with TIMI III flow distally. (b) Non-crossable lesion with TIMI 0 flow distally. The distal artery

is visualised through the collaterals following a contralateral injection into the left coronary system. (c) Non-dilatable lesion with TIMI III flow distally. (d) Non-dilatable lesion (*arrow*) with TIMI 0 flow distally

Table 3.1 Comparison between Excimer Laser Coronary Atherectomy (ELCA) and Rotational Atherectomy (RA)

Feature	ELCA	RA
Size of catheters (mm)	0.9, 1.4, 1.7 and 2.0	1.25, 1.5, 1.75, 2.0, 2.5
Compatibility with French size (F)	6 F: 0.9 and 1.4 mm 8 F: 1.7 and 2.0 mm	6 F: 1.25 and 1.5 mm 8 F: 1.75 and 2.0 mm 9 F: 2.5 mm
Dedicated wire required	No	Yes
Dedicated wire length	Standard guidewire	325 cm
Mechanism	Photothermal ablation	Differential cutting
Training required	++	++++
Severe calcification	Not effective	Effective
Machine console	Large	Small
Air supply set up	Not needed	Needed
Eye protection	Needed	Not needed
Complications	Dissection Perforation	Ischemia Slow flow/no reflow Perforation Burr entrapment Wire fracture

Basic Principles and Laser-Plaque Interactions

Since the discovery of LASER (Light Amplification by Stimulated Emission of Radiation) in the early twentieth century, this technology has gained widespread acceptance in the medical field [28]. Available medical laser devices contain laser-based generators which produce intense electromagnetic energy to stimulate an active medium which results in the emission of monochromatic light of a specific wavelength. At an atomic level, the electromagnetic energy is used to stimulate electrons to elevate them to a state of higher energy. Subsequently, as the electrons return to their baseline low-energy levels, photons are released which form the basis of the monochromatic light emission. This is the basis of ELCA [26].

The CVX-300 cardiovascular laser excimer system (Spectranetics, Colorado Springs, CO, USA) uses Xenon chloride (XeCl) as the active medium. Consequently, the light emitted is pulsed and lies in the ultraviolet B (UVB) region of the spectrum with a wavelength of 308 nm and a tissue penetration depth between 30 and 50 microns. This shallow absorption depth limits medial and adventitial tissue damage in standard PCI. Significant thermal ablation is avoided because of the pulsed delivery of high energy pulses which last only a fraction of a second. The number of pulses emitted during a 1 s period is known as the 'pulse repetition rate'. The duration of each pulse is termed a 'pulse width', which can be modified according to the nature of the treated lesion.

Tissue breakdown via photo-ablation occurs in three steps. Firstly, rapid UV light absorption occurs resulting in severing of carbon-carbon bonds, with subsequent dissipation of energy. This energy dissipation leads to evaporation of intracellular water to produce a steam bubble that advances ahead of the laser catheter. Tissue breakdown occurs due to rapid expansion and contraction of these steam bubbles. The threshold energy required for the penetration of UV light into the surrounding tissue and the subsequent creation of a steam bubble is called 'fluence' (range: 30–80 mJ/mm²). High pulse energy delivery is more efficacious in managing calcified lesions. The resultant debris particles are <10 microns in diameter with minimal risk of distal embolization [26].

ELCA Technique

ELCA catheters are compatible with a standard 0.014' guidewire and are available in 4 diameters for use in the coronary artery 0.9 mm, 1.4 mm, 1.7 mm, and 2.0 mm sizes. The larger diameter devices (1.7 mm and 2.0 mm catheters) are primarily used in straight sections of large diameter vessels for example saphenous vein grafts. They require 7 F and 8 F guide catheters respectively. Both the 0.9 mm and 1.4 mm

are 6 F compatible catheters but only the 0.9 mm, X-80 ELCA catheter is routinely used in balloon failure and CTO cases because of its excellent deliverability and high power and repetition rate settings. The 0.9 mm catheter contains 65 fibres of 50 µm diameter each and the radio-opaque marker on this catheter is set back from the tip making the device extremely deliverable (Fig. 3.3).

In balloon failure cases, this rapid-exchange ELCA catheter is advanced to the lesion and, during continuous saline flush, lasing commences with gentle, slow, forward traction of the catheter. As the pulsed ultraviolet light emitted has a shallow penetration depth there is a low risk of dissection and vessel perforation. However, it is imperative to advance the catheter slowly and cautiously when dealing with very resistant lesions. Often in these cases there is a tendency for even a supportive guide catheter to "back out" of the coronary artery, which would prevent saline from reaching the point of laser-plaque interaction, and potentially increase the risk of complications.

When dealing with CTO lesions, it is advisable not to use the saline technique for several reasons. Often when crossing the CTO with a guidewire a section of the guidewire passage may be outside the true lumen of the vessel. Any anterograde injection may result in propagation of a dissection plane and ultimately result in a longer length of stenting if not immediate no-reflow phenomena. Furthermore the saline infusion is unlikely to reach the intended target given the lack of run off from the lesion and will be therefore ineffective. It is also likely that using ELCA without saline in this setting will permit greater energy at the proximal or distal cap of the occlusion ultimately facilitating the ELCA effect [29].

It should be noted that ELCA is not ideally recommended when the operator is aware that there is a long length of sub-intimal guidewire positioning as may occur during a typical anterograde dissection re-entry case. ELCA catheters are relatively indiscriminate in performing tissue ablation and will essentially 'modify' any tissue in their field of delivery. Within the sub-intimal space the catheter would lie in closer proximity to the media and adventitia of the vessel which may cause perforation.

For non-crossable and non-expansile lesions whether or not in the context of CTO, the highly deliverable 0.9 mm X-80 catheter is favoured with maximum fluence (energy) 80 mJ/mm² and repetition rate 80 Hz attainable. Activation of 10 s is followed by a mandatory rest of 5 s between each lasing period, which is continued until either the catheter has traversed the lesion, or sufficient lesion modification has occurred to permit balloon crossing or expansion.

As mentioned above, the major advantage of ELCA is that as the catheter is utilized on the standard 0.014' guidewire and so unlike RA, it can be operational more readily without the requirement to exchange wires. This becomes of particular importance during CTO cases since it prevents

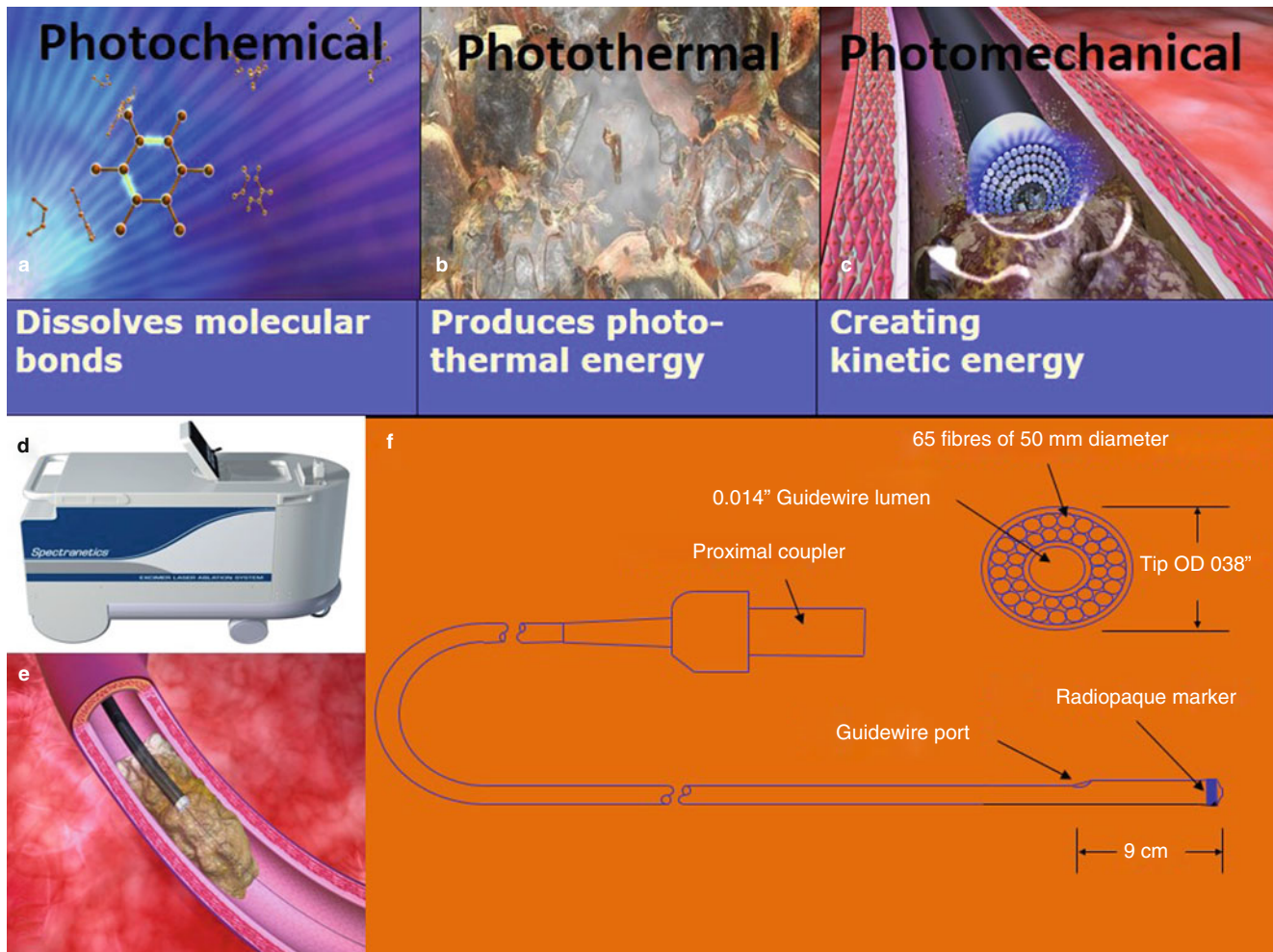


Fig. 3.3 Principles and equipment for excimer laser coronary atherectomy. (a-c) Principles to demonstrate how laser ablates tissue. (d) Laser machine. (e) A laser catheter is seen advancing through a coronary stenosis. (f) Parts of a laser catheter

any potential loss of distal wire position once the lesion has been crossed. Once ELCA has successfully traversed the lesion the case can be completed with balloon angioplasty and stenting. Alternatively, ELCA may provide the pilot channel to permit passage of a RotaWire™ either independently or with the assistance of a microcatheter to first debulk the artery with RA before balloon dilation and final stenting. We have described and previously reported the combined use of ELCA and RA as the “RASER” technique (see cases 9, 10, 11, 12) [30].

Lesions that cannot be treated with RA initially, due to an inability to advance a RotaWire™, can first be treated with ELCA with the understanding that the device will not fully debulk the lesion to permit stenting. However, the “pilot hole” created by ELCA can then be used to pass a RotaWire™, either independently or via a microcatheter exchange technique, to permit subsequent RA and achieve procedural success.

ELCA for Non-dilatable Lesions and Chronic Total Occlusions

ELCA may have additional beneficial properties than simply being able to cross or adequately debulk the resistant lesion. The ablative effect will be transmitted across the atherosclerotic plaque, any organised thrombus, fibrosis and calcification which comprise the main architecture of a CTO. During recanalization attempts, the friable thrombus may induce platelet aggregation and promote the release of vasoconstrictor agents. This leads to a pro-thrombotic milieu that present an additional challenge to an already technically demanding procedure. ELCA has a suppressive effect on platelet aggregation and can sever links within the fibrin mesh leading to clot dissolution [30–32]. ELCA is unlikely to have any significant effect on the calcification within a lesion but the ablation of material supporting the calcified plaque weakens the overall lesion to permit successful balloon traversing and expansion.

ELCA was first approved for use in cases of balloon failure during PCI in the USA in 1992 by the U.S. Food and Drug Administration. There is, however, little data on its use, particularly in contemporary practice. There are several case reports of its use for balloon failure in the balloon angioplasty era [24, 25]. In addition, the percutaneous ELCA (PELCA) multicentre registry enrolled 37 patients with balloon failure (24 with failure of balloon to dilate and 14 with failure to cross) from 1989 to 1993 [33]. The technology available at that time was limited to 1.4, 1.7 and 2.0 mm laser catheters and the laser energy delivered was much lower than current practice with a maximum of 60 fluence and 25 Hz. It was also prior to the introduction of continuous saline flushing during lasing, which has been shown to decrease complications [34]. Complication rates in these patients were high (8 % significant dissection, 3 % perforation, 3 % acute stent thrombosis and 3 % emergency bypass surgery) and laser success rates were only 37 %, although clinical success was obtained in 89 %.

Advances in PCI (with improved wire and balloon technology, the near universal use of coronary stents and the introduction of various drug-eluting stents) have increased the range of indications for PCI and improved outcomes since the 1990s. There has been a resulting increase in case complexity. At the same time there have also been significant advances in ELCA technology, particularly with the introduction of a 0.9 mm laser catheter, an increase in the laser energies delivered and the use of a continuous saline flush system [34–36].

Bilodeau et al. studied the novel 0.9 mm catheter and saline flush technique in 100 calcified and complex lesions (including 35 in which there was primary “balloon failure” although this was not defined or analyzed independently) [22]. They also utilised higher laser energies and demonstrated that increased laser energies increased laser success rates without an obvious increase in complications. In this study, overall laser and procedural success rates were over 90 %. Complications included in-hospital death (2 %), myocardial infarction (4 %) and coronary dissection (5 %).

Shen et al. have more recently reported a series of 33 cases in which they utilized ELCA, although without the saline flush technique (including 21 patients with failure of balloon to cross, 15 in the context of CTOs) [25]. They reported a success rate of 90 % and no complications directly related to laser catheter treatment.

ELCA has a clearly established role in the treatment of non-dilatable lesions occurring due to mild-moderate calcification or non-crossable lesions. However, despite an increase in the number of European PCI centres which have the ability to offer ELCA on site over the last 4 years, there is a paucity of data on the overall success rates of ELCA for balloon failure in patients undergoing contemporary PCI and particularly in CTOs [3, 29, 37]. In

addition, there is little guidance on the safety aspects. The latter is important given that previous studies using earlier generation ELCA equipment and techniques reported specific risks, including major coronary dissection (in up to 5 % of cases) and coronary perforation (0.6 % of cases) [33, 38].

Our group has recently published data from a 4-year retrospective analysis of ELCA cases performed following balloon failure from our institute [3]. This has demonstrated ELCA to be an effective and safe adjunctive treatment. We identified 58 cases of balloon failure treated with ELCA ± rotational atherectomy (RA), representing 0.84 % of all PCI performed in our centre during this period. Balloon failures were classified according to: (1) mechanism of balloon failure; and (2) whether this occurred in the context of treating a CTO. ELCA was performed following balloon failure using the CVX-300 Excimer Laser System and a 0.9 mm catheter with saline flush. For the entire cohort, procedure success was achieved in 91 % (with ELCA successful: alone in 76.1 %, after RA failure in 6.8 % and in combination with RA for 8.6 %). Only in one case did RA succeed where ELCA had failed. There were four procedure-related complications, including transient no-reflow, side branch occlusion and two coronary perforations, of which one was directly attributable to ELCA and led to subsequent mortality (Table 3.2).

ELCA in Under Expanded Stents

The ablative capabilities of ELCA are based on absorption of its energy in the atheroma, leading to photomechanical and photothermal processes. Using high power energy, the 0.9 X-80 catheter has shown to cross even heavily calcified lesions. Even if the target lesions are not directly in the focus of laser beam, the specific interaction of ELCA energy in blood vessels induces acoustic shock waves propagating onto the surrounding structures.

This effect becomes even more desirable when treating under expanded coronary stents. Under expanded coronary stents pose a significant risk for stent thrombosis and subsequent adverse clinical outcomes. There are very few case reports on the successful use of ELCA to treat under expanded stents [20, 39]. In our experience, this is a very good indication, in the presence of calcific coronary stenosis, for the use of ELCA [20]. The laser catheter ablates tissue underneath the stent allowing lesion modification and subsequent expansion of an originally under expanded stent. Recently, the ELLEMENT registry has reported the successful use of ELCA in treating under expanded coronary stents in 28 patients [40]. Importantly,

Table 3.2 Patient and lesion characteristics in patients with chronic total occlusions or non-dilatable stenosis treated with excimer laser coronary atherectomy [3]

		Total	Failed to cross		Failed to expand	
			TIMI 3	CTO	TIMI 3	CTO
Number		58	20	16	20	2
Patient	Age	72±8.5	71±7.5	71.1±8.7	74±9.2	71±11.3
	>75	50 %	7	7	14	1
	Male	83.9 %	17	11	19	1
Vessel	LAD	25 %	2	3	11	0
	RCA	46.4 %	9	10	7	1
	LCX	28.5 %	9	3	2	1
Lesion	C	78.5 %	16	15	13	2
	B2	16.2 %	3	1	5	0
	B1	5.3 %	1	0	2	0
	A	0	0	0	0	0
	Length (mm)	44.1±26.8	34.1±22.1	64.5±27.2	36.7±21	57±46.7
	> mod calcium	82.1 %	16	15	14	2
	> mod angle	20 %	3	1	4	1
Devices Used	ELCA alone-success	76.1 %	10	13	18	2
	ELCA alone-failure	6.8 %	3	1	0	0
	ELCA success after RA failure	6.8 %	3	0	1	0
	RA success after ELCA failure	1.7 %	0	0	1	0
	ELCA & RA combined – success	8.6 %	4	1	0	0
	ELCA and RA combined – failure	1.7 %	0	1	0	0
Procedure	Transradial access	28	9	6	13	0
	6 F Guide catheter	36	17	12	6	1
	7 F Guide catheter	8	3	4	0	1
	8 F Guide catheter	1	0	0	1	0
	Mean number of balloons used	2.8	2.5	3.5	2.8	4.0
	Pulses delivered	6698±5496	10,700±6575	4525±2934	4997±4094	3079±1525
	Contrast (ml)	270±86	263±105	283±71	263±72	280±170
	X-ray dose (μGy/m ²)	11,196±5826	11,625±6698	11,734±7198	9884±3426	16,037±5525
	Procedure time (min)	109±34.9	102±27.5	126±36.8	99±35.8	138±31.5
	Outcome	Procedure success	91 %	89.4 % (17)	87.5 % (14)	100 % (20)
Procedural complications		3	0	2	0	1
ELCA specific complications		1	1	0	0	0

a blood and contrast interface was utilized without saline infusion to enhance the dissipation of laser energy. Using quantitative coronary angiography and IVUS, it was noted that the minimal stent diameter increased by 63 % post ELCA. In addition, the cross-sectional area increased by two-fold following ELCA therapy. This translated into an overall success of 97 % (27 patients) with only one case of cardiac death and target lesion revascularization each at 6 months.

Clinical Case Examples

Non-balloon Crossable Coronary Lesions with TIMI Three Distal Flow Fully Crossed with ELCA

Case 1 (Fig. 3.4)

A 65-year old male with an acute coronary syndrome (ACS) was admitted to our hospital. His cardiac enzymes were

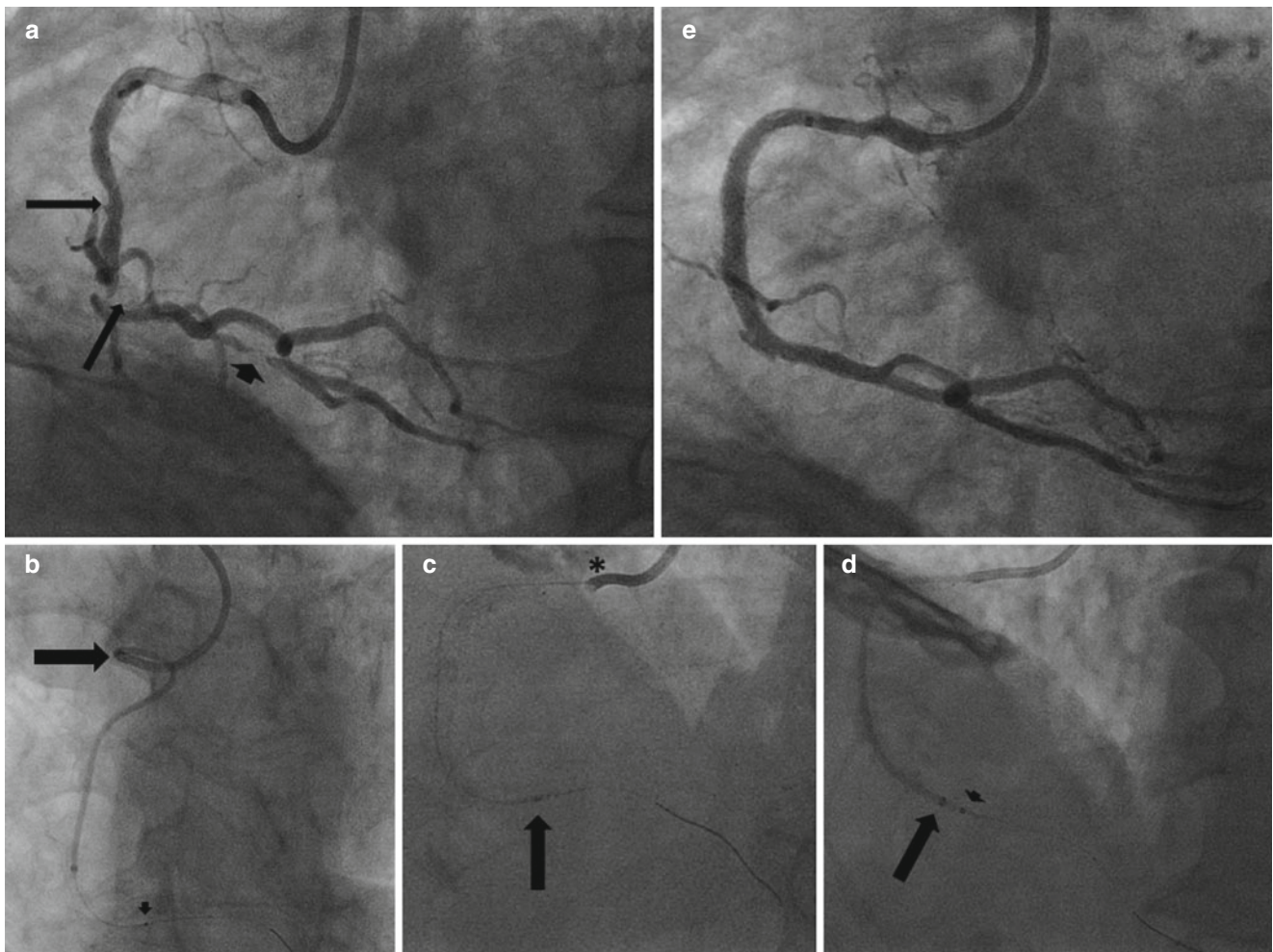


Fig. 3.4 Refer to case 1. (a) Shows the RCA with in-stent restenosis (arrows) and a de novo lesion distally (arrow head). (b) A balloon is seen in the RCA (arrow head) and despite a Guideliner™ the guide

catheter is seen curling up in the aortic root. (c) The balloon cannot be advanced (arrow) and the guide catheter is seen to back out (asterisk). (d) A Guideliner™ is seen (arrow) with a laser catheter (arrow head)

raised and there were dynamic inferior ECG changes. An echocardiogram demonstrated well-preserved left ventricular systolic function. Subsequently, a coronary angiogram (CAG) revealed severe disease in the dominant right coronary artery (RCA) with sub-total occlusion of the posterior descending artery (PDA). A BMW™ (Abbott Vascular, Ill, USA) guidewire was easily advanced into the distal PDA but the lowest profile balloon would not cross beyond the PDA ostium despite a Guideliner™ (Vascular Solutions, MN, USA) advanced up to the lesion. The more proximal RCA was treated with 3 overlapping bare metal stents (3.5×18 mm, 3.5×18 mm and 3.5×23 mm) Tsunami Gold™ (Terumo, Japan). Subsequently, an outpatient cardiac magnetic resonance imaging (MRI) was organised to establish whether there was significant ischemia in the inferior wall subtended by the distal RCA. This proved to be the case, and he was scheduled to return for a further attempt at PCI to the PDA lesion.

At subsequent CAG from the right radial artery (RRA) in addition to the non-crossable PDA lesion, there was significant ISR due to neointimal hyperplasia. The RCA was engaged with an AL 1.0 guide catheter and a Luge™ (Boston Scientific, Natick, MA, USA), wire was advanced distally into the PDA. A Guideliner™ catheter was again positioned at the PDA ostium to maximise support. A 0.9 mm X-80 laser catheter was delivered with six trains of 60 mJ/mm^2 at 60 Hz. However, during lasing he developed significant ST segment changes necessitating the Guideliner™ to be withdrawn back into the guide with a further seven trains of ELCA 80 mJ/mm^2 at 80 Hz for a total time of 2 min until the catheter fully crossed the lesion. A 1.25×15 mm RyuJin™ (Terumo Corporation, Shizuoka, Japan) balloon easily crossed the lesion and was followed by 2.0×12 mm and 2.5×12 mm Apex™ (Boston Scientific, Natick, MA, USA) balloons which were observed to expand fully. Finally, 4 overlapping (2.25×12 mm, 2.75×20 mm, 3.5×20 and 3.5×24 mm)

Promus Element™ stents (Boston Scientific, Natick, MA, USA) were implanted and post-dilated with appropriately sized balloons to ensure adequate stent apposition angiographically and using intravascular ultrasound (IVUS, EagleEye™, Volcano Corp, CA, USA).

Non-balloon Crossable Coronary Lesions with TIMI 0 Distal Flow (CTO) Fully Crossed with ELCA

Case 2 (Fig. 3.5)

A 66-year old gentleman underwent elective PCI to a CTO of his RCA. He had CCS Class II angina status despite optimal medical therapy (OMT) and had concomitant disease in the LAD and LCX. In addition, non-invasive imaging had revealed a large burden of ischemia in the RCA territory.

Coronary artery bypass grafting (CABG) had been discussed with him but he had declined.

The CTO was located in the proximal RCA with a blunt stump and ambiguous proximal cap was with an adjacent side branch visible. The distal vessel was very well visualised from contra-lateral injections of the left coronary artery (LCA) which revealed a relatively short occlusion. The J-CTO score was calculated as 3 suggesting a complex lesion [6].

Initially, a MiracleBros 3™ (Asahi Intecc, Aichi, Japan) guidewire penetrated the proximal cap but did not make further progress. With over the wire balloon support, a MiracleBros 6™ (Asahi Intecc, Aichi, Japan) guide wire advanced through the lesion but would not exit the distal cap. A polymer-jacketed Pilot 150 (Abbott Vascular, Ill, USA) wire did however successfully puncture the distal cap and exited into the true lumen distally. Unfortunately, the lowest profile balloons available including a 0.85 mm × 10 mm NIC Nano™ balloon

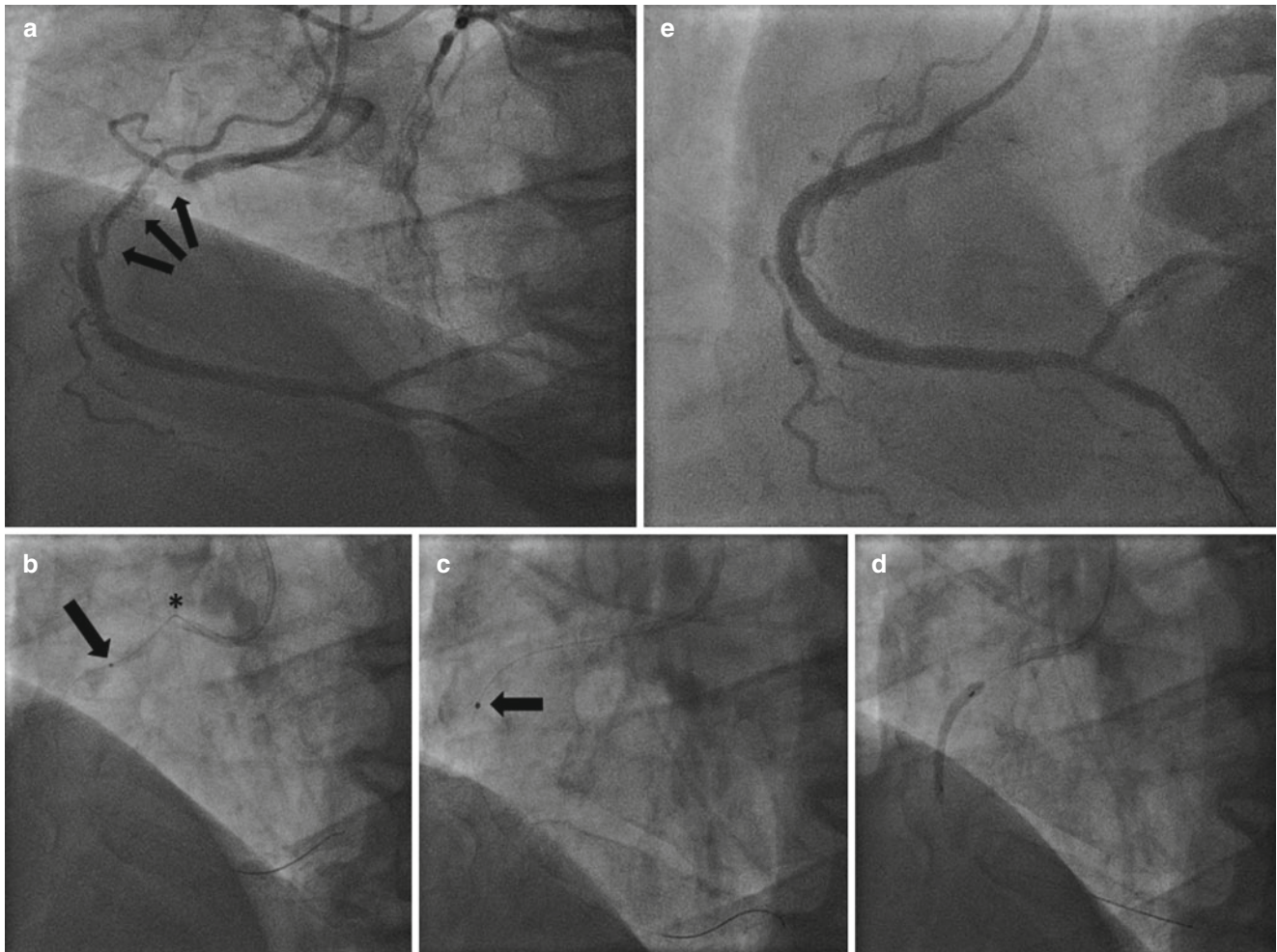


Fig. 3.5 Refer to case 2. (a) Demonstrates the CTO in RCA which appears to be heavily calcified (*arrows*). (b) Failure to advance a low-profile 0.85 × 10 mm balloon (*arrow*) across the CTO resulting in ‘buckling’ of the guide-wire and disengagement of the guide-catheter

(*asterisk*). (c) 0.9 mm X-80 ELCA catheter is used to debulk the lesion following which a 2.5 × 20 mm balloon is used to pre-dilate the lesion (d) and the final result can be seen (e)

(Vascular Perspectives, Manchester, UK) would not cross the lesion. The proximal branch was considered too small for an anchor balloon so therefore, ELCA was used with a 0.9 mm X-80 catheter advanced into the lesion. A total of 1966 pulses (eight trains) of 45 mJ/mm² at 25 Hz for a duration of 1:16 min was successful with the catheter fully crossing the lesion. Two overlapping 3.5 × 32 mm and 4.0 × 16 mm Taxus™ (Boston Scientific, Natick, MA, USA) DES were deployed and post-dilated with a 4.0 × 20 mm non-compliant balloon to ensure satisfactory stent expansion.

Case 3 (Fig. 3.6)

A 63-year old lady underwent PCI to the CTO of her LCX at our institute. Her cardiovascular risks included dyslipidaemia, peripheral vascular disease and a strong family history. She had recently presented with inferior Non-ST elevation MI (NSTEMI) and had undergone PCI to the dominant RCA. She continued to experience CCS class II angina

despite being on OMT. An echocardiogram had revealed good left ventricular systolic function while an exercise tolerance test was strongly positive at a low-workload.

A left radial artery (LRA) approach for PCI was used. On CAG, the CTO had a blunt stump with some proximal cap ambiguity and there was moderate calcification within the lesion with a J-CTO score of 2. A BMW™ wire was advanced into the LAD for added guide catheter stability. Subsequently, the CTO was successfully crossed with a Fielder XT™ wire. However, it proved impossible to cross the lesion with a 2.0 × 20 mm Apex™ or a 1.2 × 12 mm Mini Trek™ (Abbott Vascular, Ill, USA) balloon. ELCA with a 0.9 mm X-80 laser catheter was therefore utilised delivering a cumulative of 2270 pulses (6 trains) of 60 mJ/mm² at 40 Hz for 54 s. Subsequently, the lesion was successfully crossed and dilated sequentially with 1.2 × 12 mm Mini Trek™ and 2.0 × 20 mm Apex™ balloons. Finally, using IVUS four overlapping Cypher Select™ (2.25 × 18 mm, 2.5 × 23 mm, 3.0 × 28 mm and 3.0 × 8 mm,

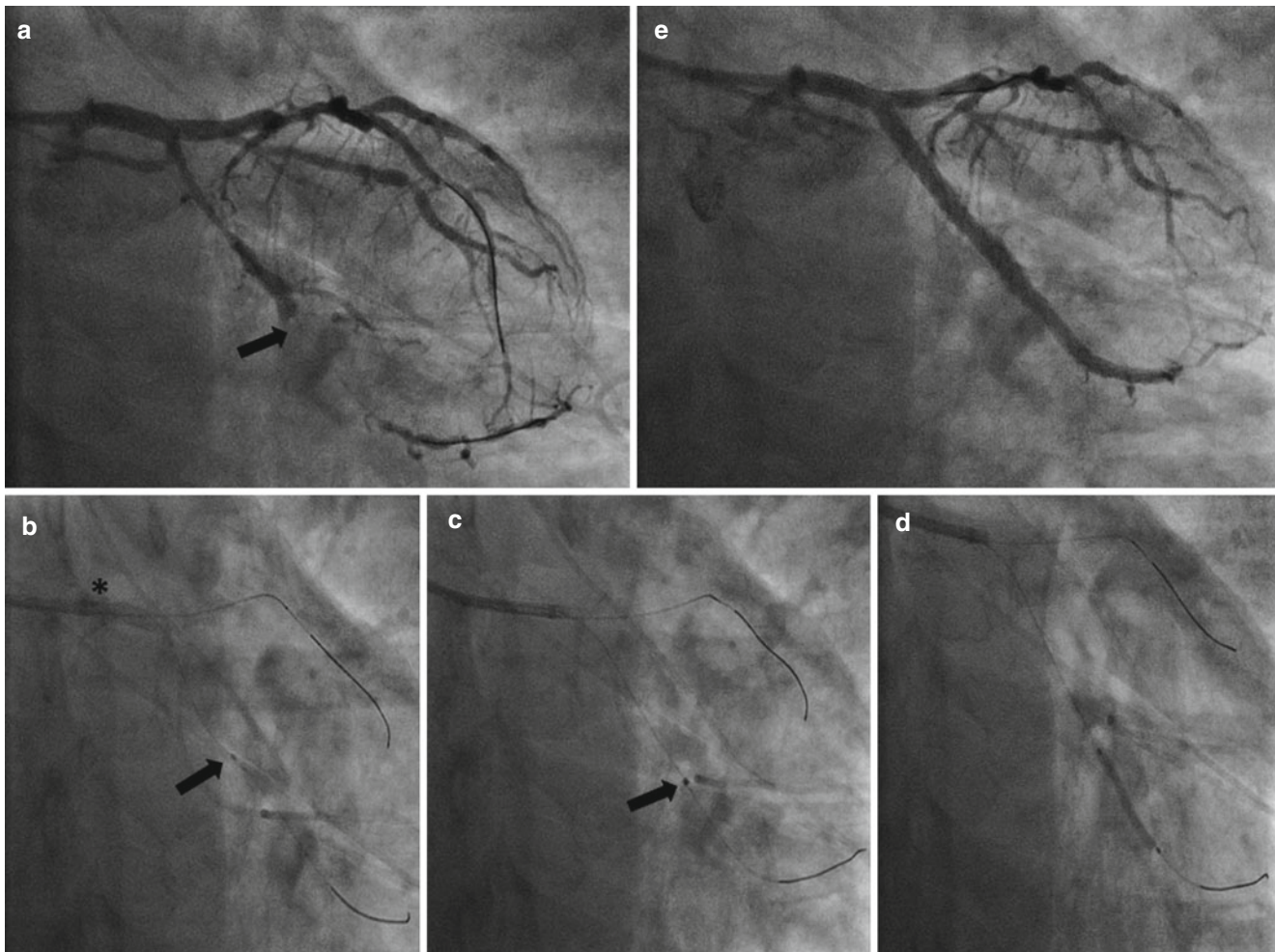


Fig. 3.6 Refer to case 3. (a) A LCX CTO is successfully crossed with a Fielder XT™ guide wire (*arrow*). (b) A 1.2 × 12 mm balloon cannot be advanced across (*asterisk*) the lesion. (c) A 0.9 mm X-80 ELCA

catheter is seen (*arrow*). (d) Following ELCA, balloon predilatation is successful. (e) Final stent result

Cordis Corporation, NJ, USA) DES were deployed back to the ostium and were post-dilated with 2.5×20 mm, 3.0×20 mm and 3.5×8 mm non-compliant balloons.

Case 4 (Fig. 3.7)

A 74-year old female underwent elective PCI to her RCA CTO at our hospital for CCS class III angina. Her past history included hypertension, cerebrovascular disease and good left ventricular function on echocardiography. The LCA was smooth and unobstructed.

An 8 F right femoral artery (RFA) approach was used with an 8 F AL0.75 engaged into the RCA and a 6 F JL 3.5 catheter engaging the LCA via the RRA for contra-lateral injections. A Fielder XT™ with Finecross™ microcatheter support failed to penetrate the proximal cap of the occlusion which was subsequently crossed with a Pilot 200™ (Abbott Vascular, Ill, USA) guide wire. However, the lowest profile balloons would not cross the CTO (2.5×20 mm Emerge™, Ryuji™ 1.25×15 mm and an ACROSS CTO 1.1×10 mm)

ELCA was undertaken using a 0.9 mm X-80 catheter and with delivery of 8336 pulses (11 trains) of 80 mJ/mm^2 at 80 Hz for 1:43 min. The lesion could then easily be crossed and pre-dilated with 1.25×15 mm Ryuji™, 2.5×12 mm Emerge™, and 3.0×20 mm Quantum Apex™ balloons. Finally, three overlapping DES with the aid of a Guideliner™ catheter (Biomatrix 3.5×36 mm, 3.5×24 and 4.0×14 mm stents) were delivered. The stents were post-dilated distally and proximally using a 3.75×20 mm and 4.5×8 mm non-compliant balloons respectively.

Non-balloon Crossable Coronary Lesions with TIMI 3 Distal Flow Partially Crossed with ELCA

Case 5 (Fig. 3.8)

A 65-year old male was admitted to his local hospital with a diagnosis of unstable angina. At the time of his original

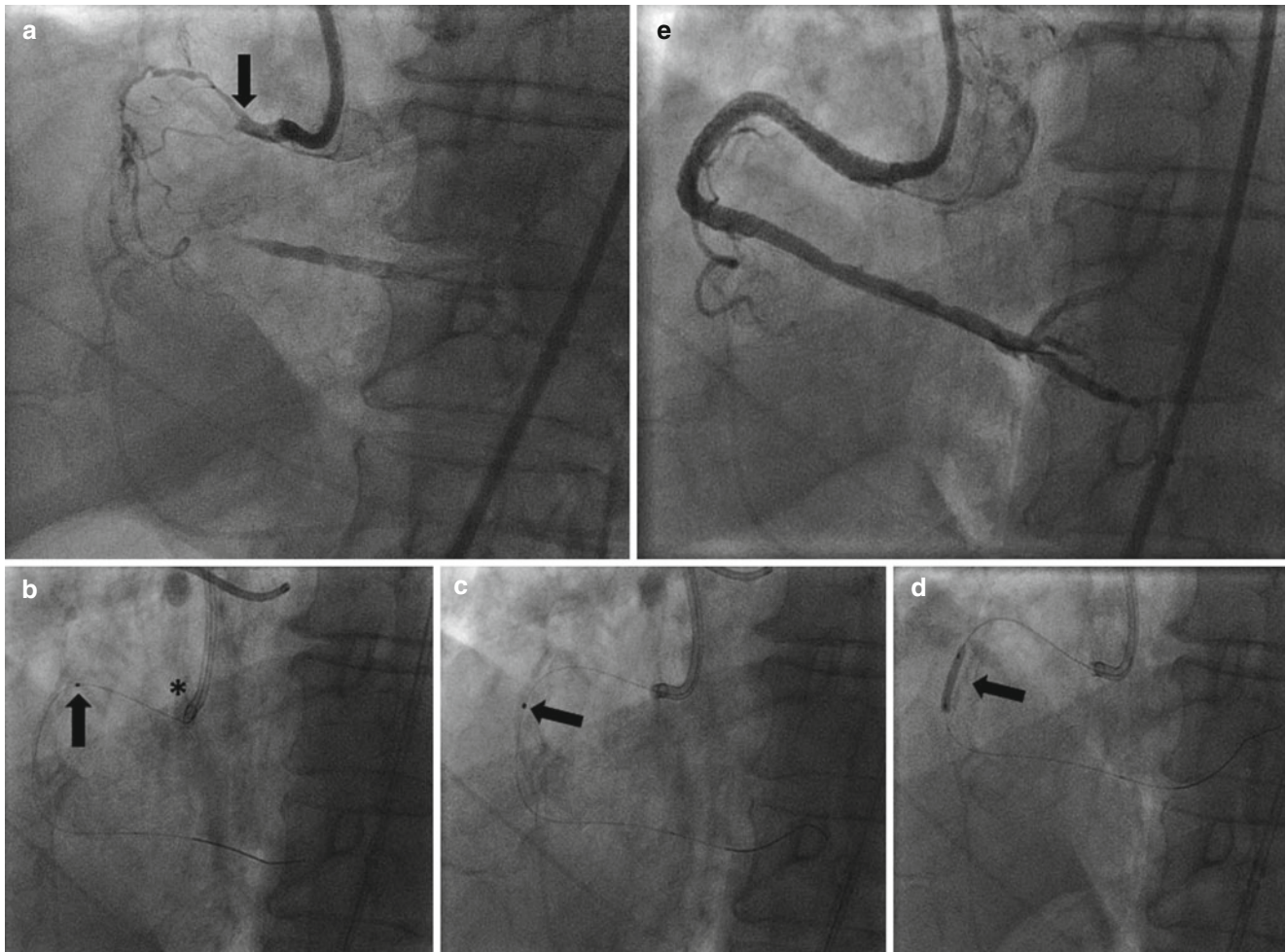


Fig. 3.7 Refer to case 4. (a) RCA CTO lesion is seen (arrow). (b) A 1.1×10 mm balloon cannot cross the lesion (arrow) as the guide catheter is seen backing out (asterisk). (c) A 0.9 mm X-80 laser catheter is seen.

(d) Following ELCA, successful pre-dilatation was possible (arrow). (e) Final stent result

CAG, the culprit lesion was considered to be in the mid RCA. However, this lesion proved non-crossable despite using multiple small profile balloons including a 1.0 × 10 mm Falcon™ balloon (Medtronic, Interventional Vascular, CA, USA). Therefore, he was transferred to our centre for consideration of ELCA to modify and debulk the lesion.

The RCA was intubated with an ART4 guide catheter using a RRA approach. Although, a BMW™ guide wire was easily able to cross the lesion, a 1.25 × 15 mm Ryujin™ balloon could not. As a result, ELCA with a 0.9 mm X-80 laser catheter was used to and deliver a total of 22,551 pulses (10 trains) of 60 mJ/mm² at 40 Hz and subsequently at 80 mJ/mm² and 80 Hz (24 trains) for 5:30 min. The ELCA catheter traversed approximately 75 % the length of the lesion but could not be advanced into the very distal vessel. However, it was still then possible to cross the lesion with a 1.5 × 15 mm Apex™, 3.0 × 20 mm Apex™ and 3.0 × 10 mm Flexotome™ cutting balloon to sufficiently prepare the

vessel for stenting. Two overlapping DES were deployed into the RCA (3.0 × 20 mm and 3.5 × 24 mm Promus Element™) with post-dilation to complete the case.

Non-balloon Crossable Coronary Lesions with TIMI 0 Distal Flow (CTO) Partially Crossed with ELCA

Case 6 (Fig. 3.9)

A 68-year old male underwent primary PCI to his LCX for a lateral ST-elevation myocardial infarction (STEMI). His past medical history included treated hypertension and PCI to the LCX 10 years ago with two bare metal stents (2.75 × 18 mm Zeta™ Multi-Link and 2.5 × 8 mm Pixel™ Multi-Link, Abbott Vascular, Ill, USA). Using a RRA access and a JL3.5 guide catheter it was noted that the LCX had occluded at the proximal end of the previous stent.

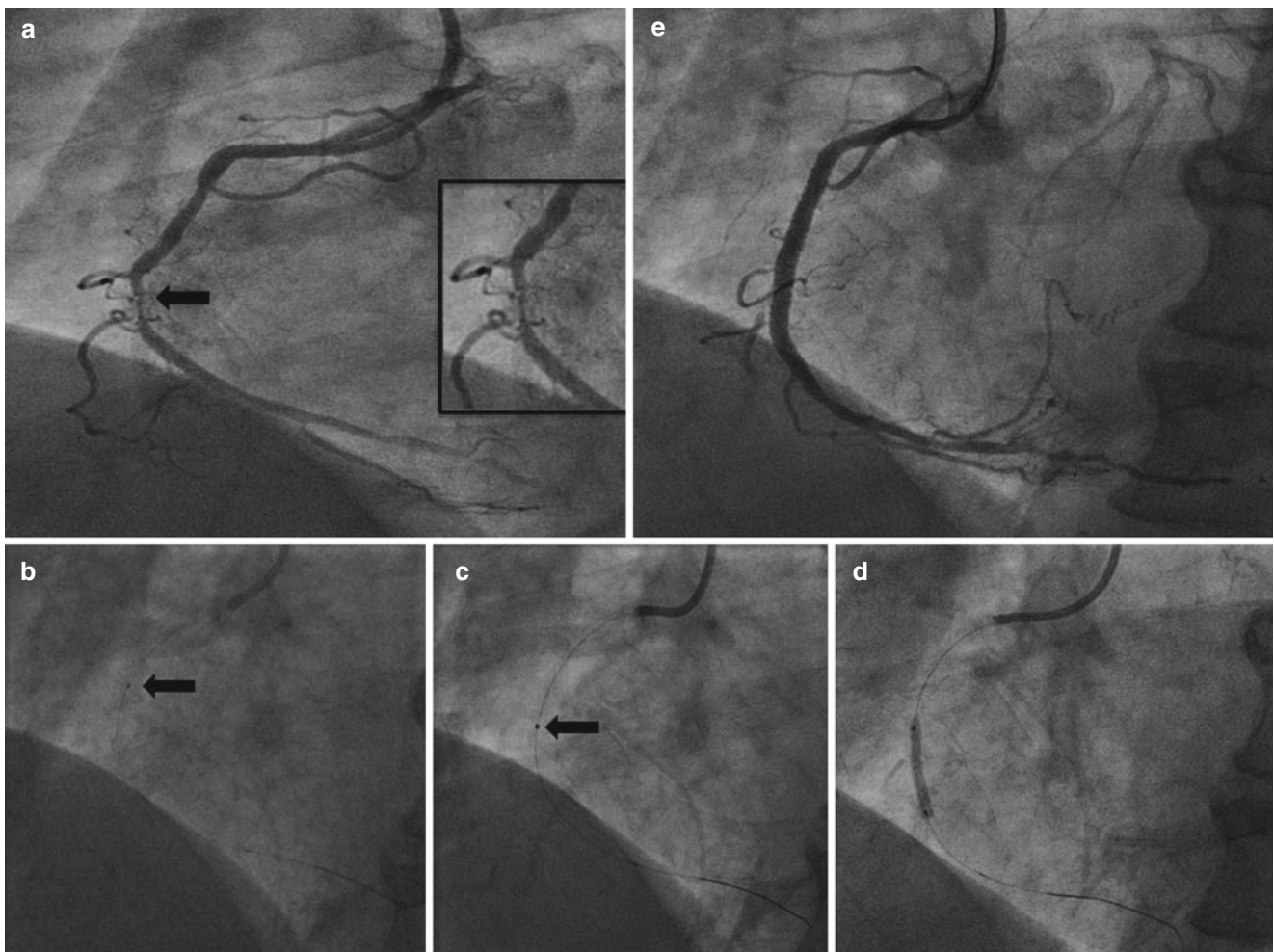


Fig. 3.8 Refer to case 5. (a) A critical RCA lesion (*arrow*) is seen with moderate calcification which is magnified in the inset. (b) A 1.25 × 10 mm balloon cannot be advanced across the lesion (*arrow*). (c)

A 0.9 mm X-80 ELCA catheter is used to laser the lesion (*arrow*). (d) A 3.0 × 20 mm balloon is used to pre-dilate the lesion. (e) Final stent result

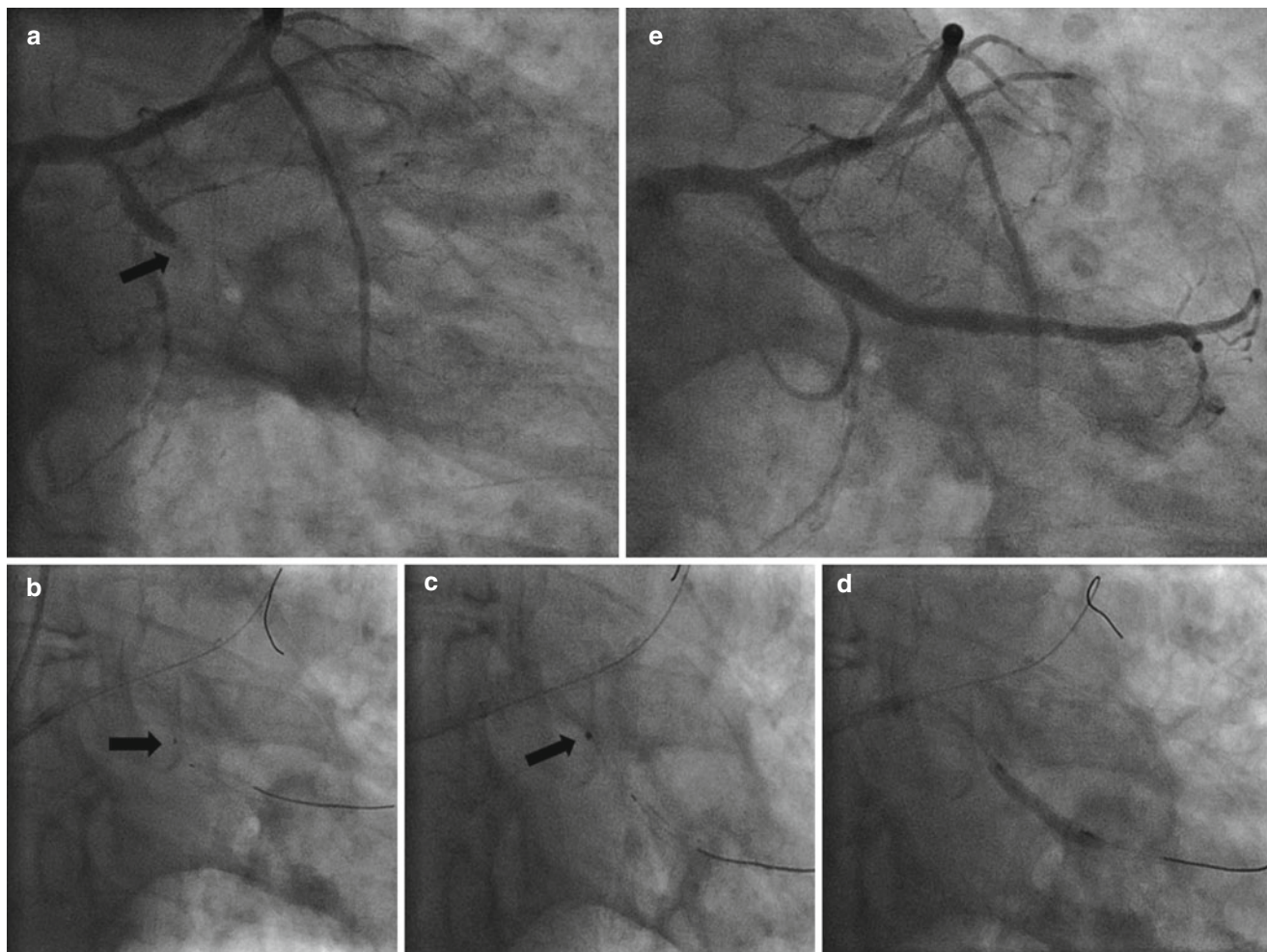


Fig. 3.9 Refer to case 6. (a) A CTO of the LCX artery is seen. (b) A 1.25×10 mm balloon cannot cross the lesion following successful advancement of the guide wire (arrow). (c) A 0.9 mm X-80 ELCA catheter is used followed by (d) successful balloon pre-dilatation and (e) final stent result

The occlusion was crossed using a Luge™ guidewire, but the lesion could not be crossed using a 1.25×15 mm Ryujin™ or 0.85×10 mm NIC Nano™ balloon. ELCA was used with a 0.9 mm X-80 laser catheter. A total of 8000 pulses of 60 mJ/mm^2 at 40 Hz for 3:10 min over 23 trains was delivered. The ELCA catheter did not fully traverse the occlusive lesion but was used intermittently interposed with low profile balloons. Despite only partial ELCA crossing it was possible to eventually cross with a balloon and fully dilate the lesion sequentially with 0.85×10 mm NIC Nano™, 1.25×15 mm Ryujin™ and 2.5×20 mm Maverick™ balloons (Boston Scientific, Natick MA, USA). Four overlapping DES were used to reconstruct the LCX artery (2.75×13 mm, 3.0×13 mm, 3.5×13 mm and 3.5×13 mm Cypher Select™).

Non-balloon Expandable Coronary Lesions with TIMI 3 Distal Flow

Case 7 (Fig. 3.10)

An 84-year old male underwent elective PCI to his LAD at our institute for stable angina. He had been treated with primary PCI to his RCA, 3 months prior to the current procedure. It was noted at the time, that there was a severe mid LAD stenosis that did not appear calcified. He continued to experience angina despite on OMT and had a positive ETT.

The procedure was performed trans-femorally using a 6 F EBU 3.5 guide catheter. A BMW™ wire was advanced distally into the vessel. Pre-dilation of the LAD stenosis with a 2.5×15 mm Apex™ balloon was unsuccessful as the balloon did not fully expand and burst at 18 atmosphere.

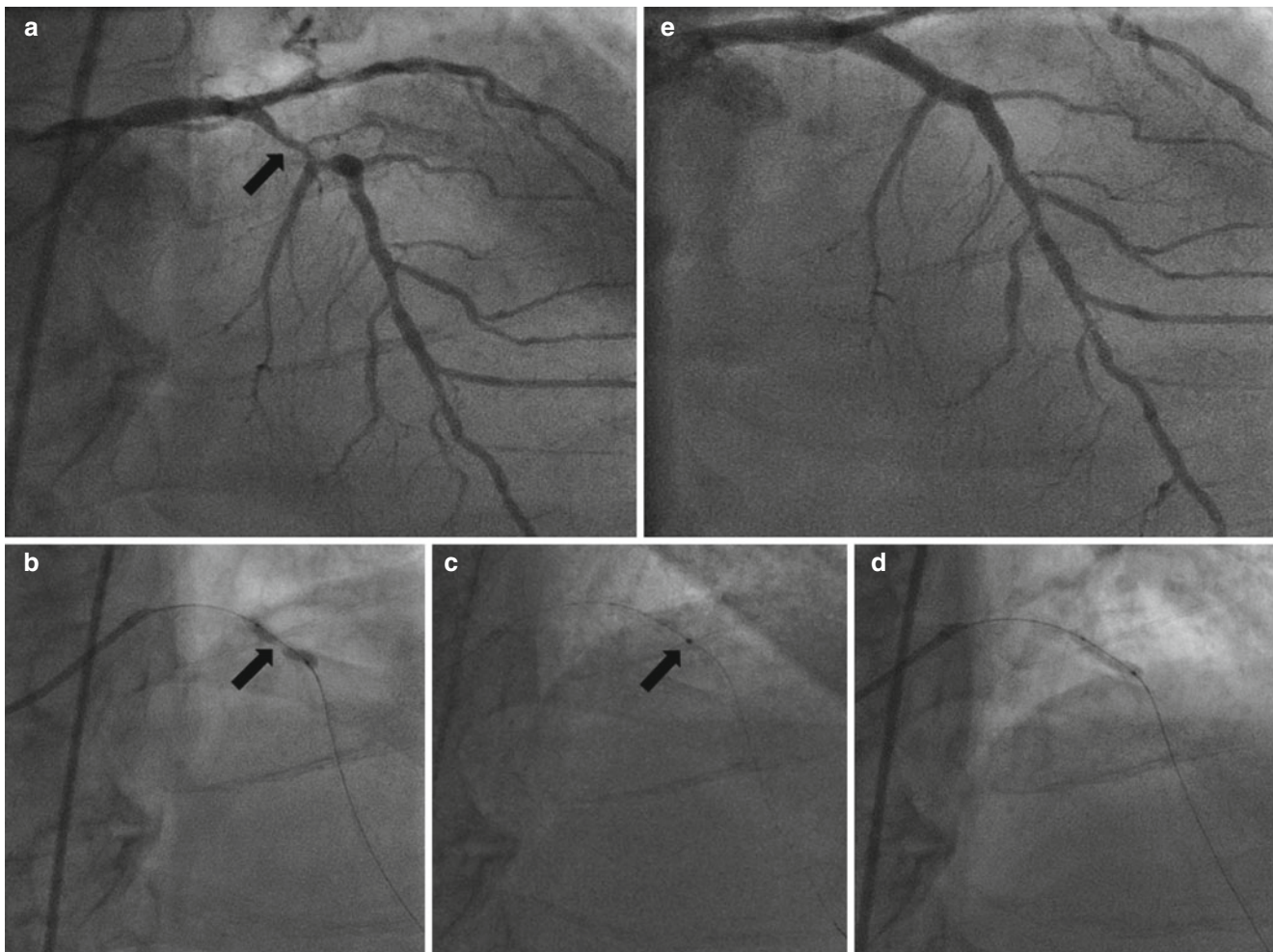


Fig. 3.10 Refer to case 7. (a) An LAD stenosis with moderate calcification is seen. (b) A 2.5×15 mm balloon is seen which has not fully expanded (*arrow*). (c) A 0.9 mm X-80 ELCA catheter is seen. (d) Successful balloon dilatation with full balloon expansion. (e) Final stent result

Instead of further balloon dilation with larger diameter or non-compliant balloons, ELCA was undertaken. Only 2800 pulses (5 trains) of 80 mJ/mm^2 at 80 Hz over a period of 50 s with a 0.9 mm X-80 laser catheter were necessary. Following this, a 2.5×15 mm Apex™ balloon was positioned with full expansion of the balloon at 14 atmospheres. Two overlapping DES to the LAD (3.0×20 mm and 3.0×8 mm Taxus™ stents) and a third back to the body of the LMS completed the PCI with an excellent final angiographic result confirmed on IVUS.

Non-balloon Expandable Coronary Lesions with TIMI 0 Distal Flow (CTO)

Case 8 (Fig. 3.11)

A 76-year old man underwent PCI to his LAD CTO at our centre. His cardiovascular risk factors included a previous myocardial infarction and hypertension. CAG confirmed an

occluded LAD and an inpatient MRI demonstrated that the LAD territory was viable with evidence of ischemia. Arterial access was obtained using a bi-femoral approach with a 7 F EBU 3.5 guide catheter for the LMS artery and a 6 F JR4 for the RCA. The CTO was short with a tapered end and moderate amount of calcification in the arterial wall. The LAD occlusion was attempted initially with a Sion™ (Asahi Intecc, Aichi, Japan), Fielder XT™ and MiracleBros 4.5 g™ (Asahi Intecc, Aichi, Japan) guidewires but these proved unsuccessful. Subsequently, the CTO was crossed with a Confianza™ 9 g guidewire with a Corsair™ microcatheter support. The lesion was pre-dilated with a 2.0×20 mm and 2.5×20 mm non-compliant balloon but the lesion proved non-dilatable. Therefore, ELCA was performed with a 0.9 mm X-80 catheter and 6000 pulses were delivered 6000 pulses of 80 mJ/mm^2 at 80 Hz. Following this, a 2.5×20 mm balloon was easily expandable at 12 atmospheres. The LAD was treated with three overlapping DES (2.5×12 mm, 3.0×20 mm and 3.5×28 mm Promus Element™). These were

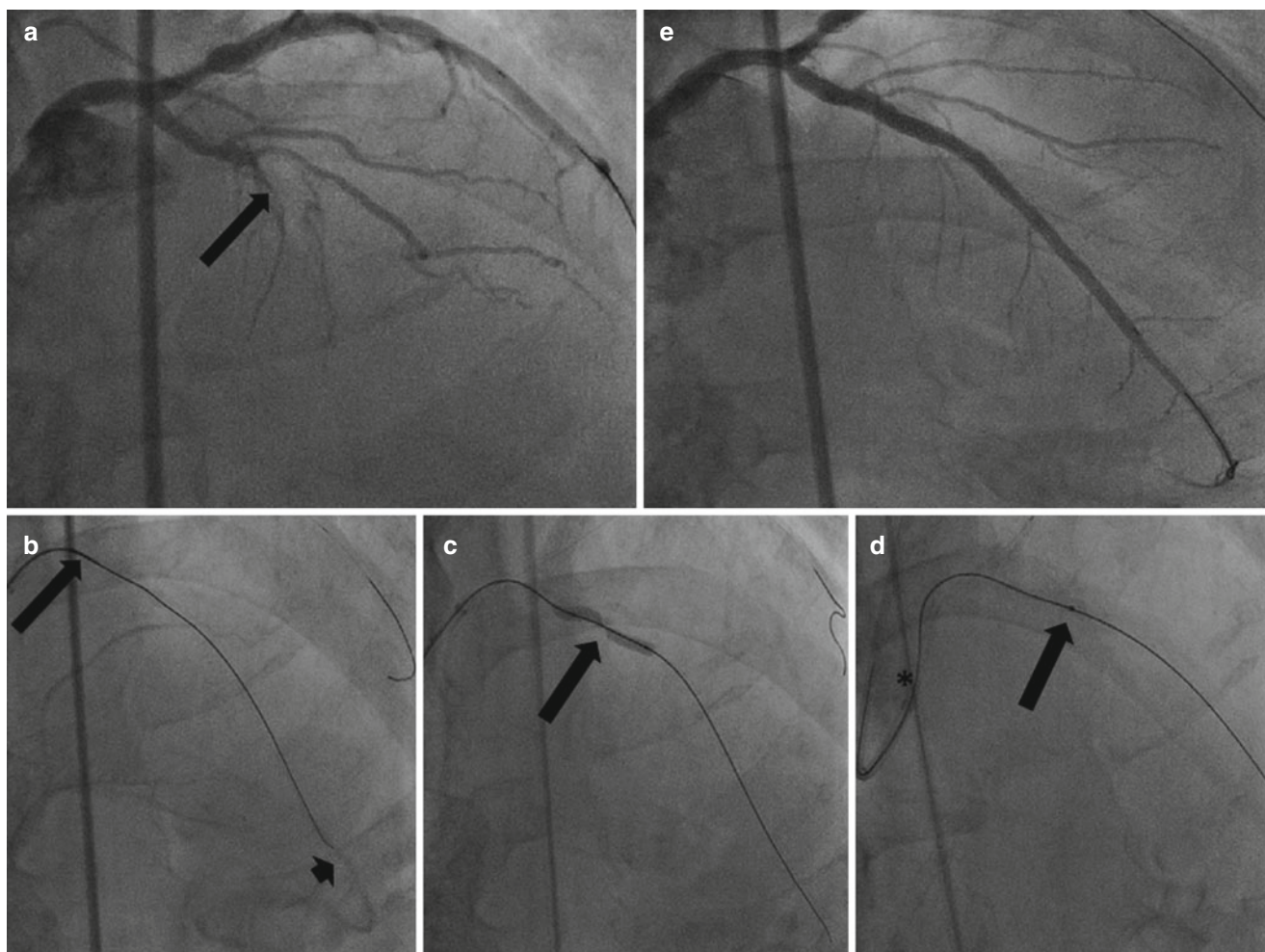


Fig. 3.11 Refer to case 8. (a) A calcified CTO is seen in a LAD. (b) Successful anterograde wire advancement into the distal true lumen as confirmed following contra lateral injection (*arrowhead*). A Corsiar™

microcatheter is also seen. (c) Balloon failure is seen suggesting a non-dilatable lesion. (d) A 0.9 mm X-80 ELCA catheter is seen (*arrow*). The guide catheter is seen to backing out (*asterisk*). (e) Final stent result

post-dilated with appropriate size non-compliant balloons to ensure full stent optimisation.

Balloon Failure Coronary Lesions with TIMI 3 Distal Flow Requiring Combined Use of ELCA and RA – ‘RASER’ Cases

Case 9 (Fig. 3.12)

A 64-year old gentleman was admitted acutely as he developed transient ST segment elevation in the lateral leads during an exercise stress echocardiogram. His cardiovascular risk factors included hypertension and he had undergone CABG 6 years previously with a LIMA graft to his LAD artery, a right internal mammary artery (RIMA) graft to his intermediate artery and vein grafts to his LCX and RCA. Left ventricular function was within normal limits.

CAG revealed an occluded native LAD and RCA. The left main stem artery had a critical, hazy distal stenosis that involved the LCX ostium with severe stenosis in a large obtuse marginal (OM) artery. The bilateral internal mammary grafts were patent, however, the SVGs were found to be occluded. In view of the ECG changes and angiogram findings, it was likely that the distal LMS and OM lesion was the culprit.

A 7 F EBU3.5 guide catheter was used to engage the LMS artery. A BMW™ wire was successfully passed distal to the stenosis into the OM branch. In view of the heavy burden of calcified plaque and the long standing coronary atheroma, it was desirable to debulk the vessel with RA prior to stenting. A RotaWire™ could not be delivered through the lesion and a Finecross™ microcatheter would also not cross to permit wire exchange.

ELCA was therefore undertaken with a 0.9 mm X-80 laser catheter and delivered 14,799 pulses (19 trains) of

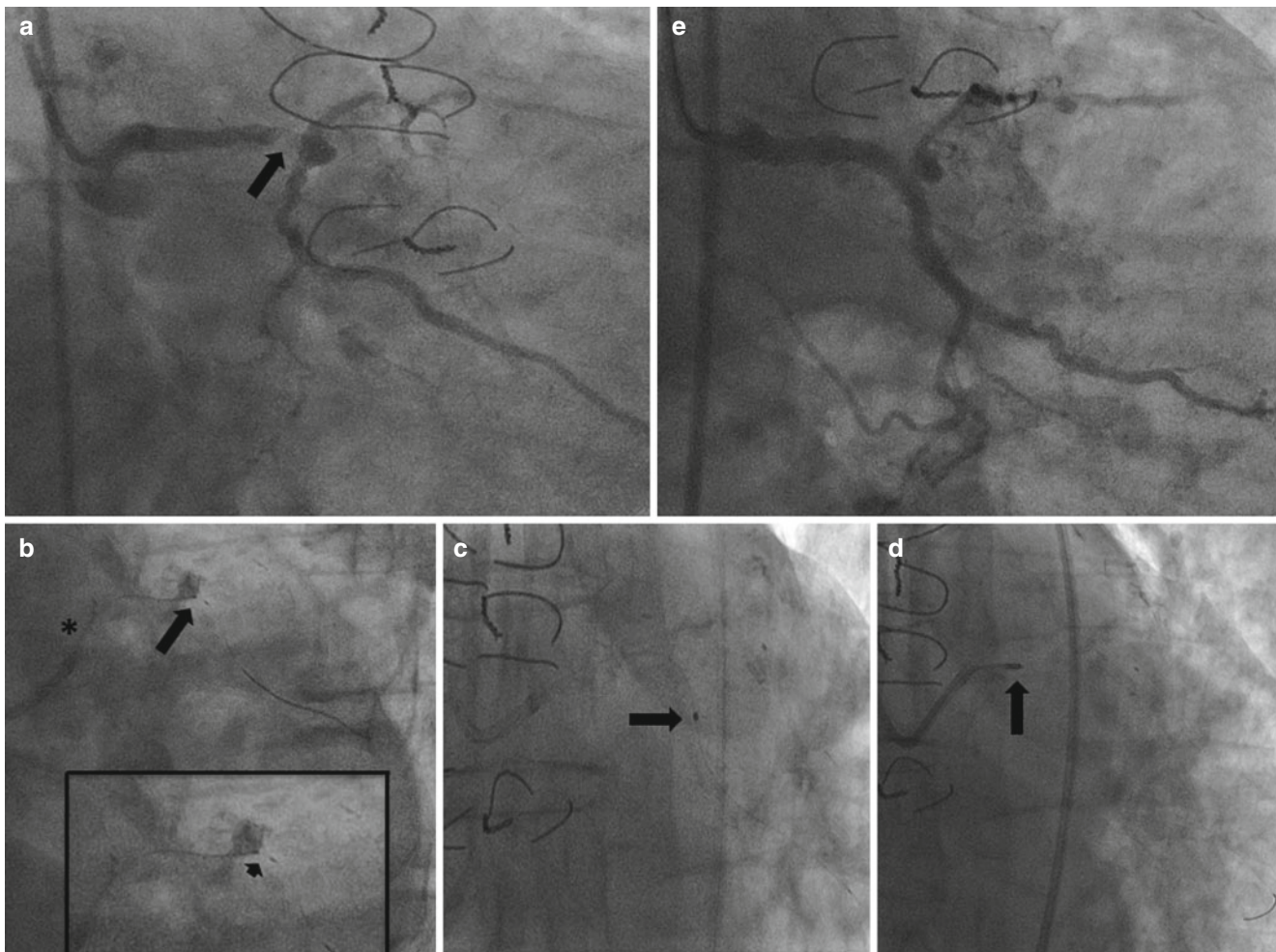


Fig. 3.12 Refer to case 9. (a) A critical stenosis is seen in the distal left main stem artery extending into the LCX artery (arrow). (b) A 1.25 × 15 mm balloon cannot cross the stenosis with backing of the guide cath-

eter (asterisk). This can be better appreciated with the magnified image in the inset (arrow head) (c) A 0.9 mm X-80 ELCA catheter is seen. (d) A 1.25 mm rotablation burr. (e) Final stent result

80 mJ/mm² at 80 Hz for a total of 3:03 min. The lesion was now easily crossed with a Finecross™ microcatheter to and the BMW™ wire was exchanged for a RotaWire™. RA was performed by sequentially using 1.5 mm and 1.75 mm rotablation burrs for a total time of 2 min.

Pre-dilation of the lesion with 2.75 × 20 mm and 3.0 × 20 mm non-compliant balloons was followed by delivery of two overlapping Biomatrix™ stents (3.5 × 20 mm and 4.0 × 15 mm) which were deployed and post-dilated with 3.5 × 20 and 4.0 × 15 mm non-compliant balloons to complete the case.

Case 10 (Fig. 3.13)

A 57-year old male was admitted to our hospital with an ACS. His cardiac risk factors included, a history of heavy smoking and a strong family history. An echocardiogram had revealed good left ventricular systolic function. Subsequent CAG via the RFA demonstrated mild plaque disease in the left coronary system and a heavily calcified RCA with a

critical mid-vessel stenosis. A 7 F JR4 guide catheter was engaged into the RCA. The initial plan was to advance a guide wire across the lesion and then exchange for a RotaWire™ to perform RA. The lesion could not be crossed with multiple guide wires including a BMW™, Fielder FC™ and Confianza Pro 9™ (Asahi Intecc, Aichi, Japan). Finally, a tapered Fielder XT™ was able to cross the lesion successfully. However, the Finecross™ could not be advanced across the stenosis to facilitate wire exchange for a RotaWire™. As a result, ELCA was performed using a 0.9 mm X-80 catheter and delivered 10,839 pulses (17 trains) of 80 mJ/mm² at 80 Hz for 2:08 min. Following this, the Finecross™ could be advanced distally into the RCA to allow wire exchange for a RotaWire™. However, a 2.5 × 20 mm balloon failed to dilated fully and hence RA was performed using a 1.5 mm rotablation burr. Subsequently, the lesion was pre-dilated with 3.0 × 20 mm and 3.5 × 20 mm non-compliant balloons. Finally, we were able to deploy three overlapping DES (3.5 × 23 mm, 3.5 × 33 mm and 3.5 × 23 mm Cypher Select™)

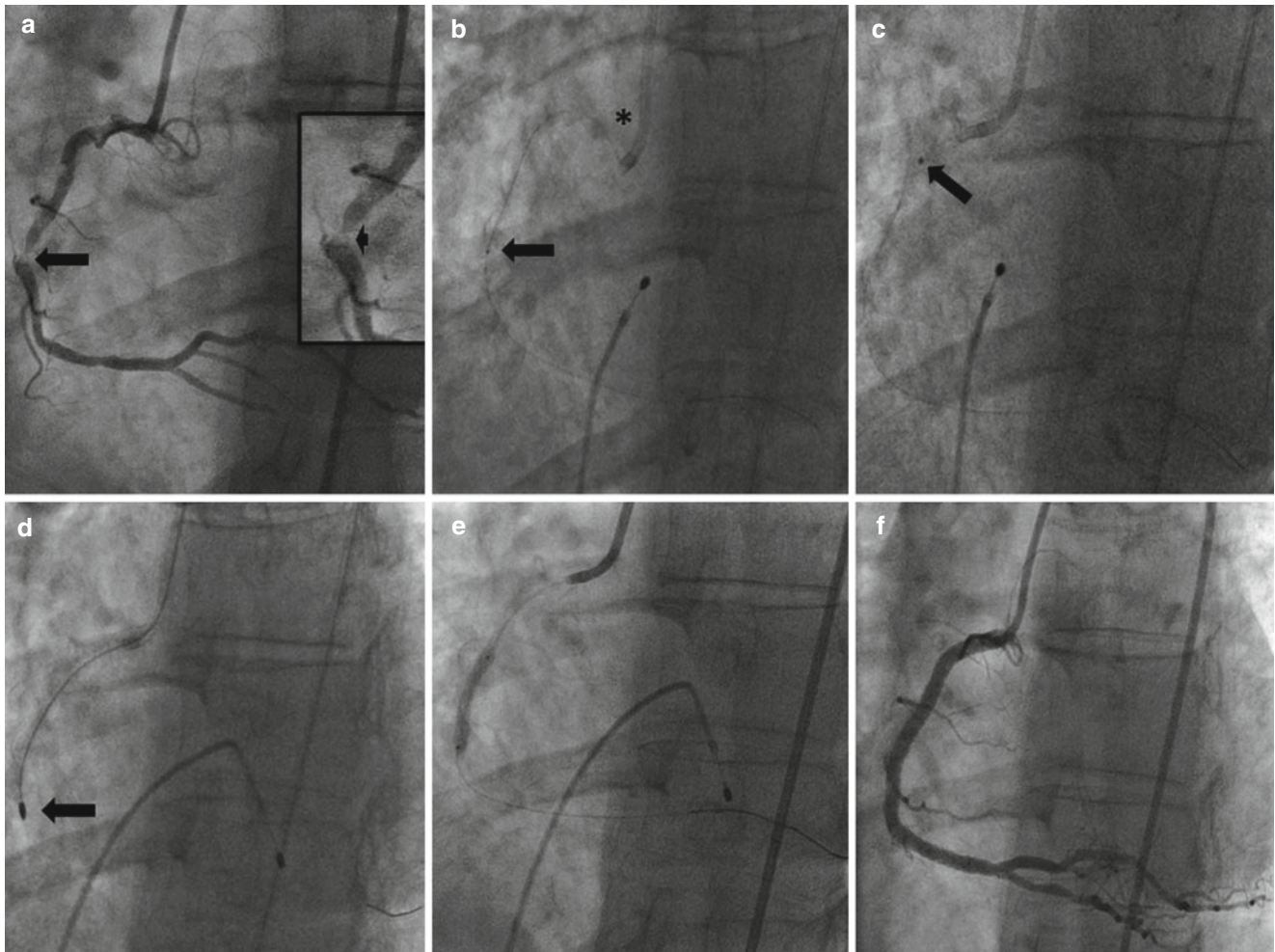


Fig. 3.13 Refer to case 10. (a) A calcified RCA stenosis is seen (arrow) which can be appreciated in greater detail in the inset (arrow head). (b) A Finecross™ catheter cannot cross the lesion (arrow) and

causes the guide catheter to back out (asterisk). (c) A 0.9 mm X-80 ELCA catheter is seen. (d) A 1.5 mm rotablation catheter is seen. (E) Successful balloon pre-dilatation of the lesion. (f) Final stent result

which were post-dilated with a 3.75×20 mm non-compliant balloon to ensure maximal stent expansion.

Balloon Failure Coronary Lesions with TIMI 0 Distal Flow (CTO) Requiring Combined Use of ELCA and RA – ‘RASER’ Cases

Case 11 (Fig. 3.14)

A 67-year old male underwent PCI to his RCA at our centre for ongoing angina refractory to OMT. His echocardiogram had revealed good left ventricular systolic function and a cardiac MRI had revealed a significant burden of ischemia in the inferior left ventricular wall. A 7 F AL0.75 guide catheter was engaged into the RCA while a JL3.5 catheter was engaged into the LMS artery for retrograde contrast injections via the RFA and RRA approach respectively. The site of the occlusion was located in the proximal RCA. The proximal

cap was tapered with no bridging collaterals with moderate ring of calcification within the vessel wall. The distal RCA was collateralised from the LAD via grade 2 collateral channels and the J-CTO score of the lesion was calculated as 4 [6, 41]. A CrossBoss™ device (Boston Scientific, Natick, MA, USA) was used to cross the lesion and a Pilot 200™ wire was advanced distally into the RCA. Following this, an Apex™ 2.5×20 mm balloon would not cross the lesion. Subsequently, a Tornus™ microcatheter followed by a 1.2×12 mm Mini Trek™ balloon were used in an attempt to cross the lesion but they proved unsuccessful. Subsequently, ELCA was utilized with a 0.9 mm X-80 catheter and delivered 3200 pulses (5 trains) of 80 mJ/mm^2 at 80 Hz for 40 s. This allowed the aforementioned balloons to cross the CTO. However, in the proximal RCA, a non-dilatable lesion was identified secondary to ring calcification. It was necessary then to perform RA to the non-dilatable lesion using a 1.75 mm burr. The RA burr successfully debulked the non-dilatable lesion and the

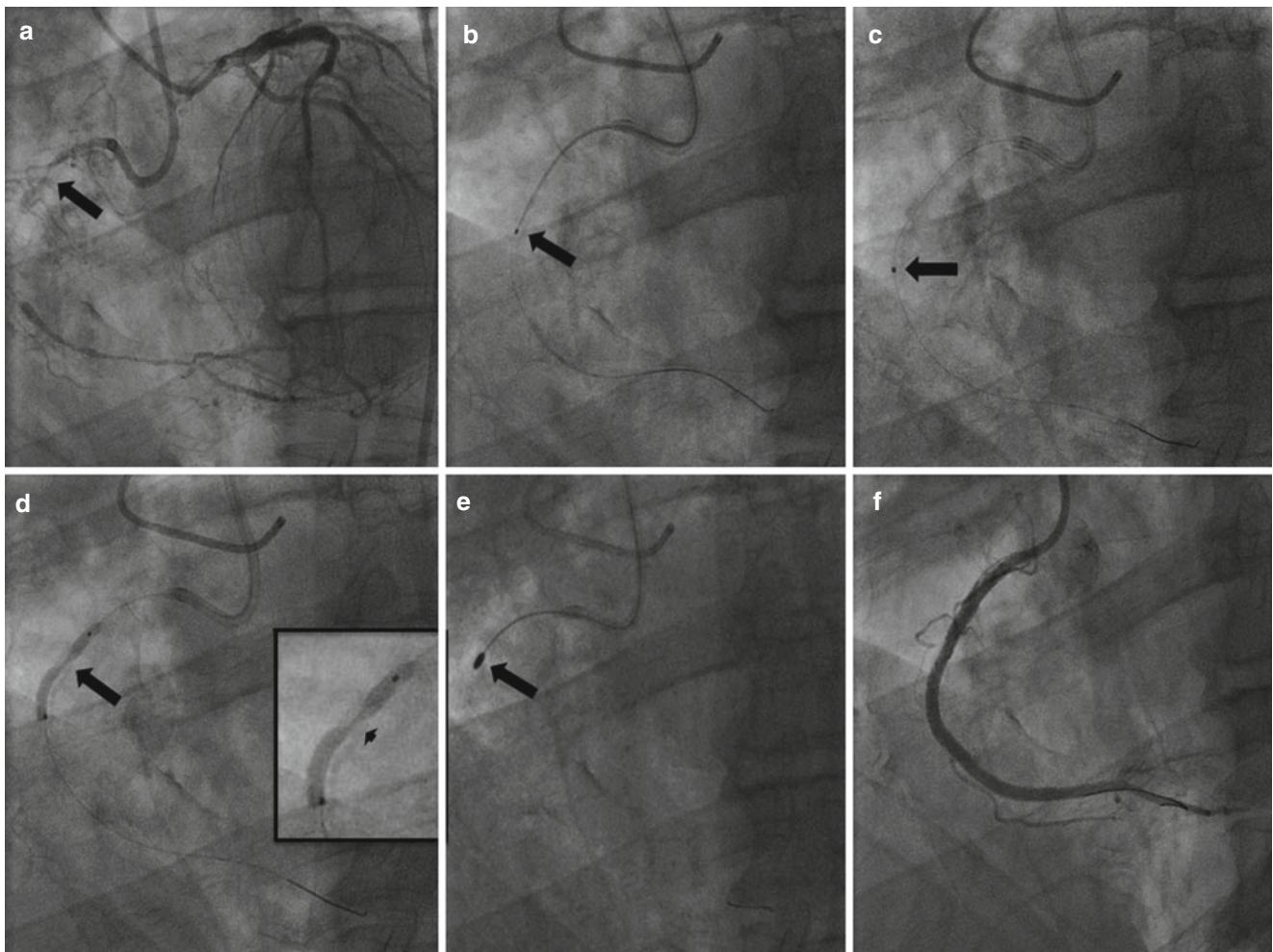


Fig. 3.14 Refer to case 11. (a) A CTO in the RCA is seen. (b) A Cross Boss™ device is seen. (c) A 0.9 mm X-80 ELCA catheter is seen. (d) A non-dilatable lesion is seen with incomplete balloon expansion (arrow)

with a magnified view in the inset (arrow head). (e) A 1.75 mm rotablator burr is seen. (f) Final stent result

artery was pre-dilated with a 2.5×20 mm Apex™ balloon. The RCA was reconstructed using five DES (2.5×18 mm, 3.0×36 mm, 3.5×33 mm and 4.0×28 mm Biomatrix™ as well as a 3.0×12 Promus Element™ stent). The stents were post-dilated using 3.0×20 , 3.5×20 and 4.0×20 mm non-compliant balloons to complete the case.

Case 12 (Fig. 3.15)

A 74-year old male was admitted with acute dyspnoea and heart failure. He had been a life-long smoker, suffered from intermittent claudication and had had a transient ischaemic attack in the past. A chest X-ray had confirmed pulmonary edema and an echocardiogram revealed severe left ventricular impairment with a thin and akinetic inferior left ventricular wall. The left ventricular ejection fraction was calculated as 10 %. He required aggressive intravenous diuretics to stabilise him with the use of inotropic agents. He remained in CCS class IV angina which was only controlled with a

continuous intra-venous nitrate infusion. CAG revealed an occluded RCA with a heavily calcified, sub-totally LAD and minor atheroma in a non-dominant LCX artery. Given the refractory angina and heart failure it was felt that there was no option but to revascularise the LAD territory. Cardiac Magnetic Resonance Imaging (MRI) revealed that the anterior wall was the only viable territory. With such significant LV systolic impairment, the risks for CABG were deemed unacceptably high and following a multi-disciplinary team (MDT) assessment and keeping in view patient's views, a plan was formulated to perform PCI on the LAD with haemodynamic support provided by an Impella™ (Abiomed Inc, Danvers, MA, USA) device [42]. Arterial access was gained via the RRA and LFA using 6 F and 14 F sheaths respectively. There was a severe stenosis in the common iliac artery which required balloon angioplasty to allow the passage of further equipment. The Impella™ device was advanced across the aortic valve and placed within the left

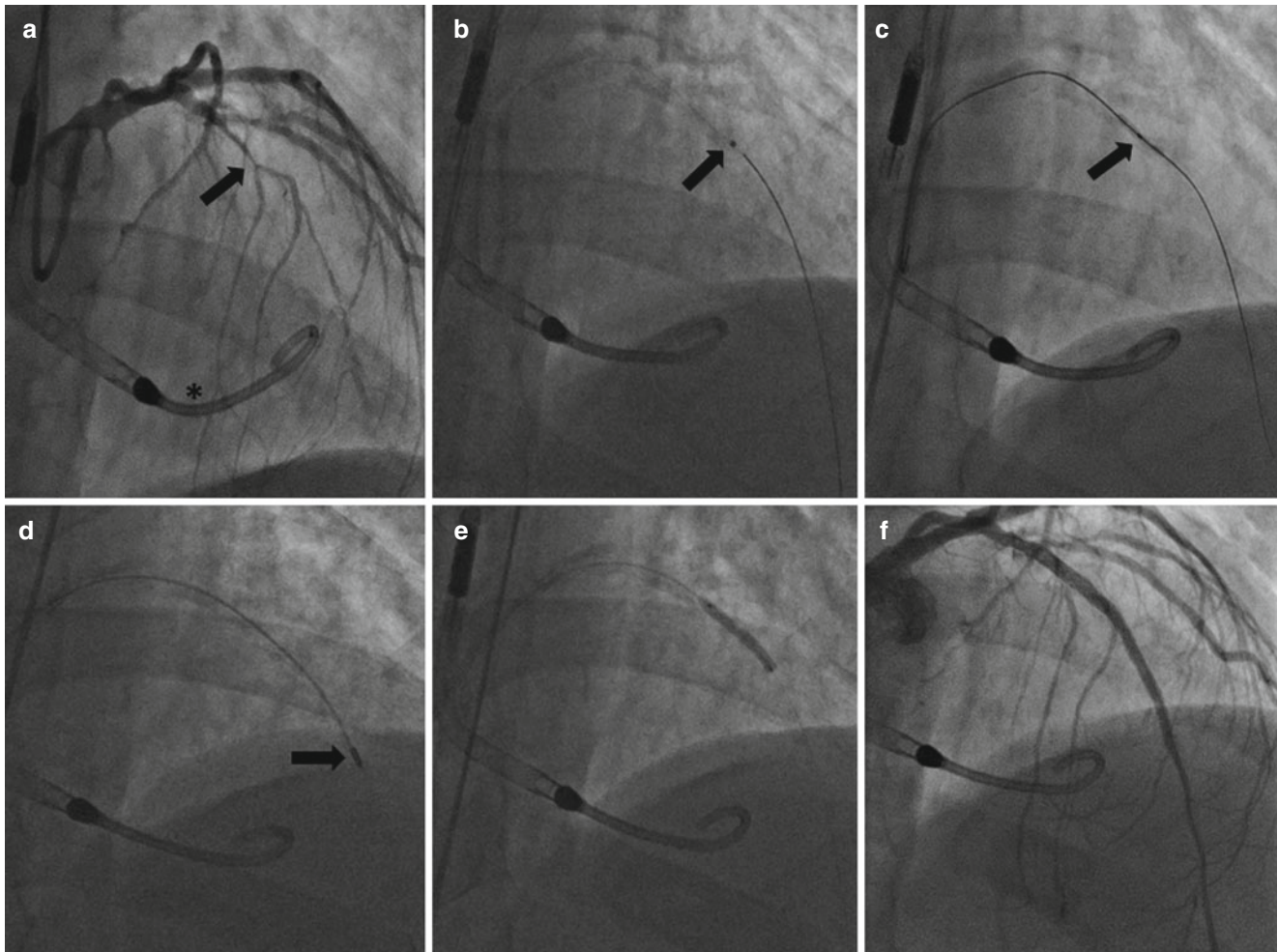


Fig. 3.15 Refer to case 12. (a) An LAD CTO is seen (*arrow*) with an Impella™ also visualised in the background (*asterisk*). (b) A 0.9 mm X-80 ELCA catheter is seen. (c) Balloon failure is seen as a 1.1×10 mm

balloon fails to expand (*arrow*). (d) A 1.25 mm rotablation burr is seen (*arrow*). (e) Successful balloon dilatation. (f) Final stent result

ventricle to increase cardiac output. The LMS artery was engaged using a 6 F EBU3.5 guide catheter and a Fielder XT™ guide wire was advanced distally into the LAD. However, a microcatheter (Finecross™ or Corsair™) could not be advanced beyond the lesion to facilitate wire exchange for a RotaWire™. In consequence, ELCA was performed with a 0.9 mm X80 catheter and delivered 14,016 pulses (18 trains) of 80 mJ/mm^2 at 80 Hz for a duration of 2:53 min. Subsequently, the Finecross™ catheter was advanced distally into the LAD and the Fielder XT™ wire was exchanged for a RotaWire™ as a 2.5×15 mm, 1.5×15 mm and 1.1×10 mm balloons could not be fully expanded. A 1.25 mm RA burr was used for RA which took several minutes as the lesion proved very resistant. Of note, despite the use of an Impella™ device, the patient had a systolic blood pressure of 40 mmHg during RA which recovered as soon as it stopped. With the help of a Grandslam™ buddy wire (Asahi Intecc, Aichi, Japan) we were able to deliver a 2.5×20 mm balloon into the LAD which could be fully

expanded. Finally, three DES were delivered into the LAD (Promus Element™, 2.25×12 mm, 2.5×28 mm and 2.75×24 mm) with an excellent angiographic result. The Impella™ device was successfully removed and the LFA puncture was secured by a vascular surgical colleague. The patient was alive with no further cardiac events, 24 months following the successful procedure.

Under-Expanded Stents Treated with ELCA Either Alone or in Combination with Other Techniques Including RA

Case 13 (Fig. 3.16)

A 54-year old male underwent primary PCI to his LAD at his local hospital for an anterior ST-elevation myocardial infarction. There was a strong family history of premature coronary disease. A BMW™ wire was advanced successfully across the occlusion into the LAD. Following manual throm-

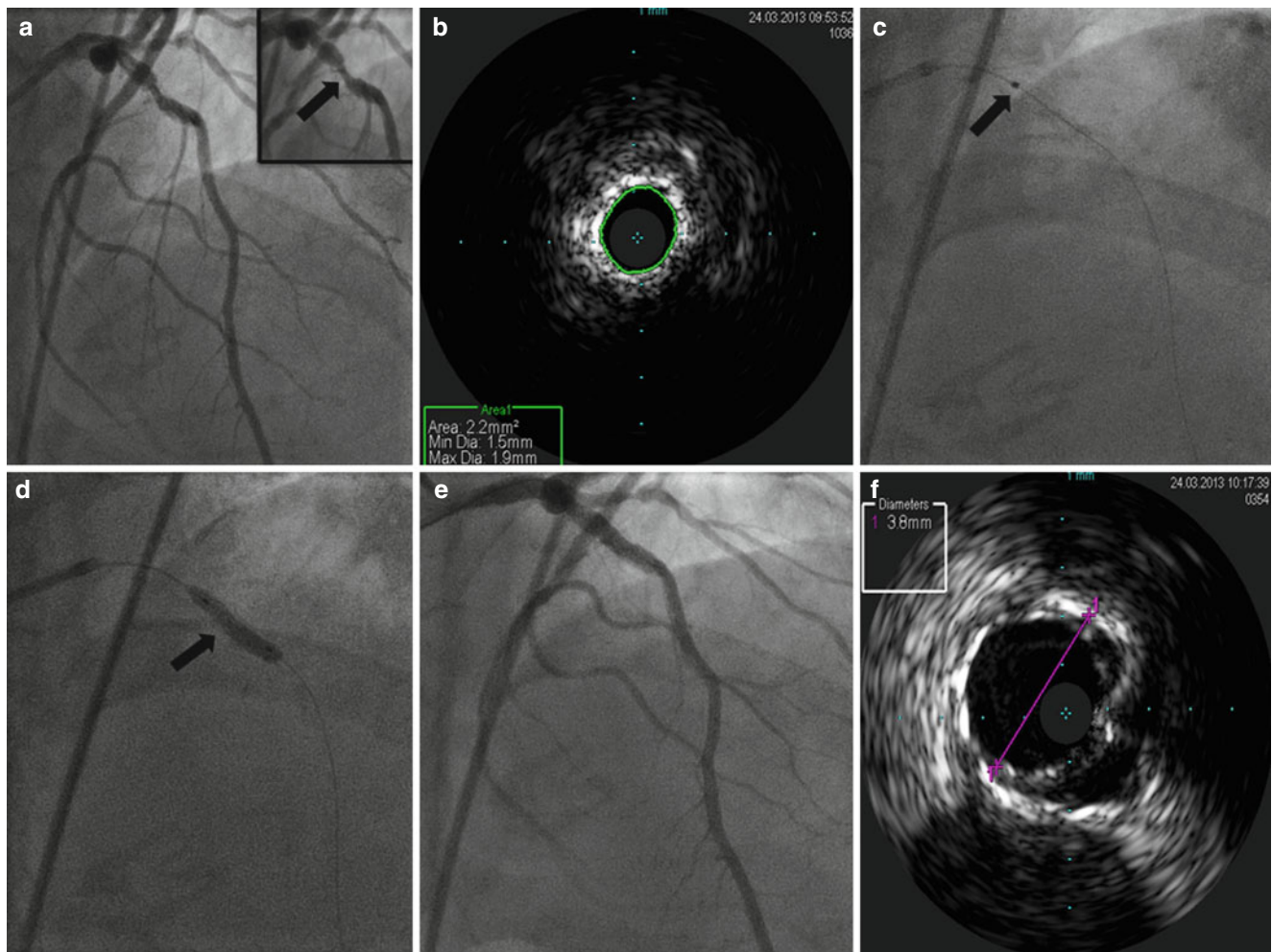


Fig. 3.16 Refer to case 13. (a) An under expanded stent is seen in the proximal LAD which has been magnified in the inset (*arrow*). (b) IVUS assessment reveals the stent to be severely under expanded with

an MLS of 2.2 mm². (c) A 0.9 mm X-80 ELCA catheter is seen (*arrow*). (d) Successful balloon dilatation. (e) Final angiographic result. (f) Final IVUS assessment with a luminal diameter of 3.8 mm

bectomy, it appeared that the lesion was moderately calcified. The lesion was pre-dilated with a 2.0 × 15 mm Maverick™ balloon following which a 2.75 × 18 mm Xience™ DES (Medtronic, Interventional Vascular, CA, USA) was deployed. It was quite clear that the stent was under expanded. Subsequently, the stent was post-dilated with 3.0 × 15 mm, 3.0 × 8 mm and 3.25 × 8 mm non-compliant balloons at 20 atmospheres for up to 30 s. Despite these measures, the mid-stent section remained under expanded significantly. The patient was then transferred to our unit for consideration of ELCA. A trans-femoral approach was undertaken to maximise guide catheter support and the LMS artery was engaged with a 6 F EBU 3.5 guide catheter. A BMW™ wire was advanced into the distal LAD following which we performed IVUS which demonstrated that the minimal stent luminal area was 2.2 mm² with an internal stent diameter of 1.9 mm. Furthermore, we were able to visualise on IVUS that there was a significant amount

of fibro-calcific tissue which was restricting stent expansion. ELCA was used with 5200 laser pulses (7 trains) of 80 mJ/mm² at 80 Hz for a duration of 64 s using a 0.9 mm X-80 laser catheter. Following this, we were able to dilate the under-expanded stent using sequential non-compliant balloons (3.0 × 15 mm and 3.5 × 12 mm). However, a repeat IVUS scan demonstrated that the original stent was severely under-sized as the luminal diameter of the LAD was 4.0 mm. Therefore, we deployed a 3.5 × 14 mm Biomatrix™ DES at 14 atmospheres with an excellent final angiographic result.

Case 14 (Fig. 3.17)

An 80-year old male was treated with PCI to his proximal LAD at our centre for CCS class II stable angina despite being on OMT. His cardiovascular risk factors included dyslipidaemia and hypertension. Furthermore, an echocardiogram had revealed good left ventricular systolic function. The RCA and LCX arteries had mild atheroma only. The

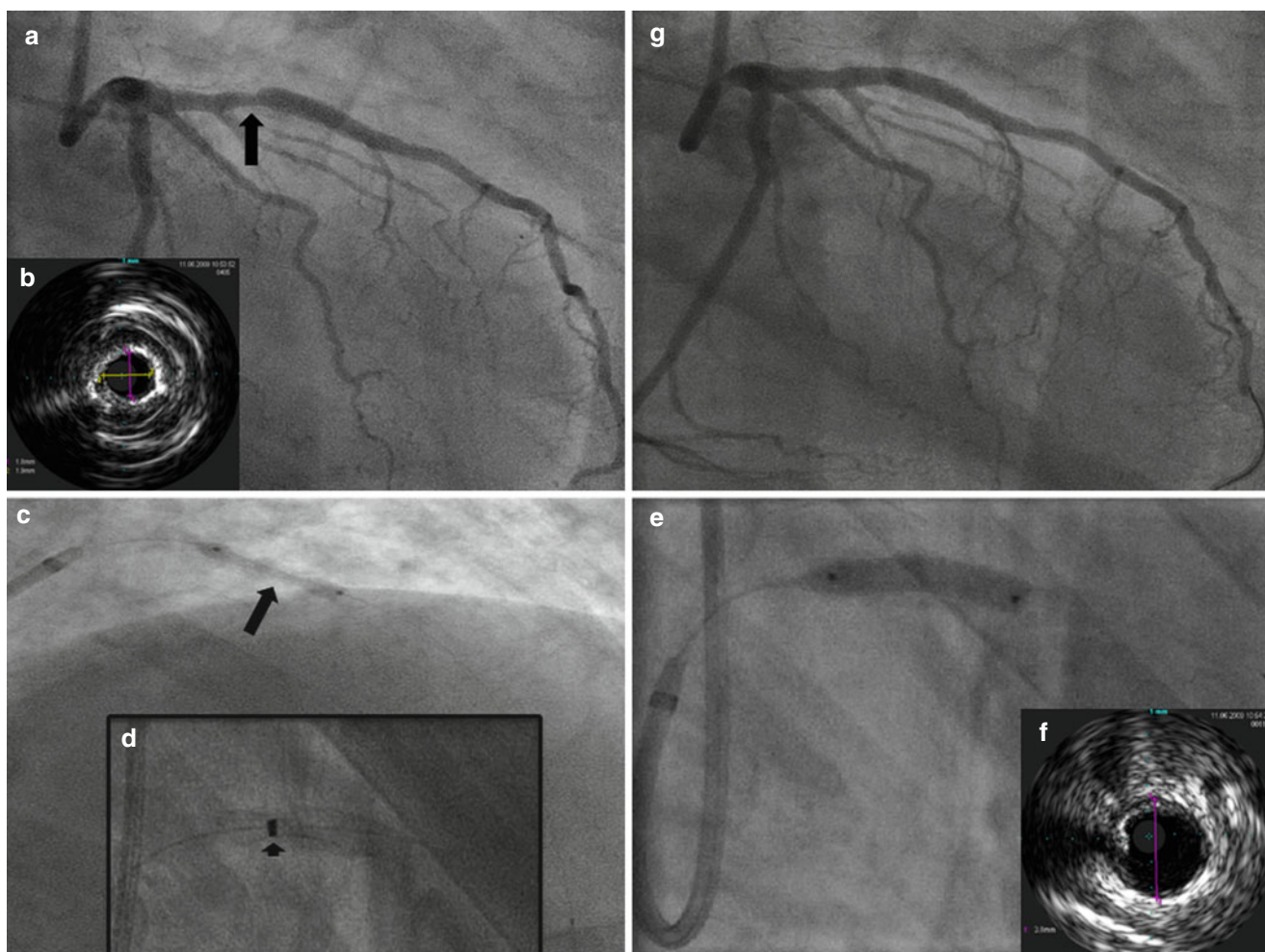


Fig. 3.17 Refer to case 14. (a) An under expanded stent is visualised in the proximal LAD (*arrow*). (b) IVUS demonstrating an under expanded stent. (c) Demonstrates balloon failure in the LAD following RA prior to stent deployment (*arrow*). (d) A 2.0 mm ELCA catheter is

seen within the stent (*arrow head*). (e) Successful balloon dilatation with a 4.25 × 10 mm balloon. (f) Post-laser IVUS shows a well expanded stent. (g) Final stent result

proximal LAD was heavily calcified and had a severe stenosis which had a fractional flow reserve of 0.80. It was decided to debulk the LAD lesion using RA prior to stent insertion. The LMS artery was engaged using an 8 F EBU3.5 guide catheter. A Luge™ wire was advanced distally into the LAD which was exchanged to a RotaWire™ using a Finecross™ microcatheter. Subsequently, a 1.75 mm rotablation burr was used to debulk the LAD stenosis for 90 s. However, the lesion was non dilatatable with a 3.0 × 20 mm non compliant balloon. Following this, further RA was delivered using a 2.0 mm burr for a further 90 s. The RotaWire™ was then exchanged with a Luge™ wire and the lesion was pre-dilated with 3.0 × 20 mm and 3.25 × 20 mm non-compliant balloons followed by a 3.5 × 10 mm Flexotome™ cutting balloon. Although there was evidence of balloon under expansion, it was felt that the lesion had been adequately debulked and more importantly, there was a localised dissection which necessitated the need to deliver two overlapping 3.5 × 22 mm

and 3.5 × 13 mm Titan 2™ stents. Despite use of non-compliant balloons for post-dilatation (3.5 × 20 mm and 3.75 × 20 mm) it was evident that there was a distinct area of stent under-expansion which corresponded to a focal ring of calcification on IVUS. As the patient remained stable, it was decided to stop the case and to treat the area of stent under expansion at a subsequent date. Two weeks later, the patient was readmitted electively as a day-case to undergo ELCA to his under-expanded stent. The LMS artery was engaged using an 8 F EBU3.5 guide catheter. A BMW wire was advanced distally into the LAD and IVUS assessment of the under-expanded section revealed a minimal luminal area of 2.5 mm². A 2.0 mm laser catheter was initially used to deliver 4500 laser pulses (20 trains) of 60 mJ/mm² at 40 Hz. However, it was noted that the 2.0 mm laser catheter was not advancing beyond the under expanded stent section and hence a 0.9 mm X-80 laser catheter was used. An additional 5000 pulses (12 trains) of 80 mJ/mm² at 80 Hz were delivered

with a total laser time of 3:15 min. Finally, the stent was post-dilated with a 3.75 × 20 mm non-compliant balloon with satisfactory stent expansion visualised on CAG and with IVUS assessment to finish the case.

Conclusion

Fibro-calcific lesions often create problems during PCI by restricting passage of pre-dilatation balloons or micro-catheters for wire exchange when rotational atherectomy is being contemplated. In these situations ELCA has a definitive role in safely debulking lesions to ensure sufficient plaque modification to permit balloon dilation or Rotawire delivery to maximise PCI success. In addition, interventional cardiologists may encounter balloon failure when lesions are non-dilatable and where aggressive high pressure balloon dilatation may be hazardous for perforation whilst inadequately prepared lesions may lead to under-expanded stents in the coronary stents; a harbinger of potential catastrophe. In our experience of non-dilatable lesions, ELCA can also be successfully and effectively utilised even when the lesion is within a CTO or in the situation of an under-expanded stent.

We hope that the aforementioned case-based examples will help educate the reader in selecting suitable cases for ELCA delivery in complex coronary disease and using this device with confidence and success.

References

- National population projections 2010-based statistical bulletin. London: Office for National Statistics. 2011. Available from: http://www.ons.gov.uk/ons/dcp171778_235886.pdf.
- Rana O, Moran R, O'Kane P, Boyd S, Swallow R, Talwar S, et al. Percutaneous coronary intervention in the very elderly (≥85 years): trends and outcomes. *Br J Cardiol*. 2013;20:27–31.
- Fernandez JP, Hobson AR, McKenzie D, Shah N, Sinha M, Wells TA, Levy T, Swallow R, Talwar S, O'Kane P. Beyond the balloon: excimer coronary laser atherectomy used alone or in combination with rotational atherectomy in the treatment of chronic total occlusions, non-crossable and non-expandable coronary lesions. *EuroIntervention*. 2013;9:243–50.
- Spratt J, Lombardi W. Chronic total occlusion percutaneous coronary intervention as mainstem therapy: are we at a tipping point? *Interv Cardiol*. 2013;5:481–4.
- Patel VG, Brayton KM, Tamayo A, Mogabgab O, Michael TT, Lo N, et al. Angiographic success and procedural complications in patients undergoing percutaneous coronary chronic total occlusion interventions. *J Am Coll Cardiol Interv*. 2013;6:128–36.
- Morino Y, Abe M, Morimoto T, Kimura T, Hayashi Y, Muramatsu Y, et al. Predicting successful guidewire crossing through chronic total occlusion of native coronary lesions within 30 minutes: the J-CTO (multicentre CTO registry in Japan) score as a difficulty grading and time assessment tool. *J Am Coll Cardiol Interv*. 2011;4: 213–21.
- Whitlow P, Burke NM, Lombardi WL, Wyman MR, Moses JW, Brilakis ES, et al. Use of a novel crossing and re-entry system in coronary chronic total occlusions that have failed standard crossing techniques: results of the FAST-CTOs (facilitated antegrade steering technique in chronic total occlusions) trial. *J Am Coll Cardiol Interv*. 2012;5:393–401.
- Karpaliotis D, Micheal TT, Brilakis ES, Papayannis AC, Tran DL, Kirkland BL, et al. Retrograde coronary chronic total occlusion revascularization: procedural and in-hospital outcomes from a multicentre registry in the United States. *J Am Coll Cardiol Interv*. 2012;5:1273–9.
- Prati F, Di Mario C, Moussa I, Reimers B, Mallus MT, Parma A, et al. In-stent neointimal proliferation correlates with the amount of residual plaque burden outside the stent: an intravascular study. *Circulation*. 1999;99:1011–4.
- MacIsaac AI, Bass TA, Buchbinder M, Cowley MJ, Leon MB, Warth DC, et al. High speed rotational atherectomy: outcome in calcified and noncalcified coronary artery lesions. *J Am Coll Cardiol*. 1995;26:731–6.
- Wei-Hsian Y. Rotational atherectomy: an update. *J Geriatr Cardiol*. 2013;10:211–2.
- Barbato E, Colombo A, Heyndrickx GY. Rotational atherectomy. In: Eeckhout E, Serruys PW, Wijns W, Vahanian A, Sambeek MV, De Palma R, editors. *Percutaneous interventional cardiovascular medicine. The PCR-EAPCI textbook*, vol. II. 1st ed. 2012; Minneapolis: Cardiotext Publishing.
- Rathore S, Matsuo H, Terashima M, Kinoshita Y, Kimura M, Tsuchikane E, et al. Rotational atherectomy for fibro-calcific coronary artery disease in drug eluting stent era: procedural outcomes and angiographic follow-up results. *Catheter Cardiovasc Interv*. 2010;75:919–27.
- Khattab AA, Otto A, Hochadel M, Toelg R, Geist V, Richardt G. Drug-eluting stents versus bare metal stents following rotational atherectomy for heavily calcified coronary lesions: late angiographic and clinical follow-up results. *J Interv Cardiol*. 2007;20:100–6.
- Furuichi S, Sangiorgi G, Godino C, Airoldi F, Montorfano M, Chieffo A, et al. Rotational atherectomy followed by drug-eluting stent implantation in calcified coronary lesions. *EuroIntervention*. 2009;5:370–4.
- Chiang M-H, Yi H-T, Tsao C-R, Chang W-C, Su C-S, Liu T-J, et al. Rotablation in the treatment of high-risk patients with heavily calcified left-main coronary lesions. *J Geriatr Cardiol*. 2013;10:217–25.
- Sambu N, Fernandez J, Shah NC, O'Kane P. The guideliner®: an interventionist's experience of their first 50 cases: 'the mostly good, rarely bad, beware of the ugly!'. *Interv Cardiol*. 2013;5:389–404.
- Asakura Y, Furukawa Y, Ishikawa S, Asakura K, Sueyoshi K, Sakamoto M, et al. Successful predilatation of a resistant, heavily calcified lesion with cutting balloon for coronary stenting: a case report. *Cathet Cardiovasc Diagn*. 1998;44:420–2.
- Karvouni E, Stankovic G, Albiero R, Takagi T, Corvaja N, Vaghetti M, et al. Cutting balloon angioplasty for treatment of calcified coronary lesions. *Catheter Cardiovasc Interv*. 2001;54:473–81.
- Fernandez JP, Hobson AR, Mckenzie DB, Talwar S, O'Kane P. How should I treat severe calcific coronary artery disease. *EuroIntervention*. 2011;7:400–7.
- Fang HY, Fang CY, Hussein H, Hsueh SK, Yang CH, Chen CJ, et al. Can a penetration catheter (Tornus) substitute traditional rotational atherectomy for recanalizing chronic total occlusions? *In Heart J*. 2010;51:147–52.
- Bilodeau L, Fretz EB, Taeymans Y, Koolen J, Taylor K, Hilton DJ. Novel use of a high-energy excimer laser catheter for calcified and complex coronary artery lesions. *Catheter Cardiovasc Interv*. 2004;62:155–61.
- Israel DH, Marmur JD, Sanborn TA. Excimer laser-facilitated balloon angioplasty of a nondilatable lesion. *J Am Coll Cardiol*. 1991;18:1118–9.
- Ahmed WH, Al-Anazi MM, Bittl JA. Excimer laser-facilitated angioplasty for undilatable coronary narrowings: study of 39 patients from the percutaneous excimer laser coronary angioplasty

- (PELCA) multicentre registry in the PTCA balloon failure to cross or dilate indication. *Am J Cardiol.* 1996;78:1045–7.
25. Shen ZJ, García-García HM, Schultz C, van der Ent M, Serruys PW. Crossing of a calcified “balloon uncrossable” coronary chronic total occlusion facilitated by a laser catheter: a case report and review recent four years’ experience at the thoraxcenter. *Int J Cardiol.* 2010;145:251–4.
 26. Topaz O, Das T, Dahm JB, Madynoon H, Perin E, Ebersole D. Excimer laser revascularisation: current indications, applications and techniques. *Lasers Med Sci.* 2001;16:72–7.
 27. O’Kane P, Redwood S. Laser. In: Redwood S, Curzen N, Thomas M, editors. *Oxford textbook of interventional cardiology.* 1st ed. 2010; Kettering, Northants: Oxford University Press.
 28. Haude M, Papalexandris M, Degen H. Laser therapy. In: Eeckhout E, Serruys PW, Wijns W, Vahanian A, Sambeek MV, De Palma R, editors. *Percutaneous interventional cardiovascular medicine. The PCR-EAPCI textbook, vol. II.* 1st ed. 2012; Minneapolis: Cardiotext Publishing.
 29. Topaz O. Laser for CTO recanalization. In: Waksman R, Saito S, editors. *Chronic total occlusions.* 2nd ed. 2013; Hoboken: Wiley-Blackwell Publishers.
 30. McKenzie DB, Talwar S, Jokhi PP, O’Kane P. How should I treat severe coronary artery calcification when it is not possible to dilate a balloon or deliver a RotaWire™? *EuroIntervention.* 2011;6:779–83.
 31. Topaz O. On the hostile massive thrombus and means to eradicate it. *Catheter Cardiovasc Intervent.* 2005;65:280–1.
 32. Topaz O, Minisi AJ, Bernardo NL, McPherson RA, Martin E, Carr SL, et al. Alteration of platelet aggregation kinetics with ultraviolet emission: the stunned platelet phenomenon. *Thromb Haemost.* 2001;86:1087–93.
 33. Bittl JA, Ryan Jr TJ, Keaney Jr JF, Tchong JE, Ellis SG, Isner JM, et al. The percutaneous excimer laser coronary angioplasty registry. Coronary artery perforation during excimer laser coronary angioplasty. *J Am Coll Cardiol.* 1993;21:1158–65.
 34. Deckelbaum LI, Natarajan MK, Bittl JA, Rohlf K, Scott J, Chisholm R, et al. Effect of intracoronary saline infusion on dissection during excimer laser coronary angioplasty: a randomized trial. The percutaneous excimer laser angioplasty (PELCA) investigators. *J Am Coll Cardiol.* 1995;26:1264–9.
 35. Badr S, Ben-Dor I, Dvir D, Barbash IM, Kitabata H, Minha S, et al. The state of the excimer laser for coronary intervention in the drug-eluting stent era. *Cardiovasc Revasc Med.* 2013;14:93–8.
 36. Fracassi F, Roberto M, Niccoli G. Current interventional coronary applications of excimer laser. *Expert Rev Med Devices.* 2013;10:541–9.
 37. Taylor K, Harlan K, Branam B. Small 0.7 mm diameter laser catheter for chronic total occlusions, small vessels, tortuous anatomy, and balloon-resistant lesions – development and initial experience. *Eurointervention.* 2006;2:265–9.
 38. Ellis SG, Ajluni S, Arnold AZ, Popma JJ, Bittl JA, Eigler NL, et al. Increased coronary perforation in the new device era: incidence, classification, management, and outcome. *Circulation.* 1994;90:2725–30.
 39. Lam SC, Bertog S, Sievert H. Excimer laser in management of underexpansion of a newly deployed coronary stent. *Catheter Cardiovasc Interv.* 2014;83(1):E64–8.
 40. Latib A, Takagi K, Chizzola G, Tobis J, Ambosini V, Niccoli G, et al. Excimer laser lesion modification to expand non-dilatable stents: the ELLEMENT registry. *Cardiovasc Revasc Med.* 2014;15(1):8–12.
 41. Werner GS, Ferrari M, Heinke S, Kueth F, Surber R, Richartz BM, et al. Angiographic assessment of collateral connections in comparison with invasively determined collateral function in chronic coronary occlusions. *Circulation.* 2001;107:1972–7.
 42. Dixon SR, Henriques JP, Mauri L, Sjaauw K, Civitello A, Kar B, et al. A prospective feasibility trial investigating the use of the impella 2.5 system in patients undergoing high-risk percutaneous coronary intervention (the protect I trial): initial U.S. experience. *J Am Coll Cardiol Interv.* 2009;2:91–6.

On Topaz and Allyne Topaz

Background

Atherosclerotic coronary plaque rupture and subsequent thrombus formation are the main pathophysiologic processes that account for acute myocardial infarction (AMI). Primary percutaneous coronary intervention (PCI) is the contemporary optimal reperfusion therapy for management of AMI, especially in patients presenting with either STEMI (S-T Elevation Myocardial Infarction) or with evolving non-STEMI (NSTEMI) and those requiring rescue intervention post failure of initial administration of thrombolytic agents [1, 2]. A PCI based AMI revascularization reduces the rate of death, stroke and re-infarction when compared with the long standing strategy that relied on select fibrinolytic agents as the first line therapy [3]. However, while many lesions treated by PCI in AMI require only standard balloons and stents, a complex morphology of the offensive plaque, especially with thrombotic content, frequently necessitates a dedicated lesion-specific approach [4]. This calls for utilization of specific devices that provide adequate plaque debulking and thrombus extraction [4, 5] and facilitate resistant-free delivery and precise deployment of intracoronary stents [5–7]. Hence, laser offers a reliable, user-friendly technology which has been successfully applied in select AMI patients. The treatment targets include atherosclerotic and thrombotic plaques, in-stent restenosis and chronic total occlusions occupying infarct related vessels such as coronary arteries and degenerated saphenous vein bypass grafts [8]. When optimal thrombus removal during PCI for AMI mandates

incorporation of mechanical thrombectomy devices [9, 10], the laser energy becomes a valid option as lasers are recognized for their dual capabilities of performing simultaneously precision plaque debulking and thrombus removal [11–13]. Altogether, this chapter aims to provide comprehensive report on the vast experience which had been gained with the use of laser during AMI interventions along the last two decades. It reviews the current criteria for use of the laser, describes the catheter technology, comments on the effective and safe lasing techniques and presents analysis of the results of pivotal clinical laser studies.

The Evolution of Laser Revascularization in AMI

The introduction of laser for PCI in AMI was initially reported in 1993 when a mid-infrared, solid-state, pulse-wave holmium: YAG (2.1 μm wave length) was first used by Eduardo de Marchena and colleagues in three patients at the Jackson Memorial Medical center of the University of Miami, Florida [14]. Another early experience in nine patients who sustained complicated AMI and needed urgent percutaneous intervention was reported by interventionalists from the St. Paul Ramsey hospital of the University of Minnesota [12]. Successful revascularization and excellent clinical outcome were observed in that small series of patients. The issue of proper lasing technique during revascularization for AMI cannot be underestimated. Noteworthy, in the early experience with coronary laser angioplasty, the recommended lasing technique relied upon rapid catheter advancement and continuous energy delivery mode of energy. Over time however, operators began to realize that this method frequently induced vessel and plaque complications. Thus, the technique was subsequently replaced to incorporate slow catheter advancement and intermittent lasing emission [15]. This modification reduced the rate and scope of laser related complications, and, consequently, enabled further exploration of the use of laser [mainly the

O. Topaz, MD, FACC, FACP, FSCAI (✉)
Professor of Medicine, Duke University School of Medicine,
Director, Interventional Cardiology, Chief, Division of Cardiology,
Charles George Veterans Affairs Medical Center,
1100 Tunnel Road, Asheville, NC 28805, USA
e-mail: on.topaz@va.gov

A. Topaz, MD
Department of Emergency Medicine, Hackensack University
Medical Center, 30 Prospect Ave., Hackensack, NJ 07601, USA
e-mail: topazax@gmail.com

dye, holmium:YAG and xenon chloride] in urgent percutaneous AMI revascularization covering the entire spectrum of acute ischemic coronary syndromes [16, 17]. To date, this technique remains safe and efficacious in coronary and peripheral applications alike.

Noteworthy, both the dye and the Holmium: YAG mid-infrared wavelength lasers were considered reliable revascularization tools [18, 19], however, they are no longer in common use in the US. The ultraviolet 308 nm excimer laser [CVX-300, Spectranetics, Colorado Springs, Colorado, US] thus remains the dominant system wavelength available for cardiovascular interventions in the US and globally. This laser is FDA approved [for physician's discretionary use] in acute coronary syndromes such as unstable angina (Fig. 4.1), the STEMI (Figs. 4.2, 4.3, and 4.4) and the non STEMI type of AMI (Figs. 4.5 and 4.6) [8, 20, 21]. Currently, the excimer laser enables AMI revascularization for targeted thrombus and plaque debulking in native coronary arteries and old saphenous vein grafts alike [8, 20]. Overall, the excimer laser has been shown as an efficient and safe technology for the treatment of challenging, high risk coronary lesions such as left main stenosis, stent restenosis, ostial lesions, arterial and saphenous vein bypass grafts stenoses and chronic total occlusions [21–23]. Noteworthy, this laser is also used for revascularization in acute, chronic and critical peripheral arterial disease with target lesions located in the superficial femoral, popliteal, subclavian and renal arteries [24]. Table 4.1 summarizes the current clinical and angiographic criteria for utilization of laser in the management of AMI.

Technical Characteristics of Cardiovascular Lasers

The pulsed-wave excimer [Xenon Chloride] laser operates at 308 nm wavelength with a pulse duration of 135 ns and output of 200 mJ/pulse. The laser energy is delivered via either over-the-wire or rapid exchange catheters containing flexible optic fibers. The modern laser catheters have improved fiber array with concentric or eccentric tip configuration [25]. Table 4.2 displays the technologic profile of coronary excimer laser catheters which are used in PCI for AMI.

Experiments with Laser- Tissue Effects Pertinent to PCI for AMI

The excimer laser energy interacts with the nonaqueous components of the atherosclerotic plaque [proteins, nucleic acids]. Absorption within atheromatous plaques and thrombotic material results in initiation of photomechanical and photo-thermal processes that lead to vaporization [26]. Laser activation generates acoustic shock waves which mechanically

break and dissolve fibrin fibers, a major constituent of thrombus [27] and considerably suppresses platelet aggregation [28] (Fig. 4.7). A series of in vitro experiments studied the effect of laser emission on thrombolytics, providing strong evidence that laser energy significantly enhances fibrinolysis in fibrin clots initially treated by t-PA. Moreover, despite the known decline in the rate of t-PA induced fibrinolysis with increasing clot age, application of laser energy results in significant enhancement of fibrinolysis [29]. Table 4.3 describes basic research phenomena related to laser activation and their clinical manifestations as pertaining to revascularization in AMI.

Clinical Outcome of Laser Application in AMI

The last two decades led to growing experience with the utilization of excimer laser for revascularization in stable and unstable angina patients who present with a spectrum of hemodynamic conditions, particularly in AMI [32, 33]. Table 4.4 presents the main findings originating from studies of laser application in AMI. It is well established that patients presenting within the first 2–3 h of STEMI commonly exhibit a less complex plaque morphology and smaller thrombus burden compared to patients arriving late; either 5–6 h or even later arrivals such as 12–24 h after the onset of the AMI. Thus, an intriguing practical question arose as to what would be the effect of laser during *every* stage of evolving AMI. Consequently, investigators set forth to explore the laser outcome not only during the early, acute phase of STEMI but also in later phases of AMI. Accordingly, the pivotal, all-comers CARMEL (Cohort of Acute Revascularization in Myocardial Infarction by Excimer Laser) study was launched [21]. The project entailed an investigator sponsored, international, multicenter study enrolling 151 patients in various stages of evolving AMI who were treated in 8 laser experienced facilities in the US, Canada and Germany. While many of the study's patients presented within the first few hours of STEMI, other patients who were late arrivals (later than 6 h after chest pain onset), patients who failed to respond to thrombolytic agents, those with cardiogenic shock (21 %), and infarct related lesions in degenerated saphenous vein grafts (26 %) were intentionally included to ensure maximal clinical challenge for the laser technology. Thus the intention to enroll *every* type of AMI offered real life representation of different clinical scenarios. This approach contrasted considerably with the more restricted, leading studies of PCI in AMI. To complement the study's high standards, the quantitative and statistical analyses were performed by the independent core laboratories of Stanford university, Palo Alto, California and Duke university, Raleigh, North Carolina, respectively. The baseline angiographic left ventriculography demonstrated left ventricular ejection fraction (LVEF) of 44 ± 13 % (normal >55 %). Then a large proportion (74 %) of

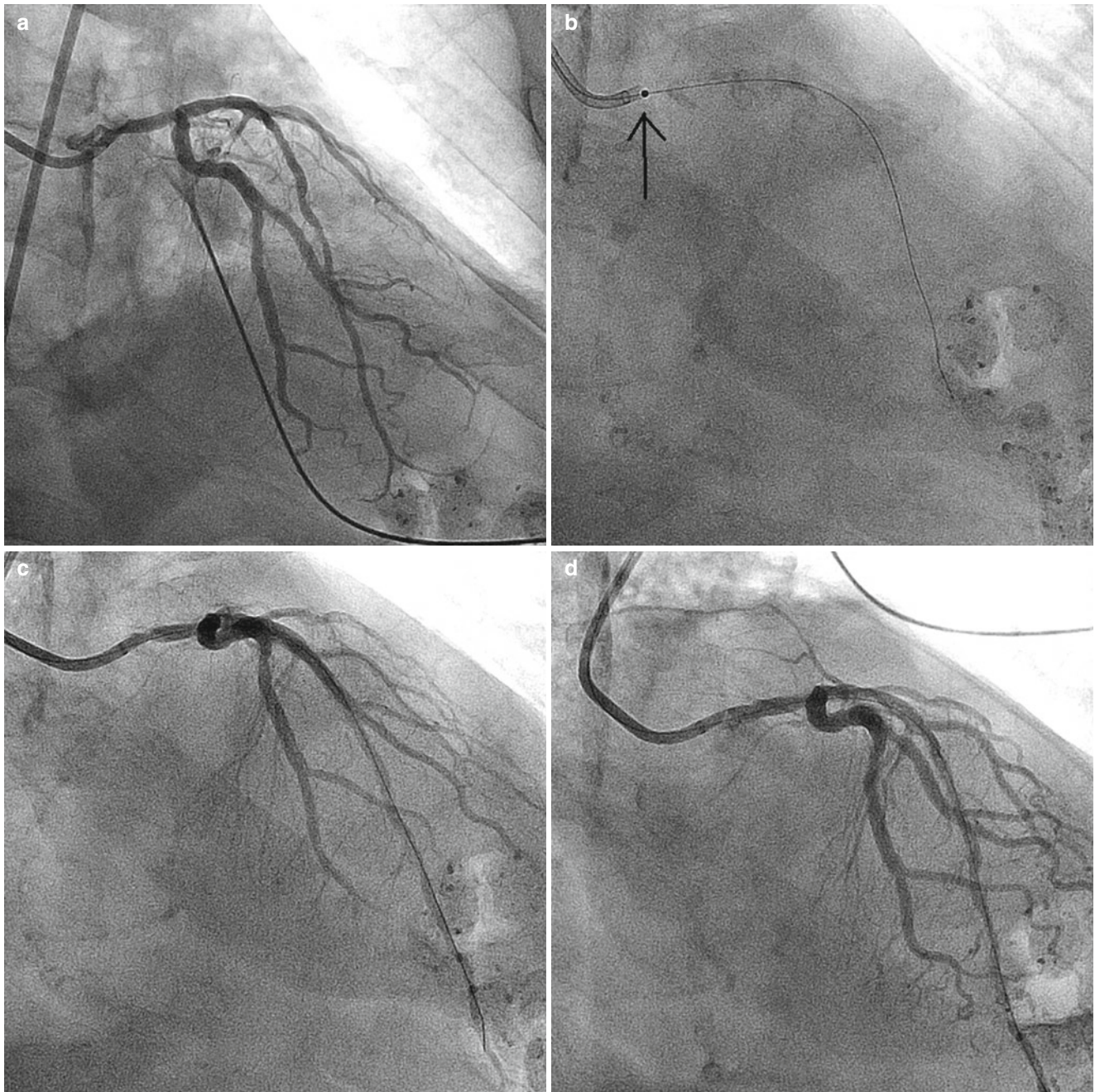


Fig. 4.1 (a) A 90 % eccentric, calcified ostial left main coronary artery stenosis in an 86 year old patient with severe unstable angina and marked anterior-lateral ischemia. The pt. had critical chronic kidney disease receiving permanent dialysis and multiple other medical problems. Surgical approach was deemed too high risk and also rejected by the patient. (b) A 0.9 mm X-80 excimer laser catheter (Spectranetics, Colorado springs, CO) in the ostium of the left main artery before activation. The energy settings were 45 mJ/mm²/25 Hz with antegrade and

retrograde delivery of 250 pulses during intermittent emission and saline flush, totaling of 4 trains. No protection device was used. (c) Selective angiogram demonstrating a smooth recanalization channel as created by the laser. No distal embolization or thrombosis occurred. (d) Angiographic appearance of the left main coronary artery following short balloon inflations and adjunct stenting. The chest pain and ischemia disappeared and the patient was discharged home the next day

of the patients presented critical stenosis of the infarct related vessel (95–100 % stenosis). Specifically, total occlusion (100 % stenosis marked by TIMI 0 flow) was present in 37 % of the patients. These critical occlusions were caused by

plaques with significant thrombus burden, a common finding in many AMI patients [35]. Accordingly, a large thrombus burden-TIMI thrombus grade of 3 or 4 was detected in as many as 65 % of the cases. For the laser revascularization,

small-size catheters (0.9 and 1.4 mm) were the first tool in 34 % of the lesions whereas larger size catheters (1.7 and 2.0 mm) were used initially in 66 %. The final laser catheter size was 2.0 mm in 23 % of the lesions, 1.7 mm in 43 %,

1.4 mm in 25 % and 0.9 mm in 9 %. By visual angiographic assessment the baseline stenosis of 95 ± 6 % was decreased by laser emission to 48 ± 23 % ($p < 0.001$), followed by further decrease as achieved with balloon and stenting, to a final

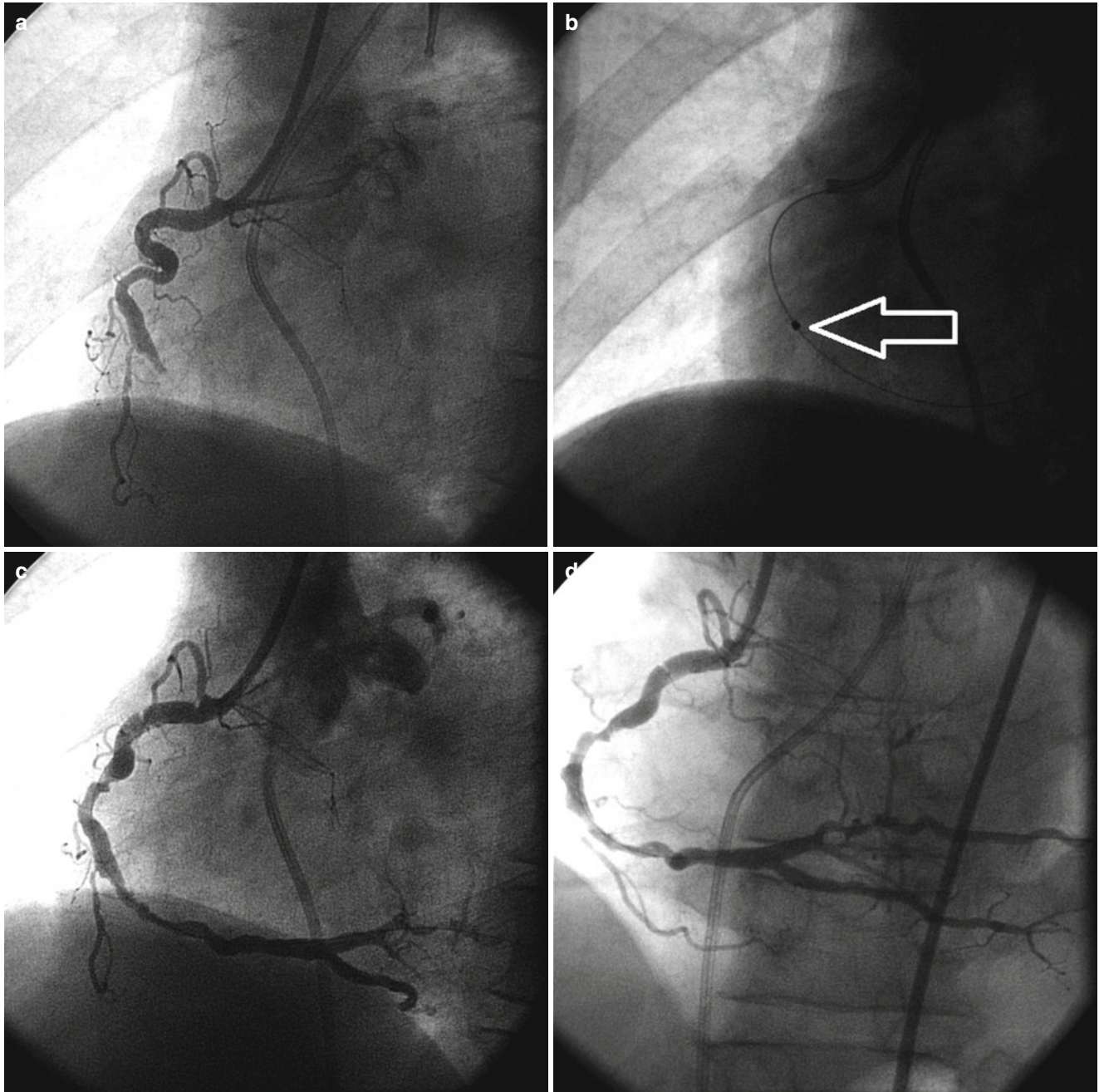


Fig. 4.2 (a) Angiogram from a patient who presented with an Inferior wall ST-elevation myocardial infarction (STEMI). The AMI was caused by a critical atherosclerotic plaque and adherent thrombus which together formed a total occlusion of the distal right coronary artery (RCA). The RCA anatomy is unfavorable for revascularization exhibiting the challenging “Sheppard’s crook” morphology. (b) A 1.7 mm concentric excimer laser catheter (Spectranetics, Colorado Springs, CO) with the catheter’s tip positioned in the occlusion (arrow). This catheter was delivered over a stiff guide wire then activated and

advanced using the slow lasing technique and concomitant saline injections. (c) Angiographic appearance of the infarct-related artery in the left anterior oblique view after completion of laser debulking. Adequate restoration of antegrade flow was observed within less than 2 min from the activation of the laser therapy. (d) The restored antegrade flow demonstrates the posterior descending and the posterior-lateral branches of the RCA. Anterior-posterior angiographic view, (e) Final angiogram showing achievement of the optimal TIMI grade 3 antegrade flow and complete patency of the infarct related vessel and its distal branches

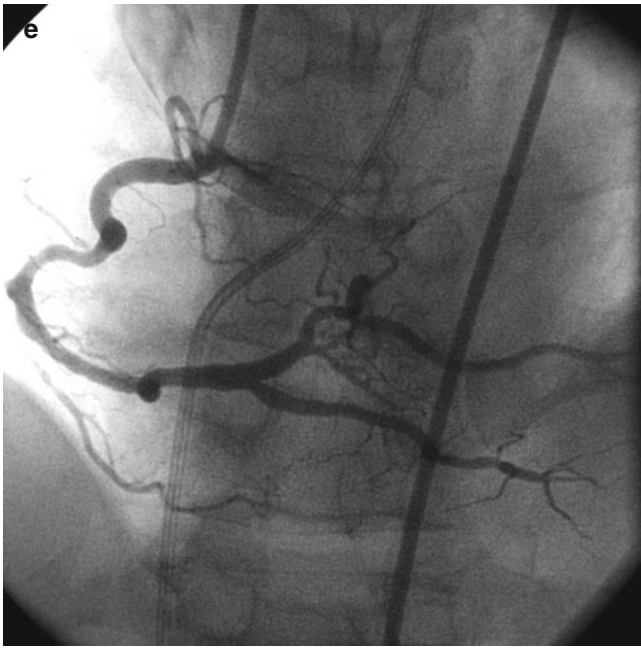


Fig. 4.2 (continued)

of $3 \pm 9\%$ ($p < 0.001$ versus baseline and post laser). The markedly low baseline TIMI flow of 1.2 ± 1.1 increased significantly by the excimer laser to grade 2.8 ± 0.5 ($p < 0.001$), reaching a final post stenting TIMI grade of 3.0 ± 0.2 ($p < 0.001$ vs. baseline). The minimal luminal diameter (MLD) of the treated vessels increased with the application of laser emission from a baseline of 0.5 ± 0.5 to 1.6 ± 0.5 mm (mean \pm SD, $p < 0.001$), reaching a final 2.7 ± 0.6 mm after adjunct stenting (baseline vs. post laser, $p < 0.001$). A 95 % device success, 97 % angiographic success and an overall 91 % procedural success rate were reported. A total of 6 patients (4 %) died, each arrived to the emergency room already in a state of cardiogenic shock. Admittedly, while the study was not powered to examine the role of laser in cardiogenic shock, intriguingly among the 20 patients who presented in this devastating hemodynamic condition there was a relatively low post procedure mortality rate of 30 %, suggesting that the laser might have had a positive impact on survival. The markedly low rate of complications included 0.6 % perforation, 5 % major dissection (all managed successfully with stent), 0.6 % acute closure, 3 % bleeding and 2 % distal embolization. The investigators discovered that the maximal gain in effective removal of the targeted thrombi was directly proportional to the initial angiographic burden, i.e. the larger the thrombotic content, the higher the laser effectiveness. This crucial finding corroborated earlier studies which recorded successful removal of 80 % of the initial thrombotic burden [35].

Overall, the CARMEL study provided the first quantitative sound evidence demonstrating the successful yield of

mechanical thrombectomy devices as applied in PCI for AMI. When further sub-analysis of the study was performed the investigators found that a specific laser related gain was achieved in those who presented later than the optimal 6 h window after AMI onset [34]. Another analysis focused on the challenging sub-group of AMI patients presenting with complete (100 %) occlusion of the infarct related artery. In most of these patients the critical TIMI flow grade 0 was attributed to the combined effect of an underlying plaque and a heavy burden, TIMI grade 5 thrombus. Nevertheless, despite the unfavorable baseline clinical condition and the heavy thrombus load in this selective group, an 89 % laser success rate was achieved as well as 93 % angiographic success and 86 % overall procedural success. Noteworthy, the baseline TIMI 0 flow increased to grade 2.7 ± 0.5 with the laser ($p < 0.001$). Then the final, post stenting TIMI flow was grade 3.0 ± 0.2 ($p < 0.001$ vs. baseline). The rate of complications in this study was considerably low. Distal embolization occurred in only 4 %, a rate serving as a testimony to the reliability of the laser in complex lesions. The “no reflow” phenomenon was detected in 2 %, target vessel dissection in 4 % [lower rate than in standard balloon angioplasty] and perforation occurred in only 0.6 %. The total MACE of 13 % was considered a low rate [37]. Another challenging, high risk sub-group of the CARMEL study patients included 31 subjects whose saphenous vein graft was the infarct related vessel [36]. Unsurprisingly, 39 % of these patients exhibited total occlusion of the old graft (TIMI 0 flow) and 23 % had sub-total (95–99 %) stenosis. Despite the morphologic and thrombotic challenge, the laser was able to increase the minimal luminal diameter in these vessels from a baseline of 0.6 ± 0.6 to 1.6 ± 0.5 mm and facilitated stent deployment resulting in a final MLD of 2.8 ± 0.6 mm. Overall, the laser success rate in this group was 87 % and only 3 (10 %) patients sustained a MACE, a rate considered low for acute interventions in such degenerated target vessels. Notably, there was no case of distal embolization and in only 3 % of the patients, a transient “no reflow” phenomenon occurred. This was achieved without insertion of distal protection devices during the laser interventions. Thus, the unique ability of the excimer laser to concomitantly debulke the plaque, suppress platelet aggregation and vaporize thrombus is unmistakable, serving as a considerable asset in the challenging context of revascularization for AMI. Table 4.5 depicts the excimer laser effect on thrombus laden lesions in AMI.

Lasering Technique in AMI Intervention

Routine patient preparation and anticoagulation for PCI are required. With the commonly used excimer laser the energy settings include a fluence of 45 mJ/mm^2 with 25 Hz. Supporting guiding catheters and guide wires are beneficial in laser proce-

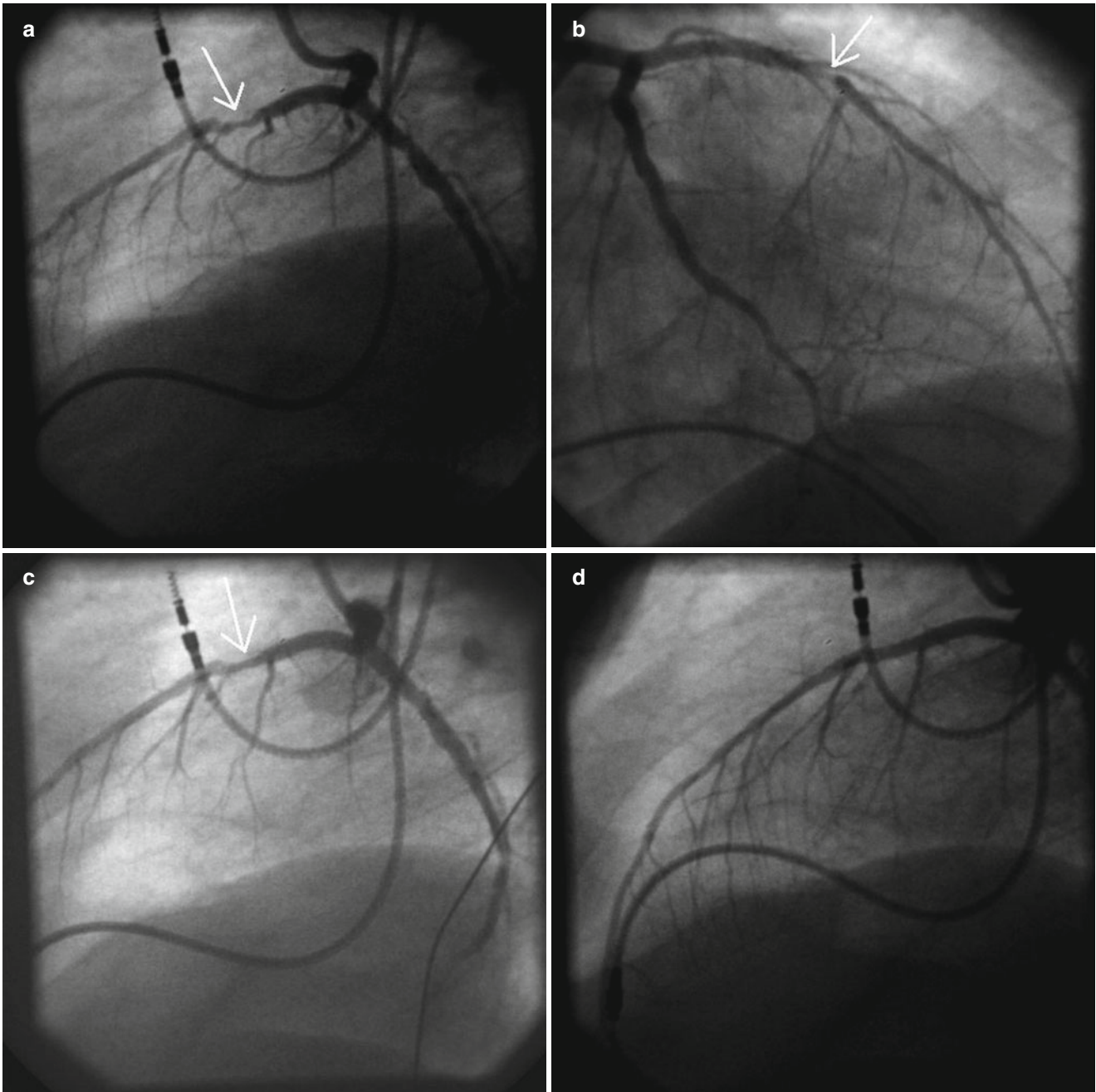


Fig. 4.3 (a) Coronary arteriography in the lateral -caudal projection in a patient who sustained STEMI of the anterior wall. The patient complained of severe chest pain which was accompanied by hemodynamic instability. The Left anterior descending artery (LAD) exhibited a 90 % eccentric lesion with irregular contour located in the proximal-middle segment of the LAD, between two septal perforator branches (*white arrow*). (b) The infarct related vessel and the target stenosis (*white arrow*) in the right anterior oblique view. (c) The target lesion was successfully debulked and adequate post laser channel created within the plaque. The successful debulking incorporated a 0.9 mm X-80 excimer

laser catheter (Spectranetics, Colorado Springs, CO). Activation was performed in a slow (0.2 mm/s) antegrade lasing along the entire length of the lesion, followed by slow debulking retrogradely. Lasing in both directions was combined with saline injections. (d) Final view of the infarct related vessel post stenting in the lateral -caudal view. Complete patency and optimal antegrade flow are present. No distal embolization occurred. (e) final view in the RAO projection. The patient had no further chest pain, the ST segment returned to baseline and hemodynamic stability was observed

dures. Catheter size selection relates inversely to the stenosis severity whereby the greater the stenosis the smaller the initial catheter size [38]. Proper lasing technique is crucial to ensure

success with laser angioplasty [39]. Since the depth of the excimer laser penetration is shallow (35–50 μm) a slow catheter advancement (0.5 mm/s) is recommended. The CVX-300

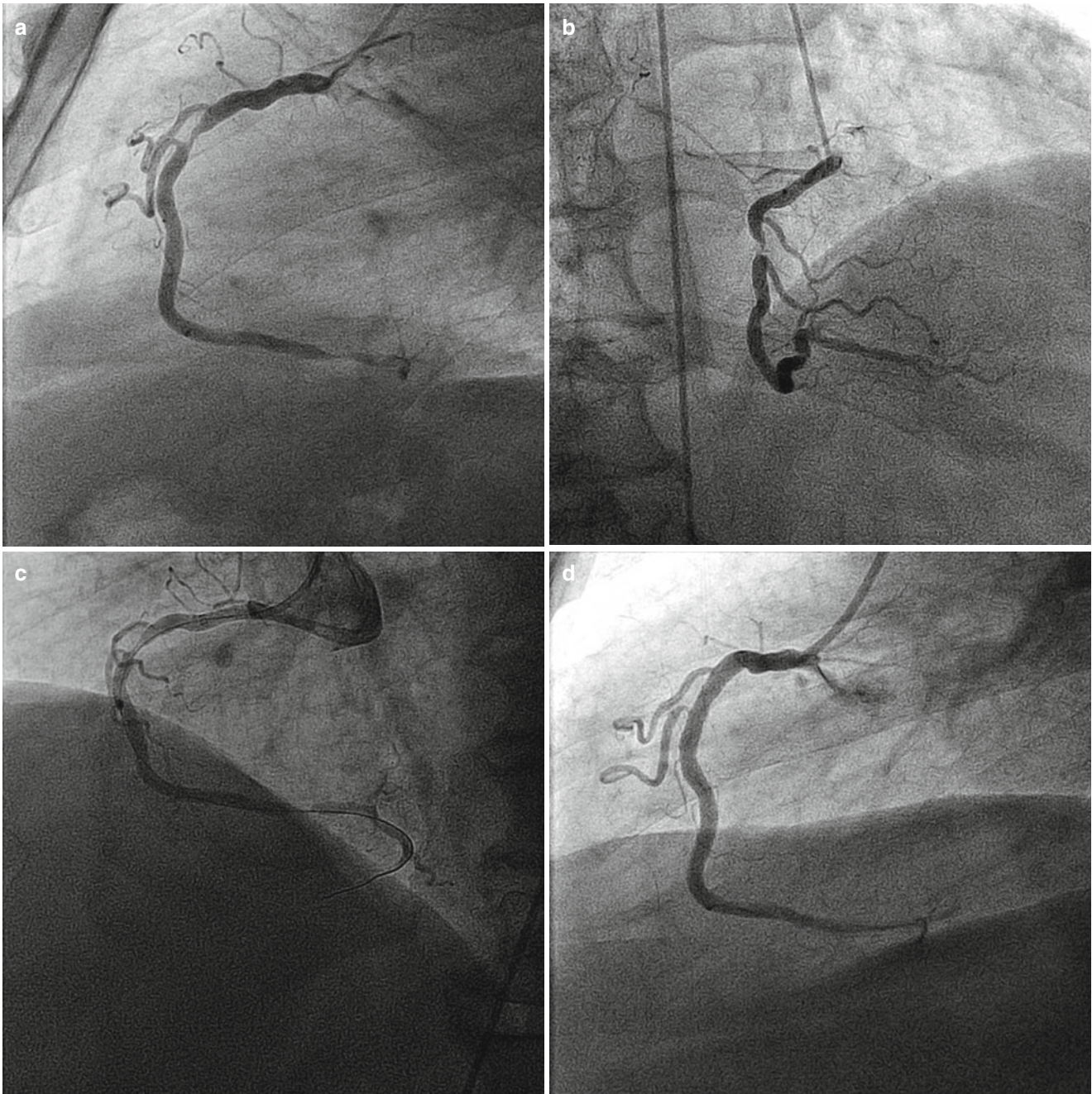


Fig. 4.4 A 59 year old man with inferior-lateral STEMI. Cardiac catheterization performed within 1 h from the onset of chest pain. The pt. had severe chest pain and shortness of breath. (a) the right coronary artery is the infarct related vessel containing a 90–95 % eccentric plaque. Angiogram in the left anterior oblique projection. (b) The right coronary artery in a right anterior oblique view. The marked eccentricity of the lesion is noted. (c) Angiogram post laser application for expedient revascularization of the vessel. A 1.4 COS excimer laser catheter (Spectranetics, Colorado Springs, CO) was used with energy settings of

45 mJ/mm²/25 Hz. The operator incorporated slow (0.2–0.5 mm/s) antegrade and retrograde lasing along the entire length of the lesion. The laser delivered total of 298 pulses. The laser emission debulked adequately the target plaque, thus creating a smooth recanalization channel without any adverse sequela. This channel permitted rapid stent delivery and positioning with optimal deployment. (d) Final angiogram post stenting with a drug eluting stent. The infarct related vessel is markedly open with TIMI 3 flow and no residual stenosis. The chest pain disappeared and patient recovered

console computer limits each lasing train to an interval of 5 s except for the X-80 0.9 mm catheter which is designed for 10 s emissions. Reaching the distal end of the stenosis, the operator may consider slow retrograde [pull back] lasing for maximiz-

ing thrombus removal. Since contrast media significantly amplifies the laser generated acoustic shock waves [40], any contrast in the vessel must be removed prior to laser activation. This step eliminates potential vessel trauma. This is accom-

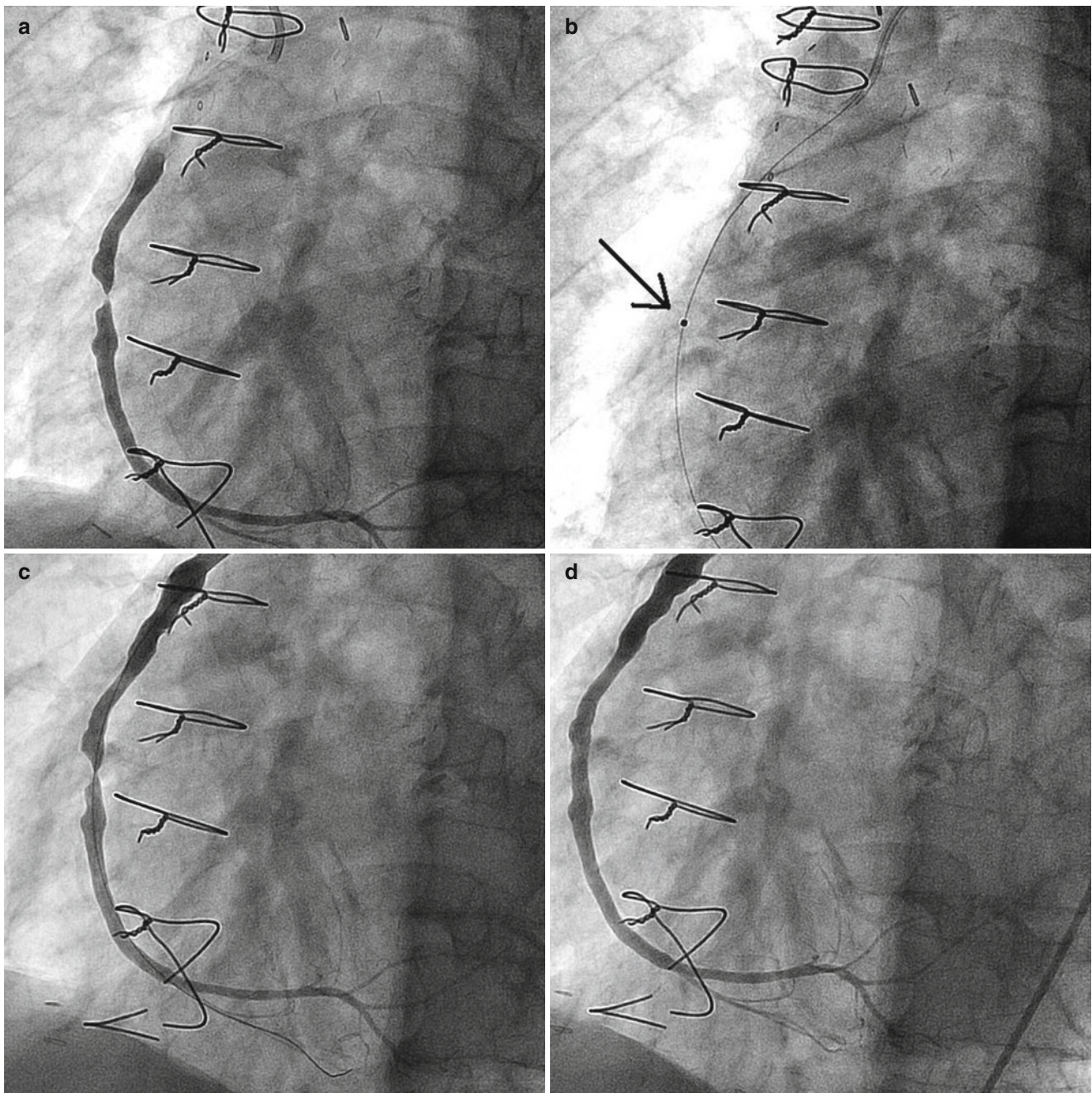


Fig. 4.5 A 70 year old patient with a large size non STEMI accompanied by severe chest pain and ischemia in the inferior-lateral EKG leads. The patient underwent coronary artery bypass surgery twice, 27 and 14 years earlier, respectively. Cardiac catheterization demonstrated total occlusion of the three major native coronary vessels at the aortic origin, thus, the entire cardiac perfusion was dependent on the old bypass grafts. The left internal mammary artery graft to the left anterior descending artery was patent and a saphenous vein bypass graft to the obtuse marginal branch of the circumflex artery was diffusely and severely diseased. (a) A 14 year old saphenous vein graft to the posterior descending artery containing a 99 %, eccentric, thrombotic lesion resulting in a decreased antegrade TIMI 2 flow. (b) The target was treated with a 1.4 mm COS laser catheter (Spectranetics, Colorado Springs, CO) delivering 450 pulses during slow antegrade and retrograde lasing (arrow). Saline injections accompanied deposition of the

laser energy emission. The patient received iv 4000 units of heparin and neither 2b/3a platelet receptor antagonist nor filter protection were used. (c) Angiography immediately post laser application. Adequate debulking of the obstructive plaque is noted. The smooth contour of the residual plaque is a result of the homogeneous distribution of the laser beam. This angiographic appearance is recognized as a unique marker of laser recanalization. The laser utilization achieved immediate cessation of the myocardial ischemia. Excellent flow along the graft and adequate filling of the distal to the anastomosis coronary segment were observed as well. (d) Final appearance of the revascularized old saphenous vein bypass graft post adjunct stenting with a 4.0x18 mm stent. The stent was positioned accurately without any resistant from the residual plaque. No distal embolization or thrombosis occurred. The patient made a complete clinical recovery

plished by initial injection of 10 cc saline into the guiding catheter and then injection of 3–5 cc saline along the intervals of laser advancement. Infrequently, the saline may increase

the Q-T interval and/or ischemia ensues. In such instances decreasing the saline volume to 1–2 cc and ensuring longer pauses between the laser trains are indicated [41]. Laser safety

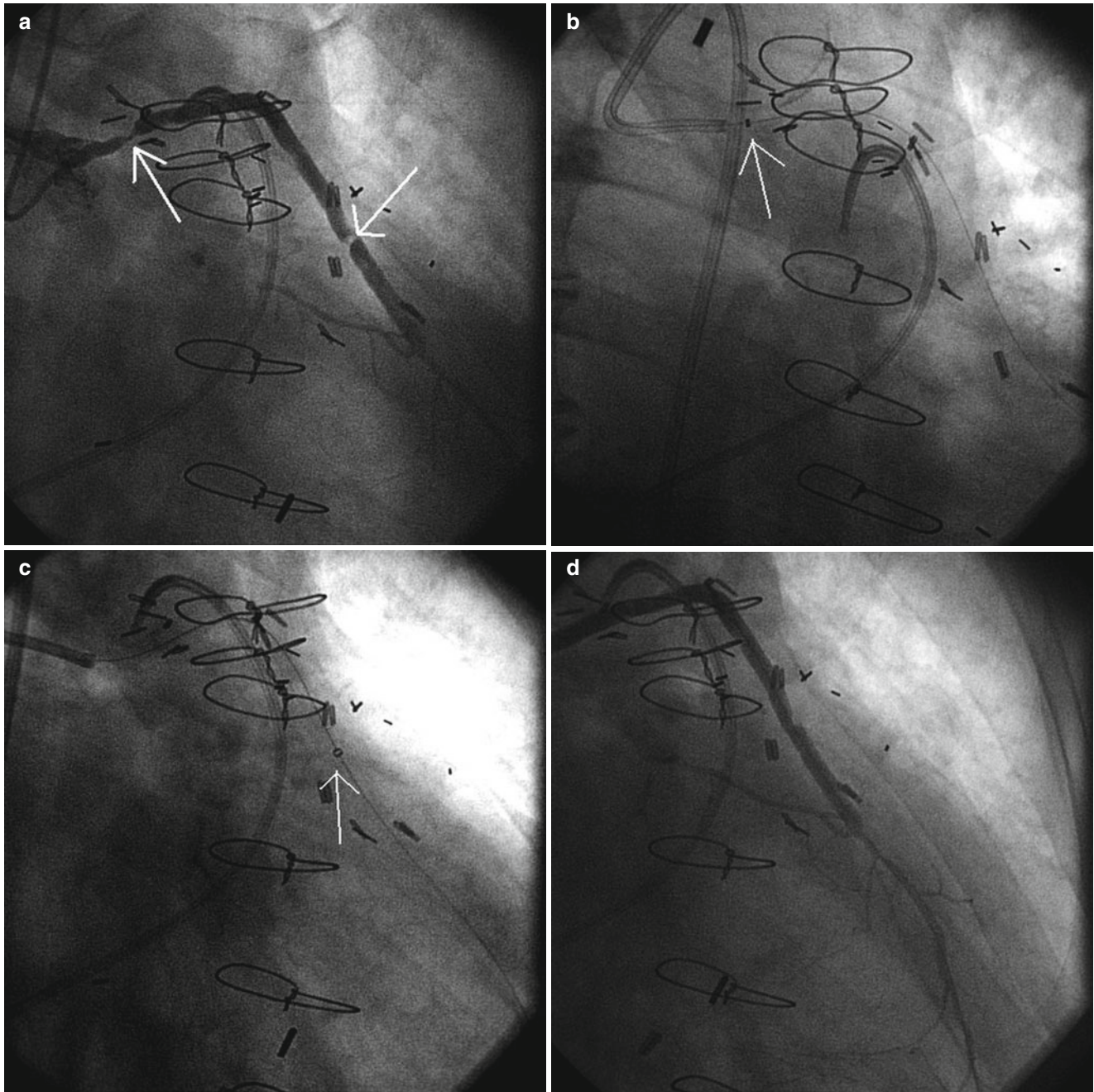


Fig. 4.6 (a) An elderly patient who underwent coronary artery bypass surgery 15 years earlier presented with a large size non STEMI complicated by congestive heart failure and relentless chest pain. Echocardiography demonstrated severely depressed left ventricular ejection fraction. The native coronary vessels were totally occluded and the saphenous vein graft to the LAD was the only remaining vascular conduit. This old bypass graft contained two critical lesions (*white arrows*): proximal 95 % stenosis and middle-distal 99 % eccentric, thrombotic stenosis. The patient had contraindications to the administration of pharmacologic 2b/3a platelets receptor antagonists. (b) A

0.9 mm X-80 COS excimer laser catheter (Spectranetics, Colorado Springs, CO) in the proximal stenosis. Activation was followed by low pressure balloon dilatation and then stenting of the lesion. (c) The same laser catheter was advanced to the distal stenosis. Delivery of laser emission was followed by low pressure balloon dilatation and then stenting. (d) Angiographic appearance of the treated bypass graft following successful laser debulking of both lesions. No filter protection device was used. (e) The final angiographic view of the old saphenous vein graft post stenting. The patient made clinical recovery and was discharged home the next day

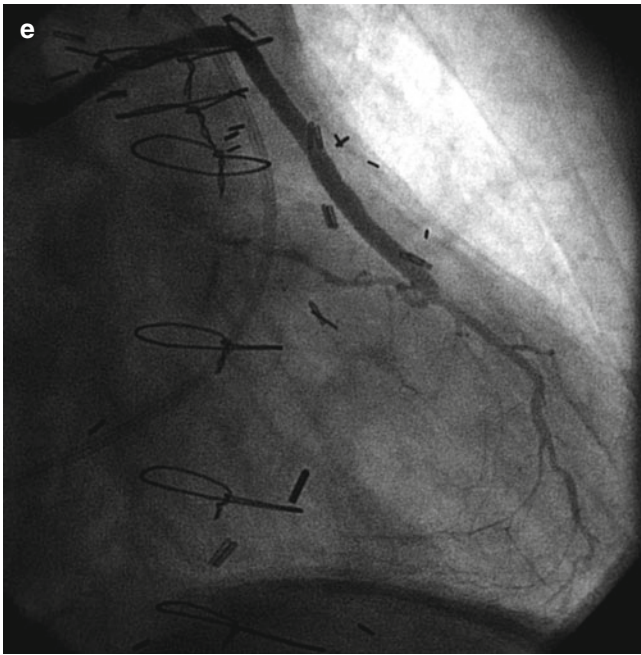


Fig. 4.6 (continued)

Table 4.1 Criteria for utilization of laser in AMI

1. STEMI or non STEMI types of AMI—including late presentation or failed thrombolytic therapy
2. Rescue intervention due to AMI expansion and/or hemodynamic instability
3. Complex lesion morphology in the infarct-related vessel, e.g., heavy plaque burden, eccentric plaque, thrombotic plaque, total occlusion, ostial stenosis, stent restenosis
4. Decreased TIMI flow in the infarct related vessel
5. TIMI Thrombus Grades 2–5—represented by medium-to-extensive thrombus burden
6. Calcified target lesion—containing low-moderate calcium burden
7. Failed thrombus removal by an aspiration catheter
8. Balloon failure to open the infarct-related vessel and/or dilate the target lesion
9. Contraindication for administration of platelet 2b/3a receptor antagonists

is an important component of the intervention and personnel and the patient alike must wear special protective goggles whenever the laser is enabled.

Altogether, based on the abovementioned findings the rationale for using laser in PCI for AMI is summarized as follows:

1. The laser is a user friendly technology which enables rapid preparation and activation for treatment of emergency cardiovascular conditions.
2. The laser offers highly selective absorption within the target plaque and thrombus resulting in expedient plaque debulking and thrombus removal are observed.

3. Laser enhances the effect of pharmacolytics on intracoronary thrombus, even in old, organized or resistant thrombus.
4. Laser induces unique, selective suppression of platelet aggregation kinetics.
5. Laser creates rapid restoration of adequate antegrade coronary flow in the infarct-related vessel.
6. Laser facilitates adjunct stenting.
7. The contemporary coronary laser has an established record of reliability, safety and efficiency as observed in coronary and peripheral interventions.

Complications Associated with the Use of Laser in AMI

As with any other PCI device the laser operators should recognize that it can cause specific complications with serious adverse impact on the targeted lesions, vessels and myocardium and the procedure outcome. These complications include perforation, dissection, spasm, acute closure, thrombosis, distal embolization, “no reflow” phenomenon and failure to achieve the acute revascularization goals. In most instances, complications though relatively rare, mainly relate to mistakes in the operator judgment mistakes and faulty lasing practices [42]. Thus understanding proper lasing techniques and the unique physical characteristics of the laser are imperative for elimination of laser induced complications.

Summary

The laser is a useful technology for application in PCI along each of the various stages of evolving acute myocardial infarctions. The merits of this device are attributed to its reliance upon sound physics principles, the user friendly technology, and, uniquely, the simultaneous ability to vaporize atherosclerotic obstructive plaques, rapidly remove thrombi and suppress platelet aggregation. Due to the precision of the laser debulking emission and the incorporation of slow advancement lasing techniques, the excimer laser does not require placement of adjunct of distal protection devices. Incorporating proper lasing technique is a prerequisite for procedural success including emphasis on slow laser catheter advancement along the target lesion, constant injections of intracoronary saline during laser emission and use intermittent laser debulking mode.

Acknowledgment The authors appreciate the invaluable assistance of Matthew Holtz CVT, RCIS in the preparations of this chapter.

Table 4.2 Coronary excimer laser catheters for PCI in AMI

Laser catheter diameter	Rapid exchange (RX)						
	0.9 mm	0.9 mm X 80	1.4 mm	1.7 mm	1.7 mm E	2.0 mm	2.0 mm E
Vessel size (mm)	≥1.5	≥2.0	≥2.2	≥2.5	≥2.5	≥3.0	≥3.0
Guide wire size	0.014"	0.014"	0.014"	0.014"	0.014"	0.014"	0.014"/0.018"
Guide catheter compatibility (F)	6	6	6/7	7	7	8	8
Max. tip diameter	0.038"	0.038"	0.057"	0.069"	0.066"	0.080"	0.079"
Max. shaft outer diameter	0.049"	0.049"	0.062"	0.072"	0.072"	0.084"	0.084"
Working catheter's length (cm)	130	130	130	130	130	130	130
Fluence (mJ/mm ²)	30–60	30–80	30–60	30–60	30–60	30–60	30–60
Repetition rate (Hz)	25–40	25–80	25–40	25–40	25–40	25–40	25–40
Laser on/off time (s)	5/10	10/5	5/10	5/10	5/10	5/10	5/10

Fig. 4.7 Effect of in-vitro laser emission on platelet aggregation kinetics. *Upper panel:* the purple curve depicts the normal response to ADP induced aggregation of platelets [control]. With delivery of laser energy, step wise increase in fluence (from the blue to orange and then green curve) results in marked suppression of platelets aggregation, a condition termed the "stunned platelets phenomenon". This unique laser effect is advantageous in clinical applications such as PCI of AMI. *Lower panel:* collagen induced platelet aggregation and the effect of increased laser fluence on the platelets aggregation kinetics (From Topaz et al. [28]. Schattauer GmbH, Publishers for Medicine and Natural Sciences, Stuttgart, Germany. With permission)

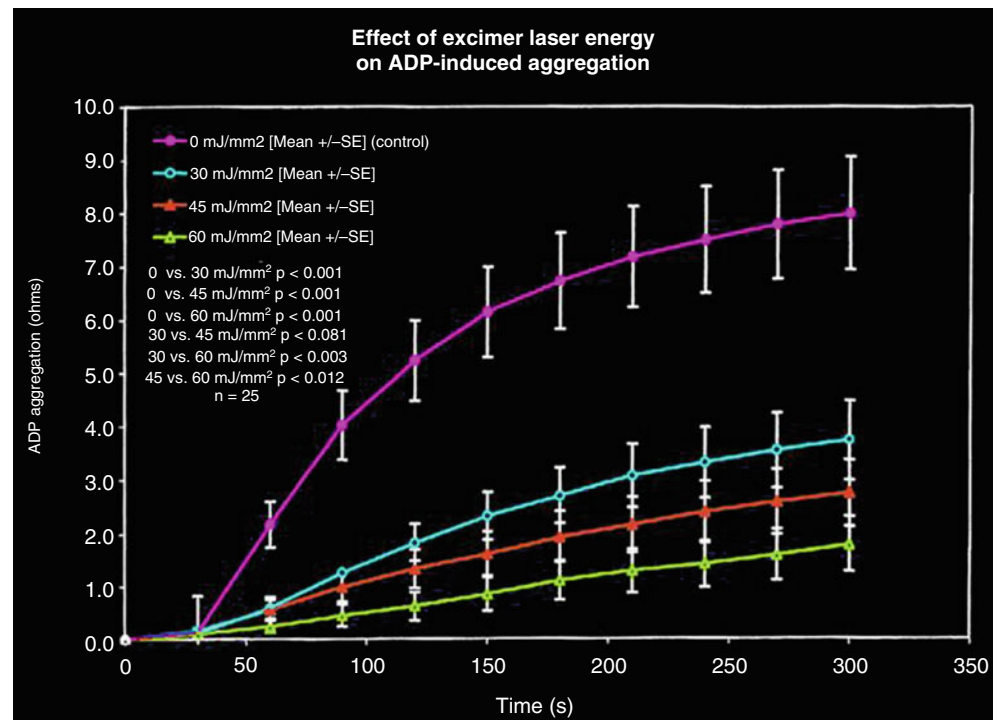


Table 4.3 Correlation of laser induced physical processes with resultant clinical effects in AMI

Process	Laser effect	Reference
Laser irradiation of plaque	No injurious effect on the vessel and plaque	[30]
Absorption in plaque	Vaporization of atherosclerotic material	[31]
Acoustic shock waves formation	Mechanical weakening of the thrombus components	[13, 26]
	Photoacoustic fibrinolytic effect on fibrin in the thrombus	
Thrombolysis	Enhanced action of lytics on old, resistant thrombus	[27, 29]
Laser absorption in platelets	Inhibiting platelet aggregation (“stuffed platelets effect”)	[28]

Table 4.4 Clinical observations—laser application in AMI

	Reference
Feasible and safe for plaque ablation and thrombolysis in complex and complicated AMI	[12]
Laser can be used successfully in AMI patients with depressed left ventricular fraction	[33]
In AMI and unstable angina pectoris, laser efficiently removes 80 % of the targeted thrombus content	[20, 32]
Maximal laser gain in AMI is achieved in infarct-related vessels containing large-to-heavy thrombus burden	[34]
In AMI with continuous chest pain and ischemia: 98 % laser success rate, very low complication rate	[35]
In AMI including STEMI, non-STEMI, late presentation, failed thrombolytic therapy, cardiogenic shock, old SVGs—a 95 % device success is observed	[21]
With laser, unlike most percutaneous devices, thrombus does not adversely impact the procedure outcome	[21, 32]
When degenerated SVG is the infarct-related vessel—no need for insertion of distal protection device	[36]

Table 4.5 Excimer laser effect on thrombus-laden lesions in AMI

Angiographic thrombus size:	Small	Extensive
Pre-laser baseline plaque:		
% DS	76 ± 16	89 ± 15
MLD (mm)	0.7 ± 0.4	0.4 ± 0.5
Laser specific acute gain:		
% DS	25 ± 15	36 ± 20
MLD (mm)	0.8 ± 0.5	1.2 ± 0.7*
Final angiographic results:		
%DS	16 ± 17	22 ± 16
MLD (mm)	3.0 ± 0.6	2.8 ± 0.6

Table based on select data from Topaz et al. [21]

MLD minimal luminal diameter, DS diameter stenosis

*p < 0.03 extensive versus small

References

- Kushner FG, Hand M, Smith Jr SC, et al. 2009 focused updates: ACC/AHA guidelines for management of patients with ST-elevation myocardial infarction and ACC/AHA/SCAI guidelines on percutaneous coronary intervention; a report of the American College of Cardiology Foundation/American Heart Association task Force on Practice Guidelines. *J Am Coll Cardiol.* 2009;54:2205–41.
- Van de Werf F, Bax J, Betriu A, et al. Management of acute myocardial infarction in patients presenting with persistent ST-segment elevation: the Task Force on the Management of ST-Segment Elevation Acute Myocardial Infarction of the European Society of Cardiology. *Eur Heart J.* 2008;29:2909–45.
- Keeley EC, Boura JA, Grines CL. Primary angioplasty versus intravenous thrombolytic therapy for acute myocardial infarction: a quantitative review of 23 randomised trials. *Lancet.* 2003;361:13–20–468.
- Topaz O. Chapter 26. The thrombus containing lesion. In: Topol EJ, Teirstein PS, editors. *Textbook of interventional cardiology.* 6th ed. Philadelphia: Elsevier; 2011. p. 336–56.
- Topaz O, Perin EC, Jesse RL, Mohanty PK, Carr Jr M, Rosenschein U. Power thrombectomy in acute ischemic coronary syndromes. *Angiology.* 2003;54:457.
- Topaz O. Editorial. Comparison between thrombus removal devices: aspirations meet reality. *Catheter Cardiovasc Interv.* 2011;78:20–2.
- Topaz O. Editorial. Thrombectomy during primary PCI for STEMI – call of the thrombus. *Catheter Cardiovasc Interv.* 2012;80:1181–2.
- Topaz O, Ebersole D, Dahm J, Das T, Madyoon H, Perin EC. Excimer laser revascularization: current indications, applications and techniques. *Lasers Med Sci.* 2001;16:72–7.
- Topaz O, Vetrovec GW. Laser for optical thrombolysis and facilitation of balloon angioplasty following failed pharmacologic thrombolysis. *Cathet Cardiovasc Diagn.* 1995;36:38–42.
- Topaz O. Editorial. Novel thrombus displacement technology for STEMI revascularization. *Catheter Cardiovasc Interv.* 2012;80:65–6.
- Topaz O. Editorial. Excimer laser thrombolysis: an emerging option for acute ischemic coronary syndromes. *Lasers Med Sci.* 2001;16:130–2.
- Topaz O, Rozenbaum EA, Battista S, Peterson C, Wysham DG. Laser facilitated angioplasty and thrombolysis in acute myocardial infarction complicated by prolonged or recurrent chest pain. *Cathet Cardiovasc Diagn.* 1993;28:7–16.
- Topaz O. Holmium laser-induced coronary thrombolysis. *J Thromb Thrombolysis.* 1996;3:327–30:22:228–239.
- de Marchena E, Mallon S, Posada J, Joshi B, Correa L, Myerburg RJ. Direct holmium laser assisted balloon angioplasty for acute myocardial infarction. *Am J Cardiol.* 1993;71:1223–5.
- Topaz O. A new safer lasing technique for laser facilitated coronary angioplasty. *J Interv Cardiol.* 1993;6:297–306.
- Topaz O. Coronary laser angioplasty. In: Topol EJ, editor. *Textbook of interventional cardiology.* 2nd ed (Suppl). Philadelphia: WB Saunders Company; 1995. p. 235–55.
- Heuser RR. Editorial. Lasers in coronary disease. *Cathet Cardiovasc Diagn.* 1993;28:17.
- Topaz O. Holmium laser angioplasty. *Semin Interv Cardiol.* 1996;1:149–61.

19. Topaz O, McIvor M, Stone GW, Krucoff MW, Perin EC, Fosschi AE, Sutton J, Nair R, deMarchena E, and the Holmium: YAG laser multicenter investigators. Acute results, complications and effect of lesion characteristics on outcome with the solid-state, pulsed-wave, mid-infrared laser angioplasty system: final multicenter registry report. *Lasers Surg Med.* 1998;22:228–39.
20. Dahm JB, Topaz O, Woenckhaus C, et al. Laser facilitated thrombectomy: a new therapeutic option for treatment of thrombus laden coronary lesions. *Catheter Cardiovasc Interv.* 2002;56:365–72.
21. Topaz O, Ebersole D, Das T, et al. Excimer laser angioplasty in acute myocardial infarction (the CARMEL multicenter trial). *Am J Cardiol.* 2004;93:694–701.
22. Topaz O, Polkampally PR, Rizk M, Mohanty PK, Bangs J, Bernardo NL. Excimer laser debulking for percutaneous coronary intervention in left main coronary artery disease. *Lasers Med Sci.* 2009;24:955–60.
23. Topaz O. Lasers in CTO. In: Waksman R, Saito S, editors. *Chronic total occlusions.* Chichester: Wiley; 2009. p. 150–64.
24. Topaz O, Polkampally PR, Topaz A, Polkampally CR, Jara J, Rizk M, McDowell K, Feldman G. Utilization of excimer laser debulking for critical lesions unsuitable for standard renal angioplasty. *Lasers Surg Med.* 2009;41:622–7.
25. Topaz O, Lippincott R, Bellendir J, et al. Optimally spaced excimer laser coronary catheters: performance analysis. *J Clin Laser Med Surg.* 2001;19:9–14.
26. Topaz O. Plaque removal and thrombus dissolution with pulsed-wave lasers' photoacoustic energy-biotissue interactions and their clinical manifestations. *Cardiology.* 1996;87:384–91.
27. Topaz O, Minisi AJ, Morris C, et al. Photoacoustic fibrinolysis: pulsed wave mid infrared laser-clot interaction. *J Thromb Thrombolysis.* 1996;3:209–14.
28. Topaz O, Minisi AJ, Bernardo NL, et al. Alterations of platelet aggregation kinetics with ultraviolet laser emission: the “stunned platelet phenomenon”. *Thromb Haemost.* 2001;86:1087–93.
29. Topaz O, Morris C, Minisi AJ, Mohanty PK, Carr Jr M. Enhancement of t-PA induced fibrinolysis with laser energy: in –vitro observations. *Lasers Med Sci.* 1999;14:123–8.
30. Topaz O, Minisi AJ, Mohanty PK, et al. In-vivo effect of coronary laser angioplasty on atherosclerotic plaques: histopathologic analysis. *Cardiovasc Pathol.* 2001;10:223–8.
31. Topaz O, Rozenbaum E, Schumacher A, Luxenberg MG. Solid-state, mid-infrared laser facilitated coronary angioplasty: clinical and quantitative angiographic results in 112 patients. *Lasers Surg Med.* 1996;19:260–72.
32. Topaz O, Bernardo NL, Shah R, et al. Effectiveness of excimer laser coronary angioplasty in acute myocardial infarction or in unstable angina pectoris. *Am J Cardiol.* 2001;87:849–55.
33. Topaz O, Minisi A, Bernardo NL, et al. Comparison of effectiveness of excimer laser angioplasty in patients with acute coronary syndromes in those with versus those without normal left ventricular ejection fraction. *Am J Cardiol.* 2003;91:797–802.
34. Topaz O, Ebersole D, Dahm JB, et al. Excimer laser in myocardial infarction: a comparison between STEMI patients with established Q-wave versus patients with non-STEMI (non-Q). *Lasers Med Sci.* 2008;23:1–10.
35. Topaz O, Shah R, Mohanty PK, McQueen RA, Janin Y, Bernardo NL. Application of excimer laser angioplasty in acute myocardial infarction. *Lasers Surg Med.* 2001;29:185–92.
36. Ebersole D, Dahm JB, Das T, et al. Excimer laser revascularization of saphenous vein grafts in acute myocardial infarction. *J Invasive Cardiol.* 2004;16:177–80.
37. Dahm JB, Ebersole D, Das T, et al. Prevention of distal embolization and no-reflow in patients with acute myocardial infarction and total occlusion in the infarct-related vessels. *Catheter Cardiovasc Interv.* 2005;64:67–74.
38. Topaz O, Safian RD. Excimer laser coronary angioplasty. In: Safian RD, Freed MS, editors. *Manual of interventional cardiology.* 3rd ed. Royal Oaks: Physicians Press; 2001. p. 681–91.
39. Topaz O. Laser. In: Topol EJ, editor. *Textbook of interventional cardiology.* 4th ed. Philadelphia: WB Saunders; 2003. p. 675–703.
40. Tchong JE. Saline infusion in excimer laser coronary angioplasty. *Semin Interv Cardiol.* 1996;1:135–41.
41. Topaz O. Laser. In: Topol EJ, editor. *Textbook of interventional cardiology.* 3rd ed. Philadelphia: WB Saunders; 1998. p. 615–33.
42. Topaz O. Editorial. Whose fault is it? Notes on “true” versus “pseudo” laser failure. *Cathet Cardiovasc Diagn.* 1995;36:1–4.

William R. Davies, Tiffany Patterson,
and Simon R. Redwood

Introduction

Coronary artery bypass surgery has revolutionised the treatment of symptomatic coronary atherosclerosis. However, the lack of long term patency of saphenous vein grafts has been a barrier to lasting procedural success. Recent estimates suggest that only 50 % of vein grafts will be patent and free of significant luminal stenosis at 10 years. The therapeutic options available to symptomatic patients facing further revascularisation are limited and hazardous. Re-do surgery is offered but at a higher risk of both morbidity and mortality than at initial operation, especially in the common situation of a patent internal mammary graft. The percutaneous option is, therefore, usually the preferred option by both the Heart Team and the patient.

The nature of vein graft stenosis makes percutaneous intervention technically challenging, and carries more risk than intervention on the native coronary arteries. Vein graft disease tends to be diffuse and friable, and often carries a high thrombotic burden. The evolution of adjunctive thera-

pies to prevent no-reflow, such as filter wire placement, have gone some way to mitigating this risk, but their use has been limited despite class I evidence of efficacy.

Percutaneous excimer coronary laser angioplasty has evolved into a useful adjunctive therapy for saphenous vein graft intervention over the last 20 years. Procedural success rates have climbed, complications have been minimised and long-term patency rates improved, due to a combination of increased operator experience and technological advancement.

In this chapter we will examine the unique pathological process that underlies saphenous vein graft stenosis and relate this to the technical challenges facing the laser operator. We will also review the evidence for laser use and discuss our experience, illustrated with case histories. Finally, we will consider the future role for this useful adjunctive therapy in the fight against coronary atherosclerosis.

Aortocoronary Saphenous Vein Grafts

Coronary artery bypass surgery has revolutionised the treatment of angina that is refractory to medical therapy. Following an initial report of surgical technique by Favaloro in 1969 [1], DeBakey's group [2] were the first to publish a series of patients who had undergone successful aortocoronary bypass using a saphenous vein graft (SVG) conduit. Bypass grafting using vein conduit has since become a key component of cardiac and vascular surgical practice beginning with these early successes only 40 years ago. Since the pioneering days, surgical techniques have been refined, suture materials have improved and adjunctive pharmacology for prevention of restenosis or thrombosis has led to an increase in graft survival. However, the aggressive nature of the sclerotic process that occurs in SVGs does severely limit their long term patency. The attrition rate of these SVGs remains alarming. During the first year after bypass surgery 15 % of venous grafts are occluded [3] and by 10 years 40 % have occluded (Fig. 5.1). Of the remaining patent grafts only 50 % are free of significant stenoses [4, 5]. When considered in conjunction

W.R. Davies, BSc, PhD, MB ChB, MRCP, MRCS
Papworth Hospital NHS Foundation Trust,
Papworth Everard,
Cambridge, CB23 3RE, UK
e-mail: wrdavies@nhs.net

T. Patterson, BSc, MBBS, MRCP
Cardiovascular Division,
King's College London British Heart Foundation
Centre of Research Excellence, Rayne Institute,
St Thomas' Hospital, St Thomas' Campus,
Westminster Bridge Road, London SE1 7EH, UK
e-mail: tiffanypatterson05@gmail.com

S.R. Redwood, MBBS, MD, FRCP, FACC, FSCAI (✉)
Cardiovascular Department,
Guy's and St Thomas' NHS Foundation Trust,
6th Floor East Wing, Westminster Bridge Road,
London SE1 7EH, UK

Cardiovascular Division, King's College London British Heart
Foundation Centre of Research Excellence, Rayne Institute,
St Thomas' Hospital, St Thomas' Campus,
Westminster Bridge Road, London SE1 7EH, UK
e-mail: simon.redwood@gstt.nhs.uk

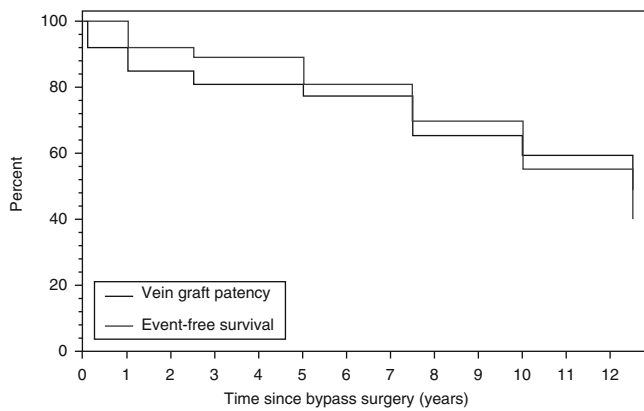


Fig. 5.1 Vein graft patency and time since coronary artery bypass surgery. The *thin line* represents the event free survival with time following coronary artery bypass surgery. The *bold line* represents vein graft patency over the same time period (Adapted from Motwani and Topol [3])

with an expected progression of native coronary disease in the same patient, it becomes apparent that coronary artery surgery is, perhaps, best considered as a palliative procedure.

The healthcare burden presented by symptomatic patients in whom initially successful revascularisation has occurred is significant. Further revascularisation following CABG is required in 4 % of patients by 5 years, 19 % of patients by 10 years and 31 % of patients by 12 years post-operatively [6]. More recently, the adoption of the radial artery as the second conduit of choice has led to an improved early and late patency rate above that expected of a venous graft [7]. However, a new phenomenon of a positive ‘string sign’ seen at coronary angiography demonstrating severe, diffuse atherosclerosis throughout the length of the arterial conduit has been reported. Either percutaneous or repeat surgical revascularisation in these patients comes at some considerable risk. Redo surgery has a higher mortality, especially in the context of a patent internal mammary graft, and is less likely to provide total relief from anginal chest pain when compared to initial bypass grafting [8]. Percutaneous intervention is, therefore, considered to be the preferable therapeutic strategy in SVG disease, and accounts for between 5 and 10 % of all PCI procedures [9]. The percutaneous option for revascularisation of diseased SVGs is, however, less successful than intervention performed on the native coronary artery, and can be fraught with technical challenges and pitfalls.

Pathogenesis of Vein Graft Sclerosis

It is important to understand the exact nature of vein graft disease to appreciate the most effective therapeutic options. The low pressure and thin walled vein is not an ideal candidate for transposition into the high pressure arterial

Table 5.1 Mechanisms of vein graft failure

Intrinsic	Extrinsic
Poor vein quality	Anastomotic problems
Missed valve/branch (<i>in-situ</i>)	Inflow tract stenosis or occlusion
Branch ligature placement	Outflow tract stenosis or occlusion
Intimal flaps	Thromboembolism
Intimal hyperplasia (anastomotic or intra-graft)	Graft sepsis
Accelerated atherosclerosis	Mechanical compression of the graft (entrapment or kinking)
Aneurysmal degeneration	

Adapted from Davies and Hagen [10]

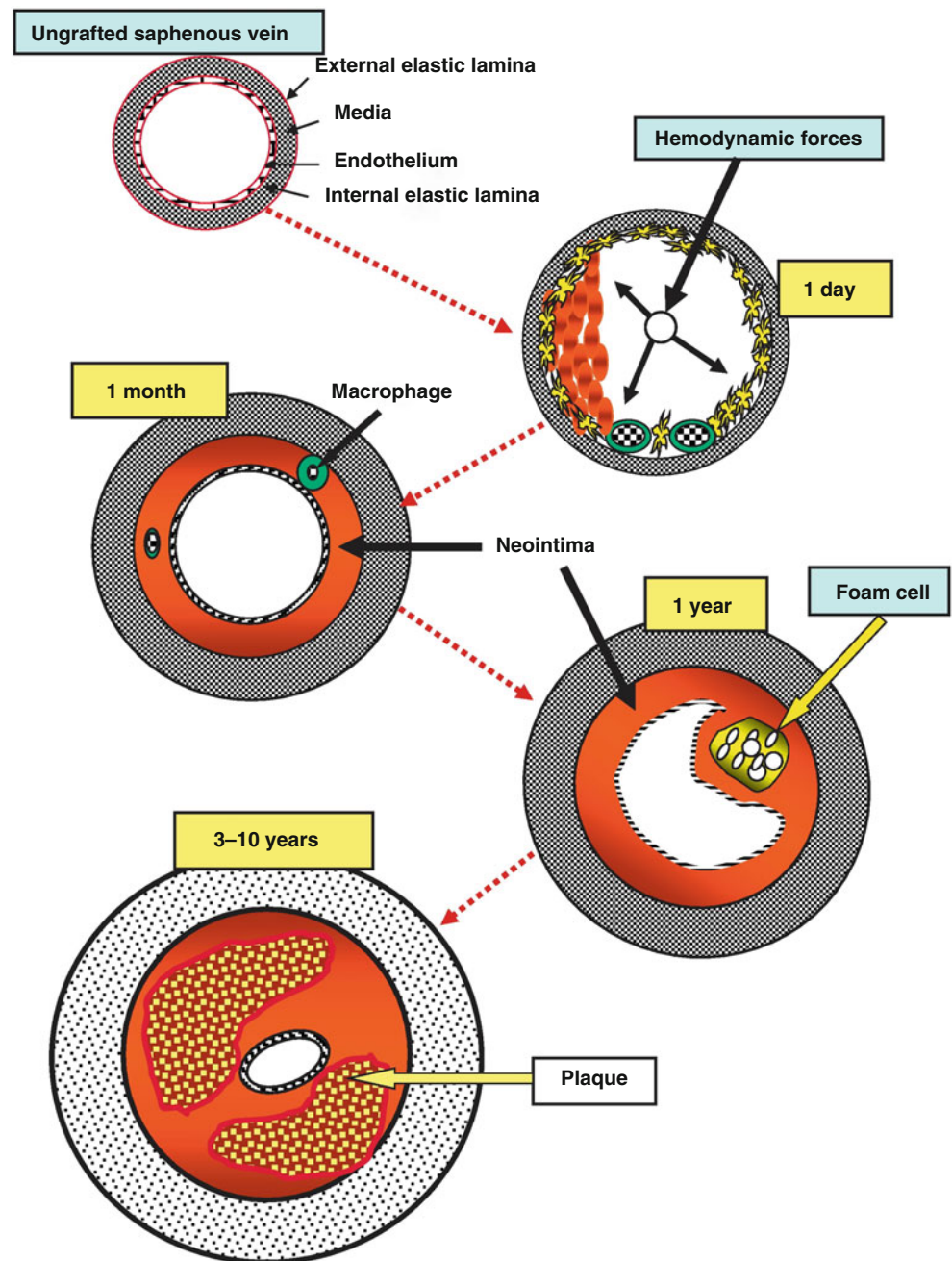
These can be divided into intrinsic and extrinsic factors. Early failures are defined as within 30 days, short-term failures as between 30 days and 2 years, and long-term failures are seen after 2 years. Many short-term failures can be attributed to technical aspects of the surgery at the anastomosis, for example poor distal run-off or graft length mismatch leading to kinking and low flow

system. The vein is divided into three anatomical layers: the intima, the media and the adventitia. Histologically the intima is a thin layer of endothelial cells, many of which have been seen to be disrupted by the process of venous harvesting [10]. The smooth muscle cells in the media are arranged into an inner longitudinal layer and an outer circumferential pattern, with interposed elastic fibres. The adventitia is often thicker than the media and is composed mainly of fibroblasts and collagen bundles. The vasa vasorum supply the vessel wall and run within the adventitial layer.

The manipulation of the SVG prior to anastomosis has been shown to cause endothelial dysfunction due to mechanical and bariatric trauma. Both endothelial and smooth muscle cell disruption appear to be important mechanisms in the subsequent pathogenesis of intimal proliferation [11]. Much work has been performed on the optimal conditions for vein harvest and storage prior to implantation in an attempt to reduce the destructive nature of the smooth muscle proliferation [10].

The mechanisms of vein graft failure can usefully be classified into intrinsic and extrinsic factors (Table 5.1 [10]). Early failures are defined as within 30 days, short-term failures occur between 30 days and 2 years, and long-term failures are seen after 2 years. Many early failures can be attributed to technical aspects at the time of anastomosis, for example poor distal run-off, graft kinking or an inadequate anti-thrombotic strategy. Short-term failures are predominantly due to the formation of neo-intimal hyperplasia within the graft. In the longer-term a combination of intimal hyperplasia and a progressive ‘atherosclerosis like’ disease causes eventual graft failure. Some of this histological differentiation is likely to be as part of an adaptive

Fig. 5.2 Natural history of vein graft failure. Early surgical trauma factors such as vein inflation with normal saline cause endothelial denudation which in turn leads to platelet aggregation. The subsequent medial thickening is caused by vascular smooth muscle cell proliferation. Over time, atheromatous lesions rich in foam cells lead to luminal narrowing. Plaque rupture is the final event that leads to graft occlusion, in a process similar to that observed in native coronary atheroma (Adapted from Shukla and Jeremy [13])



process that the vein graft undergoes secondary to the higher perfusion pressure it endures whilst positioned in the arterial tree. However, there is also immunohistochemical and ultrastructural evidence that antigen-presenting dendritic cells play an important role in the subsequent stenotic process [12]. Various factors have been implicated in the failure of vein grafts including adhesion of platelets and leucocytes, rheological factors, matrix metalloproteinase expression, neointima formation and superimposed atherogenesis. Figure 5.2 outlines the natural history of vein graft failure [13].

The typical intravascular ultrasound appearances of vein graft neo-intimal hyperplasia can be seen in Fig. 5.3 [3]. It is these lesions that are the most likely to cause a return of symptoms due to myocardial ischaemia and are thus the target for the majority of percutaneous interventions.

Although much research effort has been expended on the attempted amelioration of vein graft degeneration, no effective therapeutic strategy has, as yet, made a significant impact on graft longevity. Certainly aggressive secondary prevention measures including optimisation of anti-platelet regimens, smoking cessation and high dose statin therapy are

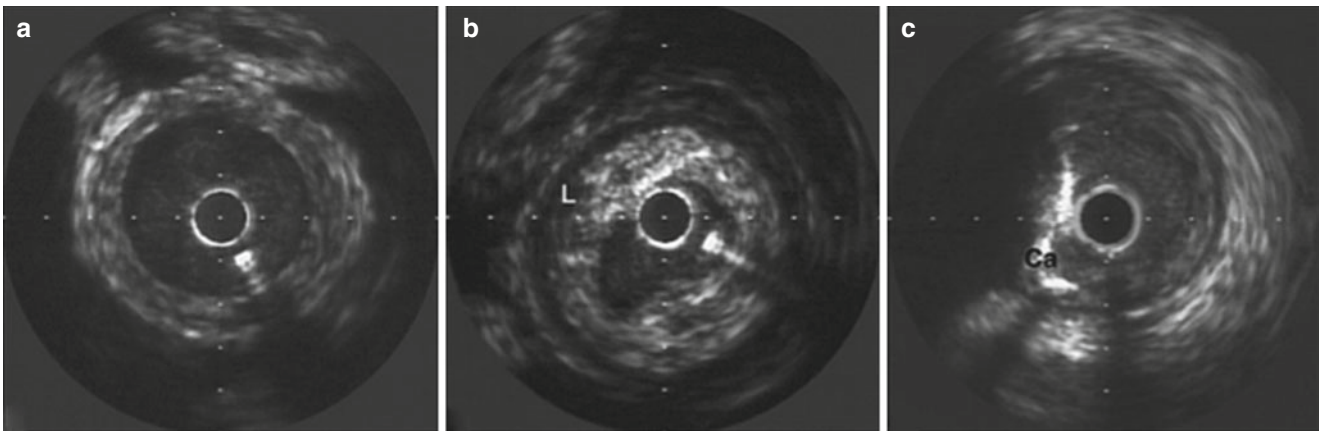


Fig. 5.3 Typical intravascular ultrasound appearances of saphenous (a) vein graft neo-intimal hyperplasia. (b) L–lipid rich plaque. (c) Ca–calcified appearance of atheroma in native vessel. (Adapted from Motwani and Topol [3])

appealing in that they would also aim to reduce the progression of the underlying native coronary artery disease. The use of adenoviral vectors for therapeutic gene transfer prior to anastomosis is also attractive and has shown promise in vitro, but is yet to translate into clinical practice [14]. The future quest for lower attrition rates of bypass grafts may hinge on the more widespread use of arterial conduit, rather than further attempts to modify the triple threat of thrombosis, intimal hyperplasia and atherosclerosis currently observed.

Technical Challenges in Percutaneous SVG Intervention

The decision to intervene in SVG disease is much the same as the decision in native coronary disease. The intervention should be symptom led, should show evidence of myocardial ischaemia in a non-invasive study, and the region with ischaemia should be subtended by an SVG with a significant stenosis. Due to the higher risk nature of intervention, clinical decisions should be made by a heart team, consisting of both an interventional cardiologist and a cardiothoracic surgeon. Treatment modalities could be percutaneous coronary intervention, redo-coronary artery bypass grafting or optimisation of medical therapy and anti-anginal pharmacology. The factors that should be considered during this discussion are outlined in Table 5.2 [15].

The role of fractional flow reserve (FFR) assessment of SVG stenoses has been poorly studied. In clinical practice, a cut off of between 0.75 and 0.80 is generally used, although as the SVG disease does progress more rapidly than native vessel atherosclerosis the decision to defer intervention is

Table 5.2 Decision nomogram to aid revascularisation decisions in patients with vein graft stenosis following coronary artery bypass grafting

Favors Repeat CABG Surgery	Favors Graft PCI
Clinical presentation	
Late graft failure	Early graft failure STEMI
Angiographic parameters	
Multiple graft lesions	Single graft lesion
Diffuse graft lesions	Focal graft lesion
No patent LIMA graft	Patent LIMA graft
Diseased LAD graft	Patent LAD graft
Echocardiograph parameters	
Near normal LVF	Poor LVF
Valvular disease (requiring future surgery)	No significant valvular disease
Technical aspects	
Adequate venous or arterial material	Inadequate conduit material
Acceptable surgical access	Difficult surgical access
Anterior or lateral target vessel	Posterior lateral target vessel
Limited mediastinal scarring	Mediastinal scarring
Favorable target vessels	Radiation, infection, pericarditis, prior pectoralis muscle transfer closure
Patient factors	
Patient's preference after fully informed consent from a surgeon and a cardiologist	Patient's preference after fully informed consent from a surgeon and a cardiologist
Acceptable pulmonary and renal function, life expectancy >5 years	Poor pulmonary or renal function, life expectancy <5 years

Adapted from Harskamp et al. [15]

LIMA indicates left internal mammary artery, LVF left ventricular function, STEMI ST-segment elevation myocardial infarction

less evidence based. The VELETI Trial (Treatment of Moderate Vein Graft Lesions with Paclitaxel Drug-Eluting Stents) [16, 17] examined the prophylactic stenting of intermediate SVG stenoses due to the rapid natural progression of these lesions. The conclusion of this small 57-patient study was that plaque sealing of lesions between 30 and 60 % severity with a drug eluting stent resulted in and improvement in 1- and 3-year MACE when compared to optimal medical therapy. The results for PCI in the chronic total occlusion of a SVG are poor. In a study of 34 patients a procedural success of 68 % was achieved, but further target vessel revascularisation was required in over 60 % of those at 18 months [18]. Perhaps more successful would be an attempt to recanalise the native coronary artery in those cases where the ischaemic myocardium is subtended by an occluded SVG.

The underlying pathological process in SVG stenosis results in particular challenges for the subsequent intervention. The sclerotic plaques are more friable, have either very thin or absent fibrous caps, contain more foam and inflammatory cells and usually are non-calcified [19]. The SVG is, therefore, more prone to an extensive thrombotic burden potentially leading to distal embolization during intervention. Grafts of an older age are more ectatic with a greater plaque burden, resulting in a higher risk of the slow-flow or no-reflow phenomenon. This is manifest as a reduction, or sometimes total loss, of the antegrade flow to the microvascular circulation without obvious angiographic evidence of obstruction. Although the mechanism of no-reflow is poorly understood, a contribution of endothelial swelling, neutrophil infiltration and platelet aggregation is likely to be contributory [20]. The use of glycoprotein (GP) IIb/IIIa inhibitors have been shown to be effective in the primary PCI setting for acute myocardial infarction. However, no such improvement in major adverse cardiovascular events (MACE) has been shown in the setting of SVG intervention either with distal embolic device protection in the SAFER trial [21] or without distal protection [22, 23]. Indeed, in the SAFER trial the patients randomised to the GP IIb/IIIa group had a higher incidence of MACE.

Several authors have studied the optimal interventional strategy to be adopted when PCI has been chosen as the best therapeutic option. The choice of stent deployed is between a bare metal (BMS), a drug eluting (DES) or a covered stent. Although more commonly used to exclude coronary artery aneurysms or to seal a coronary perforation, the covered stent does have several theoretical advantages in SVG stenoses. They may allow the trapping of graft plaque and thrombus between the stent and the vessel wall, reducing the risk of distal embolization and no-reflow. It was also hypothesized that the covered nature of the stent would reduce subsequent neo-intimal hyperplasia and restenosis. The disadvantage to this strategy is that the covered stent is more

bulky to prepare and deploy. Although initial registry results were favourable [24], the randomised controlled trials were disappointing [25, 26], with a similar restenosis rate and a higher incidence of non-fatal MI in the covered stent group when compared to those patients receiving a bare metal stent.

More work has been done on the comparison of a DES versus a BMS strategy in the SVG. Lee et al. [9, 27] undertook a meta-analysis of 19 studies, 2 of which were randomised trials and 17 registries, including 3420 patients in total. Target vessel revascularisation was less frequent in patients that had undergone intervention with a DES, as was the incidence of myocardial infarction. No differences were found in the risk of death or stent thrombosis between the two groups. These results support the use of DES in SVG for superior clinical outcomes. The clinical outcomes of six randomised stent studies are summarised in Table 5.3 [9].

Although a DES strategy provides the optimal long-term benefit, there is still a considerable incidence of procedure related complications at the time of placement. As previously discussed, the nature of SVG stenosis is such that there is likely to be a high clot burden associated within the diseased segment. Some authors have reported that the incidence of MACE (predominantly myocardial infarction) or reduced antegrade flow (the no-reflow phenomenon) to be approximately 20 % [21]. The first multi-centre randomised controlled trial to report was the SAFER trial (Saphenous vein graft Angioplasty Free of Emboli Randomised) [21]. This was the pivotal trial that led to the US Food and Drug Administration approving distal protection in the form of the PercuSurge GuardWire® (Medtronic, Minneapolis, MN USA) for commercial use. This device relies on a distal occlusion balloon to trap the emboli within the SVG until the intervention is complete and the proximal vessel is aspirated. 801 patients were enrolled between June 1999 and August 2000 over 47 sites. The safety committee halted the trial early due to a significant benefit in the active treatment arm. Three hundred and ninety-five patients were assigned to a stent placement over a conventional angioplasty wire, whilst 401 patients underwent stent placement using a distal protection device. The primary composite end point of death, myocardial infarction, emergency bypass or target lesion revascularisation by 30 days was seen in 16.5 % of patients in the control group and 9.6 % of patients in the embolic protection group. This 42 % relative risk reduction in MACE was mainly driven by MI and no-reflow phenomenon, suggesting the effective recovery of embolic particles. However, the 9.6 % MACE in the distal protection arm only underlines the difficulty in percutaneous intervention in this high risk population. The SAFER investigators subsequently reported in 2005 [28] that the cost and technical complexity of the GuardWire® device had limited its use. Further subgroup analysis of the original trial showed that patients with more

Table 5.3 Clinical outcomes of randomised controlled trials examining stent deployment in stenosed saphenous vein grafts

	SYMBIOT III		BARRICADE		RECOVERS		SOS		RRISC		ISAR-CABG		
	PTFE	BMS	PTFE	BMS	PTFE	BMS	PES	BMS	SES	BMS	DES	BMS	
	p value	p value	p value	p value	p value	p value	p value	p value	p value	p value	p value	p value	
MACE													
1 year	30.6	26.6	39.2 ^a	28.0 ^a	23.1 ^b	15.9 ^b	0.15	37	49	15.8 ^b	29.7 ^b	15.4	22.1
3 years	NA	NA	60.2	37.0	NA	NA	NA	54	77	58	41	NA	NA
5 years	NA	NA	68.3	51.8	NA	NA	NA	NA	NA	NA	NA	NA	NA
Death													
1 year	2.6 ^c	4.7 ^c	7.0	5.0	2.6 ^b	2.8 ^b	0.92	12	5	2.6 ^b	0 ^b	5.2	4.7
3 years	NA	NA	18.8	11.2	NA	NA	NA	24	13	29	0	NA	NA
5 years	NA	NA	29.8	22.3	NA	NA	NA	NA	NA	NA	NA	NA	NA
MI													
1 year	9.2	10.9	14.2	11.3	14.1 ^b	5.5 ^b	0.02	15	31	2.6 ^b	0 [†]	4.2	6.0
3 years	NA	NA	21.0	14.1	NA	NA	NA	17	46	18	5	NA	NA
5 years	NA	NA	26.2	17.4	NA	NA	NA	NA	NA	NA	NA	NA	NA
TLR													
1 year	23.5	15.6	28.2	21.1	9.6 ^b	8.3 ^b	0.84	5	28	5.3 ^b	21.6 ^b	7.2	13.1
3 years	NA	NA	37.4	21.8	NA	NA	NA	41	41	24	30	NA	NA
5 years	NA	NA	43.9	29.6	NA	NA	NA	NA	NA	NA	NA	NA	NA

Adapted from Lee et al. [9]

BARRICADE Barrier Approach to Restenosis: Restrict Intima to Curtail Adverse Events study, **BMS** = bare-metal stent(s), **DES** drug-eluting stent(s), **ISAR-CABG** Prospective, Randomized Trial of Drug-Eluting Stents Versus Bare Metal Stents for the Reduction of Restenosis in Bypass Grafts, **MACE** major adverse cardiac event(s), **MI** myocardial infarction, **NA** not available, **PTFE** polytetrafluoroethylene, **RECOVERS** Randomized Evaluation of Polytetrafluoroethylene-Covered Stent in Saphenous Vein Grafts, **RRISC** Reduction of Restenosis in Saphenous Vein Grafts with Cypher Sirolimus-Eluting Stent, **SOS** Stenting of Saphenous Vein Grafts, **SYMBIOT III A** Prospective, Randomized Trial of a Self-Expanding PTFE Stent Graft During SVG Intervention—Late Results, **TLR** target lesion revascularization

^aTarget vessel failure (composite of all-cause death, MI, or clinically driven target vessel revascularization)^b6 months^cCardiac death

diffusely diseased grafts and bulkier lesions had the highest MACE rate. However, a significant benefit in MACE reduction was seen across all levels of risk, regardless of the pre-procedure perception of lower risk by the operator.

More contemporaneous practice was reviewed by Sturm et al. in 2012 [29]. Three types of device are currently used for distal embolic protection: distal balloon occluders together with proximal aspiration; distal filters; and proximal balloon occlusion and aspiration systems. The FilterWire EX Randomised Evaluation (FIRE) study showed non inferiority of the FilterWire EX distal filter system when compared to the GuardWire system [30]. The Saphenous Vein Graft protection In a Distal Embolic Protection Randomised Trial (SPIDER) study [31] showed non-inferiority of the Spider Rx to both the GuardWire and the FilterWire EX. As a result, DPDs have become the standard of care. However, their use is not without limitations. The absence of a suitable landing zone can preclude the use of DPD as in cases of vein graft tortuosity, close proximity to the distal anastomoses [32] or vessel occlusion [33]. The lesion itself may be impossible to cross with a filterwire or lead to further embolisation of thrombotic material. In light of this evidence, the American College of Cardiology recommend use of distal embolic protection in SVG PCI wherever technically possible (Class I recommendation, level of evidence B) [34]. Despite this, embolic protection is only used in 22 % of cases [29]. There is no evidence to date for the effectiveness of rheolytic thrombectomy, for example the AngioJet (Medrad Interventional/Possis, Minneapolis, MN, USA) in the treatment of SVG disease, either in the acute or elective setting.

Early Reports of Successful Laser Therapy in SVGs

Percutaneous coronary intervention in SVGs remains a high risk area of interventional cardiological practice. The use of distal protection is beneficial, but take up is low, perhaps due to the technical difficulty encountered in deploying the available devices. MACE rates remain high despite concomitant improvement in both short and long-term results in the drug eluting stent era. Several characteristics of SVG disease appear to be particularly attractive to the use of laser revascularisation. As we have seen, SVG lesions are friable and diffuse, with significant thrombotic material increasing the potential for distal embolization. Albert Einstein first conceived the idea of a laser in 1905. The ultraviolet pulsed excimer (**excited dimer**) laser has several potential advantages in the setting of SVGs. The laser ablates material by photochemical means, without the generation of significant heating. The early use of laser in interventional cardiology was hampered by the incidence of perforation of the coronary artery and significant flow-limiting dissections. These

two complications have largely been overcome by the improvement in catheter based laser technology and the technique itself. The ability to debulk a lesion in the absence of a systemic lytic state, the shortened thrombus clearing time with concomitant plaque modification, and the facilitation of subsequent balloon angioplasty and stent deployment [35] are all attractive properties that potentially could be exploited in the setting of SVG therapy.

Excimer coronary laser angioplasty (ECLA) has been successfully used to treat lesions within SVGs. The first case reports of ECLA therapy in aortocoronary SVGs were published in 1989 by Litvack and colleagues [36]. The first patient was an 85 year old female with two previous operations for coronary artery surgery. Within 18 months of the redo procedure she represented with a symptomatic 99 % stenosis of the graft to the posterior descending artery. This was successfully treated using a 308 nm xenon-chloride laser via an 8 F sheath in the femoral artery using a multipurpose guide catheter. Following slow passage of the laser catheter over the stenosis, repeat fluoroscopic angiography revealed a residual 30 % stenosis. Subsequent balloon angioplasty was performed but only a marginal improvement in luminal diameter was achieved. The patient remained well at 8 months post discharge and was angina free. This early report demonstrated the feasibility of laser revascularisation in this unique patient population. However, following this initial success, early adopters of laser therapy did encounter significant levels of complications which hindered further progress through the 1990s.

Laser Therapy in SVGs – The Evidence

Laser light had been shown *in vitro* to obliterate atherosclerotic plaque and much was promised for this novel therapeutic intervention in the 1980s. In the haste to adopt this novel technology, a poorly refined technique produced a high initial complication rate and an unacceptable restenosis rate. The laser was removed from the cardiac catheter suite and innovation was confined to the vascular surgical use in distal complex lesions below the knee. Success in this field led to a rejuvenated, if more cautious return to the therapeutic intervention in coronary atherosclerosis.

Eigler and colleagues [37] were the first to report a series of 200 patients that underwent excimer laser therapy to aorto-ostial lesions. This group of patients were considered at the time to be poor candidates for the conventional balloon angioplasty that was available. Twenty eight percent of those patients reported underwent ECLA to a saphenous vein graft. The ECLA registry was a multicentre prospective registry of all patients undergoing ECLA and was a record of procedures performed in 20 centres in the United States, Canada, Great Britain and Japan. Patients were included if they had a

symptomatic stenosis with provokable ischaemia on stress. Patients with a recent MI were excluded. A 308 nm xenon chloride excimer laser (Advanced Interventional Systems Inc, Irvine, California, USA) was used with catheter sizes ranging from 1.3 to 2.2 mm in diameter. Acute procedural success was achieved in 90 % of patients, but one-third of failures were associated with major complications. The incidence for in-hospital complications was 3.9 % with seven patients requiring bypass surgery, one patient suffering a Q wave infarct and four patients having an extensive dissection. Coronary perforation occurred in two patients. Sixteen percent required repeat intervention for symptoms at clinical follow-up. The SVG patients had a 6 month mortality of 1.2 % and a repeat revascularisation procedure was required in 14.3 %. Eighty percent of patients in the SVG group remained event free.

One year later, Bittl et al. [38] studied 495 patients who underwent ECLA for 545 saphenous vein graft stenoses. Clinical success was achieved in 455 (92 %) as indicated by a less than 50 % residual stenosis in each target lesion. In hospital complications were death (1 %), bypass surgery (0.6 %), and myocardial infarction 4.6 %. Ostial lesions and lesions in smaller vein grafts had a greater likelihood of success. These results were obtained in the pre-stent era using older laser technology.

The evolution of the laser technology was rapid, with improved delivery systems and more malleable catheters leading to improved results. Topaz et al. [39] reported a large series of 1862 patients with 2038 lesions who underwent laser angioplasty using a novel solid-state, mid-infrared holmium:YAG laser with a 2.1 μm wavelength. 10.6 % of these lesions were in saphenous vein grafts. Stenosis reduction occurred in 87 % of lesions without the need for balloon angioplasty. In-hospital bypass surgery was required in 2.5 % of patients, Q-wave MI in 1.2 % and death in 0.8 %. Perforation occurred in 2.2 % of patients and a major dissection in 5.8 %. Clinical restenosis occurred in 34 % of patients at 6-months. In this series, there were no significant outcome differences between the lesions treated in the native coronary vessel and those in SVGs. Although the immediate procedural success rates were good, with an acceptable complication rate, the disappointing restenosis rates required further refinement of the technique.

It should be also recalled that the field of percutaneous coronary intervention was rapidly developing at the same time in the mid 1990s. Strauss et al. [40] performed the first detailed quantitative angiographic analysis of immediate procedural and late follow-up lesions in patients who had undergone percutaneous ECLA exclusively to SVG lesions. ECLA was performed in 125 SVG lesions throughout eight centres. Acute angiographic success (lesion stenosis reduced by more than 50 %) occurred in 54 % of lesions after ECLA and 94 % of lesions with adjunctive balloon angioplasty. The

dissection rate was high at 48 % but these were generally of mild severity. Dissections were more likely in longer lesions and those in the body of the graft. Clinical success was achieved in 89 % within hospital complication rates at 0.9 % death, 4.5 % MI and 0.9 % need for emergent bypass surgery. In keeping with this high risk cohort, 1-year mortality was 8.9 % with the 1-year event-free survival being 48 %. The authors acknowledge that the late restenosis and occlusion rate of the SVGs mitigated the early benefits of the procedure.

The New Approaches to Coronary Intervention (NACI) registry [41] was the next to report progress, with 887 patients electively treated with ECLA. 16.6 % of these underwent intervention to the SVG. Procedural success was achieved in 84 % of the 887 patients, with complications including 1.2 % mortality, 0.7 % MI and 2.7 % emergent surgery. The target lesion revascularisation rate was 31 % at 1 year. There was no reported difference in either complication rate or outcome success in the SVG group versus those patients that had ECLA to the native coronaries.

In the Laser Angioplasty of Restenosed Coronary Stents (LARS) trial [42] the investigators report on a total of 440 patients with restenosis or occlusions in 537 stents. Laser angioplasty success was achieved in 92 % of cases. Twelve percent of lesions treated were in SVGs, but again, no significant differences could be elucidated between the graft cases and those treatments to native coronary vessels. Serious adverse events included death (1.6 %), MI 3.2 %, tamponade 0.5 % and perforation (0.9 %). Bypass surgery was much less frequent than previously reported at 0.2 %. Although the authors were able to conclude that the safety of the procedure was improving and that immediate results were encouraging, the lack of long-term follow-up hampered wider acceptance of the results. One year follow-up was reported by the Washington Hospital Center group for 320 patients with 340 SVG aorto-ostial lesions treated with either debulking laser and stenting or stenting alone [43]. Procedural success (98 %) and complications (2.6 %) continued to improve. However, there appeared to be no benefit to laser debulking at the 1 year follow-up point, as there was no difference in procedural outcomes, late clinical events and target lesion revascularisation between the two groups. Ajani et al. [44] reported on a series of 175 patients treated with ECLA combined with intracoronary radiation. Interestingly, angiographic restenosis was significantly reduced at 6 month follow-up without a significant rise in procedural complications in those patients receiving radiation plus ELCA.

Arguably the most influential of all the trials in ECLA is the CARMEL multicentre analysis [33, 39, 45]. This multicentre, international trial called Cohort of Acute Revascularisation in Myocardial Infarction with Excimer Laser (CARMEL) aimed to document the feasibility, safety and acute procedural results of ECLA in patients with acute

MI. The particular challenge in this group was thought to be the thrombus-laden lesions, and SVGs were the target vessel in 21 % of procedures. One hundred and fifty-one patients were enrolled with quantitative coronary angiography and statistical analyses being performed by a core laboratory. Procedural success was achieved in 91 % of cases, with the most laser gain achieved in those lesions with the biggest thrombus burden. Although 4 % of patients died, each was in cardiogenic shock pre-procedure. Complications included perforation (0.6 %), dissection (4 %) acute vessel closure (0.6 %), distal embolization 2 % and bleeding (3 %). These much improved results can be attributed to not only operator experience, but also the refinement of the laser technique, with slow advancement over the target lesion and the “saline flush” procedure reducing the risk of vessel dissection. The refinement of the laser catheters with enhanced ablation capability also contributed to this substantial reduction in device related complications.

The Coronary graft Results Following Atherectomy with Laser (CORAL) trial was a prospective multicentre registry of laser therapy for degenerative SVG stenoses [46]. This registry was designed to prospectively evaluate the safety and efficacy of excimer laser in patients presenting for PCI to SVG lesions. In total, 98 patients were enrolled in 18 centres between 2003 and 2004. Patients were excluded if the operator planned to use a distal protection device. Inclusion and exclusion criteria were aligned to those of the SAFER trial to allow exact comparisons to be made. The primary endpoint of 30-day MACE occurred in 18.4 % driven primarily by non-Q wave infarct. Major procedural complications included no reflow (5 %) and major dissection (1 %). There were no cases of vessel perforation. There was a high primary technical success rate despite smaller vessel diameter when compared to the SAFER trial population. However, the assertion that ECLA would reduce the need for distal protection devices was not supported, and the authors recommended that the underutilisation of distal protection device in clinical practice be addressed to improve outcomes.

Finally, Niccoli et al. [47] published a case-control registry of ECLA versus distal protection devices in patients with acute coronary syndromes due to SVG disease. The authors outlined the technical limitations of DPD although reaffirmed the support for their use when technically feasible. Seventy one consecutive patients with non-ST elevation ACS underwent either filter-assisted or ECLA-assisted PCI of a degenerative SVG. Baseline demographic data was the same in both groups. ECLA was used in 34 % of patients, notably for SVG lesions in which the filter could not be positioned in 14 cases. The other cases were through operator choice. Type IVa myocardial infarction was significantly higher in the DPD group 49 % vs 21 %, $p=0.04$, with troponin T levels being significantly lower in the ECLA group. The angiographic index of reperfusion (TIMI flow and blush grade) was also better in the ECLA group. Although this was an observational study, the results are encouraging and pave the way for a randomised controlled trial of the use of ECLA in SVG stenosis causing non-ST elevation acute coronary syndromes.

St Thomas' Experience

In a retrospective analysis of 50 consecutive ECLA treated SVGs at St Thomas' Hospital, London (2014) angiographic success was achieved in 98 % of cases, with 6 % having a Type IVa myocardial infarction. Clinical follow-up at a mean of 2.8 ± 1.6 years demonstrated 10 % mortality, a further 10 % TLR and 22 % hospitalisation with angina.

Case Examples of ECLA in SVG lesions

Case 1 (Fig. 5.4)

A 77-year-old male with a history of coronary artery bypass grafting in 1993 with a LIMA to the LAD, SVG to RCA and SVG to D1 was admitted for urgent elective PCI

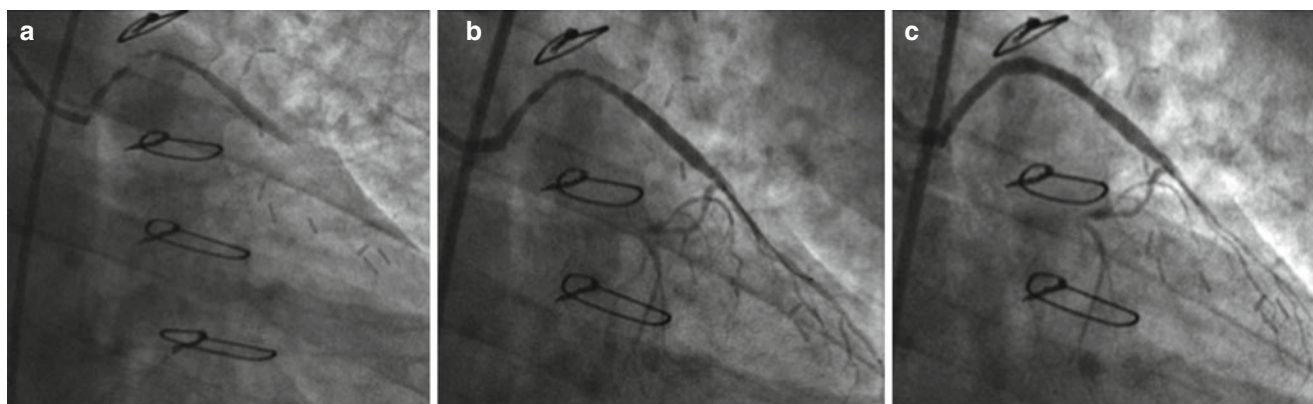


Fig. 5.4 (a) Severe proximal disease of SVG-D1 with mid-vessel occlusion. (b) After 1.7 mm Excimer laser. (c) Final image after single stent

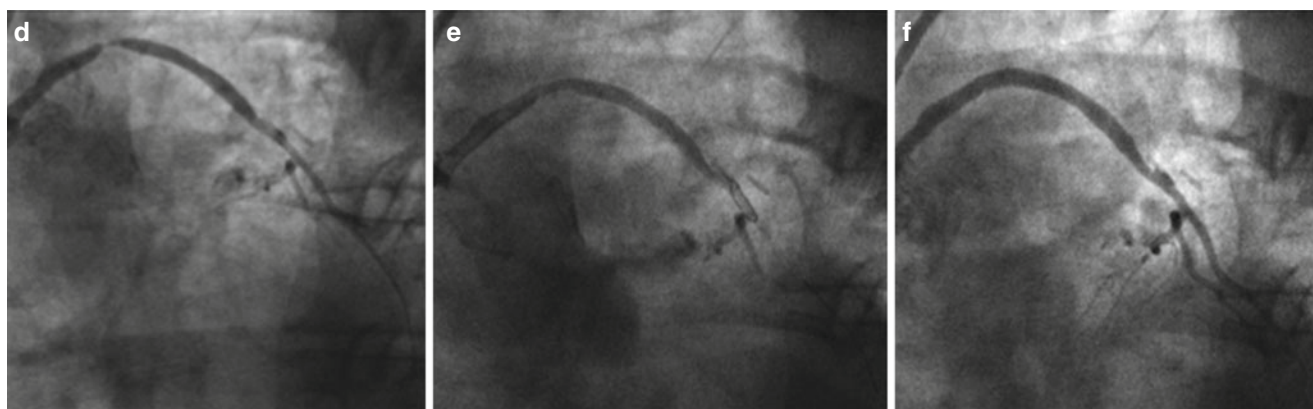


Fig. 5.5 (d) Tight proximal SVG-D1 lesion. (e) After debulking with excimer laser coronary atherectomy. (f) Final result

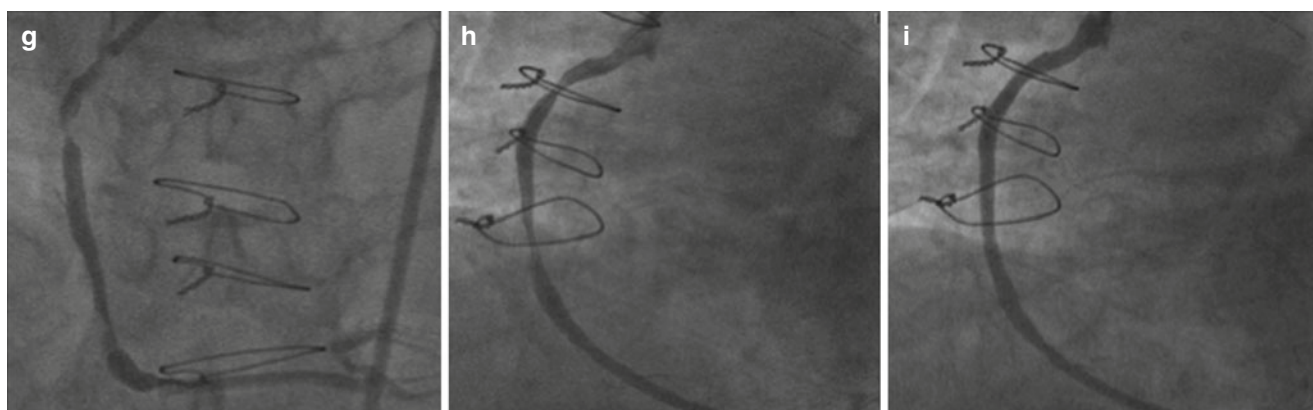


Fig. 5.6 (g) Severe proximal and distal lesions in the RCA-SVG. (h) Following debulking with ECLA. (i) Final result

to his diagonal vein graft. Eight French right femoral arterial access was obtained and a left coronary bypass (LCB) guide catheter (Medtronic) was used to intubate the SVG. A severe proximal lesion with mid-vessel occlusion was demonstrated in the diagonal graft with high thrombus burden and Thrombolysis In Myocardial Infarction (TIMI) flow grade I. Primary use of a distal protection device was precluded by vessel occlusion. A Whisper MS (Guidant) wire was advanced to the distal native diagonal vessel. The Spectranetics CVX-300 (CO, USA) excimer laser catheter system was used to debulk the lesion using a 1.7 mm laser fibre. Vessel recanalization was achieved following several passes with marked debulking and vaporisation of thrombotic material achieving TIMI III flow. The Whisper MS wire was exchanged for a distal protection device (DPD), Filterwire EZ (Boston Scientific, MA, US). The vessel was pre-dilated using a 2.5×12 mm Apex™ (Boston Scientific, Natick, US) balloon, and a 3.5×38 mm drug-eluting stent (Xience Prime; Abbott Vascular, CA, US) was deployed. An excellent angiographic result was achieved with TIMI III flow. There was no measurable rise in CK 24 h post-procedure.

Case 2 (Fig. 5.5)

A 73-year-old male was admitted to hospital with an acute coronary syndrome with ST-segment depression in the posterior ECG leads. He had undergone previous coronary artery bypass grafting with LIMA to LAD, SVG to RCA, SVG to OM and SVG to Diagonal in 1995. Coronary angiography demonstrated a severe proximal lesion in the diagonal vein graft. Using an 8 Fr LCB (Medtronic) guide catheter to intubate the graft, a Whisper MS wire (Guidant) was advanced into the distal native diagonal vessel. Excimer coronary laser atherectomy (ECLA) was performed (Spectranetics CVX-300®) with a 1.7 mm laser fibre. The severe proximal lesion was debulked and the whisper wire was exchanged for a FilterWireEZ™ (Boston Scientific, MA, US) distal protection device that was positioned in the distal graft. A 3.5×12 mm drug-eluting stent (PROMUS Element, Boston Scientific, US) was deployed with excellent angiographic result, TIMI III flow and no measurable CK rise at 24 h.

Case 3 (Fig. 5.6)

A 69-year-old male was admitted for elective PCI to SVG RCA. He had a history of increasing angina with a positive myocardial perfusion scan on a background of previous

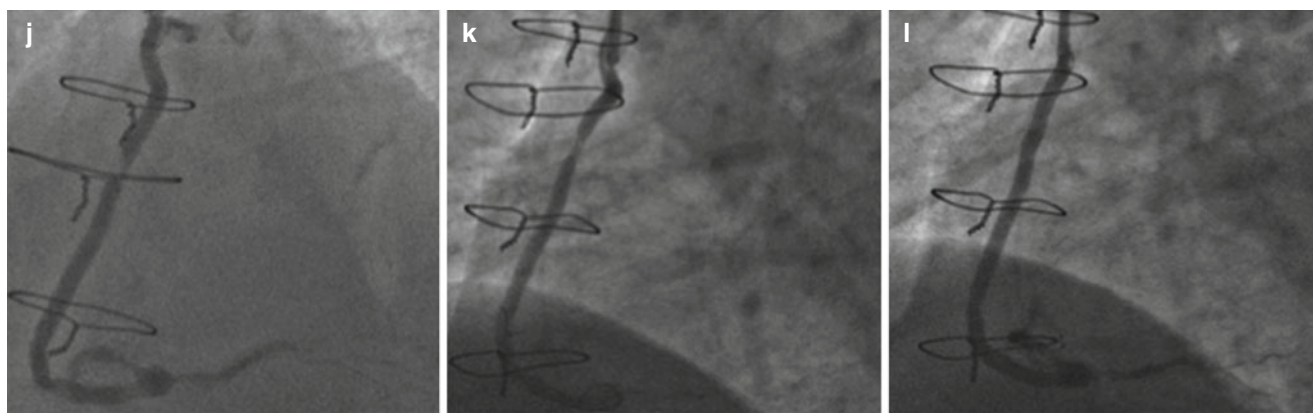


Fig. 5.7 (j) Tight proximal SVG-RCA lesion. (k) Post-excimer laser coronary atherectomy. (l) Final result following deployment of single stent

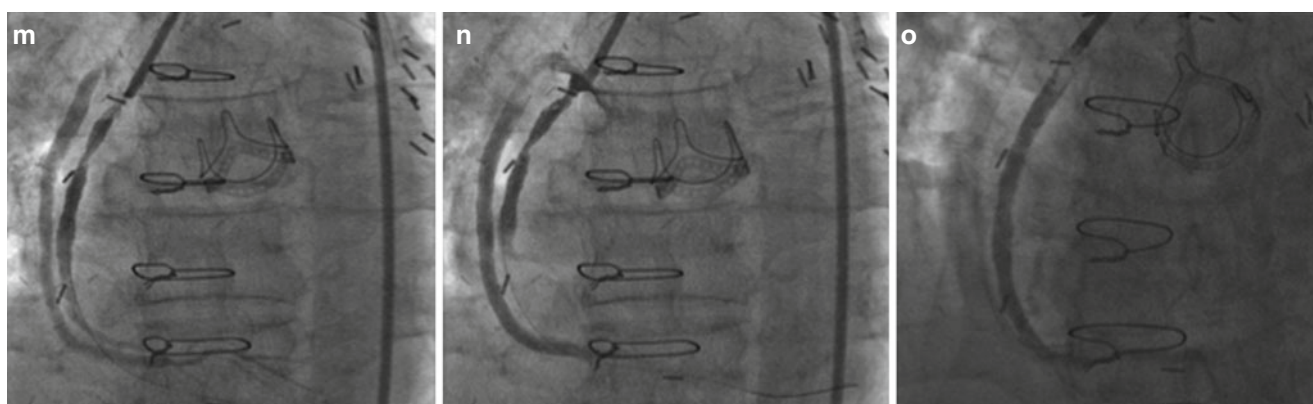


Fig. 5.8 (m) Thrombosed SVG to RCA, patent SVG-PDA with two severe focal lesions. (n) Excimer laser coronary atherectomy. (o) Final result on delivery of single stent

coronary artery bypass graft surgery in 1993 with a LIMA to LAD, SVG to RCA, SVG to Diagonal and SVG to OM. Diagnostic imaging demonstrated proximal occlusion of his native left and right coronary arteries with loss of OM and diagonal grafts, a patent LIMA to LAD with TIMI III flow and an SVG to RCA with two significant stenoses. An 8 Fr Multipurpose A (MPA) catheter was used to intubate the vein graft. A Luge® wire (Boston Scientific, MA, US) was advanced into the distal native RCA. ELCA was performed using a 1.7 mm laser fibre with the CVX-300® laser system (Spectranetics, CO, US). This resulted in considerable debulking of the vessel lesions and sufficient atherectomy to enable positioning of distal protection device, FilterWireEZ™ (Boston Scientific, MA, US). A primary drug-eluting stent (DES) (Taxus™ 3.5×32 mm) was deployed distally at 16 atm, followed by an overlapping DES (Taxus™ 3.5×24 mm) to treat the proximal lesion. Excellent angiographic result was obtained with TIMI III flow and no CK rise at 24 h.

Case 4 (Fig. 5.7)

A 69-year-old male was admitted for elective PCI to SVG-RCA prior to renal transplant surgery for end-stage renal failure. He

had been experiencing progressive exertional chest pain and non-invasive imaging had demonstrated extensive ischaemia. He had undergone coronary artery bypass grafting 18 years previously and diagnostic coronary angiography demonstrated occlusion of all native vessels, with a patent LIMA to LAD and only one remaining SVG to RCA with a tight proximal stenosis. An 8 Fr Multipurpose A (MPA) guide catheter with side holes was used to intubate the SVG-RCA, the tight proximal stenosis precluded use of DPD; a Luge® wire (Boston Scientific, MA, US) was advanced distally and into the native RCA. ELCA was performed using the CVX-300® laser system (Spectranetics, CO, US) and a 2.0 mm laser fibre. FilterWireEZ™ (Boston Scientific, MA, US) was then positioned distally with deployment of a Yukon® 3.5×16 mm drug-eluting stent (Translumina, Germany) inflated to 16 atm and post-dilated using a NC Quantum™ Apex balloon (Boston Scientific, MA, US) to 4.0 mm. Excellent angiographic result was obtained with TIMI III flow and no measurable CK rise at 24 h post-procedure.

Case 5 (Fig. 5.8)

A 73-year-old gentleman attended for elective PCI to his SVG-PDA. This was on a background of increasing angina and max-

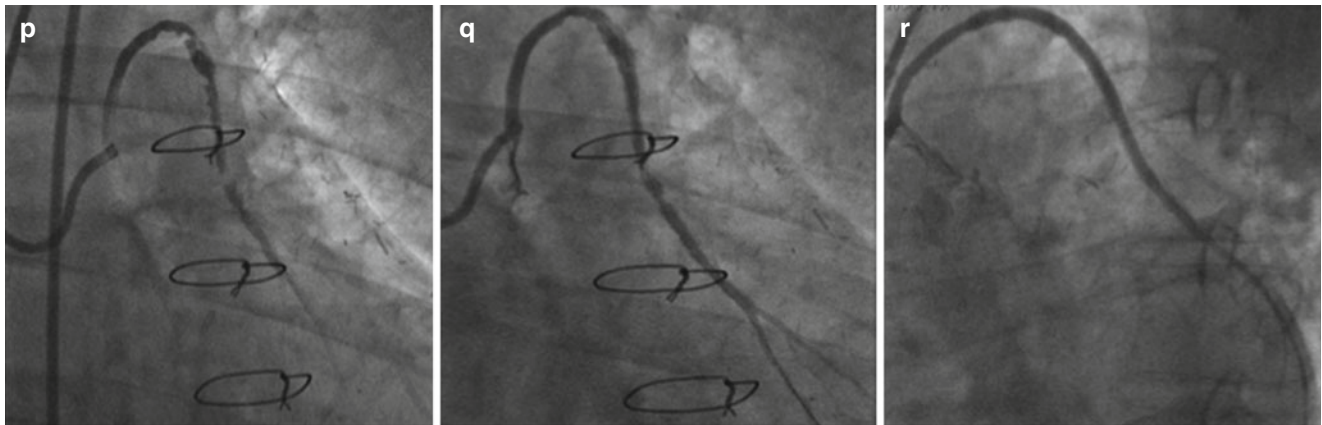


Fig. 5.9 (p) In-stent restenosis of SVG-OM with thrombus burden. (q) Following debulking with ECLA. (r) Final result

imal anti-anginal therapy. Coronary artery bypass grafting had been performed in 1989 with LIMA to LAD, SVG to PDA, OM, circumflex and diagonal vessels. He then underwent redo CABG with SVG to RCA, Circumflex, OM and a free RIMA to his diagonal vessel with a 23 mm Perimount bioprosthetic aortic valve replacement. Diagnostic angiography demonstrated a patent LIMA to LAD, SVG to OM and two severe focal lesions of the SVG-PDA and completely thrombosed previous SVG to RCA. The SVG to PDA was intubated using an 8 Fr MPA guide catheter and a Luge[®] wire (Boston Scientific, MA, US) was advanced distally. ELCA was performed using the CVX-300[®] laser system (Spectranetics, CO, US) with a 2.0 mm laser fibre to debulk the vessel. Luge[®] wire was exchanged for distal protection device FilterWireEZ[™] (Boston Scientific, MA, US), positioned just beyond the second focal lesion. A Liberte 4.0×28 mm bare metal stent was delivered and deployed at 16 atm. Post-dilatation was performed with an NC Quantum[™] Apex balloon (Boston Scientific, MA, US) to 4.5 mm. Good angiographic result was obtained with TIMI III flow with no measurable rise in CK at 24 h.

Case 6 (Fig. 5.9)

A 48-year-old male attended for elective PCI to his SVG-OM. He underwent coronary-artery bypass grafting 7 years previously with LIMA to LAD, SVG to OM and SVG to Cx with PCI to SVG-OM 2 years later. He represented with increasing exertional chest pain and breathlessness, diagnostic angiography demonstrated in-stent restenosis of his proximal SVG-OM stent with high-thrombus burden. Eight French Amplatz Left 1 (AL1) (Cordis Corp, FL, US) guiding catheter with side holes was used to intubate the SVG-OM. Luge wire advanced to the distal native OM. ELCA was performed using a 1.7 mm laser fibre and the Spectranetics CVX-300[®] laser system (CO, US). This resulted in marked debulking of the diseased vein graft with vaporisation of thrombotic material. A distal protection device FilterWireEZ[™] (Boston Scientific, MA, US), was positioned distally just prior to the anastomosis and

three overlapping, TAXUS[®] Liberte[®] drug eluting stents: 3.5×20, 3.5×32, 3.5×24 mm, were deployed in the OM vein graft with excellent angiographic result and TIMI III flow. No measurable rise in CK was demonstrated at 24 h.

Conclusions

Coronary artery bypass grafting has been instrumental in the treatment of coronary atherosclerosis over the last four decades. However, the long term patency of saphenous vein grafts has been disappointing, and redo revascularisation in this cohort of patients is at some considerable risk. The option of percutaneous intervention in these grafts is attractive, although technically challenging due to the unique pathological process observed in the venostenotic phenomenon. The use of distal protection devices has improved both short term procedural success and event free survival, but their utilization is far from ubiquitous. Several anatomical and pathophysiological factors prevent their use in a routine fashion.

Percutaneous excimer coronary laser angioplasty had a difficult early developmental period with widespread use in inexperienced hands leading to poor outcomes. As experience has been gained, registry data has very much supported the use of ECLA as a useful adjunct in the treatment of SVG stenoses. With higher success rates and lower complication rates it is likely that the use of this exciting technology will increase further in the future.

References

1. Favaloro RG. Saphenous vein graft in the surgical treatment of coronary artery disease: operative technique. *J Thorac Cardiovasc Surg.* 1969;58:178–85.
2. Garrett HE, Dennis EW, DeBakey ME. Aortocoronary bypass with saphenous vein graft: seven-year follow-up. *JAMA.* 1973;223:792–4.
3. Motwani JG, Topol EJ. Aortocoronary saphenous vein graft disease. Pathogenesis, predisposition and prevention. *Circulation.* 1998;97:916–31.

4. Campeau L, Enjalbert M, Lesperance J, Bourassa MG, Kwiterovich Jr P, Wacholder S, Sniderman A. The relation of risk factors to the development of atherosclerosis in saphenous vein bypass grafts and the progression of disease in the native circulation: a study 10 years after aortocoronary bypass surgery. *N Engl J Med*. 1984;311:1329–32.
5. Fitzgibbon GM, Kafka HP, Leach AJ, Keon WJ, Hooper D, Burton JR. Coronary bypass graft fate and patient outcome: angiographic follow-up of 5,065 grafts related to survival and reoperation in 1,388 patients during 25 years. *J Am Coll Cardiol*. 1996;28:616–26.
6. Weintraub WS, Jones EL, Craver JM, Guyton RA. Frequency of repeat coronary bypass or coronary angioplasty after coronary artery bypass surgery using saphenous venous grafts. *Am J Cardiol*. 1994;73:103–12.
7. Cao C, Ang SC, Wolak K, et al. A meta-analysis of randomized controlled trials on mid-term angiographic outcomes for radial artery versus saphenous vein in coronary artery bypass graft surgery. *Ann Cardiothorac Surg*. 2013;2(4):401–7.
8. Loop FD, Lytle BW, Cosgrove DM, Woods EL, Stewart RW, Golding LAR, Goormastic M, Taylor PC. Reoperation for coronary atherosclerosis: changing practice in 2509 consecutive patients. *Ann Surg*. 1990;212:378–86.
9. Lee MS, Park S-J, Kandzari DE, et al. Saphenous vein graft intervention. *JACC Cardiovasc Interv*. 2011;4:831–43.
10. Davies MG, Hagen PO. Reprinted article “pathophysiology of vein graft failure: a review”. *Eur J Vasc Endovasc Surg*. 2011;42: S19–29.
11. Quist WC, LoGerfo FW. Prevention of smooth muscle cell phenotypic modulation in vein grafts: a histomorphometric study. *J Vasc Surg*. 1992;16:225e31.
12. Cherian SM, Bobryshev YV, Liang H, et al. Immunohistochemical and ultrastructural evidence that dendritic cells infiltrate stenotic aortocoronary saphenous vein bypass grafts. *Cardiovasc Surg*. 2001;9(2):194–200.
13. Shukla N, Jeremy J. Pathophysiology of saphenous vein graft failure: a brief overview of interventions. *Curr Opin Pharmacol*. 2012;12:114–20.
14. Chen SJ, Wilson JM, Muller DWM. Adenovirus-mediated gene transfer of soluble vascular cell adhesion molecule to porcine interposition vein grafts. *Circulation*. 1994;89:1922–8.
15. Harskamp RE, Lopes RD, Baisden CE, et al. Saphenous vein graft failure after coronary artery bypass surgery. Pathophysiology, management, and future directions. *Ann Surg*. 2013;257:824–33.
16. Rodés-Cabau J, Bertrand OF, Larose E, et al. Comparison of plaque sealing with paclitaxel-eluting stents versus medical therapy for the treatment of moderate nonsignificant saphenous vein graft lesions: the moderate vein graft lesion stenting with the Taxus stent and intravascular ultrasound (VELETI) pilot trial. *Circulation*. 2009;2:1978–86.
17. Rodés-Cabau J. Plaque sealing with paclitaxel-eluting stents for the treatment of moderate non-significant saphenous vein graft lesions. Three-year follow-up of the VELETI (moderate vein graft lesion stenting with the taxus stent and intravascular ultrasound) trial. Paper presented at: i2 Summit 2010, Atlanta, 14 March 2010.
18. Al-Lamee R, Ielasi A, Latib A, et al. Clinical and angiographic outcomes after percutaneous recanalization of chronic total saphenous vein graft occlusion using modern techniques. *Am J Cardiol*. 2010;106:1721–7.
19. Hindnavis V, Sung-Hae C, Goldberg S. Saphenous vein graft intervention: a review. *J Invasive Cardiol*. 2012;24(2):64–71.
20. van Gaal WJ, Banning AP. Percutaneous coronary intervention and the no-reflow phenomenon. *Expert Rev Cardiovasc Ther*. 2007;5(4): 715–31.
21. Baim DS, Wahr D, George B, et al. Randomized trial of a distal embolic protection device during percutaneous intervention of saphenous vein aortocoronary bypass grafts. *Circulation*. 2002;105(11):1285–90.
22. Mathew V, Grill DE, Scott CG, et al. The influence of abciximab use on clinical outcome after aortocoronary vein graft interventions. *J Am Coll Cardiol*. 1999;34(4):1163–9.
23. Roffi M, Mukherjee D, Chew DP, et al. Lack of benefit from intravenous platelet glycoprotein IIb/IIIa receptor inhibition as adjunctive treatment for percutaneous interventions of aortocoronary bypass grafts: a pooled analysis of five randomized clinical trials. *Circulation*. 2002;106(24):3063–7.
24. Baldus S, Koster R, Elsner M, et al. Treatment of aortocoronary vein graft lesions with membrane-covered stents: a multicenter surveillance trial. *Circulation*. 2000;102(17):2024–7.
25. Schachinger V, Hamm CW, Munzel T, et al; STING (STents IN Grafts) Investigators. A randomized trial of polytetrafluoroethylene-membrane-covered stents compared with conventional stents in aortocoronary saphenous vein grafts. *J Am Coll Cardiol*. 2003;42(8): 1360–9.
26. Stankovic G, Colombo A, Presbitero P, et al. Randomized Evaluation of polytetrafluoroethylene COVERed stent in Saphenous vein grafts (RECOVERS) Trial. *Circulation*. 2003;108(1):37–42.
27. Lee MS, Yang T, Kandzari DE, et al. Comparison by meta-analysis of drug-eluting stents and bare metal stents for saphenous vein graft intervention. *Am J Cardiol*. 2010;105:1076–82.
28. Giugliano GR, Kuntz RE, Popma JJ, Cutlip DE, Baim DS. Determinants of 30-day adverse events following saphenous vein graft intervention with and without a distal occlusion embolic protection device. Saphenous Vein Graft Angioplasty Free of Emboli Randomized (SAFER) Trial Investigators. *Am J Cardiol*. 2005;95(2):173–7.
29. Sturm E, Goldber G, Goldberg S. Embolic protection devices in saphenous vein graft and native vessel percutaneous intervention: a review. *Curr Cardiol Rev*. 2012;8:192–9.
30. Stone G, Rogers C, Hermiller J, et al. Randomized comparison of distal protection with a filter-based catheter and a balloon occlusion and aspiration system during percutaneous intervention of diseased saphenous vein aorto-coronary bypass grafts. *Circulation*. 2003; 108:548–53.
31. Dixon SR. Saphenous vein graft protection in a distal embolic protection randomized trial. Paper presented at: Transcatheter Cardiovascular Therapeutics, Washington, DC, Oct 2005.
32. Mathew V, Lennon RJ, Rihal CS, Bresnahan JF, Holmes Jr DR. Applicability of distal protection for aortocoronary vein graft interventions in clinical practice. *Catheter Cardiovasc Interv*. 2004;63:148–51.
33. Ebersole D, Dahm JB, Das T, et al. Excimer laser revascularisation of saphenous vein grafts in acute myocardial infarction. *J Invasive Cardiol*. 2004;16(4):177–80.
34. Levine GN, Bates ER, Blankenship JC, Bailey SR, Bittl JA, Cercek B, Chambers CE, Ellis SG, Guyton RA, Hollenber SM, Khot UN, Lange RA, Mauri L, Mehran R, Moussa ID, Mukherjee D, Nallamothu BK, Ting HH. 2011 ACCF/AHA/SCAI Guideline for Percutaneous Coronary Intervention: a report of the American College of Cardiology Foundation/American Heart Association Task Force on Practice Guidelines and the Society for Cardiovascular Angiography and Interventions. *Circulation*. 2011;124(23):e574–651.
35. Topaz O, Das T, Dahm J, et al. Excimer laser revascularisation: current indications, applications and techniques. *Laseres Med Sci*. 2001;16(2):72–7.
36. Litvack F, Grundfest WS, Goldenberg T, et al. Percutaneous excimer laser angioplasty of aortocoronary saphenous vein grafts. *J Am Coll Cardiol*. 1989;14(3):803–8.
37. Eigler NL, Weinstock B, Douglas JS, et al. Excimer laser coronary angioplasty of aorto-ostial stenoses. Results of the excimer laser coronary angioplasty (ELCA) registry in the first 200 patients. *Circulation*. 1993;88:2049–57.
38. Bittl JA, Sanborn TA, Yardley DE, et al. Predictors of outcome of percutaneous excimer laser coronary angioplasty of Saphenous vein bypass graft lesions. The Percutaneous Excimer Laser Coronary Angioplasty Registry. *Am J Cardiol*. 1994;74(2):144–8.
39. Topaz O, Ebersole D, Das T, et al. Excimer laser angioplasty in acute myocardial infarction (the CARMEL multicentre trial). *Am J Cardiol*. 2004;93:694–701.

40. Strauss BH, Natarajan MK, Batchelor WB, et al. Early and late quantitative angiographic results of vein graft lesions treated by excimer laser with adjunctive balloon angioplasty. *Circulation*. 1995;92:348–56.
41. Holmes DR, Mehta S, Geogre CJ, et al. Excimer laser coronary angioplasty: the New Approaches to Coronary Intervention (NACI) experience. *Am J Cardiol*. 1997;80(10A):99K–105.
42. Köster R, Hamm CW, Seabra-Gomes R, et al. Laser angioplasty of restenosed coronary stents: results of a multicenter surveillance trial. *J Am Coll Cardiol*. 1999;34:25–32.
43. Ahmed JM, Hong MK, Mehran R, et al. Comparison of debulking followed by stenting versus stenting alone for saphenous vein graft aortoostial lesions: immediate and one-year clinical outcomes. *J Am Coll Cardiol*. 2000;35:1560–8.
44. Ajani AE, Waksman R, Kim H-S, et al. Excimer laser coronary angioplasty and intracoronary radiation for in-stent restenosis: six-month angiographic and clinical outcomes. *Cardiovasc Radiat Med*. 2001;2:191–6.
45. Dahm JB, Ebersole D, Das T, et al. Prevention of distal embolisation and no-reflow in patients with acute myocardial infarction and total occlusion in the infarct-related vessel: a subgroup analysis of the cohort of acute revascularisation in myocardial infarction with excimer laser – CARMEL multicentre study. *Catheter Cardiovasc Interv*. 2004;64:67–74.
46. Giugliano GR, Falcone MW, Mego D, Ebersole D, Jenkins S, Das T, Barker E, Ruggio JM, Maini B, Bailey SR. A prospective multicenter registry of laser therapy for degenerated saphenous vein graft stenosis: the COronary graft Results following Atherectomy with Laser (CORAL) trial. *Cardiovasc Revasc Med*. 2012;13(2):84–9.
47. Niccoli G, Belloni F, Cosentino N, et al. Case-control registry of excimer laser coronary angioplasty versus distal protection devices in patients with acute coronary syndromes due to SVG disease. *Am J Cardiol*. 2013;112:1586–91.

Waleed Alharbi and Luc Bilodeau

Introduction

Calcified coronary and peripheral vessel stenosis are one of the leading causes of mortality and morbidity in US. Despite being a relatively common problem, vascular calcification has been underappreciated. Due to suboptimal procedural results and poor clinical outcomes, including high major adverse cardiovascular events and angiographic complications, most drug-eluting stent clinical trials have excluded moderate to severe calcified lesions. Another challenging aspect is that angiography underestimates the presence, extent and axial depth of calcium, which makes other imaging modalities such as IVUS a valuable aid in assessment of calcified lesions. Debulking technique is occasionally an essential facilitator as endovascular treatment in subset of patients with such complex coronary or peripheral vessel lesions where the straightforward dilatation and stenting of vessel are not feasible. Plaque shift, uncrossable lesions and undilatable vessels are possible challenges to the simple PTCA and PCI. To avoid balloon failure, technical failure, incomplete revascularization or complications, excimer laser coronary angioplasty is an attractive additional resource to deal with these challenging lesions. Herein, we will discuss the decision matrix, detailed technique and the role of ELCA in calcified lesions.

W. Alharbi, MD, FRCPC (✉)
Libin Cardiovascular Institute of Alberta,
Foothills Interventional Cardiology Service,
Foothills Medical Center, University of Calgary,
Room C805, 1403 29 Street NW,
Calgary, AB T2N 2T9, Canada
e-mail: WALEED.ALHARBI@me.com

L. Bilodeau, MD, FRCPC
Cardiac Catheterization Laboratory, Cardiology Department,
Royal Victoria Hospital, McGill University,
687 Pine Ave, Montreal, QC H3A 1A1, Canada
e-mail: luc.bilodeau@mcgill.ca

Historical Considerations

Twenty years ago, the excimer laser coronary angioplasty developed and introduced as one of the potential competitors to balloon angioplasty for the treatment of stenotic coronary arteries. ELCA designed to ablate the obstructive atherothrombotic plaque compared to PTCA, which increases vessel lumen dimension. However, ELCA has been plagued by technical challenge and serious concerns regarding complications compared to PTCA. When the coronary stents emerged as superb procedure in regards of safety outcomes and lower restenosis rates, ELCA technology faded out of interest and became limited to subsets of specific lesions such as undilatable lesions, diffuse in-stent restenosis and chronic total occlusions. The setback caused no further development in design technology of ELCA over the years regarding safety and efficacy.

The renaissance of ELCA technology is dependent on its mere use as debulking and crossing tool in heavily calcified CTOs with the emergence of improved techniques to treat CTOs percutaneously rather than coronary artery bypass graft surgery. We believe with further improvement in adaptability, availability and teachability of ELCA technique, could lead to dramatically increased number of successful challenging CTO revascularizations (Fig. 6.1).

Laser Technology Design

LASER stands for light amplification by stimulated emission of radiation. The energy produced by laser is from an excited active medium such as Xenon Chloride by an electrical energy and emits either continuous or pulsed monochromatic, coherent light. This is the basic principle in all laser energy applications. In coronary application the only approved laser system is a pulsed excited dimer (excimer) laser system that utilizes Xenon Chloride with wavelength of 308 nm. The utility of using ultraviolet light lies in its short penetration depth of 50 micromillimeters. Tissue ablation

Fig. 6.1 Major uses of ELCA in the current era is what make this modality significant nowadays

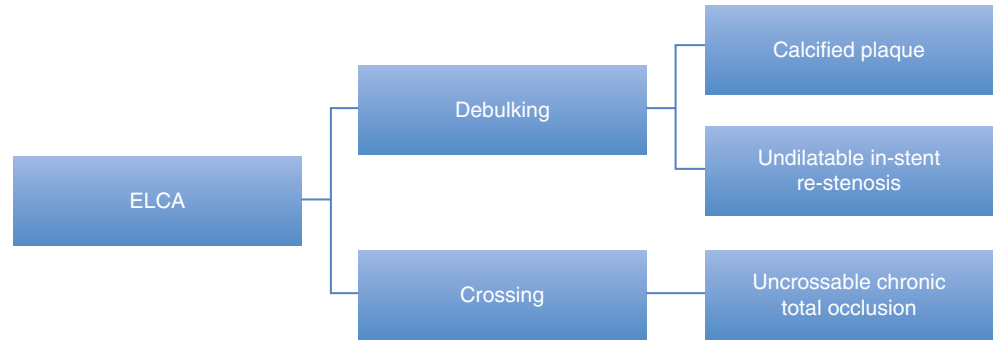
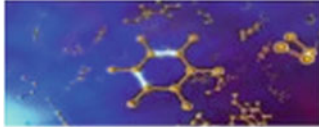

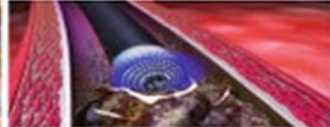


Fig. 6.2 Mechanisms of action for ELCA

Three mechanisms of action

1	2	3
Photochemical	Photothermal	Photomechanical
Breaking molecular bonds	Producing thermal energy	Creating kinetic energy
		

takes place by one of three major mechanisms of action by ELCA: photochemical (breakdown of molecules), photothermal (vaporization of tissue) and photomechanical (Fig. 6.2). Each ELCA mechanism of action is optimal for specific target tissue type. With each pulse of energy from the excimer laser catheter, 10 micromillimeters of tissue layer is eliminated. The beauty of this technology is only the contacted tissue is ablated without surrounding tissue damage. For calcified lesions, the photomechanical action is the main implicated action for calcified vessel lesions. Localized atheroablation executed by ELCA can be observed in intravascular ultrasound examination [1]. ELCA actually in addition changes vessel compliance [2]. As in the (Fig. 6.3), by IVUS the lumen area increases post laser administration where 45 % of the gain came from plaque removal and 55 % came from vessel compliance expansion.

Calcified Lesion Morphology

To understand the calcified lesion “anatomy” will start to understand the main differences of atherosclerotic intimal calcification versus medial calcification (Table 6.1) [3]. Atherosclerotic calcification is lipid driven disease with

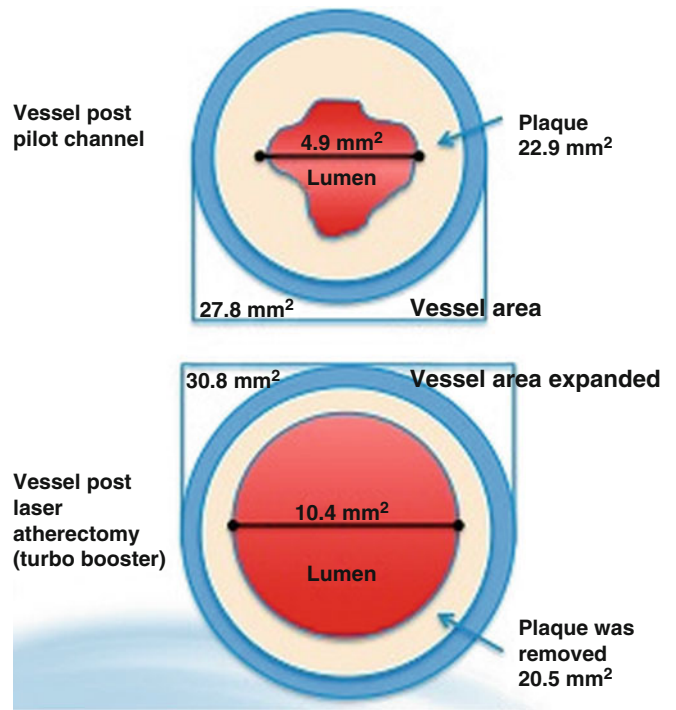


Fig. 6.3 Cartoon demonstration of vessel lumen pre and post ELCA use

small and focal calcified deposits, which commonly seen in coronary arteries [4]. Medial calcification (Monckeberg's sclerosis) in the other hand, the calcification occurs in smooth muscle cell commonly seen in peripheral arteries (Fig. 6.4). Medial calcification is primarily believed to be in response to metabolic and hormonal dysfunction, where long sheets of calcium along the elastin fibers in the media are formed (Fig. 6.5) [5]. The problem with medial calcification, that it can encompass the entire vessel circumference causing stiffening of the vessel [6, 7]. Surprisingly medial calcification is widely prevalent in peripheral artery disease up to 77 % of all vessels with atherosclerotic plaques. The literature showed wide variability in prevalence of calcium in peripheral arterial disease 32–75 %, but the severe form of calcification was found in medial calcification cohort compared to intimal atherosclerotic calcification which mostly soft material [7]. The disparity in medial versus intimal atherosclerotic calcium is found larger in diabetics [8]. Only 10 % with severe intimal calcium and 80 % had no or sparse calcium compared to 100 % severe medial calcification (Table 6.2).

Table 6.1 Pathological difference between atherosclerotic and medial calcification

Atherosclerotic (Subintimal lipid driven disease)	Medial Calcium (metabolic, smooth muscle cells regulated disease)
Eccentric	Concentric
Lumen deforming	Vessel stiffening
Fibrous intimal cap	Medial fibrosis & calcification
Small, focal calcium deposits	Sheets of calcium along elastin fibers

Medial calcification correlated to the most difficult patient populations and it is highly correlated to cardiac risk factors such as diabetes, smoking, dyslipidemia, end-stage renal disease and coronary artery disease [9–11]. Recognizing this entity is paramount because trying to remove medical calcium directly would be ineffective and has a high risk of triggering restenosis and vessel damage especially in the severe form due to subintimal tear from balloon injury, which subsequently will cause restenosis [12]. ELCA still an option if the case did not show evidence of severe luminal calcification with cobblestone in multiple quadrants as assessed by IVUS, which are markers of hard heavily calcific vessel with high risk of complications (Fig. 6.6) is an overview decision tree when facing with calcification. Vascular calcified lesions harbors broad known complications:

1. Prone to dissection during balloon angioplasty or predilation [13].
2. Difficulty to completely dilate [14].
3. Prevent adequate stent expansion [15].
4. May result in stent malapposition [16].
5. Insufficient drug penetration and subsequent restenosis [17].
6. Perforation
7. Restenosis due to excessive balloon dilation.

Patient Selection

The main use of laser revascularization are two major utilities: As debulking tool and crossing tool to facilitate the preparation of the action area for stenting, form a channel to

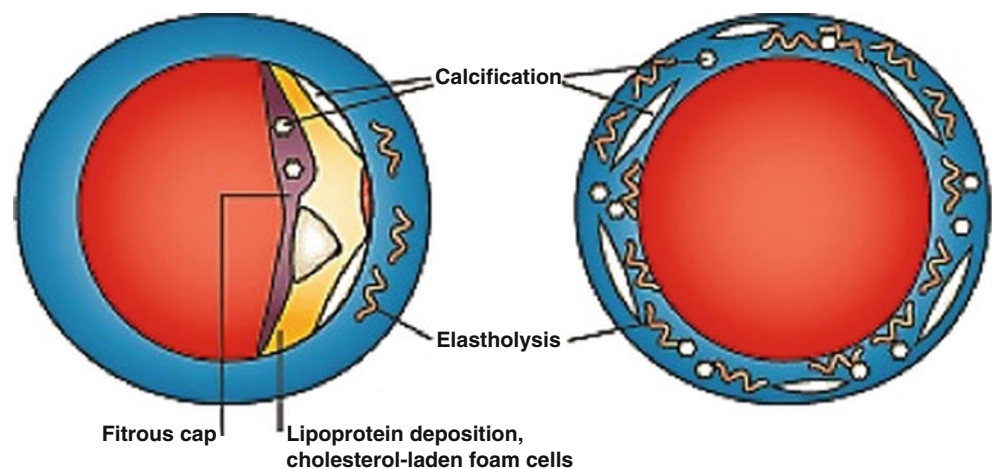


Fig. 6.4 Atherosclerotic vs. medial calcification

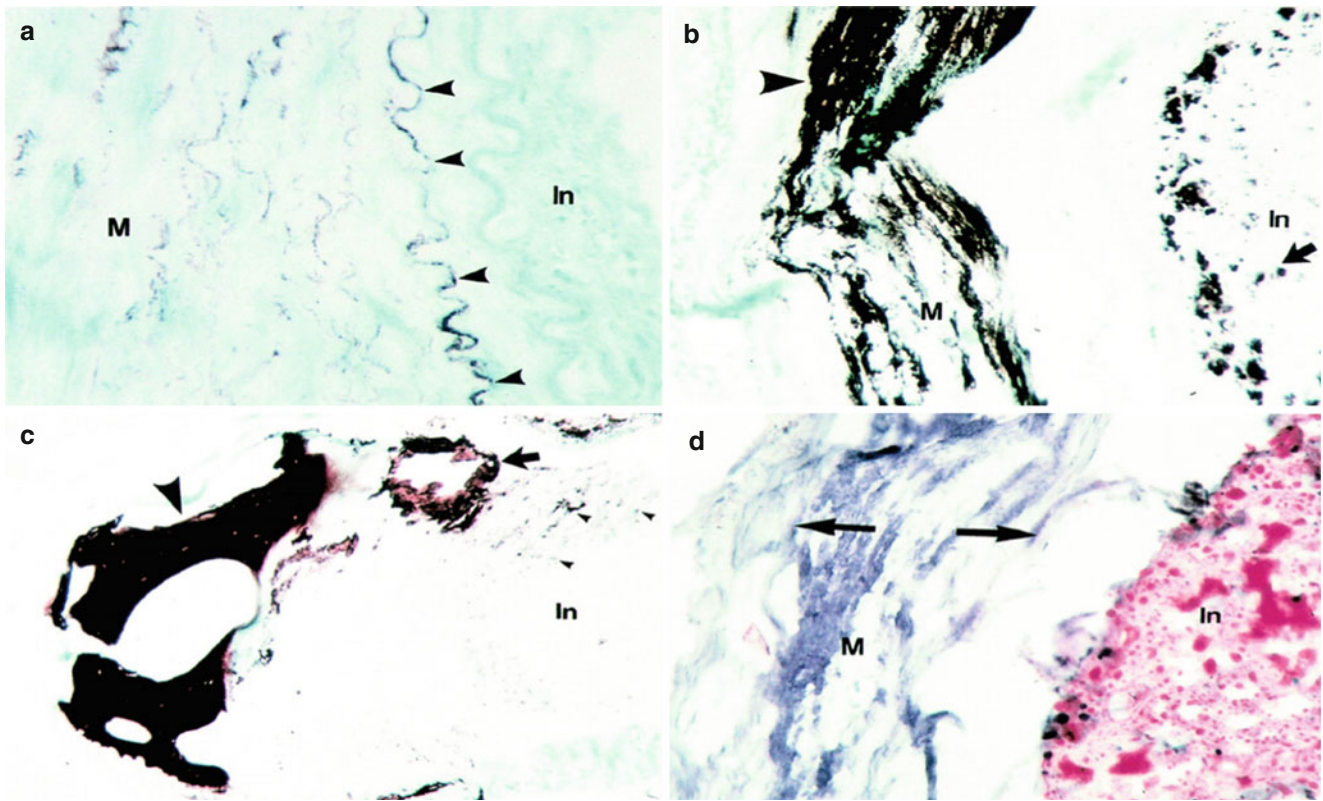


Fig. 6.5 Histopathological differences between medial and intimal calcification. (a) Presence of mild medial calcium but no intimal calcium present. (b) Presence of advanced medial calcium with evidence of focal intimal calcification. (c) Presence of severe medial calcification

with bone formation and evidence of sparse intimal calcium. (d) Presence of heavy medial calcification with sparse intimal calcification and high lipid content

Table 6.2 Incidence of calcification severity between intimal and medical calcification

Degree of calcification	Medial calcium (Monckeberg's sclerosis)	Intimal calcium (atherosclerosis)
None	36 % (all non diabetics)	64 %
Sparse	5 %	18 %
Mild/Moderate	9 %	9 %
Severe	50 % (100 % in diabetics)	9 %

cross the lesion and to tackle with improperly expanded coronary stent. The following lesion subsets are mainly indicated in ELCA:

In-Stent Restenosis

ELCA is an ideal technique for lesions that an adequately sized stent is not able to expand the lesion completely despite high pressures of up to 20 atm or more, where the unique capability of ELCA in preparing non-compliant plaque lesions for stenting proved efficacious and powerful aid. ELCA competes with rotational atherectomy or cutting-balloon catheters for this indication [18, 19]. The reason behind that, its ablative role and its induction of imploding

vapour bubbles which creates microfissures to the obstructive plaque which allow complete balloon inflation during post-dilatation. For non-compliant plaques already stented where high-pressure balloon, buddy wire balloon inflation or cutting balloon inflation have failed to optimize stent implantation, ECLA remains the only choice of treatment.

Uncrossable Chronic Total Occlusions

Traditionally, chronic total occlusions have been one of the challenging lesion subsets in percutaneous vessel intervention. Some of these CTOs have calcified, densely fibrotic, angulated or severely stenotic artery lesions are uncrossable by the smallest balloons preventing proper dilatation (Fig. 6.7). The estimated wired lesions not be crossed by balloons is 1–2 %. The interventionist will start to entertain other options for treating an uncrossable CTO such as CABG, medical therapy or using other multiple CTO tools exist for the challenging uncrossable CTO lesion profile such as development of smallest balloon catheter crossing profile, single marker balloon, rotational atherectomy, Tornus catheter (Asahi Intec Co) and ELCA.

The use of ELCA in CTO is to achieve two major goals. First is debulking for preparation of the vessel for balloon

Fig. 6.6 Angiographic, pathological and Histopathological correlation in different types of vessel lesions

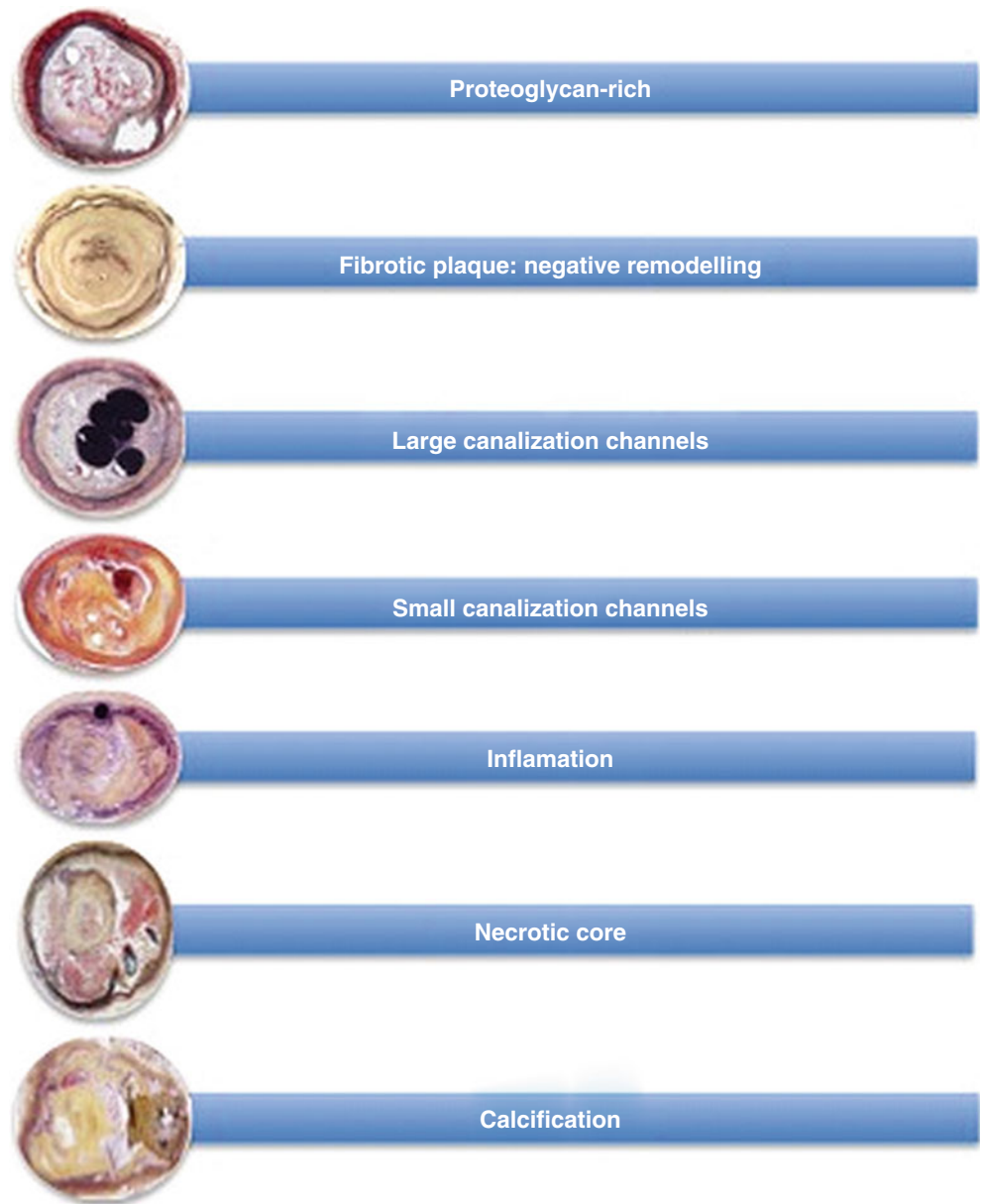
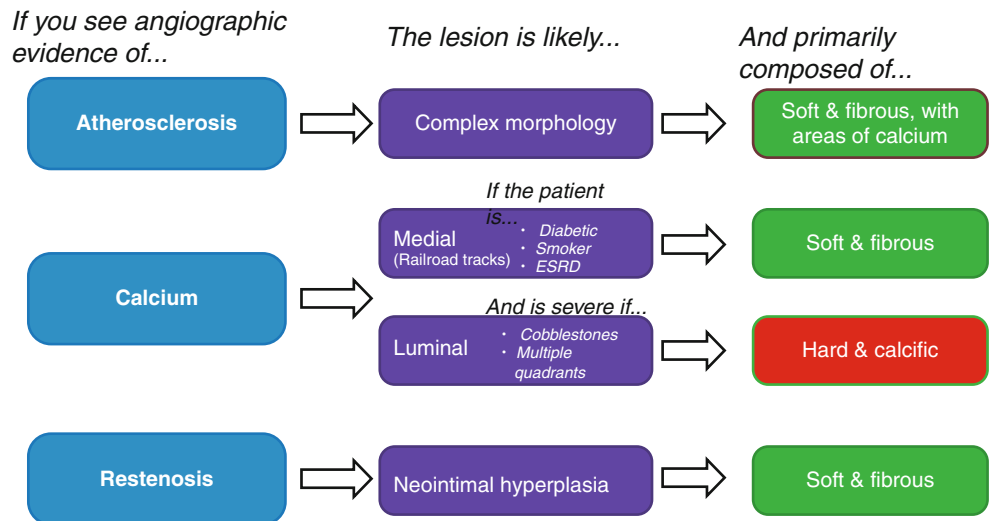


Fig. 6.7 Spectrum of Lumen Morphology in CTO

Table 6.3 Comparison between different ELCA catheter types and sizes

Device description	0.9 mm RX	0.9 mm RX	1.4 mm RX	1.7 mm RX	2 mm RX	1.7 mm E RX	2 mm E RX	0.9 mm OTW	0.9 mm OTW
Tip Design	Concentric	X-80 Catheter	Concentric	Concentric	Concentric	Eccentric	Eccentric	Concentric	X-80 catheter
Max guidewire compatibility	0.014	0.014	0.014	0.014	0.014	0.014	0.018	0.014	0.014
Max tip outer diameter	0.038	0.038	0.057	0.069	0.080	0.069	0.079	0.038	0.038
Shaft diameter	0.049	0.049	0.062	0.072	0.084	0.072	0.084	0.049	0.049
Guide catheter Compatibility	5 Fr	5 Fr	7 Fr	7 Fr	8 Fr	7 Fr	8 Fr	5 Fr	5 Fr

crossing with low distal embolization rate compared to other debulking devices. Second is lesion modification for optimizing stent apposition. Even after successful wire passage across a CTO PCI is sometimes limited similarly by the inability to pass with a balloon catheter. In this particular setting ELCA is a valuable option since, in contrast to rotational atherectomy, it can be advanced along standard guidewires. The laser can create a channel through the CTO, which allows a balloon catheter to pass afterwards in order to facilitate final vessel reconstruction by stent implantation [19].

A subgroup analysis of the randomized AMRO trial in patients with functional or total coronary occlusions >10 mm evaluated the safety and efficacy of ELCA plus PTCA versus PTCA alone [20]. Angiographic success rates were similar in both groups at 65 and 61 %. Net lumen gain at 6 months was also not significantly different (0.81 ± 0.74 mm versus 1.04 ± 0.68 mm), whilst there was at least a trend towards a lower restenosis rate in the PTCA group alone (48.5 % versus 66.7 %; $p=0.15$). A special 018-in. laser wire was introduced to address those CTOs, which cannot be passed with standard or dedicated crossing wires [21]. This wire was quite rigid and wire exits during the crossing attempt were not infrequent.

Equipment

Laser Catheters

Laser catheters are available as rapid exchange devices or over-the-wire. The laser catheter consists of 50 μ m fibers that arranged either in eccentric or concentric fashion around 0.014-in. guidewire or 0.018 in. for the 2 mm eccentric laser catheter. The eccentric ELCA catheters were developed to increase the size of ablation and deals with eccentric coronary lesions. The operator targets these eccentric lesions by rotating the eccentric ELCA catheter and apposes the lasing part of the catheter tip towards the plaque eccentric lesion. The recommended laser size

catheter size should not exceed 50 % the reference vessel diameter, though 0.9 mm catheter size 0.9 mm is mainly used in most cases. The laser wire 0.018 and 0.7 mm concentric catheter were abandoned due to complications from inconsistent energy delivery with 0.7 mm catheter. Detailed catheter sizes and comparison between them in this following (Table 6.3). These laser catheters evolved over time in design to achieve homogenous distribution of light to reduce vessel wall trauma and less energy density without losing tissue penetration efficacy by designing thicker laser fibers and minimizing dead space around the fibers in the ELCA catheter [22].

Technical Strategy

General Steps of ELCA Procedure

- Confirm the patient received dual antiplatelet therapy at least 6 h before the procedure in elective cases.
- The laser unit should be set up and the warm-up time started for 5 min.
- Patient and all personnel in the catheterization laboratory must wear laser eye protection glasses.
- Calibration of the intended laser catheter size.
- Establish vascular access
- Administration of unfractionated heparin to achieve target activated clotting time of 300 s.
- Choose guide catheter sizes according to the planned ELCA catheter size.
- Position the guide catheter in the ostium of the target arterial vessel.
- Secure correct guidewire positioning in the vessel lumen and should be passed across the target lesion under fluoroscopic guidance.
- The laser catheter is then advanced over the wire to come into contact with the target lesion and insure proper back up either active or passive from guiding catheter to properly apply laser therapy on target lesion.

- Guide catheter is flushed with at least 10–20 cc of normal saline to wash out blood or contrast (Flush & Bathe Technique.)
- First pass laser activation should be performed with a fluence of 45 mJ/mm² and a repetition rate of 25 Hz.
- If resistance noticed, fluence and repetition rates can be increased to a maximum fluence of 80 mJ/mm² and repetition rate of 80 Hz depending on the laser catheter used. Also, could use laser without flush to get increased local reaction.
- During each lasing pass continuous infuse 1 cc/s normal saline in the guide catheter, or no flush in resistant lesions.
- During laser activation the ELCA catheter is advanced slowly at 0.5–1 mm per second.

Coronary Optimal Revascularization Strategy

1. Calcified plaque (high energy 100 %):

- (a) Laser energy emitted from the catheter tip was calibrated at 35–60 mJ/mm². Experience showed that higher-energy fluences are often required for successful ablation, particularly with heavily calcified lesions, which treated with energy fluences of 45–50 mJ/mm²; even higher fluences were used if the lesion was heavily calcified or attempted laser angioplasty at a lower fluence was unsuccessful.
- (b) After calibration of laser tip energy, the laser catheter was advanced over the guidewire until it reaches immediately proximal to the lesion. Under fluoroscopic control, the laser catheter is advanced slowly across the lesion while laser pulses were delivered at 20 Hz.
- (c) After each passage through the lesion, the catheter was withdrawn, and angiographic contrast was injected. Multiple passes were might be required through the lesion based on angiographic debulked area.

2. **Uncrossable calcified lesions (regular energy):** In the attempt of trying to cross a lesion with wire but unsuccessful in crossing the lesion with a balloon that's define uncrossable lesions. In this type of lesions, using laser facilitates in preparing the lesion for balloon passage. The steps of recanalization uncrossable lesion has five major general milestones:

- (a) Crossing proximal fibrous cap:

With the laser wire 0.9 mm X-80 catheter, you create a channel for the balloon to cross the occlusion and penetrate the proximal cap. Then, exchange for

conventional wire and advance wire to distal cap. If conventional wire will not penetrate distal cap, exchange again for laser wire. Rather than drilling the distal cap with stiff wire, an attempt to puncture the cap with a forward movement directed exactly perpendicular to the tangent of the convex curvature of the cap. This is the advantage of laser wire where it can penetrate distal fibrous cap without need for rotation.

- (b) Crossing distal fibrous cap

- (c) Crossing lesion with balloon

- (d) Opening lesion to prepare the lesion for stenting

3. Suboptimal non-dilatable stent (high energy, no flush and Bathe technique)

Calcified balloon-resistant coronary lesion is an important cause of stent underexpansion if the lesion is not well prepared for stenting. Laser could play a major role in facilitating stent expansion in balloon resistant lesions. The steps are as follow [23]:

1. Perform pre-dilatation with a non-compliant balloon prior to ECLA of the target lesion. Once balloon underexpansion was confirmed at angiography, calibration of the catheter was then performed and the desired energy level was set up.
2. The ELCA catheter (Turbo Elite catheter®, 0.9–2.0 mm; Spectranetics Corporation, Colorado Springs, CO, USA) used to pass over the guidewire, then inserted within the stent and advanced slowly toward the underexpanded zone. The catheter tip is maintained in close contact with the undilatable zone without necessarily crossing the lesion. The speed of this advancement was limited to 0.5–1.0 mm per second to avoid dotter effects, dissections and suboptimal ablation.
3. The laser 6 Fr-compatible catheter incorporates 65 concentric 50 lm fibers with the potential of delivering excimer energy from 30 to 80 mJ/mm (fluence) at pulse repetition from 25 to 80 Hz, using a 10-s on and 5-s off lasing cycle [24].
4. For example you can start with laser energy at 60 fluence and 40 Hz. Laser energy is then increased to 80 fluence and 80 Hz for two additional sequences without applying the classical “flush and bathe” technique, which is usually used to replace all blood and contrast within the vessel with crystalloid before activating the laser to decrease vapour bubble formation and its corresponding acousto-mechanical trauma.

An illustrated example of a technical strategy of suboptimal stent deployment case using excimer laser is in Figs. 6.8, 6.9, 6.10, 6.11, and 6.12 [24].

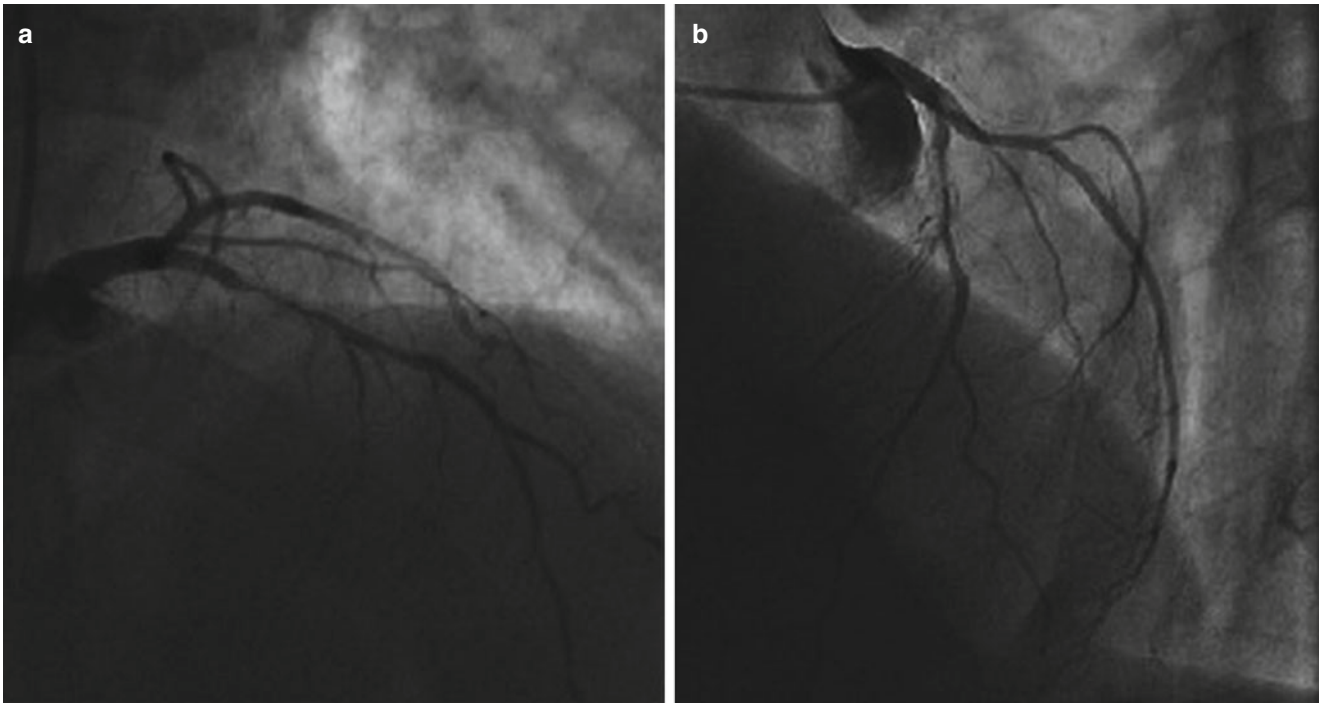


Fig. 6.8 (a, b) Diagnostic coronary angiogram in both RAO cranial (*Right*) and LAO cranial (*Left*) showing severe diffuse in-stent restenosis (Mehran classification type II) in the proximal segment of the bare-metal stent in the mid left anterior descending

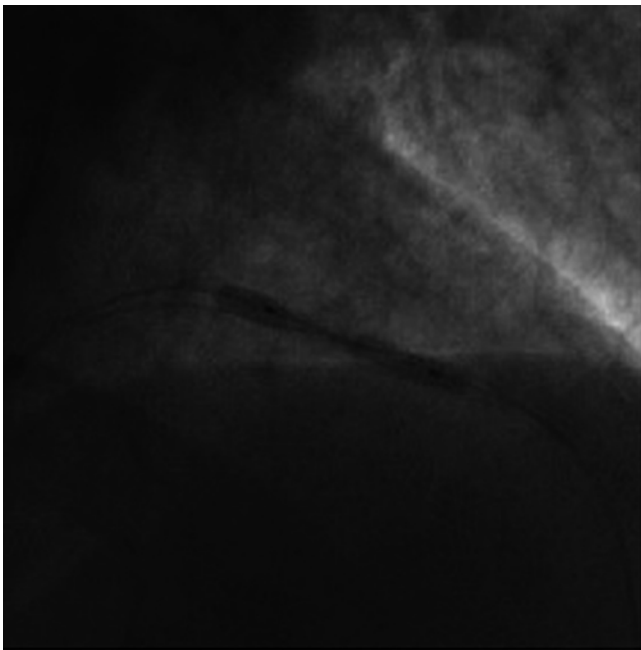


Fig. 6.9 In-stent restenosis with stent underexpansion, which could not be disrupted by repeated high atmosphere balloon inflations

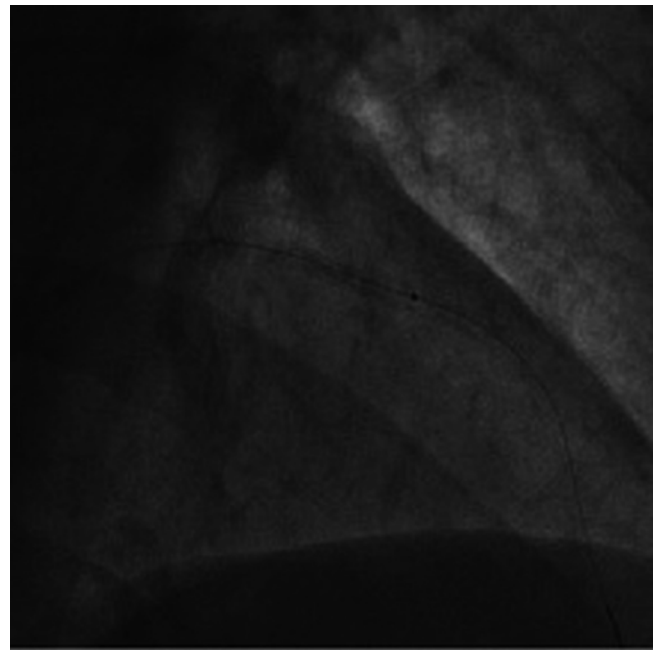


Fig. 6.10 Excimer laser use started with laser energy at 60 fluence and 40 Hz. Laser energy was increased to 80 fluence and 80 Hz for two additional sequences without applying the classical “flush and bathe” technique

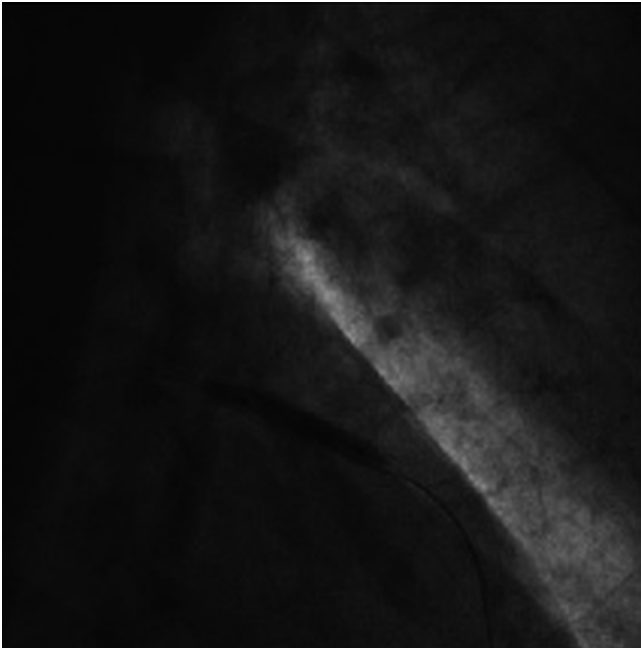


Fig. 6.11 After excimer use, complete balloon expansion resulted in fully expanded stent

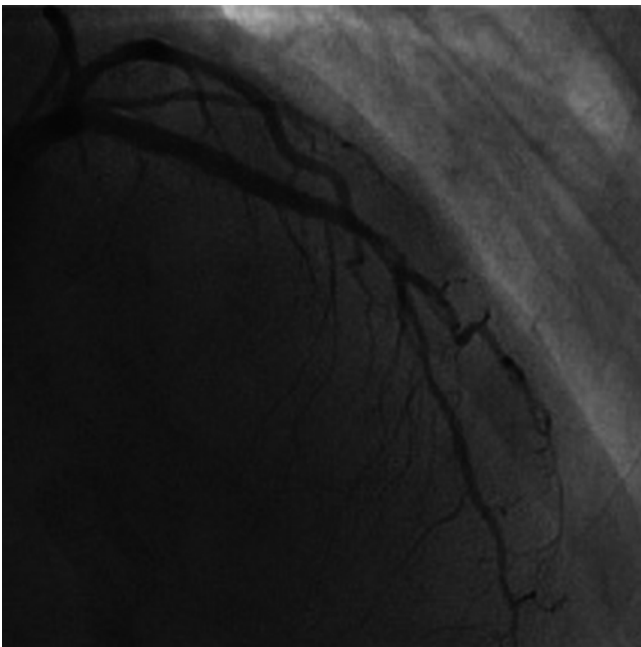


Fig. 6.12 Final result after excimer laser and drug-eluting stents implantation showing no residual stenosis and complete apposition of the stents to the vessel wall in the RAO cranial view

Peripheral Optimal Revascularization Strategy

Laser “Step-By-Step” Technique Figs. 6.13 and 6.14

This technique first described by Biamino and Schinert [25]. This technique not performed in coronary revascularization technique due to high perforation risk in this anatomical subset compared to peripheral arterial vessels. The concept of the “Step-By-Step” technique involves use of ELCA ahead of the wire to cross the uncrossable lesions or occlusions with concentric laser and use of support catheter. The technique is particularly beneficial in superficial femoral artery CTOs to enter flush occlusions without visible stump or to pass a segment that was resistant to crossing with a guide-wire. The steps as follows:

1. **Angiographic assessment:** The initial angiogram assessment used to determine feasibility of the ELCA procedure by assessing the following Fig. 6.15:
 - (a) Vessel take off
 - (b) Vessel stump
 - (c) Visibility of target vessel
2. **Wire insertion:** insert hydrophilic wire 0.018/0.035 wire and do the following:
 - (a) Approximate the proximal cap as accurately as possible
 - (b) Look for wire buckle or prolapse for angiographic confirmation. Be careful not to force the wire, it may create subintimal track, which laser will follow.
3. **Laser positioning:** Fig. 6.16
 - (a) Initially position the laser catheter proximal and directly on top of the occlusion with wire inside laser catheter.
 - (b) Ensure the laser tip is not forced into dissection track or off-center.
 - (c) Lead with the wire 1–2 mm ahead of the laser catheter.
4. **Initial laser activation:** Fig. 6.17
 - (a) Activate Laser 5–10 s without advancing with setting 45/25 that assists in modifying the resistant proximal cap.
 - (b) Attempt wire advancement slowly (proceeding <1 mm/s)

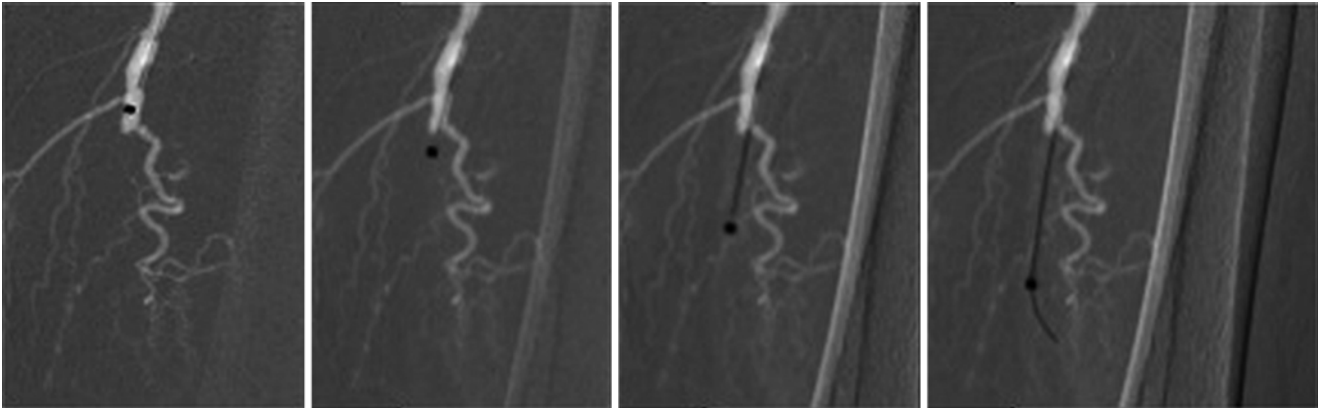


Fig. 6.13 Step-by Step Technique of superficial femoral artery

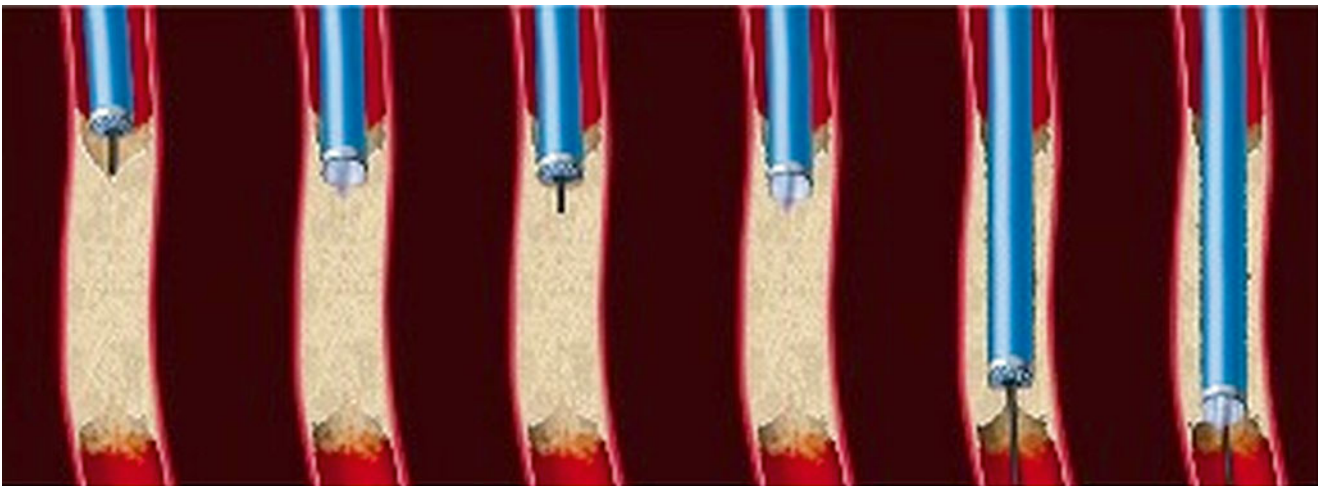


Fig. 6.14 Cartoon illustration of “Step-by-Step Technique”

5. **Initial wire advancement:** if successful continue passing wire distally into the lumen until either recanalize into distal bed or encounter resistance within the CTO Fig. 6.18.
6. **Unsuccessful wire advancement:** if unsuccessful in advancing the wire after initial laser activation do the following:
 - (a) Increase rate setting for second attempt
 - (b) Continue to increase rate settings for third and subsequent attempts
 - (c) Repeat previous steps
 - (d) If still unable to fully cross the lesion, but have wire partially down the CTO, lase over wire to point of wire tip, adjust and attempt to re-advance wire/laser as described earlier.
7. **Intraluminal confirmation:** confirm intraluminal placement by using multiple angles and 50 % contrast injection via laser catheter. If the wire position is intraluminal repeat the process. If the wire is extraluminal, pull the catheter back to most probable intraluminal location and redirect wire.
8. **Entering the patent distal segment:** prior to entering target vessel, use multiple angles to confirm position, then cross the last 2 cm of the occlusion with guidewire first. Due to the nature of the distal cap formation, it is not unusual for the laser alone to create subintimal space at distal cap.
9. **Multiple Laser passes:** perform at least two to three attempts with Laser catheter at low settings first. If it didn't work increase the settings as needed for second and third additional attempts. Next, exchange 0.035 with 0.018 guidewire to allow saline flushing through the lumen during subsequent laser passes.
10. **Determine vessel run-off:** perform angiogram to determine vessel run-off then determine what is your next planned step whether your decision the case is complete, the need of larger laser, PTCA or need of stenting Fig. 6.19.

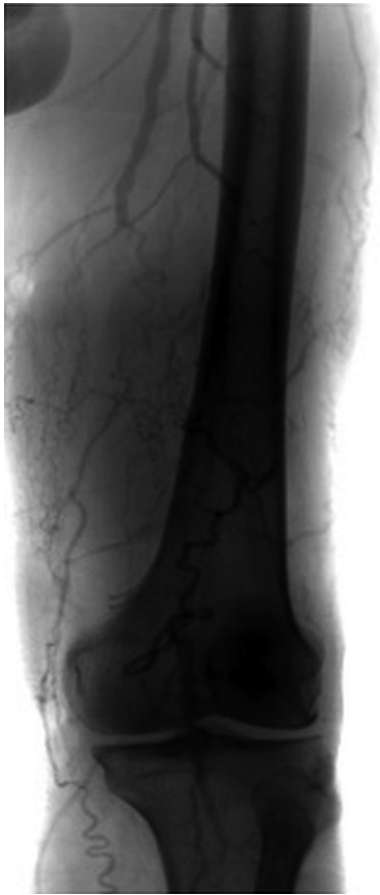


Fig. 6.15 Angiographic assessment of superficial femoral artery to determine feasibility of the “Step-by-Step Technique” using the excimer laser



Fig. 6.16 Wire insertion and excimer laser catheter positioning

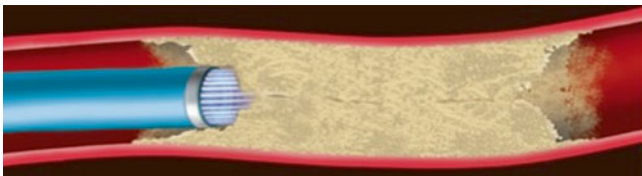


Fig. 6.17 Initial excimer laser activation

The “Step-By-Step” technique has contributed to the low rate of occlusive arterial wall dissections, with a resultant stent frequency of only 7.3 % [26]. Other relevant complications

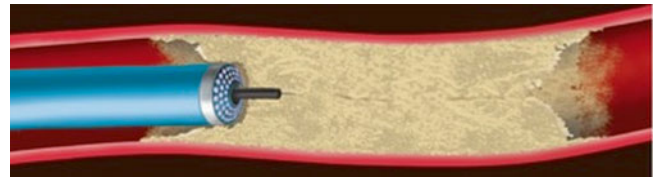


Fig. 6.18 Initial wire advancement



Fig. 6.19 (a, b) After intraluminal confirmation, entering the patent distal segment, performance of multiple excimer laser passes and the distal vessel run-off is determined, a transluminal balloon angioplasty and stenting performed successfully to the superficial femoral artery

reported were acute occlusion of 1 %, perforation 2.2 % and distal embolization of 3.9 %. In the LACI trial where “Step-By-Step” technique used in 17 % of lesions resistant to guidewire navigation in critically ischemic limbs, it helped to achieve crossing in 88 % of these cases [25].

Complications

Over the years of laser technology evolution and application, interventionists and engineers realized that ultraviolet laser energy is absorbed in blood or contrast medium, inducing acoustic effects generating imploding vapor bubbles which

produce rapid microsecond dilation followed by invagination of the adjacent arterial segment. This will result in extensive tissue wall damage with medial necrosis and intramural hematoma, resulting in dissections and perforations [20, 27]. However this photo acoustic effect could be useful for plaque modification if lesion remains resistant.

The observed unwanted effect of ELCA is the generation of imploding vapor bubbles creating local dissections or causing perforations especially in context of ELCA activation in blood or contrast medium, which continuous saline flush during laser activation minimized this issue by displacement of blood or contrast medium from the arterial vessel [28].

Coronary Complications

The rate of major complication rates with ELCA is low and similar to conventional PTCA. The statistical data report from US and Europe PELCA registry (Percutaneous excimer laser coronary angioplasty) revealed mortality rates <1 %, emergent CABG in 3.1 % and STEMI in 2.3 %. Complications incidence from ELCA can be divided into two eras: Pre-saline flush era and saline flush era. The incidence of complications reduced dramatically after the introduction of saline flushing during ELCA application. The possible complications as follows [29–32]:

1. Arterial dissections: they were common in pre-saline flush era that was reported up to 24 % that make it the most frequently observed ELCA complication. The complicated dissections followed by abrupt closure occur in 5–6 % [32]. There are other major factors that might impact on dissection risk such as laser catheter size especially with 1.2 mm compared to 0.9 mm device, technical strategy, vessel size and area of action.
2. Perforations: They occur in about 2 % with 1.5 % are usually benign and easily sealed by prolonged inflation or stenting [33, 34].
3. Distal plaque embolization: this complication occurs in 2.3 % and it is most commonly seen in patients with saphenous graft lesions where target lesion is composed of atherothrombotic material. Rates of embolization remains high regardless of tools used up to 50 %, and it mandates the use of protection devices (proximal & distal). These filter devices are being compatible with laser as opposed to other atherectomy devices.
4. In-hospital death reported from 0 to 2 % [33, 35].

The above complications are minimized by increased operator experience, slow catheter advancement with easy pushability and use of saline flushing.

The major predictors of dissection and perforation based on PELCA registry were the following:

1. Female gender
2. Catheter use of >1.4 mm diameter
3. At vessel branch points
4. Chronic total occlusion lesions
5. Novice operator

Peripheral Complications

Use of excimer laser in peripheral vessel revascularization is more forgiving than its coronary counterpart in regards of treatment strategies to treat the complications. There are few trials and case series and they vary in incidence with evolution of technique and experience. The following are reported complications in the literature from LACI trial and other case series [36–38]:

1. Vessel perforation: It varies between 2.2 and 3.1 % but most of the peripheral vessel perforations are managed promptly without need for surgical intervention.
2. Acute re-occlusion 1 %
3. Distal embolization 3.1–3.9 %
4. Major dissection 34.6 %
5. Pseudoaneurysms 2.4 %

Conclusion

A number of developments of ELCA therapy have evolved over the years to sidestep the difficulties and complications of laser treatment. ELCA stands out in subset of challenging lesions such as undilatable, uncrossable and calcified vessel. The safety and efficacy of ELCA use is dependent on experience of using this tool and understanding the laser system and its limitations. ELCA has the potential to gain broader use especially in below knee peripheral artery disease and uncrossable CTOs. The renaissance of ELCA will be dependent on the availability of the laser system to the experienced interventionist or the novice interventionist with proctorship during the initial learning curve. The lack of data for the last decade, create a challenge, but with conducting and designing prospective randomized trials to address the role of ELCA as debulking tool in challenging lesions such as calcified uncrossable CTOs will clarify if ELCA will be a reasonable strategy option in these cases.

References

1. Mintz GS, et al. Mechanisms of lumen enlargement after excimer laser coronary angioplasty. An intravascular ultrasound study. *Circulation*. 1995;92(12):3408–14.
2. Dave RM, et al. Excimer laser recanalization of femoropopliteal lesions and 1-year patency: results of the CELLO registry. *J Endovasc Ther*. 2009;16(6):665–75.

3. Thompson B, Towler DA. Arterial calcification and bone physiology: role of the bone-vascular axis. *Nat Rev Endocrinol*. 2012;8(9):529–43.
4. Wexler L, et al. Coronary artery calcification: pathophysiology, epidemiology, imaging methods, and clinical implications. A statement for health professionals from the American Heart Association Writing Group. *Circulation*. 1996;94(5):1175–92.
5. Leopold JA. Vascular calcification: an age-old problem of old age. *Circulation*. 2013;127(24):2380–2.
6. Soor GS, et al. Peripheral vascular disease: who gets it and why? A histomorphological analysis of 261 arterial segments from 58 cases. *Pathology*. 2008;40(4):385–91.
7. Shanahan CM, et al. Medial localization of mineralization-regulating proteins in association with Monckeberg's sclerosis: evidence for smooth muscle cell-mediated vascular calcification. *Circulation*. 1999;100(21):2168–76.
8. Johnson RC, Leopold JA, Loscalzo J. Vascular calcification: pathological mechanisms and clinical implications. *Circ Res*. 2006;99(10):1044–59.
9. Ouriel K. Peripheral arterial disease. *Lancet*. 2001;358(9289):1257–64.
10. Amann K. Media calcification and intima calcification are distinct entities in chronic kidney disease. *Clin J Am Soc Nephrol*. 2008;3(6):1599–605.
11. Gross ML, et al. Calcification of coronary intima and media: immunohistochemistry, backscatter imaging, and x-ray analysis in renal and nonrenal patients. *Clin J Am Soc Nephrol*. 2007;2(1):121–34.
12. Leimgruber PP, et al. Influence of intimal dissection on restenosis after successful coronary angioplasty. *Circulation*. 1985;72(3):530–5.
13. Fitzgerald PJ, Ports TA, Yock PG. Contribution of localized calcium deposits to dissection after angioplasty. An observational study using intravascular ultrasound. *Circulation*. 1992;86(1):64–70.
14. Cavusoglu E, et al. Current status of rotational atherectomy. *Catheter Cardiovasc Interv*. 2004;62(4):485–98.
15. Moussa I, et al. Coronary stenting after rotational atherectomy in calcified and complex lesions. Angiographic and clinical follow-up results. *Circulation*. 1997;96(1):128–36.
16. Mosseri M, et al. Impact of vessel calcification on outcomes after coronary stenting. *Cardiovasc Revasc Med*. 2005;6(4):147–53.
17. Nakano M, et al. Human autopsy study of drug-eluting stents restenosis: histomorphological predictors and neointimal characteristics. *Eur Heart J*. 2013;34(42):3304–13.
18. Ahmed WH, al-Anazi MM, Bittl JA. Excimer laser-facilitated angioplasty for undilatable coronary narrowings. *Am J Cardiol*. 1996;78(9):1045–6.
19. Bilodeau L, et al. Novel use of a high-energy excimer laser catheter for calcified and complex coronary artery lesions. *Catheter Cardiovasc Interv*. 2004;62(2):155–61.
20. Isner JM, et al. Factors contributing to perforations resulting from laser coronary angioplasty: observations in an intact human post-mortem preparation of intraoperative laser coronary angioplasty. *Circulation*. 1985;72(3 Pt 2):II191–9.
21. Hamburger JN, et al. Recanalization of total coronary occlusions using a laser guidewire (the European TOTAL Surveillance Study). *Am J Cardiol*. 1997;80(11):1419–23.
22. Gijsbers GH, Hamburger JN, Serruys PW. Homogeneous light distribution to reduce vessel trauma during excimer laser angioplasty. *Semin Interv Cardiol*. 1996;1(2):143–8.
23. Latib A, et al. Excimer Laser LEsion modification to expand non-dilatable sTents: the ELLEMENT registry. *Cardiovasc Revasc Med*. 2014;15(1):8–12.
24. Noble S, Bilodeau L. High energy excimer laser to treat coronary in-stent restenosis in an underexpanded stent. *Catheter Cardiovasc Interv*. 2008;71(6):803–7.
25. Scheinert D, Biamino G. Femoropopliteal occlusions: experience with peripheral excimer laser angioplasty. *Curr Interv Cardiol Rep*. 2001;3(2):130–8.
26. Wissgott C, et al. Treatment of long superficial femoral artery occlusions with excimer laser angioplasty: long-term results after 48 months. *Acta Radiol*. 2004;45(1):23–9.
27. van Leeuwen TG, et al. Intraluminal vapor bubble induced by excimer laser pulse causes microsecond arterial dilation and invagination leading to extensive wall damage in the rabbit. *Circulation*. 1993;87(4):1258–63.
28. Deckelbaum LI, et al. Reduction of laser-induced pathologic tissue injury using pulsed energy delivery. *Am J Cardiol*. 1985;56(10):662–7.
29. Holmes Jr DR, et al. Excimer laser coronary angioplasty: the New Approaches to Coronary Intervention (NACI) experience. *Am J Cardiol*. 1997;80(10A):99K–105.
30. Hong MK, et al. Frequency and predictors of major in-hospital ischemic complications after planned and unplanned new-device angioplasty from the New Approaches to Coronary Intervention (NACI) registry. *Am J Cardiol*. 1997;80(10A):40K–9.
31. Litvack F, et al. Percutaneous excimer laser coronary angioplasty: results in the first consecutive 3,000 patients. The ELCA Investigators. *J Am Coll Cardiol*. 1994;23(2):323–9.
32. Baumbach A, et al. Acute complications of excimer laser coronary angioplasty: a detailed analysis of multicenter results. Coinvestigators of the U.S. and European Percutaneous Excimer Laser Coronary Angioplasty (PELCA) registries. *J Am Coll Cardiol*. 1994;23(6):1305–13.
33. Bittl JA, Sanborn TA. Excimer laser-facilitated coronary angioplasty. Relative risk analysis of acute and follow-up results in 200 patients. *Circulation*. 1992;86(1):71–80.
34. Bittl JA, et al. Coronary artery perforation during excimer laser coronary angioplasty. The percutaneous Excimer Laser Coronary Angioplasty Registry. *J Am Coll Cardiol*. 1993;21(5):1158–65.
35. Bittl JA, et al. Clinical success, complications and restenosis rates with excimer laser coronary angioplasty. The Percutaneous Excimer Laser Coronary Angioplasty Registry. *Am J Cardiol*. 1992;70(20):1533–9.
36. Scheinert D, et al. Excimer laser-assisted recanalization of long, chronic superficial femoral artery occlusions. *J Endovasc Ther*. 2001;8(2):156–66.
37. Steinkamp HJ, et al. Percutaneous transluminal laser angioplasty versus balloon dilation for treatment of popliteal artery occlusions. *J Endovasc Ther*. 2002;9(6):882–8.
38. Laird JR, et al. Limb salvage following laser-assisted angioplasty for critical limb ischemia: results of the LACI multicenter trial. *J Endovasc Ther*. 2006;13(1):1–11.

Itsik Ben-Dor and Ron Waksman

Introduction

Excimer laser coronary atherectomy (ELCA) has been used for coronary intervention for more than 20 years for the treatment of obstructed coronary arteries. This technology is designed to ablate the obstructive atherothrombotic plaque. The initial data have failed to show better angiographic, procedural, or clinical outcome results when compared to balloon angioplasty or stenting. Advances in delivery systems for laser energy using the xenon-chlorine pulsed laser catheter deliver higher energy density with lower heat production and have led to better results in terms of efficacy and safety with low complication rate. The Spectranetics CVX-300® (Spectranetics Corporation, Colorado Springs, CO) excimer laser catheter system has been used for the treatment of several coronary indications. This chapter will focus on complex coronary lesions, including balloon-resistant lesions, chronic total occlusions, in-stent restenosis (ISR), and underexpanded stents in calcified lesions. ELCA is used for thrombus containing lesions in acute myocardial infarction and degenerated saphenous vein graft lesions (not discussed in this chapter).

Initial Clinical Data ELCA vs. Balloon Angioplasty

Randomized trials one to two decades old failed to demonstrate the superiority of ELCA technique over balloon angioplasty in complex lesions. The Amsterdam-Rotterdam (AMRO) trial [1] compared ELCA to balloon angioplasty in 308 patients with stable angina and coronary lesions longer than 10 mm. The primary clinical endpoint was the composite of death, myocardial infarction (MI), coronary surgical revascularization, or repeat coronary angioplasty after 6 months following the index

procedure. ELCA followed by balloon angioplasty provides no benefit additional to balloon angioplasty alone with respect to the initial and long-term clinical and angiographic outcome in the treatment of obstructive coronary artery disease. There were no significant differences in angiographic success (79 % versus 80 %). However, there was a tenfold higher transient occlusion rate in the ELCA group (0.7 % versus 7 %) in periprocedural complications and a trend toward higher restenosis rate in the ELCA group (41.3 % versus 51.6 %) at 6 months, but there was no difference in angiographic net lumen gain (0.40 mm versus 0.48 mm). The Excimer Laser Rotational Atherectomy Balloon Angioplasty Comparison (ERBAC) trial [2] randomly assigned 685 patients with complex lesions to excimer laser angioplasty, conventional balloon angioplasty, or rotational atherectomy. The patients who underwent rotational atherectomy had a higher rate of procedural success (89 %) than did those who underwent ELCA (77 %) or conventional balloon angioplasty (80 %) ($p=0.0019$). At 6 months' follow-up, revascularization of the original target lesion was performed more frequently in the rotational atherectomy group (42.4 %) and in the excimer laser group (46.0 %) than in the angioplasty group (31.9 %, $p=0.013$). Meta-analysis of randomized trials of balloon angioplasty versus coronary atherectomy, laser angioplasty, or cutting balloon atherectomy evaluating the effects of plaque modification during percutaneous coronary intervention found significant increase in restenosis for ELCA with OR 1.55 [95 % CI 1.09–2.20] [3].

In-stent Restenosis

ELCA has been used as an alternative approach for the treatment of ISR. The use of ELCA as adjunctive treatment for ISR has been previously evaluated in 440 patients. There was a 92 % procedural success rate and low complication rates: Q-wave MI in 0.5 %, non-Q-wave MI in 2.7 %, tamponade in 0.5 %, and dissection in 4.8 % [4]. Similarly, the Laser Angioplasty for Restenotic Stents (LARS) multicenter registry comparing 146 patients with ISR treated with balloon only or ELCA demon-

I. Ben-Dor, MD • R. Waksman, MD (✉)
Division of Cardiology, Washington Hospital Center,
110 Irving Street, NW, Suite 4B-1, Washington, DC 20010, USA
e-mail: itsikbd@gmail.com; ron.waksman@medstar.net

Unexpanded stents with recurrent restenosis

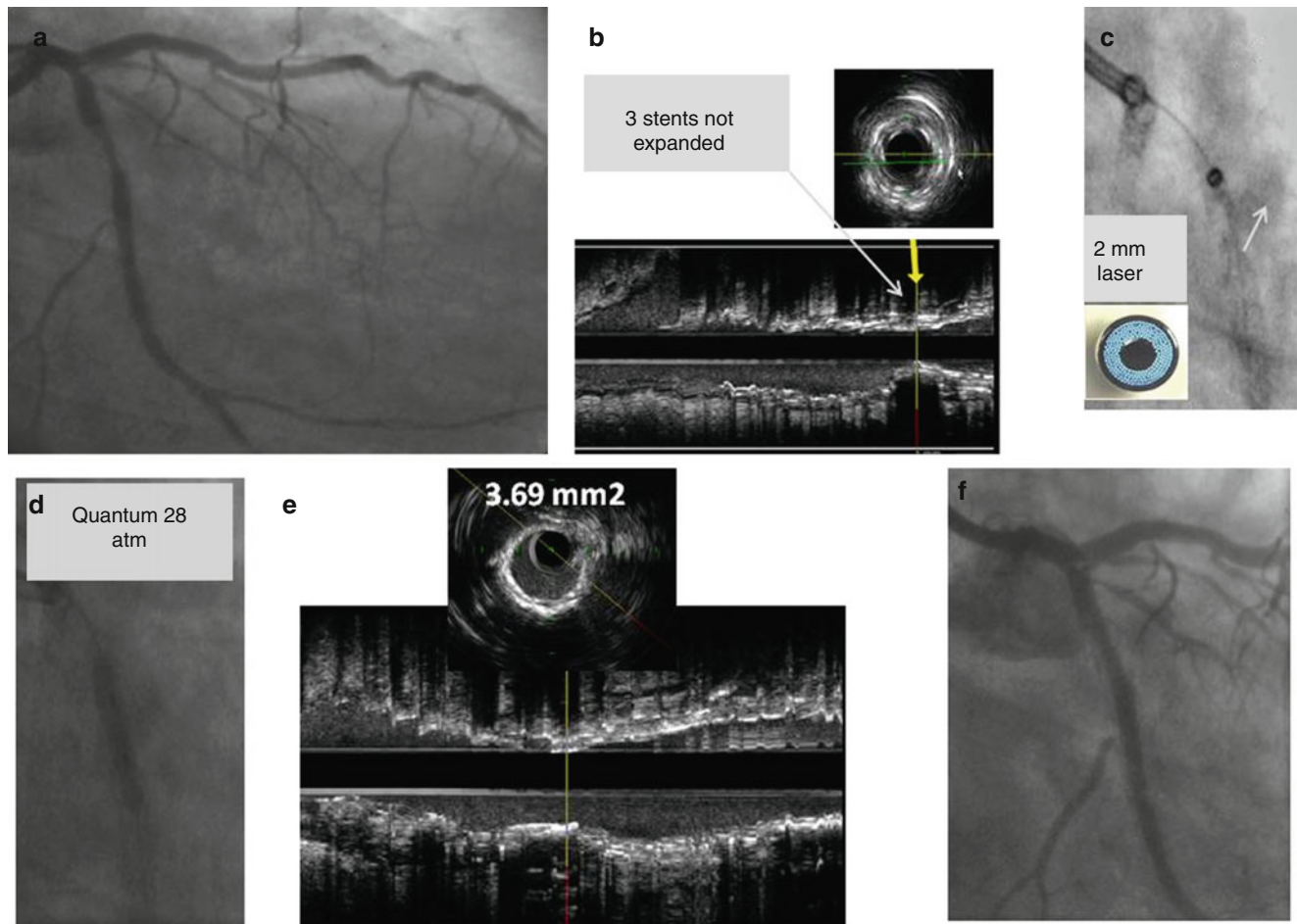


Fig. 7.1 Underexpanded stent with recurrent in-stent restenosis. Coronary angiogram revealed focal ISR in the proximal circumflex artery of the multiple overlapped stents (a). Intravascular ultrasound showed under expanded stents in an area of severe underlying concentric calcification. Minimal luminal area was 1.3 mm² (b). Multiple

attempts at dilatation with noncompliant balloons at pressures up to 24 atm failed. The stenosis was then treated with a 2-mm excimer laser (c), followed by high pressure Quantum balloon (Boston Scientific) inflation (28 atm) (d) with good angiographic and ultrasound results (e, f), thereby increasing the minimal luminal area to 3.68 mm²

strated that ELCA is as safe and effective as balloon angioplasty alone [5]. Intravascular ultrasound-based data documented effective ablation of neointimal tissue adjunct balloon angioplasty extrudes neointimal tissue out of the stent and also further expands the stent [6]. However follow-up data showed high incidence of recurrent restenosis in this group of patients with up to 68 % ISR in 6 months, suggesting that this technique is unlikely to reduce recurrent in-stent restenosis and that other approaches are necessary [7]. In a meta-analysis of 3012 patients with in-stent restenosis, 474 patients receiving ELCA as the treatment presented the highest probability, 34.8 %, to develop major cardiac events (death, myocardial infarction, or revascularization) at follow-up [8]. For the treatment of in-stent restenosis, rotablation had higher acute ablation efficacy as compared to ELCA with similar clinical outcomes at 1 year [9].

Today with the use of drug eluting stents and the introduction of drug eluting balloon, the need of ELCA as a treatment for ISR is rarely needed and is mainly used for underexpanded stents.

Underexpanded Stent

Underexpanded stents are frequently difficult to fully expand once deployed. The application of ELCA is to expand an undilatable stent using contrast injection during laser angioplasty to amplify the energy and shock waves to successfully expand a stent refractory to balloon dilatation [10]. ELCA is used also for the management of underexpansion of a newly deployed coronary stent [11]. The ELLEMENT study reported 28 patients with an underexpanded stent despite high-pressure balloon inflation. Laser-assisted stent dilatation was successful in 27 cases (96.4 %), with an improvement in minimal stent diameter 1.6 at baseline to 2.6 post-procedure and minimal stent area by IVUS 3.5 mm² to 7.1². The target lesion revascularization was 4.3 % at 6 months [12].

Figure 7.1 demonstrates ELCA assist in late dilatation of an underexpanded stent, and Fig. 7.2 shows a newly deployed stent.

Unexpanded stents with recurrent restenosis

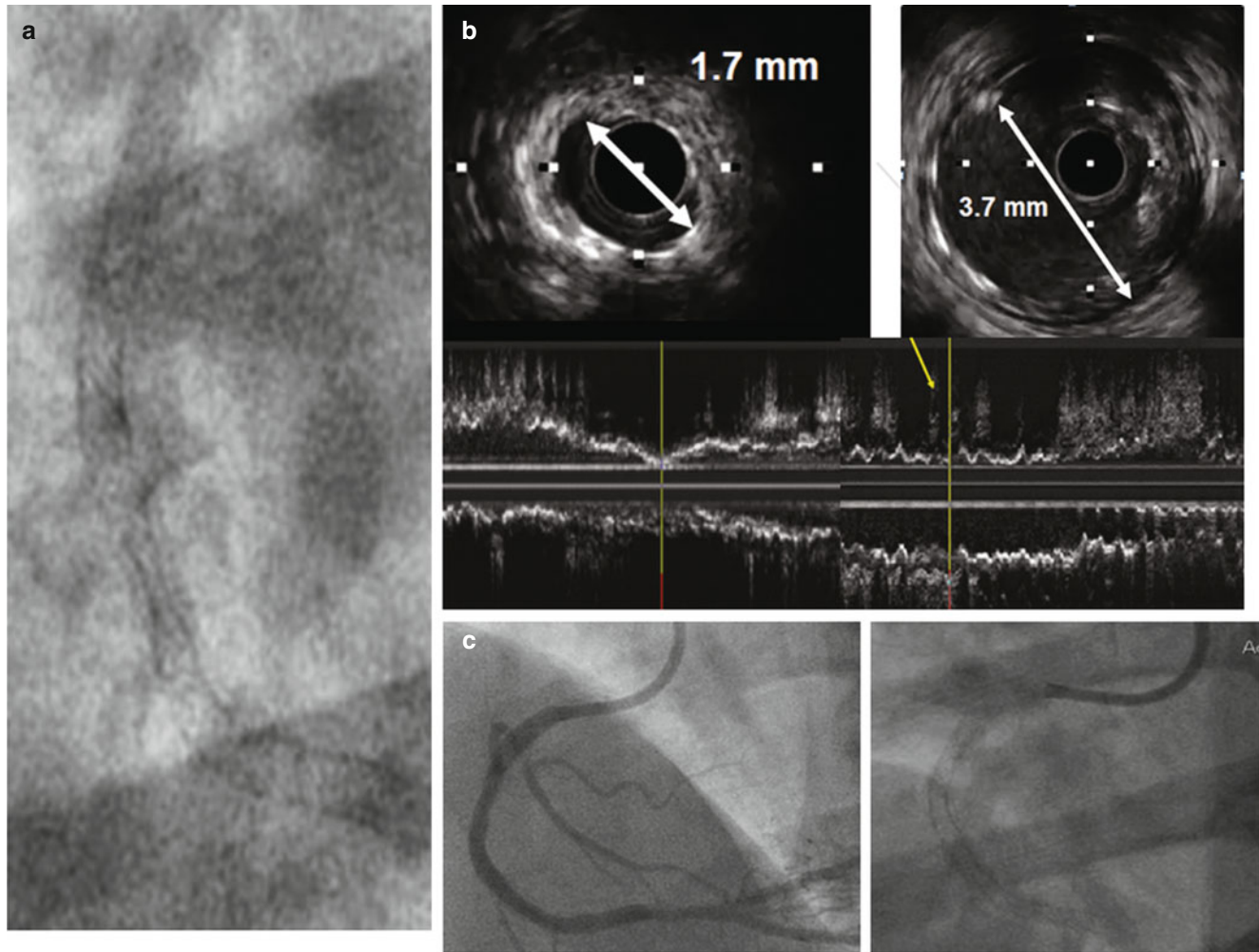


Fig. 7.2 New deployed underexpanded stent. Fluoroscopy revealed underexpanded stent in distal RCA after multiple attempts at dilatation with noncompliant balloon (a). Intravascular ultrasound showed underexpanded stents in an area of severe underlying concentric

calcification. Minimal luminal diameter 1.7 mm², after 1.4 mm laser with contrast injection followed by high pressure balloon inflation (24 atm) diameter increases to 3.7 mm (b). Angiographic and fluoro after laser and balloon (c)

Undilatable Lesion and Calcified Lesion

In some lesions resistance is so high that an adequately sized balloon is not able to expand completely despite high pressures of up to 20 atm or more. Ahmed et al [13] reported the use of ELCA to facilitate angioplasty for undilatable coronary narrowing. In 100 calcified and/or balloon-resistant lesions, using a 0.9-mm Excimer Laser catheter at standard or higher energy levels resulted in procedural success in 88 lesions (93 %) and clinical success in 82 lesions (86 %). Increased laser parameters were used for 29 resistant lesions. Using higher energy parameters seems to be safe and effective for the management of calcified and undilatable lesions [14]. Shen et al [15] reported a series of 33 cases in using ELCA, including 21 patients with failure of balloon to cross and 15 chronic total occlusion. They reported a success rate of 90 % and no complications directly related to laser catheter

treatment. Recently, Fernandez et al [16] reported 58 cases of balloon failure treated ELCA 0.9 mm catheter with saline flush. Procedure success was achieved in 91 %, with ELCA successful alone in 76.1 %, after rotational atherectomy failure in 6.8 %, and in combination with rotational atherectomy for 8.6 %. There were four procedure-related complications, including transient no-reflow, side branch occlusion, and two coronary perforations, of which one was directly attributable to ELCA.

The most commonly used device for heavily calcified coronary lesions is rotational atherectomy. There are occasions that the dedicated RotaWire (Boston Scientific, Natick, MA, USA) cannot be delivered beyond the lesion, either independently or using a microcatheter exchange system. The advantage of the ELCA after successful wire passage across a chronic total coronary occlusion or calcified lesion, when balloon catheter or the exchange catheter cannot cross,

Balloon resistant lesion

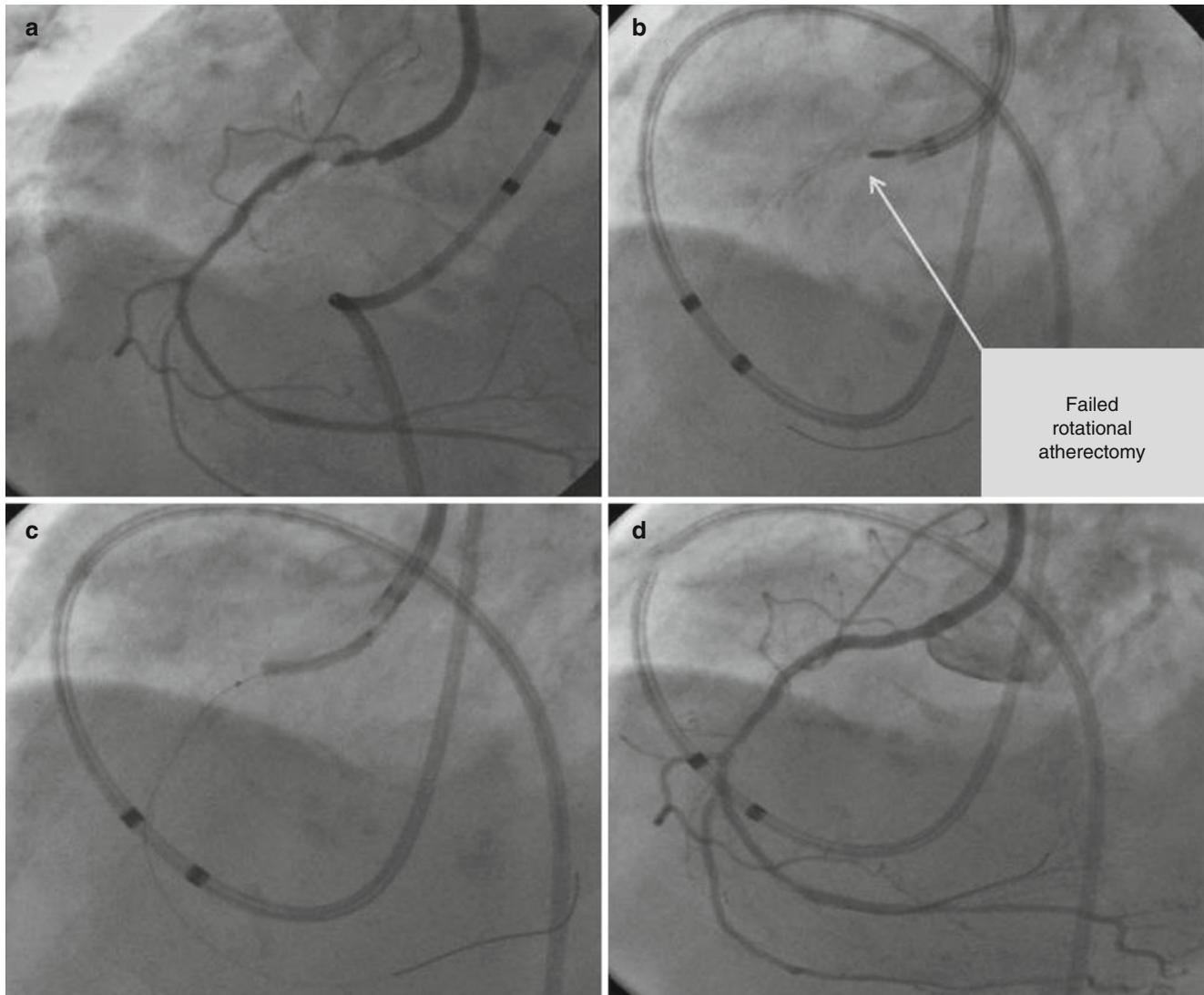


Fig. 7.3 ELCA for balloon-resistant lesion. Severely calcified 95 % stenotic lesion was found in the proximal right coronary artery (RCA) (a). A 0.014" BMW guidewire (Guidant Corp., Santa Clara, CA) crossed the lesion, but 2.5/20-mm and a 1.5/15-mm Sprinter balloons (Medtronic, Minneapolis, MN) did not. The BMW guidewire was exchanged over a microguide catheter (FineCross MG, Terumo, Ann Arbor, MI) for a Rota Extra Support guidewire (Boston Scientific, Natick, MA). Rotational atherectomy with Rotablator catheters (Boston Scientific, Natick, MA) was attempted. A 1.5-mm burr did not cross the lesion, and a 1.25-mm burr decelerated without crossing (b). The lesion

was successfully crossed with the Spectranetics 0.9-mm excimer laser catheter. Laser energy was initiated with a repetition rate of 40 Hz and fluence of 60 mJ/mm² and was then increased to a repetition rate 80 Hz and a fluence of 80 mJ/mm². Subsequent to passage of the laser catheter, rotational atherectomy with 1.5-mm burr was successful. The Rota Extra Support guidewire was exchanged for a BMW guidewire, and a 2.5/20-mm Sprinter balloon was inflated at 12 atm (c). A Micro-Driver 2.5/14-mm bare metal stent (BMS) (Medtronic, Minneapolis, MN) was deployed at high pressure (16 atm) (d)

is the ability to be advanced along standard guidewire 0.014" in contrast to rotational atherectomy. The laser can create a channel through the CTO, which allows a balloon catheter to pass afterward to facilitate final vessel reconstruction by stent implantation (Fig. 7.3). In some cases, the channel created by the ELCA can then be used to pass a RotaWire to permit rotational atherectomy. The combination of ELCA and rotational atherectomy has been reported and termed

RASER angioplasty for heavily lesion unresponsive to either modality alone [17, 18].

Our center reports the safety and efficacy of ELCA in 124 complex coronary lesions. The overall ELCA success rate was 88.7 %, while angiographic success was 91 %. Despite such lesion complexity, the complication rate was low (8 %). The most common complication was the presence of dissection [19]. ELCA has a high success rate and low complication

Chronic total occlusion

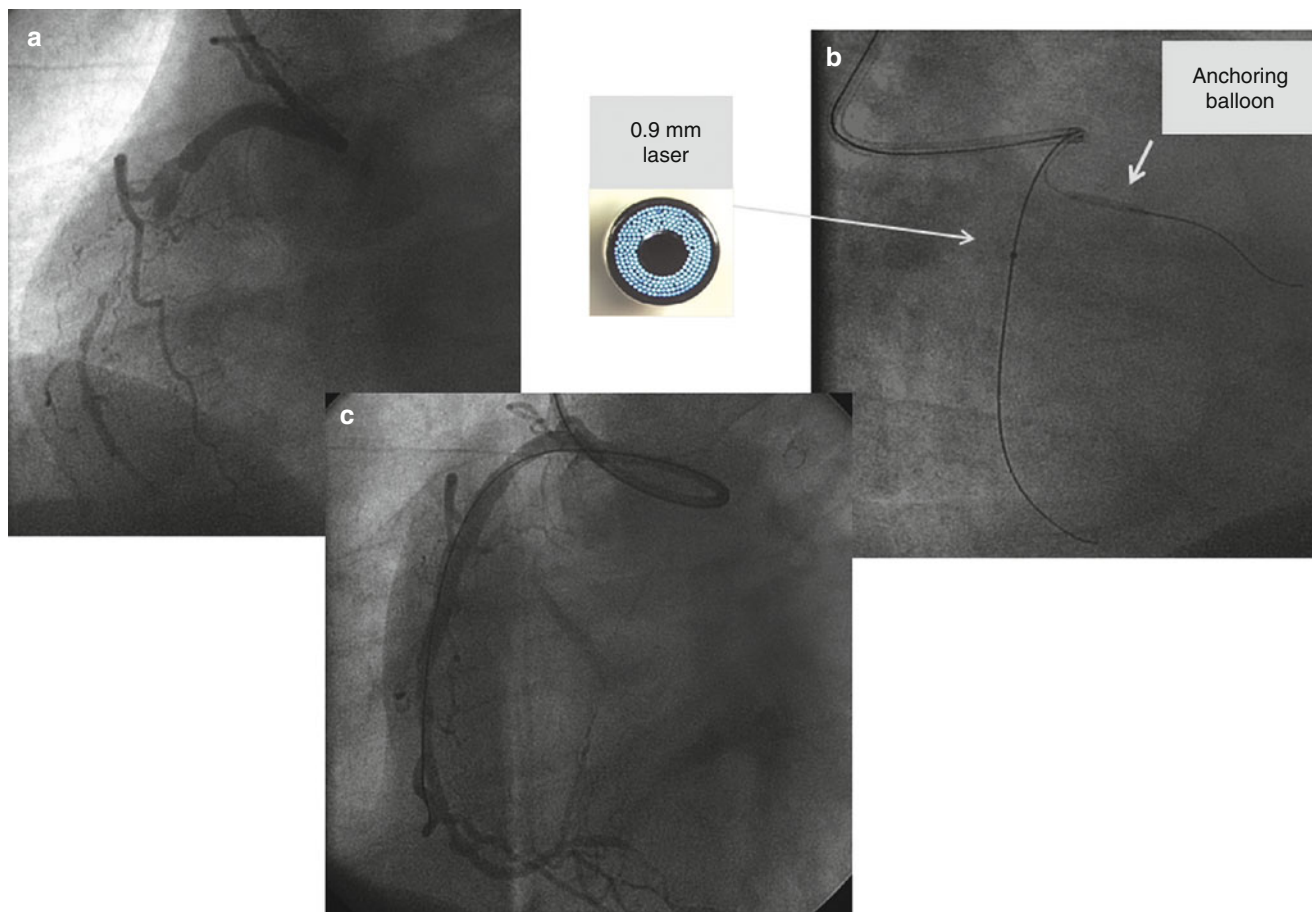


Fig. 7.4 ELCA for chronic total occlusion. Total occlusion in the proximal third of the RCA (a). The occlusion could not be crossed with a MiracleBros 6 guidewire (Abbott Vascular, Abbott Park, IL); however, successful crossing was attained with a 2.1 F Tornus catheter (Abbott Vascular) and a Confianza guidewire (Abbott Vascular). An Apex 1.5-mm balloon (Boston Scientific, Natick, MA) could not be passed. Initially, the Spectranetics excimer laser (0.9 mm) also failed but did

cross with the use of a proximal anchoring balloon. Laser treatment with a repetition rate of 80 Hz and a fluence of 80 mJ/mm² allowed passage (b) of an Apex 1.5/15-mm balloon followed by a 2.5/30-mm Maverick balloon (Boston Scientific). Both were inflated at high pressure, and a long Cypher (2.5/30-mm) drug-eluting stent (DES) (Cordis Corporation, Miami Lakes, FL) was deployed at high pressure with excellent angiographic results (c)

rate for treatment of calcified or undilatable lesions, but the follow-up rate of repeat revascularization is high with one study up to 46 % in 12 months [20], and another study reports major adverse cardiac events up to 33.3 %, with 22.2 % repeat revascularization in 6 months [21].

Chronic Total Coronary Occlusions

The use of ELCA for chronic coronary occlusion was compared in 303 patients randomized to treatment with either a laser guidewire (n=144) or a conventional guidewire (n=159). Treatment success using the laser guidewire versus the mechanical guidewire was not significantly different (52.8 % versus 47.2 %, p=0.33). No serious adverse events

followed the initial laser guidewire attempt; adverse events were found in only 0.6 % following the use of the mechanical guidewire. Further, there was no difference in either the rate of binary restenosis at 6 months on angiographic follow-up or in event-free survival at 12 months [22]. This device is no longer available and has been replaced by dedicated mechanical crossing wires and techniques. Appellam et al [23] reported the use of ELCA-assisted balloon angioplasty for chronic total occlusion and found no benefit over balloon angioplasty with respect to initial and long-term clinical and angiographic outcome. The laser catheter can be useful in selected patients, including those with CTO where a balloon would not pass despite a guidewire in the distal true lumen [15]. Today the ELCA is used in CTO mainly to facilitate balloon advancement or stent deployment after crossing with guidewire (Fig. 7.4).

ELCA, when used for specific “niche” lesions, may be effective even though randomized trials of “unselected” lesions did not show any benefit. The variety of lesions that may be treated by using a 0.9-mm catheter requires careful case selection; appropriate utilization of equipment; and the application of safe lasing techniques for complex coronary interventions, such as calcified or nondilatable lesions. The undilatable coronary lesion (following successful wire passage) is a very good indication to use ELCA and, in terms of efficacy, competes with rotational atherectomy with the advantage of the ability to be advanced along standard guidewire. Other indications are failure to cross with balloons, which is a well-recognized cause of failure to recanalize a chronic total occlusion, and in cases of unexpanded stents with recurrent restenosis.

References

- Appelman YE, Piek JJ, Strikwerda S, Tijssen JG, de Feyter PJ, David GK, Serruys PW, Margolis JR, Koelemay MJ, Montauban van Swijndregt EW, Koolen JJ. Randomised trial of excimer laser angioplasty versus balloon angioplasty for treatment of obstructive coronary artery disease. *Lancet*. 1996;347:79–84.
- Reifart N, Vandormael M, Krajcar M, Göhring S, Preusler W, Schwarz F, Störger H, Hofmann M, Klöpffer J, Müller S, Haase J. Randomized comparison of angioplasty of complex coronary lesions at a single center. Excimer Laser, Rotational Atherectomy, and Balloon Angioplasty Comparison (ERBAC) Study. *Circulation*. 1997;96:91–8.
- Bittl JA, Chew DP, Topol EJ, Kong DF, Califf RM. Meta-analysis of randomized trials of percutaneous transluminal coronary angioplasty versus atherectomy, cutting balloon atherotomy, or laser angioplasty. *J Am Coll Cardiol*. 2004;43:936–42.
- Köster R, Hamm CW, Seabra-Gomes R, Herrmann G, Sievert H, Macaya C, Fleck E, Fischer K, Bonnier JJ, Fajadet J, Waigand J, Kuck KH, Henry M, Morice MC, Pizzulli L, Webb-Peploe MM, Buchwald AB, Ekström L, Grube E, Al Kasab S, Colombo A, Sanati A, Ernst SM, Haude M, Serruys PW, et al. Laser angioplasty of restenosed coronary stents: results of a multicenter surveillance trial. The Laser Angioplasty of Restenosed Stents (LARS) Investigators. *J Am Coll Cardiol*. 1999;34:25–32.
- Giri S, Ito S, Lansky AJ, Mehran R, Margolis J, Gilmore P, Garratt KN, Cummins F, Moses J, Rentrop P, Oesterle S, Power J, Kent KM, Satler LF, Pichard AD, Wu H, Greenberg A, Bucher TA, Kerker W, Abizaid AS, Saucedo J, Leon MB, Popma JJ. Clinical and angiographic outcome in the laser angioplasty for restenotic stents (LARS) multicenter registry. *Catheter Cardiovasc Interv*. 2001;52:24–34.
- Mehran R, Mintz GS, Satler LF, Pichard AD, Kent KM, Bucher TA, Popma JJ, Leon MB. Treatment of in-stent restenosis with excimer laser coronary angioplasty: mechanisms and results compared with PTCA alone. *Circulation*. 1997;96:2183–9.
- Köster R, Kähler J, Terres W, Reimers J, Baldus S, Hartig D, Berger J, Meinertz T, Hamm CW. Six-month clinical and angiographic outcome after successful excimer laser angioplasty for in-stent restenosis. *J Am Coll Cardiol*. 2000;36:69–74.
- Radke PW, Kaiser A, Frost C, Sigwart U. Outcome after treatment of coronary in-stent restenosis; results from a systematic review using meta-analysis techniques. *Eur Heart J*. 2003;24:266–73.
- Mehran R, Dangas G, Mintz GS, Waksman R, Abizaid A, Satler LF, Pichard AD, Kent KM, Lansky AJ, Stone GW, Leon MB. Treatment of in-stent restenosis with excimer laser coronary angioplasty versus rotational atherectomy: comparative mechanisms and results. *Circulation*. 2000;101:2484–9.
- Goldberg SL, Colombo A, Akiyama T. Stent under-expansion refractory to balloon dilatation: a novel solution with excimer laser. *J Invasive Cardiol*. 1998;10:269–73.
- Lam SC, Bertog S, Sievert H. Excimer laser in management of underexpansion of a newly deployed coronary stent. *Catheter Cardiovasc Interv*. 2014;83:E64–8.
- Latib A, Takagi K, Chizzola G, Tobis J, Ambrosini V, Niccoli G, Sardella G, DiSalvo ME, Armigliato P, Valgimigli M, Tarsia G, Gabrielli G, Lazar L, Maffeo D, Colombo A. Excimer laser LEsion modification to expand non-dilatable stents: the ELLEMENT registry. *Cardiovasc Revasc Med*. 2014;15:8–12.
- Ahmed WH, al-Anazi MM, Bittl JA. Excimer laser-facilitated angioplasty for undilatable coronary narrowings. *Am J Cardiol*. 1996;78:1045–6.
- Bilodeau L, Fretz EB, Taeymans Y, Koolen J, Taylor K, Hilton DJ. Novel use of a high-energy excimer laser catheter for calcified and complex coronary artery lesions. *Catheter Cardiovasc Interv*. 2004;62:155–61.
- Shen ZJ, García-García HM, Schultz C, van der Ent M, Serruys PW. Crossing of a calcified “balloon uncrossable” coronary chronic total occlusion facilitated by a laser catheter: a case report and review recent four years’ experience at the Thoraxcenter. *Int J Cardiol*. 2010;145:251–4.
- Fernandez JP, Hobson AR, McKenzie D, Shah N, Sinha MK, Wells TA, Levy TM, Swallow RA, Talwar S, O’Kane PD. Beyond the balloon: excimer coronary laser atherectomy used alone or in combination with rotational atherectomy in the treatment of chronic total occlusions, non-crossable and non-expandable coronary lesions. *EuroIntervention*. 2013;9:243–50.
- McKenzie DB, Talwar S, Jokhi PP, O’Kane PD, Osheroov A, Strauss B, Dahm J. How should I treat severe coronary artery calcification when it is not possible to dilate a balloon or deliver a RotaWire™? *EuroIntervention*. 2011;6:779–83.
- Egred M. RASER angioplasty. *Catheter Cardiovasc Interv*. 2012;79:1009–12.
- Badr S, Ben-Dor I, Dvir D, Barbash IM, Kitabata H, Minha S, Pendyala LK, Loh JP, Torguson R, Pichard AD, Waksman R. The state of the excimer laser for coronary intervention in the drug-eluting stent era. *Cardiovasc Revasc Med*. 2013;14:93–8.
- Tarsia G, De Michele M, Viceconte N, Takagi K, Biscione C, Del Prete G, Polosa D, Osanna R, Lisanti P. Immediate and midterm follow-up results of excimer laser application in complex percutaneous coronary interventions: report from a single center experience. *Interv Med Appl Sci*. 2013;5:10–5.
- Niccoli G, Giubilato S, Conte M, Belloni F, Cosentino N, Marino M, Mongiardo R, Crea F. Laser for complex coronary lesions: impact of excimer lasers and technical advancements. *Int J Cardiol*. 2011;146:296–9.
- Serruys PW, Hamburger JN, Koolen JJ, Fajadet J, Haude M, Klues H, Seabra-Gomes R, Corcos T, Hamm C, Pizzulli L, Meier B, Mathey D, Fleck E, Taeymans Y, Melkert R, Teunissen Y, Simon R. Total occlusion trial with angioplasty by using laser guidewire. The TOTAL trial. *Eur Heart J*. 2000;21:1797–805.
- Appelman YE, Koolen JJ, Piek JJ, Redekop WK, de Feyter PJ, Strikwerda S, David GK, Serruys PW, Tijssen JG, van Swijnregt E, Lie KI. Excimer laser angioplasty versus balloon angioplasty in functional and total coronary occlusions. *Am J Cardiol*. 1996;78:757–62.

Optical Coherence Tomography for Assessment of Percutaneous Coronary Intervention with Excimer Laser Coronary Atherectomy

John Rawlins, Suneel Talwar, and Peter O’Kane

Introduction

Excimer laser coronary atherectomy (ELCA) has been applied in the treatment of arterial atheroma for nearly 30 years. The concept of utilising laser to remove atherosclerotic material in coronary arteries developed as an alternative to simple modification of an obstructed lumen as was the case with plain old balloon angioplasty (POBA). However, despite enthusiasm amongst interventional cardiologists and registry data in over 3000 patients early results when compared with conventional percutaneous coronary intervention (PCI) techniques were disappointing resulting in limited uptake of the technology [1, 2]. However, advances in laser catheters and PCI technique has led to a resurgence of interest, reflected in recent literature [3–5]. Contemporary challenges in PCI include an ability to deal with calcified lesions, chronic total occlusions (CTO), thrombotic lesions and repeat intervention in vessels already containing devices (in stent re-stenosis and under expanded stents). All of these provide an indication for ELCA.

In parallel with advances in laser catheter technology, intra-vascular imaging has become an integral part of modern interventional practice. Optical coherence tomography (OCT) is a recently developed intra-vascular imaging modality. It uses near-infrared light to provide high resolution (12–15 μm) images of the coronary vessel lumen and wall. It can clearly identify and differentiate intravascular thrombus, and

provides detailed information on the effects of intervention on the coronary intima and media [6]. When compared to IVUS (Table 8.1), the high resolution images that are produced allow a more comprehensive assessment of vessel intima, stent architecture and the composition of arterial atherosclerosis.

The aim of this chapter is to describe the coronary OCT appearance after ELCA, using case examples, to aid PCI decision making. Firstly, the process of OCT image acquisition is described, followed by a brief summary of common findings. This is followed by a series of cases that cover the current indications for ELCA, each accompanied by a detailed analysis of the OCT images acquired during the case.

“Let There Be Light” – Common Properties of Laser and OCT

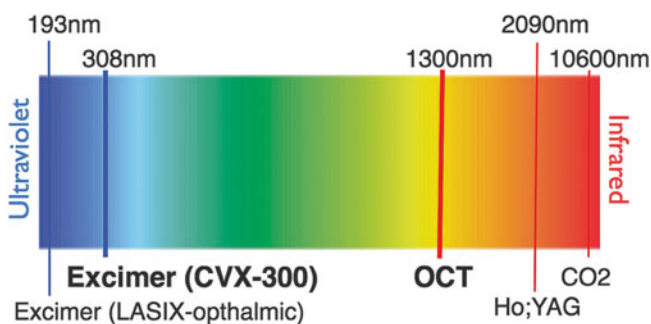
Individual lasers emit light with a characteristic wavelength, which is determined by the lasing medium used to create the energy (Fig. 8.1). For coronary laser atherectomy the xenon chloride excimer lasing properties result from a high voltage electrical discharge placed across a mixture of inert gas (xenon) and a dilute halogen compound (hydrogen chloride). The light subsequently emitted has a wavelength of 308 nm. Light at this end of the spectrum has a shallow penetration depth of only 50 μm because it is absorbed by non-aqueous cellular macromolecules such as proteins and nucleic acids [1]. In contrast to laser emitted from Nd-YAG source, excimer laser energy is therefore less likely to produce charring or deep vessel injury and in turn permits safe tissue ablation in the absence of coronary artery dissection or perforation. Thermal injury is further reduced in the contemporary excimer system owing to the pulsed nature of emission rather than more traditional continuous wave output. The current excimer laser fires high-energy pulses that last only a fraction of a second restricting the thermal effect only to the irradiated tissue.

Disclosures Drs O’Kane & Talwar are Proctors for Spectranetics. No other author has any particular disclosures or conflicts of interest. All authors have been involved in the design, preparation, and revision of this article and consent to its submission.

J. Rawlins, BSc, MBBS, MRCP, MD (Res)
S. Talwar, BSc, MBBS, MD • P. O’Kane, BSc, MBBS,
FRCP, MD (✉)
Dorset Heart Centre, Royal Bournemouth Hospital,
Castle Lane East, Bournemouth BH7 7DW, UK
e-mail: john.rawlins@doctors.net.uk; Suneel.talwar@rbch.nhs.uk;
peter.o’kane@rbch.nhs.uk

Table 8.1 Summary of basic fundamental differences between Optical Coherence tomography (OCT) and intravascular ultra-sound (IVUS)

	OCT	IVUS
Axial resolution	12–15 μm	100–200 μm
Penetration depth	1.5–2 mm	4–8 mm
Probe size	OCT = 0.92 mm (2.7 F)	IVUS = 1.1 mm (3.5 F)
Pullback speed	up to 40 mm/s	Up to 40 mm/s
Blood free imaging field	Yes	No
Tissue characterisation	Yes	Yes
Fibrous cap measurement	Yes	No
Vessel Remodelling	No	Yes
Stent endothelisation	Yes	No
Thrombus differentiation	Yes	No

**Fig. 8.1** A figurative representation of the spectrum of light demonstrating the wavelength of light used in Excimer laser systems (308 nm for the CVX-300 used in coronary intervention) relative to that used in OCT (1300 nm – within the infra-red spectrum), and other forms of industrial Laser (Ho:YAG and CO₂)

Optical coherence tomography (OCT) is an imaging modality that uses in the infra-red spectrum (central wavelength between 1250 and 1350 nm) to generate detailed images of the tissue structure being studied (Fig. 8.1). This particular spectral range provides the ideal window for imaging of biological tissues since the absorption of light by water, protein, lipids and haemoglobin is low for these wavelengths. OCT can be considered analogous to ultra-sound but uses light instead of sound. The imaging resolution in the axial direction is dependent on both wavelength and bandwidth, which are related to the speed of light ($3 \times 10^8 \text{ ms}^{-1}$) and are much higher for OCT compared to intravascular ultrasound (IVUS). The result is an axial resolution that is an order of magnitude greater for OCT (10–20 μm .) compared to IVUS (100–200 μm). However, the properties of vascular tissues limit the depth of light penetration to between 1 and 3 mm, when compared to 4–8 mm with IVUS [6] (Table 8.1).

The fundamental principles that underpin current OCT technology evolved from optical 1-dimensional low-coherence reflectometry. In the early 1990s, 2-dimensional imaging was enabled with the addition of transverse scanning (termed B-scan) [7]. This technique was named OCT by

James Fujimoto, one of the early pioneers in the field. It was first used to image the retina [6], and its use has been rapidly expanded to numerous biomedical and clinical applications. Although originally developed for use in transparent tissues, by applying light sources with longer wavelengths with larger penetration depths in non-transparent media, OCT could eventually be used to image opaque tissue.

Intravascular OCT uses a single optical fibre that both emits light and records its reflection, whilst rotating and being retracted back through the artery. An image is generated by measuring the time it takes for the emitted light to travel between the target tissue and back to the lens (echo time delay), and the intensity of light that is reflected/backscattered from the tissue structures being examined. Multiple scan lines are constantly acquired as the catheter rotates, and a complete revolution allows acquisition of a full cross sectional view of the arterial lumen. The speed of light ($3 \times 10^8 \text{ m/s}$) is many magnitudes greater than the speed of sound (1500 m/s), and hence it is not possible to measure the echo delay directly. Measurement is achieved with the use of interferometric techniques, and then resulting signals processed to produce an image. An interferometer (or 50/50 coupler) is used to split the image beam, one half being directed at tissue and the other half at a reference mirror. After reflection of both waves, the reference wave is then re-combined with the tissue sample wave. Constructive interference results when the path length of the light to the reference mirror and back equals that of the light reflected from the tissue sample. The precise mirror position gives a measure of depth and reflectivity within the tissue sample where reflection took place. These are combined and computed to produce a high resolution visual representation of the coronary artery intimal and medial walls. The maximum depth of penetration remains between 0.5 and 3 mm [8], with a maximal scan diameter (with modern Fourier Domain or Frequency Domain (FD)-OCT systems) of up to 11 mm [9, 10].

There are two main modalities of OCT available, Time domain (or TD-OCT) and FD-OCT. TD-OCT was the first commercially available system, and used broadband light and a reference mirror that moved in pre-determined, calibrated distances to produce known echo delays [11]. The reflected reference wave and tissue wave could then be combined, and then analysed within a photo detector, amplified and an image created from the resulting signal (Fig. 8.2). This technology has largely been replaced with FD-OCT systems. Here, the reference mirror is fixed, and the light source used is of variable frequency, but of near monochromatic wavelength – allowing a much higher frame rate and speed of data acquisition. This allows the simultaneous detection of reflections from all echo time delays, shortening the time taken to produce OCT images. This technology has replaced TD-OCT in modern interventional practice due to its ease of use, with significant improvements in pullback speed and image quality [10]. All the images used in this chapter were produced using FD-OCT systems.

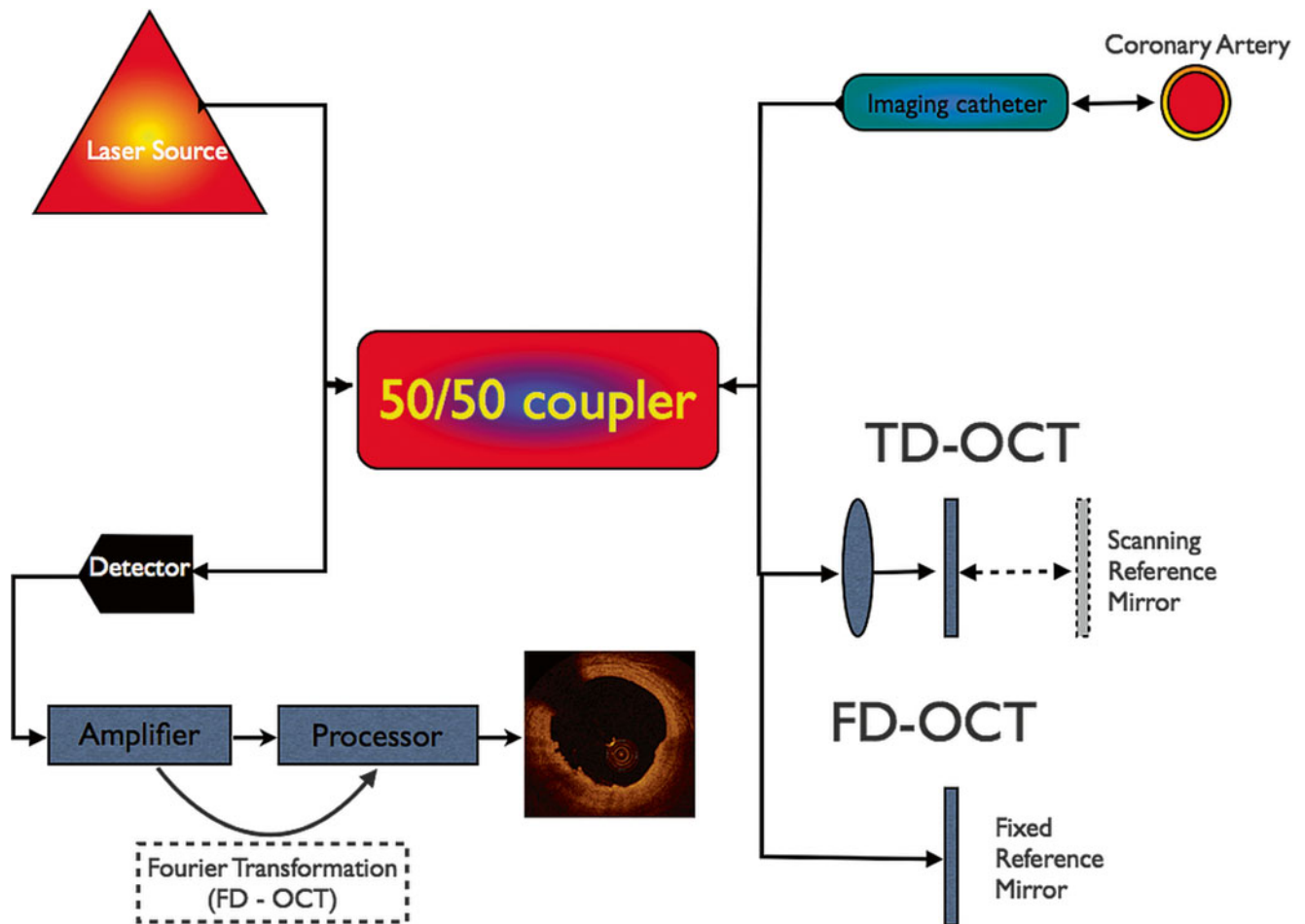


Fig. 8.2 A schematic representation of an OCT image acquisition system. Infra-red light is generated by the laser source and directed into the 50/50 Coupler (or interferometer). Here the beam is divided into a tissue arm, directed via an imaging catheter into the coronary artery, and a reference arm. Using a TD-OCT system (*upper panel*), the beam is mechanically scanned by a constantly moving mirror to produce a time

delay. In contrast, FD-OCT (*lower panel*) uses a fixed reference mirror, and uses a post amplification frequency sweep to analyse the returned beam detecting interference between the reference and tissue samples. This oscillates according to the frequency difference (indicating the depth of the reflected signal), and this is transformed (using a fourier calculation) to produce a measurable echo-delay

Commercially, FD-OCT systems are available from St Jude, the C7-XR/LUMIEN™ system (Dragonfly™ FD-OCT catheter) and Terumo LUNAWAVE^R (Fastview™ OFDI catheter & Lunawire™ OFDI system, with a further similar system in development from Volcano, but this is not yet available.

Image Acquisition

All commercially available OCT systems are essentially a single optical fibre, with a lens at the distal end. The system is advanced into the coronary artery, either directly (TD-OCT) or using a mono-rail casing (FD-OCT) [11]. The main barrier to the use of intravascular OCT in clinical practice is that images must be produced in a lumen free from blood. Inadequate blood clearance during image acquisition can dramatically degrade image quality. After clearing the blood from the arterial lumen, an acquisition run can be commenced,

using an automated pullback system retracting the system back towards the artery ostium. The use of an automated pullback is advised to enable accurate measures of length and to minimise movement artefact [12].

The first commercially available TD-OCT systems utilised an occlusive technique to establish a blood free lumen. A proximal over-the-wire occlusion balloon was first advanced over the OCT-wire, and an infusion of a crystalloid solution was administered through an end-hole in the balloon catheter to flush the lumen free of blood. Inflation and infusion times were dictated by the severity of patient symptoms and/or ECG changes, with the infusion times set to a maximum of 35 s to avoid haemodynamic instability [12, 13]. A power injector was usually required to inject fluid at a constant rate.

The occlusive technique is associated with a number of significant disadvantages, in addition to the induction of ischaemia (albeit transient). If the balloon is non-occlusive, then it may not be possible to achieve a blood free imaging

field despite saline flush. This may be exacerbated by retrograde flow from well-developed collaterals. It is also not possible to image ostial or very proximal lesions due to the length of the balloon. Due to the speed of the pullback – it was also difficult to image lesions in which the length exceed 30 mm [8].

With the development of FD-OCT, the majority of these limitations have been overcome. FD-OCT allows rapid imaging of the coronary artery lumen using a non-occlusive acquisition technique. The first FD-OCT catheter to become commercially available was the Dragonfly™, produced by St Jude Medical. The Dragonfly™ catheter comprises a single-mode OCT fibre encased in a metallic hollow torque wire that rotates at 100 rpm. It is advanced over a standard 0.014" guide wire, with a short monorail tip. A blood free field is still required, and created with an injection of a single bolus of crystalloid solution (usually angiographic iodinated contrast or a dextran solution) timed with the acquisition run. This can be done by hand, but the use of an automated contrast injection system is usually recommended to optimise the image quality. The imaging depth is approximately 1.5 mm with an axial resolution of 10–20 µm and lateral resolution of 25–30 µm. Images are acquired at a speed of 100 frames per second and the acquisition speed can be altered up to 25 mm/s to facilitate assessment of lesions over 54 mm in length.

A similar system is now available from Terumo (termed OFDi, the Lunawave™ system). The imaging depth, axial and lateral resolution are similar to the St Jude system but images are acquired at a frame rate of 158 frames per second with a maximum pullback speed of 40 mm/s permitting assessment of up to 150 mm in a single pullback. In addition, the Fastview™ OFDI catheter is “closed”, so there is no requirement to flush before imaging runs which is in contrast to the Dragonfly™ FD-OCT catheter. A third FD-OCT catheter technology remains in development by Volcano.

FD-OCT technology such as that described above has been shown to be safe [10, 11, 14] and reproducible [15] for the assessment of coronary artery luminal diameter, area and length. However image quality is dependant upon attaining co-axial guide catheter engagement to maximise contrast flow and a blood free arterial lumen.

Image Assessment (Table 8.1)

The following section will address the common appearances and define structures that are encountered during an OCT assessment within the coronary artery, focusing on pathology that is likely to be encountered when undertaking Excimer Coronary Laser Atherectomy.

The axial resolution of OCT gives the operator an opportunity to undertake a highly detailed assessment of the lesion

Table 8.2 Summary of the key atherosclerotic tissue characteristics identified with intra-coronary imaging highlighting the differences in tissue appearance observed between OCT and IVUS

Tissue type	Image characteristics	
	OCT	IVUS
Fibrotic plaque	Homogeneous High reflectivity/signal Low attenuation Poorly delineated margins	Homogeneous High reflectivity/ signal
Calcific plaque	Inhomogeneous signal Well delineated margins Low reflectivity Low attenuation	Very high reflectivity Acoustic shadow
Lipid plaque	Moderately delineated margins High reflectivity High attenuation High penetration	Low backscatter High penetration
Red thrombus	Medium reflectivity High attenuation	Medium-high reflectivity
White thrombus	Medium reflectivity Low attenuation	

that has been treated with Laser atherectomy. Correct interpretation of the OCT findings can alter the interventional strategy employed, and has the potential to affect patient outcomes. However, this is not intended to be an exhaustive description of all the findings that may be seen during an OCT assessment of a coronary artery, as this is beyond the scope of this article.

Particular features that may be recognised include vascular calcification, thrombus, the presence and integrity of stent architecture and the composition of the atherosclerotic plaque around the area of laser atherectomy.

Atherosclerotic Findings at OCT (Table 8.2)

Calcification within the coronary media may be identified by sharply delineated, homogeneous zones, with a low degree of back-scatter (Fig. 8.3). The thickness of most superficial calcium can be determined, as well as its relationship to the overlying intima and other media structures. In a similar fashion to that seen on IVUS, the arc of calcification can also be examined, and graded by the number of involved quadrants (from 1 to 4). The penetration depth of OCT, and relative properties of calcific plaque also allow a limited assessment of the depth and extent of medial calcification that may be obscured during IVUS. The limitation remains the depth of light penetration into the media that at present is constrained to between 1.5 and 3 mm [12].

Fibrous tissue is seen as homogeneous tissue that has a high reflectivity and low signal attenuation (Fig. 8.3). In contrast, lipid pools are less well demarcated, with a diffuse edge appearance and more heterogeneous back-scattering

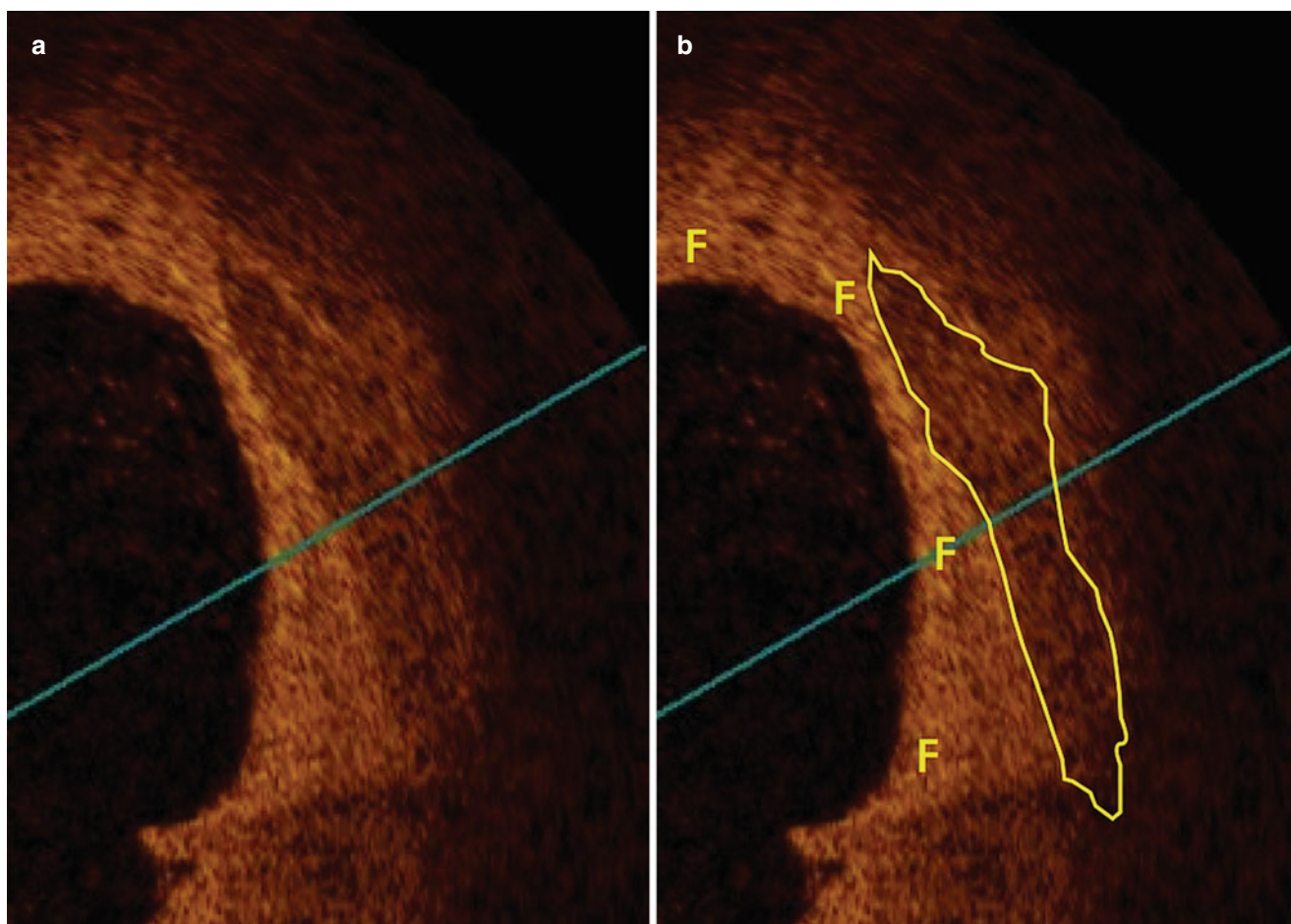


Fig. 8.3 Medial Calcification – seen as a well delineated low signal homogenous zone within the media (a), highlighted in panel (b). Note the extensive intimal thickening overlying the calcified region (indicated by *F*), consistent with fibrotic atherosclerosis

than predominately fibrous atheromatous lesions (Fig. 8.4). There is a strong contrast between fibrous and lipid filled lesions on OCT with lipid filled plaques appearing as diffuse low-density homogenous regions with overlying signal-rich bands that histologically correspond to fibrous caps. The axial resolution of OCT allows the operator to make precise assessment of fibrous cap thickness. Pathological studies indicate that a fibrous cap thickness of less than 65 μm is the threshold that identifies a vulnerable lesion [16] – increasing the likely-hood of plaque rupture and a subsequent acute coronary syndrome [17–19]. OCT remains the only imaging modality with the resolution to reliably and reproducibly assess for thin-capped fibro-atheroma with an acceptable degree of sensitivity and specificity [17–19] (Fig. 8.4).

In the setting of ELCA, thin capped fibro-atheroma (TFCA) is most likely to be identified in acute coronary syndromes – often associated with significant intra-coronary thrombus. OCT is able to identify and assess the presence of thrombus within the coronary artery with a higher degree of sensitivity and specificity than with IVUS alone

[20]. Thrombus is identifiable as a mass that protrudes into the vessel lumen that appears not to be in continuity with the vessel wall. OCT is able to differentiate clearly between red and white thrombus (Fig. 8.5). Red thrombus, composed largely of red blood cells, has a characteristic high degree of signal attenuation, with a resulting large amount of signal dropout that is seen as a shadow behind the protuberance. In contrast, white thrombus, composed largely of platelets and white blood cells, is seen as identifiable as signal rich projections that extend into the vessel lumen that lack the backscattering seen in red thrombus [21] (Fig. 8.5).

OCT is highly sensitive at the detection of arterial dissection, both spontaneous and iatrogenic. Dissection is seen as a linear rim of tissue that extends into the lumen, with clear separation from the vessel wall (Fig. 8.6). These may be associated with underlying atheromatous plaque and ulceration – with or without overlying thrombus. In particular, the use of OCT during coronary intervention (e.g. after balloon angioplasty and at stent edges) will identify vessel dissection

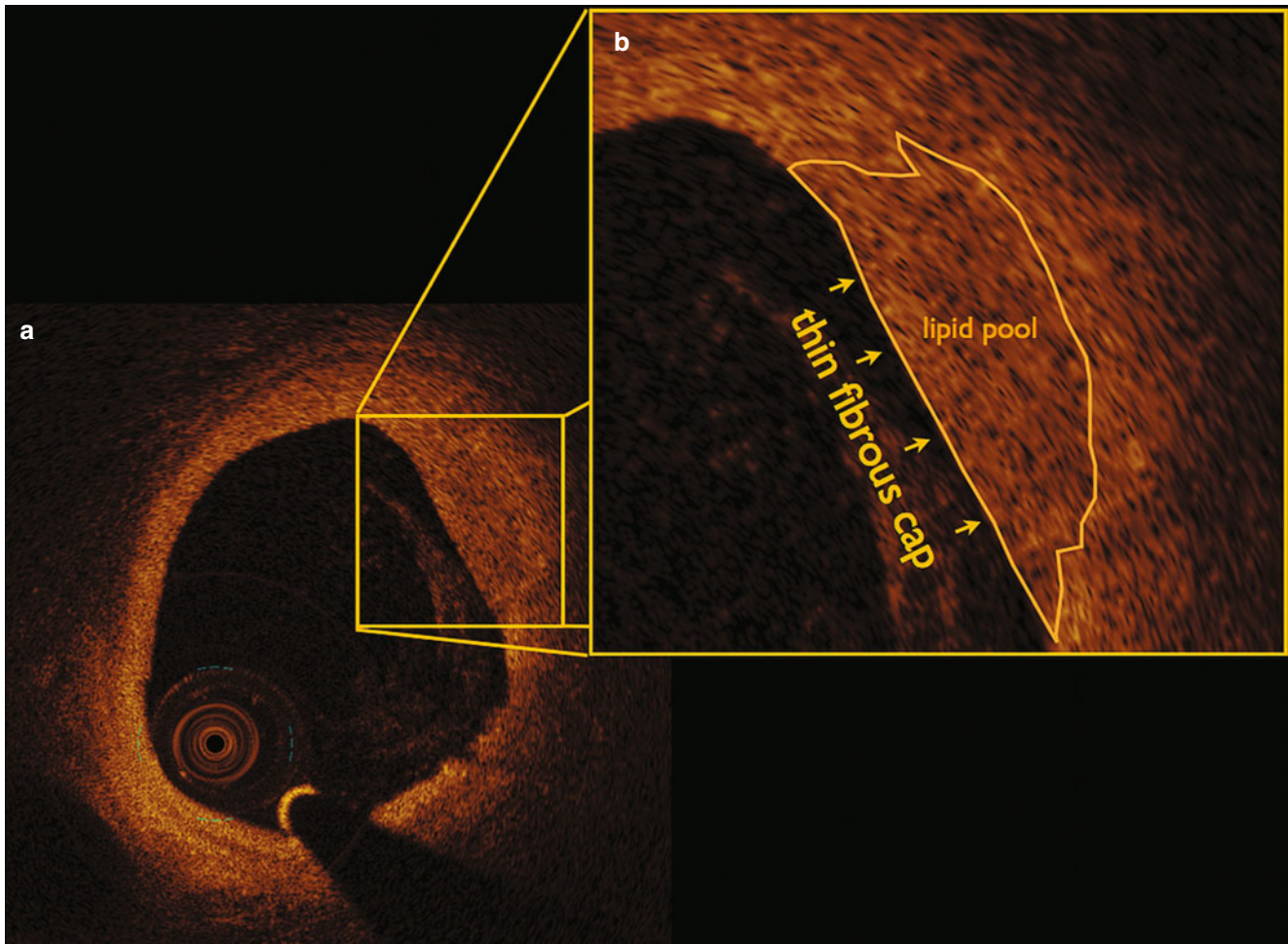


Fig. 8.4 Thin capped non obstructive lipid plaque (Panel **a**) – the lipid pool is seen as a low density homogenous region with poorly defined margins, within the thickened fibrotic intimal layer (highlighted in

panel **b**). The overlying fibrous cap extremely thin, as is shown in panel **b**, but is intact and not associated with any visible thrombus nor ulceration

that may not be apparent angiographically. These can be described by their length (mm), depth, width and circumferential extension (expressed in degrees or quadrants).

Stent Architecture

Optical coherence tomography has become established as the gold standard for assessing the luminal stent architecture and deployment *in vivo*. In particular, the high axial resolution of OCT allows a clear and accurate assessment of stent endothelialisation and healing [6]. In addition, with the increasing use of bio-absorbable scaffolds (BVS), the use of high definition intravascular imaging technology has become an important part of artery sizing and assessment of scaffold deployment.

A metallic stent can be identified on OCT as a highly reflective spot associated with a clear defined drop-out shadow behind the stent strut. A metallic stent is a highly

reflective structure, and as such, only the reflection of the luminal surface is visible and OCT is unable to provide a direct measurement of strut thickness (Fig. 8.7). Stent overlap can be identified in an axial section by the presence of two concentric layers of stent struts. Incomplete Stent Apposition (ISA) can be identified if there is a separation of the stent strut from the vessel wall. As the full stent thickness is not visible on OCT, at a strut level, ISA is defined as a measured distance from the vessel intimal surface that is greater than the strut thickness (alone for bare metal stents), or strut plus polymer (or similar) for drug eluting stents (Fig. 8.7).

ISA may be acute – i.e. at the time of stent deployment, or late – observed at follow-up and as a consequence of positive arterial remodelling. OCT studies after stent deployment consistently demonstrate a higher proportion of malapposed struts – even after extensive post dilatation – when compared to IVUS [22]. This is particularly evident over areas of stent overlap, and when treating a long segment of stent (particularly in calcific disease). It was considered that a strut was

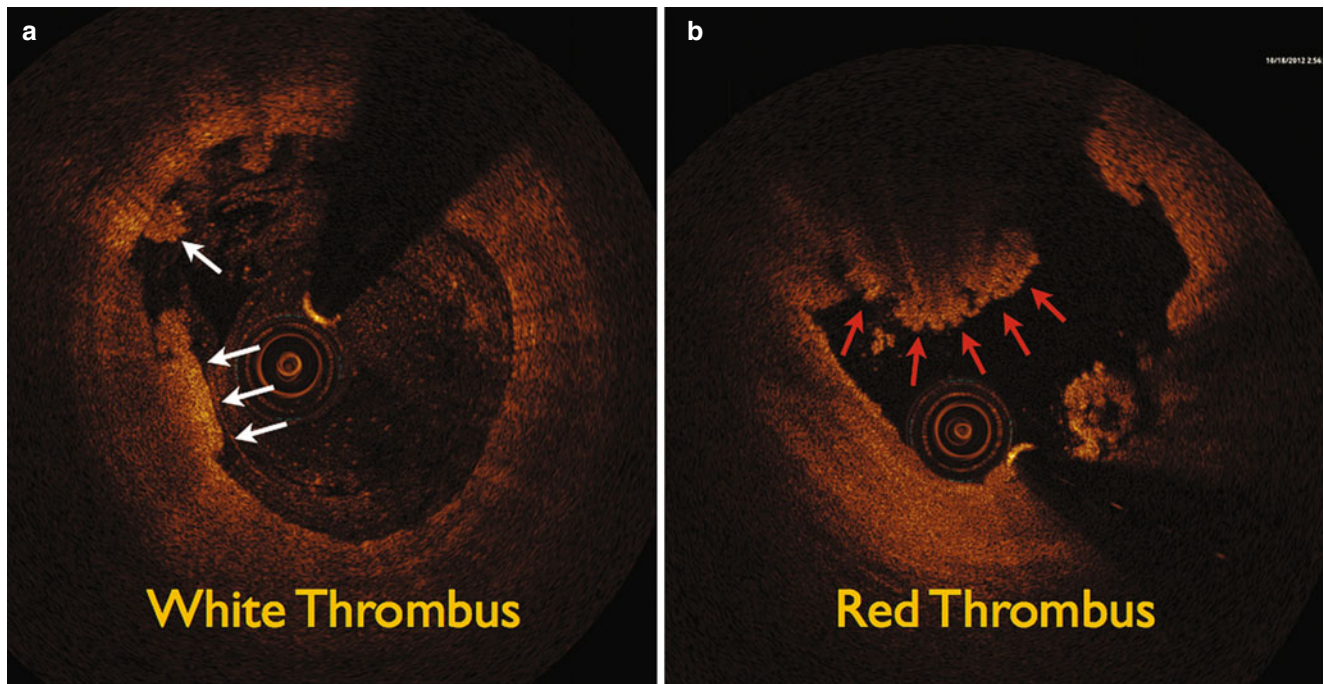


Fig. 8.5 Panel **a** illustrates the appearance of white thrombus, indicated by the *white arrows*, as a signal rich projection into the lumen, with a relatively low degree of backscatter and the intimal surface visible underneath. In contrast, Panel **b** demonstrates a large volume of red thrombus (indicated by the *red arrows*), as a highly reflective mass projecting into

the lumen, with a large amount of backscatter – obscuring the underlying arterial surface. In reality, most arterial thrombus is a mixture of red and *white thrombus*, and these are rarely identified in isolation. Incidentally, note the artifactual appearance within the lumen that results from inadequate clearing of the blood pool during image acquisition

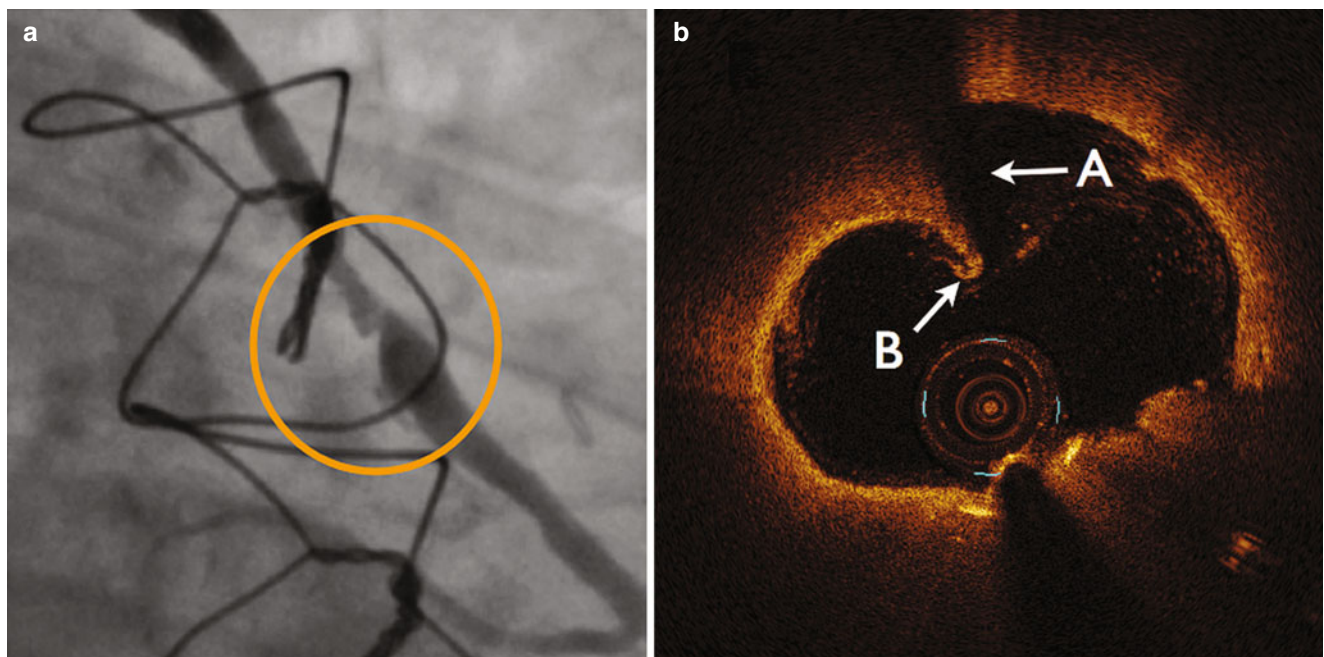


Fig. 8.6 An angiogram (Panel **a**) and OCT frame (Panel **b**) taken from an assessment of a degenerative vein graft prior to any intervention. A flap is evident angiographically (highlighted with circle – Panel **a**), confirmed on OCT as a dissection flap (Panel **b**, *arrow A*), as a linear

portion of tissue that is clearly separated from the vessel wall, that extends into the lumen. The intimal disruption can be seen (*arrow B*), with a frond of redundant intima evident. In this example, the dissection is not associated with significant overlying thrombus

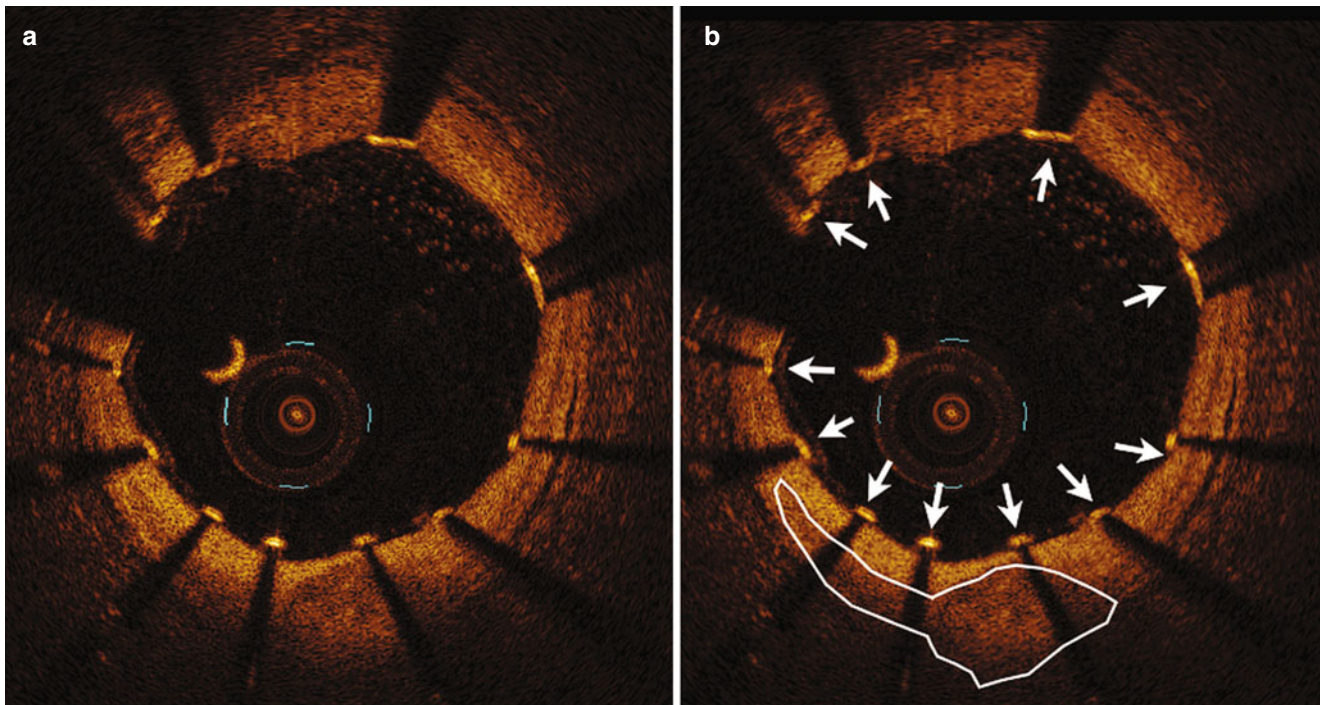


Fig. 8.7 A single OCT cross sectional image demonstrating a well deployed stent (Panel **a**). The stent struts (indicated by the *white arrows*) are highly reflective structures with a large amount of backscatter. All struts in this case are well apposed to the intimal surface. This stent was

inserted during the case, so there is no neo-intimal coverage at this stage. This would be seen as a homogeneous layer covering the bright, reflective stent strut. Of note in this image is the large lipid pool in the media – highlighted in image (**b**) – with a thick overlying fibrous cap

malapposed if >200 μm from the vessel wall when taking into account the strut thickness of the individual stent. However, more recent data suggests that ISA of <280 μm (for sirolimus eluting stents) and <260 μm (for Pacitaxel eluting stents) is likely to be clinically benign [23].

In contrast to metallic stents, bio-resorbable scaffolds (BVS) have a significantly lower degree of light reflectivity. Therefore, the entire strut is visible, and thickness can be assessed accurately (Fig. 8.8). OCT has become the modality of choice for assessment of BVS post deployment, including the pattern of degradation and neo-intimal coverage (Fig. 8.8). As the BVS is absorbed, the degradation process results in spaces replacing scaffold struts, but with the second generation of devices – mechanical integrity is maintained [24], as the device fragments. The treated artery appears to positively remodel, without loss of luminal diameter.

The use of OCT in the evaluation of in-stent restenosis has redefined the way that ISR is evaluated and treated. There is a wide heterogeneous clinical presentation of patients with ISR, ranging from dramatic acute infarction (e.g. STEMI), to progressive silent occlusion and gradual formation of a chronic total occlusion (CTO). In particular, ISR of drug eluting stents often have highly variable imaging characteristics – both at angiography and with the use of

intra-vascular imaging. The presence of concentric fibrosis, neo-vascularisation and calcification within the ISR can define the clinical presentation [25] and guide the interventionist towards an appropriate treatment strategy.

Within bare metal stents, early in-stent restenosis with a concentric dense fibrotic layer within the margins of the stent struts can be clearly identified with OCT. Over time, this layer can become thicker, and accumulate significant quantities of lipid plaque within the re-stenotic segment [26]. Thin-capped fibro-atheroma may also develop – observed in 16 % of BMS late re-stenotic lesions in one series [27]. Within drug eluting stents, the pattern of restenosis differs to that observed in BMS. In early DES re-stenosis, a mixed heterogeneous fibrinous layer is often observed, with low signal images in the deep tissue layer that are considered to represent fibrin surrounded proteoglycan extra-cellular matrix. Neo-atheroma may be seen more frequently, and progress more rapidly in DES when compared to BMS [28]. As yet, the differences in the in-stent atheroma observed do not alter the interventional strategy employed, but may determine the initial clinical presentation (e.g. stable angina vs. an acute coronary syndrome).

Having considered the common OCT appearances prior to ELCA, the following section will detail the appearance of the coronary artery following deliver of Laser energy.

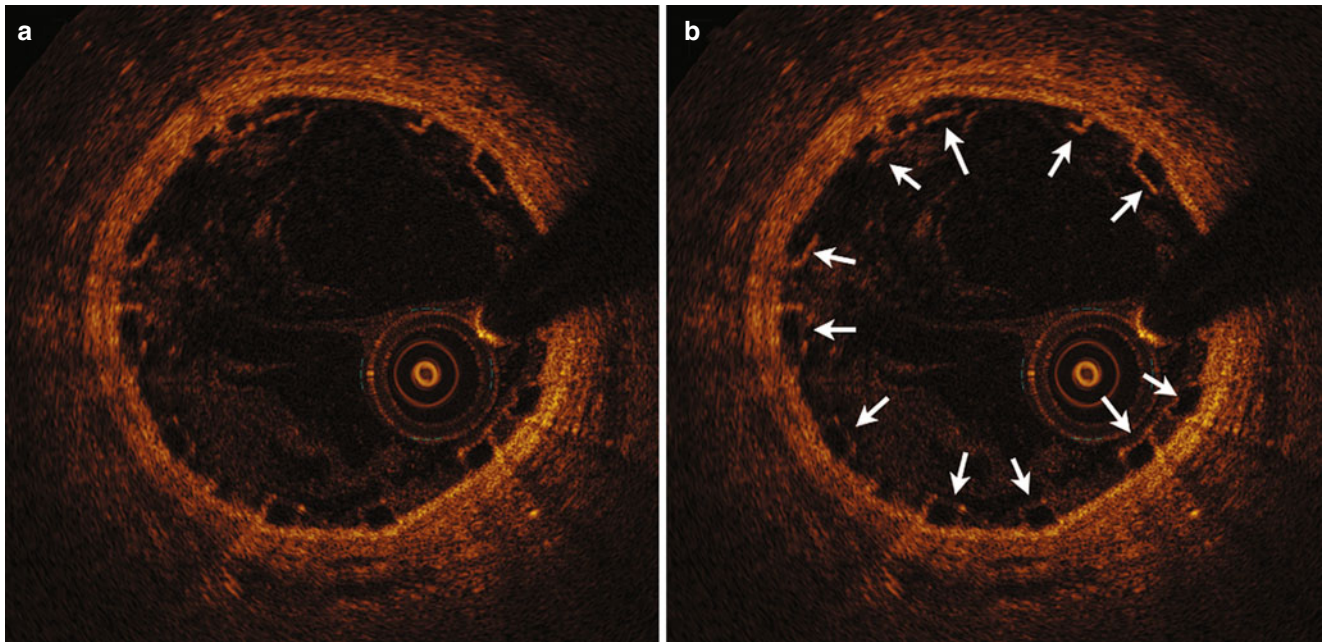


Fig. 8.8 An OCT cross section demonstrating a bio-resorbable scaffold (BVS) immediately post deployment (Panel A). In contrast to the stent seen in Fig. 8.6, the whole scaffold strut is clearly visible (Panel B – indicated with *white arrows*) and sharply demarcated. The scaffold is well opposed to the intimal surface, and in time the struts will be covered by neo-intima and be absorbed into the vascular

wall. First generation BVS will leave an empty space as the strut is dissolved – but the second generation device appears to maintain its mechanical properties during the process of stent fragmentation, without loss of functional luminal diameter as the artery positively remodels

Indication 1: In-Stent Re-stenosis (ISR)

Despite significant advances in drug eluting stents (DES), target lesion revascularisation (TLR) remains a limitation of PCI, with angiographic ISR of up to 10 % in patients with DES [29].

ELCA is a safe and effective technique in the treatment of ISR [30]. Examination of 107 re-stenotic lesions in 98 patients, with both IVUS and quantitative angiography (QCA), demonstrated that lesions treated with ELCA, compared to balloon angioplasty (POBA) alone, had a greater cross sectional area and luminal gain, with more intimal hyperplasia ablation. There was a trend towards a less frequent need for target vessel revascularisation (TVR) at 6 months, but this did not reach statistical significance (TVR 21 % vs. 38 % $p=0.083$) [30].

Case 1 (Fig. 8.9)

A 57-year-old with previous multi-vessel PCI (using a 3.0×24 mm sirolimus eluting stent) 3 years previously underwent angiography, via the right radial artery (RRA) identifying a severe fibrotic re-stenotic lesion in the proximal LAD (Fig. 8.9ai). Due to the dense fibrotic restenosis, laser atherectomy was undertaken, to maximise luminal gain, in this

large vessel that is likely to supply a large area of myocardial territory and therefore of prognostic significance.

A 1.4 mm concentric ELCA catheter was used, delivered through a standard 6 french guide, using an energy of 60 mJ/mm^2 at a pulse repetition rate (PRF) of 40 Hz, delivered approximately 8000 pulses over 20 runs. The OCT appearance post ELCA (Fig. 8.9b) demonstrates a reduction in neo-intimal material, and creating a cleft/dissection plane having, extending to the media (Fig. 8.9b (zoom)). Stent expansion was achieved with sequential non-compliant (NC) and Paclitaxel eluting balloon inflations (Pantera Lux, Biotronik, Berlin, Germany) (Fig. 8.9ci).

ELCA proved effective in debulking the lesion, an effect that is not a consequence of thermal injury [31], as in-vivo models have demonstrated acceptable temperature changes within stented porcine arteries. Neither does ELCA distort stainless steel stent architecture, when 1000 pulses of energy are applied [32]. The process of Laser tissue ablation disrupted the neo-intima, creating tissue planes to facilitate balloon expansion, and provide maximal luminal gain and full stent apposition. Subsequent delivery of Paclitaxel to arrest the early healing phase and minimise late loss is likely to be more effective when the stent is maximally expanded within minimal neo-intimal tissue.

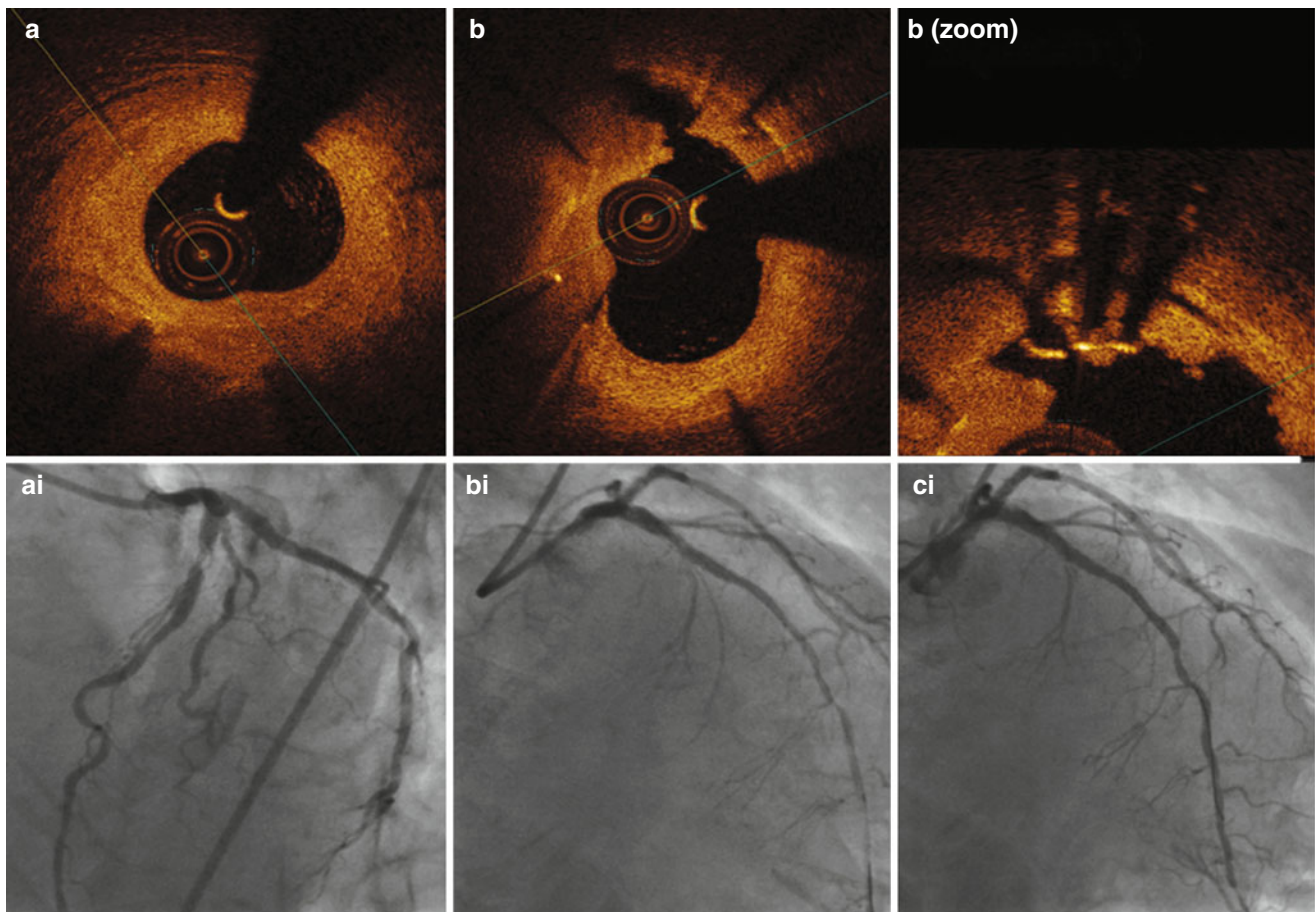


Fig. 8.9 Severe concentric fibrotic In-stent restenosis in the proximal LAD DES on angiography (panel **ai**) and the corresponding OCT (panel **a**). Post ELCA, a cleft/dissection plane is evident (panel **b**),

extending to the true intimal layer (panel **b**-zoom). This was subsequently treated with sequential non-compliant and paclitaxel eluting balloon inflations with an excellent final angiographic result (panel **ci**)

Indication 2: Coronary Calcification and Uncrossable Lesions

With an ageing population, the frequency with which complex, calcific coronary disease is encountered during PCI is increasing. The presence of a CTO or calcific/non-compliant stenoses can make intervention challenging, often requiring adjuvant techniques. When the lesion can be crossed with a guide-wire but not with a low-profile balloon, ELCA is well established as an effective and simple technique, that works on the standard 0.014" guide-wire to provide an efficient and safe solution. Similarly, when the lesion fails to expand adequately to balloon dilation, ELCA is usually effective, particularly when there is a focal fibro-calcific lesion preventing balloon expansion.

However, within heavily calcified arteries, rotational atherectomy remains the most effective plaque modification therapy. This technique still requires delivery of a specific 0.009" stainless steel guide wire (Rotawire™, Boston Scientific, Boston, USA), which is much less deliverable than standard 0.014"

wires. Indeed, a proportion of lesions cannot be crossed with either Rotawire™ directly or using a micro-catheter exchange system. In these circumstances, an ELCA catheter can be advanced over a standard 0.014" guide wire first to create a sufficient channel to permit subsequent Rotawire™ passage. We have termed the combined use of ELCA and rotational atherectomy the "Raser" technique [3], with a comprehensive explanation of the technique contained within Chap. 3. Furthermore, our group has recently published our experience of ELCA in 58 patients where the lesion was non-crossable or non-expandable [5]. It should be noted that the delivery of one or more trains of laser energy, even if the lesion is not transversed, will often induce sufficient plaque modification to allow passage of a micro-catheter or Rotawire™.

Case 2 – (Fig. 8.10)

A 70 year. old with angina was referred for intervention to his right coronary CTO. He had previously undergone complex intervention to his circumflex artery via the right radial route, so this procedure was conducted via the left radial

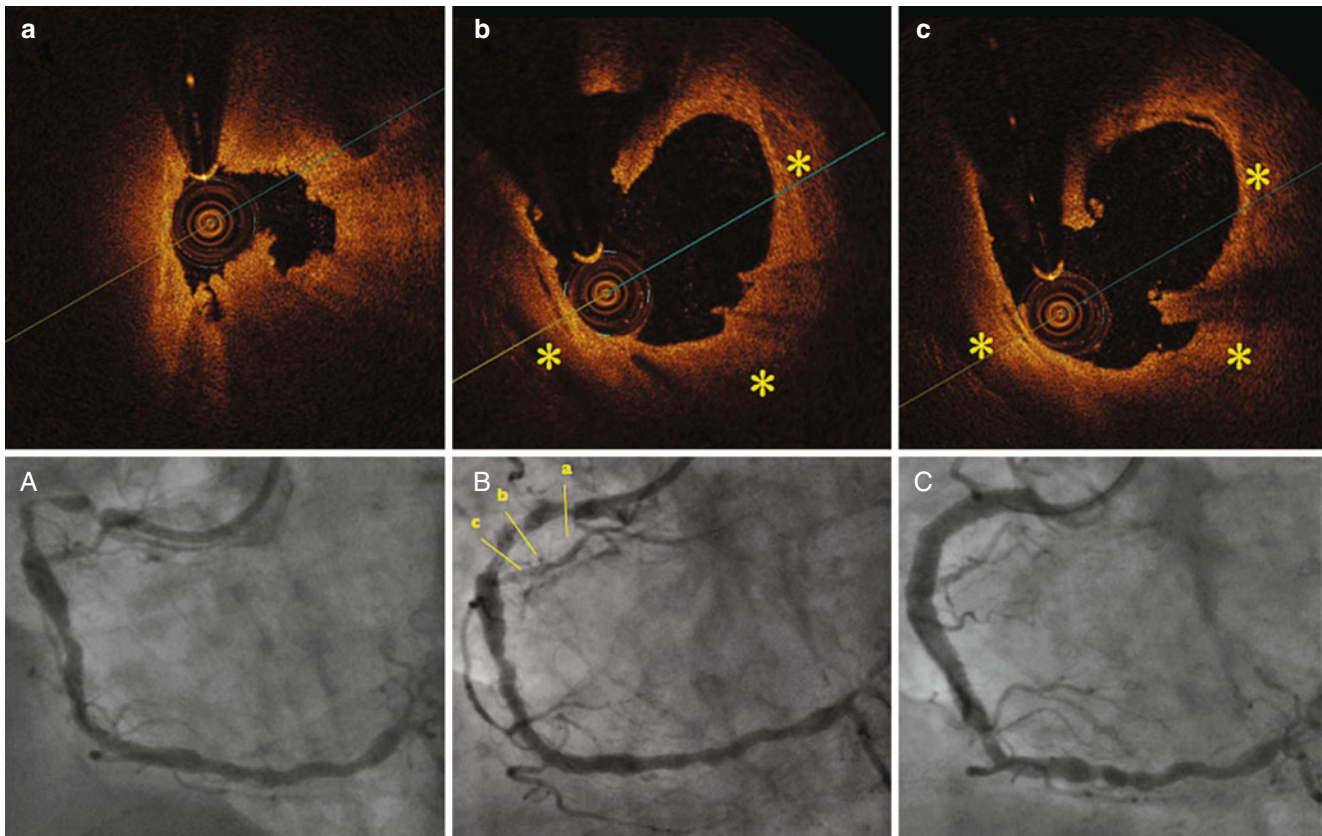


Fig. 8.10 Panel A demonstrates a severe calcific lesion in the proximal RCA. This proved uncrossable. ELCA was undertaken, and the OCT taken post-ELCA is shown in panels a–c, with the position in the RCA indicated on panel B. A variegated fibro-thrombotic lesion is seen in the proximal artery with the appearance of white thrombus on the inferior border (a). Extensive media calcification is evident, but little involving

the intima directly (shown with *in panel b, c) Multiple dissection planes are evident distally, within the diseased intimal layer, not extending into the calcific media (panel b, c), and not apparent angiographically (panel B). The lesion was now easily crossable with an NC balloon. After pre-dilatation, the case was completed with 2 DES, with the final angiographic appearance shown in panel C

artery. An AllRight 4.0 6 french guide catheter was used, and a Sion Blue (Asahi, Abbott Vascular, Illinois, USA) 0.014" wire was successfully advanced to the distal vessel.

The proximal lesion (Fig. 8.10A) proved un-crossable with either a low profile (1.0 mm diameter) balloon or micro-catheter—and ELCA was undertaken. There was an expectation that rotational atherectomy would be required in this case, but as the lesion was difficult to cross with a Sion wire, a Rotawire™ would not be deliverable. Therefore, an X80 0.9 mm catheter, at an energy of 80 mJ/mm² with a PRF of 80 Hz, was used to deliver 7900 pulses over 12 trains with full traversing of the lesion.

OCT taken post-ELCA demonstrates a variegated fibro-thrombotic lesion in the proximal artery – with white thrombus apparent on the inferior border (Fig. 8.10a). Extensive media calcification is evident, but little involving the intima directly (Fig. 8.10b). Multiple dissection planes are observed distally, within the diseased intimal layer, not extending into the calcific media (Fig. 8.10b, c), and not apparent angiographically (Fig. 8.10B).

In view of the lack of intimal calcification, the decision was made to attempt crossing with a non-compliant balloon

(4.0 mm × 20 mm) which was successful, and this expanded fully at 10 atm. Once adequately prepared, the lesion was treated with two overlapping drug eluting stents (4.0 × 24 mm & 4.0 × 28 mm Biomatrix Flex, Biosensors, Singapore). Rotational atherectomy was therefore not required as predicted by the OCT images despite an ambiguous angiographic image.

When a lesion proves to be uncrossable, ELCA is an effective strategy to facilitate PCI. Here, ELCA debulked the atheroma, increasing vessel compliance allowing large calibre balloon inflation and stent delivery with minimal further preparation. OCT supports this – illustrating the focused tissue ablation resulting from ELCA (Fig. 8.10b, c).

Indication 3: Saphenous Vein Graft Intervention

Atheromatous degeneration of saphenous vein grafts (SVGs) is characterised by multi-focal, diffuse, degenerative lesions that often contains significant athero-thrombotic material

[33]. This is prone to distal embolisation and subsequent no-reflow. Hence, distal protection devices (DPD) are advocated when attempting SVG-PCI [34].

ELCA has been proposed as an alternative to a DPD, as particulate matter released during tissue ablation is below the diameter of a capillary and can be easily be resorbed by the reticulo-endothelial system. Where a lesion is too severe for initial DPD passage, a small diameter ELCA catheter can safely traverse the lesion, avoiding distal embolisation, to facilitate subsequent DPD delivery and case completion with stenting. Alternatively a larger diameter ELCA catheter may be the preferred option either with or without DPD to offer maximal debulking of the vein graft before stenting.

ELCA in SVG-PCI has been studied in a number of registries. Data from the original laser registry showed that distal embolisation occurred in only 18/546 (3.3 %) of SVG stenoses treated [35] Prospective data from the CORAL multi-centre registry compared 98 patients who underwent SVG-ELCA, where DPD delivery was not possible, with the SAFER (Saphenous Vein Graft Angioplasty Free of Emboli) control group. They demonstrated that ELCA was safe and feasible but failed to demonstrate an advantage over standard treatment [36]. In contrast, in retrospective cohort of 119 patients who presented with acute myocardial infarction (AMI) and underwent ELCA SVG revascularisation, the peri-procedural MI (CK-MB release) rate was dramatically lower than that seen in the SAFER group (2.4 % vs. 8.4 %, $p=0.02$). (36) There are no randomised control trails of ELCA versus DPD to date [37].

Case 3 – (Fig. 8.11)

An 82 years. old lady with previous CABG and recurrent angina attended for treatment of a severe SVG lesion. This was a high risk case, as this was the last remaining vein graft, supplying a dominant right coronary system. The native vessel had a long length of disease and was not amenable to percutaneous intervention.

Angiography was conducted through the right femoral artery, and a 50 cm 8 french long sheath was required to access the aorta due to excessive tortuosity. An 8 F MPA guide was used to intubate the graft. OCT was undertaken to examine the lumen of the vein graft and confirm the most significant area area stenosis in the proximal SVG (Fig. 8.11a, ai). ELCA was to used in attempt to maximise luminal gain and reduce the risk of distal embolisation. Passage of a DPD was attempted, but would not pass easily – so was abandoned. The stenosis was treated with a 2.0 mm concentric Eximer laser catheter, at an energy of 60 mJ/mm² with a PRF of 40 Hz, delivering 4000 pulses in 10 trains.

OCT post ELCA (Fig. 8.11b), demonstrated dramatic reduction in the atheroma burden. However, the laser-tissue interaction created a friable intimal surface (a mixture of white thrombus and fibro-atheroma), despite the theoretical

micro-particle generation [37, 38]. Distal embolisation therefore is a risk with passage of any device, supporting the position that DPD should be used, if possible, before stent deployment in a SVG.

The OCT images demonstrate that despite the use of large diameter ELCA catheters, large fragments of friable potentially embolic material remain on the lesions surface and supports the use of DPD, despite upstream ELCA.

This case was completed (without DPD), with a single pericardial covered stent (Over and Under, Trendymed, Toronto, Canada) (Fig. 8.11c).

Case 4 (Fig. 8.12)

A 76 years. man with a previous history of severe 3 vessel ischaemic heart disease and coronary artery bypass surgery, presented to the catheter lab acutely with recurrent angina despite optimal medical therapy. Coronary angiography demonstrated a severe lesion in the vein graft to OM2 (Fig. 8.12a)

OCT confirmed the severity of the disease within the degenerative graft, with an MLA of only 3.4 mm². In an attempt to reduce the atheroma burden, and maximise lumen diameter, ELCA was undertaken. Using a 1.7 mm concentric catheter at an energy of 45 mJ/mm², and a PRF of 25 Hz, 22 trains of Laser were delivered (a total of 3000 pulses). A DPD was not used due to the severity and complexity of the lesion at initial OCT assessment. OCT assessment following delivery of ELCA demonstrates a reduction in the atheroma burden without any angiographic nor electrocardiographic evidence of distal embolisation.

The lesion was treated with a single drug eluting stent with an excellent angiographic result. Here, ELCA was used in the absence of distal protection without adverse complications. There remains however friable material within the lesion, and maybe use of a DPD should be advocated if such a device can be delivered across a lesion.

Indication 4: Intra-coronary Thrombolysis and Primary PCI

Primary PCI (PPCI) for the management of acute ST elevation myocardial infarction (STEMI) is accepted as current optimal treatment [39]. Performing PCI with significant arterial thrombus is often challenging and may increase complications, in particular from distal thrombus embolisation and microvascular obstruction. There have been multiple adjunct devices that have been developed aiming to facilitate effective and safe revascularisation in this setting. These include a variety of simple aspiration thrombectomy catheters, mechanical thrombectomy devices, mesh covered stents and infusion catheters designed to deliver glycoprotein IIb/IIIa antagonists and/or vasodilators downstream from the

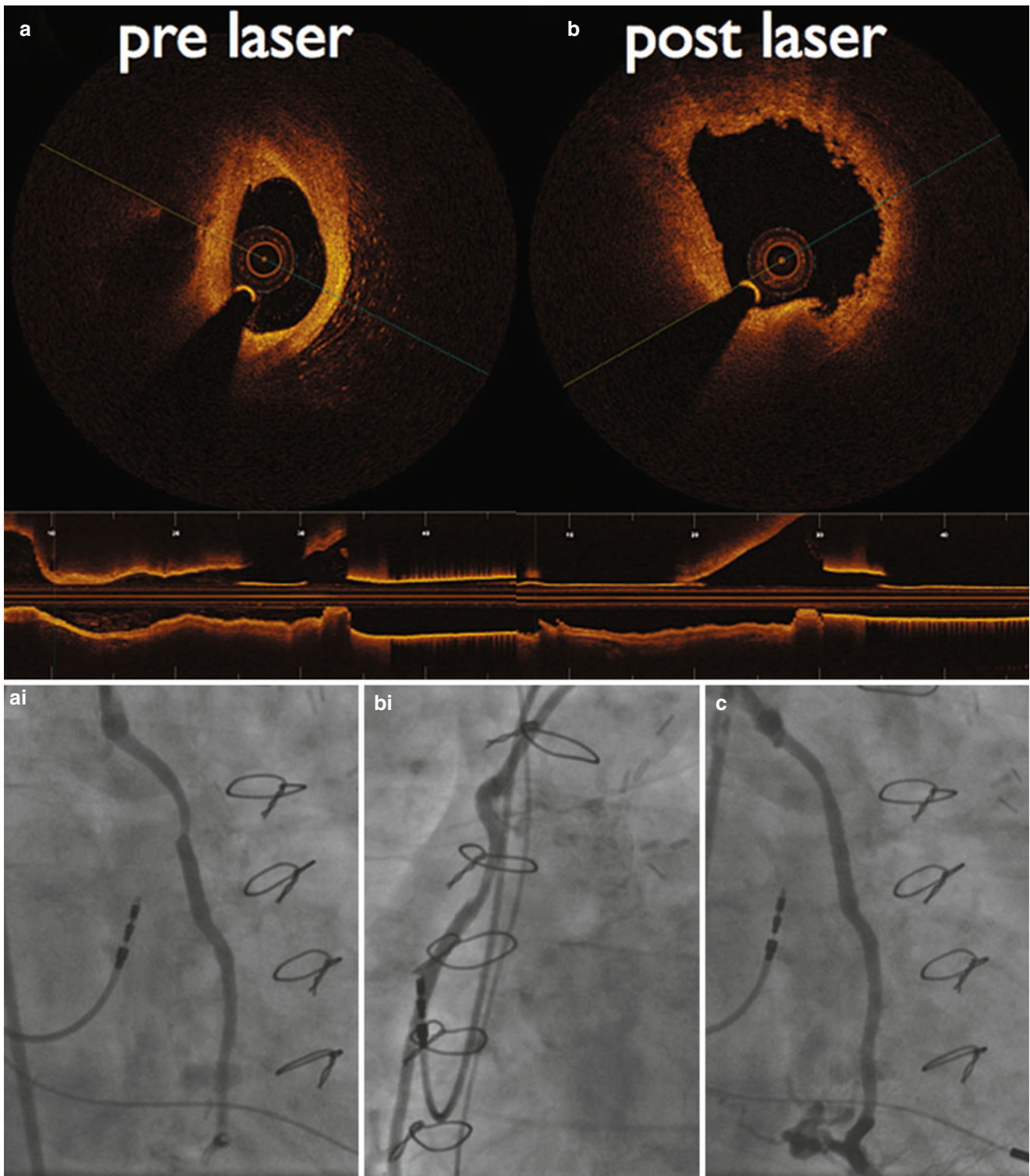


Fig. 8.11 Angiographic (panel ai) and OCT (panel a) images demonstrating a severe lesion in a saphenous vein graft. OCT post ELCA (panel b, bi), demonstrated dramatic reduction in the atheroma burden, with panels a, b taken from identical angiographic positions. However, the laser-tissue interaction created a friable intimal surface (a mixture

of red thrombus and fibro-atheroma), despite the theoretical properties of tissue ablation micro-particle generation, and not seen angiographically. This case was completed using a single pericardial covered stent (panel c), with an excellent angiographic result

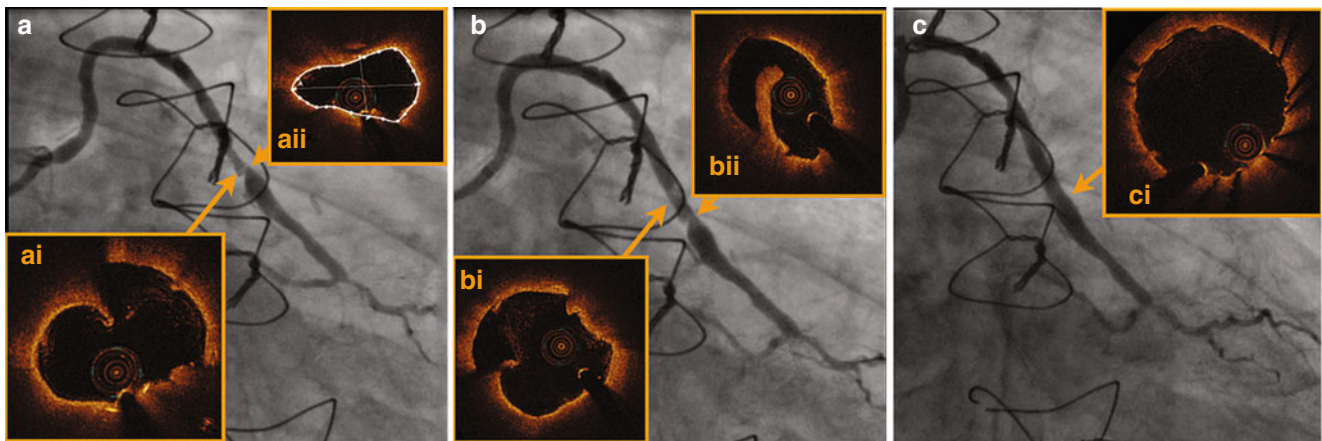


Fig. 8.12 Panel **a** demonstrates a severe lesion in the mid portion of a diffusely diseased saphenous vein graft. Upon OCT interrogation, a dissection flap is evident (panel **ai**) proximal to a severe stenosis, with an MLA of 3.38 cm (Panel **aai**). ELCA was undertaken – on this occasion without a distal protection device. Analysis of the OCT image post

ELCA demonstrates a significant reduction in atheromatous plaque burden. Extension of the atheromatous dissection is clearly shown in panel **bii**, that is not clearly seen angiographically. The case was completed with deployment of a single DES with an excellent angiographic and OCT result (panel **c**)

point of occlusion. However, when subjected to large scale robust randomised control trials, none have proved superior to conventional PCI technique.

With respect to the most widely adopted technology, simple aspiration thrombectomy, the TAPAS (Thrombus Aspiration during Primary Angioplasty Study) trial (n= 1000 patients), demonstrated significantly lower all cause mortality rate in the thrombus aspiration arm at 1 year, when compared to balloon angioplasty alone [40]. However, the larger TASTE study of over 7000 patients failed to reproduce this finding at 30 days [41]. There is a small positive dataset to support the use of the M-guard mesh covered bare metal stent in PPCI [42], with a large randomised study in STEMI currently underway [43].

Although there are no significantly powered endpoint trials of using ELCA in PPCI, there is growing recognition amongst ELCA users that the device is very effective in this situation. Using laser energy to treat coronary thrombus has a number of potential advantages. ELCA facilitates removal of organised thrombus, destroys pro-coagulant mediators, augments tissue plasminogen factor [44] and appears to suppress platelet aggregation [45]. Exposure of healthy blood, in-vivo, to incremental doses of laser energy resulted in a dose dependant suppression of ADP and collagen-induced whole blood aggregation, with suppression of platelet contraction force at higher energies. The precise mechanism for this inhibition of function remains unclear, but no morphological changes were apparent within ELCA exposed platelets on electron microscopy [45]. In addition, spectrophotometric studies have demonstrated that thrombus absorbs laser light emitted at a optimal wave length of 415-514 nm, within the blue-green spectrum in close

proximity to the Excimer laser (wavelength 308 nm). Therefore laser energies are directly transmitted into the thrombus, leading to vaporisation and penetration into the clot in a linear dose response fashion [46].

In the pre-PPCI era, a number of registries report the use of ELCA in AMI. In a cohort of 50 patients who presented with STEMI (56 %)/NSTEMI (44 %) requiring emergency revascularisation, ELCA success rate was 100 %, and significant reduction in thrombus was observed in 83 %. TIMI flow increased from 1.7 (± 1.1) to 2.8 (± 0.4), with only a single ELCA-induced dissection. This demonstrated safety, feasibility and relative efficacy for ELCA in AMI [47].

The multi-centre CARMEL registry, reported on 151 patients with AMI (54 % Q-wave, 46 % non-q-wave) who underwent ELCA [48]. Laser energy was delivered in 95 % of cases, with a 97 % angiographic success rate and TIMI flow restoration (1.2 ± 1.1 to 2.8 ± 0.5 ($p < 0.001$)). A large thrombus burden was present in 65 % cases and it was in these cases that ELCA had the greatest effect on luminal diameter. Complications included dissection (5 % major, 3 % minor), perforation (0.6 %), acute vessel closure (0.6 %) and distal embolisation (2 %). The authors concluded that application of ELCA in AMI was most effective in lesions with extensive thrombus.

There is limited data examining ELCA in PPCI for STEMI. In a single centre study of 66 consecutive patients, ELCA was used during primary/rescue PCI. Myocardial blush grade was increased from 0.12 ± 0.4 to 2.5 ± 0.5 (42) with TIMI flow increasing from 0.2 ± 0.4 to 2.65 ± 0.5 [49]. The increase in myocardial blush grade is an indication that ELCA may improve outcome, as was observed in TAPAS [40].

There is only a single published randomised trial of ELCA-PCI compared to a conventional strategy in STEMI. The LaserAMI study examined only 27 patients, and not powered for superiority. It demonstrated that ELCA was safe and effective – with no significant complications [44]. There were no differences observed in TIMI flow, myocardial blush score, nor corrected TIMI frame count, although in the latter, the gain from baseline was higher in the ELCA group – maybe suggesting an advantage towards ELCA.

Despite the theoretical advantages ELCA offers in AMI – in particular STEMI – there is a lack of randomised data in comparison to aspiration thrombectomy. In particular, ELCA may offer benefit in cases of massive thrombus – where aspiration thrombectomy may be ineffective.

Case 5 – (Fig. 8.13)

A 32 years. old presented to the catheter lab with an anterior STEMI. He was admitted 2 weeks previously following a renal haemorrhage – requiring 4U of blood. During this admission – he had a transient episode of chest discomfort, associated with anterior ST elevation that rapidly resolved without treatment. A CT angiogram, organised during this admission, as a the diagnosis was uncertain and to avoid an invasive procedure, had indicated that his coronary arteries appeared free from atheroma,

Emergent coronary angiography was undertaken through the right radial artery, initially using 6 F equipment. This demonstrated a massive thrombus in the proximal LAD (Fig. 8.13a). Aspiration thrombectomy extracted a small volume of white thrombus, but had little angiographic effect. OCT was used to assess the detailed vascular architecture in an attempt to establish the presence/absence of atheroma. OCT imaging revealed extensive red and white thrombus, with multiple layers of organised lamina thrombus (Fig. 8.13c). The varying thrombus densities would suggest multiple vessel thromboses – correlating with the clinical history. There was no atheroma evident.

A 1.4 mm Excimer catheter, using an energy of 45 mJ/mm² with a PRF of 45 Hz, was employed to deliver 3000 pulses of energy with a dramatic improvement in thrombus burden. Repeat OCT demonstrated a reduction in macroscopic thrombus, but there remained a significant quantity of lamina thrombus within the artery. The radial guide was then upsized to a 7 F system, allowing mechanical thrombectomy to be undertaken. Using the Thrombcath XT rotational thrombectomy device (Spectranetics, Colorado Spings, USA), the amount of thrombus visible on both angiography and OCT was significantly reduced. This was all conducted in combination with optimal anti-thrombotic and anti-platelet therapy. Post thrombectomy, OCT demonstrated no evidence of vascular trauma that would necessitate further PCI (Fig. 8.13d, e).

Case 6 – Large Thrombus Burden (Fig. 8.14)

A 26 year old man diabetic, current smoker, presented via a remote emergency department with an anterior STEMI. He had a history of an anterior STEMI treated 6 months previously in another institution with simple balloon angioplasty and thrombus aspiration as IVUS demonstrated only mild atheromatous plaque in the proximal vessel, associated with occlusion of the very distal LAD. No stent was deployed and there was no significant lesion noted on IVUS.

Once again, emergent coronary angiography was undertaken through a right radial approach using 6 F equipment. On this occasion, it demonstrated a proximally occluded LAD, with a large burden of organised thrombus (Fig. 8.14a). Aspiration thrombectomy had little effect and retrieved no macroscopic thrombus. ELCA was undertaken, and using a 0.9 mm concentric ELCA catheter with an energy of 45 mJ/mm² and a PRF of 25 Hz, 3750 pluses were delivered. TIMI 3 flow was restored, with a dramatic reduction in angiographically apparent thrombus (Fig. 8.14b).

Unlike case 5, the high organised thrombus burden obscured the underlying arterial intima and media (Fig. 8.14ai). There was no atheroma visible either proximal or distal to the point of occlusion, but given the clinical context, it was likely that an underlying plaque rupture was the cause of his acute presentation. In view of his young age and diabetes mellitus, and the likelihood of the need for further revascularisation in the future, his artery was treated with a 3.0×28 mm bio-absorbable scaffold (BVS, Abbott Vascular, Illionis, USA), that was post dilated with a 3.25×12 mm NC balloon. OCT imaging post deployment confirmed good scaffold apposition (Fig. 8.14ci). Of note, residual thrombus is apparent prolapsing through the struts of the scaffold. (Fig. 8.14cii) This emphasises the need for optimal pharmacotherapy in the treatment of massive organised thrombus, as residual thrombus will often remain after treatment. As with the previous case, the use of ELCA in this artery with little disease but massive organised thrombus was not associated with any significant vascular trauma.

Case 7 (Fig. 8.15)

A 52 year old man presented via the emergency department with an inferior STEMI. He was pre-treated with aspirin, clopidogrel and a bolus and infusion of Bivalirudin, and taken directly to the catheter lab for emergent coronary angiography. This was undertaken via the right radial artery using 6 F equipment. This demonstrated a proximal occlusion of the right coronary artery, associated with massive organised coronary thrombus (Fig. 8.15a).

Percutaneous intervention was then undertaken via a 6 F AL1 guide. The lesion was crossed with a PT graphix wire (Abbott Vascular, Illionis, USA), without complication. Simple aspiration thrombectomy had little effect on either

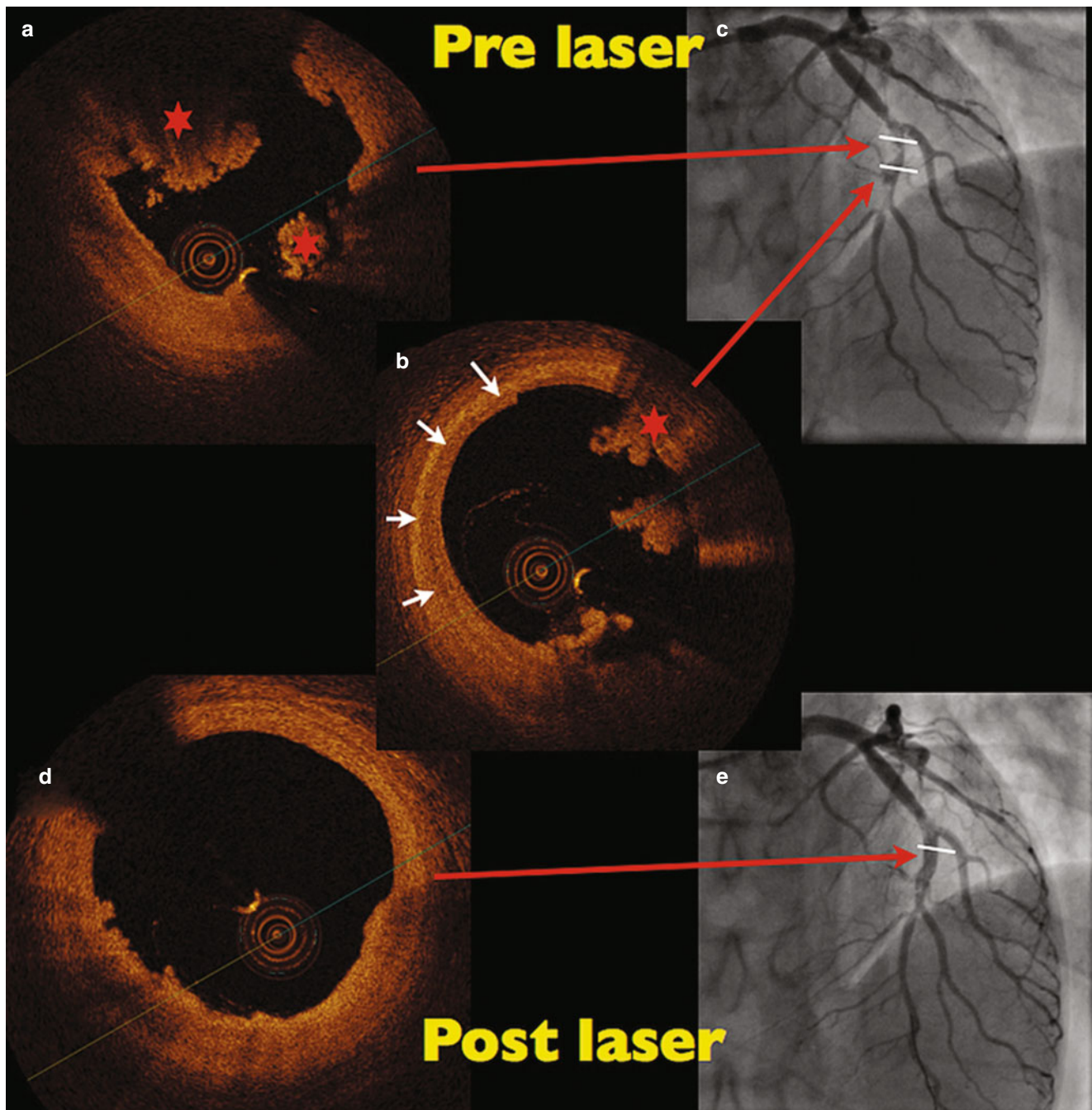


Fig. 8.13 A coronary angiographic still demonstrating a massive organised thrombus in the proximal LAD (panel c). OCT imaging revealed extensive red thrombus (panel a, indicated by *red stars*), with multiple layers of organised lamina thrombus (panel b, indicated by the *white arrows*). The varying lamina thrombus densities would suggest

multiple vessel thromboses – correlating with the clinical history. There was no evidence of vascular atheroma. Post ELCA, a dramatic reduction in thrombus burden is seen (panels d, e) with no evidence of vascular trauma that would necessitate further PCI

flow nor on the quantity of thrombus present. Hence, ELCA was initiated – with a 1.4 mm concentric catheter using an energy of 45 mJ/mm^2 at a PRF of 25 Hz, delivering 5000 pulses of Laser energy in 12 trains.

This had a dramatic effect of the amount of visible thrombus and re-established TIMI 3 flow. further aspiration thrombec-

tomy was undertaken with retrieval of a small amount of organised thrombus, and the artery was treated with delivery of three overlapping DES ($3.5 \times 33 \text{ mm}$, $4.0 \times 28 \text{ mm}$, $4.0 \times 28 \text{ mm}$ Biomatrix Flex, Biosensors, Singapore). TIMI 3 flow was maintained, and his ST elevation settled – but with significant thrombus remaining in the proximal artery (Fig. 8.15c). Further

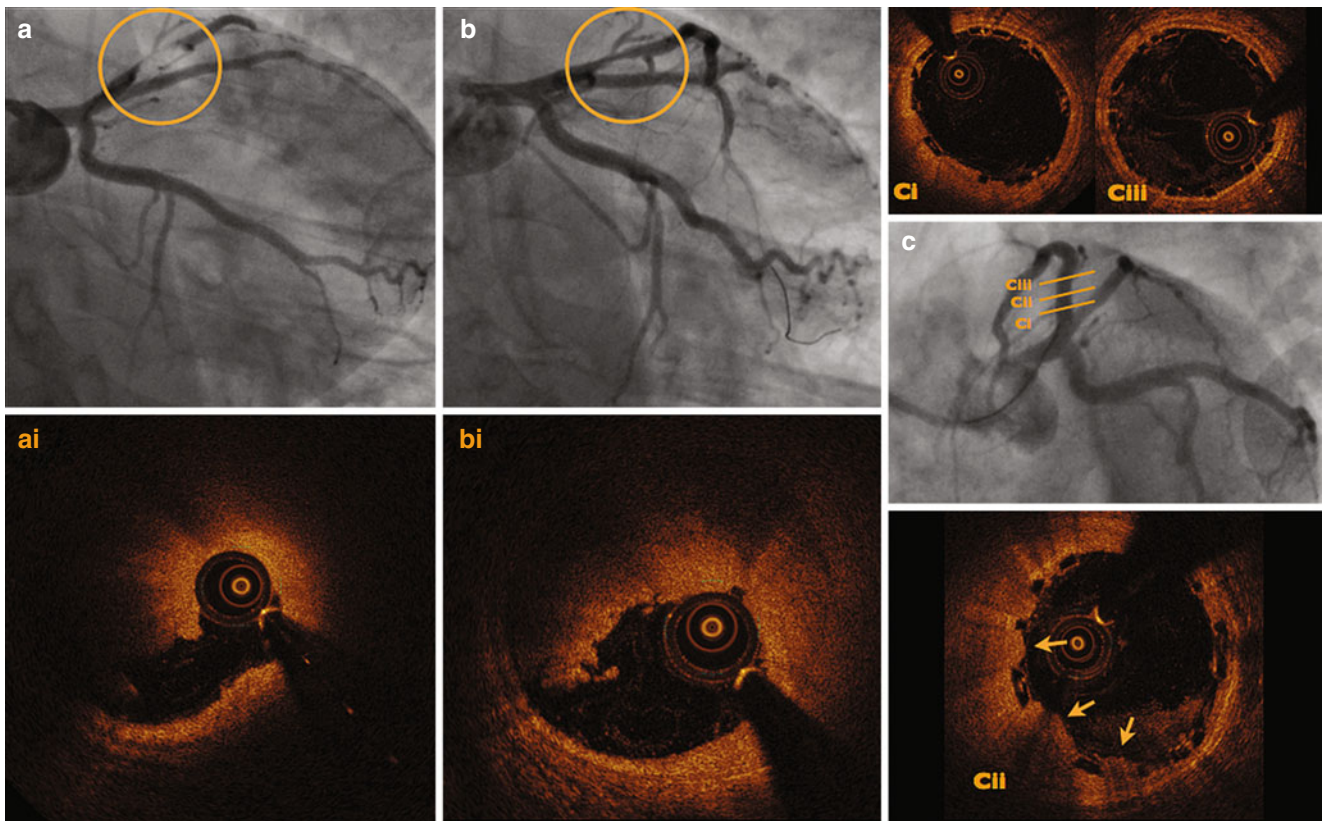


Fig. 8.14 An angiographic (Panel a) and OCT cross section (Panel ai), demonstrating a large organised thrombus in the proximal LAD (circled), with a massive red thrombus burden. ELCA was then undertaken, with a dramatic improvement in thrombus burden – observed on both angiographic (Panel b) and OCT (panel bi) imaging. The underlying artery has been obscured by *red thrombus*, and the culprit atheromatous

plaque is not visible. The lesion was treated with a bio-resorbable vascular scaffold (BVS) – with an excellent angiographic (Panel c) and OCT result (Panel ci–iii). The BVS has been appropriately sized and is well opposed throughout (Panel ci and ciii), with no evidence of vascular trauma. The thrombus has been contained and can be seen prolapsing through the scaffold struts (Panel cii – indicated by arrows)

aspiration thrombectomy and ELCA was undertaken – with an increase in energy (to 60 mJ/mm² at a PRF of 40 Hz), but with little effect on the angiographic appearance. He was started on eptifibatid and returned to the CCU.

He remained on eptifibatid for a period of 5 days, during which he continued to experience transient chest discomfort associated with ST segment elevation. At this point, it became apparent that medical therapy had been unsuccessful in thrombus dissolution, so he returned to the lab for further assessment of his RCA. Intervention was again performed via the RRA, using a specific sheathless 7.5 F guide. OCT assessment of the RCA revealed significant red thrombus remained within the proximal vessel (Fig. 8.15di). The stents were well deployed within the artery, but thrombus was apparent surrounding the stent struts, and in a layer between the struts and the true arterial wall. There was no intimal damage or dissection evident as a consequence of ELCA.

Further aspiration thrombectomy had little effect, so mechanical thrombectomy, using the Thrombcat XT (Spectranetics, Colorado Springs, USA) rotational thrombectomy device, was undertaken. A distal protection device

(Filterwire EZ, Boston Scientific, Boston) was positioned prior to Thrombcat deployment to minimise distal embolisation. A number of runs with the Thrombcat device were performed, with a significant reduction in the amount of angiographically visible thrombus. A further run of ELCA was also performed, using a 1.7 mm catheter at an energy of 60 mJ/mm² and a PRF of 40 Hz, in an attempt to treat any thrombus that may not have been within reach of the thrombectomy device. In addition, the stents were post dilated using a 4.0 mm and 4.5 mm non-compliant balloon to ensure true intimal apposition. An OCT was repeated and demonstrated a dramatic reduction in the amount of thrombus, with only a small amount seen adherent to the stent struts (Fig. 8.15fi). The patient completed a further 2 days of eptifibatid, and remained pain free until discharge without complication.

This case demonstrates the effectiveness of ELCA in the treatment of massive organised coronary thrombus. Crucially in this case, this was combined with further adjuvant interventional techniques and optimal pharmacotherapy to achieve an excellent final result.

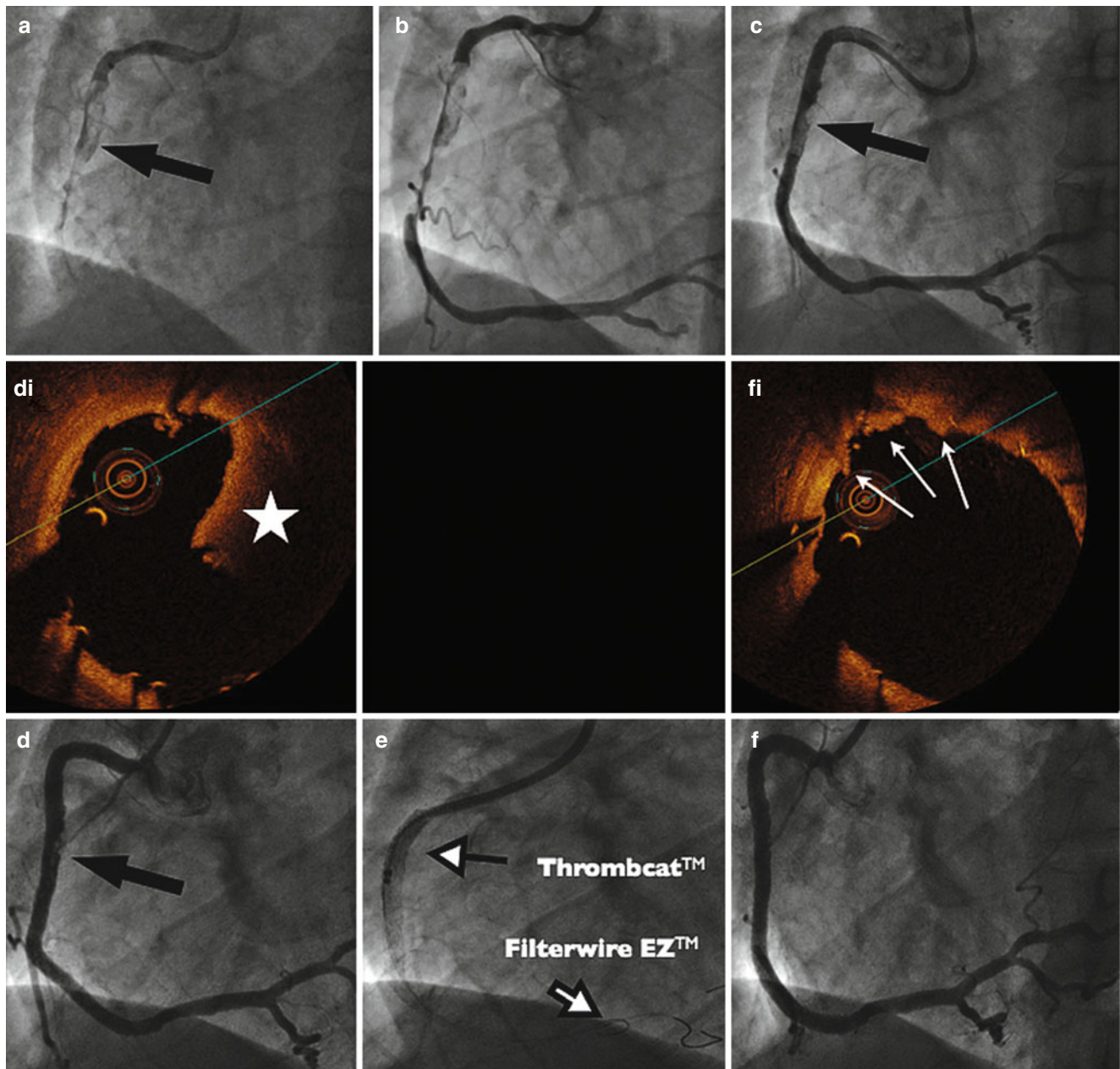


Fig. 8.15 A series of angiographic stills that demonstrate: (a) An occluded dominant right coronary artery. The *black arrow* marks the presence of a massive intra-coronary thrombus. (b) Establishment of TIMI 2 flow following excimer laser atherectomy. (c) Final result after treatment with three overlapping drug eluting stents (Biomatrix, Biosensors, Singapore), with thrombus still evident in the proximal segment of the artery. (d) Evidence

of proximal red thrombus remains (*Black arrow*), shown on OCT to overly the stent struts (panel **di** – star indicating residual thrombus). (e) Passage of Thrombcat XT (Spectranetics, CA, USA) over a distal protection device. (f) Final angiographic and OCT appearance (Panel **fi**), with near complete thrombus resolution – with *white arrows* indicating a small volume of red thrombus that remains adherent to the stent struts

Indication 5 – Under-Expanded Stent (Fig. 8.16)

The presence of significant calcification within a lesion can lead to a failure of balloon dilatation. In such cases, de-bulking and plaque modification techniques (such as rotablation) are typically employed to facilitate stent expansion. Despite this, stent under-expansion remains a risk of treating such vessels.

Post intervention luminal diameter and minimal luminal area can predict the risk of subsequent stent thrombosis. Once a stent has deployed and failed to expand – despite high pressure balloon dilatation, then therapeutic strategies are limited.

Excimer laser atherectomy for the treatment of a non-dilatable stented lesions was first reported in 1998 [50]. Since then, the technique has been modified, with operators replacing the saline infusion with intravenous contrast. Upon

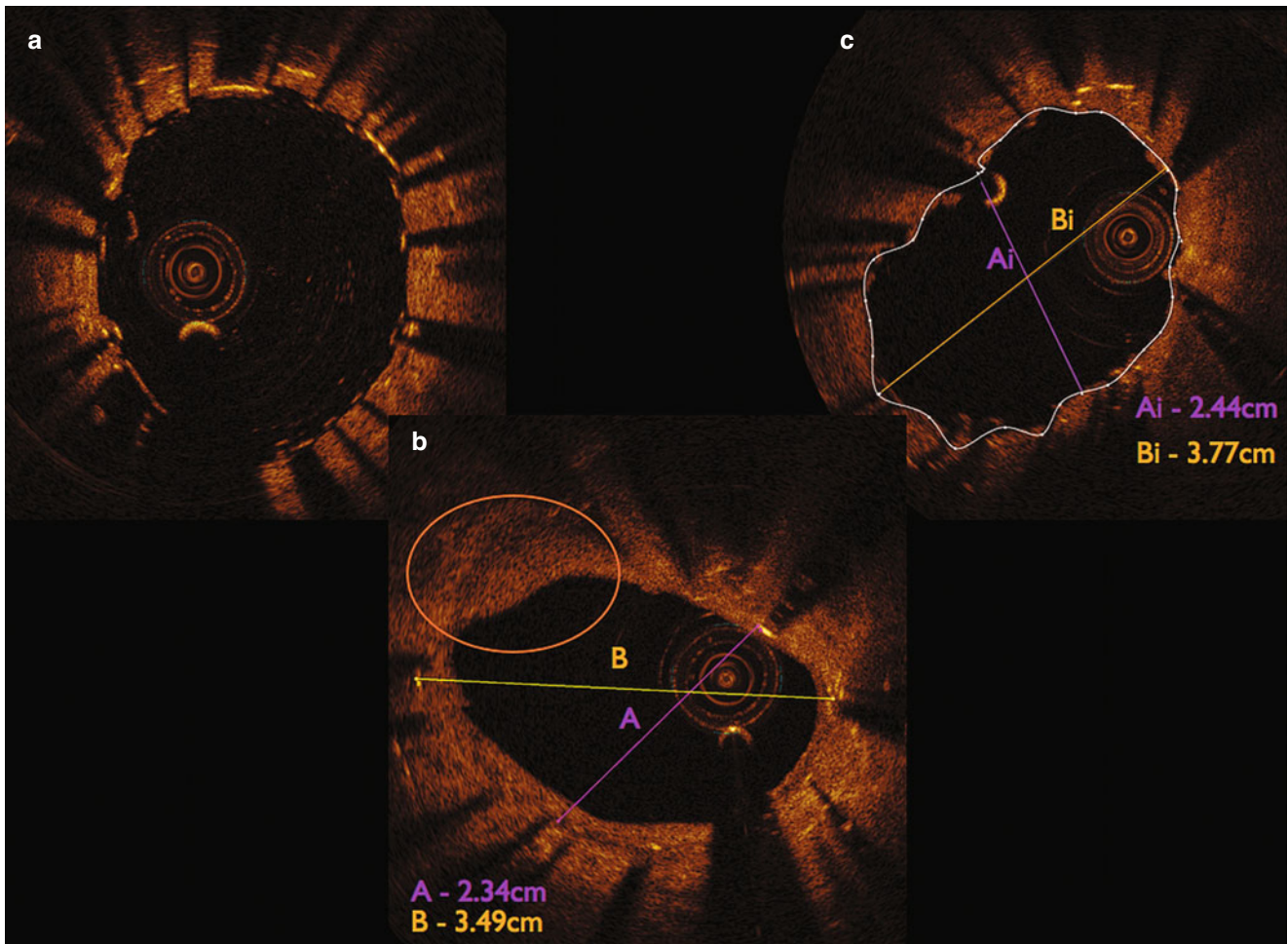


Fig. 8.16 Panel **a** is an OCT cross section taken from the proximal vessel demonstrating multiple layers of stent. Panel **b** is distal to panel **a**, and illustrates the worst area of re-stenosis. Within this area is an area of poorly defined neo-intima (within the *yellow circle*), although this is

not associated with any overlying thrombus or plaque rupture. Panel **c** demonstrates the same area after intervention with ELCA, rotablation and further stent deployment. There has been a significant increase in MLA, with no evidence of further thrombus formation

Excimer laser activation, large bubbles can develop within the viscous contrast liquid, that upon rupture can produce a significant localised force within the vessel lumen. This produces focused localised plaque disruption that within the vessel containing the under-deployed stent and within the media constraining stent deployment. This plaque modification may be sufficient to allow stent expansion with subsequent non-compliant balloon dilatation [51].

This technique, first described in a number of case reports, has now been systematically evaluated in the ELLEMENT registry of 28 patients [52]. Using an increase of 1 cm² on IVUS or an increase of at least 10 % in minimal stent diameter by QCA as a definition of procedural success, this was achieved in 96.4 % (27/28) of cases. Peri-procedural MI occurred in 7.1 %, with transient slow-flow in 3.6 % and ST elevation in 3.6 %. During follow-up there was one cardiac death, and TLR occurred in 6.7 %. There were no cases of perforation nor tamponade. Despite the theoretical risks, this strategy does not appear to be associated with a significantly

higher complication rate when compared to the limited alternative strategies for this scenario.

Case 8 (Fig. 8.16)

A 72 year old gentleman with a long history of ischaemic heart disease, CABG, and native vessel coronary intervention presented to the lab for treatment of a segment of in-stent restenosis within the distal left main stem involving the ostium and proximal portion of the circumflex. This portion of the artery had been previously treated on 5 separate occasions for in-stent restenosis, and contained 3 layers of stent (implanted on three separate occasions). In addition to recurrent stent deployment, additional ISR modification techniques had been used – including cutting and drug eluting balloons – in an attempt to treat ISR. He presented to a remote hospital with 2 separate non-ST elevation myocardial infarctions, having failed medical therapy that included high dose oral anti-platelets and aggressive lipid and blood glucose control.

Coronary intervention was undertaken through the right femoral artery using 7 F equipment (Fig. 8.16a). After predilation with sequential 3.5 and 3.75 non compliant balloons, ELCA was undertaken, utilising a 0.9 mm concentric catheter at a power of 80 mJ/mm² and a PRF of 80 Hz, delivering 24 trains of energy. This was repeated with a 2.0 mm concentric catheter – again using a power of 80 mJ/mm² and a PRF of 80 Hz. During these runs, saline was replaced with contrast.

OCT following ELCA demonstrated a significant increase in MLA (Fig. 8.16b), with clefts within the intima layer that allowed full balloon expansion. There did however remain a segment of calcific disease that prevented full balloon expansion. The case was completed with rotablation to this area of the vessel, further large calibre NC balloon dilatation and deployment of a further 4.0 mm drug eluting stent to maximise vessel luminal diameter (Fig. 8.16c).

This case illustrates the both the advantages and limitations of ELCA. Laser energy is not constrained by the physical boundary of the stent, and is able to act within the heavily fibrosed intimal layer to maximise stent expansion. Its action is however limited by the presence of large volumes of dense calcification. In these circumstances, currently rotational atherectomy offers the most effective solution for lesion debulking/modification to facilitate stent expansion – as is demonstrated in this case.

Conclusions

These eight cases span the current main indications for ELCA which remains a safe and effective technique in these clinical scenarios. The OCT appearances offer an insight into both the mechanism of ELCA, and its potential uses in PCI. In particular, they illustrate the effectiveness of ELCA thrombus ablation. However, despite the theoretical advantages of ELCA over simple aspiration – particularly in massive thrombus – further data is needed to support its routine use in STEMI. We have also illustrated the importance of DPDs in SVG intervention to minimise the risk of no-reflow in addition to the use of ELCA.

As increasingly challenging and complex cases are encountered during PCI, it is likely that intra-coronary imaging (OCT), will increasingly be used in combination with adjunctive techniques such as ELCA and rotational atherectomy. The interventional cardiologist should therefore be aware of the typical OCT findings before and after ELCA to facilitate decision making during the case.

References

- O'Kane P, Redwood S. Laser for PCI. In: Oxford textbook of interventional cardiology. London: Oxford University Press; 2010.
- Litvack F, Eigler N, Margolis J, et al. Percutaneous excimer laser coronary angioplasty: results in the first consecutive 3,000 patients. The ELCA Investigators. *J Am Coll Cardiol.* 1994;23:323–9.
- Fernandez JP. Treatment of calcific coronary stenosis with the use of excimer laser coronary atherectomy and rotational atherectomy. *Interv Cardiol.* 2010;2:801–6.
- Badr S, Ben-Dor I, Dvir D, et al. The state of the excimer laser for coronary intervention in the drug-eluting stent era. *Cardiovasc Revasc Med.* 2013;14:93–8.
- Fernandez JP, Hobson AR, McKenzie D, et al. Beyond the balloon: excimer coronary laser atherectomy used alone or in combination with rotational atherectomy in the treatment of chronic total occlusions, non-crossable and non-expandable coronary lesions. *EuroIntervention.* 2013;9:243–50.
- Bezerra HG, Costa MA, Guagliumi G, Rollins AM, Simon DI. Intracoronary optical coherence tomography: a comprehensive review clinical and research applications. *JACC Cardiovasc Interv.* 2009;2:1035–46.
- Huang D. Optical coherence tomography. *Science.* 1991;254:1178–81.
- Jang IK, Tearney GJ, MacNeill B, et al. In vivo characterization of coronary atherosclerotic plaque by use of optical coherence tomography. *Circulation.* 2005;111:1551–5.
- Tearney GJ, Waxman S, Shishkov M, et al. Three-dimensional coronary artery microscopy by intracoronary optical frequency domain imaging. *JACC Cardiovasc Imaging.* 2008;1:752–61.
- Takarada S, Imanishi T, Liu Y, et al. Advantage of next-generation frequency-domain optical coherence tomography compared with conventional time-domain system in the assessment of coronary lesion. *Catheter Cardiovasc Interv.* 2010;75:202–6.
- Prati F, Regar E, Mintz GS, et al. Expert review document on methodology, terminology, and clinical applications of optical coherence tomography: physical principles, methodology of image acquisition, and clinical application for assessment of coronary arteries and atherosclerosis. *Eur Heart J.* 2010;31:401–15.
- Prati F, Guagliumi G, Mintz GS, et al. Expert review document part 2: methodology, terminology and clinical applications of optical coherence tomography for the assessment of interventional procedures. *Eur Heart J.* 2012;33:2513–20.
- Jang IK, Bouma BE, Kang DH, et al. Visualization of coronary atherosclerotic plaques in patients using optical coherence tomography: comparison with intravascular ultrasound. *J Am Coll Cardiol.* 2002;39:604–9.
- Imola F, Mallus MT, Ramazzotti V, et al. Safety and feasibility of frequency domain optical coherence tomography to guide decision making in percutaneous coronary intervention. *EuroIntervention.* 2010;6:575–81.
- Gonzalo N, Serruys PW, García-García HM, et al. Quantitative ex vivo and in vivo comparison of lumen dimensions measured by optical coherence tomography and intravascular ultrasound in human coronary arteries. *Rev Esp Cardiol.* 2009;62:615–24.
- Burke AP, Farb A, Malcom GT, Liang YH, Smialek J, Virmani R. Coronary risk factors and plaque morphology in men with coronary disease who died suddenly. *N Engl J Med.* 1997;336:1276–82.
- Barlis P, Serruys PW, Gonzalo N, van der Giessen WJ, de Jaegere PJ, Regar E. Assessment of culprit and remote coronary narrowings using optical coherence tomography with long-term outcomes. *Am J Cardiol.* 2008;102:391–5.
- Barlis P, Serruys PW, Devries A, Regar E. Optical coherence tomography assessment of vulnerable plaque rupture: predilection for the plaque 'shoulder'. *Eur Heart J.* 2008;29:2023.
- Yabushita H, Bouma BE, Houser SL, et al. Characterization of human atherosclerosis by optical coherence tomography. *Circulation.* 2002;106:1640–5.
- Prati F, Capodanno D, Pawlowski T, et al. Local delivery versus intracoronary infusion of abciximab in patients with acute coronary syndromes. *JACC Cardiovasc Interv.* 2010;3:928–34.
- Kume T, Akasaka T, Kawamoto T, et al. Assessment of coronary arterial thrombus by optical coherence tomography. *Am J Cardiol.* 2006;97:1713–7.

22. Bezerra HG, Attizzani GF, Sirbu V, et al. Optical coherence tomography versus intravascular ultrasound to evaluate coronary. *JACC Cardiovasc Interv.* 2013;6:228–36.
23. Kawamori H, Shite J, Shinke T, et al. Natural consequence of post-intervention stent malapposition, thrombus, tissue prolapse, and dissection assessed by optical coherence tomography at mid-term follow-up. *Eur Heart J Cardiovasc Imaging.* 2013;14:865–75.
24. Serruys PW, Onuma Y, Ormiston JA, et al. Evaluation of the second generation of a bioresorbable everolimus drug-eluting vascular scaffold for treatment of de novo coronary artery stenosis: six-month clinical and imaging outcomes. *Circulation.* 2010;122:2301–12.
25. Gonzalo N, Serruys PW, Piazza N, Regar E. Optical coherence tomography (OCT) in secondary revascularisation: stent and graft assessment. *EuroIntervention.* 2009;5(Suppl D):D93–100.
26. Goto K, Takebayashi H, Kihara Y, et al. Appearance of neointima according to stent type and restenotic phase: analysis by optical coherence tomography. *EuroIntervention.* 2013;9:601–7.
27. Nakazawa G, Otsuka F, Nakano M, et al. The pathology of neoath-erosclerosis in human coronary implants bare-metal and drug-eluting stents. *J Am Coll Cardiol.* 2011;57:1314–22.
28. Park S-J, Kang S-J, Virmani R, Nakano M, Ueda Y. In-stent neoath-erosclerosis a final common pathway of late stent failure. *J Am Coll Cardiol.* 2012;59:2051–7.
29. Dangas GD, Claessen BE, Caixeta A, Sanidas EA, Mintz GS, Mehran R. In-stent restenosis in the drug-eluting stent era. *J Am Coll Cardiol.* 2010;56:1897–907.
30. Mehran R, Mintz GS, Satler LF, et al. Treatment of in-stent restenosis with excimer laser coronary angioplasty: mechanisms and results compared with PTCA alone. *Circulation.* 1997;96:2183–9.
31. Papaioannou T, Yadegar D, Vari S, Shehada R, Grundfest WS. Excimer laser (308 nm) recanalisation of in-stent restenosis: thermal considerations. *Lasers Med Sci.* 2001;16:90–100.
32. Burris N, Lippincott RA, Elfe A, Tchong JE, O’Shea JC, Reiser C. Effects of 308 nanometer excimer laser energy on 316 L stainless-steel stents: implications for laser atherectomy of in-stent restenosis. *J Invasive Cardiol.* 2000;12:555–9.
33. Webb JG, Carere RG, Virmani R, et al. Retrieval and analysis of particulate debris after saphenous vein graft intervention. *J Am Coll Cardiol.* 1999;34:468–75.
34. Baim DS, Wahr D, George B, et al. Randomized trial of a distal embolic protection device during percutaneous intervention of saphenous vein aorto-coronary bypass grafts. *Circulation.* 2002;105:1285–90.
35. Bittl JA, Sanborn TA, Yardley DE, et al. Predictors of outcome of percutaneous excimer laser coronary angioplasty of saphenous vein bypass graft lesions. The percutaneous excimer laser coronary angioplasty registry. *Am J Cardiol.* 1994;74:144–8.
36. Giugliano GR, Falcone MW, Mego D, et al. A prospective multi-center registry of laser therapy for degenerated saphenous vein graft stenosis: the COronary graft Results following Atherectomy with Laser (CORAL) trial. *Cardiovasc Revasc Med.* 2012;13:84–9.
37. Ebersole D, Dahm JB, Das T, et al. Excimer laser revascularization of saphenous vein grafts in acute myocardial infarction. *J Invasive Cardiol.* 2004;16:177–80.
38. Topaz O. Plaque removal and thrombus dissolution with the photoacoustic energy of pulsed-wave lasers-biotissue interactions and their clinical manifestations. *Cardiology.* 1996;87:384–91.
39. Steg PG, James SK, Atar D, et al. ESC Guidelines for the management of acute myocardial infarction in patients presenting with ST-segment elevation. *Eur Heart J.* 2012;33:2569–619.
40. Vlaar PJ, Svilaas T, van der Horst IC, et al. Cardiac death and reinfarction after 1 year in the Thrombus Aspiration during Percutaneous coronary intervention in Acute myocardial infarction Study (TAPAS): a 1-year follow-up study. *Lancet.* 2008;371:1915–20.
41. Fröbert O, Lagerqvist B, Olivecrona GK, et al. Thrombus aspiration during ST-segment elevation myocardial infarction. *N Engl J Med.* 2013;369:1587–97.
42. Stone GW, Abizaid A, Silber S, et al. Prospective, randomized, multicenter evaluation of a polyethylene terephthalate micronet mesh-covered stent (MGuard) in ST-segment elevation myocardial infarction: the MASTER trial. *J Am Coll Cardiol.* 2012;60(19):1975–84.
43. Costa JR, Abizaid A, Dudek D, Silber S, Leon MB, Stone GW. Rationale and design of the MGuard for acute ST elevation reperfusion MASTER trial. *Catheter Cardiovasc Interv.* 2013;82:184–90.
44. Topaz O, Das T, Dahm J, Madyhoon H, Perin E, Ebersole D. Excimer laser revascularisation: current indications, applications and techniques. *Lasers Med Sci.* 2001;16:72–7.
45. Topaz O, Minisi AJ, Bernardo NL, et al. Alterations of platelet aggregation kinetics with ultraviolet laser emission: the “stunned platelet” phenomenon. *Thromb Haemost.* 2001;86:1087–93.
46. Lee G, Ikeda RM, Stobbe D, et al. Effects of laser irradiation on human thrombus: demonstration of a linear dissolution-dose relation between clot length and energy density. *Am J Cardiol.* 1983;52:876–7.
47. Topaz O, Shah R, Mohanty PK, McQueen RA, Janin Y, Bernardo NL. Application of excimer laser angioplasty in acute myocardial infarction. *Lasers Surg Med.* 2001;29:185–92.
48. Topaz O, Ebersole D, Das T, et al. Excimer laser angioplasty in acute myocardial infarction (the CARMEL multicenter trial). *Am J Cardiol.* 2004;93:694–701.
49. Ambrosini V, Cioppa A, Salemm L, et al. Excimer laser in acute myocardial infarction: single centre experience on 66 patients. *Int J Cardiol.* 2008;127:98–102.
50. Sunew J, Chandwaney RH, Stein DW, Meyers S, Davidson CJ. Excimer laser facilitated percutaneous coronary intervention of a nondilatable coronary stent. *Catheter Cardiovasc Interv.* 2001;53:513–7; discussion 518.
51. Lam SC, Bertog S, Sievert H. Excimer laser in management of underexpansion of a newly deployed coronary stent. *Catheter Cardiovasc Interv.* 2014;83(1):E64–8.
52. Latib A, Takagi K, Chizzola G, et al. Excimer laser {LEsion} modification to expand non-dilatable sTents: the {ELLEMENT} Registry. *Cardiovasc Revasc Med.* 2014;15(1):8–12.

308 Nanometer Excimer Laser in the Therapy of Peripheral Vascular Disease

Craig M. Walker

Three hundred and eight nanometer excimer laser energy is being increasingly utilized for the interventional treatment of occluded peripheral arteries and bypass grafts. It is utilized as a crossing tool in some cases and as an atherectomy and thrombus removal device facilitating revascularization in others. Excimer laser has been FDA approved to cross and treat instent occlusions of peripheral arteries. Excimer laser coupled with thrombolytic drugs is not FDA approved to treat occluded synthetic femoral-popliteal grafts but has been utilized by several clinicians for this purpose [1].

Excimer laser energy is delivered via fiber-optic catheters with up to 150 cm delivery length in over the wire and rapid exchange configurations. Catheter sizes of 0.9, 1.4, 1.7, 2.0, 2.3, and 2.5 mm are available.

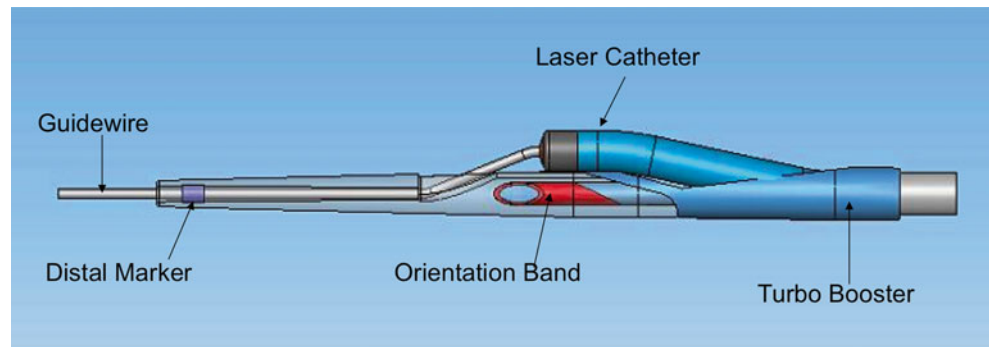
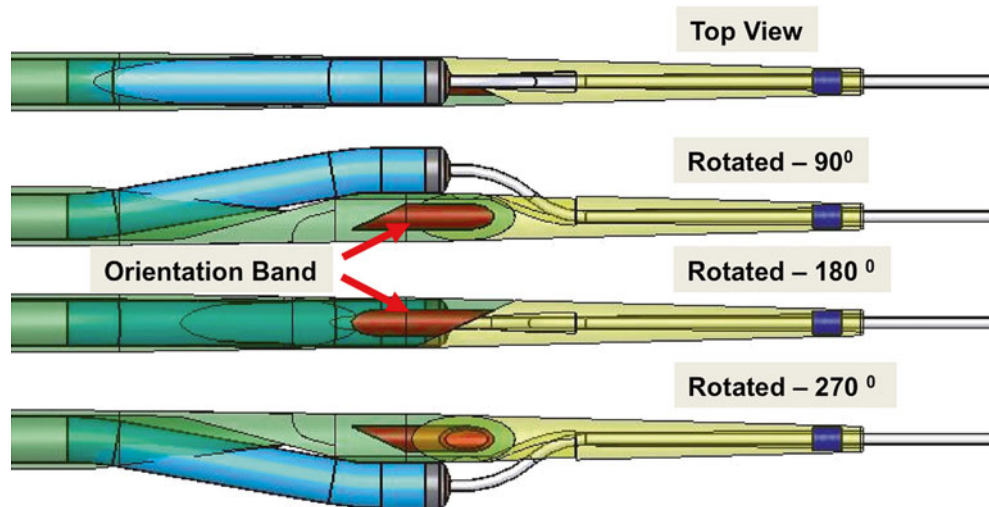
308 nm excimer laser energy ablates obstructive tissue by three recognized mechanisms: (1) photochemical, (2) photo-thermal, and (3) photomechanical. The photo-chemical effect is characterized by disruption of molecular bonds as excimer laser light energy is absorbed by obstructive plaque and thrombus. The photo-thermal effect is the result of the conversion of absorbed light energy into heat secondary to conversion of the absorbed laser energy into vibrational energy. Because the laser energy is administered only in 125 ns bursts (energy is delivered <1 % of the treatment time) there is only a minimal thermal effect at the catheter tip with temperatures rarely exceeding 50° Celsius. There are no oxidative by-products indicative of burning. The photomechanical effect is secondary to the creation of a vapor bubble caused by the photo-thermal effect. The vapor bubble is typically larger than the cross sectional area of the catheter allowing the laser treatment to create a lumen larger than the catheter cross-sectional area. The size of the vapor bubble is directly related to the Fluence (surface energy measured in

mj/mm²) and is inversely proportional to the rate of advancement. Energy delivery is at the distal tip of the fiber optic catheter with no “dead space” interacting with diseased segment before atherectomy occurs. To create even larger lumens a device, which eccentrically displaces the laser catheter (Turbo-Booster or Turbo-Tandem) (Fig. 9.1) can be utilized. Directed passes create incremental luminal gain. (Intravascular ultrasound has confirmed lumens of up to 5.5 mm in diameter following treatment with Turbobooster alone.) This device does however have distal “dead space” interacting with the treated area before the ablative energy is delivered (Fig. 9.2).

Excimer laser energy photoablates plaque and thrombus at a depth of approximately 50 μm per 125 ns burst of energy. Delivery frequencies of up to 80 bursts per second are available in all catheter sizes. This allows catheter advancement rates of no more than 0.5–1.0 mm/s if the operator desires optimal tissue ablation. Advancement rates faster than this result in a suboptimal laser effect (less tissue ablation) as well as an increased risk of embolization [2]. Catheter surface energies (Fluence) of up to 80mj/mm² can be delivered with the .9 mm catheter but only 45 mj/mm² via the 2.5 mm probe. All of the other laser catheters can deliver energy densities up to 60 mj/mm². Peripheral vascular excimer laser catheters do not automatically shut off at pre-specified treatment times like coronary catheters (“constant on”) allowing the operator to determine the treatment run time and avoid untreated gaps in treated long segments of disease.

Excimer laser can be used as definitive therapy or as partial debulking therapy (of thrombus, intimal hyperplasia, and plaque) prior to balloon angioplasty or stenting. Laser atherectomy is utilized to achieve greater luminal gain with diminished risk of dissection. Interventional treatment with laser should be conducted utilizing saline flush. There should be no contrast in the area of treatment as this creates percussive waves, which increase the risk of dissection, perforation, and embolization. Rapid catheter advancement rates result in suboptimal debulking and an increased risk of embolization [2]. Laser catheters can be utilized as a crossing tool in

C.M. Walker, MD
Cardiovascular Institute of the South, Houma, LA, USA
Tulane University School of Medicine, New Orleans, LA, USA
LSU Medical School, New Orleans, LA, USA
e-mail: drcrwalker@gmail.com

Fig. 9.1 Turbo booster**Fig. 9.2** A view directly down on the device with the catheter above the Turbo Booster

totally occluded vascular segments “Step by Step technique” described by Biamino [3]. This author has found this to be very useful in crossing long areas of in-stent occlusion, as the devices are typically larger than the stent interstices therefore the device is held in an intraluminal position by the stent. This approach debulks simultaneously as crossing occurs.

The Step-by-Step Technique is demonstrated in Fig. 9.3.

Multiple trials have been conducted utilizing 308 nm excimer laser energy to treat peripheral arterial disease.

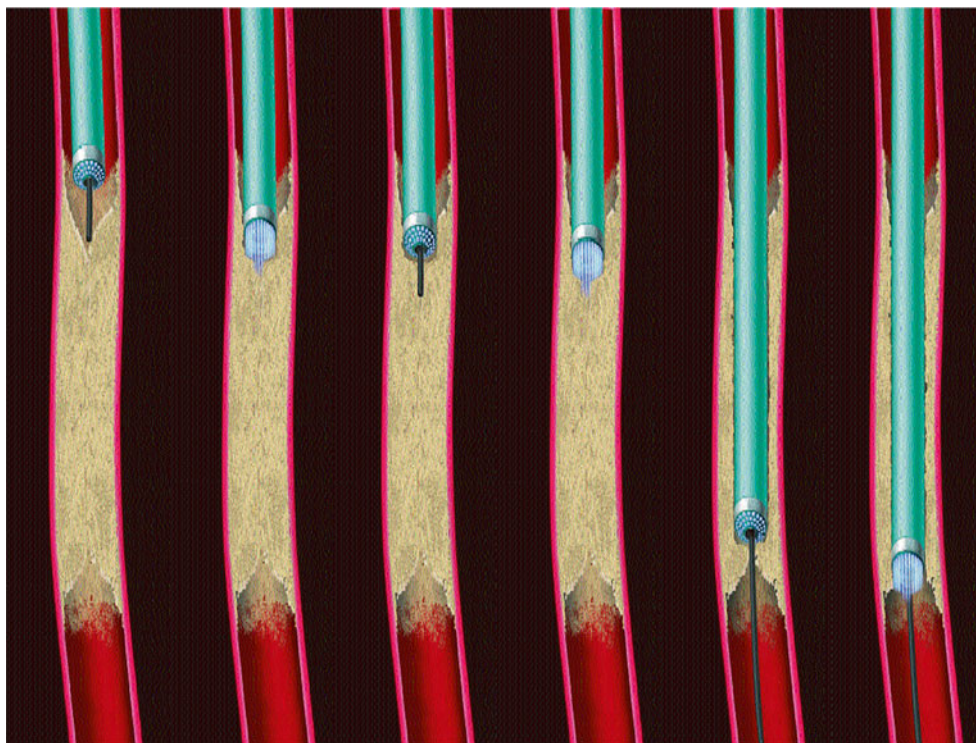
One of the first randomized trials was the PELA (Peripheral Excimer Laser Angioplasty) trial in which 251 patients with total superficial femoral artery occlusions and claudication were randomized to PTA or laser assisted PTA [4]. Results at 1 year suggested no clinical patency benefit in the patients who were treated with laser and PTA over PTA alone. It should be noted, however that this trial was performed with no probes larger than 2.3 mm in diameter. Strict control of technique was not mandated. In this trial, the excimer laser catheter was frequently utilized as a crossing tool via the “Step by Step” technique popularized by Dr. Biamino with excellent crossing success [3]. With this technique the laser is advanced to the area of total SFA occlusion then activated at low energies

and advanced several mm to cross the cap of the occlusion while carefully monitoring for pain. Further attempts at wire crossing are made and if unsuccessful the process of blind laser advancement repeated followed by attempts at wire crossing repeated until the total occlusion was crossed.

The LACI (Laser Angioplasty in Critical Limb Ischemia) trial [5, 6] enrolled 145 patients with critical limb ischemia that were poor surgical candidates at 15 sites in the United States and Germany. Laser angioplasty was performed in 99 % of cases with 96 % receiving adjunctive PTA and 45 % stenting respectively. Blood flow was restored in 89 %. There was a 92.5 % six-month limb salvage rate and a 10 % mortality at 6 months (which is typical in CLI patients). The ABI improved from 0.54+ or -.21 to .84+ or -.2, there was no active control group in this trial (historical controls were used) leading many to criticism of the outcome data.

The CELLO (ClirPath Excimer Laser System to Enlarge Luminal Openings) [7] trial was a 17 center international trial that enrolled 65 patients with denovo SFA lesions for laser treatment utilizing the Turbo-Booster laser device to increase plaque ablation in vessels with at least 70 % stenosis. The Turbo-Booster treatment reduced stenosis from 77.3

Fig. 9.3 Laser catheter advanced to occlusion attempt wire crossing. If that fails, activate laser at low energy and advance several mm monitoring pain. STOP IF PAIN. Try to advance wire again. If unsuccessful repeat steps until lesion crossed (use low energy)



to 42.5 % immediately with no major adverse events at 6 months. At 1 year ABI had increased from .78 to .9. Walking impairment questionnaire had improved from 45.6 to 65.1 and Rutherford category had improved from 2.4 to 1.3 at 12 months. All of these secondary endpoints were statistically significant.

Excimer laser was utilized to debulk in-stent restenotic lesions prior to balloon angioplasty in the EXCITE trial [8]. There were 250 patients enrolled with in-stent stenosis greater than 4 cm. that were randomized 2:1 to laser atherectomy followed by PTA versus PTA alone. Procedural success was higher in the group treated with laser (93.5 % vs. 82.7 %). The group treated with laser had less dissections (7.7 % vs. 17.2 %) and less need for repeat stenting (4.7 vs. 13.6 %). There were similar rates of procedural complications. Laser has received FDA approval for the treatment of in-stent restenosis.

There is an ongoing study being conducted in the interventional treatment of “in-stent restenosis prior to drug-eluting balloon therapy of diffuse in-stent obstructions (PHOTOPAC) [9].

Although other frequencies of laser energy were historically utilized in the therapy of PAD, they were limited by the creation of thermal injury and thrombogenic effects. These lasers are no longer utilized. At present the 308 nm excimer laser is the only FDA approved laser used to treat PAD.

Several case studies will demonstrate the use of laser in treating PAD.

Cases

Case 1

68 year old male with 1 cm plantar ulcer on foot, with true ischemia rest pain (Figs. 9.4, 9.5, 9.6, 9.7, 9.8 and 9.9).

Case 2

41 year old female with multiple failed angioplasty/stent procedures (Fig. 9.10).

Case 3

60 year old male, post femoral stenting (Fig. 9.11).

Case 4

57 year old male with chronic in-stent occlusion (Fig. 9.12).

Case 5

62 year old male de-nova SFA occlusion (Figs. 9.13, 9.14, and 9.15).

Case 6

49 year old female de-nova SFA occlusion (Fig. 9.16).

Infrapopliteal Case 1

54 year old male with ischemic ulcer second toe (Figs. 9.17 and 9.18).

Infrapopliteal Case 2

56 year old male with severe rest pain (Figs. 9.19, 9.20 and 9.21).

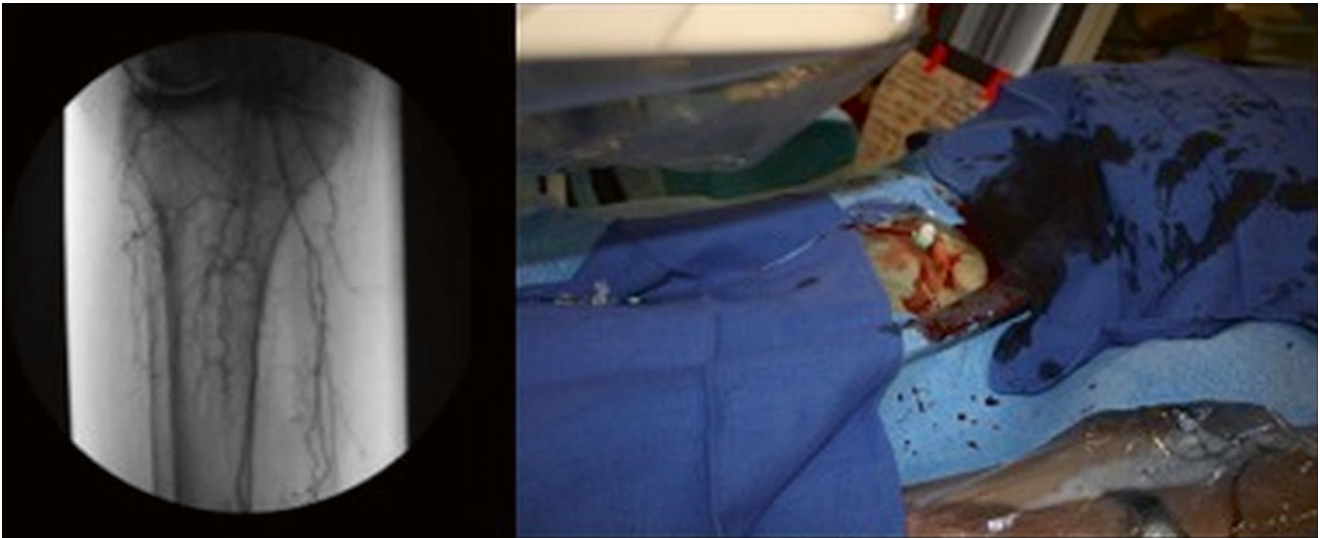


Fig. 9.4 Occluded popliteal artery and proximal infra-popliteal vessels that could not be crossed in ante-grade manner

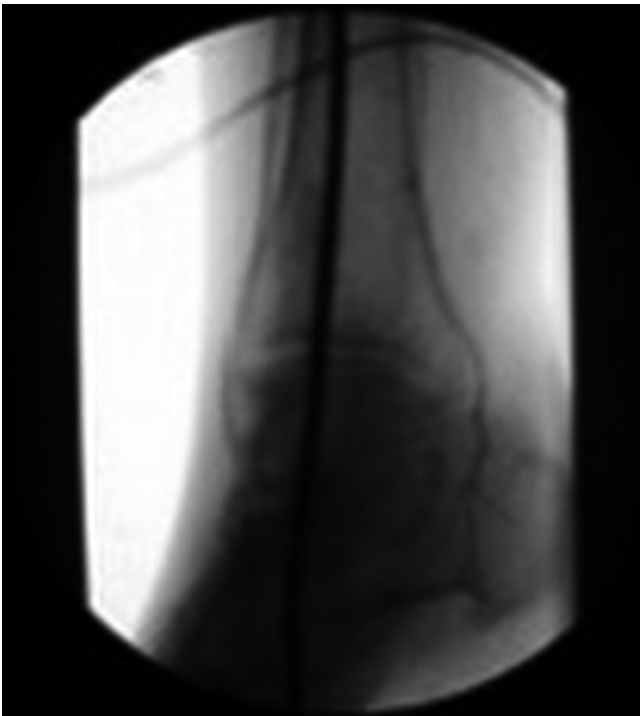


Fig. 9.5 Patent infra-popliteal arteries at ankle

Step by step (Figs. 9.22 and 9.23).

1. Allows for breaking of proximal cap
2. Slow advancement
3. Probe with wire
4. Carefully monitor pain

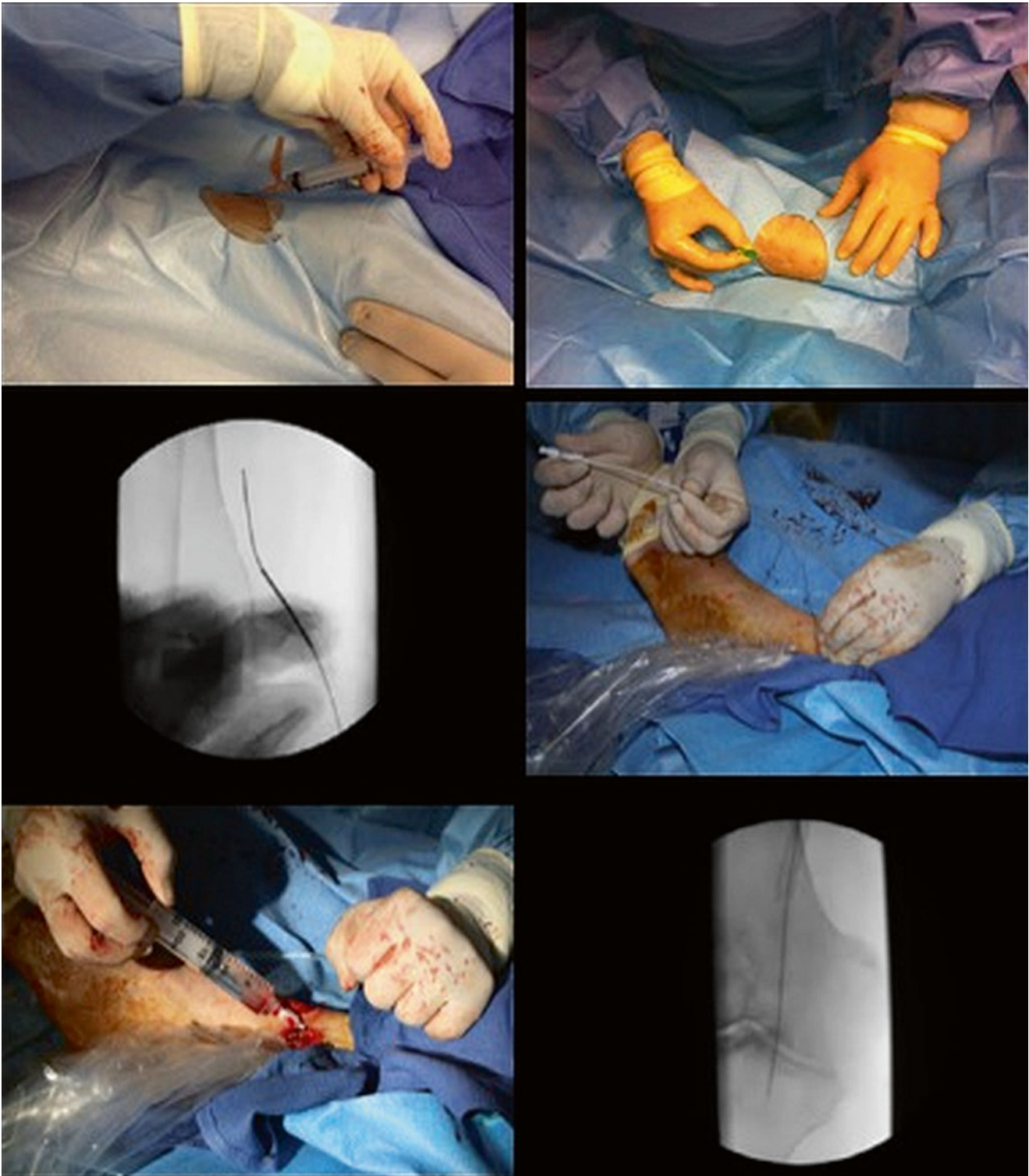


Fig. 9.6 Following posterior tibial artery access at the ankle a 2.9 F sheath was placed then the lesion was crossed with a .018 guidewire

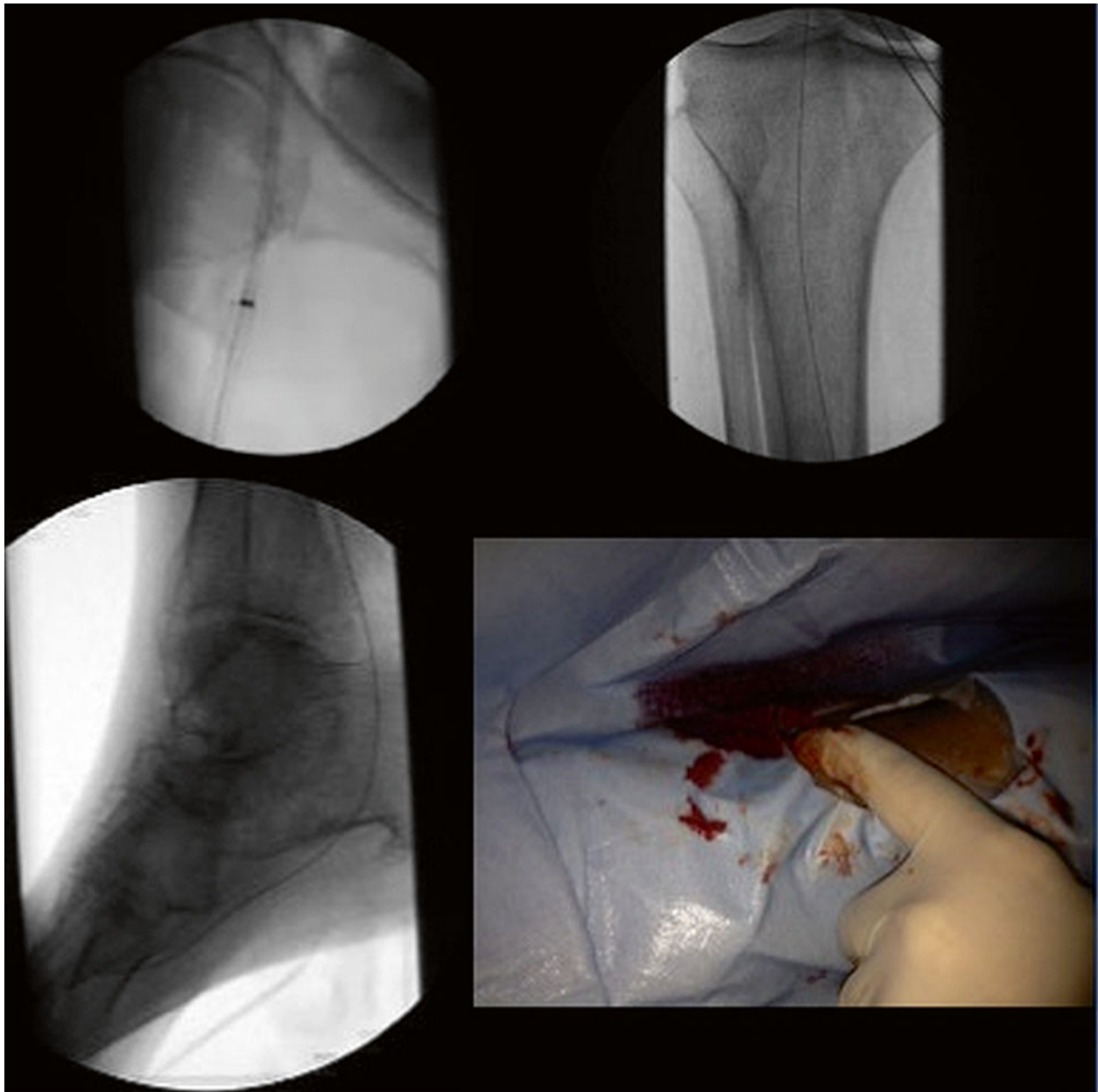


Fig. 9.7 The guidewire was snared into the femoral sheath then the lesion was crossed over this wire following which the soft distal wire tip was advanced beyond the arterial entry site. The posterior tibial

sheath was then removed and light digital pressure applied for one minute to achieve hemostasis

Fig. 9.8 *Left:* The occluded segment was treated with a 2 mm laser atherectomy device followed by low-pressure balloon inflation. *Right:* Final angiographic result

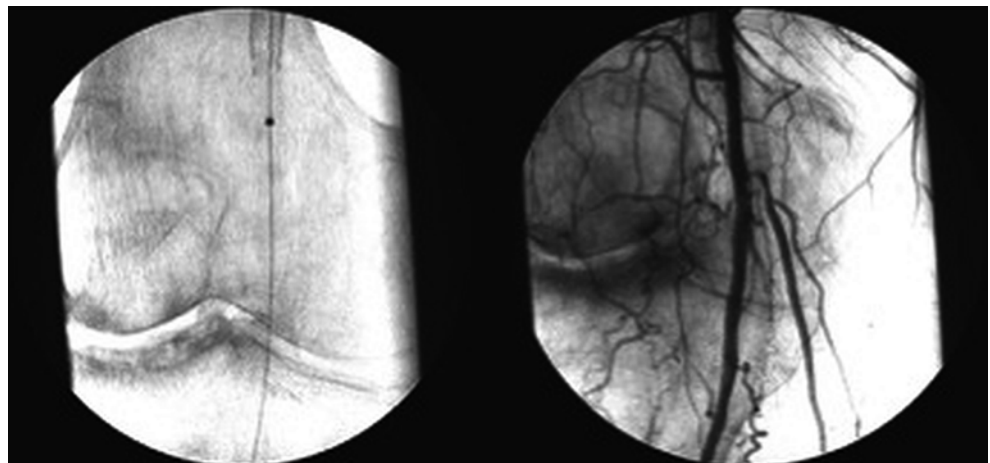




Fig. 9.9 Occluded synthetic femoral-below the knee popliteal arterial graft with rest pain

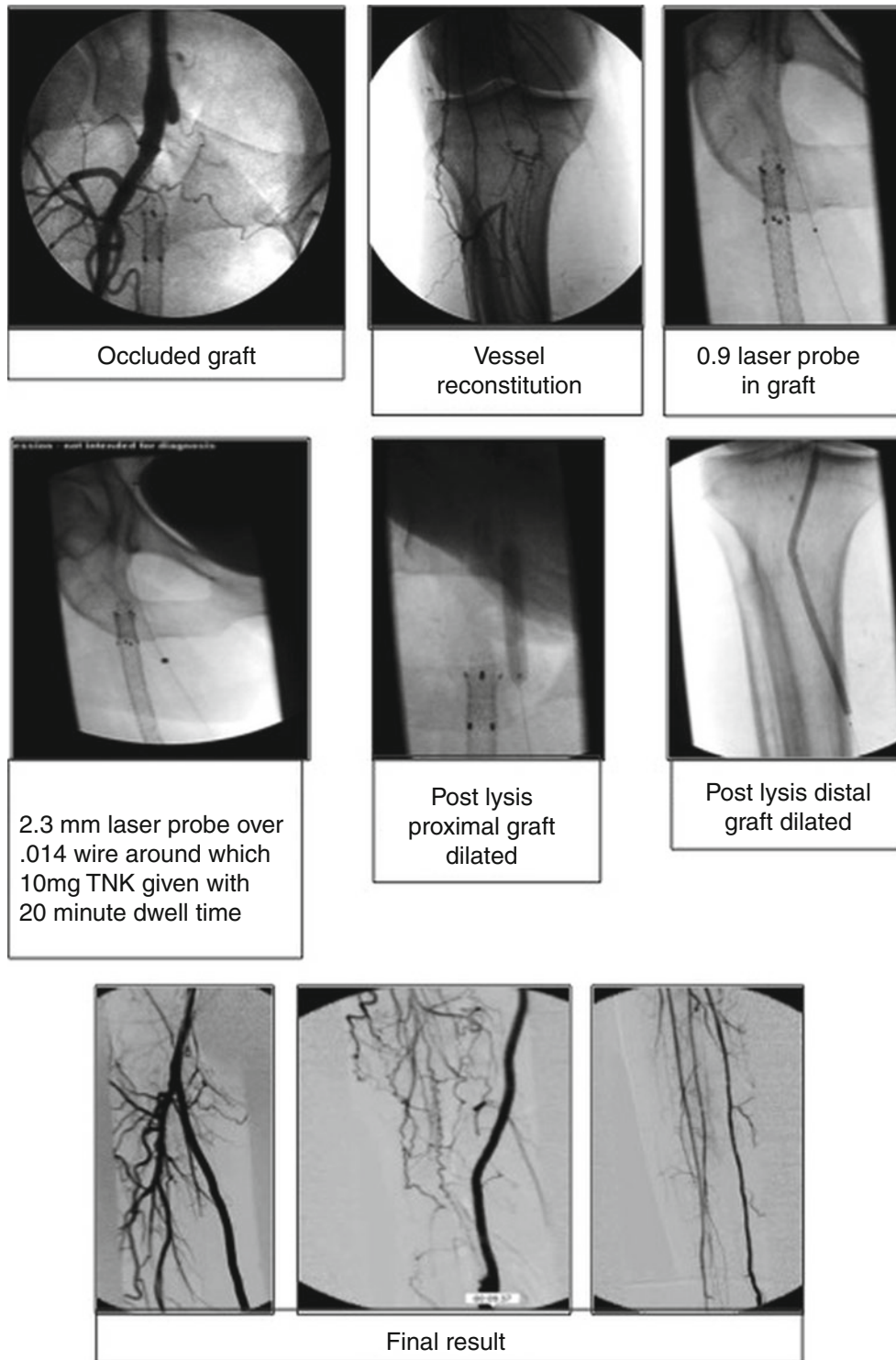


Fig. 9.10 41 year old female with multiple failed angioplasty/stent procedures and two failed femoral to below knee bypass grafts. Patients presented with angiographically confirmed graft occlusion for three months and true ischemia rest pain

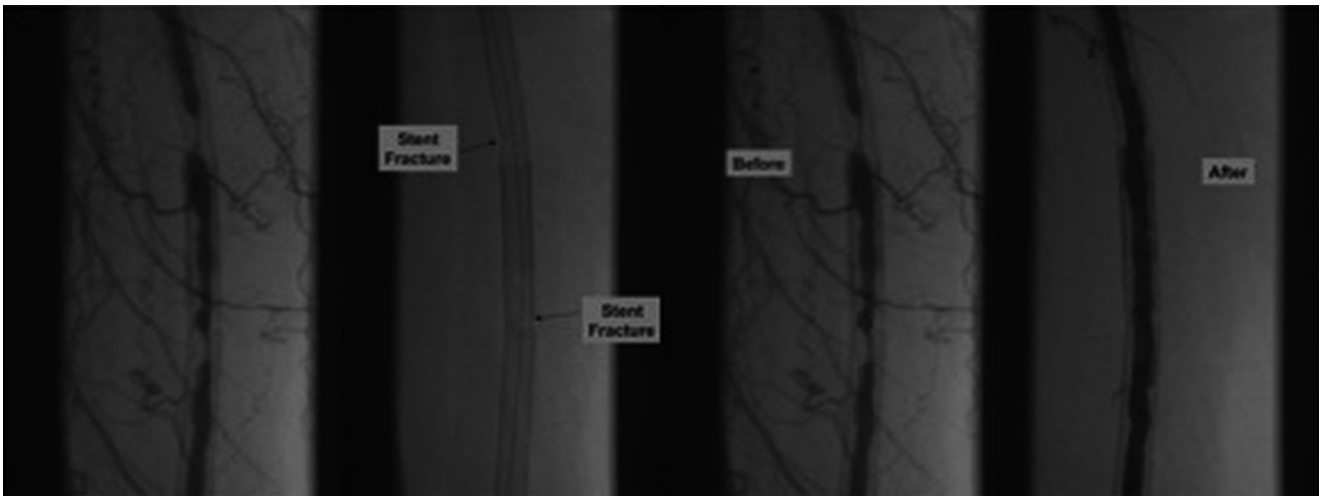


Fig. 9.11 60 year old male, post femoral stenting 2 years prior who developed Rutherford 3 claudication, secondary to in-stent restenosis. Patient successfully treated with laser atherectomy followed by balloon angioplasty

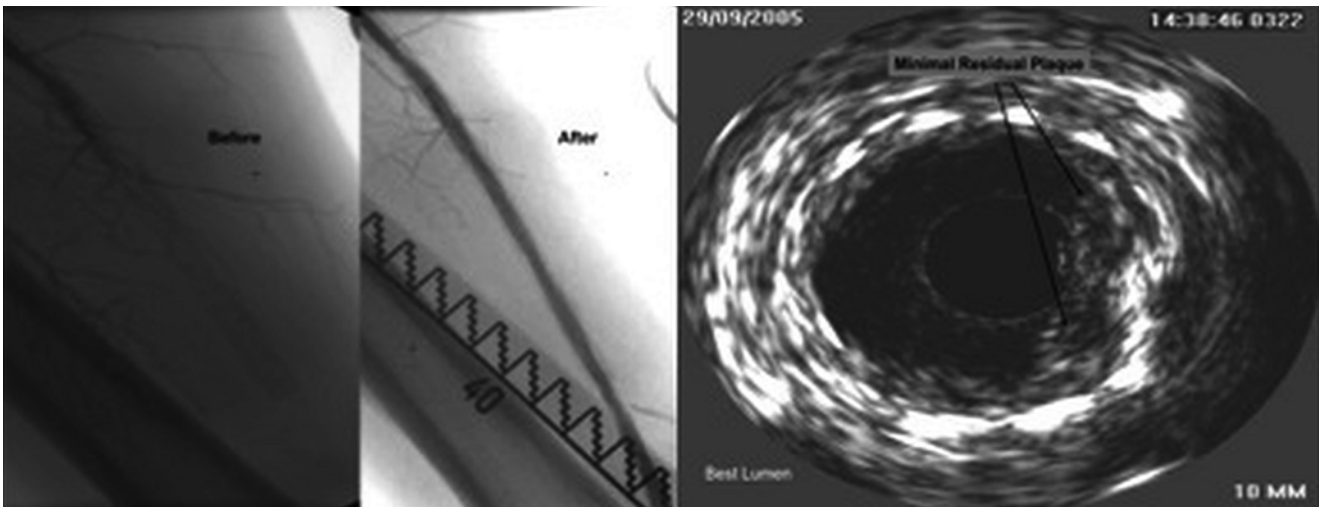
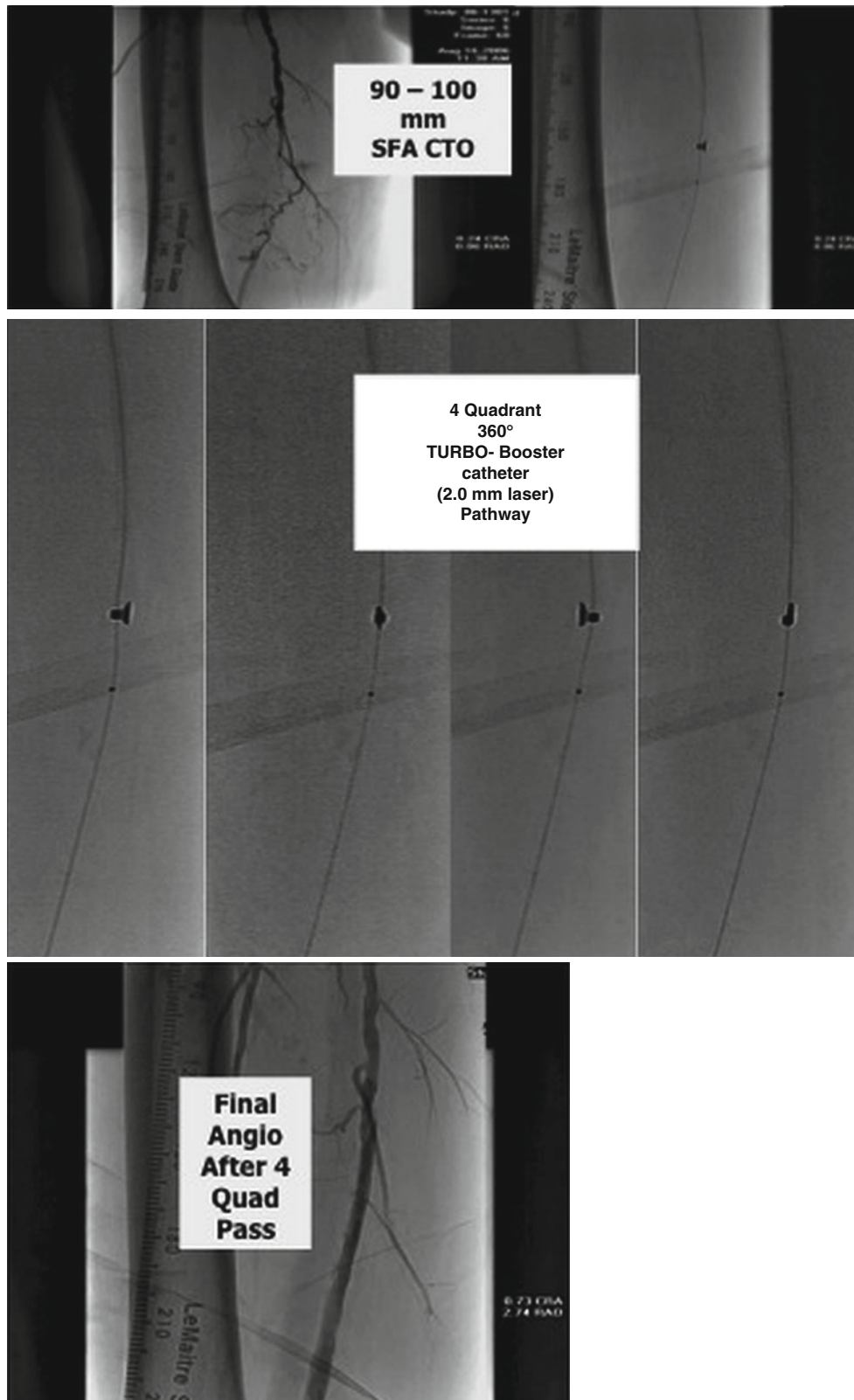


Fig. 9.12 57 year old male with chronic in-stent occlusion and true ischemia rest pain. Treated with turbo booster laser Atherectomy with no angioplasty



Figs. 9.13, 9.14, and 9.15 62 year old male de-nova SFA occlusion with Rutherford 3 claudication. Treated with Turbo Booster atherectomy with no adjunctive PTA

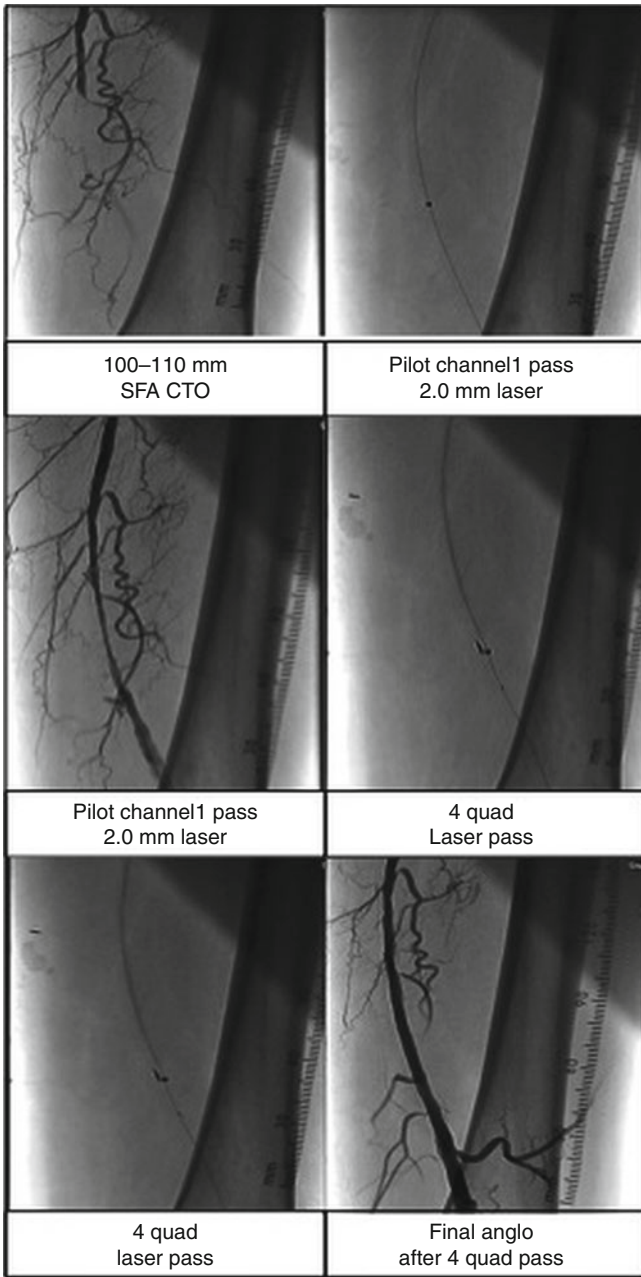
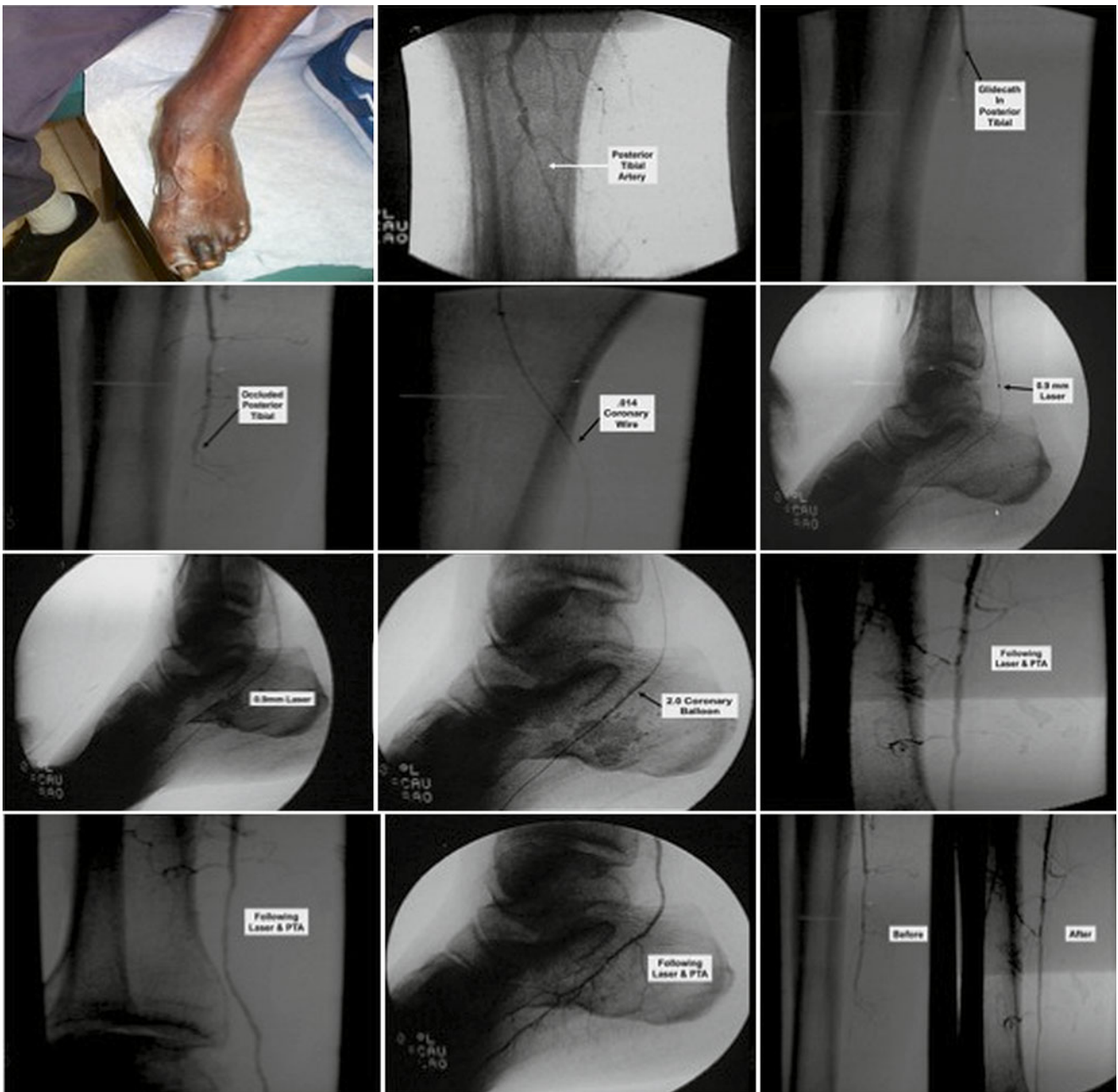


Fig. 9.16 49 year old female de-nova SFA occlusion with Rutherford 3 claudication. Treated with Turbo Booster Atherectomy as sole therapy



Figs. 9.17 and 9.18 54 year old male with ischemic ulcer second toe, with history of two prior failed femoral-tibial bypass grafts. Patient had true ischemic rest pain. Lesion crossed with guide wire then treated with .9 mm laser followed by balloon angioplasty



Figs. 9.17 and 9.18 (continued)



Fig. 9.19 A 56-year-old male with severe rest pain and a history of multiple failed distal bypass surgical procedures. Gangrenous toes with active infection

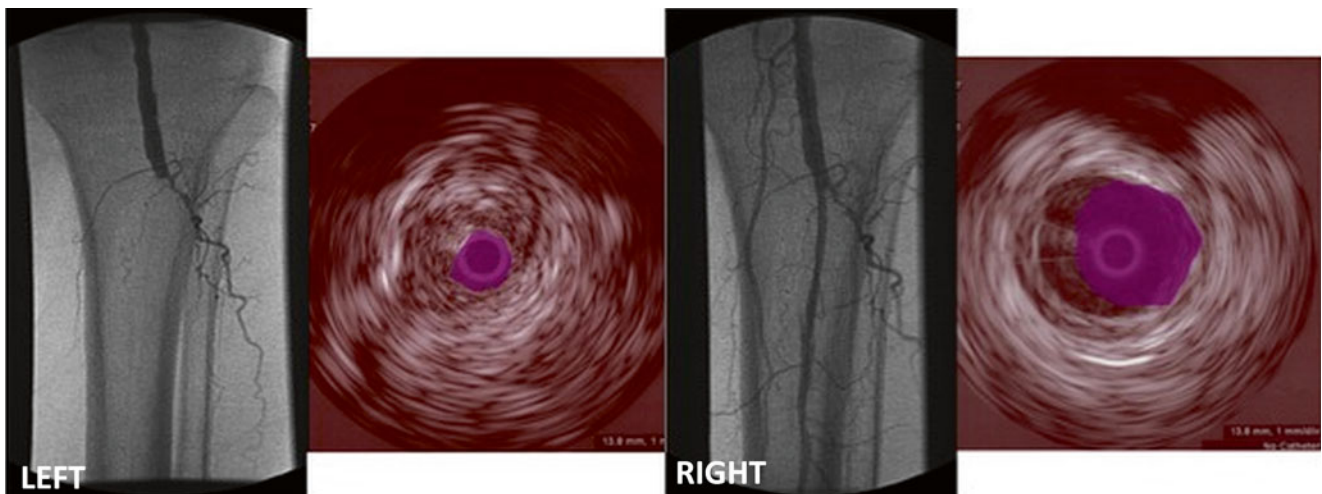


Fig. 9.20 *Left:* Initial angiogram showing totally occluded distal popliteal artery with no distal filling by angiography. CTA and MRA also showed no distal targets. *Right:* Lesion could not be crossed with a guide wire. Step by step technique was utilized to cross revealing a widely patent channel after laser alone (Subsequent PTA was performed with a 3mm balloon not shown here)



Fig. 9.21 Foot post minor amputation and skin grafting (13 years post procedure)

Fig. 9.22 Guide wire could not be advanced past this point. IVUS confirmed this was intraluminal in SFA

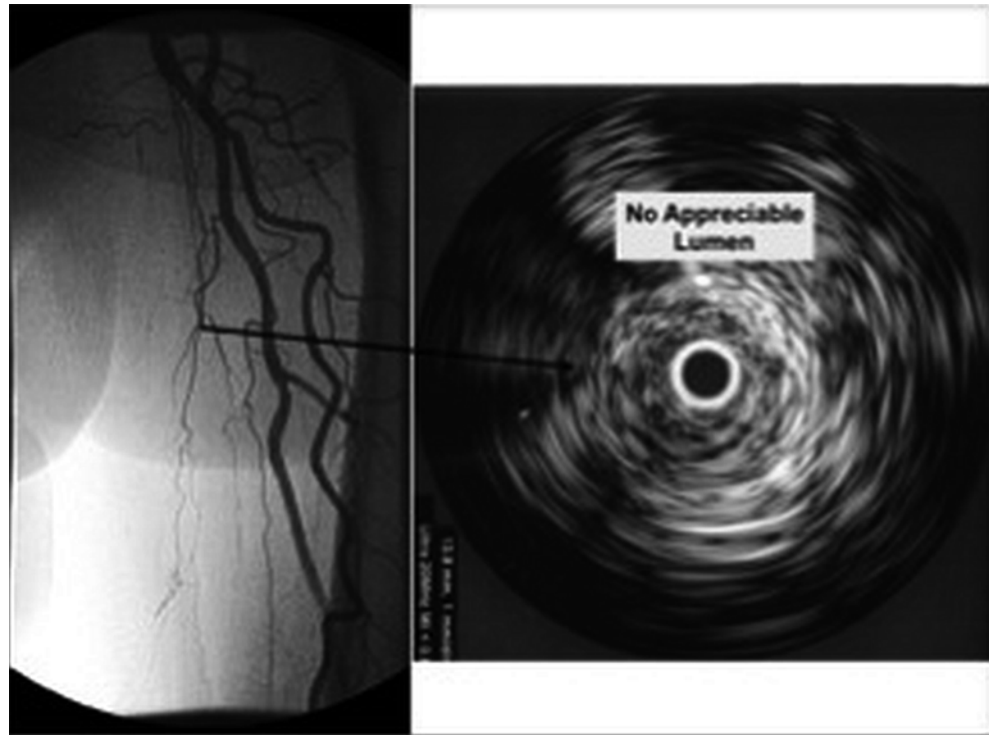
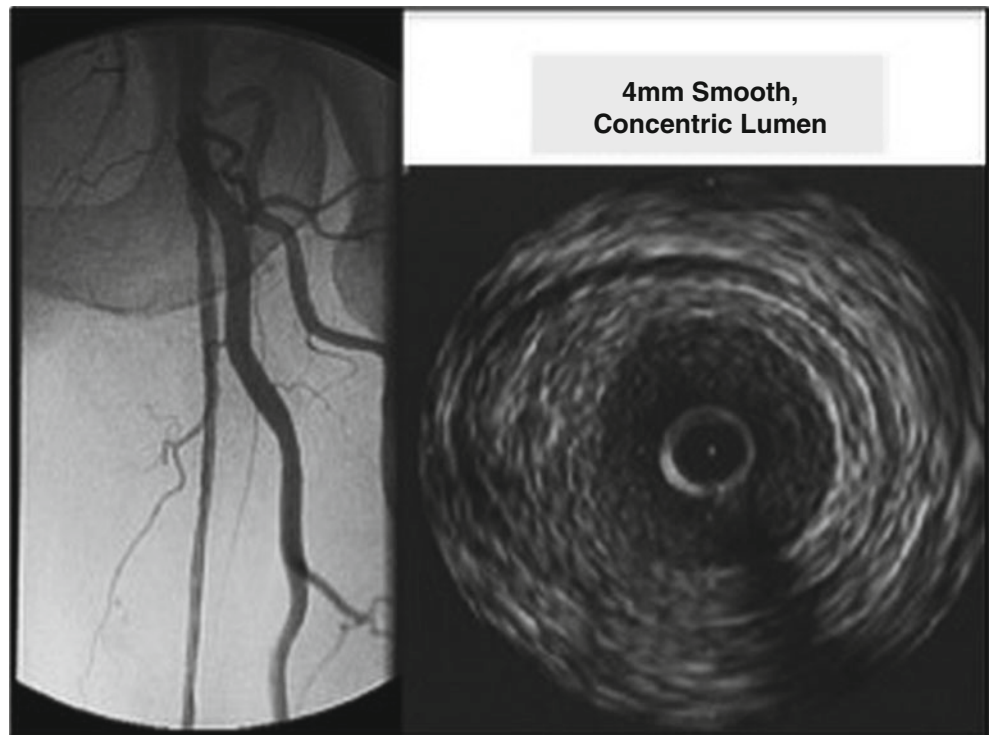


Fig. 9.23 2 mm laser probe advanced using step-by-step technique to cross and establish a pilot channel (Subsequent PTA was performed but is not shown)



Conclusions

Three hundred and eight nanometer excimer laser is a versatile and useful tool in the interventional therapy of PAD when utilized appropriately. It can remove obstructive plaque and thrombus without thermal injury as solo or adjunctive therapy.

References

1. Walker C, Patlola R, et al. Laser-facilitated lysis of occluded synthetic femoropopliteal bypass grafts. *Vasc Dis Manag.* 2013;10(3): E63–6.
2. Topaz O et al. “Optimally Spaced” excimer laser coronary catheters: performance analysis. *J Clin Laser Med Surg.* 2001;19:9–14.
3. Biamino G, Scheinert D. Excimer laser treatment of SFA occlusions. *Endovasc Today.* 2003;45. Available at: evtoday.com/2003/06/0503_101.html.
4. Laird J. PELA trial: peripheral excimer laser angioplasty. Presented at Transcatheter Cardiovascular Therapeutics 2002. Available at: <http://www.medscape.com/viewarticle/442691>.
5. Laird JR, Zeller T, Gray BH, et al. Limb salvage following laser-assisted angioplasty for critical limb ischemia: results of the LACI multicenter trial. *J Endovasc Ther.* 2006;13:1–11.
6. Allie D, Walker C. Excimer laser-assisted angioplasty in severe infrapopliteal disease and CLI: the CIS “LACI equivalent” experience. Available at: <http://vasculardiseasemanagement.Com/article/3248>. Accessed 8 Sept 2008.
7. Dippel E, Dave RM, Patlola R, Kollmeyer K, et al. Excimer laser revascularization of femoropopliteal lesions and 1-year patency: results of the CELLO registry. *J Endovasc Ther.* 2009;16(6): 665–75. doi:10.1583/09-2781.1.
8. Dippel E. Excite trial: the latest data. Presented at New Cardiovascular Horizons 2014, New Orleans, LA.
9. Van den Berg J. 4F lower limb intervention: pulsar stent technology. Presented at New Cardiovascular Horizons 2014, New Orleans, LA.

Gagan D. Singh, Ehrin J. Armstrong, and John R. Laird

Introduction

Critical limb ischemia (CLI) results from severe arterial insufficiency and is characterized by rest pain, non-healing ulceration or gangrene. Angiographically, CLI often involves progressive multi-level atherosclerosis of the iliac, superficial femoral, popliteal, and/or infrapopliteal arteries. Many diabetic CLI patients will present with severe occlusive disease of all three of the infrapopliteal arteries. CLI is associated with major amputation rates of 40 % and mortality rates of 25 % at 1 year [1, 2]. Medical therapy remains an important component of the care of CLI patients in order to reduce the burden of modifiable risk factors (e.g., diabetes, hypertension, smoking) and to treat the associated cardiovascular comorbidities of such patients [3]. At the same time, the majority of patients require adjunctive endovascular or surgical revascularization to maximize limb salvage and amputation-free survival. Establishment of “straight line” flow to the foot in one or more of the infrapopliteal arteries is necessary to allow for adequate tissue healing, and avoidance of major (above the ankle) amputation.

Percutaneous transluminal angioplasty (PTA) is the most common endovascular intervention for treatment of CLI [3–5].

G.D. Singh, MD

Division of Cardiovascular Medicine, Department of Internal Medicine, University of California Davis Medical Center, 4860 Y Street, Suite 2820, Sacramento, CA 95817, USA
e-mail: drsingh@ucdavis.edu

E.J. Armstrong, MD, MSc, MAS

Division of Cardiovascular Medicine, Department of Internal Medicine, VA Eastern Colorado Healthcare System, 1055 Clermont Street, Denver, CO 80220, USA

Division of Cardiology, University of Colorado School of Medicine, 1055 Clermont Street, Denver, CO 80220, USA
e-mail: Ehrin.armstrong@gmail.com

J.R. Laird, MD (✉)

Professor of Medicine, Division of Cardiovascular Medicine, UC Davis Vascular Center, 4860 Y Street, Suite 3400, Sacramento, CA 95817, USA
e-mail: jrlaird@ucdavis.edu

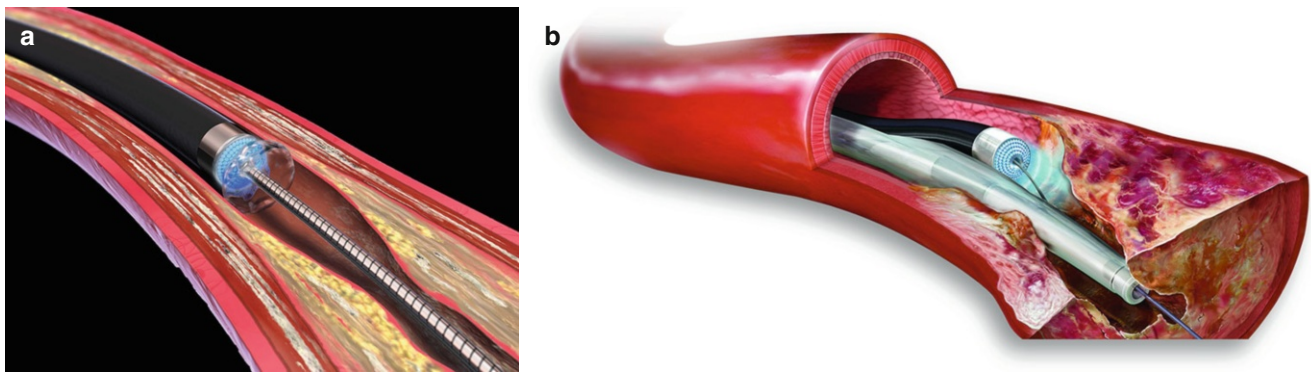
PTA alone can obtain durable results in focal aorto-iliac lesions [3], but is associated with higher rates of restenosis for longer lesions and smaller caliber vessels, and is limited by elastic recoil, and vessel injury [4, 5]. Additionally, the frequent presence of chronic, infrainguinal occlusions among patients with CLI limits the utility of isolated PTA as such lesions have a high rate of restenosis. With advances in new technologies for treatment of anatomically complex PAD [6] and refinement in recanalization techniques, improved procedural success rates and outcomes are possible in the endovascular treatment of CLI. Among these modalities, laser atherectomy has been well studied and holds particular promise for the successful treatment of challenging femoropopliteal and infrapopliteal lesions that are frequently encountered in patients with CLI. The goal of this chapter is to delineate the technical aspects of laser atherectomy for treatment of complex lower extremity lesions and to review the clinical literature supporting the use of laser atherectomy in the treatment of CLI.

Technical Aspects of Laser Atherectomy in Patients with Critical Limb Ischemia

Peripheral arterial applications of laser atherectomy utilize a 308 nm excimer laser similar to the system utilized in the coronary arteries (Spectranetics, Colorado Springs, CO). Catheters are available in both rapid exchange and over the wire configurations (Table 10.1). For larger femoropopliteal vessels, catheter diameters up to 2.5 mm can be used, whereas smaller 0.9–1.7 mm catheters are available for infrapopliteal applications. The 2.5 mm TurboElite® laser catheter (Fig. 10.1a) can be delivered through an 8 Fr sheath, while a 2.3 mm catheter can be delivered through a 7 Fr sheath. The TurboTandem® laser atherectomy (Fig. 10.1b) catheter also provides circumferential laser atherectomy for larger debulking applications, and has been shown to have utility for cases of femoropopliteal in-stent restenosis. Each of these available catheters can utilize a wide range of repetition rates and fluency to deliver optimal atherectomy at the

Table 10.1 Excimer laser (Spectranetics, Colorado Springs CO) device specifications

Device	Device size	Sheath size	Working length (cm)	Guidewire (inches)
Turbo Elite OTW	0.9–2.5 mm	4 F: 0.9 mm device	110 for 2.5 mm	0.014 for 0.9 and 1.4 mm 0.014 or 0.018 for 1.7, 2.0, 2.3 and 2.5 mm
		5 F: 1.4 and 1.7 mm	120 for 2.3 mm	
		6 F: 2.0 mm	150 for others	
		7 F: 2.3 mm		
		8 F: 2.5 mm		
Spectranetics Turbo Elite Rx	0.9–2.0 mm	4 F: 0.9 mm device	150	0.014
		5 F: 1.4 mm		
		6 F: 1.7 mm		
		7 F: 2.0 mm		
Turbo Booster Laser Guide Catheter	Custom guide sheath that allows the laser to directionally ablate tissue to obtain a larger lumen	7 F: 1.4 and 1.7 mm devices	110	Guidewire sizing according to laser device
		8 F: 1.4, 1.7, and 2.0 mm		

**Fig. 10.1** Turbo-Elite (a) and Turbo-Tandem (b) laser guidecatheter

target lesion site. In each case, the laser catheter should be advanced slowly (typically 0.5–1.0 mm/s) in order to maximize lesion debulking.

Because patients with CLI often have chronic occlusions, it is worth noting that laser atherectomy techniques have been developed specifically for crossing occlusions of the superficial femoral artery or infrapopliteal vessels. This “step by step” technique is particularly useful when there is a hard, fibrous proximal cap or when prominent collaterals are present at the proximal end of the occlusion, and the guidewire gets repetitively deflected into the collateral vessels. In the “step by step” technique, a wire is initially advanced to a site of occlusion (Fig. 10.2). The laser is then advanced to the tip of the wire at the proximal end of the cap. Laser atherectomy is then performed after withdrawal of the wire tip, so that the laser performs focal ablation at the proximal cap. The wire is then advanced into the site of ablation, and the laser is again advanced and activated (in a stepwise manner) to provide lesion debulking and to facilitate crossing of the occlusion. By serially repeating this process, it is possible to successfully advance the guidewire and laser through the occlusion, across the distal cap, and into the true lumen beyond the occlusion.

Clinical Studies of Laser Atherectomy in Critical Limb Ischemia

The efficacy of laser debulking therapy was first noted more than two decades ago, but initial clinical utility was limited by device profile [7]. The current generation of laser debulking devices have led to marked improvement in patient-centered outcomes. The use of laser atherectomy for patients with CLI has been studied in multicenter trials as well as smaller retrospective cohorts. The following discussion reviews the published literature of laser atherectomy for treatment of patients with CLI. Because patients with CLI often have diabetes and are at high risk for the development of in-stent restenosis, the potential application of laser atherectomy for these two clinical situations is also discussed.

Initial Studies of Laser Atherectomy in Claudication and CLI

One of the first studies of laser atherectomy for endovascular intervention evaluated 318 patients with long superficial femoral artery (SFA) occlusions undergoing 411 consecutive

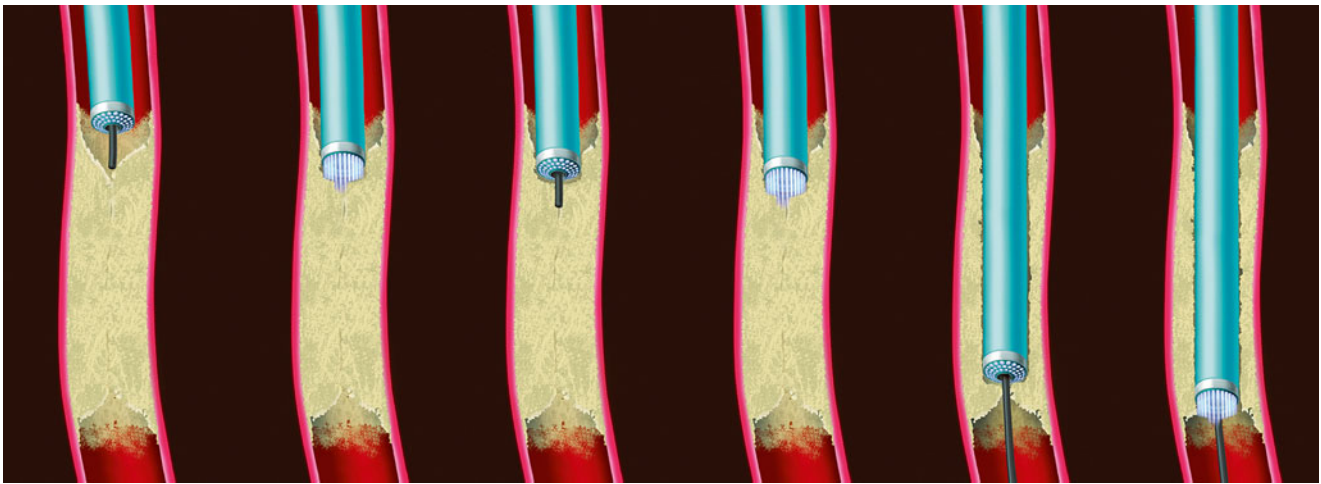


Fig. 10.2 The “step by step” technique. The excimer laser catheter is used to penetrate the fibrous cap of the chronic total occlusion. The laser catheter and guidewire are advanced in tandem through the occlusion until access to the true lumen beyond the occlusion is achieved

excimer laser-assisted recanalization procedures [8]. While many of the patients in this study had significant risk factors contributing to advanced PAD (76 % smokers, 31 % diabetes, mean occlusion length of 19.4 cm, 24 % with one vessel runoff), the majority did not have CLI (7 % of patients were Rutherford category 4–6). In this population primarily of claudicants, the technical success rate of laser-assisted angioplasty was 91 %, with provisional stenting in only 7 % of cases. Given the presence of very long occlusions, a primary patency of 34 % was not surprising; however with careful surveillance and early reintervention, 1-year primary assisted (re-intervention for restenosis) and secondary patency (re-intervention for reocclusion) rates for long SFA occlusions were 65 % and 75 %, respectively. Immediately post-procedure, the majority of patients had significant symptomatic improvement: 69 % of patients were asymptomatic post-intervention, with a remaining 25 % had mild to moderate claudication only. The authors reported low procedural complication rates consisting of acute reocclusion (1 %), perforation (2.2 %) and embolization/distal thrombosis (3.9 %). At 1 year, the limb salvage rate (LSR) and amputation free survival (AFS) was 100 % [8]. Although only a small percentage of patients in this initial cohort had CLI, this study provided technical proof of concept that laser atherectomy could be an effective therapy for long SFA occlusions.

In a separate prospective randomized study with similar patient characteristics (i.e., primarily claudicants and long SFA lesions) comparing PTA to laser-assisted PTA, procedural success was high (91 % PTA vs. 85 % laser-assisted PTA) and complication rates were comparable [9, 10]. There was a greater use of self-expanding nitinol stents in the PTA group (59 %) vs. the laser-assisted PTA group (42 %). At 12 months, the patency rates and functional status were similar between the two groups [9].

In both of the above studies, procedural success rates were high, complications rates were low, and significant clinical improvement was demonstrated during follow-up in patients with claudication. Collectively, these investigations also provided evidence suggesting a reduced need for stenting after laser-assisted angioplasty, with similar rates of restenosis when compared to PTA alone. These studies were also the first to demonstrate reduced distal embolization rates when using laser assisted PTA when compared to PTA alone, with the former approach having a slightly increased risk of minor vessel perforation. In the majority of cases, minor vessel perforation can be treated with prolonged balloon dilatation with virtually no long-term clinical sequelae. In comparison, treatment of distal embolization represents a greater challenge with potentially greater long-term consequences.

Table 10.2 compares the initial studies of PTA and laser-assisted PTA vs. a more contemporary study evaluating PTA alone in SFA occlusions for patients with claudication [11]. When compared to the initial laser-assisted angioplasty data for claudicants, the more contemporary PTA study appears to demonstrate superior 1-year patency rates; however, a greater percentage of patients were also treated with adjunctive stent placement.

The above studies highlighted the safety and 1-year efficacy of laser-assisted angioplasty for endovascular treatment of patients primarily with claudication. The first prospective evaluation of laser-assisted endovascular revascularization in patients with CLI was performed by Gray and colleagues in 25 limbs (23 patients) [12]. In that study, the authors reported limb salvage rates after laser-assisted angioplasty with provisional stenting in initially inoperable patients (i.e., significant cardiac comorbidities, absence of autologous venous conduits, or inadequate bypass targets for distal anastomosis) with Rutherford 5 or 6 disease. Multi-level interventions (aorto-iliac, femoropopliteal, and infrapopliteal) were performed in nearly all patients,

Table 10.2 Excimer laser for claudication

Series	Scheinert et al. [8]	Gray et al. [12]		Siracuse et al. [11]
Year published	2001	2002		2012
Treatment modality	Laser	Laser	PTA	PTA
Patients	318	101	88	105
Mean age (years)	64	66	65	69
% Male	65 %	75	77	63 %
Occlusion length (cm)	19.4	20.2	20.8	
Anatomic segment	SFA	SFA	SFA	SFA
<u>Acute procedural results</u>				
Procedural success	91 %	85 %	91 %	100
Stent implanted	7 %	42 %	59 %	57 %
<u>Procedural complications</u>				
Death	0	0	0	0
Amputation	0	0	0	NR
Surgical intervention	0	1 (0.9 %)	0	NR
Acute reocclusion	4 (1.3 %)	1 (0.9 %)	0	0
Perforation	9 (2.2 %)	9 (8.9 %)	3 (3.4 %)	NR
Embolization	16 (3.9 %)	2 (2.0 %)	7 (8.0 %)	NR
<u>6 month results</u>				
Primary patency	82 %	NR	NR	80 %
Survival	100 %	NR	NR	100 %
<u>12 month results</u>				
Primary patency	34 %	49 %	59 %	70 %
Survival	100 %	100 %	100 %	95 %

Modified from Laird et al. [9]

with occlusions in 24 % of the limbs, occlusion and stenosis in 60 % of limbs, and the remaining 16 % having stenosis without occlusion. The procedural success was 88 % with a mean of 3.1 lesions treated per limb. Provisional stenting was performed in 40 % of limbs. The authors reported a mean wound area reduction of 70 % at 3 months, which increased to 89 % at 6 months (Fig. 10.3). Owing to improved flow distal to revascularization sites, four patients became candidates for subsequent surgical revascularization. In successfully treated patients receiving adjuvant surgical revascularization, limb salvage was 90 % at 6 months but only 69 % in those who were not candidates for surgical revascularization [12]. Although this was a small study, the authors demonstrated a successful multi-modality approach for the treatment of CLI with favorable outcomes. This study also provided reassuring initial results with laser-assisted angioplasty for the treatment of CLI that led to the first multicenter trial evaluating the efficacy of excimer laser therapy in CLI [13].

The LACI Trial

The Laser Angioplasty for Critical Limb Ischemia (LACI) trial enrolled 145 patients (155 limbs) with CLI who were poor or non-surgical candidates [13]. In this multicenter trial

spanning 14 sites, enrolled patients had a high prevalence of baseline comorbidities including hypertension (83 %), diabetes (66 %), active or former smoking (53 %), and ASA class 4 (46 %). All patients had CLI, with 71 % of patients having Rutherford class 5 or 6 disease. Chronic occlusions were present in 91 % of the 423 lesions treated (SFA 41 %, popliteal 15 %, infrapopliteal 41 %) with a mean treatment length of 16 cm for the overall cohort. Nearly all (96 %) of the patients underwent laser-assisted angioplasty with 45 % receiving provisional nitinol stenting. Overall procedural success was 85 % (Fig. 10.4) with few complication rates (4 % major dissection, 3 % acute thrombus formation, 3 % distal embolization, 2 % perforation).

Despite challenging lesion characteristics, excellent survival and LSRs of 87 % and 92 %, respectively, were achieved at 6 months (Fig. 10.5). This study was also one of the first to prospectively report a series of patients treated with the “step-by-step” laser technique for chronic occlusions that could not be crossed successfully with a guidewire. A total of 26 lesions were encountered that could not be crossed with standard guidewire and support catheter in an antegrade manner. Utilizing the “step-by-step” laser technique (Fig. 10.2), 88 % of these lesions were successfully crossed, thereby salvaging a procedure that would have otherwise been unsuccessful. Hence, despite a failed guidewire



Fig. 10.3 (a) Ischemic forefoot pre-intervention. (b) Three months post laser assisted angioplasty, the forefoot has completely healed (Reproduced from Gray et al. [12])

crossing in 8 % of the cases, laser treatment was delivered to 99 % of the cases with adjunctive PTA performed successfully in 96 % of the cases and a straight-line flow established in 89 % of the cohort. Overall in-hospital and 6-month follow-up adverse events rates were low (Table 10.3).

The LACI trial demonstrated feasibility, safety, and high limb salvage and survival rates of laser-assisted PTA in a highly morbid patient population unsuitable for surgical revascularization. The subsequent LACI Belgium study confirmed these findings in a similar patient cohort and using similar study design, and follow-up [14]. Despite the treatment of a high-risk cohort not suitable for surgical revascularization, the LACI investigations showed applicability of laser-assisted angioplasty in a safe and efficacious manner with minimal peri-procedural risk.

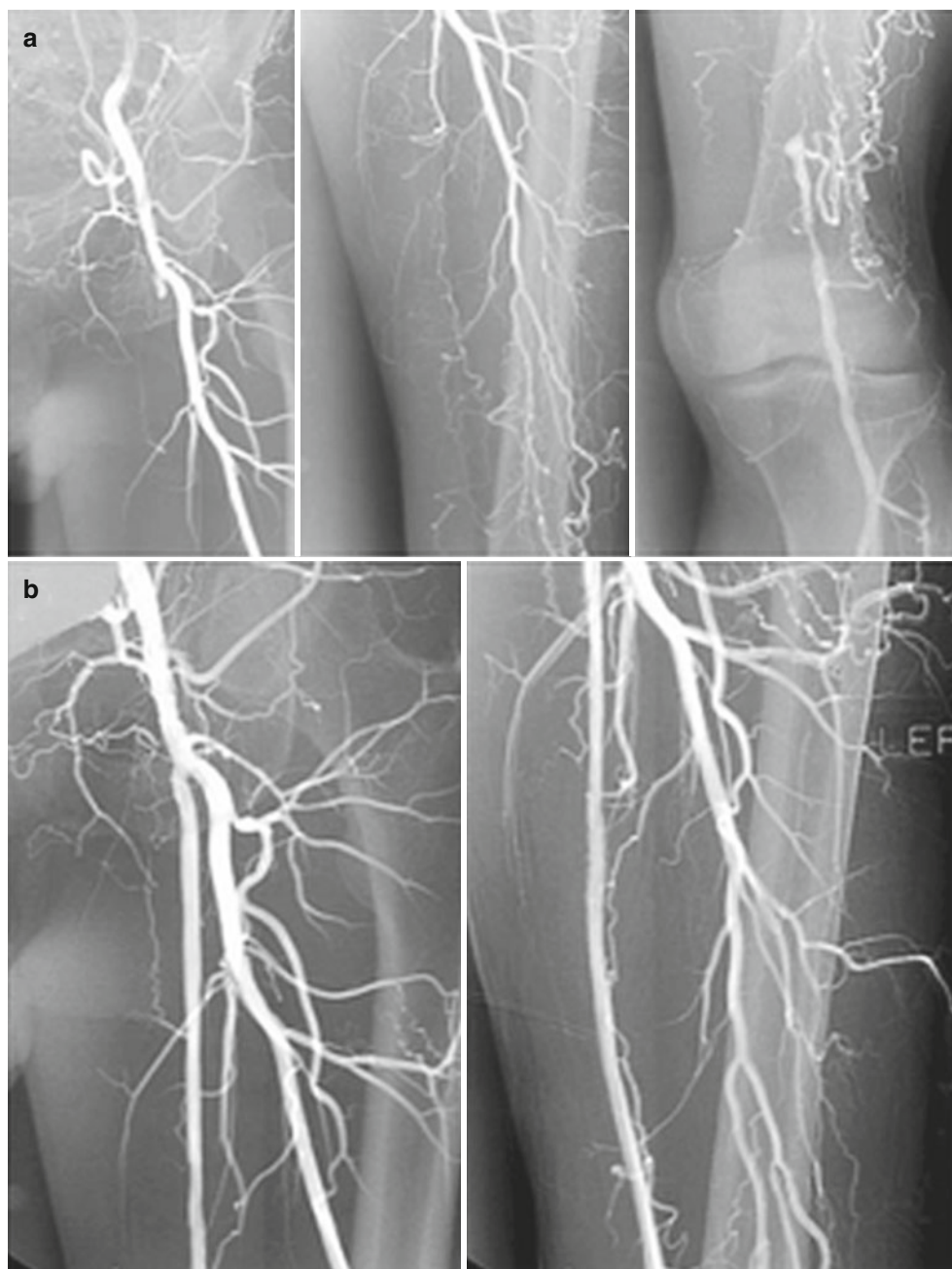
Multiple smaller studies published since the LACI trial have evaluated the role of laser-assisted PTA for the treatment of CLI (Table 10.3). Most of these reports are based on retrospective personal and institutional criteria rather than a prospective trial. One retrospective study of 40 patients at high-surgical risk reported disappointing one-year patency and limb salvage results with laser-assisted angioplasty [15]. The results of this study are a significant outlier when compared to other laser assisted angioplasty studies [16–18]. The authors noted that the studied cohort [16] included patients with many high-risk comorbidities (i.e., DM and ESRD) that may have contributed to the higher rate of adverse outcomes. Owing to the higher adverse event rates in this study, operator

experience and an initial learning curve with the system may also have been a contributor to the lower patency, lower limb salvage rates, and higher adverse event rates [16].

Laser Atherectomy with Balloon Angioplasty Versus Balloon Angioplasty Alone for De Novo Stenosis

The only prospective study comparing laser-assisted angioplasty ($n=42$) to PTA ($n=38$) alone was recently published with a non-randomized and non-blinded design [18]. This small investigation enrolled CLI patients solely (100 %) with a high proportion of diabetics with chronic occlusions and long diseased infrapopliteal segments. Laser-assisted angioplasty demonstrated superior 3-year patency and, more importantly, AFS rates when compared to PTA alone. In the PTA cohort, AFS (89 %) was significantly better than patency rates (55 %) at 3-year follow-up with a re-intervention rate of 36 %. The authors of this study [18] published follow-up data of 3 years and noted superior patency results in patients receiving laser atherectomy for infrapopliteal CLI versus PTA. The PTA group had patency rates of 55 % at 3 years but amputation free survival of 89 % highlighting the notion that patency is required for adequate tissue healing alone and that long-term patency may not be important once the affected tissue has healed. However, the authors also note that the AFS in the PTA cohort was achieved with a re-intervention

Fig. 10.4 Panel (a) representative angiography of a chronically occluded proximal SFA. The occlusion extends from the proximal to the distal SFA. The vessel reconstitutes at the level of the proximal popliteal artery. Panel (b) after laser assisted angioplasty, there is full recanalization of the previously occluded SFA in its entirety (Reproduced from Laird et al. [13])



rate of 36 %. In the laser atherectomy group, patency rates were quite impressive (83 %) at 3 years. While the follow-up time periods are different, the patency rates in this investigation mirrored those seen in the earlier laser studies [13, 14, 16]. More interesting is that these patency rates were achieved with very low re-intervention rates (5 %) and achieved statistically significant higher AFS (95 %) when compared to PTA (89 %) alone for infrapopliteal CLI. This is the first study with laser atherectomy study was associated with superior patency rates and amputation free survival with a significant follow-up period (3 years) when compared to PTA alone [18].

Laser Atherectomy in Diabetic Patients with CLI

Patients with CLI often have concomitant diabetes. Patients with diabetes are more likely to have infrapopliteal arterial occlusive disease, and patients with diabetes additionally have higher rates of restenosis and target lesion failure after endovascular intervention. As a result, patients with CLI and diabetes may have as much as a tenfold increase in the risk of amputation [2]. In a small study (51 lesions) of diabetics with CLI and occlusive arterial disease, treatment with laser and adjunctive PTA (64 %) and/or stenting (25 %) yielded

Fig. 10.5 Patient survival (a) and limb salvage rates (b) at 6 month followup (Reproduced from Laird et al. [13])

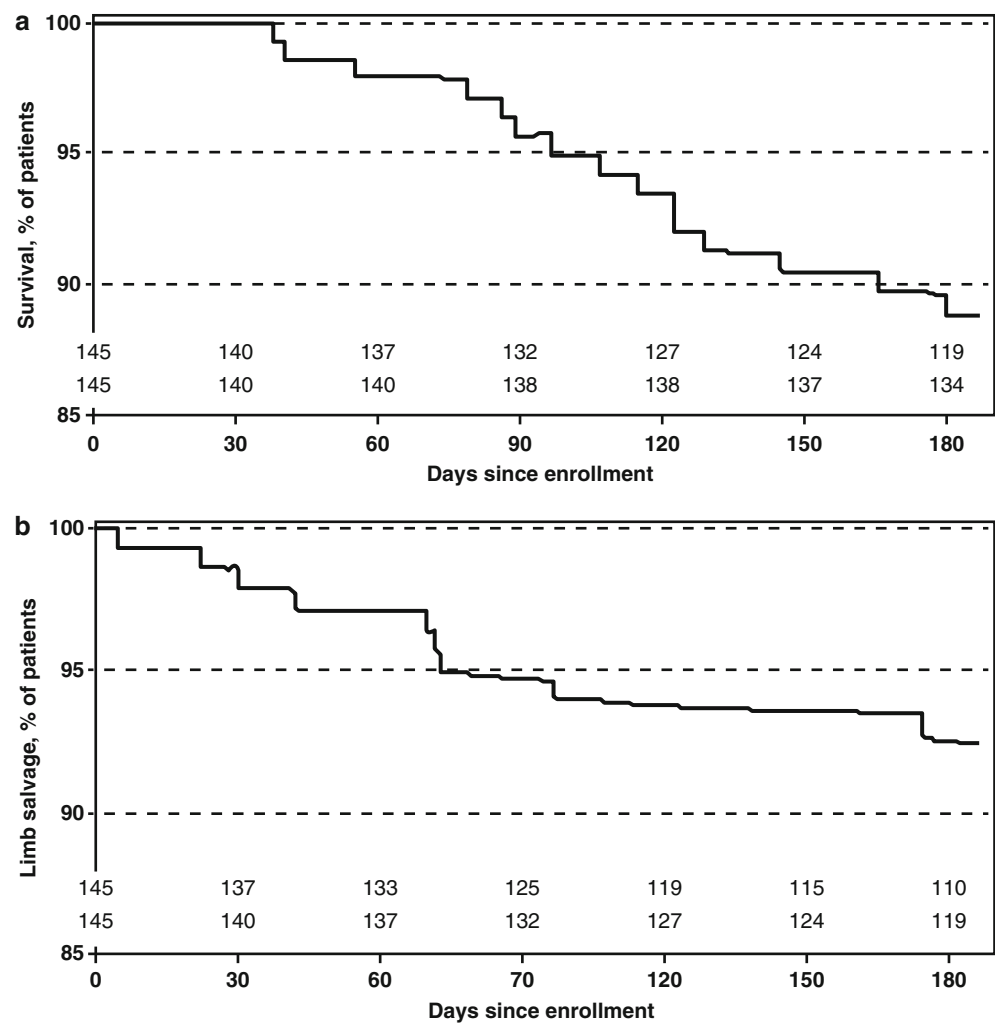


Table 10.3 Adverse event rates from the LACI trial [13]

Event	In hospital	6 months followup
Death any cause	0 (0 %)	15 (10 %)
Nonfatal MI or stroke	0 (0 %)	2 (1 %)
Acute limb ischemia	0 (0 %)	1 (1 %)
Hemataoma with surgery	1 (1 %)	0 (0 %)
Major amputation	2 (1 %)	9 (6 %)
Bypass Surgery	0 (0 %)	3 (2 %)
Endarterectomy	0 (0 %)	1 (1 %)

2-year patency rates of 83 % with LSR of 94 % with only a 6 % need for re-intervention[16]. Unlike the LACI cohort, all of these patients had a much more favorable overall risk factor profile and were pre-selected for an endovascular strategy. Hence, the lower degree of co-morbidities along with the single center nature of the study may partly explain better patency and limb salvage rates when compared to LACI. Overall, nearly all published studies evaluating laser debulking therapy have had a substantial (at least 50 % or more) proportion of diabetics (Table 10.4). However, this

study [16] included the lowest rate of adjunctive stenting (only 25 %) and still reported favorable outcomes. Because diabetic patients are more likely to develop restenosis, laser atherectomy may provide some promise in obtaining greater luminal gain during the initial intervention, thereby lowering the likelihood of symptomatic restenosis. Whether this theoretical benefit of laser atherectomy in diabetic patients with CLI translates into improved clinical outcomes remains uncertain.

Laser Atherectomy for Treatment of In-Stent Restenosis in Patients with CLI

In-stent restenosis (ISR) is a frequent clinical problem encountered in the endovascular management of patients with CLI [19]. Laser atherectomy may offer advantages for the treatment of ISR, including significant debulking of neointima. Covered stent grafts may also have additional benefit by excluding the neointima within a PTFE (Polytetrafluoroethylene)-covered stent graft. The

Table 10.4 Outcomes of LACI and other laser-assisted angioplasty trials in patients with CLI

	LACI [13]	LACI Belgium [14]	Stoner et al. [15]	Serrino et al. [16]	SALVAGE [17]	Sultan et al. [18]	
						Laser	PTA
Study time period	2000–2001	2003	2004–2006	2007–2009	2008–2009	2005–2010	
Patients/limbs	145/155	48/51	40/47	35/51	27/NR	42/44	38/40
CLI (%)	100 %	100 %	65 %	100 %	74 %	100 %	100 %
Diabetes	66 %	47 %	55 %	100 %	59 %	82 %	77 %
Patient selection	All poor surgical candidates	All poor surgical candidates	Selected for EVI	Selected for EVI	Selected for EVI	Selected for EVI	Selected for EVI
TASC D or chronic occlusions	91 %	NR	41 % FP/69 % IP	100 %	81 %	100 %	100 %
Total treated length	16.2		NR	4–23 cm	21 cm	16	17 %
Lesion/limb	2.7	NR	NR	1.5	NR	1.95	2
Lesion location	Multilevel	Multilevel	Multilevel	Multilevel	Fem-pop	Infrapopliteal	Infrapopliteal
Primary treatment	Laser	Laser	Laser	Laser	Laser	Laser	PTA
Adjuvant treatment type (%)	PTA (96 %)	PTA (80 %)	PTA (75 %)	PTA (64 %)	PTA (100 %)		
Adjuvant treatment type (%)	Stenting (45 %)	Stent (53 %)	Stent (13 %)	Stent (25 %)	Stent Graft (100 %)	Stent (30 %)	Stent (36 %)
Procedural success	85 %	NR	88 %	88 %	100 %	81 %	74 %
Followup duration	6 months	6 months	12 months	12/24 months	12 months	3 year	3 year
Primary patency	83 %	76 %	44 %	97 %/83 %	48 %	83 %	55 % ^a
Reintervention (%)	15 %	4 %	NR	6 %	17 %	5 %	36 %
Bypass (n)	2 %	2 %	NR		1	2	4
Survival (%)	92 %	87 %	NR		100 %	95 % ^b	89 % ^{a, b}
Limb salvage rate (%)	87 %	90 %	55 %	100 %/94 %	NR	96 %	91 %

EVI endovascular intervention

^ap<0.05 vs laser

^bAmputation free survival

SALVAGE [17] trial evaluated 27 patients, all of whom received heparin-coated VIABAHN® covered stent grafts after laser-assisted angioplasty. All patients received treatment for femoropopliteal in-stent restenosis in setting of claudication (26 %) or CLI (74 %). The 1-year patency rates were disappointing at 48 %, with a high (17 %) re-intervention requirement. Despite these findings, all patients had substantial clinical improvement at 1-year follow-up. In the SALVAGE study, the reduced patency rates were felt to be secondary to edge stent restenosis, rather than luminal narrowing. These results emphasize the important of stent sizing when using covered stent grafts, as an oversized stent is more likely to develop edge restenosis. While laser atherectomy did not change the incidence of restenosis when using a covered stent graft, the superior debulking obtained with laser atherectomy of neointimal hyperplasia prior to covered stent graft placement likely improves the cross sectional area of the stented lumen, thereby limiting restenosis within the stented region. It remains to be determined whether combination of laser atherectomy with a covered stent graft offers additional clinical benefit.

Two recent studies have examined use of laser atherectomy plus balloon angioplasty for treatment of bare metal stent ISR. The PATENT (Photo-Ablation using the TURBO-Booster® and Excimer Laser for In-Stent Restenosis Treatment) trial enrolled 90 patients at two sites in Germany who had symptomatic Rutherford Class 1–5 disease due to femoropopliteal ISR [20]. At 6 and 12 months, the freedom from target lesion revascularization was 88 % and 64 %, respectively. Although this was a registry study, these results are significantly improved compared to historical controls of patients with femoropopliteal-ISR [21]. The EXCITE ISR (EXCimer Laser Randomized Controlled Study for Treatment of Femoropopliteal In-Stent Restenosis) randomized trial was a study of Turbo Tandem® laser atherectomy with PTA versus PTA only for the treatment of femoropopliteal ISR of bare nitinol stents [22]. The inclusion criteria consist of patients with Rutherford class 1–4 symptoms, femoropopliteal ISR of a 5.0–7.0 mm vessel, and a lesion stenosis of ≥50 % and ≥40 mm in length. Patients were randomized in a 2:1 fashion to laser-assisted PTA vs. PTA alone. The primary outcome is target lesion revascularization at 6 months,

as well as major adverse events within the first 30 days post-procedure. The total enrollment goal was 318 patients; however, the study was terminated early at 250 patients due to early efficacy demonstrated in a prespecified interim analysis. The authors noted a significant improved TLR in the laser assisted PTA versus PTA alone (74 % versus 52 %, $P < 0.005$) at 6 months. Additionally, laser assisted PTA was associated with a 52 % reduction in TLR (HR 0.48; 95 % CI 0.31–0.74). A more formal analysis and publication of a concurrent chronic occlusion registry Although the majority of patients enrolled in this study had symptomatic claudication rather than CLI, the results of this study should also be applicable to treatment of threatened limbs due to femoropopliteal ISR.

The advantages and disadvantages of drug eluting stents to maintain patency in the coronary circulation have been well established. However, the benefit of deploying drug eluting stents to vessels of the lower extremities remains to be confirmed [23, 24]. However, the use of drug-coated balloons is a relatively new and promising strategy to inhibit vascular smooth muscle proliferation after local delivery of anti-neoplastic drug (e.g., paclitaxel) combined with PTA for lower extremity occlusive arterial disease [25]. Laser atherectomy may have additional benefit when combined with drug-coated balloon angioplasty for the treatment of femoropopliteal-ISR. An initial study of ten patients (five with CLI) with symptomatic femoropopliteal-ISR reported that combination of laser atherectomy with paclitaxel-coated balloon angioplasty resulted in vessel patency in seven of ten patients at 7 months [26, 27]. At a recently reported mean follow-up of 16 months, five of those patients were recently reported to have no evidence of recurrent restenosis [27]. In another recently published study, Gandini et al. reported a randomized trial of 48 patients with CLI due to stent occlusion from FP-ISR who were randomized to laser atherectomy and drug coated balloon angioplasty vs. drug coated balloon angioplasty alone [28]. The authors reported a 12 month target lesion revascularization rate of 16.7 % for laser atherectomy and drug-coated balloons, versus 50 % for the patients randomized to drug-coated balloons only. Importantly, the rates of major amputation were also significantly lower in the laser and drug-coated balloons (8 %) vs. drug-coated balloons only group (46 %). If these results are replicated in a larger randomized study, the combination of laser atherectomy and drug coated balloon angioplasty may emerge as a particularly promising therapy for the treatment of femoropopliteal-ISR. The ongoing PHOTOPAC (Photoablative Atherectomy Followed by a Paclitaxel-Coated Balloon to Inhibit Restenosis in Instent Femoropopliteal Obstructions) randomized study, which is enrolling up to 50 patients at four sites in Europe, will further assess this question [29].

Sample Case 1: Superficial Femoral Artery In-Stent Restenosis

History

An 84 year old male with a long standing history of coronary artery disease and chronic renal insufficiency was originally referred for peripheral angiography due to progressive critical limb ischemia (Rutherford 4) of the left leg. Non-invasive vascular testing demonstrated an ankle brachial index of 0.33 of the left lower extremity. Duplex ultrasonography indicated left superficial femoral artery occlusion. Diagnostic angiography confirmed a chronic occlusion of the proximal SFA with under-filled and diffusely diseased distal vasculature. Percutaneous revascularization was undertaken with Viabahn Stent Grafts resulting in successful recanalization of the left SFA and popliteal artery. Approximately 2 years after treatment with stent, the patient was seen for routine follow-up and noted to have progressive left lower extremity ulceration and rest pain. Follow-up angiography (Fig. 10.6) demonstrated occluded Viabahn stent grafts with the popliteal artery reconstituted via collaterals.

Procedure

The chronic occlusion was successfully crossed with a 0.014" PT Graphix (Boston Scientific, Natick MA) hydrophilic wire and navigated into an infrapopliteal artery. Next a 2 mm Turbo Elite catheter (Spectranetics Corporation, Colorado Springs CO) was advanced and laser atherectomy was performed of the occluded segment using previously described techniques. This created a channel allowing for straight-line flow down into the popliteal artery (Fig. 10.7). Next prolonged balloon angioplasty was performed successively starting from the distal occlusion to the proximal SFA. Final angiography demonstrated brisk flow down the entire left lower extremity (Fig. 10.8).

Sample Case 2: Treatment of Infrapopliteal Occlusive Disease with Laser Atherectomy

History

A 67 year old male with diabetes and known infrapopliteal peripheral arterial occlusive disease is referred for 6 months of non-healing lower extremity ulcerations (Rutherford Stage 6). Prior attempts at lower extremity revascularization with balloon angioplasty by the referring institution were unsuccessful. A diagnostic angiogram demonstrated patent common femoral, SFA, and popliteal arteries. However, all three infrapopliteal arteries are occluded with the distal foot vascular reconstituted via collaterals (Fig. 10.9).

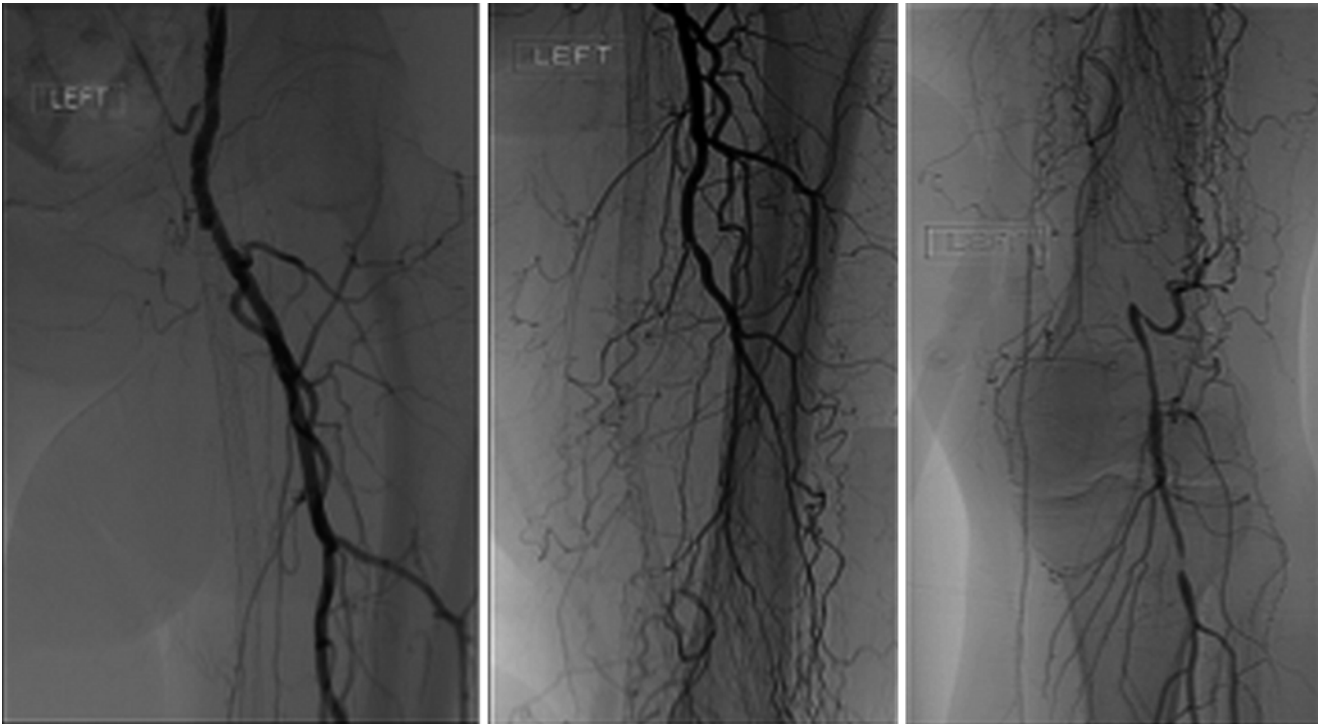


Fig. 10.6 Sample Case 1. Left lower cineangiography demonstrates an occluded previously placed Viabahn Stent Grafts used to treat de-novo femoropopliteal disease in a patient with CLI. The occlusion begins in the proximal SFA (*left panel*). The popliteal artery reconstitutes via collaterals (*right panel*). Also noted is an area of focal stenosis at the distal popliteal artery

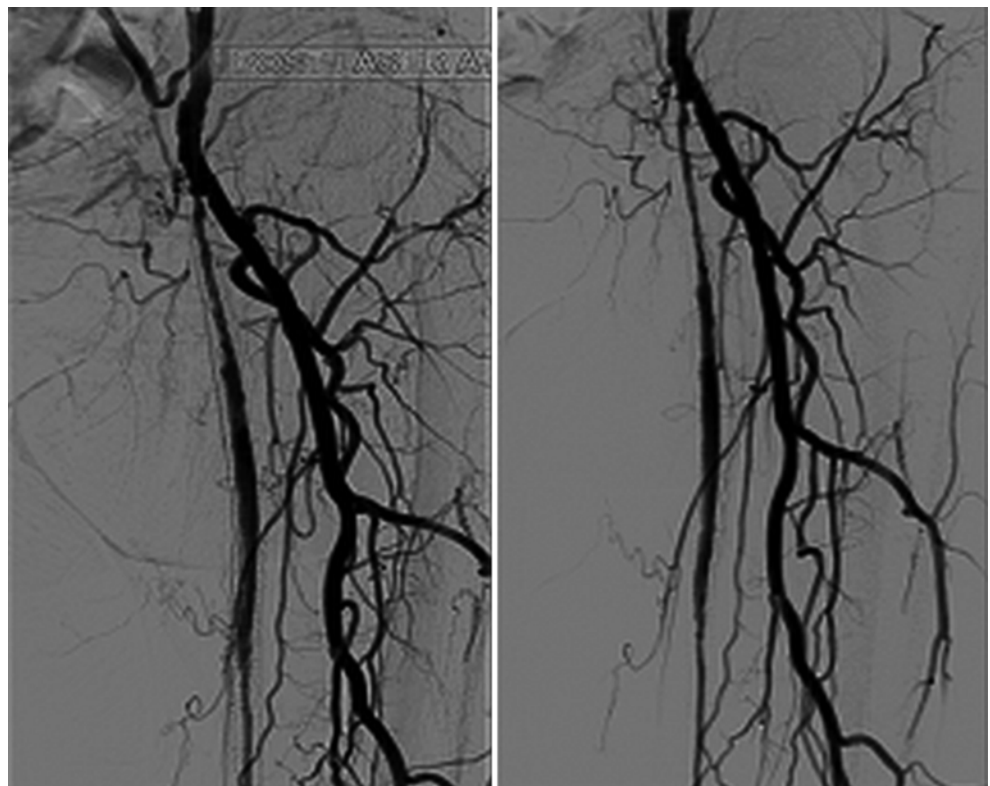
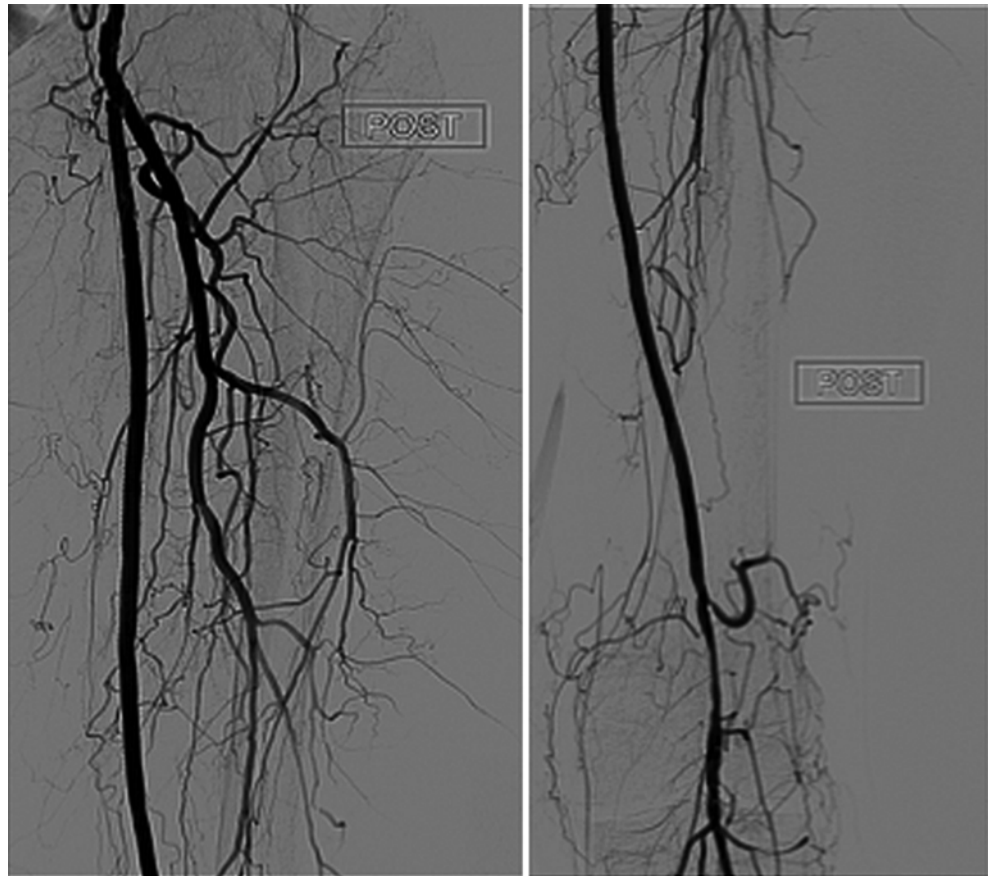


Fig. 10.7 Sample Case 1. Debulking with laser atherectomy is performed to establish a straight line of flow down to the lower extremities

Fig. 10.8 Sample Case 1. Prolonged adjunctive balloon angioplasty is performed after debulking with laser atherectomy. Angiography demonstrates reconstituted Viabahn stent grafts. The distal popliteal artery stenosis was also treated with prolonged balloon angioplasty



Procedure

The peroneal artery was successfully crossed with the assistance of a TruePath Occlusion Device (Boston Scientific, Natick MA). After removal of the Occlusion Device, laser atherectomy was performed with a 0.9 mm Turbo Elite laser atherectomy device (Spectranetics Corporation, Colorado Springs CO). Multiple passes were made through the chronic occlusion and into the distal vessel. After a successful straight line of flow was established, successive balloon angioplasty was performed to the entire length of the peroneal artery (Fig. 10.10). The chronic occlusion of the anterior tibial artery was crossed using a hydrophilic 0.014" guidewire followed by laser atherectomy and balloon angioplasty. Final angiography (Fig. 10.11) revealed minimal residual stenosis with two-vessel runoff to the lower extremity.

Conclusion

The fundamental benefit of laser atherectomy lies in its ability to evaporate and debulk tissue without substantially increasing the risk of complications such as distal embolization or vessel perforation. The current generation of laser atherectomy devices allow for treatment of the most severe forms of PAD with excellent short- and long-term outcomes for both claudication and CLI. Laser debulking systems are also a viable option for chronic occlusions that cannot otherwise be successfully crossed in an antero-grade manner by utilizing the "step by step" approach. With the current technology and evidence available to date, excimer laser has a role in endovascular therapy as an option for patients at high surgical risk, either as definitive treatment of appropriately selected lesions or as an adjunctive therapy for debulking lesions. Laser atherectomy should be considered part of the standard armamentarium for a successful endovascular revascularization strategy.



Fig. 10.9 Sample Case 2. Widely patent femoropopliteal system feeding diffusely diseased infrapopliteal vasculature. All the three major infrapopliteal vessels are chronically occluded with the ankle vessels filling via collaterals

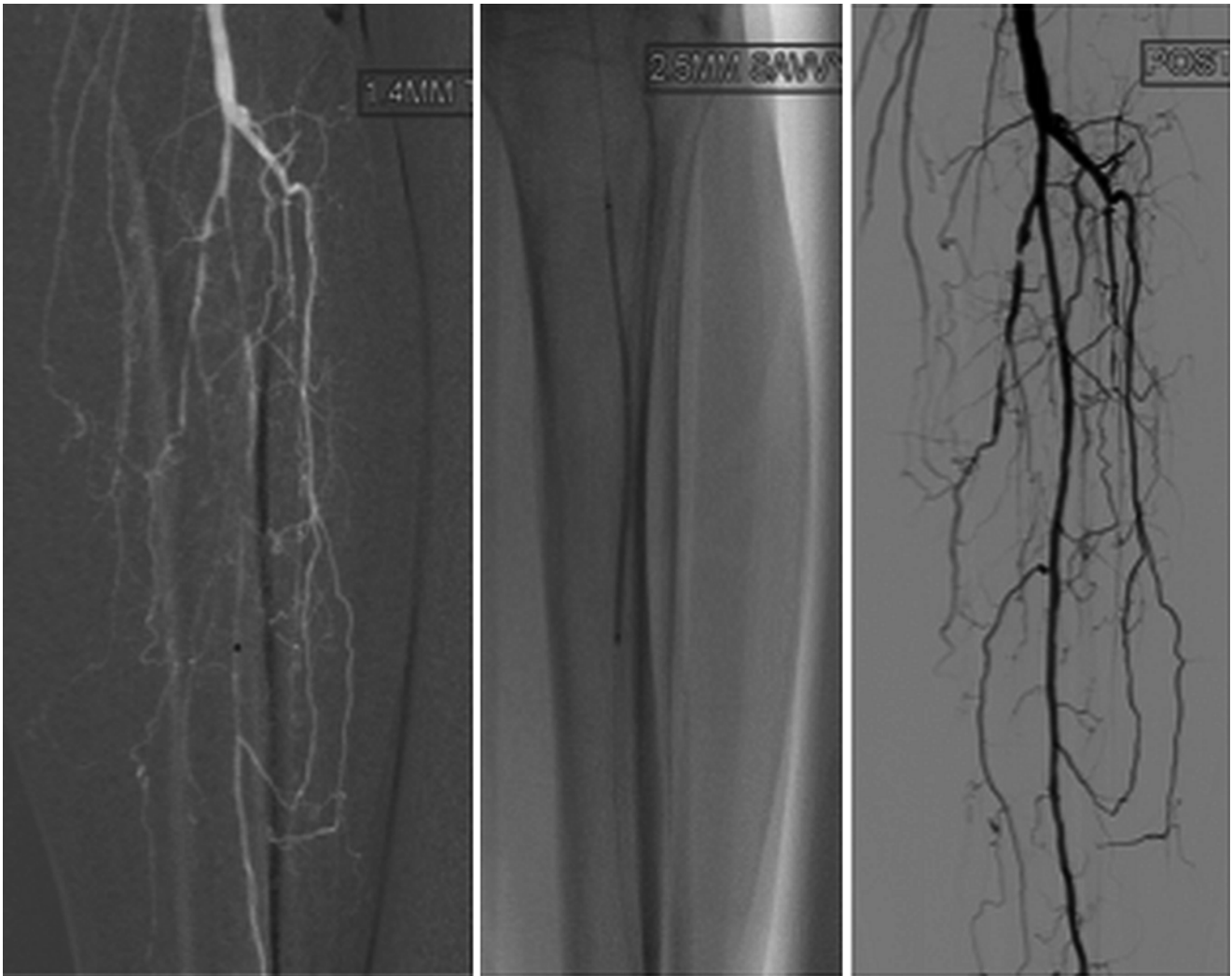


Fig. 10.10 Sample Case 2. After treatment with laser atherectomy and adjunctive balloon angioplasty to the peroneal artery, flow is re-established to the foot



Fig. 10.11 Sample Case 2. After treatment of the peroneal artery, the anterior tibial artery is treated with laser atherectomy and adjunctive balloon angioplasty re-establishing two vessel runoff to the lower extremity

References

- Ouriel K. Peripheral arterial disease. *Lancet*. 2001;358(9289):1257–64.
- Norgren L, Hiatt WR, Dormandy MR, Nehler KA, Fowkes FGR. Inter-Society Consensus for the Management of Peripheral Arterial Disease (TASC II). *J Vasc Surg*. 2007;45(1):S5A–67.
- Dormandy JA, Rutherford RB. Management of peripheral arterial disease (PAD). TASC Working Group. TransAtlantic Inter-Society Consensus (TASC). *J Vasc Surg*. 2000;31(1 Pt 2):S1–296.
- Matsi PJ, Manninen HI, Suhonen MT, Pirinen AE, Soimakallio S. Chronic critical lower-limb ischemia: prospective trial of angioplasty with 1–36 months follow-up. *Radiology*. 1993;188(2):381–7.
- Parsons RE, Suggs WD, Lee JJ, Sanchez LA, Lyon RT, Veith FJ. Percutaneous transluminal angioplasty for the treatment of limb threatening ischemia: do the results justify an attempt before bypass grafting? *J Vasc Surg*. 1998;28(6):1066–71.
- Rogers JH, Laird JR. Overview of new technologies for lower extremity revascularization. *Circulation*. 2007;116(18):2072–85.
- Wollenek G, Laufer G. Comparative study of different laser systems with special regard to angioplasty. *Thorac Cardiovasc Surg*. 1988;36 Suppl 2:126–32.
- Scheinert D, Laird Jr JR, Schroder M, Steinkamp H, Balzer JO, Biamino G. Excimer laser-assisted recanalization of long, chronic superficial femoral artery occlusions. *J Endovasc Ther*. 2001;8(2):156–66.
- Laird Jr JR, Reiser C, Biamino G, Zeller T. Excimer laser assisted angioplasty for the treatment of critical limb ischemia. *J Cardiovasc Surg (Torino)*. 2004;45(3):239–48.
- Laird JR. Peripheral excimer laser angioplasty (PELA) trial results. Presented at late breaking clinical trials. Transcatheter cardiovascular therapeutics (TCT) annual meeting, 24–28 Sept 2002, Washington, DC.
- Siracuse JJ, Giles KA, Pomposelli FB, Hamdan AD, Wyers MC, Chaikof EL, Nedeau AE, Schermerhorn ML. Results for primary bypass versus primary angioplasty/stent for intermittent claudication due to superficial femoral artery occlusive disease. *J Vasc Surg*. 2012;55(4):1001–7.
- Gray BH, Laird JR, Ansel GM, Shuck JW. Complex endovascular treatment for critical limb ischemia in poor surgical candidates: a pilot study. *J Endovasc Ther*. 2002;9(5):599–604.
- Laird JR, Zeller T, Gray BH, Scheinert D, Vranic M, Reiser C, Biamino G, Investigators L. Limb salvage following laser-assisted angioplasty for critical limb ischemia: results of the LACI multicenter trial. *J Endovasc Ther*. 2006;13(1):1–11.
- Bosiers M, Peeters P, Elst FV, Vermassen F, Maleux G, Fourneau I, Massin H. Excimer laser assisted angioplasty for critical limb ischemia: results of the LACI Belgium Study. *Eur J Vasc Endovasc Surg*. 2005;29(6):613–9.

15. Stoner MC, De Freitas DJ, Phade SV, Parker FM, Bogey WM, Powell S. Mid-term results with laser atherectomy in the treatment of infrainguinal occlusive disease. *J Vasc Surg.* 2007;46(2):289–95.
16. Serino F, Cao Y, Renzi C, Mascellari L, Toscanella F, Raskovic D, Tempesta P, Bandiera G, Santini A. Excimer laser ablation in the treatment of total chronic obstructions in critical limb ischaemia in diabetic patients. Sustained efficacy of plaque recanalisation in mid-term results. *Eur J Vasc Endovasc Surg.* 2010;39(2):234–8.
17. Laird Jr JR, Yeo KK, Rocha-Singh K, Das T, Joye J, Dippel E, Reddy B, Botti C, Jaff MR. Excimer laser with adjunctive balloon angioplasty and heparin-coated self-expanding stent grafts for the treatment of femoropopliteal artery in-stent restenosis: twelve-month results from the SALVAGE study. *Catheter Cardiovasc Interv.* 2012;80(5):852–9.
18. Sultan S, Tawfick W, Hynes N. Cool excimer laser-assisted angioplasty (CELA) and tibial balloon angioplasty (TBA) in management of infragenicular arterial occlusion in critical lower limb ischemia (CLI). *Vasc Endovascular Surg.* 2013;47(3):179–91.
19. Armstrong EJ, Singh S, Singh GD, Yeo KK, Ludder S, Westin G, Anderson D, Dawson DL, Pevac WC, Laird JR. Angiographic characteristics of femoropopliteal in-stent restenosis: association with long-term outcomes after endovascular intervention. *Catheter Cardiovasc Interv.* 2013;82(7):1168–74.
20. Schmidt A, Zeller T, Sievert H, Krankenberg H, Torsello G, Stark MA, Scheinert D. Photoablation using the turbo-booster and excimer laser for in-stent restenosis treatment: twelve-month results from the PATENT study. *J Endovasc Ther.* 2014;21:52–60.
21. Tosaka A, Soga Y, Iida O, Ishihara T, Hirano K, Suzuki K, Yokoi H, Nanto S, Nobuyoshi M. Classification and clinical impact of restenosis after femoropopliteal stenting. *J Am Coll Cardiol.* 2012;59(1):16–23.
22. Dippel EJ, Makam P, Kovach R, George JC, Patlola R, Metzger DC, Mena-Hurtado C, Beasley R, Soukas P, Colon-Hernandez PJ, et al. Randomized controlled study of excimer laser atherectomy for treatment of femoropopliteal in-stent restenosis: initial results from the EXCITE ISR trial (EXCimer Laser Randomized Controlled Study for Treatment of Femoropopliteal In-Stent Restenosis). *JACC Cardiovasc Interv.* 2015;8(1 Pt A):92–101.
23. Schillinger M, Sabeti S, Loewe C, Dick P, Amighi J, Mlekusch W, Schlager O, Cejna M, Lammer J, Minar E. Balloon angioplasty versus implantation of nitinol stents in the superficial femoral artery. *N Engl J Med.* 2006;354(18):1879–88.
24. Scheinert D, Scheinert S, Sax J, Piorowski C, Braunlich S, Ulrich M, Biamino G, Schmidt A. Prevalence and clinical impact of stent fractures after femoropopliteal stenting. *J Am Coll Cardiol.* 2005;45(2):312–5.
25. Tepe G, Zeller T, Albrecht T, Heller S, Schwarzwald U, Beregi JP, Claussen CD, Oldenburg A, Scheller B, Speck U. Local delivery of paclitaxel to inhibit restenosis during angioplasty of the leg. *N Engl J Med.* 2008;358(7):689–99.
26. Van Den Berg JC, Pedrotti M, Canevascini R, Chimchila Chevili S, Giovannacci L, Rosso R. Endovascular treatment of in-stent restenosis using excimer laser angioplasty and drug eluting balloons. *J Cardiovasc Surg (Torino).* 2012;53(2):215–22.
27. van den Berg JC. Commentary: laser debulking and drug-eluting balloons for in-stent restenosis: a light at the end of the tunnel? *J Endovasc Ther.* 2013;20(6):815–8.
28. Gandini R, Del Giudice C, Merolla S, Morosetti D, Pampana E, Simonetti G. Treatment of chronic SFA in-stent occlusion with combined laser atherectomy and drug-eluting balloon angioplasty in patients with critical limb ischemia: a single-center, prospective, randomized study. *J Endovasc Ther.* 2013;20(6):805–14.
29. Photoablative atherectomy followed by a paclitaxel-coated balloon to inhibit restenosis in instent femoro-popliteal obstructions (PHOTOPAC). [Clinicaltrials.gov](http://clinicaltrials.gov). Retrieved 30 Dec 2013 from <http://clinicaltrials.gov/show/NCT01298947>.

Treatment of Subacute and Chronic Thrombotic Occlusions of the Lower Extremity Peripheral Arteries: The Role of Excimer Laser

Nicolas W. Shammass

Prevalence of Thrombotic Lesions in Peripheral Arterial Disease

Thrombotic lesions are highly prevalent in patients with peripheral arterial disease (PAD) particularly those with occlusive disease [1–4]. PAD is associated with thrombotic conditions including diabetes, smoking and coexistent cardiovascular disease [5–9]. Furthermore, stenotic lesions, restenotic or de novo, disrupt laminar flow predisposing to thrombus formation. Finally, a higher inflammatory state is present in patients with PAD. Rossi et al. [10] have shown that patients with PAD display a high baseline inflammatory state comparable to patients with unstable angina. Similarly, patients with critical limb ischemia (CLI) have a higher baseline fibrinogen, high sensitivity-C reactive protein (hs-CRP) and von Willebrand factors than claudicants [11]. In addition to baseline heightened inflammation, inflammatory markers rise significantly after peripheral arterial interventions (Fig. 11.1) [12–16]. Thrombosis and inflammation are strongly linked [17] and quite often coexists as seen in patients with PAD.

The presence of thrombus, however, is highly underestimated with angiography alone. Studies have shown the discrepancy between the actual presence of intra-arterial thrombus using intravascular ultrasound and its visualization on angiography. Using intravascular ultrasound (IVUS), thrombus was present in the majority of patients with symptom onset less than 6 months and a totally occluded culprit vessel [2]. In the Dethrombosis of the Lower Extremity Arteries Using the Power-Pulse Spray (P-PS) Technique in Patients with Recent Onset Thrombotic Occlusions

(DETHROMBOSIS) registry [2], the majority of patients (94.1 %) had a definite thrombus identified by IVUS whereas angiography revealed only 11.8 % of patients with a definite grade 3 thrombus and 29.4 % of patients with a grade 1 thrombus (modified TIMI scale) at baseline. Furthermore, patients with critical limb ischemia are likely to have more thrombotic lesions than claudicants likely because of higher prevalence of total occlusions. In the limb salvage following laser-assisted angioplasty for critical limb ischemia (LACI) prospective multicenter registry, total occlusions were present in 92 % of limbs [18].

The presence of intravascular thrombus is likely to increase the rate of distal embolization, reocclusion after revascularization, contrast use, radiation exposure and intra-procedural complications [2, 19–23]. Intravascular thrombus also prolongs procedure time (Fig. 11.2) [24]. Treatment of thrombus with balloon angioplasty alone or stenting carries a higher risk of distal embolization and reocclusion [22, 23, 25, 26].

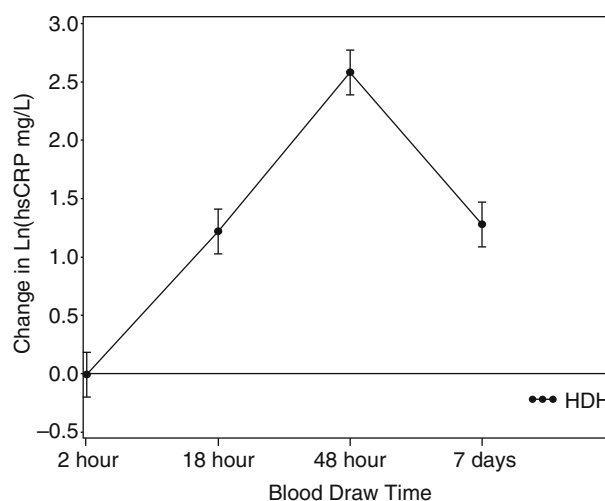
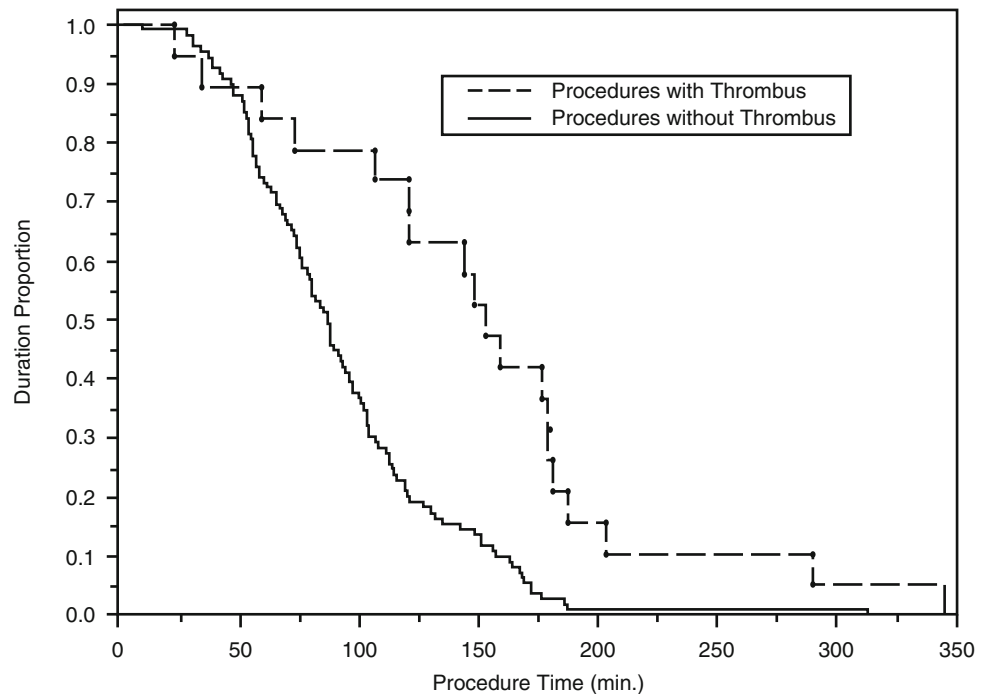


Fig. 11.1 Change in high sensitivity-C Reactive Protein (hs-CRP) with percutaneous peripheral intervention. Hs-CRP peaks at about 48 h post intervention (From Shammass et al. with permission from Journal of Invasive Cardiology, HMP Communications)

N.W. Shammass, MD, EJD, MS, FACC, FSCAI, FICA
 President and Research Director,
 Midwest Cardiovascular Research Foundation,
 Adjunct Clinical Associate Professor of Medicine,
 University of Iowa Interventional Cardiologist,
 Cardiovascular Medicine, PC Davenport, IA, USA
 e-mail: shammass@mchsi.com

Fig. 11.2 Procedure time in patients with and without intraprocedural thrombus during peripheral intervention (From Shammam et al. with permission from Vascular Disease Management. HMP communications)



Non Excimer Laser Therapy of Subacute and Chronic Thrombotic Lesions

Subacute and chronic thrombi are harder to treat with aspiration embolectomy alone without added lytic treatment. The use of 6 F or 7 F aspiration catheters is rarely effective given the larger size of the thrombotic lesions relative to the effective lumen size of the catheters [27]. Also, these thrombotic lesions tend to strongly adhere to the vessel wall making aspiration embolectomy ineffective.

Following delivery of lytic therapy via the power pulse spray (PP-S) technique [2] or porous balloon infusion [4] directly into the thrombotic lesion, only a partial resolution of the organized thrombus was seen when followed with angiojet rheolytic thrombectomy (RT) (Boston Scientific, Maple Grove, MN, USA).

The use of intravenous glycoprotein IIb/IIIa receptor antagonists alone is unlikely to be effective in treating the organized thrombus although it may reduce the incidence of slow flow and distal embolization during peripheral intervention [28, 29]. Furthermore, the use of continuous 8–48 h catheter-directed thrombolysis (CDT) is likely to be partially effective in reducing thrombus burden [30–32] but at a considerable price including prolonged hospital stay, increase risk of bleeding, distal embolization and the need for repetitive visit to the angiography suite during the same hospital stay. Both CDT and surgery continued to have high amputation and mortality rates in the acute-subacute patient population [33, 34]. More data on ultrasound-assisted lysis [35] in treating these lesions is still lacking.

Organized thrombus coexists with relatively new, fresh thrombus, the latter generally responds to lytic treatment and/or aspiration methods. However, the more organized thrombus is unlikely to respond to the above described methods because of its cellular nature. As thrombus ages (beyond 5 days), there is an in-growth of smooth muscle cells with or without connective tissue and the development of intra-thrombus capillary vessels [36].

Mechanical approaches as a stand-alone therapy without lytic treatment have been attempted to shorten procedure time and reduce bleeding complications [37]. Data in subacute and chronic thrombotic lesions is however still lacking.

Excimer Laser in Treating Subacute and Chronic Thrombotic Occlusions in Peripheral Arterial Interventions

Thrombus displays a strong optical absorption in the ultraviolet, visible and mid-infrared wavelengths making it a clear target for laser treatment with distinct advantages (Table 11.1). Laser dissolves thrombus by emitting energy that initiates photomechanical, photochemical and photo-thermal transformation within the plaque-thrombus [38]. The xenon-hydrogen chloride excimer laser (ultraviolet spectrum) (Spectranetics, Colorado Springs, CO) is now widely used in the treatment of atherosclerotic-thrombotic disease. Emitting light at a wavelength of 308 nm and in discrete pulses, excimer laser creates a high pressure within the

Table 11.1 The use of laser in treating subacute and chronic thrombotic lesions

<i>Indications</i>
Primary post wire crossing ablation of thrombotic lesions
Facilitate wire crossing of chronic total occlusions
Pre-lysis laser assisted treatment
Post-lysis residual lesion treatment
Treatment of distal embolic thrombotic lesions
Treatment of in-stent thrombotic occlusions
<i>Advantages</i>
Reduce thrombus burden
Reduce distal embolization burden
Suppresses platelet aggregation
Enhances chemical lysis
Ease of use with lesser need for multiple catheter exchanges
Reduces the need or time for lysis
Shorter procedure time than lysis
Reduces the need to return to the cath lab for repetitive angiography
Reduced risk of bleeding when compared to lysis

targeted plaque and gas bubble formation that subsequently lead to non thermal ablation of the plaque and thrombus [38]. In addition to its photoablative therapy, excimer laser also suppresses platelet aggregation which reduces the chance of thrombus formation and enhances chemical lysis. Topaz et al. [39] investigated the effect of excimer laser on platelets. Blood samples were exposed to increased levels (0, 30, 45, 60 mJ/mm²; 25 Hz) of excimer laser fluence and then tested for ADP and collagen induced platelet aggregation, platelet concentration, and platelet contractile force development. Dose dependent suppression of platelet and collagen-induced aggregation was seen with the laser. Platelet contractile force declined with higher laser energy indicating a progressive platelet stunning. The most pronounced response on the platelet was obtained at higher energy levels of 60 mJ/mm². Whether this fluence level represents an optimal threshold to treat subacute and chronic thrombotic lesions because of its most pronounced antiplatelet effect remains unclear.

Excimer laser has been shown to ablate thrombus in patients with acute coronary syndrome including acute myocardial infarction and improves flow in the infarct-related artery [40, 41]. In a single-center retrospective analysis by Shishikura et al. [42] in consecutive acute coronary patients treated with excimer laser (n=50) and age- and sex-matched to patients treated with manual aspiration (n=48) crossing the lesions was higher in the laser group (96.2 % vs. 82.6 %, P=0.04). Also the laser group had higher thrombolysis in myocardial infarction (TIMI) 3 flow (86.0 % vs. 68.8 %, P=0.04) and myocardial blush grade 3 (76.0 % vs. 54.2 %, P=0.02) than the aspiration group. Major adverse events were reported more in the aspiration group. Topaz and colleagues [43] also evaluated the role of excimer laser in patients presenting for urgent revascularization with established Q-wave myocardial infarction (QI) versus those with

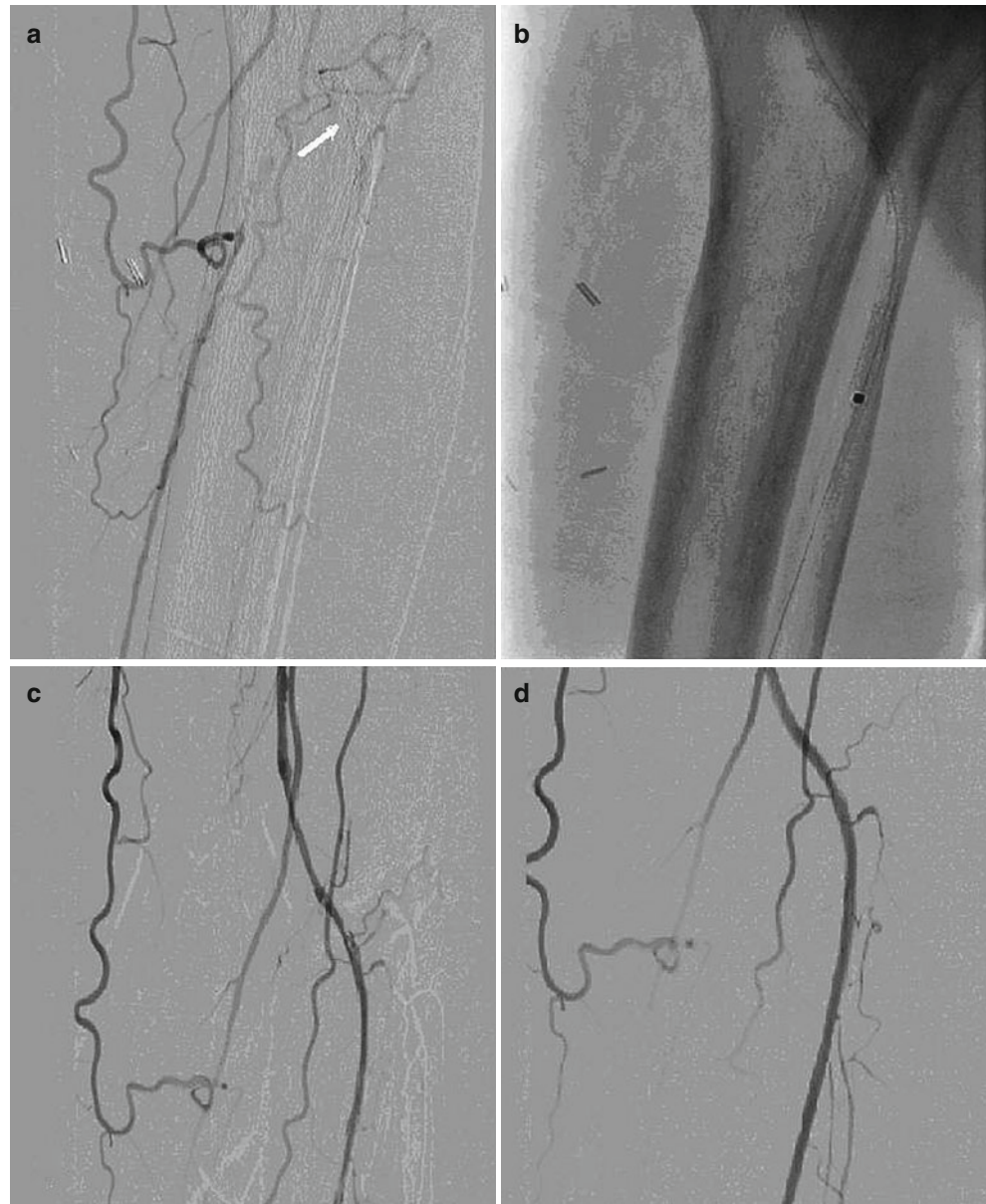
non-STEMI in 151 patients with continuous chest pain and ischemia presenting within 24 h of symptom onset. Quantitative coronary arteriography was performed by an independent core laboratory. Among the QI patients, the larger the thrombus burden, the higher acute gain was recorded with the laser. Baseline TIMI flow grade (0.9 for QI vs 1.5 for NSTEMI) increased with laser and reached a final level of TIMI 3 in both groups. A high procedural success rate was seen in both groups with low complication rates. This study illustrates that lasing thrombus is effective resulting in larger acute minimal luminal gain with heavy thrombus burden typically seen in PAD patients.

Excimer laser has also been applied in treating deep venous chronic thrombotic occlusions of the lower extremities and acute and subacute thrombotic occlusions of hemodialysis shunts with good results [44]. Dahm et al. [58] reported their findings on 21 patients with a thrombotic occlusion of their hemodialysis shunt with a mean occlusion time of 4.1 days. All patients were treated initially with excimer laser with 85.7 % of them receiving adjunctive thrombolysis for residual thrombus. Excimer laser reduced the occlusion from 100 to 63 %. Following lytic treatment, residual stenosis averaged 36 %. TIMI flow increased significantly from grade 0–2.7 after laser ablation and to 3.0 after adjunctive treatment. Procedural success was 95.2 %. Primary patency was 85 %. At 6-week follow up, all successfully treated shunts were used for dialysis.

Excimer laser is more likely to be used in more complex and longer lesions than other forms of atherectomy [45]. When operators' preferences were analyzed in treating restenotic femoropopliteal lesions with SilverHawk atherectomy versus excimer laser, the latter was applied more frequently in longer lesions, TASC D lesions, total occlusions and thrombotic lesions and with less distal embolization (Fig. 11.3). This is likely because the use of excimer laser is user-friendly and effective in treating total occlusions and does not require the frequent removal and reinsertion of the device.

Shammas et al. [46] reported their experience with excimer laser in treating patients with subacute (n=12; >24 h, <30 days), and chronic (n=8; between 1 and 6 months) symptoms and totally occluded vessels. The author lasing technique is described in Table 11.2. In this single center prospective registry, 20 consecutive patients were enrolled (8 males, mean age 69.5 ± 11.1 years). 15/20 (75 %) had restenotic occlusions. Intravascular ultrasound (IVUS) (Volcano, Rancho Cordova, CA) was performed at baseline after crossing the lesion and after laser treatment prior to adjunctive therapy. The laser Elite (2.3 mm (n=4); 2.5 mm (n=6)) and Tandem laser (2.5 mm (n=10)) (Spectranetics, Colorado Springs, CO) were utilized. Lasing was performed at 0.5 mm per second with continuous saline flush. A total of 4.9 ± 2.3 runs were performed per lesion using a fluence of

Fig. 11.3 Total occlusion of distal popliteal and anterior tibialis (*white arrow*) (**a**) treated with excimer laser (**b**) with results after no adjunctive therapy (**c**) and post adjunctive therapy (**d**)



60 mJ/mm² and a repetition rate of 45 Hz. Spider Embolic Filter protection device (Covidien, Minneapolis, MN) was used at the discretion of the operator. Bail out stenting was performed for residual stenosis of more than 30 % after adjunctive balloon angioplasty. Procedural success was defined as the ability of the laser after adjunctive final treatment to reduce stenosis to <30 % in the treated vessel as qualitatively assessed by the operator and with no visible angiographic thrombus at the end of treatment.

In this study, a typical high risk PAD population was seen. Patients had high prevalence of hyperlipidemia (70 %), smoking (85 %), diabetes (40 %) and prior peripheral interventions (85 %). Over half these patients had critical limb ischemia (Rutherford class IV and V). 95 % of segments treated were femoropopliteal. Embolic filter protection was

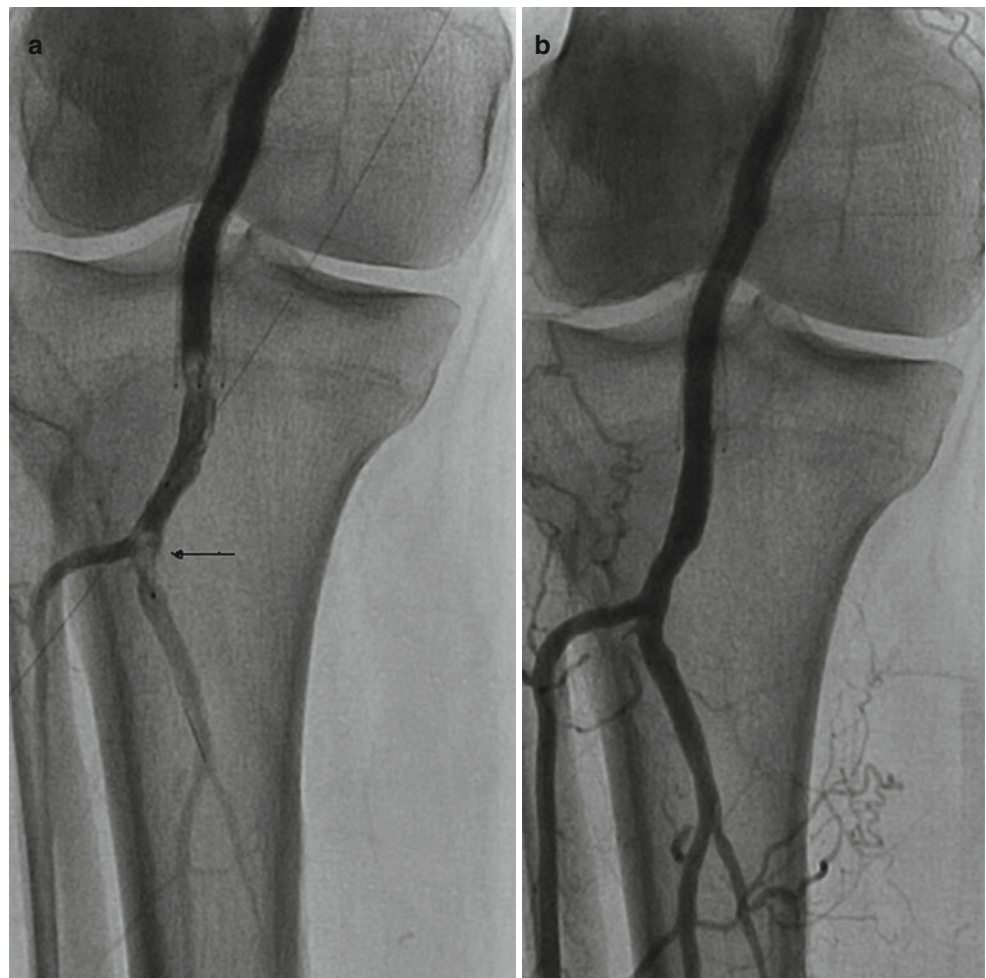
used in 75 % of patients. Procedural success was 100 % with no deaths or amputations. There were no in-hospital or 30-day reocclusions. A significant reduction in residual angiographic stenosis post laser alone (100 % vs. 66.75 ± 23.9 %, p=0.001) was seen. Macrodebris were collected in 85.7 % of all filters but only one patient had a minor distal embolization beyond the filter that did not require further intervention.

In the prospective, single-center, open-label Distal Embolic Event Protection Using Excimer Laser Ablation in Peripheral Vascular Interventions (DEEP EMBOLI) registry [23], excimer laser was applied in 20 patients under embolic filter protection. 28.6 % of patients had total occlusions. Visible thrombus was seen in 14.3 % of patients. Adjunctive angioplasty and stenting were performed in 96.4 % and

Table 11.2 The author lasing technique using Excimer laser

Patient pretreated with clopidogrel (600 mg po load) and aspirin (325 mg po load)
6 F sheath is inserted in the contralateral common femoral artery under fluoroscopic guidance
After placement of 0.034 inch Wholey wire (Covidien) in the contralateral leg, the sheath is exchanged with a 7 F Pinnacle Destination sheath (Terumo)
Parenteral anticoagulant administered (bivalirudin (the Medicines Co.) or less frequently unfractionated heparin)
Lesion is then crossed (with a 0.034 inch wire [angled glide or the Wholey wire] over a supporting catheter or an angioplasty balloon)
In total and/or long occlusions, 0.034 inch wire is then exchanged with a 0.014 inch wire and an embolic filter is deployed prior to lasing (we commonly use the Spider filter)
An appropriately sized Laser Elite catheter is then selected and advanced over the Spider filter wire or if the filter is not used, the catheter is advanced over a stiff, 0.014 inch non hydrophilic wire
Saline flush to remove contrast and blood is initiated through the laser catheter
The CVX-300 Excimer laser system is used and after calibration it is generally set at 60 mJ/mm ² at 45 Hz
Laser catheter is then advanced very slowly at 0.5 mm/s
Typically lasing is repeated twice
Angiography is performed and if significant residual is seen, we proceed with the use of the Turbo Tandem catheter and/or adjunctive balloon angioplasty with 90 s inflation twice at lower pressure (enough to yield full balloon inflation)
Stenting is avoided unless required for bail out
Filter is then removed and angiography is repeated including digital subtraction to the tibial vessels

Fig. 11.4 Embolic filter filled with thrombus (*black arrow*) (a) after treating with excimer laser of total proximal occlusion. Flow normalized after retrieval of the filter (b)



60.7 % of lesions respectively. Procedural success was met in 100 % of patients. Although large macrodebris was found in 22.2 % of filter after excimer laser (Fig. 11.4), only 1/20

(5 %) distal embolization occurred after filter removal and prior to completion of definitive treatment. No other adverse events were noted.

In the multicenter prospective laser-assisted angioplasty for critical limb ischemia (LACI) trial [18], 145 patients with 155 critically ischemic limbs were included. Diabetes was present in 66 % of patients. Occlusions were present in 92 % of limbs and median lesion length was 11 cm. Procedural success was 86 %. On follow-up, limb salvage was achieved in 92 % of surviving patients. Procedural complications occurred in 12 % of the limbs; major dissection in 4 %, acute thrombus formation in 3 %, distal embolization in 3 %, and perforation in 2 %. The authors noted that excimer laser effectively removed plaque-thrombus in these total occlusions reducing the rate of complications when compared to historic control with balloon angioplasty of complex lesions. Balloon angioplasty alone appears to have lower salvage rate, higher rate of distal embolization, perforation and acute vessel closure.

Scheinert et al. [47] reported data on 318 consecutive patients who underwent excimer laser of 411 superficial femoral arteries with total chronic occlusions. Lesion length was 19.4 ± 6.0 cm. Overall technical success was 90.5 %. There was no death, amputation or emergent surgical intervention. The primary patency at 1 year was 33.6 % with 1-year assisted primary and secondary patency rates of 65.1 % and 75.9 %, respectively. Complications included acute reocclusion (1.0 %), perforation

(2.2 %), and distal thrombosis/embolization (3.9 %). Embolization consisted of plaque-thrombotic debris and the majority of patients (11/16) were successfully treated with mechanical recanalization and local thrombolysis with recombinant tissue plasminogen activator (10-mg bolus followed by 1 mg/h infusion for 24 h) with resolution of thrombotic debris.

With the advent of the Turbo-Booster and recently the Turbo-Tandem catheters, more effective laser photoablation can be accomplished. Directional lasing allows more plaque-thrombus removal and larger lumen above what can be obtained with the Turbo-Elite catheter. In the Excimer laser recanalization of femoropopliteal lesions and 1-year patency (CELLO) trial [48], the Turbo-Booster was utilized in treating femoropopliteal lesions leading to 100 % increase in minimal luminal area above initial treatment with the Turbo-Elite catheter ($4.9\text{--}10.4$ mm²). In this study, total occlusions were 20 % of treated lesions and thrombus was visualized in 4.6 % of patients. Laser ablation reduced diameter stenosis from 77 % at baseline to 34.7 %. Patency rates were 59 % and 54 % at 6 and 12 months, respectively. There were no major adverse events.

Based on the above observational data, excimer laser appears to be an effective method in treating subacute and chronic total occlusions which typically have multilayered thrombus at various stages of organization. Figure 11.5

Protocol Algorithm for the Treatment of Subacute (> 24 hours, < 1 mo) and Chronic (> 1 mo, < 6 mo) Thrombotic Vessel Occlusions using Excimer Laser

UFH = unfractionated heparin; IVUS = intravascular ultrasound, CDT = catheter directed thrombolysis, tPA = tissue plasminogen activator

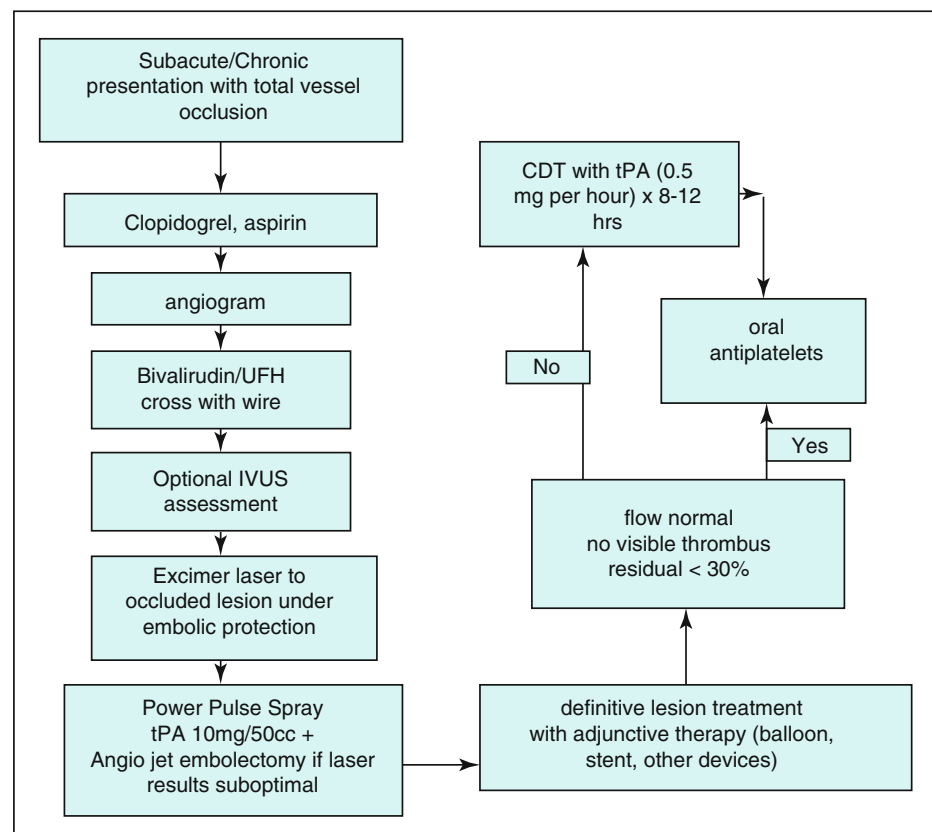


Fig. 11.5 Proposed algorithm to treat subacute (>24 h, <1 month) and chronic (>1 month, <6 months) thrombotic occlusions using excimer laser as a first line therapy with bailout use of power-pulse spray and catheter directed lysis with tPA as needed. UFH unfractionated heparin, IVUS intravascular ultrasound, CDT catheter directed thrombolysis, tPA tissue plasminogen activator

illustrates an algorithm that incorporates excimer laser in treating these lesions. Depending on the thrombus age, adjunctive lytic treatment may be needed. This laser-facilitated lytic approach appears to be effective in subacute and chronic lesions if laser alone is insufficient to achieve optimal results.

Distal Embolization in Treating Thrombotic Lesions

Irrespective of the device used in the periphery, the presence of thrombotic lesions is a high predictor of distal embolization. The use of embolic protection in peripheral interventions has gained significant momentum [49, 50] and appears effective in capturing debris, large enough to interrupt tibial flow which may lead to significant complications [51–53, 55].

Although distal embolization is encountered less frequently with excimer laser, this remains however a significant problem in treating thrombotic lesions (Fig. 11.4). In the DEEP EMBOLI [23] prospective registry, excimer laser was associated with significant distal embolization. In this study, moderately calcified, ulcerated, long, or totally occluded lesions were included. Two filters were used per patient; one prior to excimer laser and the other prior to final adjunctive balloon angioplasty and/or stenting. Macrodebris was found in 66.7 % of patients treated with the laser under filter protection; however, only 22.2 % of filters contained clinically significant debris (>2 mm in longest axial length). Interestingly, adjunctive therapy with balloon angioplasty or stenting was also associated with macrodebris in 35.0 % of filters, of which 20.0 % were clinically significant debris. In another study of subacute and chronic thrombotic occlusions [46], embolic filters were used in 15/20 (75 %) of patients treated with excimer laser. Macrodebris >2 mm were seen in 85.7 % of these filters supporting prior findings that excimer laser in thrombotic lesions may embolize distally. Finally, using continuous doppler monitoring, Lam et al. [52] reported the presence of distal embolization after angioplasty, stenting, SilverHawk atherectomy, and excimer laser therapy in the superficial femoral artery. The average number of embolic signals was 12 for angioplasty, 28 for stenting, 49 for SilverHawk, and 51 for laser, although sizes of these debris are unknown.

The mechanism of distal embolization with the laser remains undefined. One hypothesis is that mechanical manipulation of thrombotic lesions with any catheter including the laser could dislodge the thrombus from the vessel wall. Also, limited data suggest the formation of irregular channels with large amount of tissue remnants following excimer laser treatment that may become a risk factor for embolization of debris [54]. Even after laser ablation of these lesions, adjunctive treatment with balloon angioplasty and stenting continues to contribute to distal embolization [23]. When treating thrombotic lesions we have adopted the use of embolic filter protection to avoid significant distal embolization and its consequences.

Bail Out Stenting with Excimer Laser

Excimer laser also appears to be associated with higher rate of stenting than is historically seen with other atherectomy devices (range 10–60 %) [18, 23, 46–48]. This may be related to a higher dissection rate possibly secondary to plaque bursting under buildup of very high intra-plaque pressure and gas bubbles. Another hypothesis is that the rate of dissection can be proportional to the speed of lasing not allowing the gas bubble to always lead the tip of the lasing catheter. Inadequate flushing of the catheter from the contrast dye may also contribute to dissections and aggressive flushing of contrast is recommended during lasing.

In treating subacute and chronic thrombotic lesions, bail out stenting was performed in up to 50 % of patients for sub-optimal results (>30 % residual) [46]. Also, in the LACI trial [18], stents were implanted in 45 % of limbs (61 % in the superficial femoral, 38 % popliteal, 16 % tibial). In addition, in the CELLO study [48] laser ablation followed by adjunctive stenting was performed in 23.3 % of patients. Furthermore, Scheinert et al. [47] reported a 7.3 % of limbs treated for chronic superficial femoral artery occlusions with excimer laser to require stenting. Finally in the DEEP EMBOLI registry [23], adjunctive angioplasty and stenting were performed in 96.4 % and 60.7 % of lesions respectively.

This stenting rate with the laser was similar to historic controls with balloon angioplasty (provisional stenting ranged from 10 to 50 %). Bail out stenting, however was not a prespecified endpoint in these studies and was left to operator's discretion. The true bail out stenting rate with the laser in subacute and chronic thrombotic lesions is unknown and requires further studies.

Laser-Facilitated Lysis in Treating Subacute and Chronic Thrombus in the Periphery

Pretreatment of thrombotic occlusions with the laser may facilitate lytic treatment and was described in treating acute thrombotic coronary syndromes [56, 57]. This concept was also tested in acutely and subacutely occluded hemodialysis shunts [58]. In 21 patients with mean occlusion time of 4 days and lesion length ranged from 5 to 27 cm, thrombus was present in all lesions. 85.7 % of patients were pretreated with excimer laser followed by local lysis for residual thrombus. The majority of patients then underwent angioplasty of underlying anastomatic lesions. Excimer laser reduced the occlusion from 100 % to a mean of 63 %. Following lysis with 20 mg tissue plasminogen activator therapy this was further reduced to 36 %. Procedural success was 95.2 % and primary and secondary patency were 85 % and 100 % respectively at 6 weeks. All successfully treated shunts were usable at 6 weeks follow-up.

Laser-assisted lysis of organized thrombus was also applied in patients with deep vein thrombosis and post-thrombotic syndrome. Moritz et al. [59] presented data on nine symptomatic patients (three upper and eight lower limbs; total 16 segments) with total deep vein occlusions ranging in age from 2 months to 15 years. Laser was used as follows: two occluded segments were crossed by guidewires but laser treatment was needed to pass a balloon through chronic thrombus. Four segments could not be crossed with wires and laser successfully created a channel allowing wire passage. In four segments laser was utilized as a primary means of clot lysis. Two vessels could not be recanalized. The authors concluded that laser was effective in recanalization of these thrombotic occlusions facilitating wire and balloon passage and allowing a successful treatment of these deep vein thrombotic lesions.

Use of Base Anticoagulants and Antiplatelets with Excimer Laser Treatment in Thrombotic Lesions

There is no data on the ideal anticoagulant during excimer laser treatment in thrombotic lesions. Unfractionated heparin has been the most commonly used anticoagulant during peripheral vascular interventions and this remains the same during treatment with excimer laser. Bivalirudin, a direct thrombin inhibitor, has more predictable anticoagulation profile and carries significantly less bleeding risk when used in acute coronary syndrome patients compared to unfractionated heparin [60, 61]. It has a short half-life in patients with normal renal function and inhibits free and bound thrombin and thrombin-induced platelet activation and aggregation [62]. These properties may have a distinct advantage in treating atherosclerotic/thrombotic lesions. Major bleeding with unfractionated heparin in peripheral interventions has been reported in the range of 2.1–4.6 % [63]. Heparin is an indirect thrombin inhibitor that binds to serum proteases, endothelial cells and macrophages with unpredictable anticoagulation profile. It is also partly neutralized by platelet factor 4 and only inhibits soluble thrombin. Heparin also activates platelets [64, 65].

Observational studies suggest a safe and reliable profile with the use of bivalirudin during peripheral interventions [66–69]. In the Angiomax Peripheral Procedure Registry of Vascular Events Trial (APPROVE) bivalirudin showed predictable anticoagulation during peripheral interventions. A low rate of ischemic events (1.4 %) and major hemorrhage (0.4 %) were reported [66]. APPROVE however, included low-risk patients including iliac and renal interventions. In a real world-registry of 369 unselected consecutive bivalirudin-treated patients, limb ischemia was present in 28 % and angiographic thrombus in 8.2 % of patients. Glycoprotein (GP)

IIB/IIIa inhibitors were co-administered in 4.6 % of patients. Bivalirudin was safe with 0.5 % major bleeding risk. Other adverse events included stroke 0.3 %, acute renal failure 0.3 %, distal embolization 3 %, vascular access complications 0.5 %, and minor amputation 0.5 % [67]. This data compares favorably to historic controls with unfractionated heparin [24]. Finally, In 20 patients with subacute and chronic thrombus, Shammam et al. [46] have used bivalirudin with excimer laser during peripheral intervention. There was no reported major bleeding despite procedural complexity and the occasional use of adjunctive GpIIB/IIIa inhibitors.

Mechanical manipulation or disruption of thrombotic lesions often exposes more thrombin and theoretically potentiates additional thrombus accumulation. Bivalirudin along with aspirin, ADP-receptor antagonists (clopidogrel) and occasionally glycoprotein IIB/IIIa inhibitors as clinically deemed necessary appear to be a logical pharmacologic base in patients undergoing laser treatment for thrombotic occlusions. Randomized trials are needed to determine effectiveness and safety outcomes of UFH versus bivalirudin in peripheral vascular interventions in general and with the use of excimer laser in specific particularly in high risk thrombotic lesions.

Conclusion

Data indicate that subacute and chronic thrombotic lesions are difficult to treat using a single modality. Laser atherectomy is effective in treating these lesions as a stand-alone therapy, or to facilitate wire crossing or as an adjunct to CDT. In the experience of the author, embolic protection in treating these lesions is preferred because of the high rate of distal embolization of clinically significant debris. It is hypothesized that targeting thrombus with excimer laser and reducing its burden prior to a more definitive treatment may result in more successful acute and long-term outcomes, a hypothesis that remains to be proven in randomized trials.

References

1. Harris LM, Dosluoglu HH. Endovascular management of subacute lower extremity ischemia. *Semin Vasc Surg.* 2008;21:167–79.
2. Shammam NW, Dippel EJ, Shammam G, et al. Dethrombosis of the lower extremity arteries using the power-pulse spray technique in patients with recent onset thrombotic occlusions: results of the DETHROMBOSIS Registry. *J Endovasc Ther.* 2008;15:570–9.
3. Kasirajan K, Gray B, Beavers FP, et al. Rheolytic thrombectomy in the management of acute and subacute limb-threatening ischemia. *J Vasc Interv Radiol.* 2001;12:413–21.
4. Shammam NW, Weissman NJ, Coiner D, et al. Dethrombosis of lower extremity thrombus by local delivery of thrombolysis using ClearWay transcatheter balloon irrigation: a feasibility study. *Cardiovasc Revasc Med.* 2011;12:350–4.
5. Shammam NW, Dippel EJ. Evidence-based management of peripheral vascular disease. *Curr Atheroscler Rep.* 2005;7:358–63.

6. Athyros VG, Mikhailidis DP, Papageorgiou AA, Didangelos TP, Ganotakis ES, Symeonidis AN, Daskalopoulou SS, Kakafika AI, Elisaf M, METS-GREECE Collaborative Group. Prevalence of atherosclerotic vascular disease among subjects with the metabolic syndrome with or without diabetes mellitus: the METS-GREECE Multicentre Study. *Curr Med Res Opin.* 2004;20:1691–701.
7. Hamalainen H, Ronnema T, Halonen JP, Toikka T. Factors predicting lower extremity amputations in patients with type 1 or type 2 diabetes mellitus: a population-based 7-year follow-up study. *J Intern Med.* 1999;246:97–103.
8. Bhatt D. REACH (Reduction of Atherothrombosis for Continued Health) registry. American College of Cardiology Annual Scientific Session, 8 Mar 2005.
9. Ness J, Aronow WS. Prevalence of coexistence of coronary artery disease, ischemic stroke, and peripheral arterial disease in older persons, mean age 80 years, in an academic hospital-based geriatrics practice. *J Am Geriatr Soc.* 1999;47:1255–6.
10. Rossi E, Biasucci LM, Citterio F, Pelliccioni S, Monaco C, Ginnetti F, Angiolillo DJ, Grieco G, Liuzzo G, Maseri A. Risk of myocardial infarction and angina in patients with severe peripheral vascular disease: predictive role of C-reactive protein. *Circulation.* 2002;105:800–3.
11. Cassar K, Bachoo P, Ford I, Greaves M, Brittenden J. Markers of coagulation activation, endothelial stimulation and inflammation in patients with peripheral arterial disease. *Eur J Vasc Endovasc Surg.* 2005;29:171–6.
12. Schillinger M, Exner M, Mlekusch W, Haumer M, Ahmadi R, Rumpold H, Wagner O, Minar E. Inflammatory response to stent implantation: differences in femoropopliteal, iliac and carotid arteries. *Radiology.* 2002;224:529–35.
13. Shammass NW, Dippel EJ, Lemke JH, et al. Eptifibatid does not reduce inflammatory markers in patients undergoing peripheral vascular interventions: results of the INFLAME trial. *J Invasive Cardiol.* 2006;18:6–12.
14. Schillinger M, Exner M, Mlekusch W, Haumer M, Rumpold H, Ahmadi R, Sabeti S, Wagner O, Minar E. Endovascular revascularization below the knee: 6-month results and predictive value of C-reactive protein level. *Radiology.* 2003;227:419–25.
15. Mlekusch W, Exner M, Schillinger M, Sabeti S, Mannhalter C, Minar E, Wagner O. E-Selectin and restenosis after femoropopliteal angioplasty: prognostic impact of the Ser128Arg genotype and plasma levels. *Thromb Haemost.* 2004;91:171–9.
16. Schillinger M, Minar E. Restenosis after percutaneous angioplasty: the role of vascular inflammation. *Vasc Health Risk Manag.* 2005;1:73–8.
17. Freedman JE, Loscalzo J. Platelet-monocyte aggregates. Bridging thrombosis and inflammation. *Circulation.* 2002;105:2130–2.
18. Laird JR, Zeller T, Gray BH, Scheinert D, Vranic M, Reiser C, Biamino G, LACI Investigators. Limb salvage following laser-assisted angioplasty for critical limb ischemia: results of the LACI multicenter trial. *J Endovasc Ther.* 2006;13:1–11.
19. Allie DE, Hebert CJ, Lirtzman MD, et al. Novel simultaneous combination chemical thrombolysis/rheolytic thrombectomy therapy for acute critical limb ischemia: the power-pulse spray technique. *Catheter Cardiovasc Interv.* 2004;63:512–22.
20. Kasirajan K, Haskal ZJ, Ouriel K. The use of mechanical thrombectomy devices in the management of acute peripheral arterial occlusive disease. *J Vasc Interv Radiol.* 2001;12:405–11.
21. Wholey MH, Maynar MA, Wholey MH, et al. Comparison of thrombolytic therapy of lower-extremity acute, subacute, and chronic arterial occlusions. *Cathet Cardiovasc Diagn.* 1998;44:159–69.
22. Shammass NW, Shammass GA, Dippel EJ, et al. Predictors of distal embolization in peripheral percutaneous interventions: a report from a large peripheral vascular registry. *J Invasive Cardiol.* 2009;21:628–31.
23. Shammass NW, Coiner D, Shammass GA, et al. Embolic event protection using excimer laser ablation in peripheral vascular interventions: results of the DEEP EMBOLI registry. *J Endovasc Ther.* 2009;16:197–202.
24. Shammass NW, Lemke JH, Dippel EJ, et al. In-hospital complications of peripheral vascular interventions using unfractionated heparin as the primary anticoagulant. *J Invasive Cardiol.* 2003;15:242–6.
25. Siablis D, Karnabatidis D, Katsanos K, et al. Outflow protection filters during percutaneous recanalization of lower extremities' arterial occlusions: a pilot study. *Eur J Radiol.* 2005;55:243–9.
26. Shammass NW, Dippel EJ, Coiner D, et al. Preventing lower extremity distal embolization using embolic filter protection: results of the PROTECT registry. *J Endovasc Ther.* 2008;15:270–6.
27. Topaz O. Revascularization of thrombus-laden lesions in AMI – the burden on the interventionalist. *J Invasive Cardiol.* 2007;19:324–5.
28. Shammass NW, Dippel EJ, Shammass GA, Kumar A, Jerin M, Kennedy L. Utilization of GP IIb/IIIa inhibitors in peripheral percutaneous interventions: current applications and in-hospital outcomes at a tertiary referral center. *J Invasive Cardiol.* 2008;20:266–9.
29. Allie DE, Hebert CJ, Lirtzman MD, et al. A safety and feasibility report of combined direct thrombin and GP IIb/IIIa inhibition with bivalirudin and tirofiban in peripheral vascular disease intervention: treating critical limb ischemia like acute coronary syndrome. *J Invasive Cardiol.* 2005;17:427–32.
30. Mahler F, Schneider E, Hess H, Steering Committee, Study on Local Thrombolysis. Recombinant tissue plasminogen activator versus urokinase for local thrombolysis of femoropopliteal occlusions: a prospective, randomized multicenter trial. *J Endovasc Ther.* 2001;8:638–47.
31. Robertson I, Kessel DO, Berridge DC. Fibrinolytic agents for peripheral arterial occlusion. *Cochrane Database Syst Rev.* 2010;(3):CD001099. doi:10.1002/14651858.CD001099.pub2.
32. Weaver FA, Comerota AJ, Youngblood M, Froehlich J, Hosking JD, Papanicolaou G. Surgical revascularization versus thrombolysis for nonembolic lower extremity native artery occlusions: results of a prospective randomized trial. The STILE Investigators. Surgery versus Thrombolysis for Ischemia of the Lower Extremity. *J Vasc Surg.* 1996;24:513–21.
33. Ouriel K, Shortell CK, DeWeese JA, et al. A comparison of thrombolytic therapy with operative revascularization in the initial treatment of acute peripheral arterial ischemia. *J Vasc Surg.* 1994;19:1021–30.
34. Ouriel K, Veith FJ, Sasahara AA. Thrombolysis or peripheral arterial surgery: phase I results. TOPAS Investigators. *J Vasc Surg.* 1996;23:64–73.
35. Schrijver AM, Reijnen MM, van Oostayen JA, Hoksbergen AW, Lely RJ, van Leersum M, de Vries JP. Initial results of catheter-directed ultrasound-accelerated thrombolysis for thromboembolic obstructions of the aortofemoral arteries: a feasibility study. *Cardiovasc Intervent Radiol.* 2012;35:279–85.
36. Kramer MC, van der Wal AC, Koch KT, Rittersma SZ, Li X, et al. Histopathological features of aspirated thrombi after primary percutaneous coronary intervention in patients with ST-elevation myocardial infarction. *PLoS One.* 2009;4(6), e5817. doi:10.1371/journal.pone.0005817.
37. Wissgott C, Kamusella P, Richter A, Klein-Wiegel P, Steinkamp HJ. Mechanical rotational thrombectomy for treatment thrombolysis in acute and subacute occlusion of femoropopliteal arteries: retrospective analysis of the results from 1999 to 2005. *Rofo.* 2008;180:325–31. doi:10.1055/s-2008-1027144.
38. Topaz O. Plaque removal and thrombus dissolution with the photoacoustic energy of pulsed-wave lasers-biotissue interactions and their clinical manifestations. *Cardiology.* 1996;87:384–91.
39. Topaz O, Minisi AJ, Bernardo NL, et al. Alterations of platelet aggregation kinetics with ultraviolet laser emission: the “stunned platelet” phenomenon. *Thromb Haemost.* 2001;86:1087–93.

40. Topaz O, Bernardo NL, Shah R, et al. Effectiveness of excimer laser coronary angioplasty in acute myocardial infarction or in unstable angina pectoris. *Am J Cardiol.* 2001;87:849–55.
41. Topaz O, Shah R, Mohanty PK, et al. Application of excimer laser angioplasty in acute myocardial infarction. *Laser Surg Med.* 2001;29:185–92.
42. Shishikura D, Otsuji S, Takiuchi S, Fukumoto A, Asano K, Ikushima M, Yasuda T, Hasegawa K, Kashiyama T, Yabuki M, Hanafusa T, Higashino Y. Vaporizing thrombus with excimer laser before coronary stenting improves myocardial reperfusion in acute coronary syndrome. *Circ J.* 2013;77:1445–52. Epub 2013 Mar 26.
43. CARMEL Excimer Laser Interventional Study Group, Topaz O, Ebersole D, Dahm JB, Alderman EL, Madyoon H, Vora K, Baker JD, Hilton D, Das T. Excimer laser in myocardial infarction: a comparison between STEMI patients with established Q-wave versus patients with non-STEMI (non-Q). *Lasers Med Sci.* 2008;23:1–10. Epub 2007 Apr 11.
44. Moritz M, Agis H, Kabnick LS, et al. Treatment of chronic major deep vein thrombosis with excimer laser rechanneling. Abstract presented at: 2007 American Venous Forum Symposium; 14–17 Feb 2007; San Diego.
45. Shammam NW, Shammam GA, Jerin M. Differences in patients' selection and outcomes of Silverhawk atherectomy versus laser atherectomy in treating in-stent restenosis of the femoropopliteal arteries: a retrospective analysis from a single center. Abstract #5. Page 9, Proceedings of the 14th annual new cardiovascular horizons abstract book New Orleans, LA, 5–7 June 2013. https://www.ncvh.org/ncvh-annual-conference_108_1970938390.pdf.
46. Shammam NW, Weissman NJ, Coiner D, Shammam GA, Dippel E, Jerin M. Treatment of subacute and chronic thrombotic occlusions of lower extremity peripheral arteries with the excimer laser: a feasibility study. *Cardiovasc Revasc Med.* 2012;13:211–4.
47. Scheinert D, Laird Jr JR, Schröder M, Steinkamp H, Balzer JO, Biamino G. Excimer laser-assisted recanalization of long, chronic superficial femoral artery occlusions. *J Endovasc Ther.* 2001;8:156–66.
48. Dave RM, Patlola R, Kollmeyer K, Bunch F, Weinstock BS, Dippel E, Jaff MR, Popma J, Weissman N, CELLO Investigators. Excimer laser recanalization of femoropopliteal lesions and 1-year patency: results of the CELLO registry. *J Endovasc Ther.* 2009;16:665–75.
49. Covidien's SpiderFX Embolic protection device approved for use in lower extremities. *Endovasc Today.* <http://bmctoday.net/evtoday/2011/11/article.asp?f=covidiens-spiderfx-embolic-protection-device-approved-for-use-in-lower-extremities>.
50. Shammam NW. Balloon angioplasty with built-in embolic protection mechanism: the dual role of the proteus balloon. *J Endovasc Ther.* 2012;19:617–9.
51. Banerjee S, Iqbal A, Sun S, Master R, Brilakis ES. Peripheral embolic events during endovascular treatment of infra-inguinal chronic total occlusion. *Cardiovasc Revasc Med.* 2011;12:134.e7–10. Epub 2010 Dec 30.
52. Lam RC, Shah S, Faries PL, McKinsey JF, Kent KC, Morrissey NJ. Incidence and clinical significance of distal embolization during percutaneous interventions involving the superficial femoral artery. *J Vasc Surg.* 2007;46:1155–9.
53. Davies MG, Bismuth J, Saad WE, Naoum JJ, Mohiuddin IT, Peden EK, Lumsden AB. Implications of in situ thrombosis and distal embolization during superficial femoral artery endoluminal intervention. *Ann Vasc Surg.* 2010;24:14–22.
54. Larrazet FS, Dupouy PJ, Rande JL, Hirotsuka A, Kvasnicka J, Geschwind HJ. Angioscopy after laser and balloon coronary angioplasty. *J Am Coll Cardiol.* 1994;23:1321–6.
55. Shammam NW, Shammam GA, Dippel EJ, Jerin M. Intraprocedural outcomes following distal lower extremity embolization in patients undergoing peripheral percutaneous interventions. *Vasc Dis Manag.* 2009;6:58–61.
56. Dahm JB, Topaz O, Woenckhaus C, et al. Laser-facilitated thrombectomy: a new therapeutic option for treatment of thrombus-laden coronary lesions. *Catheter Cardiovasc Interv.* 2002;56:365–72.
57. Topaz O, Morris C, Minisi AJ, et al. Enhancement of t-PA induced fibrinolysis with laser energy: in-vitro observations. *Lasers Med Sci.* 1999;14:123–8.
58. Dahm JB, Ruppert J, Doerr M, et al. Percutaneous laser-facilitated thrombectomy: an innovative, easily applied, and effective therapeutic option for recanalization of acute and subacute thrombotic hemodialysis shunt occlusions. *J Endovasc Ther.* 2006;13:603–8.
59. Moritz MW, Ombrellino M, Agis H. Excimer laser for debulking and lysing chronic venous thrombi and occlusions. *Vasc Endovascular Surg.* 2009;43:370–3.
60. Lincoff AM, Bittl JA, Harrington RA, et al. Bivalirudin and provisional glycoprotein IIb/IIIa blockade compared with heparin and planned glycoprotein IIb/IIIa during percutaneous coronary intervention; the REPLACE-2 randomized trial. *JAMA.* 2003;289:853–63.
61. Stone GW, McLaurin BT, Cox DA, et al. Bivalirudin for patients with acute coronary syndromes. *N Engl J Med.* 2006;355:2203–16.
62. Shammam NW. Bivalirudin: pharmacology and clinical applications. *Cardiovasc Drug Rev.* 2005;23(4):345–60.
63. Shammam NW. Complications in peripheral vascular interventions: emerging role of direct thrombin inhibitors. *J Vasc Interv Radiol.* 2005;16(2 Pt 1):165–71.
64. Burgess JK, Chong BH. The platelet proaggregating and potentiating effects of unfractionated heparin, low molecular weight heparin and heparinoid in intensive care patients and healthy controls. *Eur J Haematol.* 1997;58:279–85.
65. Xiao Z, Théroux P. Platelet activation with unfractionated heparin at therapeutic concentrations and comparisons with a low-molecular-weight heparin and with a direct thrombin inhibitor. *Circulation.* 1998;97:251–6.
66. Allie DE, Hall P, Shammam NW, et al. The Angiomax Peripheral Procedure Registry of Vascular Events Trial (APPROVE): in-hospital and 30-day results. *J Invasive Cardiol.* 2004;16:651–6.
67. Shammam NW, Shammam GA, Jerin M, Dippel EJ, Shammam AN. In-hospital safety and effectiveness of bivalirudin in percutaneous peripheral interventions: data from a real-world registry. *J Endovasc Ther.* 2010;17:31–6.
68. Katzen BT, Ardid MI, MacLean AA, et al. Bivalirudin as an anticoagulation agent: safety and efficacy in peripheral interventions. *J Vasc Interv Radiol.* 2005;16:1183–7.
69. Shammam NW, Lemke JH, Dippel EJ, et al. Bivalirudin in peripheral vascular interventions: a single center experience. *J Invasive Cardiol.* 2003;15:401–4.

Robert A. Gallino

In this chapter I will discuss the use of the Laser for the treatment of complex SFA disease.

The most commonly used Laser catheters for the SFA are the 2.0, 2.3 and less commonly the Turbo Tandem, the 2.5 and the smaller (>2.0) catheters. The 2.0 can be used with a 6 F sheath whereas the 2.3 requires a 7 F sheath. There's significant luminal gain with the 2.3 laser compared with the 2.0 and hence it's my catheter of choice for most SFA lesions. The 2.5 laser requires an 8 F sheath and doesn't offer much gain above the 2.3 laser. The smaller catheters are limited by the amount of luminal gain in these 4–6 mm diameter arteries. The 2.0 and 2.3 laser work over a 0.018 Guide Wire. Although the V 18 Control wire is frequently used to traverse SFA lesions and occlusions, I prefer not to work over this wire because of the potential of the distal hydrophilic tip to create distal dissections or perforations. Usually the laser is advanced over a non hydrophilic (0.018 Road Runner, Steelcore,) wire. Any supportive 0.014 wire (Grandslam, Ironman, BHW) can also be used.

Most commonly the laser is used for lesion preparation prior to the use of balloons or stents. It's particularly useful here for several reasons. First, a single laser catheter can treat a long (>30 cm) segment of disease with a single catheter, not removed from the body, with minimal use of contrast and fluoroscopy. Some comments regarding the technique are important to discuss. The contralateral approach is the most commonly used however, if the SFA is extensively calcified the antegrade approach is preferred for maximal support and pushability. The Arrow Sheath is not recommended because the ridges within the sheath inhibit the passage of the laser. The general principles of the laser are discussed elsewhere, but suffice to say, saline flush is delivered not through the sheath, but more effectively through the distal port of the laser. Flushing saline through the sheath often doesn't reach

the tip of laser. Therefore I recommend flushing saline through the distal tip of the laser in order to maximize delivery beyond the laser tip. This is accomplished by connecting a Co-Pilot or any Touey Borst Y adapter to the guide wire as it exists the back of the laser. Saline is flushed through the side arm of the Y adapter.

I usually start with lower energy (i.e.; 45 J) at a repetition rate 55 pulses/s. The lower energy is used in an attempt to minimize dissections. Higher energies, 80 J, create a larger vapor bubble and within a tight lesion are prone to create acoustic trauma and subsequent dissections. After one or two passes are made at the lower energies, a pass can be made at the highest energy and rate (60/80). After the higher energies there's usually significant luminal gain achieved. The gain occurs not only by vaporizing plaque, but by having the large vapor bubble produced by the high energy, render the vessel more compliant. This effect was seen in the CELLO trial where by IVUS, the majority of the luminal gain was seen by the increase in the external elastic membrane not plaque reduction. The more compliant artery post laser permits 1:1 sizing of the balloon which usually completely expands at low atms. Typically a 6 mm diameter for men and a 5 mm for women, covering the entire segment, (balloons up to 300 mm) is inflated to low atms (4–6) up to 3 min. As always, in order to get the maximal luminal gain, without dissections, the laser needs to be advanced slowly (1 mm/s) in a blood and contrast free space.

The laser has a unique property of being an Atherectomy catheter that can be used to initially cross the CTO. The initial use of the laser to cross CTOs was by Professor Giancarlo Biamino. He described a provocative method of using the laser without a leading wire to cross CTOs. He termed this technique "Step by Step". The laser catheter is positioned proximal to the SFA occlusion (with the wire withdrawn into the catheter) The laser is then activated for about 10 s a few mm proximal to the cap. Then the laser is again activated, and gently passed into the cap (with the wire still behind the tip), After slowly penetrating the cap a few mm the wire can now gently probe the channel. Sometimes simply penetrating

R.A. Gallino, MD
Department of Cardiology, Medstar Montgomery Medical Center
and Washington Hospital Center, Olney, MD, USA
e-mail: robert.a.gallino@medstar.net

the fibrotic proximal cap will allow wire passage through the softer organized thrombus. If resistance is encountered, the laser is activated over the advanced wire. At the point of resistance the wire is withdrawn, and the laser activated with slow gentle forward pressure (similar to what was done at the proximal cap) After advancing the laser, the wire then can probe the channel. The laser is then advanced as above, (Step by Step). This technique is very effective in straight occlusions, it becomes less so in the bends of the adductor canal. At the adductor canal it's useful to probe with a wire either through the laser, or exchanging for an angled catheter. Trying to advance the laser, without the leading wire, through tortuous calcified occlusions can lead to dissection and perforation.

After the wire traverses the occlusion the laser is again activated into the distal true lumen. Usually we withdraw the laser back to the proximal cap and ablate the entire occlusion. Following this, standard angioplasty techniques can be used. Because of the laser vapor bubble (discussed below) the vessel is rendered more compliant and only low atmosphere inflations are needed for full balloon expansion. Often, post laser and a long (3 min) low pressure (<8 atms) inflation stenting is not needed.

The laser is ideally suited for the treatment of SFA in stent restenosis (ISR). Stents that have been chronically occluded are very difficult to cross. The hard, rubbery restenotic scar tissue makes guide wire passage not only difficult to engage the proximal cap but once within the stent the wire frequently exists the stent struts at the points of significant resistance. The laser can be placed at the proximal cap and advanced in a step by step manner similar for native SFA occlusions. The laser energy is usually sufficient to disrupt the proximal cap. Once within the stent the laser which is larger than the stent struts remains within the stent. Typically a 2.3 Laser is used at the highest energies (60/80) within the stent. At the distal aspect of the stent lower energies are used to avoid dissection. Several passes are made to achieve maximal debulking. This is one instance where I usually will use distal protection (with a filter). To achieve maximal luminal gain the Turbo Tandem laser can be used. The treatment of the occluded SFA stent is likely the best indication for the Turbo Tandem Laser. The major downside to the Turbo Tandem Laser is the cost of using another laser and this is why I usually just use the 2.3 Laser to cross and debulk the occluded stent. Following laser, a 1:1 balloon to stent size, covering the entire stent usually leads to an excellent acute result. Unfortunately, the acute result is not well maintained with frequent restenosis occurring (The Patent trial). A randomized study of POBA vs Laser for the treatment of SFA ISR is in progress (Excite Trial PI Dr Eric Dipple) at the time of this writing. Presently, post Laser ISR is being treated with Drug Eluting Balloons (DEB) and Drug Eluting Stents (DES). No long term data of this approach is presently available.

The laser cannot only treat the chronically occluded stent, but can treat a focal recalcitrant stenosis within a stent. It's not uncommon to have a focal portion of the stent not fully expand, despite high pressure balloon inflations, secondary to an bulky calcified plaque. The vapor bubble of the laser works beyond the stent struts to weaken the calcified plaque and permit subsequent balloon expansion of the stent. This is well recognized in the treatment of the unexpanded coronary stent. The laser is the only atherectomy device that can modify the tissue behind the stent struts. The treatment of the calcified lesion will be discussed below.

The laser is usually not thought of as a device for the treatment of calcified SFA lesions. However, at high energies, the vapor bubble does disrupt calcium. IVUS clearly shows the arcs of calcium have been fragmented. Following laser, for the I prefer to use a scoring balloon to further modify the lesion. The Angioscore balloon is an excellent choice because it has the ability to inflate to high atms within the calcified lesion. I will not place a stent if the balloon has a persistent waist, fortunately this is rare following high energy passes with the laser.

The most commonly used Laser catheters for the SFA are the 2.0, 2.3 and less commonly the Turbo Tandem, the 2.5 and the smaller (>2.0) catheters. The 2.0 can be used with a 6 F sheath whereas the 2.3 requires a 7 F sheath. There's significant luminal gain with the 2.3 laser compared with the 2.0 and hence it's my catheter of choice for most SFA lesions. The 2.5 laser requires an 8 F sheath and doesn't offer much gain above the 2.3 laser. The smaller catheters are limited by the amount of luminal gain in these 4–6 mm diameter arteries. The 2.0 and 2.3 laser work over a 0.018 Guide Wire. Although the V 18 Control wire is frequently use to traverse SFA lesions and occlusions, I prefer not to work over this wire because of the potential of the distal hydrophilic tip to create distal dissections or perforations. Usually the laser is advanced over a non hydrophilic (0.018 Road Runner, Steelcore,) wire. Any supportive (Grandslam, Ironman, BHW) 0.014 wire can also be used.

There are several limitations of the laser. It's not effective as a stand alone treatment for complex SFA disease. Dissections and modest luminal gain are common post laser alone. Fortunately, ballooning post laser leads to excellent luminal gain and tacking up of the dissections. Also, the long term patency of Laser and POBA especially in long lesions is accompanied by significant restenosis. DEB post laser appears to be a promising strategy, although no data is presently available. It's likely that the laser will be an important device for lesion preparation prior to DEB, DES and Bioabsorbable Stents.

In conclusion, the laser has a long term track record of being an effective tool for the treatment of a variety of SFA lesions. It's relatively easy to use with very predictable results. It can work over standard guide wires and usually

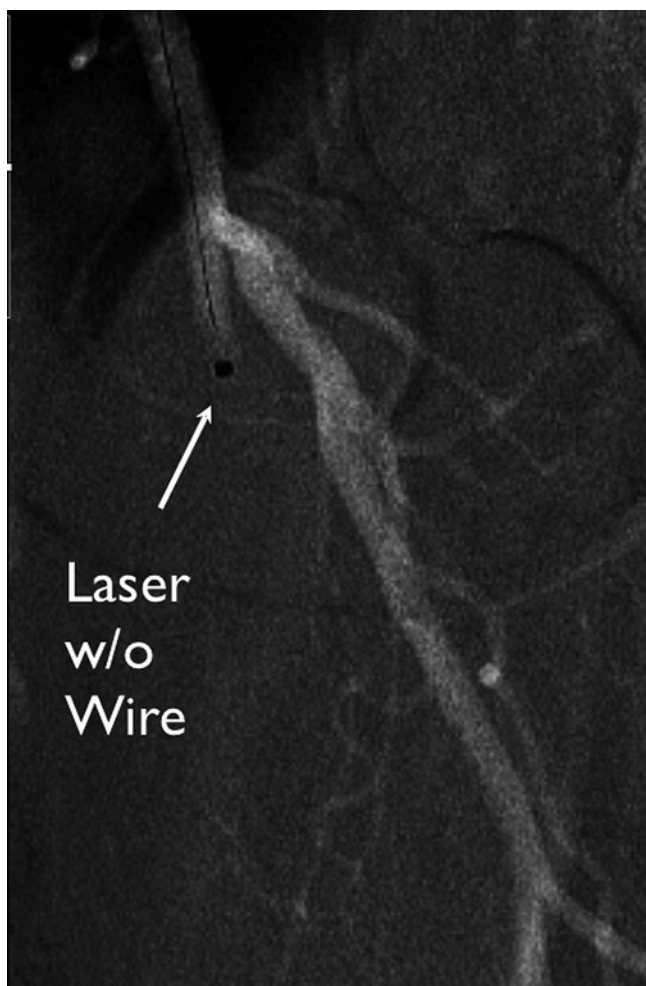


Fig. 12.1 The Laser at the proximal cap with the trailing guide wire (note the laser is activated a few mm proximal to the cap)

doesn't require the use of a distal filter. It has unique properties of being able to cross and the debulk CTOs. It probably is the catheter of choice for the treatment of the occluded stent.

Laser Step by Step Technique

1. Advance the Laser ~5 mm proximal to the SFA stump (Fig. 12.1). As discussed in the text, I prefer a larger laser (2.0 or 2.3) for this technique. **Clear all the contrast from the system, this is imperative** (discussed in the text)
2. Using a fluency and rate of 42/25 activate the laser on the proximal cap. **Without advancing** activate for approximately 10 s and sit on the cap
3. Next, activate and **gently advance** the Laser across the proximal cap (Fig. 12.2)
4. Post activation, probe with a heavy tip (i.e. Cook Approach CTO Wires 6, 12,18 & 25 g tip or the Asahi Astato 30 g tip) Advance the wire until resistance is encountered (Fig. 12.3)
5. Activate and advance the Laser over wire
6. Withdraw the wire into the laser, activate and advance the laser. Repeat step 4
7. If the distal re-entry is in a straight section of the vessel, advance the laser into the distal true lumen. The wire should then easily pass forward (Fig. 12.4). Remove the heavy tipped wire and exchange for a standard softer tipped wire (any workhorse wire is fine)
8. If the re-entry zone is at an angle, consider advancing the laser to the angle and then probe with the heavy tipped wire (I prefer non hydrophilic wires)
9. If the Laser encounters resistance, don't push, advance the sheath over the laser. This will provide more support to cross the stubborn spot.
10. After crossing the occlusion, withdraw the laser to the proximal cap and re laser the entire occlusion at a rate of ~1 mm per second. This slow rate achieves maximal ablation



Fig. 12.2 The Laser has advanced across the proximal cap while the wire continues to trail the tip

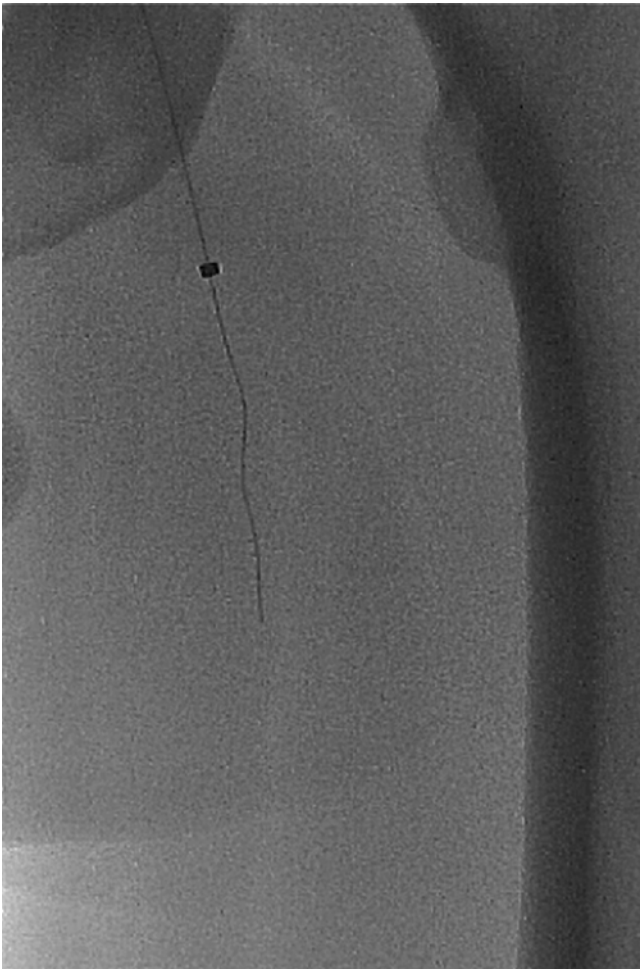


Fig. 12.3 The heavy tipped guide wire (Cook 25 g Approach wire) is advanced now ahead of the laser. It's not uncommon to have free wire passage after penetrating the fibrotic proximal cap. If resistance is met, the laser is advanced up to that point, the wire withdrawn, and the laser activated (similar to the proximal cap)



Fig. 12.4 If the wire doesn't encounter resistance it is advanced across the distal occlusion into the true lumen. Be especially careful at the distal cap, forceful pushing of either the wire or laser leads to Subintimal passage

Laser Synergism with Drug Eluting Balloon for Treatment of In-Stent Restenosis in the Lower Extremities

13

Jos C. van den Berg

Introduction

In the last years new techniques and technologies have been developed for the endovascular treatment of arterial occlusive disease affecting the superficial femoral artery (SFA) and infrapopliteal arteries. With the availability of dedicated stents the problem of elastic recoil, flow-limiting dissection and residual stenosis after balloon angioplasty can be dealt with efficaciously, and this development has therefore allowed the treatment of very complex and extensive lesions with a low complication rate. Restenosis, and in particular in-stent restenosis, remains a problem that significantly affects mid- and long-term outcome of SFA stenting [1]. Two studies that demonstrated a statistically significant benefit of primary stenting of the SFA over angioplasty with bail-out stenting still yielded high restenosis rates with Duplex derived primary patency of 81.3 % [2] at 1 year and 63 % at 2 years [3]. The rate of recurrent stenosis in below-the-knee lesions after PTA and stenting is even higher than after femoropopliteal procedures [4]. As a result of the favorable outcomes achieved, endovascular treatment with stenting is used more liberally and this leads to a situation where we are faced more and more with the problem of in-stent restenosis. In-stent restenosis cannot be treated efficiently with plain balloon angioplasty, cutting balloon angioplasty or cryoplasty [5, 6]. Directional atherectomy as stand-alone treatment has also demonstrated to be inadequate in the treatment of in-stent restenosis with patency rates around 50 % [7].

This chapter will provide a description of the process of (in-stent) restenosis with special attention to the histopathological changes that occur. Furthermore it will give an overview of the current status of drug-eluting balloon technology and will present results from the literature with the treatment

of in-stent restenosis using a combination of laser atherectomy and drug-eluting balloons.

The Problem of Restenosis

All endovascular procedures (balloon angioplasty with or without stenting) produce a more or less controlled injury to the arterial wall, with intimal plaque disruption typically accompanied by medial injury. Deep vessel injury caused by stent struts (damaging the internal elastic lamina), is one of the causes of restenosis [8].

The local arterial response to stenting as demonstrated by experimental animal and human autopsy studies follows a response-to-injury sequence of events, similar to wound healing [9–11]. The superficial femoral artery, like the coronary arteries, is a so-called muscular or distributing artery. Muscular arteries contain fewer elastic and more smooth muscle cells than elastic arteries (that typically contain high amounts of collagen and elastin fiber in the media, and exhibit a lower incidence of in-stent restenosis) [12]. The in-stent restenosis mechanism in coronary and peripheral muscular arteries is supposed to be similar [13]: in human coronary arteries, stents cause platelet and fibrin deposition around struts and an initial acute inflammatory cell response within the first 3 days. Afterwards the acute inflammation subsides and is followed by a granulation tissue response with neovascularization, smooth muscle cell migration and proliferation, and replacement of acute inflammatory cells by chronic inflammatory cells by 2–4 weeks: proliferating smooth muscle cells are seen in the early neointima and are associated with organizing thrombus and a thin extracellular matrix. After 30 days the presence of fibrin and chronic inflammation may persist, and the neointima is enriched further by smooth muscle cells and extracellular matrix. The formation of intimal hyperplasia (restenosis) consists of three different processes: cell replication, cell migration, and accumulation of extracellular matrix in the arterial wall [14]. The

J.C. van den Berg, MD, PhD
Service of Interventional Radiology, Ospedale Regionale di Lugano, Via Tesserete 46, Lugano 6903, Switzerland
e-mail: jos.vandenberg@eoc.ch

extracellular matrix molecules are synthesized by neointimal smooth muscle cells. The extracellular matrix is composed of a variety of molecules, including collagen (type I and III), elastin, glycoproteins, and proteoglycans (versican, biglycan and decorin). Proteoglycans and hyaluronan participate in the regulation of vascular permeability, lipid metabolism, and thrombosis. In a muscular (coronary) artery, type III collagen is the most abundant matrix protein. Experimental arterial injury studies have demonstrated that remodelling of the neointima occurs with replacement of the type III collagen with type I collagen. The extracellular matrix accumulates mainly around stent struts and in the outer intima [14, 15]. Around the struts, in addition to the extracellular matrix, inflammatory cells (leukocytes, macrophages and T-lymphocytes) can be found. The outer intima is characterized by lower cell density or lower cell replication as compared with the inner intima, which suggests that matrix accumulation is more critical than the increase of cell number because of cell replication. Smooth muscle cell components are concentrated at the intimal surface, and demonstrate cell replication even at 7–19 months after stent implantation [14]. This dense neointimal layer is typically the first 250 μm of the intra luminal section. Studies with animal models that have evaluated the responses to balloon angioplasty injury of arteries with preexisting intimal lesions showed similar findings in the intima after balloon angioplasty. Intimal size increases in the late phase after balloon angioplasty, and matrix accumulation (and not intimal cell replication) accounts for most of the increase of intimal size [14]. A difference exists in restenosis mechanism between balloon angioplasty and stenting. Intimal hyperplasia accounts for all late lumen loss following stenting, but for less than 40 % after balloon angioplasty (the remainder being caused by so-called constrictive remodelling). Stenting causes an even greater increase in collagen accumulation, in both arterial intima and media/adventitia layers compared with balloon angioplasty. This is likely due to extensive tissue damage and persistent circumferential stretching, that are both well recognized stimuli for enhanced collagen synthesis [16, 17].

All these processes lead to the heterogenous nature of in-stent restenotic lesions with a cell-dense intimal layer that has been described as “rubbery” in consistency and a significant volume of cell-poor, hydrated matrix in the outer intima to the stent struts.

The major histological findings can be summarized as follows:

- In-stent restenotic lesions are complex and differ significantly from de-novo atherosclerotic lesions.
- In-stent restenotic lesions are heterogeneous and consist primarily of collagen and smooth muscle cells. They have

an innermost intimal layer of dense smooth muscle cell tissue and an outermost intimal layer that can be described as a cell-poor scaffold or “sponge” comprised of collagen. This outermost intimal layer is the largest volume constituent of an in-stent restenotic lesion.

- Calcium is rare in in-stent restenotic lesions.
- Thrombus can be present, but typically constitutes a small part of the total volume (the exception may be in acute occlusions that occur within a short time frame after stent placement).

Due to this unique morphology (the majority of the volume being extra-cellular matrix), in-stent restenotic lesions tend to feel “spongy” and recoil quickly. The extracellular matrix accounts for 50 % of the total volume of neointimal restenotic lesions, and explain the fact why balloon angioplasty alone does not work in restenotic lesions [17]. Therefore many clinicians have abandoned this approach to treat in-stent restenosis, particularly in long or occlusive disease, and started a quest for alternative treatments.

Current Status of Drug-Eluting Balloon Technology

The concept of drug-eluting balloons is based on the local delivery of drugs on site, with an exact control of the drug dosage, thus achieving an effective and sufficient local concentration, and avoiding systemic exposure to the drug. Advantages of the technology are the possibility of a homogeneous drug transfer as compared to stent-mediated drug release where the drug is only delivered at the level of contact of the stent struts with the vessel wall. Because approximately 85 % of the stented vessel wall area is not covered by the stent struts, stent-mediated drug release results in low tissue concentrations of the antiproliferative agent in these areas [18]. Furthermore drug-eluting balloons allow for a drug concentration that is highest at the time of the vessel wall injury that occurs during balloon angioplasty and therefore can prevent the initiation of the chain of events that will eventually lead to neointimal proliferation. The absence of metal struts makes the technique suitable for treatment of long lesions (especially in small diameter vessels), and areas where flexion and compression of stents may occur. Finally the absence of a stent allows the artery’s original anatomy to remain intact, which is especially of importance in lesions at the level of a bifurcation. The absence of polymer that is needed in most drug-eluting stents could decrease chronic inflammation and the trigger for late thrombosis and thus obviate the need for long-term dual antiplatelet therapy [19, 20]. By not using stents follow-up treatment options (re-PTA, treating a potential anastomosis-site for surgical bypass

without compromising the distal anastomosis site) are preserved. Most currently available drug-eluting balloons use dry state paclitaxel. This drug is the active ingredient of Taxol® (Bristol-Myers-Squibb) that has been approved and widely used in oncological therapy. In oncological applications, paclitaxel is typically infused intravenously up to a dose of 175 mg/m² body surface equivalent, a dosage that is equivalent to about 300 mg/patient. Usually, the treatment is repeated several times with a treatment-free interval of 1 month. The dose of paclitaxel that is used by almost all manufacturers of drug-eluting balloons is either 2 or 3 µg/mm² of the balloon surface. With this dosage regimen the total dose of paclitaxel administered to the patient remains well below the dosage schemes used in cancer treatment (for example 3 µg paclitaxel/mm² balloon surface results for the largest balloon (Ø 6 × 120 mm) in about 8 mg). Paclitaxel is a cytotoxic agent and a potent inhibitor of smooth muscle cell (SMC) proliferation, SMC migration, and extracellular matrix formation in vitro, with all three phases of the restenosis process inhibited effectively [21]. Paclitaxel is a lipophilic substance. The effective transfer of drug to the arterial wall is controlled by how the drug is loaded on the balloon (coating engineering) and by the relative solubility of the drug between the cell wall and the coating. Several techniques are available to make the drug adhere to the balloon, and to optimize drug release. Paclitaxel can be made to adhere to the balloon surface by using ethyl acetate or acetone as a solvent [22]. More recent developments in balloon coating technology used the contrast agent iopromide as a hydrophilic spacer (Paccocath). In this way the solubility of paclitaxel is increased and the transfer of paclitaxel to the vessel wall is enhanced [22]. The second method (FreePac coating, Medtronic Invatec) uses urea as a matrix to improve adherence of the drug to the balloon and facilitates drug elution by separating paclitaxel molecules and balancing hydrophilic and lipophilic properties. Urea is a natural degradation product of protein and one of the most common substances in human serum (100–500 mg/l). Urea is synthesized in the liver in an amount of ca. 18–35 g per day to detoxify and excrete nitrogen derived from proteins. Urea has very low toxicity and causes no hypersensitivity reactions. The dose of urea on the balloon is about 0.5 µg/mm² balloon surface, which results for a large balloon (Ø 6 × 120 mm) in a total dose of urea of 1.1 mg. This is the amount of urea contained in 10 ml serum or <0.01 % of the urea synthesized during one day, and this can be considered totally harmless. The third type of balloon uses a coating matrix that consists of a natural resin (composed of shellolic and alleuritic acid; Shellac coating, Eurocor; more recently another balloon using shellolic acid base coating covering so-called nanocrystalline paclitaxel has become available; Cardionovum). Once in contact with blood the hydrophilic network of the composite swells and opens the structure to allow

pressure-induced release of paclitaxel. The fourth type of balloon uses Butyryl-tri-hexyl citrate (BTHC) (Biotronik): BTHC is a compound that is used in medical devices and cosmetics. It is approved to be dissolved into the blood and used in the body, and degrades to citric acid and alcohol. BTHC disrupts the crystalline structure of paclitaxel and makes the compound better absorbable to the tissue. The last types of balloon (that both use a dose of 2 µg/mm² of paclitaxel) use sorbitol and polysorbate (Lutonix/BARD) and polyethylene glycol (Spectranetics) as carrier.

Although technically similar to the use of non-coated angioplasty balloons, there are several issues that must be considered when using drug-eluting balloons. The presence of the coating on the balloon will increase its crossing profile only slightly, and therefore the drug-eluting balloon will not require a larger introduction sheath size. However it is generally recommended to upsize 1 F size, in order to avoid ‘scraping off’ the coating while crossing the sheath. The inflation time recommended for optimal release of the drug (up to 80 % of the total amount) is between 30 and 60 s (shorter inflation should be avoided in all cases, longer inflation times will not lead to a significant additional release of drug) [1]. Balloon length should always exceed lesion length, and predilation is recommended not only to avoid loss of drug from the balloon when crossing the lesion to be treated (especially in total occlusions and heavily calcified lesions), but also to ensure an equal distribution of the drug across the vessel surface. When treating lesions with a length that exceeds the total balloon length an additional balloon or additional balloons should be used in order to cover the whole lesion length (as mentioned before, 80 % of the drug is released after one inflation, which renders the balloon inapt for a second drug release). In an animal study it was demonstrated that increase of local dose due to overlapping balloons does not lead to an increase in adverse reactions and does not influence the efficacy of reduction of neointimal proliferation. No adverse reactions were seen as dose was increased to more than three times the clinically tested dose [23]. It is of utmost importance to avoid a so-called geographic miss, that is, a segment of the lesion not being treated with the drug-eluting balloon. Bony landmarks or a ruler can be used to ensure proper overlapping of the drug-eluting balloons. As a reliable alternative, the roadmap feature of the angiography system can be used: with the first balloon inflated, the roadmap is activated (without injecting contrast), and when after balloon deflation and exchange for the second balloon the fluoroscopy is used, the image of the first balloon and its markers will be visible as a ‘negative image’. The markers of the second balloon will be projected on this image as ‘positive’, and the most distal marker of the first balloon and the most proximal marker of the second balloon can be easily superimposed.

Endovascular Treatment of In-Stent Restenosis Using Excimer Laser Angioplasty and Drug Eluting Balloons

With the development of drug-eluting balloon technology a potential novel treatment modality for in-stent restenosis has become available (with or without debulking), and first results look promising. The technique of the combined therapy of laser debulking and drug-eluting balloon angioplasty for in-stent restenosis will be discussed hereafter and will be put in perspective with other treatment strategies.

Technique

Either an ipsilateral, antegrade approach or a retrograde, contralateral approach with cross-over can be used. After obtaining arterial access a 4 F introducer sheath is placed, and a diagnostic angiography of the whole affected limb is obtained. After successful crossing of the lesion with a hydrophilic guide wire (Glidewire, Terumo) a diagnostic catheter is advanced and contrast injected distally from the lesion to confirm intraluminal position. In case of a total occlusion the lesion should preferably be crossed with the guide wire 'looped' in order to avoid exiting of the wire through the struts of the stent in a 'subintimal' fashion. The 4 F introducer sheath can then be subsequently exchanged for a 5 F–7 F sheath (depending on the size of the laser catheter that is to be used), while maintaining the guide wire in a position with its tip distally from the lesion. Then the hydrophilic guide wire should be exchanged for a 0.014" guide wire or a 0.018" guide wire, again this depending on which type of laser catheter is used. A Turbo Elite laser catheter (diameter ranging from 1.4 mm till 2.0 mm) is subsequently introduced, while applying continuous saline flush on both the introducer sheath and through the laser catheter. The laser catheter is then slowly advanced through the lesion under fluoroscopic control (speed <1 mm/s). It is recommended to perform two passages with the laser catheter. Fluence and pulse repetition rate settings for the first passage should be intermediate, and this will allow for more efficacious ablation of any soft (thrombotic) material present, thus minimizing the risk of distal embolization. The second passage will be performed using the maximum Fluence and frequency (as set by the manufacturer). At maximum settings the vapor bubble that is typically formed around the tip of the laser catheter (and that is contributing significantly to the ablative effect) is larger, and thus the debulking will be more efficient. After removal of the laser catheter, balloon angioplasty of the treated segment is performed using standard angioplasty balloons, with a size 1 mm less than the reference vessel diameter. This

is followed by angioplasty using drug-eluting balloons according to the technical considerations described above (inflation time, avoidance of geographical miss etc.). A representative case is depicted in Fig. 13.1a–g.

Alternatively the Turbo-Tandem system can be used for debulking. The Turbo Tandem requires a 7 F sheath, and consists of a guiding catheter with a ramp and a pre-mounted laser catheter that can be advanced onto the ramp allowing for an off-center position of the laser catheter during ablation. This technique allows to obtain a larger luminal gain [24]. The Turbo Tandem catheter can only be used after creating a so-called pilot channel in the occlusion (the minimum diameter required is 2 mm). The pilot channel can be obtained by using a small size Turbo Elite catheter, or predilatation of the occlusion with an angioplasty balloon of the above mentioned sizes. After the first pass of the Turbo Tandem through the occlusion the laser catheter is retracted off the ramp, the whole system is withdrawn, and a new pass is performed. It is recommended to perform a total of 4 quadrant passes (at 0°, 90°, 180° and 270°).

Sometimes it is impossible to enter the stent proximally, or to cross the entire length of the stent occlusion with the guide wire (inability to create the 'loop', with the guide wire exiting the stent struts). In these cases either a puncture distally from the stent or a direct puncture of the stent can be performed (placing a 4 F introducer sheath), and retrograde crossing of the occlusion can be attempted [25]. After successful retrograde passage, the guide wire can be snared from above and the procedure can be completed in an antegrade fashion as described above.

Review of Results in Literature

The first indication that the outcome of combining laser debulking and drug-eluting balloon angioplasty was better than previously reported studies using plain balloon angioplasty, came from a paper that described the short-term follow up of a cohort of 10 patients treated with this novel combination therapy [26]. This paper described the follow-up at a mean of 7 months. The cohort consisted of 8 female and 2 male patients with a mean age of 78.6 years (range 69–88 years). The mean time to recurrence was 7.2 months (range 2–16 months) and the mean lesion length was 115 mm (range 10–300 mm). Half of the patients presented with critical limb ischemia (5/10). The arterial segments involved were the superficial femoral artery (n=4), superficial femoral and popliteal artery (n=3), popliteal artery, superficial femoral/popliteal and crural artery, and popliteal and crural artery (each n=1). Two patients had a Tosaka class [27] I lesion, the remaining 8 were all Tosaka class III. All procedures were technically successful. No residual stenosis was seen angiographically. There were 2 cases of distal embolization (both

in patients with a history of acute on chronic occlusion). Both could be treated successfully with aspiration embolectomy ($n=2$) and local (on-the-table) intra-arterial thrombolysis using a bolus of urokinase of 250,000 U ($n=1$). No access site related complications were seen. Mean follow-up was 7.6 months (range 2–20 months). Six patients had Duplex follow up, one patient had an angiographic control (during angioplasty of an ipsilateral superficial femoral artery stenosis proximal of the treated segment a year after the index procedure), and the remaining 3 patients had clinical follow-up with ABI measurements. No target lesion revascularization was performed. The clinical stage improved in all patients, with 9 patients becoming asymptomatic, and one patient having a Fontaine class IIa (Rutherford class 2). The patients that were evaluated with Duplex and/or angiography ($n=7$; mean

follow-up 7 months) did not demonstrate any signs of neointimal hyperplasia. One patient underwent a (pre-planned) amputation of a toe shortly after the revascularization procedure. No major-amputations or deaths occurred. These outcomes compare favorable to what is currently known on the outcome of balloon angioplasty as stand-alone treatment for in-stent restenosis, especially considering the relatively long mean lesion length. In a randomized study that compared conventional balloon-angioplasty with peripheral cutting-balloon angioplasty in patients with in-stent restenosis with lesion lengths upto 20 cm (mean lesion length 80 mm) it was found that restenosis rates at 6 months were 65 % after cutting balloon angioplasty and even worse with conventional PTA (73 % restenosis). Thus the overall patency for both treatment modalities was disappointing. Cryoplasty for

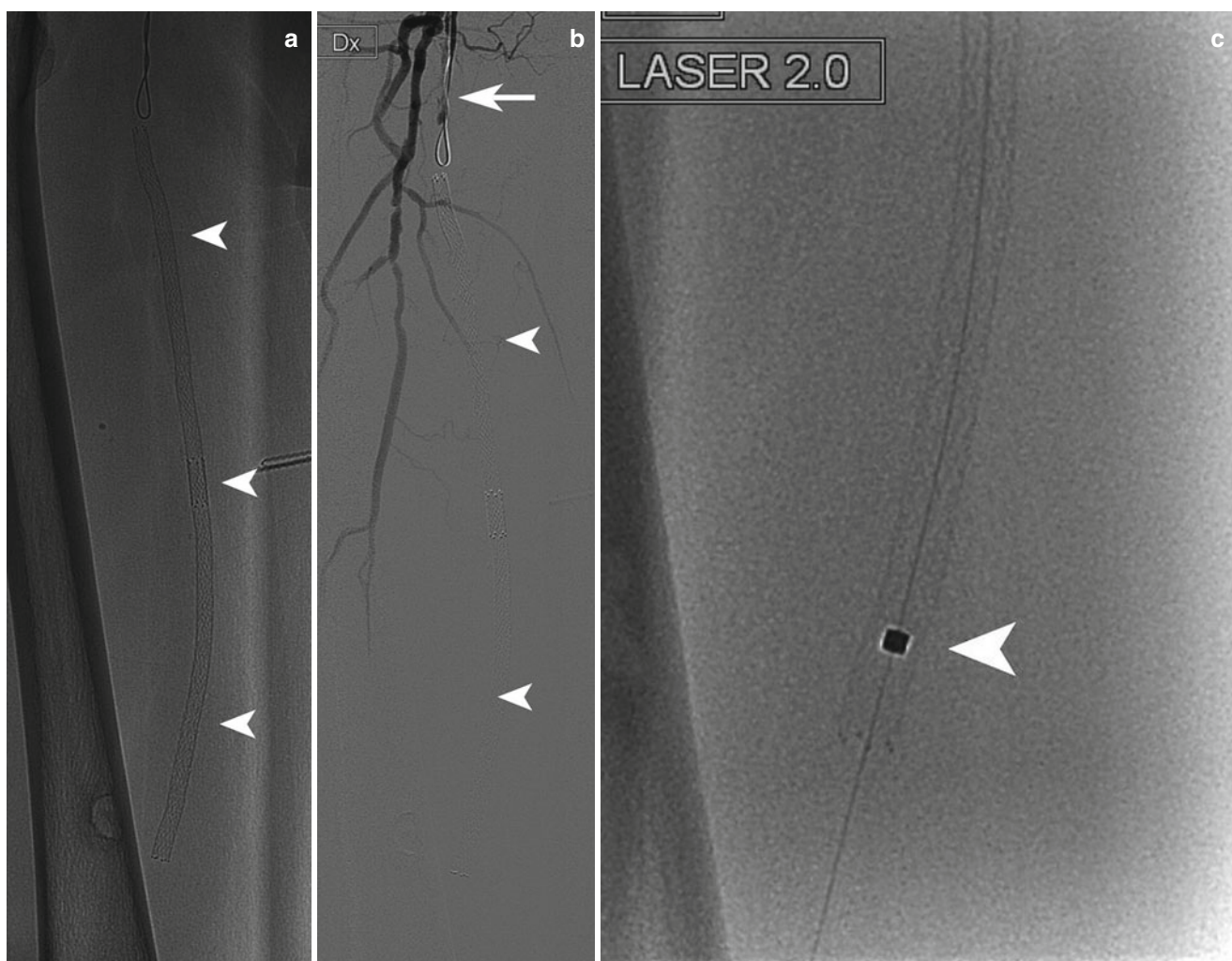


Fig. 13.1 (a) Fluoroscopic image of a long stented segment (arrowheads) of the right superficial femoral artery (two overlapping stents of 6×120 mm). (b) Digital subtraction angiography demonstrating stenosis of the proximal SFA (arrow) and stent occlusion (Tosaka class III; arrowheads). (c) Fluoroscopic image of laser catheter (Turbo Elite 2.0 mm; arrow) in distal stented segment. (d) Roadmap image obtained

after 2 passages of the laser catheter showing antegrade flow; note the significant luminal gain. (e) Fluoroscopic image of predilation with 4×250 mm angioplasty balloon. (f) Fluoroscopic image of dilation of the middle segment of the SFA with drug-eluting balloon (5×120). (g) Digital subtraction angiography: detail demonstrating complete restoration of the angiographic lumen at the level of the stent

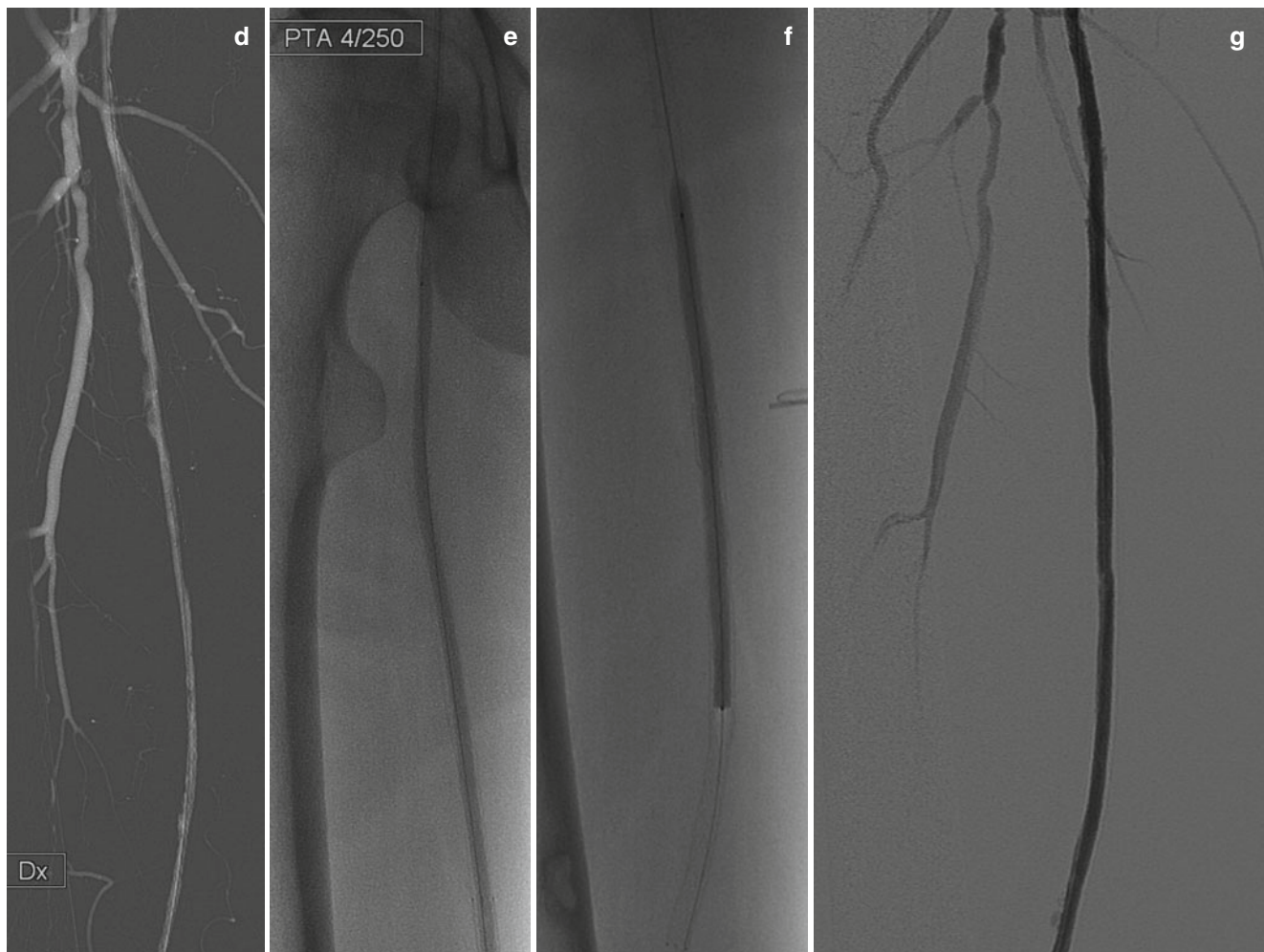


Fig. 13.1 (continued)

instant restenosis resulted in even worse outcome data, with a 100 % failure rate at 12 months [6].

The longer term follow-up of the above mentioned cohort of 10 patients has recently been published, and it appears from this that the effect of laser debulking followed by DEB is sustained also at 2 years [28]. The duration of clinical follow-up was $22.2 \text{ months} \pm 8.4 \text{ months}$ (range 15–38 months) and for Duplex follow-up $23.8 \text{ months} \pm 8.5 \text{ months}$ (range 13–38 months). Two patients were lost to follow-up after 13 and 14 months respectively (and were asymptomatic at that time). One patient demonstrated a binary restenosis (>50 % stenosis as demonstrated by Duplex using a peak systolic velocity ratio threshold of >2.4) at 36 months. This led to a target lesion revascularization ($n=1$) at 36 months (angiographically a focal 60 % stenosis in the distal popliteal artery was seen). In the remaining patients no clinically significant restenosis was seen with Duplex. Five patients (5/10; 50 %) showed absence of restenosis at a mean follow-up of 16.2 months (range 15–20 months), while 4/10 (40 %) demonstrated a 25–50 % stenosis (mean follow-up of this sub group 25 months; range 19–38 months).

Similar good results were seen in a study that involved 48 patients that were randomly assigned to treatment using combination therapy of laser debulking and drug eluting balloon angioplasty ($n=24$), or drug eluting balloon angioplasty alone ($n=24$) [25]. All patients were suffering from chronic critical limb ischemia and presented with a total occlusion of the superficial femoral artery (Tosaka class III). Mean length of the treated stent was $20.0 \pm 10.1 \text{ cm}$ in the combination therapy group and $23.3 \pm 9.1 \text{ cm}$ in the DEB only group ($p=\text{NS}$). The treated lesion length was $22.4 \pm 9.4 \text{ cm}$ vs. $25.9 \pm 8.7 \text{ cm}$, respectively ($p=\text{NS}$). The occluded tract was limited to the stent only in 3 patients, in the remaining cases stent obstruction was associated with proximal and/or distal thrombosis. Two cases of distal embolization were seen in the drug-eluting balloon group, and in one patient that was treated with combined therapy. The patency rates at 6 and 12 months in the combined therapy group (91.7 % and 66.7 % respectively) were significantly higher than in the drug-eluting balloon group (58.3 % and 37.5 % respectively; $p=0.01$). TLR at 12 months was 16.7 % in the combination

therapy group, and 50 % in the drug-eluting balloon angioplasty only group ($p=0.01$). Also the number of major amputations was significantly reduced (8 % versus 46 %; $p=0.003$). Ulcer healing was better in the patients that underwent combination therapy.

To put these positive results in perspective a comparison should be made with the outcomes as seen with drug-eluting balloon angioplasty as stand-alone therapy or with atherectomy (debulking) as single therapy. Results of 2 studies in patients with coronary in-stent restenosis have demonstrated the efficacy of a balloon that is coated with a paclitaxel-iodopromide mixture. Two-year follow-up data of a randomized trial comparing uncoated balloons with paclitaxel-coated balloons in patients with coronary in-stent restenosis demonstrated a statistically significant reduction of target lesion revascularization [29]. In this study in-segment late lumen loss after 6 months was 0.81 ± 0.79 mm in the uncoated balloon group vs. 0.11 ± 0.45 mm ($P < 0.001$) in the drug-coated balloon group. This resulted in a binary restenosis rate of 25/49 (uncoated) vs. 3/47 (coated; $P < 0.001$). Until 12 months post procedure 20 patients in the uncoated balloon group compared to two patients in the coated balloon group required target lesion revascularization ($P=0.001$). Similar results were obtained in a randomized comparison of paclitaxel-coated balloon angioplasty versus a paclitaxel-coated stent for the treatment of coronary in-stent restenosis [18]. In this study at 6 months follow-up, in-segment late lumen loss was 0.38 ± 0.61 mm in the drug-eluting stent group versus 0.17 ± 0.42 mm ($P=0.03$) in the drug-coated balloon group, resulting in a binary restenosis rate of 12 of 59 (20 %) versus 4 of 57 (7 %; $P=0.06$). At 12 months, the rate of major adverse cardiac events were 22 % and 9 %, respectively ($P=0.08$). It was concluded that treatment of coronary in-stent restenosis with the paclitaxel-coated balloon was at least as efficacious and as well tolerated as the paclitaxel-eluting stent, and furthermore that for the treatment of in-stent restenosis, inhibition of re-restenosis does not require a second stent implantation. One study evaluated the use of drug-eluting balloons for the treatment of superficial femoral artery in-stent restenosis, and demonstrated a 92.1 % primary patency rate at 1 year follow-up in a patient cohort with a mean lesion length of $82.9 \text{ mm} \pm 78.9 \text{ mm}$. In this study the number of Class III lesions was relatively low (20.5 %) [30]. The results of 2-year follow-up in this cohort were recently presented during the LINC 2014 meeting in Leipzig, and showed a decrease in primary patency to 70.3 % and a freedom from TLR of 78.4 %. Class I lesions showed a better primary patency rate (between 10 and 15 %) as compared to class III lesions (with a primary patency rate of around 35 %). The data from these three studies evaluating drug-eluting balloon angioplasty in the coronary (at 6 months) and SFA in-stent restenosis (at 1 and 2 years) show higher restenosis rates as compared to the treatment using

combined therapy of debulking and drug-eluting balloon angioplasty in the SFA as found in the above mentioned studies. This improvement of outcome can most probably be explained by the additional use of debulking.

Laser debulking as a stand-alone therapy has been evaluated in the PATENT registry [24]. In this study relatively long and complex lesions were treated (mean lesion length 123 ± 95.9 mm, with 34.1 % of lesions being total occlusions). The primary patency at 6 months (64.1 %) compared favorable to that seen in the study by Dick et al. (despite shorter lesion length the patency rate was only 27 % in the balloon angioplasty group; see above [5]). At 12 months the overall primary patency showed a drop to 37.8 %. The primary patency at 12 months as stratified by Tosaka class was 54.5 % for class I, 27.6 % for class II, and 24.0 % for class III. Although it was calculated that, when comparing the 3 classes, primary patency at 12 months was not significantly different, this indicates that longer and more complex lesions tend to do worse. From this study (and also from studies using directional atherectomy [7]) it can be concluded that after debulking additional therapy is needed in order to prevent recurrence of in-stent restenosis.

Because the burden of intima hyperplasia-associated restenosis and in-stent restenosis in the peripheral arteries is quite considerable, especially in long lesions, the data obtained in the studies mentioned above, support the approach of combining debulking with drug-eluting balloons, thus avoiding additional stenting procedures. Further back-up for this approach comes from a study where positive results were obtained using directional atherectomy for debulking [31]. All current atherectomy modalities rely on mechanical scraping or grinding which are generally inappropriate for softer tissues such as thrombus or neointimal hyperplasia and the moving components pose an elevated risk for stent disruption and fragmentation. Directional atherectomy is actually contraindicated in the treatment of in-stent restenosis and this technique is therefore not recommended [32].

In-stent restenosis should probably be treated in an early stage, even when the patient is asymptomatic (cf. surveillance of surgical bypass), in order to maintain high primary assisted patency rates. In addition, treatment of in-stent restenosis will be less complex as compared to treatment of a totally occluded stent where wire crossing is not always possible. Furthermore treatment before an acute (thrombotic) occlusion occurs will reduce the incidence of distal embolization. The 2 cases in the above mentioned series where distal embolization was seen occurred in patients that presented with acute clinical symptoms, in retrospect caused by acute thrombosis of a chronic stenosis. By using the previously described technique with 2 passages at a different energy setting the risk of distal embolization can be reduced (no instances of distal embolization were seen in the

subsequent 15 patients treated). In the Gandini study distal embolization was seen less frequent in the combined therapy group than in the drug-eluting balloon only group, emphasizing the safety of the procedure.

Class III lesions (total occlusions >5 cm) of the SFA are probably more difficult to treat, because of the large amount of re-stenotic material that needs to be dealt with. Given the fact that the innermost layer of the substance that forms the in-stent restenosis consists of non-cellular material the cytotoxic effect of the drug paclitaxel may not be able to reach the cellular (outermost) layer. Atherectomy offers the possibility to remove the smooth muscle cell inner intimal layer and the aqueous outer intimal layer that mainly consists of extra-cellular matrix. The effectiveness of laser atherectomy followed by DEB as a joint therapy is currently under evaluation in the PHOTOPAC trial (Photoablative Atherectomy Followed by a Paclitaxel-Coated Balloon to Inhibit Restenosis in In-stent Femoro-popliteal Obstructions; co-principal investigators: Thomas Zeller, MD and Dierk Scheinert, MD). The objective of this study is to evaluate the safety and efficacy of preparing a vessel with photoablation with Excimer laser and laser catheters prior to local paclitaxel delivery compared to local paclitaxel delivery without initial photoablation. This is a prospective, two-arm randomized study. Subjects meeting the definitions of Rutherford Clinical Categories 1–5 with in-stent lesions located in superficial femoral artery and the popliteal artery above the knee joint are eligible for enrollment. Primary outcome is Target Lesion Percent Stenosis at 1 year. Secondary outcomes are procedural success, MAE rate at 30 days and 1 year, improvement in WIQ Score, improvement in EQ-5D Score, improvement in Rutherford clinical category, improvement in Ankle-Brachial Index, clinically-driven target lesion revascularization, patency rate (Peak Systolic Velocity ≤ 3.5) and alternative patency rate (Peak Systolic Velocity ≤ 2.4) all at 6, 12 and 24 months; and minimum lumen diameter, net lumen gain, angiographic patency rate and secondary patency rate all at 1 and 2 years. Hopefully this and future studies, together with the growing experience in daily clinical practice (as in the case series described herein) will further define the optimal treatment of in-stent restenosis. A subsequent step that needs to be made is to evaluate the cost-effectiveness of this therapy.

Conclusion

In the treatment of in-stent restenosis, debulking is probably key. There is a growing body of evidence that by adding drug-eluting balloon angioplasty to debulking results can be achieved that compare favorable to those described in the literature that were obtained with standard balloon angioplasty, cutting-balloon angioplasty or debulking alone. Especially in long and complex lesions (Tosaka class III) this synergy is more pronounced.

Long-term follow-up and randomized studies are underway that will further define the role of combined excimer laser and drug-eluting balloon angioplasty in the treatment of in-stent restenosis.

References

1. Diehm NA, Hoppe H, Do DD. Drug eluting balloons. *Tech Vasc Interv Radiol.* 2010;13(1):59–63.
2. Laird JR, Katzen BT, Scheinert D, Lammer J, Carpenter J, Buchbinder M, et al. Nitinol stent implantation versus balloon angioplasty for lesions in the superficial femoral artery and proximal popliteal artery: twelve-month results from the RESILIENT randomized trial. *Circ Cardiovasc Interv.* 2010;3(3):267–76.
3. Schillinger M, Sabeti S, Dick P, Amighi J, Mlekusch W, Schlager O, et al. Sustained benefit at 2 years of primary femoropopliteal stenting compared with balloon angioplasty with optional stenting. *Circulation.* 2007;115(21):2745–9.
4. Siablis D, Karnabatidis D, Katsanos K, Diamantopoulos A, Spiliopoulos S, Kagadis GC, et al. Infrapopliteal application of sirolimus-eluting versus bare metal stents for critical limb ischemia: analysis of long-term angiographic and clinical outcome. *J Vasc Interv Radiol.* 2009;20(9):1141–50.
5. Dick P, Sabeti S, Mlekusch W, Schlager O, Amighi J, Haumer M, et al. Conventional balloon angioplasty versus peripheral cutting balloon angioplasty for treatment of femoropopliteal artery in-stent restenosis: initial experience. *Radiology.* 2008;248(1):297–302.
6. Karthik S, Tuite DJ, Nicholson AA, Patel JV, Shaw DR, McPherson SJ, et al. Cryoplasty for arterial restenosis. *Eur J Vasc Endovasc Surg.* 2007;33(1):40–3.
7. Zeller T, Rastan A, Sixt S, Schwarzwald U, Schwarz T, Frank U, et al. Long-term results after directional atherectomy of femoropopliteal lesions. *J Am Coll Cardiol.* 2006;48(8):1573–8.
8. Sullivan TM, Ainsworth SD, Langan EM, Taylor S, Snyder B, Cull D, et al. Effect of endovascular stent strut geometry on vascular injury, myointimal hyperplasia, and restenosis. *J Vasc Surg.* 2002;36(1):143–9.
9. Carter AJ, Laird JR, Farb A, Kufs W, Wortham DC, Virmani R. Morphologic characteristics of lesion formation and time course of smooth muscle cell proliferation in a porcine proliferative restenosis model. *J Am Coll Cardiol.* 1994;24(5):1398–405.
10. Farb A, Sangiorgi G, Carter AJ, Walley VM, Edwards WD, Schwartz RS, et al. Pathology of acute and chronic coronary stenting in humans. *Circulation.* 1999;99(1):44–52.
11. Farb A, Virmani R, Atkinson JB, Kolodgie FD. Plaque morphology and pathologic changes in arteries from patients dying after coronary balloon angioplasty. *J Am Coll Cardiol.* 1990;16(6):1421–9.
12. Adiguzel E, Ahmad PJ, Franco C, Bendeck MP. Collagens in the progression and complications of atherosclerosis. *Vasc Med.* 2009;14(1):73–89.
13. Farb A, Weber DK, Kolodgie FD, Burke AP, Virmani R. Morphological predictors of restenosis after coronary stenting in humans. *Circulation.* 2002;105(25):2974–80.
14. Inoue S, Koyama H, Miyata T, Shigematsu H. Pathogenetic heterogeneity of in-stent lesion formation in human peripheral arterial disease. *J Vasc Surg.* 2002;35(4):672–8.
15. Iida O, Uematsu M, Soga Y, Hirano K, Suzuki K, Yokoi H, et al. Timing of the restenosis following nitinol stenting in the superficial femoral artery and the factors associated with early and late restenoses. *Catheter Cardiovasc Interv.* 2011;78(4):611–7.
16. Osherov AB, Gotha L, Cheema AN, Qiang B, Strauss BH. Proteins mediating collagen biosynthesis and accumulation in arterial repair: novel targets for anti-restenosis therapy. *Cardiovasc Res.* 2011;91(1):16–26.

17. Farb A, Kolodgie FD, Hwang JY, Burke AP, Tefera K, Weber DK, et al. Extracellular matrix changes in stented human coronary arteries. *Circulation*. 2004;110(8):940–7.
18. Unverdorben M, Vallbracht C, Cremers B, Heuer H, Hengstenberg C, Maikowski C, et al. Paclitaxel-coated balloon catheter versus paclitaxel-coated stent for the treatment of coronary in-stent restenosis. *Circulation*. 2009;119(23):2986–94.
19. Karnabatidis D, Katsanos K, Spiliopoulos S, Diamantopoulos A, Kagadis GC, Siablis D. Incidence, anatomical location, and clinical significance of compressions and fractures in infrapopliteal balloon-expandable metal stents. *J Endovasc Ther*. 2009;16(1):15–22.
20. Waksman R, Pakala R. Drug-eluting balloon: the comeback kid? *Circ Cardiovasc Interv*. 2009;2(4):352–8.
21. Wiskirchen J, Schober W, Schart N, Kehlbach R, Wersebe A, Tepe G, et al. The effects of paclitaxel on the three phases of restenosis: smooth muscle cell proliferation, migration, and matrix formation: an in vitro study. *Invest Radiol*. 2004;39(9):565–71.
22. Scheller B, Speck U, Abramjuk C, Bernhardt U, Bohm M, Nickenig G. Paclitaxel balloon coating, a novel method for prevention and therapy of restenosis. *Circulation*. 2004;110(7):810–4.
23. Cremers B, Speck U, Kaufels N, Mahnkopf D, Kuhler M, Bohm M, et al. Drug-eluting balloon: very short-term exposure and overlapping. *Thromb Haemost*. 2009;101(1):201–6.
24. Schmidt A, Zeller T, Sievert H, Krankenberg H, Torsello G, Stark MA, et al. Photoablation using the turbo-booster and excimer laser for in-stent restenosis treatment: twelve-month results from the PATENT study. *J Endovasc Ther*. 2014;21(1):52–60.
25. Gandini R, Del GC, Merolla S, Morosetti D, Pampana E, Simonetti G. Treatment of chronic SFA in-stent occlusion with combined laser atherectomy and drug-eluting balloon angioplasty in patients with critical limb ischemia: a single-center, prospective, randomized study. *J Endovasc Ther*. 2013;20(6):805–14.
26. Van Den Berg JC, Pedrotti M, Canevascini R, Chimchila CS, Giovannacci L, Rosso R. Endovascular treatment of in-stent restenosis using excimer laser angioplasty and drug eluting balloons. *J Cardiovasc Surg (Torino)*. 2012;53(2):215–22.
27. Tosaka A, Soga Y, Iida O, Ishihara T, Hirano K, Suzuki K, et al. Classification and clinical impact of restenosis after femoropopliteal stenting. *J Am Coll Cardiol*. 2012;59(1):16–23.
28. Van Den Berg JC. Commentary: laser debulking and drug-eluting balloons for in-stent restenosis: a light at the end of the tunnel? *J Endovasc Ther*. 2013;20(6):815–8.
29. Scheller B, Hehrlein C, Bocksch W, Rutsch W, Haghi D, Dietz U, et al. Two year follow-up after treatment of coronary in-stent restenosis with a paclitaxel-coated balloon catheter. *Clin Res Cardiol*. 2008;97(10):773–81.
30. Stabile E, Virga V, Salemm L, Cioppa A, Ambrosini V, Sorropago G, et al. Drug-eluting balloon for treatment of superficial femoral artery in-stent restenosis. *J Am Coll Cardiol*. 2012;60(18):1739–42.
31. Sixt S, Carpio Cancino OG, Treszl A, Beschoner U, Macharzina R, Rastan A, et al. Drug-coated balloon angioplasty after directional atherectomy improves outcome in restenotic femoropopliteal arteries. *J Vasc Surg*. 2013;58(3):682–6.
32. Trentmann J, Charalambous N, Djawanscher M, Schafer JP, Jahnke T. Safety and efficacy of directional atherectomy for the treatment of in-stent restenosis of the femoropopliteal artery. *J Cardiovasc Surg (Torino)*. 2010;51(4):551–60.

Synergistic Strategy of Laser Atherectomy and Drug Eluting Balloon Angioplasty for Treatment of In-Stent Restenosis in the Superficial Femoral Artery

Roberto Gandini and Costantino Del Giudice

Background

Currently, endovascular procedure is the treatment of choice for femoropopliteal occlusive lesions up to 10 cm and surgical therapy is preferred for chronic total occlusions of common femoral artery and superficial femoral artery >20 cm according to TASC II [1]. Nevertheless, thanks to the results of multicenter trials, primary stenting diffused in common practice to treat claudication and critical limb ischemia due to femoral artery stenosis or occlusion [2–5].

Several multicenter randomized trials compared percutaneous transluminal angioplasty (PTA) associated to a bailout stenting to primary stenting demonstrating that femoral stent may obtain better immediate results with a reduction of flow limiting dissection and plaque elastic recoil.

Although case series and single-arm studies suggested safe and efficacious short-term results with nitinol stents, randomized trials compared to balloon angioplasty and bailout stenting helped to define the real value of this technology. In the 2 published randomized trials, primary stenting offered greater efficacy for primary patency and clinical impact in longer lesions (mean length ≥ 130 mm) [2, 5] but not for short lesions (mean length ≤ 45 mm) [3].

In the recent RESILIENT trial, PTA with bailout stenting was compared to self-expandable nitinol stenting in patient with claudication. Acute angiographic result was superior for the stent group compared with the angioplasty group (95.8 % versus 83.9 %; $P < 0.01$). Moreover At 12 months, freedom from target lesion revascularization was significantly higher from stent group compared with patients treated with angioplasty, respectively 87.3 % versus 45.1 % [4].

Even if several new devices have been introduced in the market with improvements in design and material, several limits

persist in superficial femoral artery stenting due to the occurrence of struts fractures, torsion, restenosis and thrombosis.

Restenosis remains “the Achilles’ heel” of this approach, with rates between 14 and 50 % reported [2–5]. Worse outcomes have been reported for patients with CLI and several other risk factors [6].

Also drug eluting stent recently introduced for treatment of femoropopliteal disease have a restenosis rate of about 17 %, significantly reduced compared with patients treated with bare-metal stents but still not negligible [7].

As a direct consequence of high rates of restenosis, an increased number of patients have recurrence of rest pain and delay or arrest of ulcer healing.

Recently, Tosaka et al. [8] have reported results of balloon angioplasty for femoral-popliteal ISR, considering the relationship to pattern of restenosis. In this study they observed that totally occluded stents (class III) were associated with an increased risk of recurrent ISR, recurrent occlusion and surgical revascularization. Compared to the stenotic ISR group (classes I and II), the freedom from recurrent ISR of class III was remarkably low with higher occlusion rate. This confirms the inadequacy of simple PTA and the need for more sophisticated endovascular techniques to try to obtain an improvement of the results in this category of patients.

In-Stent Restenosis Management

SFA stent occlusion remains a significant clinical problem for the endovascular specialist. Often the first clinical manifestation is the appearance of a claudication, but patients with CLI have more severe consequences associated with an increased risk of amputation and death. Stenting causes reorganization of the plaque and a continuous barotrauma to the vessel intima which triggers complex molecular processes initiating smooth muscle cell migration, proliferation and production of extracellular matrix. The resulting intimal hyperplasia causes a narrowing of the lumen that leads to the generation of clinically detectable restenosis or occlusion.

R. Gandini, MD (✉) • C. Del Giudice, MD
Department of Diagnostic and Molecular Imaging, Interventional Radiology and Radiation Therapy, Fondazione IRCCS Policlinico Tor Vergata, Viale Oxford 81, Rome 00133, Italy
e-mail: roberto.gandini@fastwebnet.it;
costantino.delgiudice@gmail.com

Inadequate antiplatelet therapy, a lack of response to therapy, poor distal run off, elastic characteristics, length and fracture of the stent, excessive overlapping of multiple stents, inadequate stent placement with flow limit in flexion, lifestyle and cardiovascular risk factors of the patients are some of the variables associated with reduced patency at long term follow-up in previous studies [9].

Although bypass surgery is currently considered the gold standard for treatment of this condition, many patients, particularly diabetics with CLI, are not candidates for bypass surgery due to several associated comorbidities and high surgical risk. Despite the occurrence of femoropopliteal stent occlusion in clinical practice [4, 8], there is limited data available regarding the effectiveness of endovascular interventions for this condition.

As previously described, Tosaka et al. demonstrated poor outcomes of patients treated with PTA alone, particularly in type II and III ISR, where this approach should be considered insufficient [8].

These results are comparable with those of Dick et al. [10], who compared efficacy of PTA and cutting balloon technique in the treatment femoropopliteal ISR. In this study length of stented SFA was 10.5 ± 8.8 cm in patients treated with PTA and 10.1 ± 8.1 cm in patients treated with cutting balloon technique without any differences between the two groups. Both techniques obtained excellent immediate results but restenosis rate was high at 6 months follow-up, 65 % in patients treated with PTA and 73 % in patients treated with cutting balloon respectively. The main problem with this approach is that the cutting balloon angioplasty get improved immediate results, but does not prevent the recurrence intimal hyperplasia during follow-up.

Several authors attempted the ISR treatment using a debulking approach. The main purpose of these studies was to demonstrate an increase in patency obtained by removing intimal hyperplasia and organized thrombus rather than through the remodeling obtained with percutaneous angioplasty and stenting. Zeller et al. [11] evaluated the efficacy of percutaneous directional atherectomy in 131 femoropopliteal occlusive lesions, of which 45 were occluded stents. In this study primary and secondary patency rates were higher in de novo lesions compared to in-stent occlusions ($p < 0.002$), and there was no difference between restenotic lesions and in ISR with primary patency rate at 12 months of a 54 %. Trentmann et al. [20] reported 68 % patency rates at 6 months follow-up for femoropopliteal ISR with a medium stent length of 14.1 ± 8 cm treated by percutaneous directional atherectomy. The main limit of this approach should be the difficulty to treat long stent occlusions. In fact the use of directional atherectomy to treat lesions longer than 15 cm could be challenging with long time treatment and poor results. Furthermore, the risk of embolic complications during the procedure is still high.

Moreover directional atherectomy is characterized by an increased risk of distal embolization that could be considered. Drug-eluting balloons have been used for the treatment of ISR in the coronary initially [12, 13] and more recently at the femoral level, demonstrating preliminary positive efficacy and safety results. The choice to perform a DEB angioplasty is based on clinical evidence of a greater inflammatory response of femoropopliteal vascular district after stenting, compared with other elastic arteries such as the iliac ones [14]. The preliminary results of multicenter trials with DEB technology have suggested the usefulness for the treatment of ISR, although the initial trial included only a small number of patients with ISR (17 % of patients in the Thunder trial [15] and 4 % of patients in the FemPac trial [16]). Stabile et al. [17] reported an experience on 39 patients with SFA ISR treated with DEB, demonstrating the safety and efficacy of this therapeutic strategy in this kind of disease with mean lesion length of 82.9 ± 78.9 mm. In this trial a primary patency rate at 12 months of 92.1 % was obtained with lack of recurrent restenosis at 1 year follow-up.

The poor results obtained with conventional PTA associated to the encouraging outcomes obtained with debulking and drug eluting approaches have recently stimulated some authors to perform a combined approaches using laser debulking in association to drug balloon angioplasty in order to improve the patency of the stent with restenosis.

A laser debulking procedure reduces the thrombus and neointimal hyperplasia material within the stent decreasing the procedural risk of distal embolization. Moreover as previously demonstrated the laser debulking is efficacious to obtain a recanalization of long occluded stent compared to the directional atherectomy. Furthermore, the debulking before drug eluting balloon angioplasty has many synergic effects, including the creation of a smooth lumen to improve the DEB-wall contact and the reduction in wall thickness, that allow a more homogenous Paclitaxel uptake in the vessel wall, reducing the jeopardization of the paclitaxel effect due to presence of neointimal hyperplasia. All these aspects lead to better angiographic and clinical outcomes as demonstrated in our experience.

Laser Atherectomy and Drug Eluting Balloon Angioplasty for Treatment of In-Stent Restenosis: Our Experience

Between December 2009 and March 2011 all patients with SFA stent occlusion, from a cohort of 790 patients with critical limb ischemia treated in our diabetic foot care center with endovascular revascularization, were enrolled in a single center randomized study. All patients included in the study were poor candidate for surgical bypass (for several medical co-morbidities or anatomical features), not treatable with

local thrombolysis and with at least a patent BTK vessel. The diagnosis of critical limb ischemia was performed based on the presence of ischemic rest pain or non-healing ulcers/gangrene of the foot.

SFA stent occlusions were treated in 24 patients using a combined laser debulking and drug eluting balloon angioplasty and in 24 patients with drug eluting balloon angioplasty. All patients had associated BTK lesions.

Table 14.1 summarizes baseline demographic characteristics and cardiovascular risk factors.

A dual antiplatelet therapy (Aspirin 100 mg/die and clopidogrel 75 mg/die) was started 3 days before the procedure. In the post-procedural period, the dual antiplatelet therapy was continued for life.

All procedures were performed in dedicated angiographic suites under local anesthesia (Lidocainechlorhydrate 2 %) associated with a mild sedation, from an antegrade puncture of the ipsilateral common femoral artery using a 6 cm 6 F Radifocus introducer II (Terumo, Tokyo Japan), except in an obese patient with a SFA femoral occlusion at the origin,

who was treated performing a contralateral approach. All patients enrolled presented with a type III ISR (total occlusion) following the Tosaka et al classification [8]. An initial intra-arterial heparin bolus (3000–5000 units) followed by a 750–1000-U/h infusion was administered during the procedure to obtain an activating clotting time >250 s.

A fundamental phase of the treatment was to cross the occluded tract to recanalize the stent. This step is particularly hard to perform when the occluded stent is suspended without an in-flow and out-flow. For this reason an adequate pre-procedural imaging using echo-color Doppler, magnetic resonance angiography and computed tomography angiography, consistent with renal function, it is important to understand if the stent is located in the intraluminal or subintimal (Figs. 14.1 and 14.2). In our experience it's crucial to know the position of the stent previously implanted to perform a stent revascularization, as the strategy changes in the presence of an intraluminal or subintimal stent: if the stent is intraluminal stent, a 0.035" hydrophilic straight-tip guide-wire (Terumo, Tokyo, Japan) could be used to cross it

Table 14.1 Demographic characteristics and cardiovascular risk factors

Variable	Group 1 (no ^c = 24)	Group 2 (no ^c = 24)	p
Age, years \pm SD ^a	74.1 \pm 7.2	70.1 \pm 11.6	NS
Sex, male (%)	18 (75)	21 (87.5)	NS
<i>Cardiovascular Risk Factors:</i>			
Hypertension, no (%)	21 (87.5)	18 (75)	NS
Systolic blood pressure (mmHg)	138.3 \pm 1.2	139.7 \pm 0.3	NS
Diastolic blood pressure (mmHg)	75.3 \pm 0.3	78.2 \pm 0.4	NS
Smoker no (%)	17 (70.8)	15 (62.5)	NS
Dislipidemia (yes-%)	21 (87.5)	18 (75)	NS
Family CAD ^b history (yes-%)	12 (50)	9 (37.5)	NS
<i>Associated disease</i>			
Chronic renal failure (yes-%)	3 (12.5)	6 (25)	NS
Ischemic heart disease (yes-%)	9 (37.5)	6 (25)	NS
Previous cerebrovascular disease (yes-%)	6 (25)	3 (12.5)	NS
<i>Symptoms and foot ulcer characteristics</i>			
Rest pain	5 (20.8)	4 (16.7)	NS
Foot ulcer	19 (79.1)	20 (83.3)	NS
Ulcer dimension >5 cm (no ^c -%)	11 (45.8)	8 (37.5)	NS
Infection (yes-%)	13 (54.2)	15 (62.5)	NS
<i>Transcutaneous oxygen and carbon dioxide levels</i>			
Basal TcPO ₂ ^d	14.5 \pm 0.6	13.3 \pm 0.4	NS
Basal TcPCO ₂ ^e	56.7 \pm 0.8	58.3 \pm 1.2	NS
<i>Contraindication to surgical bypass</i>			
Several medical comorbidities with an ASA score 3–4	15 (62.5)	9 (37.5)	NS
Previous failed SFA surgical bypass	3 (12.5)	5 (20.8)	NS
Calcified SFA without distal site anastomosis	6 (25)	10 (41.7)	NS

^aSD standard derivation

^bCAD cardiovascular artery disease

^cNo number

^dTcPO₂ transcutaneous oxygen pressure

^eTcPCO₂ transcutaneous carbon dioxide pressure

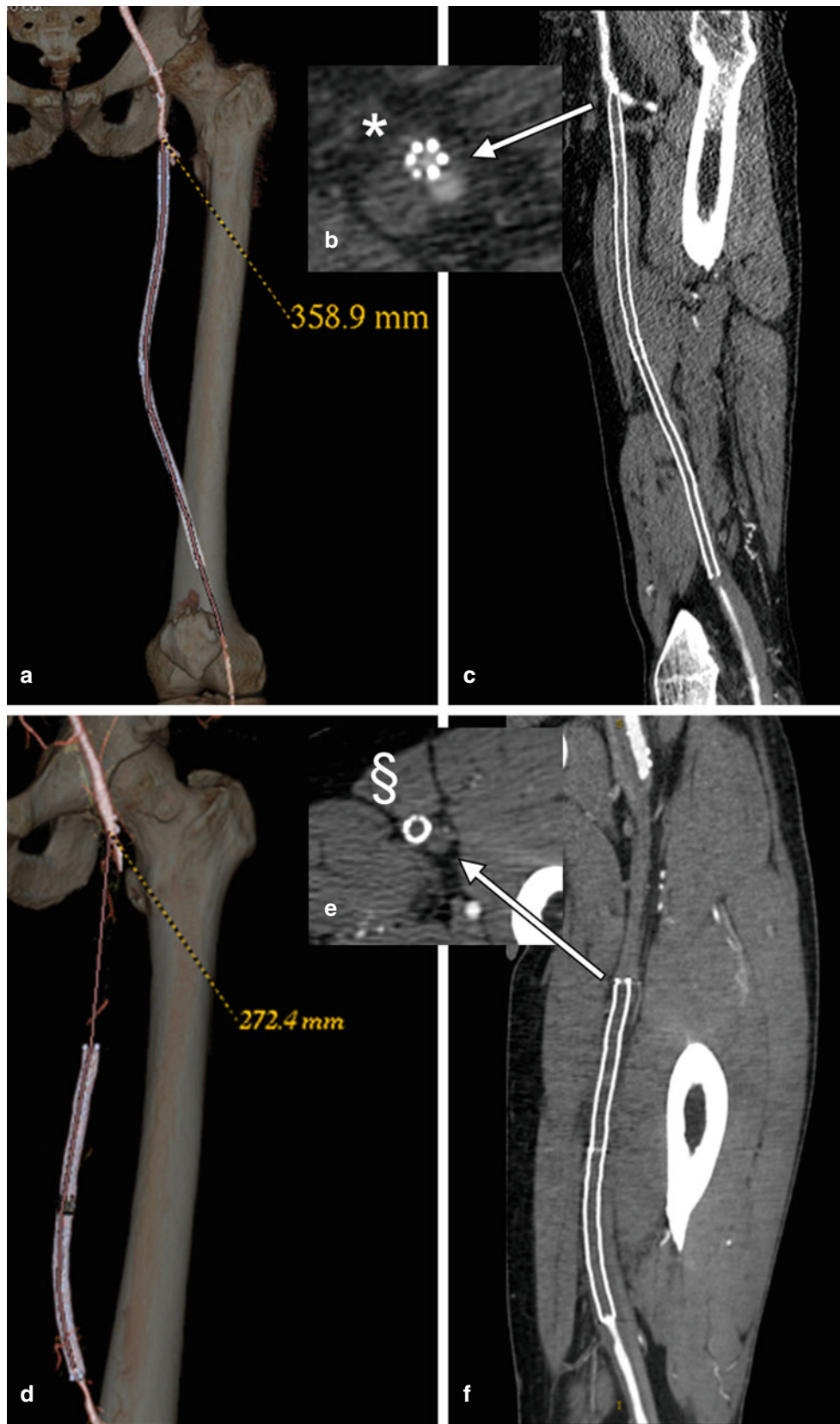


Fig. 14.1 Preprocedural computed tomography angiography with volume rendering (a, d), curved (c, f) and axial view (b, e) showing an example of intraluminal occluded femoral stent (*) (a-c) and a subintimal occluded femoral stent (§) (d-f)

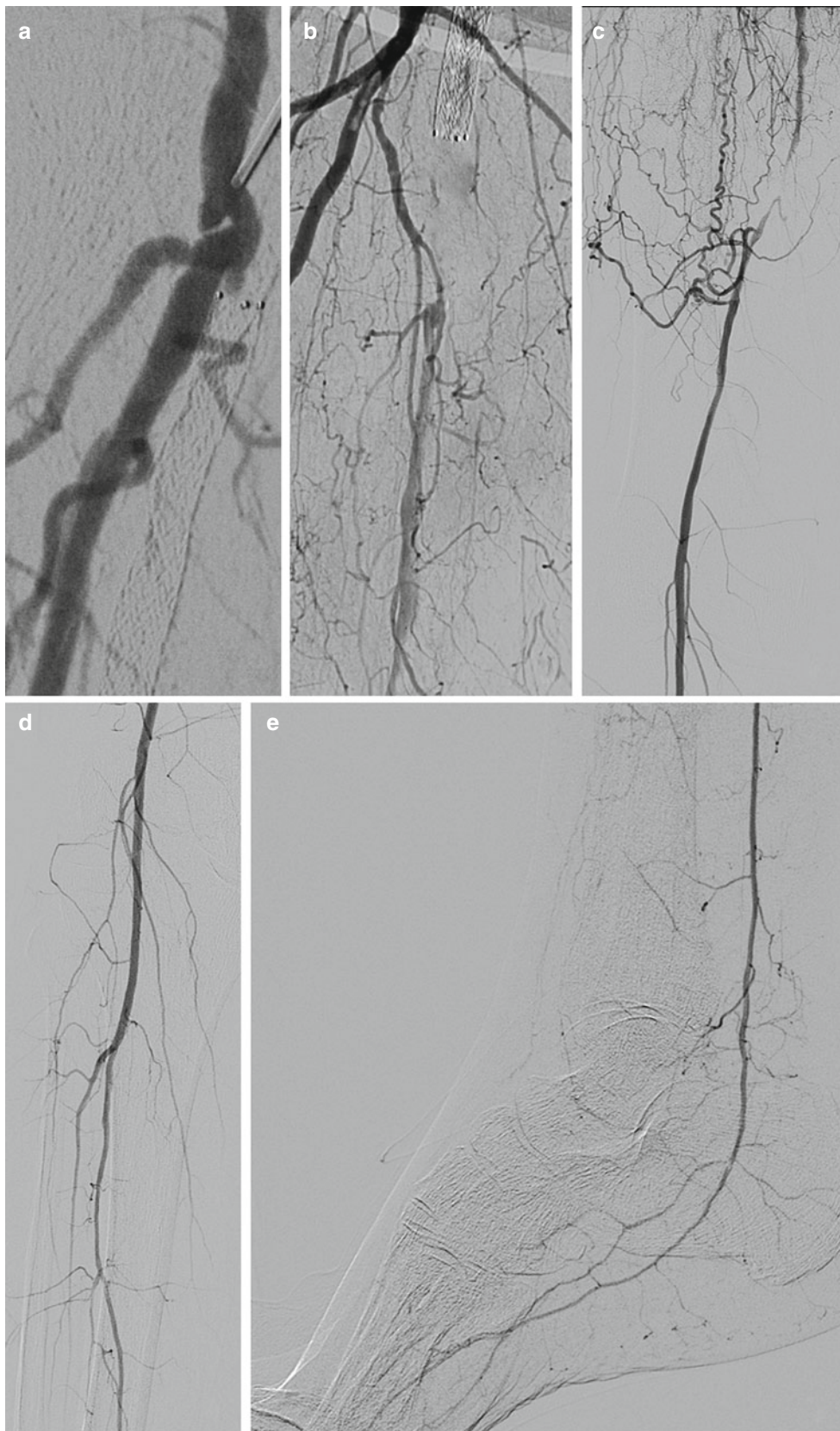


Fig. 14.2 A 56 years old patient with rest pain, previously treated with a in-traluminal femoral stenting. Preprocedural angiography showing an occlusion of the femoral stent at the origin and collateral flow from

the deep femoral artery to the distal superficial femoral (a, b). Pre-occlusive stenosis of the distal superficial femoral artery (c). Occlusion of the peroneal and anterior tibial artery below the knee (d, e)

supported by a diagnostic catheter. If the stent is subintimal a first attempt to recanalize the stent could be performed with a J tip 0.035" guidewire supported by a 5 Fr diagnostic catheter. If the guidewire fails to cross the occluded stent a double approach with puncture of the popliteal artery or a direct stent puncture were performed and the recanalization could be achieved through a dual approach during the same procedure (Fig. 14.3).

In patient treated with laser debulking, a guidewire exchange with a 0.014" guidewire (Pilot 300, Abbott Vascular, Santa Clara, CA, USA) was performed at this time of the procedure and a debulking of the occluded tract was performed with an over the wire 308-nm excimer laser catheter system (Turbo Elite, Spectranetics, Colorado Springs, CO, USA). In all patients we used a 2.0 mm laser fiber catheter with an energy density of 40–60 mJ/mm² (mean 50.6±5.8 mJ/mm²) and a repetition rate of 60 Hz. Three Laser passage were performed for each occluded stent to perform a debulking creating a smooth tunnel in the occluded stent. A better debulking procedure should be obtained with larger laser catheters or turbo booster technology, but a sufficient plaque excision was obtained, as confirmed by our results, without the need to increase post procedural bleeding risk using larger femoral sheaths (Fig. 14.4).

After debulking a low pressure PTA was performed with 4–6 mm conventional catheter balloon for at least 1 min,

followed by a 5–7 mm DEB angioplasty with a standardized inflation time of 1–2 min. No distal filter protection were used considering the reduced embolic risk using the laser debulking.

In patients treated with DEB angioplasty alone, the 0.035 guidewire was maintained and only a low pressure PTA and DEB angioplasty were performed using the same kind of catheter balloons used in the other group (Figs. 14.5 and 14.6).

In our experience no differences were observed in terms of baseline demographics and cardiovascular risk factors in the two groups. Mean length of the treated stent was similar in both group (respectively 20±10.1 cm in group 1 and 23.3±9.1 cm in group 2; p=NS). Treated lesion length was 22.4±9.4 in group 1 vs 25.9±8.7 in group 2 respectively (p=NS).

Procedural success was obtained in all patients. Stents were re-canalized with an antegrade intraluminal approach in 41 patients (85.4 %), respectively 20 in group 1 and 22 patients in group 2 (p=NS). In 1 patients (4.1 %) in group 1 and 1 patients (4.1 %) in group 2 a retrograde recanalization of the stent through puncture of the popliteal artery was performed. In 3 patients (12.5 %) in group 1 and 1 patients (4.1 %) in group 2 a puncture of the stent with a combined double approach was performed. An SFA re-stenting was performed in 2 patients (8.3 %) in group 1. No further stents were released in group 2 at the end of the procedures.

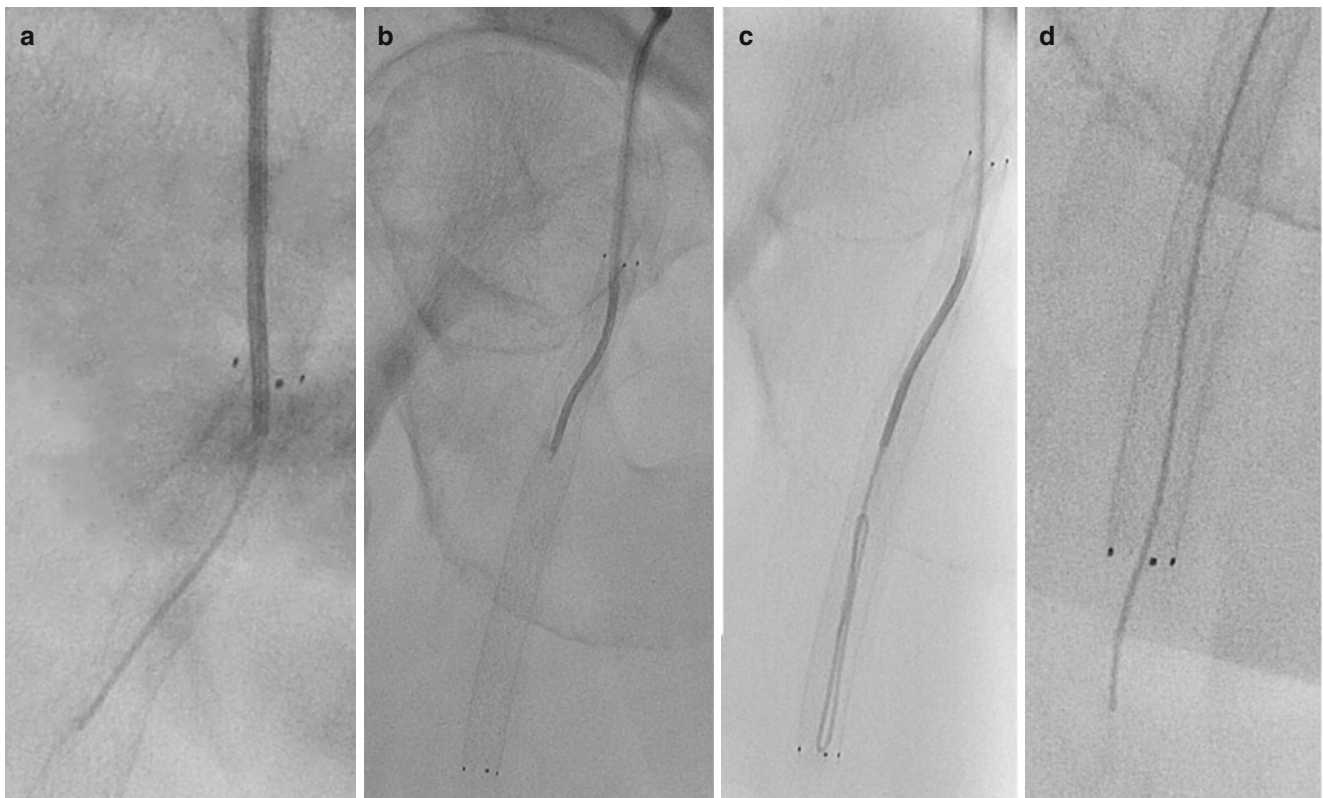


Fig. 14.3 Recanalization of the occluded stent using a straight 0.035" guidewire supported by a 5Fr diagnostic catheter (a–d)

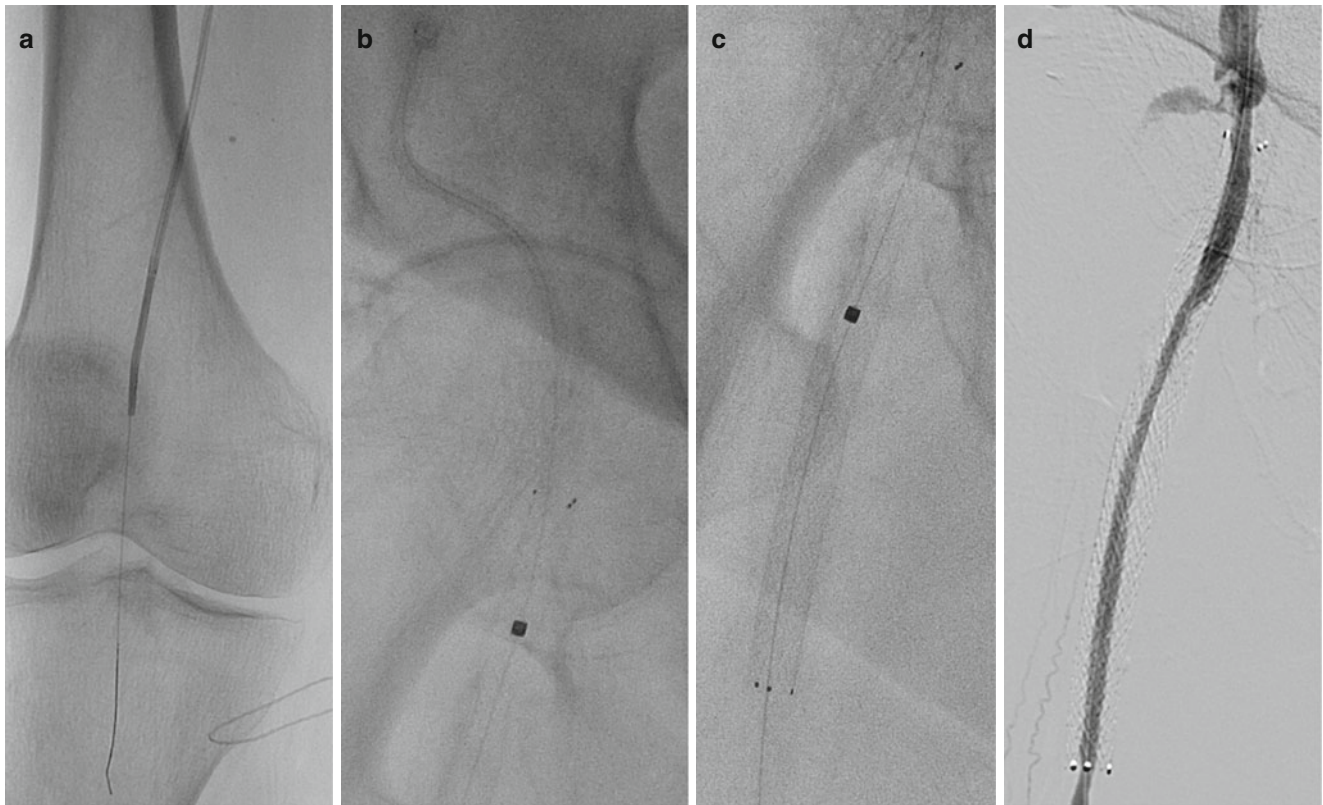


Fig. 14.4 0.014" guidewire exchange (a) and laser debulking of the occluded stent (b, c) with an angiography showing the smooth channel created by the Excimer laser catheter (d)

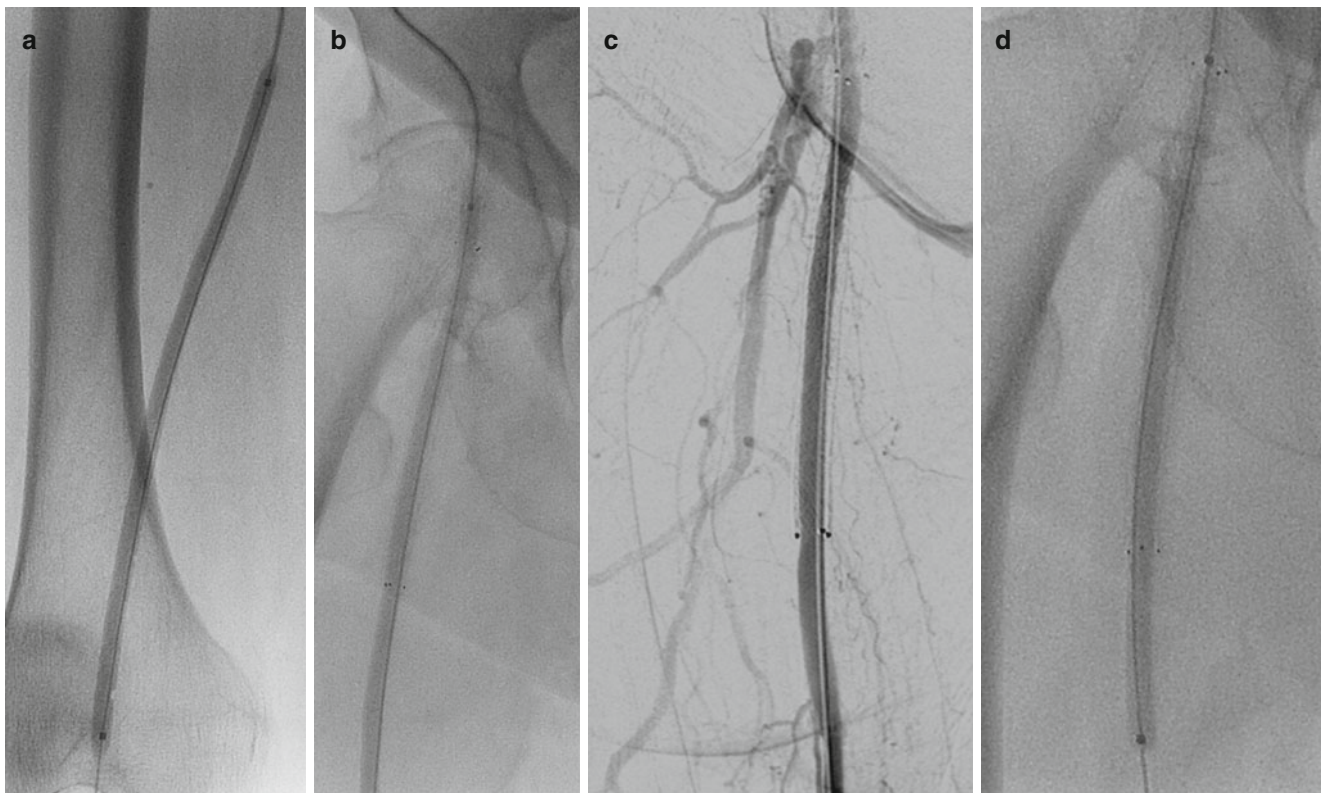


Fig. 14.5 Percutaneous angioplasty of the pre-occlusive distal stenosis (a) and the recanalized stent using a common (b, c) and Paclitaxel eluting balloon (d)

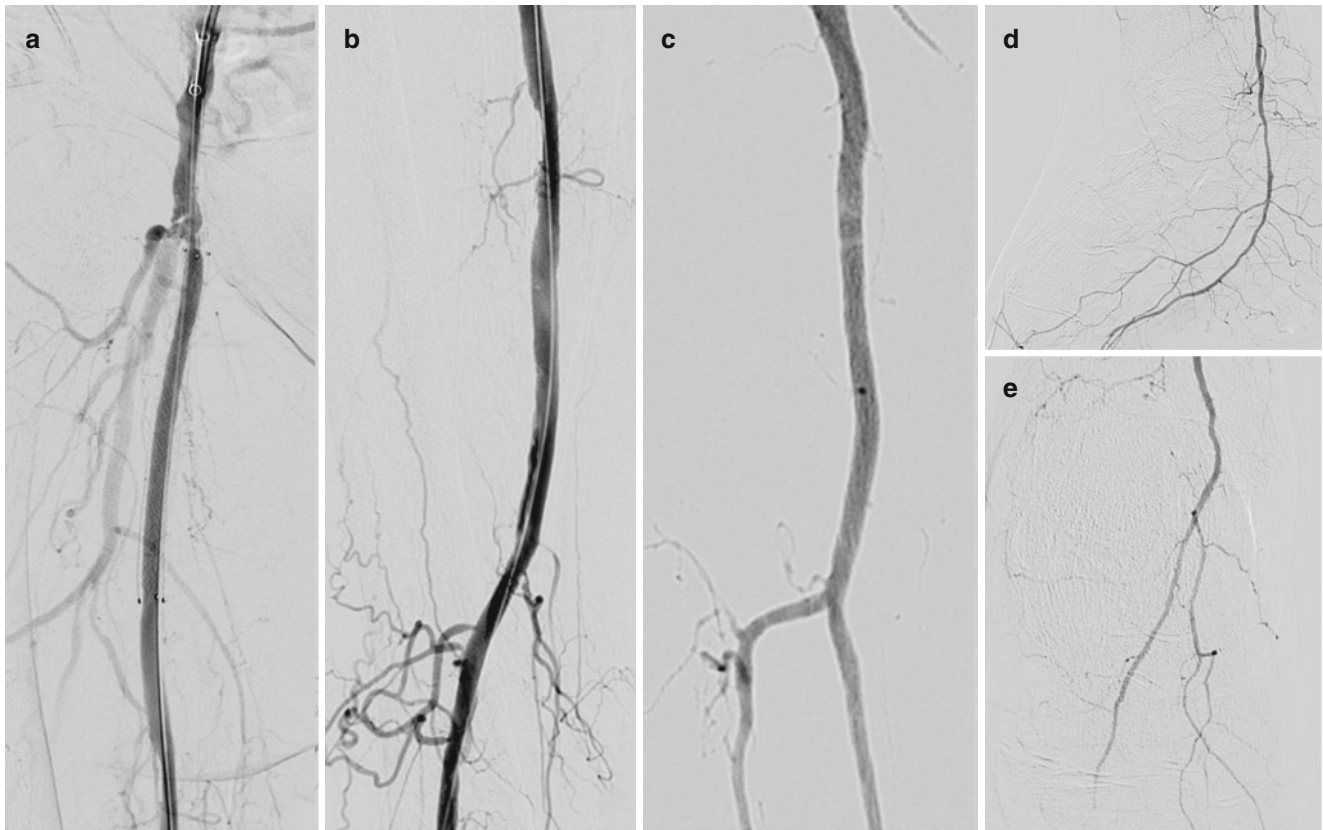


Fig. 14.6 Postprocedural angiography showing the treatment of the femoral artery (a, b) without any distal embolization (c–e)

Immediate angiographic results were similar in both groups, without any difference in term of runoff score. Procedural variables, drug eluting balloon and laser parameters and complications are reported in Table 14.2.

No adverse events related to laser debulking or the drug coating were recorded in either group. Ultrasound control showed a primary patency rate of 100 % at 1 month follow-up in both groups ($p=NS$). At 6 and 12 months the patency rate was significantly higher in patients treated with LD and DEB compared to DEB alone (respectively 91.7 % and 66.7 % in group 1 and 58.3 % and 37.5 % in group 2, $p=0.01$).

TLR at 12 months follow-up was 16.7 % in group 1 and 50 % in group 2 ($p=0.01$).

These technical results were confirmed by clinical outcomes that showed improved results in term of amputation, ulcer healing and death in patients treated with the combined laser debulking and drug eluting balloon angioplasty. Two patients (8.3 %) treated with the combined treatment plan (LD and DEB angioplasty) needed major amputations at 4 and 8 months FU. In contrast, 11 patients (45.8 %) in the group 2 cohort (DEB alone) were subjected to major amputations for extensive gangrene at a mean time to amputation of 5 months FU ($p=0.003$).

Healing of the foot ulcer was recorded in 17 patients (89.4 %) in group 1 and 11 patients of 20 patients (55 %) in group 2 ($p=0.03$). Three patients (12.5 %) died in group 1 during the 12 months follow-up for myocardial infarction. Nine patients (37.5 %) in group 2 died during the 12 months follow-up (7 due to myocardial failure, 1 from stroke and 1 from sepsis), 6 of whom had previously undergone major amputations. this studies in literature.

Many studies in the literature have focused on primary patency of the femoral stents but little is known on the effectiveness and results of treatment after occlusion and restenosis. Particularly in patients with critical limb ischemia, the use of stents should be limited where necessary, as in the case of occlusion of a stent, the prognosis is worse inevitably. Our experience suggest the usefulness of a complete approach using a laser debulking associated to drug eluting balloon angioplasty to treat complex cases as in stent restenosis and occlusions.

The future results of the currently enrolling PHOTOPAC study (Photoablative Atherectomy Followed by a Paclitaxel Coated Balloon to Inhibit Restenosis in In-stent Femoropopliteal Obstructions) will help strengthen the utility of laser debulking in combination with balloon angioplasty in the treatment of medicated stent restenosis.

Table 14.2 Procedure and complications

Variable	Group 1 (no ^a =24)	Group 2 (no ^a =24)	p
Technical success (no ^a -%)	24 (100)	24 (100)	NS
<i>Treated vessels</i>			
Associated femoral re-stenting (no ^a -%)	2 (8.3)	0	NS
Associated below the knee treatment (no ^a -%)	–	–	–
Anterior tibial artery	14 (58.3)	13 (54.2)	NS
Peroneal artery	10 (41.6)	9 (37.5)	NS
Posterior tibial artery	13 (54.2)	11 (45.8)	NS
Postprocedural Runoff score \pm SD ^b	2.3 \pm 0.5	2.5 \pm 0.3	NS
<i>Drug Eluting balloon angioplasty</i>			
Number of DEB used per patients \pm SD ^b	1.8 \pm 1.2	2.1 \pm 2.3	NS
Mean diameter of DEB	5.72 \pm 1.2	5.65 \pm 2.4	NS
Mean length of DEB	13.2 \pm 0.5	13.4 \pm 0.7	NS
<i>Laser parameters</i>			
Energy density (mJ/mm ² \pm SD ^b)	50.6 \pm 5.8	/	–
Repetition rate (Hz \pm SD ^b)	60 \pm 0	/	–
<i>Major periprocedural complications</i>			
Periprocedural death (no ^a -%)	0	0	NS
Periprocedural Limb threatening ischemia (no ^a -%)	0	0	NS
Need of surgical conversion (no ^a -%)	0	0	NS
<i>Minor periprocedural complications</i>			
Peripheral embolization (no ^a -%)	1 (4)	2 (8)	NS
Thrombosis (no ^a -%)	0	0	NS
Vessel dissection (no ^a -%)	0	0	NS
Retroperitoneal bleeding (no ^a -%)	0	0	NS
Hematomas (no ^a -%)	1 (4)	2 (8)	NS

^aNo number^bSD standard derivation

Bibliography

- Norgren L, Hiatt WR, Dormandy JA, Nehler MR, Harris KA, Fowkes FG, et al. Inter-society consensus for the management of peripheral arterial disease (TASC II). *J Vasc Surg.* 2007;45 (Suppl S):S5–67. doi:10.1016/j.jvs.2006.12.037.
- Schillinger M, Sabeti S, Dick P, Amighi J, Mlekusch W, Schlager O, et al. Sustained benefit at 2 years of primary femoropopliteal stenting compared with balloon angioplasty with optional stenting. *Circulation.* 2007;115(21):2745–9. doi:10.1161/CIRCULATIONAHA.107.688341.
- Krankenbergh H, Schluter M, Steinkamp HJ, Burgelin K, Scheinert D, Schulte KL, et al. Nitinol stent implantation versus percutaneous transluminal angioplasty in superficial femoral artery lesions up to 10 cm in length: the femoral artery stenting trial (FAST). *Circulation.* 2007;116(3):285–92. doi:10.1161/CIRCULATIONAHA.107.689141.
- Laird JR, Katzen BT, Scheinert D, Lammer J, Carpenter J, Buchbinder M, et al. Nitinol stent implantation versus balloon angioplasty for lesions in the superficial femoral artery and proximal popliteal artery: twelve-month results from the RESILIENT randomized trial. *Circ Cardiovasc Interv.* 2010;3(3):267–76. doi:10.1161/CIRCINTERVENTIONS.109.903468.
- Schillinger M, Sabeti S, Loewe C, Dick P, Amighi J, Mlekusch W, et al. Balloon angioplasty versus implantation of nitinol stents in the superficial femoral artery. *N Engl J Med.* 2006;354(18):1879–88. doi:10.1056/NEJMoa051303.
- Soga Y, Iida O, Hirano K, Suzuki K, Tosaka A, Yokoi H, et al. Utility of new classification based on clinical and lesional factors after self-expandable nitinol stenting in the superficial femoral artery. *J Vasc Surg.* 2011;54(4):1058–66. doi:10.1016/j.jvs.2011.03.286.
- Dake MD, Ansel GM, Jaff MR, Ohki T, Saxon RR, Smouse HB, et al. Sustained safety and effectiveness of paclitaxel-eluting stents for femoropopliteal lesions: 2-year follow-up from the Zilver PTX randomized and single-arm clinical studies. *J Am Coll Cardiol.* 2013;61(24):2417–27. doi:10.1016/j.jacc.2013.03.034.
- Tosaka A, Soga Y, Iida O, Ishihara T, Hirano K, Suzuki K, et al. Classification and clinical impact of restenosis after femoropopliteal stenting. *J Am Coll Cardiol.* 2012;59(1):16–23. doi:10.1016/j.jacc.2011.09.036.
- Soga Y, Iida O, Hirano K, Yokoi H, Nanto S, Nobuyoshi M. Mid-term clinical outcome and predictors of vessel patency after femoropopliteal stenting with self-expandable nitinol stent. *J Vasc Surg.* 2010;52(3):608–15. doi:10.1016/j.jvs.2010.03.050.
- Dick P, Sabeti S, Mlekusch W, Schlager O, Amighi J, Haumer M, et al. Conventional balloon angioplasty versus peripheral cutting balloon angioplasty for treatment of femoropopliteal artery in-stent restenosis: initial experience. *Radiology.* 2008;248(1):297–302. doi:10.1148/radiol.2481071159.
- Zeller T, Rastan A, Sixt S, Schwarzwald U, Schwarz T, Frank U, et al. Long-term results after directional atherectomy of femoropopliteal lesions. *J Am Coll Cardiol.* 2006;48(8):1573–8. doi:10.1016/j.jacc.2006.07.031.
- Scheller B, Clever YP, Kelsch B, Hehrlein C, Bocks W, Rutsch W, et al. Long-term follow-up after treatment of coronary in-stent

- restenosis with a paclitaxel-coated balloon catheter. *JACC Cardiovasc Interv.* 2012;5(3):323–30. doi:[10.1016/j.jcin.2012.01.008](https://doi.org/10.1016/j.jcin.2012.01.008).
13. Stella PR, Belkacemi A, Waksman R, Stahnke S, Torguson R, von Strandmann RP, et al. The Valentines Trial: results of the first one week worldwide multicentre enrolment trial, evaluating the real world usage of the second generation DIOR paclitaxel drug-eluting balloon for in-stent restenosis treatment. *EuroIntervention.* 2011;7(6):705–10. doi:[10.4244/EIJV7I6A113](https://doi.org/10.4244/EIJV7I6A113).
 14. Schillinger M, Exner M, Mlekusch W, Haumer M, Ahmadi R, Rumpold H, et al. Inflammatory response to stent implantation: differences in femoropopliteal, iliac, and carotid arteries. *Radiology.* 2002;224(2):529–35. doi:[10.1148/radiol.2241011253](https://doi.org/10.1148/radiol.2241011253).
 15. Tepe G, Zeller T, Albrecht T, Heller S, Schwarzwald U, Beregi JP, et al. Local delivery of paclitaxel to inhibit restenosis during angioplasty of the leg. *N Engl J Med.* 2008;358(7):689–99. doi:[10.1056/NEJMoa0706356](https://doi.org/10.1056/NEJMoa0706356).
 16. Werk M, Langner S, Reinkensmeier B, Boettcher HF, Tepe G, Dietz U, et al. Inhibition of restenosis in femoropopliteal arteries: paclitaxel-coated versus uncoated balloon: femoral paclitaxel randomized pilot trial. *Circulation.* 2008;118(13):1358–65. doi:[10.1161/CIRCULATIONAHA.107.735985](https://doi.org/10.1161/CIRCULATIONAHA.107.735985).
 17. Stabile E, Virga V, Salemme L, Cioppa A, Ambrosini V, Sorropago G, et al. Drug-eluting balloon for treatment of superficial femoral artery in-stent restenosis. *J Am Coll Cardiol.* 2012;60(18):1739–42. doi:[10.1016/j.jacc.2012.07.033](https://doi.org/10.1016/j.jacc.2012.07.033).

Richard E. Redlinger Jr., Sadaf S. Ahanchi,
and Jean M. Panneton

Introduction

Acute pathologies of the descending thoracic aorta can involve the left subclavian artery, complicating the proximal landing zone during thoracic endovascular aneurysm repair (TEVAR). Involvement of the left subclavian can mandate either traditional open repair or TEVAR with coverage of the left subclavian artery with or without revascularization. Emergent open repair for acute aortic pathology confers mortality rates approaching 20 %, and significant morbidity, including an 18.6 % post-operative spinal cord ischemia rate [1, 2]. Early experience with intentional endograft coverage of the left subclavian without revascularization was thought to be a viable alternative to extend the applicability of TEVAR in this setting of great vessel encroachment [3]. Unfortunately, expanding experience with intentional left subclavian artery coverage without revascularization has been found to portend a significantly increased risk of subclavian steal syndrome, arm claudication, vertebral territory stroke, and spinal cord ischemia by eliminating collateral blood supply to the spinal cord from the vertebral artery [4, 5].

As such, obtaining an adequate proximal seal without compromising left subclavian artery patency has remained an important challenge as TEVAR experience increases and expands. Adjunctive options to revascularize the left subclavian artery include elective debranching prior to TEVAR, the chimney technique by deploying a left subclavian stent parallel to the thoracic endograft, prefabricated branched endograft deployment, or surgeon modified endografts [6–9]. Elective bypass to or transposition of the

left subclavian often requires long operative times and the need for multiple surgical interventions if staged endografting is planned. Open subclavian revascularization performed as an adjunct to TEVAR has been reported to carry a 30-day postoperative stroke and combined stroke/death rates of 8.9 % and 12.9 %, respectively [10]. Open revascularization also has the potential for vocal cord paralysis and injury to the thoracic duct, brachial plexus, and phrenic nerve. Prefabricated, patient customized devices require extensive planning with precise preoperative imaging, time for graft manufacturing, and are currently not commercially available in the United States. For this reason, these modalities are often not advisable or feasible for patients presenting with acute thoracic aortic pathologies requiring emergent repair.

The limited options to maintain left subclavian artery patency in the setting of TEVAR in an urgent or emergent setting has led to the technique of a physician modified endograft utilizing retrograde laser fenestration to revascularize the left subclavian during zone II deployment [11]. This relatively simple intraoperative method of laser-mediated endograft modification provides a rapid, reproducible method of fenestrating the endograft material to revascularize aortic branches for a variety of acute thoracic aortic pathologies.

Ex Vivo Experiments

Laser fenestration of the Dacron fabric of a Talent stent-graft (Medtronic Vascular, Santa Rosa, CA, USA) was first described by Murphy et al. in bench-top experiments. In their description, a 2.3-mm fenestration was created that maintained the integrity of the surrounding Dacron fabric even after balloon dilation of the laser-cut opening [12]. These results were then replicated by our facility to verify feasibility prior to clinical application. These tests demonstrated a clean and sealed 2.5–3-mm fenestration created within 3–5 s after application of laser energy (45 mJ/mm² fluence at a rate of 25 pulses per second) using a 2.0–2.5-mm Turbo Elite laser catheter (Spectranetics, Colorado Springs, CO). The gross

R.E. Redlinger Jr., MD • J.M. Panneton, MD, FRCSC, FACS (✉)
S.S. Ahanchi, MD
Division of Vascular Surgery,
Eastern Virginia Medical School,
Norfolk, VA, USA
e-mail: rredlinger@gmail.com; pannetjm@evms.edu;
ssahanch@sentara.com

integrity of the fabric was maintained even after balloon dilation and stent placement [11]. During *ex vivo* experiments of laser and endograft interactions, the laser beam was also noted to deflect off the nitinol stents of the endograft. The nitinol stents were examined after laser energy exposure, and their integrity also remained grossly intact. Furthermore, the gross integrity of the fabric was maintained after balloon dilation and stent placement (Fig. 15.1).

Collaborative work from our institution additionally examined the microscopic alteration to endograft fabrics following laser fenestration [13]. The Medtronic Valiant endograft, made of nitinol stents and monofilament woven Dacron fabric, and the Cook Zenith TX2 (Cook Inc., Bloomington, IN) comprised of stainless steel stents and multifilament woven Dacron fabric were subjected to laser fenestration. The fenestrations were subsequently dilated with 8, 10 or 12-mm diameter angioplasty balloons. The fenestrations were then observed under light and scanning electron microscopy. The fenestrations were shown to be reproducible in both Dacron-based endograft devices, but both devices demonstrated elements of fraying (more with the multifilament TX2) and/or tearing (more with the monofilament Valiant). The size and directions of the fenestrations were more predictable with the 8-mm diameter balloon whereas the results obtained with the 10 and 12-mm diameter balloons were more dispersed. The diameter of balloon used for dilation of the laser fenestration was felt to play the most important role to control the overall size of the graft

fenestration. The larger sized 10 and 12 mm balloons were felt to be more likely to lead to a long tear of the graft fenestration, which could damage the structural integrity of the endograft.

Initial Descriptions of Branch Vessel Fenestration

The recognized clinical benefit for aortic branch vessel revascularization led to an exploration for alternative techniques for graft modification, McWilliams and colleagues first evaluated percutaneous *in situ* graft fenestration and found it to be a promising avenue for endograft modification [9]. In both an *in vitro* and an *in vivo* canine model, fenestration of a Dacron stent-graft was found to be technically feasible. Initial graft puncture was performed with the stiff end of a 0.014-inch coronary guidewire followed by fabric dilation with a cutting balloon to create a fenestration. The authors recognized that an immediate application of this technique would be fenestration of the left subclavian artery when covered intentionally to extend the neck of a thoracic aneurysm. The same authors expounded upon this experience with the first clinical report of *in situ* graft fenestration after deliberate coverage of the left subclavian artery during TEVAR. Short-term follow-up demonstrated technical success with stent patency on imaging and a symmetrical upper extremity blood pressures following left subclavian fenestration [14].

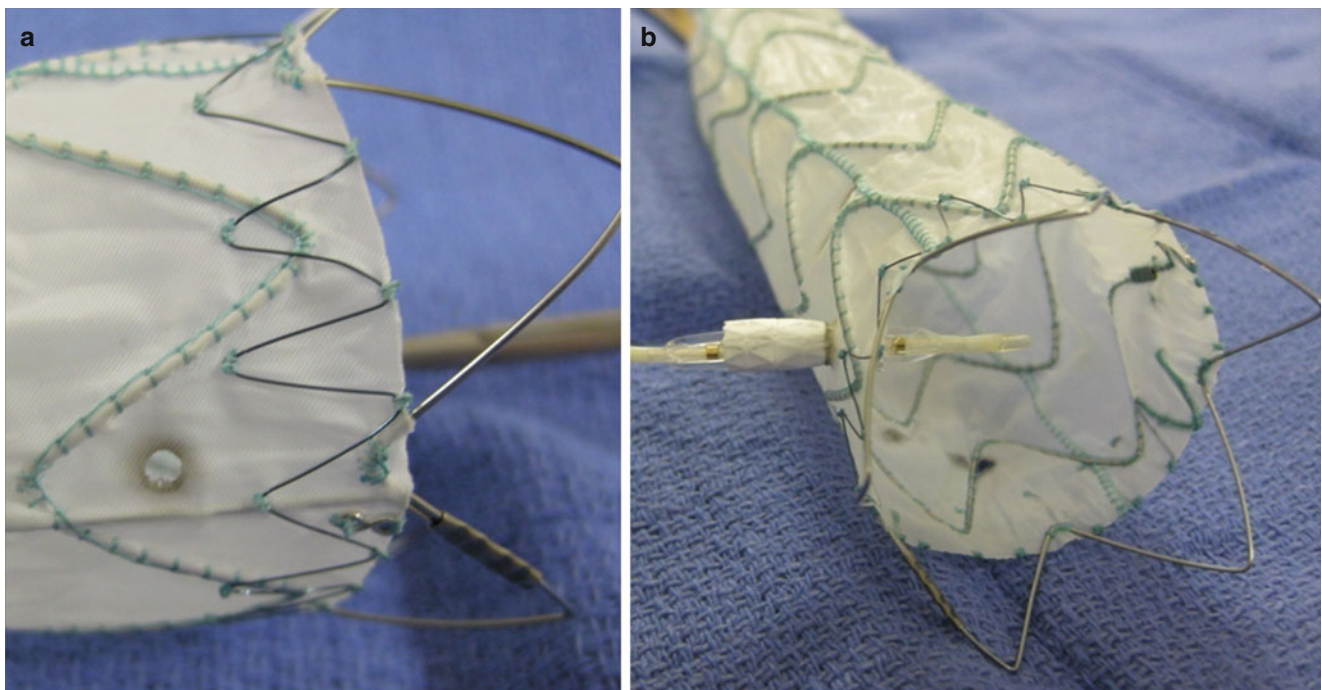


Fig. 15.1 (a) *Ex vivo* application of laser energy to a Dacron endograft demonstrated a clean and sealed fenestration (b) gross fabric integrity was maintained after balloon dilation and covered stent placement

Murphy et al. expounded on the premise of endograft modification to maintain aortic branch vessel patency with the first description of percutaneous in situ laser graft fenestration to rescue a left subclavian artery covered during repair following blunt traumatic aortic injury [12]. The authors described a 26-year-old man with a partially contained acute aortic transection just distal to the takeoff of the left subclavian artery following blunt chest trauma. The operating surgeon elected to perform thoracic endografting with in-situ graft fenestration to decrease the risk of posterior circulation stroke, spinal cord ischemia, and subclavian steal syndrome. A laser catheter was advanced through the left subclavian to fenestrate the Dacron thoracic stent-graft endograft and the fenestration was dilated and stented with a covered stent. Follow up of this initial case report documented uneventful patient recovery with TEVAR and left subclavian artery patency on follow-up imaging. The authors expounded that retrograde fenestration of the left subclavian artery combined with endovascular repair extended the indications of TEVAR for the management of acute traumatic thoracic aortic injuries to further minimize the risks associated with traditional open surgical repair in this setting.

In Situ Fenestration Technique & Considerations

The authors' experience employing TEVAR with retrograde laser fenestration to revascularize the left subclavian artery has been utilized thus far in an urgent or emergent basis secondary to unremitting symptoms or rupture on a compassionate use basis after proper informed consent of patients. Emergent cases were generally performed within hours of patient presentation while urgent cases varied in timing, as these patients underwent repair following an initial, failed attempt at medical management and ultimately were deemed to require urgent operative intervention.

For in situ laser fenestration during TEVAR, pre-operative computed tomography (CT) scan with 3D reconstruction is very helpful with pre-operative planning. CT scan measurements should be used to document the length and diameters of the aorta and the left subclavian artery, identify the takeoff of the vertebral artery from the left subclavian and to fully understand the arch anatomy. These measurements then guide the selection of endograft and left subclavian stent diameters and lengths in preparation for the procedure. The proposed location of the fenestration on the endograft and its final relationship within the aortic arch can also be predicted. During our experience, we have found that in addition to the routine measurements gathered during TEVAR, preoperative analysis of the angle of the left subclavian artery to the aorta is also helpful to predict technical feasibility of fenestration,

with the optimal angle of the laser (and as such the subclavian artery) oriented 90° to the endograft fabric. Routine pre-operative intracranial imaging is not mandatory, but carotid duplex ultrasound can be obtained pre-operatively to determine patency or dominance of the vertebral arteries.

Once in the operating theater, we obtain open femoral artery access, percutaneous contralateral femoral artery access with a 5 French sheath, and finally left brachial artery access (either open or percutaneously) proximal to the antecubital fossa with a 7 or 8 French sheath. Intravascular ultrasound (IVUS) is performed to measure the proximal normal aorta, mark the location of arch vessels, and in the setting of aortic dissection to verify true lumen location and localize the entry tear of the dissection. The remainder of the aorta from the left subclavian distally is then inspected with IVUS noting the location of the visceral vessels.

An 8 French Lamp sheath (St. Jude Medical, St. Paul, MN) with preformed angle at the tip is placed via retrograde left brachial artery access at the ostium of the left subclavian artery. A 2.0–2.5-mm Turbo Elite laser catheter (Spectranetics, Colorado Springs, CO) is placed at the ostium of the left subclavian over a 0.018-inch Platinum Plus wire (Boston Scientific, Natick, MA) (Fig. 15.2).

Both the sheath and laser catheter are positioned prior to stent graft deployment and within minutes the laser fenestration is performed, limiting potential ischemia time to less than 5 min in a majority of cases. Thoracic endografts deployed in our experience have been either Medtronic Talent/Valiant or Cook TX2 stent-grafts. The endograft is inserted into the aorta over a stiff wire and an angiogram is performed to mark the location of the arch vessels. The endograft is then deployed after positioning the fabric of the endograft in the appropriate landing position based upon the arch anatomy. The proximal bare metal stent portion of the endograft is released allowing removal of the delivery system. Next, judicious use of multiple C-arm projections is performed to verify the most perpendicular angle of the sheath and laser fiber to the endograft material prior to laser fenestration (Fig. 15.3). This maneuver ensures that the laser fiber is aligned appropriately with the endograft and is facilitated by the preformed lamp sheath.

The laser fiber is gently advanced to make contact with the deployed Dacron endograft, followed by laser energy application (45 mJ/mm² fluence at a rate of 25 pulses per second) for 3–5 s to create the fenestration. The 0.018-inch wire is then advanced through the laser catheter and fenestration into the main endograft lumen and the laser fiber is removed. A Quick-Cross support catheter (Spectranetics, Colorado Springs, CO) is then advanced into the ascending aorta from the brachial access. This catheter is then used to carefully exchange for a stiff 0.035" wire while maintaining brachial sheath position (Fig. 15.4). The endograft fenestration is then pre-dilated using a 6-mm balloon. Again,

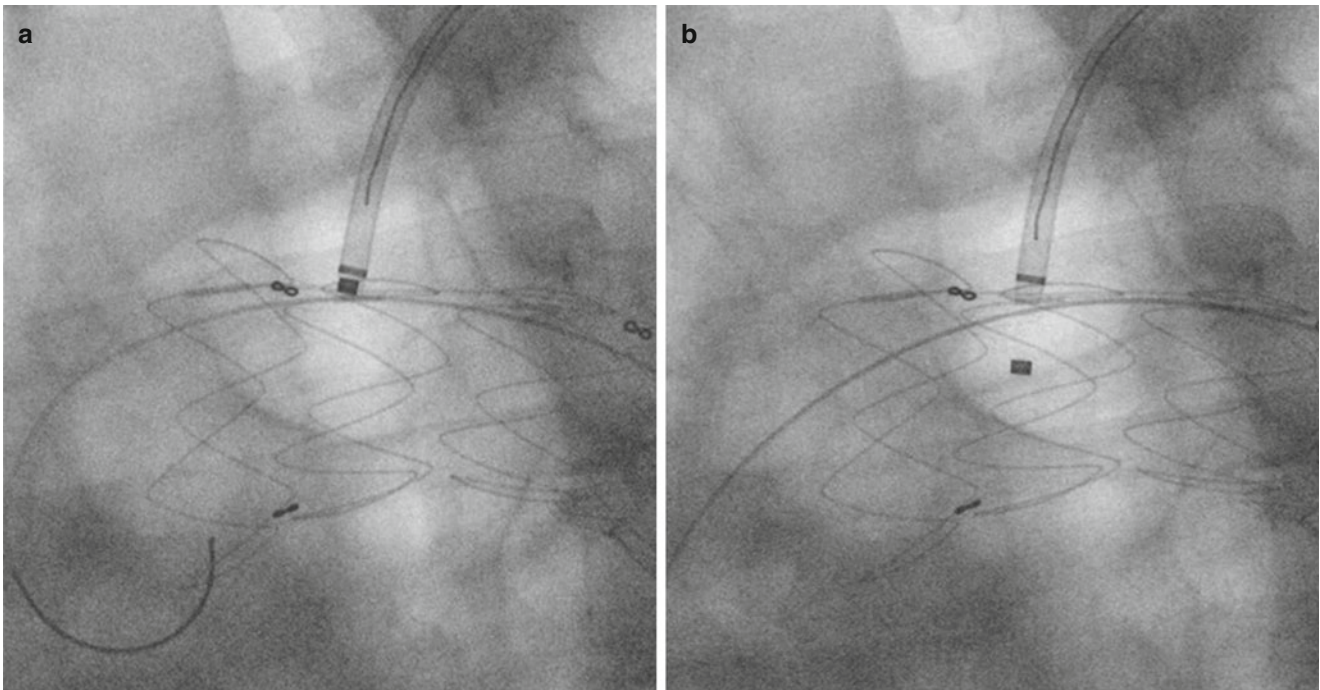


Fig. 15.2 (a) The laser catheter is placed at the ostium of the left subclavian artery perpendicular to the endograft over a 0.018-inch wire. To create a clean, circular fenestration, the laser fiber should ideally be

oriented at a 90° angle to the endograft. (b) Laser energy is applied in conjunction with gentle laser to endograft contact pressure for 3–5 s

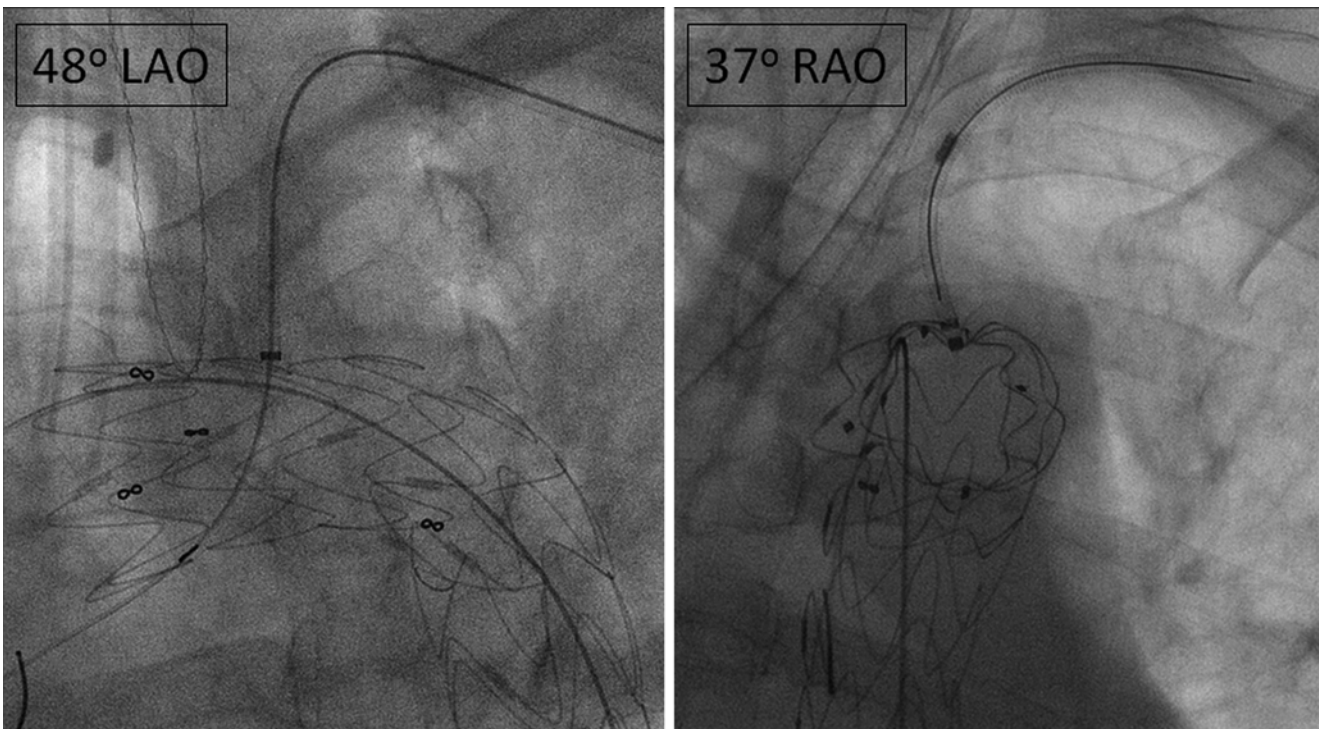


Fig. 15.3 The judicious use of multiple C-arm projections is essential to verify the most perpendicular angle of the sheath and laser fiber to the endograft material prior to laser application. This maneuver ensures that the laser fiber is aligned appropriately with the endograft fabric



Fig. 15.4 Once laser fiber contact with the Dacron endograft is confirmed, laser energy is applied to create the fenestration. An 0.018-inch wire is advanced through the laser catheter and fenestration into the endograft lumen. A Quick-Cross support catheter is then advanced into the ascending aorta from the brachial access to carefully exchange for a stiff 0.035" wire, while maintaining brachial sheath position

multiple angiographic projections are used to verify the correct position of the fenestration and balloon. This is followed by deployment of an 8- to 10×38-mm balloon-expandable iCAST covered stent (Atrium, Hudson, NH). The stent is deployed approximately one quarter into the endograft lumen and three quarters into the branch vessel being aware of the position of the vertebral artery. The intra-endograft portion of the covered stent is then flared using a 14×20-mm balloon introduced from the brachial access. Finally, completion aortography is performed to confirm endograft and LSA fenestration patency without endoleak (Fig. 15.5).

The most important factor that will determine technical ease and success of laser fenestration is the angle of the LSA takeoff from the aortic arch. To create a clean, circular fenestration the laser fiber ideally must be oriented at a 90° angle to the endograft and too acute an angle (<30°) will not allow the fenestration to be created. This anatomic scenario should preclude in situ laser fenestration. Other unfavorable anatomic criteria that are contraindications for the use of this technique include: subclavian artery origin dilatation greater than 12-mm (which would be greater than the size of the largest available iCast covered stents and compromise seal), a low vertebral artery take off not allowing for an appropriate

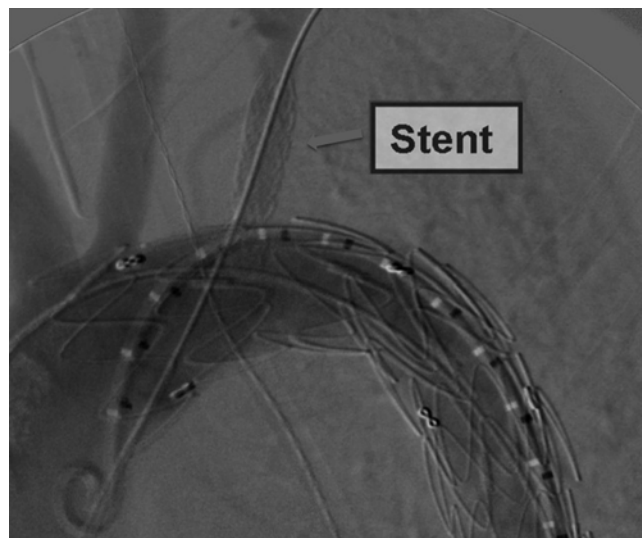


Fig. 15.5 The iCAST stent is deployed from the brachial access approximately one quarter into the endograft lumen and three quarters into the branch vessel with the intra-endograft portion of the covered stent flared with an angioplasty balloon introduced from the brachial access. Completion aortography confirms endograft and left subclavian fenestration patency without endoleak

landing zone for the covered stent and involvement of the left subclavian artery by dissection or aneurysmal disease.

Laser Fenestration Results

Our published institutional experience reported TEVAR with in situ retrograde laser fenestration of the left subclavian artery successfully performed on 22 patients in an urgent or emergent setting [15]. The indications for TEVAR included large symptomatic thoracic aortic aneurysm, acute symptomatic type B aortic dissection and intramural hematoma and/or penetrating aortic ulcer. Four of these patients had evidence of aortic rupture. All 22 patients underwent technically successful TEVAR. The proximal graft through which the fenestration was created was a Medtronic Talent or Valiant endograft in 19 of the 22 patients, while in the remaining 3 patients the fenestrated graft was a Cook TX2. An average of two endografts (range 1–4) were placed during TEVAR, with 18 patients having multiple endografts placed. The left subclavian iCAST covered stents that were deployed ranged in diameter from 8 to 10 mm. The mean operative time for TEVAR with laser fenestration was 154±65 min with an average of 20 min of the total case time required for obtaining brachial access, fenestration of the graft and LSA stent deployment.

Percutaneous left brachial artery access was performed in 8 patients and the remaining 14 patients underwent open left brachial exposure. While there were no major in situ laser fenestration related operative complications, the two minor

operative complications noted in our series were related to brachial artery access. These two patients required early post-operative re-intervention in the form of exploration and repair of a left brachial artery following percutaneous access and evacuation of both a groin and left arm hematoma in a patient who had open left brachial access.

Our mid-term follow at a mean of 11 months has found 100 % primary patency of the left subclavian artery stents as demonstrated by routine follow up CT angiogram imaging (Fig. 15.6). There is one patient with an asymptomatic left subclavian stent stenosis. Re-intervention was required in two patients noted to have type II endoleaks from the left subclavian artery. Both of these patients underwent successful endovascular coil embolization via combined percutaneous femoral and brachial artery access. Endoleak obliteration after re-intervention was confirmed with completion

angiography and follow-up CT angiogram. There were no fenestration-related Type I or III endoleaks. There have been no left arm claudication symptoms or vertebral basilar symptoms on follow up examination in any of the patients with retrograde LSA fenestration.

Conclusion

The technique of in situ retrograde laser fenestration offers a relatively simple, rapid and reproducible method of in vivo endograft modification during emergent TEVAR that can be applied in a spectrum of acute thoracic aortic pathologies. The high technical success, low fenestration-related morbidity, and excellent mid-term patency support this technique of intraoperative emergency endograft modification in the absence of available branched devices for arch deployment.



Fig. 15.6 A representative CT scan obtained at 39-month follow-up CTA after in situ retrograde laser fenestration demonstrates left subclavian artery stent patency, without evidence of endoleak, and stable aortic size

References

1. Galloway AC, Schwartz DS, Culliford AT, Ribakove GH, Esposito RA, Baumann FG, et al. Selective approach to descending thoracic aortic aneurysm repair: a ten-year experience. *Ann Thorac Surg.* 1996;62:1152–7.
2. Conrad MF, Cambria RP. Contemporary management of descending thoracic and thoracoabdominal aortic aneurysms: endovascular versus open. *Circulation.* 2008;117(6):841–52.
3. Alsac JM, Boura B, Desgranges P, Fabiani JN, Becquemin JP, Leseche G. Immediate endovascular repair for acute traumatic injuries of the thoracic aorta: a multicenter analysis of 28 cases. *J Vasc Surg.* 2008;48:1369–74.
4. Rizvi AZ, Murad MH, Fairman RM, Erwin PJ, Montori VM. The effect of left subclavian artery coverage on morbidity and mortality in patients undergoing endovascular thoracic aortic interventions: a systematic review and meta-analysis. *J Vasc Surg.* 2009;50:1159–69.
5. Chung J, Kasirajan K, Veeraswamy RK, Dodson TF, Salam AA, Chaikof EL, et al. Left subclavian artery coverage during thoracic endovascular aortic repair and risk of perioperative stroke or death. *J Vasc Surg.* 2011;54:979–84.
6. Lee TC, Andersen ND, Williams JB, Bhattacharya SD, McCann RL, Hughes GC. Results with a selective revascularization strategy for left subclavian artery coverage during thoracic endovascular aortic repair. *Ann Thorac Surg.* 2011;92:97–102.
7. Criado FJ. A percutaneous technique for preservation of arch branch patency during thoracic endovascular aortic repair (TEVAR): retrograde catheterization and stenting. *J Endovasc Ther.* 2007;14:54–8.
8. Saito N, Kimura T, Odashiro K, Toma M, Nobuyoshi M, Ueno K, et al. Feasibility of the Inoue single-branched stent-graft implantation for thoracic aortic aneurysm or dissection involving the left subclavian artery: short- to medium-term results in 17 patients. *J Vasc Surg.* 2005;41:206–12.
9. McWilliams RG, Fearn SJ, Harris PL, Hartley D, Semmens JB, Lawrence-Brown MM. Retrograde fenestration of endoluminal grafts from target vessels: feasibility, technique, and potential usage. *J Endovasc Ther.* 2003;10:946–52.
10. Scali ST, Chang CK, Pape SG, Feezor RJ, Berceli SA, Huber TS, et al. Subclavian revascularization in the age of thoracic endovascular aortic repair and comparison of outcomes in patients with occlusive disease. *J Vasc Surg.* 2013;58:901–9.
11. Ahanchi SS, Almaroof B, Stout CL, Panneton JM. In situ laser fenestration for revascularization of the left subclavian artery during emergent thoracic endovascular aortic repair. *J Endovasc Ther.* 2012;19:226–30.
12. Murphy EH, Dimaio JM, Dean W, Jessen ME, Arko FR. Endovascular repair of acute traumatic thoracic aortic transection with laser-assisted in-situ fenestration of a stent-graft covering the left subclavian artery. *J Endovasc Ther.* 2009;16:457–63.
13. Udgiri N, Lin J, Guidoin R, Zhang Z, Dexter D, Guan X, et al. Scanning electron microscope analysis of ex-vivo laser fenestration of thoracic endografts: variables for optimal fenestrations? Society for Clinical Vascular Surgery 42nd Annual Symposium, 18 Mar 2014, Carlsbad.
14. McWilliams RG, Murphy M, Hartley D, Lawrence-Brown MM, Harris PL. In situ stent-graft fenestration to preserve the left subclavian artery. *J Endovasc Ther.* 2004;11:170–4.
15. Redlinger RE, Ahanchi SS, Panneton JM. In situ laser fenestration during emergent thoracic endovascular aortic repair is an effective method for left subclavian artery revascularization. *J Vasc Surg.* 2013;58(5):1171–7.

Robert Splinter

Introduction

Worldwide the two main causes for macro-reentry ventricular arrhythmias are coronary artery disease and associated post-infarction ischemia and Chagas' disease. Post myocardial infarction (MI) ventricular tachycardia (VT) is the leading clinical concern in the northern hemisphere. Atrial diseases also cause arrhythmias, primarily resulting from anatomical anomalies along the long axis of the crista terminalis in the right atrium, next to cell-to-cell coupling delays at the root of the coronary sinus, as well as electrical distortions at the root of the pulmonary vein of the left atrium, next to a minority of random diffuse anatomical damage in non-specific locations of the atrial tissue in less than 30 % of the patient population. All result in various forms of atrial fibrillation [1]. Additionally, both ventricular and atrial fibrillation can be treated in specific fashion, particular to the anatomic and/or electro-physiologic data that can be obtained from imaging and sensing [2].

In general, the guidelines for patients with arrhythmogenic episodes resulting from either non-ischaemic cardiomyopathy (NICM) or ischaemic cardiomyopathy (ICM) single out the biological integration of an implantable cardioverter-defibrillator (ICD). These patients are at risk for sudden cardiac death and require treatment. The ICD imposes several constraints on the life-style of the recipient. A more permanent solution would be beneficial and improves the quality of life.

Cardiac arrhythmias are the direct result of an anatomical, and consequently physiological, disruption of the three-dimensional depolarization path in the cell-to-cell communication of the myocardial muscle tissue. The electrical communication pattern is generally identified from electrical activation mapping by means of a multi-pole

electro-cardiogram (ECG), as illustrated in Fig. 16.1. The multiple electrodes may be attached to a sock, which can be placed over the epicardium of the heart during open-chest surgery for high resolution depolarization tracking, or alternatively by transcatheter mapping from the endocardial side during minimally invasive electro-physiologic examination. During open-chest surgery there may also be visual indications that reveal cell damage resulting from (post-infarction) myocardial scarring or margins from an aneurysm.

The quality of life for a person with arrhythmias, in particular ventricular tachycardia (VT) is generally compromised and specifically the treatment with a pace-maker or cardiac-defibrillator can place significant constraints on the freedom of movement of the individual.

Ventricular arrhythmias resulting from infections by the *Trypanosoma cruzi* parasite are prevalent in South American countries, with increasing occurrences around the world [3]. Post-myocardial infarction tachycardias and the ventricular arrhythmias in Chagas' disease share significant similarities. Both are macroreentrant circuits, involving any myocardial wall segment (not limited to the endo- or epicardial surface), and are entrainable. The Chagasic patient population generally tends to be younger than patients with post-MI VT, and due to the aetiology, have a higher left ventricular ejection fraction. Chagasic myocarditis can result in the modification of cell-to-cell communications within the electrophysiologic substrate that show potential of developing fatal VT's that closely resemble the effects of coronary infarct damage. A person with Chagas Disease may receive a heart-transplant, but this offers only a temporary solution. The *Trypanosoma cruzi* parasite will nevertheless revive and the same inflammatory scenario will follow thereafter with associated arrhythmias. Additionally, the use of endo and epicardial radio-frequency (RF) ablation still leaves a lot to be desired with respect to elimination of VT's for Chagasic patients [4].

Ventricular Tachycardia (VT) and other arrhythmias can result in disabling symptoms at unpredictable times. Arrhythmias can be disrupting the patients' lives, next to mortality. An implantable cardiac defibrillator (ICD) on the

R. Splinter
Department of R&D, Splinter Consultants,
318 Albright Avenue, Graham, NC 27253, USA
e-mail: rsplinter@gmail.com

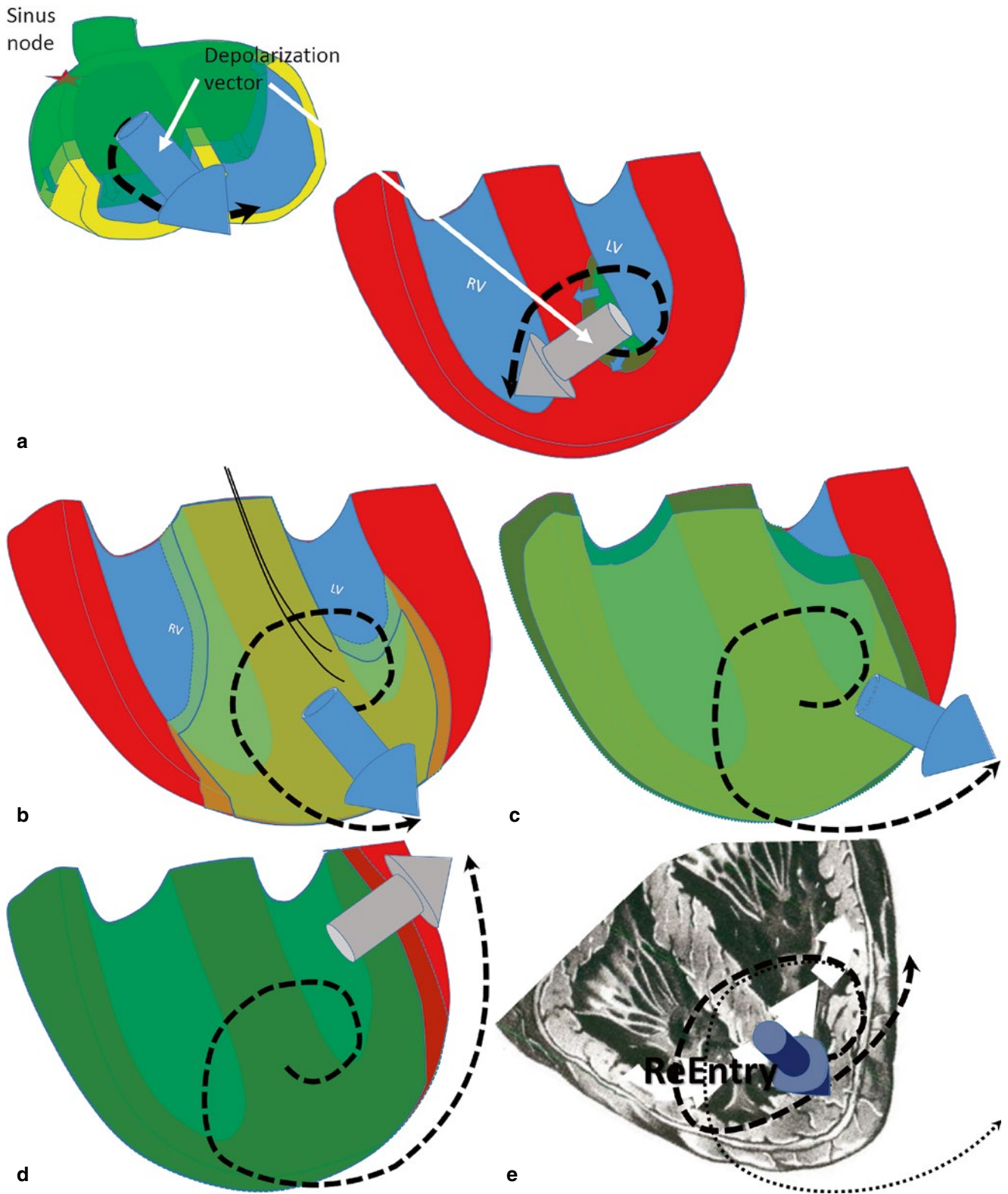


Fig. 16.1 Representative depolarization vector revolution based on simulated 12-point ECG recording for a normal heart. (a) SA-node firing followed by atrial depolarization leading to AV-node conduction and initiation of ventricular depolarization from the HIS bundle, (b) ventricular depolarization wavefront propagation, (c) depolarization

progression and associated depolarization vector gyration, (d) completion of depolarization process, end systolic, (e) hypothetical re-entry path resulting from a localized aneurysm, with depiction of deviation in depolarization vector orientation path as curve with long dashes, in comparison to the 'healthy' dotted line

other hand may still require ongoing medical treatment and may not be considered a cure. Specifically, the arrhythmogenic substrate remains unchanged although the treatment effectively terminates ventricular arrhythmias. Patients may still be at risk of an arrhythmia, involving unconsciousness or cardiac arrest. Patients may no longer have all driving privileges removed when wearing an ICD, however recipients must still be required to abstain from driving for up to 6 months following any shock administered by their device.

In general, cardiac arrhythmias can be attributed to the following four types of processes: (1) Ventricular arrhythmias, (2) Atrial arrhythmias, (3) atrial and ventricular fibrillation and (4) Sinus node depolarization rate [5–9].

Therapeutic arrhythmia applications currently available, next to implanted cardiac pacemaker or defibrillator, are the following (but not limited to, or combinations of) six thermal and mechanical treatment mechanisms: chemical ablation; cryo-ablation; electrical ablation (specifically Direct-Current or Radio-Frequency respectively micro-wave heating), laser photo-ablation, surgical intervention, and ultrasonic heating [8, 10, 11]. Additional treatment options are available as well, such as pharmacological intervention. Specifically, laser coagulation will be discussed as a viable and verified treatment option [12, 13].

The use of conversion of light into thermal energy provides a mechanism to achieve tissue coagulation. Targeted thermal denaturation can be used to electively modify the electrophysiological properties of excitable cells as well as alter the passive electrical conductivity of diseased tissues.

When targeting diseased tissues in a discriminatory fashion by means of directional light delivery and/or suitable wavelength selection, a therapeutic application can selectively remove unwanted electro-chemical components from within the cardiac muscle. It is frequently virtually impossible to selectively target and treat only the diseased tissue, both from an anatomic and from an optical delivery standpoint. The differences in optical properties between healthy and diseased tissues are not fundamentally large enough to generate a statistically significantly different temperature rise in the respective tissues to selectively destroy the diseased tissues while salvaging the healthy tissues that are fully integrated from an anatomical standpoint. The goal is now to minimize the tissue volume that is raised to coagulation temperature to the segment containing most, and preferably all, of the diseased tissues that are involved in the modified depolarization path-way, while concurrently minimizing functional damage to the surrounding healthy cardiac muscle tissue.

In this chapter the mechanism of action and the positive clinical results from irradiation of arrhythmogenic foci by means of Neodymium: Yttrium Aluminum Garnet laser (Nd:YAG, operating at a wavelength of 1064 nm) and several diode laser sources, also operating in the near-infrared, providing the laser photocoagulation for therapeutic practices is described.

The Origins of Cardiac Arrhythmias

Tissues identified as the arrhythmogenic foci are segments with electronic transmission with enough delay to hold the depolarization signal past the repolarization period of the cardiac cells bordering the diseased volume, and subsequently induce re-entry of the original depolarization during intra-cellular communication.

Slow intra-cellular communication may result from integration of collagen strands within the cardiac muscle. Historically anatomical locations of scar tissue and fibrosis discovered during open-chest surgery have been associated with the initiation and formation of arrhythmias. The recognition of anatomic substrates may require full open-chest surgery, or the use of high-resolution imaging (e.g. MRI, ultrasound). Collagen results from cell-death in response to deprivation of blood-flow. Other causes of collagen formation are found in parasitic and viral infections, specifically the infiltration by the parasite *Trypanosoma cruzi* [3]. An illustration of the biologically and anatomically diverse tissue composition in fibrotic myocardium is presented in Fig. 16.2. The respective tissues all have specific biological, electrical, mechanical and optical characteristics.

There are several ways of locating the target tissues; under exposed heart by means of visual identification of pathological regions, under electrophysiologic monitoring (both open chest and closed chest), as well as under Magnetic Resonance Imaging (MRI) [14] and by means of ultrasound [11]. Atrial arrhythmias can also be localized by intravascular echocardiography (ICE), primarily based on the anatomy and

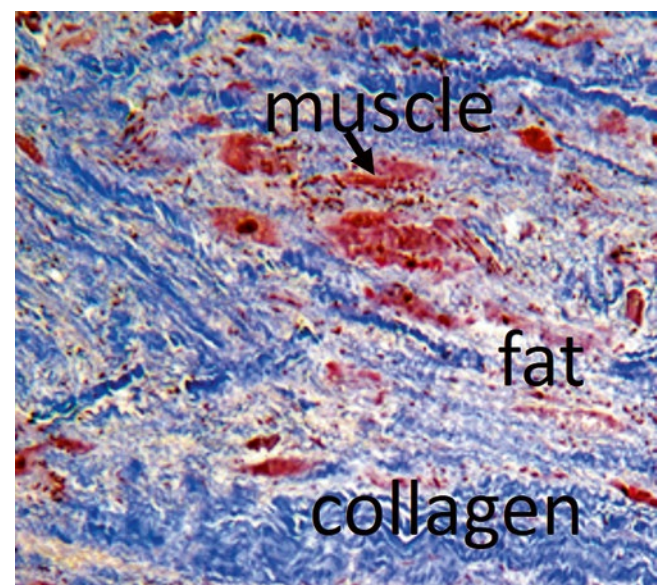


Fig. 16.2 Illustration of the complex and heterogeneous tissue assembly in fibrotic myocardium. The collagen and fatty tissues will have different electrical propagation characteristics as well as unique optical characteristics

pathology of the diseased tissues [1]. After localization of anatomical markers the placement of an electrophysiology catheter may be required for verification of target location, if possible.

During both open chest surgery and via minimally invasive closed-chest transcatheter techniques, electrophysiologic measurements can provide the physiologic path of propagation for the depolarization pathway, and the locations of delay that may result in re-entry of the depolarization wave. Based on electrophysiologic feedback the physiologic and anatomic origins of arrhythmogenic foci can be identified with a high degree of accuracy in location and pathological impact. Tissues with modified electronic transmission that can sustain enough delay to induce arrhythmias can selectively be treated. The electrical insulation by the non-depolarizing diseased tissue matrix may still provide passive conduction, however delayed.

There are four specific therapeutic applications related to arrhythmogenic phenomena: (1) ventricular ablation of arrhythmogenic foci [15], (2) ablation of atrial fibrillation; by means of the inscription of a maze pattern or by isolation of the pulmonary vein [16], (3) modification of the atrio-ventricular node in signal transmission [17], and (4) limiting the firing rate of the sinus-node [18]. Additional treatment options do also exist but are outside the main focus of this discussion.

Electrophysiologic Diagnostic Modalities for the Determination of the Origins of Arrhythmias

The methods available for electrical activation mapping are a direct function of accessibility. During open chest surgery the heart is exposed and a multi-electrode sock may be wrapped around the heart for full instantaneous surface depolarization wavefront propagation recording.

Additional details may be obtained by plunge-needle electrodes, providing a three-dimensional depolarization wavefront propagation investigation, revealing potential invisible sub-surface volumes of diseased, slow conducting tissues. A representative depolarization wavefront progression and associated three-dimensional ECG in ischemic myocardium measured by plunge-needle mapping is illustrated in Fig. 16.3.

During minimally transcatheter diagnostics only the endocardial surface is fully accessible, however transcatheter electrode placement can add location specific epicardial depolarization data if needed. Apart from electrophysiologic mapping from the coronaries additional “non-restrictive” depolarization sensing has been performed with transthoracic epicardial mapping [4].

The use of multi-pole electrodes, such as the use of a “basket mapping” catheter can capture an instantaneous surface

wavefront. A graphical representation of a deployed “basket” catheter with 254 electrodes is shown in Fig. 16.4. Alternatively, a linear array of electrodes only provides a one-dimensional surface impression of the line of propagation.

Generally, the level of diagnostic detail will depend on the number of electrodes used in the mapping device for instantaneous recordings, and their respective spacing. During patient examination standard twelve-lead chest electrode ECG is usually performed in combination with transcatheter mapping, if not minimally a three-point ECG. The 12 lead ECG provides extensive detail about the time-resolved “revolution” of the depolarization-vector which can be used to identify deviations in the vector movement resulting from locations in the heart with deviating cell-to-cell transmission and hence elude to potential arrhythmogenic foci, as illustrated in Fig. 16.1 for the average depolarization path and derived vector [5]. During catheter mapping (EP-catheter) with only two to four electrodes it will be required to repeatedly move the EP catheter and analytically link the latest recording to a reference point established in the prior measurement for full high-resolution location specific diagnostic identification of the arrhythmogenic foci.

In order to obtain feedback during endocardial energy delivery for coagulation of arrhythmogenic foci the use of the coronary vessels can provide electrophysiologic information about the progress of the signal degradation. Specifically the use of the coronary sinus to access the epicardial surface of the left ventricle has proven beneficial [19].

Atrial fibrillation has been identified by anatomical characterization, generally followed by electrophysiologic verification [1, 2, 20]. Traditionally, atrial fibrillation has been treated by the maze-procedure during open-chest surgery [16, 10]. With new information based on clinical experience, the specific anatomical landmarks in the atria that have been identified as primary potential locations of arrhythmogenic foci are the attachment of the superior vena cava, or the root of the pulmonary vein, the tricuspid annulus or the Crista Terminalis, which are subsequently verified by electrophysiologic mapping as standard procedure for treatment. The later methods can be performed by transcatheter approach.

The Available Treatment Options for Arrhythmias

Depending on the type and persistence of the arrhythmia the following anatomical and respective functional zones can be treated: (1) the ventricular wall (predominantly left ventricle), (2) atrium (both left and right), (3) atrio-ventricular node, and (4) sinus-node. Traditionally arrhythmias have been treated by surgical means, removing or circumventing the anatomical substrate essential to the cause for the arrhythmia. Wolf-Parkinson-White syndrome has primarily benefitted the most

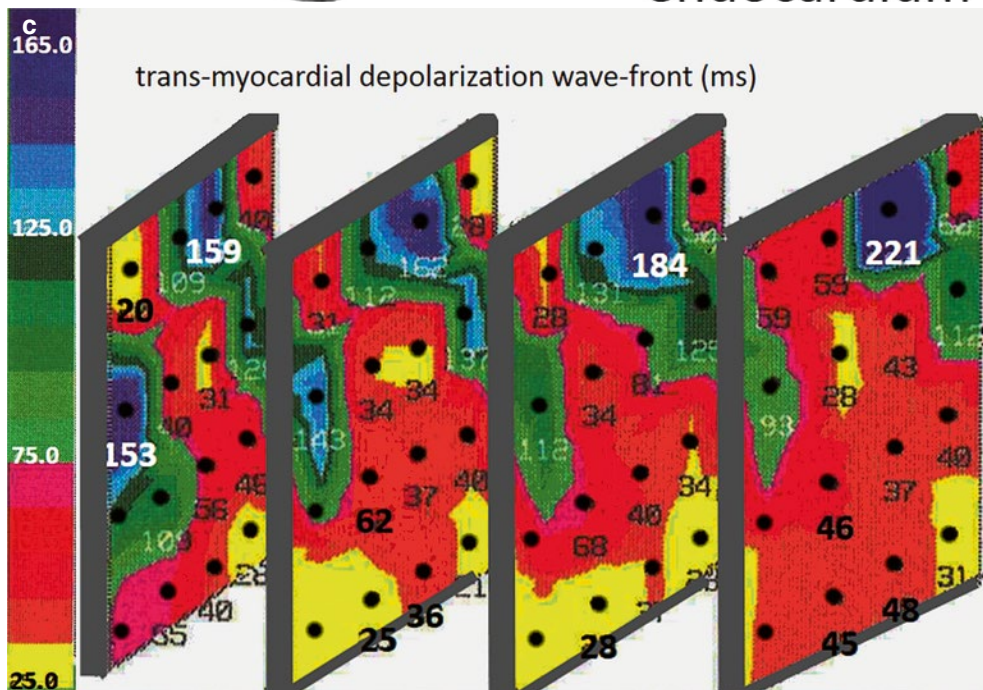
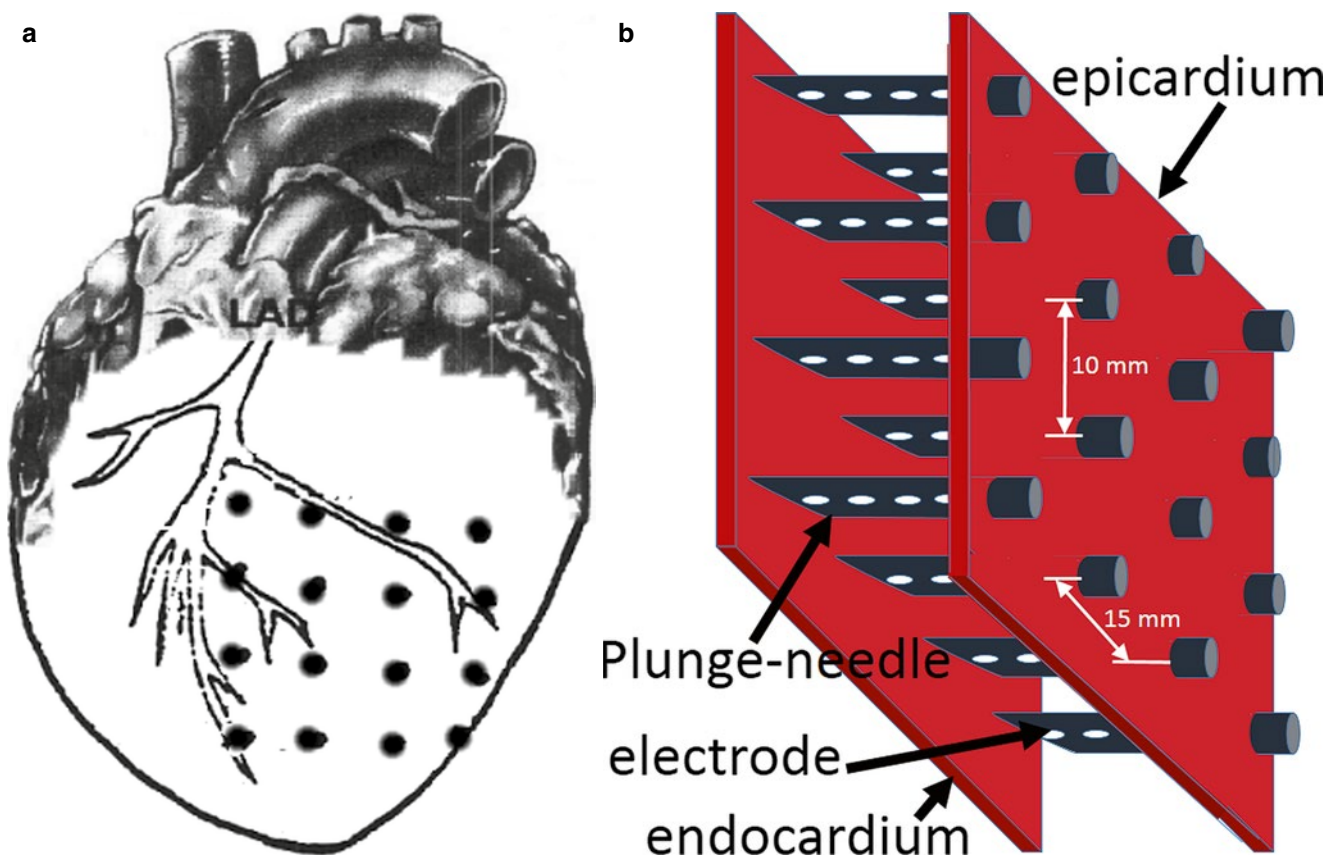


Fig. 16.3 Instantaneous three-dimensional ventricular depolarization in a region affected by a coronary occlusion. (a) Placement outline of plunge needles, (b) detail of electrode arrangement, (c) three-dimensional

ECG map of the ventricular section, illustrating the drastic delay as the preferential location for treatment by laser photocoagulation

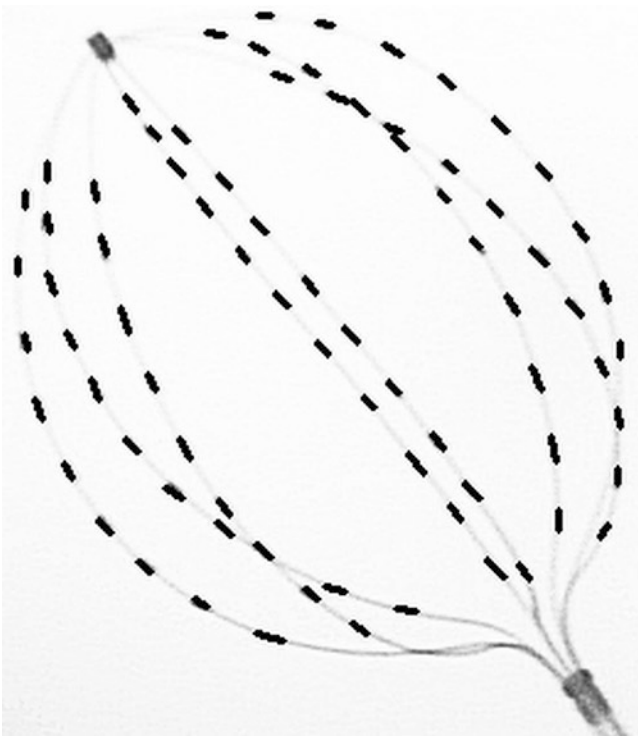


Fig. 16.4 Transcatheter “basket” electrode mapping device outline, providing minimally invasive three-dimensional time-resolved mapping of the endocardial depolarization wavefront

from the surgical approach [21]. Not all post-infarction ventricular tachycardias can be attributed to the presence of discrete fibrotic regions within the ventricular wall. For that matter, the reentry-pathways may be deep in the ventricular wall, out of sight or out of reach from certain mechanisms used for modification of the electrical depolarization or delayed conduction. Over the years several ablative techniques have been developed to alter the depolarization path to achieve synchronization of the total ventricular depolarization with the refractory period. Specifically, drug-resistant tachy-arrhythmias present a special challenge. The available treatment options next to surgical intervention are the following: pharmacologica therapy, chemical ablation, next to a range of thermal applications, including but not limited to: cryo-ablation, electrical ablation (ranging from Direct-Current, to Microwave and Radio-Frequency), laser photocoagulation and ultrasonic heating and coagulation. Each thermal mechanism has its own active or passive mechanism-of-action, where passive heat conduction forms the basis of several techniques. Most thermal techniques are relatively non-directional, leaving the target volume ill-defined. Laser light however, can be applied in a targeting fashion, inherently minimizing the risk for peripheral damage and consequently salvaging the functionality of properly functioning cardiac muscle tissues [12, 13].

Redirecting the three-dimensional depolarization path to avoid the temporal superposition of several depolarization

waves has been shown to provide the tools to reduce and permanently eliminate the incidence of arrhythmias.

Most treatment options have inherent limitations that reduce the efficacy and clinical benefits of these procedures. Chemical ablation has been shown to result in myocardial infarction with associated clinical concerns and follow-up requirements. Cryo-ablation results in a reduced feedback for procedural quality control due to the suppression of electronic signaling between the cells under reduced local temperatures [10, 22, 23]. Even though Radio-Frequency (RF) cardiac ablation is the most popular therapeutic application in use to this day, the success rate is still limited [24, 25] (Takemoto 2005). Additionally, the radio-frequency signal generates interference with the ability to accurately detect and monitor the ECG signal due to the inherent electrical activity of the treatment. During open-chest surgery other opportunity for controlling the heart rate are available as well.

On an elementary rhythm control level the following two options are clinically explored by various groups: sinus node or Atrio-Ventricular node (AV-node) modification. The Sinus node has a well-defined discrete distribution of pace-maker cells of specific maximum depolarization rate, ranging from slow to fast in an anatomically gradient fashion, which respectively can selectively be eliminated. The conduction of the AV-node can be influenced in the same manner in transcatheter approach to set an upper limit to the transmitted depolarization frequency [26]. These two mechanisms form specific solutions to certain well defined arrhythmogenic conditions. Both Sinus and AV node can be modified by pharmacological and thermal means, as well as chemical modification of the physiology. Alternatively, the Sinus-Node and Atrio-Ventricular Node functionality can be modified by thermal mechanisms to set an upper limit of depolarization frequency from a biological control perspective. Examples of the available thermal mechanisms are direct-current, radio-frequency and laser irradiation as well as cryo-ablation and ultrasonic heating.

Atrial fibrillation under open chest surgery has in the past been treated by surgical incision or by means of radio-frequency, microwave coagulation or cryoablation in a pre-set pattern, the maze procedure [10]. Other therapeutic solutions rely on the isolation of specific anatomical entities, such as the pulmonary vein, tricuspid annulus and the Crista Terminalis [1]. In certain cases this may also be attempted under transcatheter approach. The prevailing treatment option for atrial-fibrillation has been intraoperatively by application of the ‘maze procedure’ [16]. The maze procedure carves a maze pattern of scar, traditionally induced by surgical incision or by radio-frequency coagulation, drawing lines creating a forced path of depolarization and propagation.

The selective electrical isolation of the superior vena cava from the atrium, or the pulmonary vein by means of circular coagulation at the root [27, 20] can be achieved with the use of thermal coagulation means.

The frequent requirement for electrical modification of tissues that are several millimeters below the endocardial, respectively epicardial surface can be satisfied by thermal means through conversion of one form of energy into heat, thus raising the local temperature resulting in rendering the depolarization of the cellular membrane inactive.

LASER Therapy for Cardiac Arrhythmia Ablation

Light of specific wavelengths can scatter and reach deep seated locations before ultimately being converted into a temperature rise through absorption with imparted temperature gradient and distribution of heat. The heat generated during this light absorption with cause a rise in temperature cumulative with exposure time and rate of absorption as a function of location [28, 29]. The use of light in general can be unpredictable when light of a broad range of wavelengths is applied. The use of a high-powered infrared lamp for instance, may not result in the desired confined deep-tissue heating. The use of a well-defined, narrow bandwidth, small delivery spot-size, laser source will provide the tools to selectively control the surface size and target volume to be heated, while intentionally sparing surrounding healthy tissues. A laser provides a monochromatic collimated light source that, when coupled into a fiber-optic delivery system, can be delivered in a narrow cone of tissue volume. Since the optical properties are a function of the particular wavelength(s) used during the irradiation process, the wavelength selection becomes of critical importance to the success of the treatment [12].

Laser is the acronym representing the mechanism-of-action used to generate coherent and monochromatic high power light, it stands for Light Amplification by Stimulated Emission of Radiation. The stimulated process of emission guarantees the generation of single wavelength electromagnetic radiation. This stands in contrast to spontaneous emission of light from an excitable medium, which will be broad-band. Phosphor is the most well-known example of an excitable medium that provides broad-band spontaneous emission. Other broad-band light-sources include the incandescent bulb and arc-lamps. The latter use electric current as the driving energy source for emission of light. The laser excitation process for the Neodymium:Yttrium-Aluminum-Garnet laser (Nd:YAG laser, operating at 1064 nm) for instance uses a broad-band flash-lamp to excite the susceptible Neodymium doping elements in the Garnet crystal to

raise the electrons to a specific energy level from which they will momentarily decay to produce a single energy photon with a wavelength of $\lambda = 1064 \text{ nm}$ that corresponds to the molecular electron energy transition: $E = h\nu = h \frac{c}{\lambda}$, where $h = 6.62606957 \times 10^{-34} \text{ m}^2 \text{ kg/s}$ is Planck's constant, ν the frequency of the electromagnetic radiation and $c = 2.99792458 \times 10^8 \text{ m/s}$ the speed of light. The coherent property of laser light is generally unimportant in the therapeutic applications.

The laser wavelength is a direct function of the material configuration used to produce the electro-magnetic radiation. The light that can be produced by laser ranges from very short wavelength, high energy Ultraviolet to long-wavelength, low photon energy Far Infrared.

The continuously growing selection and increasing power output of diode lasers can offer a relatively low-cost opportunity for the development of laser assisted therapeutic devices.

The inherent tissues will be comprised of certain optical characteristics, specific to the pertinent tissues in the target volume. The optical properties are all a function of wavelength. Selecting the appropriate wavelength to achieve deep tissue heating is one of the requirements for successful treatment of deep seated arrhythmogenic foci within the ventricular wall. Specifically treating sub-endocardial and sub-epicardial areas during minimally invasive transcatheter methods form a significant challenge.

One of the specific advantages of laser photocoagulation for the treatment of ventricular tachycardia is the ability to perform treatment under normothermic conditions while avoiding interfering with the electrophysiologic monitoring principles. Immediate and real-time verification of the success of treatment is extremely beneficial. The electrophysiologically guided ablation allows for a systematic approach with simultaneous validation of initial success. Due to the relatively homogeneous distribution of the photon energy in the turbid tissue medium the resulting coagulation process results in a solid volume with well demarcated boundaries. As a result, when properly applied and executed, the laser lesion renders negligible risk of sustaining reentry pathways within the treatment area.

The frequent requirement for electrical modification of tissues that are several millimeters below the endocardial, respectively epicardial surface can be satisfied by thermal means through conversion of light energy by means of absorption at the appropriate wavelength. In ventricular laser photocoagulation the use of laser light delivery by fiber-optic means creates a three-dimensional light distribution inside the ventricular wall. The local absorption of light as a function of location specific fluence causes a temperature rise proportional to the absorbed local light quantity as a function

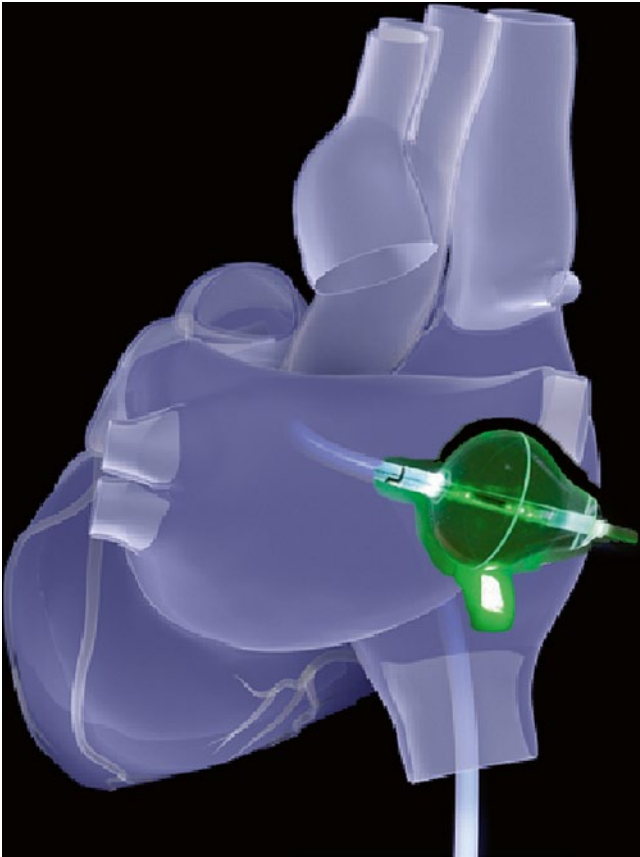


Fig. 16.5 Diagram of the electrical isolation procedure of the pulmonary vein by means of circumferential laser irradiation provided by the CardioFocus® catheter

of exposure time. One example of atrial treatment in specific, uses a fiber-optic with diffusing tip that is placed against the endocardium of the atrium to induce linear coagulation lines for creation of an electrophysiologic maze [10]. The interesting aspect of the laser assisted fiber-optic treatment is the addition of spectroscopic feedback on the progression and extend of the induced coagulation process. Additionally under surgical access the fiber-optic delivery of laser light can be used to draw lines of coagulation through slow linear advancement of the fiber-optic in perpendicular delivery. One of the most widely used treatments for atrial fibrillation is isolation of the pulmonary vein by various means. One method in specific uses a diode laser operating at 980 nm for balloon assisted circumferential coagulation of the base of the pulmonary vein [20]. The CardioFocus device used for laser coagulation pulmonary vein isolation is illustrated in Fig. 16.5. The selective electrical isolation of the superior vena cava from the atrium, or the pulmonary vein by means of circular coagulation at the root [27, 20] can effectively be achieved with the use of thermal coagulation means. The root isolation has proven to be initially successful for the treatment of atrial fibrillation through minimally invasive

transcatheter ablation [20]. In line with the earlier mentioned four mechanisms of rate control, both the Sinus-Node and Atrio-Ventricular Node can be treated by laser irradiation to modify the upper limit of depolarization frequency from a biological control perspective. The absorbed light respectively selectively renders pacing cells inactive or blocks the transmission rate above a specific (monitored) frequency. The progress is generally measured by means of lengthening of the RR-interval.

Mechanism-of-Action of the LASER in Photocoagulation

LASER light, based on its electro-magnetic field composition, produces electric and magnetic field interactions with the charged particles and/or segments in molecular configurations; ions, charge-polarized branches of a molecule (i.e. dipole formation) or even interacting with the elementary electron building-blocks under short wavelength interaction. The charged constituents, under influence of Coulomb and Lorentz forces, can perform a single or combined mechanical motion consisting of vibration, scissor-action or rotation [30–32]. The local tissue temperature in the irradiated volume is directly related to the kinetic energy (KE) of motion on the molecular level of the constituents as:

$$T = \frac{2}{3} \frac{1}{k_b} \langle KE \rangle = \frac{2}{3} \frac{1}{k_b} \left\langle \sum_i \frac{1}{2} m_i v_i^2 \right\rangle, \text{ where } \left\langle \sum_i \frac{1}{2} m_i v_i^2 \right\rangle \text{ is}$$

the average kinetic energy for a mixture of masses (m_i) with respective velocities for their collection of various movements, on average: v_i [33]. The increase in kinetic energy associated with an associated temperature rise will eventually reach a point where a phase transition will occur, specifically coagulation. The thermal effects resulting from electro-magnetic radiation are directly concomitant with the light energy distribution inside the irradiated medium, while thermal diffusion only yields as a secondary mechanism for heat distribution, contingent on the exposure time. In contrast, most other available thermal mechanisms rely primarily on thermal diffusion for inflicting cell-damage. Thermal diffusion will result in lesion-width growth concurrent with lesion-depth, thus increasing the risks for damaging healthy tissues when targeting deep-seated arrhythmogenic foci.

The cell-death resulting from thermal injury relies on modification of the cellular membrane, cytoskeleton and/or the nucleus. Denaturation of proteins in the membrane will stop the transfer of nutrients and oxygen. The cytoskeleton for various cell types will have a range of thermal responses. In human erythrocytes, the protein spectrin forms the building block of the cytoskeleton. Spectrin has been shown to be thermally inactivated at 50 °C, leading eventually to cell-death but may recover [34].

Disintegration of the nucleus, at higher temperatures, causes instantaneous cell-death. The irreversible coagulation process is a time dependent mechanism that is governed by an inverse proportional relationship between temperature and exposure time. Exposure to 43 °C will require several dozen minutes to hours for achieving coagulation of the volume. Generally, temperatures exceeding 60 °C result in virtually instantaneous cell-death. Tissue temperatures in excess of 100 °C can result in boiling and hence vaporization, whereas temperatures exceeding 225 °C will provide the risk of carbonization. During transcatheter ablation specifically carbonization needs to be prevented. Carbonized tissues may break loose from their base and can lead to obstruction of vascular flow in case the debris does not disintegrate. Thorough understanding of the interaction of light of a specific wavelength with the tissue constituents can provide the means of predicting the prevailing coagulation effects as well as gauge the volumetric extend.

The process of the energy transfer effects on the local tissues is a function of the phase transition energy requirements, converting the proteins in the coagulation process and hence causing cell-death by means of destruction of the cell-membrane or by denaturing the cell nucleus. The coagulation energy is a direct function of the cumulative absorption of all electro-magnetic radiation as a function of location, in the tissue volume located at position \vec{r} expressed as the light radiance: ($\Psi(\vec{r}, t)$), see [Appendix](#).

The energy involved in a phase transition is represented by the Gibbs Free Energy (on a chemical level). This represents the reaction energy for the protein denaturation at a constant temperature. At this point the light energy is converted into chemical energy. The denaturation (coagulation) process can be defined by the change in Gibbs Free energy of the system as: $\Delta G_{den} = \Delta H_{den} - T\Delta S_{den}$, where the denatur-

ation enthalpy is defined as $\Delta H_{den} = U + \Delta nRT$ and the entropy (S_{den}) is connected to the latent heat of latent heat of coagulation (h_c): $T\Delta S_{den} = h_c$. The incremental changes in Gibb's free energy of a system undergoing denaturation is represented as: $\Delta G = \Delta U - T\Delta S - S\Delta T + \Delta nRT + nR\Delta T$; technically comprised of a summation over all constituents, where $R = 8.3144621 \frac{J}{Kmol}$ is the universal Gas Constant,

n the number(s) of molecules of chemicals involved in the processes and respective phase-transitions, and U the internal energy of the system.

This denaturation process can be represented by the chemical process: $aA + bB \rightarrow cC + dD$, providing the

change in Gibbs energy: $\Delta G_{den} = \Delta G_{native} + RT \ln \left[\frac{[C]^c [D]^d}{[A]^a [B]^b} \right]$,

where A, B, C , and D are the respective constituents of the chemical breakdown with concentrations $[A]$ and $[B]$ for the respective concentrations of hypothetical native molecules, and $[C]$ and $[D]$ the respective molecular concentrations of the denatured states. The entropy change ΔS_{den} will be positive, defined as: $\Delta S_{den} = k_b \ln \left(\frac{\omega_{c,denatured}}{\omega_{c,native}} \right)$, which

was defined by Boltzmann [35] in the form of the natural log of the number of all configurations possible in a system: ω_c , multiplied by the Boltzmann constant:

$$k_b = 1.3806488 \times 10^{-23} \frac{m^2 kg}{s^2 K}, \text{ and } \frac{\omega_{denatured}}{\omega_{native}} \gg 1,$$

with the respective molecular fractions: $\omega_{c,denatured}$ and $\omega_{c,native}$. The volume of denaturation can be derived from the Damage Integral, which is a function of the radiant exposure to laser light. The temperature under continuous laser light exposure provides the location (\vec{r}) and time (t) specific coagulation energy within the total volume of tissue ($E_{coagulation}(\vec{r}, t)$) defined as: $E_{coagulation}(\vec{r}, t) = m(h_c + c_v \Delta T)$.

Where $\Delta T = T_b - T_0$ is the temperature rise from steady state (T_0) to coagulation temperature (T_b), c_v is the specific heat of the generalized protein medium, h_c the latent heat of coagulation for the medium, and m is the mass that has been coagulated. The Gibb's Free energy also depends on the entropy of the system ($S = k_b \ln \omega_c$). The mass (m) will roughly be equivalent to the lesion volume (V) times the density of muscle ($\rho_{muscle} = 1.06 \frac{g}{cm^3}$): $m = \rho V$.

The coagulation process depends on the number of amino acids involved in the protein conversion process and for a single protein molecule the energy requirement ranges from $h_{c, molecule} = 4 eV = 6.40870628 \times 10^{-19} J$ for 21 amino acids to $h_{c, molecule} = 16 eV = 2.56348251 \times 10^{-18} J$ for 100 amino acids in one single protein.

The full extent of the inflicted thermal damage process can be described by the so-called **damage integral**, linking the elevated temperature magnitude and duration to the inflicted ultimate cell-death as a function of location within the irradiated volume. The process of calculating the generated volume of cellular damage will be discussed next.

Damage Integral

Healthy tissue initially contains N_0 molecules of one species in a volume. The number of surviving molecules (N) after thermal denaturation is directly proportional to the native number. The number of denatured molecules $dN_{denatured}$ as a function of time obeys the heuristic

Table 16.1 Typical energetic values associated with the denaturation and phase transition process in representative biological media

Tissue	Phase change entropy; ΔS	Phase change enthalpy; ΔH	Phase change temperature; T
Muscle (Tomberg 2005) [36]		7.2–8.3 cal/g	36–80 °C
Protein; Wort (Jin et al. 2009) [37]		0.47–1.06 J/g	
Hydrogen bond separation of 0.28 nm. (Jacques 2006, Floume et al. 2010) [38, 39]		28–29 kJ/mol	
Hydrocarbon ($-CH_2$) separation from water (H_2O). (Jacques 2006, Floume et al. 2010) [38, 39]		8 kJ/mol	
Range of stability between folded and unfolded protein strands. (Splinter 2010) [33]		7–15 kJ/mol	37 °C
Rat prostate (Floume et al. 2010) [39]	-82.9 kJ/molK	71.8 kJ/mol	~60 °C

equation: $dN_{denatured} = k_r N(t) dt$, where k_r is the reaction coefficient. The solution yields the number of surviving native molecules ($N(t)$) as a function of time as: $N(t) = N_0 e^{-\Omega(t)}$. This provides the damage integral: $\Omega(t) = \int_0^t k_r(t') dt' = \int_0^t \frac{kT(t)}{h} e^{\Delta S/R} e^{-\Delta H/(RT(t))} dt$. At any given

time, the number of denatured molecules, $N_{denatured}(t)$, equals the debit $N_0 - N(t)$. In general the damage integral incorporates the cumulative average values of all molecules involved in the denaturation process in a volume of tissue.

The value of k_r depends on the temperature of exposure, the specific chemical reactions (each reaction influenced by the temperature in their own respective manner) and the characteristic values of ΔS and ΔH for specific measurable phase transitions in the tissue. An example of a phase transition is the irreversible loss of enzymatic activity, the denaturation and aggregation process of proteins. Other processes are the coagulation of collagenous tissues which transform into gelatin with associated loss of collagen fiber bundle structure. For example: a second degree burn is defined for $\Omega > 10$, while a third degree burns yields $\Omega > 10,000$.

Typical values of ΔS and ΔH are listed in Table 16.1 as indications of thermal coagulation. Generally the integration constant is defined with respect to the exposure time required to achieve $\Omega = 1$, ($t_{\Omega} = 1/k_r$ (s)) as a function of the tem-

perature. The more complex the molecular structures that are being denatured, the faster will the rate constant change with temperature. This is an immediate result of the fact that the change in entropy (ΔS) is greater. Additionally, the number of bonds to be broken simultaneously (ΔH) will be equivalently larger in number.

The irreversible phase change associated with coagulation has an entropy change (ΔS) which is in first approximation

directly proportional to the enthalpy (ΔH) of the transition. The enthalpy is conceptually connected to the energy of all molecular bonds that simultaneously hold a molecular matrix together. The greater entropy is the dependent variable that describes the entropic energy change involved with the cellular structure and the energy requirements of breaking the bonds.

The damage integral calculates the fraction of the conversion of normal tissue to the coagulated state as a standard reaction equation as a function of applied energy and exposure duration as:

$$\Omega(t) = \ln \left(\frac{[N_{total}]}{[N_{total}] - [N_{denatured}]} \right) = A \int_0^t \exp \left(\frac{-E_{act}}{RT} \right) dt. \text{ Where}$$

the total number of cells in the tissue volume being irradiated ($[N_{total}]$) is compared to the number of denatured cells after laser irradiation ($[N_{denatured}]$), with $R = 8.314 \times 10^3 \text{ J/kmolK}$ is the universal gas constant, A is the rate constant (e.g. $A = 3.1 \times 10^{98} \text{ s}^{-1}$), E_{act} the activation energy for burn injury ($6.28 \times 10^5 \text{ J/mol}$), and T is the temperature of the tissue obtained from the absorption of light at the point of phase transition.

The solution to the volumetric extent of laser photocoagulation is not easily obtained by trying to obtain an analytical solution to the damage integral, specifically since the light distribution is a complex three-dimensional matrix parameter. Generally, the irradiated tissue light distribution, thermal distribution and resulting ultimate damage predictions as a function of exposure time will require a numerical approach, using computer modeling.

The Damage State

Next to the physical temperature change as a function of location within the tissues in the path of irradiation, it will be useful to understand the impact of the thermal damage to the functional status and biological capabilities of the tis-

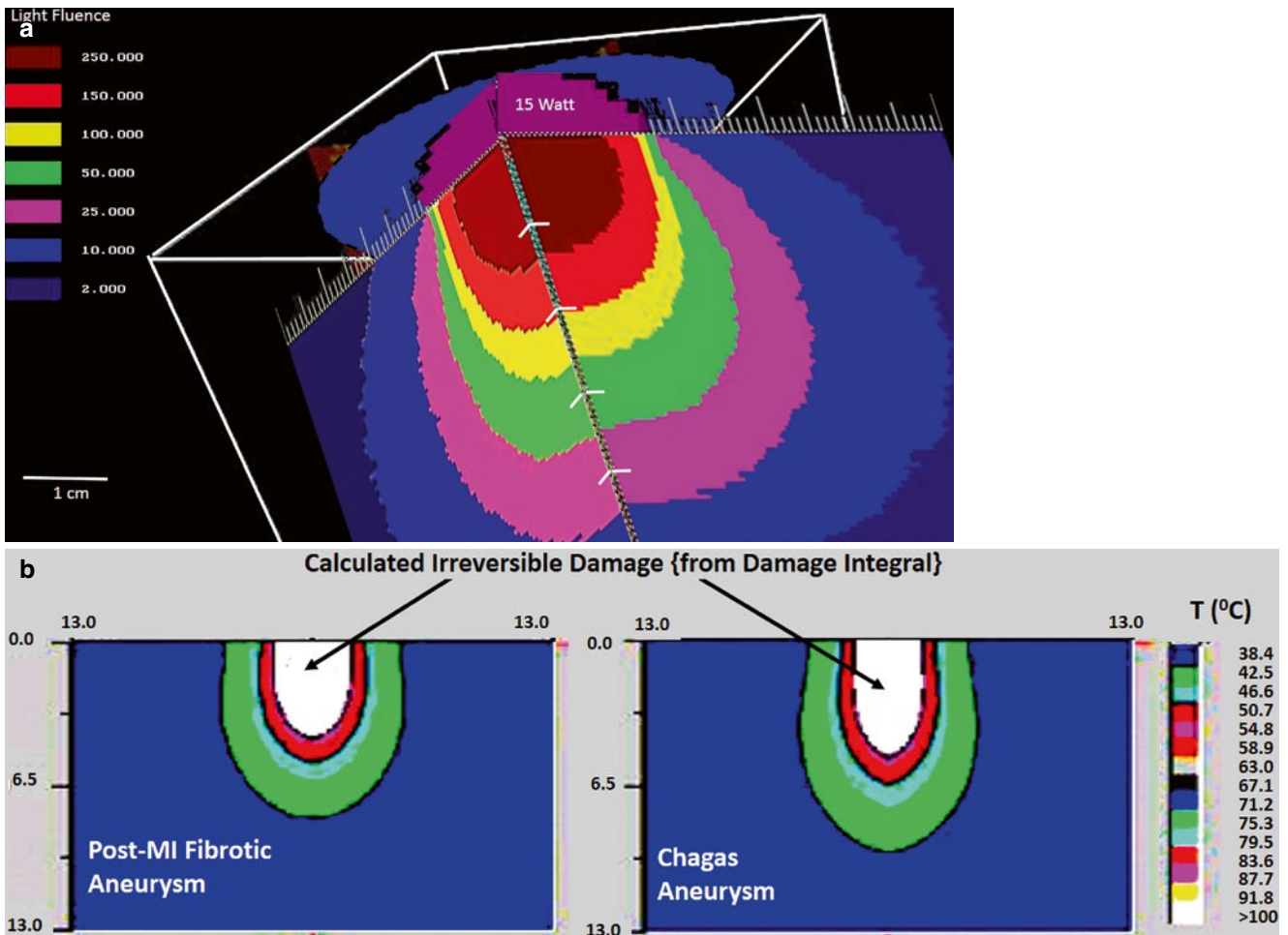


Fig. 16.6 Laser photocoagulation process under low power density near-infrared irradiation. (a) Computer simulation of the light distribution in homogeneous myocardial muscle based on in-vitro optical properties, resulting from a close-contact fiber-optic laser spot with 8 mm diameter. The muscle has an assumed thickness of 13 mm, the radiance

scaling indicates the localized fluence in incremental (logarithmic) steps, (b) computer calculated temperature profile (in °C) resulting from 10 s exposure with the light distribution outlined in a) however adjusted for prominent differences between post-MI myocardium and respective Chagasic myocardium

sues. The damage state is an indication of the ‘severity’ of the inflicted damage. The damage state: D can be determined numerically as the result of exposure duration from laser irradiation by integration over various discrete time intervals. For instance the damage calculation for time increments in 0.1 s intervals yields:

$$D = \Omega(0.1) = A \exp\left\{\left(\frac{-E}{RT}\right)(0.1)\right\}$$

The total damage inflicted by a laser procedure follows from cumulative processes over the total time of laser irradiation. These processes will require that the local tissue conditions after each interval have changed and these local values delineated in the thermal equations will need to be updated as well. Specifically, the light distribution can change as a result of the coagulation process [33].

In the damage process the following three operational ranges can be distinguished:

1. $0 \leq D \leq 0.53$ Tissue resides in normal functioning state, potential reversible damage.
2. $0.53 < D < 1$ Tissue volume where the damage parameter reaches this range is coagulated.
3. $D \geq 1$ Local tissue will be carbonized.

The carbonization state is generally avoided due to the inherent risks associated with the fragile nature of carbonized tissues.

The interaction of electromagnetic radiation with turbid media can be formulated as a diffusion process, pertaining to photons in this case. The “source” for diffusion is however based on the injection of photons from a point-of-contact, the illuminated spot on the tissue surface.

Figure 16.6 illustrates a cross-section of the light distribution for the established optical parameters with respect to cardiac muscle as well as the thermal profile after a certain exposure duration along with the inherent

cumulative irreversible damage. The representation of the resulting thermal lesion is shown in Fig. 16.7. Since the light is providing the primary energy source for tissue heating in the applications described, the light distribution aspect is described in the Appendix. Examples of the chromophores involved in the optical penetration are hemoglobin and water, as well as a wide range of inter and extra-cellular chemicals with specific molecular spectral signatures. The spectral attenuation profile for water and blood is provided in Fig. 16.8.

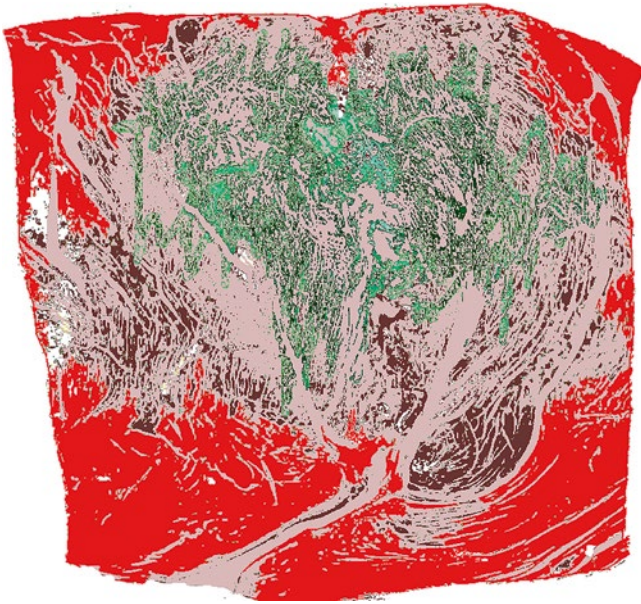


Fig. 16.7 Observed representative onion shape thermal lesion resulting from close contact fiber-optic laser irradiation of myocardium over 40 s continuous exposure

LASER-Tissue Interaction

Experimental and clinical procedures have been performed using Neodymium-Yttrium Aluminum Garnet (Nd:YAG) laser photocoagulation at 1064 nm to modify the depolarization wave-front propagation pattern [19, 40, 41]. The most promising mechanism so far has been the use of Neodymium-Yttrium Aluminum Garnet (Nd:YAG) laser photocoagulation at 1064 nm.

Both open chest and transcatheter closed-chest procedures have been used in FDA approved clinical trials. Modification of the depolarization access route and local tissue conduction by means of laser irradiation have resulted in the successful eradication of incidences of ventricular arrhythmias and cure in human patients.

The specific operational tools and procedures used by select groups in the treatment of cardiac arrhythmias will be outlined next.

Therapeutic Device Design

All laser systems use a fiber-optic delivery system to provide the convenience of catheter approach or delivery by hand using an ergonomic wand. The individual fiber-optic delivers a circular spot size that will vary in diameter inversely proportional to distance with the target.

Ventricular Approach

The work of several groups has explored the opportunities for minimally invasive treatment of ventricular tachycardias. During minimally invasive ablation a catheter has been used

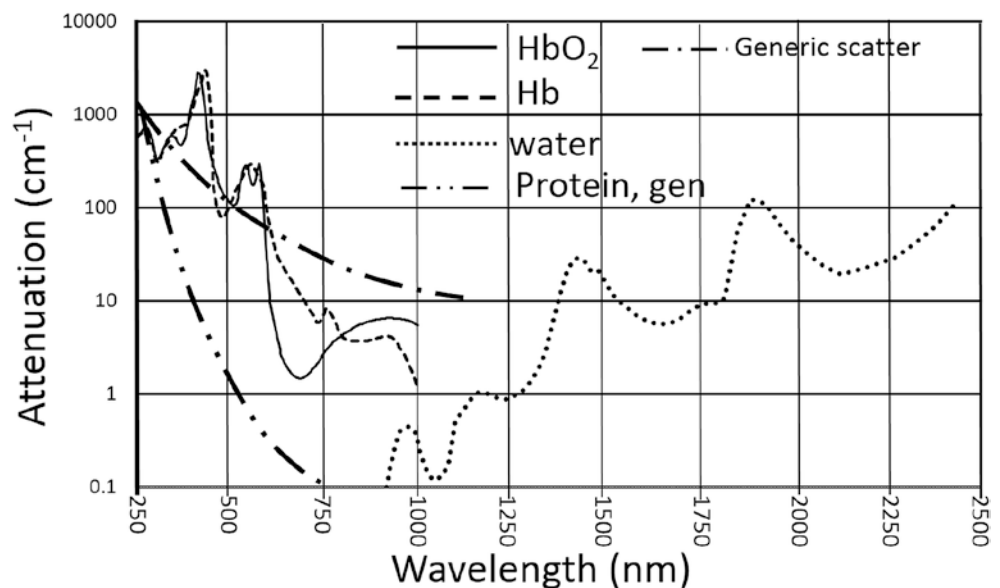


Fig. 16.8 Optical attenuation as a function of wavelength due to absorption and scattering for specific elementary media encountered during laser photocoagulation. Data from Buiteveld [66] and Jacques [67], while the portrayed scattering curve is representative for the verified Rayleigh scattering function

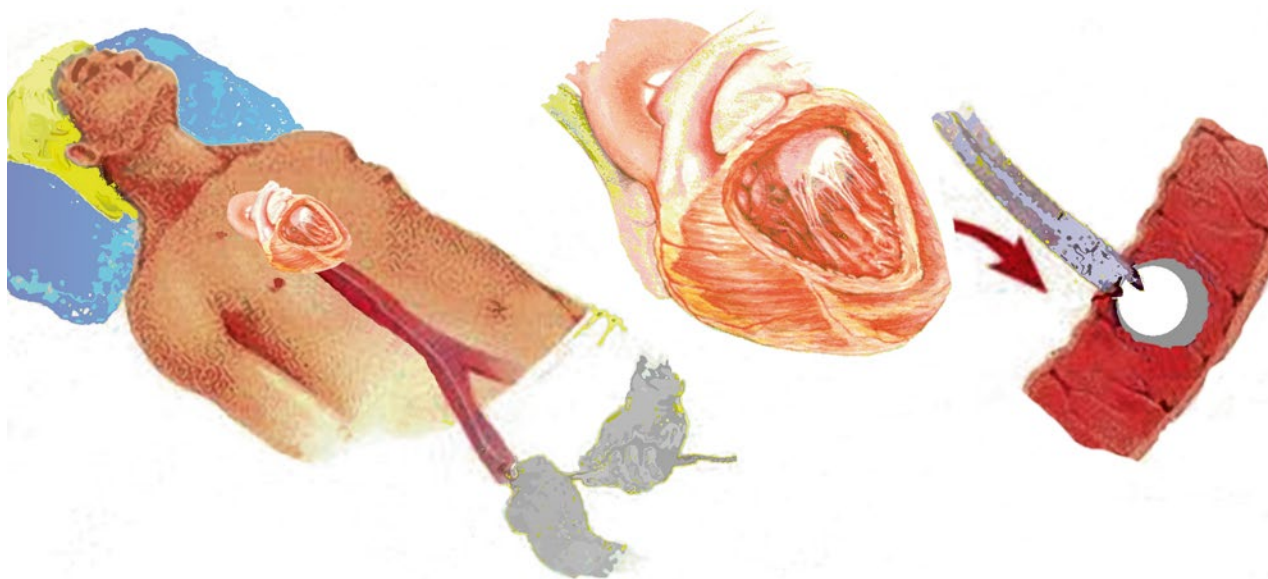


Fig. 16.9 Graphic representation of a transcatheter laser ablation protocol with a 600 μm fiber-optic flanked by two electrodes and two thermocouples, as illustrated in Fig. 16.10

for both electrophysiologic location determination as well as ablative light delivery. The catheter design of the Charlotte, NC group [19, 42] used in the treatment of ventricular tachycardia, has a centrally located 600 μm diameter fiber-optic with a bare distal tip and is connected on the proximal side to a laser. An illustration of the clinical procedure is outlined in Fig. 16.9. Two types of laser have been used in clinical applications. The initial therapeutic laser used by the Charlotte group [43] was an MBB Medilas 3 Nd:YAG: capable of generating up to 80 W emitting at 1064 nm, but for the clinical procedures only operating to a maximum of 25 W. The choice of laser in this case was primarily based on the availability of a high-powered laser in the near-infrared, not specifically resulting from a calculated optimal wavelength. In another set of clinical trials a 25 W CeramOptec diode laser operating at 830 nm was used by the Charlotte group [44], based on more stringent requirements both on wavelength and size as well as electrical power settings and cooling requirements. The diode laser is generally not dependent on water cooling nor requires high voltage/high current in contrast to the critical water cooling for the Medilas 3 Nd:YAG as well as specialized electric connections.

The use of a fiber-optic delivery in both catheter or delivery wand systems generates a circular spot size that will increase in diameter with increasing distance to the target, hence reducing the power-density delivered on impact. The power-density has important implications on the light distribution in the tissue.

The catheter consists of an extrusion tube that has wires imbedded for electrophysiologic mapping and temperature monitoring at the ablation site. The built-in radiographic

opacity pattern of the catheter ensures the tools for establishing location and guided positioning under x-ray fluoroscopy. Two electrodes protrude from the distal tip, each with a length of 2 mm. The electrodes are slanted to provide a sharp point in order to easily penetrate the endocardial surface, see Fig. 16.10. The electrodes are used for site selection based on the measured location-specific time-frames obtained during cardiac depolarization. Additional benefits of the sharp needle electrodes is in mechanical fixation of the catheter tip during laser irradiation in a beating heart. The anchored catheter, in this manner, provides a steady, reliable single entry-point for the laser energy, confining the treatment to the isolated volume of interest. Two thermocouples placed on the face of the catheter tip provide feedback on the tissue temperature, accounting for safety aspects, for instance related to the potential for tissue vaporization. Additionally, tracking the temperature with two sensors at opposite side of the annulus yields information with respect to catheter placement in orthogonal position to the endocardial surface. Perfectly perpendicular incident of the laser light will have the greatest likelihood of high-efficiency and directional tissue penetration and hence obtains the best results for tissue coagulation and subsequent cure rate.

Under low radiance the lesion will match the onion shape light-distribution as illustrated in Fig. 16.5 as predicted by the Radiative Transfer Equation (Appendix), [29, 45, 46]. The scattering dominated light propagation uses a probability distribution of the likelihood of the end-point of a photon after multiple scattering events, each changing the photon direction, ultimately terminated by absorption. However,

Fig. 16.10 Diagram of a catheter delivery tip using fiber-optic irradiation, with thermal and electrophysiological feedback

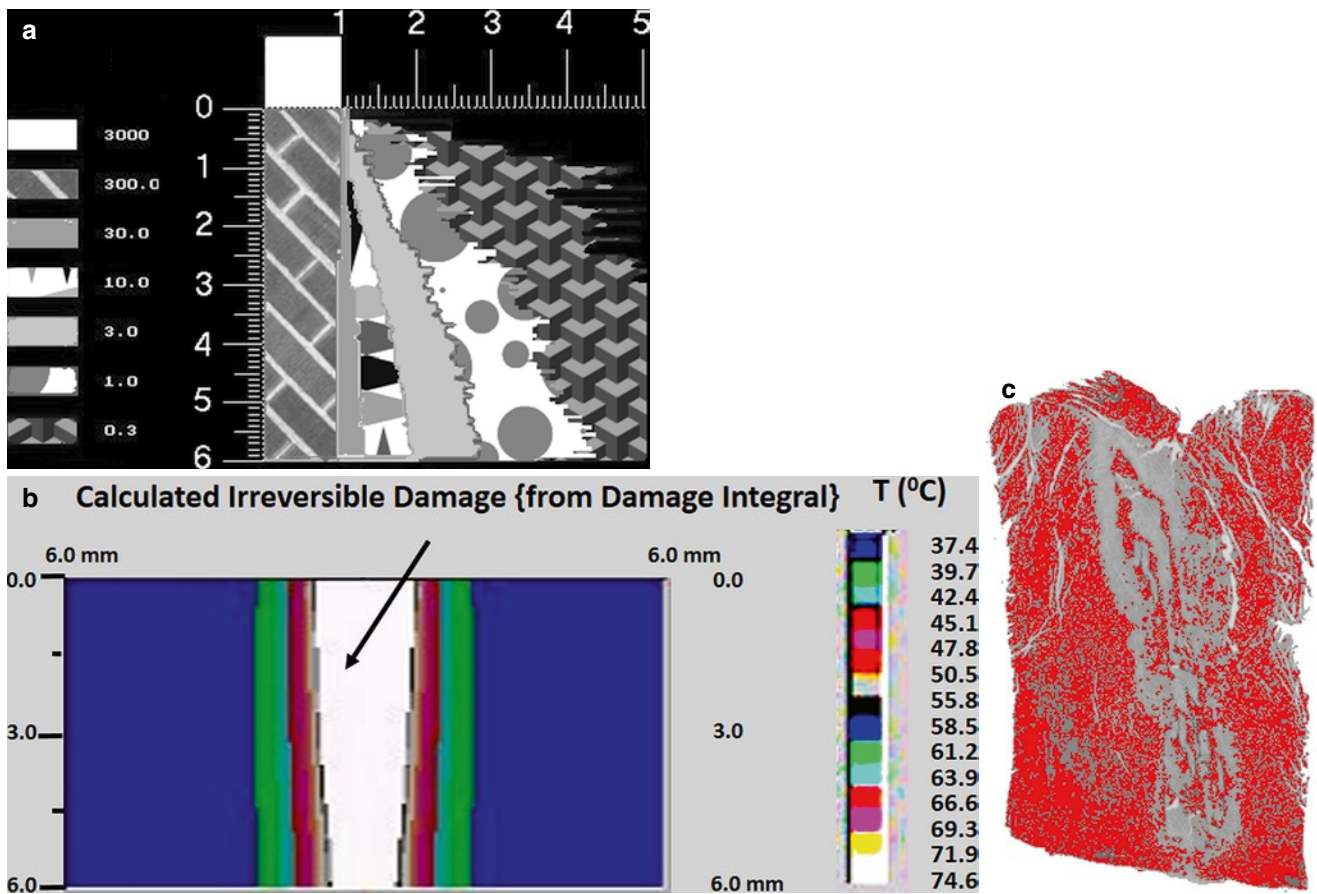
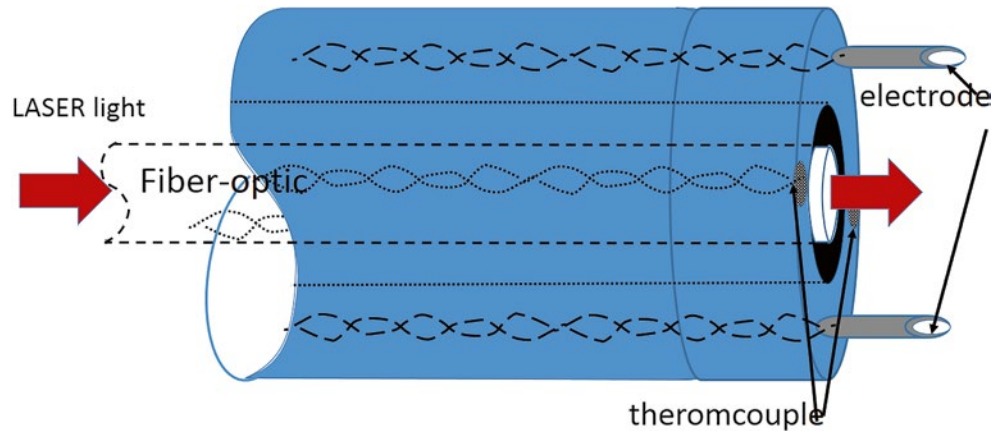


Fig. 16.11 Representative illustration of observed non-linear optical effects resulting from high power density laser irradiation under contact fiber-optic therapy. (a) Computer simulated cylindrical light distribution under the assumption that absorption is saturated, where the column on the left represents the calculated localized light radiance, (b) computer simulated thermal profile cross-section for the light

distribution in (a) after 6 s exposure, (c) observed representative, and reproducibly obtained, cylindrical transmural ventricular photocoagulation lesion resulting from irradiation by 1064 nm Nd:YAG laser light over 10 s at 20 W with the fiber-optic in direct tissue contact, for a tissue thickness of 6 mm, under irradiation by 2 mm laser spotsize

when a certain threshold power density is exceeded ($\sim 10 \text{ kW/cm}^2$ [19]), the scattering will encounter saturation and optical nonlinearity will occur. The resulting saturation will provide a light-distribution resembling a cylinder with resulting

cylindrical lesion shape as illustrated in Fig. 16.11. The saturation effects provide the means to create relatively narrow transmural lesions, affecting only a limited volume of peripheral damage.

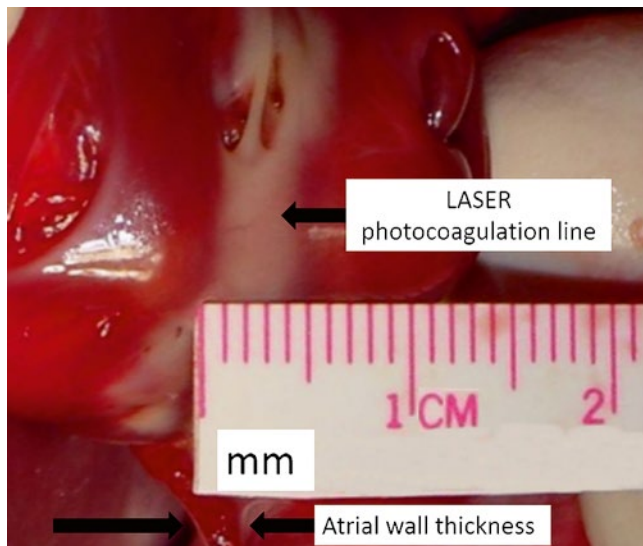


Fig. 16.12 Endocardial view of a representative narrow transmural photocoagulation line drawn in the atrial wall resulting from direct epicardial contact irradiation while moving a special catheter, without spikes and electrodes, in a linear fashion at a slow and steady rate using a 1064 nm Nd:YAG laser

Atrial Approach

For the atrial tissue the wall-thickness is considerably less than the left ventricular wall. In this situation the choice in coagulation wavelength becomes less stringent. The general laser light delivery application under open chest procedure can mimic the surgical blade or RF probe in the standard maze procedure. Applying the bare fiber-optic tip perpendicularly in direct epicardial contact while gradually advancing the fiber-optic in a linear motion along the epicardium will draw a line of coagulation (Fig. 16.12). The observed transmural narrow line of coagulation provides an excellent maze with minimal peripheral damage, maintaining confined functional atrial tissue.

Additionally, the inherently reduced penetration depth will impose less of a constraint on the power density. The lower power density requirement tolerates diffuse light delivery, specifically allowing for the use of a frosted fiber-optic tip that delivers light along a length of fiber in radial direction. Under transcatheter application of a diffusing linear probe, coagulation lines can be drawn with a relatively high success rate for elimination or reduction of atrial fibrillation [10, 40, 47–49]. The ablation wavelengths used in these applications were 980 nm, and 1064 nm as well as 1168 nm (anecdotal evidence only at the 1168 nm wavelength). Additional success has been achieved by electrical isolation of the pulmonary vein from the left atrium by means of circumferential laser coagulation with a catheter system positioned by means of a balloon in transcatheter approach [1], as illustrated in Fig. 16.5. Based on anatomical and

physiological findings the electrical isolation of the Crista Terminalis in the right atrium by means of laser photocoagulation have also shown clinical efficacy for the reduction of atrial fibrillation in patients [1].

Experimental and Clinical Results

Since the mid 80s both the Charlotte group under the leadership of Dr. Robert H. Svenson, Dr. Laszlo Littmann and Gregory Brucker, PhD, in consistent collaboration with Drs. John Selle and John Gallagher (and an additional host of critical clinical and technical individuals as well as support personnel that cannot be listed in its entirety) in Charlotte, NC, USA, as well as other groups such as Dr. G.M. Vincent in Salt Lake City, UT, USA, Dr. H.P. Weber in Munich, Germany and Dr. R. Moosdorf in Germany have investigated the use of laser-light for the modification of cardiac cellular depolarization and reshaping the excitation wave-front [12, 13, 41, 50]. Specifically, operating in the optical-window provides deep coagulation while providing the safety of minimizing the risks of carbonization and tissue removal, as found to occur with lasers operating at wavelengths below 580 nm and above 1600 nm [51, 52].

After extensive animal studies on dogs and pigs with the Nd:YAG laser the treatment options were validated for human use [17–19, 43].

The initial clinical procedures were performed on patients that did not respond to any of the classical available treatments in a life-saving emergency interventions. All patients from this worst case population responded with excellent clinical results under open-chest laser photocoagulation procedures [53].

All clinical and animal studies were performed under approved USA FDA investigational device exemption procedures, using human experimental protocols approved by the Human Subjects Committee of Carolinas Healthcare System as well as the Institutional Review Board (under which Carolinas Medical Center) Charlotte, NC; USA, respectively of the unit of Cardiac Arrhythmia at the Heart Institute (InCor) of the University of São Paulo Medical School, São Paulo; Brazil. All patients signed the approved informed consent forms in advance of the procedures.

Experimental and Animal Learning Curve

Our group in Charlotte, NC, USA, has experimentally verified the successful use of Nd:YAG and diode laser for the termination of ventricular tachycardia in dogs. Additional work with the Nd:YAG laser was validated for applying the Cox-Maze procedure under minimally invasive coagulation for the treatment of atrial fibrillation in dogs. Additional

work on limiting the sinus rhythm has proven beneficial in canine studies and was applied to human cases in limited trials. Isolation of the pulmonary vein on canine test subjects as well as pigs under open chest conditions validated the opportunity to treat the etiological bases for atrial fibrillation and initiated the development of a device suitable for transcatheter therapeutic applications on humans.

The fundamental understanding of the electrophysiologic cardiac depolarization-wave propagation for the root of targeted ventricular methodologies. Following the determination of the upper output power limit of the catheter under animal studies, the human clinical results were virtually identical, certainly within the statistical variance at $p < 0.05$. The power output is a critical issue in both patient safety as well as efficacy. The laser power as a function of laser wavelength will need to be set below a maximum wattage in order to prevent routine vaporization and specifically avoid carbonization. Since the magnitude of the light-distribution and absorbed radiance is directly proportional to the fiber-optic output power and power density, the absorption of light at the contact point with the tissue will result in an expedited temperature rise under higher output power.

Adding additional sensing safeguards to the temperature effects by means of real-time thermal feedback from the irradiated surface area provided a mechanism to account for inter-subject biological and histological variability.

Human Clinical Applications

The coagulation of depolarizing cells has been shown effective in selectively eradicating deviant depolarization pathways that were the result of physiological or anatomical tissue anomalies, as well as changing the depolarization on an individual cellular level with respect to sinus node excitation rate and atrio-ventricular node transfer-function [17, 18]. The “tear-drop” shape of the sinus node has an anatomically outlined depolarization rate distribution that is extremely well demarcated and lends itself to hyperfine graduated elimination of specific upper thresholds in pacing rhythm [18]. Under open-chest surgical intervention the sinus-node can be operationally defined and charted by electrophysiological examination using probing/pacing needles and specialty electrodes. Under continuous feedback by means of electrophysiologic mapping the application of laser irradiation has been shown to provide a graduated elimination of the functionality of cells with identified specific depolarization rate when applying the fiber-optic laser-light delivery in close-contact. In close-contact only a well demarcated tissue region equivalent to the diameter of the fiber-optic is denatured, in the order of 400–600 μm in diameter. The depth of coagulation is directly proportional to the exposure time.

The modifications to the atrio-ventricular node by means of laser photocoagulation have shown the potential for controlling the ventricular depolarization rate under the conditions of sustained rapid atrial rhythms without forming total atrio-ventricular block [17, 54]. Laser irradiation with the Nd:YAG laser operating at 1064 nm was applied to an area between the coronary sinus orifice and the electrophysiologically identified site of the most proximally recorded His-signal deflection. Laser photocoagulation was induced to create second degree AV block while the atrial pacing rate was greater or equal to 200 beats/min. In long-term follow-up the effects on AV node function were monitored during a 3 month duration. In the study 9 out of 12 dogs preserved 1:1 conduction, while three canine subjects developed chronic AV block. The nine success cases showed an average increase in AV node Wenckebach periodicity from $183 \pm 6 \text{ ms}$ to $261 \pm 24 \text{ ms}$, which corresponds to a 43 % increment. During induced atrial fibrillation the minimal RR-interval was raised to $275 \pm 20 \text{ ms}$ with respect to $215 \pm 11 \text{ ms}$. The effects were non-reversible by isoproterenol infusion. These results indicate the potential for laser assisted sustained modification anterograde AV node transmission. The ventricular rate under rapid atrial rhythms is permanently restrained to a significantly lower level, showing the potential for a nonpharmacologic mechanisms to permanently control the heart rate in patients with restrictive atrial arrhythmias.

Laser ablation of ventricular arrhythmias has proven successful in a multi-center study design over a 15 year period in Charlotte, North Carolina; USA, as well as Bonn; Germany and São Paulo; Brazil. The use of laser photocoagulation for the treatment and cure of human ventricular tachycardia has been validated with a better than 90 % success rate in a study on 30 patients with 85 arrhythmogenic morphologies, using a 1064 Nd:YAG laser [55].

The use of laser photocoagulation was first attempted in clinical trials by Dr. Helmut P. Weber as published in 1994 [56]. The use of laser photocoagulation in human atrial fibrillation treatment on a population approaching 2000 using a CardioFocus balloon for isolation of the pulmonary vein has yielded an initial success rate of better than 60 % while follow-up treatment of the unsuccessful first attempts provided a total cure rate of greater than 90 % [57]. The treatment of Chagasic patients with 830 nm diode laser ($n=8$) provided 65 % success [44].

The Charlotte study of laser ablation of Ventricular Tachycardia involved the treatment of more than 30 patients over a period of 15 years with a success rate of better than 90 % for post-infarction VT in the US trials with follow-up as long as 5 years post-procedure. Additional human clinical trials by G. Hindricks [58] were also likewise successful. The Chagas patients treated in Brazil’s Heart Institute (InCor), University of São Paulo Medical School in São

Paulo provided a success rate of 75 % (n=7) altogether, and a 78 % success rate (n=9) was achieved in the German human study with a follow-up of 17 ± 11 months; patients fell in mean NYHA class 2.2 ± 0.4 [59].

The additional benefits from modifications to sinus-node response rate under laser irradiation yields a powerful treatment tool. Modification of atrio-ventricular node conduction rate modification also yields treatment options for selectively blocking transfer of atrial fibrillation while specifically maintaining AV node functionality.

In contrast, several other techniques applied to the HIS bundle have resulted in total AV block and hence the need for pacemaker implants.

Opportunities for Therapeutic Applications

In cardiac photocoagulation the future lies in the development of spatially configurable high-power light delivery. The device design opportunities include structures that allow for location appropriate and accurate light delivery from validated diode laser energy sources geared to targeted coagulation. The device design includes both the target optical delivery orientation as well as efficiency of light delivery with minimal loss to inappropriate media. Specifically, the delivery of a linear irradiation pattern for transcatheter atrial maze procedures can benefit from limiting to irradiation of tissue in a perpendicular manner, avoiding irradiation of ambient blood as was the case under diffuse fiber-optic probe irradiation. The inherent requirement is in the reduction of peripheral damage (for instance to the circulating blood), as well as limiting the treatment volume to produce thin lines of block, significantly preserving contractile functionality of the remaining atrium. The directional delivery of a linear source (device that delivers light in a radial direction within a narrow spatial angle over a fixed length with uniform radiance) would require the knowledge of the orientation in which the light is emitted. In order to obtain this kind of information the probe may need to include a spectral analysis of the media in front of the window of irradiation, thus recognizing blood versus tissue orientation, or combinations (specifically, when placed in non-perpendicular position). Irradiation of blood may result in undesirable damage. In case light is not delivered in a perpendicular fashion the light penetration may be constrained or directed in an undesirable part of the atrial tissue, with a reduction in therapeutic efficacy. Light delivered at grazing angle has the potential of being reflected from the tissue surface or travel along the boundary, hence forming a thin layer of coagulation at the endocardial surface not a deep (preferentially transmural) and narrow line.

Additional feedback mechanisms for assessment of depth and width of coagulation have been developed but have so far not been implemented for additional qualitative and quantitative feedback on the perceived permanence of the detected physiological results [60, 61]. Verification of the ablation range can be beneficial for establishing boundaries in the treatment protocol.

Furthermore, the full impact and opportunities of non-linear optical mechanisms in the coagulation process require supplemental research and controlled mechanisms for delivery as well as irradiation.

Conclusions and Recommendations for Future Therapeutic Direction

Laser ablation of cardiac arrhythmias has shown the potential to cure better than 75 % of the total patient population, including those excluded from other treatment options due to the high risk associated with their conditions or after failing beneficial response to several other treatment mechanisms as well as remaining drug resistant. The use of monochromatic light provides the means to minimize peripheral damage and target deep-seated arrhythmogenic foci.

With the development of powerful small profile diode lasers operating over a broad wavelength range the device development can move forward with a low cost alternative for cure.

The minimally invasive catheter approach also provides a health benefit and quick recovery time.

In line with the growing elderly population, and associated increase in cardiac arrhythmias the transcatheter laser treatment opportunities will offer a low cost device as well as short recovery with equivalent reductions in healthcare costs.

Acknowledgments In acknowledgment for the clinical work, scientific contributions and practical conversations the following people require honorable mention: Dr. Robert H. Svenson, Dr. Laszlo Littmann, Dr. J. Selle, Dr. John J. Gallagher, Gregory Brucker, PhD, Kathleen Tuntelder-Seifert, Jan Tuntelder, Kathy R. Dezern, Katie Linder, Ernest Pruitt, Dr. Andre d'Avila, Dr. Eduardo Sosa, and Sergei Y. Semenov, PhD.

Appendix

Light-Distribution in Turbid Media

In order to provide a mechanism to predict the tissue volume that can potentially be coagulated, the light-distribution inside the tissue needs to be known first. Once the optical parameters for the different tissues over a range of wavelengths are known the most suitable wavelength can be

selected on a theoretical basis to provide the desired deep tissue effects for the clinical application. Concurrently, the theoretical analysis can provide the selection criteria for wavelength bands that should be avoided for risk mitigation, such as vaporization and carbonization.

Radiative transport theory provides the Equation of Radiative Transfer which is in many aspects similar to the Boltzmann equation used in kinetic gas theory, only now for photons [29]. The time-dependent angular and spatial photon energy rate distribution is described by the light power incident on a cross-sectional area flowing within a solid angle, and is designated by the parameter Radiance: $\bar{L}(\vec{r}, \vec{s}, t)$ (W/sr.cm²). In this notation the vector \vec{r} denotes the position of the location where the radiance is quantified, \vec{s} is the direction vector for the photon migration (within a small segment solid angle (i.e. cone of light) $d\Omega$, since the light is diffuse at this point), all as a function of time: t .

The Radiance follows from the Poyting vector: \vec{S} The Poynting vector is the energy vector describing the magnitude and direction of electro-magnetic radiation defined as:

$$\vec{S} = \frac{\vec{E} \times \vec{B}}{\mu} = \frac{|E| * |B| \sin \alpha}{\mu} \quad (\text{where } \vec{E} \text{ is the electric field,}$$

\vec{B} the magnetic field, \times designates the ‘‘cross-product’’ resulting in a vector with magnitude derived from the magnitude of both the electric and magnetic field with direction resulting from the right-hand rule (orthogonal to both vectors) and $\mu = \mu_r * \mu_0$ the dielectric permeability of the medium which is the product of the relative permeability μ_r and the permeability of free space: $\mu_0 = 4\pi \times 10^{-7} \text{ H/m}$). The Radiance is defined as the time average of the length of the Poynting vector, averaged over one or more cycle-lengths:

$$\bar{L}(\vec{r}, \vec{s}, t) = \left\langle \frac{\vec{E} \times \vec{B}}{\mu} \right\rangle \quad \text{The radiance } (\bar{L}(\vec{r}, \vec{s}, t)) \text{ is linked to}$$

the fluence ($\Psi(\vec{r}, t)$) as: $\Psi(\vec{r}, t) = \int_{4\pi} \bar{L}(\vec{r}, \vec{s}, t) d\Omega'$, integrated

over the full solid angle, hence without direction-specific details, representing all the electromagnetic radiation incident on the small but finite surface of a spherical tissue volume.

Since there are no external forces acting, the energy in the system is conserved. A general balance equation (such as those used to model chemical reactions) can be used to help develop an illumination model. For example the general energy balance follows the following rules: *Accumulation within a system is equal to the sum of the in-flow through system boundaries and the generation within the system complemented by the depletion by out-flow through system boundaries and consumption within the system.*

For light this is defined by the time dependent Equation of Radiative Transfer:

$$\frac{1}{c} \frac{\partial L(\vec{r}, \vec{s}, t)}{\partial t} = -\vec{s} \cdot \nabla L(\vec{r}, \vec{s}, t) - (\mu_a(\vec{r}) + \mu_s(\vec{r})) L(\vec{r}, \vec{s}, t) + \mu_s(\vec{r}) \int_{4\pi} P(\vec{s}, \vec{s}') L(\vec{r}, \vec{s}', t) d\Omega' + S(\vec{r}, \vec{s}', t)$$

The optical parameters defining the tissue in the following three terms: the absorption coefficient: μ_a , the scattering coefficient: μ_s , and the probability for a photon entering into a volume of scattering medium from direction \vec{s}' to be redirected in a narrow solid angle with direction \vec{s} represented by $P(\vec{s}, \vec{s}')$. The scattering probability $P(\vec{s}, \vec{s}')$ yields the scattering anisotropy factor (g) as the weighted average cosine of scattering angle (θ): $g = \langle \cos \theta \rangle$. One of the derived optical parameters is the total attenuation coefficient: $\mu_t = \mu_a + \mu_s$, which is equal to the sum of the absorption and scattering and represents the probability of per unit path length that a photon will encounter either an absorption or scattering event. When the anisotropy coefficient g is not known, the reduced scattering coefficient $\mu_s' = (1-g)\mu_s$ is useful to describe the scattering event. The Equation of Radiative Transfer provides a three-dimensional probability distribution for the final resting place of every photon directed at the tissue from the light-source. Hence the local cumulative energy absorption can be estimate and used to predict the volumetric spatial temperature rise as a function of location with respect to the entry point of the laser beam.

This equation can be seen as the composite effects of the following components of radiation transfer within a small but finite volume V of turbid medium. The first term represents the change in radiance per unit volume:

The first term after the equal sign signifies the radiance lost through the boundaries of the volume. The following term indicates the loss due to absorption and due to scattering into a different direction. The subsequent term identifies the recovery of radiance into the original direction as a result of scattering. The final term is the irradiation source. The deposited light energy translates in the volumetric thermal coagulation described by the three dimensional light distribution fluence ($\Psi(\vec{r}, t)$) as:

$$E_{coagulation}(\vec{r}, t) = \int_{4\pi} \int_t \mu_a L'(\vec{r}, \vec{s}, t) dt d\omega = \int_t \mu_a \Psi(\vec{r}, t) dt = \sum_{i \text{ constituents } V} \int_V \rho_i (h_{c,i} + c_{v,i} \Delta T) dV$$

The Radiative Transfer equation describing the light distribution can not be solved analytically but can be described numerically. Examples of numerical light distribution

computer simulation for Nd:YAG irradiation (1064 nm) in cardiac tissues are represented in Figs. 16.6 and 16.11. In Figs. 16.7 and 16.11c the representative thermal lesion resulting from long-term laser light exposure does resemble the respective light distribution and associated thermal profile.

The window of opportunities for laser assisted coagulation in the treatment of cardiac arrhythmias is in the 800–1100 nm emission range, even extending to 1200 nm in the atrial application; the proverbial “optical window”, as illustrated in Fig. 16.8.

Light Propagation Under Dominant Absorption

The simplest situation to solve the light distribution inside a turbid medium for is where absorption is much greater than scattering. This is however not the most favorable situation for deep tissue coagulation. This situation can be verified for ultraviolet light irradiation of biological media. In the wavelength range below 400 nm absorption is much greater than scattering (for instance for muscle in comparison to irradiation at 1064 nm has at least three times greater attenuation at 400 nm and ten times greater at 308 nm [62]), increasingly so for shorter wavelength. Under these conditions the light propagation simply reduces to the Beer – Lambert law. The light propagation can be described by a one dimensional attenuation proportional to the distance, with respect to absorption only: $\psi(z) = \psi_0 e^{-\mu_a z}$. Note that

after one optical-free path length $\left(\delta = \frac{1}{\mu_a + (1-g)\mu_s} \right)$ 63 %

of the light energy has been converted into other forms of energy (e.g. chemical dissociation, vaporization) due to absorption.

Dominant absorption will only provide surface effects, without significant tissue penetration. The surface effects are represented as vaporization (e.g. Trans-Myocardial Revascularization: TMR [63]) or carbonization [41]. No large volume tissue coagulation can be achieved under absorption dominated light-tissue interaction.

Absorption dominated light-tissue interaction occurs at short wavelengths (below 550 nm, green) and at attenuation peaks in the near and mid infrared (see Fig. 16.8).

The practical implementation of light propagation theory is often a compromise between mathematical feasibility and physical accuracy.

The use of lasers for photocoagulation falls primarily in the so-called optical window of low attenuation, ranging from yellow to near-infrared. The most frequently used and beneficial laser wavelengths are 810 nm [64], 830 nm [44],

980 nm [20, 57], and 1064 nm [22, 55, 65]. Additional work with an 1168 nm laser irradiation has insufficient data available to show efficacy for ventricular ablation but has proven successful for pulmonary vein isolation procedures (Private communication Gregory Brucker, PhD; Innovations in Medicine/MedCV). The introduction of diode lasers has provided a few more wavelengths in the 900–1200 nm range that are showing the potential for deep coagulation when avoiding specific spectral absorption lines, mainly of water.

Generally, wavelengths between 580 and 700 nm have relatively low absorption and do not produce significant thermal effects, although the laser selection in this wavelength range is still rather limited.

Shorter wavelengths have strong absorption and are not clinically relevant due to the risk of carbonization and fall in the ‘absorption dominated’ range of operation. The use of the Argon laser operating at 488 nm or 514.5 nm (green) has been shown to be ineffective for reaching deep photocoagulation, with associated low clinical success rate and the considerable risk of carbonization [41].

It is recommended to avoid absorption dominated light-tissue interaction due to the risks of potential adverse effects (e.g. carbonization and high degree of peripheral damage).

References

1. Kalman JM, Olgin JE, Karch MR, Hamdan M, Lee RJ, Lesh MD. “Cristal tachycardias”: origin of right atrial tachycardias from the crista terminalis identified by intracardiac echocardiography. *J Am Coll Cardiol.* 1998;31(2):451–9.
2. Wyndham CRC. Atrial fibrillation: the most common arrhythmia. *Tex Heart Inst J.* 2000;27(3):257–67.
3. Chagas C. *Mem Inst Oswaldo Cruz.* 1909;1:159–218.
4. Sosa E, Scanavacca M, d’Avila A, Piccioni J, Sanchez O, Velarde JL, Silva M. Endocardial and epicardial ablation guided by non-surgical transthoracic epicardial mapping to treat recurrent ventricular tachycardia. *J Cardiovasc Electrophysiol.* 1998;9:229–39.
5. Aliot EM, Stevenson WG, Almendral-Garrote JM, Bogun F, Calkins CH, Delacretaz E, Bella PD, Hindricks G, Jais P, Josephson ME, Kautzner J, Kay GN, Kuck KH, Lerman BB, Marchlinski F, Reddy V, Schalij MJ, Schilling R, Soejima K, Wilber D, European Heart Rhythm A, European Society of C, Heart Rhythm S. EHRA/HRS Expert Consensus on Catheter Ablation of Ventricular Arrhythmias: developed in a partnership with the European Heart Rhythm Association (EHRA), a Registered Branch of the European Society of Cardiology (ESC), and the Heart Rhythm Society (HRS); in collaboration with the American College of Cardiology (ACC) and the American Heart Association (AHA). *Europace.* 2009;11:771–817.
6. Brugada P, de Swart H, Bar WHM, J. Smeets LRM, van Ommen FV, Wellens HJJ. Transcoronary chemical ablation of ventricular tachycardia. In: Zipes DP, Jalife J, editors. *Cardiac electrophysiology: from cell to bedside.* Amsterdam, The Netherlands: Elsevier; 1990. pp. 1006–14.
7. Goodacre S, Irons R. ABC of clinical electrocardiography: atrial arrhythmias. *BMJ.* 2002;324(7337):594–7.

8. Friedman PL. Catheter cryoablation of cardiac arrhythmias. *Curr Opin Cardiol.* 2005;20(1):48–54.
9. Huang SKS, Wood MA. Catheter ablation of cardiac arrhythmias. 2nd ed. Philadelphia: Elsevier Saunders; 2011.
10. Keane D. New catheter ablation techniques for the treatment of cardiac arrhythmias. *Card Electrophysiol Rev.* 2002;6:341–8.
11. Wu Q, Zhou Q, Zhu Q, Rong S, Wang Q, Guo R, Deng C, Liu D, Yang G, Jiang Y, Wang Z, Lei H, He TC, Wang Z, Huang J. Noninvasive cardiac arrhythmia therapy using High-Intensity Focused Ultrasound (HIFU) ablation. *Int J Cardiol.* 2013; 166(2):e28–30.
12. Vincent GM, Fox J, Benedick BA, Hunter J, Dixon JA. Laser catheter ablation of simulated ventricular tachycardia. *Lasers Surg Med.* 1987;7(5):421–5.
13. Vincent GM, Fox J, Knowlton K, Dixon JA. Catheter-directed neodymium:YAG laser injury of the left ventricle for arrhythmia ablation: dosimetry and hemodynamic, hematologic, and electrophysiologic effects. *Lasers Surg Med.* 1989;9(5):446–53.
14. Dickfeld T, Tian J, Ahmad G, Jimenez A, Turgeman A, Kuk R, Peters M, Saliaris A, Saba M, Shorofsky S, Jeudy J. MRI-Guided ventricular tachycardia ablation: integration of late gadolinium-enhanced 3D scar in patients with implantable cardioverter-defibrillators. *Circ Arrhythm Electrophysiol.* 2011;4(2):172–84.
15. Prystowsky EN, Padanilam BJ, Joshi S, Fogel RI. Ventricular arrhythmias in the absence of structural heart disease. *J Am Coll Cardiol.* 2012;59(20):1733–44.
16. Cox JL, Boineau JP, Schuessler RB, Kater KM, Lapps DG. Five-year experience with the maze procedure for atrial fibrillation. *Ann Thorac Surg.* 1993;56(4):814–23.
17. Littmann L, Svenson RH, Tomcsanyi I, Hehrlein C, Gallagher JJ, Bharati S, Lev M, Splinter R, Tatsis GP, Tuntelder JR. Modification of atrioventricular node transmission properties by intraoperative neodymium-YAG laser photocoagulation in dogs. *J Am Coll Cardiol.* 1991;17(3):797–804.
18. Littmann L, Svenson RH, Gallagher JJ, Bharati S, Lev M, Linder KD, Tatsis GP, Nichelson C. Modification of sinus node function by epicardial laser irradiation in dogs. *Circulation.* 1990;81(1):350–9.
19. Svenson RH, Splinter R, Littmann L, Tatsis GP. Photoablation of ventricular arrhythmias: past results and future applications to ventricular and other arrhythmias. Chapter 25. In: Liem LB, Downar E, editors. *Progress in catheter ablation: clinical application of new mapping and ablation technology: developments in cardiovascular medicine*, vol. 241. New York: Springer; 2001.
20. Dukkupati SR, Neuzil P, Skoda J, Petru J, d'Avila A, Doshi SK, Reddy VY. Visual balloon-guided point-by-point ablation: reliable, reproducible, and persistent pulmonary vein isolation. *Circ Arrhythm Electrophysiol.* 2010;3(3):266–73.
21. Cobb FR, Blumenschein SD, Sealy WC, Boineau JP, Wagner GS, Wallace AG. Successful surgical interruption of the bundle of Kent in a patient with Wolff-Parkinson-White syndrome. *Circulation.* 1968;38:1018–29.
22. Avitall B, Khan M, Krum D, Hare J, Lessila C, Dhala A, Deshpande S, Jazayeri M, Sra J, Akhtar M. Physics and engineering of transcatheter cardiac tissue ablation. *J Am Coll Cardiol.* 1993;22(3): 921–32.
23. Avitall B, Lafontaine D, Rozmus G, Adoni N, Dehnee A, Urbonas A, Le KM, Aleksonis D. Ablation of atrial-ventricular junction tissues via the coronary sinus using cryo balloon technology. *J Interv Card Electrophysiol.* 2005;12(3):203–11.
24. Takemoto M, Yoshimura H, Ohba Y, Matsumoto Y, Yamamoto U, Mohri M, Yamamoto H, Origuchi H. Radiofrequency catheter ablation of premature ventricular complexes from right ventricular out-flow tract improves left ventricular dilation and clinical status in patients without structural heart disease. *J Am Coll Cardiol.* 2005;45(8):1259–65.
25. Wissner E, Stevenson WG, Kuck K-H. Catheter ablation of ventricular tachycardia and non-ischaemic cardiomyopathy; where are we today? A clinical review. *Eur Heart J.* 2012;33(12):1440–50.
26. Feld GK, Fleck RP, Fujimura O, Prothro DL, Bahnson TD, Ibarra M. Control of rapid ventricular response by radiofrequency catheter modification of the atrioventricular node in patients with medically refractory atrial fibrillation. *Circulation.* 1994;90(5):2299–307.
27. Hsu LF, Jaïs P, Keane D, Wharton JM, Deisenhofer I, Hocini M, Shah DC, Sanders P, Scavée C, Weerasooriya R, Clémenty J, Haïssaguerre M. Atrial fibrillation originating from persistent left superior vena cava. *Circulation.* 2004;109(7):828–32.
28. Weber HP, Heinze A, Hauptmann G, Ruprecht L, Unsöld E. In vivo temperature measurement during transcatheter endomyocardial Nd-YAG laser irradiation in dogs. *Lasers Med Sci.* 1997;12(4): 352–6.
29. Splinter R, Hooper B. *Introduction to biomedical optics.* Boca Raton: CRC Press/Taylor & Francis; 2007.
30. Tipler P, Mosca G. *Physics for scientists and engineers: electricity, magnetism, light, and elementary modern physics.* 5th ed. New York: W. H. Freeman/Macmillan; 2004.
31. Mielnik B. An electron trapped in a rotating magnetic field. *J Math Phys.* 1989;30(2):537–49.
32. Whittaker ET. *A history of the theories of aether and electricity.* New York: Dover Publications; 1951.
33. Splinter R. *Handbook of physics in medicine and biology.* Boca Raton: CRC Press/Taylor & Francis Group; 2010.
34. Parshina EY, Yusipovich AL, Platonova AA, Grygorczyk R, Maksimov GV, Orlov SN. Thermal inactivation of volume-sensitive K^+ , Cl^- cotransport and plasma membrane relief changes in human erythrocytes. *Pflugers Arch Eur J Physiol.* 2013;465(7):977–83.
35. Boltzmann L. *Wiener Berichte.* 1866;53:195–220.
36. Tornberg E. Effects of heat on meat proteins – implications on structure and quality of meat products. *Meat Sci.* 2005;70(3):493–508. doi:10.1016/j.meatsci.2004.11.021.
37. Jin B, Li L, Liu G-Q, Li B, Zhu Y-K, Liao L-N. Structural changes of malt proteins during boiling. *Molecules.* 2009;14(3):1081–97. doi:10.3390/molecules14031081A.
38. Jacques SL. Ratio of entropy to enthalpy in thermal transitions in biological tissues. *J Biomed Opt.* 2006;11(4):041108.
39. Floume T, Syms RR, Darzi AW, Hanna GB. Optical, thermal, and electrical monitoring of radio-frequency tissue modification. *J Biomed Opt.* 2010;15(1):018003. doi:10.1117/1.3323089.
40. Keane D, Ruskin JN. Linear atrial ablation with a diode laser and fiberoptic catheter. *Circulation.* 1999;100(14):e59–60.
41. Saksena S. Catheter ablation of tachycardias with laser energy: issues and answers. *PACE.* 1989;12:196–203.
42. Splinter R, Semenov SY, Nanney GA, Littmann L, Tuntelder JR, Svenson RH, Chuang CH, Tatsis GP. Myocardial temperature distribution under cw Nd:YAG laser irradiation in in vitro and in vivo situations: theory and experiment. *Appl Opt.* 1995;34:391–9.
43. Svenson RH, Littmann L, Cola Vita PG, Zimmern SH, Gallagher JJ, Fedor JM, Selle JG. Laser photoablation of ventricular tachycardia: correlation of diastolic activation times and photoablation effects on cycle length and termination-observations supporting a macroreentrant mechanism. *J Am Coll Cardiol.* 1992;19(3): 607–13.
44. d'Avila A, Splinter R, Svenson RH, Scanavacca M, Pruitt E, Kasell J, Sosa E. New perspectives on catheter-based ablation of ventricular tachycardia complicating Chagas' disease: experimental evidence of the efficacy of near infrared lasers for catheter ablation of Chagas' VT. *J Interv Card Electrophysiol.* 2002;7(1):23–38.
45. Splinter R, Svenson RH, Littmann L, Chuang C-H, Tuntelder JR, Thompson M, Tatsis GP, Keijzer M. Computer simulated light distributions in myocardial tissues at the Nd-YAG wavelength of 1064 nm. *Lasers Med Sci.* 1993;8(1):15–21.

46. Heinze A, Weber HP, Gottschalk W, Unsöld E. Simulation of heat generation for transcatheter Nd-YAG laser photocoagulation of myocardium. *Lasers Med Sci*. 1994;9(2):119–25.
47. Fried NM, Lardo AC, Berger RD, Calkins H, Halperin HR. Linear lesions in myocardium created by Nd:YAG laser using diffusing optical fibers: in vitro and in vivo results. *Lasers Surg Med*. 2000;27(4):295–304.
48. Williams MR, Casher JM, Russo MJ, Hong KN, Argenziano M, Oz MC. Laser energy source in surgical atrial fibrillation ablation: pre-clinical experience. *Ann Thorac Surg*. 2006;82(6):2260–4.
49. Peshko I, Rubtsov V, Vesselov L, Sigal G, Laks H. Fiber photocoagulation catheters for laser treatment of atrial fibrillation. *Opt Lasers Eng*. 2007;45(4):495–502.
50. Wagshall A, Abela GS, Maheshwari A, Gupta A, Bowden R, Huang SK. A novel catheter design for laser photocoagulation of the myocardium to ablate ventricular tachycardia. *J Interv Card Electrophysiol*. 2002;7(1):13–22.
51. Smith AM, Mancini MC, Nie S. Bioimaging: second window for in vivo imaging. *Nat Nanotechnol*. 2009;4(11):710–1.
52. Tsai C-L, Chen J-C, Wang W-J. Near-infrared absorption property of biological soft tissue constituents. *J Med Biol Eng*. 2001;21(1):7–14.
53. Selle JG, Svenson RH, Sealy WC, Gallagher JJ, Zimmern SH, Fedor JM, Marroum MC, Robicsek F. Successful clinical laser ablation of ventricular tachycardia: a promising new therapeutic method. *Ann Thorac Surg*. 1986;42(4):380–4.
54. Weber HP, Kaltenbrunner W, Heinze A, Steinbach K. Laser catheter coagulation of atrial myocardium for ablation of atrioventricular nodal reentrant tachycardia. First clinical experience. *Eur Heart J*. 1997;18(3):487–95.
55. Svenson RH, Littmann L, Splinter R, Selle JG, Gallagher JJ, Tatsis GP, Linder KD, Seifert KT. Application of lasers for arrhythmia ablation. Chapter 107. In: Zipes DP, Jalife J, editors. *Cardiac electrophysiology: from cell to bedside*. Dordrecht: Elsevier; 1990.
56. Weber HP, Heinze A. Laser catheter ablation of atrial flutter and of atrioventricular nodal reentrant tachycardia in a single session. *Eur Heart J*. 1994;15(8):1147–9.
57. Dukkupati SR, Kuck KH, Neuzil P, Woollett I, Kautzner J, McElderry HT, Schmidt B, Gerstenfeld EP, Doshi SK, Horton R, Metzner A, d'Avila A, Ruskin JN, Natale A, Reddy VY. Pulmonary vein isolation using a visually guided laser balloon catheter: the first 200-patient multicenter clinical experience. *Circ Arrhythm Electrophysiol*. 2013;6(3):467–72. doi:10.1161/CIRCEP.113.000431. Epub 4 Apr 2013.
58. Hindricks G, Haverkamp W, Gülker H, Kramer T, Russel U, Teutemacher H, Borggrefe M, Breithardt G. Perkutane endokardiale Nd-YAG-Laserapplikation: Experimentelle Untersuchungen zur Ablation ventrikulären Myokards. *Z Kardiologie*. 1991;80:673–80.
59. Pfeiffer D, Moosdorf R, Svenson RH, Littmann L, Grimm W, Kirchhoff PG, Lüderitz B. Epicardial neodymium. YAG laser photocoagulation of ventricular tachycardia without ventriculotomy in patients after myocardial infarction. *Circulation*. 1996;94(12):3221–5.
60. Splinter R, Farahi F, Raja MYA, Svenson RH. Tissue diagnostics by depth profiling of optical characteristics using broadband fiber optic interferometry. *Proc. SPIE 2732*. Valery V. Tuchin, editor. *CIS selected papers: Coherence-Domain methods in biomedical optics*. Bellingham: SPIE; 1996. pp. 242–50.
61. Fleming CP, Wang H, Quan KJ, Rollins AM. Real-time monitoring of cardiac radio-frequency ablation lesion formation using an optical coherence tomography forward-imaging catheter. *J Biomed Opt*. 2010;15(3):030516.
62. Tuchin VV. Light scattering study of tissues. *Phys – Uspekhi*. 1997;40(5):495–515.
63. Kim CB, Kesten R, Javier M, Hayase M, Walton AS, Billingham ME, Kernoff R, Oesterle SN. Percutaneous method of laser transmural myocardial revascularization. *Cathet Cardiovasc Diagn*. 1997;40(2):223–8.
64. Hamman BL, Theologes TT. Surgical treatment of atrial fibrillation with diode-pumped laser. *Proc (Bayl Univ Med Cent)*. 2009;22(3):230–3.
65. Oeff M, Hug B, Müller G. Transcatheter laser photocoagulation for treatment of cardiac arrhythmias. *Lasers Med Sci*. 1991;6:355–61.
66. Buiteveld H, Hakvoort JMH, Donze M. The optical properties of pure water. *SPIE Proc Ocean Optics XII*. edited by J. S. Jaffe. 1994;2258:174–83.
67. Jacques SL. Optical properties of biological tissues: a review. *Phys Med Biol*. 2013;58:R37–61.

Helmut P. Weber and Michaela Sagerer-Gerhardt

Experimental Studies

Introduction

With the invention of the laser (Light Amplification by Stimulated Emission of Radiation), many clinical disciplines have taken advantage of this new energy source. Its precision, intensity and energy density is superior to all other known surgical devices. Based on the principle of light amplification from photon-emitting resonator monochromaticity, collimation and coherence provide the high-energy density of the laser beam for medical applications. Among medical lasers continuous wave (cw) 1064 nm Nd:YAG laser light is best suited for thermal coagulation of myocardium with arrhythmia ablation [1]. Similar to the eye ball the Nd:YAG laser crosses through transparent or translucent tissue such as the endocardium, epicardium and scarred fibrous myocardium without substantial heat generation [2]. Initially, photons are scattered penetrating in the myocardium and are eventually absorbed by Chromophoren, by myoglobin, inducing heat deep intramurally [3].

By application of laser light we do not ablate, we coagulate the myocardium rendering it electrically inactive. The coagulated myocardium is devoid of electrical potentials, the electrical activity of the arrhythmogenic substrate is eliminated or at least modified, the arrhythmia is “ablated”. The anatomical integrity of the culprit myocardium is not destroyed. The acute laser lesion of coagulation necrosis is healing to a dense fibrous scar without thickening of the

cardiac wall, without aneurysm formation, and without adjacent angiogenesis.

In the past decades, a total of 153 anesthetized dogs, mainly beagles, over 500 acute or chronic experiments with cardiovascular laser applications, 1–24 per dog were performed by using the 1064 nm laser light via open irrigated laser catheter systems. Along with rabbits, dogs display similar channel distributions and channel activity as the human cardiac conduction system.

The dog has been described as the most predictive pre-clinical species with regard to human electrophysiology. Various canine models of atrial and ventricular arrhythmias have been employed to study the underlying mechanisms of these arrhythmias [4, 5].

The investigations complied with the principles outlined in the Declaration of Helsinki, animal experimental studies were conforming to the *Directive 86/609/EEC on the protection of Animals used for Experimental and other scientific purposes*, adopted in 1986 by the European commission, 1986 Retrieved February 8, 2007, and comply with all applicable *Laws and Regulations and Guidelines of the United States Food and Drug Administration regarding Good Laboratory Practice and Non-clinical Research (CFR Title 21, Parts 11 and 58)*.

In the following we report our experience with experimental and clinical catheter directed cardiovascular laser applications since 1984 performed in various research institutions including:

1. Research Laboratory of Donier MedTech, Rosenheimer Landstr. 114, Ottobrunn, Germany
2. Central Laser Laboratory and Animal Experimental Facilities of the Helmholtz Institute Neuherberg/Munich, Germany
3. Experimental Animal Laboratory of the German Heart Center (DHZ), Munich, Germany
4. Animal Experimental Laboratory of the Anadaal Hospital Maastricht, Netherlands
5. King Faisal Specialist Hospital & Research Center, Riyadh, Saudi-Arabia

H.P. Weber, MD (✉)
Department of Research, Development and Education,
CCEP Center Taufkirchen, Taufkirchen, D-82024, Germany
e-mail: hw@ccep.de

M. Sagerer-Gerhardt, MD
Department of Anesthesiology, Hospital Neuperlach, Teaching
Hospital of the LM-University of Munich, Munich, Germany
e-mail: misage@t-online.de

6. Experimental Laboratory of the Surgical Department LM-University Munich, Germany
7. Laser and Applied Technologies Laboratory, Charlotte, NC, USA
8. Experimental Electrophysiology Laboratory of the UCLA, CA, USA
9. Animal Experimental Facilities of the Semmelweis University Budapest, Hungary
10. Animal Experimental Laboratory of the Cardiac Department University of Tübingen, Germany
11. Research Laboratories of Hanson Medical, Mountain-View, CA, USA
12. Experimental Electrophysiology Laboratory, The University of Oklahoma, Health Science Center, Oklahoma City, OK, USA

The Laser

Power source was a *MediLas* fibertom Model 4060 N, a medical laser system from Dornier MedTech, provided with a Light-guide protection system (LPS). The LPS switched off the laser automatically in case of imminent overheating at the optical fiber tip. More recently a novel diode laser designed for cardiovascular laser application was used, the *MediLas D 1064* Cardiovascular Laser Application, LasCor GmbH, Taufkirchen, Germany. This is provided with a standard continuous wave (cw) application mode for radiation at powers of 2–30 W in 1 W steps (Fig. 17.1).

Besides the LPS the diode laser is provided with two additional safety chains: one for control of the saline irrigation flow assured by a peristaltic pump, another for control of the esophageal temperature with a light sensor [6]. Each of the safety chains can stop the laser automatically in case of



Fig. 17.1 Diode laser *MediLas D 1064*, LPS, LasCor GmbH, designed for cardiovascular laser applications, with the peristaltic pump for catheter irrigation on it

imminent catheter damages, or of insufficient catheter irrigation flow, or in case of imminent overheating prior to the occurrence of thermal damages to the esophagus.

The Catheter

The electrode-laser mapping and ablation (ELMA) catheter *RytmoLas* and its variant the *RytmoLas.m*, LasCor GmbH, Taufkirchen, Germany consist of a 400 μm core diameter and 300 cm long optical fiber fed into the central lumen of an 8 F flexible plastic tube, working length 115 cm. In addition, for magnetic navigation the distal segment of the *RytmoLas.m* is provided with three cylindrical magnets (Fig. 17.2). The tip of the optical fiber is mounted at a given distance from the end hole of the catheter and is protected within the catheter hose. In front of the end hole the divergent laser beam creates a ring shaped laser spot, a “donut”, on the illuminated field (Fig. 17.3).

For cardiovascular laser application the catheter is irrigated continuously with heparinized saline (5000 IU/L) at a flow rate of 15 mL/min, assured by a peristaltic pump. Irrigation flow washes away the blood and creates a clear path for the laser light in front of the end hole of the catheter to illuminate the targeted endocardial area. During laser application irrigation flow is increased automatically with the foot switch of the laser to a preset value of 30–40 mL/min, “working flow”. The two symmetrically arranged tip electrodes of the catheter are connected to the manifold via cables running in the lumen of the catheter along with the optical fiber. Electrodes are riding symmetrically upon the radiation field and allow for continuous intracardiac local bipolar or unipolar electrical recordings. Local electrograms (LEGs) recorded directly from around the illuminated endocardial area were displayed on the monitor without noise, also during laser application.

Catheter Ablation

For a safe and effective cardiovascular laser application contact of the optical fiber with tissue or with the blood has to be avoided. Therefore the fiber tip is mounted in the catheter lumen at a given distance from its end-hole and the catheter is rinsed continuously. Such contact would result in an instant temperature rise up to several 100 $^{\circ}\text{C}$ with vaporization and carbonization of tissue and the risk of cardiac wall perforation (Fig. 17.4, left). However, intramural cavitation may occur also without optical fiber tip to tissue contact when too high power levels are applied (Fig. 17.4, right). Such unwanted effects can be avoided by applying optimal energy settings, namely, lower levels of power with longer application times. By applying optimal energy settings larger lesions of clear-cut coagulation necrosis can be achieved without intramural cavitation (Fig. 17.4 mid).

Fig. 17.2 Overview of the open-irrigated electrode-laser mapping and ablation (ELMA) catheter *RytmoLas* and the distal end of its variant, the *RytmoLas.m* (top, right) provided with three magnetic rings for remote magnetic navigation

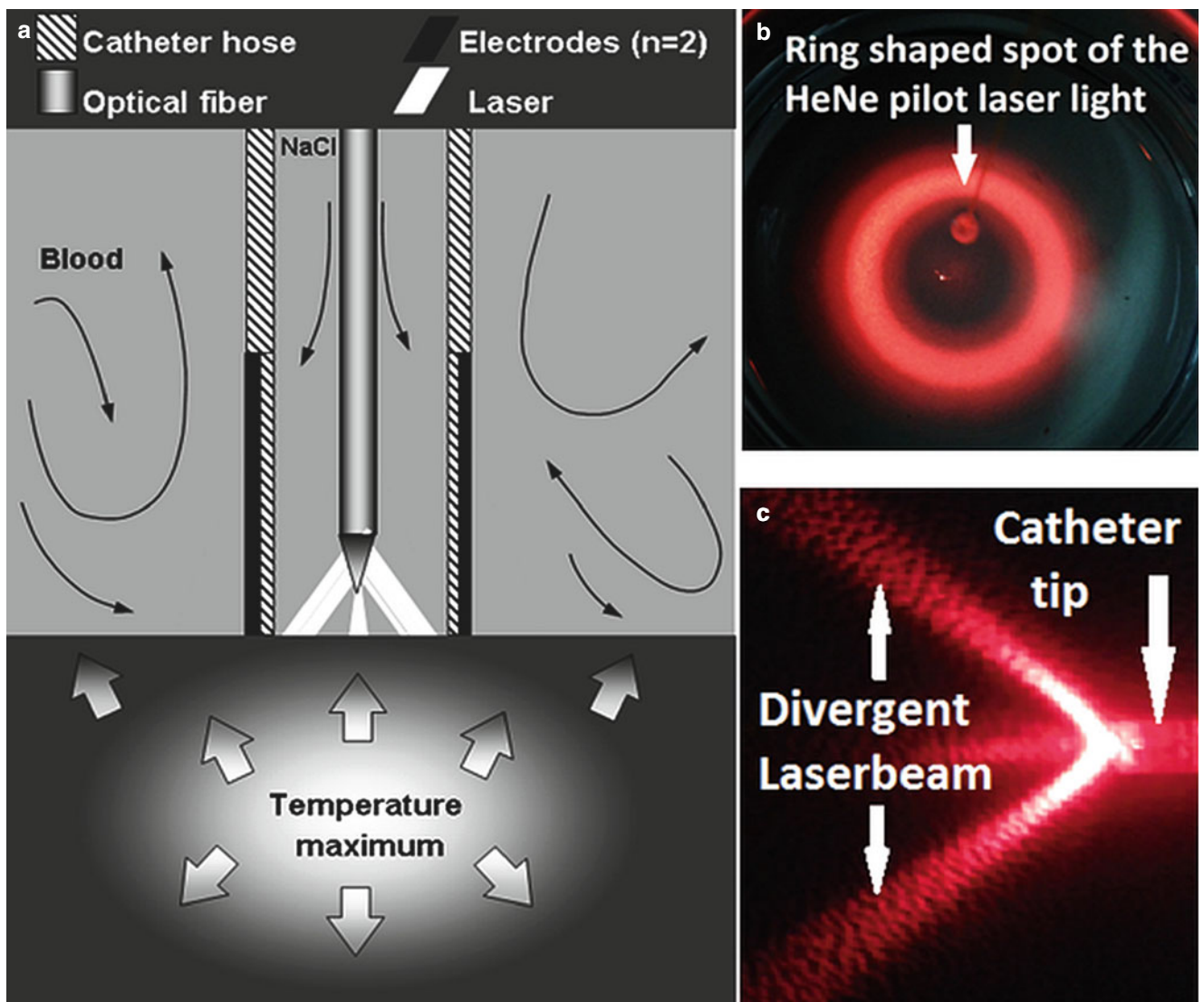
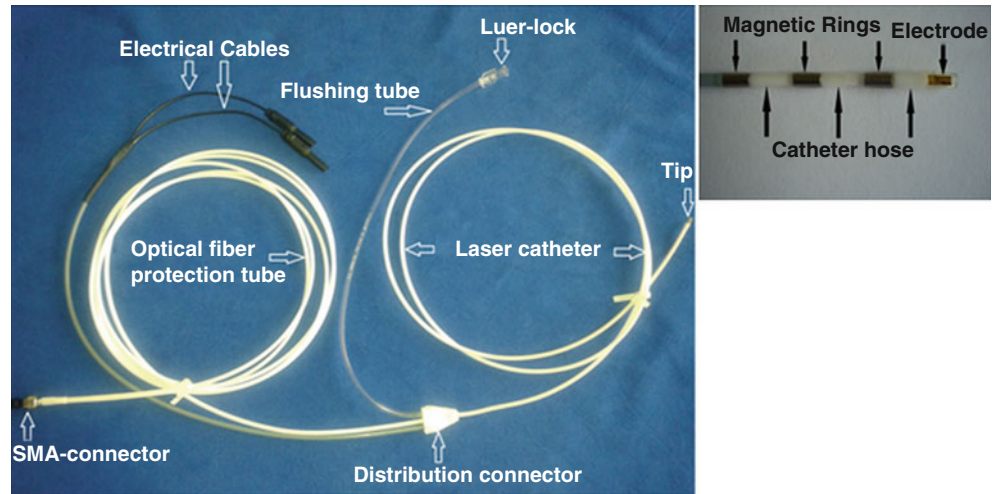


Fig. 17.3 (a) Scheme showing the distal end of the laser catheter *RytmoLas* framing and shielding the ring-shaped spot of the laser light, and the two electrodes overriding the margins of the spot, and (b) the

laser beam profile frontal and (c) in lateral view with the tip of the 8 F catheter emanating the divergent light beam of the HeNe pilot laser light from its end-hole

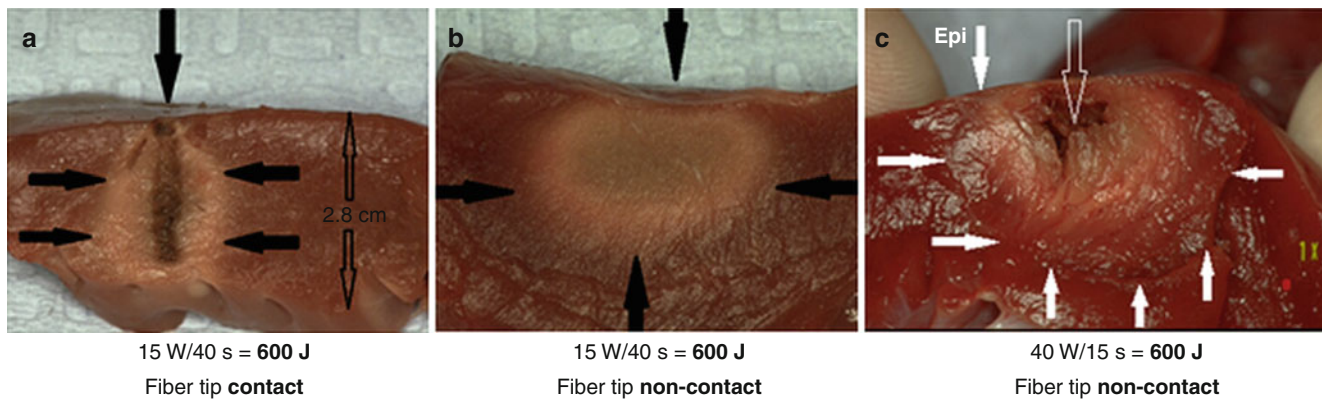
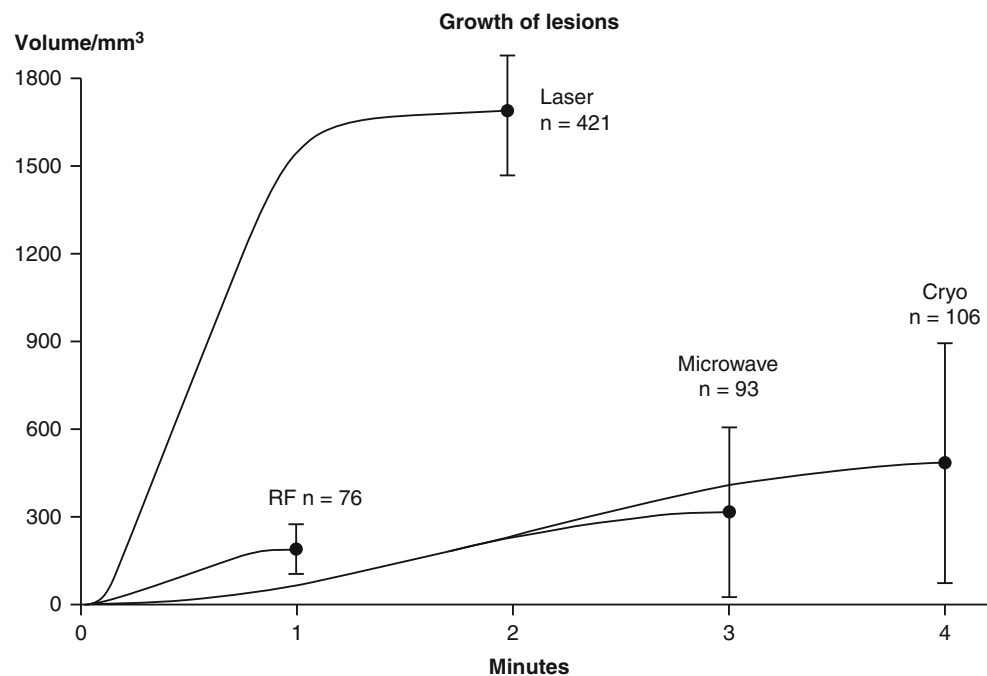


Fig. 17.4 Epicardial lesions achieved by laser application on bovine myocardium with the same level of energy, **600 J**, but with two different energy settings, (a) with the bare fiber tip in intimate contact showing a deep channel burned into the tissue (*black vertical arrow*), and (b) with the fiber tip **mounted** at a given distance from the end hole of the cath-

eter showing a not fat a clear-cut homogenous coagulation necrosis without tissue vaporization with crater formation, without central cavitation, and (c) with intramural cavitation (*vertical clear arrow*). Black and white arrows indicate the margins of lesions

Fig. 17.5 Diagram showing volumes of myocardial lesions achieved in dog hearts by laser catheter applications via an open irrigated electrode laser mapping and ablation (ELMA) catheter, as compared to Not fat: the volumes of lesions achieved by using other methods of ablation when applying a comparable level of energy. Laser lesions were transmural after one minute (No further increase of volume achievable)



Energy Settings

By using the open irrigated ELMA catheter *RytmoLas* transmural lesions can be achieved in dog hearts within seconds (Fig. 17.5). In order to avoid unwanted effects energy delivery must be adapted to the thickness of the myocardial wall [6]. At a given power higher energy can be used for coagulation of thicker ventricular walls by lengthening radiation times and a lower energy by shortening radiation times when thinner atrial structures are targeted. Adapted energy settings are important for both safety and efficacy of the method and help avoid collateral damages to the lungs and esophagus,

malignant arrhythmias and intramural cavitations (Fig. 17.6). In our experience, optimal energy settings for in-vivo laser applications aimed at the atrial walls are 10 W for 10–20 s and at the ventricular walls 15 W/15–40 s.

Collateral Damages

Laser catheter applications at too high power levels or with too long application times may result in collateral damages. Besides intramural cavitations and ventricular arrhythmias, damages to structures in the mediastinum including the lungs and esophagus may occur (Fig. 17.7). This emphasizes the

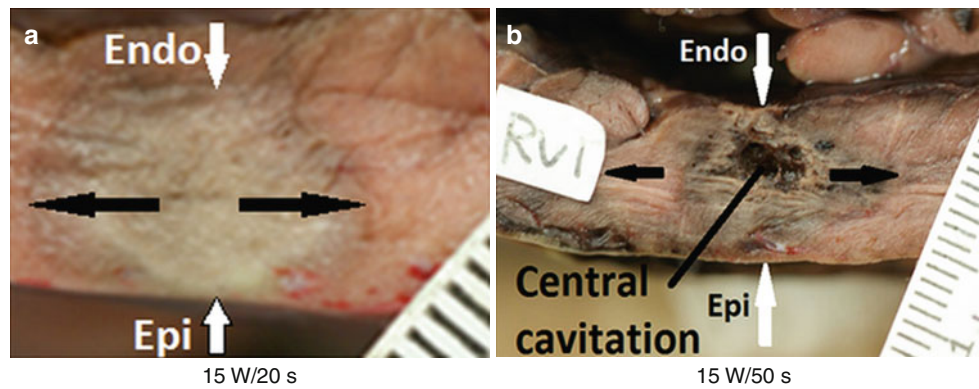
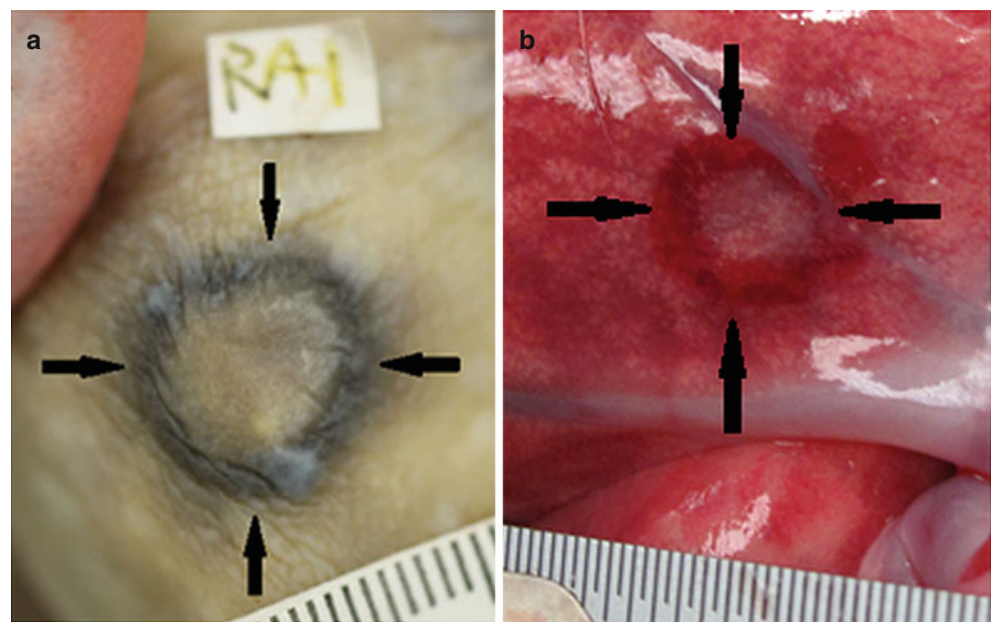


Fig. 17.6 Transmural lesions achieved with the ELMA catheter *RytmoLas* in the right ventricular free wall of dogs by laser applications at 15 W. (a) After a radiation time of 20 s diameter of the lesion of clear

cut homogenous coagulation necrosis is 10.8 mm. (b) After 50 s of radiation diameter is 18.2 mm but a central cavitation is present (oblique indicator). The horizontal black arrows indicate the margins of lesion

Fig. 17.7 Collateral damages to the lung and to the esophagus after laser applications aimed at the posterior right and left atrial walls, showing a ring-shaped carbonization of the irradiated lung lobe (a) a red inflammatory ring around the transmural lesion at the anterior aspect of the esophagus. (b) Arrows indicate the margins of lesions



crucial importance of optimal energy settings, adapted to the thickness of the myocardial wall during laser catheter ablation.

Control of Laser Lesion Formation

For control of laser lesion formation LEG is helpful [7, 8]. Laser light is not competitive with the mapping electrograms recorded via the tip electrodes of the ELMA catheter. During laser application the LEG is displayed on the monitor without noise. The electrodes are riding upon the irradiated area and allow for online electrical control directly from the illuminated field.

Attenuation of amplitudes of local electrical potentials is always conspicuous on the monitor simultaneously with the

start of laser application. Gradual attenuation of the local potential amplitudes reflects the spread of coagulation necrosis, the growing of the lesion in the myocardial wall (Fig. 17.8). After abolishment of the electrical potentials amplitudes the lesions achieved were transmural (Fig. 17.9). In contrast to that, stop of radiation prior to the permanent abolishment of potential amplitudes the amplitudes will recover, will increase to their initial heights (Fig. 17.10). In such instances the initially induced myocardial hyperemia with edema and slight hemorrhagic infiltration are also reversible and histopathologically no tissue damage, no lesion can be found. In general, laser effects on myocardium are reversible when radiation times are limited to 3–5 s. These phenomena of electrical potential amplitude attenuation during and the recovery of amplitudes after limited laser impacts are the basis for the laser mapping.

Fig. 17.8 (a) Surface leads I and II, and intracardiac right atrial (MAP RAE) and (b) left ventricular (MAP 1–3) LEGs recorded via the tip electrodes of the **ELMA catheter RytmoLas** during laser application at 10 W aimed at the atrial wall and at 15 W aimed at the left ventricular free wall, showing: gradual attenuation of voltage, of potential amplitudes, with the start of the laser. Amplitudes are practically abolished (vertical arrows) after 10 s of radiation aimed at the atrial wall (A–A1) and after 20 s in the ventricle (V–V1)

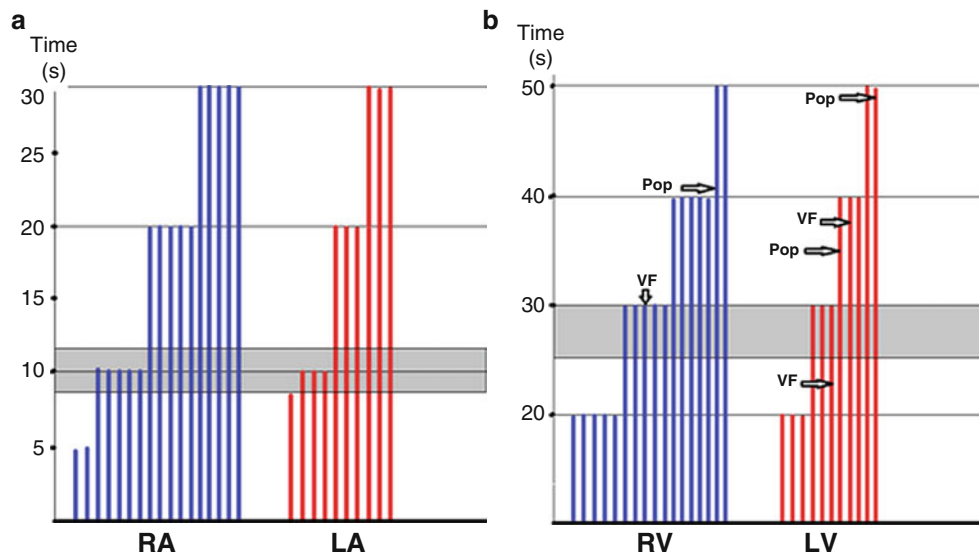
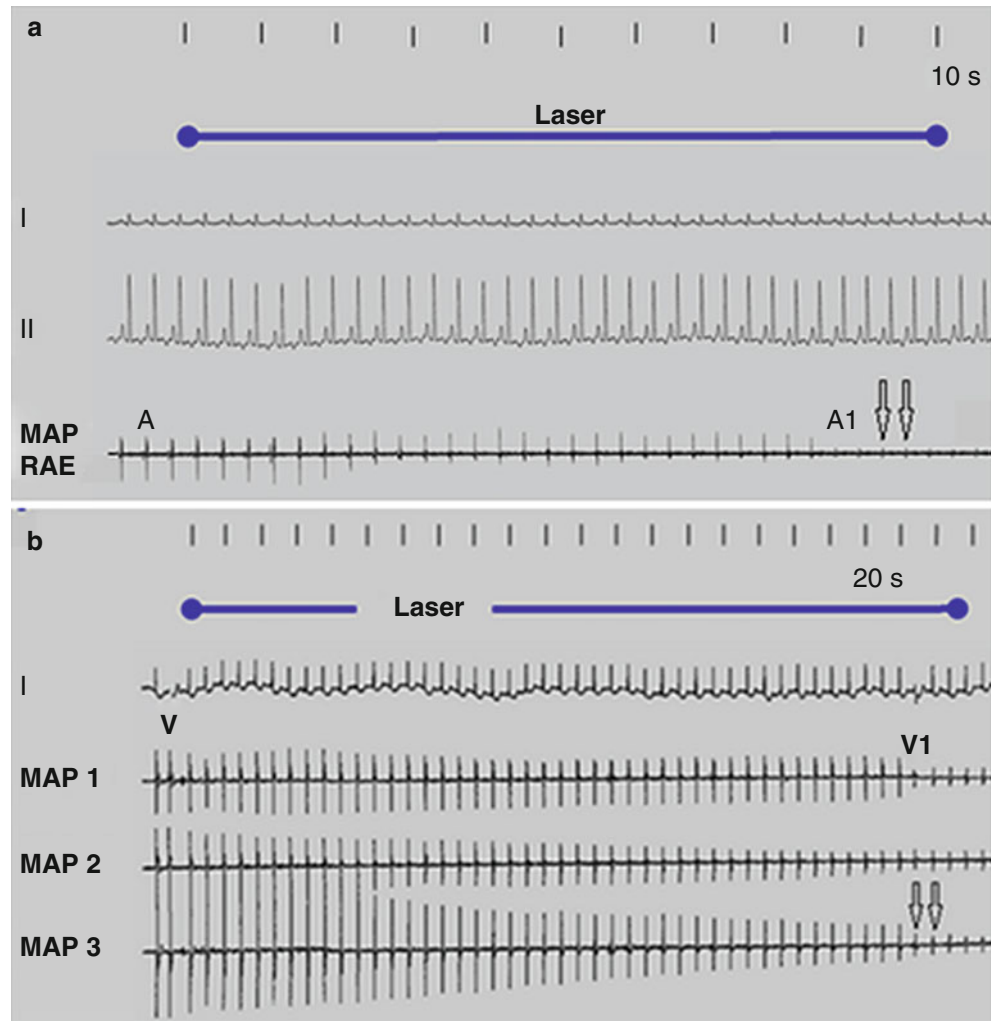
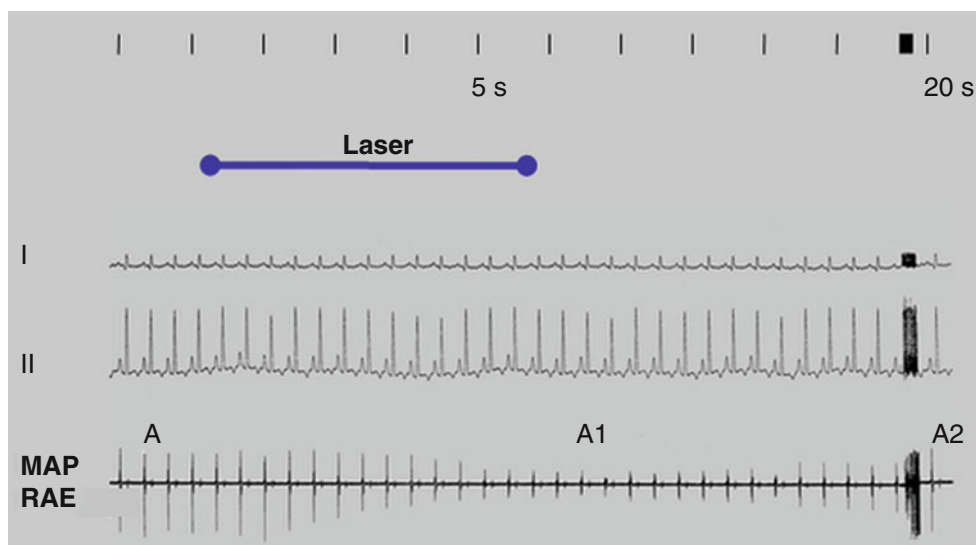


Fig. 17.9 Diagram showing the time intervals when local potentials were abolished permanently (a) after 8–12 s of laser application aimed at the atrial walls, and (b) after 25–30 s of laser application aimed at the ventricular walls (grey bars). After right atrial (RA) laser applications limited to 5 s amplitudes of local potentials recovered. The first four impacts aimed at the left atrial (LA) walls were stopped automatically after 8–10 s by the esophageal sensor. Collateral lesions to the lungs

and esophagus occurred after atrial radiation times >20 s, time well beyond the 8–12 s of the abolishment of atrial potentials. Similarly, steam pops or ventricular fibrillation (VF) occurred >35 s of radiation, >5 s after abolishment of ventricular potentials; except in one instance of non-sustained VF in the LV (20 W/23 s). The VF in the RV occurred after 30 s of radiation but 5 s after permanent abolishment of potentials

Fig. 17.10 Reversible laser effect after the stop of radiation aimed at right atrial lateral wall in the fifth second when local potential amplitudes were not yet abolished permanently (A–A1). Voltages increase again; amplitudes reach again their initial heights 20 s after the start of radiation (A1–A2)



Laser Mapping

Unwanted effects on impulse formation and conduction, especially on the atrioventricular conduction such as iatrogenic laser induced complete AV-block have to be avoided. LEG during laser application allows for online control of laser effects on myocardium. Reversibility of laser effects in instances of the occurrence of unwanted effects is possible by a timely stop of radiation. Aim of our following studies was to test the feasibility of laser mapping by using the ELMA catheter *RytmoLas* for mapping guided laser applications aimed at the sinus nodal (SN) and AV-nodal areas, at the His-bundle and the bundle branches in dogs [9–12].

SN Mapping

By mapping of the sinus nodal area with the ELMA catheter the earliest high right atrial activation was localized by recording spikes at least 30 ms prior to the earliest onset of the P-wave in the surface lead Electrograms. Mapping guided laser application aimed at that area in 14 dogs always produced gradual abatement of the amplitudes of SN-potentials. In addition, lengthening of the sinus cycle was conspicuous in the LEG. With the stop of radiation after 5–8 s both the phenomena reversed. However, laser applications of 20s repeated in the same catheter position produced chronic low amplitudes of local potentials and sinus cycles lengthened from 430–470 ms to 450–610 ms permanently (Fig. 17.11).

Electropharmacologic testing performed prior to, following immediately and after 4–11 months showed a mean percent decrease in 24 h heart rate (21.2 ± 7.5), maximum heart rate (24.0 ± 4.2), heart rate during beta blockade (31.4 ± 3.3), and maximum heart rate on isoproterenol (18.8 ± 5.1). SN recovery times remained unchanged. Acute, 3 h old lesions showed oval shaped transmural necrosis

surrounded by hemorrhage and edema but without crater formation. Chronic lesions showed patches of homogenous clear-cut transmural fibrosis at diameters of 6.4–17.5 mm.

We concluded that mapping guided laser catheter coagulation of SN areas persistently limits maximum heart rate without causing bradycardia. The method could become a form of heart rate control in patients with inappropriate sinus tachycardia.

AVN Mapping

Laser catheter applications were aimed at the central regions of Koch's triangle in nine dogs, from where no or only a very small His potential could be recorded. It could be demonstrated that a stop of the laser impact aimed at the AV-nodal regions immediately after the occurrence of the Wenckebach period or the Mobitz type 2:1 block, but prior to the occurrence of complete heart block, AV-conduction is always reversible [13]. Local potential amplitudes recover in up to 16 s (Fig. 17.12).

Besides a progressive dwindling of local potential amplitudes there was a mean increase of AH intervals of 29 ± 2.5 ms (+38 %) and of the AV node Wenckebach periodicity from 176 ± 15 to 260 ± 10 ms (+48 %). Mean RR-intervals during induced atrial fibrillation increased by approximately 30 %. These effects were not reversed by isoproterenol infusion. Histologic examination of acute, 3 h old lesions (in four dogs) showed circular to oval shaped coagulation necrosis or transmural fibrosis after 5–11 months of follow up (in five dogs).

Weekly electrocardiographic controls showed that anterograde AVN transmission properties do not progress to higher degrees of AV conduction disturbances. The animals survived the procedures without complications, and their follow up was uneventful. We concluded that the method could become a form of heart rate control in patients with disabling atrial tachycardia.

Fig. 17.11 Laser application at 10 W/20 s aimed at the sinus nodal area induces gradual attenuation of voltage, potential amplitudes diminish (*oblique arrow*), and sinus cycle lengths (SCL) increase from 470 to 610 ms. *I, II* surface lead Electrograms, *SNE* sinus nodal Electrogram, *S* atrial potential recorded from the sinus nodal area, *SP* Sino-atrial interval, and *P* p-wave

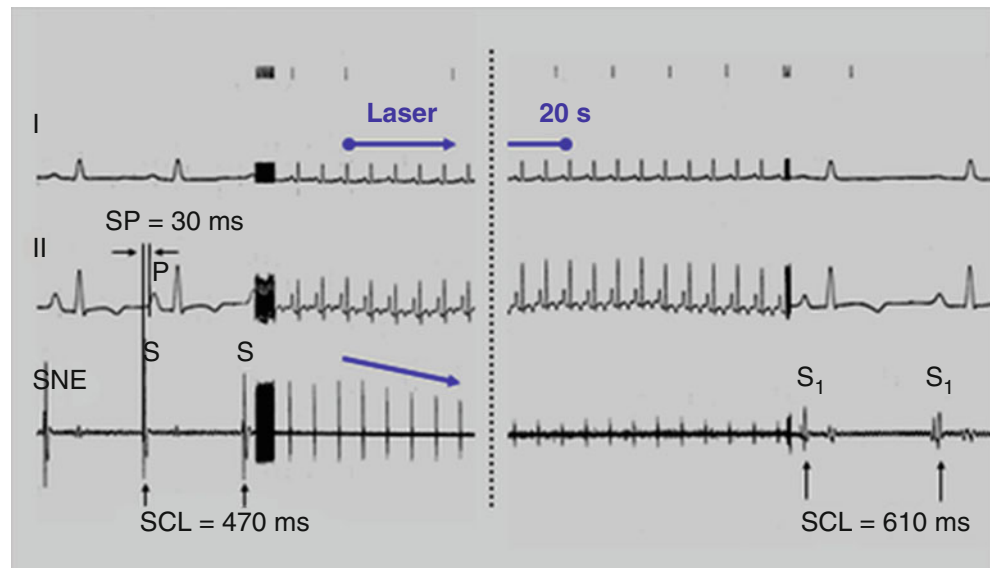
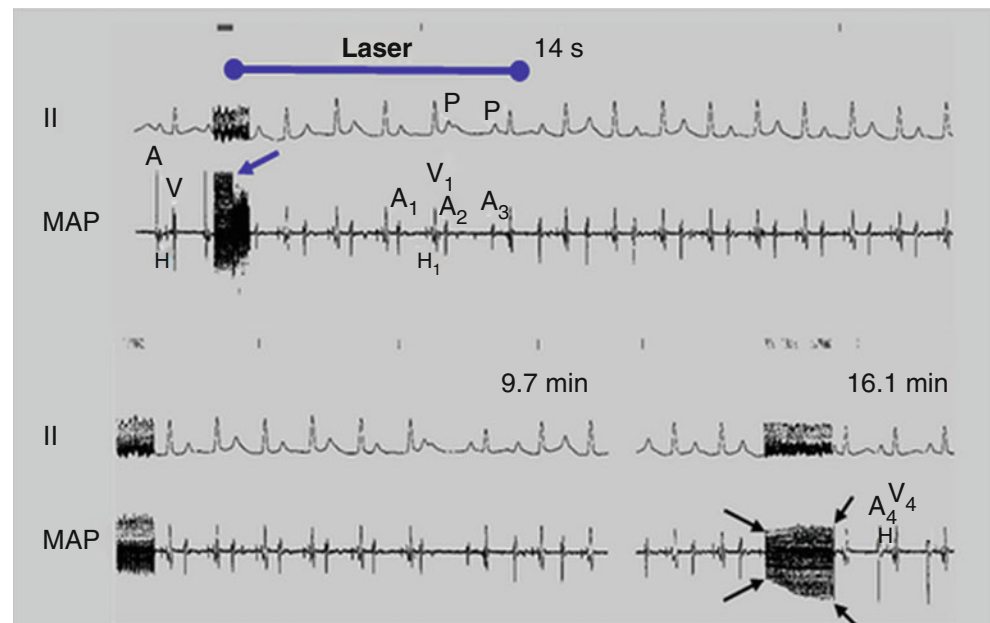


Fig. 17.12 Laser application at 15 W aimed at the AV-nodal area induces a gradual attenuation of atrial potential amplitudes (A–A1), and a gradual lengthening of the AH interval (Wenckebach period). The A_1 – H_1 interval is followed by AV block (A2–A3, and P–P). Stop of radiation after the first blocked AV-conduction allows for recovery of voltage. Local potential amplitudes and AV-conduction normalizes after 16 min (A4HV4, as compared to AHV prior to radiation). *II* surface lead Electrograms, *MAP* local mapping recordings, *A* atrial, *H* His-bundle, *V* ventricular potentials, and *P* p-waves



His-Bundle and Fascicular Mapping

Laser effects on the His-bundle and fascicles were observed already after radiation times of 4–6 s ($n=5$ dogs, each). After laser impacts aimed at the His-bundle second degree AV-block is followed by a complete conduction block. Laser radiation limited to <5 s allowed for recovery of AV conduction within 9–14 s (Fig. 17.13a). Short laser impacts aimed at the fascicles induced transitory conduction disturbances characterized by sequences of deviation of the electrical axis of the heart (Fig. 17.13b).

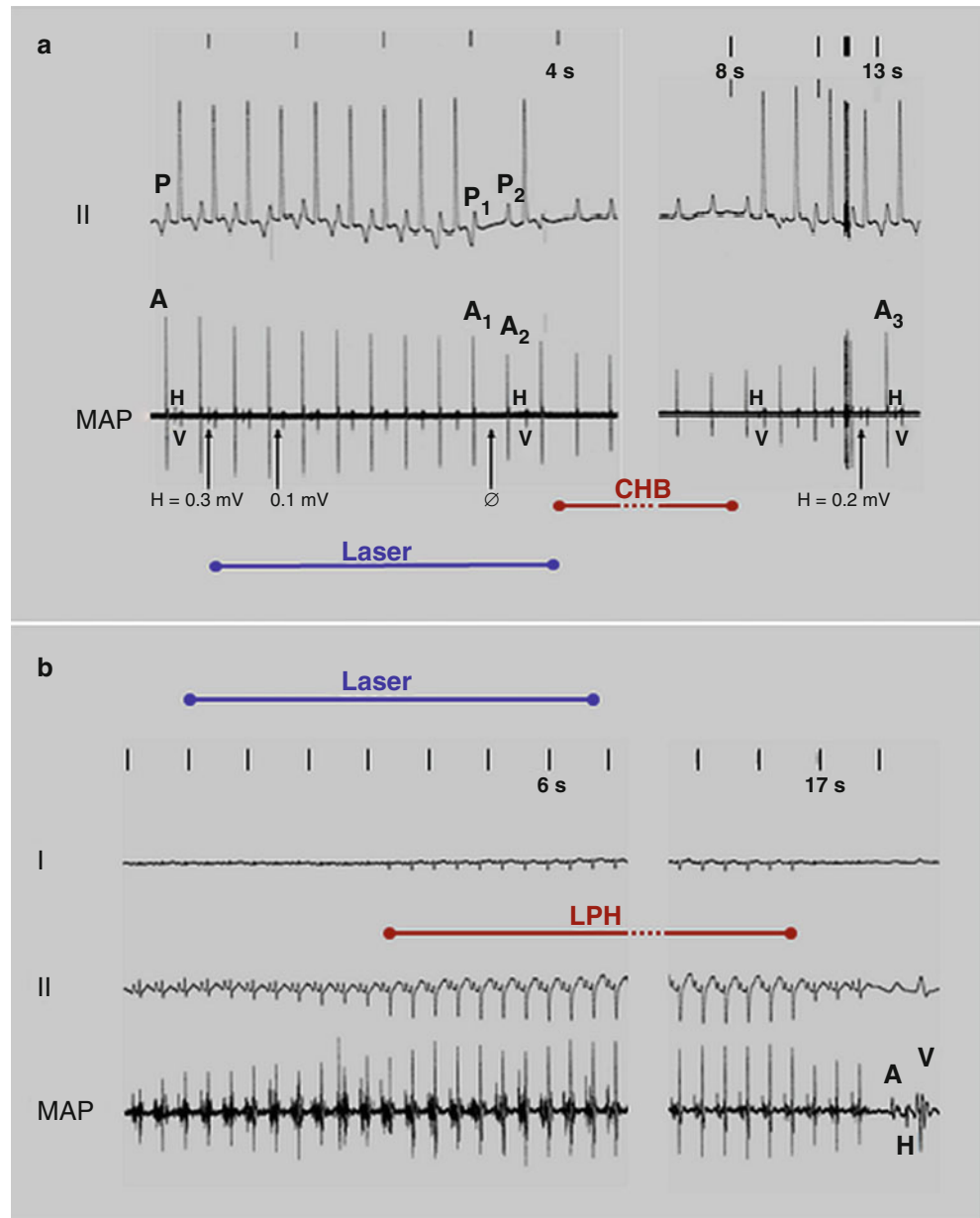
Weekly electrocardiographic control during a follow up of 3–5 months showed no kind of conduction disturbances.

There were no lesions found in the His-bundle and fascicular areas. We concluded that timely limited laser applications aimed at the His-bundle or the fascicles can avoid inadvertent AV conduction disturbances.

Catheter Irrigation

For cardiovascular catheterization with an open end catheter continuous rinsing of its lumen is mandatory. Otherwise blood could enter the end hole, obliterate the catheter, and produce blood clotting with thrombus formation, with its attendant risks of stroke and infarction. Especially for laser

Fig. 17.13 (a) Occurrence of complete heart block (CHB) after gradual attenuation of His-potential amplitudes ($H=0.3\text{--}0.1\text{ mV}$) and its abolishment after 3 s of laser application. In the 4 s of radiation the laser is stopped and His as well as atrial potentials recover, His potentials (H) reappear, and Potentials as well as AV-conduction normalizes after 13 s (Compare AHV prior to with A3HV after radiation). II surface lead Electrogram, MAP mapping Electrogram. (b) Transitory deviation of the electrical axis of the heart after a laser impact at 10 W limited to 7 s aimed at the fascicular segment of the His bundle. Normal proximal and distal conduction intervals AHV are preserved during laser application. LPH left posterior hemiblock, I and II surface lead Electrogram, MAP local mapping electrogram



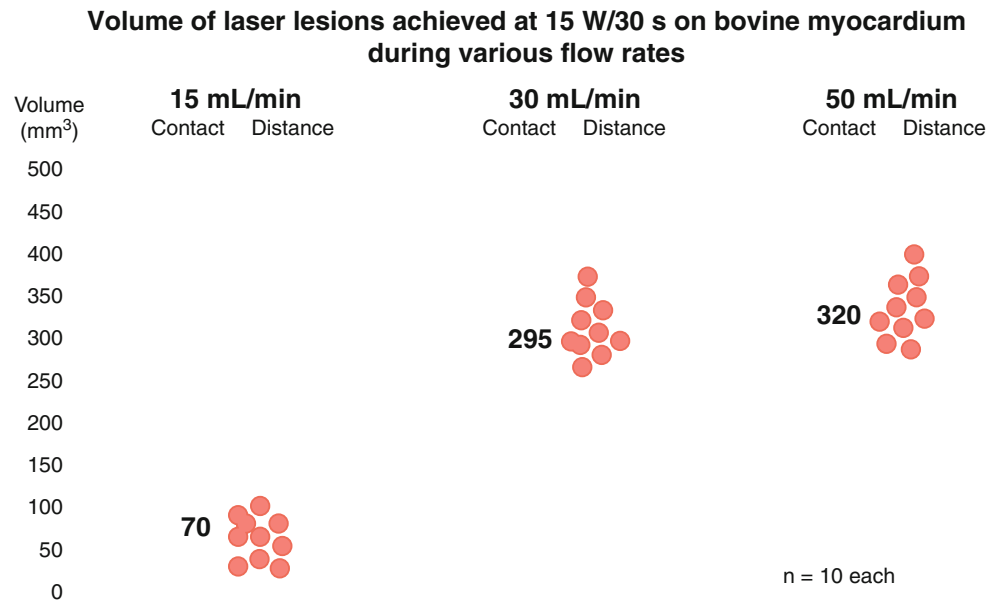
catheters which need a clear path for the light to heat up and coagulate myocardium catheter irrigation is crucial. Saline catheter irrigation washes away the blood and protects the tip of the optical fiber from contact with blood. In addition, cools the illuminated endocardial area. Irrigation flow also influences laser lesion formation. It could be demonstrated that open-irrigated laser catheter ablation produces flow dependent sizes of lesions [12]. With an increase of flow rate from 15 to 30 mL/min volumes of laser lesions produced at 15 W/30 s increased significantly from 70 ± 25.5 to $295 \pm 43\text{ mm}^3$ (Fig. 17.14).

Continuous irrigation flow needed for myocardial laser coagulation by using the ELMA catheter *RytmoLas* is 15 mL/min, whereas during laser application the optimal “working

flow” is 30–40 mL/min. It can be assumed, that a higher flow does better wash away the blood and will create a larger clear path for the laser light. A higher irrigation flow also more effectively cools the superficial myocardial layers. The significant increase of lesions achieved with the higher flow rate is of importance for ablation of ventricular arrhythmogenic foci located >8.0 mm deep intramurally or subepicardial not amenable for ablation by other techniques [13].

Saline irrigation from the catheter goes directly into the patient’s bloodstream. Awareness and management of the irrigation volume is important. Patients with normal renal function will respond to the volume infused by excreting it through the kidneys. However, many patients who undergo ablation have risk factors that reduce their ability to handle

Fig. 17.14 Diagram showing the influence of catheter irrigation flow rate on the lesion volumes. Means \pm STD in mm are: 70 ± 25.5 vs. 295 ± 43 ; $p=0.0001$; 295 ± 43 vs. 320 ± 45.5 ; $p=0.218$ NS (P=values)



this volume load developing pulmonary edema or heart failure during the procedure. Patients with congestive heart failure or renal insufficiency and the elderly are particularly susceptible.

The total amount of saline administered depends on procedure duration, flow rate, number of lesions, and duration of each lesion. Power titration and fluid management for optimal safety and efficacy of irrigated RF ablation was the topic of a series of publications [14–17]. During RF-ablation mapping irrigation flow is 2 mL/min whereas during ablation is 30 mL/min plus 5 s of flow before and after each lesion. For a procedure time of 90 min and a total of 30 lesions of 90s volume of irrigation fluid totalizes 1580 mL. As compared to that, mapping irrigation during laser procedures is 15 mL/min and during laser applications is 30 ml/min. Applying a total of 30 lesions of 30s each during a procedure time of 90 min, irrigation fluid totalizes a volume of about 1575 mL. Thus, total volume of irrigation flow during laser ablation is not higher as compared to that of the RF-method. Moreover, taking into consideration that RF ablation procedures frequently require more applications during a longer procedure time total volume of irrigation flow during laser ablation is rather less as that of the RF-method.

Patients with heart failure or hypertension have to be advised to reduce the sodium in their diet to 2.4 g daily prior to the ablation. If a long procedure is anticipated, placement of a urinary catheter and a central venous line are needed. Development of agitation, increase in respiratory rate, or falling oxygen saturation may be manifestations of volume overload, warranting diuresis. If fluid balance becomes markedly positive (e.g., >1–1.5 L), administration of an intravenous diuretic agent such as furosemide may be

considered. Blood electrolytes, especially potassium, should be monitored in cases of frequent administration of diuretics. In patients with poor cardiac function treatment of obvious volume overload includes inotropic agents such as dobutamine. In addition to the volume load, each liter of saline irrigation contains 5,000 Int. Units of heparin. Thus, monitoring of ACT is mandatory during long procedures.

Catheter Stability

For effective lesion formation stable intimate contact of the ablation catheter with the arrhythmogenic substrate in the beating heart is decisive for a successful treatment. Experimental tests have shown that an important factor to effective RF lesion formation is the contact force between catheter tip and tissue [18, 19]. Insufficient contact will result in ineffective lesions, whereas excessive contact force may result in complications such as heart wall perforation, steam pop, thrombus formation, and esophageal injury [20]. Recently, a novel open irrigated radiofrequency ablation catheter with a contact force sensor at the distal tip is available for clinical use [21]. In contrast to that, our experiments suggest that for laser lesion formation catheter pressure on the targeted tissue is not needed [6, 12]. To evaluate the influence of contact pressure on laser lesion formation laser applications at 15 W/30 s, irrigation flow 35 ml/min, contact pressure 100, 10, 1.0 g, and at distances of 2 and 5 mm, n=10 each, were performed in stagnant blood on bovine myocardium at room temperature by using the open irrigated laser catheter *RyimoLas*. Lesions were evaluated morphometrically and comparison of lesion sizes was performed by using a two-sample *t*-Test.

Lesions showed clear cut circular to oval shaped areas of homogenous coagulation necrosis of myocardium. Endocardial surfaces were translucent without tissue vaporization with crater formation regardless of catheter pressure applied (Fig. 17.15). Maximum sizes of lesions achieved with pressure of 100 g, of 10 g and without pressure did not differ significantly. However, significant differences were found between the sizes of contact lesions and the lesions achieved at a distance of 2 mm away from the endocardial surface (Fig. 17.16).

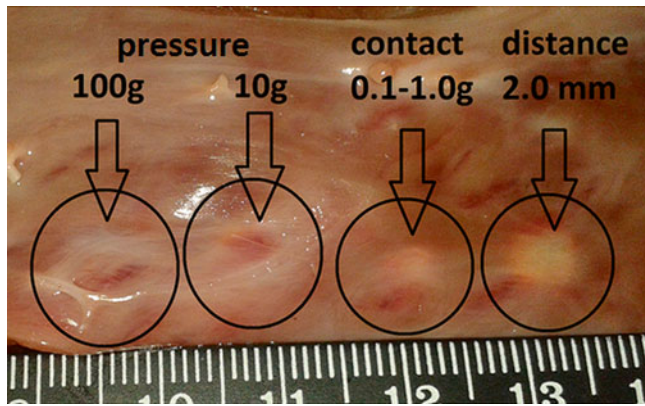


Fig. 17.15 Endocardial surface of a bovine specimen showing pale areas of coagulation necrosis with increasing diameters (from right to left, within black circles) produced in stagnant blood by laser applications at 15 W/30 s, catheter irrigation 35 ml/min, with and without catheter pressure on the endocardial surface and at a distance of 2 mm. Note: Continuity of endomyocardial layers is always preserved; there is no tissue vaporization with crater formation

Collateral Laser Effects on Coronary Vessels

To determine the influence of Nd:YAG laser coagulation of myocardium on coronary vessels, a total of 48 transcatheter laser impacts at 10 W/10 s, 7 W/mm², catheter irrigation flow 30 ml/min, were aimed at the left ventricular free wall, endocardial approach, 24 lesions in two dogs, or at the branches of the epicardial left coronary arteries, epicardial approach, 24 lesions in two other dogs (12 lesions in each of the 4 dogs). Sizes of lesions were evaluated morpho-histopathologically.

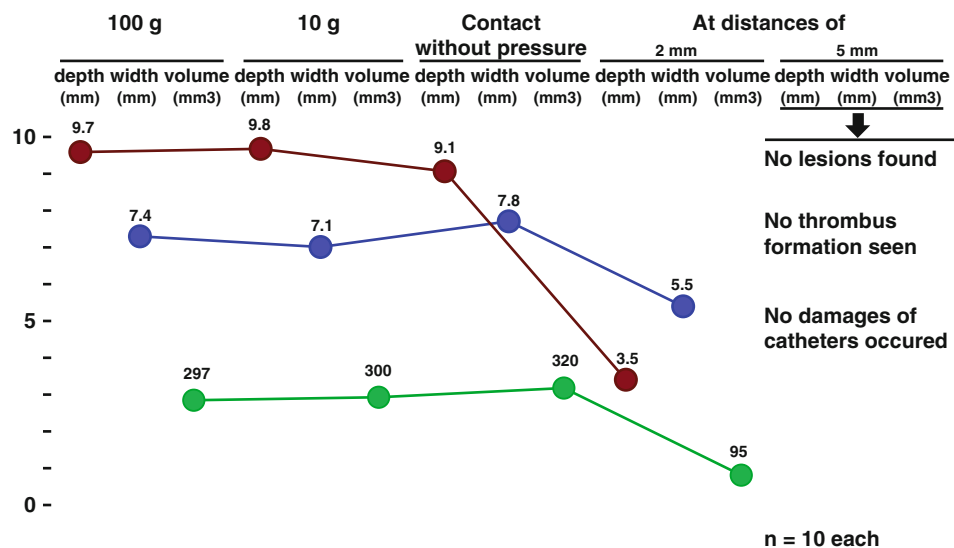
In 8 of the 24 endomyocardial lesions (2–6 months old) coronary vessels with a diameter of >50 μm were found within the coagulation zones. The volume of these lesions was significantly smaller (139 ± 43 mm³) than those (n=16) containing coronary vessels measuring <50 μm (311 ± 87 mm³), p<0.01. Volumes of epimyocardial lesions (1–2 h old) produced by transcatheter laser applications were significantly smaller when the coronary blood flow was normal (31 ± 17 mm³) as compared to those produced across coronaries with reduced (73 ± 22 mm³) or interrupted blood flow (119 ± 34 mm³, p<0.019) by means of a tourniquet placed around the artery proximal to the irradiated vessel segment (Fig. 17.17).

Both directly radiated vessels and those found within the coagulation zones appeared histologically normal through all layers with an intact intima and without thrombi in their lumen. The ultrastructure of radiated vessels was no different from that of non-radiated controls [22].

Thus, coronary blood flow significantly reduces the volume of coagulated myocardium, whereas the medium sized and larger coronaries themselves appear to remain

Sizes of lesions achieved by Nd:YAG laser applications at 15 W/30 s, 35 ml/min with and without pressure of the catheter on bovine myocardium

Fig. 17.16 Diagram showing the mean values of lesion sizes achieved on bovine myocardium with and without catheter pressure on the endocardial surface and at a distance of 2.0 mm. Only sizes of lesions achieved at a distance of 2 mm away from the irradiated endocardial surface diminished significantly: in depth from 9.1 ± 0.74 vs. 3.5 ± 0.47 mm, p<0.0001, in width of 7.8 ± 0.4 vs. 5.5 ± 0.5 mm, p<0.0001, and volumes from 320 ± 24.3 vs. 95 ± 13.8 mm³, p<0.0001



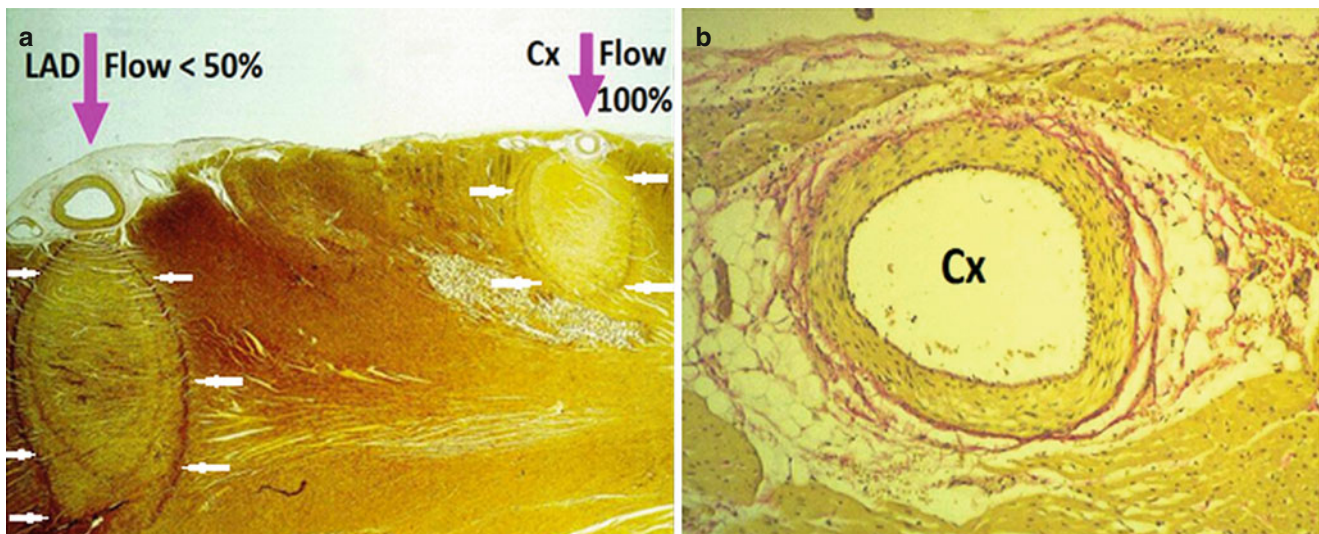


Fig. 17.17 (a) Clear-cut lesions of homogenous coagulation necrosis achieved by open chest hand held laser catheter application at 10 W/15 s, aimed at epicardial coronary arteries with normal (100 %), and with reduced blood flow (<50 %), showing different sizes of lesions achieved after radiation through the arteries (*small white arrows*). Orientation of the catheter during laser application is shown by the vertical arrows. (b) Section through the circumflex (Cx) coronary artery

after Nd:YAG laser radiation directed through the epicardium and the lumen of the artery into the myocardium is showing a normal intima and media of the vessel wall. The vessel lumen is open without thrombus formation. *Note:* the normal vascular intima and media. Only a slight focal infiltration of the adventitia and a mild inflammation of the epicardium are conspicuous. Elastica van Gieson stained

undamaged by laser radiation as used for myocardial coagulation with the ELMA catheter *RytmoLas*. Owing to the cooling blood flow coronary vessels are protected from overheating; vessel intima and media remain undamaged. Only a focal infiltration of the adventitia by mild inflammation of the epicardium was conspicuous.

Laser of Scarred Myocardium

Larger lesions would increase success rates of catheter ablation especially for ventricular arrhythmias. Transcatheter application of Nd:YAG laser produces significantly larger and better reproducible lesions than RF current, without undesirable effects on the ventricular walls [23]. RF ablation success rate in patients with ventricular tachycardia is limited mainly due to insufficient depth of lesions [13, 24]. Therefore, besides improvement of RF current application techniques alternative energy sources are being investigated. The laser can achieve transmural ventricular lesions in dog hearts within seconds. However, results achieved in healthy myocardium of dogs are difficult to apply to patients with diseased ischemic or scarred myocardium. Therefore we have tested morphology and dimensions of ventricular lesions induced by laser catheter applications on scarred ventricular myocardium in a dog model [25].

A total of 244 laser lesions (1064 nm, 10–30 W/15–60 s, catheter irrigation flow 30 mL/min) were produced percutaneously (endocardial approach, n = 124) and under visual control

(epicardial approach, n = 124) in the left ventricular free walls of 24 anesthetized dogs. Dimension of lesions increased with the amount of energy applied. Laser impacts at 20 W/60 s produced transmural lesions (depth = 12.6 ± 1.1 mm), width = 15.0 ± 2.8 mm, and volumes = 1582 ± 777 mm³.

It could be shown that volumes of lesions did not change significantly when induced through previously scarred myocardium. We concluded that the laser method might be a promising alternative for ablation of ventricular arrhythmias in patients with ischemic heart disease or even with a post infarction scarred ventricular myocardium.

Catheter Tilt

Catheter orientation towards the target area may influence lesion formation when using an open irrigated catheter emanating a divergent laser beam from its end hole. Irradiation area may change corresponding to the contact angle and the cooling effect could be affected as well, so that temperature distribution in the vicinity of the tissue surface would vary. However, a strong and stable perpendicular catheter orientation during laser application in the beating heart is rather the exception. By mounting the catheter with a support that allowed catheter orientation at various angles towards the endocardial surface we have tested in-vitro laser lesion formation in heparinized stagnant blood on bovine myocardium. It could be demonstrated, that only catheter tilting at an angle of 22° and more significantly reduces depth but less the width of lesions (Fig. 17.18).

This can be explained by the divergent laser beam with partially downwards orientated beam that hits the endocardial surface almost vertically. From a circular to oval shaped lesion achieved in perpendicular position, a more oblique catheter orientation produces wooden shoe like lesions, “en sabot”. In a horizontal position the catheter produces again oval shaped lesions almost at the same diameters as the tilt of 45° but less in depth (Fig. 17.19).

It can be assume that for an experienced operator it is not a problem to manipulate the catheter in an approximately perpendicular position in almost all regions of the heart chambers. This will not jeopardize lesion formation and the success of the ablation procedure. With a catheter tilt at an angle of about 45° transmural lesion can be achieved in the relative thick left ventricular free wall of a dog heart very similar in size and shape to those achieved in a perpendicular catheter orientation (Fig. 17.20).

Myocardial Temperature Measurement

Intramural temperature was measured during endomyocardial laser applications by using an open-irrigated laser catheter [3]. Temperatures were monitored by means of a

linear array of thermocouples inserted epicardially (Fig. 17.21). Thermocouples were thermally insulated inside 0.8 mm cannulas mounted at distances of 5 mm from each other. The thermocouples were connected to a DMT D/A registration unit [26]. In order to maintain a stable insertion depth, a mobile distal bar was adjusted along the cannulas according to the thickness of the ventricular wall. A total of 30 cw 1064 nm laser impacts at 25 W/15 s, 20 W/30 s, and 15 W/45 s (n=10 each) were aimed at various sites of the left ventricular free walls in four anesthetized dogs.

Temperatures increased gradually after the start of the laser. Maximum values were measured in the central areas attaining 100±15 °C at 25 W, 78±23 °C at 20 W and 80±13 °C at 15 W. Rise of intramural temperature was accompanied by gradual attenuation of electrical potential amplitudes in the LEG recorded via the pin electrodes of the ELMA catheter (Fig. 17.22).

Lesions achieved were transmural regardless of the level of energy applied. There was no crater formation. In the heart of dogs, transmural laser coagulation of healthy ventricular myocardium can be performed in a safe and controllable manner at energy settings of 15 W/25–45 s without the risk of pop with crater formation.

Laser lesions achieved at 15 W/30 s, 30 ml/min, on bovine myocardium in heparinized stagnant blood with the open-irrigated laser catheter in various orientations, in contact but without pressure on the endocardial surface

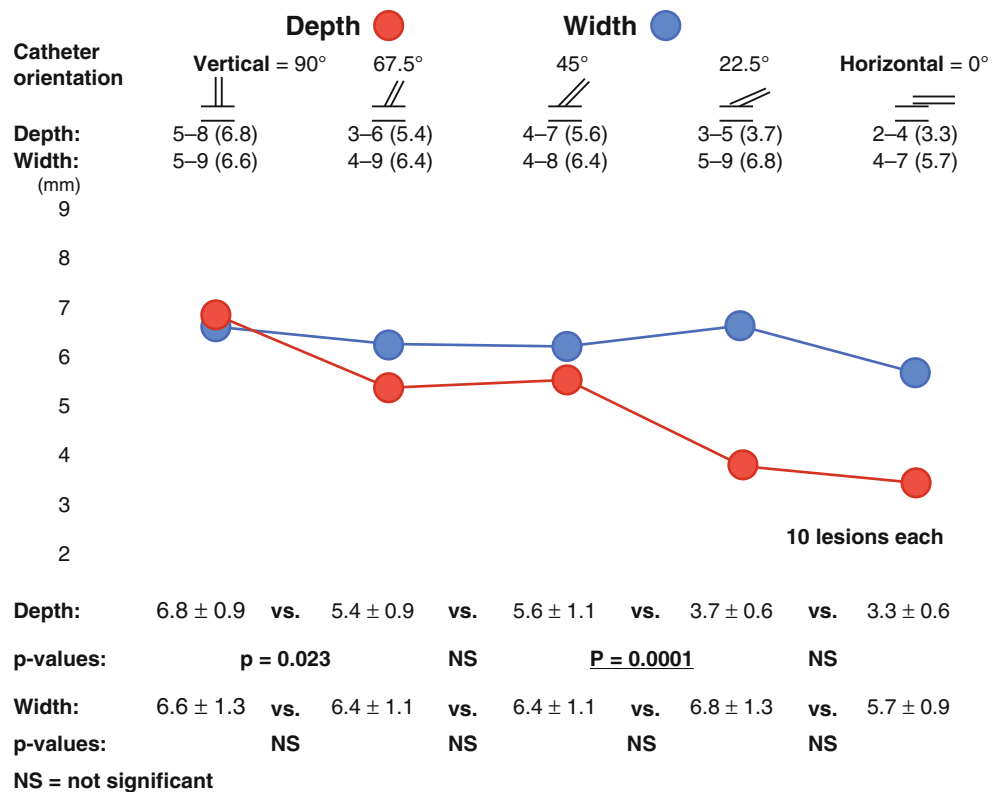


Fig. 17.18 Diagram showing highly significant decrease of laser lesions in depth, when laser application was performed with a catheter tilting at an angle of 22.5° or more. However, substantial coagulation is achieved with the ELMA catheter in a flat, horizontal position

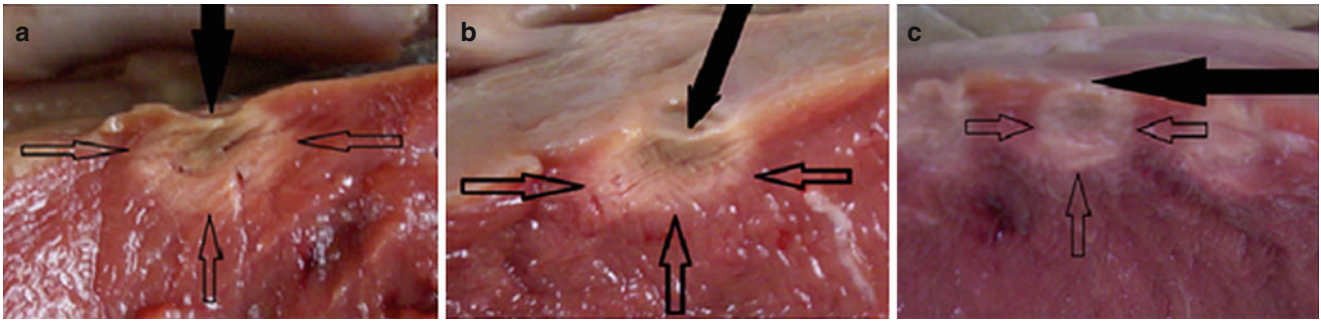


Fig. 17.19 Shapes of laser lesions achieved at 15 W/30 s, irrigation flow 30 ml/min, in stagnant heparinized blood, on bovine myocardium with the catheter in perpendicular position (a), at an angle of 45° (b),

and in horizontal, flat position on the endocardial surface (c). The lesion is sabot shaped in b and circular in a and c. Catheter orientation is indicated by black arrows, lesion margins in clear arrows

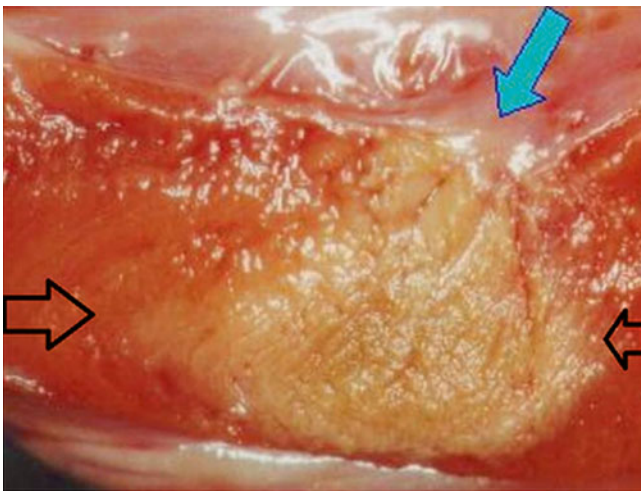


Fig. 17.20 Section through the left ventricular free wall of a dog heart showing a transmural lesion achieved at 15 W/40 s, irrigation flow 30 ml/min, with the catheter at an angle of approximately 45°. The oblique arrow upon the endocardial surface indicates the assumed orientation of the catheter during laser application. The horizontal clear arrows indicate the margins of the lesion. *Note:* the clear-cut homogeneous coagulation necrosis and the gleaming translucent endocardium in the irradiation field; without tissue vaporization with crater formation, and without central cavitation

Laser Catheter Ablation of Arrhythmias (CALCAM Study Trial)

Introduction

Electrode catheter exploration performed in patients during the arrhythmic state in the electrophysiology laboratory of the Department of Pediatric Cardiology University of Göttingen in the mid 70s of the last century allowed for localization of subendocardial areas suggesting accessory pathways or arrhythmogenic foci, the arrhythmogenic substrate of the arrhythmia mechanism. A catheter mapping guided DC shock aimed at the area of an antero-septal accessory atrio-ventricular pathway in August 1982 successfully

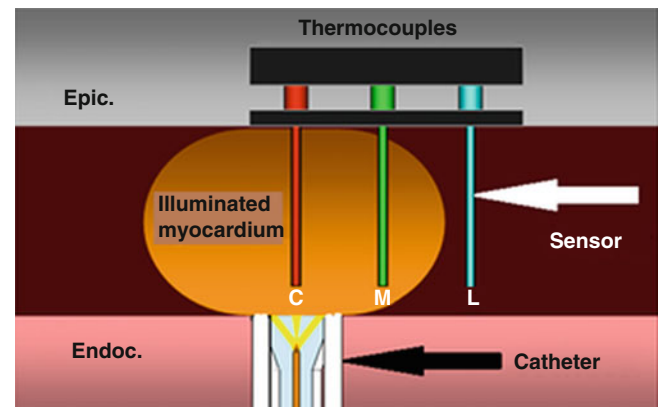
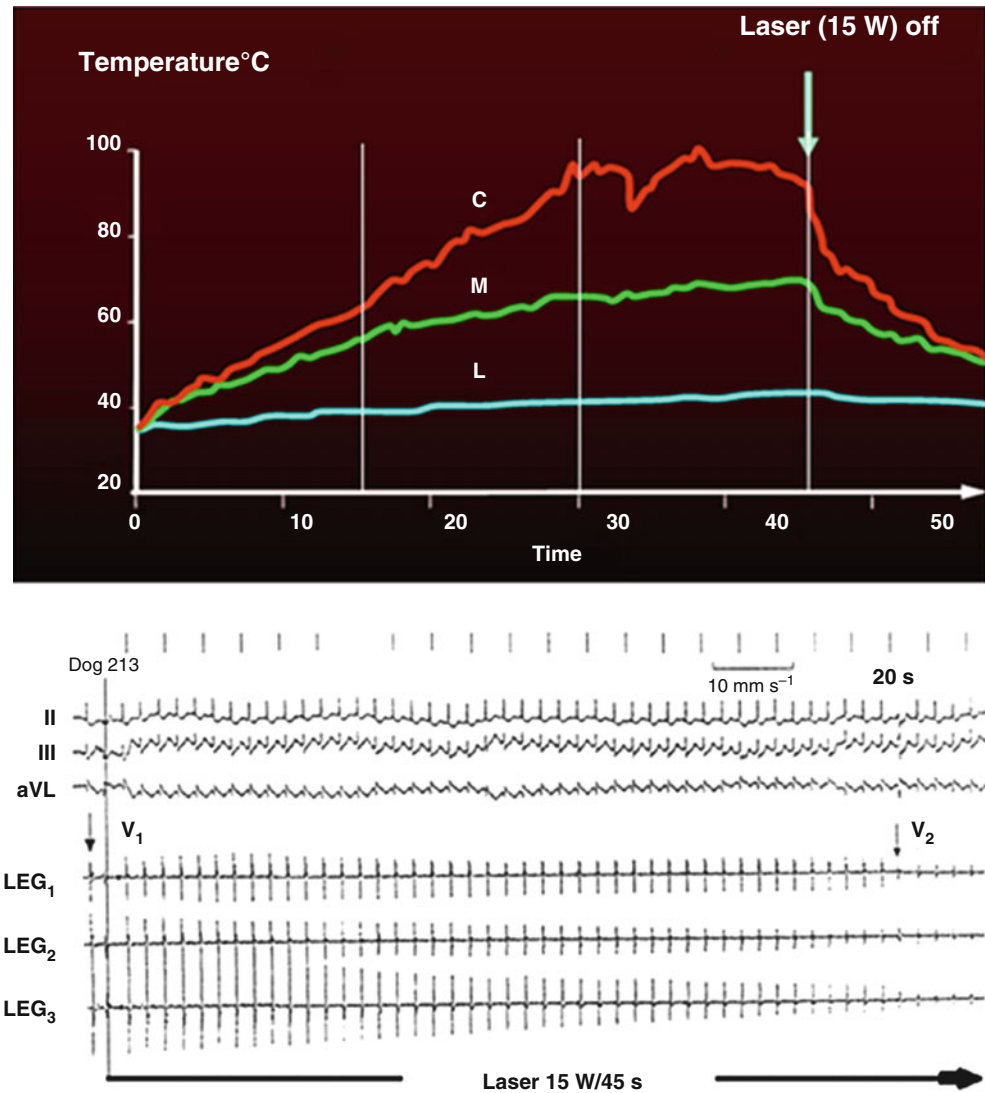


Fig. 17.21 Scheme demonstrating the position of the laser sensors (C central, M middle, and L lateral) positioned at 5 mm from each other, and of the laser catheter during laser application. *Endoc.* epicardial and *Epic.* epicardial sites

abolished conduction through that pathway, ablated the arrhythmia [27].

Encouraged by this result we have started to investigate alternative power sources including RF current, microwave, ultrasound and lasers. Eventually, with the cw 1064 nm laser we achieved superior results when using the open irrigated ELMA catheter [1, 28]. In contrast to that, when using plane polished bare fibers or catheters with lateral light beam, that was difficult to control, results were unsatisfactory. Endoscopically guided laser balloon techniques were highly sophisticated, cost intensive and limited to pulmonary vein applications. In addition, thrombus formation in the stagnant blood in front of the balloon has the potential risk of stroke and infarction [29]. Laser ablation in photosensitized tissues with cold laser effects by using photodynamic therapy is also experimentally feasible [30]. Ought to our successful tests without photodynamic therapy we did not consider the method in our laboratory. Based on our good experimental results we have started in early 1988 with laser ablation of cardiac arrhythmias in patients by using the cw 1064 nm laser in combination with the open-irrigated ELMA catheter

Fig. 17.22 *Top*: Myocardial temperature curves and *bottom*: local electrograms (LEGs) recorded simultaneously during laser application at 15 W/45 s (3×15 s, vertical lines) showing, a gradual increase of temperature, and, simultaneously a gradual and eventually a permanent voltage attenuation in the LEGs (V1–V2) during transmural lesion maturation



in a first multicenter study trial, the CALCAM (*Catheter Laser Coagulation of Arrhythmogenic Myocardium*) study trial.

Patients signed an informed consent which together with the study protocol was approved by the ethics committee of the Land of Bavaria. The CALCAM study was performed in the following electrophysiology laboratories:

1. Heart Center, Hospital Munich Bogenhausen, Teaching Hospital of the Technical University of Munich, Munich, Germany
2. Laser Center and applied technologies, first Medical Department, Electrophysiology, Hospital Harlaching, Teaching Hospital of the University of Munich, Munich, Germany
3. Section of Adult cardiology, Department of Cardiovascular Diseases, King Faisal Specialist Hospital, Riyadh 11211, Saudi Arabia
4. Third Medical Department, Cardiology and Nephrology, Wilhelminenspital, Vienna, Teaching Hospital of the University of Vienna, Austria
5. Electrophysiological Laboratory, German Heart Center Munich, Munich, Germany
6. Electrophysiology Laboratory, first Department Internal Medicine, Cardiology, University Bonn, Bonn, Germany
7. Electrophysiology Laboratory, third Medical Department, Cardiology, University of Tübingen, Tübingen, Germany

Patients and Methods

From March 1988 until July 2003 in a total of 80 patients, aged 59 ± 17 years, 44 males, with symptomatic arrhythmias since >12 months including atrial fibrillation (AF, paroxysmal = 19, long persistent = 13), typical atrial flutter (AFL = 11),

atrioventricular nodal reentrant tachycardia (AVNRT=14), accessory atrioventricular pathways (AP=9), ventricular tachycardia (VT=9), and atrial tachycardia (AT=5) laser ablation of the arrhythmias was attempted by using the open-irrigated ELMA catheter. All of the patients received 1–4 antiarrhythmic drugs that were discontinued >24 h prior to the intervention.

Power source was a cw1064 nm laser fibertom from Dornier MedTech, Wessling, Germany, provided with a Light-guide protection system (LPS) that stopped the laser automatically prior to overheating of the catheter. The catheter, RytmoLas LasCor GmbH Taufkirchen, Germany, was an 8 F flexible plastic tube with 20 % BaSO₄ connected via a SubMiniature version A (SMA) connector to the laser, via a Luer connector to the peristaltic pump for catheter irrigation, and through two plugs to the manifold for the display of intracardiac Electrograms recorded via the tip electrodes of the catheter.

The catheter was introduced pervenously from the groin and advanced and manipulated by a steerable Agilis sheath into the right atrium. For left heart catheterization transseptal laser puncture procedure was performed with a novel laser atrial septal puncture set [31]. For localization of arrhythmogenic substrates in the heart anatomical and electrical catheter mapping was used. Laser applications were aimed at the earliest activation during the arrhythmia or by localization of accessory pathway potentials. For AF ablation reentry circuits, foci and fractionated potentials were stepwise targeted. In the majority with AF extensive contiguous coagulation of the posterior left atrial wall was performed and right atrial applications were added. Lines, with the laser method rather stripes of 5–10 mm in width, of ablation and focal applications were added whenever thought opportune. Ablation numbers, total radiation and procedure times were kept to a practicable minimum. Pulmonary veins were always spared. Radiations at 10 W were aimed at atrial walls and at 15 W at ventricular walls. Catheter Irrigation flow was 15 mL/min. During radiation it was augmented automatically via the foot switch of the laser to 30 mL/min. Procedures are displayed in Table 17.1.

In 25 patients relative D-dimer serum levels (immunofluorescence technique VIDA-D-Dimer) were estimated prior to, immediately following and 2 days after laser ablation [30]. Follow-up was 5–8 years with 24 h Holter monitoring after the ablation procedure and surface lead ECGs with medical check-up every week (3×), every month (3×), and

subsequently every 6 months, and whenever symptoms occurred or recurrence of the arrhythmia was suspected.

Results and Follow-up

In the first patient of this study laser ablation of a left sided AP was successfully attempted in March 1988 (Fig. 17.23). For the ablation of AVNRT and typical atrial flutter procedure times were less than 1 h. The longest procedure times of up 3 h were needed for the ablation of AF. In general, atrial endocardial mapping in atrial fibrillation displayed various LEGs, including rapid local reentry, fractionated potentials and even torsade de point like recordings. All these types of tracings were sometimes present in the same patient (Fig. 17.24).

With the start of laser applications electrical potential amplitudes in the LEGs were attenuated gradually and were abolished after 15–20 s in the atria and after 25–40 s in the ventricles. No audible pops or malignant arrhythmias occurred. The arrhythmias could be stopped in all of the patients and were not inducible acutely except in five patients with AF. Arrhythmias were ablated after one to eight laser applications except for AF where 8–14 applications were needed. In all of the patients with AF extensive contiguous lesions were aimed at in the left and sometimes in both of the atria. Best results were achieved by laser applications aimed at areas with rapid local reentry suggesting a “rotor” as the arrhythmogenic substrate (Fig. 17.25). D-dimer serum levels did not increase significantly ($p>0.05$) after Laser ablation (Fig. 17.26).

During the follow-up 11 patients were lost for various reasons. One patient died 5 days after a Maze procedure for AF in another hospital 9 months after successful ablation of an AP. A second patient died after 9 months on the ICU of another hospital because of hemothorax after a house accident, and a third patient died after 16 months because of liver cancer. In the other eight patients complete data of follow-up were not available due relocations and too far distances abroad. However, telephonic contact with the practitioner did not give indication for arrhythmia recurrences in these 8 patients. Follow-up of 5–8 years of the remainder 69 patients is summarized in Table 17.2.

Except for patients with atrial tachycardia repeated studies were needed in 14 out of 55 patients for the cure of the arrhythmia. In addition, in one patient a back-up ICD was

Table 17.1 Laser catheter ablation procedures in 80 patients

Ablation		Laser	
Procedure duration (min)	X-ray exposure (min)	Applications n=524 (means ± STD)	Radiation time (s)
118	13.2	7.2	155
±72	±12.2	±6.7	±186

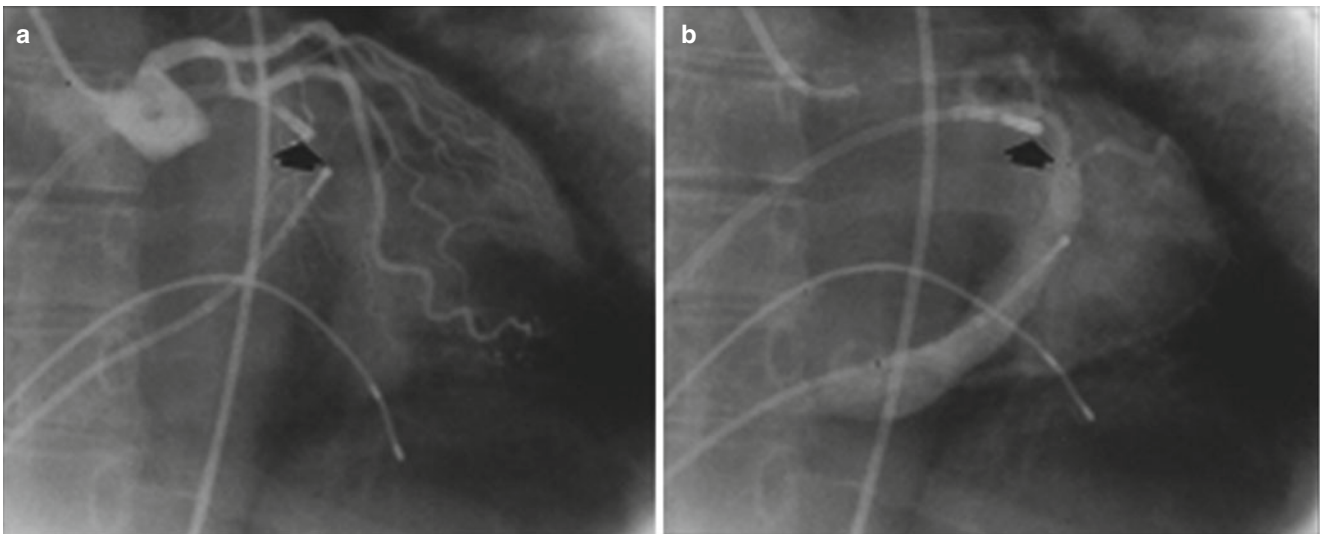
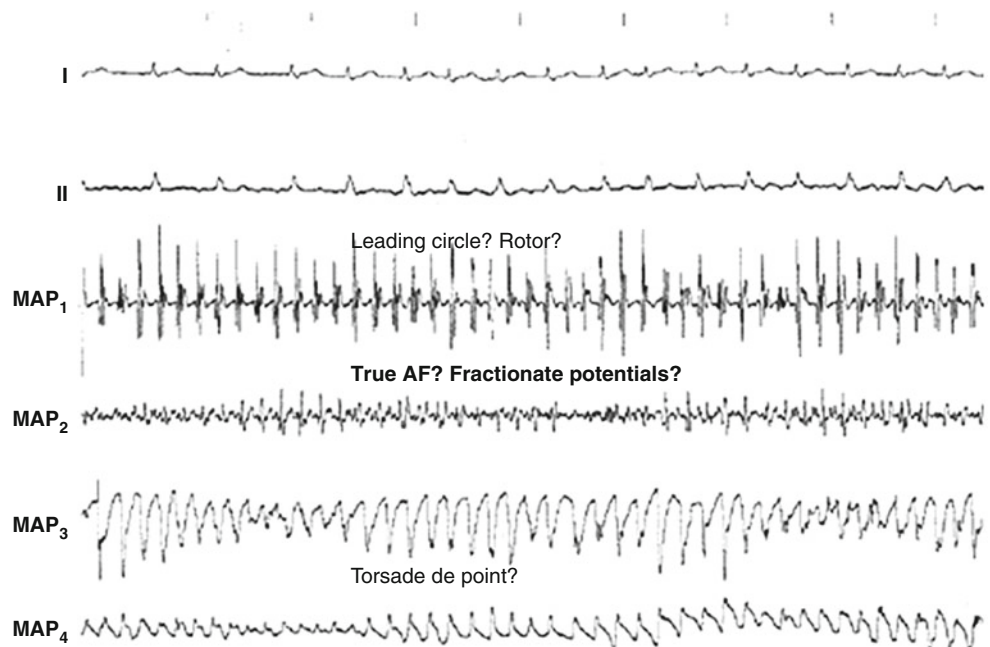


Fig. 17.23 (a) Left coronary angiogram (RAO) with (b) subsequent coronary sinus contrast filling, showing the electrode laser mapping and ablation (ELMA) catheter *RytmoLas* with its tip (*black arrow*) pointing towards the site where the first successful laser catheter ablation procedure was performed by using the ELMA catheter *RytmoLas*, in March

1988. The patient with a *left* sided atrioventricular accessory pathway suffered from weekly paroxysmal atrial fibrillation and syncope. Electrode catheters are positioned in the coronary sinus and in the *right* ventricular apex

Fig. 17.24 Surface lead electrograms I and II, and intracardiac local mapping electrograms (MAP1-4) recorded simultaneously from *right* (MAP_{1,2}) and *left* (MAP_{3,4}) atrial endocardial sites of a patient with atrial fibrillation, prior to the AF ablation attempts. MAP1 recorded from the right atrial lateral wall suggests a circuit (rotor?), a rapid local reentry; whereas recordings in MAP₂ suggest fractionated potentials, and in MAP3-4 torsade like tracings



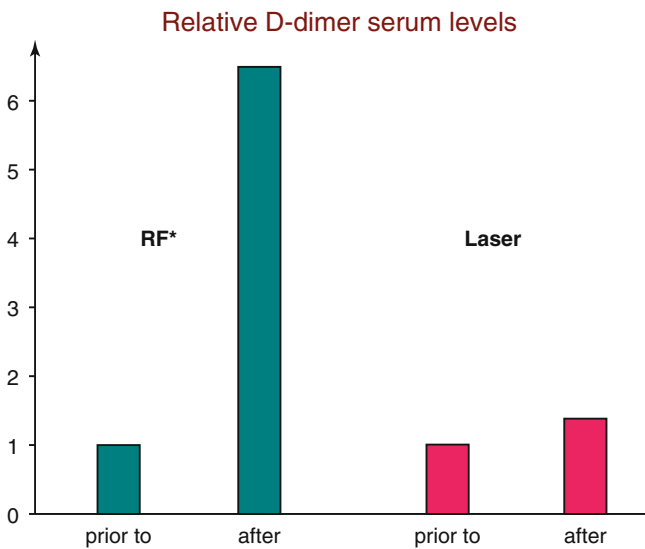
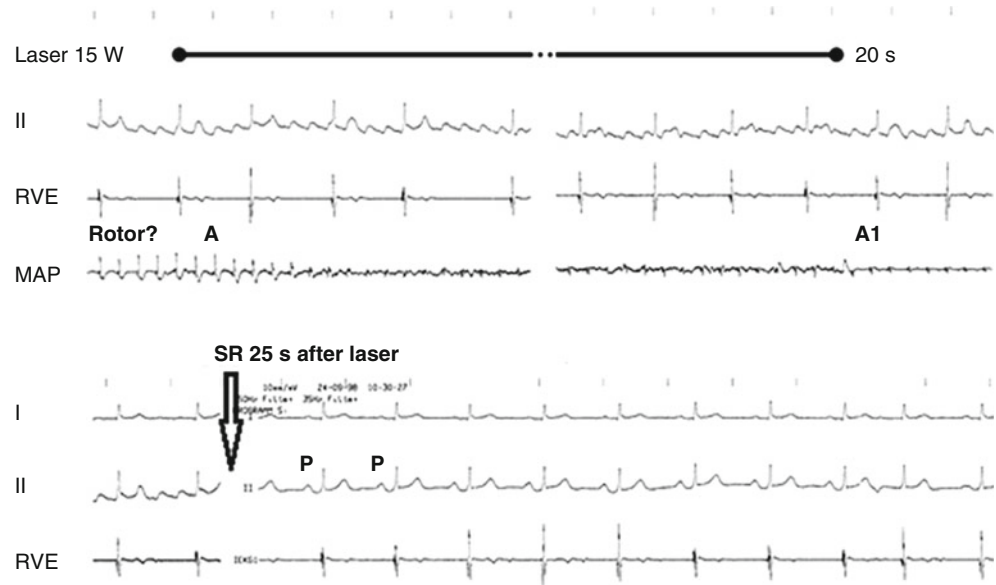
implanted after ablation of an idiopathic left ventricular tachycardia. The ICD could be removed after 2 years of uneventful follow-up. The cured patients were in sinus rhythm, had normal exercise capacity and were off medication including anticoagulants.

The 13 patients with improved clinical condition were intermittently in sinus rhythm but all needed antiarrhythmic medication, e.g. “pill in the pocket”, that was not effective prior to ablation. AF patients continued treatment with

Warfarin. In four patients with paroxysmal AF a permanent pacemaker was implanted because of (in two already pre-existent) symptomatic bradyarrhythmia. In all of the patients clinical symptomatology was reduced and exercise capacity improved. Eventually, in one patient AF could be abolished but temporarily and is now considered as permanent AF.

Except minor bleedings in the groin after venous access in three patients there were no complications encountered during laser ablation procedures or during the follow-up period.

Fig. 17.25 Surface lead I and II, and intracardiac right ventricular (RVE) and mapping (MAP) electrograms during catheter ablation of AF by laser application at 15 W/20 s aimed at the right atrial lateral wall, the area suggesting a rotor. With the start of radiation amplitudes of potential in the LEG gradually dwindle from A to A1. Stable sinus rhythm (SR) is achieved 25 s after radiation. P p-wave in the surface lead Electrogram



* Manolis at al. JACC 1996

Fig. 17.26 Diagram showing D-Dimer relative serum levels prior to and after radiofrequency (RF) ablation as compared to those prior to and after laser ablation

Discussion

Modern mapping guided catheter ablation techniques such as electroanatomical mapping and Navix, or robotic guides (Hanson, Stereotaxis) were not available for the CALCAM study trial. However, the high success rate achieved in this small group of patients with various arrhythmias including AF and VT demonstrates the importance of a safe and effective power source in combination with a catheter adapted to the laser. Both these criteria are met by the cw 1064 nm laser *MediLas* and the ELMA catheter *RytmoLas*. As demonstrated

Table 17.2 Results of laser ablation in 69 patients, follow-up 5–8 years

	AF		AVNRT	AFI	AP	VT	AT	%
	px	ps/pt						
Cured (in SR)	14	10	15	8	4	2	2	81
After re-study	1	5	2	4	1	1		
+ ICD						1		
Improvement	3	8				2		18
After re-study	1	1				2		
+ Pm		4						
Unchanged		1						1.5

AF atrial fibrillation, px paroxysmal, ps persistent (long), pt long persistent, AVNRT atrioventricular nodal reentrant tachycardia, AFI atrial flutter, AP accessory pathway, VT ventricular tachycardia, AT atrial tachycardia, Pm pacemaker (perm.), ICD implantable cardioverter/defibrillator device

experimentally, a unique advantage is the fact that the 1064 nm laser light deeply penetrates into the myocardium creating transmural lesions within seconds regardless of normal or scarred tissue. This unique effect allowed for successful treatment of patients with fibrous scarred myocardium, with structural heart diseases characterized by a tissue mixture of fibrosis with normal myocardium. With the laser large areas were rendered electrically inactive with a relative small number of applications. Ablated areas became rapidly devoid of electrical potentials as documented by the LEG.

Attenuation of the amplitudes of electrical potentials in the LEG during laser application allowed for monitoring of lesion formation, for indirect visualization of lesion maturation in the myocardial wall. This was achievable without sophisticated additional equipment. The electrodes arranged symmetrically at the catheter tip overriding the targeted area allowed for electrical potential recordings closely from the

illuminated field. Potential amplitudes of the LEG were displayed on the monitor. This method for control of lesion maturation we have used routinely during experimental tests and during arrhythmia ablation procedures in patients [25, 32]. More recently, similar techniques for monitoring of lesion maturation were described [33, 34]. With the *RytmoLas*, tip electrodes for endocardial voltage mapping allowed assessment of electrical activity and lesion efficacy by monitoring local electrogram amplitudes. Gradual attenuation of the amplitudes of local potentials reflects lesion maturation, the growth of laser lesion in the myocardial wall during laser application whereas abolishment of potential amplitudes in the LEG is consistent with the achievement of transmural lesions. Energy settings adapted to the thickness of the myocardial walls and stop of laser application after the abolishment of local potentials helped avoid myocardial and collateral damages [35]. By doing so we did not encounter pop or malignant arrhythmias during or after laser applications aimed at the atrial or ventricular walls. Thus, monitoring of potential amplitudes has an important safety aspect for laser ablation of arrhythmias. However, voltage mapping allows only an indirect visualization of lesion formation. In contrast to that, real-time MRI based ablation systems have the advantage of scar identification and localization, of lesion formation visualization during laser delivery. MRI system can be used to identify and acutely target gaps in atrial ablation lesion sets. Acute targeting of gaps in ablation lesion sets can potentially lead to significant improvement in clinical outcomes [36–38]. As the ELMA catheter *RytmoLas* is MR-safe it would be intriguing to verify lesion visualization by producing laser lesions under MR control, preferably in a multicenter study trial for arrhythmia ablation in a larger number of patients.

Pulmonary vein isolation (PVI) is the cornerstone for paroxysmal AF ablation [39]. In our experience multiple arrhythmogenic areas scattered all over the right and left atrial sites were found in patients with AF regardless of which form of AF, paroxysmal, persistent or permanent. In general, laser applications aimed at areas with a fast rate high frequency regular depolarization suggesting a rotor almost instantly ablated AF. By targeting step by step selectively these areas good results were achieved without pulmonary vein isolation (PVI) as routinely used in other electrophysiology centers. Recently, it has been shown that results of AF ablation do not correlate with PVI [40]. September 1st 2013, during the ESC Congress in Amsterdam Dr. Marrouche said: *“we do ablation around the pulmonary veins because we have assumed for years that the trigger for AF comes from the vein – that’s the standard of care. But what we found in DECAAF is that ablation of the veins did not predict outcome. In fact, the most important predictor of outcome, along with stage of atrial fibrosis, was the degree of ablation of the fibrotic tissue. Rather than targeting the pulmonary veins,*

procedures which ablated fibrotic tissue produced better outcomes – the more that was targeted, the better the outcome.”

These new insights support our concept not to target primarily pulmonary veins and in the same time can explain the reason of the good results achieved by the laser method due to the penetration of laser light through scarred tissue. To improve results of PVI research is very active. A recently developed visually guided laser ablation balloon catheter achieved PVI in virtually all of the AF patients. However, efficacy was similar to RF ablation [41].

We always saved the pulmonary veins because it is difficult to achieve durable PVI, and for safety reasons because pulmonary vein stenosis is a well-known possible and severe complication of RF ablation after PVI. Besides that, laser applications around the PV Ostia anyway isolate the veins. We did not perform PVI but we were successful.

Although off anticoagulants in our successfully ablated AF patients cerebrovascular or other vascular incidents were not encountered during the follow-up. The new guide-lines in this regard indicate continuation of anticoagulants even after successful ablation. This might be different in our group of AF patients with successful AF ablation documented for a relative long follow-up. However, in the new knowledge of this field for prevention of stroke we nowadays would recommend one of the new anticoagulants. Of importance for the lower thromboembolic risk in our patients is also the fact that in contrast to the RF method the laser method is not thrombogenic as demonstrated by estimation of the relative D-Dimer serum levels [42].

Laser Applications in the Management of Structural Heart Conditions

HOCM Ablation

Hypertrophic non-obstructive cardiomyopathy (HCM) is often a familial cardiomyopathy with hypertrophic left ventricular myocardium predominantly in the septum. This may result in a left ventricular outflow tract obstruction, the hypertrophic obstructive cardiomyopathy (HOCM). Reduced septal longitudinal strain is associated with ventricular arrhythmias in these patients. Total amount of fibrosis was found to be a marker of ventricular arrhythmias in these patients [43]. Interstitial fibrosis seemed to be more important compared with replacement fibrosis in arrhythmogenesis, and was related to reduced septal myocardial function. The patients with ventricular arrhythmias were reported to have lower septal longitudinal strain compared with those without arrhythmia ($p=0.006$). These findings suggest that interstitial fibrosis may play an important role as the arrhythmogenic substrate.

Ought to the thickness and fibrosis of the myocardial wall RF and alcohol catheter ablation is disappointing and septal myectomy the therapy of choice. With the deep penetration of the laser light in fibrous tissue laser catheter ablation technique has the potential to successfully ablate ventricular arrhythmias originating from the hypertrophied septum. In the same time it can reduce or abolish left ventricular outflow tract obstruction. In the majority of patients with predominantly septal hypertrophy, laser ablation of the septum can be performed from the right side of the septum.

By using the venous approach from the groin, a more risky arterial puncture and transaortic left heart catheterization can be avoided. This procedure was successful applied in a first attempt at septal ablation in three patients with HOCM (Fig. 17.27).

After this promising feasibility test catheter ablation of arrhythmogenic and/or hypertrophic Cardiomyopathy in a larger series of patients by using the open-irrigated ELMA catheter *RytmoLas* is warranted.

Chagas Disease

Chagas' disease is an endemic disease in Latin America caused by a unicellular parasite, the *Tripanosoma cruzi*. Almost 18 million people are infected and 25 % of them develop chronic myocardial disease after years or decades.

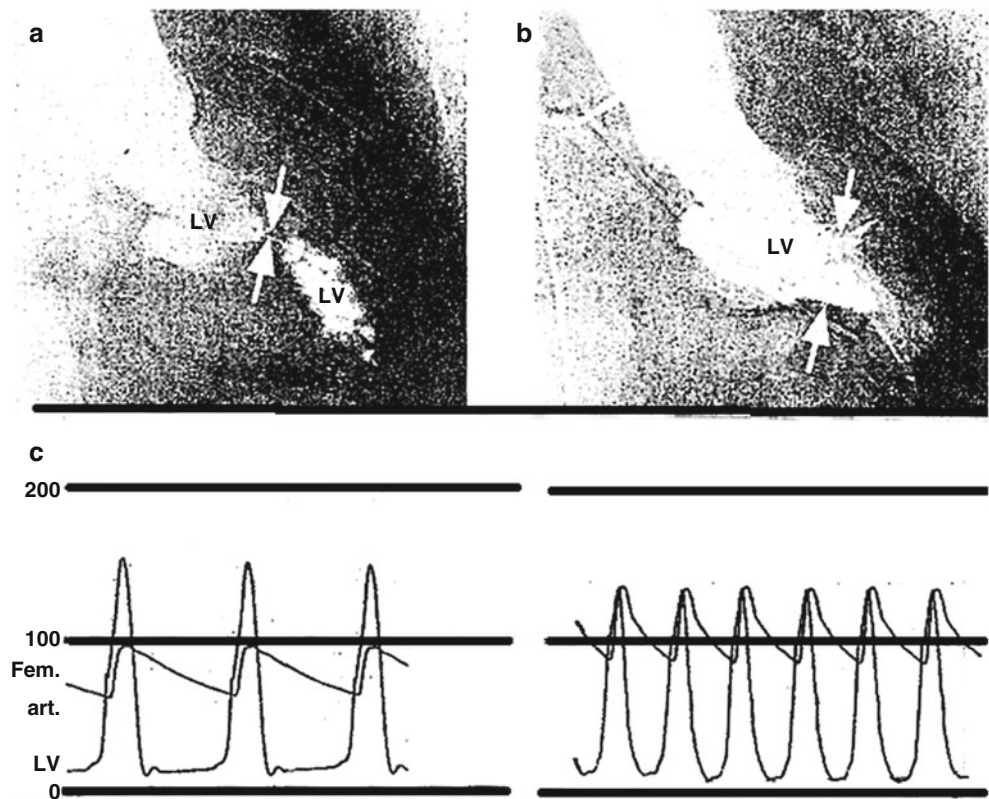
The intermediate phase may last for two to three decades, and the only manifestation of the disease is the immunological reaction. Causes of death are congestive heart failure and sudden cardiac death. Although malignant ventricular arrhythmias are thought to be the main cause of sudden death, bradyarrhythmia and thromboembolic events also account for some of the sudden death.

Chagas' disease has become a worldwide problem, given the new patterns of immigration. Physicians around the world should become aware of its existence and how to recognize and treat it [44]. Implantable cardioverter defibrillators (ICDs) are considered a first-line tool for primary and secondary prevention of sudden death. Ought to the deep intramurally located arrhythmogenic myocardium catheter ablation is of limited value. However, in rare cases RF catheter ablation was reported to be effective [45]. Taking into consideration the deep penetration of laser light into the myocardium and the direct effect of laser light heating up the *Tripanosoma cruzi* effective laser ablation of Chagas' arrhythmias can be anticipated. To prove this assumption experimental and clinical tests would be appropriate.

Renal Sympathetic Denervation

Hypertension is highly prevalent in the overall population and both stroke and myocardial infarction show a linear

Fig. 17.27 (a) Left ventricular angiograms in RAO projection showing severe systolic left ventricular (LV) obstruction (white arrows) prior to laser radiation aimed at the ventricular septum from the right side after pervenous access with the open-irrigated ELMA catheter *RytmoLas*. (b) After two laser applications at 15 W/40 s each, the obstruction is practically abolished. (c) Left ventricular and femoral artery (needle puncture) pressure measurements prior to and after the right septal HOCM laser ablation procedure showing the abolishment of (LV/Fem art) pressure gradient



relation with blood pressure (BP) levels [46]. Unfortunately, many patients are not controlled to target BP values, even with the availability of safe and effective antihypertensive drugs known to reduce the risk of major cardiovascular complications. It has been shown that activation of the renal sympathetic nervous system plays a major role in the progression and development of hypertension [47].

Recently, a catheter-based approach to denervate the kidneys has been successfully introduced into clinical practice, shown to reduce BP and sympathetic activity in patients with resistant hypertension without significant side effects. The first evidence on the clinical effectiveness and safety of this procedure in patients with resistant hypertension was documented in the simplicity hypertension trials [48]. Renal nerve ablation significantly decreased BP by $-30/10$ mmHg over the follow-up period of 36 months. However, patients must have a suitable renal anatomy, i.e. renal arteries 4 mm in diameter, and a single renal artery supplying each kidney without prior renal artery interventions. Up to six ablations are applied in a spiral fashion from the distal part of the renal artery to its origin. In rare cases secondary rise in blood pressure, renal artery dissection, pseudo aneurysm, or renal artery stenosis after renal RF denervation were reported [22, 49, 50]. In addition, more recently failure of the Symplicity HTN-3 trial to achieve primary efficacy end point was reported. However, as compared to the RF the laser could have major advantages for renal sympathetic catheter denervation. The 1064 nm laser light penetration through the vessel walls without thermal damages [22] and the divergent laser beam would ablate renal nerves with a lower risk (Fig. 17.3).

The divergent beam would hit a cylindrical segment with the entire circumference of the arterial wall. Thus, a single application could interrupt sympathetic connections. In addition, the dark Nissl's bodies sensitize the sympathetic nerve cells to the laser light (Fig. 17.28). Of growing importance is renal denervation also for its beneficial effects on glucose metabolism and insulin resistance, and the sleep apnea syndrome [51, 52]. Although speculative, animal experimental research in this regard is warrantable.

Interatrial Transseptal Laser Puncture

Safe and reproducibly effective transseptal puncture and access to the left atrium and ventricle is now a prerequisite for the practicing invasive electrophysiologists. During the past years a variety of left heart catheter intervention were developed beside left atrial and ventricular catheter mapping and ablation including left atrial occlusion procedures, mitral valve clipping and prosthesis, etc. To achieve that goal side selective puncture for targeting these specific anatomical structures is helpful. However, puncture of a thicker atrial septum or a fibrotic septum after repeated punctures may be difficult and routine procedures may fail. Side selective puncture was performed successfully in our patients by using the laser. For this purpose a special laser transseptal introducer and puncture set was developed, the *TransLas* LasCor GmbH (Fig. 17.29). By using this catheter side selective transseptal puncture was successfully performed independent of the thickness and anatomy of the interatrial septum [31].

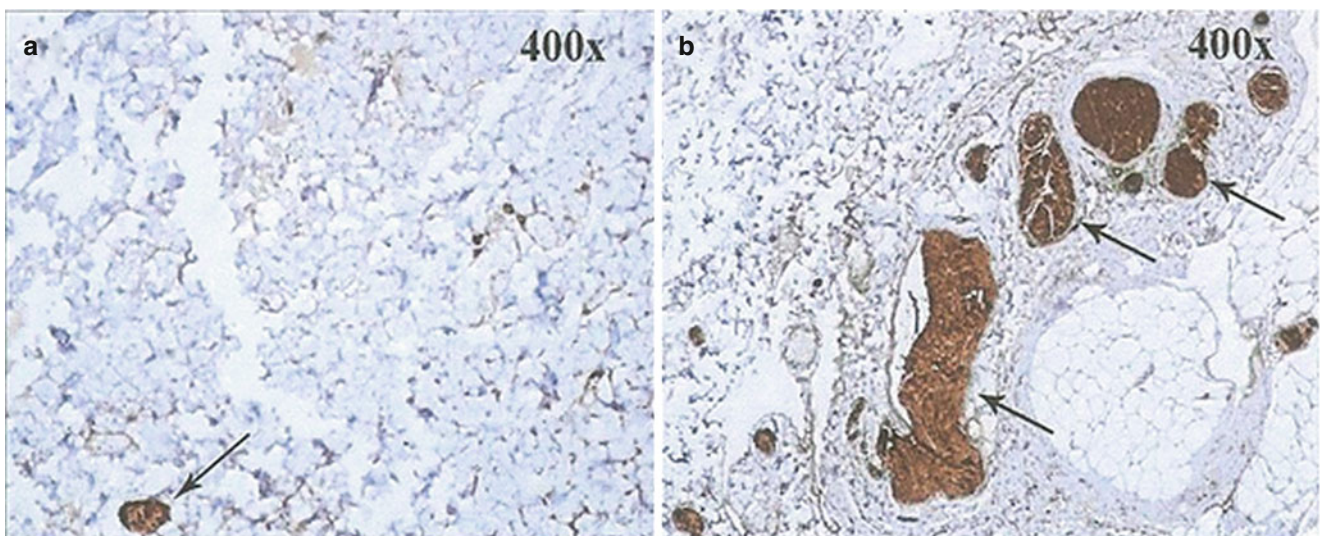


Fig. 17.28 Immune stain with neuron specific Enolase of perirenal tissue (a) after completely destroyed renal sympathetic nerves reflected by the disappearance of (b) Nissl's bodies, dark bodies (arrows) that highly sensitize sympathetic cells to the 1064 nm laser light

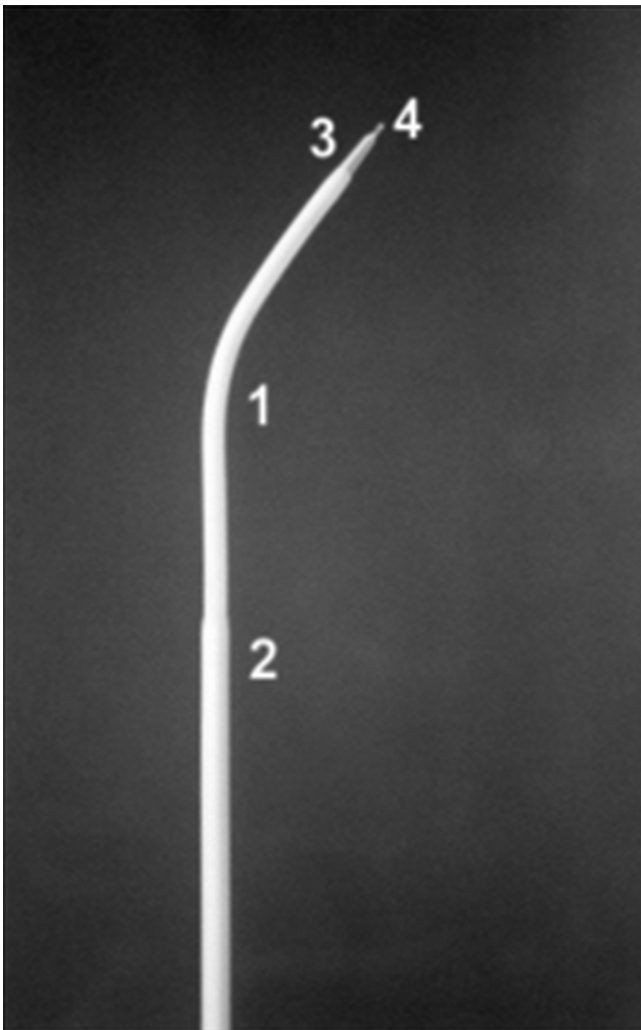


Fig. 17.29 Distal end of the laser transeptal puncture set *TransLas* as used in these studies showing: the tip of the optical fiber (4) advanced approximately 3 mm beyond the end hole of the dilator tip (3) which is fed into a preshaped (1) and a telescoping straight sheath (2) overriding each other

Summary and Conclusions

Laser energy is light waves that are converted to heat to coagulate and create scar tissue. It may be a safer heat-based energy for arrhythmia ablation than unipolar radiofrequency energy. With laser energy, the optical fiber doesn't need to be in direct contact with tissue and the catheter is not heated up, which could mean it will have fewer complications than radiofrequency energy. Unlike other energy sources, contact force is not a factor in whether a clear-cut homogenous laser lesion is transmural. In addition, laser energy can be adjusted when ablating tissues of varying thickness, with higher energy applied to thicker tissue and lower energy applied to thinner structures in the heart. Larger laser lesion enhances the prospects that lesions will be contiguous (without gaps) and could shorten procedure times. In addition, attenuation

of potentials in the intracardiac Electrograms during laser application allows for indirect control of lesion formation.

The results of our experimental and clinical studies detailed above suggest that the laser method is an intriguing alternative for catheter ablation of arrhythmias and for the treatment of various other cardiovascular conditions. With the invention of the multipurpose ELMA catheter percutaneous transluminal catheter directed application of laser light in the cardiovascular system has become safely and effectively practicable. At powers of 10–15 W/10–50 s, energies as low as 100–750 J, the laser light transmitted via the ELMA catheter *RytmoLas* without pressure creates transmural lesions of homogenous coagulation necrosis within seconds healing to dense fibrous scar tissue. Laser lesions can reach arrhythmogenic substrates located deep intramurally or contained in scarred post infarction or in Chagas myocardium.

We conclude that cardiovascular laser catheter applications represent an intriguing technology for a minimally invasive treatment of a series of major cardiovascular disorders. With its LPS, the TLS, and the monitoring of catheter irrigation the laser method has a unique safety profile.

References

1. Weber H, Ischinger T. Cardiovascular application of Nd:YAG laser. *Lasers Med Surg*. 1988;4:54–8.
2. Boulnois J-L. Photophysical processes in recent medical laser developments: a review. *J Lasers Med Sci*. 1986;1:47–66.
3. Weber H, Heinze A, Enders S, Hauptmann G, Ruprecht L, Unsöld E. In vivo temperature measurement during transcatheter endomyocardial Nd:YAG laser radiation. *Lasers Med Sci*. 1997;12:352–6.
4. Gralinski MR. The dog's role in the preclinical assessment of QT interval prolongation. *Toxicol Pathol*. 2003;31:11–6.
5. Eckardt L, Meissner A, Kirchof P, Weber T, Borggreffe M, Breithardt G, Van Aken H, Haverkamp W. In vivo recording of monophasic action potentials in awake dogs – new applications for experimental electrophysiology. *Basic Res Cardiol*. 2001;96:169–74.
6. Weber H, Sagerer-Gerhardt M. Open-irrigated laser catheter ablation: relationship between the level of energy, myocardial thickness, and collateral damages in a dog model. *Europace*. 2013. 2014;16:142.48. doi:10.1093/Europace/eut150.
7. Weber H, Heinze A. Reversible laser mapping: experimental and clinical results. *PACE*. 2001;24:S68 (abstr 269).
8. Weber H, Heinze A. Hot versus cool ablation. *J Cardiovasc Electrophysiol*. 2002;13:440–1.
9. Weber H, Enders S, Heinze A, Ruprecht L, Unsoeld E. Transcatheter mapping guided laser irradiation of the AV-conduction system. *PACE*. 1993;16:1109 (Part II).
10. Weber H, Heinze A, Enders S, Ruprecht L, Unsoeld E. Modification of sinus node functions by endocardial catheter directed laser irradiation in dogs. *PACE*. 1994;17:797 (Part II).
11. Weber H, Heinze A, Enders S, Ruprecht L, Unsoeld E. Modification of atrioventricular node transmission properties by transcatheter endocardial laser irradiation in dogs. *PACE*. 1994;17:832 (Part II).
12. Helmut P. Weber, Sagerer-Gerhardt M. Monitoring of laser effects on the conduction system by using an open-irrigated electrode-laser mapping and ablation catheter: laser catheter mapping. *Europace*. 2015;17:664–70.

13. Weber H. Hot versus cool ablation. *J Cardiovasc Electrophysiol.* 2002;13:440–441.
14. Stevenson WG, Cooper J, Sapp J. Optimizing RF output for cooled RF ablation. *J Cardiovasc Electrophysiol.* 2004;15:24–7.
15. Nakagawa H, Wittkamp FH, Yamanashi WS, Pitha JV, Imia S, Campbell B, Arruda M, Lazzara R, Jackman WM. Inverse relationship between electrode size and lesion size during RF ablation with active electrode cooling. *Circulation.* 1998;98:458–65.
16. Matsudaira K, Nakagawa H, Wittkamp FH, Yamanashi W, Imia S, Pitha JV, Lazzara R, Jackman WM. High incidence of thrombus formation without impedance rise during RF ablation using electrode temperature control. *PACE.* 2003;26:1227–37.
17. Scavee C, Jais P, Hsu LF, Sanders P, Hocini M, Weerasooriya R, Macle L, Raybaud F, Clementy J, Haissaguerre M. Prospective randomized comparison of irrigated-tip and large-tip catheter ablation of cavotricuspid isthmus-dependent atrial flutter. *Eur Heart J.* 2004;25:963–9.
18. Shah DC, Lambert H, Nakagawa H, Langenkamp A, Aeby N, Leo G. Area under real time contact force curve (force time integral) predicts radiofrequency lesion size in an in-vitro contractile model simulating beating heart. *J Cardiovasc Electrophysiol.* 2010;21:1038–43.
19. Thiagalingam A, D'Avila A, Foley L, et al. Importance of catheter contact forceduring irrigated radiofrequency ablation: evaluation in a porcine ex vivo model using a force sensing catheter. *J Cardiovasc Electrophysiol.* 2010;21:806–11.
20. Cappato R, Calkins H, Chen SA, et al. Updated worldwide survey on the methods, efficacy and safety of catheter ablation for human atrial fibrillation. *Circ Arrhythm Electrophysiol.* 2010;3:32–8.
21. Kuck KH, Reddy VY, Schmidt B, et al. A novel radiofrequency ablation catheter using contact force sensing: TOCCATA Study. *Heart Rhythm.* 2012;9:18–23.
22. Weber H, Enders S, Coppenrath C, Murray AB, Schad H, Mendler N. Effects of Nd:YAG laser coagulation of myocardium on coronary vessels. *Lasers Surg Med.* 1990;10:133–9.
23. Weber H, Heinze A, Enders S, Ruprecht L, Unseold E. Laser versus radiofrequency catheter ablation of ventricular myocardium: a comparative test. *Cardiology.* 1997;88:346–52.
24. Haines D. Biophysics of ablation: application to technology. *J Cardiovasc Electrophysiol.* 2004;15:S2–11.
25. Weber HP, Heinze A, Enders S, Ruprecht L, Unsöld E. Laser catheter coagulation of normal and scarred ventricular myocardium in dogs. *Lasers Surg Med.* 1998;14:109–19.
26. Splinter R, Svenson RH, Littman L, et al. Significance of optical characterization of Myocardium in laser ablation of ventricular Tachycardia. In: Splinter R, editor. Dissertation, University of Amsterdam; 1990. p. 77–92.
27. Weber H, Schmitz L. Catheter technique for closed-chest ablation of an accessory atrioventricular pathway. *N Engl J Med.* 1983;308:653–4.
28. Weber H, Heinze A. Laser catheter ablation of atrial flutter and of atrio-ventricular nodal reentrant tachycardia in a single session. *Eur Heart J.* 1994;15:1147–9.
29. Ischinger T, Coppenrath C, Weber H, Enders S, Ruprecht L, Unseold E, et al. Laser balloon angioplasty: technical realization and vascular tissue effects of a modified concept. *Lasers Surg Med.* 1990;10:112–23.
30. Kimura T, Takatzski S, Miyoshi SH, Fukumoto K, Takahashi M, Ogawa E, et al. Nonthermal cardiac catheter ablation using photodynamic therapy. *Circ Arrhythm Electrophysiol.* 2013;6:1025–31.
31. Weber H, Sagerer-Gerhardt M. Side-selective atrial transseptal laser puncture. *Innov CRM.* 2013;4:1481–5.
32. Weber H, Kaltenbrunner W, Heinze A, Steinbach K. Laser catheter coagulation of atrial myocardium for ablation of atrioventricular nodal reentrant tachycardia. *Eur Heart J.* 1997;18:487–95.
33. Price A, Leshen Z, Hansen J, Singh I, Arora P, Koblish J, Avitall B. Novel ablation catheter technology that improves mapping resolution and monitoring of lesion maturation. *Innov CRM.* 2012;3:599–609.
34. Migliore F, Zorzi A, Silvano M, Bevilacqua M, Leoni L, Perazzolo Marra M, Elmaghavi M, Brugnaro L, Dal Lin C, Bauce B, Rigato I, Tarantini G, Basso C, Buja J, Thiene G, Iliceto S, Corrado D. Prognostic value of endocardial voltage mapping in patients with arrhythmogenic ventricular cardiomyopathy/dysplasia. *Circ Arrhythm Electrophysiol.* 2013;6:167–76.
35. Weber H, Sagerer-Gerhardt M. Open-irrigated laser catheter ablation: relationship between the level of energy, myocardial thickness, and collateral damages in a dog model. *Europace.* 2014;16:142–8.
36. Ranjan R, Kholmovski EG, Blauer J, Vijayakumar S, Volland NA, Salama ME, Parker DL, MacLeod R, Marrouche NF. Identification and acute targeting of gaps in atrial ablation lesion sets using a real-time magnetic resonance imaging system. *Circ Arrhythm Electrophysiol.* 2012;5:1130–5.
37. Oakes RS, Badger TJ, Kholmovski EG, Akoum N, Burgon NS, Fish NE, Blauer JJE, Rao SN, DiBella EVR, Segerson NM, Daccarett M, Windfelder J, McGann DHJ, Parker D, McLeod RS, Marrouche NF. Detection and quantification of left atrial structural remodeling with delayed enhancement magnetic resonance imaging in patients with atrial fibrillation. *Circulation.* 2009;119:1758–67.
38. Akoum N, Daccarett M, McGann CH, Segersen N, Verara G, Kuppahally S, Badger T, Burgon N, Haslam T, Kholmovski E, McLeod R, Marrouche N. Atrial fibrosis helps select the appropriate patient and strategy in catheter ablation of atrial fibrillation: a DE-MRI guided approach. *J Cardiovasc Electrophysiol.* 2011;22:16–22.
39. Calkins H, Kuck KH, Cappato R, Brugada J, Camm AJ, Chen SA, et al. Expert consensus statement of catheter and surgical ablation of atrial fibrillation. *Europace.* 2012;14:528–606.
40. Kawata H, Schricker A, Lalani GG, Baykauer T, Krummen DE, Narayan SM. Focal impulse and rotor modulation for paroxysmal atrial fibrillation. *Innov CRM.* 2013;4:1101–7.
41. Dukkipati SR, Kuck KH, Neuzil P, Woollett J, Kautzner J, McElderry HT, Schmidt B, Gerstenfeld EP, Doshi AK, Horton R, Metzner A, d'Avila A, Ruskin JM, Natale A, Reddy VY. Pulmonary vein isolation using a visually guided laser balloon catheter: the first 200-patient multicenter clinical experience. *Circ Arrhythm Electrophysiol.* 2013;6:467–72.
42. Zhuang S, Weber H, Heinze A, Wanner G, Weiss L. D-dimer serum level after laser catheter ablation of tachyarrhythmias. *PACE.* 1999;22:A94 (P196).
43. Furushima H, Chinushi M, Iijima K, Sanada A, Izumi D, Hosaka Y, Aizawa Y. Ventricular tachyarrhythmia associated with hypertrophic cardiomyopathy: incidence, prognosis, and relation to type of hypertrophy. *J Cardiovasc Electrophysiol.* 2010;21:991–9.
44. Muratore CA, Batista Sa LA, Chiale PA, Eloy R, Tentori MCH, Escudero J, Cavalcanti Lima AM, Medina LE, Garillo R, Maloney J. Implantable cardioverter defibrillators and Chagas' disease: results of the ICD Registry Latin America. *Europace.* 2009;11:164–8.
45. Hadid C, Gallino S, Di Toro D, Celano L, Lopez C, Duce E, Labadet C. Multiple morphologies of ventricular tachycardia assessed by implantable cardioverter-defibrillator electrograms in a patient with Chagas disease, successfully treated with catheter ablation: modern problems, old solutions. *Europace.* 2012;14:1660.
46. Calhoun DA, Jones D, Textor S, Goff DC, Murphy TP, Toto RD, White A, Cushman WC, White W, Sica D, Ferdinand K, Giles TD, Falkner B, Carey RM. Resistant hypertension: diagnosis, evaluation, and treatment: a scientific statement from the American Heart Association Professional Education Committee of the Council for High Blood Pressure Research. *Circulation.* 2008;117:e510–26.
47. Krum H, Barman N, Schlaich M, Sobotka P, Esler M, Mahfoud F, Böhm M, Dunlap M. Catheter-based renal sympathetic denervation

- for resistant hypertension: durability of blood pressure reduction out to 24 months. *Hypertension*. 2011;57:911–7.
48. Esler MD, Krum H, Sobotka PA, Schlaich MP, Schmieder RE, Boehm M. Renal sympathetic denervation in patients with treatment-resistant hypertension (The Symplicity HTN-2 Trial): a randomized controlled trial. *Lancet*. 2010;376:1903–9.
49. Vonend O, Antoch G, Rump LC, Blondin D. Secondary rise in blood pressure after renal denervation. *Lancet*. 2012;380:778.
50. Kaltenbach B, Id D, Franke JC, Sievert H, Hennersdorf M, Maier J, Bertog SC. Renal artery stenosis after renal sympathetic denervation. *J Am Coll Cardiol*. 2012;60:2694–5.
51. Mahfoud F, Ukena C, Cremers B, Kindermann I, Kindermann M, Sobotka P, Schlaich M, Boehm M. Renal denervation improves glucose metabolism in patients with resistant hypertension. *Circulation*. 2011;123:1940–6.
52. Witkowski A, Prejbisz A, Florczak E, Kadziela J, Sliwinski P, Bielen P, Michalowska I, Kabat M, Warchol E, Januszewicz M, Narkiewicz K, Somers VK, Sobotka PA, Januszewicz AE. Effects of renal sympathetic denervation on blood pressure, sleep apnea course, and glycemic control in patients with resistant hypertension and sleep apnea. *Hypertension*. 2011;58:559–65.

Roger Carrillo and Chris Healy

Introduction

The rate of cardiac implantable electronic device (CIED) implantation continues to increase, thus the number of CIED leads in use and the inevitable complications associated with these leads also continues to rise [1, 2]. As the knowledge and techniques associated with CIED implantation have advanced, so have the knowledge and techniques associated with transvenous lead extraction. A great deal is now known about the risks, benefits, indications, and contraindications associated with lead extraction. This was comprehensively addressed in the most recent expert consensus document from the Heart Rhythm Society (HRS) [3].

History

Laser sheaths were introduced as power tools for lead extraction in 1997 (Table 18.1). The catheter brings fiber optics laser energy to the tip from a generator (CVX-300®, Spectranetics, Colorado) (Fig. 18.1). The Excimer Laser uses an ultraviolet spectrum light at 380 nm. The length of the catheter is 50 cm. It has a metal tip beveled to 15° and comes in three sizes: 12 French (color code blue), 14 French (color code grey), and 16 French (color code black). It has a precision cutting tip of 50 µm (the diameter of a human hair). The laser is pulsed at 135 ns to mitigate heat radiation inside the venous lumen. In 1997, the pulses were emitted at 40 Hz. Since 2012, a new sheath named GlideLight® has the programmability to increase the repetition rate from 40 to 80 Hz.

R. Carrillo, MD (✉)

Department of Cardiothoracic Surgery, University of Miami Hospital, 1295 NW 14th Street, Suite H, Miami, FL 33125, USA
e-mail: rogercar@aol.com

C. Healy, MD

Division of Cardiology, University of Miami, Clinical Research Building Room 1107, 1120 NW 14th Street, Miami, FL 33136, USA
e-mail: CHealy@med.miami.edu; healycr@gmail.com

This provides a more powerful tool and a more efficient pulse repetition rate [4].

Technique

Pre-procedure planning is very important. A detailed judgment of the risks versus benefits of the procedure should be tailored to every patient. There are three important elements: (a) Patient medical condition, (b) Indications for extraction, (c) Leads (Fig. 18.2).

Patient medical condition refers to comorbidities such as renal failure, congestive heart failure, a history of body radiation, steroid intake, and body mass index (BMI). The assessment of the indication is important: in the case of infection, all leads should be removed [5], while in non-infectious cases not all the hardware needs to be removed. In reference to leads one should take into account the lead model, their fixation mechanism (active versus passive), the material (silicone versus polyurethane), the time of implantation, and the number of leads. In addition, pacemaker dependency of the patient should be established.

The pre-procedure planning should also include a posteroanterior and lateral chest X-ray. Some authors have suggested the use of Gated CT scan of the chest to verify the intra-cardiac position of the leads [6].

A simple tool for stratification is the allocation of patients into low, medium, and high risk. This can only be done if intra-cardiac position of the leads is confirmed. The risk stratification is based on the time of implantation of the oldest lead (pacemaker or defibrillating):

- Low risk: less than 2 years of oldest lead implantation
- Medium risk: between 2 and 5 years of oldest lead implantation
- High risk: between 6 and 20 years of oldest lead implantation
- Severe risk: greater than 20 years of oldest lead implantation

Table 18.1 Progression of laser sheath characteristics over time

Model	Year	Repetition rate	Characteristics
SLS I®	1997	40 Hz fixed	Firm
SLS II®	2002	40 Hz fixed	Flexible and lubricious
GlideLight®	2012	40–80 Hz programmable	Flexible and lubricious

**Fig. 18.1** Laser sheath used for lead extraction

If the BMI is less than 25 kg/m² the risk level should be elevated to the next one (e.g. a woman with a BMI of 19 kg/m² within 1 year of lead implantation should be classified as medium risk instead of low risk). Major adverse events have been linked to low body mass index [7].

A successful lead extraction program involves a medical team. A skilled extractor should be complimented with a well-trained laser extraction team. An open line of communication is mandatory among members. The anesthesiologist, the scrub nurse, the circulating nurse, X-ray tech, the pacemaker representative, the laser representative, and the backup surgeon are all essential. Each team member should have a checklist that details his or her role in an emergency. Rehearsing of emergency drills is beneficial to develop teamwork. Improvements for successful performance are clarified after a debriefing meeting following this drill.

A survey in 2010 revealed that Electrophysiologists performed 89 % of the lead extraction procedures, Cardiac Surgeons 6 % and Cardiologists 5 % [8]. Most of the responders performed less than 25 procedures per year. The survey stated that 36 % of the lead extractions were done in the Operating Room, while 64 % were conducted in an Electrophysiology Laboratory. The 2009 guidelines state that the procedure can be performed either in the Operating Room or in the Electrophysiology laboratory [3]. There is data favoring the Operating Room [9] as well as the Electrophysiology Laboratory [10]. However, the extraction team must decide which is the optimal location for them.

Lately, Hybrid Operating Rooms are becoming a popular procedure location for many hospitals.

The procedure is performed under general anesthesia in many centers, while others use local anesthesia and sedation. Anesthesia management includes the use of an arterial line and a large bore femoral intravenous line. Cardiac function is often monitored with a transesophageal echocardiogram (TEE), which can be a useful tool for the early detection of intraoperative complications. Alternatively, either a transthoracic echocardiogram (TTE) or an intra-cardiac echocardiogram (ICE) is an adequate choice. Pacing and defibrillating pads should be placed on the skin of the patient.

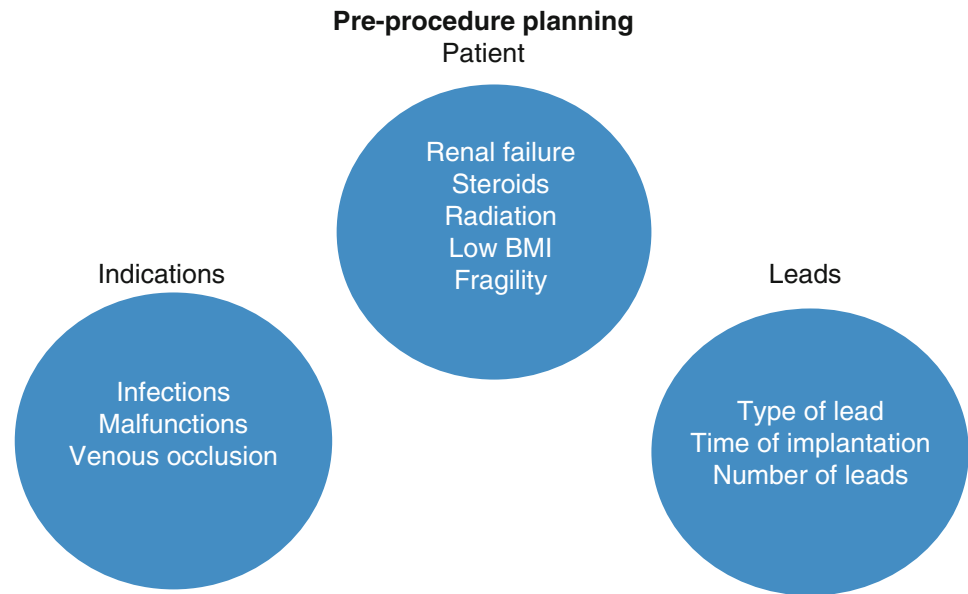
After the infraclavicular incision is made, the generator is removed, and the leads are dissected into the subclavicular space. Active fixation leads should be retracted if feasible. The leads are prepared by the use of a specialized lead locking device. The complete preparation includes securing conductor cables and insulation. An appropriately sized laser sheath is used. While keeping traction, the scar tissue surrounding the lead is ablated by advancing the laser sheath. Several steps are identified during laser advancement: (a) Subclavian-Innominate vein, (b) Superior Vena Cava, (c) Right atrium and Tricuspid valve, (d) Detachment of the myocardial interface.

The laser sheath must be aligned with the lead; in other words, you must stay **coaxial** to the lead. The lead should be used as a rail that guides the laser sheath into the endovenous space. Technically, the most difficult section is the adhesions in the upper superior vena cava. The leads may take a posterior turn in this area, and at times this may not be detected by 2D fluoroscopy. The use of multiplanar fluoroscopic views could be helpful in navigating this treacherous anatomic landmark. The presence of a superior vena cava coil in a defibrillating lead adds complexity to the procedure [11].

The **bevel** of the laser sheath should be aligned in such a way that the tip should point towards the lumen and the base of the bevel should point towards the wall of the superior vena cava.

As the time of lead implantation lengthens, calcifications occur concentrically in the area closest to the lead. At times, the laser fails to advance due to bunching up of tissue or insulation plastic. This issue is often referred to as “snow plowing” or “accordion.” The lack of advancement of the laser can be overcome by pushing the outer sheath past the laser tip. This technique is called **telescoping**.

Fig. 18.2 Factors involved in preprocedure planning for lead extraction



Once the laser has entered the right atrium, the traction should be decreased to avoid damage to the tricuspid valve and right ventricular invagination. Excess traction may cause hypotension; therefore, the extractor should constantly communicate with the anesthesiologist to avoid unnecessary use of vasoactive drugs.

Laser ablation should be paused a few millimeters before reaching the tip of the lead. A gentle tug will detach the lead from the myocardial interface. This maneuver is called **counter traction**. The advancement of a catheter over the lead tip at the myocardial interface minimizes the shearing forces on the right ventricular wall. In contrast, forceful direct traction of the leads without the use of the catheter could avulse myocardial tissue.

Results

Three major registries have addressed the results of laser assisted lead extraction [12, 13]. The first of these was the PLEXES trial, which randomized patients to CIED lead extraction with a laser sheath vs. a non-laser sheath. In this trial, complete lead removal was achieved in 94 % of the laser group as opposed to only 64 % of the non-laser group (failed non-laser extraction was completed with the laser sheath in 88 % of cases) [13]. Subsequently, an analysis of over 2500 attempted lead extractions at 89 sites in the United States reported a 90 % success rate for complete lead removal and a 3 % rate of partial removal [12]. These two reports represent early experience with the laser sheath.

The LEXiCon study is a more contemporary experience with this technology. It reported the outcomes of over 2400 leads treated at predominantly high-volume centers. The

rate of complete lead removal was 96.5 %, and the rate of clinical success (goals associated with indication for lead extraction were achieved) was 97.7 %. Conditions associated with procedural failure include BMI <25 kg/m², leads implanted >10 years, and procedures performed in low volume centers [6].

In these three registries, the rate of major adverse events associated with the procedure was 1.4–2.0 %, and the procedural mortality was 0.27–0.65 % (Fig. 18.3). However, in the LEXiCon study the major adverse event rate was <1 % in procedures performed in high volume centers. Factors associated with in-hospital mortality in the LEXiCon study include pocket infection, device-related endocarditis, diabetes, and serum creatinine ≥2.0 [12, 13].

Undue traction over the leaflets of the tricuspid valve may cause significant tricuspid insufficiency. A study stated that tricuspid insufficiency is uncommon but concerning during percutaneous lead extraction [14, 15]. In contrast, several reports involving hundreds of patients have suggested laser lead removal has no effect on the increased incidence of tricuspid insufficiency [16]. In addition, they reported that laser extraction is not associated with clinical development of severe tricuspid insufficiency [17].

Indications

When evaluating a patient for possible lead extraction, as with any procedure, it is important to keep in mind the strength of the clinical indication for the procedure. Here, the strength of the indication will be reported as in the HRS consensus document (Class I, IIa, IIb, or III) and is summarized in Table 18.2. The strength of the indication must be weighed

Fig. 18.3 Results of major registries of lead extraction outcomes

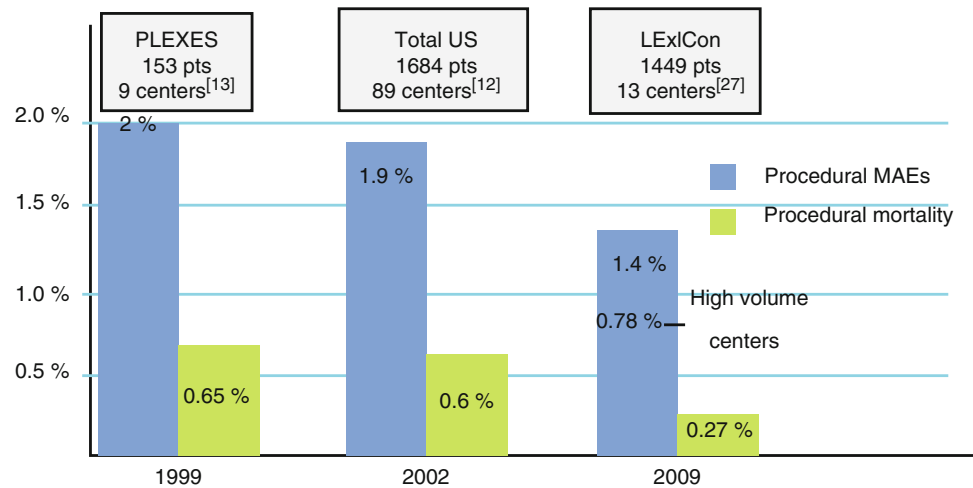


Table 18.2 Strength of indication for transvenous lead extraction

Class I
Conditions where evidence and/or general agreement exists that the procedure is useful and effective
Class II
Conditions where there is conflicting evidence and/or a divergence of opinion about the usefulness/efficacy of a procedure or treatment
IIa: The weight of evidence/opinion is in favor of usefulness/efficacy
IIb: Usefulness/efficacy is less well established by evidence/opinion
Class III
Conditions where evidence and/or general agreement exists that the procedure is not useful or effective, and in some cases may be harmful (NOT INDICATED)

in relation to the value of the desired outcome and the risk of the procedure.

This decision is unique for every patient; it must take into account the training and experience of both the extractor and the entire extraction team. These topics are discussed elsewhere in more detail in this text.

The indications for lead extraction can be generally divided into two categories: infectious and non-infectious. In the LExICon study, a multi-center retrospective analysis of laser-assisted lead extraction, over half of all lead extractions were done for infectious indications. Together, functional and non-functional leads were responsible for slightly over a third of all extractions and venous stenosis/occlusion was responsible for less than 5 % of procedures, while chronic pain was the indication in fewer than 1 % of all extractions [7].

Infectious Indications

Infection of a CIED is the strongest indication for complete CIED system removal. However, the possible clinical presentations of CIED related infection can vary widely [18, 19]. CIED related infection can manifest as nothing more than pain in the device pocket, or can be associated with valvular endocarditis

and sepsis. When an infection is discovered, every effort should be made to remove all components of the CIED system (device, leads, sutures, etc.) and as much of the infected tissue as possible in order to give the patient the best chance to clear the infection [20, 21]. The infectious indications for extraction are listed in Table 18.3. Rarely, will a patient's clinical condition and long-term prognosis be so precarious that chronic suppressive antibiotic therapy would be favored over extraction. This is the exception, not the rule, and an attempt at extraction should be undertaken whenever feasible.

Device related infections might be obvious when they present with fever, bacteremia, vegetations, or sepsis. However, it may prove difficult to diagnose or associate infection with the implantable device. Cultures may be negative, even in patients with documented device related infection who are not receiving antibiotics. Studies have shown that the highest yield for documenting the pathologic organism requires culture of tissue debrided from the fibrotic material surrounding the pulse generator pocket. Yet, even this yields positive results in just over two-thirds of clinically infected patients [22]. When device infection is suspected, diagnosis and treatment should be expedited, as delay to definitive therapy with removal of all components of the CIED system has been associated with increased mortality [23].

Table 18.3 Infectious indications for transvenous lead extraction

Class I – Evidence and/or general agreement exists that the procedure is useful and effective
Definitive CIED system infection, as evidenced by valvular endocarditis, lead endocarditis, or sepsis
CIED pocket infection as evidenced by pocket abscess, device erosion, skin adherence, or chronic draining sinus
Valvular endocarditis without definitive involvement of the lead(s) and/or device
Occult gram-positive bacteremia (not contaminant)
Class IIa – Weight of evidence/opinion is in favor of usefulness/efficacy of the procedure
Persistent occult gram-negative bacteremia
Class III – Evidence and/or general agreement exists that the procedure is not useful or effective, and in some cases may be harmful (NOT INDICATED)
Superficial or incisional infection without involvement of the device and/or leads
Chronic bacteremia due to a source other than the CIED, when long-term suppressive antibiotics are required

Adapted from the 2009 HRS Expert Consensus Document on Transvenous Lead Extraction

CIED(s) cardiovascular implantable electronic device(s)

It is important to note that patients presenting with signs/symptoms of pocket infection typically have involvement of the intravascular components as well [24]. This is likely related to the biofilm formed by staphylococcal bacteria, the most common pathogen responsible for device infection. The biofilm adheres to foreign bodies (devices, leads, etc.), making the infection resistant to antibiotics and the patient's immune system. Thus, even in the absence of an overt indication of infection, when pocket pain is severe enough to require intervention, some experts recommend that consideration be given to treating the patient as if the cause is an infection [3].

Occasionally, the only evidence of infection is positive blood cultures. If only a single blood culture is positive without clinical evidence of infection, extraction should not be pursued. However, in the setting of persistent bacteremia (positive blood cultures for the same organism on different days, particularly gram-positive organisms), even without a clear source of infection involving the heart, leads, or other body site (occult infection) extraction is recommended [3]. CIED infection is not typically related to gram-negative bacteremia and other sources of infection should be investigated and treated before pursuing extraction [20, 21].

Infection or erythema that involves only the skin or superficial incision should not be treated as an infection of the CIED and does not warrant extraction. These patients should be followed closely to prevent and/or identify progression to a deeper infection, as this would necessitate extraction.

In spite of the advances made in transvenous lead extraction technology, situations still exist where open surgery is necessary or more desirable. One factor that may necessitate an open procedure is the presence of large vegetations. No specific rules exist as to the size of vegetation that requires an open surgical technique. However, there is growing clinical evidence that vegetations smaller than 2.5 cm could be removed percutaneously without major clinical complications [25]. Factors that must be considered include vegetation shape and friability, presence or absence of a patent

foramen ovale, atrial or ventricular septal defect, and the health or hemodynamic stability of the patient must be considered [1]. The decision about whether a transvenous or an open approach is best must be individualized to each patient and clinical situation.

Non-infectious Indications

While the benefits of device extraction in the setting of an infection are clear, lead extraction for non-infectious indications is a more nuanced decision. In these circumstances, the option of abandoning failed or unnecessary leads and reimplantation through the same or an alternative route often exists. It should be noted, however, that putting 4 or more leads through a single vein or 5 or more leads through the superior vena cava is discouraged [3]. For the majority of non-infectious indications, an immediate risk of mortality is not present, making calculation of the risk/benefit ratio more complicated. This makes individualization of the decision for each patient even more important. The non-infectious indications as laid out in the HRS expert consensus document on lead extraction are listed in Table 18.4.

When making the decision about whether or not to extract a lead for a non-infectious indication, the long-term prognosis of the patient as well as the number of likely future procedures must be considered. When a lead has been in place for a longer period of time, extraction becomes more challenging, and the risk of a major complication increases [7]. This fact must be carefully considered when deciding whether or not to extract a lead. The same non-infectious indication for lead extraction may result in different management strategies for a 24-year-old patient with congenital complete heart block and multiple failed leads as opposed to a 92-year-old patient with a 3–4 year life expectancy and a single malfunctioning lead.

The decision about whether or not to extract a lead and/or a CIED system for chronic pain is perhaps the most

Table 18.4 Non-infectious indications for transvenous lead extraction

Chronic pain
Class IIa – Weight of evidence/opinion is in favor of usefulness/efficacy of the procedure
Severe, chronic pain at the device or lead insertion site that causes significant discomfort, is not manageable by medical or surgical techniques, and for which there is no acceptable alternative
Thrombosis or venous stenosis
Class I – Evidence and/or general agreement exists that the procedure is useful and effective
Clinically significant thromboembolic events associated with thrombus on a lead or lead fragment
Bilateral subclavian vein or SVC occlusion precluding implantation of a needed transvenous lead
Planned stent deployment in a vein containing a transvenous lead, in order to avoid entrapment of the lead
SVC stenosis or occlusion with limiting symptoms
Ipsilateral venous occlusion preventing access to the venous circulation for required placement of an additional lead when a contraindication exists to using the contralateral side (contralateral AV fistula, shunt, or vascular access port, mastectomy, etc.)
Class IIa – Weight of evidence/opinion is in favor of usefulness/efficacy of the procedure
Ipsilateral venous occlusion preventing access to the venous circulation for required placement of an additional lead, when there is no contraindication to using the contralateral side
Functional leads
Class I – Evidence and/or general agreement exists that the procedure is useful and effective
Life threatening arrhythmias secondary to retained leads
Leads that, due to their design or failure, may pose an immediate threat to the patient if left in place
Leads that interfere with the operation of implanted cardiac devices
Leads that interfere with the treatment of a malignancy (radiation/reconstructive surgery)
Class IIb – Usefulness/efficacy of the procedure is less well established by evidence/opinion
Abandoned functional leads that pose a risk of interference with the operation of the active CIED system
Functioning leads that due to their design or failure pose a potential future threat to the patient if left in place
Leads that are functional but not being used (RV pacing lead after upgrade to ICD)
Patients who require specific imaging techniques (MRI) that cannot be imaged due to the presence of the CIED system, for which there is no other available imaging alternative
To permit the implantation of an MRI conditional CIED system
Class III – Evidence and/or general agreement exists that the procedure is not useful or effective, and in some cases may be harmful. (NOT INDICATED)
Functional but redundant leads if the patient has a life expectancy of less than 1 year
Patients with known anomalous placement of leads through structures other than normal venous and cardiac structures (subclavian artery, aorta, pleura, atrial or ventricular wall, mediastinum, etc.) or through a systemic venous atrium or systemic ventricle (Additional techniques including surgical backup may be used if the clinical scenario is compelling)
Non-functional leads
Class I – Evidence and/or general agreement exists that the procedure is useful and effective
Life threatening arrhythmias secondary to retained leads or lead fragments
Leads that, due to their design or failure, may pose an immediate threat to the patient if left in place
Leads that interfere with the operation of implanted cardiac devices
Leads that interfere with the treatment of a malignancy (radiation/reconstructive surgery)
Class IIa – Weight of evidence/opinion is in favor of usefulness/efficacy of the procedure
Leads that due to their design or failure pose a threat to the patient, that is not immediate or imminent if left in place
If CIED implantation would require more than 4 leads on one side or more than 5 leads through the SVC
Patients who require specific imaging techniques (MRI) that cannot be imaged due to the presence of the CIED system, for which there is no other available imaging alternative
Class IIb – Usefulness/efficacy of the procedure is less well established by evidence/opinion
At the time of an indicated CIED procedure, if contraindications are absent, to permit the implantation of an MRI conditional CIED system
Class III – Evidence and/or general agreement exists that the procedure is not useful or effective, and in some cases may be harmful. (NOT INDICATED)
If the patient has a life expectancy of less than 1 year
Patients with known anomalous placement of leads through structures other than normal venous and cardiac structures (subclavian artery, aorta, pleura, atrial or ventricular wall, mediastinum, etc.) or through a systemic venous atrium or systemic ventricle (Additional techniques including surgical backup may be used if the clinical scenario is compelling)

Adapted from the 2009 HRS Expert Consensus Document on Transvenous Lead Extraction

CIED(s) cardiovascular implantable electronic device(s), *SVC* superior vena cava, *AV* arteriovenous, *RV* right ventricle, *ICD* implantable cardioverter defibrillator

challenging decision that exists in the field of lead extraction. As mentioned previously, pain at the implant site should increase suspicion for device infection [3]. If there are no signs/symptoms of infection, the decision of whether or not to extract a lead for chronic pain must involve a thorough discussion of the risks/benefits of the procedure with the patient. Furthermore, an extensive evaluation for other causes of pain should be undertaken prior to subjecting the patient to an invasive procedure.

The problems of venous stenosis and thrombosis will exist as long as CIEDs involve transvenous leads. The management and prevention of central venous stenosis is particularly important among patients with or at risk for end-stage renal disease. In these patients, central venous access is a requirement for dialysis, a life-prolonging therapy that cannot be delayed for any significant amount of time. The treatment of central venous stenosis involves multiple therapeutic options including venoplasty, stenting, and lead extraction when necessary. While lead extraction should not be a first-line therapy, it certainly has a role in the management of these patients. For instance, trapping a transvenous lead against the vein wall when stenting open a vein should be avoided whenever possible as it eliminates the option of future transvenous extraction if necessary.

While the use of transvenous leads will always mean a risk of central venous stenosis, similarly the use of transvenous leads will always result in a risk of lead malfunction. Lead technology and clinical experience with any particular lead is constantly advancing. Failure rates change over time, and attempting to predict them is an exercise fraught with folly. Any physician who intends to extract leads must stay up to

date on the failure rates and management strategies of leads that have proven troublesome (Sprint Fidelis, Riata, etc.).

As more patients are living with CIEDs, the number of patients with CIEDs who need radiation and/or surgical procedures in the area of the device or magnetic resonance imaging (MRI) is also increasing. Malignancy is a life-threatening condition and when the location of a CIED interferes with the treatment of a malignancy, the decision to extract the device in order to allow for proper treatment of the malignancy is a fairly simple one. The U.S. Food and Drug Administration has classified pacemaker systems as either MRI safe, MRI conditional, or MRI unsafe [26]. While the increased use of more MRI conditional devices will result in more patients with CIEDs having the option to undergo an MRI, for many patients, extraction will continue to be necessary.

Complications

Although uncommon, intra-procedure complications may occur [7]. Early recognition of the complication and appropriate management increases the chances of surviving a major adverse event. The immediate availability of an informed cardiothoracic surgeon and support personnel (cardiopulmonary bypass perfusionist, surgical team) facilitates the initiation of a rescue procedure.

The complications can be divided by their anatomic location as (a) extrapericardial or (b) intrapericardial (Fig. 18.4). Extrapericardial complications include subclavian vein, innominate vein, and high superior vena cava lacerations. Intrapericardial complications include lower superior vena

Potential Complications

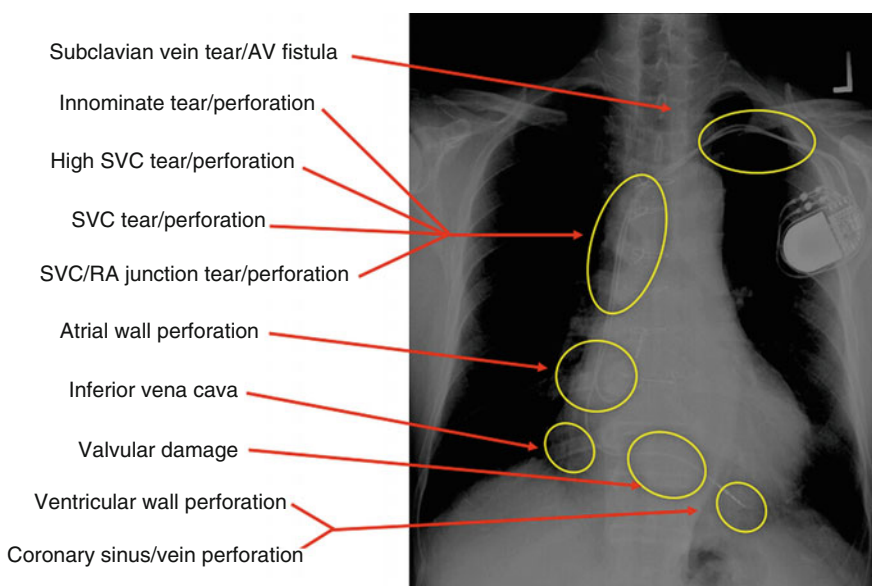


Fig. 18.4 Anatomic locations of potential complications of laser lead extraction. AV arteriovenous, RA right atrium, SVC superior vena cava

cava, right atrial wall, inferior vena cava, right ventricular wall, and coronary sinus perforations.

Signs of complications include tachycardia and hypotension. If the anesthetic ventilator has CO₂ monitoring, a decrease on exhaled CO₂ may herald hypoperfusion. The diagnosis of extrapericardial complications is made by a simple fluoroscopy of the pleural space. Any evidence of hemothorax will provide the diagnostic clue needed to assume a venous laceration. At times, opacification of the right or left chest may be due to atelectasis. A low endotracheal tube or endobronchial mucus plug may produce atelectasis. The absence of hypotension and tachycardia is associated with atelectasis. Intrapericardial injuries are evidenced by pericardial tamponade. During the procedure we can confirm the diagnosis by (a) Fluoroscopy of the heart border, or (b) echocardiogram. The fluoroscopic evidence of pericardial effusion is the lack of movement of the left ventricular border. TEE, TTE, or ICE can visualize a pericardial effusion and impending cardiac tamponade.

Extrapericardial injuries can be managed by median sternotomy. If the patient had a previous open-heart surgery, a high anterior thoracotomy could prove a faster alternative. Femoral-Femoral cardiopulmonary bypass may be needed to manage this complication. Digital compression of the injury followed by resuscitation of hypovolemic shock are surgical priorities. Patch repair of the superior vena cava laceration is at times necessary.

Intrapericardial injuries can be managed by a subxyphoid or median sternotomy. If the patient is hemodynamically unstable or if the surgeon is unfamiliar, avoid the subxyphoid approach. However, if the patient is hemodynamically stable, a subxyphoid approach could be attempted. Emergency percutaneous pericardiocentesis has a limited role in patients that are hemodynamically unstable. Atrial and ventricular wall tears can be repaired off bypass, while complex injuries to the lower superior vena cava may require the use of cardiopulmonary bypass.

Successful interventions of major adverse events require a team approach. When everyone works as a single unit during the development of a complication, good outcomes follow. A strong commitment is required from the facility to ensure the availability of equipment and personnel. Emergency drills allow the institution to develop the required level of teamwork [3].

Summary

Extraction for patients with an infection should be aggressively pursued, but the decision regarding whether or not to extract a lead in a patient without an infection can often be considerably more challenging. Every decision must be individualized to the patient and clinical situation. Furthermore, this decision must take into account the skill and experience of the extractor and the entire extraction team.

References

- Zhon C, Boine WB, Sedrokyan A, Steiner C. Cardiac device implantation in the United States from 1997 through 2004: a population-based analysis. *J Gen Intern Med.* 2008;23:13–9.
- Uslan DZ, Tleyjeh IM, Baddour LM, Friedman PA, Jenkins SM, St Sauver JL, et al. Temporal trends in permanent pacemaker implantation: a population-based study. *Am Heart J.* 2008;155(5):896–903.
- Wilkoff BL, Love CJ, Byrd CL, Bongioni MG, Carrillo RG, Crossley GH, et al. Transvenous lead extraction: heart rhythm society expert consensus on facilities, training, indications, and patient management. *Heart Rhythm.* 2009;6(7):1085–104.
- Tanawuttiwat T, Gallego D, Carrillo RG. Lead extraction experience with high frequency excimer laser. *Pacing Clin Electrophysiol.* 2014;37(9):1120–8.
- Rodriguez Y, Garisto J, Carrillo RG. Management of cardiac device-related infections: a review of protocol-driven care. *Int J Cardiol.* 2013;166(1):55–60.
- Lewis RK, Pokorney SD, Greenfield RA, Hranitzky PM, Hegland DD, Schroder JN, et al. Preprocedural ECG-gated computed tomography for prevention of complications during lead extraction. *Pacing Clin Electrophysiol.* 2014;37(10):1297–305.
- Wazni O, Epstein LM, Carrillo RG, Love C, Adler SW, Riggio DW, et al. Lead extraction in the contemporary setting: the LExIcon study: an observational retrospective study of consecutive laser lead extractions. *J Am Coll Cardiol.* 2010;55(6):579–86.
- Henrikson CA, Zhang K, Brinker JA. A survey of the practice of lead extraction in the United States. *Pacing Clin Electrophysiol.* 2010;33(6):721–6.
- Gaca JG, Lima B, Milano CA, Lin SS, Davis RD, Lowe JE, et al. Laser-assisted extraction of pacemaker and defibrillator leads: the role of the cardiac surgeon. *Ann Thorac Surg.* 2009;87(5):1446–51.
- Franceschi F, Dubuc M, Deharo JC, Mancini J, Page P, Thibault B, et al. Extraction of transvenous leads in the operating room versus electrophysiology laboratory: a comparative study. *Heart Rhythm.* 2011;8(7):1001–5.
- Epstein LM, Love CJ, Wilkoff BL, Chung MK, Hackler JW, Bongioni MG, et al. Superior vena cava defibrillator coils make transvenous lead extraction more challenging and riskier. *J Am Coll Cardiol.* 2013;61(9):987–9.
- Byrd CL, Wilkoff BL, Love CJ, Sellers TD, Reiser C. Clinical study of the laser sheath for lead extraction: the total experience in the United States. *Pacing Clin Electrophysiol.* 2002;25(5):804–8.
- Wilkoff BL, Byrd CL, Love CJ, Hayes DL, Sellers TD, Schaerf R, et al. Pacemaker lead extraction with the laser sheath: results of the pacing lead extraction with the excimer sheath (PLEXES) trial. *J Am Coll Cardiol.* 1999;33(6):1671–6.
- Franceschi F, Thuny F, Giorgi R, Sanaa I, Peyrouse E, Assouan X, et al. Incidence, risk factors, and outcome of traumatic tricuspid regurgitation after percutaneous ventricular lead removal. *J Am Coll Cardiol.* 2009;53(23):2168–74.
- Sanaa I, Thuny F, Giorgi R, Assouan X, Perrouse E, Franceschi F, et al. Incidence, predictive factors and long term follow-up of severe tricuspid regurgitation after percutaneous ventricular lead extraction. *Eur Heart J.* 2008;29:415.
- Rodriguez Y, Mesa J, Arguelles E, Carrillo RG. Tricuspid insufficiency after laser lead extraction. *Pacing Clin Electrophysiol.* 2013;36(8):939–44.
- Coffey JO, Sager SJ, Gangireddy S, Levine A, Viles-Gonzalez JF, Fischer A. The impact of transvenous lead extraction on tricuspid valve function. *Pacing Clin Electrophysiol.* 2014;37(1):19–24.
- Uslan DZ, Sohail MR, St Sauver JL, Friedman PA, Hayes DL, Stoner SM, et al. Permanent pacemaker and implantable

- cardioverter defibrillator infection – a population-based study. *Arch Intern Med.* 2007;167(7):669–75.
19. Wilkoff BL. How to treat and identify device infections. *Heart Rhythm.* 2007;4(11):1467–70.
 20. Chua JD, Wilkoff BL, Lee I, Juratli N, Longworth DL, Gordon SM. Diagnosis and management of infections involving implantable electrophysiologic cardiac devices. *Ann Intern Med.* 2000;133(8):604–8.
 21. Sohail MR, Uslan DZ, Khan AH, Friedman PA, Hayes DL, Wilson WR, et al. Management and outcome of permanent pacemaker and implantable cardioverter-defibrillator infections. *J Am Coll Cardiol.* 2007;49(18):1851–9.
 22. Chua JD, Abdul-Karim A, Mawhorter S, Procop GW, Tchou P, Niebauer M, et al. The role of swab and tissue culture in the diagnosis of implantable cardiac device infection. *Pacing Clin Electrophysiol.* 2005;28(12):1276–81.
 23. Chamis AL, Peterson GE, Cabell CH, Corey GR, Sorrentino RA, Greenfield RA, et al. *Staphylococcus aureus* bacteremia in patients with permanent pacemakers or implantable cardioverter-defibrillators. *Circulation.* 2001;104(9):1029–33.
 24. Klug D, Lacroix D, Savoye C, Goullard L, Grandmougin D, Hennequin JL, et al. Systemic infection related to endocarditis on pacemaker leads – clinical presentation and management. *Circulation.* 1997;95(8):2098–107.
 25. Grammes JA, Schulze CM, Al-Bataineh M, Yesenosky GA, Saari CS, Vrabel MJ, et al. Percutaneous pacemaker and implantable cardioverter-defibrillator lead extraction in 100 patients with intracardiac vegetations defined by transesophageal echocardiogram. *J Am Coll Cardiol.* 2010;55(9):886–94.
 26. Faris OP, Shein M. Food and drug administration perspective – magnetic resonance imaging of pacemaker and implantable cardioverter-defibrillator patients. *Circulation.* 2006;114(12):1232–3.
 27. Wazni O, et al. The LEXIcon Study: a multicenter observational retrospective study of consecutive laser lead extractions. *Heart Rhythm.* 2009;6(5 Suppl):Ab AB 39–5.

Application of Excimer Laser for Percutaneous Extraction of Pacemaker and Defibrillator Leads: Experience from the Hunter Holmes McGuire Veterans Administration Medical Center and the Virginia Commonwealth University

Karoly Kaszala, Alex Tan, Harsimran Saini, Yuhning L. Hu, Jennifer Winfield, Jayanthi Koneru, Richard K. Shepard, Kenneth A. Ellenbogen, and Jose F. Huizar

Introduction

Over the last decades, the clinical need for managing the consequences of chronically implanted intravascular cardiac pacemaker or defibrillator leads has grown exponentially. Lead failure and new indications for an upgraded device therapy often requires new lead implantation in a limited central venous “real estate”. In addition, device implantation in patients with increasing comorbidities resulted in higher infection rates and cure in these cases is unlikely without complete system removal. While removal with simple traction of recently implanted leads is often sufficient, once significant fibrosis takes place around the lead (usually after 6 -12 months), use of special extraction tools often becomes necessary as traction may cause complications or incomplete lead removal. Among the numerous older and newer advanced lead management modalities, the most extensive

clinical experience and supporting data from multicenter trials has come from the use of the excimer laser technology.

In this chapter, we discuss the main principles of lead extraction, including indications, perioperative management with particular focus on the laser lead removal technique and present outcome data from the Hunter Holmes McGuire VA Medical Center and the Virginia Commonwealth University.

Technological Consideration of Laser Technology for Lead Extraction

The CVX-300 excimer laser is based on a 308 nm wavelength xenon chloride cold cutting (approximately 50 °C) laser light. In the mammal tissue, the excimer laser energy is absorbed by lipids and proteins but not by water (in contrast to other forms of laser energy). This feature is particularly

K. Kaszala, MD, PhD (✉) • A. Tan, MD • J.F. Huizar, MD
Cardiac Electrophysiology Laboratory,
Hunter Holmes McGuire VA Medical Center
and Division of Cardiology, VCU Pauley Heart Center,
Medical College of Virginia and VCU School of Medicine,
1201 Broad Rock Blvd. Room 111(J3), Richmond,
VA 23249, USA
e-mail: Karoly.Kaszala@va.gov

H. Saini, MD • Y.L. Hu, MD • J. Koneru, MBBS
K.A. Ellenbogen, MD
Division of Cardiology, VCU Pauley Heart Center,
Medical College of Virginia and VCU School of Medicine,
1200E. Marshall Street, 3rd Floor, Electrophysiology Division,
Room 3-223, Richmond, VA 23219, USA

J. Winfield, BSN, RN
Cardiac Electrophysiology Laboratory, Hunter Holmes McGuire VA
Medical Center, 1201 Broad Rock Blvd. Room 111(J3),
Richmond, VA 23249, USA

R.K. Shepard, MD
VCU Pauley Heart Center, Medical College of Virginia
and VCU School of Medicine, 1200E. Marshall Street, 3rd Floor,
Electrophysiology Division, Room 3-223, Richmond,
VA 23219, USA

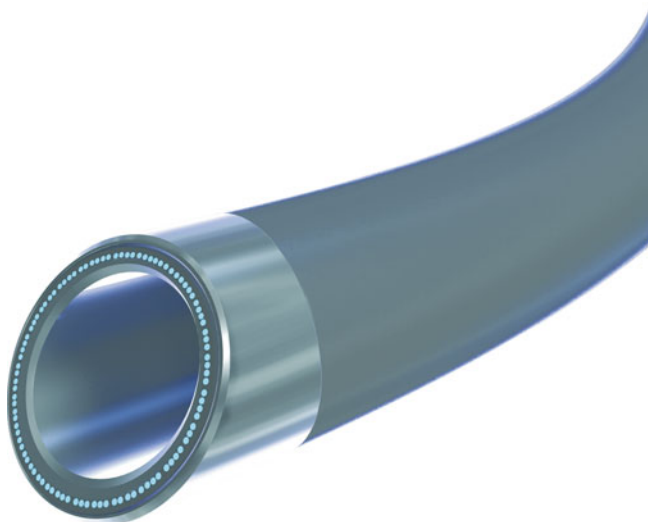


Fig. 19.1 Illustration of the Glidelight™ (Spectranetics, USA) laser sheath tip (Courtesy of Spectranetics)

advantageous to selectively disrupt fibrous tissue around the leads but without affecting the blood or nearby other leads. As the energy of the excimer laser is largely absorbed by 0.2 mm tissue depth, there is limited chance to affect even nearby vascular structures.

For the purpose of cardiac lead extraction, three sizes of laser sheaths are currently used (12, 14 and 16 Fr). Each sheath contains over 80 longitudinal fiberoptic cables (diameter 100 μm) that emit light at the tip of the sheath (Fig. 19.1). Based on the original clinical studies using the SLS II™ sheath, the laser console in current practice is programmed with fixed repetition rate of 40 Hz and fluence (output energy per unit area fiber) of 60 mJ/mm^2 . It has become clear that in certain clinical situations, more energy is required to achieve the desired clinical effects. More recently the Glidelight™ sheath has been introduced to clinical practice which allows a faster repetition rate (up to 80 Hz) and higher energy (may be titrated between 25 and 80 mJ/mm^2). The physical properties of these sheaths are the same, only the control chip is modified to allow changes in the above parameters. Published outcomes and clinical experience with the Glidelight™ sheath is limited at the current time but based on bench research data [1], the technology allows equal or better tissue dissection with less mechanical force application (55 % less force), potentially limiting the chance of a vascular tear [2].

Teflon or polypropylene based outer sheaths may be used over the laser sheath to provide support and also help if needed with counter pressure at the lead tip site (discussed below under “Technical details of laser lead extraction”). These sheaths have a beveled and flat end and more recent upgrades include a radiopaque marker for better visualization under fluoroscopy (Fig. 19.2). The beveled end of the

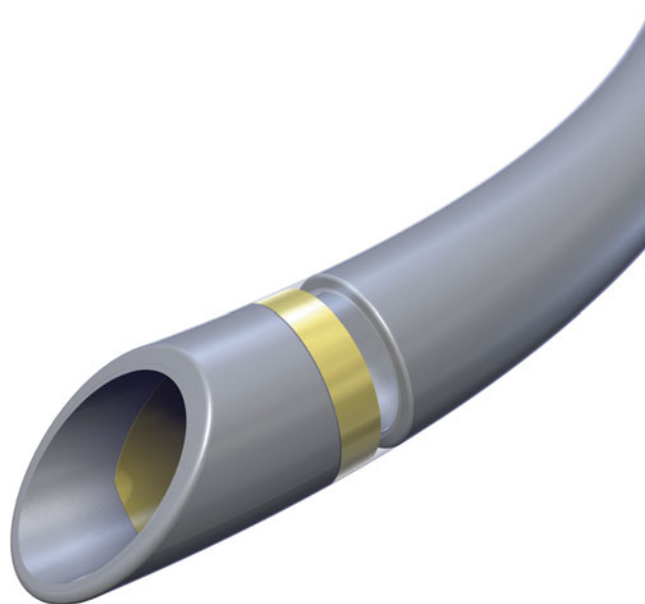


Fig. 19.2 Illustration of the Visi Sheath (Spectranetics, USA) (Courtesy of Spectranetics)

outer sheath should not be used near the myocardium due to risk of perforation. In our center, we exclusively use the flat end for dissection and support.

Indications for Lead Extraction

Current recommendations by the Heart Rhythm Society provide comprehensive and up-to-date guidance for lead management in common clinical situations (summarized in Table 19.1) and institutional standards to perform lead extraction safely [3]. Patient selection, as with any invasive treatment, is crucial to maximize safety and efficacy. The risks and benefits have to be estimated and considered for each individual patient. The risks calculation should take into consideration implant and patient characteristics, comorbidities, availability of a physician with adequate training and experience in lead extraction, as well as of an operating room with cardiopulmonary bypass capability and cardiac surgical backup. Benefit calculation should consider the life expectancy of the patient and consequences of not doing the procedure. Due to a high risk associated with this procedure, lead extractions should be performed when benefits outweigh potential risks or complications. The indication for lead extraction should be independent of the choice of the extraction tools. In optimal conditions, there are five major clinical categories to consider (detailed in Table 19.1): (a) CIED infection; (b) thrombosis or venous stenosis; (c) non-functional leads; (d) superfluous functional leads; and (e) chronic pain. In general, there is no absolute mandatory indication for lead extraction that applies regardless of the clinical situation.

Table 19.1 Indications for lead extraction

<u>Infection</u>		
<i>Class I</i> (Complete device and lead removal is recommended)	Definite CIED system infection, as evidenced by valvular endocarditis, lead endocarditis or sepsis.	<i>Level of evidence: B</i>
	CIED pocket infection as evidenced by pocket abscess, device erosion, skin adherence, or chronic draining sinus without clinically evident involvement of the transvenous portion of the lead system	<i>Level of evidence: B</i>
	Valvular endocarditis without definite involvement of the lead(s) and/or device	<i>Level of evidence: B</i>
<i>Class IIa</i> (Complete device and lead removal is reasonable)	Persistent occult gram-negative bacteremia	<i>Level of evidence: B</i>
<i>Class III</i> (Device and lead removal is not indicated)	Extraction is not indicated in superficial or incisional infection without involvement of the device and/or leads	<i>Level of evidence: C</i>
	Extraction is not indicated to treat chronic bacteremia due to a source other than the CIED, when long-term suppressive antibiotics are required	<i>Level of evidence: C</i>
<u>Thrombosis or venous stenosis</u>		
<i>Class I</i> (Lead removal is recommended)	Clinically significant thromboembolic events associated with thrombus on a lead or a lead fragment	<i>Level of evidence: C</i>
	Bilateral subclavian vein or SVC occlusion precluding implantation of a needed transvenous lead	<i>Level of evidence: C</i>
	Planned stent deployment in a vein already containing a transvenous lead, to avoid entrapment of the lead	<i>Level of evidence: C</i>
	Superior vena cava stenosis or occlusion with limiting symptoms	<i>Level of evidence: C</i>
	Ipsilateral venous occlusion preventing access to the venous circulation for required placement of an additional lead when there is a contraindication for using the contralateral side (e.g. contralateral AV fistula, shunt or vascular access port, mastectomy)	<i>Level of evidence: C</i>
<i>Class IIa</i> (Lead removal is reasonable)	Ipsilateral venous occlusion preventing access to the venous circulation for required placement of an additional lead, when there is no contraindication for using the contralateral side	<i>Level of evidence: C</i>
<u>Functional leads</u>		
<i>Class I</i> (Lead removal is recommended)	Life threatening arrhythmias secondary to retained leads	<i>Level of evidence: B</i>
	Leads that, due to their design or their failure, may pose an immediate threat to the patients if left in place. (e.g. Telectronics ACCUFIX J wire fracture with protrusion)	<i>Level of evidence: B</i>
	Leads that interfere with the operation of implanted cardiac devices	<i>Level of evidence: B</i>
	Leads that interfere with the treatment of a malignancy (radiation/reconstructive surgery)	<i>Level of evidence: C</i>
<i>Class IIb</i> (Lead removal maybe considered)	Abandoned functional lead that poses a risk of interference with the operation of the active CIED system	<i>Level of evidence: C</i>
	Leads that due to their design or their failure pose a potential future threat to the patient if left in place. (e.g. Telectronics ACCUFIX without protrusion)	<i>Level of evidence: C</i>
	Leads that are functional but not being used. (i.e. RV pacing lead after upgrade to ICD)	<i>Level of evidence: C</i>
	Patients who require specific imaging techniques (e.g. MRI) that cannot be imaged due to the presence of the CIED system for which there is no other available imaging alternative for the diagnosis	<i>Level of evidence: C</i>
	Patients in order to permit the implantation of an MRI conditional CIED system	<i>Level of evidence: C</i>
<i>Class III</i> (Lead removal is not indicated)	Patients with functional but redundant leads if patients have a life expectancy of less than 1 year	<i>Level of evidence: C</i>
	Patients with known anomalous placement of leads through structures other than normal venous and cardiac structures, (e.g. subclavian artery, aorta, pleura, atrial or ventricular wall or mediastinum) or through a systemic venous atrium or systemic ventricle. Additional techniques including surgical backup may be used if the clinical scenario is compelling	<i>Level of evidence: C</i>

(continued)

Table 19.1 (continued)

<u>Non-functional leads</u>		
<i>Class I</i> (Lead removal is recommended)	Patients with life threatening arrhythmias secondary to retained leads or lead fragments	<i>Level of evidence: B</i>
	Leads that, due to their design or their failure, may pose an immediate threat to the patients if left in place. (e.g. Telectronics ACCUFIX J wire fracture with protrusion)	<i>Level of evidence: B</i>
	Leads that interfere with the operation of implanted cardiac devices	<i>Level of evidence: B</i>
	Leads that interfere with the treatment of a malignancy (radiation/reconstructive surgery)	<i>Level of evidence: C</i>
<i>Class IIa</i> (Lead removal is reasonable)	Leads that due to their design or their failure pose a threat to the patient, that is not immediate or imminent if left in place. (e.g. Telectronics ACCUFIX without protrusion)	<i>Level of evidence: C</i>
	If a CIED implantation would require more than 4 leads on one side or more than 5 leads through the SVC	<i>Level of evidence: C</i>
	Require specific imaging techniques (e.g. MRI) and cannot be imaged due to the presence of the CIED system for which there is no other available imaging alternative for the diagnosis	<i>Level of evidence: C</i>
<i>Class IIb</i> (Lead removal maybe considered)	At the time of an indicated CIED procedure, in patients with non-functional leads, if contraindications are absent	<i>Level of evidence: C</i>
	To permit the implantation of an MRI conditional CIED system	<i>Level of evidence: C</i>
<i>Class III</i> (Lead removal is not indicated)	Non-functional leads if patients have a life expectancy of less than 1 year	<i>Level of evidence: C</i>
	Known anomalous placement of leads through structures other than normal venous and cardiac structures, (e.g. subclavian artery, aorta, pleura, atrial or ventricular wall or mediastinum) or through a systemic venous atrium or systemic ventricle. Additional techniques including surgical backup may be used if the clinical scenario is compelling	<i>Level of evidence: C</i>
<u>Chronic pain</u>		
<i>Class IIa</i> (Device or lead removal is reasonable)	Severe chronic pain, at the device or lead insertion site with significant discomfort unable to be managed by medical or surgical techniques and for which there is no acceptable alternative	<i>Level of evidence: C</i>

Note: Level of Evidence

A: Data derived from multiple randomized clinical trials or meta-analyses

B: Data derived from a single randomized trial, or non-randomized studies

C: Consensus opinion of experts, case studies, or standard of care

Level of Evidence B or C should not be construed as implying that the recommendation is weak

An infection of the CIED is the most compelling indication for complete system extraction. There is a wide range of disease spectrum from chronic device pocket pain to severe pocket erythema, erosion and sepsis and endocarditis. Experience is required to make appropriate management decision in each individual case.

Indication of lead extraction in a non-infected system is less clear and may be controversial (Table 19.1). It is in these cases that all clinical circumstances have to be taken into consideration prior to recommending lead extraction. As a general guide for the management of superfluous leads in asymptomatic patients, 4 or less leads in a single vein or 5 or less leads in the superior vena cava are considered acceptable. Clinical circumstances should be also considered, such as the age of the patient, projected longevity, ease or difficulty of lead explantation. For example if lead extraction is recommended for a failed atrial lead in a biventricular system, it should be considered that the left ventricular lead may also suffer damage during the explant and if coronary sinus branches are limited, a new percutaneous lead implant may not be feasible.

Clinical Experience with Lead Extraction

As the number of cardiac implantable defibrillator (ICD) and permanent pacemaker (PPM) implants and life expectancy have increased over the years, the number of ICD and PPM system malfunction and infections requiring extraction has also risen. An estimated 10,000–15,000 PPM and ICD leads are extracted annually worldwide [4]. New indications for ICD therapy have led to an increasing number of ICDs placed, and cardiac resynchronization therapy (CRT) requiring more leads per patient have contributed to increased need for lead extractions. Infection rates have also increased as the number and complexity of devices increased [5]. Additionally, lead recalls and malfunctions have added to the increasing number of lead extractions [6]. With the advent and safety of laser-assisted transvenous lead extraction (TLE), the trend worldwide has been toward utilizing the available and developing technology for transvenous lead removal and increased operator volumes, leading to improved operator experience, safety profile and procedural and patient outcomes [5, 7]. In Europe,

Table 19.2 Comparison of US and European Data on practice patterns and outcomes [6–8, 10, 11]

		US [6, 7, 10, 11]	Europe [8]
Institutional volume/year		<10 procedures/year: 15	50 leads/year: 84
		10–25 procedures/year: 42	50–100 leads/year: 11.5
		26–50 procedures/year: 23	>100 leads/year: 4.5
		>50 procedures/year: 19	
Onsite and available CTS backup (%)		75	60
OR or hybrid OR (%)		36	25
Cardiologist/EP primary op (%)		83	88
Indication (% infection)		27 (1996–1999)	70 (data from 2001 to 2011)
Leads (%)	Pacing	60	73
	ICD	39	24
	Other	1	2
Equipment (%)	Laser sheath	NA	26–28
	Locking stylet	NA	88
Major complication (%)		1–5 (perceived); 1.9 (real)	1–5
Mortality (%)		0.5–1 (perceived); 0.8 (real)	0.5–1
Procedural success (radiological)	Complete (%)	93	88
	Partial (%)	5	7
	Failed (%)	2	5

very few surveyed centers (5 %) performed or attempted TLE before 1988; whereas from 2000 to 2011 TLE was performed in 60 % of centers [8, 9]. In the US, the use of laser cautery in 1994–1999 was 6 %, [6] and is expected to be much higher now (summarized in Table 19.2) [5, 10].

Worldwide Practice Patterns of Transvenous Lead Extractions

It is instructive to first understand the worldwide practice patterns of transvenous lead extraction as practice is critically tied to outcomes. Table 19.2 provides a snapshot of worldwide practice, based on European and United States (US) single center experience, multicenter registries and surveys of physician practices over the past 15 years [6–8, 11]. There is broad similarity in European and US practices. First, cardiologists and electrophysiologists form the majority (over 80 %) of operators with cardiac surgeons making up the balance. However, only between 60 and 75 % of lead extraction procedures are performed in the presence of immediately available and onsite cardiac surgical backup. Procedural volumes also vary significantly. Although most centers (>80 %) perform at least ten procedures/year or 50 leads/year, only 4.5 % of European centers perform >100 lead extractions per year. A minority (25–36 %) of procedures are performed in an operating room or hybrid laboratory and the rest in the cardiac catheterization or EP laboratory. In terms of equipment used, most procedures (88 %) in Europe are performed with at least a locking stylet, and a quarter of the laboratories use a laser cautery sheath [8]. Overall, European procedures are more frequently

performed without available surgical backup and within the cardiac catheterization or EP laboratory rather than in the OR [8, 10]. Beyond US and Europe, practice patterns have not been systematically evaluated.

Outcomes of Transvenous Lead Extractions

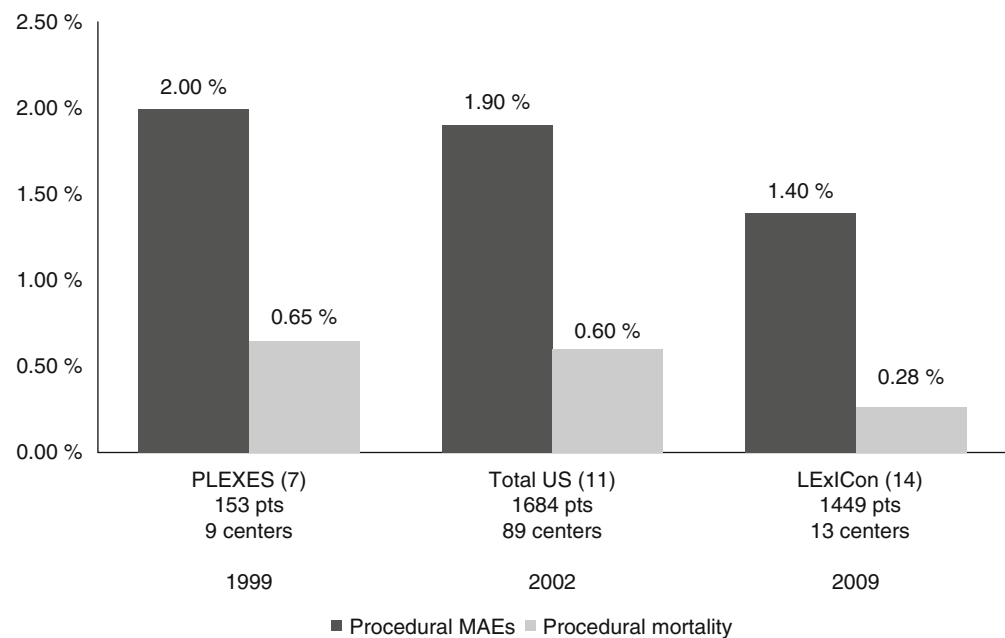
Despite differences in European versus US practices related to availability of surgical back-up, outcomes are generally similar, with complete procedural success in 90 %, partial success in 5 %, overall mortality of 0.5–1 % and major complication rates of 1–5 % [4–8, 11]. The Heart Rhythm Society defines partial or complete procedural success radiologically. Partial success is defined retained lead insulation or lead segment >4 cm. Clinical success is the achievement of the desired clinical outcome [3, 12]. For example, leaving a small portion of the lead within the heart in the case of device pocket infection is considered an incomplete procedural success however; complete resolution of infection means having achieved the desired clinical outcome [3, 12]. Notwithstanding the differences in reporting owing to variable definitions of procedural versus clinical success, or partial versus complete procedural success, lead extractions can be performed safely, although not without complications [4, 5, 7, 11]. Table 19.3 lists potential major and minor complications of lead extraction [3].

Over the past 30 years, improvements in extraction techniques and technology, and surgical preparedness have resulted in a gradual decline in major adverse events and mortality (Fig. 19.3). Major complication rates are less than 2 %, and in-hospital mortality is less than 1 % in experienced centers [13, 14]. A Multivariate analysis of US registry data

Table 19.3 Potential major and minor complications of lead extraction [3, 11]

Major complications	Minor complications
Death	Pericardial effusion not requiring intervention
Cardiac avulsion requiring intervention (percutaneous or surgical)	Hemothorax not requiring intervention
Vascular injury requiring intervention (percutaneous or surgical)	Pocket hematoma requiring reoperation
Pulmonary embolism requiring surgical intervention	Upper extremity thrombosis resulting in medical treatment
Respiratory arrest/anesthesia-related complication prolonging hospitalization	Vascular repair near implant site or venous entry site
Stroke	Hemodynamically significant air embolism
CIED infection at previously noninfected site	Migrated lead fragment without sequelae
	Blood transfusion as a result of intraoperative blood loss
	Pneumothorax requiring a chest tube
	Pulmonary embolism not requiring surgical intervention

Fig. 19.3 Procedural outcome of laser-assisted lead extraction demonstrating major adverse events (MAEs) and procedural mortality. *PLEXES* Pacemaker lead extraction with the laser sheath: results of the pacing lead extraction with the excimer sheath (Adapted from Birgersdotter-Green and Pretorius [24])



from 1994 to 1999 demonstrated four predictors of major complications using the definitions described in the North American Society for Pacing and Electrophysiology (NASPE) recommendations document. The major complication rate was 1.6 % [12]. Predictors of major complications are implant duration of oldest lead, female gender, presence of ICD lead, non-use of laser extraction technique and lower procedural volume [12]. Additionally, renal failure, and low body mass index are also independent predictors of major complications in a retrospective observational study [5]. In the only US randomized trial of laser versus non-laser TLEs performed to date for PPM leads, [7] complete lead removal rate was 94 % in the laser group and 64 % in the non-laser group ($p=0.001$). Failed non-laser extraction was completed with the laser tools 88 % of the time. From a procedural suc-

cess standpoint, infected leads are extracted as successfully as leads with functional defects, however, complications from infection (Table 19.3) can arise.

Another major determinant of outcome is the experience of the operator and volume at the extraction center. Byrd et al. [6] included retrospective data from 226 centers, 2338 patients and 3540 leads, and reported major complications in 1.4 % (<1 % for centers with >300 extraction procedures). Risk of incomplete or failed extraction decreased when procedural experience is greater than or equal to 20 prior procedures. After 20 procedures, subsequent decline in complication rate reaches a plateau [6] (Fig. 19.4). The overall complication rates will continue to decline as experience with laser lead extraction increases (Fig. 19.4) [7] and adherence to guidelines improves [3].

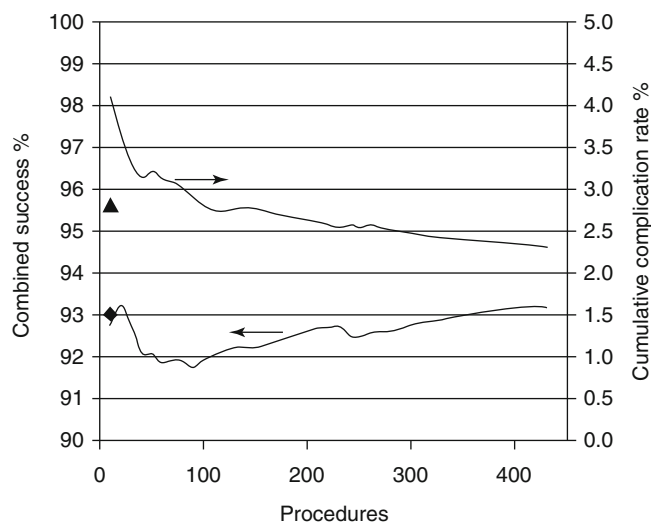


Fig. 19.4 The figure illustrates the difference in combined success rate and complication rate related to operator experience. There is rapid decline in complications following the first 20 cases with continued slow improvement up to 400 cases (graph on *top*). Similarly, success rate gradually increases with additional experience (*bottom* graph) [11]

Single center study showed that experienced device implanters may achieve adequate results following a short intensive course on lead extraction [15]. From a systems prospective, the ability to promptly initiate an emergent surgical procedure with an experienced cardiothoracic surgeon cannot be overemphasized.

More contemporary lead extraction data (for leads implanted >1 year) was also reported from analysis of the National Cardiovascular Data Registry for a 2-year period (from 2010 to 2012) [16]. In a “real-world” experience in 11,304 patients from 762 centers, the peri-procedural major complication rate for ICD and pacemaker leads was 2.3 % and 2 %, respectively. Urgent surgery was required in 0.3 %. Intraoperative and in-hospital mortality was 0.16 % and 0.9 %, respectively. The mortality of patients who needed emergency cardiothoracic surgery was 34 %. Multivariate analysis identified female gender, infection, ≥ 3 leads extracted, lead dislodgement during prior procedure, heart failure, older age as patient related predictors for major complications. Specific adverse characteristics to ICD leads included smaller lead diameter, flat coil design and greater proximal surface coil area. While the data has only been published in abstract form at the current time and clinical data was not complete, it is reassuring to see that safety and efficacy of lead extraction in a very broad patient and institutional population was similar to prior studies from large volume institutions [6, 7, 11, 12, 17].

Prophylactic Lead Extractions: An Emerging Paradigm?

Several studies [9, 14] have reported outcomes with prophylactic extraction of leads that are on manufacturer’s advisory during generator change in young patients who are expected to have a long lead indwelling time. A recent report [14] modeled the risk-benefit ratio in such a prophylactic extraction strategy during generator change, in various hypothetical clinical and patient permutations, and found that the benefits outweigh the risks in young patients with fewer comorbidities and long indwelling times. Although this practice remains controversial, as experience with laser extraction technology improves and centers and operator volumes increase, the shift will likely to occur towards a more aggressive approach in carefully selected patients.

Outcomes of Percutaneous Lead Extraction; Data from Hunter Holmes McGuire VAMC and Virginia Commonwealth University

In the following section, we review the combined lead extraction data from the Virginia Commonwealth University and the Hunter Holmes McGuire VAMC, Richmond, Virginia, USA. The data was gathered from the locally collected lead extraction database, reviewed for a 5-year period between 2009 and 2014. Lead extraction was defined as removal of a chronic lead implanted >12 months or need for use of advanced tools (i.e. locking stylet, sheath). During the review period 123 patients were identified. Patient characteristics are summarized in Table 19.4. All procedures were performed in the operating room with cardiopulmonary bypass service and cardiothoracic surgeon on stand-by. General anesthesia was used in >95 % of the cases. Laser sheath was used in 72 % of the cases and in combination with other modalities (femoral work station, snare etc) in another 6 %. In 18 %, non-laser based advanced tools were used. Simple traction with lead locking device was successfully used as a primary technique in 4 %. The indication for extraction was infection in 62 %, lead integrity failure in 34 % and “prophylactic” extraction of a recalled lead in 4 %. Extraction was successful in 98 %, partially successful in 2 % (lead fragment >4 cm remained in the body). Major complications related to lead extraction occurred in one case in a critically ill patient with sepsis. Dissection of the coronary sinus during laser ablation of an active fixation coronary sinus lead required open heart surgery for repair. The patient subsequently expired due to disseminated intravascular coagulation. The overall in-hospital mortality was 2.4 %, all deaths

Table 19.4 Basic patient characteristics of patients

Number of patients	123
Age (years)	61 ± 15
Male Gender (%)	75
Diabetes mellitus type II (%)	31
NYHA Class	1.8 ± 0.7
Pacemaker dependency (%)	44
Coronary artery disease (%)	56
Prior sternotomy (%)	28
Ejection fraction (%)	40 ± 15
Age of oldest lead at explant (months)	84 ± 65 (range 6–300 months)
Average number of leads per patient	2 ± 0.9
Patients with defibrillation lead (%)	63 %
Total number of leads removed	244

Data from retrospective data analysis from the Virginia Commonwealth University and the Hunter Holmes McGuire VAMC

resulted from sepsis. The median hospital stay was 8 days (mean 12 ± 14 days; range: 2–91 days).

Data from our centers mimic the experience of other high volume institutions. Lead extraction may be performed with relatively low risk if trained personnel are available and an institutional environment and safety safeguards are adequately maintained. Despite of a relative procedural safety, device infection identifies a patient cohort with higher morbidity and mortality.

Technical Details of Laser Lead Extraction

Preoperative Patient Preparation

Careful preoperative patient management for any invasive procedure is important. While lead extraction in a low-risk profile patient is not a high risk intervention per se, if complications occur those tend to be severe. Outcomes are further compromised by frequent serious comorbidities and reduced physiologic reserve. Optimal management of complications would involve a multidisciplinary approach and well-organized team work. A full assessment and detailed planning would help to mitigate potential problems during and after the procedure and help to respond to unexpected events. In this section, rather than reviewing all possible clinical scenarios, we will provide a general overview and highlight common, important clinical decision points.

The first step of the preoperative evaluation is to identify any treatable underlying medical problems before the surgery (Table 19.5). The first decision point is to determine the urgency of the operation. At the extremes of examples, a patient with acute bacterial endocarditis and septic embolization from a pacemaker lead vegetation would require an urgent, lifesaving intervention and pre-operative work should focus on treatment of quickly reversible major abnormalities (i.e. optimize fluid status, heart rate control

etc). On the other hand, a non-pacemaker dependent patient who requires a system revision and needs lead extraction to allow access to the central venous system should have all or most non-urgent medical problems optimized (such as blood sugar control, blood pressure control etc) in order to minimize perioperative risks. Several aspects of pre-operative patient preparation may be standardized and use of pre-specified check lists should be encouraged to help minimize risk of oversight (Table 19.6). In the scheduling and early preoperative phase, arrangements need to be made for availability of industry support if needed (for example Spectranetics or pacemaker/ICD device company) and tools be available. In terms of location of the procedure, this is a center-specific decision with careful consideration for resources (operating room vs. cardiac catheterization laboratory). In general, a setting should be chosen that allows adequate fluoroscopic visualization during the case but also a very quick access to an urgent open heart intervention. In our opinion, despite some debate, the ideal location for this procedure is in a hybrid operating room with high quality fluoroscopy and immediate availability of a heart-lung perfusion system.

In our center, we perform all high risk lead extractions (lead implant >12 months) in the operating room with cardiothoracic surgery backup. The patients undergo preoperative screening visit by the electrophysiology and the anesthesia team. Routinely performed preoperative blood tests and imaging studies are summarized in Table 19.6. Individualized decision is made regarding the need for general anesthesia or conscious sedation. Patient is advised to maintain NPO status for 8 h and all oral anticoagulants and antiplatelet agents (except aspirin) are stopped for at least 5 days with individualized bridging strategy. It is important to assess the pacemaker or ICD lead position with chest X-ray, echocardiography and electrocardiogram (is there inadvertent left atrial or left ventricular lead position?), identify the lead fixation mechanism and course of the leads as well as

Table 19.5 General principles of preoperative patient preparation

Task	Specific focus
Preoperative history 13 point system assessment	Cardiovascular history (MI, stroke, VT, AF)
	Cardiac, vascular or thoracic surgeries
	Other major surgeries
	Anesthesia history
	Device implant history
	Indication for device therapy
	Ongoing infection
	Diabetes care
	Dialysis needs
Preoperative physical exam	Blood pressure control
	Fluid status
	Heart failure status
	Device site
	Nutritional status
	NPO status
Medications	Watch with predominant renal clearance
	Watch with narrow therapeutic margin
	Antidiabetics (stop or modify dose)
	Anticoagulant (stop)
	Antiplatelet (stop if feasible except ASA)
	Steroid use (risk of perforation)
Social history	Illicit drug use (consider screening)
	Smoking (increased complications)
	Postoperative care (especially for long term antibiotics or wound care if needed)
Laboratory evaluation and imaging	Basic chemistry
	Liver and renal panel
	Coagulation panel
	Electrocardiogram (paced/non-paced if possible)
	Chest X-ray (AP/lateral)
	Echocardiogram (Chest CT)

Table 19.6 Lead extraction specific preoperative considerations

Task	Specific focus
Determine indication for extraction	Urgency, adequacy of indication
Device history	Device type
	Implant date
Specific lead history	Company
	Model
	Type (active/passive fixation)
	Serial number(s)
	Lead diameter
	Prior lead interventions (any cut leads)
Indication of device therapy and intervention	Need for reimplantation during the case
	Consider other access sites, alternative techniques

the number of leads and possible calcifications around the leads. Prior operative reports should be available to identify any difficulties during the implant and specific details of the implanted hardware, including lead manufacturer and lead model. In some centers, chest CT is performed to evaluate for possible lead perforation or extravascular course of the lead [18].

Intraoperative Technical Details

In the preoperative area, all critical aspects of the case are reviewed in collaboration with the anesthesia team. We confirm the availability of all team members, including CT surgeon on stand-by, equipment (laser console, fluoroscopy, transesophageal echocardiogram) and an unchanged clinical

status of the patient. We have four units of packed red blood cells available in the room at the start of the case. We utilize a special portable locker for all necessary extraction and emergency tools (i.e. special wires, sheaths, extraction kits, snares, pericardiocentesis tray) and the list of tools is evaluated weekly to assure adequate reserve.

Patients undergo prepping from the neck to the mid thighs and drapes are placed to allow access to the groins, subxyphoid region and also to the thorax in case of a need for thoracotomy. Hemodynamic parameters are monitored with an arterial line (brachial or femoral), end tidal CO₂ monitor and EKG. Two large bore venous sheaths are placed in the right femoral vein. Temporary pacer is only inserted for pacemaker dependent patients but access and equipment for pacing is readily available. The second access is used to advance an exchange length stiff wire (0.035 mm Wholey; Covidien, Plymouth, MN) to the left or right subclavian vein to assist with access for balloon insertion and venous tamponade in case of a vascular tear.

Preparation of Equipment

In designing the site and length of skin incision, consideration should be given to permit access to all lead segments in the pocket but also to allow alignment of laser sheath with the lead entry site and the initial subclavian segment of the lead. Some centers perform two incisions to achieve these goals. After the pocket is opened, the leads are freed from the fibrous tissue and suture sleeves removed. Once the leads are disconnected, a soft stylet is introduced to clear the lead lumen. Excessive lead manipulation should be avoided especially when older leads (>5 years old) are involved. Following an attempt to retract the lead screw (in active fixation leads), gentle traction may be applied under fluoroscopy guidance to assess adhesion and adherence to the vascular structures. If gentle traction fails to move the lead, a few rounds of clockwise and counterclockwise rotations may be used to free adhesions. If the lead is older or a lead fracture is suspected, we prefer to introduce a lead locking device early and before any lead manipulation to minimize the risk of losing access to the inner coil channel. Before the lock-in device is introduced, the lead should be cut close to the lead pin or the yolk (ICD leads) with sharp scissors and lead insulation carefully peeled off with a blade. Once the pace-sense coil is exposed, the lead locking tool is advanced all the way to the lead tip under fluoroscopy and manually deployed. Failure to advance the locking device to the tip is associated with unsuccessful extraction. We predominantly use the Lead Locking Device (LLD™) or LLD EZ™ (Spectranetics, Colorado Springs, CO, Fig. 19.5). Each individual components of the lead, including defibrillator coils and lead body, is secured with 0 silk ties. Alternatively, a Bulldog Extender (Cook Medical, Bloomington Indiana, USA) may be used to lock the defibrillator coils. The laser sheath is then calibrated, flushed and the

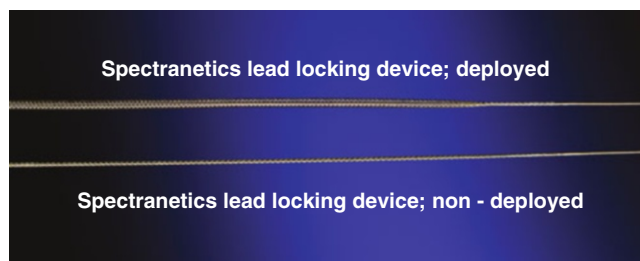


Fig. 19.5 Illustration of Spectranetics lead locking device (Courtesy of Spectranetics)

prepared lead apparatus is fed back through the laser sheath. We always load an outer sheath. We cut the outer sheath by 5–8 cm at the angled end but the cut part would not enter the body. We find it helpful to support the laser sheath with the outer sheath at the subclavian vein and on occasion in the innominate vein and the shortened sheath allows a better control of the laser sheath at the vein entry site. If support is needed in a more proximal section, the outer sheath may need to be changed out to a longer, uncut one. The outer sheath may also serve as a vehicle to maintain vascular access after successful lead extraction. We invariably choose the smallest laser sheath that would accommodate the lead. A helpful guide for sizing of the sheath is available at the Spectranetics website (<http://www.spectranetics.com/physicians/lead-management/lead-lookup/>; accessed January 22, 2015).

Technical Details of Extraction

The basic technical principle of the laser lead extraction technique is that the lead is used as a rail for support as the laser sheath apparatus is advanced while lasing. This is accomplished by steady pull (“countertraction”) while the laser is gradually advanced or pushed (“counterpressure”). If there is an imbalance between these forces, there is a risk of injury to the venous structures or disintegration of lead components (i.e. laser sheath is pushed more forcefully or leads pulled excessively). There is significant variability in the force of countertraction and counterpressure between experienced operators but invariably, the balance between the two forces should be always maintained. With experience, tactile feedback during the extraction process will also help to readjust the applied forces so that the lead integrity is maintained as much as possible. It is important to remember that the goal of this technique is to use laser energy to vaporize the adhesion sites and minimize the need for mechanical separation of the leads using forceful movement of the sheaths as the latter is more likely to cause venous tear. In general, gradual progression of the laser sheath is preferred to maintain control of the movement in the vasculature. Newer generation laser sheaths (GlideLight™) with higher pulse frequency and increased energy has been shown to allow improved efficacy with less use of mechanical force. The increased power may

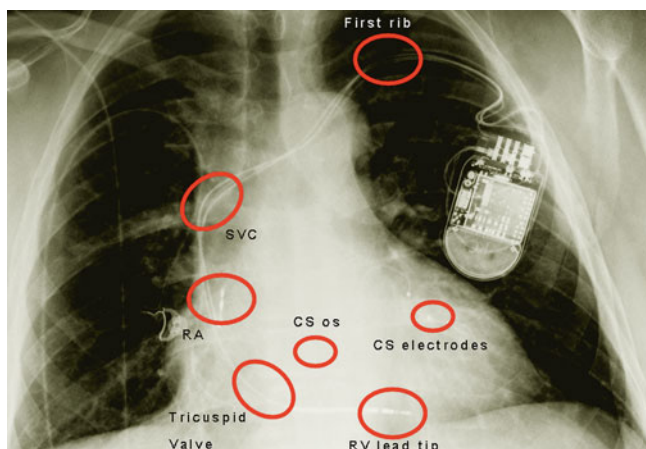


Fig. 19.6 Illustration of intravascular and intracardiac sites that are commonly associated with increased lead adhesions. CS coronary sinus, RA right atrium, RV right ventricle, SVC superior vena cava

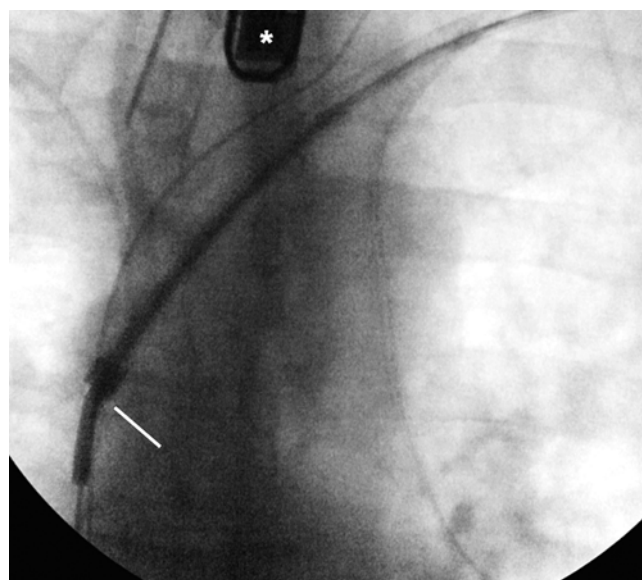


Fig. 19.8 Fluoroscopy image of the laser sheath at the superior vena cava. Lead dissection at the innominate vein-SVC-RA junction is the most dangerous area for a venous tear. This case is further complicated by the presence of a non-back-filled superior vena cava lead coil (dual coil ICD lead). In the current technological era of effective intracardiac defibrillation, dual coil lead implant should be rarely required. Note the bevel orientation of the laser sheath (approximated by the *white line*). Adequate traction on the lead allows a completely coaxial orientation of the sheath during lasing. This area was safely cleared with a 16 Fr sheath. Transesophageal echocardiogram probe is also seen (*). It is withdrawn to the superior esophagus to allow optimal fluoroscopic visualization of the leads

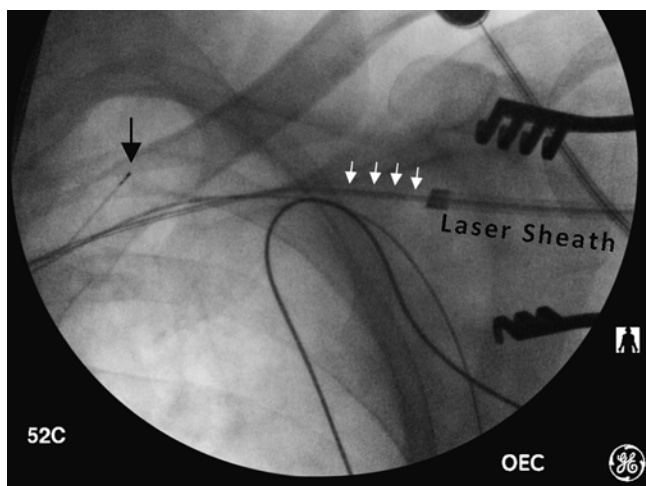


Fig. 19.7 Fluoroscopy image of the laser sheath as it enters the central venous circulation. Note a completely parallel orientation with the lead (marked with *white arrows*). The bevel points up and away from the minor curvature of the course of the lead. A *black arrow* points to the tip of the Wholey wire, inserted via the femoral vein

potentially be associated with higher risks. There are several general vascular areas that are associated with difficulty and increased complications (illustrated in Fig. 19.6). At the lead entry site, calcification may be encountered and external compression from skeletal structures at the first rib/clavicle region may cause further challenge in advancing the apparatus. In addition, the change in course of the lead, as in other parts of the vascular system warrants increased vigilance. As the laser sheath is aligned, a parallel course with the lead has to be assured (Fig. 19.7). The bevel of the laser tip needs to be directed in such a way that the distal part is kept in line with the inner curvature of the course of the lead (Figs. 19.7 and 19.8) so as the sheath is advanced, the distal, sharp part of the sheath remains closest to the lead

and minimize risk of “shaving off” the venous wall further away from the lead. Maintaining proper sheath orientation is important throughout the procedure but especially at the subclavian vein and the junction of the innominate vein and superior vena cava. This latter region is a common site for lead adhesion and also for risk to venous tears. As the laser sheath is advanced further, adhesions may be seen at the tricuspid annulus and the right ventricle. Lasing in this region is commonly associated with development of extrasystoles or ventricular tachycardia. These usually subside with cessation of lasing. On occasion, the whole distal length of the lead is fibrosed to the surrounding cardiac tissue and lasing is required all along the course. Once the sheath reaches approximately 1 cm from the lead tip, further lasing should not be done as the risk of perforation is increased. It is recommended to advance the outer sheath at this time all the way to the myocardium. Counter-pressure should be applied via the outer sheath to prevent invagination of the right ventricular myocardium as the lead is pulled back with gentle traction. Similar approach is used for the right atrial lead. While percutaneously implanted left ventricular leads tend to pull out easily in most instances, special precautions should be applied in select cases and this will be discussed in the section “Special situations”.

Special Situations

Fineline Lead Extraction

Discussion of the structural composition of each lead type is beyond the scope of this chapter, but one particular commonly used lead deserves a special mention due to unusual lead design. The Fineline lead family from Boston Scientific (formerly Guidant; Marlborough, MA) has been used with great long term results since 2000. The lead has a co-radial design, which means that the insulated cathode and anode coil wound together in parallel around the stylet tube (Fig. 19.9). The weakest link of the Fineline lead is the anode ring bond. If there is significant traction proximal to the anode ring, the coil may break off and also the coils may stretch. As the LLD stylet locks along the whole lead length, uncoiling is more frequent with its use. We therefore prefer to use the Cook Liberator stylet (Cook Medical, Bloomington Indiana, USA) which locks only at the most distal lead point. We also recommend keeping the lead pin intact as cutting the lead makes the coils more likely to unwind. In order to pass a 12 Fr laser sheath over the lead apparatus, the sealing ring has to be carefully shaved off the pin. During extraction, counter-traction should be applied carefully during advancement of the laser to preserve lead integrity.

Coronary Sinus Lead Extraction

Cardiac resynchronization therapy commonly requires placement of pacing leads in the coronary sinus system. Most leads are designed in such a way that the pace-sense coil is open at the tip and accommodates a 0.014 mm angioplasty wire. If a lock-in stylet or any other wire is introduced via the lumen, close fluoroscopy-based monitoring is

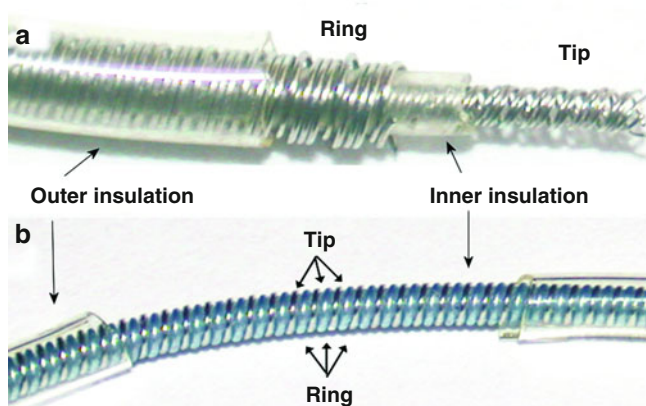


Fig. 19.9 Illustration of the difference in lead design between coaxial and co-radial pacemaker leads. *Panel A:* coaxial lead. The tip electrode is wrapped with insulation and the ring electrode is coiled around it. The ring electrode is covered by the outer insulation. *Panel B:* coradial lead design. Ring and tip electrode is individually covered with insulation and coiled down along the lead parallel to each other. The final layer is formed by the outer insulation

important in order to avoid perforation as the wire exits the distal tip. Common adhesion sites for coronary sinus leads are similar to other leads (first rib area, innominate vein/SVC junction). Adhesions in the coronary veins are rare (10 %) and mostly seen at the electrode sites. These leads are often explanted with gentle manual traction only. While currently an off-label application, small series have confirmed the safety of laser application in the cardiac venous system in case manual traction fails but a venous tear commonly requires open heart surgery. Special consideration should be given if an active fixation coronary lead is present in the coronary sinus. The only FDA approved, Attain Starfix model 4195 lead (Medtronic, Minnesota, MN) is designed with deployable lobes to maximize stability in the vein. While the lobes are retractable by design, long term follow-up data has shown that the lobes would not withdraw in the majority of the cases after implantation. Successful removal of these leads frequently requires laser application within the coronary veins with significantly increased risk of complications. If difficulties encountered during laser application, cardiothoracic, open-chest approach should be considered.

Extraction of Leads on Advisory

While lead failure may occur with any lead, over the history of device therapy, changes in lead design had resulted in products with higher than average failure rate. A historic example is the Teletronics Accufix J shaped pacing lead. This lead was placed on recall in 1994 because patient injuries and deaths occurred as a result of fracture of a retention J wire with subsequent cardiac or vascular laceration [19]. While prophylactic lead extraction was feasible, due to a low overall spontaneous event rates the risk/benefit ratio favored conservative management for most patients [19]. More contemporary lead problems were related to ICD lead failures. The Sprint Fidelis leads (Medtronic, Minneapolis, MN) have been shown to have an increased risk of lead failure mainly due to pace-sense or high voltage conductor fracture. Lead failures resulted in loss of pacing or inappropriate ICD shocks. As these leads are designed with back-filled defibrillation coils, tissue in-growth in the critical portion of the leads is markedly reduced and lead extractions have been safely performed and without an increased risk. The other recent lead advisory is related to the Riata lead family by St. Jude Medical. These leads are at risk to develop insulation failure. There is a 20–40 % chance to develop an inside-out erosion and externalization of the high voltage cables [20, 21]. As these cables have an additional ethylene tetrafluorethylene (ETFE) coating, visual integrity failure does not mean an electrical abnormality. In addition, shorting of high voltage cables to defibrillation coil or ICD can has been shown with arcing and resultant ineffective defibrillation. Particular challenges may occur with these leads during the extraction due to increased bulk

of the lead and possible thrombus formation at the site of an externalization [22]. Pre-operative imaging studies, such as CT or echocardiography should be encouraged. There are several points to consider during extraction. During preparation of the leads, it is recommended to make adjustment to the high voltage coil extrusion by pulling back individually on these components. This maneuver will minimize the lead bulk and often allows proceeding through the externalized area without upsizing of the sheath. “Snowplowing” effect is commonly encountered despite the best efforts and upsizing of the laser sheath is commonly required. Another challenge with the Riata™ leads is the lack of coil backfill and increase tissue ingrowth in these areas. Despite these challenges, in experienced hands the safety and efficacy of lead extraction with the advisory leads are comparable to other leads [23].

The Difficult Lead Extraction

Even the most experienced extractor will on occasion run into difficult cases. As with all complex procedures, the difficulties may be alleviated by appropriate preparation, thinking several steps ahead and expecting the next possible challenge in the case. Several factors have been identified as predictors of a more difficult or riskier extraction (Table 19.7). By the virtue of the laser extraction procedure, access to the proximal lead is obligatory in order to advance the laser. Thus if leads are cut back too short or maybe pulled back into the venous circulation during a previous procedure, alternative methods would be needed for extraction. A chest X-ray would help to clarify this. If there is lead fracture and locking stylet cannot be advanced all the way to the lead tip, chance of failed extraction increases. In these cases counter-traction has to be limited in order avoid further lead integrity disruption. If despite the best efforts the lead breaks, the remaining lead fragment would be explanted via another vascular access using a snare (via the femoral or jugular vein).

Table 19.7 Predictors of difficult extraction or complications

Multiple leads
ICD lead
Presence of SVC coil
Lead implantation >5 years
Multiple leads
Prior extraction attempt
Tined lead fixation mechanism
Active fixation coronary sinus lead
Non-isodiametric lead design (step-ups along the course of the lead)
Non-back filled ICD coils
Female gender
BMI <25
Operator experience

The most common difficulty is failure of advancing the laser sheath. The main reasons are vascular calcification, inter-lead adhesions and lead interactions and “snowplowing” of the insulation, vascular/fibrous tissue or other lead components (see “Extraction of leads on advisory” section). An example is shown in Fig. 19.10. Known vascular calcification is contraindication for laser extraction but it is very difficult to ascertain except in extreme cases. If the calcification occurs at the first rib/clavicular section, other mechanical tools may be used to dilate and cross the area. More commonly, failure to advance occurs in the innominate vein and SVC region. In our experience, this is mainly due to snowplowing. On occasion advancing the outer sheath may help to equalize or “re-distribute” the build-up but commonly upsizing of the sheath is required for continued progress. Once the largest sheath is used, the options are very limited in case another tissue build-up develops; in those cases either mechanical dissection with the outer sheath or use of different technology (such as snare from a different access) may be required. Fibrous ingrowth affecting multiple leads is commonly seen and poses a significant challenge.

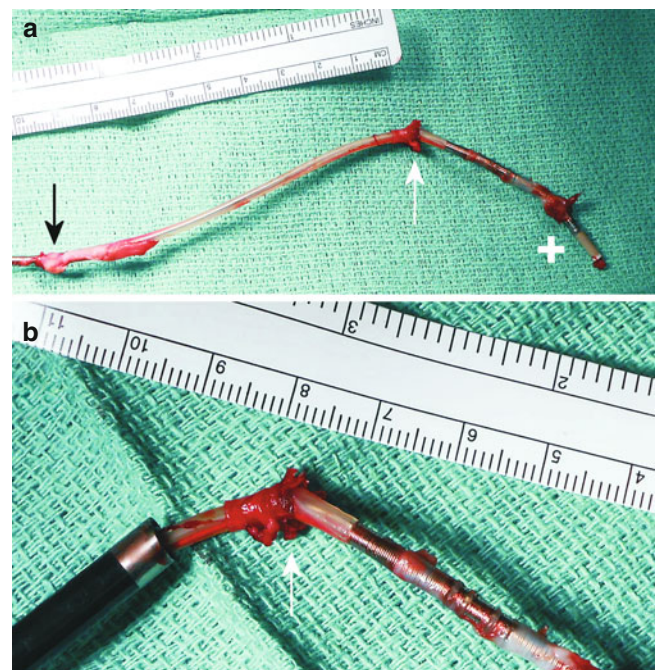


Fig. 19.10 Difficult lead extraction due to snowplowing effect. The figure illustrates an explanted right ventricular ICD lead. *Panel A* shows three areas of significant fibrosis at the distal lead area. At the *black arrow* site, the 14 Fr laser sheath did not progress and it was upsized to a 16 Fr sheath. The 16 Fr sheath easily cleared this area but could not be advanced beyond the *white arrow* area due to a second incident of snowplowing. There was also a severe bend in the lead, partially due to extensive manipulations. The area at the *white arrow* and the distal coil/ring electrode region (marked with a *cross*) was cleared with manual traction. The lead was withdrawn in its entirety and without any complications. *Panel B* shows the laser sheath and lead as they were pulled out from the patient. *White arrow* marks the same area as in *Panel A*

In case there is more than one lead present, we routinely prepare each lead with a locking stylet and maintain traction on all leads. We routinely start the explant with the “easiest” lead, the one with the highest chance for extraction (most recently implanted lead first; coronary sinus lead – >atrial lead – >ventricular lead). If progress is unsatisfactory with the first lead, it is worthwhile to switch to another lead to free up adhesions or “debulk” using a different route.

A special situation is when the lead tip is released from the myocardium but the mid segment of the lead remains locked due to adhesions. In these cases, especially if the Cook stylet is used, there is no good way to provide traction on the lead. This may be mitigated by snaring and holding the freed-up lead tip via a femoral access and thereby allowing adequate traction on the lead to advance the laser sheath.

Management of Complications

Multiple factors influence the outcomes following a complication. The type and degree of injury and the physiologic reserve of the patient are primary determinants but these factors cannot be modified beyond a certain degree. Another, modifiable component is related to a system response. This includes presence of adequate, well-trained staff, adequate monitoring, availability of emergency imaging and ancillary services and timely recognition of the abnormality with rapid intervention if needed. All emergency equipment and supportive measures need to be present as detailed in the “[Preoperative patient preparation](#)”

section. As most serious complications result in sudden hemodynamic catastrophe, all team members have to know their role so the appropriate treatment steps may be followed at the most efficient fashion. Periodic mock simulations may help to build a strong team cohesion and more effective response in case of an emergency. Management options for common and serious complications are summarized in [Table 19.8](#).

Postoperative Care

After successful lead extraction, the device pocket is managed according to the presenting abnormality. Acute pocket infection is best managed by debridement and packing of the site to allow healing with secondary intention. Once drainage is improved, a negative pressure device may be used to enhance healing (wound V.A.C.TM therapy). Alternatively, a Penrose or Jackson-Pratt drain may be inserted and the pocket loosely closed. If infection is not present, the pocket is closed in a standard fashion. Before extubation, a transesophageal echocardiogram is repeated to assess cardiac and gross valvular function and evidence of pericardial effusion. All central lines are removed before transfer to the postoperative observation unit and subsequently to the step-down unit or intensive care unit with vigilance for possible subacute complications. We delay treatment with oral anticoagulants or antiplatelet therapy for 24 h unless a high risk condition exists in which case a bridging strategy may be individualized.

Table 19.8 Management of common complications of lead extraction

Complication	Treatment
Pocket bleeding/hematoma	Careful attention to hemostasis
	Diffuse oozing: consider packing of the pocket
Deep venous thrombosis following extraction	Oral anticoagulation for 3–6 months
A-V fistula formation	Emergency vascular surgery intervention
Pneumothorax	Consider chest tube if moderate to large
Hemothorax	Emergency CT surgery intervention
Air embolization	Attempt to aspirate or “break up” with catheter if loculated
	Hemodynamic support
Pulmonary embolism	Embolectomy
Venous tear	Emergency CT surgery intervention
	Consider temporizing with large intravascular ballon
Cardiac perforation	Pericardiocentesis (often does not “seal” spontaneously)
	Emergency CT surgery evaluation
Stroke (embolization via PFO/ASD; arterial implant)	Supportive measures
	Determine intracardiac shunt, lead entry before extraction
Tricuspid valve rupture	Manage heart failure symptoms
Cardiac avulsion	Emergency CT surgery intervention
Respiratory complications (anesthesia, intubation)	Supportive care
Arrhythmia	Treat reversible causes
	Consider retained lead fragment

Conclusions

The clinical need for implantable cardiac lead management is expected to increase as the number of implanted devices grows in a population with greater risk of infection and limited venous access. As experience with transvenous laser lead extraction continued to accumulate with increased procedural volume and operator experience, the safety and efficacy of extractions have improved over the past 30 years. A greater adherence to the 2009 Heart Rhythm consensus statement which recommends a systematic, multidisciplinary approach to an extraction procedure with available personnel and facilities for emergent backup surgery, it is expected that outcomes will continue to improve as surgical variability declines. Yet, because major complications with the current technology will not be entirely eliminated, a detailed assessment of individual risk-benefit ratio and appropriate preparations to deal with complications emergently are paramount in order to maximize safety and optimize clinical outcomes.

References

- Coe MS, Taylor KD, Lippincott RA, Sorokoumov O, Papaioannou T, editors. Proceedings of SPIE 4244, Lasers in surgery: advanced characterization, therapeutics, and systems 2001;XI:454. doi:10.1117/12.427834; <http://dx.doi.org/10.1117/12.427834>.
- Summary of P960042/s031 Glide Light 80Hz laser sheath (12, 14 or 16Fr), spectranetics. Department of Health and Human Services; 2012. Accessed: 25 Feb 2015. Available from: http://www.access-data.fda.gov/cdrh_docs/pdf/p960042s031m.pdf.
- Wilkoff BL, Love CJ, Byrd CL, Bongiorno MG, Carrillo RG, Crossley 3rd GH, et al. Transvenous lead extraction: Heart Rhythm Society expert consensus on facilities, training, indications, and patient management: this document was endorsed by the American Heart Association (AHA). *Heart Rhythm*. 2009;6(7):1085–104.
- Hauser RG, Katsiyannis WT, Gornick CC, Almquist AK, Kallinen LM. Deaths and cardiovascular injuries due to device-assisted implantable cardioverter-defibrillator and pacemaker lead extraction. *Europace*. 2010;12(3):395–401.
- Greenspon AJ, Patel JD, Lau E, Ochoa JA, Frisch DR, Ho RT, et al. 16-year trends in the infection burden for pacemakers and implantable cardioverter-defibrillators in the United States 1993 to 2008. *J Am Coll Cardiol*. 2011;58(10):1001–6.
- Byrd CL, Wilkoff BL, Love CJ, Sellers TD, Turk KT, Reeves R, et al. Intravascular extraction of problematic or infected permanent pacemaker leads: 1994–1996. U.S. Extraction Database, MED Institute. *Pacing Clin Electrophysiol*. 1999;22(9):1348–57.
- Wilkoff BL, Byrd CL, Love CJ, Hayes DL, Sellers TD, Schaerf R, et al. Pacemaker lead extraction with the laser sheath: results of the pacing lead extraction with the excimer sheath (PLEXES) trial I. *J Am Coll Cardiol*. 1999;33(6):1671–6.
- Bongiorno MG, Blomström-Lundqvist C, Kennergren C, Dagnes N, Pison L, Svendsen JH, et al. Current practice in transvenous lead extraction: a European Heart Rhythm Association EP Network Survey. *Europace*. 2012;14(6):783–6.
- Van Erven L, Morgan JM. Attitude towards redundant leads and the practice of lead extractions: a European survey. *Europace*. 2010;12(2):275–6.
- Henrikson CA, Zhang K, Brinker JA. A survey of the practice of lead extraction in the United States. *Pacing Clin Electrophysiol*. 2010;33(6):721–6.
- Byrd CL, Wilkoff BL, Love CJ, Sellers TD, Reiser C. Clinical study of the laser sheath for lead extraction: the total experience in the United States. *Pacing Clin Electrophysiol*. 2002; 25(5):804–8.
- Wilkoff BL, Byrd CL, Love CJ, Sellers TD, Van Zandt HJ. Trends in intravascular lead extraction: analysis of data from 5339 procedures in 10 years (XIth World Symposium on Cardiac Pacing and Electrophysiology: Berlin). *Pacing Clin Electrophysiol*. 1999;22(6 (pt. II)):A207.
- Di Monaco A, Pelargonio G, Narducci ML, Manzoli L, Boccia S, Flacco ME, et al. Safety of transvenous lead extraction according to centre volume: a systematic review and meta-analysis. *Europace*. 2014;16(10):1496–507.
- Mendenhall GS, Saba S. Prophylactic lead extraction at implantable cardioverter-defibrillator generator change. *Circ Arrhythm Electrophysiol*. 2014;7(2):330–6.
- Ghosh N, Yee R, Klein GJ, Quantz M, Novick RJ, Skanes AC, et al. Laser lead extraction: is there a learning curve? *Pacing Clin Electrophysiol*. 2005;28(3):180–4.
- Sood N, Martin D, Clancy J, Curtis J, Parzynski CS, Lampert R. Incidence and predictors of peri-procedure complications with transvenous lead extractions in the real world: data from NCDR ICD registry. *Circulation*. 2014;130 Suppl 2:A19603.
- Kennergren C, Schaerf RH, Sellers TD, Wilkoff BL, Byrd CL, Tyres GF, et al. Cardiac lead extraction with a novel locking stylet. *J Interv Card Electrophysiol*. 2000;4(4):591–3.
- Vlay SC. Concerns about the Riata ST (St. Jude Medical) ICD lead. *Pacing Clin Electrophysiol*. 2008;31(1):1–2. [Comment Editorial].
- Kay GN, Brinker JA, Kawanishi DT, Love CJ, Lloyd MA, Reeves RC, et al. Risks of spontaneous injury and extraction of an active fixation pacemaker lead: report of the Accufix Multicenter Clinical Study and worldwide registry. *Circulation*. 1999;100(23):2344–52.
- Theuns DA, Elvan A, de Voogt W, de Cock CC, van Erven L, Meine M. Prevalence and presentation of externalized conductors and electrical abnormalities in Riata defibrillator leads after fluoroscopic screening: report from the Netherlands Heart Rhythm Association Device Advisory Committee. *Circ Arrhythm Electrophysiol*. 2012;5(6):1059–63.
- Parvathaneni SV, Ellis CR, Rottman JN. High prevalence of insulation failure with externalized cables in St. Jude Medical Riata family ICD leads: fluoroscopic grading scale and correlation to extracted leads. *Heart Rhythm*. 2012;9(8):1218–24.
- Goyal SK, Ellis CR, Rottman JN, Whalen SP. Lead thrombi associated with externalized cables on Riata ICD leads: a case series. *J Cardiovasc Electrophysiol*. 2013;24(9):1047–50.
- Bongiorno MG, Di Cori A, Segreti L, Zucchelli G, Viani S, Paperini L, et al. Transvenous extraction profile of Riata leads: procedural outcomes and technical complexity of mechanical removal. *Heart Rhythm*. 2015;12(3):580–7.
- Birgersdotter-Green UM, Pretorius VG. Lead extractions: indications, procedural aspects, and outcomes. *Cardiol Clin*. 2014;32(2):201–10. [Review].

Transmyocardial Laser Revascularization: Physiology, Pathology, and Basic Research Concepts

20

Anthony J. Minisi, Deepak D. Banerjee,
and Laxmi B. Mohanty

Significant improvements in the outcome of cardiac surgery and percutaneous coronary intervention (PCI) have led to enhanced survival among patients with severe coronary artery disease. However, it has also created a population of patients never before encountered in the field of Cardiovascular Medicine. These patients, who often have had coronary bypass surgery and/or PCI multiple times, are characterized by far advanced, end-stage coronary artery disease and disabling anginal symptoms which are refractory to medical therapy with maximal doses of antianginal drugs such as nitrates, beta blockers, calcium channel blockers, and ranolazine.

The treatment of patients with end-stage coronary artery disease and refractory, disabling anginal symptoms represents a complicated and increasingly prevalent problem for clinicians. One recent report estimated that over 100,000 patients each year may be diagnosed with this condition [1]. Due to the failure of saphenous vein coronary bypass grafts, the progression of atherosclerotic disease, and/or the development of restenosis, severe symptoms have recurred and further traditional revascularization measures are not feasible.

It has become clear that new therapeutic modalities are required to treat this group of patients. One of these modalities is transmyocardial laser revascularization (TMLR). TMLR is a procedure in which laser light is used to create channels through the left ventricular myocardium. This can be done surgically via a thoracotomy (open chest procedure), in which case transmural channels are made from the epicardium to the endocardium. The procedure can also be done percutaneously, in which case non-transmural channels are created from the endocardial surface. This technique has been shown to improve symptomatic status in patients with end-stage coronary artery disease who cannot receive further traditional surgical or percutaneous revascularization.

To date, surgical TMLR has been studied in a large number of patients with end-stage coronary disease and severe angina [2–9]. The results of these studies have been fairly consistent and have shown that TMLR improves subjective anginal symptoms compared to continued medical therapy. These results suggest that TMLR may be a promising therapeutic modality for this group of patients. However, evidence of improvement in objective parameters such as myocardial perfusion has not been demonstrated consistently. Most troubling, the mechanism whereby TMLR results in improved anginal symptoms is not completely understood.

A.J. Minisi, MD, FACC (✉)
Division of Cardiology, McGuire VA Medical Center and Medical
College of Virginia, Campus of Virginia Commonwealth
University, Richmond, VA, USA
e-mail: anthony.minisi@va.gov

D.D. Banerjee, MD, FSCAI
Division of Cardiology, McGuire VA Medical Center and Medical
College of Virginia, Campus of Virginia Commonwealth
University, Richmond, VA, USA

Interventional Cardiology, Memorial Hospital of Martinsville
and Henry Counties, Martinsville, VA, USA

L.B. Mohanty, MD
Division of Cardiology, McGuire VA Medical Center and Medical
College of Virginia, Campus of Virginia Commonwealth
University, Richmond, VA, USA

Department of Pathology and Laboratory Medicine,
McGuire VA Medical Center, Richmond, VA, USA

Clinical Experience with TMLR

Surgical TMLR has been widely applied to the treatment of patients with end-stage coronary artery disease and refractory anginal symptoms. TMLR has been used both in conjunction with coronary bypass surgery and as sole therapy in patients who are not candidates for further revascularization procedures. A multicenter registry of patients undergoing TMLR showed significant improvement in anginal class at 3, 6, and 12 months compared to baseline symptoms before treatment [2]. The number of annual admissions for angina was reduced in the year after TMLR compared to the year before treatment. There was also a decrease in the number of

nuclear perfusion defects observed in the treated regions of the left ventricle.

There have been six randomized trials comparing surgical TMLR to maximal medical therapy in over 1000 patients with end-stage coronary disease and refractory angina [3–5, 7–9]. All of these studies showed significantly improved anginal symptoms in the groups randomized to TMLR, whether this was expressed as mean angina class [8] or percentage of patients with a decrease of ≥ 2 anginal classes during follow-up [3–5, 7, 9]. Patients treated with TMLR also had greater freedom from cardiac-related rehospitalization, increased exercise tolerance, decreased use of cardioactive medications, and higher quality of life scores. One of the studies showed improved perfusion by nuclear imaging in the TMLR group compared to the medical therapy group [5]. However, four other studies did not demonstrate any significant differences in myocardial perfusion imaging [3, 4, 8, 9].

Operative mortality ranged from 1 to 5%. These favorable results reflect the strict enrollment criteria for these studies as well as refinement in the procedural techniques. Based on previous clinical observations of high operative mortality in patients with high risk features such as active, unstable angina and/or impaired left ventricular ejection fraction (<25–30%), these patients were excluded from the randomized trials. Of note, none of the randomized trials showed significant differences in survival between the treatment groups at 1 year. In addition, the two largest randomized trials allowed crossover of patients during the follow-up period with 32% and 59% of patients crossing over from medical therapy to TMLR [4, 5]. Nevertheless, based on the results of these studies, the Food and Drug Administration has approved both a CO₂ laser and a holmium:YAG laser for use in TMLR. An additional randomized trial showed improvement of angina symptoms following TMLR with an xenon chloride laser compared to maximal medical therapy but this study was limited by a very small number of participants [10].

Two of the randomized trials have reported long-term results at 3–5 years. Both studies showed sustained angina relief in those randomized to TMLR compared to maximal medical therapy at a mean follow-up of 43 months [11] and 5 years [12] (Table 20.1). In the cohort studied by Aaberge et al., there appeared to be attenuation of the symptomatic

benefit during long term follow up. Allen et al. actually reported a higher percentage of patients in both the TMLR and maximal medical therapy groups who had a decrease of ≥ 2 anginal classes at 5 year follow up. These results most likely represent differences in study methodology. Aaberge et al. had no crossover between treatment groups during long term follow up while the cohort studied by Allen et al. were allowed to cross over from maximal medical therapy to TMLR and to have additional revascularization procedures during long term follow up. In addition, only 77% of the original randomized cohort had data available for analysis in the study by Allen et al.

These two randomized trials also reported long term survival data. Aaberge et al. found no significant differences in survival between the randomized groups at a mean follow up of 43 months. Survival was 78% in those randomized to TMLR and 76% in those randomized to maximal medical therapy ($p=NS$). In contrast, using an intention to treat analysis, Allen et al. did find a survival benefit for those randomized to TMLR compared to maximal medical therapy (65% vs. 52%; $p=0.05$). When crossovers were analyzed as a separate group, survival remained higher in the TMLR group but this difference was no longer statistically significant.

Long term follow up has also been reported for a registry study [13]. At a mean follow up period of 5 years, there were 78 of the original cohort of 195 patients who remained alive and had not had any additional revascularization procedures. In this select group of 78 patients, TMLR appeared to have a durable effect in improving anginal symptoms. At baseline, all of the patients had CCS class III or IV angina. At 1 year, 77% of these patients had ≥ 2 angina class decrease in symptoms. At the 5 year follow up, a decrease of ≥ 2 anginal classes was observed in 68% of these patients.

In contrast, other nonrandomized reports indicate that recurrent angina is more prevalent following TMLR [14, 15]. In a cohort of 34 patients who underwent TMLR for refractory angina, anginal status at 3 years remained improved compared to baseline but had deteriorated slightly compared to 1 year follow up [14]. At 12 years, only 9 of the original 34 patients remained alive and the majority of survivors had a return of their anginal symptoms. The 12 year actuarial freedom from major adverse cardiac events was only $13 \pm 8\%$ [15].

Table 20.1 Percentage of patients with decrease of ≥ 2 angina classes at 12 months and 3–5 years

Author	% improved at 12 months		% improved at 3–5 years	
	TMLR	MMT	TMLR	MMT
Allen et al. [12]	76	32	88	44
Aaberge et al. [11]	39	0	24	3

TMLR transmyocardial laser revascularization, MMT maximal medical therapy

Mechanisms of Action of TMLR

The mechanism by which TMLR results in improvement in anginal symptoms has been the subject of intense research efforts. Despite the abundant evidence of subjective improvement outlined above, the mechanism for this beneficial effect is not clear. There remains controversy as to how and why

this technique seems to work. Several theories have been proposed and studied:

1. Direct myocardial perfusion via patent lased channels.

The initial rationale for TMLR was based on the concept of the reptilian heart. There are no coronary arteries in the hearts of reptiles. Rather, oxygenated blood perfuses the myocardium through a system of sinusoids that communicate directly with the left ventricular cavity. Early pathologic studies suggested that the human heart might also contain a system of sinusoids [16]. Thus, direct myocardial perfusion was initially felt to be the mechanism of action for TMLR. The creation of intramyocardial channels by the laser would allow oxygenated blood from the left ventricular cavity to enter the sinusoidal system and perfuse the heart. Although this concept of direct myocardial perfusion was initially appealing, subsequent observations have raised serious doubt about this potential mechanism. Recent studies have disputed the existence of a network of sinusoids in the human heart [17]. In addition, several experimental and clinical studies have demonstrated that the long-term patency rate of these lased, intramyocardial channels is very low [18–21].

2. Angiogenesis.

Several experimental studies have shown anatomical and molecular evidence of neovascularization in the region of the lased channels [22–28]. Microscopic analysis of lased myocardium reveals an inflammatory process evident within weeks. This inflammation promotes angiogenesis and increased expression of various angiogenic growth factors such as vascular endothelial growth factor, matrix metalloproteinases, and platelet-derived endothelial growth factor [22, 27, 28]. Neovascularization is present throughout the lased myocardium but it predominates along the periphery between the TMLR channel remnants and the surrounding muscle [25], with extension into the adjacent muscle [24]. These neovessels have a highly disorganized pattern suggestive of angiogenesis. Immunohistochemical staining has confirmed the presence of endothelial cells within these neovessels [24, 25]. TMLR also appears to significantly enhance the normal compensatory development of collateral channels in the lased myocardium. These vascular structures have been shown to augment perfusion to the laser treated area of the left ventricular myocardium during pharmacologic stress induced by vasodilators [27]. This latter observation is particularly pertinent because it suggests that enhanced perfusion through these microchannels could improve regional myocardial blood flow and ameliorate symptoms of angina.

Finally, autopsy and case reports in patients have also documented histologic evidence of angiogenesis in the

regions surrounding lased channels [20, 21, 29]. This was described as “a developing network of capillaries” in the early study of Krabatsch et al. [20]. Of note, the case report of a patient whose heart was harvested at the time of transplant 9 months after TMLR showed evidence of red blood cells within the lumen of the neovessels [29].

3. Placebo effect.

Some have contended that the long term improvement in anginal symptoms noted after TMLR mitigates against a placebo effect. However, given the dire circumstances of the typical patient who would be a candidate for TMLR, a significant placebo effect associated with any operative procedure cannot be overlooked. In this regard, there has never been a blinded, placebo-controlled study of surgical TMLR. Percutaneous TMLR does afford the opportunity to perform blinded, placebo-controlled trials and one such study failed to demonstrate significant differences in anginal status or exercise times between patients receiving active treatment and those with sham treatment [30]. It is unclear whether these observations can be extrapolated to surgical TMLR since there are major differences between surgical and percutaneous TMLR.

4. Cardiac deafferentation (denervation).

In considering that the beneficial effect of TMLR may be related to cardiac deafferentation, one must consider the neural basis for the perception of anginal pain. The left ventricle is a sensory organ that is innervated by receptors with both sympathetic and vagal afferent fibers. The sensation of anginal pain is most likely multifactorial in origin. However, a neural component for the perception of anginal pain is strongly suggested by the observation that cardiac transplant patients in whom neural structures to the ventricles are severed often do not experience anginal symptoms despite the presence of advanced transplant atherosclerosis [31]. Further observations from experimental studies suggest that left ventricular receptors with sympathetic afferent fibers are the cardiac nociceptors [32, 33]. Unlike the vagal afferents that are preferentially distributed to the inferoposterior wall, the sympathetic afferents are uniformly distributed throughout the left ventricle [34]. These receptors are polymodal in nature and can be activated by both mechanical and chemical stimuli [35–37]. Activation of these receptors results in reflex excitatory responses such as hypertension, tachycardia, and vasoconstriction [38–40]. These reflex excitatory responses are mediated by both increases in efferent sympathetic outflow and decreases in efferent parasympathetic outflow from the central nervous system.

The perception of anginal pain is felt to be mediated by activation of left ventricular sympathetic afferents by

myocardial ischemia. During coronary occlusion, left ventricular receptors with sympathetic afferent fibers can be activated mechanically by increases in cardiac pressures and chemically by release of noxious substances from the ischemic myocardium [33, 36, 37, 41]. This activation has been demonstrated by direct recordings from sympathetic afferent nerve fibers [42, 43]. However, afferent input from sympathetic afferent fibers may be heavily modulated by inhibitory supraspinal mechanisms [44, 45]. Therefore, measurement of an efferent response such as sympathetic outflow is necessary to confirm that these afferent impulses have been successfully transmitted to the higher centers of the central nervous system. This transmission of afferent input to the higher neural centers is a requirement for nociception.

Pathologic studies have shown that the application of laser energy to the myocardium results in destruction of all cardiac structures within the lased channel [46]. Thus, it is reasonable to speculate that TMLR improves anginal symptoms by deafferentation of the left ventricle. Interruption of cardiac sympathetic afferents following TMLR may eliminate afferent input during myocardial ischemia and prevent nociception.

Several studies in humans and experimental animals have provided anatomical evidence that TMLR damages cardiac neural structures. Kwong and colleagues studied dogs 2 weeks following TMLR and demonstrated reduced concentration of tyrosine hydroxylase in the treated myocardium [47]. This enzyme is involved in the synthesis of norepinephrine from tyrosine and is felt to be a specific marker for efferent sympathetic nerve terminals [48]. Similar findings were reported by Hughes et al. [49]. They studied pigs 3 days after TMLR and found that tyrosine hydroxylase concentrations were reduced in the lased segments of the heart compared to nonlased regions of the treated hearts as well as untreated, control hearts. This group also studied animals 6 months after TMLR in a model of chronic myocardial ischemia. At 6 months, there were no differences in tyrosine hydroxylase concentrations between laser treated areas and control hearts. On the basis of these observations, the investigators postulated that reinnervation had occurred and suggested that the long term benefit of TMLR should be attributed to mechanisms other than denervation.

Al-Sheikh and colleagues observed similar findings in humans [50]. They demonstrated cardiac sympathetic neuronal injury as manifested by decreased myocardial uptake of [11C] hydroxyephedrine in patients who had previously undergone TMLR. This tracer is a catecholamine analog that reflects norepinephrine uptake-1 and vesicular storage mechanisms of viable sympathetic nerve terminals [51]. Beek and colleagues also examined the effects of TMLR on cardiac innervation using pre- and post-operative imaging with iodine 123-labeled meta-iodobenzylguanide (^{123}I -MIBG) scintigraphy [52]. ^{123}I -MIBG is also a catecholamine analog

whose uptake in the heart is felt to be a measure of sympathetic innervation. In their patient cohort, 45 % of treated segments exhibited decreased uptake of ^{123}I -MIBG after TMLR. These results were confirmed in a study from Muxi et al. [53]. They performed ^{123}I -MIBG imaging before and 3 and 12 months after TMLR. At 3 months, 58 % of TMLR treated segments showed evidence of neuronal damage as reflected by decreased uptake of ^{123}I -MIBG. On 12 month imaging, 60 % of these segments showed improved radio-tracer uptake, suggesting reinnervation. Of interest, there was scintigraphic evidence of reinnervation in four of the five patients whose anginal status worsened between the 3rd and 12th months.

These studies show clear anatomical evidence of cardiac neural damage following TMLR in both humans and experimental animals. However, the markers used are not specific for cardiac afferent nerves and these anatomical observations provide no functional information about the ability of left ventricular receptors to transmit sympathetic afferent traffic to the brain and spinal cord.

Kwong et al. did assess the effects of TMLR on the functional integrity of cardiac reflexes [47]. They measured reflex changes in arterial pressure that occurred in response to epicardial application of bradykinin before and 2 weeks after TMLR in anesthetized dogs. Prior to TMLR, epicardial bradykinin elicited decreases in arterial pressure. Following TMLR, changes in arterial pressure in response to epicardial bradykinin were abolished. Based on these findings, Kwong and colleagues concluded that TMLR resulted in both anatomical and functional "denervation" of the left ventricle.

Hirsch and colleagues also assessed the effects of TMLR on the function of cardiac nerves in anesthetized dogs [54]. Both cardiac afferent and efferent nerves were studied. Left ventricular receptors were stimulated chemically by epicardial bradykinin and veratridine. Responses were measured by direct recordings from intrinsic cardiac afferent neurons. In addition, left ventricular efferent nerves were electrically and chemically activated and changes in heart rate, arterial pressure, and cardiac contractility were measured. Observations were made immediately before and after TMLR. In this study, TMLR had no apparent effect on the function of cardiac afferent or efferent nerves. In particular, the increased afferent neuronal activity that was elicited by epicardial bradykinin and veratridine was not significantly diminished by TMLR. In a separate study from this group, experiments performed 4 weeks following TMLR revealed similar findings [55].

Thus, although there is abundant anatomical evidence that TMLR damages cardiac neural structures, studies to assess the effects of TMLR on the function of cardiac nerves have yielded conflicting results.

Although the seminal experiments performed by Kwong et al. suggested that TMLR resulted in functional cardiac

deafferentation, we had several concerns about the methodology employed in these studies [47]. For instance, Kwong and colleagues used changes in arterial pressure to quantitate the response to epicardial bradykinin. This is a rather insensitive parameter for the study of autonomic reflexes. In addition, they studied animals with all reflexes intact. This represents a potential shortcoming for several reasons. Responses mediated by left ventricular sympathetic afferents are heavily influenced by other neurocirculatory reflexes such as the sinoaortic baroreflex and the vagal cardiopulmonary reflex [44]. The confounding influence of these other reflexes is especially problematic when bradykinin is used to activate cardiac receptors and elicit a response. Bradykinin is not a selective agonist for left ventricular sympathetic afferents. It also activates cardiac vagal afferents and can engage the vagal cardiopulmonary reflex [56]. Bradykinin also is a powerful vasodilator and its administration can lead to direct changes in arterial pressure that can engage the sinoaortic baroreflex.

Thus, when all reflexes are intact, responses to epicardial application of bradykinin may not be specific for left ventricular sympathetic afferents. In this experimental model, interpretation of these responses can be difficult and may be unreliable, particularly when the parameter used to measure these responses is changes in arterial pressure.

These methodologic concerns led us to reassess the effects of TMLR on reflexes mediated by left ventricular receptors with sympathetic afferent fibers in response to bradykinin administration [57]. We performed experiments in anesthetized dogs with sinoaortic denervation and vagotomy. This experimental preparation was used to facilitate the investigation of reflex responses mediated by left ventricular sympathetic afferents. Sinoaortic denervation prevented changes in arterial pressure associated with bradykinin administration from affecting the reflex response mediated by cardiac sympathetic afferents. Vagotomy prevented the activation of cardiac vagal afferents by bradykinin from contributing to these reflex responses. Thus, elimination of the effects of the sinoaortic baroreflex and the vagal cardiopulmonary reflex ensured that reflex changes elicited by bradykinin were mediated solely by left ventricular receptors with sympathetic afferent fibers.

In addition, we measured the reflex effects of bradykinin administration by direct recording of sympathetic outflow from efferent renal sympathetic nerve activity. This technique provides a more quantitative and rigorous assessment of the reflex changes in sympathetic outflow from the central nervous system, particularly in response to activation of cardiac receptors.

Thirteen mechanically ventilated dogs anesthetized with barbiturate and alpha chloralose were studied. We measured reflex changes in efferent renal sympathetic nerve activity (RSNA) in response to epicardial and intracoronary

bradykinin administration before and approximately 45 min after TMLR. Epicardial bradykinin was applied to the anterior wall of the left ventricle. Intracoronary bradykinin was administered through a cannula placed into a diagonal coronary artery. TMLR was performed according to the protocol that has been utilized in humans [4]. A 1 mm hand-held, pulsed holmium:YAG laser fiber was used to create transmyocardial channels. A mean of 44.5 ± 1.0 channels were made mainly in the anterior, anterolateral, and apical regions.

Renal nerve responses to epicardial bradykinin are shown in Fig. 20.1. As expected, epicardial bradykinin activated left ventricular sympathetic afferents and elicited reflex increases in RSNA prior to TMLR. Following TMLR, there were no significant differences in the reflex responses to epicardial bradykinin.

Renal nerve responses to intracoronary bradykinin are shown in Fig. 20.2. Intracoronary bradykinin also elicited reflex increases in RSNA before TMLR. There were no significant differences in reflex renal nerve responses to intracoronary bradykinin after TMLR.

In three experiments, reflex changes in renal nerve activity to graded doses of intracoronary bradykinin were assessed before and 45 min after TMLR. The results from these experiments are shown in Fig. 20.3. Prior to TMLR, an incremental relationship between increasing doses of intracoronary bradykinin and reflex increases in RSNA was observed. TMLR had no significant effect on the increase in RSNA in response to any dose of intracoronary bradykinin.

Pathologic analysis of two explanted hearts revealed three major findings (Fig. 20.4). In areas remote from the lased channels, intact neural structures were observed. In areas showing evidence of laser-induced myocardial damage, there was also evidence of neural damage with edema and vacuolization. However, undamaged nerve fibers were also present within the inflammatory zone created by laser-induced myocardial trauma. We speculate that this latter

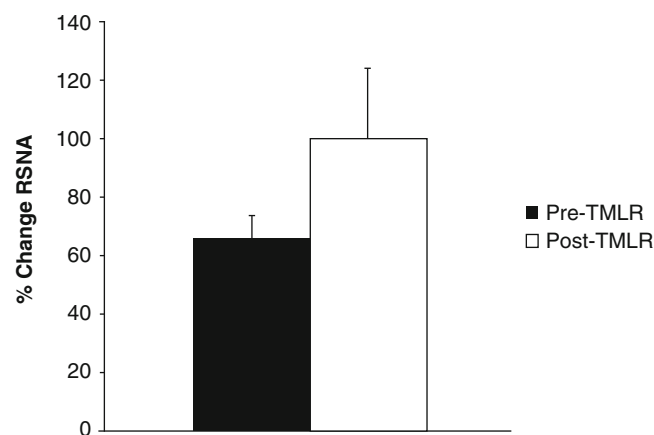


Fig. 20.1 Mean (\pm SEM) percent changes in RSNA in response to epicardial bradykinin

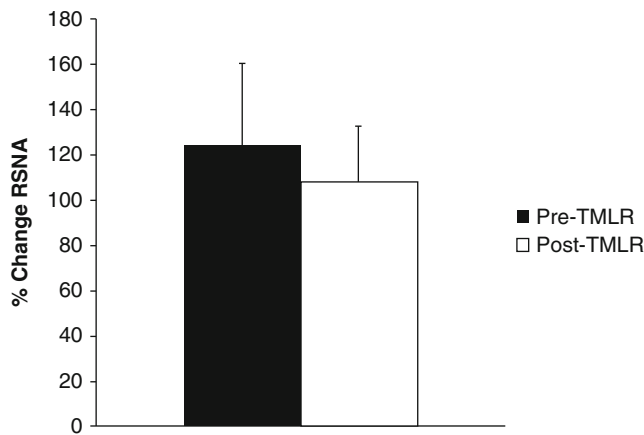


Fig. 20.2 Mean (\pm SEM) percent changes in RSNA in response to intracoronary bradykinin

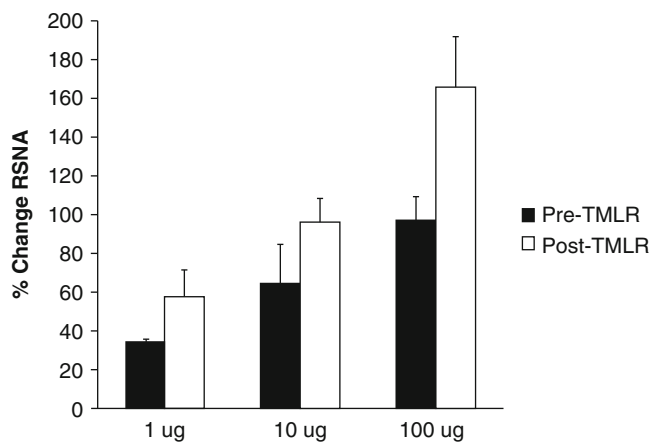


Fig. 20.3 Mean (\pm SEM) percent changes in RSNA in response to graded doses of intracoronary bradykinin

finding is related to non-uniform propagation of acoustic shock waves generated by laser energy and/or variable susceptibility of cardiac tissue to the effects of laser energy [58].

Although we expected to replicate the findings of Kwong and colleagues utilizing a refined experimental model, we found that reflexes mediated by left ventricular sympathetic afferents in response to chemical activation were unaffected by acute TMLR. Our results indicate that the receptors that represent the afferent pathway for the perception of anginal pain remain functional immediately following TMLR. We speculate that the discrepancy between the anatomical and functional data is related to the fact that the pattern of afferent innervation of the left ventricle represents a neural network. As a result, the damage to these neural structures from TMLR is not sufficient to cause functional deafferentation. Since cardiac deafferentation would attenuate or abolish responses mediated by left ventricular receptors with sympathetic afferent fibers, our results do not support the neural hypothesis for the relief of angina by TMLR.

Although our experimental results are not consistent with the observations of Kwong and colleagues, they studied responses to bradykinin 2 weeks after TMLR. We assessed the effects of TMLR on reflexes mediated by left ventricular sympathetic afferents in the acute experimental model. It is possible that the effects of TMLR on cardiac neural structures may be progressive over time and that deafferentation can only be demonstrated in a chronic model. Hence, we performed a second set of experiments to evaluate the effects of chronic TMLR on reflexes mediated by left ventricular receptors with sympathetic afferent fibers [59].

Two groups of 17 dogs underwent thoracotomy with either TMLR of the anterior, anterolateral, and apical regions or a sham procedure. After a recovery period of at least 4 weeks, animals were re-anesthetized and an acute protocol was performed in which responses to intracoronary and epicardial bradykinin were measured. In addition, we also measured responses to transmural myocardial ischemia of the anterior wall in this set of experiments. As in our previous experiments, sinoaortic denervation and vagotomy were performed to ensure that reflex changes elicited by bradykinin and myocardial ischemia were mediated solely by left ventricular receptors with sympathetic afferent fibers. Direct recordings of RSNA were again used to quantitate reflex responses.

The reflex responses to injection of graded doses of intracoronary bradykinin into the anterior descending (LAD) and left circumflex (LCx) coronary arteries are shown in Fig. 20.5a, b. As expected, there were escalating responses to incremental doses of bradykinin in both groups. For both the TMLR and Sham groups, injection into the LAD elicited similar responses as injection into the LCx for each dose of bradykinin. For the Sham group, this finding supports previous observations that cardiac receptors with sympathetic afferent fibers are uniformly distributed throughout the left ventricle [34]. For the TMLR group, this finding indicates that efferent responses to chemical stimulation of left ventricular nociceptors are not significantly different in the laser treated anterior wall compared to the untreated posterior region.

The reflex responses to anterior myocardial ischemia are shown in Fig. 20.6. Cardiac receptors with sympathetic afferent fibers are located mainly in the superficial epicardial layers of the left ventricle [34, 60, 61]. As a result, transmural myocardial ischemia is required to activate these receptors and elicit reflex excitatory responses. In dogs, extensive coronary collateral circulation limits the extent of transmural ischemia during simple coronary occlusion. In these experiments, we measured renal nerve responses to complete occlusion of the LAD while a collateral flow-limiting stenosis was in place on the LCx. Previous experiments from our laboratory validated that this technique results in greater transmural ischemia than simple coronary

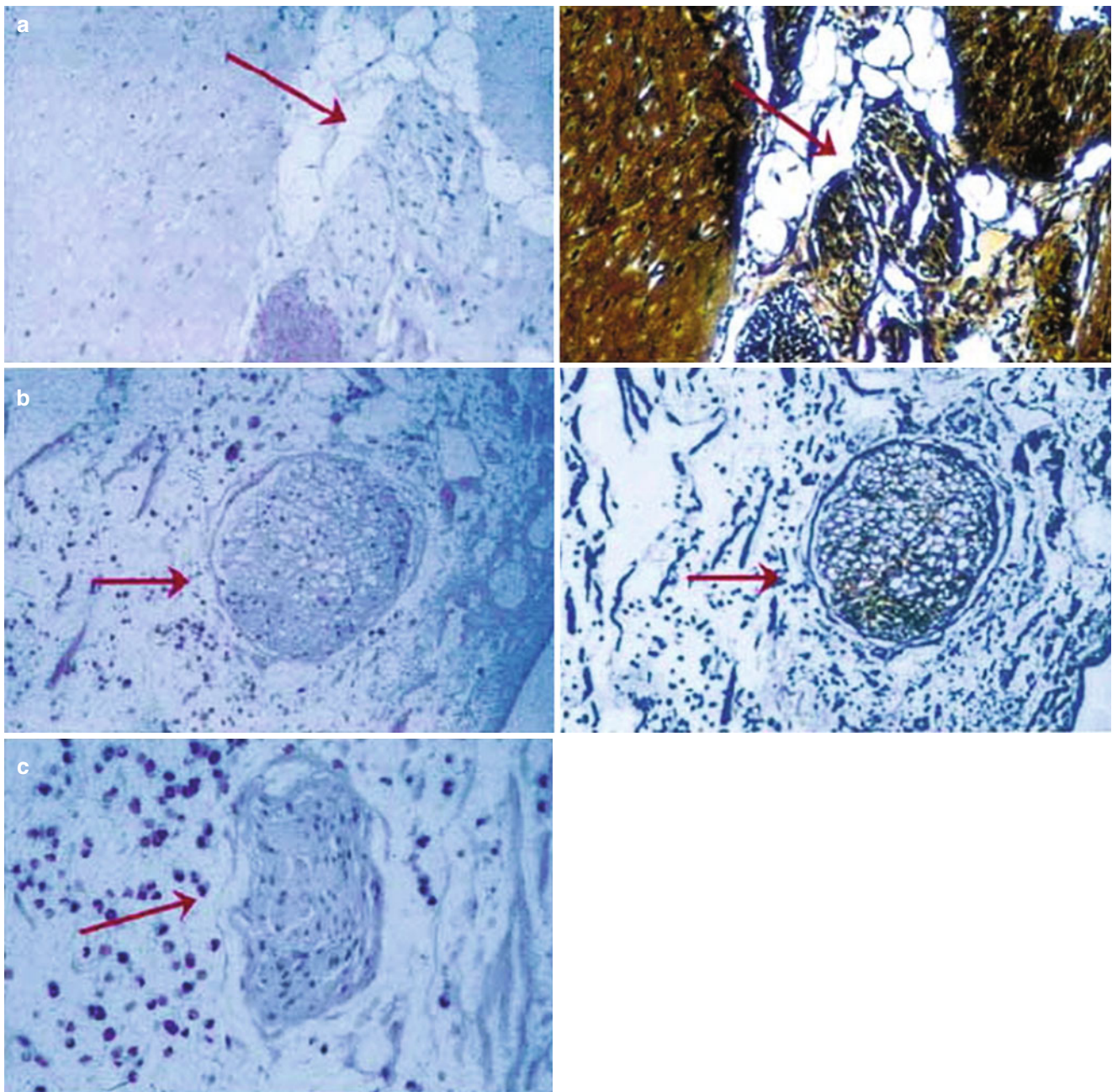


Fig. 20.4 Representative photomicrographs of pathologic specimens obtained from lased hearts. Panel (a) shows both hematoxylin and eosin (left) and Bielschowsky (right) stains of a neurovascular bundle containing intact neural structures (arrows) remote from a lased channel (original magnification, 50 \times). Panel (b) shows hematoxylin and eosin

(left) and Bielschowsky (right) stains of a damaged nerve (arrow) within a region of laser-induced myocardial damage (original magnification, 50 \times). Panel (c) shows hematoxylin and eosin stain of an undamaged nerve within the zone of laser-induced myocardial inflammation (original magnification, 100 \times)

occlusion alone and elicits significantly greater reflex increases in RSNA [61].

Transmural anterior myocardial ischemia elicited reflex increases in RSNA in both groups of animals. There were no significant differences in the reflex responses to ischemia between the laser-treated animals and the sham-treated control group. These results indicate that reflex responses to activation of cardiac receptors with sympathetic afferent

fibers by transmural anterior ischemia are not significantly attenuated by TMLR.

The results of our two series of experiments indicate that the neural pathways responsible for the perception of anginal pain remain fully functional both immediately and 4 weeks following TMLR. Although it is clear that any neural structures in the path of the laser beam will be damaged during TMLR, the results of our chronic studies indicate that this neural damage is

not progressive over time. Based on these results, we conclude that the extent of neural damage during TMLR is not sufficient to attenuate reflex responses mediated by left ventricular receptors with sympathetic afferent fibers. These results refute the hypothesis that TMLR results in functional denervation/deafferentation of the treated segments of the left ventricle.

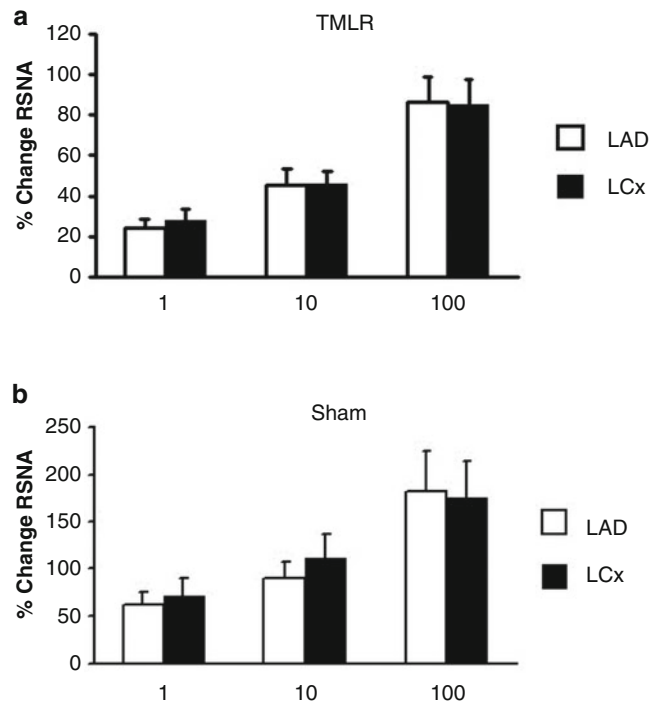


Fig. 20.5 Mean (\pm SEM) percent changes in RSNA in the anterior (LAD) and posterior (LCx) left ventricular walls in response to graded doses of bradykinin. Panel (a) shows results in TMLR treated dogs and Panel (b) shows results in sham group

Failure to demonstrate that TMLR causes denervation/deafferentation could be paradoxically fortuitous. Deafferentation as the mechanism for relief of angina by TMLR would imply that the procedure merely disables the anginal warning system without treating ongoing ischemia. Deafferentation following TMLR could also result in catecholamine supersensitivity which could be potentially arrhythmogenic. Both of these effects could be associated with negative prognostic implications after TMLR and could explain why TMLR has not been shown to improve survival.

TMLR as Adjunctive Therapy

In addition to the clinical experiences with TMLR as stand-alone therapy described above, the use of TMLR in conjunction with both traditional coronary artery bypass grafting (CABG) and cell therapy has been described. When used as an adjunct to CABG, TMLR has the potential to provide more complete revascularization. TMLR provides an option for treatment of regions of the left ventricle that are supplied by coronary arteries which are unsuitable for bypass grafting. Incomplete revascularization is not uncommon during CABG and it has been shown to be an independent predictor of operative mortality and other adverse outcomes following surgery [62–65]. In one cohort of patients, 5-year cardiac survival was significantly diminished in patients with incomplete revascularization compared to patients in whom surgical revascularization was considered complete (75 % vs. 93 %; $p < 0.001$) [65].

There have been three prospective, randomized trials comparing TMLR+CABG to CABG alone in patients who

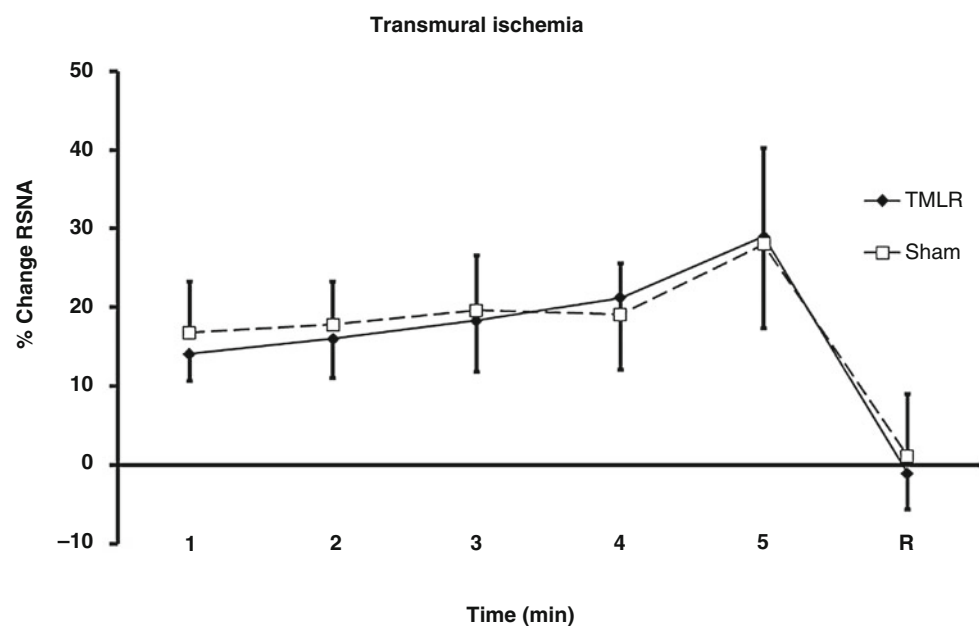


Fig. 20.6 Mean (\pm SEM) percent changes in RSNA in the laser and sham dogs in response to transmurial, anterior myocardial ischemia

could not be completely revascularized by bypass surgery only [66–68]. The largest of these trials was performed by Allen and colleagues who randomized 263 patients with one or more ischemic areas not amenable to bypass grafting to either TMLR+CABG (n=132) or CABG alone (n=131) [66]. The group randomized to TMLR+CABG had significantly reduced operative (30 day) mortality compared to the group randomized to CABG alone (1.5 % vs. 7.6 %; $p=0.02$). At 1 year, Kaplan Meier survival estimates continued to favor the group randomized to TMLR+CABG (95 % vs. 89 %; $P=0.05$). Freedom from death and myocardial infarction was significantly higher in the TMLR+CABG group at 30 days (97 % vs. 91 %; $p=0.04$). However, at 1 year, these differences were no longer statistically significant. Compared to baseline, both groups had significant and similar improvements in angina and exercise treadmill time at 3, 6, and 12 months following surgery.

Long term follow-up is available for 83 % (218/263) of the original cohort of randomized patients [69]. In this subset of patients, there were no significant differences in Kaplan Meier survival at 6 years. Compared to the CABG alone patients, the group randomized to TMLR+CABG had significantly improved control of angina as reflected by fewer patients with class III/IV anginal symptoms (0 % vs. 10 %; $p=0.009$) and more patients who were angina free (78 % vs. 63 %; $p=0.08$). These differences were especially pronounced in the randomized patients with diabetes. In this subset, 93 % of patients assigned to TMLR+CABG were free of angina at 5 years compared to 63 % of patients treated with CABG alone ($p=0.02$).

The other two randomized trials were hampered by very small sample sizes and limited statistical power. A meta analysis of all three trials of TMLR+CABG compared to CABG alone has been published [70].

There has been limited clinical experience with the use of TMLR in conjunction with cell therapy for the treatment of patients with end-stage coronary artery disease and ischemic cardiomyopathy. Cell therapy has the potential to facilitate regeneration of cardiac tissue and induce angiogenesis. Patel et al. examined animals with experimental myocardial infarction that were treated by injection of mesenchymal stem cells into the infarcted tissue [71]. They observed that TMLR performed prior to cell therapy improved early cell survival compared to cell therapy without TMLR. These results suggest a potential synergistic relationship between TMLR and cell therapy.

There have been several small case series describing the use of TMLR as an adjunct to cell therapy with autologous bone marrow derived stem cells in patients with end-stage coronary artery disease and refractory angina [72–75]. All of these studies have shown an improvement in symptomatic status and quality of life following the procedure. Some patients had improvement in myocardial perfusion and left

ventricular ejection fraction/regional wall motion, but this was not a consistent finding. Thirty three of the 35 patients described in these reports survived the procedure and no safety concerns emerged during the follow-up period. In general, the results appear to be very similar to those reported for TMLR as sole therapy. There have been no studies that have compared TMLR plus cell therapy to TMLR alone.

Other than for the impact of laser energy on stem cell retention described above, the mechanism for any synergy between TMLR and cell therapy remains a matter of speculation. The inflammatory response to the creation of a laser channel has a variety of effects that could facilitate myocardial regeneration and enhanced perfusion that is associated with cell therapy [76–78]. ***We have made a unique observation in our laboratory which may have relevance to the potential synergy between TMLR and cell therapy.***

The application of infrared laser energy to the left ventricular myocardium creates a transmural channel by the generation of heat with tissue vaporization. Local temperatures in the regions of laser application reach 60–70 °C [46, 79]. During TMLR, the creation of multiple channels in the myocardium with a laser generates local thermal stress. The thermal injury associated with TMLR could be a potent stimulus for the expression and synthesis of heat shock proteins. Heat shock proteins are a family of proteins that are cytoprotective [80]. A number of heat shock proteins of varying molecular size have been described. The heat shock protein with a molecular size of 70 kDa (Hsp70) has been extensively evaluated in the heart. Both thermal and ischemic stress result in increased production of Hsp70 in cardiac myocytes [81–84].

Preliminary data from our laboratory support this contention. We have observed that Hsp70 levels are increased 1 month following TMLR. The results of Western blots are shown in Fig. 20.7. The heart treated with TMLR (right blot) is compared to a heart from an animal with sham treatment (left blot). Qualitatively, Hsp70 levels are clearly increased in the tissue harvested from the TMLR treated heart.

Hsp70 levels were also measured in the hearts of four additional Holmium:YAG TMLR-treated dogs. In these animals, Western blots were performed on tissue from the treated anterior wall and from the untreated posterior wall.

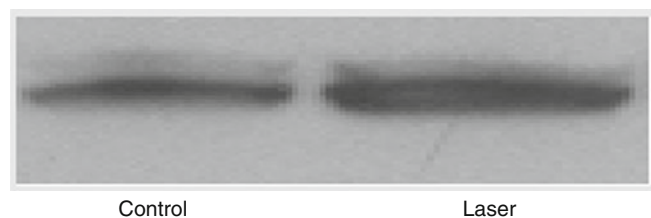


Fig. 20.7 Results of Western blot analysis of Hsp70 expression in a TMLR-treated heart (*Laser*) compared to a sham treated heart (*Control*). Protein sample sizes in each lane were 100 μ g

The results of this analysis are shown in Fig. 20.8. Four weeks following TMLR, Hsp70 levels were significantly higher in the treated anterior region compared to the untreated posterior region. These hearts did not express increased levels of Hsp32, another heat shock protein with a cardioprotective effect.

To our knowledge, this is the first demonstration that cardiac Hsp70 expression is increased 4 weeks following TMLR. In fact, we are not aware of any cardiac stimulus that has resulted in increased expression of Hsp70 for such an extended period of time. We postulate that the prolonged expression of Hsp70 is related to the intense thermal stimulus associated with the application of laser energy directly to the myocardium. No previous experimental studies of Hsp70 have utilized this unique thermal stimulus.

This observation is relevant to TMLR as an adjunct to cell therapy because experimental studies have shown that overexpression of heat shock proteins can improve stem cell viability and protect against hypoxic and ischemic stress [85–87]. These findings have been documented in both in vitro and in vivo experimental models. By increasing the expression of heat shock proteins, TMLR may create an environment that is conducive to the survival and function of transplanted stem cells.

Preconditioning as a Mechanism for TMLR

The finding of a sustained increase in the expression of Hsp70 following TMLR has significance beyond potentially improving the efficacy of stem cell therapy. Preconditioning is a phenomenon whereby the left ventricular myocardium is rendered resistant to the consequences of decreased coronary blood flow. In the experimental setting, ischemic

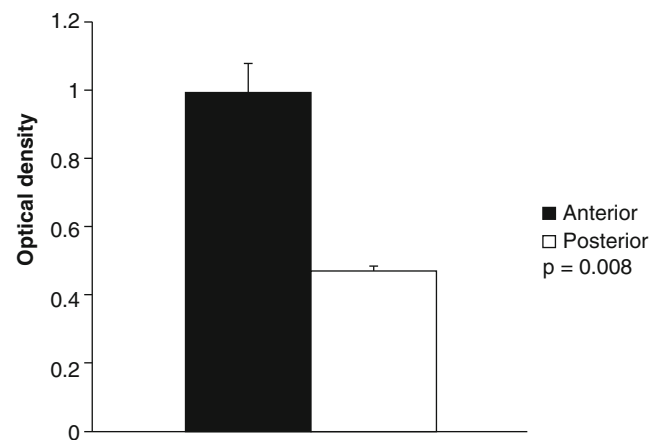


Fig. 20.8 Mean (\pm SEM) densitometric quantification values for Hsp70 expression in myocardial tissue from the treated anterior wall and the untreated posterior wall. Samples for Western blots each contained 100 μ g of protein

preconditioning has been studied extensively. Ischemic preconditioning is usually induced by repetitive short cycles of coronary occlusion followed by reperfusion. These cycles have been shown to provide protection against the deleterious effects of prolonged myocardial ischemia. This protection is apparent when ischemia occurs within a few hours (acute or early preconditioning) and when it occurs 24–48 h later (delayed or late preconditioning) [81, 88–90].

In addition to ischemic stress, preconditioning can be induced by exercise, rapid ventricular pacing, systemic hypoxia, various pharmacologic agents and by thermal stress. Preconditioning associated with thermal stress results in increased intracellular synthesis of heat shock proteins [81]. Since heat shock proteins are cytoprotective, they have been implicated as a potential mediator of the beneficial anti-ischemic effects of preconditioning. The appearance and the amount of Hsp70 synthesis correlate with the extent of myocardial protection after ischemia/reperfusion injury [81, 91–93]. Cultured cardiac myocytes in which the expression of Hsp70 is augmented by gene transfer techniques demonstrate tolerance to simulated ischemic conditions [94, 95]. Similar findings have been observed in the intact heart injected with an adenoviral vector encoding the Hsp70 gene [96]. Finally, the hearts of transgenic mice overexpressing the Hsp70 gene are protected from the deleterious effects of ischemia/reperfusion injury [97–100].

Thus, there is considerable experimental evidence that Hsp70 has an integral role in the myocardial protection observed following whole body thermal stress. Considering the intense thermal stimulus associated with TMLR, it is plausible that the symptomatic benefit associated with this procedure could be due to preconditioning initiated by increased expression and synthesis of Hsp70. Improved anginal status after TMLR could be related to this inducible resistance to myocardial ischemia. To our knowledge, this possibility has not been investigated previously.

Conclusions

Although some are skeptical about the safety and efficacy of TMLR as a therapeutic intervention, it cannot be denied that there is an expanding pool of patients with end-stage coronary disease who are not candidates for traditional revascularization procedures and who continue to be severely symptomatic despite maximal medical therapy. Novel treatment modalities such as TMLR are required for these patients. Based on an extensive database accumulated from clinical registries and randomized clinical trials, there was considerable enthusiasm for TMLR as a therapeutic modality and it was added to the practice guidelines of the American College of Cardiology/American Heart Association (ACC/AHA), the Society of Thoracic Surgeons (STS), and the International Society

of Minimally Invasive Cardiothoracic Surgeons (ISMICS) as early as 2002.

These guidelines are evidence based recommendations that are designed to evaluate various medical interventions and to assist health care providers in appropriately utilizing these interventions. A class I recommendation is given when available evidence indicates that the benefits of an intervention far outweigh the risks. As a result, the procedure or treatment *should be performed or administered*. A class II recommendation indicates that the benefit exceeds or equals the risk and that it is *reasonable to perform or administer* the procedure or treatment (class IIa) or that the procedure or treatment *may be considered* (class IIb). Finally, a class III recommendation indicates that the procedure or treatment is of no benefit or may cause harm. Any intervention with a class III recommendation *should not be performed*.

In addition to the recommendations, the guidelines also rate the quality of evidence that is used to make these determinations. The highest quality level of evidence is Grade A. This designation is utilized when the data is derived from multiple randomized clinical trials or meta-analyses that have evaluated multiple patient populations. Grade B level of evidence indicates that the intervention has been evaluated in limited patient populations and that the data is derived from a single randomized trial or non-randomized studies. Level of evidence C refers to situations in which very limited patient populations have been evaluated and the recommendation is based on expert opinion regarding the appropriate standard of care or case studies.

The ACC/AHA guidelines from 2002 gave a class IIa recommendation with a grade A level of evidence for TMLR when used as alternative treatment in stable patients with angina refractory to medical therapy who were not candidates for conventional revascularization procedures [101]. Stronger endorsements were provided by the STS and ISMICS who gave TMLR a class I recommendation with grade A level of evidence as sole therapy in these “no option” patients [102, 103]. When used as an adjunct to CABG, TMLR was given a class I recommendation by ISMICS and a class IIa recommendation by the STS. In both cases, the level of evidence was grade B.

The ACC/AHA guidelines for management of patients with stable ischemic heart disease were most recently updated in 2012. In this version, TMLR as an alternative therapy for the relief of symptoms in patients with refractory angina was given a class IIb recommendation with level of evidence B. This applies to TMLR both as sole therapy and as an adjunct to CABG [104].

A report from the STS tracked the utilization of TMLR following approval by the FDA [105]. In their

database, the number of sites performing TMLR increased from 33 in 1998 to 131 in 2001. The latter figure represents 36 % of sites that submitted data to the STS. The number of TMLR procedures rose from 59 in the first half of 1998 to 572 in the second half of 2001. From 1998 to 2001, a total of 3,717 TMLR procedures were performed. Of note, only 661 (17 %) of these procedures were TMLR as sole therapy. The remainder were performed for “off-label” indications and included TMLR with CABG (67 %) and TMLR with another cardiac procedure (16 %).

There has been a gradual decline in the utilization of this procedure. There are several potential reasons for this waning enthusiasm. TMLR is a highly invasive procedure with associated morbidity and mortality. The complication rate is higher in patients with unstable anginal syndromes and/or left ventricular dysfunction. Unfortunately, the prevalence of episodic acute coronary syndromes and left ventricular dysfunction in the typical “no option” patient with refractory angina is high. This reduces the number of patients who may be considered good candidates for this procedure.

TMLR has not been shown to improve survival. Of greater concern, the mechanism for improvement in anginal symptoms remains undetermined. Arguments have been made against a placebo effect but this possibility has not been excluded because a placebo controlled trial of TMLR is not feasible. Placebo controlled trials can be performed with percutaneous myocardial revascularization and these studies have failed to demonstrate differences in anginal status between patients randomized to active therapy and those who received sham treatment [30]. This finding has dampened enthusiasm for TMLR as a treatment modality. However, there are major differences between TMLR and percutaneous myocardial revascularization and these differences should invalidate any comparisons or correlations between the two procedures.

In conclusion, TMLR is a surgical treatment that has been shown to improve anginal status, prevent cardiac-related hospitalizations, increase exercise tolerance, decrease use of cardiac medications, and improve quality of life in properly selected patients. These patients typically have end-stage coronary artery disease that is not amenable to further conventional revascularization procedures with CABG or PCI. They are extremely symptomatic with refractory angina that cannot be controlled with maximal medical therapy. Although TMLR has not been shown to improve survival, the circumstances of the typical “no option” patient are dire and the importance of any intervention that can improve quality of life endpoints should not be minimized or dismissed.

References

- Mukherjee D, Bhatt DL, Roe MT, Patel V, Ellis SG. Direct myocardial revascularization and angiogenesis—how many patients might be eligible? *Am J Cardiol.* 1999;84:598–600.
- Horvath KA, Cohn LH, Cooley DA, Crew JR, Frazier OH, Griffith BP, Kadipasaoglu K, Lansing A, Mannting F, March R, Mirhoseini MR, Smith C. Transmyocardial laser revascularization: results of a multicenter trial with transmyocardial laser revascularization used as sole therapy for end-stage coronary artery disease. *J Thorac Cardiovasc Surg.* 1997;113:645–53.
- Schofield PM, Sharples LD, Caine N, Burns S, Tait S, Wistow T, Buxton M, Wallwork J. Transmyocardial laser revascularization in patients with refractory angina: a randomised controlled trial. *Lancet.* 1999;353:519–24.
- Allen KB, Dowling RD, Fudge TL, Schoettle GP, Selinger SL, Gangahar DM, Angell WW, Petracek MR, Shaar CJ, O'Neill WW. Comparison of transmyocardial revascularization with medical therapy in patients with refractory angina. *N Engl J Med.* 1999;341:1029–36.
- Frazier OH, March RJ, Horvath KA. Transmyocardial revascularization with a carbon dioxide laser in patients with end-stage coronary artery disease. *N Engl J Med.* 1999;341:1021–8.
- Horvath KA, Mannting F, Cummings N, Shernan SK, Cohn LH. Transmyocardial laser revascularization, operative techniques, and clinical results at two years. *J Thorac Cardiovasc Surg.* 1996;111:1047–53.
- Aaberge L, Nordstrand K, Dragsund M, Saatvedt K, Endresen K, Golf S, Geiran O, Abdelnoor M, Forfang K. Transmyocardial revascularization with CO₂ laser in patients with refractory angina pectoris. *J Am Coll Cardiol.* 2000;35:1170–7.
- Jones JW, Schmidt SE, Richman BW, Miller CC, Sapire KJ, Burkhoff D, Baldwin JC. Holmium:YAG laser transmyocardial revascularization relieves angina and improves functional status. *Ann Thorac Surg.* 1999;67:1596–602.
- Burkhoff D, Schmidt S, Schulman SP, Myers J, Resar J, Becker LC, Weiss J, Jones JW. Transmyocardial laser revascularisation compared with continued medical therapy for treatment of refractory angina pectoris: a prospective randomised trial. *Lancet.* 1999;354:885–90.
- van der Sloot JA, Huikeshoven M, Tukkie R, Verberne HJ, van der Meulen J, van Eck-Smit BL, van Gemert MJ, Tijssen JG, Beek JF. Transmyocardial revascularization using an XeCl excimer laser: results of a randomized trial. *Ann Thorac Surg.* 2004;78:875–81.
- Aaberge L, Rootwelt K, Blomhoff S, Saatvedt K, Abdelnoor M, Forfang K. Continued symptomatic improvement three to five years after transmyocardial revascularization with CO₂ laser. *J Am Coll Cardiol.* 2002;39:1588–93.
- Allen KB, Dowling RD, Angell WW, Gangahar DM, Fudge TL, Richenbacher W, Selinger SL, Petracek MR, Murphy D. Transmyocardial revascularization: 5 year follow-up of a prospective randomized multicenter trial. *Ann Thorac Surg.* 2004;77:1228–34.
- Horvath KA, Aranki SF, Cohn LH, March RJ, Frazier OH, Kadipasaoglu KA, Boyce SW, Lytle BW, Landolfo KP, Lowe JE, Hattler B, Griffith BP, Lansing AM. Sustained angina relief 5 years after transmyocardial laser revascularization with a CO₂ laser. *Circulation.* 2001;104:181–4.
- De Carlo M, Milano AD, Pratali S, Levantino M, Mariotti R, Bortolotti U. Symptomatic improvement after transmyocardial laser revascularization: how long does it last? *Ann Thorac Surg.* 2000;70:1130–3.
- Pratali S, Chiamonti F, Milano A, Bortolotti U. Transmyocardial laser revascularization 12 years later. *Interact Cardiovasc Thorac Surg.* 2010;11:480–1.
- Wearn JT, Mettier SR, Klumpp TG, Zschesche LJ. The nature of the vascular communications between the coronary arteries and the chambers of the heart. *Am Heart J.* 1933;9:143–64.
- Tsang JC-C, Chiu RC-J. The phantom of “myocardial sinusoids”: a historical reappraisal. *Ann Thorac Surg.* 1995;60:1831–5.
- Gassler N, Wintzer H-O, Stubbe H-M, Wullbrand A, Helmchen U. Transmyocardial laser revascularization: histological features in human nonresponder myocardium. *Circulation.* 1997;95:371–5.
- Burkhoff D, Fisher PE, Apfelbaum M, Kohmoto T, DeRosa CM, Smith CR. Histologic appearance of transmyocardial laser channels after 4-1/2 weeks. *Ann Thorac Surg.* 1996;61:1532–5.
- Krabatsch T, Schaper F, Leder C, Tulsner J, Thalmann U, Hetzer R. Histological findings after transmyocardial laser revascularization. *J Cardiac Surg.* 1996;11:326–31.
- Sigel JE, Abramovitch CM, Lytle BW, Ratliff NB. Transmyocardial laser revascularization: three sequential autopsy case. *J Thorac Cardiovasc Surg.* 1998;115:1381–5.
- Horvath KA, Chiu E, Maun DC, Lomasney JW, Greene R, Pearce WH, Fullerton DA. Up-regulation of vascular endothelial growth factor mRNA and angiogenesis after transmyocardial laser revascularization. *Ann Thorac Surg.* 1999;68:825–9.
- Spanier T, Smith CR, Burkhoff D. Angiogenesis: a possible mechanism underlying the clinical benefits of transmyocardial laser revascularization. *J Clin Laser Med Surg.* 1997;15:269–73.
- Kohmoto T, DeRosa CM, Yamamoto N, Fisher PE, Failey P, Smith CR, Burkhoff D. Evidence of vascular growth associated with laser treatment of normal canine myocardium. *Ann Thorac Surg.* 1998;65:1360–7.
- Hughes CG, Lowe JE, Kypson AP, St. Louis JD, Phippen AM, Peters KG, Coleman RE, DeGrado TR, Donovan CL, Annex BH, Landolfo KP. Neovascularization after transmyocardial laser revascularization in a model of chronic ischemia. *Ann Thorac Surg.* 1998;66:2029–36.
- Malekan R, Reynolds C, Narula N, Kelley ST, Suzuki Y, Bridges CR. Angiogenesis in transmyocardial laser revascularization: a nonspecific response to injury. *Circulation.* 1998;98:II62–6.
- Yamamoto N, Kohmoto T, Gu A, DeRosa C, Smith CR, Burkhoff D. Angiogenesis is enhanced in ischemic canine myocardium by transmyocardial laser revascularization. *J Am Coll Cardiol.* 1998;31:1426–33.
- Li W, Chiba Y, Kimura T, Morioka K, Uesaka T, Ihaya A, Muraoka R. Transmyocardial laser revascularization induced angiogenesis correlated with the expression of matrix metalloproteinases and platelet-derived endothelial cell growth factor. *Eur J Cardiothorac Surg.* 2001;19:156–63.
- Domkowski PW, Biswas SS, Steenbergen C, Lowe JE. Histological evidence of angiogenesis 9 months after transmyocardial laser revascularization. *Circulation.* 2001;103:469–71.
- Stone GW, Teirstein PS, Rubenstein R, Schmidt D, Whitlow PL, Kosinski EJ, Power JA. A prospective, multicenter, randomized trial of percutaneous transmyocardial laser revascularization in patients with nonrevascularizable chronic total occlusions. *J Am Coll Cardiol.* 2002;15:1581–7.
- Bristow M. The surgically denervated, transplanted heart. *Circulation.* 1990;82:658–60.
- White JC. Cardiac pain: anatomic pathways and physiologic mechanisms. *Circulation.* 1957;16:644–55.
- Baker DG, Coleridge HM, Coleridge JCG, Nerdrum T. Search for a cardiac nociceptor: stimulation by bradykinin of afferent sympathetic nerve endings in the cat. *J Physiol.* 1980;306:519–36.
- Minisi AJ, Thames MD. Distribution of left ventricular sympathetic afferents demonstrated by reflex responses to transmural myocardial ischemia and to intracoronary and epicardial bradykinin. *Circulation.* 1993;87:240–6.
- Malliani A, Recordati G, Schwartz PJ. Nervous activity of afferent cardiac sympathetic fibres with atrial and ventricular endings. *J Physiol.* 1973;229:457–69.

36. Lombardi F, Della Bella P, Casati R, Malliani A. Effects of intracoronary administration of bradykinin on the impulse activity of afferent sympathetic unmyelinated fibers with left ventricular endings in the cat. *Circ Res*. 1981;48:69–75.
37. Uchida Y, Kamisaka K, Murao S, Ueda H. Mechanosensitivity of afferent cardiac sympathetic nerve fiber. *Am J Physiol*. 1974;226:1088–93.
38. Bishop VS, Malliani A, Thoren P. Cardiac mechanoreceptors. In: Shepherd JT, Abboud FM, editors. *Handbook of physiology: peripheral circulation and organ blood flow*. Washington, DC: American Physiological Society; 1983. p. 497–555.
39. Brown A. Cardiac reflexes. In: Berne RM, editor. *Handbook of physiology: the heart*. Washington, DC: American Physiological Society; 1983. p. 667–89.
40. Malliani A. Afferent cardiovascular sympathetic nerve fibers and their function in the neural regulation of the circulation. In: Hainsworth R, Kidd C, Linden RJ, editors. *Cardiac receptors*. Cambridge, UK: Cambridge University Press; 1979. p. 319–38.
41. Uchida Y, Murao S. Bradykinin-induced excitation of afferent cardiac sympathetic nerve fibers. *Jpn Heart J*. 1974;15:84–91.
42. Brown AM. Excitation of afferent cardiac sympathetic nerve fibers during myocardial ischemia. *J Physiol (London)*. 1967;190:35–53.
43. Uchida Y, Murao S. Excitation of afferent cardiac sympathetic nerve fibers during coronary occlusion. *Am J Physiol*. 1974;226:1094–9.
44. Felder RB, Thames MD. Interaction between cardiac receptors and sinoaortic baroreceptors in the control of efferent cardiac sympathetic nerve activity during myocardial ischemia in dogs. *Circ Res*. 1979;45:728–36.
45. Felder RB, Thames MD. The cardiocardiac sympathetic reflex during coronary occlusion in anesthetized dogs. *Circ Res*. 1981;48:685–92.
46. Whittaker P. Detection and assessment of laser-mediated injury in transmyocardial revascularization. *J Clin Laser Med Surg*. 1997;15:261–7.
47. Kwong KF, Kanellopoulos GK, Nickols JC, Pogwizd SM, Saffitz JE, Schuellser RB, Sundt III TM. Transmyocardial laser treatment denervates canine myocardium. *J Thorac Cardiovasc Surg*. 1997;114:883–9.
48. Wooten GF, Coyle JT. Axonal transport of catecholamine synthesizing and metabolizing enzymes. *J Neurochem*. 1973;20:1361–71.
49. Hughes GC, Baklanov DV, Biswas SS, Phippen AM, DeGrado TR, Coleman RE, Landolfo CK, Lowe JE, Annex BH, Landolfo KP. Regional cardiac sympathetic innervation early and late after transmyocardial laser revascularization. *J Card Surg*. 2004;19:21–7.
50. Al-Sheikh T, Allen KB, Straka SP, Heimansohn DA, Fain RL, Hutchins GD, Sawada SG, Zipes DP, Engelstein ED. Cardiac sympathetic denervation after transmyocardial laser revascularization. *Circulation*. 1999;100:135–40.
51. Allman KC, Wieland DM, Muzik O, DeGrado TR, Wolfe Jr ER, Schwaiger M. Carbon-11 hydroxyephedrine with positron emission tomography for serial assessment of cardiac adrenergic neuronal function after acute myocardial infarction in humans. *J Am Coll Cardiol*. 1993;22:368–75.
52. Beek JF, van der Sloot JAP, Huijkeshoven M, Verberne HJ, van Eck-Smit BLF, van der Meulen J, Tijssen JGP, van Gemert MJC, Tukkie R. Cardiac denervation after clinical transmyocardial laser revascularization: short-term and long-term iodine 123-labeled meta-iodobenzylguanide scintigraphic evidence. *J Thorac Cardiovasc Surg*. 2004;127:517–24.
53. Muxi A, Magrina J, Martin F, Josa M, Fuster D, Setoain FJ, Perez-Villa F, Pavia J, Bosch X. Technetium 99m-labeled tetrofosmin and iodine 123-labeled metaiodobenzylguanidine scintigraphy in the assessment of transmyocardial laser revascularization. *J Thorac Cardiovasc Surg*. 2003;125:1493–8.
54. Hirsch GM, Thompson GW, Arora RC, Hirsch KJ, Sullivan JA, Armour JA. Transmyocardial laser revascularization does not denervate the canine heart. *Ann Thorac Surg*. 1999;68:460–9.
55. Arora RC, Hirsch GM, Hirsch K, Armour JA. Transmyocardial laser revascularization remodels the intrinsic cardiac nervous system in a chronic setting. *Circulation*. 2001;104:1115–20.
56. Kaufman MP, Baker BG, Coleridge HM, Coleridge JCG. Stimulation by bradykinin of afferent vagal C-fibers with chemosensitive endings in the heart and aorta of the dog. *Circ Res*. 1980;46:476–84.
57. Minisi AJ, Topaz O, Quinn MS, Mohanty L. Cardiac nociceptive reflexes following transmyocardial laser revascularization: implications for the neural hypothesis of angina relief. *J Thorac Cardiovasc Surg*. 2001;122:712–9.
58. Van Gemert MJC, Welch AJ, Jacques SL, Cheong WF, Star WM. Light distribution, optical properties, and cardiovascular tissues. In: Abela GS, editor. *Lasers in cardiovascular medicine and surgery: fundamentals and techniques*, vol. 8. Boston: Kluwer Academic Publishers; 1990. p. 99–110.
59. Banerjee DD, Quinn MS, Mohanty LB, Minisi AJ. Failure of chronic transmyocardial laser revascularization to alter cardiac nociceptive reflexes: implications for the treatment of angina pectoris. *Lasers Med Sci*. 2008;23:155–61.
60. Barber MJ, Mueller TM, Davies BG, Zipes DP. Phenol topically applied to canine left ventricular epicardium interrupts sympathetic but not vagal afferents. *Circ Res*. 1984;55:532–44.
61. Minisi AJ, Thames MD. Activation of cardiac sympathetic afferents during coronary occlusion: evidence for reflex activation of the sympathetic nervous system during transmural myocardial ischemia in the dog. *Circulation*. 1991;84:357–67.
62. Lawrie GM, Morris Jr GC, Silvers A, Wagner WF, Baron AE, Beltangady SS, Glaeser DH, Chapman DW. The influence of residual disease after coronary bypass on the 5-year survival rate of 1274 men with coronary artery disease. *Circulation*. 1982;66:717–23.
63. Bell MR, Gersh BJ, Schaff HV, Holmes Jr DR, Fisher LD, Alderman EL, Myers WO, Parsons LS, Reeder GS. Effect of completeness of revascularization on long-term outcome of patients with three-vessel disease undergoing coronary artery bypass surgery. A report from the Coronary Artery Surgery Study (CASS). *Circulation*. 1992;86:446–57.
64. Osswald BR, Blackstone EH, Tochtermann U, Schweiger P, Thomas G, Vahl CF, Hagl S. Does the completeness of revascularization affect early survival after coronary artery bypass grafting in elderly patients? *Eur J Cardiothorac Surg*. 2001;20:120–5.
65. Kleisli T, Cheng W, Jacobs MJ, Mirocha J, Derobertis MA, Kass RM, Blanche C, Fontana GP, Raissi SS, Magliato KE, Trento A. In the current era, complete revascularization improves survival after coronary artery bypass surgery. *J Thorac Cardiovasc Surg*. 2005;129:1283–91.
66. Allen KB, Dowling RD, DeRossi AJ, Realyvasques F, Lefrak EA, Pfeffer TA, Fudge TL, Mostovych M, Schuch D, Szentpetery S, Shaar CJ. Transmyocardial laser revascularization combined with coronary artery bypass grafting: a multicenter, blinded, prospective, randomized, controlled trial. *J Thorac Cardiovasc Surg*. 2000;119:540–9.
67. Frazier OH, Tuzun E, Eichstadt H, Boyce SW, Lansing AM, March RJ, Sartori M, Kadipasaoglu KA. Transmyocardial laser revascularization as an adjunct to coronary artery bypass grafting. A randomized, multicenter study with 4-year follow-up. *Tex Heart Inst J*. 2004;31:231–9.
68. Loubani M, Chin D, Leverment JN, Galinanes M. Mid-term results of combined transmyocardial laser revascularization and coronary artery bypass. *Ann Thorac Surg*. 2003;76:1163–6.

69. Allen KB, Dowling RD, Schuch DR, Pfeffer TA, Marra S, Lefrak EA, Fudge TL, Mostovych M, Szentpetery S, Saha SP, Murphy D, Dennis H. Adjunctive transmyocardial revascularization: five-year follow-up of a prospective, randomized trial. *Ann Thorac Surg.* 2004;78:458–65.
70. Cheng D, Diegeler A, Allen K, Weisel R, Lutter G, Sartori M, Asai T, Aaberge L, Horvath K, Martin J. Transmyocardial laser revascularization: a meta-analysis and systematic review of controlled trials. *Innovations.* 2006;1:295–313.
71. Patel AN, Spadaccio C, Kuzman M, Park E, Fischer DW, Stice SL, Mullangi C, Toma C. Improved cell survival in infarcted myocardium using a novel combination transmyocardial laser and cell delivery system. *Cell Transplant.* 2007;16:899–905.
72. Klein HM, Ghodsizad A, Borowski A, Saleh A, Draganov J, Poll L, Stoldt V, Feifel N, Piecharczek C, Burchardt ER, Stockschrader M, Gams E. Autologous bone marrow-derived stem cell therapy in combination with TMLR. A novel therapeutic option for end-stage coronary heart disease: report on 2 cases. *Heart Surg Forum.* 2004;7:E416–9.
73. Gowdak LHW, Schettert IT, Rochitte CE, Rienzo M, Lisboa LAF, Dallan LAO, Cesar LAM, Krieger JE, Ramires JAF, de Oliveira SA. Transmyocardial laser revascularization plus cell therapy for refractory angina. *Int J Cardiol.* 2008;127:295–7.
74. Reyes G, Allen KB, Alvarez P, Alegre A, Aguado B, Olivera M, Caballero P, Rodriguez J, Duarte J. Mid term results after bone marrow laser revascularization for treating refractory angina. *BMC Cardiovasc Disord.* 2010;10:42.
75. Babin-Ebell J, Sievers HH, Charitos EI, Klein HM, Jung F, Hellberg AK, Depping R, Sier HA, Marxsen J, Stoelting S, Kraatz EG, Wagner KF. Transmyocardial laser revascularization combined with intramyocardial endothelial progenitor cell transplantation in patients with intractable ischemic heart disease ineligible for conventional revascularization: preliminary results from a highly selected small patient cohort. *Thorac Cardiovasc Surg.* 2010;58:11–6.
76. Atluri P, Panlilio CM, Liao GP, Suarez EE, McCormick RC, Hiesinger W, Cohen JE, Smith MJ, Patel AB, Feng W, Woo YJ. Transmyocardial revascularization to enhance myocardial vasculogenesis and hemodynamic function. *J Thorac Cardiovasc Surg.* 2008;135:283–91.
77. Yamamoto N, Kohmoto T, Roethy W, Gu A, DeRosa C, Rabbani LE, Smith CR, Burkhoff D. Histologic evidence that basic fibroblast growth factor enhances the angiogenic effects of transmyocardial laser revascularization. *Basic Res Cardiol.* 2000;95:55–63.
78. Lutter G, Attmann T, Heilmann C, von Samson P, von Specht B, Beyersdorf F. The combined use of transmyocardial laser revascularization (TMLR) and fibroblastic growth factor (FGF-2) enhances perfusion and regional contractility in chronically ischemic porcine hearts. *Eur J Cardiothorac Surg.* 2002;22:753–61.
79. Hardy RI, Bove KE, James FW, Kaplan S, Goldman L. A histologic study of laser-induced transmyocardial channels. *Lasers Surg Med.* 1987;6:563–73.
80. Benjamin IJ, McMillan DR. Stress (heat shock) proteins: molecular chaperones in cardiovascular biology and disease. *Circ Res.* 1998;83:117–32.
81. Marber MS, Latchman DS, Walker JM, Yellon DM. Cardiac stress protein elevation 24 hours after brief ischemia or heat stress is associated with resistance to myocardial infarction. *Circulation.* 1993;88:1264–72.
82. Benjamin IJ, Kroger B, Williams RS. Activation of the heat shock transcription factor by hypoxia in mammalian cells. *Proc Natl Acad Sci U S A.* 1990;87:6263–7.
83. Mehta HB, Popovich BK, Dillmann WH. Ischemia induces changes in the level of mRNAs coding for stress protein 71 and creatine kinase M. *Circ Res.* 1988;63:512–7.
84. Knowlton AA, Brecher P, Apstein CS. Rapid expression of heat shock protein in the rabbit after brief cardiac ischemia. *J Clin Invest.* 1991;87:139–47.
85. Suzuki K, Smolenski RT, Jayakumar J, Murtuza B, Brand NJ, Yacoub MH. Heat shock treatment enhances graft cell survival in skeletal myoblast transplantation to the heart. *Circulation.* 2000;102:III216–21.
86. McGinley LM, McMahon J, Stocca A, Duffy A, Flynn A, O'Toole D, O'Brien T. Mesenchymal stem cell survival in the infarcted heart is enhanced by lentivirus vector-mediated heat shock protein 27 expression. *Hum Gene Ther.* 2013;24:840–51.
87. Feng Y, Huang W, Meng W, Jegga AG, Wang Y, Cai W, Kim HW, Wen Z, Rao F, Modi RM, Yu X, Ashraf M. Heat shock improves sca-1+ stem cells survival and directs ischemic cardiomyocytes towards a prosurvival phenotype via exosomal transfer: a critical role for HSF1/miR-34a/HSP70 pathway. *Stem Cells.* 2014;32:462–72.
88. Kuzuya T, Hoshida S, Yamashita N, Fuji H, Oe H, Hori M, Kamada T, Tada M. Delayed effect of sublethal ischemia on the acquisition of tolerance to ischemia. *Circ Res.* 1993;72:1293–9.
89. Murry CE, Jennings RB, Reimer KA. Preconditioning with ischemia: a delay of lethal cell injury in ischemic myocardium. *Circulation.* 1986;74:1124–36.
90. Murry CE, Richard VJ, Jennings RB, Reimer KA. Myocardial protection is lost before contractile function recovers from ischemic preconditioning. *Am J Physiol.* 1991;260:H796–804. *Heart Circ Physiol* 29.
91. Donnelly TJ, Sievers RE, Vissern FL, Welch WJ, Wolfe CL. Heat shock protein induction in rat hearts: a role for improved myocardial salvage after ischemia and reperfusion? *Circulation.* 1992;85:769–78.
92. Currie RW, Tanguay RM, Kingma Jr JG. Heat-shock response and limitation of tissue necrosis during occlusion/reperfusion in rabbit hearts. *Circulation.* 1993;87:963–71.
93. Hutter MM, Sievers RE, Barbosa V, Wolfe CL. Heat-shock protein induction in rat hearts: a direct correlation between the amount of heat-shock protein induced and the degree of myocardial protection. *Circulation.* 1994;89:355–60.
94. Williams RS, Thomas JA, Fina M, German Z, Benjamin IJ. Human heat shock protein 70 (hsp70) protects murine cells from injury during metabolic stress. *J Clin Invest.* 1993;92:503–8.
95. Mestrlil R, Chi SH, Sayen MR, O'Reilly K, Dillman WH. Expression of inducible stress protein 70 in rat heart myogenic cells confers protection against stimulated ischemia-induced injury. *J Clin Invest.* 1994;93:759–67.
96. Okubo S, Wildner O, Shah MR, Chelliah JC, Hess ML, Kukreja RC. Gene transfer of heat shock protein 70 reduces infarct size in vivo after ischemia/reperfusion in the rabbit heart. *Circulation.* 2001;103:877–81.
97. Plumier JC, Ross BM, Currie RW, Angelidis CE, Kazlaris H, Kollias G, Pagoulatos GN. Transgenic mice expressing the human heat shock protein 70 have improved post-ischemic myocardial recovery. *J Clin Invest.* 1995;95:1854–60.
98. Marber MS, Mestrlil R, Chi SH, Sayen MR, Yellon DM, Dillmann WH. Overexpression of the rat inducible 70-kD heat stress protein in a transgenic mouse increases the resistance of the heart to ischemic injury. *J Clin Invest.* 1995;95:1446–56.
99. Radford NB, Fina M, Benjamin IJ, Moreadith RW, Graves KH, Zhao P, Gavva S, Wiethoff A, Sherry AD, Malloy CR, Williams RS. Cardioprotective effects of 70-kDa heat shock protein transgenic mice. *Proc Natl Acad Sci U S A.* 1996;93:2339–42.
100. Hutter JJ, Mesril R, Tam WK, Sievers RE, Dillmann WH, Wolfe CL. Overexpression of heat shock protein 72 in transgenic mice decreases infarct size in vivo. *Circulation.* 1996;94:1408–11.
101. Gibbons RJ, Abrams J, Chatterjee K, Daley J, Deedwania PC, Douglas JS, Ferguson Jr TB, Fihn SD, Fraker Jr TD, Gardin JM,

- O'Rourke RA, Pasternak RC, Williams SV. ACC/AHA 2002 guideline update for the management of patients with chronic stable angina—summary article: a report of the American College of Cardiology/American Heart Association Task Force on practice guidelines (Committee on the Management of Patients With Chronic Stable Angina). *Circulation*. 2003;107:149–58.
102. Bridges CR, Horvath KA, Nugent WC, Shahian DM, Haan CK, Shemin RJ, Allen KB, Edwards FH. The Society of Thoracic Surgeons practice guideline series: transmyocardial laser revascularization. *Ann Thorac Surg*. 2004;77:1494–502.
103. Diegeler A, Cheng D, Allen K, Weisel R, Lutter G, Sartori M, Asai T, Aaberge L, Horvath K, Martin J. Transmyocardial laser revascularization: a consensus statement of the International Society of Minimally Invasive Cardiothoracic Surgery (ISMICS) 2006. *Innovations*. 2006;1:314–22.
104. Fihn SD, Gardin JM, Abrams J, Berra K, Blankenship JC, Dallas P, Douglas PS, Foody JM, Gerber TC, Hinderliter AL, King III SB, Kligfield PD, Krumholz HM, Kwong RYK, Lim MJ, Linderbaum JA, Mack MJ, Munger MA, Prager RL, Sabik JF, Shaw LJ, Sikkema JD, Smith Jr CR, Smith Jr SC, Spertus JA, Williams SV. 2012 ACCF/AHA/ACP/AATS/PCNA/SCAI/STS guideline for the diagnosis and management of patients with stable ischemic heart disease: a report of the American College of Cardiology Foundation/American Heart Association Task Force on Practice Guidelines, and the American College of Physicians, American Association for Thoracic Surgery, Preventive Cardiovascular Nurses Association, Society for Cardiovascular Angiography and Interventions, and Society of Thoracic Surgeons. *Circulation*. 2012;126:e354–471.
105. Peterson ED, Kaul P, Kaczmarek RG, Hammill BG, Armstrong PW, Bridges CR, Ferguson TB. From controlled trials to clinical practice: monitoring transmyocardial revascularization use and outcomes. *J Am Coll Cardiol*. 2003;42:1611–6.

The Impact of Various Wavelength Lasers on Myocardial Function following Transmyocardial Laser Revascularization

21

Keith A. Horvath and Cristian Militaru

Introduction

The treatment of angina has gone a long way and has taken many turns. Procedures like coronary artery bypass grafting (CABG) and percutaneous coronary intervention (PCI) have proven themselves as viable solutions for many, but not all. A growing number of patients are unable to be treated by these methods primarily because of the diffuse nature of their disease. It is for these end-stage coronary disease patients, that transmyocardial laser revascularization (TMLR) was developed. This chapter will explore the influence of specific laser parameters on laser-tissue interactions, the results of studies involving TMLR or TMLR in conjunction with CABG, and finally will analyze the possible mechanisms of TMLR.

Historical Perspective

The concept of myocardial vascularization directly from the ventricular cavity was developed over many years through the strenuous work and forward thinking of pioneers. Their work helped in the development of new and better treatment techniques, and, perhaps even more importantly, in the understanding of the anatomy and pathophysiology of coronary disease. While a detailed history of their findings in this field is beyond the scope of this chapter, we feel that a brief

summary would help the reader better comprehend the development of ideas and methods in use today.

The discovery of direct vascular communications between coronary arteries and ventricles, by Vieussens (royal physician of Louis XIV) and Thebesius, dates back to the beginning of the 18th century [1, 2]. These communications were later named the Thebesian veins. Two hundred years later, examining in the morgue, the hearts of two patients who had suffered from chronic syphilitic aortitis, American doctors Leary and Wearn discovered that both patients' coronary orifices had been occluded by the disease. The finding was surprising because although the lesions were obviously chronic, the patients had no apparent physical effort limitations in the years prior to their death, "These two people were able to work and go about their daily lives with their coronary arteries completely occluded" [3]. The discovery begged the question: where did the heart get sufficient blood supply from? The only viable answer in the authors' opinion was the Thebesian veins.

Another doctor whose contributions are worth mentioning is Claude Beck. He postulated that the inflammatory response in the myocardium stimulates arteriogenesis. He successfully tested his theory by adding foreign objects like powdered beef bone or asbestos to the surface of the heart and thus producing inflammation [4]. He also performed myopexy and omentopexy in an effort to stimulate collateral blood flow. After that, Beck tried to bring oxygenated blood to the coronaries by "arterialization of the coronary sinus", a surgery that used the brachial artery as a graft connecting the aorta to the coronary sinus [5]. This operation was first applied to patients in 1948, on a beating heart, years before the development of cardiopulmonary bypass and CABG.

The procedure that probably received the most attention was the Vineberg surgery. Dr. Arthur Vineberg, a Canadian cardiac surgeon, began implanting the left internal mammary artery (IMA) into the myocardium in 1946 (Fig. 21.1). The technique relied on the idea that anastomosis between the graft and the microcirculation of the myocardium would develop [6]. Angiographic, histologic and functional

K.A. Horvath, MD (✉)

Cardiothoracic Surgery Research Program, National Heart, Lung, and Blood Institute, National Institutes of Health, Bethesda, MD, USA

e-mail: horvathka@nhlbi.nih.gov

C. Militaru, MD

Cardiothoracic Surgery Research Program, National Heart, Lung, and Blood Institute, National Institutes of Health, Bethesda, MD, USA

Department of Surgery, Carol Davila University of Medicine and Pharmacy, Bucharest, Romania

e-mail: crmilitaru@gmail.com

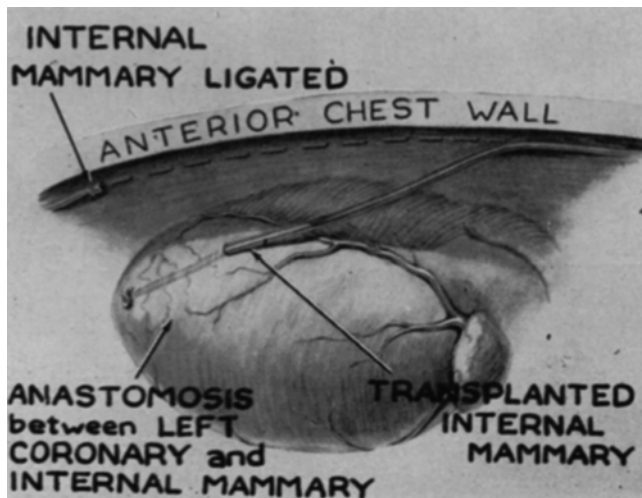


Fig. 21.1 Drawing showing internal mammary artery implant into the myocardium (Vineberg surgery) (From Vineberg and Miller [7] with permission)

evidence confirmed his theory. It showed that the IMA implant was patent, that it had extensive communications with the myocardial circulation, and that it improved survival after coronary artery ligation in an animal model [7]. The first human Vineberg surgery took place in 1950 and, although the patient died 62 h later, the second patient to undergo the operation lived for another 10 years. Afterwards, the method was improved and, consequently, so were the results [8]. Interestingly, angiographic evaluation of a patient, 21 years after the procedure, confirmed that the mammary implant was still permeable and still supplying blood to the myocardium [9].

In 1965 Dr. P. K. Sen, of Bombay, India, reported the use of a unique approach to direct myocardial revascularization [10]. Based on the observation of the reptilian heart, where most of the blood supply comes directly from the ventricular cavity, Sen used needles to create small channels in the myocardium, which would communicate directly to the ventricular chamber. Using a canine model with the left anterior descending coronary artery (LAD) ligation, he showed that the technique resulted in decreased mortality, increased long-term survival, and decreased infarct size.

Later, in 1981, Mirhoseini and Cayton used a carbon dioxide (CO₂) laser (0–400 W), instead of needles, to create channels in the canine myocardium [11]. After ligation of the LAD, they divided the dogs into four groups: the first group received laser treatment to the entire area perfused by the LAD, the second group had only 1 cm² of their myocardium treated, the third had the entire area perfused by the LAD laser-perforated prior to the coronary ligation, and the fourth group was the control group with no laser treatment. All the animals in the control group died within 20 min, whereas the survival rate in the other groups was: group I – 83 %, group

II – 33 % and group III – 100 %. In 1983, Mirhoseini et al. used transmyocardial laser revascularization in conjunction with CABG on a patient, with satisfying results [12].

Laser-Tissue Interactions

The subject of laser-tissue interactions has been an area of significant debate over the last decades, ever since laser first found its medical application. Obviously, an exhaustive discussion of all aspects of laser-tissue interaction is not practical, so we will just focus on understanding the fundamental mechanisms in the context of TMLR.

The type of interactions between the photon beam and the molecules of the target tissue is determined on the one hand by laser parameters and on the other hand by tissue characteristics. We will now present the most important laser and tissue characteristics when it comes to TMLR, the types of interactions that may occur, and their dependence on the aforementioned characteristics.

Laser Parameters

Laser stands for “light amplification by stimulated emission of radiation” and is basically an intense beam of coherent light. Its coherence is both spatial, which means that the light is focused on a small spot, and also temporal, i.e., the light has a very narrow spectrum. The light produced by the laser can be continuous or pulsatile. A pulsed laser can deliver pulses of light at varying frequencies (number of pulses per unit of time) and of varying durations. On the other hand, a continuous wave laser emits a photon beam whose output power is constant over time.

The most important laser parameters are wavelength, energy, exposure time, power (energy/time) and irradiance (power/area). The wavelength of the photons determines the color of the light produced, and since all the photons emitted by the laser have basically the same wavelength, the laser light is monochromatic (Fig. 21.2). The wavelength also determines which elements of the target tissue (proteins, DNA, melanin, hemoglobin, or water) absorb the photon energy, but this will be discussed in length in the next subchapter. The wavelength (λ) is inversely proportional to the frequency (ν), which in turn is directly proportional to the energy (E) of the photon, as shown by *Planck’s relation*:

$$E = h\nu$$

where h is *Planck’s constant* = $6.62606957 \times 10^{-34}$ m²kg/s.

Another relevant parameter is the power of the laser, i.e., the energy delivered in a unit of time. Lasers with a small pulse duration (e.g., Ho:YAG laser, excimer laser) produce higher power than lasers with longer pulse duration (e.g., CO₂

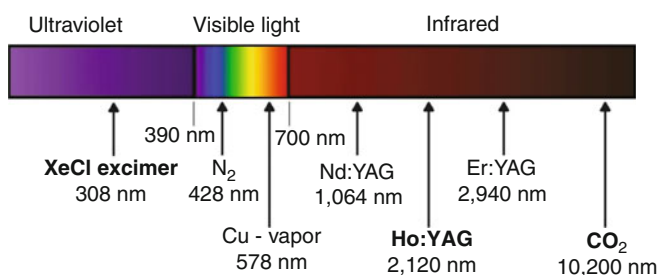


Fig. 21.2 A diagram of the electromagnetic spectrum, showing lasers across the range of wavelengths. In bold lasers used in TMLR

laser), even though they poses less energy. As we will see later in the chapter, the relationship between these two parameters will be essential in the effects lasers have on myocardial tissue, both on the depth of ablation and on the degree of collateral damage.

Optic Tissue Characteristics

Firstly, it is worth mentioning that when interacting with biological tissue laser light is treated as photons. This is because biological tissue is “an inhomogeneous mix of compounds, many with unknown properties, at unknown and varying quantities and distributed in variable and largely unknown fashion” [13]. So, trying to apply Maxwell’s equations (i.e., treat light as a wave) would only result in an insoluble mathematical problem. Thus, light is considered to be made up of particles (photons) and, this way, probabilistic mathematical formulas can be used.

When the laser photons collide with the target tissue, one of the following can happen:

1. Some photons will reflect off the tissue surface; this is determined by the refractive index (n) of the tissue. Note that the refractive index of the same surface can vary depending on the light wavelength (see Sellmeier’s formula), so different lasers reflect in different proportions off the same myocardial surface.
2. The majority of the photons will enter the tissue, upon which the following can happen:
 - (a) Some photons are absorbed (their energy is absorbed by the molecules) and can trigger thermal, chemical or mechanical reactions.
 - (b) Some photons are not absorbed, but deflected towards other molecules (*scattered*), and the process repeats itself until the photon may be absorbed.

The type of interaction is determined not only by the laser wavelength, but also by the composition of the tissue. If the target molecule naturally vibrates at frequencies similar to the frequencies of the photon that hits it, this molecule

absorbs most of the photon’s energy. If, on the other hand, the frequencies are not similar, only a small portion of the photon energy is absorbed and the photon is scattered towards other molecules with which it interacts in the same way, and the process continues until the all the photon’s energy is absorbed. If scattering is significant, photons are determined to travel from molecule to molecule in directions other than the one intended, thus producing collateral damage. Likewise, if absorption is dominant, the photons will quickly penetrate the tissue, theoretically in the direction chosen by the operator. Unfortunately laser-tissue interactions are not as simple as we, deliberately, made them look. For example, even if the energy of the photons is absorbed only by target molecules and none others, the type of interaction it determines can still produce mechanical collateral damage, as is the case of tissue rupture after explosive vaporization. Not to mention the fact that a certain degree of collateral damage may even be benefic in the specific case of TMLR. It is vital, therefore, to choose the types of lasers whose wavelengths are appropriate for the tissue they target, and also for the type of effects they seek to produce.

Let’s turn the discussion to absorption in particular since energy absorption is the crucial event that allows for any further effect to take place. How much of this outside energy is absorbed in the unit of time and space determines whether the effects are benefic or destructive, and whether the type of reaction it produces inside the molecules is photochemical, photothermal, or photomechanical. Light of different wavelengths is absorbed by different molecules. The substances that absorb light are called *chromophores*.

The principal myocardial tissue chromophores in relationship to the laser wavelength are as follows [14]:

- I. In ultraviolet (UV) light the principal chromophores are proteins, DNA and melanin. At shorter wavelengths, the peptide bond ($O=C-N-H$), which is the brick of all proteins, is the principal light absorber; its maximal absorption being around 190 nm, although it remains significant to 240 nm. As the wavelength becomes longer, DNA, the aromatic amino acid residues, and melanin, start absorbing most of the light. The only UV laser used in TMLR is the XeCl excimer laser, which has a λ of 308 nm. Other excimer lasers, like ArF excimer laser ($\lambda=193$ nm), could also be used in theory, but either have not been sufficiently studied, or are believed to be cytotoxic and mutagenic because of their effect on DNA.
- II. In the visible spectrum, melanin and hemoglobin dominate the absorption. Melanin absorption drops monotonically with the increase in wavelength; as such, the absorption at 780 nm is roughly 5 times lower than that at 400 nm [15, 16]. Hemoglobin is more important when it comes to the myocardial tissue, and can be present in both deoxygenated (Hb) and oxygenated (HbO₂) forms.

Hb absorption peaks in the violet at $\lambda=433$ nm, then drops, only to have another peak at $\lambda=556$ nm. HbO₂ has a similar behavior, with maximum absorptions at $\lambda=414$, 542, and 576 nm. Although the absorption drops with infrared radiation, hemoglobin still plays a significant role in highly vascularized tissues, as proven by Horecker back in 1943 [17]. At the moment there are no lasers that emit light in the visible spectrum that are used in TMLR.

- III. In the infrared (IR) light, water is the most important chromophore. As mentioned before, hemoglobin plays a role, as do proteins (especially collagen), but, by and large, water absorption is the one that counts. The absorption coefficient (μ_a) increases constantly in relation to the wavelength, achieving peaks at 960, 1440, 1950, 2940, 4680 and 6100 nm [100], the maximum being at 2940 nm. Optical absorption continues to be important through wavelengths of 10–15 μm , and even in the far IR. The only two Food and Drug Administration (FDA) approved lasers for TMLR are IR lasers: Ho:YAG, $\lambda=2100$ nm, and CO₂ at $\lambda=10,200$ nm.

Types of Laser-Tissue Interactions

The multitude of combinations between the laser parameters and tissue characteristics result in an almost infinite number of potential interactions. Even so, these interactions can be divided into five main groups: photochemical, photothermal, photoablation, plasma-induced ablation and photodisruption. Each of these will be discussed briefly with emphasis on the specific case of TMLR. For a more detailed review we highly recommend the reader see the *Interaction Mechanisms* chapter from Markolf Niemz' book [18].

Before going further, two observations are worth making. Firstly, the fact that even though the lasers' radiant exposure (energy/area) ranges just from approximately 1 J/cm² to 1000 J/cm², the irradiance (power/area) ranges by 15 orders of magnitude. Thus, one can conclude that a sole parameter, the time of exposure, has the greatest influence on the mechanism of interaction. Secondly, it is important to understand that these types of interactions cannot be completely separated and that often they overlap. For example, ultrashort pulses of 100 ps, which taken separately have no thermal effect, when applied in repetition at rates of 20 Hz or higher, may add up to significant increases in temperature [18].

Photochemical Interactions

Photochemical interactions are negligible when it comes to TMLR, so we will only briefly address them. Empirical observations have shown that light can produce chemical reactions within the molecules and tissue that it is applied to.

One obvious example is the process of photosynthesis that takes place in plants. Photochemical interactions take place when low irradiance light (generally about 1 W/cm²) is applied over very long periods of time, ranging from seconds to hours. In most cases the wavelengths fall within the visible spectrum and scattering is dominant. Their most preeminent medical use is during *photodynamic therapy* (PDT), a form of phototherapy that combines a drug (photosensitizer) with laser light of a specific wavelength. The photosensitizer is a nontoxic drug that, when exposed to a certain wavelength, becomes toxic. PDT is mostly used in cancer treatment, and relies on the fact that the photosensitizer is absorbed by cells all over the body but stays in malignant cells longer than it does in normal cells. After the photosensitizer has been eliminated from all but the cancer cells, laser light is applied, which makes the photosensitizer to produce reactive oxygen species, thus harming the tumor.

Photothermal Interactions

The term *photothermal interactions* stands for a large group of interaction types resulting from the transformation of absorbed light energy to heat. While the photochemical interactions are governed by precise laws and follow a specific reaction pathway, photothermal reactions tend to be non-specific. Depending on the duration and temperature increase, one of the following processes can be distinguished: coagulation, vaporization, carbonization and melting (Table 21.1). Often more than one thermal effect is induced in the biological tissue, even ranging from carbonization at the surface to just hyperthermia a few millimeters inside the tissue. As such, the exact threshold of cell necrosis at a given depth is hard to determine and depends largely on the time of exposure. Given sufficient time, heat transfer inside the myocardial tissue is also governed by the laws of thermodynamics that apply to any other material: firstly, energy is conserved, and secondly, heat flows from areas of high temperature to areas of lower temperature. Typically, photothermal processes take place at pulse durations of 1 μs up to 1 s and irradiances of 10–10⁶ W/cm², and are the most prevalent interaction when it comes to the lasers used in TMLR.

Collateral thermal damage can be caused in two particular ways: either by direct deposition of heat below the point where the energy density is sufficient enough for ablation, or by thermal diffusion from the heated tissue to the surrounding cooler tissue. Apart from these though, there is still a very important way of causing collateral damage, photomechanical interactions. As the temperature increases to 100 °C most water molecules start to vaporize. At first this vaporization is advantageous because the generated vapor carries away excess heat and helps prevent a further increase in temperature. But as the laser beam advances and the vapor

Table 21.1 Thermal effects of laser radiation in relationship to the temperature achieved (Adapted from Niemz [18])

Temperature (°C)	Biological effect
37	Normal
45	Hyperthermia
50	Reduction in enzyme activity, cell immobility
60	Denaturation of proteins and collagen, coagulation
80	Permeability of membranes
100	Vaporization, thermal decomposition (ablation)
>100	Carbonization
>300 °C	Melting

cannot quickly evaporate up the portion of the channel already created, the large increase in volume leads to gas bubbles formation. While trying to escape out of the tissue, the bubbles will likely tear the tissue along the path of least resistance, which is along the long axis of the muscle cells. The rapid volume expansion will also produce acoustic shock waves that damage nearby tissue. This entire process is called *explosive vaporization* and is particularly important during TMLR. It is very likely that this type of laser-tissue interaction is detrimental to cardiac architecture, function and electrical conduction, and should be avoided.

With regards to the heat diffusion and subsequent thermal collateral damage, it is obvious that the longer the pulse, the more time for heat to dissipate and damage the surrounding tissue. The irony is that by trying to avoid this side effect and making the pulses shorter, the laser's power (energy/time) will increase, causing the ablation process to be even more explosive and potentially do more mechanical damage. While the exact optimal laser parameters are unknown, it appears that the Ho:YAG laser has been associated with greater tissue injury due to its multiple short pulses, while the single pulse CO₂ laser seems to produce less damage. More on that in the section *TMLR-specific laser parameters* below.

Photoablation

Photoablation relies on the fact that, when exposed to high intensity laser radiation, the monomers, that make up a polymer, can change from an attractive to a repulsive state. This chance is associated with an increase in the volume occupied by each monomer, leading to expulsion, and thus to the process of ablation. For simplicity's sake, the process of photoablation can be divided into five stages, as follows:

1. absorption of high-energy UV photons
2. promotion to repulsive excited states
3. dissociation
4. ejection of fragments (but no necrosis)
5. ablation.

In contrast to explosive vaporization, the entire process is closer to a photochemical interaction in nature, and thus more exact. The main advantages of this ablation technique lie in the precision of the etching process, its excellent predictability, and the theoretical lack of collateral damage to adjacent tissue [13]. If however the photon energy is not high enough, the molecule is only promoted to a vibrational state, rather than to a repulsive state. The absorbed energy then dissipates to heat and the molecule returns to its original state.

In theory, lasers with wavelengths shorter than 350 nm have high enough photon energy for monomers' promotion to repulsive states and the dissociation of the C–C bonds. In reality, pure photoablation is only observed for wavelengths such as that of the 193 nm ArF excimer laser [18]. Higher wavelengths are usually associated with a more prevalent thermal component [19–21]. In particular the XeCl laser ($\lambda=308$ nm) used in TMLR was a dominant photothermal effect, similar to the infrared lasers. Also similar to the CO₂ and Ho:YAG lasers is the resulting mechanical damage produced by the vapor bubble formation.

Plasma-Induced Ablation

Plasma-induced ablation involves the use of ultrashort pulses (in the order of magnitude of femtoseconds and picoseconds) and peak irradiances of 10^{11} – 10^{13} W/cm², which are not characteristic to lasers currently used for TMLR. Using such parameters causes the target material to become ionized. The result is a small cloud of free positive ions and negative electrons known as *plasma*. The entire process, also called *dielectric breakdown*, is based on an avalanche effect caused by a free electron absorbing a photon, accelerating, colliding with an atom, ionizing it, resulting in another two free electrons that can follow the same path. This process continues as long as the electric field strength E produced by the laser remains strong enough. So, E is the crucial parameter for the onset and continuation of plasma-induced ablation and is directly proportional to the power density (irradiance) of the laser.

Once formed, the plasma becomes self-absorbing, causing the subsequent laser energy to be efficiently coupled in the growing plasma. The important consequence of this phenomenon is the efficient energy deposition in nominally weakly absorbing tissue. This is due to the increased absorption coefficient of the induced plasma.

Photodisruption

For didactic purposes, we neglected any secondary side effects when discussing plasma-induced ablation. Those side effects (shock wave formation, cavitation and jet formation)

will be briefly discussed below as part of what is called *photodisruption*. At higher laser energies, and thus higher plasma energies, these mechanical side effects become increasingly significant. This is due to the fact that mechanical effects scale linearly with the absorbed energy. Plasma-induced ablation is limited to a rather narrow range of pulse durations up to approximately 500 ps. At longer pulse durations, the energy density necessary for achieving breakdown already induces significant mechanical side effects [18].

During plasma formation, local temperature can reach thousands of degrees Celsius, causing rapid volume expansion and formation of shock waves that diffuse in the surrounding medium, in a way similar to the explosive vaporization caused by the photothermal interactions. Roughly 50–150 ns after the initial laser pulse, tissue water evaporates, resulting in vapor induced mechanical stress and formation of a cavitation bubble. The cavitation bubble performs several oscillations of expansion and collapses within a period of a few hundred microseconds, rupturing the surrounding tissue and producing an explosive ablation process.

TMLR-Specific Laser Parameters

Numerous mechanical devices [22, 23], including ultrasound [24], cryoablation [25], radiofrequency [26] and needles [27, 28], have been used to create channels through the myocardium. Additionally, a large variety of laser wavelengths have also been employed experimentally: neodymium:YAG (Nd:YAG) [29], erbium:YAG (Er:YAG) [30], xenon chloride (XeCl), holmium:YAG (Ho:YAG) and carbon dioxide (CO₂), with the latter three also being used clinically. Still, the only ones approved by the FDA and used in large-scale clinical practice are the Ho:YAG and the CO₂ lasers. The characteristics of these lasers and their specific ablation process will be presented below, followed by the operative TMLR technique.

The Ho:YAG laser is an infrared (2,120 nm) pulsed laser, producing pulses of 200 μs that are emitted through a flexible 1 mm optical fiber. The CardioGenesis Corp laser system, the most widely used Ho:YAG laser, produces energies of 1–2 J/pulse, resulting in an average power of 6–8 W/pulse and irradiances of 6–8 W/mm². It takes approximately 20 pulses to create a transmural channel. Despite the relatively low energy level, there are high peak power levels delivered to the tissue, resulting in explosive vaporization with each pulse (Fig. 21.3). Another potential shortcoming arises from the fact that the optic fiber has to be manually advanced through the myocardium, and it is therefore difficult to know if the channel is being created by the laser ablation or the mechanical kinetic effect of the advancing fiber.

By contrast, the CO₂ laser uses a single laser pulse to create the channel, and because of this the process has also been called continuous laser ablation (to differentiate from pulsed laser ablation). The clinically approved PLC Medical Systems CO₂ laser system is set to deliver 800 W in a pulse 1–99 ms long at energies of 8–80 J to create 1 mm diameter channels (Fig. 21.4). It should be noted that although the average pulse duration is 25–40 ms, the actual interaction time within a single myocardial zone is approximately 24 μs because the ablation front moves at a speed of 500 mm/s [13]. Under these conditions, the laser photons do not cause explosive ablation and the collateral structural damage is minimized (Fig. 21.3). Additionally, the CO₂ laser is synchronized to fire on the R wave of the ECG when there is maximal ventricular filling and electrical quiescence. The Ho:YAG laser device is unsynchronized, and also due to the motion of the fiber through the myocardium during the cardiac cycles, it is more prone to ventricular arrhythmias.

When compared side-by-side, the results indicate that although the Ho:YAG laser can create channels smaller in diameter, it causes up to six times more collateral damage compared to the CO₂ laser [31]. This is likely due to both laser-tissue interactions at different wavelengths, as previously detailed, as well as to the differences in laser system parameters and actual laser delivery method. Kitade et al. also found that the Ho:YAG laser created a layer of 760 ± 288 μm of thermal damage, while the CO₂ laser only caused 249 ± 83 μm of damage to the surrounding tissue [32]. Another histopathology report also confirmed the fact that collateral damage is initially greater when using the Ho:YAG laser, but was unable to see a significant scar difference at 6 weeks [33]. Even though the exact mechanism of TMLR is still debatable, a strong case can be made that the explosive vaporization garnered by the Ho:YAG laser ablation does not improve cardiac function or perfusion [31, 34, 35]. This is also supported by the results of the randomized clinical trials that showed improved perfusion tests for the CO₂ treated patients, but not for those treated with holmium laser. More on that in the section *Clinical trials* below.

Finally, the XeCl laser operates with ultraviolet (308 nm) light and uses a 1 mm fiber embedded steel tip to advance through the myocardium, much like the Ho:YAG laser. The standard operating parameters for the laser are pulses of 110 ns with energies of 32–40 mJ/pulse, resulting in an average power of 0.2 W per pulse and irradiances of 0.26 W/mm². The maximum number of pulses per cardiac cycle is 5 and it takes 3–4 triggered cardiac cycles to create the transmural channel. As previously discussed, even if theoretically, being an UV laser, the XeCl excimer should employ photobleaching, in reality, its action mechanism is mostly photothermal, much like the IR lasers. And finally, also being a pulsed laser, its ablation process is closely related to the one of the Ho:YAG laser.

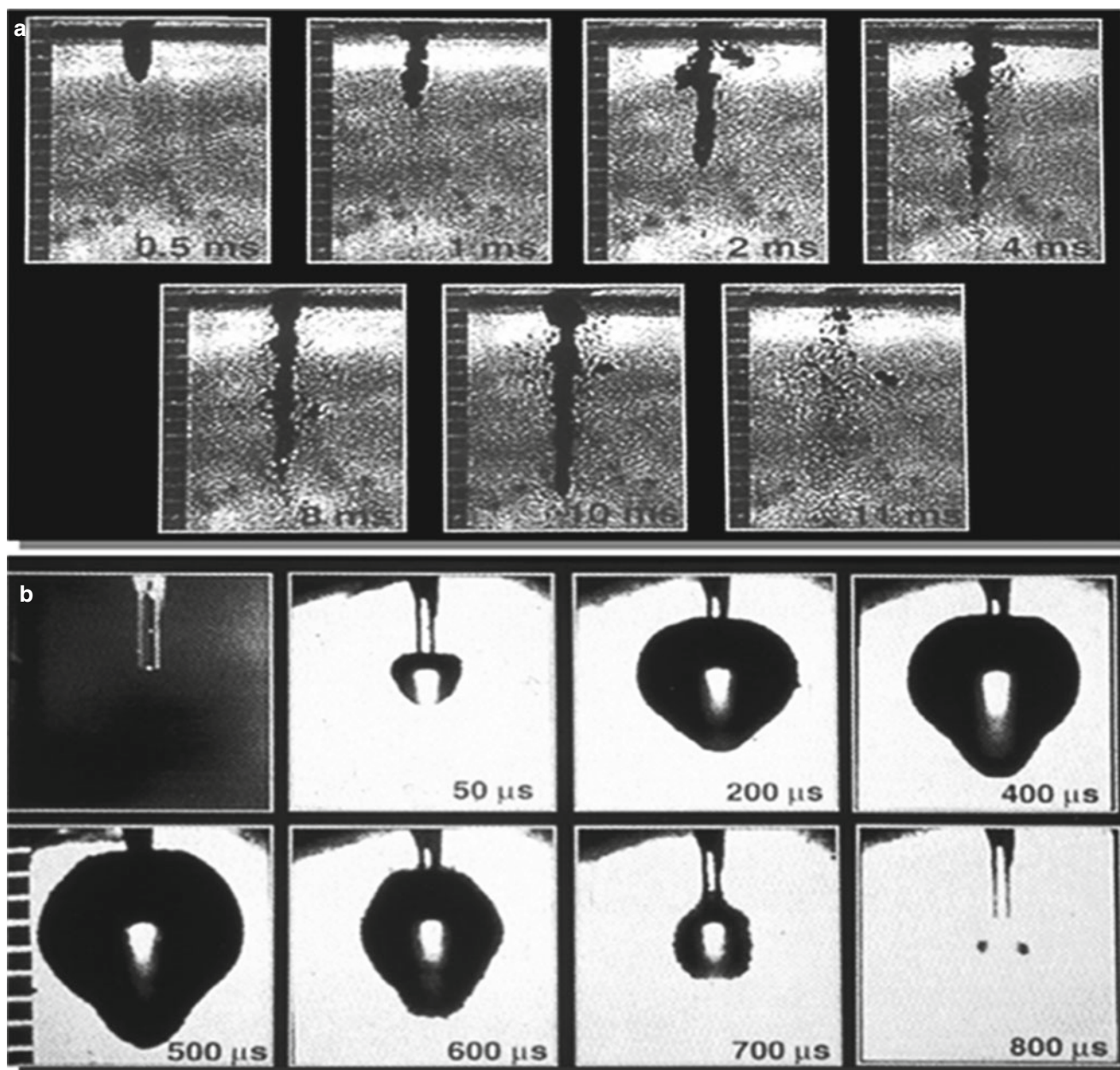


Fig. 21.3 Sequential photography of the firing of a single pulse from a CO₂ laser (a) and a Ho:YAG laser (b) into water. The pulse duration and energy levels are the same as those being used clinically

Operative Technique

TMLR can be used as a sole-therapy or in conjunction with CABG. When used as a sole-therapy, the patient undergoes a left anterior thoracotomy in the fifth intercostal space after general anesthesia is established. Once the ribs are spread by a retractor, the left lung is deflated and the pericardium is open to expose the epicardial surface of the left heart (Fig. 21.4). Care must be taken to avoid previous bypass grafts and to physically manipulate the heart as little as possible. Channels are created starting at the base of the heart

and then serially in lines approximately 1 cm apart towards the apex, starting inferiorly and working superiorly to the anterior surface of the heart. The exact number of channels created depends upon the ischemic area and the size of the heart. The areas where the myocardium is thinned by scar should be avoided, as TMLR will not be beneficial and excessive bleeding may become a problem. Transesophageal echography can be used to confirm transmural penetration of the laser beam. The vaporization of blood as the laser jet enters the ventricle creates a characteristic acoustic effect easily seen through an echography. For select patients, in

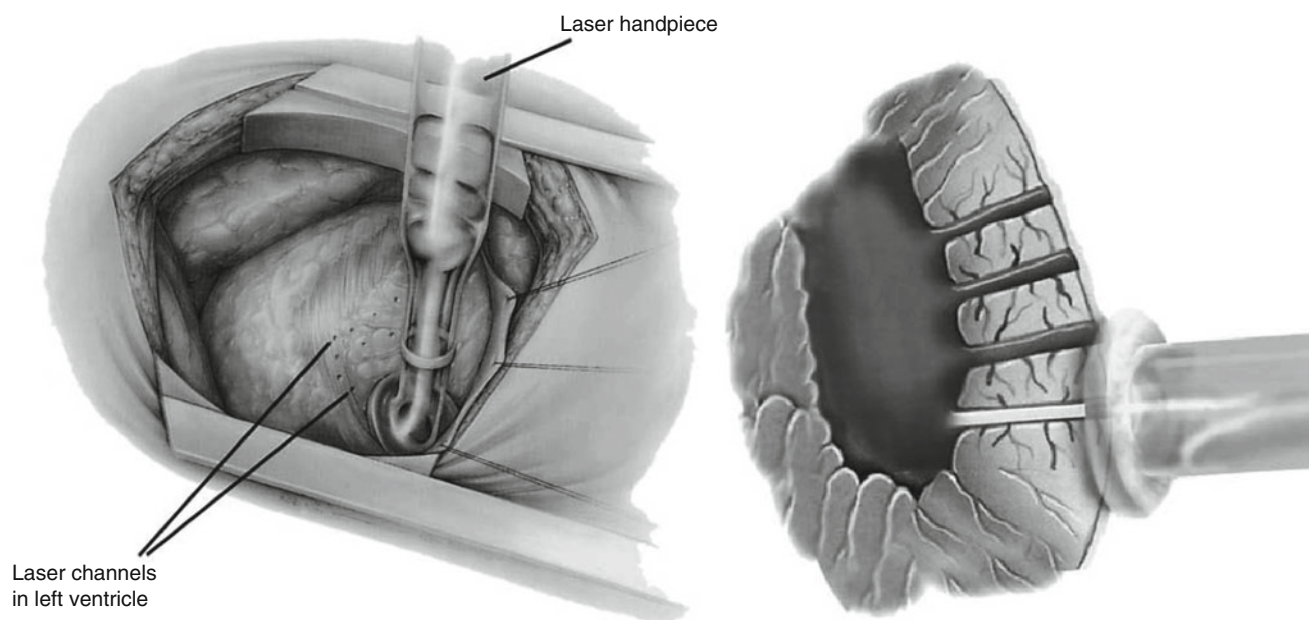


Fig. 21.4 Open transmyocardial revascularization with the CO₂ laser system (From Estvold et al. [31] with permission from John Wiley and Sons)

order to minimize postoperative incisional pain, the procedure can also be performed robotically or with video-assisted thoracoscopy [36]. When it comes to performing TMLR in conjunction with on-pump CABG, the main difference is that the heart is not moving and this facilitates creation of the channels with the exact desired distribution.

Clinical Trials

Sole TMLR Therapy

The safety and efficiency of TMLR, previously demonstrated in a series of nonrandomized studies [35, 37–42], was also confirmed by the controlled randomized trials [43–48] (Table 21.2). As part of these pivotal studies, over 1000 patients with severe refractory angina were enrolled and randomized to receive either TMLR or conservative medical therapy. The common inclusion criteria were the following: patients suffered from severe refractory angina that was not amendable to standard reperfusion therapy (PCI or CABG), and had a left ventricular ejection fraction (LVEF) greater than 25%. The patients were randomly assigned to TMLR or medical management (MM), and as such, there were no significant demographic or risk factors differences between the TMLR and the MM group. The characteristics of the TMLR group in each of the six studies are presented in Table 21.2. Patients' average age was 62, the majority were male and had a mildly diminished ejection fraction (48%). All patients had classes III (39%) or IV (61%) angina according to the Canadian Cardiovascular Society (CCS) class. A large

portion of the patients had undergone CABG or PCI prior to the TMLR. Two studies [43, 44] permitted crossover from MM to TMLR in case the failure criteria was met (angina unweanable from intravenous antianginal medication), while the others did not. Finally, three of the studies were multi-center and the other three were developed in a single center.

Results

Mortality (Table 21.3)

Although mortality rates had been previously reported in the 10–20% range [35, 37–39, 41, 42], the prospective randomized studies reported lower perioperative mortality of 1–5% [43–48] (Fig. 21.5). The essential predicting factor of mortality appeared to be whether or not patients were suffering from unstable angina or were on IV nitroglycerin at the moment of the intervention. If patients were able to be weaned from IV medication before going into surgery, the mortality rate was as low as 1% [43]. One-year survival of the TMLR patients ranged from 84 to 95%, while the MM patients survival was reported to be 79–96%. Meta-analysis done indicated no statistically significant difference between the two groups [49].

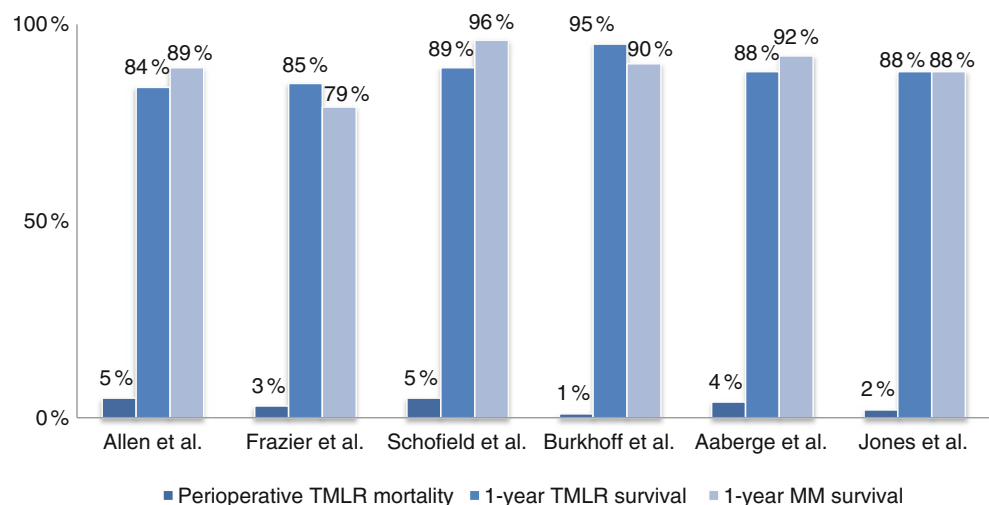
Morbidity

The exact definitions and inclusion of various conditions and complications varied between the studies' protocols making morbidity data much harder to analyze. In general, however, patients who underwent TMLR had a lower incidence of cardiac-related hospitalizations, myocardial infarction, heart

Table 21.2 Randomized control trials of transmyocardial revascularization

Characteristic	Allen et al. [43]	Frazier et al. [44]	Schofield et al. [45]	Burkhoff et al. [46]	Aaberge et al. [47]	Jones et al. [48]
Laser used	Ho:YAG	CO ₂	CO ₂	Ho:YAG	CO ₂	Ho:YAG
Number of centers	18	12	1	16	1	1
Patients (N)	275	192	188	182	100	86
Age (years)	60	61	60	63	61	62
Male gender (%)	74	81	88	89	92	100
LVEF (%)	47	50	48	50	49	46
CCS class III/IV (%) ^a	0/100	31/69	73/27	37/63	66/34	23/77
CHF (%)	17	34	9	NR	NR	NR
Diabetes (%)	46	40	19	36	22	NR
Hypertension (%)	70	65	NR	74	28	63
Prior MI (%)	64	82	73	70	70	73
Prior CABG (%)	86	92	95	90	80	87
Prior PCI (%)	48	47	29	53	38	51
Number of channels	39	36	30	18	48	NR

^a Canadian Cardiovascular Society (CCS) class [43–46, 48]; New York Heart Association (NYHA) class [47]

Table 21.3 Perioperative TMLR mortality and 1-year survival comparison between TMLR and MM in the randomized trials

failure, arrhythmias, coronary-artery bypass grafting or percutaneous angioplasty [43–48]. For example Allen et al. [43] reported Kaplan–Meier estimates of freedom from cardiac-related rehospitalization at 1 year to be significantly higher in the TMLR group (61 % vs. 33 %, $P < 0.001$).

Angina Improvement

Angina improvement is the main benefit for laser therapy. Significant angina reduction was defined as a reduction of two or more angina classes (CCS) from the baseline. Such a reduction was observed in all of the randomized trials [43–48] through the 1-year follow-up period, and this reduction was highly significant ($p < 0.001$) when compared to MM (Table 21.4). Success rates ranged from 25 to 76 % and were directly proportional to the percentage of patients who had baseline class IV angina [43–47] (Jones et al. [48] reported 83 % reduction in angina class, but was not clear about the

number of angina classes dropped). The broad range of success rates can be attributed to the differences in baseline characteristics for the patients enrolled. As stated above, the studies that had a higher percentage of patients with initial class IV angina [43, 44] had higher success rates. This is of course because it is easier to achieve a two-class angina drop when baseline angina class is IV, compared to a baseline of class III angina.

Exercise Tolerance

Four of the trials considered exercise tolerance time (ETT) as an endpoint and demonstrated improvement after TMLR [45–48]. Schofield et al. [45] employed both a symptom-limited modified Bruce treadmill test and a 12-min walk test to compare 1-year changes between TMLR and MM patients. The exercise tests showed that TMLR patients lasted an average of 40 s longer on the treadmill ($p = 0.15$) and needed to

stop the test due to angina less frequently than MM patients ($p < 0.001$). Also, the mean 12-min walk distance was 33 m longer in the TMLR group ($p = 0.1$). Burkhoff et al. [46] also used a modified Bruce treadmill exercise test and reported significant ETT improvement after TMLR (+65 vs. -46 s with MM; $p < 0.0001$). Using a cycle ergometer exercise test, Aaberge et al. [47] showed an increase in time to onset of angina at 12 months (+66 vs. -3 s, TMLR vs. MM patients; $p < 0.01$). Finally, even with preprocedure baseline ETT slightly in favor of the MM group, Jones et al. [48] reported a 1-year follow-up mean *exercise time to angina* of 490 vs. 294 s in TMLR vs. MM groups ($p = 0.0001$).

Quality of Life and Medical Treatment

Three trials used standardized questionnaires to assess the quality of life subjectively perceived by the patients. Two trials chose the Seattle Angina Questionnaire [44, 46] (Frazier

[44] also employed the 36-item Medical Outcomes Study Short-Form General Health Survey – SF36) and another used the Duke Activity Status Index [43]. The findings were consistent and statistically significant in favor of TMLR. The results also showed a significant increase in event-free survival at 1-year ($p < 0.0001$) [43, 44]. Hospital admissions reduction can also be considered an indicator of efficiency and increased quality of life. A meta-analysis of the trials’ data found out that 1-year hospital admissions were in fact four times more frequent in the MM group than the laser-treated patients [49].

All the patients included in the studies were suffering from severe refractory angina and were on a maximal anti-anginal medical therapy. Although at baseline the medication profile was similar for both arms of the trials, 1-year follow-up demonstrated reduction in nitrates, beta-blockers and Ca blockers use for the TMLR patients. One trial’s data shows that 83 % of TMLR-treated patients’ medication decreased or remained unchanged, while 86 % of MM patients’ medication increased or remained the same [44]. This goes to prove that the TMLR’s angina reduction and exercise tolerance improvements were not due to change or increase in medication.

Perfusion Tests

Most of the prospective trials obtained perfusion scans pre-operatively and as part of the follow-up [43–46, 48]. The lesions determined on the scans were deemed either as scar tissue (fixed defects) or as ischemia (reversible defects). Although the exact methodology of the nuclear scanning differs, the results are consistent in demonstrating improvement of perfusion in CO₂ laser-treated patients, and, conversely, no improvement in the Ho:YAG laser trials. Frazier et al. [44] reported a 20 % decrease in the ischemic area after TMLR and a 27 % increase of ischemia in the MM patients, but no differences in the number of fixed defects. In the other

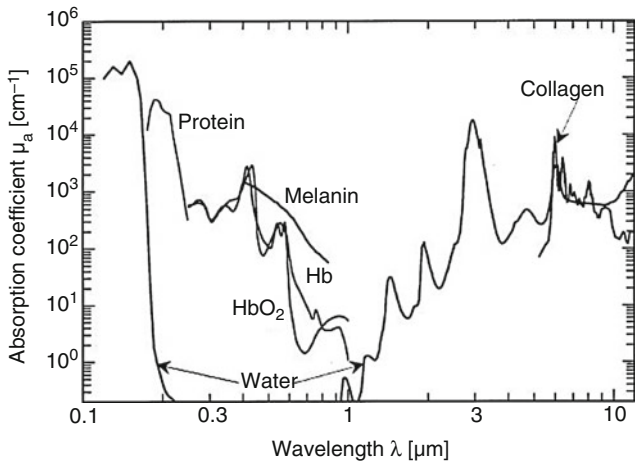


Fig. 21.5 Optical absorption coefficients of principal chromophores, in relationship to light wavelength (From Vogel and Venugopalan [14] with permission)

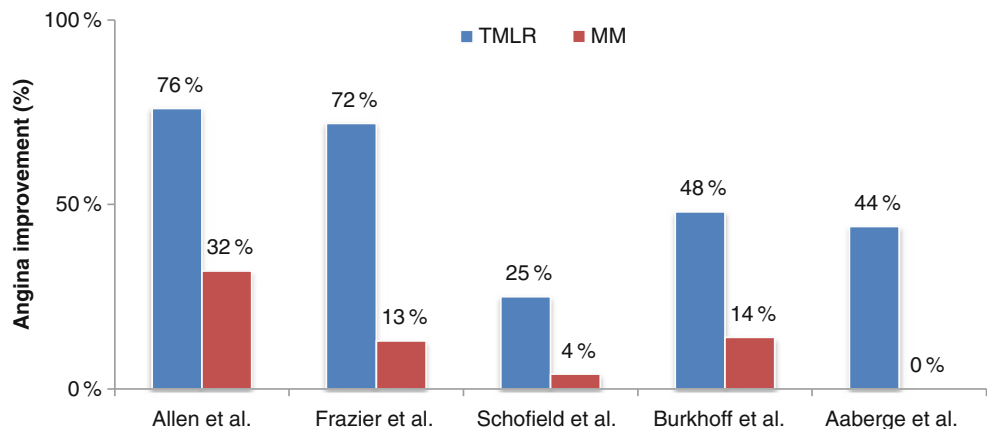


Table 21.4 Percentage of patients with improved angina (reduction of two or more CCS angina classes) after TMLR compared to MM

Meta analysis of angina improvement TMLR vs MM by Horvath [18]
 Summary odds ratio = 9.3 $p < 0.0000001$

CO₂ laser trial, Schofield et al. [45] observed a significant decrease in reversible defects in both the TMLR and MM groups. Still, a difference was evident when comparing scar tissue (fixed defects) after the 1-year follow-up. The number of fixed defects did not increase in the TMLR group but doubled under sole medical therapy. As mentioned above, none of the Ho:YAG trials [43, 46, 48] reported any significant difference in myocardial perfusion after TMLR.

Nonrandomized data had previously demonstrated improvement of perfusion in both fixed and reversible defects using isotope scanning in CO₂ TMLR-treated patients [37]. Using position emission tomography (PET) scanning, arguably the most sensitive test for myocardial perfusion, Frazier et al. [50] showed an increase in the relative perfusion of the subendocardial to epicardial areas after CO₂ TMR treatment. Interestingly, these changes were seen in patients who displayed no significant improvement in thallium scans, thus raising questions about the accuracy of the commonly used isotope scans.

Long-Term Results

Two of the studies included a long-term follow-up of the randomized patients. With regards to mortality, Aaberge et al. [51] reported four-year survival to be 78 % after TMLR and 76 % with MM (no statistical significance), while Allen et al. [52] demonstrated survival of 65 % versus 52 % in favor of TMLR ($p=0.05$) with an average annual mortality beyond 1 year of 8 % versus 13 % ($p=0.03$). With regards to angina reduction, one trial determined that 88 % TMLR vs. 44 % MM ($p<0.001$) patients were still experiencing at least a two-class angina improvement after 5 years. Importantly, 33 % of the laser-treated group were free from angina symptoms altogether, versus just 11 % of the sole medical therapy ($p=0.05$) [52]. The other long-term study also reported angina improvement (24 % vs. 3 %, TMLR vs. MM, $p=0.001$) and unstable angina hospitalizations reduction ($p<0.05$) at a mean follow-up of 43 months [51]. Nonrandomized data from a 5-year follow-up study of TMLR patients supports these findings and shows continued improvements in symptoms and quality of life [53].

Because none of the trials involving TMLR were blinded, it has been suggested that angina relief after TMLR may have resulted from the placebo effect induced by the surgical incision and the novelty of the procedure. The overwhelmingly positive 1-year results [43–48] and continued long-term improvement [51–53] mitigates the concern of placebo effect. The placebo effect would be expected to influence early outcomes in such trials, but that those outcomes would persist long-term is unlikely. Another important argument in favor of TMLR is the objective data attesting to the reduction of myocardial ischemia after isotope nuclear scanning [37, 44, 45], PET scan [50], dobutamine stress echocardiography [54] and contrast enhanced magnetic resonance imaging [55].

Based on an assessment of the cumulative results from these multiple randomized trials, the American College of Cardiology/American Heart Association (ACC/AHA) practice guidelines [56], Society of Thoracic Surgeons (STS) practice guidelines [57], and a consensus statement from the International Society of Minimally Invasive Cardiac Surgery [58] have determined that the weight of the evidence strongly favors the use of TMR in the treatment of stable, medically refractory angina patients.

TMLR as an Adjuvant to CABG

Incomplete revascularization of multivessel coronary artery disease after CABG occurs in up to 25 % of cases [59, 60] and is a strong predictor of perioperative adverse events and long-term poor prognosis [59–65]. Due to the success of TMLR as a sole therapy, it also has been evaluated in conjunction with CABG for patients with diffuse coronary disease who could not be completely revascularized with CABG alone. The safety and feasibility of the method was assessed in a couple of non-randomized trials [66–68], but the assessment was made difficult mostly due to the multitude of other factors that contribute to CABG, as well as the lack of randomized controls arms.

Two prospective, randomized trials have been performed using TMLR in conjunction with CABG [69, 70]. The baseline and operative characteristics were similar between groups in both trials, including the location and number of bypass grafts placed (3.1 ± 1.2 , CABG+TMR; 3.4 ± 1.2 , CABG alone, $p=0.07$). Importantly, patients were also blinded to their treatment group through the 1-year follow-up.

Allen and associates [69] using a Ho:YAG laser reported improved outcomes following TMLR+CABG versus CABG alone in terms of a reduced operative mortality rate (1.5 % vs. 7.6 %, $p=0.02$), reduced postoperative inotropic support required (30 % vs. 55 %, $p=0.001$) and increased 30-day freedom from major adverse cardiac events (97 % vs. 91 %, $p=0.04$). The 1-year follow-up also showed significantly increased 1-year survival (95 % vs. 89 %, $p=0.05$) and freedom from major cardiac events, defined as death or myocardial infarction (92 % vs. 86 %, $p=0.05$) in favor of the patients who also received adjuvant TMLR.

A 5-year follow-up of the patients was also performed [71]. Based on blinded independent evaluations the TMLR group experienced significantly lower mean angina scores compared to the CABG alone group (0.4 ± 0.7 vs. 0.7 ± 1.1 , $p=0.05$), a lower proportion of patients with severe angina (class III or IV), and a trend towards a greater number of angina-free patients (78 % vs. 63 %, $p=0.08$). Finally, the survival rate was similar between the groups.

In a similar randomized, prospective, multicenter study, Frazier et al. [70] also reported reduced operative mortality

(9 % vs. 33 %, $p=0.09$) and increased angina improvement at 1 year (63 % vs. 34 %, $p=0.34$) for the TMLR+CABG patients. At the 1 year mark the rate of treatment failure, defined as death, repeat revascularization, or failure to improve angina class) was nonsignificantly reduced for TMLR+CABG. During the 4-year follow-up [72] the incidence of repeat revascularization was higher after CABG alone (24 % vs. 0 %, $p<0.05$) but the mortality was similar.

Excimer Laser Trials

The CO₂ and Ho:YAG lasers operate in the infrared range and their mechanism of ablation involves vaporizing tissue water, which causes thermal and mechanical damage to the surrounding tissue (photothermal interactions). This type of ablation does not allow precise control over the collateral damage created by the bursting vapor bubbles. By contrast, the excimer XeCl laser uses ultraviolet light (308 nm), which removes tissue in a more precise manner. The nature of the process mostly involves photoablation and reduces the collateral damage created. In theory this would be a good thing, but practice has proved that a certain degree of collateral damage may be desirable particularly in triggering angiogenesis.

The efficiency and safety of the XeCl laser had been demonstrated in several uncontrolled trials [73–75] and also one randomized study [76]. Van der Sloot and associates randomized 30 patients with refractory angina to either TMLR using excimer laser or maximal medical therapy who were followed-up over 1 year. After 12 months patients treated with TMLR experienced an angina decreased from a mean class of 3.8 to a class of 1.9 and reported an increase in the quality of their lives, while angina in conservatively treated patients only decreased from 3.9 to 3.7 CCS ($p=0.000001$). Still, myocardial perfusion or exercise time was not significantly improved for the laser treated patients versus the control group. These results are in line with the ones produced by the other 2 lasers, those being an improved quality of life and decreased angina and a debatable evidence of improved cardiac perfusion or function [76].

Mechanism of Action

Channel Patency

The initial premise of TMLR was that the created transmural channels would allow oxygenated blood to flow directly from the ventricle cavity into the myocardium. This initial theory appears to be false and not the reason behind TMLR's clinical success. Although there is work showing some evidence of patency [77–80], the majority of histological

evidence has found the channels occluded, initially by thrombus and later by scar tissue [81–85]. Even if the channels were to remain open, the intramyocardial pressure during the cardiac cycle exceeds that within the ventricle cavity, making the flow of blood into the channels impossible [86–88]. The consensus is that while occasionally channels may remain open, this is not the principal mechanism of TMLR.

Denervation

Laser-induced denervation may be responsible for the angina relief experienced following TMLR. The nervous system of the heart consists of afferent neurons, postganglionic neurons, and sympathetic or parasympathetic efferent neurons. This system can function independent of the extracardiac inputs regulating cardiac functions through reflex action. Kwong and colleagues were the first to demonstrate myocardial denervation 2 weeks after Ho:YAG TMLR in a nonischemic canine model [89, 90]. Hirsch et al. and Minisi et al. [91, 92], to the contrary, found that TMLR does not affect afferent or efferent axonal function, while another study concluded that even though laser treatment may not affect afferent or extracardiac efferent neuronal function, it does “remodel” the intrinsic cardiac nervous system [93]. Al-Sheik and colleagues [94] studied regional sympathetic denervation using PET scan and demonstrated denervation in lased regions 2 months postoperatively. Other experimental work suggests that although denervation is important in the acute stage, reinnervation occurs afterwards [95, 96]. Although the studies were thoroughly carried out, the difference in results can be attributed to the fact it is difficult to isolate the nerve fibers and assess their individual function. Still, the weight of evidence suggests that TMLR does produce myocardial denervation, but whether or not it is responsible for the angina reduction is unclear.

Angiogenesis

Stimulation of angiogenesis is likely the most important mechanism behind the efficacy of TMLR. This would explain both the relief in symptoms and the improved myocardial perfusion and function as seen with the CO₂ laser. Numerous reports have demonstrated a histological increase in perfusion as a result of TMLR [33, 82, 85, 97–99] and some have attributed it to a nonspecific response to injury similar to that seen with mechanical (needle) channel creation [23, 100, 101]. Important molecular evidence of angiogenesis was derived from studies showing upregulation of vascular endothelial growth factor (VEGF) messenger RNA, expression of fibroblast growth factor 2 (FGF2), as well as matrix metalloproteinases following TMR [102–104].

In a provocative trial, Hughes et al. [105] compared neovascularization and contractile reserve on an ischemic porcine model after TMLR with either a CO₂, Ho:YAG or XeCl excimer laser to a control sham thoracotomy. Using dobutamine stress echocardiography and PET scanning, they reported significantly improved neovascularization, perfusion, and function following CO₂ or Ho:YAG treatment. None of these changes were seen with the XeCl laser TMLR or the sham thoracotomy. Improved cardiac function and perfusion with the CO₂ laser has also been demonstrated in other studies using a variety of imaging techniques including isotope nuclear scanning [37, 44, 45], PET scanning [50], dobutamine stress echocardiography [54] and contrast enhanced magnetic resonance imaging [55]. On the other hand, randomized trials using Ho:YAG laser failed to show improved perfusion [43, 46, 48].

Percutaneous Myocardial Laser Revascularization

Myocardial laser revascularization has been performed via thoracoscopy [35, 37–48], sternotomy [66–70], thoroscopically [36], and also percutaneously [106–110]. Percutaneous myocardial laser revascularization (PMLR) was performed using a flexible optical fiber to reach the left ventricle cavity via a peripheral artery. The laser of choice was the Ho:YAG laser because it could be delivered through the optic fiber, unlike the CO₂ laser. Even with the use of electromechanical mapping to verify the position of the fiber and the creation of the channel, the results from PMLR have been less favorable than those seen with TMLR. In a randomized, blinded trial, Stone et al. [109] performed PCI to patients suffering from class III or IV angina, and if the procedure was unsuccessful and uncomplicated, the patient was randomized to either PMLR plus MM or to MM only. The patients were blinded to the procedure being performed through heavy sedation and dark goggles, and remained blinded during the follow-up period. At 6 months there was no statistically significant improvement in angina, exercise tolerance or mortality. Another study randomized and blinded 298 patients to low or high dose laser revascularization or a sham procedure [110]. The results showed no difference between the three groups in terms of angina class, exercise duration, or myocardial perfusion.

The failure of PMLR to achieve the same results as TMLR may be due to several important limitations. The first of these is the difficulty to create channels in an exact location and with the desired distribution from inside a moving ventricle. Secondly, channels created percutaneously have a maximum estimated depth of 6 mm, which is not enough to achieve transmural ablation, as with TMLR. Finally, there are limitations of the Ho:YAG laser, which has proven less efficient

than the CO₂ laser for TMLR. As a result of these limitations and the unsatisfactory trial results, the FDA has deemed PMLR unapprovable.

Future Uses of TMLR

TMLR has also been performed in combination with other innovating methods of promoting angiogenesis. Experimental work investigating the use of TMLR in combination with gene therapy has shown promising results [111–114]. The use of endothelial or fibroblast growth factors was associated with increased angiogenesis and, perhaps more importantly, improvement of cardiac function versus laser therapy alone. Beneficial results have also been reported for TMLR coupled with stem cell-based therapies, experimentally and clinically [115–119].

Conclusions

Cardiac surgeons are increasingly faced with more complex cases of patients suffering from diffuse coronary artery disease not amenable to classical revascularization methods. Concordant results from multiple randomized trials and long-term follow-up studies have validated the safety, effectiveness, and substantially improved health outcomes of TMLR for the treatment of selected patients with severe refractory angina. It is also imperative that research continues to elucidate the influence of laser parameters on the mechanism and outcomes of TMLR, as well as the adjuvant gene or stem cell therapies.

References

1. Vieussens R. *Nouvelles découvertes sur le coeur*. Toulouse: Jean Guillemette; 1706.
2. Thebesius AC. *De circulo sanguinis in corde*. Leiden: Elsevier; 1708.
3. Leary T, Wearn JT. Two cases of complete occlusion of both coronary orifices. *Am Heart J*. 1930;5(4):412–23.
4. Schildt P, Stanton E, Beck CS. Communications between the coronary arteries produced by the application of inflammatory agents to the surface of the heart. *Ann Surg*. 1943;118(1):34–45.
5. Beck CS, Stanton E. Revascularization of heart by graft of systemic artery into coronary sinus. *JAMA*. 1948;137(5):436–42.
6. Vineberg AM. Development of an anastomosis between the coronary vessels and a transplanted internal mammary artery. *Can Med Assoc J*. 1946;55(2):117–9.
7. Vineberg A, Miller D. Functional evaluation of an internal mammary coronary artery anastomosis. *Am Heart J*. 1953;45(6):873–88.
8. Vineberg A. Experimental background of myocardial revascularization by internal mammary artery implantation and supplementary techniques, with its clinical application in 125 patients: a review and critical appraisal. *Ann Surg*. 1964;159:185–207.
9. Topaz O, Pavlos S, Mackall JA, Nair R, Hsu J. The Vineberg procedure revisited: angiographic evaluation and coronary artery

- bypass surgery in a patient 21 years following bilateral internal mammary artery implantation. *Cathet Cardiovasc Diagn.* 1992;25(3):218–22.
10. Sen PK, Udawadia TE, Kinare SG, Parulkar GB. Transmyocardial acupuncture: a new approach to myocardial revascularization. *J Thorac Cardiovasc Surg.* 1965;50:181–9.
 11. Mirhoseini M, Cayton MM. Revascularization of the heart by laser. *Microsurgery.* 1981;2(4):253–60.
 12. Mirhoseini M, Fisher JC, Cayton M. Myocardial revascularization by laser: a clinical report. *Lasers Surg Med.* 1983;3(3):241–5.
 13. Jansen ED, Whittaker P. Laser-tissue interactions. In: Bridges CR, Horvath KA, Chiu R, editors. *Myocardial laser revascularization.* 1st ed. Malden: Blackwell Publishing; 2006. p. 16–30.
 14. Vogel A, Venugopalan V. Mechanisms of pulsed laser ablation of biological tissues. *Chem Rev.* 2003;103(2):577–644.
 15. Wolbarsht ML, Walsh AW, George G. Melanin, a unique biological absorber. *Appl Opt.* 1981;20(13):2184–6.
 16. Zonios G, Dimou A, Bassukas I, Galaris D, Tsolakidis A, Kaxiras E. Melanin absorption spectroscopy: new method for noninvasive skin investigation and melanoma detection. *J Biomed Opt.* 2008;13(1):014017.
 17. Horecker BL. The absorption spectra of hemoglobin and its derivatives in the visible and near infra-red regions. *J Biol Chem.* 1943;148(1):173–83.
 18. Niemi M. *Laser-tissue interactions.* 3rd ed. Berlin: Springer; 2007.
 19. Clarke RH, Isner JM, Donaldson RF, Jones G. Gas chromatographic-light microscopic correlative analysis of excimer laser photoablation of cardiovascular tissues: evidence for a thermal mechanism. *Circ Res.* 1987;60(3):429–37.
 20. Oraevsky AA, Jacques SL, Pettit GH, Saidi IS, Tittel FK, Henry PD. XeCl laser ablation of atherosclerotic aorta: optical properties and energy pathways. *Lasers Surg Med.* 1992;12(6):585–97.
 21. Gijssbers GHM, Sprangers RLH, Keijzer M, Bakker JMT, Leeuwen TG, Verdaasdonk RM, et al. Some laser-tissue interactions in 308 nm excimer laser coronary angioplasty. *J Interv Cardiol.* 1990;3(4):231–41.
 22. Shawl FA, Kaul U, Saadat V. Percutaneous myocardial revascularization using a myocardial channeling device: first human experience using the AngioTrax system. *J Am Coll Cardiol.* 2000;35(2s1):61A.
 23. Malekan R, Reynolds C, Narula N, Kelley ST, Suzuki Y, Bridges CR. Angiogenesis in transmyocardial laser revascularization. A nonspecific response to injury. *Circulation.* 1998;98(19 Suppl):II62–5; discussion II66.
 24. Smith NB, Hynynen K. The feasibility of using focused ultrasound for transmyocardial revascularization. *Ultrasound Med Biol.* 1998;24(7):1045–54.
 25. Khairy P, Dubuc M, Gallo R. Cryoapplication induces neovascularization: a novel approach to percutaneous myocardial revascularization. *J Am Coll Cardiol.* 2000;35(2s1):5A–6A.
 26. Yamamoto N, Gu A, DeRosa CM, Shimizu J, Zwas DR, Smith CR, et al. Radio frequency transmyocardial revascularization enhances angiogenesis and causes myocardial denervation in canine model. *Lasers Surg Med.* 2000;27(1):18–28.
 27. Horvath KA, Belkind N, Wu I, Greene R, Doukas J, Lomasney JW, et al. Functional comparison of transmyocardial revascularization by mechanical and laser means. *Ann Thorac Surg.* 2001;72(6):1997–2002.
 28. Whittaker P, Rakusan K, Kloner RA. Transmural channels can protect ischemic tissue: assessment of long-term myocardial response to laser- and needle-made channels. *Circulation.* 1996;93(1):143–52.
 29. Whittaker P, Spariosu K, Ho ZZ. Success of transmyocardial laser revascularization is determined by the amount and organization of scar tissue produced in response to initial injury: results of ultraviolet laser treatment. *Lasers Surg Med.* 1999;24(4):253–60.
 30. Genyk IA, Frenz M, Ott B, Walpoth BH, Schaffner T, Carrel TP. Acute and chronic effects of transmyocardial laser revascularization in the nonischemic pig myocardium by using three laser systems. *Lasers Surg Med.* 2000;27(5):438–50.
 31. Estvold SK, Mordini F, Zhou Y, Yu ZX, Sachdev V, Arai A, et al. Does laser type impact myocardial function following transmyocardial laser revascularization? *Lasers Surg Med.* 2010;42(10):746–51.
 32. Kitade T, Okada M, Tsuji Y, Nakamura M, Matoba Y. Experimental investigations on relationships between myocardial damage and laser type used in transmyocardial laser revascularization (TMLR). *Kobe J Med Sci.* 1999;45(3–4):127–36.
 33. Fisher PE, Khomoto T, DeRosa CM, Spotnitz HM, Smith CR, Burkhoff D. Histologic analysis of transmyocardial channels: comparison of CO₂ and holmium:YAG lasers. *Ann Thorac Surg.* 1997;64(2):466–72.
 34. Eckstein FS, Scheule AM, Pauncz Y, Schmid ST, Zucker M, Ziemer G. Transmyocardial laser revascularization with the Holmium:YAG laser does not improve myocardial perfusion in the acutely ischemic heart: an experimental study measuring myocardial perfusion by a thermal imaging camera. *Thorac Cardiovasc Surg.* 1999;47(5):293–7.
 35. Milano A, Pratali S, Tartarini G, Mariotti R, De Carlo M, Paterni G, et al. Early results of transmyocardial revascularization with a holmium laser. *Ann Thorac Surg.* 1998;65(3):700–4.
 36. Horvath KA. Thoracoscopic transmyocardial laser revascularization. *Ann Thorac Surg.* 1998;65(5):1439–41.
 37. Horvath KA, Mannting F, Cummings N, Shernan SK, Cohn LH. Transmyocardial laser revascularization: operative techniques and clinical results at two years. *J Thorac Cardiovasc Surg.* 1996;111(5):1047–53.
 38. Cooley DA, Frazier OH, Kadipasaoglu KA, Lindenmeier MH, Pehlivanoglu S, Kolff JW, et al. Transmyocardial laser revascularization: clinical experience with twelve-month follow-up. *J Thorac Cardiovasc Surg.* 1996;111(4):791–7; discussion 797–9.
 39. Horvath KA, Cohn LH, Cooley DA, Crew JR, Frazier OH, Griffith BP, et al. Transmyocardial laser revascularization: results of a multicenter trial with transmyocardial laser revascularization used as sole therapy for end-stage coronary artery disease. *J Thorac Cardiovasc Surg.* 1997;113(4):645–53; discussion 653–4.
 40. Krabatsch T, Tambeur L, Lieback E, Shaper F, Hetzer R. Transmyocardial laser revascularization in the treatment of end-stage coronary artery disease. *Ann Thorac Cardiovasc Surg.* 1998;4(2):64–71.
 41. Hattler BG, Griffith BP, Zenati MA, Crew JR, Mirhoseini M, Cohn LH, et al. Transmyocardial laser revascularization in the patient with unmanageable unstable angina. *Ann Thorac Surg.* 1999;68(4):1203–9.
 42. Dowling RD, Petracek MR, Selinger SL, Allen KB. Transmyocardial revascularization in patients with refractory, unstable angina. *Circulation.* 1998;98(19 Suppl):II73–5; discussion II75–6.
 43. Allen KB, Dowling RD, Fudge TL, Schoettle GP, Selinger SL, Gangahar DM, et al. Comparison of transmyocardial revascularization with medical therapy in patients with refractory angina. *N Engl J Med.* 1999;341(14):1029–36.
 44. Frazier OH, March RJ, Horvath KA. Transmyocardial revascularization with a carbon dioxide laser in patients with end-stage coronary artery disease. *N Engl J Med.* 1999;341(14):1021–8.
 45. Schofield P, Sharples L, Caine N, Burns S, Tait S, Wistow T, et al. Transmyocardial laser revascularisation in patients with refractory angina: a randomised controlled trial. *Lancet.* 1999;353(9152):519–24.
 46. Burkhoff D, Schmidt S, Schulman SP, Myers J, Resar J, Becker LC, et al. Transmyocardial laser revascularisation compared with continued medical therapy for treatment of refractory angina

- pectoris: a prospective randomised trial. ATLANTIC Investigators. *Angina Treatments-Lasers and Normal Therapies in Comparison*. *Lancet*. 1999;354(9182):885–90.
47. Aaberge L, Nordstrand K, Dragsund M, Saatvedt K, Endresen K, Golf S, et al. Transmyocardial revascularization with CO₂ laser in patients with refractory angina pectoris. Clinical results from the Norwegian randomized trial. *J Am Coll Cardiol*. 2000;35(5):1170–7.
 48. Jones JW, Schmidt SE, Richman BW, Miller CC, Sapire KJ, Burkhoff D, et al. Holmium:YAG laser transmyocardial revascularization relieves angina and improves functional status. *Ann Thorac Surg*. 1999;67(6):1596–601; discussion 1601–2.
 49. Horvath KA. Results of prospective randomized controlled trials of transmyocardial laser revascularization. *Heart Surg Forum*. 2002;5(1):33–9; discussion 39–40.
 50. Frazier OH, Cooley DA, Kadipasaoglu KA, Pehlivanoglu S, Lindenmeir M, Barasch E, et al. Myocardial revascularization with laser. Preliminary findings. *Circulation*. 1995; 92(9 Suppl):II58–65.
 51. Aaberge L, Rootwelt K, Blomhoff S, Saatvedt K, Abdelnoor M, Forfang K. Continued symptomatic improvement three to five years after transmyocardial revascularization with CO₂ laser. *J Am Coll Cardiol*. 2002;39(10):1588–93.
 52. Allen KB, Dowling RD, Angell WW, Gangahar DM, Fudge TL, Richenbacher W, et al. Transmyocardial revascularization: 5-year follow-up of a prospective, randomized multicenter trial. *Ann Thorac Surg*. 2004;77(4):1228–34.
 53. Horvath KA, Aranki SF, Cohn LH, March RJ, Frazier OH, Kadipasaoglu KA, et al. Sustained angina relief 5 years after transmyocardial laser revascularization with a CO₂ laser. *Circulation*. 2001;104(Suppl 1):I-81–4.
 54. Donovan CL, Landolfo KP, Lowe JE, Clements F, Coleman RB, Ryan T. Improvement in inducible ischemia during dobutamine stress echocardiography after transmyocardial laser revascularization in patients with refractory angina pectoris. *J Am Coll Cardiol*. 1997;30(3):607–12.
 55. Horvath KA, Kim RJ, Judd RM, et al. Contrast enhanced MRI assessment of microinfarction after transmyocardial laser revascularization. *Circulation*. 2000;104(Suppl 2):II-765.
 56. Gibbons RJ. ACC/AHA 2002 guideline update for the management of patients with chronic stable angina—summary article: a report of the American College of Cardiology/American Heart Association Task Force on Practice Guidelines (Committee on the Management of Patients). *Circulation* (Lippincott Williams & Wilkins). 2003;107(1):149–58.
 57. Bridges CR, Horvath KA, Nugent WC, Shahian DM, Haan CK, Shemin RJ, et al. The Society of Thoracic Surgeons practice guideline series: transmyocardial laser revascularization. *Ann Thorac Surg*. 2004;77(4):1494–502.
 58. Diegeler A, Cheng D, Allen K, Weisel R, Lutter G, Sartori M, et al. Transmyocardial laser revascularization: a consensus statement of the International Society of Minimally Invasive Cardiothoracic Surgery (ISMICS) 2006. *Innovations (Phila)*. 2006;1(6):314–22.
 59. Garcia S, Sandoval Y, Roukoz H, Adabag S, Canoniero M, Yannopoulos D, et al. Outcomes after complete versus incomplete revascularization of patients with multivessel coronary artery disease: a meta-analysis of 89,883 patients enrolled in randomized clinical trials and observational studies. *J Am Coll Cardiol*. 2013;62(16):1421–31.
 60. Weintraub WS, Jones EL, Craver JM, Guyton RA. Frequency of repeat coronary bypass or coronary angioplasty after coronary artery bypass surgery using saphenous venous grafts. *Am J Cardiol*. 1994;73(2):103–12.
 61. Lawrie GM, Morris GC, Silvers A, Wagner WF, Baron AE, Beltangady SS, et al. The influence of residual disease after coronary bypass on the 5-year survival rate of 1274 men with coronary artery disease. *Circulation*. 1982;66(4):717–23.
 62. Schaff HV, Gersh BJ, Pluth JR, Danielson GK, Orszulak TA, Puga FJ, et al. Survival and functional status after coronary artery bypass grafting: results 10 to 12 years after surgery in 500 patients. *Circulation*. 1983;68(Suppl 2):II200–4.
 63. Bell MR, Gersh BJ, Schaff HV, Holmes DR, Fisher LD, Alderman EL, et al. Effect of completeness of revascularization on long-term outcome of patients with three-vessel disease undergoing coronary artery bypass surgery. A report from the Coronary Artery Surgery Study (CASS) Registry. *Circulation*. 1992;86(2):446–57.
 64. Osswald BR, Blackstone EH, Tochtermann U, Schweiger P, Thomas G, Vahl CF, et al. Does the completeness of revascularization affect early survival after coronary artery bypass grafting in elderly patients? *Eur J Cardiothorac Surg*. 2001;20(1):120–5; discussion 125–6.
 65. Graham MM, Chambers RJ, Davies RF. Angiographic quantification of diffuse coronary artery disease: reliability and prognostic value for bypass operations. *J Thorac Cardiovasc Surg*. 1999;118(4):618–27.
 66. Trehan N, Mishra M, Bapna R, Mishra A, Maheshwari P, Karlekar A. Transmyocardial laser revascularisation combined with coronary artery bypass grafting without cardiopulmonary bypass. *Eur J Cardiothorac Surg*. 1997;12(2):276–84.
 67. Stamou SC, Boyce SW, Cooke RH, Carlos BD, Sweet LC, Corso PJ. One-year outcome after combined coronary artery bypass grafting and transmyocardial laser revascularization for refractory angina pectoris. *Am J Cardiol*. 2002;89(12):1365–8.
 68. Wehberg KE, Julian JS, Todd JC, Ogburn N, Klopp E, Buchness M. Improved patient outcomes when transmyocardial revascularization is used as adjunctive revascularization. *Heart Surg Forum*. 2003;6(5):328–30.
 69. Allen KB, Dowling RD, DeRossi AJ, Realyvasques F, Lefrak EA, Pfeffer TA, et al. Transmyocardial laser revascularization combined with coronary artery bypass grafting: a multicenter, blinded, prospective, randomized, controlled trial. *J Thorac Cardiovasc Surg*. 2000;119(3):540–9.
 70. Frazier OH, Boyce SW, Griffith BP, Hattler BG, Kadipasaoglu KA, Lansing AM, March RJ. Transmyocardial revascularization using a synchronized CO₂ laser as adjunct to coronary artery bypass grafting: results of a prospective, randomized, multicenter trial with 12-month follow-up [abstract]. *Circulation*. 1999;100(Suppl 1):I-248.
 71. Allen KB, Dowling RD, Schuch DR, Pfeffer TA, Marra S, Lefrak EA, et al. Adjunctive transmyocardial revascularization: five-year follow-up of a prospective, randomized trial. *Ann Thorac Surg*. 2004;78(2):458–65; discussion 458–65.
 72. Frazier OH, Tuzun E, Eichstadt H, Boyce SW, Lansing AM, March RJ, et al. Transmyocardial laser revascularization as an adjunct to coronary artery bypass grafting: a randomized, multicenter study with 4-year follow-up. *Tex Heart Inst J*. 2004;31(3):231–9.
 73. Morgan I, Campanella C. Transmyocardial laser revascularisation in Edinburgh. *Br J Theatre Nurs*. 1998;7(12):4–9.
 74. Lee LY, O'Hara MF, Finnin EB, Hachamovitch R, Szulc M, Kligfield PD, et al. Transmyocardial laser revascularization with excimer laser: clinical results at 1 year. *Ann Thorac Surg*. 2000;70(2):498–503.
 75. Kavanagh GJ, Whittaker P, Prejean CA, Firth BR, Kloner RA, Kay GL. Dissociation between improvement in angina pectoris and myocardial perfusion after transmyocardial revascularization with an excimer laser. *Am J Cardiol*. 2001;87(2):229–31, A9.
 76. Van der Sloot JAP, Huikeshoven M, Tukkies R, Verberne HJ, van der Meulen J, van Eck-Smit BLF, et al. Transmyocardial revascularization using an XeCl excimer laser: results of a randomized trial. *Ann Thorac Surg*. 2004;78(3):875–81; discussion 881–2.

77. Mirhoseini M, Shelgikar S, Cayton M. Clinical and histological evaluation of laser myocardial revascularization. *J Clin Laser Med Surg.* 1990;8(3):73–7.
78. Cooley DA, Frazier OH, Kadipasaoglu KA, Pehlivanoglu S, Shannon RL, Angelini P. Transmyocardial laser revascularization. Anatomic evidence of long-term channel patency. *Tex Heart Inst J.* 1994;21(3):220–4.
79. Hardy RI, James FW, Millard RW, Kaplan S. Regional myocardial blood flow and cardiac mechanics in dog hearts with CO₂ laser-induced intramyocardial revascularization. *Basic Res Cardiol.* 1990;85(2):179–97.
80. Horvath KA, Smith WJ, Laurence RG, Schoen FJ, Appleyard RF, Cohn LH. Recovery and viability of an acute myocardial infarct after transmyocardial laser revascularization. *J Am Coll Cardiol.* 1995;25(1):258–63.
81. Gassler N, Wintzer HO, Stubbe HM, Wullbrand A, Helmchen UA. Transmyocardial laser revascularization. Histological features in human nonresponder myocardium. *Circulation.* 1997;95(2):371–5.
82. Burkhoff D, Fisher PE, Apfelbaum M, Kohmoto T, DeRosa CM, Smith CR. Histologic appearance of transmyocardial laser channels after 4 1/2 weeks. *Ann Thorac Surg.* 1996;61(5):1532–4; discussion 1534–5.
83. Sigel JE, Abramovich CM, Lytle BW, Ratliff NB. Transmyocardial laser revascularization: three sequential autopsy cases. *J Thorac Cardiovasc Surg.* 1998;115(6):1381–5.
84. Kohmoto T, Fisher PE, Gu A, Zhu SM, Yano OJ, Spotnitz HM, et al. Does blood flow through holmium:YAG transmyocardial laser channels? *Ann Thorac Surg.* 1996;61(3):861–8.
85. Kohmoto T, Fisher PE, Gu A, Zhu SM, DeRosa CM, Smith CR, et al. Physiology, histology, and 2-week morphology of acute transmyocardial channels made with a CO₂ laser. *Ann Thorac Surg.* 1997;63(5):1275–83.
86. Pifarré R, Jasuja ML, Lynch RD, Neville WE. Myocardial revascularization by transmyocardial acupuncture. A physiologic impossibility. *J Thorac Cardiovasc Surg.* 1969;58(3):424–31.
87. Stein PD, Sabbah HN, Marzilli M, Blick EF. Comparison of the distribution of intramyocardial pressure across the canine left ventricular wall in the beating heart during diastole and in the arrested heart. Evidence of epicardial muscle tone during diastole. *Circ Res.* 1980;47(2):258–67.
88. Denys BG, Aubert AE, Ector H, Kesteloot H, De Geest H. Intramyocardial pressure in the canine heart. An experimental study. *J Thorac Cardiovasc Surg.* 1985;90(6):888–95.
89. Kwong KF, Kanellopoulos G, Nikols J, Pogwizd S, Saffitz J, Schuessler R, et al. Transmyocardial laser treatment denervates canine myocardium. *J Thorac Cardiovasc Surg.* 1997;114(6):883–90.
90. Kwong KF, Schuessler RB, Kanellopoulos GK, Saffitz JE, Sundt TM. Nontransmural laser treatment incompletely denervates canine myocardium. *Circulation.* 1998;98(19 Suppl):II67–71; discussion II71–2.
91. Hirsch GM, Thompson GW, Arora RC, Hirsch KJ, Sullivan JA, Armour JA. Transmyocardial laser revascularization does not denervate the canine heart. *Ann Thorac Surg.* 1999;68(2):460–8; discussion 468–9.
92. Minisi AJ, Topaz O, Quinn MS, Mohanty LB. Cardiac nociceptive reflexes after transmyocardial laser revascularization: implications for the neural hypothesis of angina relief. *J Thorac Cardiovasc Surg.* 2001;122(4):712–9.
93. Arora RC, Hirsch GM, Hirsch K, Armour JA. Transmyocardial laser revascularization remodels the intrinsic cardiac nervous system in a chronic setting. *Circulation.* 2001;104(12 Suppl 1):II15–20.
94. Al-Sheikh T, Allen KB, Straka SP, Heimansohn DA, Fain RL, Hutchins GD, et al. Cardiac sympathetic denervation after transmyocardial laser revascularization. *Circulation.* 1999;100(2):135–40.
95. Hughes GC, Baklanov DV, Biswas SS, Phippen AM, DeGrado TR, Coleman RE, et al. Regional cardiac sympathetic innervation early and late after transmyocardial laser revascularization. *J Card Surg.* 2004;19(1):21–7.
96. Muxí A, Magriñá J, Martín F, Josa M, Fuster D, Setoain FJ, et al. Technetium 99 m-labeled tetrofosmin and iodine 123-labeled metaiodobenzylguanidine scintigraphy in the assessment of transmyocardial laser revascularization. *J Thorac Cardiovasc Surg.* 2003;125(6):1493–8.
97. Yamamoto N, Kohmoto T, Gu A, DeRosa C, Smith CR, Burkhoff D. Angiogenesis is enhanced in ischemic canine myocardium by transmyocardial laser revascularization. *J Am Coll Cardiol.* 1998;31(6):1426–33.
98. Spanier T, Smith CR, Burkhoff D. Angiogenesis: a possible mechanism underlying the clinical benefits of transmyocardial laser revascularization. *J Clin Laser Med Surg.* 1997;15(6):269–73.
99. Hughes GC, Lowe JE, Kypson AP, St Louis JD, Phippen AM, Peters KG, et al. Neovascularization after transmyocardial laser revascularization in a model of chronic ischemia. *Ann Thorac Surg.* 1998;66(6):2029–36.
100. Chu VF, Giaid A, Kuang JQ, McGinn AN, Li CM, Pelletier MP, et al. Thoracic Surgery Directors Association Award. Angiogenesis in transmyocardial revascularization: comparison of laser versus mechanical punctures. *Ann Thorac Surg.* 1999;68(2):301–7; discussion 307–8.
101. Mueller XM, Tevaearai HT, Chaubert P, Genton CY, von Segesser LK. Does laser injury induce a different neovascularisation pattern from mechanical or ischaemic injuries? *Heart.* 2001;85(6):697–701.
102. Pelletier MP, Giaid A, Sivaraman S, Dorfman J, Li CM, Philip A, et al. Angiogenesis and growth factor expression in a model of transmyocardial revascularization. *Ann Thorac Surg.* 1998;66(1):12–8.
103. Horvath KA, Chiu E, Maun DC, Lomasney JW, Greene R, Pearce WH, et al. Up-regulation of vascular endothelial growth factor mRNA and angiogenesis after transmyocardial laser revascularization. *Ann Thorac Surg.* 1999;68(3):825–9.
104. Li W, Chiba Y, Kimura T, Morioka K, Uesaka T, Haya A, et al. Transmyocardial laser revascularization induced angiogenesis correlated with the expression of matrix metalloproteinases and platelet-derived endothelial cell growth factor. *Eur J Cardiothorac Surg.* 2001;19(2):156–63.
105. Hughes GC, Kypson AP, Annex BH, Yin B, St Louis JD, Biswas SS, et al. Induction of angiogenesis after TMR: a comparison of holmium: YAG, CO₂, and excimer lasers. *Ann Thorac Surg.* 2000;70(2):504–9.
106. Oesterle SN, Sanborn TA, Ali N, Resar J, Ramee SR, Heuser R, et al. Percutaneous transmyocardial laser revascularisation for severe angina: the PACIFIC randomised trial. Potential Class Improvement From Intramyocardial Channels. *Lancet.* 2000;356(9243):1705–10.
107. Lauer B, Junghans U, Stahl F, Kluge R, Oesterle SN, Schuler G. Catheter-based percutaneous myocardial laser revascularization in patients with end-stage coronary artery disease. *J Am Coll Cardiol.* 1999;34(6):1663–70.
108. Gray TJ, Burns SM, Clarke SC, Tait S, Sharples LD, Caine N, et al. Percutaneous myocardial laser revascularization in patients with refractory angina pectoris. *Am J Cardiol.* 2003;91(6):661–6.
109. Stone GW, Teirstein PS, Rubenstein R, Schmidt D, Whitlow PL, Kosinski EJ, et al. A prospective, multicenter, randomized trial of percutaneous transmyocardial laser revascularization in patients with nonrevascularizable chronic total occlusions. *J Am Coll Cardiol.* 2002;39(10):1581–7.
110. Leon MB, Kornowski R, Downey WE, Weisz G, Baim DS, Bonow RO, et al. A blinded, randomized, placebo-controlled trial of

- percutaneous laser myocardial revascularization to improve angina symptoms in patients with severe coronary disease. *J Am Coll Cardiol.* 2005;46(10):1812–9.
111. Fleischer KJ, Goldschmidt-Clermont PJ, Fonger JD, Hutchins GM, Hruban RH, Baumgartner WA. One-month histologic response of transmyocardial laser channels with molecular intervention. *Ann Thorac Surg.* 1996;62(4):1051–8.
112. Sayeed-Shah U, Mann MJ, Martin J, Grachev S, Reimold S, Laurence R, et al. Complete reversal of ischemic wall motion abnormalities by combined use of gene therapy with transmyocardial laser revascularization. *J Thorac Cardiovasc Surg.* 1998;116(5):763–9.
113. Lutter G, Attmann T, Heilmann C, von Samson P, von Specht B, Beyersdorf F. The combined use of transmyocardial laser revascularization (TMLR) and fibroblastic growth factor (FGF-2) enhances perfusion and regional contractility in chronically ischemic porcine hearts. *Eur J Cardiothorac Surg.* 2002;22(5):753–61.
114. Horvath KA, Doukas J, Lu C-YJ, Belkind N, Greene R, Pierce GF, et al. Myocardial functional recovery after fibroblast growth factor 2 gene therapy as assessed by echocardiography and magnetic resonance imaging. *Ann Thorac Surg.* 2002;74(2):481–7.
115. Klein H-M, Ghodsizad A, Borowski A, Saleh A, Draganov J, Poll L, et al. Autologous bone marrow-derived stem cell therapy in combination with TMLR. A novel therapeutic option for endstage coronary heart disease: report on 2 cases. *Heart Surg Forum.* 2004;7(5):E416–9.
116. Gowdak LHW, Schettert IT, Rochitte CE, Lisboa LAF, Dallan LAO, César LAM, et al. Cell therapy plus transmyocardial laser revascularization for refractory angina. *Ann Thorac Surg.* 2005;80(2):712–4.
117. De Oliveira SA, Gowdak LHW, Buckberg G, Krieger JE. Cell biology, MRI and geometry: insight into a microscopic/macrosopic marriage. *Eur J Cardiothorac Surg.* 2006;29 Suppl 1:S259–65.
118. Patel AN, Spadaccio C, Kuzman M, Park E, Fischer DW, Stice SL, et al. Improved cell survival in infarcted myocardium using a novel combination transmyocardial laser and cell delivery system. *Cell Transplant.* 2007;16(9):899–905.
119. Gowdak LHW, Schettert IT, Rochitte CE, Rienzo M, Lisboa LAF, Dallan LAO, et al. Transmyocardial laser revascularization plus cell therapy for refractory angina. *Int J Cardiol.* 2008;127(2):295–7.

Chartchai Kositprapa, On Topaz, Arun Samidurai,
Shinji Okubo, Vigneshwar Kasirajan,
and Rakesh C. Kukreja

Introduction

Cardiovascular disease is the leading cause of death in Western countries. In 2007, almost eight million individuals were affected by acute myocardial infarction (AMI). Clinically the goal is to re-establish blood flow to the ischemic area as quickly as possible to salvage cardiomyocytes that would be damaged by ischemia. While reperfusion is necessary for tissue survival, it is worth noting that reperfusion itself can also cause tissue damage, termed “reperfusion injury”. As more tissue is irreversibly injured, the prognosis becomes worse

C. Kositprapa, MD
Division of Cardiology, Department of Medicine, Pauley Heart Center, Virginia Commonwealth University, Richmond, VA 23298, USA

Division of Cardiology, Department of Internal Medicine, Virginia Commonwealth University Medical Center, Richmond, VA USA

O. Topaz, MD, FACC, FACP, FSCAI
Professor of Medicine, Duke University School of Medicine, Director, Interventional Cardiology, Chief, Division of Cardiology, Charles George Veterans Affairs Medical Center, 1100 Tunnel Road, Asheville, NC 28805, USA

A. Samidurai, PhD • R.C. Kukreja, PhD (✉)
Division of Cardiology, Department of Medicine, Pauley Heart Center, Virginia Commonwealth University, Richmond, VA 23298, USA

Department of Internal Medicine, Virginia Commonwealth University Medical Center, Pauley Heart Center, Richmond, VA USA
e-mail: rakesh.kukreja@vcuhealth.org

S. Okubo, MD, PhD
Division of Cardiology, Department of Medicine, Pauley Heart Center, Virginia Commonwealth University, Richmond, VA 23298, USA

Tokyo Medical University, Ibaraki Medical Center, Ibaraki, Japan

V. Kasirajan, MD
Division of Cardiology, Department of Medicine, Pauley Heart Center, Virginia Commonwealth University, Richmond, VA 23298, USA

Department of Surgery, Virginia Commonwealth University Medical Center, Richmond, VA USA

because terminally differentiated cardiac myocytes cannot regenerate. Loss of contractile mass puts an inordinate load on surviving tissue thereby causing the remaining cells to enlarge and results in hypertrophy and adverse remodeling of the ventricle ending ultimately in heart failure. Therefore, strategies that would render heart cells resistant to death from ischemia/reperfusion injury would greatly improve the prognosis of AMI. Since the 1970s, virtually hundreds of direct cardioprotective therapies have been claimed to reduce myocardial infarct size in experimental animals. However, only a few of them have been reproducible, and none has been translated into clinical therapies [1]. As a result, after investing an enormous amount of time, money, and resources into the search for cardioprotective therapies, we still do not have a drug that has been specifically approved for the reduction of infarct size in patients with AMI.

Transmyocardial Revascularization

The concept of improving blood flow using myocardial channels was first introduced by Sen et al. [2]. Laser transmyocardial revascularization, a procedure originally intended to simulate the perfusion mechanism of the reptilian heart, has evolved into an effective treatment for angina when traditional revascularization is not an option. Percutaneous myocardial revascularization is a less-invasive catheter-based procedure that has been adapted from trans-myocardial laser revascularization. This technique can also be applied percutaneously [percutaneous myocardial revascularization (PMR) or direct myocardial revascularization (DMR)]. TMR was first introduced by Mirhoseini et al. [3] by making channels directly through the LV wall using laser energy via a left anterior thoracotomy approach. The idea behind the development of TMR was that the oxygenated blood could flow directly from the LV and perfuse the myocardium. Thereafter, it was anticipated that such artificially created channels would remain patent. Unlike standard revascularization techniques (CABG or PCI), there is probably no immediate revascularization benefit achieved by TMR. It has also been demonstrated

that these channels occlude soon after their creation, with no demonstrable direct camerosinusoidal blood flow on long-term follow-up [4, 5]. Clinically, numerous reports of reduction in frequency and severity of anginal symptoms, improved exercise tolerance and quality of life have appeared from non-blind registry-type studies as well as non-blind randomized clinical trials of TMR or TMR versus continued medical therapy. TMR was not associated with a significant improvement in survival compared with the medical therapy alone in randomized trials. However, improvements in angina stages, quality of life, and perfusion of the myocardium have been demonstrated with TMR [6]. In fact, over 50,000 procedures have been performed worldwide using TMR. More recent work has shown that the combination of cell therapy and TMR facilitate mesenchymal stem cell (MSC) engraftment in rat hearts, with associated increase in the expression of stem cell factor, stromal derived factor-1, c-kit, and chemokine receptor type 4 [7, 8]. Clinical studies of MSCs plus TMR include individual case reports or series of patients with angina refractory to CABG or percutaneous coronary intervention. All of these studies demonstrated that injection of stem cells in addition to TMR was safe and showed an improvement in angina class. Several studies showed some evidence of improvement in perfusion and left ventricular contractility [9–11].

Currently, there are two laser devices approved by the US Food and Drug Administration for TMR – holmium:yttrium–aluminum–garnet and CO₂. The two devices differ in regard to energy outputs, wavelengths, ability to synchronize with the heart cycle, and laser–tissue interactions. These differences have led to studies showing different efficacies between the two laser devices [6].

Animal studies have shown that TMR reduces infarct size, preserve contractile function [12], stimulate angiogenesis [13, 14] and denervate the myocardium [15]. Positron emission tomography (PET) imaging of sympathetic innervation of the heart using ¹¹C-hydroxyephedrine (HED) showed marked increases in HED defects after TMR, consistent with sympathetic denervation [16]. This function may be important in explaining its anti-anginal effect. In addition, the injury produced by laser energy may result in the elaboration of vascular growth factors that stimulate angiogenesis and neovascularization in ischemic myocardial tissue following TMR [17]. The early improvement may be related to myocardial denervation whereas later improvement could be mediated by the angiogenic effect of TMR.

Myocardial Preconditioning –Basic Concepts

In 1986, Murry, Jennings and Reimer [18] discovered that if the prolonged ischemia was preceded by four brief episodes of 5 min of ischemia each followed by 5 min of reperfusion,

the infarct size was reduced to only 25 % of that in the control group. This phenomenon was termed ischemic preconditioning (IPC). IPC causes two phases of protection. The first phase, termed “early” or “first window” IPC, protects the heart for an hour or two and then wanes; the second phase, “delayed” or “late” IPC or “second window of protection” (SWOP), appears 24 h after the IPC protocol and can last for 3 days. Unlike previously reported interventions, IPC was shown to be highly reproducible phenomenon [19, 20]. Subsequently, this powerful protective function of IPC was shown to occur in all species tested including the mouse, rat, rabbit, feline, canine, sheep, monkey and even human hearts. Although IPC is not amenable for treating AMI since those patients are present with ischemia already in progress, its discovery proved once and for all that myocardial protection was possible [21]. Besides the short episodes of ischemia, IPC was shown to be triggered by a number of other cellular stresses including the reversible ischemia, heat stress, ventricular pacing, or exercise (reviewed in [22, 23]). These non-lethal stresses cause release of chemical signals [nitric oxide (NO), reactive oxygen species (ROS), adenosine, and possibly opioid receptor agonists] that serve as triggers for the development of late PC as outlined in Fig. 22.1. These substances activate a complex signal transduction cascade that includes protein kinase C (PKC; specifically, the δ -isoform), protein tyrosine kinases (specifically, Src and/or Lck), and probably other as yet unknown kinases. A similar activation of PKC and downstream kinases can be elicited pharmacologically by a wide variety of agents, including naturally occurring—and often noxious—substances (e.g., endotoxin, interleukin-1, TNF- α , TNF- β , leukemia inhibitor factor, or ROS), as well as clinically applicable drugs including the NO donors, adenosine A1 or A3 receptor agonists, endotoxin derivatives, or δ 1-opioid receptor agonists. The recruitment of PKC and distal kinases leads to activation of NF- κ B and other transcription factors, resulting in increased transcription of multiple cardioprotective genes and synthesis of multiple of redundancy cardioprotective proteins that serve as comediators of protection for 2–4 days after the IPC stimulus. The mediators of late PC identified thus far include inducible nitric oxide synthase (iNOS), cyclooxygenase (COX)-2, heme oxygenase (HO)-1, SOD, and heat shock proteins. Opening of ATP-sensitive K⁺ (K_{ATP}) channels is also essential for the protection against infarction to become manifest (reviewed in [24]).

Generation of ROS plays an essential role in the protective mechanism of IPC. Murry et al. [25] had proposed that ROS signaling might be involved in IPC because the intravenous administration of the free radical scavengers including superoxide dismutase and catalase abolished IPC with ischemia in some, but not all, of their dog hearts. IPC’s protection was also shown to be mimicked by transient exposure to an oxygen radical generating system, and, conversely, a ROS scavenger abolished protection from IPC [26, 27].

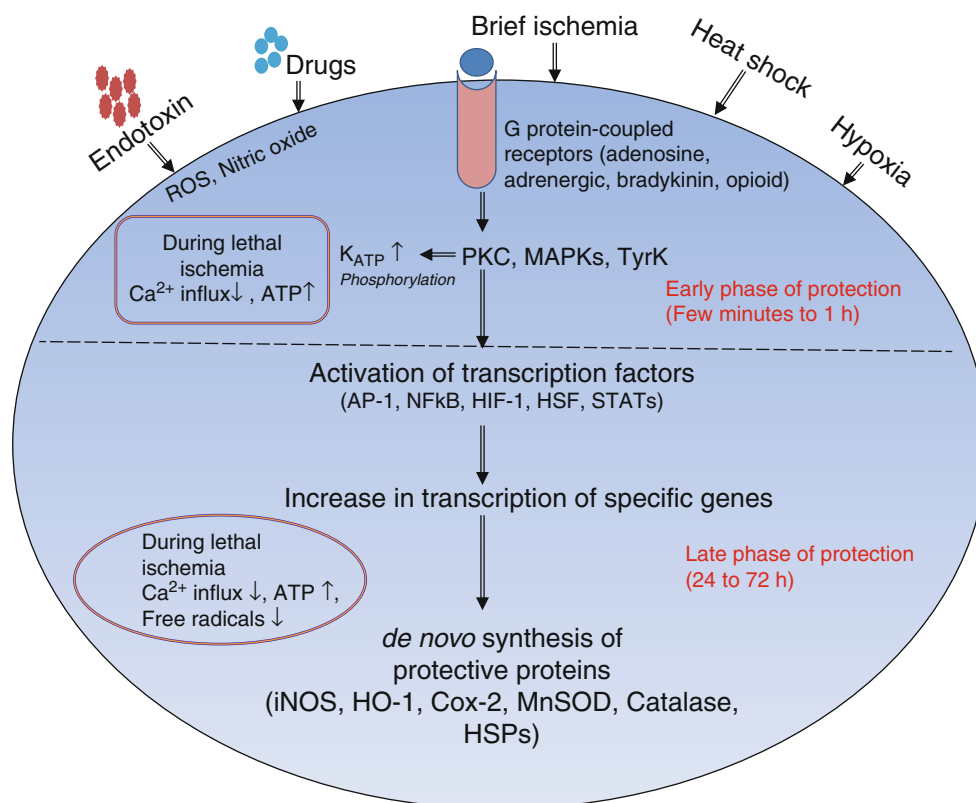


Fig. 22.1 Schematic representation of the mechanism of myocardial preconditioning. Non-lethal cellular stresses such as reversible ischemia, heat stress, hypoxia, exercise and drugs including endotoxin cause release of chemical signals including the nitric oxide (NO), reactive oxygen species (ROS), adenosine, and possibly opioid receptor agonists. These substances trigger signal transduction cascade that includes activation of protein kinase C, protein tyrosine kinases and probably other as yet unknown kinases. The PKC and other kinases activate transcription factors including AP1, NF- κ B, hypoxia inducible

factor 1 α (HIF1 α) and STAT3 which have a role in increased transcription of multiple cardioprotective genes including inducible nitric oxide synthase (iNOS), cyclooxygenase (COX)-2, heme oxygenase (HO)-1, superoxide dismutase (SOD) and heat shock protein 70 (HSP70). These proteins have been implicated in the late phase of preconditioning. Opening of mitochondrial ATP-sensitive K⁺ (mitoK_{ATP}) channels is also essential for the protection against infarction during early and late phase of preconditioning

MPG(2-Mercaptopropionylglycine), is a cell-permeant ROS scavenger. It has been reported that MPG does not scavenge either superoxide or hydrogen peroxide [28] appears to scavenge both peroxynitrite (a product of superoxide and nitric oxide interaction) and hydroxyl radical. By administering MPG during either the ischemic or the reperfusion phases of IPC, it was shown that the protective redox signaling occurred when oxygen is reintroduced following the brief occlusion [29].

Transmyocardial Revascularization and Myocardial Preconditioning

It has been suggested that laser phototherapy causes accumulation of safe levels of ROS, which may potentially trigger protective signaling leading to accelerated healing [30]. Considering the essential role of ROS in IPC as discussed above [26, 27, 29], we hypothesized that laser treatment could

potentially induce cardioprotection via generation of ROS following exposure to the laser energy by TMR. The studies were performed in a rabbit model of myocardial ischemia/reperfusion injury as described previously [31–33]. After the rabbits were anesthetized with ketamine HCl (35 mg/kg) and xylazine (5 mg/kg), a left thoracotomy was performed to expose the heart. Myocardial ischemia was induced by occlusion of coronary artery for 30 min, followed by reperfusion for 3 h. Laser treatment was given through Xenon chloride excimer laser generator at 308-nm wavelength, pulse duration 135 ns, output 200 mJ/pulse. Energy was delivered via a 0.9 mm catheter. Lasing parameters were set at a fluence of 30 mJ/mm² and 25 Hz. In the treatment group, laser was given directly through myocardium to create approximately 15 small channels along the LAD artery territory in each animal. Another group received MPG by intravenous infusion starting 15 min prior to and continued through 15 min after the laser treatment. Sham group of rabbits were subjected to the identical procedure without the laser delivery. After 30 min

(for early phase) and 24 h (for late phase and MPG-group) of laser treatment, the animals were subjected to 30 min of ischemia followed by 3 h of reperfusion. After completion of ischemia-reperfusion protocol, 500 IU of heparin were injected and the heart was quickly removed and mounted on a Langendorff apparatus. The coronary arteries were perfused with 0.9 % NaCl containing 2.5 mM CaCl_2 . After the blood was washed out, the ligation around the coronary artery was retightened and ~ 2 ml of 10 % Evans blue dye were injected as a bolus into the aorta until most of the heart turned blue. The heart was perfused with saline to wash out the excess Evans blue. Finally, the heart was removed, frozen, and cut into 8–10 transverse slices from apex to base of equal thickness (~ 1 mm). The slices were then incubated in a 1 % triphenyltetrazolium chloride solution in an isotonic phosphate buffer (pH 7.4) at 37 °C for 30 min. The areas of infarcted tissue, the risk zone, and the whole left ventricle were determined by computer morphometry using a Bioquant imaging software. Infarct size was expressed as a percentage of ischemic risk area. Total pulses delivered and time of laser treatment were identical in all groups. Compared with sham surgery, laser treatment significantly decreased infarct size from 51.5 ± 3.3 % to 36.5 ± 4.3 % in early phase and from 52.6 ± 3.29 % to 31.8 ± 1.65 % in late phase (mean \pm SE, $n=6$ /group, Fig. 22.2). Interestingly, MPG completely blocked the late protective effect of the laser treatment as demonstrated by significant increase in infarct size from 31.8 ± 1.7 % to 54.2 ± 4.9 %. There was no significant difference in risk areas in all groups (not shown). Laser and MPG did not have any effect on hemodynamics compared with sham (not shown). These data suggest that direct myocardial laser treatment

induces early and late cardioprotective effect which is mediated by generation of ROS from the laser energy.

It is interesting that laser treatment caused significant reduction in infarct size both immediately (early) and after 24 h of laser treatment which appears to be similar to the effects of the dynamics of IPC induced by short episodes of ischemia. It is not clear how long is the protective effect of laser-induced preconditioning persists. However, the degree of infarct size reduction with laser treatment, particularly during early phase is lower as compared to previously reported infarct size following IPC [34]. The blockade of cardioprotection with MPG suggests that ROS generated, or the generated ROS immediately following laser treatment in the myocardium could trigger signaling event that lead to reduction of infarct size during early and late phase of IPC. ROS are generated not only as by-products of mitochondrial metabolism but also by a variety of cellular enzyme systems, including nicotinamide adenine dinucleotide phosphate (NADPH) oxidase (NOX), uncoupled endothelial nitric oxide synthase (eNOS), xanthine oxidase, and arachidonic acid–metabolizing enzymes [35, 36]. When cellular production of ROS exceeds the antioxidant capacity of cardiovascular cells, proteins, lipids, and nucleic acids become damaged and may eventually contribute to the development of cardiovascular diseases such as atherosclerosis, hypertension, diabetic cardiovascular complications, and ischemic/reperfusion injury. Conversely, low concentrations of ROS play a critical role in regulating cardiovascular functions such as angiogenesis and tissue repair [37–39]. ROS are required for vascular endothelial growth factor (VEGF)–induced endothelial migration, proliferation, and tube formation [40, 41]. During ischemia/ reperfusion, ROS generation

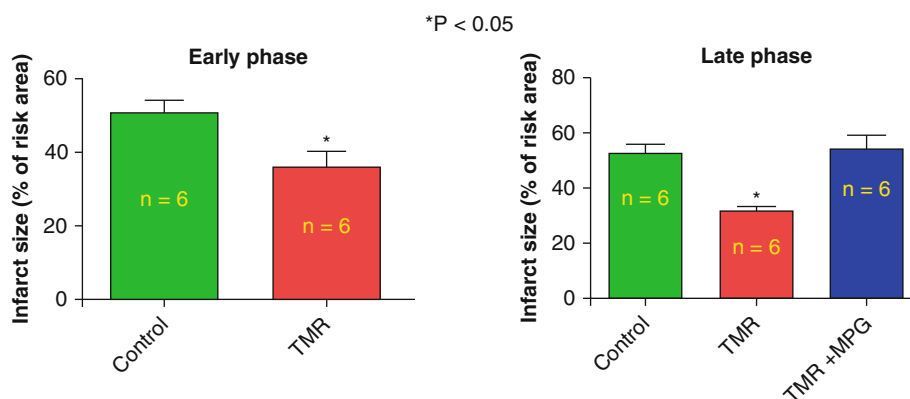


Fig. 22.2 Effect of transmyocardial revascularization on myocardial infarct size following ischemia/reperfusion: Infarct size (expressed as percentage of area at risk) during early phase and late phase of cardioprotection with **transmyocardial Revascularization (TMR)** in rabbits. After anesthetization, a left thoracotomy was performed to expose the heart. Laser treatment was given through Xenon chloride excimer laser generator at 308-nm wavelength, pulse duration 135 ns, output 200 mJ/pulse. Energy was delivered via a 0.9 mm catheter. In the treatment group, laser was given directly through myocardium to create

approximately 15 small channels along the LAD artery territory in each animal. Another group received 2-Mercaptopropionylglycine (MPG, 50 mg/kg) by intravenous infusion starting 15 min prior to and continued through 15 min after the laser treatment. Sham (control) group of rabbits were subjected to the identical procedure without the laser delivery. After 30 min (for early phase) and 24 h (for late phase and MPG-group) of laser treatment, the animals were subjected to 30 min of ischemia followed by 3 h of reperfusion ($N=6$ /group)

promotes capillary tube formation in human microvascular endothelial cells [40, 42] and the heart [43] whereas, inhibiting ROS through treatment with antioxidants or superoxide dismutases blocks vascularization and growth of tumors. The precise molecular mechanisms, however, by which ROS mediate angiogenic responses are incompletely understood. ROS are second messengers of preconditioning and have long been known to be required for cardioprotective signaling as discussed above. The mechanism of increased ROS is reasonably well understood: signaling from the plasma membrane leads to opening of the mitochondrial ATP-sensitive K⁺ channel (mitoK_{ATP}) [44], and the increased K⁺ influx into the matrix causes an increase in ROS, which derive during normoxia from complex I of the respiratory chain [45]. Although not studied in our current experiments, it is likely that opening of mitoK_{ATP} channels are possibly the downstream mediators of cardioprotection with the laser treatment [46].

Conclusions

TMR is a surgical procedure that has been shown to provide angina relief to patients with diffuse coronary disease. Most commonly accepted mechanism for the beneficial effects involves myocardial angiogenesis that ultimately leads to increased perfusion. In the present study, for the first time we have demonstrated that TMR also triggers cardioprotective effect similar to IPC which was responsible for significant reduction of infarct size both acutely as well as 24 h after laser treatment in rabbits. Interestingly, such infarct limiting effect was abolished when rabbits were treated with MPG suggesting that ROS are important triggers of cardioprotection. Further studies are necessary to delineate the downstream signaling targets of ROS. In particular, it would be interesting to study the expression of cardioprotective proteins including the antioxidants enzymes including such as superoxide dismutase, HSP70 [47–49] or the nitric oxide synthase [50–54] that have been implicated in the development of late phase of IPC [24, 33, 55]. These studies may help in expanding our current understanding of the mechanisms by which TMR provides relief from angina.

Acknowledgements This research was supported by the National Institutes of Health Grants R37 HL51045, R01 HL 59469 R01 HL79424, R01HL93685 and R01 HL118808 to RCK.

References

- Bolli R, Becker L, Gross G, Mentzer Jr R, Balshaw D, Lathrop DA. Myocardial protection at a crossroads: the need for translation into clinical therapy. *Circ Res*. 2004;95(2):125–34.
- Sen PK, Udawadia TE, Kinare SG, Parulkar GB. Transmyocardial acupuncture: a new approach to myocardial revascularization. *J Thorac Cardiovasc Surg*. 1965;50:181–9.
- Mirhoseini M, Cayton MM. Revascularization of the heart by laser. *J Microsurg*. 1981;2(4):253–60.
- Krabatsch T, Schaper F, Leder C, Tulsner J, Thalmann U, Hetzer R. Histological findings after transmyocardial laser revascularization. *J Card Surg*. 1996;11(5):326–31.
- Hardy RI, Bove KE, James FW, Kaplan S, Goldman L. A histologic study of laser-induced transmyocardial channels. *Lasers Surg Med*. 1987;6(6):563–73.
- Kindzelski BA, Zhou Y, Horvath KA. Transmyocardial revascularization devices: technology update. *Med Devices (Auckl)*. 2015;8:11–9.
- Shahzad U, Li G, Zhang Y, Yau TM. Transmyocardial revascularization induces mesenchymal stem cell engraftment in infarcted hearts. *Ann Thorac Surg*. 2012;94(2):556–62.
- Shahzad U, Li G, Zhang Y, Li RK, Rao V, Yau TM. Transmyocardial revascularization enhances bone marrow stem cell engraftment in infarcted hearts through SCF-C-kit and SDF-1-CXCR4 signaling axes. *Stem Cell Rev*. 2015;11:332–46.
- Reyes G, Allen KB, Alvarez P, et al. Mid term results after bone marrow laser revascularization for treating refractory angina. *BMC Cardiovasc Disord*. 2010;10:42.
- Goodarzi AA, Jeggo P, Lobrich M. The influence of heterochromatin on DNA double strand break repair: getting the strong, silent type to relax. *DNA Repair (Amst)*. 2010;9(12):1273–82.
- Gowdak LH, Schetter IT, Rochitte CE, et al. Cell therapy plus transmyocardial laser revascularization for refractory angina. *Ann Thorac Surg*. 2005;80(2):712–4.
- Horvath KA, Smith WJ, Laurence RG, Schoen FJ, Appleyard RF, Cohn LH. Recovery and viability of an acute myocardial infarct after transmyocardial laser revascularization. *J Am Coll Cardiol*. 1995;25(1):258–63.
- Kohmoto T, DeRosa CM, Yamamoto N, et al. Evidence of vascular growth associated with laser treatment of normal canine myocardium. *Ann Thorac Surg*. 1998;65(5):1360–7.
- Yamamoto N, Kohmoto T, Gu A, DeRosa C, Smith CR, Burkhoff D. Angiogenesis is enhanced in ischemic canine myocardium by transmyocardial laser revascularization. *J Am Coll Cardiol*. 1998;31(6):1426–33.
- Beek JF, van der Sloot JA, Huikeshoven M, et al. Cardiac denervation after clinical transmyocardial laser revascularization: short-term and long-term iodine 123-labeled meta-iodobenzylguanide scintigraphic evidence. *J Thorac Cardiovasc Surg*. 2004;127(2):517–24.
- Al-Sheikh T, Allen KB, Straka SP, et al. Cardiac sympathetic denervation after transmyocardial laser revascularization. *Circulation*. 1999;100(2):135–40.
- Hughes GC, Lowe JE, Kypson AP, et al. Neovascularization after transmyocardial laser revascularization in a model of chronic ischemia. *Ann Thorac Surg*. 1998;66(6):2029–36.
- Murry CE, Jennings RB, Reimer KA. Preconditioning with ischemia: a delay of lethal cell injury in ischemic myocardium. *Circulation*. 1986;74(5):1124–36.
- Gill R, Kuriakose R, Gertz ZM, Salloum FN, Xi L, Kukreja RC. Remote ischemic preconditioning for myocardial protection: update on mechanisms and clinical relevance. *Mol Cell Biochem*. 2015;402:41–9.
- Jones SP, Tang XL, Guo Y, et al. The NHLBI-sponsored consortium for preclinical assessment of cardioprotective therapies (CAESAR): a new paradigm for rigorous, accurate, and reproducible evaluation of putative infarct-sparing interventions in mice, rabbits, and pigs. *Circ Res*. 2015;116:572–86.
- Yang X, Cohen MV, Downey JM. Mechanism of cardioprotection by early ischemic preconditioning. *Cardiovasc Drugs Ther*. 2010;24(3):225–34.
- Okubo S, Xi L, Bernardo NL, Yoshida K, Kukreja RC. Myocardial preconditioning: basic concepts and potential mechanisms. *Mol Cell Biochem*. 1999;196(1–2):3–12.

23. Xi L, Tekin D, Bhargava P, Kukreja RC. Whole body hyperthermia and preconditioning of the heart: basic concepts, complexity, and potential mechanisms. *Int J Hyperthermia*. 2001;17(5):439–55.
24. Bolli R. The late phase of preconditioning. *Circ Res*. 2000;87(11):972–83.
25. Murry CE RVJRRKA. Preconditioning with ischemia: is the protective effect mediated by free radical-induced myocardial stunning? *Circulation*. 1988;78(Suppl II):II-77. (Abstract).
26. Baines CP, Goto M, Downey JM. Oxygen radicals released during ischemic preconditioning contribute to cardioprotection in the rabbit myocardium. *J Mol Cell Cardiol*. 1997;29(1):207–16.
27. Tritto I, D'Andrea D, Eramo N, et al. Oxygen radicals can induce preconditioning in rabbit hearts. *Circ Res*. 1997;80(5):743–8.
28. Bolli R, Jeroudi MO, Patel BS, et al. Marked reduction of free radical generation and contractile dysfunction by antioxidant therapy begun at the time of reperfusion. Evidence that myocardial “stunning” is a manifestation of reperfusion injury. *Circ Res*. 1989;65(3):607–22.
29. Liu Y, Yang XM, Iliodromitis EK, et al. Redox signaling at reperfusion is required for protection from ischemic preconditioning but not from a direct PKC activator. *Basic Res Cardiol*. 2008;103(1):54–9.
30. Dillenburg CS, Almeida LO, Martins MD, Squarize CH, Castilho RM. Laser phototherapy triggers the production of reactive oxygen species in oral epithelial cells without inducing DNA damage. *J Biomed Opt*. 2014;19(4):048002.
31. Bernardo NL, D'Angelo M, Okubo S, Joy A, Kukreja RC. Delayed ischemic preconditioning is mediated by opening of ATP-sensitive potassium channels in the rabbit heart. *Am J Physiol*. 1999; 276(4 Pt 2): H1323–30.
32. Kositprapa C, Ockaili RA, Kukreja RC. Bradykinin B2 receptor is involved in the late phase of preconditioning in rabbit heart. *J Mol Cell Cardiol*. 2001;33(7):1355–62.
33. Okubo S, Wildner O, Shah MR, Chelliah JC, Hess ML, Kukreja RC. Gene transfer of heat-shock protein 70 reduces infarct size in vivo after ischemia/reperfusion in the rabbit heart. *Circulation*. 2001;103(6):877–81.
34. Ytrehus K, Liu Y, Downey JM. Preconditioning protects ischemic rabbit heart by protein kinase C activation. *Am J Physiol*. 1994;266(3 Pt 2):H1145–52.
35. Kukreja RC, Hess ML. The oxygen free radical system: from equations through membrane-protein interactions to cardiovascular injury and protection. *Cardiovasc Res*. 1992;26(7):641–55.
36. Kukreja RC, Janin Y. Reperfusion injury: basic concepts and protection strategies. *J Thromb Thrombolysis*. 1997;4(1):7–24.
37. Chen W, Gabel S, Steenbergen C, Murphy E. A redox-based mechanism for cardioprotection induced by ischemic preconditioning in perfused rat heart. *Circ Res*. 1995;77(2):424–9.
38. Skyschally A, Schulz R, Gres P, Korth HG, Heusch G. Attenuation of ischemic preconditioning in pigs by scavenging of free oxyradicals with ascorbic acid. *Am J Physiol Heart Circ Physiol*. 2003;284(2):H698–703.
39. Tanaka K, Weihrauch D, Kehl F, et al. Mechanism of preconditioning by isoflurane in rabbits: a direct role for reactive oxygen species. *Anesthesiology*. 2002;97(6):1485–90.
40. Ushio-Fukai M, Tang Y, Fukai T, et al. Novel role of gp91(phox)-containing NAD(P)H oxidase in vascular endothelial growth factor-induced signaling and angiogenesis. *Circ Res*. 2002; 91(12): 1160–7.
41. Colavitti R, Pani G, Bedogni B, et al. Reactive oxygen species as downstream mediators of angiogenic signaling by vascular endothelial growth factor receptor-2/KDR. *J Biol Chem*. 2002; 277(5):3101–8.
42. Lelkes PI, Hahn KL, Sukovich DA, Karmiol S, Schmidt DH. On the possible role of reactive oxygen species in angiogenesis. *Adv Exp Med Biol*. 1998;454:295–310.
43. Maulik N. Redox regulation of vascular angiogenesis. *Antioxid Redox Signal*. 2002;4(5):783–4.
44. Garlid KD, Costa AD, Quinlan CL, Pierre SV, Dos SP. Cardioprotective signaling to mitochondria. *J Mol Cell Cardiol*. 2009;46(6):858–66.
45. Andrukhiv A, Costa AD, West IC, Garlid KD. Opening mitochondria increases superoxide generation from complex I of the electron transport chain. *Am J Physiol Heart Circ Physiol*. 2006;291(5):H2067–74.
46. Kukreja RC. Mechanism of reactive oxygen species generation after opening of mitochondrial KATP channels. *Am J Physiol Heart Circ Physiol*. 2006;291(5):H2041–3.
47. Kukreja RC, Kontos MC, Loesser KE, et al. Oxidant stress increases heat shock protein 70 mRNA in isolated perfused rat heart. *Am J Physiol*. 1994;267(6 Pt 2):H2213–9.
48. Kukreja RC, Kontos MC, Hess ML. Free radicals and heat shock protein in the heart. *Ann N Y Acad Sci*. 1996;793:108–22.
49. Yoshida K, Maaieh MM, Shipley JB, et al. Monophosphoryl lipid A induces pharmacologic ‘preconditioning’ in rabbit hearts without concomitant expression of 70-kDa heat shock protein. *Mol Cell Biochem*. 1996;156(1):1–8.
50. Yin C, Salloum FN, Kukreja RC. A novel role of microRNA in late preconditioning: upregulation of endothelial nitric oxide synthase and heat shock protein 70. *Circ Res*. 2009;104(5):572–5.
51. Xi L, Salloum F, Tekin D, Jarrett NC, Kukreja RC. Glycolipid RC-552 induces delayed preconditioning-like effect via iNOS-dependent pathway in mice. *Am J Physiol*. 1999;277(6 Pt 2): H2418–24.
52. Xi L, Jarrett NC, Hess ML, Kukreja RC. Essential role of inducible nitric oxide synthase in monophosphoryl lipid A-induced late cardioprotection: evidence from pharmacological inhibition and gene knockout mice. *Circulation*. 1999;99(16):2157–63.
53. Xi L, Kukreja RC. Pivotal role of nitric oxide in delayed pharmacological preconditioning against myocardial infarction. *Toxicology*. 2000;155(1–3):37–44.
54. Xi L, Tekin D, Gursoy E, Salloum F, Levasseur JE, Kukreja RC. Evidence that NOS2 acts as a trigger and mediator of late preconditioning induced by acute systemic hypoxia. *Am J Physiol Heart Circ Physiol*. 2002;283(1):H5–12.
55. Okubo S, Tanabe Y, Takeda K, et al. Ischemic preconditioning and morphine attenuate myocardial apoptosis and infarction after ischemia-reperfusion in rabbits: role of delta-opioid receptor. *Am J Physiol Heart Circ Physiol*. 2004;287(4):H1786–91.

Andrew C.W. Baldwin and O.H. Frazier

Introduction

Although the modern armamentarium for the treatment of coronary artery disease (CAD) includes ever-improving medical therapies, percutaneous coronary interventions (PCI), and coronary artery bypass graft operations (CABG), these modalities are not always sufficient for the treatment of advanced disease. Indeed, the number of patients with symptomatic chronic disease not amenable to intervention continues to rise, likely because of advances in medical therapy for acute heart disease. As many as 1 in 4 patients undergoing CABG are incompletely revascularized due to poor distal coronary targets—a significant predictor of poor perioperative outcomes [1–3]. As a result, researchers have long sought to develop alternative strategies to traditional revascularization techniques. In the 1990s, transmyocardial laser revascularization (TMLR) emerged as an effective treatment modality for patients with severe CAD not amenable to conventional therapy. Although the proposed mechanisms of reperfusion and the perceived effects of TMLR remain unclear, laser therapy can significantly improve angina symptoms in selected patient groups, and it is an important therapeutic option for the treatment of CAD.

History

The original rationale for the development of TMLR was based on the hypothesis that myocardial channels could allow delivery of oxygenated blood from the left ventricle into the muscle wall via myocardial sinusoidal plexuses. Whereas the existence of ventricular communication with

the surrounding vasculature was suggested as early as the eighteenth century, anatomical evidence for the existence of myocardial sinusoids was first reported by Joseph Wearn in 1933 [4, 5]. Although critics later claimed that these channels were a misinterpreted dehydration artifact, their presence was reminiscent of reptilian anatomy, which permits a substantial degree of myocardial perfusion directly from the left ventricle [6].

Surgical attempts to exploit this physiologic irregularity were developed over the ensuing decades. In 1955, Claude Beck reported relief of angina after performing experimental epicardial omentopexy, pericardiopexy, and inflammatory poudrage to enhance the surrounding vascularity [7]. Simultaneous research efforts led to the suggestion that natural or artificial conduits could potentially be developed to shunt blood from the left ventricle to the subendocardium [8, 9]. In adopting these theories, Profulla Sen, a pioneer of cardiothoracic surgery in India, has been credited with introducing the foundations of modern TMLR in 1965 by using a 16-gauge cannula to perform cardiac acupuncture and thereby establish direct perfusion of the myocardium [6, 10]. Hans Georg Borst later built upon this concept by implanting hollow tubes to assist myocardial perfusion, but his clinical success was limited [11]. In the 1970s, the widespread adoption of CABG for the treatment of CAD temporarily dampened interest in alternative revascularization methods.

Early efforts to establish direct myocardial revascularization techniques were limited by poor long-term patency, largely attributed to excessive tissue trauma. The emergence of laser technology in the 1980s led to landmark studies by Mahmood Mirhoseini [12] (in animals) and Masayoshi Okada [13] (in humans), who were the first to demonstrate the value of lasers for myocardial revascularization. Initial studies focused on lasers as adjunctive tools during CABG. Due to the limited peak energy outputs produced by early devices (restricted to 80 W) intraoperative cardiac arrest was typically required to provide sufficient time to bore transmural channels [14]. Technological advancements ultimately led to the development of lasers capable of

Disclosures None to declare

A.C.W. Baldwin, MD • O.H. Frazier, MD, FACC, FACS (✉)
Department of Cardiopulmonary Transplantation, Center for
Cardiac Support, Texas Heart Institute, MC 2-114A,
PO Box 20345, Houston, TX 77225-0345, USA
e-mail: abaldwin@texasheart.org; lschwenke@texasheart.org

producing 800 W and creating transmural channels on the beating heart, thus expanding the clinical expediency of the procedure [15]. A series of investigational studies subsequently revealed the utility of TMLR as sole therapy for CAD. In 1998, the technology was approved by the United States Food and Drug Administration for use in patients otherwise deemed ineligible for traditional therapy [16, 17].

Laser Types

In addition to laser technology, multiple alternative techniques for transmural revascularization were proposed, ranging from needle-based cauterization to cryogenic ablation and from focused ultrasonography to radiofrequency targeting [18–22]. None of these methods produced results comparable to those of laser technology. Various types and wavelengths of lasers were also tried, including carbon dioxide (CO₂), xenon chloride, and crystalized yttrium-aluminum-garnet (YAG) based devices [23–25]. Of the available options, only CO₂ and holmium-YAG (Ho:YAG) lasers have seen extensive clinical application, with the contents of this chapter specifically dedicated to the discussion of CO₂ Lasers.

With an infrared wavelength of 10.6 μm , CO₂ lasers transmit energy via thermal dissipation after the wavelength is absorbed by water molecules within the tissue. In contrast with Ho:YAG devices, CO₂ lasers use relatively high energy levels (typically 20 J) and require only a single 30–40-ms pulse to produce transmural channels (Fig. 23.1). The higher energy levels permitted with CO₂ lasers reduce structural trauma to the surrounding tissues, as shorter pulse durations minimize the accumulation of explosive thermal pressures [26]. Additionally, the CO₂ laser is designed to fire synchronously with the electrocardiographic R wave, thereby minimizing the risk of arrhythmogenic complications seen with Ho:YAG laser firings [27]. The laser system consists of a free-standing console with disposable sterile handpieces (Fig. 23.2).

Mechanisms of Action

Whereas the origins of TMLR were based upon anatomic hypotheses regarding collateral sources for myocardial perfusion, the true mechanism by which TMLR provides a therapeutic effect has been an area of considerable controversy. Several theories have been proposed to establish a causal

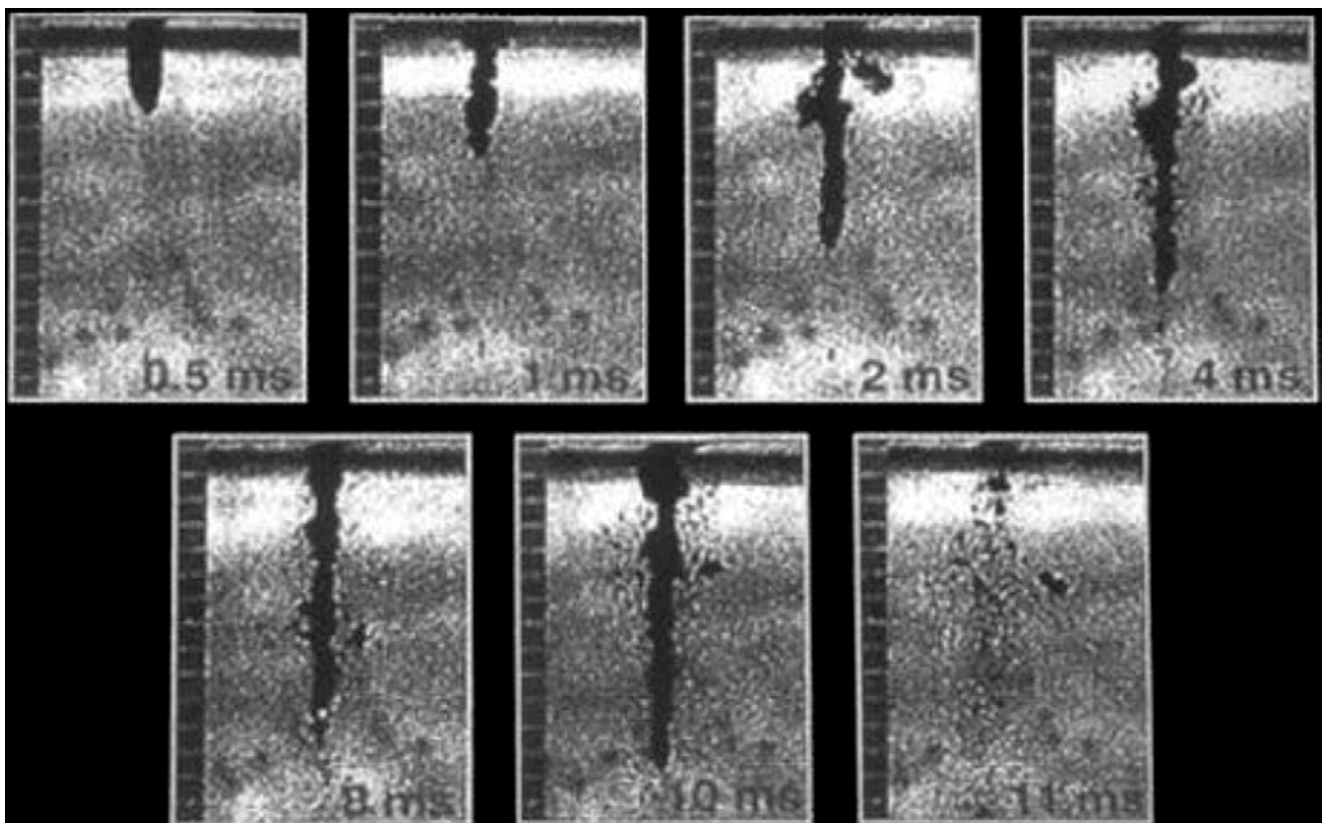


Fig. 23.1 Time-lapse photography showing a single CO₂ laser pulse in water (Reprinted with permission from Horvath and Zhou [78])



Fig. 23.2 Mobile console for the CO₂ HEART LASER system. Disposable hand pieces allow sterile manipulation of the laser arm by the surgeon (Reprinted with permission from Novadaq Technologies, Inc., Bonita Springs, Florida)

relationship between the drilling of laser channels and the symptomatic improvements documented in many patients. The evidence appears to favor certain mechanisms over others, but it is likely that a combination of factors collectively produce the observed results.

Channel Patency

The original intent of TMLR was to establish direct channels from the left ventricular lumen that were capable of delivering oxygenated blood to the myocardium. Early clinical and experimental studies revealed some evidence of long-term patency [28]. However, a number of dissenting researchers argued instead that the channels underwent deterioration and

thrombosis within a period of weeks [29, 30]. Nevertheless, patent channels have been observed with high-resolution contrast echocardiography [31]. Investigators using positron emission tomography (PET) and thallium single-photon emission tomography (TI:SPECT) have demonstrated a significant increase in subendocardial blood flow in the months after TMLR [16, 32]. Unfortunately, the prohibitive costs of these imaging modalities have limited their use, and enhanced perfusion does not prove channel patency. Whereas some channels may indeed remain patent, the general scientific consensus has moved away from the reptilian model of direct ventricular perfusion as the principal mechanism by which TMLR exerts its symptomatic benefits. Rather, drilling of the channels may indirectly lead to other tissue alterations responsible for the perceived effects.

Denervation

An alternative proposal for the mechanism of symptom relief after TMLR is the destruction of sympathetic nerve fibers leading to relief of angina. The nervous system of the heart is complex and incorporates an interwoven network of intrinsic and extrinsic neuronal components, making identification of specific disruptions to neural pathways quite difficult. However, experimental studies using Ho:YAG lasers have shown sympathetic denervation through a decreased response to epicardial bradykinin in animal models [33]. Reflecting the complexity of interpreting cardiac neuronal responses, other studies have failed to reveal significant changes in sympathetic reflexes after laser treatment [34, 35]. Regardless of the difficulty in pinpointing the neurologic mechanism involved, clinical studies utilizing postoperative PET imaging have revealed evidence of sympathetic denervation in patients treated with Ho:YAG lasers [36]. Although this finding has not yet been reproduced with CO₂ devices—which are associated with significantly less tissue destruction—evidence does suggest that some degree of neurologic disruption is associated with TMLR treatment and may contribute to symptom relief.

Angiogenesis

Angiogenesis has emerged as the most commonly cited mechanism for explaining the clinical efficacy of TMLR. The development of new blood vessels to feed the myocardium provides an explanation not only for the improvement in symptoms after laser therapy but also the enhanced blood flow seen on PET imaging in treated patients. In support of this argument, a host of animal studies have shown a dramatic increase in capillary density and histologic neovascularization after laser treatment [37–40]. Early investigations concerning the effects of laser irradiation on human tissues

revealed the production of heat-shock proteins and oxygen free radicals known to possess angiogenic properties [41]. More recently, studies have shown the upregulation and expression of various molecular regulators of neovascularization after TMLR, including vascular endothelial growth factor, fibroblast growth factor 2, and matrix metalloproteinases [42–44]. Whereas neovascularization has been shown to be a rather nonspecific reaction to tissue injury, high-energy laser pulses appear to produce a robust angiogenic response without significant scar formation or damage to the surrounding tissues [45–47].

Operative Technique

TMLR may be performed as sole therapy or concomitantly with CABG (with or without cardiopulmonary bypass). Because the majority of candidates have a lengthy history of refractory CAD often involving previous surgery, it is not uncommon to encounter significant adhesions upon reoperation. Whereas TMLR as sole therapy is most commonly performed through a left anterior thoracotomy, the procedure also has been performed via median sternotomy and thoracoscopic approaches [48, 49]. To assist with entrance into the thoracic cavity, general anesthesia is typically used, with single-lung ventilation achieved through the placement of a double-lumen endotracheal tube or a bronchial blocker. Intraoperative transesophageal echocardiography (TEE) is essential, both to monitor cardiac function and to confirm penetration of the endocardium by the laser.

The patient may be placed in the right lateral decubitus position or supine with a roll placed under the left side of the chest. The left groin is exposed for access should cardiopulmonary bypass or intraaortic balloon pump support be required. An anterolateral thoracotomy is performed through the fifth intercostal space, and the ribs are spread by using a ratcheting self-retaining retractor. On occasion, inadequate exposure may be improved by shingling the head of the 6th rib to widen the intercostal aperture. Dissection within the chest is frequently complicated by the presence of intrathoracic adhesions, and great care must be taken to avoid previous bypass grafts, friable lung tissue, and the phrenic nerve. Access to the heart is gained through a longitudinal incision along the pericardium anterior to the course of the phrenic nerve. If present, epicardial adhesions must be carefully released to allow mobilization of the heart. The left anterior descending artery is used as an anatomical landmark to identify territories selected for revascularization.

All operating-room personnel should wear protective eye-wear while the laser is in use. After the predetermined treatment zone has been identified, the surgeon creates channels by firing the laser every centimeter in a longitudinal fashion from the base of the heart toward the apex (Fig. 23.3).

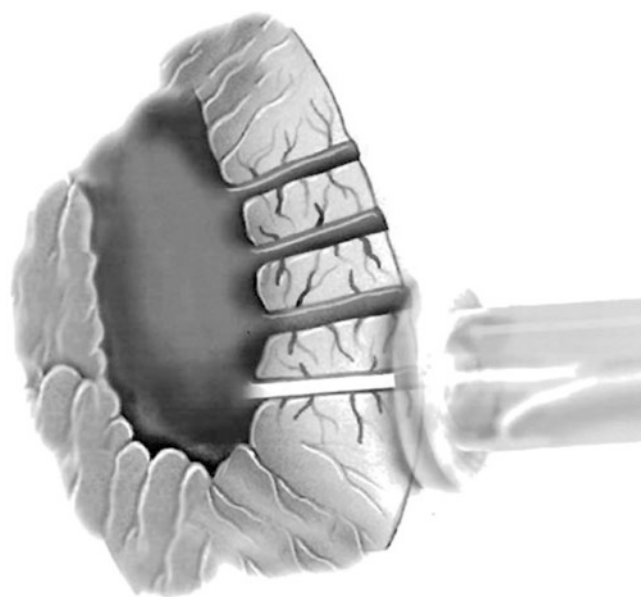


Fig. 23.3 Creation of a transmural channel using a single CO₂ laser pulse (Reprinted with permission from Horvath and Zhou [78])

Sequential rows of channels are formed as needed to cover the treatment area, and firings are minimized in areas of non-viable scarring. By beginning each row along the base of the heart, one can minimize the amount of blood collected within the active laser field. With CO₂ lasers, transmural channels are created by a single energy pulse. Transesophageal echocardiography is used to monitor each pulse and confirm a characteristic acoustic effect indicating the vaporization of blood [50]. When the entire ischemic area has been treated, the pericardial space is irrigated with saline solution, and any persistent bleeding is controlled with a 6–0 polypropylene suture. Drains are placed within the pleura and pericardial space, and the thoracotomy is closed in a standard fashion.

TMLR as Sole Therapy

In the 1990s, early small studies showed that TMLR could be used safely and effectively for patients with severe CAD not amenable to traditional intervention [16, 51]. The symptom relief observed in these early efforts quickly led to a series of large prospective, randomized, controlled trials comparing TMLR with standard medical therapy. Nearly 1000 patients were enrolled into 5 separate trials, the results of which were all reported within a 1-year period at the close of the decade [52–56]. Three of these studies involved only CO₂ lasers, and the remainder were limited to evaluating the efficacy of Ho:YAG therapy. All of the studies involved similar patient populations and a minimum follow-up period of 12 months, with two groups completing long-term follow-up studies that reached 5 years [57, 58].

A meta-analysis review revealed no statistically significant difference in 1-year survival for TMLR patients versus those undergoing medical therapy alone (survival rate, 84–95 % vs. 79–96 %, respectively) [59]. Perioperative mortality rates were low (1–5 %) and were significantly affected by the severity of the patient's preoperative clinical status. Similarly, long-term follow-up analyses revealed no statistically significant difference in survival between the TMLR and medical arms at 5 years. The reported incidence of specific postoperative complications—including myocardial infarction, heart failure, and arrhythmias—was lower after TMLR than that traditionally seen after reoperative CABG [60]. Procedure-specific risks included pericardial tamponade and chordal damage, both of which were exceedingly rare.

Whereas mortality rates were largely equivalent, the randomized studies reported consistent improvements in perioperative morbidity, hospital readmission rates, and quality of life among patients treated with TMLR. All patients continued to receive appropriate medical therapy throughout the study period, but TMLR patients experienced a significant reduction in the amount of medications required after 1 year. Moreover, 1-year hospitalization rates were significantly lower for laser-treated patients, and patients who had medical therapy alone were admitted to the hospital 4 times more often than were the laser patients within the first year. Additionally, each study documented significant improvements in quality-of-life metrics for patients treated with TMLR, and these improvements were not similarly reflected in the medical group.

Relief from angina symptoms has consistently been the most prominent result of TMLR therapy. Angina classification, as defined by the Canadian Cardiovascular Society grading scale, was used in all studies to compare symptoms before and after treatment. Although baseline characteristics were not standardized across all 5 trials, the majority of patients (69 %) were listed in class IV (severely limited; unable to perform any activity without angina, or symptoms at rest), and each study employed a blinded independent observer to perform symptomatic assessments. Overall, significant symptomatic improvement was seen in all 5 trials, 25–76 % of patients reaching the predetermined benchmark of angina improvement by two classifications (this goal was more easily reached by patients designated with severe baseline symptoms). Significantly fewer patients in the medical cohort experienced a similar improvement in angina symptoms (Fig. 23.4). In long-term follow-up studies, the apparent symptomatic advantage of TMLR therapy persisted, and at 5 years significantly more TMLR patients maintained an improved angina profile versus baseline profile [58].

As a result of these studies, the Society of Thoracic Surgeons developed a summary of consensus practice guidelines designed to standardize the use of TMLR as sole therapy (Table 23.1) [61]. The level of evidence supporting these

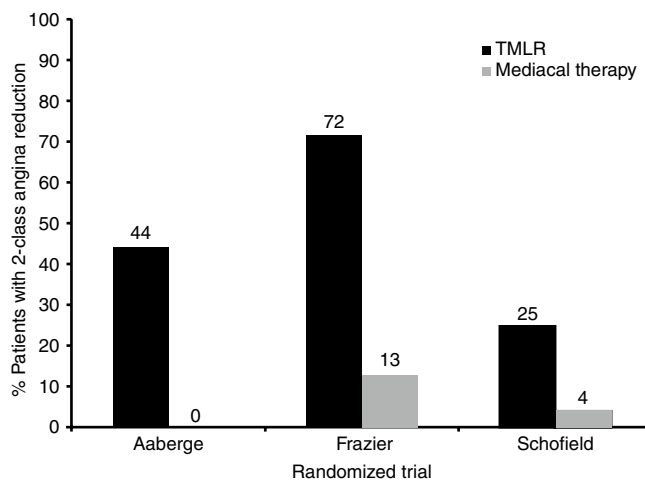


Fig. 23.4 Summary of angina relief reported by randomized controlled trials utilizing CO₂ lasers as sole therapy. The graph compares the percentage of patients reporting a reduction of 2 or more angina classes after laser revascularization (TMLR) or medical therapy (Reprinted with permission from Horvath and Zhou [78])

recommendations is categorized according to the standard American College of Cardiology and American Heart Association format, and it most strongly supports the use of TMLR in patients with severe angina, a preserved ejection fraction, and evidence of reversible ischemia not amenable to standard revascularization.

TMLR as an Adjunct to CABG

The success of TMLR as sole therapy led to interest in evaluating laser treatment as an adjunctive procedure during CABG. Anecdotal clinical experience with the concomitant procedures initially provided contradictory results, probably owing to the severity of diffuse coronary disease in many of the patients recommended for dual therapy [62, 63]. To evaluate the utility of this practice, 2 prospective randomized controlled trials were performed to evaluate the outcomes of CABG with concurrent TMLR versus CABG alone [64, 65].

Although baseline patient characteristics reflected a difference in the severity of clinical profiles between the two studies, both series revealed significantly better postoperative outcomes after combined CABG plus TMLR than after CABG alone. Perioperative mortality rates, 30-day freedom from major adverse cardiac events, and 1-year Kaplan-Meier survival rates each reflected a significant benefit for concurrent TMLR. Additionally, postoperative inotropic support, intensive-care-unit times, and the index hospitalization length of stay were all significantly reduced in the combined procedure cohort. As seen in the sole therapy studies, patients treated with TMLR also had a statistically significant postoperative reduction in angina symptoms. Long-term follow-up

Table 23.1 Recommendations for transmyocardial laser revascularization as sole therapy

<i>Class I</i>
1. Patients with an ejection fraction greater than 0.30 and CCS class III or IV angina that is refractory to maximal medical therapy. These patients should have reversible ischemia of the left ventricular free wall and coronary artery disease corresponding to the regions of myocardial ischemia. In all regions of the myocardium, the coronary disease must not be amenable to CABG or PTCA either as a result of (1) severe diffuse disease, (2) lack of suitable targets for complete revascularization, or (3) lack of suitable conduits for complete revascularization (level of evidence: A)
<i>Class IIB</i>
1. Patients who otherwise have class I indications for TMLR but who have either:
(a) Ejection fraction less than 0.30 with or without insertion of an intraaortic balloon pump (level of evidence: C)
(b) Unstable angina or acute ischemia necessitating intravenous antianginal therapy (level of evidence: B)
(c) Patients with class II angina (level of evidence: C)
<i>Class III</i>
1. Patients without angina or with class I angina (level of evidence: C)
2. Acute evolving myocardial infarction or recent transmural or nontransmural myocardial infarction (level of evidence: C)
3. Cardiogenic shock defined as a systolic blood pressure less than 80 mmHg or a cardiac index of less than $1.8 \text{ L} \cdot \text{min}^{-1} \cdot \text{min}^{-2}$ (level of evidence: C)
4. Uncontrolled ventricular or supraventricular tachyarrhythmias (level of evidence: C)
5. Decompensated congestive heart failure (level of evidence: C)

Compiled from data presented in Bridges et al. [61]

CABG coronary artery bypass grafting, CCS Canadian Cardiovascular Society, PTCA percutaneous transluminal coronary angioplasty, TMLR transmyocardial laser revascularization

Table 23.2 Recommendations for transmyocardial laser revascularization as adjunct to coronary artery bypass grafting

<i>Class IIA</i>
1. Patients with angina (class I–IV) in whom CABG is the standard of care who also have at least one accessible and viable ischemic region with demonstrable coronary artery disease that cannot be bypassed either because of (1) severe diffuse disease, (2) lack of suitable targets for complete revascularization, or (3) lack of suitable conduits for complete revascularization (level of evidence: B)
<i>Class IIB</i>
1. Patients without angina in whom CABG is the standard of care who also have at least one accessible and viable ischemic region with demonstrable coronary artery disease that cannot be bypassed either because of (1) severe diffuse disease, (2) lack of suitable targets for complete revascularization, or (3) lack of suitable conduits for complete revascularization (level of evidence: C)
<i>Class III</i>
1. Patients in whom CABG is not the standard of care (level of evidence C)

Compiled from data presented in Bridges et al. [61]

CABG coronary artery bypass grafting

studies suggest that this overall improvement is sustained and is characterized by a reduced New York Heart Association functional classification among patients treated with TMLR versus CABG alone [66]. Like the recommendations for sole therapy, practice guidelines for the use of TMLR in conjunction with CABG have been developed by the Society of Thoracic Surgeons and reflect the relative strength of supporting evidence (Table 23.2).

Percutaneous Laser Revascularization

To pursue increasingly minimally invasive treatment modalities, researchers have sought to evaluate percutaneous myocardial laser revascularization (PMLR) as a method of achieving results similar to those of external laser therapy. In PMLR, a catheter-based device is used to guide a laser fiber

in retrograde fashion from a peripheral artery into the left ventricle. Small divots are then created in target areas of the subendocardium by using electromechanical mapping [67]. In several trials, investigators have attempted to reproduce the symptomatic benefits of TMLR by using a percutaneous approach, but patients were instead found to have less favorable outcomes than those undergoing either standard TMLR or concurrent percutaneous interventions [68–70]. Additionally, this technology was not applied to CO₂ lasers and was limited to Ho:YAG delivery alone.

Future Directions

In select high-risk patients for whom more extensive surgery may not be tolerated, TMLR represents a valuable option. For example, isolated reports have indicated a potential ben-

efit for the use of TMLR in treating patients with diffuse transplant allograft atherosclerosis and reoperative patients of the Jehovah's Witness faith [71, 72].

A number of recent studies have focused on the potential use of TMLR with adjuvant cell therapy for the stimulation of therapeutic angiogenesis. Animal studies have shown that the addition of laser therapy results in increased expression of specific angiogenic chemokines and growth factors [73, 74]. Small clinical studies have shown the feasibility of combined treatment with adjuvant therapy but have yet to establish proven benefits [75–77]. Targeted application of TMLR with specific stem cell lines is believed to have the potential for effective neovascularization and reperfusion of ischemic zones with subsequent clinical improvement, and active research efforts toward this end are ongoing.

Key Points

1. Randomized controlled trials have shown that TMLR can provide significant relief of angina symptoms for patients with severe CAD otherwise not amenable to traditional therapy.
2. Both Ho:YAG and CO₂ lasers are approved by the US Food and Drug Administration for use in TMLR. CO₂ lasers require only a single pulse, may be used on the beating heart, and can be easily monitored via TEE during application.
3. To target areas not amenable to bypass and to provide more thorough revascularization, TMLR can be performed concurrently with CABG. Again, studies have shown significant angina relief with this method versus CABG alone.

References

1. Mannheimer C, Camici P, Chester MR, Collins A, DeJongste M, Eliasson T, Follath F, Hellemans I, Herlitz J, Luscher T, Pasic M, Thelle D. The problem of chronic refractory angina; report from the ESC Joint Study Group on the Treatment of Refractory Angina. *Eur Heart J*. 2002;23:355–70.
2. Osswald BR, Blackstone EH, Tochtermann U, Schweiger P, Thomas G, Vahl CF, Hagl S. Does the completeness of revascularization affect early survival after coronary artery bypass grafting in elderly patients? *Eur J Cardiothorac Surg*. 2001;20:120–5, discussion 125–126.
3. Weintraub WS, Jones EL, Craver JM, Guyton RA. Frequency of repeat coronary bypass or coronary angioplasty after coronary artery bypass surgery using saphenous venous grafts. *Am J Cardiol*. 1994;73:103–12.
4. Thebesius AC. *De circolo sanguinis in corde*. Leiden: Apud Abrahamum Elzevier; 1708.
5. Wearn JT, Mettler SR, Klumpp TG, Zschiesche LJ. The nature of the vascular communications between the coronary arteries and the chambers of the heart. *Am Heart J*. 1933;9:147–64.
6. Sen PK, Udawadia TE, Kinare SG, Parulkar GB. Transmyocardial acupuncture: a new approach to myocardial revascularization. *J Thorac Cardiovasc Surg*. 1965;50:181–9.
7. Beck CS, Leighninger DS. Scientific basis for the surgical treatment of coronary artery disease. *JAMA*. 1955;159:1264–71.
8. Goldman A, Greenstone SM, Preuss FS, Strauss SH, Chang ES. Experimental methods for producing a collateral circulation to the heart directly from the left ventricular. *J Thorac Surg*. 1956;31:364–74.
9. Massimo C, Boffi L. Myocardial revascularization by a new method of carrying blood directly from the left ventricular cavity into the coronary circulation. *J Thorac Surg*. 1957;34:257–64.
10. Mittal CM. Profulla Kumar Sen: his contributions to cardiovascular surgery. *Tex Heart Inst J*. 2002;29:17–25.
11. Walter P, Hundeshagen H, Borst HG. Treatment of acute myocardial infarction by transmural blood supply from the ventricular cavity. *Eur Surg Res*. 1971;3:130–8.
12. Mirhoseini M, Muckerheide M, Cayton MM. Transventricular revascularization by laser. *Lasers Surg Med*. 1982;2:187–98.
13. Okada M, Ikuta H, Shimizu K, Horii H, Nakamura K. Alternatives method of myocardial revascularization by laser: experimental and clinical study. *Kobe J Med Sci*. 1986;32:151–61.
14. Mirhoseini M, Shelgikar S, Cayton MM. New concepts in revascularization of the myocardium. *Ann Thorac Surg*. 1988;45:415–20.
15. Mirhoseini M, Cayton MM, Shelgikar S. Transmyocardial laser revascularization. *J Am Coll Cardiol*. 1994;1A:484.
16. Frazier OH, Cooley DA, Kadipasaoglu KA, Pehlivanoglu S, Lindenmeir M, Barasch E, Conger JL, Wilansky S, Moore WH. Myocardial revascularization with laser. Preliminary findings. *Circulation*. 1995;92:II58–65.
17. Josefson D. FDA approves heart laser treatment. *BMJ*. 1998;316:1409.
18. Dietz U, Darius H, Eick O, Buerke M, Ed Odeh R. Transmyocardial revascularization using temperature controlled HF energy creates reproducible intramyocardial channels. *Circulation*. 1998;98:3770.
19. Khairy P, Dubuc M, Gallo R. Cryoapplication induces neovascularization: a novel approach to percutaneous myocardial revascularization. *J Am Coll Cardiol*. 2000;35:5A–6.
20. Smith NB, Hynynen K. The feasibility of using focused ultrasound for transmyocardial revascularization. *Ultrasound Med Biol*. 1998;24:1045–54.
21. Whittaker P, Rakusan K, Kloner RA. Transmural channels can protect ischemic tissue. Assessment of long-term myocardial response to laser- and needle-made channels. *Circulation*. 1996;93:143–52.
22. Yamamoto N, Gu A, DeRosa CM, Shimizu J, Zwas DR, Smith CR, Burkhoff D. Radio frequency transmyocardial revascularization enhances angiogenesis and causes myocardial denervation in canine model. *Lasers Surg Med*. 2000;27:18–28.
23. Genyk IA, Frenz M, Ott B, Walpoth BH, Schaffner T, Carrel TP. Acute and chronic effects of transmyocardial laser revascularization in the nonischemic pig myocardium by using three laser systems. *Lasers Surg Med*. 2000;27:438–50.
24. Hughes GC, Kypson AP, Annex BH, Yin B, St Louis JD, Biswas SS, Coleman RE, DeGrado TR, Donovan CL, Landolfo KP, Lowe JE. Induction of angiogenesis after TMR: a comparison of holmium: YAG, CO₂, and excimer lasers. *Ann Thorac Surg*. 2000;70:504–9.
25. Jeevanandam V, Auteri JS, Oz MC, Watkins J, Rose EA, Smith CR. Myocardial revascularization by laser-induced channels. *Surg Forum*. 1994;41:225–7.
26. Kadipasaoglu KA, Frazier OH. Transmyocardial laser revascularization: effect of laser parameters on tissue ablation and cardiac perfusion. *Semin Thorac Cardiovasc Surg*. 1999;11:4–11.
27. Kadipasaoglu KA, Sartori M, Masai T, Cihan HB, Clubb Jr FJ, Conger JL, Frazier OH. Intraoperative arrhythmias and tissue damage during transmyocardial laser revascularization. *Ann Thorac Surg*. 1999;67:423–31.

28. Cooley DA, Frazier OH, Kadipasaoglu KA, Pehlivanoglu S, Shannon RL, Angelini P. Transmyocardial laser revascularization. Anatomic evidence of long-term channel patency. *Tex Heart Inst J*. 1994;21:220-4.
29. Burkhoff D, Fisher PE, Apfelbaum M, Kohmoto T, DeRosa CM, Smith CR. Histologic appearance of transmyocardial laser channels after 4 1/2 weeks. *Ann Thorac Surg*. 1996;61:1532-4; discussion 1534-1535.
30. Gassler N, Wintzer HO, Stubbe HM, Wullbrand A, Helmchen U. Transmyocardial laser revascularization. Histological features in human nonresponder myocardium. *Circulation*. 1997;95:371-5.
31. Berwing K, Bauer EP, Strasser R, Klovekorn WP, Reuthebuch O, Bertschmann W. Functional evidence of long-term channel patency after transmyocardial laser revascularization (abstract). *Circulation*. 1997;96:I-564.
32. Cooley DA, Frazier OH, Kadipasaoglu KA, Lindenmeir MH, Pehlivanoglu S, Kolff JW, Wilansky S, Moore WH. Transmyocardial laser revascularization: clinical experience with twelve-month follow-up. *J Thorac Cardiovasc Surg*. 1996;111:791-7; discussion 797-799.
33. Kwong KF, Kanellopoulos GK, Nickols JC, Pogwizd SM, Saffitz JE, Schuessler RB, Sundt 3rd TM. Transmyocardial laser treatment denervates canine myocardium. *J Thorac Cardiovasc Surg*. 1997;114:883-9; discussion 889-890.
34. Hirsch GM, Thompson GW, Arora RC, Hirsch KJ, Sullivan JA, Armour JA. Transmyocardial laser revascularization does not denervate the canine heart. *Ann Thorac Surg*. 1999;68:460-8; discussion 468-469.
35. Minisi AJ, Topaz O, Quinn MS, Mohanty LB. Cardiac nociceptive reflexes after transmyocardial laser revascularization: implications for the neural hypothesis of angina relief. *J Thorac Cardiovasc Surg*. 2001;122:712-9.
36. Al-Sheikh T, Allen KB, Straka SP, Heimansohn DA, Fain RL, Hutchins GD, Sawada SG, Zipes DP, Engelstein ED. Cardiac sympathetic denervation after transmyocardial laser revascularization. *Circulation*. 1999;100:135-40.
37. Hughes GC, Lowe JE, Kypson AP, St Louis JD, Pippen AM, Peters KG, Coleman RE, DeGrado TR, Donovan CL, Annex BH, Landolfo KP. Neovascularization after transmyocardial laser revascularization in a model of chronic ischemia. *Ann Thorac Surg*. 1998;66:2029-36.
38. Kohmoto T, Fisher PE, DeRosa C, Smith CR, Burkhoff D. Evidence of angiogenesis in regions treated with transmyocardial laser revascularization. *Circulation*. 1996;94:I-294.
39. Malekan R, Reynolds CA, Kelly ST, Suzuki Y, Bridges CR. Angiogenesis in transmyocardial laser revascularization: a nonspecific response to injury. *Circulation*. 1997;96:I-483.
40. Yamamoto N, Kohmoto T, Gu A, Derosa C, Smith CR, Burkhoff D. Transmyocardial revascularization enhances angiogenesis in a canine model of chronic ischemia. *Circulation*. 1997;96:I-563.
41. Nakagawa K. Direct observation of laser generated free radicals from a myocardium target site. *Free Radic Biol Med*. 1992;12:241-2.
42. Horvath KA, Chiu E, Maun DC, Lomasney JW, Greene R, Pearce WH, Fullerton DA. Up-regulation of vascular endothelial growth factor mRNA and angiogenesis after transmyocardial laser revascularization. *Ann Thorac Surg*. 1999;68:825-9.
43. Li W, Chiba Y, Kimura T, Morioka K, Uesaka T, Ihaya A, Muraoka R. Transmyocardial laser revascularization induced angiogenesis correlated with the expression of matrix metalloproteinases and platelet-derived endothelial cell growth factor. *Eur J Cardiothorac Surg*. 2001;19:156-63.
44. Pelletier MP, Gaiad A, Sivaraman S, Dorfman J, Li CM, Philip A, Chiu RC. Angiogenesis and growth factor expression in a model of transmyocardial revascularization. *Ann Thorac Surg*. 1998;66:12-8.
45. Chu VF, Gaiad A, Kuang JQ, McGinn AN, Li CM, Pelletier MP, Chiu RC. Thoracic Surgery Directors Association Award. Angiogenesis in transmyocardial revascularization: comparison of laser versus mechanical punctures. *Ann Thorac Surg*. 1999;68:301-7; discussion 307-308.
46. Horvath KA, Belkind N, Wu I, Greene R, Doukas J, Lomasney JW, McPherson DD, Fullerton DA. Functional comparison of transmyocardial revascularization by mechanical and laser means. *Ann Thorac Surg*. 2001;72:1997-2002.
47. Malekan R, Reynolds C, Narula N, Kelley ST, Suzuki Y, Bridges CR. Angiogenesis in transmyocardial laser revascularization. A nonspecific response to injury. *Circulation*. 1998;98:II62-5; discussion II66.
48. Horvath KA. Thoracoscopic transmyocardial laser revascularization. *Ann Thorac Surg*. 1998;65:1439-41.
49. Saatvedt K, Dragsund M, Nordstrand K. Transmyocardial laser revascularization and coronary artery bypass grafting without cardiopulmonary bypass. *Ann Thorac Surg*. 1996;62:323-4.
50. Agarwal S, Kamath MV, Castresana MR. Transesophageal echocardiography for transmyocardial laser revascularization. *Anesth Analg*. 2014;118:1146-9.
51. Horvath KA, Cohn LH, Cooley DA, Crew JR, Frazier OH, Griffith BP, Kadipasaoglu K, Lansing A, Mannting F, March R, Mirhoseini MR, Smith C. Transmyocardial laser revascularization: results of a multicenter trial with transmyocardial laser revascularization used as sole therapy for end-stage coronary artery disease. *J Thorac Cardiovasc Surg*. 1997;113:645-54.
52. Aaberge L, Nordstrand K, Dragsund M, Saatvedt K, Endresen K, Golf S, Geiran O, Abdelnoor M, Forfang K. Transmyocardial revascularization with CO2 laser in patients with refractory angina pectoris. Clinical results from the Norwegian randomized trial. *J Am Coll Cardiol*. 2000;35:1170-7.
53. Allen KB, Dowling RD, Fudge TL, Schoettle GP, Selinger SL, Gangahar DM, Angell WW, Petracek MR, Shaar CJ, O'Neill WW. Comparison of transmyocardial revascularization with medical therapy in patients with refractory angina. *N Engl J Med*. 1999;341:1029-36.
54. Burkhoff D, Schmidt S, Schulman SP, Myers J, Resar J, Becker LC, Weiss J, Jones JW. Transmyocardial laser revascularisation compared with continued medical therapy for treatment of refractory angina pectoris: a prospective randomised trial. ATLANTIC Investigators. *Angina Treatments-Lasers and Normal Therapies in Comparison*. *Lancet*. 1999;354:885-90.
55. Frazier OH, March RJ, Horvath KA. Transmyocardial revascularization with a carbon dioxide laser in patients with end-stage coronary artery disease. *N Engl J Med*. 1999;341:1021-8.
56. Schofield PM, Sharples LD, Caine N, Burns S, Tait S, Wistow T, Buxton M, Wallwork J. Transmyocardial laser revascularisation in patients with refractory angina: a randomised controlled trial. *Lancet*. 1999;353:519-24.
57. Aaberge L, Rootwelt K, Blomhoff S, Saatvedt K, Abdelnoor M, Forfang K. Continued symptomatic improvement three to five years after transmyocardial revascularization with CO(2) laser: a late clinical follow-up of the Norwegian Randomized trial with transmyocardial revascularization. *J Am Coll Cardiol*. 2002;39:1588-93.
58. Allen KB, Dowling RD, Angell WW, Gangahar DM, Fudge TL, Richenbacher W, Selinger SL, Petracek MR, Murphy D. Transmyocardial revascularization: 5-year follow-up of a prospective, randomized multicenter trial. *Ann Thorac Surg*. 2004;77:1228-34.
59. Cheng D, Diegeler A, Allen K, Weisel R, Lutter G, Sartori M, Asai T, Aaberge L, Horvath K, Martin J. Transmyocardial laser revascularization: a meta-analysis and systematic review of controlled trials. *Innovations (Phila)*. 2006;1:295-313.
60. Horvath KA. Transmyocardial laser revascularization. *J Card Surg*. 2008;23:266-76.

61. Bridges CR, Horvath KA, Nugent WC, Shahian DM, Haan CK, Shemin RJ, Allen KB, Edwards FH, Society of Thoracic Surgeons. The Society of Thoracic Surgeons practice guideline series: transmyocardial laser revascularization. *Ann Thorac Surg.* 2004;77:1494–502.
62. Horvath KA, Ferguson Jr TB, Guyton RA, Edwards FH. Impact of unstable angina on outcomes of transmyocardial laser revascularization combined with coronary artery bypass grafting. *Ann Thorac Surg.* 2005;80:2082–5.
63. Peterson ED, Kaul P, Kaczmarek RG, Hammill BG, Armstrong PW, Bridges CR, Ferguson Jr TB, Society of Thoracic Surgeons. From controlled trials to clinical practice: monitoring transmyocardial revascularization use and outcomes. *J Am Coll Cardiol.* 2003;42:1611–6.
64. Allen KB, Dowling RD, DelRossi AJ, Realyvasques F, Lefrak EA, Pfeffer TA, Fudge TL, Mostovych M, Schuch D, Szentpetery S, Shaar CJ. Transmyocardial laser revascularization combined with coronary artery bypass grafting: a multicenter, blinded, prospective, randomized, controlled trial. *J Thorac Cardiovasc Surg.* 2000;119:540–9.
65. Frazier OH, Boyce SW, Griffith BP, Hattler BG, Kadipasaoglu KA, Lansing AM, March RJ. Transmyocardial revascularization using a synchronized CO₂ laser as adjunct to coronary artery bypass grafting: results of a prospective, randomized, multicenter trial with 12-month follow-up (abstract). *Circulation.* 1999;100:I-248.
66. Eldaif SM, Lattouf OM, Kilgo P, Guyton RA, Puskas JD, Thourani VH. Long-term outcomes after CABG with concomitant CO₂ transmyocardial revascularization in comparison with CABG alone. *Innovations (Phila).* 2010;5:103–8.
67. Kim CB, Oesterle SN. Percutaneous transmyocardial revascularization. *J Clin Laser Med Surg.* 1997;15:293–8.
68. Leon MB, Kornowski R, Downey WE, Weisz G, Baim DS, Bonow RO, Hendel RC, Cohen DJ, Gervino E, Laham R, Lembo NJ, Moses JW, Kuntz RE. A blinded, randomized, placebo-controlled trial of percutaneous laser myocardial revascularization to improve angina symptoms in patients with severe coronary disease. *J Am Coll Cardiol.* 2005;46:1812–9.
69. Oesterle SN, Sanborn TA, Ali N, Resar J, Ramee SR, Heuser R, Dean L, Knopf W, Schofield P, Schaer GL, Reeder G, Masden R, Yeung AC, Burkhoff D. Percutaneous transmyocardial laser revascularisation for severe angina: the PACIFIC randomised trial. Potential Class Improvement From Intramyocardial Channels. *Lancet.* 2000;356:1705–10.
70. Stone GW, Teirstein PS, Rubenstein R, Schmidt D, Whitlow PL, Kosinski EJ, Mishkel G, Power JA. A prospective, multicenter, randomized trial of percutaneous transmyocardial laser revascularization in patients with nonrecanalizable chronic total occlusions. *J Am Coll Cardiol.* 2002;39:1581–7.
71. Frazier OH, Kadipasaoglu KA, Radovancevic B, Cihan HB, March RJ, Mirhoseini M, Cooley DA. Transmyocardial laser revascularization in allograft coronary artery disease. *Ann Thorac Surg.* 1998;65:1138–41.
72. Gregoric ID, Nolen MT, Ksela J, Chandler LB, Messner GN, Cervera RD, Smart FW, Delgado 3rd RM, Frazier OH. Posttransplant off-pump coronary bypass and laser revascularization in a Jehovah's Witness. *Tex Heart Inst J.* 2005;32:434–6.
73. Patel AN, Spadaccio C, Kuzman M, Park E, Fischer DW, Stice SL, Mullangi C, Toma C. Improved cell survival in infarcted myocardium using a novel combination transmyocardial laser and cell delivery system. *Cell Transplant.* 2007;16:899–905.
74. Shahzad U, Li G, Zhang Y, Yau TM. Transmyocardial revascularization induces mesenchymal stem cell engraftment in infarcted hearts. *Ann Thorac Surg.* 2012;94:556–62.
75. Gowdak LH, Schettert IT, Rochitte CE, Lisboa LA, Dallan LA, Cesar LA, Krieger JE, Ramires JA, Oliveira SA. Cell therapy plus transmyocardial laser revascularization for refractory angina. *Ann Thorac Surg.* 2005;80:712–4.
76. Gowdak LH, Schettert IT, Rochitte CE, Rienzo M, Lisboa LA, Dallan LA, Cesar LA, Krieger JE, Ramires JA, de Oliveira SA. Transmyocardial laser revascularization plus cell therapy for refractory angina. *Int J Cardiol.* 2008;127:295–7.
77. Reyes G, Allen KB, Alvarez P, Alegre A, Aguado B, Olivera M, Caballero P, Rodriguez J, Duarte J. Mid term results after bone marrow laser revascularization for treating refractory angina. *BMC Cardiovasc Disord.* 2010;10:42.
78. Horvath KA, Zhou Y. Transmyocardial laser revascularization and extravascular angiogenetic techniques to increase myocardial blood flow. In: Cohn LH, editor. *Cardiac surgery in the adult.* 4th ed. New York: McGraw-Hill Professional; 2012.

Mark W. Moritz, Michael Ombrellino, and Harry Agis

Introduction to Basic Principles of Laser Use

Key Points

Laser – tissue interaction depends on chromophore absorption characteristics, laser wavelength, fluence, pulse duration, and relaxation time of the target tissue, among other factors.

Hemoglobin is the targeted chromophore for surface lesions.

Hemoglobin and water are targeted for endovenous therapy.

Laser safety demands proactive, rigorous attention to avoid injury to the patient or staff.

This section will introduce the reader to the basics of laser function and its interactions with tissue, with an emphasis on venous tissue, and provide basic information for laser safety. Treatments are now routine which were barely conceivable decades ago, and procedures once done commonly have been replaced by minimally invasive procedures which are made possible with lasers. It is imperative that the provider of modern vein treatments be familiar with the various applications of laser technology in this field. Complete description in depth of this field is of course impossible in one chapter; here, we present an overview of the field. Only important elements will be reviewed which are needed for the practitioner to understand and safely apply laser technology appropriately to the care of patients with venous disease. For more material in depth, the reader is referred to a number of excellent resources on this subject, which include review articles and texts [1–3].

The term “laser” is in fact an acronym, which stands for: “Light Amplification by the Stimulated Emission of

Radiation”, i.e., the specific electromagnetic radiation we call “light”. The first lasers were produced beginning in 1960, 2 years after the theory was first developed and published. The laser’s development evolved directly from the maser (Microwave Amplification by the Stimulated Emission of Radiation), devised in 1954, using similar technology but using microwave radiation instead of light. Over the ensuing decades, many lasers have been introduced, each using different substances and electronic circuits to produce monochromatic light of specific wavelengths, each suited to particular needs. The laser works by using incident light, such as white light, which is multi-chromatic, to energize a substance to give off a characteristic monochromatic light as stimulated electrons return to their lower valence/energy levels. This is intensified with mirrors within the apparatus, causing a high-energy monochromatic light emission or flash. Substances used in lasers include argon, carbon dioxide, ruby, neodymium, yttrium, garnet, and others, each of which alone, or combined, emit specific varieties of light. Description of specific laser types and their science is beyond the scope of this chapter.

The successful treatment of clinical disorders with laser depends on interaction with tissue in a safe and predictable manner. This depends on the physics of light-tissue interaction. For instance, for laser to treat telangiectasia, the light energy must pass through overlying skin without damaging it. The safe characteristics of light which permit this are called the “optical window” of the skin, which corresponds to the wavelengths of 600–1200 nm, the interval where the skin absorption of the energy is minimized. Electromagnetic energy is absorbed by tissue elements known as “chromophores”, and for these wavelengths, they would be the hemoglobin in blood and the melanin in the skin. Water, another dominant skin element, does not absorb significantly below wavelengths of 1000 nm. The amount of melanin in epidermis also determines extent of absorption, with fair skin absorbing less than tanned skin. In dermis, hemoglobin becomes the dominant chromophore, many-fold more so than melanin. When assessing the absorption of laser energy by hemo-

M.W. Moritz, MD (✉) • M. Ombrellino, MD • H. Agis, MD
The Vein Institute of New Jersey at the Cardiovascular Care
Group, New Jersey Medical School, Rutgers University,
95 Madison Avenue, Suite 109, Morristown, NJ 07960, USA
e-mail: mmoritz@tcvcg.com; mombrellino@gmail.com;
agisharry@gmail.com

globin in the skin, the wavelength of the laser energy is important, as the absorption of 532 nm light by hemoglobin is 100-fold more than for 1064 nm light [4]. For this reason, 532 nm light penetrates tissue less deeply than does 1064 nm light. Thus for a surface lesion of the skin composed of blood vessels (hemangioma, telangiectasis), energy from 532 nm light is absorbed more effectively than that of longer wavelengths. For deeper lesions (example, subcutaneous vessels), 1064 nm would penetrate better to that level and produce a coagulum.

The size of the incident laser beam (diameter) also influences depth of penetration. When the laser beam interacts with tissue elements, there is scatter of the light in different directions. Because some scatter occurs in the forward direction, a wider beam will induce more forward scatter, as more tissue elements are encountered. Thus, a wider beam has deeper penetration than a narrow one.

A major factor of laser energy that determines outcome and success of the treatment, such as ablating telangiectasia, is the fluence, or energy density, measured in J/cm^2 , of the incident laser light. In addition, the time in which the energy is delivered (pulse duration) is very important. Longer pulse duration causes more effective heating of a vessel, and whereas a short pulse duration may cause thrombosis of a small vessel, a long pulse duration will also cause destruction of the vessel wall [5–9]. Since cooling of tissue after laser heating occurs exponentially, with a time constant characterizing the tissue, the “relaxation time”, related to the time constant for cooling, is used to determine the optimal pulse duration. The properties of the target tissue are also important. The thermal relaxation time is a tissue characteristic which quantifies the transfer of heat to and from the tissue with time. When pulse duration exceeds relaxation time, any advantage of higher absorption is lost [10]. Pulse duration should not exceed the relaxation time of the tissue for optimal efficacy [3]. In surface laser treatment of telangiectasia and small veins, higher fluencies can be administered to the target tissue if the skin surface is also cooled simultaneously, preventing skin damage from the heat generated in the target. In addition, pulsed laser delivery modality is more effective than continuous wave delivery, since it can take advantage of higher energy absorption in the target tissue [11].

Another use of laser for venous disease treatment, endoablation (see section following), utilizes laser to produce heat in either hemoglobin, water, or both, to cause destruction of the vein wall, contraction and eventual disappearance of the vein. In this application, a light-conducting fiber is placed through the vein to be ablated, usually from a distal access location to a proximal site. When the laser is energized, energy is emitted from the tip, causing heating of the vein wall, and destruction of the

endothelium. The laser wavelength for effective water absorption in the vein wall is longer, up to 1470 nm, and these lasers are therefore correspondingly selected for that property. The heating at the fiber tip is thought to produce a coagulum, which in turn produces steam bubbles in any residual blood in the lumen, which then transmit heat to the endothelium [12, 13]. However, longer wavelengths, pulsed laser, and longer pulse duration favor vessel contraction over intraluminal thrombosis [4]. Various commercial products offer a choice of wavelengths, and there is some evidence that postoperative pain and bruising is less with longer wavelengths [14]. Tumescence anesthetic containing epinephrine also constricts the vein around the fiber, producing direct contact heating as well.

Heat transfer from an endovenous laser is described more simply for clinical purposes by the “linear endovenous energy density” (LEED), a measure of the joules applied per centimeter of vein length treated. Typically, 70 J/cm is the LEED which causes irreversible closure of a vein [15], but variations in the wavelength and other characteristics between devices mean that each device will have its own recommended settings (temperature, wattage, etc.) to achieve permanent closure. For larger diameter veins, more energy needs to be applied to avoid failure to close. We typically apply 70 J/cm with good results. Higher power settings (wattage) also may be more effective [16, 17].

Descriptions of various useful laser types in venous applications are given in the appropriate sections following.

Laser Safety

The operator must not only take positive steps to prevent patient injury during laser therapy, but must proactively anticipate problems and take steps to avoid injury to the eyes of personnel. All individuals in the procedure room must wear optical protective glasses for the wavelength laser being used. Approved designs will be labeled indicating for which wavelengths they are effective, and are usually supplied with the laser generator purchase. The patient is best protected with the use of eye shields, opaque plastic or metal devices specifically made for this purpose. The laser generator should always be kept in the “standby” mode until the moment that treatment begins, to avoid accidental firing outside the patient’s body (for endoablation), or before appropriate eyewear is in place for all parties (both surface laser and endoablative treatment). A clear, visible sign must be mounted on the door to the treatment room, warning that laser is in use and the door must be kept closed, preferably locked from the inside, to prevent accidental exposure to an individual entering during treatment. OSHA rules must be followed [18].

Practical Vein Anatomy: Surface, Superficial and Deep Systems

Key Point

Knowledge of venous anatomy is essential for successful treatment

Venous therapy involves interruption of refluxing blood flow in the lower extremities by (endo)ablation or excision (phlebectomy) for pain, stasis ulcers, or other complications of reflux, obliterative treatment of blood-filled cutaneous lesions (telangiectasia, port-wine stains, angiomas). It may also include recanalization of thrombosed major veins to treat obstructive symptoms in some cases. The choice of site for treatment and method of laser application for a particular treatment need is largely dependent on the patient's venous anatomy. Selecting patients with appropriate indications for laser procedures is complex, but a significant factor in determining suitability for a procedure is the anatomy of the veins to be treated and their abnormalities. A good working knowledge of practical anatomy is the foundation of good vein treatment. Space limitations in this chapter preclude a thorough review of venous anatomy. A basic knowledge of venous anatomy is assumed on the part of the reader; anatomic illustrations are readily available in many reference sources.

It is important that the practitioner utilize the new international nomenclature recently developed to avoid confusion since the commonly accepted terms are often different from those used in clinical practice, and the non-invasive imaging technologies such as duplex ultrasound imaging, three-dimensional CT, and MRI, have changed our knowledge of venous anatomy (Table 24.1).

The venous system, for purposes of laser treatment, can be thought of as composed of cutaneous veins anywhere on the body, the superficial and deep systems in the extremities, and the major veins of the pelvis and trunk (all deep veins). Venous anatomy can vary between individuals. We describe that usu-

Table 24.1 Examples of old and new nomenclature of venous anatomy useful in laser therapy

Old nomenclature	New nomenclature
Superficial femoral vein	Femoral vein
Greater saphenous vein, long saphenous vein	Great saphenous vein
Lesser saphenous vein	Small saphenous vein
Anterior saphenous vein	Anterior accessory saphenous vein
Giacomini's vein	Intersaphenous or posterior thigh circumflex
Cockett's perforators	Posterior tibial perforating veins
Boyd's perforating vein	Medial knee perforating vein

Adapted from Caggiati et al. [44]

ally found, but the vein therapist must be knowledgeable of, and vigilant for variations or anomalies that can occur. These must be recognized on physical exam or other studies such as ultrasound, so that appropriate efficacious treatment can be done with good results and without complications. Some common variations and anomalies are shown in Table 24.2.

Cutaneous venous anatomy, including intracutaneous lesions, which while technically "superficial", is not described as part of that named system. Rather, cutaneous venous lesions include telangiectasias, hemangiomas, pigmented lesions, port wine stains, and other venous malformations of the skin, nasal and oral cavities [19].

The superficial veins include those in the subcutaneous tissues, superficial to the investing fascia of a limb or other body part. In the legs, of interest here, this includes the saphenous systems and their tributaries, subcutaneous veins of the feet, and the epigastric veins draining the trunk into the femoral veins. Deep veins, however, include those which accompany the arterial counterparts in the limbs, pelvis, etc., including the iliac and gonadal systems, and the inferior vena cava, among others. Upper extremity deep and superficial veins include respectively, the axillary and subclavian veins, and the cephalic, basilic, and brachial systems. Perforating veins connect the two saphenous systems to the deep system of the same limb, with unidirectional valves, which, if dysfunctional, can be the source for reflux (insufficiency) and pathology. When found, refluxing perforating veins often also need definitive treatment to resolve stasis ulcers and may prevent ulcer recurrence.

As a practical matter, laser therapy lends itself to treatment of several venous structures addressed in this chapter: surface laser for telanectasia and angiomas, endoablation of refluxing superficial veins (saphenous systems) and thrombolysis of large truncal veins (iliacs, brachiocephalics). Telangiectasias and angiomas are confluences of dilated intradermal venules <1 mm. in diameter. These can be treated with surface laser, where a laser beam penetrates the skin, causing a coagulum to form, with associated vasospasm, ultimately shrinking and obliterating the venules.

Below the dermis, in the subcutaneous tissue, the reticular veins can be seen as dilated veins 1–3 mm. in diameter, often tortuous, but excluding otherwise normal veins visible in pale thin skin. These do not lend themselves to laser treatment, and

Table 24.2 Some variants and anomalies found in the adult venous system of importance to laser therapy

Duplicated great saphenous vein
Bifid great saphenous vein
Subcutaneous great saphenous vein
Thigh (cranial) extension of small saphenous vein
Aplastic or hypoplastic veins
Avalvulia (absent valves)
Venous aneurysm
Phlebectasia (diffuse dilatation)

we usually treat them with microphlebectomy, a technique which is covered elsewhere [20]. Varicose veins are also subcutaneous, but are >3 mm. in diameter when the patient stands. Patients with these often present with them protruding, and they often are associated with saphenous reflux (insufficiency), which responds well to laser endoablation when present.

Surface Ablation

Key Points

Ablation of cutaneous lesions with laser requires appropriate application of wavelength, pulse duration, depth and other laser characteristics for the particular lesion(s) and body part being treated.

Application of excess laser energy can cause skin injury with bulla formation, depigmentation, and pain.

Successful treatment of surface lesions requires patience and time. Patients' expectations should be prepared for repeated treatments to the same area with lightening over time, and may take months to achieve an appearance that pleases the patient.

Telangiectasias of the face and cherry hemangiomas respond the best to laser therapy, telangiectasias of the legs, telangiectatic matting post sclerotherapy and port wine stains require in general multiple treatment sessions. Reticular veins and larger telangiectasias are best treated with sclerotherapy first, and laser used to treat the fine residual telangiectasias to achieve the best cosmetic results.

Lasers have been used to treat cutaneous lesions of the face, legs, and elsewhere on the body since the 1960s. We will here review the basic principles and contemporary tools available.

Most patients with cutaneous vascular lesions seek treatment for cosmetic purposes, and expectations must be addressed very early in the preparation of the patient for treatment including vein resolution and cosmetic appearance. The patient must be carefully counseled regarding the risks of treatment with laser: skin burns, recurrences, pain, skin color changes, and failure to improve. Perfection is difficult to achieve, and improvement of the condition should be the goal. The patient must understand that lightening of a lesion to the patient's satisfaction may require several treatment sessions.

Telangiectasias of the face are very common and are a common lesion for which treatment with laser is appropriate. When on the legs, they are more difficult to treat and usually require more than one treatment session at either location. When considering laser treatment of cutaneous lesions, the melanin content of the patient's skin is important, as darker types will have more absorption by the melanin and less by the hemoglobin. The conventional method to assess skin col-

oration type is by the Fitzpatrick scale [21, 22]. This allows for consistent communication with a common nomenclature. Laser treatment is most safe and effective for Fitzpatrick types I–III (paler skin types). As the melanin content increases (types IV–VI, darker skin types), the likelihood of depigmentation by melanin absorption and destruction with laser treatment rises, and such therapy must be considered with caution to avoid unacceptable cosmetic outcomes.

Laser Vs. Sclerotherapy for Treatment of Cutaneous and Subcutaneous Lesions

Sclerotherapy is the treatment of choice for reticular veins and telangiectasias. This can often eliminate small telangiectasias with only one treatment session, whereas laser can require more than one session for the same result. The difference for the patient is lower overall cost, and quicker resolution. Small and large varicose veins are best treated with microphlebectomy, as laser is often ineffective in their complete elimination. An individualized treatment plan is always necessary. The best candidates for surface laser treatment are those with Fitzpatrick skin types I to III (paler skin types), who present with telangiectasias of the face and legs.

In our practice, we typically utilize the laser for telangiectasias of the legs which persist after sclerotherapy is complete, such as for telangiectatic matting, which is a fine, dense area of telangiectasias that can form after sclerotherapy, and where the vessels are too small to cannulate with a needle. When the face is treated, sclerotherapy is not used, so laser is the primary treatment. A few types of lasers are useful for these indications. The shorter wavelength lasers are best for the more superficial lesions, and the longer wavelengths, which transmit more power, for the deeper lesions.

Cherry hemangiomas are very common lesions, typically occurring on the neck, trunk and proximal legs. They can grow over time to large size, and often are very numerous, constituting a significant cosmetic concern for most patients who have them. They respond very well to laser therapy, and are perhaps the easiest type of lesion to treat. Smaller lesions often require only one session to be eliminated.

Choices of Lasers for Surface Treatment

The Diode 532/940 nm laser is our preference due to its portability and the availability of two different wavelengths in the same generator. However the Pulsed Dye Laser (PDL) 595 nm, the Alexandrite 755 nm and the long-pulsed Nd:Yag 1064 Laser are alternative devices that offer satisfactory results as well. The 1064 laser can be used in all skin types I to VI. Because of its weak absorption of melanin it is best for darker skin types. Optimal parameters for devices with this

wavelength have been reported [17]. The KTP (Potassium Titanyl Phosphate) 532 nm laser also treats surface lesions effectively. The KTP 532 laser has an Nd:YAG crystal doubled with a KTP crystal to emit a wavelength of 532 nm (green) which is in the visible spectrum of light. Lesions such as telangiectasias of the face and legs, port wine stains, red tattoos, poikiloderma, cherry hemangiomas and some pigmented skin lesions are amenable to treatment with this laser, with a low incidence of purpura. It has a penetration of 0.75 mm with hemoglobin as the chromophore. Patients with Fitzpatrick types I, II and III are the best candidates for its use. Treatment parameters for the Diode 532/940 nm laser which we find are effective and usually do not damage the skin included a fluence of 16–20 J/cm, and a pulse duration of 40 ms. We use a 1 mm beam diameter in most cases.

Some other laser choices are also described below, but this list is not intended to be complete. The reader is referred to a more complete technical review elsewhere [1].

The Long Pulsed 1064 nm Nd:YAG Laser can be used to treat leg and facial telangiectasias, with a success rate of vessel clearing at 50–100 % for facial telangiectasias after one treatment for the face, and after 3–5 treatments for the legs [23]. It is useful for Fitzpatrick skin types IV, V, and VI. The occurrence of hyperpigmentation is a complication. A cooling device is required to minimize collateral skin damage due to its high power transmission and to maximize patient comfort.

The Pulse Dye Laser (PDL, 585–600 nm wavelength) can be used for facial and leg telangiectasias and port wine stains. One of the main disadvantages of this laser is the propensity to develop purpura, which can last for several days. Using proper treating parameters and subpurpuric thresholds, satisfactory results can be achieved with this laser [24].

Method for Surface Laser Treatment

The use of laser for cosmetic purposes is best done in a comfortable setting for the patient, especially since laser application involves a small amount of pain with each pulse, and many patients expect it to be painless. A warm environment with soft music provides a relaxed atmosphere. Laser safety precautions are always used (see above). The patient is placed in a recumbent position as needed to expose the area to be treated. For first-time treatment, an explanation of what the laser feels like during treatment is given. We usually compare it to a rubber band snapping on the skin. Hydrogel is used on the skin surface for lubrication and good laser light conductivity. Skin cooling with the Diode 532/940 nm laser is not necessary, however cold hydrogel can be applied for patient comfort during the treatment. Longer wavelength lasers such as the 940 and 1064 nm wavelength lasers penetrate more deeply, and produce more pain than those with

shorter wavelengths. Topical anesthetics are not routinely used. Cooling methods vary with the manufacturer and some companies incorporate various cooling devices with the laser itself, and when other longer wavelengths are used, skin cooling and topical anesthesia are useful. After the treatment, gauze soaked in ice water is wrung out and placed on the treated areas for 5 min to improve comfort.

Telangiectasias of the face or legs are treated with a spot size of 1 mm outlining the vessel wall, the endpoint being blanching or graying of the vessel. The laser is set up at a fluence of 16–20 J/cm² with pulse duration between 32 and 40 ms and a repetition rate of 2 Hz. The lower fluence number is used for facial telangiectasias. One of the main advantages of the KTP 532 laser is that at the proper parameters it rarely causes purpura, resulting in a quicker clearing of the skin and better patient satisfaction. Avoiding pulse stacking (multiple laser dosing of the same spot) is important to prevent damage to the skin, remembering that the object is to eliminate the vein leaving the skin intact. Treatments usually last between 15 and 30 min depending on the extent of the problem. Venues in the alae, which are extremely sensitive to pain, are best pretreated with topical lidocaine.

Poikiloderma de Civatte which commonly occurs as a result of actinic damage and appears on the neck and upper chest, consists of both telangiectasias and pigmentation changes, it responds to laser treatment, however even lower fluencies are recommended to avoid skin damage and worsening hypopigmentation with uneven appearance of the skin. Small ones usually require one treatment with the Diode 532 laser at a fluence of 16–18 J/cm² and pulse duration of 32–38 ms. Larger lesions require more than one treatment session. Rosacea of the face, with its many small venules, responds very well, as do cherry hemangiomas.

Written and verbal post procedure instructions are given and the patient is cautioned not to tan the skin until completely healed, to use sunblock with an SPF of 30 or higher when in the sun, and to keep the skin moisturized. The patient is instructed to expect erythema for 1–3 days, similar to a sunburn. Sessions are spaced 3–4 weeks apart to allow a complete healing cycle of the area before assessment of the result and possible retreatment. As the lesion lightens with each treatment session, a subsequent treatment is then considered for patient satisfaction. During the follow up visit the results of the treatment are assessed and further treatment is performed as indicated. Telangiectasias of the face clear after one or two treatments with the nasolabial fold usually requiring a second laser application. Leg telangiectasias usually require two or more sessions with 60–70 % or better resolution in most cases.

Potential complications of laser treatment include: hypopigmentation, skin blistering, and telangiectatic matting. Residual scarring with the above mentioned parameters is rare. Mild skin erythema and some swelling are noted

immediately after treatment and resolve in a few hours, some mild crusting is occasionally seen and usually resolves in a few weeks. Changes in pigmentation are to be avoided especially as once the skin is depigmented, restoration is usually not possible. Hyperpigmentation can resolve slowly over time.

Endovenous Ablation

Key Points

Endovenous ablation of veins has replaced some older open surgical procedures, enabling the patient to have such procedures under local anesthesia with no incisions, as ambulatory patients, with minimal limitations during recovery.

Laser is a means of providing energy as focal heat at the tip of a catheter intraluminally and is one of two commonly used energy sources for ablations (the other is radiofrequency).

Most non-thrombotic venous disease is the result of reflux (insufficiency) in the deep and superficial veins, caused by primary or secondary valve dysfunction. In the presence of an intact deep system, veins of the superficial venous system can be closed to stop the reflux; endovenous ablation is a preferred method.

Quality B mode ultrasound imaging, preferably with duplex capability, is essential for successful venous closure and for preventing thrombotic complications.

Endoablation usually must be combined with phlebectomies to accomplish complete treatment of venous reflux and its sequelae, and to prevent later varicosity-related complication.

Patient Selection and Indications

The advent of catheter-based therapy has replaced stripping of superficial veins. Endovenous ablation of the GSV, SSV, Anterior Accessory GSV and the intersaphenous vein (Giacomini) has been performed for more than a decade with excellent clinical outcomes and a low rate of complications [25]. Patients must be carefully selected for this therapy to ensure good results, and must have a superficial refluxing vein identified on duplex ultrasound which fills a contiguous varix, and through which a laser fiber can pass. Using the international system of nomenclature for describing diagnostic information in chronic venous disease (CEAP classification), most such patients will be symptomatic, corresponding to CEAP classes 2–6 (Table 24.3). While many patients present with edema and varices, and are found to have reflux, only in some will the edema respond to superficial vein

Table 24.3 CEAP clinical grades

Grade	Description
C 0	Normal – no symptoms or signs of venous disease
C 1	Telangiectasias or reticular veins
C 2	Varicose veins
C 3	Edema
C4	Skin changes due to venous disease: 4A: hyperpigmentation, eczema 4B: lipodermatosclerosis, atrophie blanche
C 5	Prior (healed) venous ulcer
C 6	Open venous ulcer

endoablation [26]. Many patients with edema alone will not benefit. Those however with CEAP 3–6 will frequently have improvement in pain (sometimes immediately after the procedure), faster healing of stasis ulcers, and fewer, less frequent ulcer recurrences [27].

Since the procedure by definition produces a coagulum in the treated vein, it is relatively contraindicated in a patient with a known thrombophilic disorder. Offering this procedure to such a patient should be done only after careful consideration of the indication and whether other means of treatment would be efficacious. These patients should have DVT prophylaxis at the time of the procedure. In the rare patients of this sort treated in our practice, prophylaxis did not prevent successful vein closure.

Method

Prior to the procedure, the vein should be mapped with ultrasound, both to demonstrate the course of the vein and its unique characteristics, if any. Size, depth, areas of stenosis or occlusion must be noted. The original scan results obtained during diagnostic workup are checked. This may not have demonstrated the same level of detail which might make a difference in operative technique, such as an anomaly or variation in the vein. For instance, a superficial subcutaneous location of the distal great saphenous vein in the thigh would lead one to exercise more caution in tumescent anesthetic administration to make sure enough was infiltrated between the vein and the skin to prevent thermal skin damage. In the case of a small saphenous vein procedure, the presence of an intersaphenous vein, extending the small saphenous up the thigh and around it medially, would lead the operator to place the laser fiber further up the thigh proximally than would otherwise be done. Occasionally, a patient will have a cutaneous sensory nerve adjacent to the GSV, which would require extra tumescent anesthetic to prevent damage by heating and can sometimes be seen on ultrasound (Fig. 24.1). Some patients will have a duplicated GSV, and treatment of both branches is necessary.

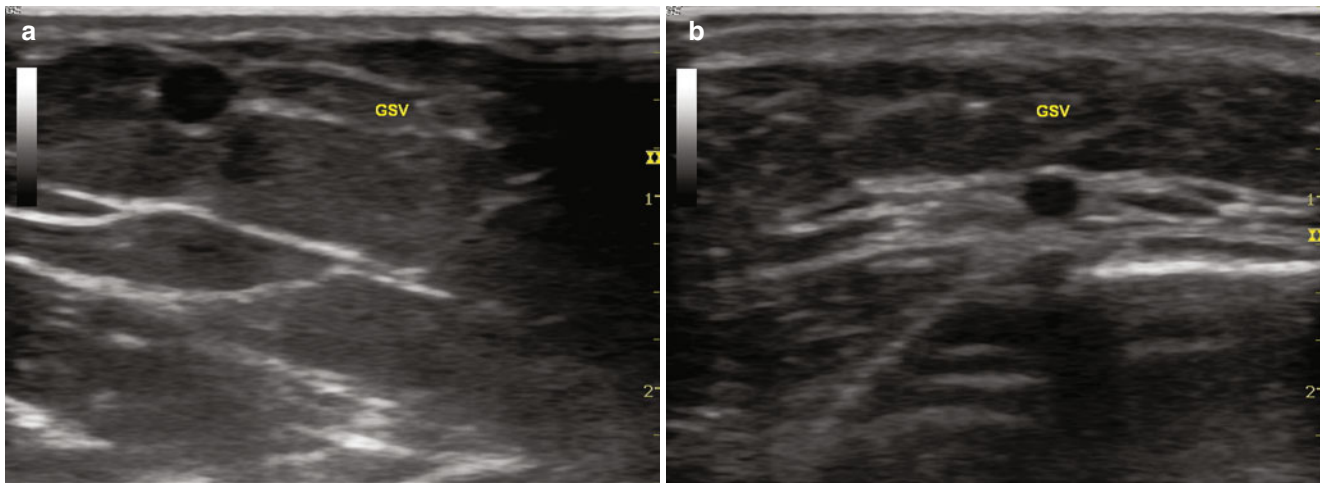


Fig. 24.1 (a) Subcutaneous vs. (b) interfascial location of GSV. More tumescent anesthesia is required for the same effect when it is not contained in the interfascial space. A vein which is in the subcutaneous

position should be traced to the saphenofemoral junction to confirm its identity before treatment

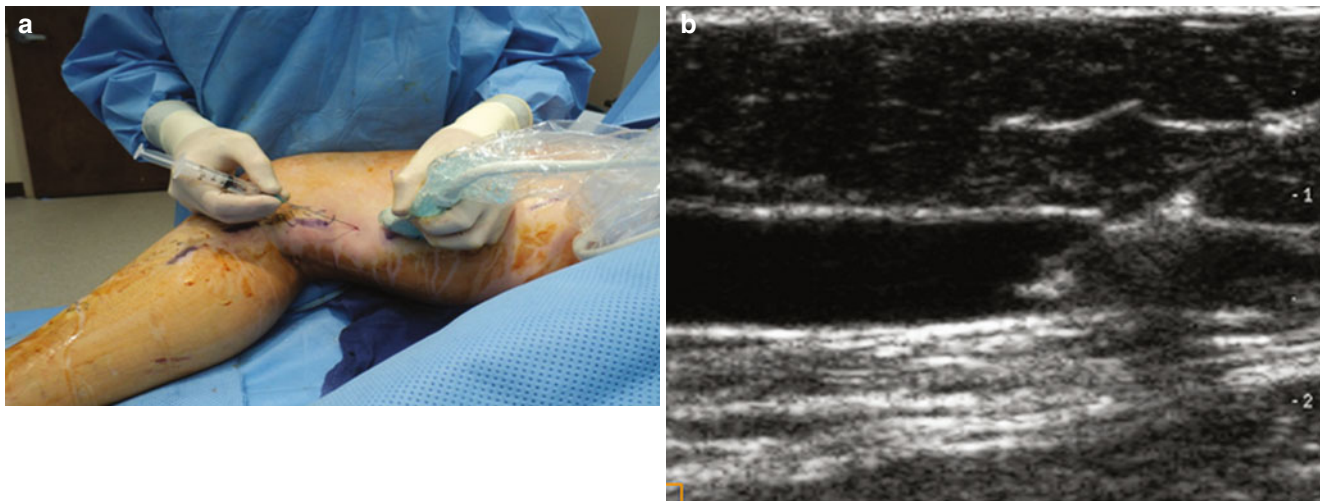


Fig. 24.2 Micropuncture antegrade cannulation of GSV. (a) An 8 MHz probe and a sterile cover are used to insulate the target vein; the probe and needle are aligned. (b) A longitudinal view best facilitates

needle entry under direct vision. The echogenic needle tip is seen as it enters the vein on the right

General anesthesia is almost never needed for this procedure. In fact the use of tumescent anesthesia (see below) allows for immediate postoperative ambulation, a desirable goal for these patients, in whom avoidance of thrombosis at the saphenofemoral junction is to be avoided. However, a small oral dose of sedative (alprazolam, 0.5 mg) 30 min or more before the procedure is helpful for most patients.

The patient is placed on the operating table either prone or supine, to expose the appropriate vein location, and sterile prep and draping are done. For the GSV, access is made just distal to the knee when possible, to allow for the maximal length of thigh vein, or just proximal to the ankle for the SSV. However, the key portion of vein to be treated is not only the most proximal portion, about 2 cm distal to the

SFJ for the GSV, or the SPJ for the SSV, but also should include the point of most distal reflux as well. Access is best done with local anesthetic, such as 1 % plain lidocaine, and a micropuncture set (available from several manufacturers), with direct vision using B-mode ultrasound. The operator must be well-practiced with ultrasound imaging, or the necessary detail required to perform a good endoablation will not be achieved, and an otherwise straightforward procedure could become very difficult. Correct technique minimizes interference with the operator's movements, provides stability for the ultrasound probe, and allows the operator complete freedom with one hand while imaging with the other (Fig. 24.2a, b). The sterile probe cover is clamped to the overlying sheets with a large clamp

(Kelly or equivalent), leaving a lax loop of cable on the patient, and preventing pulling on the probe itself from the weight of the cable. When access is done with the right hand, the left should hold the probe with the hypothenar eminence resting directly on the patient, providing a stable base from which the probe can be held still and steady during imaging. The hand holds the probe in supination, and no motion is made with the arm or elbow, only the hand and fingers (Fig. 24.2a). The opposite hand is used in a similar position to perform the micropuncture simultaneously. Using this technique, precise, non-moving images of the vein in detail allows cannulation with ease. Image orientation is according to preference. Many prefer a transverse image, but we find the longitudinal image far more useful here. The vein axis and the echogenic needle tip can be aligned precisely, and vein entry can be completely visualized in real time. The needle tip can be advanced within the vein lumen, as necessary, during wire insertion.

Most failures to access a superficial vein are due to venospasm, often occurring when the patient is cold, anxious, or when a first attempt is unsuccessful. When this occurs, the B-mode image of the vein acquires a ringed appearance, which is due to the constricted, thickened vein wall, with a minimal residual lumen, if any. Repeat attempts to cannulate are rendered more difficult as a result, and the adjacent lengths of vein are similarly affected, constricting along with the region originally penetrated. If multiple attempts at different levels are unsuccessful, or if the size of the constricted vein's lumen is so small as to prevent entry, the best course is to pause the case, warm and reassure the patient, apply sterile 2 % nitroglycerine ointment to the skin at the access site (Nitro-bid, Savage Laboratories, Melville, NY), and wait about 10 min or more for the vein to relax. This usually returns the vein to its original, unconstricted size, and another access attempt will succeed. In addition, if a particular site, usually near the knee, is not accessible after several tries, the best course is to choose a larger diameter site more proximally, treating a shorter segment than originally planned, but still ablating the vein effectively.

Another method for access entry which we have occasionally found useful is retrograde entry (Fig. 24.3). Since the superficial vein, usually a great, small or accessory anterior saphenous, is usually refluxing from its proximal end, and that position has the largest diameter along the length being treated, the access can be made from the proximal end, and the catheter passed distally, through the prolapsing valves, without difficulty. In this case, a longitudinal image of the site is essential, allowing for skin penetration over the SFJ or SPJ, and vein entry 2 cm. or more from the junction. Following passage of the catheter sheath and fiber distally, the remainder of the procedure is no different from



Fig. 24.3 Retrograde saphenous cannulation. The entry site is first clearly visualized with ultrasound and a longitudinal view allows entry just beyond the position of the inferior epigastric vein confluence. Treatment is done up to 2 cm from the terminal valve, or more distally (Photo Copyright 2014 Mark W. Moritz, M.D.)

an antegrade one, except that the endpoint of treatment is proximal, and the most proximal treated site must be at least 2 cm from the junction, mandating good ultrasound visualization.

Positioning of the access site should be done with the treatment length of the vein in mind. The GSV is not treated with heat below the knee, due to the proximity of the saphenous nerve to the vein distal to that point; the nerve is directly apposed to the vein from the proximal calf distally, and heating the vein will cause damage to the nerve, with unacceptable postoperative consequences. Similarly, the sural nerve apposes the SSV beginning at the widest point of the calf, and distally.

One manner in which fiber positioning can be problematic, is when the length of vein to be treated has a tortuosity, kink, or angulation at one or more sites. This is quite common, and is usually remedied with a guide wire for initial passage, often accompanied by manipulation of the surrounding tissues to straighten the path of the wire. Use of a 0.035" diameter wire, especially a glide wire, with both "J" and straight soft tips is usually adequate. The straight end is often required to pass through these areas, and twirling the wire back and forth while manipulating it and the surrounding tissues is necessary. However, if the vein still cannot be cannulated, perhaps due to an obstructing functional valve, more proximal access is sometimes required.

Perhaps the most important complication of an endoablation is deep venous thrombosis (DVT), occurring at the SFJ or SPJ, as a consequence of heat EHIT – endothermal heat-induced thrombosis (treatment is described in the

section on complications below) [28, 29]. Evidence has shown that the distance from the tip of the treatment fiber to the junction is critical in determining the likelihood of developing EHIT although at least one other study has shown that gender, Caprini score, CEAP class, and a prior history of thrombosis were more significant [29]. We have found in our series of more than 200 patients that a distance of at least 2.0 cm. is effective in preventing EHIT in almost all patients [30]. The laser sheath is placed up to the junction then the fiber is passed through it and positioned in this manner, measuring with ultrasound the distance from its tip to the junction.

Tumescent anesthetic is administered along the entire fiber length, from the access point to the junction, avoiding intraluminal injection. Typically, it is safe to place 7 mg/kg of lidocaine, using 1 % with epinephrine mixed 1:10 with normal saline and with 1:50 sodium bicarbonate 8.4 % as buffer (440 cc NS with 50 cc of 1 % lidocaine/epinephrine and 10 cc sodium bicarbonate 8.4 %). We avoid giving more than 500 cc of the above mixture in any one session. The tumescent anesthetic serves as a “heat sink”, absorbing heat and protecting surrounding tissues, due to the high heat capacity of water. Infiltrating the anesthetic around the vein will produce a “halo” on ultrasound, which indicates adequate protection. This is especially important to avoid cutaneous nerve damage, and there must be at least 1 cm. between the vein and the skin to avoid burn. Also, where the vein is very superficial, the anesthetic provides this space.

The laser fiber can be energized after the anesthetic is in place. The fiber is pulled back at a constant rate to heat the vein evenly. Ultrasound or, with some devices, a light at the tip of the catheter which is visible through the skin, can be used to track the fiber tip position during pullback. Treatment must be stopped when the fiber is 1 cm. from the skin surface, as it begins to exit the vein. Once laser pullback is complete and the treatment is complete, ultrasound is again used to confirm that the deep vein at the junction is compressible, and that there is no thrombosis in the junction. This can be done in B-mode, or in color mode. The treated vein will show opacity (bright reflection) and no flow, and flow will be visible in the epigastric and common femoral veins.

The patient is instructed to wear compression hose for 2 weeks post-procedure, which is important for patient comfort. (S)he is encouraged to walk every 2 h on the day of procedure, and to avoid heavy exercise during the 2 weeks.

Within the first 3 postoperative days, the patient has an ultrasound of the treated leg, at the SFJ or SPJ as appropriate, for evidence of endovenous heat-induced thrombosis (EHIT, see section on complications, below).

Complications of Endovenous Ablation

Some of the most frequently encountered complications of these procedures are relatively minor and commonly occur. These include pain, ecchymosis, mild paresthesias, minor skin burns, hematomas, ablation failure, and superficial thrombophlebitis. Other complications can be considered major and are relatively uncommon, including thermal nerve damage, DVT, pulmonary embolism, arterio-venous fistula and catheter or guide wire fragmentation with or without embolization [31].

EHIT (Endovenous heat induced thrombosis) at the sapheno-femoral junction (SFJ) is a distinct entity that occurs when the intraluminal heat induced thrombus progresses proximally from the laser fiber tip site in the GSV. It can protrude into the common femoral vein, and can progress to DVT. It is because of this possibility that an ultrasound is performed in our practice within 72 h post procedure. We have found this in about 2 % of patients, unlike other reports of a higher incidence [29, 32, 33]. This can be characterized based on its presence at the junction, protruding into the major deep vein, or having at least part of its base on the wall of the major deep vein. In all such cases, we treat the patient for 1 week with injectable enoxaparin (Lovenox®, Sanofi), 1.5 mg/kg daily. All such patients are again scanned again at 1 week, and if the repeat duplex shows retraction of the thrombus into the SFJ, anticoagulation is discontinued. These thrombi are intrinsically different from those occurring spontaneously, and prolonged anticoagulation is unnecessary in our experience. However, we also individualize the treatment and in some cases, where resolution/contraction does not occur, or the patient has a history of prior clotting disorder, longer therapy is given. With these precautions we only very rarely had any patient develop a pulmonary embolism. Pulmonary embolism is rare but has been described [34].

Heat-induced damage to nearby cutaneous nerves is not common, but patients should be cautioned preoperatively that dysesthesias, of the mid to distal thigh, medial calf, or posterior calf can occur, depending on the site of the vein treated. These typically are described as a mild burning sensation. Reassurance and anti-inflammatory drugs are very beneficial and the symptoms are usually self-limited. In order to prevent nerve damage the tumescent solution is delivered into the saphenous compartment under ultrasound visualization, creating the appearance of a halo around the vein of at least 1 cm in diameter. The ablation of the of the GSV in the calf or the SSV in its distal two-thirds is avoided in order to minimize nerve damage, due to the proximity of the saphenous or sural nerve to the GSV and SSV vein respectively.

Ablation failure can occur with large diameter veins, incomplete heating, or a procedure performed while the

patient is anticoagulated, and may only involve a part of the treated vein. The procedure can be repeated, but since most patients also undergo subsequent microphlebectomy on a different day, ligation and excision of the remaining portion can be considered at the same time, especially in thin individuals. Alternatively, sclerotherapy can close a remaining vein, usually with foam injection and ultrasound guidance. Other complications including arteriovenous fistula [35, 36], skin burns (erythema and bullae), infection, and seroma, are rare in our experience.

Prevention of the rare but potentially serious complication of catheter, laser fiber, or guide wire fragmentation or embolization requires meticulous attention to detail and inspection of all the equipment after termination of the procedure to ascertain integrity and accountability of all devices used. Once it is discovered that a fragment of wire or other foreign body has separated from the removed portion, compression should be put on the groin or popliteal site as appropriate to prevent further movement into the deep system. The ultrasound unit is then used to find it. Retrieval can be done by incising the overlying skin, palpating the object in the vein, if possible, and using a clamp to grasp it through the vein wall, or in the adjacent tissues. It can then be excised safely. If a fragment has embolized proximally, it must be located and extracted by other means.

A common reason why a fragment of wire is lost in the tissues is when the needle through which it is inserted is extravascular. The wire then does not advance through the vein lumen, but inserts into the subcutaneous tissues. Resistance is always felt to forward movement. When this happens it is imperative that both the needle and wire be removed together, and the cannulation process be started again; an attempt to remove the bent wire through the needle can result in shearing off the end of the wire, leaving it in the tissues. Removing such a fragment requires locating it with ultrasound, and excising it, as described above.

Skin burns although rare can be prevented by avoiding ablation of very superficially located veins; these are better dealt with by microphlebectomy. Exit site burns can be avoided by stopping the laser catheter pullback while several centimeters of the catheter still remain in the patient, and then placing the laser in standby mode prior to removing the laser fiber. Burns of this type are usually minor and are treated with expectant observation and measures to relieve symptoms.

Complications associated with tumescent anesthesia range from catheter damage by the needle to the more serious Lidocaine toxicity. The recommended dose of 1 % lidocaine with epinephrine is 7.0 mg /kg. or less, however doses of up to 35 mg/kg can be given during liposuction [37]. We mention this to caution against its use, since

during liposuction, tissue containing the lidocaine is removed during the procedure. When the administered dose of lidocaine without epinephrine is at or above 1.5 mg/kg, there is a likelihood of toxicity. Also, inadvertent injection of the anesthetic directly into a vein or an artery is potentially a toxic dose. Toxic reactions include light-headedness, visual disturbances, headache, sedation, perioral or tongue tingling, dysarthria, and muscle twitching, and may progress to seizures. If toxicity is suspected, the infusion must be immediately stopped, oxygen should be administered, and emergency management should be instituted.

Endolysis: The Use of Excimer Laser in Chronic Venous Obstruction

Key Points

Post-thrombotic syndrome (PTS) is a common and disabling complication of DVT, occurring in at least half of the 300,000 patients who acquire DVT each year in the United States, resulting in edema, pain, lipodermatosclerosis, and often ulceration, with disability.

DVT is amenable to thrombolysis when acute, less so with time. By about 1 month, the chronic thrombus is not responsive to lytic agents, and in fact although the vessel may recanalize, it can eventually become sclerotic.

DVT of the pelvic veins and/or vena cava produces disability due to obstruction of the venous outflow of the legs. Superior vena cava syndrome is the analogous condition of the upper extremities, with occlusion of the subclavian veins and/or superior vena cava.

Excimer laser treatment can provide an alternative for recanalizing a chronically thrombosed lesion when a wire and/or balloon catheter will not cross.

DVT is a common entity in the United States, with approximately 300,000 cases per year, half of which go on to post-thrombotic syndrome [38]. Disability resulting from the edema, pain, lipodermatosclerosis, hyperpigmentation and ulceration causes billions of dollars of lost time and productivity each year [39]. When the thrombosis is acute, and in the major truncal veins of the upper and lower limbs, lysis has been shown to decrease the frequency and severity of post-thrombotic symptoms [40]. When those lesions contain chronic, organized thrombus, conventional lysis methods are often unsuccessful.

The excimer laser (EL, Spectranetics Corporation, Colorado Springs, CO) has been used in our hands for successful recanalization of major truncal veins, facilitating

guidewire passage prior to venoplasty and stenting in cases where simple guidewire passage was impossible [41]. The adjunctive use of the EL facilitates wire passage by creating a flow channel through which further therapeutic maneuvers may be performed. It is particularly effective in those situations where older, organized thrombus limits the operator from advancing a wire across a chronic venous occlusion. The excimer laser is a pulsed laser, emitting very brief pulses of very high energy, but by vibrating the tip of the catheter and generating ultrasonic disruption of plaque (for which it was designed) does not produce heat, as with other lasers designed for use in the venous system. It can also disrupt thrombus [42, 43]. This then allows a guidewire to track unimpeded within an occluded vein facilitating subsequent interventions. While we have used this device in this application many times without incident, and with good outcomes for our patients, its use in the venous system is “off-label”.

Method

The procedure may be done in either the interventional radiology/catheterization suite or in the operating room with a portable C-arm unit. The patient is placed either supine or prone, depending on the level of access desired. For lesions involving only the iliac veins or inferior vena cava, the supine position with entry through the common femoral vein(s) is preferred, because of easier accessibility of the CFV and overall better comfort of the patient during the procedure. The prone position is preferred when accessing thrombosed popliteal or femoral veins and will also allow access to the more proximal iliac veins as well. Subclavian and innominate lesions, and the basilic, brachial, or axillar veins are approached through the ipsilateral arm, in supine position.

Under local anesthesia with or without minimal to moderate conscious sedation, and under direct ultrasound visualization, the target vein is imaged and entered using a small echogenic entry needle. The accompanying wire is advanced through the needle and a 4 Fr microcatheter is positioned within the vein. Even in a thrombosed vein, this can be done safely and easily. This is subsequently up-sized to a 5 Fr sheath (Pinnacle, Terumo Medical Corp, Elkton, MD). X-ray contrast is injected through the sheath, allowing the operator an initial view of the extent and complexity of the thrombosis. A hydrophilic glidewire (Terumo Medical Corp, Somerset, NJ) is then passed through the thrombosed segment of vein until it reaches a proximal open vessel. A catheter is then passed over the wire to the proximal vessel, and injection of contrast is done to confirm

intraluminal position and characteristics of the proximal patent vein.

In cases of chronic thrombosis, where pharmacolytic agents are not expected to work, the EL is used to debulk the site. After intraluminal position is confirmed, the glide-wire is exchanged for an 0.018" wire. An EL catheter of 2.0–2.5 mm is then passed over the wire, activated with settings of 40–60 mJ/cm² fluence and a repetition rate of 40/s or higher to lyse and debulk thrombus as the initial modality. Once the EL catheter has passed through to the proximal patent vein, it is then backed out, while activated again, leaving a newly created flow channel. In most cases the EL passes through the thrombus without difficulty, allowing for balloon venoplasty and stenting to be done as appropriate.

In cases where the initial wire cannot pass through the involved vein to a proximal patent vein, the EL can be used in a stepwise fashion to progressively work through the obstructive lesion. This is done by leading with the EL catheter under fluoroscopy through the lesion in 2 mm steps, without first advancing the guidewire, then advancing the wire a small distance ahead of the catheter, then repeating this process until the wire reaches the open proximal vein. It is important not to forcibly push the catheter through the occlusion, but rather allow it to find a natural path while the laser is fired, to limit the potential for perforation. The EL, having been passed proximally, is then brought back distally while firing continuously, through the new channel. In all cases, a venagram is done to confirm intraluminal position, and the resulting flow channel, after which venoplasty and stenting can proceed.

All patients are fully heparinized during these procedures. Each procedure is ended after venoplasty with stenting when there is a good resulting flow channel, the lesion is traversed with a wire, and there is reduction in the number of visible venous collaterals on completion fluoroscopy when compared with the initial views. The method reported here works well in large and medium-sized veins, such as the femoral and the iliac, and even the vena cava. It produces an adequate channel in chronic thrombus through which to pass wires and balloons for further treatment (Figs. 24.4, 24.5, and 24.6).

Although there is a possibility of perforation, as in the arterial system, with careful technique and use of appropriate equipment, we have not had this occur. Other complications can include recurrence of thrombosis, infection or bleeding, and persistence of PTS symptoms. The patient remains anticoagulated postoperatively, but the recurrence of thrombosis is clearly related to the cause of the original event, and should be prophylaxed and treated with that in mind.

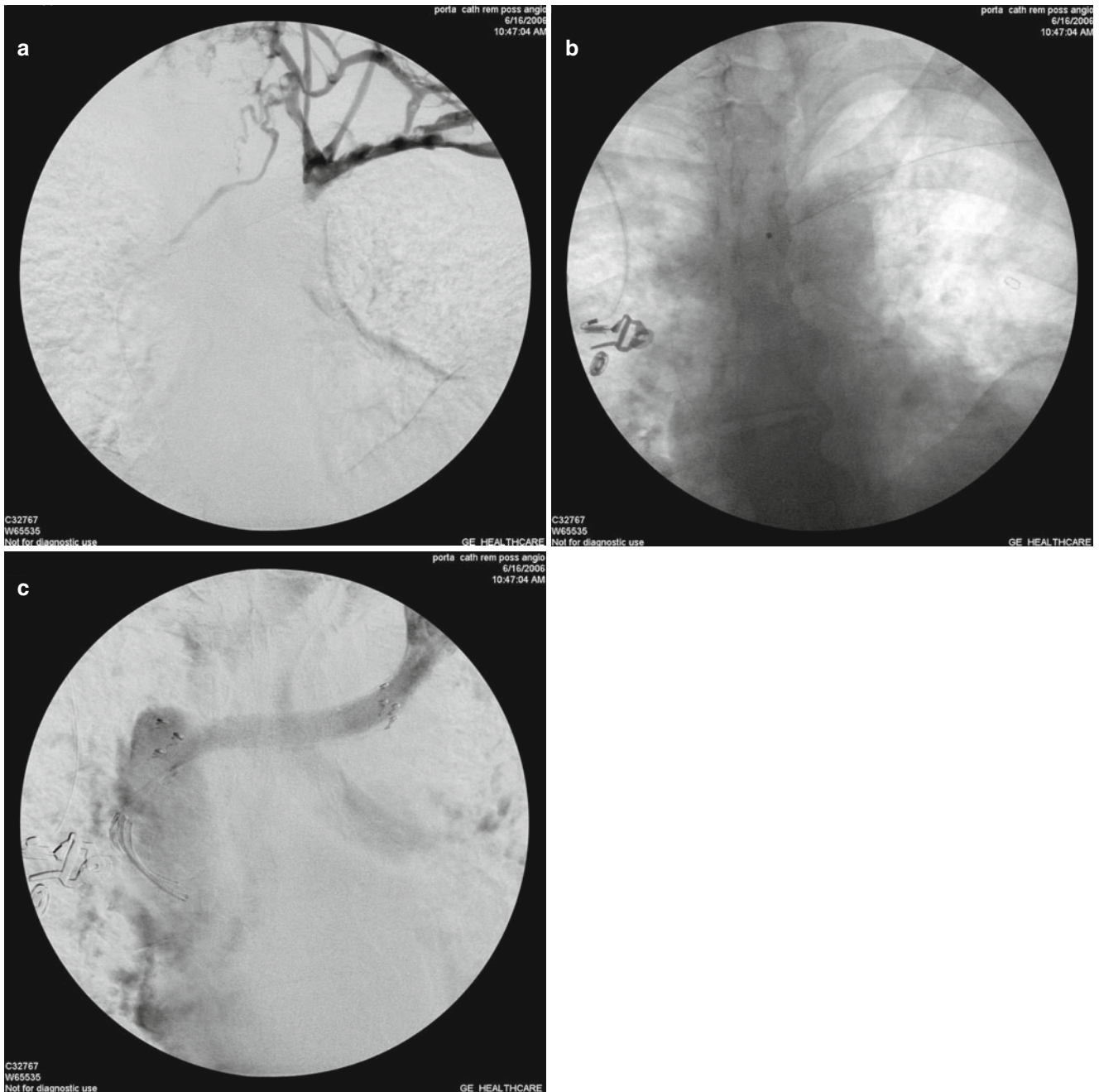


Fig. 24.4 Excimer laser used to reopen a chronically occluded brachiocephalic vein for relief of left arm pain and edema. (a) Initial venogram shows collaterals around obstruction, which could not be traversed with guidewires. (b) Passage of excimer laser. The radiopaque tip is

visible at the innominate vein – superior vena cava junction. (c) Final result with stent in place. The patient experienced prompt relief of disabling symptoms (Photos Copyright 2015 Mark W. Moritz, M.D.)

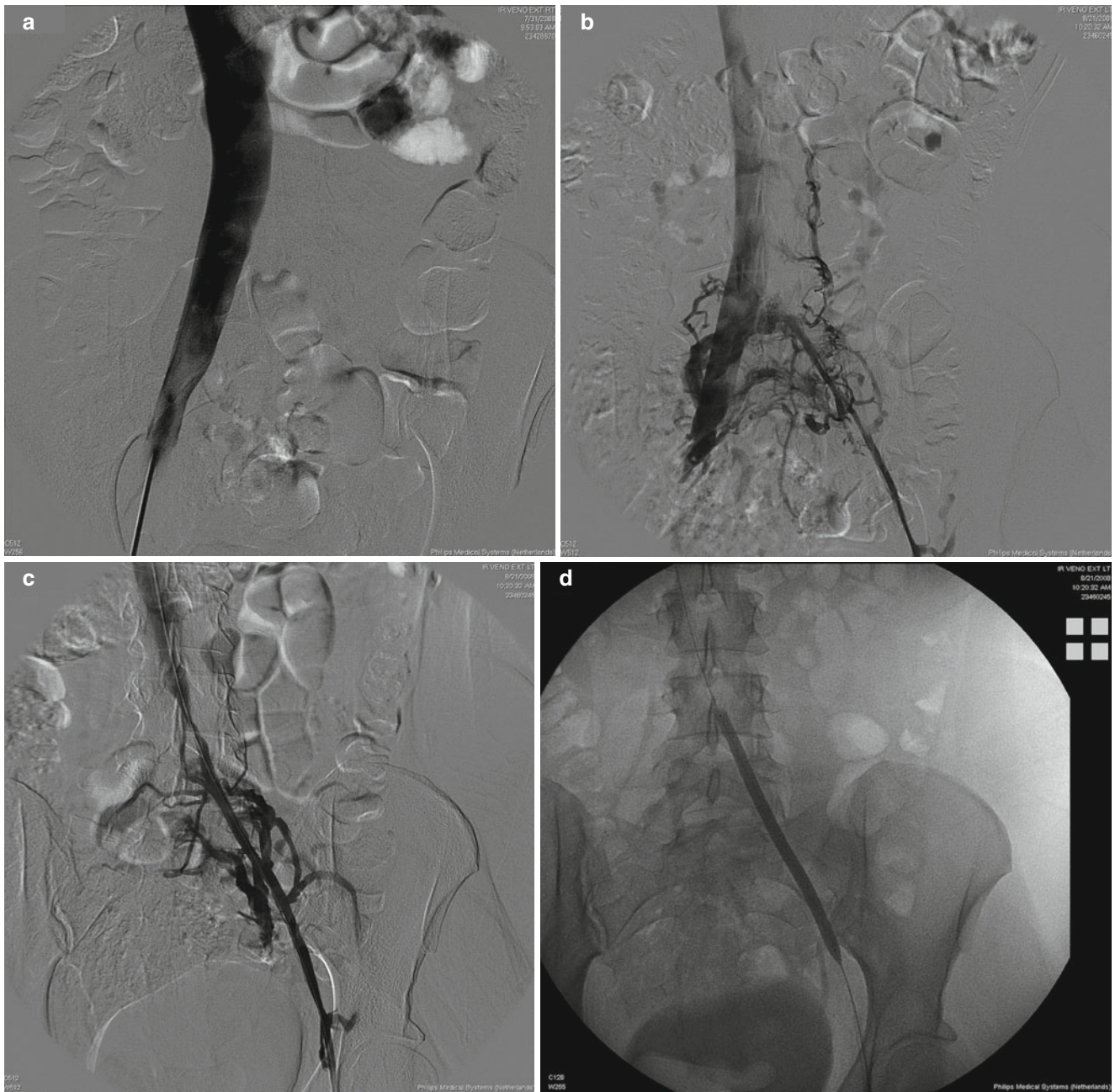


Fig. 24.5 Recanalization of an occluded left iliac vein system with excimer laser. (a, b) Initial bilateral venograms showing occlusion and collaterals. (c) Result after laser passage when guidewire could not

otherwise be passed. (d) Balloon angioplasty. (e) Ballooned and stented result, with disappearance of collaterals (Photos Copyright 2015 Michael Ombrellino, M.D.)



Fig. 24.5 (continued)

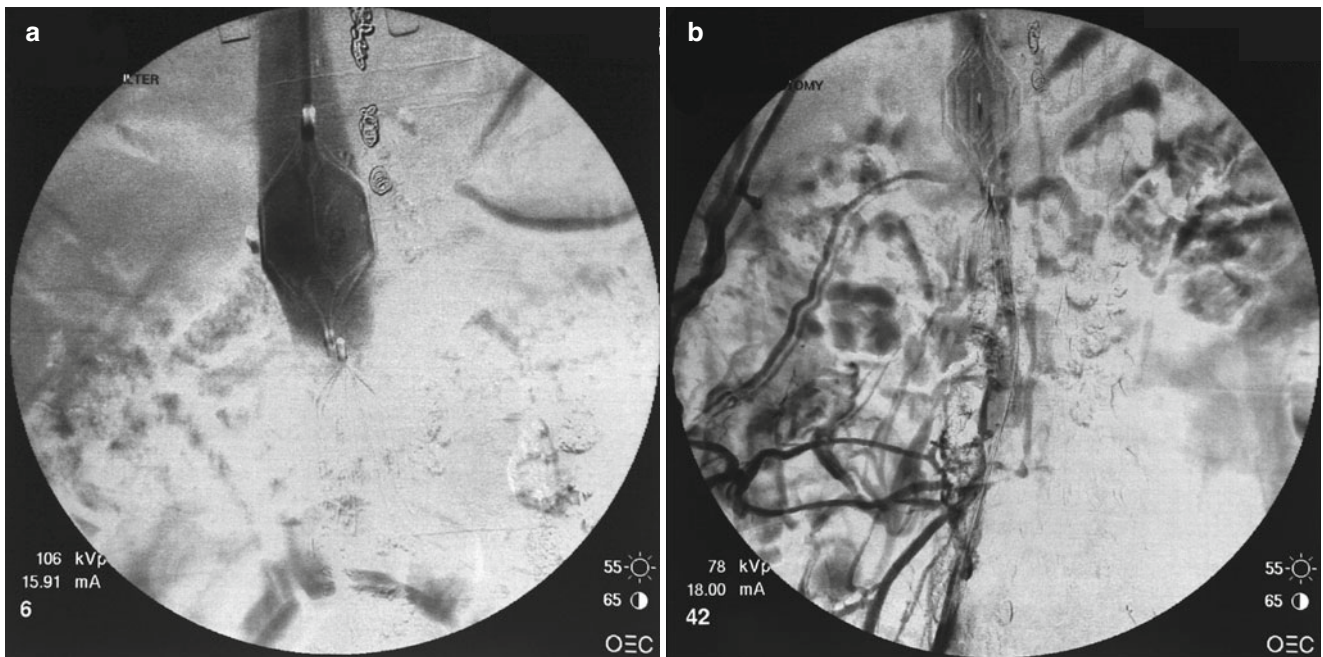


Fig. 24.6 Relief of chronic right iliac and inferior vena caval obstruction with excimer laser used to facilitate passage of guidewire and balloon catheter which otherwise could not be passed. (**a, b**) initial bilateral venography showing obstruction and collaterals. Thrombus had propagated through the original inferior vena cava filter and a second filter

was placed proximally before treatment. (**c, d**) Passage of wire and balloon venoplastics following excimer laser passage. (**e**) Patent ilio caval system after venoplasty and Palmaz stent placement in cava (Photos Copyright 2015 Mark W. Moritz, M.D.)

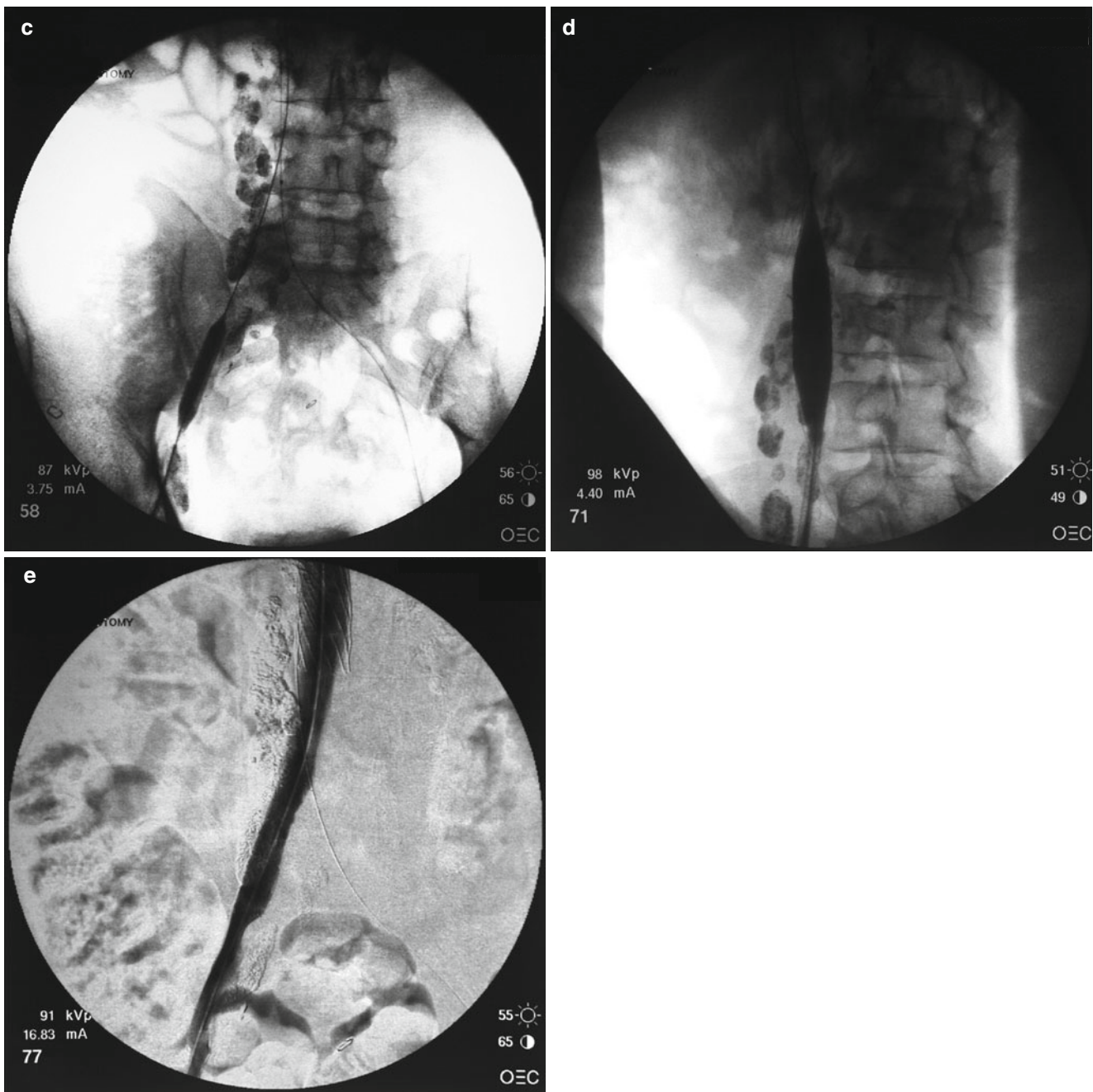


Fig. 24.6 (continued)

Conclusion

Laser technology has revolutionized venous therapies. Surface venous lesions, superficial veins, and deep veins now have treatment options available which add to the older armamentarium, and in some cases, have completely replaced older open surgical procedures with percutaneous alternatives. This versatile technology will predictably continue to improve venous therapy outcomes as it is further developed.

References

1. Goldman M, Guex J, Weiss R. Sclerotherapy: treatment of varicose and telangiectatic leg veins. 5th ed. London: Saunders Elsevier; 2011.
2. Gloviczki P, editor. Handbook of venous disorders: guidelines of the American Venous Forum. 3rd ed. London: Hodder Arnold; 2009.
3. Adamic M, Troilius A, et al. Vascular lasers and IPLS: guidelines for care from the European Society for Laser Dermatology (ESLD). *Cosmet Laser Ther.* 2007;9(2):113–24.
4. Ross E, Domankevitz Y. Laser treatment of leg veins: physical mechanisms and theoretical considerations. *Laser Surg Med.* 2005;36:105–16.

5. Goldman MP, Amiry S. Closure of the greater saphenous vein with endoluminal radiofrequency thermal heating of the vein wall in combination with ambulatory phlebectomy: 50 patients with more than 6-month follow-up. *Dermatol Surg.* 2002;28:29.
6. Merchant RF, Pichot O, et al. Four-year follow up on endovascular radiofrequency obliteration of great saphenous reflux. *Dermatol Surg.* 2006;31:129.
7. Kabnick LS, Merchant RF. Twelve and twenty-four month follow-up after endovascular obliteration of saphenous vein reflux – a report from the multi-center registry. *J Phlebol.* 2001;1:17.
8. Calcagno D, Rossi JA, et al. Effect of saphenous vein diameter on closure rate with Closure FAST radiofrequency catheter. *Vasc Endovasc Surg.* 2009;43:567.
9. Parlette E, Groff W, et al. Optimal pulse durations for the treatment of leg telangiectasias with a Neodymium YAG laser. *Lasers Surg Med.* 2006;38:98–105.
10. Anderson RR, Parrish JA. Selective photothermolysis: precise microsurgery by selective absorption of pulsed radiation. *Science.* 1983;220:524–7.
11. Massaki A, Kiripolsky M. Endoluminal laser delivery mode and wavelength effects on varicose veins in an *Ex vivo* model. *Laser Surg Med Spec Issue: Dermatol Plast Surg.* 2013;45(2):123–9.
12. Disselhoff BC, Rem AI, et al. Endovenous laser ablation: an experimental study on the mechanism of action. *Phlebology.* 2008;23:69.
13. Fan CM, Rox-Anderson R. Endovenous laser ablation: mechanism of action. *Phlebology.* 2008;23:206.
14. Doganci S, Demirkilic U. Comparison of 980 nm laser and bare-tip fibre with 1470 nm laser and radial fibre in the treatment of great saphenous varicosities: a prospective randomized clinical trial. *Eur J Vasc Surg.* 2010;40(2):254–9.
15. Pannier F, Rabe E, et al. First results with a new 1470-nm diode laser for endovenous ablation of incompetent saphenous veins. *Phlebology.* 2009;24(1):26–30.
16. Samuel N, Wallace M, et al. Comparison of 12-W versus 14-@ endovenous laser ablation in the treatment of great saphenous varicose veins: 5-year outcomes from a randomized controlled trial. *Vasc Endovasc Surg.* 2013;47(5):346–52.
17. Baumler W, Ulrich H, et al. Optimal parameters for the treatment of leg veins using Nd:YAG lasers at 1064 nm. *Br J Dermatol.* 2006;155(2):364–71.
18. Laser hazards: safety standards. Available from: <https://www.osha.gov/SLTC/laserhazards/>.
19. Scherer K, Waner M. Nd:YAG lasers (1,064 nm) in the treatment of venous malformations of the face and neck: challenges and benefits. *Lasers Med Sci.* 2007;22(2):119–26.
20. Kabnick L, Ombrellino M. Ambulatory phlebectomy. *Semin Interv Radiol.* 2005;22(3):218–24.
21. Fitzpatrick TB. “Soleil et peau” [Sun and skin]. *J de Médecine Esthétique (in French).* 1975;2:33–4.
22. Pathak MA, Jimbow K, Szabo G, Fitzpatrick TB. Sunlight and melanin pigmentation. In: Smith KC, editor. *Photochemical and photobiological reviews.* New York: Plenum Press; 1976. p. 211–39.
23. Major A, Brazzini B, et al. Nd:YAG 1064 nm laser in the treatment of facial and leg telangiectasias. *J Eur Acad Dermatol Venereol.* 2001;15(6):559–65.
24. Tanghetti E, Sherr E. Treatment of telangiectasia using the multipass technique with the extended pulse width, pulsed dye laser. *J Cosmetic Laser Ther.* 2003;5:71–5.
25. Navarro L, Min R, et al. Endovenous Laser: a new minimally invasive method of treatment for varicose veins; preliminary observations using an 810 nm diode laser. *Dermatol Surg.* 2001;27:117–22.
26. Ombrellino M, Kabnick L. Varicose vein surgery. *Semin Interv Radiol.* 2005;22(3):185–94.
27. Rasmussen L, Bjoern M, et al. Randomised clinical trial comparing endovenous laser ablation with stripping of the great saphenous vein: clinical outcome and recurrence after two years. *Eur J Vasc Endovasc Surg.* 2010;39(5):630–5.
28. Mozes G, Kalra M, et al. Extension of the saphenous thrombus into the femoral vein: a potential complication of new endovenous ablation techniques. *J Vasc Surg.* 2005;41(1):130–5.
29. Rhee S, Cantelmo N. Factors influencing the incidence of endovenous heat-induced thrombosis (EHIT). *Vasc Endovasc Surg.* 2013;47(3):207–12.
30. Agis H, Kabnick L, et al. Minimization of thermally-induced thrombosis at the saphenofemoral junction during endothermal ablation of the great saphenous vein; safe position for catheter tip placement. Presented at: XVI meeting of the Union Internationale de Phlebologie. 2009.
31. Den Bos R, Neumann M, et al. Endovenous laser ablation-induced complications: review of the literature and new cases. *Dermatol Surg.* 2009;35(8):1206–14.
32. Kabnick L, Ombrellino M, et al. Endovenous heat induced thrombus (EHIT) following endovenous vein obliteration: to treat or not to treat? Presented at: Third International Vein Congress. 2005.
33. Hingorani A, Ascher E, et al. Deep venous thrombosis after radiofrequency ablation of the great saphenous vein: a word of caution. *J Vasc Surg.* 2005;41(2):314.
34. Puggioni A, Kalra M, et al. Endovenous laser therapy and radiofrequency ablation of the great saphenous vein: analysis of early efficacy and complications. *J Vasc Surg.* 2005;42(3):488–93.
35. Dexter D, Kabnick L, et al. Complications of endovenous lasers. *Phlebology.* 2012;27 Suppl 1:40–5.
36. Yildirim E, Saba T, et al. Treatment of an unusual complication of endovenous laser therapy: multiple small arteriovenous fistulas causing complete recanalization. *Cariovasc Interv Radiol.* 2009;32:166–8.
37. Klein J. Tumescence technique for regional anesthesia permits lidocaine doses of 35 mg/kg for liposuction. *J Dermatol Surg Oncol.* 1990;16:248–63.
38. Silverstein M, Heit J, et al. Trends in the incidence of deep vein thrombosis and pulmonary embolism: a 25-year population-based study. *Arch Intern Med.* 1998;158(6):585–93.
39. Comerota A, Throm R, et al. Catheter-directed thrombolysis for iliofemoral deep vein thrombosis improves health-related quality of life. *J Vasc Surg.* 2000;32(1):130–7.
40. Grewal N, Martinez J, et al. Quantity of clot lysed after catheter-directed thrombolysis for iliofemoral deep venous thrombosis correlates with postthrombotic morbidity. *J Vasc Surg.* 2010;51(5):1209–14.
41. Moritz M, Ombrellino M, Agis H. Excimer laser for debulking and lysing chronic venous thrombi and occlusions. *Vasc Endovasc Surg.* 2009;43(4):370–4.
42. Papaioannou T, Sorocoumov O, Taylor K, Grundfest WS, et al. Excimer laser assisted thrombolysis: the effect of fluence, repetition rate and catheter size. In: Bartels KE, editor. *Lasers in surgery: advanced characterization, therapeutics, and systems XII, Proceedings of SPIE, Bellingham, USA; vol. 4609.* 2002. p. 413–8.
43. Moritz M, Ombrellino M. Excimer laser as an adjunct for popliteal aneurysm. *Endovasc Today.* 2007;6:41–2.
44. Caggiati A, Bergan J, et al. Nomenclature of the veins of the lower limb: extensions, refinements, and clinical application. *J Vasc Surg.* 2005;41:719–24.

Christof Zerweck and Thomas Schwarz

Introduction

The first report on endovenous laser ablation (EVLA) in varicose saphenous veins was published in 1999 [1]. In the last decade a lot of studies have been published, regarding the optimal laser device, wavelength, pulse duration and the optimal laser emitting fiber design. The vast majority of this research was done on the varicose saphenous veins: the great saphenous vein (GSV) and the small saphenous vein (SSV). Since 2007 when Proebstle and Herdemann reported about laser ablation of incompetent perforating veins (IPV) with a 1320 nm and a 940 nm diode laser, only few studies focused on this topic [2]. This might have been due to the fact that there were no specialized thin laser fibers available and the insertion of a thick 6 french sheath in the short perforator was tricky and almost impracticable. Proebstle and Herdemann for this reason used 16 gauge cannulas for a 600 nm fiber [2]. Ozkan used Seldinger technique for laser fiber insertion [3]. Overall, the procedure remained niched.

In 2008 a thin 400 μm fiber from Angiodynamics, used on an 810 nm diode laser was available, inserted through a 21 gauge cannula. In 2010 another 400 μm (ELVeS-radial-slim kitTM, Biolitec AG Jena, Germany) was introduced, suitable for a 1470 nm diode laser system (Cerelas DTM). At this point of time 1470 nm had proved to deliver best results in endovenous laser ablation [4]. This fiber is delivered via a 16 gauge cannula, providing excellent maneuverability and causes tolerable discomfort for the patient. A sheath to introduce the fiber is not necessary. The radial slim fiber can also be used for treatment of varicose vein in the GSV or SSV in one procedure. In a recently published study we demonstrated excellent efficacy and safety of the procedure with this fiber

treating incompetent perforating veins [5]. In 2011 Corcos et al. published their results with an 808 nm diode laser and a 600 nm fiber. Comprising 530 IPVs, this study is the largest one released so far [6].

At the moment, thin laser fibers are available from AngioDynamics Latham, USA (VenaCure EVLTTM), Biolitec AG Jena, Germany ((ELVeS-radial-slim kitTM) and Total Vein Systems Houston, USA (EasyFlex GlideFiberTM).

Anatomy, Physiology and Pathogenesis

Perforating veins in the upper or lower leg are physiological connections between the deep and the superficial venous system, draining superficial blood into the deep venous system. In the upper leg, the proximal and distal Dodd's perforator and the Hunter's perforator are known. In the lower leg, the Boyd's perforator and several paratibial (Cockett), dorsal (May, Sherman) and lateral perforating veins have been described.

In cases of pathological reflux, these veins may build the proximal insufficient point with reverse flow. More often the varicose perforator acts as the distal main drainage vein, when the GSV and the SSV show pathological reflux. Reflux in the deep venous system is highly associated to the occurrence of IPVs, in some studies 2/3 of all IPVs are correlated with deep venous reflux [7].

Moreover, Cockett and Jones described the Blow-Out-Syndrome as a result of muscular contraction as possible base for the development of IPVs [8].

Clinical Presentation

IPV represent only a small aspect in the total disease of varicose veins. Common complaints during the day with aggravation towards evening are pain, swelling, aching, itching, heaviness of the leg or nocturnal muscle cramps. Complaints are typically relieved by elevation of the extremity or by wearing compression stockings.

C. Zerweck, MD (✉) • T. Schwarz, MD
Venous Section, Department of Angiology,
Universitaets – Herzzentrum Freiburg,
Suedring 15, Bad Krozingen, Baden-Wuerttemberg
79189, Germany
e-mail: Christof.Zerweck@universitaets-herzzentrum.de

Additionally, some patients describe local pain whilst standing or walking.

In other cases, general practitioners admit patients with suspected IPV's in cases of prolonged ulcer healing. Local changes of the skin and subcutaneous tissue such as eczema, dermatitis with induration, pigment disorder, lipodermatosclerosis are possible signs for an incompetent perforator vein disease. Other patients present with deep venous thrombosis in the deep calf veins, or isolated calf muscle vein thrombosis in the soleal and gastrocnemial muscle veins probably caused by thrombus progression via perforator veins from initially superficial venous thrombosis (SVT) [9].

Indication to Treat

There is a common belief that the majority of patients with IPV do not require to be treated by surgery or thermal ablations [10]. Indication for treatment is related to the clinical complaints of the patient.

Functional testing of blood flow must be performed to get information about the relevance of the vessel in relation to the total disease. Duplex ultrasound is the accepted gold standard for this purpose [10]. The measurement of the perforator diameter completes the general view, but may not be used as the only marker value for or against treatment.

According to the recommendations of the American venous forum, IPV's are pathologic, when reflux is ≥ 500 ms, diameter exceeds 3.5 mm. Furthermore, an open or closed ulcer (CEAP class 5–6) has to be located in the proximity of the perforator.

Procedure

There is no consensus on the optimal IPV ablation procedure yet. For this reason, we describe the procedure as it is performed in our department. As we know, our procedure slightly differs from other institutions, regarding anesthesia and post-interventional care. We use a radial emitting slim fiber on a 1470 nm diode laser from Biolitec (ELVeS-radial-slim kit™ + Cerelas D™ Biolitec AG Jena, Germany).

It is recommended to use a standardized examination protocol for venous sonography [11, 12]. The procedure is started with a short run down on the saphenous veins to determine the optimal puncture site that can be marked with a permanent marker (Fig. 25.1). The perforator veins are first observed in an oblique view, then the ultrasonic probe may be turned 90° to achieve a longitudinal image of the vein. Afterwards the longitudinal direction can be marked again with a marker pen with intent to shorten and ease the following puncture procedure as the insertion of the large cannula is not comfortable for the patient.



Fig. 25.1 The procedure is started with a short run down on the saphenous veins to determine the optimal puncture site that can be marked with a permanent marker

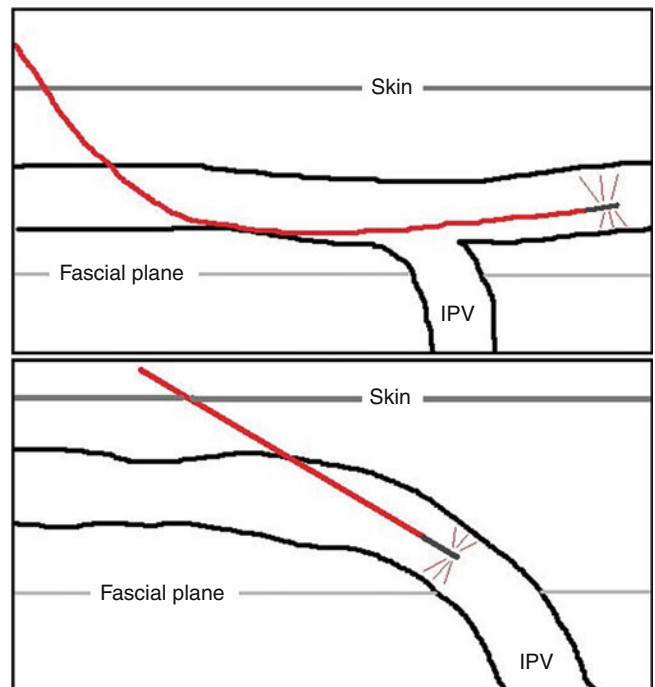
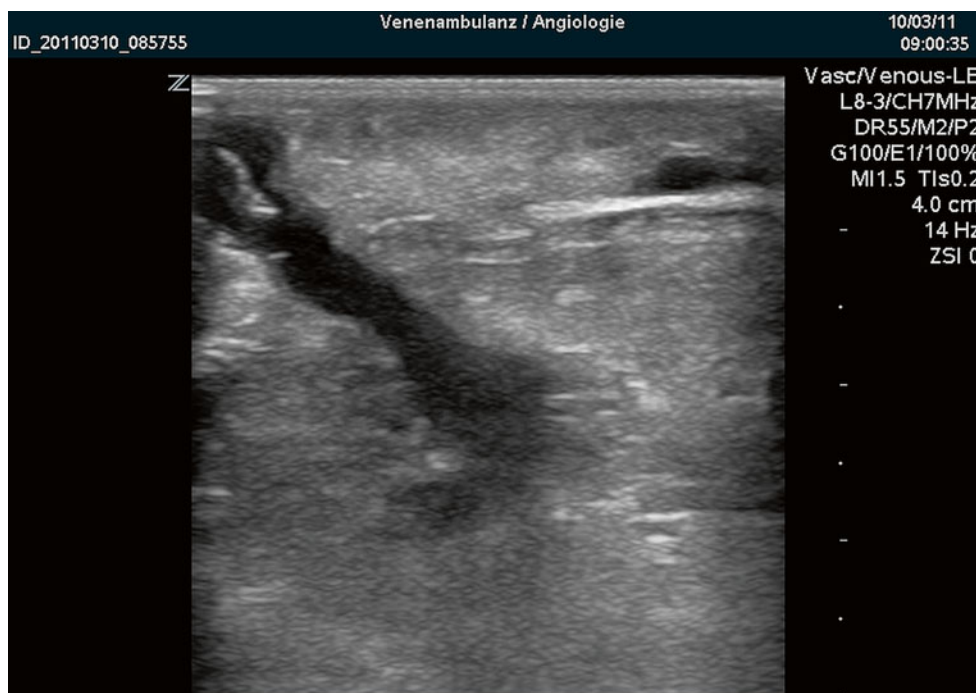


Fig. 25.2 Above: T-like IPV; below: L-like IPV with laser fiber

From an anatomical point of view there exist T- and L-like shaped perforators (Fig. 25.2). The catheter therefore may be placed in one or two ways. It is important to place the fiber tip intravenous and above the fascial plane (Fig. 25.3), intramuscular placement could lead to unexpected side effects, e.g., muscle vein thrombosis or deep venous thrombosis.

Cutaneous disinfection of the whole leg is performed. 16 gauge cannulas are placed subsequently in all varicose veins that require treatment (saphenous vein or tributaries).

Fig. 25.3 Perforator with inserted radial fiber slim



All cannulas should be placed prior to the tumescent local anesthesia injection, as the epinephrine in it causes a vessel contraction (Fig. 25.4).

Thereafter, the laser radial fiber slim is introduced firstly in the saphenous vein. Then, tumescent local anesthesia consisting of 25 ml of 2 % ultracaine, 25 ml of 8.4 % sodium carbonate, 0.5 mg epinephrine diluted in 500 ml cooled saline is injected along the perivenous space of the GSV/SSV under usage of ultrasound guidance. 5–10 ml 1 % prilocainhydrochloride is injected at the perforator area to provide a good toponarcosis. The proximal vein should be first closed to reduce blood pressure in the area around the perforator.

If necessary, treatment of the GSV or SSV has to be performed before IPV-treatment.

The laser procedure will be started in the saphenous vein after placing the laser fiber tip according to the guidelines of the manufacturer with approximately 1 cm distance to the deep vein system. Laser energy can be delivered at 8 W with the radial fiber slim. The varicose vein will be treated to approximately 1 cm above the skin entry site. The targeted linear endovenous energy density (LEED, J/cm) in the GSV and SSV is 60 J/cm [4, 14].

After treatment of the saphenous vein, the fiber is introduced in the already placed cannula in the perforator veins. The tip of the fiber should be placed ultrasonographically guided in the epifascial region above the fascial plane. After this maneuver the plastic cannula must be drawn out of the skin, sliding back over the fiber which must be kept in the correct intravenous position. Before starting the laser treatment, approximately 10 ml of cooled tumescent local

anaesthesia is injected again around the laser fiber. This has to be done for cooling reasons as Pannier could show a significantly reduced intake of analgesics with cooled tumescence fluid after the procedure [15]. During laser ablation, the fiber is pulled back 1–3 cm until the tip of the fiber exits the varicose vein. This is seen on ultrasound imaging and may be felt by the investigators hands as vibrations on the skin. In perforator veins higher energy levels than in the saphenous veins are needed for a good result, a LEED of 69–130 J/cm with 1470 nm has proved to be sufficient [5, 13]. With lower energy levels, the perforator might not be closed. Nevertheless, studies with lower energies have not been published yet. Laser energy application is controlled, modifying the velocity up until the withdrawal of the catheter.

After the procedure, venous flow is checked immediately in the proximal deep veins and in the perforator by ultrasound. Persistent reflux in tributaries or below the treated vein is checked and additional treatment with foam sclerotherapy [16] or phlebectomy [17] should be applied if needed.

Post-interventional Care

Immediately after the procedure, prophylaxis of venous thromboembolism is started (e.g., with enoxaparin 40 mg s.c.) for the following 5 days. But there is no clear evidence from clinical studies on this topic.

Compression therapy with a graduated class II stocking (30–40 mmHg) should be worn immediately with the intention



Fig. 25.4 Procedure. *Above left.* Sonographic inserted 16G cannulas (Left one in GSV, both right ones in IPVs). *Above right.* Advancement of the fiber in the GSV, navigation light is shining red through the skin. *Middle left.* Laser ablation of GSV is finished. Insertion of the fiber into

the proximal IPV. *Middle right.* Fixation of the fiber with a finger, cannula already removed. *Below left.* Treatment of the distal IPV. *Below right.* Immediately before laser activation. Additional tumescence anesthesia for cooling reason

of wearing the stockings for 72 h continuously. After that they may be worn during the day for a further 3 weeks. A non-steroidal anti-inflammatory drug (diclofenac-sodium 75 mg 3–5 days

b.i.d.) is useful for pain relief and to limit the inflammatory reaction. The patient can resume routine daily activities immediately, however strenuous exercise should be avoided for about 1 week.

After 1 week signs for superficial vein thrombosis or phlebitis should be checked, this procedure may be repeated 1 month later for patient's satisfaction. At the same time the treated veins and the surrounding area of these are observed for recanalization and to exclude DVT in the extremity.

Complications

The major complications in the laser ablation of perforators are similar to all endovascular thermal therapy options known. They include pulmonary embolism, deep or superficial venous thrombosis, nerve injury, and neurologic symptoms. Special minor complications are: skin alteration, bruising.

A special complication is the occurrence of muscle vein thrombosis in the intramuscular part of the perforator vein. It starts intramuscular near the fascial plane and may have an extension up to 2 cm. The relevance of this thrombus is unclear but it is likely that it arises as a result of hemostasis in this vessel. Thrombus progression into the deep venous system has not been reported yet.

Results from Clinical Trials

Up to this point seven studies have observed the efficacy and safety of endovenous laser ablation of IPVs with differences in sample size, perforator diameter, LEED, wavelength of the laser device and long term results (Table 25.1). Because of the different wavelength, providing maximum absorption power either in hemoglobin or water, no direct comparison of the different LEED (for successful IPV closure) can be made. Nevertheless, Darwood and Gough recommend a minimum LEED of 60 J/cm for successful ablation of varicose veins.

The first published data were presented from Proebstle and Herdemann in 2007. They used laser devices with 940 and 1320 nm. In the beginning, 5–8 W were used in both laser devices with a mean energy dose of 130 J (45–342). After this pilot phase, laser energy was doubled up to 250 J (1320 nm) and 290 J (940 nm), although closure success was mentioned sufficient in the lower dose group. The study focused on diameter shrinkage at day 1 after treatment, not on closure success. After 3 months, follow-up examination could be completed in 16 of 67 ablated IPVs, no further shrinkage compared to day 1 was noticed. In 50 % of the

patients ecchymosis was noticed, whereas 16 % complained about paresthesia in the treated skin area.

The study of Sang Woo Park et al. investigated different technical approaches regarding the location of laser energy delivery in thigh perforators [18]. Some IPVs were punctured and ablated directly whereas others were closed due to sole ablation of the connected GSV. For visualization of varicose vein anatomy during the procedure, angiographic and duplexsonographic images were used. After 1 week 96 % of the IPVs were still occluded, late closure results are sufficient but not very reliable due to a high dropout rate. Better technical results of the procedure were achieved with the GSV ablation method, because the direct advancement of the laser fiber into the IPV was reported to be more complicated. This study reports a high rate of bruising and ecchymosis, probably correlated to the bare fiber used, known for causing perforations of the venous wall [19].

Hisslink et al. reported on IPV ablation in patients with imminent, healed or florid ulcer (CEAP class C4–C6). The majority of IPVs were accompanied by reflux in the deep venous system. Three months after the procedure 78 % of the IPVs were still occluded. No ecchymosis was seen as the fiber used is designed with a gold tip, resulting in less focal charring of the vein.

The Ceralas D diode laser with 1470 nm in combination with a radial fiber slim was used in two studies. Mert et al. used a LEED of 69 J/cm, achieving a closure success of 87 % after 12 months. Zerweck et al. treated IPVs with a mean diameter of 5.1 mm and had a closure success of 96 % after one month, requiring a LEED of 132 J/cm. The latter had a lower energy delivery with 8 W, whereas the former used 10 W. Comparing the available data, lower energy levels might be sufficient in this technical setup. Both studies had a low rate of paresthesia.

Corcos et al. report about 808 nm laser ablation of 530 IPVs between the years 2002 and 2008. Energy delivery was between 6–10 W, LEED is stated being as low as 15 J/cm whilst displacement speed of the fiber was 2 mm/s. Despite the low deployed energy, the closure rate in the follow-up examination after 3 months and 6 years was 72 %. Four of five IPVs were 2–4 mm in diameter, potentially explaining the low LEED levels. With 1.5 % a remarkable low rate of paresthesia was noticed.

A case report on ablation of 7 IPVs was published by Ozkan in 2009 [3]. 6 of 7 IPVs could be closed successfully with a LEED of 50–60 J/cm and a 10 W diode laser at 940 nm. No severe complications occurred.

Table 25.1 Comparison on IPV laser ablation studies

	Corcos	Zerweck	Hissink	Sang Woo Park	Mert	Proebstle	Proebstle	Ozkan
Laser device	Diode	Diode Ceraslas D TM Biolitec AG; Jena, Germany	Diode Diomed delta 15 W; Andover, MA, USA	Daedeok Laser, Daejeon, Korea	Diode Ceraslas D TM Biolitec AG; Jena, Germany	Nd:YAG	Diode	Diode Dornier; MedTech Laser GmbH, Germering, Germany
Fiber (µm)	600 Eufoton Flat surface of emission	400 ELVeS-radial-slim kit TM	400 Angiodynamics, Queensbury, NY, USA	600 bare tip	400 ELVeS-radial-slim kit TM	600	600	600
Wavelength (nm)	808	1470	810	980	1470	1320	940	940
Perforators	530	69	58	69 (34/35)	23	47	20	7
Diameter	2–4 mm N=203 ~4 mm N=222 4–6 mm N=99 >6 mm N=10	5.1 ± 1.6 mm	No data	No data	No Data	3.3 mm (1.1–8)	3.3 mm (1.1–8)	3–4.6 mm
Energydelivery (W)	Continuous 6–10	Continuous 8	Continuous 14	Continuous 10 (14)	Continuous 10	Pulsed 5–10	Pulsed 8–30	Pulsed 8–30
LEED (J/cm)	15	132	No data	No data	69	~400	~400	~60m
Meanenergy (J)	No data	241 ±121	187 (87–325)	No data	174 ±75	290 (90–625)	250 (103–443)	No data
Early follow-up closuresuccess	No data	1 day 100 % 1 week 94.2 %	No data	1 week 96.1 %	1 day 100 %	1 day 100 %	1 day 100 %	No data
Late follow-up closuresuccess	3 month–6 years 72.2 %	1 month 95.6 %	3 months 78 %	High dropout rate	12 months 86.9 %	3 months Shrinkage, no data High dropout rate	3 months Shrinkage, no data High dropout rate	1 month 83.3 %

References

1. Boné C. Tratamiento endoluminal de las varices con láser de diodo. Estudio preliminar. *Patol Vasc*. 1999;V:31–9.
2. Proebstle TM, Herdemann S. Early results and feasibility of incompetent perforator vein ablation by endovenous laser treatment. *Dermatol Surg*. 2007;33(2):162–8.
3. Ozkan U. Endovenous laser ablation of incompetent perforator veins: a new technique in treatment of chronic venous disease. *Cardiovasc Interv Radiol*. 2009;32(5):1067–70.
4. Schwarz T, von Hodenberg E, Furtwängler C, Rastan A, Zeller T, Neumann FJ. Endovenous laser ablation of varicose veins with the 1470-nm diode laser. *J Vasc Surg*. 2010;51(6):1474–8.
5. Zerweck C, von Hodenberg E, Knittel M, Zeller T, Schwarz T. Endovenous laser ablation of varicose perforating veins with the 1470-nm diode laser using the radial fibre slim. *Phlebology*. 2014;29(1):30–6.
6. Corcos L, Pontello D, de Anna D, Dini S, Spina T, Barucchello V, Carrer F, Elezi B, Di Benedetto F. Endovenous 808-nm diode laser occlusion of perforating veins and varicose collaterals: a prospective study of 482 limbs. *Dermatol Surg*. 2011;37(10):1486–98.
7. Hissink RJ, Bruins RM, Erkens R, Castellanos Nuijts ML, van den Berg M. Innovative treatments in chronic venous insufficiency: endovenous laser ablation of perforating veins: a prospective short-term analysis of 58 cases. *Eur J Vasc Endovasc Surg*. 2010;40(3):403–6.
8. Cockett FB, Jones DE. The ankle blow-out syndrome; a new approach to the varicose ulcer problem. *Lancet*. 1953;1(6749):17–23.
9. Bozzato S, Rancan E, Ageno W. Fondaparinux for the treatment of superficial vein thrombosis in the legs: the CALISTO study. *Expert Opin Pharmacother*. 2011;12(5):835–7.
10. Gloviczki P, Gloviczki ML. Guidelines for the management of varicose veins. *Phlebology*. 2012;27 Suppl 1:2–9. doi:10.1258/phleb.2012.012S28.
11. Schwarz T, Schmidt B, Schellong SM. Inter observer agreement of complete compression ultrasound for clinically suspected deep vein thrombosis. *Clin Appl Thromb Hemost*. 2002;8:45–9.
12. Schellong SM, Schwarz T, Halbritter K, Beyer J, Siegert G, Oettelr W, Schmidt B, Schroeder HE. Complete compression ultrasonography of the leg veins as a single test for the diagnosis of deep vein thrombosis. *Thromb Haemost*. 2003;89:228–34.
13. Dumantepe M, Tarhan A, Yurdakul I, Özler A. Endovenous laser ablation of incompetent perforating veins with 1470 nm, 400 µm radial fiber. *Photomed Laser Surg*. 2012;30(11):672–7.
14. Darwood RJ, Gough MJ. Endovenous laser treatment for uncomplicated varicose veins. *Phlebology*. 2009;24 Suppl 1:50–61. doi:10.1258/phleb.2009.09s006.
15. Pannier F, Rabe E, Maurins U. 1470 nm diode laser for endovenous ablation (EVL) of incompetent saphenous veins - a prospective randomized pilot study comparing warm and cold tumescence anaesthesia. *Vasa*. 2010;39(3):249–55.
16. Rabe E, Pannier F. Sclerotherapy of varicose veins with polidocanol based on the guidelines of the German Society of Phlebology. *Dermatol Surg*. 2010;36 Suppl 2:968–75.
17. Harlander-Locke M, Jimenez JC, Lawrence PF, Derubertis BG, Rigberg DA, Gelabert HA. Endovenous ablation with concomitant phlebectomy is a safe and effective method of treatment for symptomatic patients with axial reflux and large incompetent tributaries. *J Vasc Surg*. 2013;58(1):166–72.
18. Park SW, Hwang JJ, Yun IJ, Lee SA, Kim JS, Chang SH, Chee HK, Chang IS. Randomized clinical trial comparing two methods for endovenous laser ablation of incompetent perforator veins in thigh and great saphenous vein without evidence of saphenofemoral reflux. *Dermatol Surg*. 2012;38(4):640–6. doi:10.1111/j.1524-4725.2011.02261.x. Epub 2011 Dec 30.
19. Sroka R, Weick K, Sadeghi-Azandaryani M, Steckmeier B, Schmedt CG. Endovenous laser therapy--application studies and latest investigations. *J Biophotonics*. 2010;3(5–6):269–76.

Excimer Laser Assisted Retrieval of Embedded Vena Cava Filters: Insights from the Preclinical Animal Model

Naritatsu Saito and Takeshi Shimamoto

Pulmonary thromboembolism is the sudden blockage in one or more arteries in the lung by the blood clots formed in the veins of the lower extremities or pelvis. Pulmonary thromboembolism is a serious circulatory disorder, which can be a cause of sudden death. Many types of Inferior vena cava (IVC) filters have been developed to prevent the pulmonary thromboembolism in patients with deep vein thrombosis. The permanent placement of an IVC filter effectively reduces the recurrence rate of pulmonary thromboembolism in the acute phase of deep vein thrombosis but it increases the rate of recurrent deep vein thrombosis in the chronic phase [1, 2]. The retrievable IVC filters may resolve this problem as they may be left in place as permanent filters or retrieved if the patient no longer requires vena cava interruption. The retrieval is usually recommended within a certain periods of time after its implantation to avoid fibrotic fixation of the filter to the venous wall. We previously described the feasibility of laser-assisted retrieval of embedded IVC filters in a canine model [3]. The technique has already been applied to more than 100 patients by another group and the results are favorable [4]. In this chapter, we describe the insights from the preclinical animal experiments.

The experiment employed Gunther Tulip filter (GTF; Cook, Bloomington, Indiana), which is one of the most commonly used retrievable filters. Six GTFs were implanted in six mongrel dogs and retrieved after 4 weeks. The filters were firmly attached to the venous wall at the time of retrieval. The laser-assisted retrieval was examined in this model. The retrieval system consisted of a 14-F excimer

laser sheath (Spectranetics, Colorado Springs, Colorado), an 8-F guide catheter, and a 15-mm Goose Neck snare (Fig. 26.1). The laser sheath was connected to a CVX-300 Excimer Laser System (Spectranetics Co.), which generates ultraviolet light that has a wavelength of 308 nm and maximum fluence of 60 mJ/mm² (energy output per unit area of the fiber). In the present study, a 40 Hz repetition rate was used. The retrieval technique was described as follows. The right jugular vein of each dog was surgically isolated. A longitudinal venotomy was created, and the laser sheath was advanced through the right jugular vein into the IVC, with the tip of the sheath being positioned approximately 1 cm proximal to the filter hook. After injecting 3000 units of heparin, the Goose Neck snare and 8-F guide catheter were advanced through the laser sheath to capture the hook of the filter. The filter was gently pulled into the 8-F guide catheter until a firm and persistent resistance was perceived. A cavography revealed an hourglass-shaped collapse of the caval lumen, indicating tight adhesion of the filter to the vessel wall. The laser sheath was gently advanced to the site of the adhesion while holding the Goose Neck snare and 8-F guide catheter. Excimer laser energy (10-second bursts) was applied to various points in the adhesion site by slowly rotating the beveled tip. When ablation of the adhered tissue was completed, the filter was retrieved in the laser sheath. Immediately after filter retrieval, cavography was performed to assess the morphology of the inner caval wall and check for any damage or perforation. We did not perform a continuous saline injection through the guiding catheter during the laser application, which might be necessary to minimize vessel wall damage. Figure 26.2 describes the retrieval technique. After ablation of the adhesions by excimer laser emission, all filters were successfully retrieved. Final cavography after retrieval revealed no caval damage except for minor extravasation in three dogs. Examination of the caval specimen taken from a dog immediately after filter retrieval revealed partial absence of the intima and media (Fig. 26.3). In the remaining five dogs, cavography performed 2 days after filter retrieval revealed complete hemostasis and almost

N. Saito, MD (✉)
Department of Cardiovascular Medicine,
Graduate School of Medicine, Kyoto University,
54 Shogoin Kawahara-cho, Sakyo-ku, Kyoto, Japan
e-mail: naritatu@kuhp.kyoto-u.ac.jp

T. Shimamoto, MD
Department of Cardiovascular Surgery, Kurashiki Central Hospital,
1-1-1 Miwa, Kurashiki, Okayama, Japan
e-mail: shimamo@kuhp.kyoto-u.ac.jp

indistinguishable intimal indentations. On follow-up cavography 28 days after filter retrieval, caval stenosis with 38 ± 11 % diameter narrowing was noted. The caval specimen

obtained from a dog at 28 days showed neointima formation at the level where the filter struts were in contact with the caval wall (Fig. 26.4). The other four dogs have survived for more than 3 months without any adverse events. We concluded that laser-assisted retrieval of an IVC filter incorporated into the IVC wall is feasible.

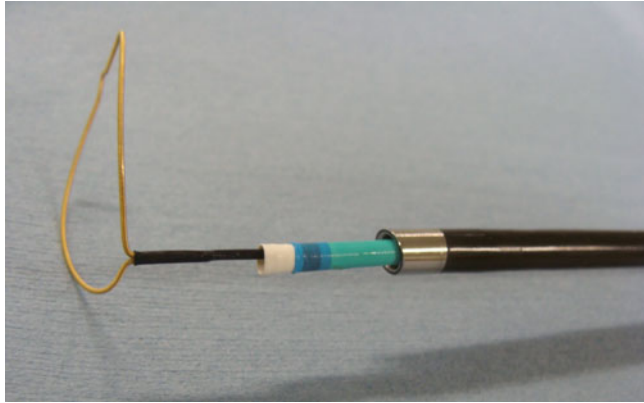


Fig. 26.1 The retrieval system consisting of a 14-F excimer laser sheath, an 8-F straight guide catheter, and a 15-mm Goose Neck snare

The laser-assisted retrieval of embedded IVC filter has already been used in humans. Kuo and colleagues present their experience in 100 consecutive patients. The procedures were successful in 98.0 % with mean implantation of 855 days. The major complication rate was 3.0 %; one patient developed IVC thrombus and two patients developed major hemorrhage requiring stent-graft placement. The results seem favorable. However, we consider that some modifications are desirable in the laser sheath because it is originally designed for pacemaker lead removal. Most importantly, the tip of the laser sheath should be slightly tapered inward. The distal tip of the laser sheath used in this study was beveled at a 15° angle,

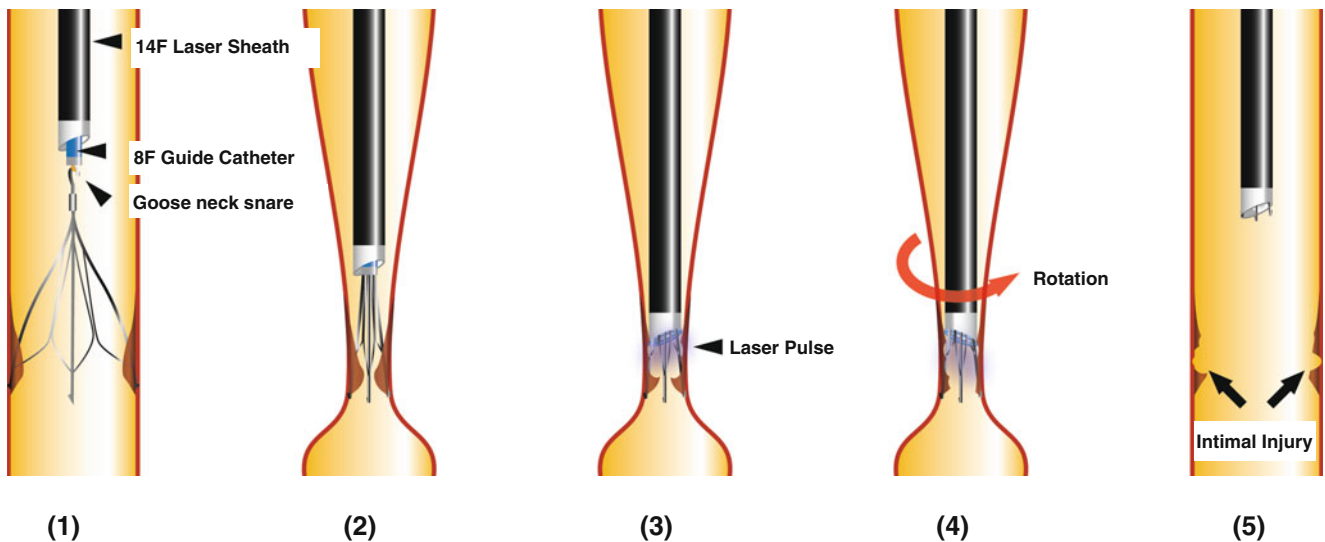


Fig. 26.2 Diagrammatic representation of the various steps of laser-assisted GTF retrieval. (1) Entrapment of the filter hook by the Goose Neck snare. (2) IVC wall collapse with the advancement of the laser

sheath. (3) Generation of the laser pulse. (4) Rotation the beveled tip of the laser sheath. (5) Filter removal

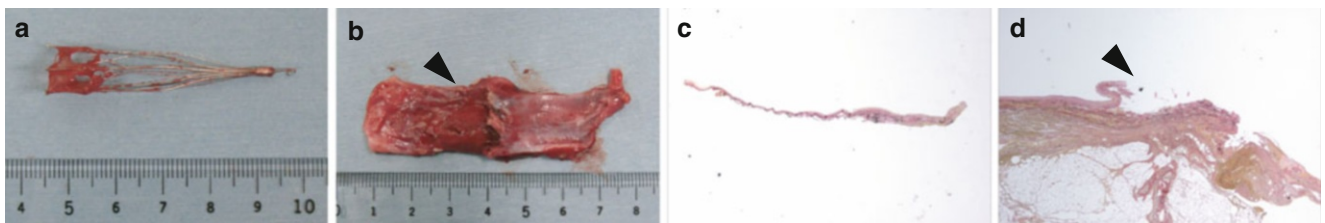


Fig. 26.3 Gross and microscopic findings of the IVC wall and retrieved filter (Van Gieson staining) immediately after retrieval. (a) Filter legs are covered with a fibrotic red membrane. (b) The intima is partially absent (arrowhead). (c) Microscopic findings of the tissue

attached to the filter struts. Vascular intima and fibrin were found. (d) Microscopic findings of the caval wall show partial absence of the endothelium, intima, and media (arrowhead)

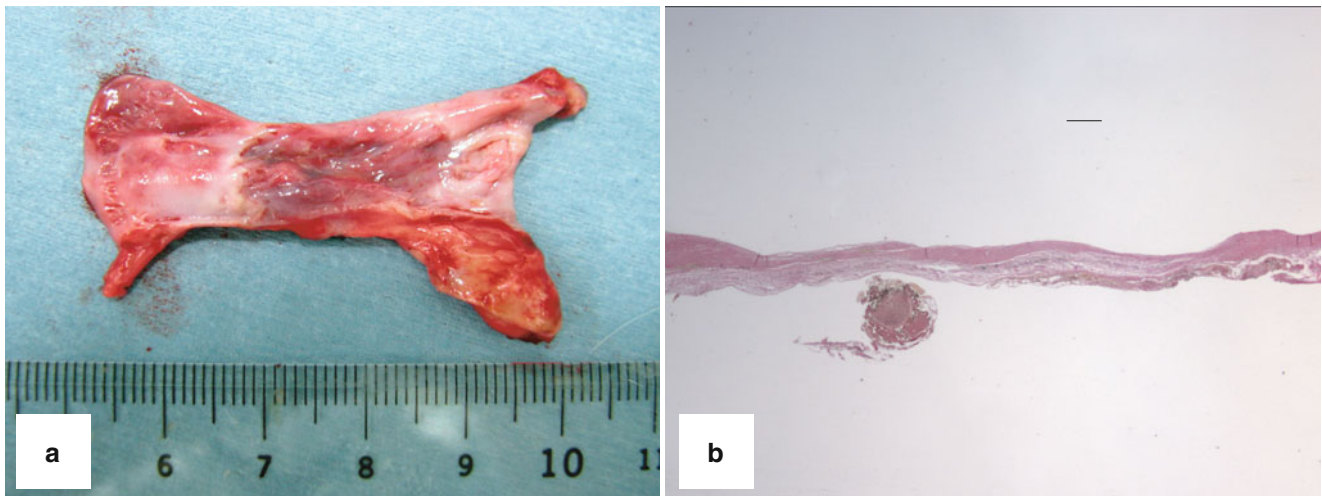
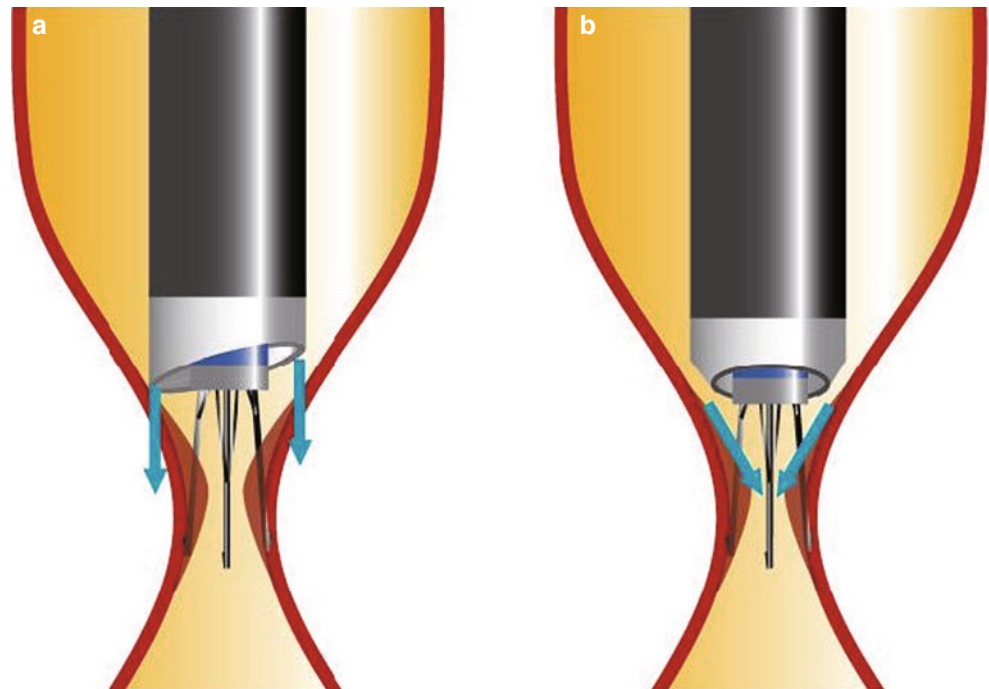


Fig. 26.4 Gross and microscopic findings of the caval wall 28 days after GTF retrieval (Van Gieson staining). **(a)** Gross findings show thin neointima formation at the site where the filter struts were in contact

with the caval wall. **(b)** Microscopic findings show proliferated neointima replacing the damaged intima

Fig. 26.5 **(a)** The excimer laser sheath used in the study. **(b)** Desirable shape of the distal tip. The distal tip of the laser sheath is tapered inward so the direction of the laser becomes parallel to that of the collapsed caval wall



which makes it easier to pass the acute pacing lead angle in the superior vena cava. However, a beveled tip is not necessary for the retrieval of filters implanted in the IVC as this vessel usually runs straight along the body axis. When the distal tip is tapered slightly inward, the direction of the laser becomes parallel to that of the collapsed IVC wall,

which may facilitate accurate and fine dissection (Fig. 26.5).

The laser assisted retrieval of embedded IVC filter is a new indication for excimer laser use. The therapeutic system requires more improvements and the true efficacy should be assessed in a control, randomized clinical trial.

References

1. England TN. A clinical trial of vena caval filters in the prevention of pulmonary embolism in patients with proximal deep-vein. 1998;13:409–15.
2. Avenue G. Eight-year follow-up of patients with permanent vena cava filters in the prevention of pulmonary embolism: the PREPIC (Prevention du Risque d'Embolie Pulmonaire par Interruption Cave) randomized study. *Circulation* [Internet]. 2005 [cited 2014 Jan 4]; 112(3):416–22. Available from: <http://www.ncbi.nlm.nih.gov/pubmed/16009794>.
3. Saito N, Shimamoto T, Takeda T, Marui A, Kimura T, Ikeda T, et al. Excimer laser-assisted retrieval of Günther Tulip vena cava filters: a pilot study in a canine Model. *J Vasc Interv Radiol* [Internet]. Elsevier Inc.; 2010 [cited 2012 Aug 4];21(5):719–24. Available from: <http://dx.doi.org/10.1016/j.jvir.2010.01.028>.
4. Kuo WT, Odegaard JI, Rosenberg JK, Hofmann LV. Excimer laser-assisted removal of embedded inferior vena cava filters: a single-center prospective study. *Circ Cardiovasc Interv*. 2013;6(5):560–6. Available from: <http://www.ncbi.nlm.nih.gov/pubmed/24065445>.

Jagadeesh Kumar Kalavakunta, Mohammad Anas Hajjar,
Prem Srinivas Subramaniyam, and George S. Abela

Historical Background of Lasers

Laser is an acronym for “light amplification by stimulated emission of radiation”. The development of lasers is based on Neil Bohr’s theory of quantum mechanics and Albert Einstein’s theory of stimulated emission [1]. Bohr theorized that energy is released in quanta of electromechanical energy from excited atoms known as photons while Einstein theorized that when an excited atom is struck by a photon of a certain wave length and direction it would release a photon of the same specific wavelength and direction. In 1958 Townes and Schawlow in the United States and Prokhorov in the Soviet Union further developed this concept leading to the first laser device to be built by Theodore Maiman in 1960 [2, 3].

Lasers are uniquely suited in the medical field because of certain features that include a monochromatic light that can be absorbed selectively by tissues with distinctive color as well as a coherent light that deposits high energy that can ablate tissue with precision cutting. Not long after the first ruby laser was developed, Dr. Leon Goldman, a dermatologist

at the University of Cincinnati started to treat skin lesions with intense color (i.e., hemangiomas) in his laboratory [4]. Soon to follow was application of laser in ophthalmology for treatment of diabetic retinopathy and in general surgery for non-contact cutting that avoids the spread of tumor cells [5]. All these applications of the laser were initially delivered by hand-held rigid devices using mirrors to direct the laser beam. However, industrial advances in fiber optics led to the ability of transmitting lasers via flexible fibers. Fibers could then be threaded into body orifices via catheters that carry the laser light to treat target lesions deep into body cavities.

Continuous Laser Wavelengths for Angioplasty Procedures

Several early brief reports demonstrating the effect of laser on atherosclerosis were published using a ruby laser by McGuff (1963) and then with an argon laser by Macruz (1980) [6, 7]. Meanwhile, in the cardiovascular field, balloon angioplasty procedures were becoming widely used for the treatment of arterial blockages in the heart and peripheral circulation. Thus, the time was right to evaluate the use of laser technology in more depth. In 1982 Abela presented an initial report at the American College of Cardiology demonstrating the effect of three laser wavelengths (CO₂; 10,600 nm, argon; 488;514 nm and Nd-Yag; 1060 nm) on atherosclerotic plaques [8]. The advantage of the argon and Nd-Yag lasers wavelengths was these could be easily transmitted via optical fibers whereas the CO₂ required articulated mechanical arms with mirrors [9]. However, all three wavelengths produced very similar tissue effects characterized by a central zone of plaque vaporization, surrounded by a zone of thermal injury and an adjacent outer layer of diffuse tissue disruption [10] (Fig. 27.1). Importantly, using fiber optic delivery systems it was possible to perform lasing in a blood filled medium with the fiber in direct contact with the tissue [11] (Fig. 27.2).

J.K. Kalavakunta, MD
Division of Cardiology, Department of Medicine,
Michigan State University (CHM), Borgess Medical Center,
East Lansing, MI, USA
e-mail: jkalavakunta@gmail.com

M.A. Hajjar, MD • P.S. Subramaniyam, MD
Division of Cardiology, Department of Medicine,
Michigan State University (CHM),
East Lansing, MI, USA
e-mail: anashajjar@hotmail.com; prem.subramaniyam@hc.msu.edu

G.S. Abela, MD, MSc, MBA, FACC, FAHA, FNLA (✉)
Division of Cardiology, Department of Medicine,
B208 Clinical Center, Michigan State University (CHM),
East Lansing, MI, USA

Division of Pathology, Department of Physiology,
Michigan State University, East Lansing, MI 48824, USA
e-mail: george.abela@ht.msu.edu

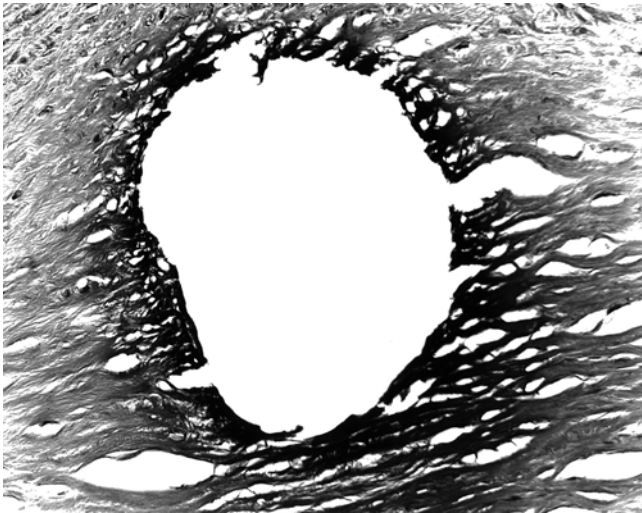


Fig. 27.1 Histology of laser effect on arterial plaque demonstrating a central zone of vaporization surrounded by a zone of thermal injury and a surrounding zone of diffuse tissue disruption (Abela et al. [10], with permission)

Fiber Optic Laser Delivery Systems

Reports on the effect of lasers in cardiovascular system began to emerge, including dissolving thrombus in cadaver hearts [12]. All these preliminary studies were conducted using continuous wavelength lasers. These lasers were adapted to optical fibers that had a small diameter (≤ 1 mm) but were flexible enough to pass through hollow catheters within the circulatory system to reach distant arterial targets under fluoroscopic guidance [13]. Meanwhile, modified fibers were also being produced. One such device had a metal ring at the tip to help with fluoroscopic visualization (Fig. 27.3). However, there were major limitations to these systems because they produced small arterial channels and caused frequent arterial perforations. Perforations were related to both the stiffness of the fiber optic tips as well as heat generated during laser delivery of continuous laser wavelengths. The focus then shifted to development of various approaches to improve optical fiber guidance and mechanical control.

Guiding Systems for Laser Angioplasty

In order to reduce arterial perforations, various guiding systems were developed and/or adapted.

Guide Wires

The initial system was to use a guide wire within the laser catheter in order to keep the fiber aligned with the vascular lumen. This was based on the work of John Simpson and that was then adapted by Anderson and Gruentzig to the

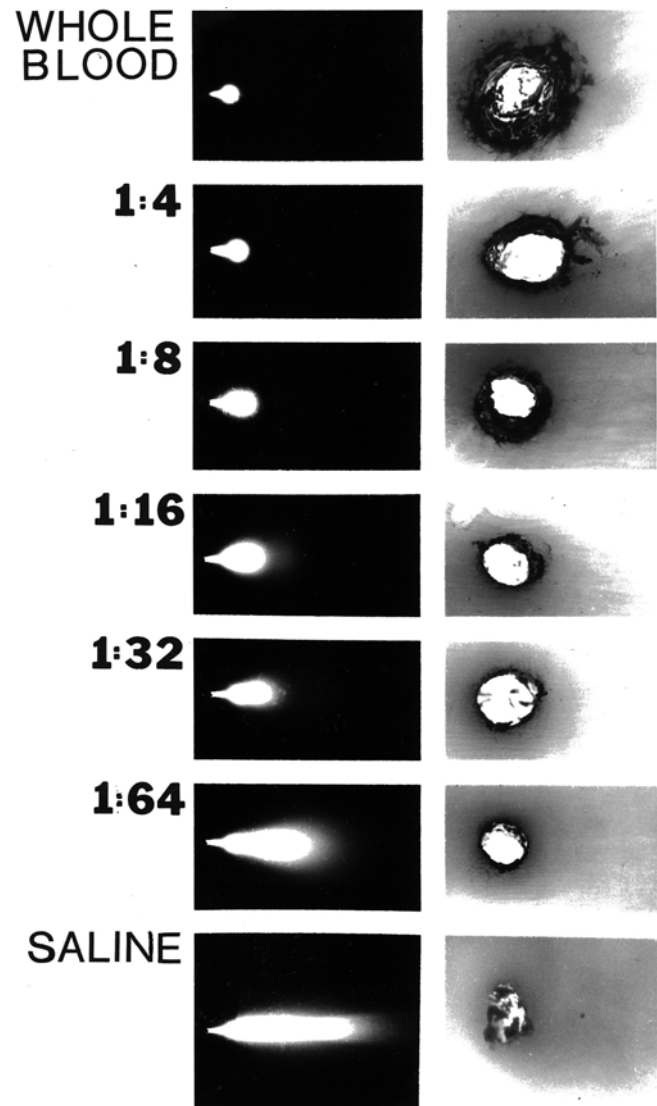


Fig. 27.2 *Left*, beam dispersion pattern in whole blood, saline solution and various blood-saline dilutions. The divergence angle increases from 15° in saline solution to 30° in 1:64. In whole blood the dispersion is spherical around the fiber tip. *Right*, larger craters are produced at increasing concentrations of blood, the largest being in whole blood. Charring at the lased site is also greater with increase concentrations of blood (Fenech et al. [11], with permission)

laser catheter system [14, 15]. Consequently, irradiation from the tip would remain centered within the arterial lumen along the course of the guide wire [16].

Angioscopy

Fiber bundles with lens tips were used to make angioscopic catheters that could be used to visualize the plaque and guide the fiber tips during irradiation of the plaque. However, these devices were often large, bulky and did not achieve the desired outcome of reduced perforation because they lacked catheter tip control. However, angioscopes advanced over

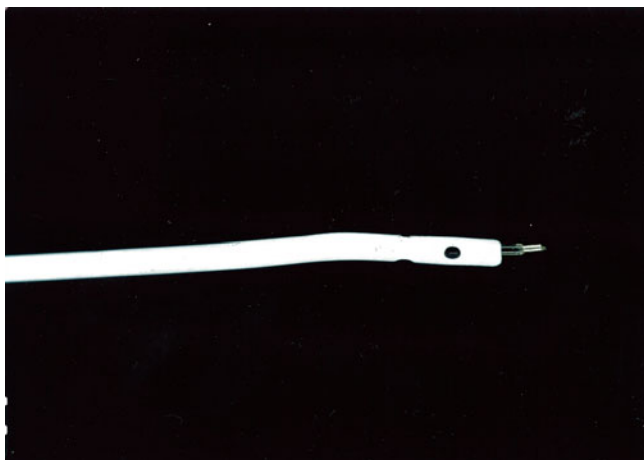


Fig. 27.3 Catheter with protruding optical fiber. The fiber has a metal ring placed at the tip to allow visualization with fluoroscopy (Courtesy of Abela GS)

guidewires evolved independently of lasers to be used for examining atherosclerotic plaques *in vivo* and identify unstable atherosclerotic plaques that may lead to acute cardiovascular events [17].

Fluorescence

Other systems were developed using tissue fluorescence as a feedback mechanism to help guide the laser procedure to localize plaque components while avoiding the native artery [18–21]. Those systems could also define the composition of the plaque by spectral signals to identify calcification, fibrous tissue and lipid content. Although this approach was able to distinguish plaques from the artery, it did not have an associated guidance system to address the limitations of the small channel size and arterial perforation with laser.

Ultrasound

Intravascular ultrasound (IVUS) was being developed at the same time when lasers were being evaluated for angioplasty. Although IVUS provided useful data on plaque morphology and composition, it did not resolve the perforation problem [22]. IVUS then evolved independently as a diagnostic tool for vascular procedures especially to identify arterial wall dissection and the severity of arterial stenosis.

Modified Fiberoptic Catheter Systems

'Hot Tip' Probe (Trimedyn, Inc, Lake Forest, CA)

In order to reduce the arterial perforation rate and also enlarge the arterial channel diameter in occluded arteries, the

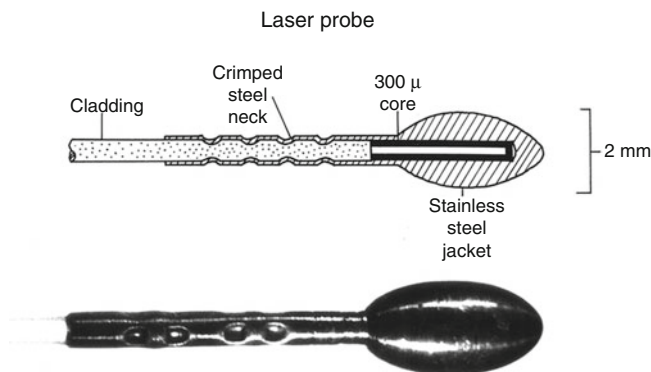


Fig. 27.4 Laser Thermal Probe with steel metal jacket enclosing the optical fiber tip. All the laser energy is absorbed by the fiber converting it into a 'hot tip' system that vaporized the atherosclerotic plaque tissue (Courtesy of Abela GS)

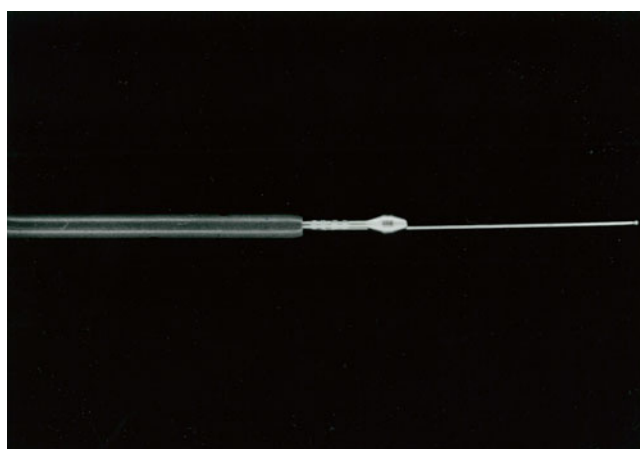


Fig. 27.5 Thermal probe with a 0.18" guide wire passing through an eccentric channel in the probe tip. The whole system is back loaded in a 7-F catheter to allow saline and contrast agent infusion (Courtesy of Abela GS)

optical fiber tip was modified by adapting an olive-shaped metallic steel cap [23, 24]. The metal cap would then absorb laser energy to thermally vaporize the tissue [25, 26] (Fig. 27.4). However, this system required direct contact with the tissue. Moreover, it would also get very hot reaching temperatures above 100 °C which could then cause arterial perforations by thermal conduction to adjacent tissue. Those perforations were larger than the size of the optical fiber. To reduce perforations, a guide wire was adapted by inserting into the body of the metallic probe tip to help keep the fiber probe aligned with the arterial lumen (Figs. 27.5 and 27.6).

Hybrid Probe (Trimedyn, Inc, Lake Forest, CA)

Given the above limitations, a hybrid probe was then developed by Abela et al. and this used the same type of metallic probe tip but had an open end with an optical fiber with

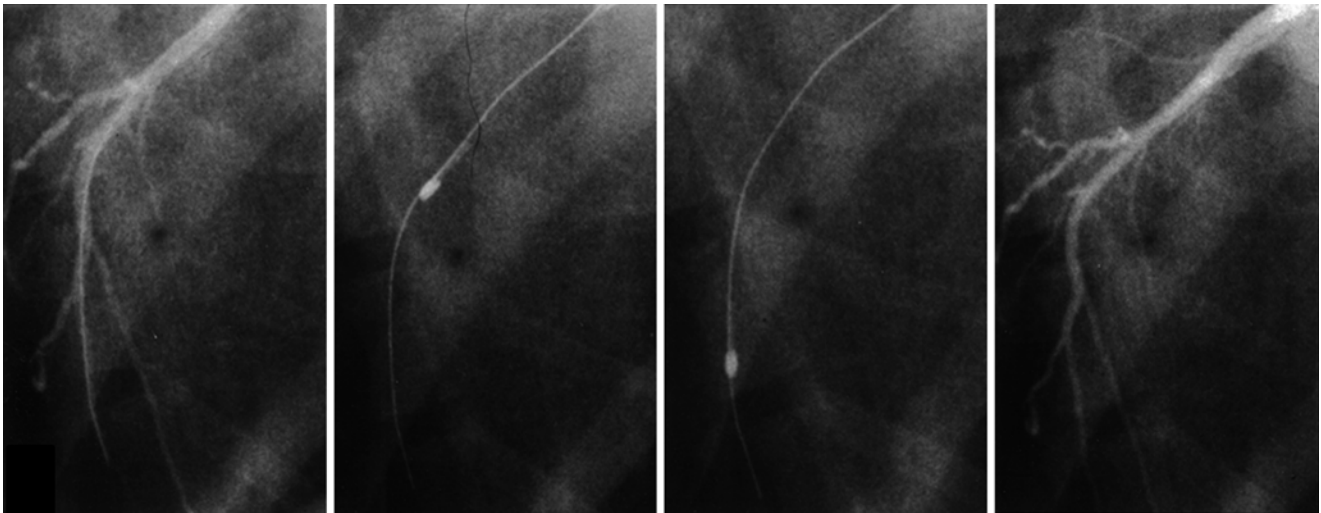


Fig. 27.6 Thermal probe passing into the coronary circulation of a dog demonstrating the flexibility of the probe to follow the guide wire (Courtesy of Abela GS)

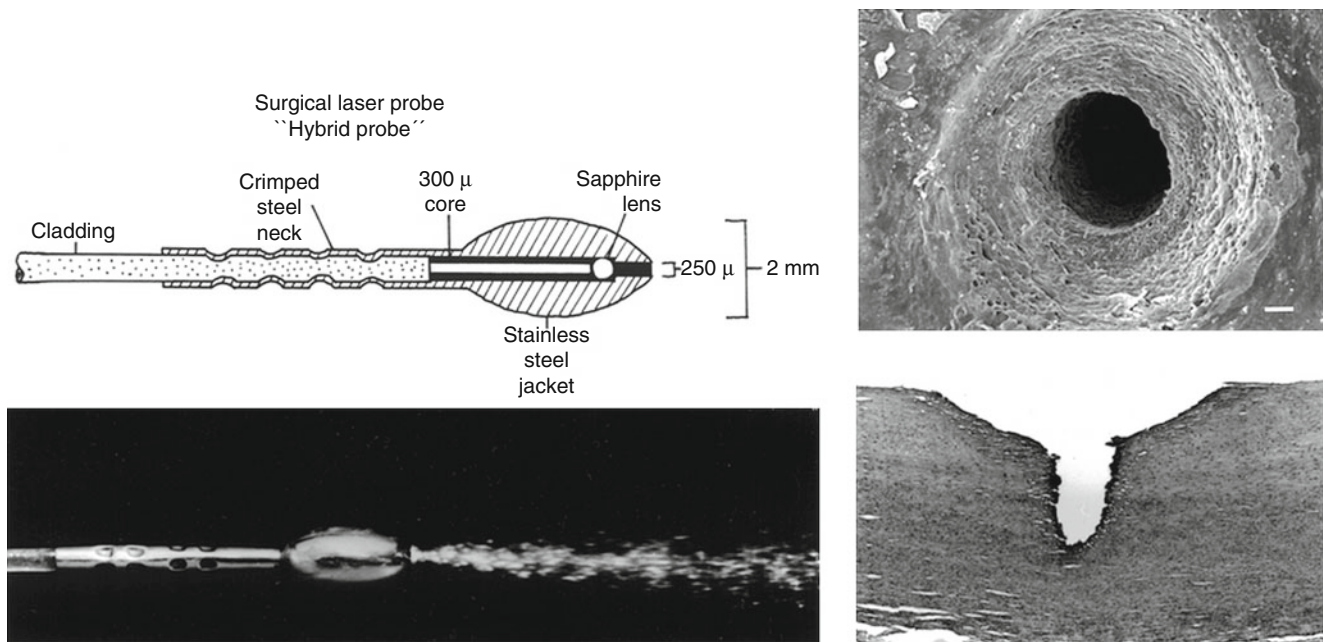


Fig. 27.7 *Left*, the Spectraprobe-PLR™ or hybrid probe has a lens tipped fiber and a metal cap. The fiber discharges a laser beam from the tip and simultaneously heats up the metal probe (Abela et al. [27]

J Am Coll Cardiol, with permission). *Right*, this creates a central channel that is further enlarged by the thermal effect of the probe (Courtesy of Abela et al. [26], with permission)

lensed tip to focus the laser beam [27]. This system created a pilot channel into which the metal probe would then follow to help orient the direction of the fiber [26] (Fig. 27.7). Although this was also a useful modification, perforations still occurred. Some of this was related to overheating of the probe. To address this problem the procedure was conducted by flushing normal saline at 22 °C during the lasing procedure to prevent thermal dispersion. Another modification was the addition of a thermocouple to the tip of the

probe so that it would cut off the laser when the probe temperature exceeded 100 °C [28]. Despite these innovations arterial perforations were still a potential problem, especially in small diameter arteries. The challenge for laser angioplasty was to be able to revascularize the artery and obtain a channel equal to the native vessel without perforation. All the thermal probe systems required tissue contact and were activated by a continuous wavelength laser systems (i.e., argon, Nd-Yag).

Lensed Fibers

Other modifications included of lensed fibers that were made with the intent of focusing the laser beam when ablating the arterial plaque [29]. However, those were quickly transformed into thermal probe system once the lens became soiled by either blood or tissue debris at the treatment site. Thus, these systems also had similar outcomes as the thermal probes.

Laser Balloon Catheter (USCI-Bard, Billerica, MA)

A unique concept was developed by Spears that dispersed laser irradiation by scattering the light through an angioplasty balloon catheter [30]. Since the balloon is transparent to the light and simultaneously displace the blood when inflated allowing a scattered laser beam to irradiate the tissue. The concept behind this system was to cause 'biological stenting' of the tissue. This could seal dissections by balloon angioplasty and stabilize the plaque. Another endpoint was to prevent the high restenosis rate that was frequent following standalone balloon angioplasty. Moreover, to further enhance this system, a photosensitizer, hematoporphyrin derivative (HPD), with high affinity to atherosclerotic plaque would result in selective absorption of the laser light at 316 nm laser wavelength [31]. Although highly innovative, in practice, the expected outcomes of reduced restenosis and biological stenting were not realized.

Pulsed Laser Systems (Excimer, Ho:Yag) for Angioplasty Procedures

Given the hurdles with the continuous wave laser systems attention turned to pulsed lasers as a method to recanalize arterial obstruction. The rationale was that pulsed laser had the ability to vaporize calcific tissues and cut more precisely with less thermal injury to surrounding tissue [32]. Two major wavelengths were used for pulsed laser, Ho:Yag (2100 nm) and Excimer (308 nm Pulse width: 125–200 ns; fluence 30–60 mJ/mm²). These effects were demonstrated by Cross and Bowker in the United Kingdom, by Clarke and Isner and Grundfest and Litvack in the United States [33–35]. Both are highly absorbed by the tissues making them precision cutting devices. A major breakthrough by Goldenberg was the ability to couple the excimer laser (XeCl 308 nm) to fiber optic bundles [36]. These were then used to deliver the laser beam in a forward direction from the catheter tip. Subsequent tip modifications were also made to disperse the beam at outward angles to achieve a wider cut of tissue than the size of the catheter tip.

High energy pulses had their own limitations including production of vapor bubbles that would expand and then implode generating photoacoustic shock waves in the immediate environment [37–40]. These shock waves produced tissue dissection especially if the lasing was done rapidly and in the presence of blood. This could lead to intramural hemorrhage with separation of the arterial wall layers forming the appearance of a multilayered French pastry known as 'Mille Feuille' [41]. Thus, clearing the local milieu of blood during lasing was required to obtain the clean cuts that were seen in the in vitro experiments [42]. This procedure required that the lasing be performed slowly without forcing the catheter into the tissue to avoid mechanical dissection but rather have the catheter lead the way by precision cutting of plaque. Pulsed HoYag was also used but had more shock wave and thermal tissue effects than the excimer [41]. Various catheter systems were built with a central channel and surrounding fibers that could then cut a precise rounded channel around a guide wire. Although successful, this approach continued to require the need for follow up balloon angioplasty to obtain the size of channel comparable to the size of native artery. Furthermore, the anticipated effect of reduced restenosis using laser was not achieved.

Laser Thrombectomy

Thrombus plays a key role in the acute coronary syndrome (ACS) and it poses a challenge for revascularization. Moreover, thrombosis is associated with increased intra and post procedural complications. Distal embolization of the thrombus during percutaneous coronary intervention (PCI) can reduce microvascular perfusion which has been shown to be associated with poor prognosis.

Mechanical thrombolysis can be achieved with laser as thrombi have a high water content which helps in the absorption of the light. Also, the laser interacts with platelets and fibrin which are key components of the thrombus. Topaz et al. demonstrated that the mid pulsed ultraviolet and infrared lasers (i.e., excimer and holmium:YAG) can create acoustic shock waves with dynamic pressure on the fibrin mesh to break up the fibrin to cause thrombolysis [43]. Lasers can also alter platelet aggregation and can cause stunning in a dose dependent manner.

During ACS laser thrombectomy can be achieved both in native coronary arteries and venous grafts. Thus, the laser may be used as an alternative to treat a high thrombus burden especially in patients who failed thrombolysis or have contraindications for thrombolytics or IIb/IIIa receptor antagonists. In a study of 50 AMI patients excimer laser was effective in thrombus reduction by 83 % and an improved Thrombolysis In Myocardial Infarction (TIMI) flow [44].

In the CARMEL (Cohort of Acute Revascularization of Myocardial Infarction with Excimer Laser) multicenter, non-randomized, observational study Topaz et al. demonstrated that excimer laser was effective in AMI by significantly increasing TIMI flow and reducing target lesion stenosis [45]. Both native coronaries stenoses (79 %) and venous grafts (21 %) were included. A 91 % overall procedural success rate was achieved with minimal complications (0.6 % balloon related perforations, 0.6 % acute closure, 3 % laser induced major dissections). No laser related perforations were noted. Other key findings were that the maximal laser effect was noted in the lesions with large thrombus burden. Also, no distal embolization was noted among the 21 % of patients who had degenerated vein grafts.

than 6 months and >10 cm total superficial femoral artery (SFA) occlusion compared balloon angioplasty with laser assisted balloon angioplasty. No differences in outcomes (clinical events or patency rates) were demonstrated at 1 year follow up between the two approaches [50].

The Laser Angioplasty in Critical Ischemia (LACI) trial included 145 critical limb ischemia patients who were deemed to be unfit candidates for vascular surgery [51]. Patients were enrolled to test the effectiveness of laser-assisted balloon angioplasty. Procedural success rate was reported as high as 86 % and stenting was performed in only 45 % of limbs. Follow up at 6 months demonstrated a high limb salvage rate of 92.5 %, with 10 % mortality and 6 % major amputation rates.

Clinical Trials with Lasers

Lasering with Continuous Wave Lasers

Abela et al. were the first to receive FDA approval in the US to perform laser angioplasty in the peripheral circulation in humans using the thermal hybrid probe system. An initial study was performed in 11 patients evaluating the immediate effects of laser angioplasty in peripheral arteries using angioscopic guidance. This was initially performed in the operating room setting during peripheral artery surgery. A new vascular channel was created in 10 of the 11 patients who had totally occluded superficial femoral arteries [27]. Meanwhile, Cumberland et al. worked on peripheral arteries in humans with a laser activated thermal probe or 'hot tip' and had a 89 % primary success in creating a channel followed by balloon dilatation [46]. Sanborn et al. also reported on the use of peripheral laser thermal angioplasty as an adjunct to conventional balloon angioplasty [47]. They demonstrated a high success rate for femoropopliteal stenosis (77 %) and total occlusions (95 %). The 1-year cumulative clinical patency was also 77 % but longer lesions had lower patency rates in 1-year. Shorter lesions had better patency with laser angioplasty compared to balloon angioplasty alone. Other studies reported similar results [48].

Using a hybrid laser/thermal probe, Barbeau et al. demonstrated the feasibility of treating complex peripheral artery lesions using a combined laser angioplasty and percutaneous balloon approach. In this study overall technical success rate was 75 % (Figs. 27.8 and 27.9) [27, 49].

Excimer Laser Angioplasty in the Peripheral Circulation

PELA (Peripheral Excimer Laser Angioplasty) was a prospective, randomized trial in 251 patients (13 US and 6 German sites) with symptoms of claudication for greater

Coronary Artery Studies

Initial results using the excimer laser catheter system (Spectranetics, Colorado Springs, CO) in the coronary circulation were very promising (Fig. 27.10). Early trials by Litvack et al. demonstrated that it was safe to ablate the atheroma and reduce coronary stenosis with the excimer laser. In a multicenter trial on 55 patients the mean minimal stenotic diameter increased from a baseline of 0.5 ± 0.4 to 1.6 ± 0.5 mm with laser treatment and to 2.1 ± 0.5 mm with balloon angioplasty [52]. Similarly Karsch. et al. in a small study (60 patients) also showed lasers were safe in treating both stable and unstable angina patients [53].

Similarly, Sanborn et al. in a multicenter trial on 141 patients demonstrated that laser assisted angioplasty was safe and feasible [54]. However, several trials have not shown benefit over conventional balloon angioplasty. LAVA (Laser Angioplasty Versus Angioplasty) trial was a randomized multicenter study in 215 patients that compared laser facilitated PTCA to balloon angioplasty alone [55]. There were more procedural complications and patient adverse events with laser without any difference in immediate and long term benefits. Similarly the AMRO (Amsterdam-Rotterdam) study in 308 stable angina patients compared excimer laser coronary angioplasty with balloon angioplasty and did not demonstrate improved angiographic success rate, myocardial infarction, coronary bypass surgery, repeat angioplasty or net mean gain in minimal lumen diameter [56]. The ERBAC (Excimer Laser, Rotational Atherectomy, and Balloon Angioplasty Comparison) study showed that the success rate of procedure was higher with rotational atherectomy compared to laser angioplasty and balloon angioplasty [57].

However, the ELLEMENT study confirmed the feasibility of ELCA during contrast injection to improve stent under expansion in undilatable stented lesions [58]. Overall, given that balloon angioplasty was required to dilate the artery following laser procedure and the lack of prevention from restenosis with the laser despite the debulking of the plaque burden

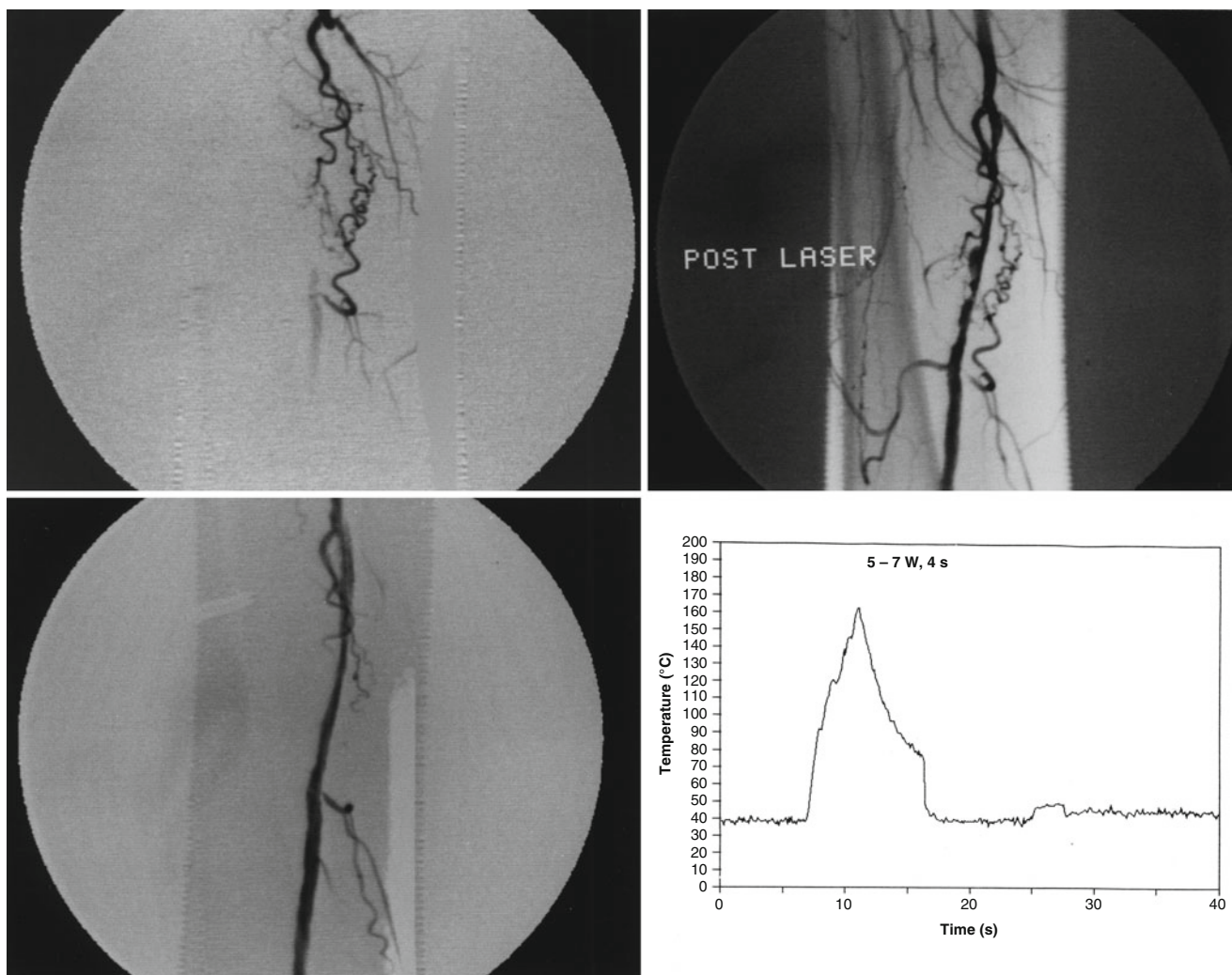


Fig. 27.8 Sequential digital angiograms of the right superficial femoral artery (*top left*) before laser recanalization with hybrid probe, (*bottom left*) after laser recanalization, and (*top right*) after balloon angioplasty. (*bottom right*) Probe temperature is plotted against time

during laser recanalization of the occluded segment shown in (*top left*). Peak probe temperature of 168 °C which resulted in recanalization was reached at a power of 6 W and 4 S exposure (Barbeau et al. [28], with permission)

at the site, laser angioplasty gradually became less frequently used. Currently few clinical uses are considered for excimer laser angioplasty. These include the re-canalization of in-stent restenosis and left main coronary artery disease. Another area that still has occasional use of laser technology is in heavily calcific peripheral vascular lesions [59].

Laser Application for Trans myocardial Revascularization (TMR)

TMR was proposed as an option to treat patients with refractory angina to medical therapy. This was used as standalone therapy but more often as an adjunct to coronary bypass graft surgery. The concept was based on the ventricular sinusoidal system that supplies blood to reptilian hearts as well as the Vineberg technique of direct myocardial revascularization

[60]. The physiological basis is that microchannels created by utilizing lasers can provide an alternative pathway for blood supply of the myocardium by direct perfusion from the left ventricle. However, autopsy studies demonstrated that the channels had become fibrosed and were occluded. Several explanations have been proposed for presumed benefits included such as stimulation of angiogenesis to improve perfusion, anesthetic effect due to destruction of the sympathetic fibers or a placebo effect. There have been multiple methods to create channels in the myocardium. Initially, P.K. Sen used acupuncture needles to create myocardial channels which inspired the use of lasers to create microchannels [61]. Mirhoseini and his colleagues used the CO₂ laser in a canine model and then in humans as an adjunct to CABG [62, 63]. Currently, the CO₂ laser (PLC Systems) and the holmium:YAG laser (Cardiogenesis, Sunnyvale, CA) are the only approved lasers for TMR in United States.

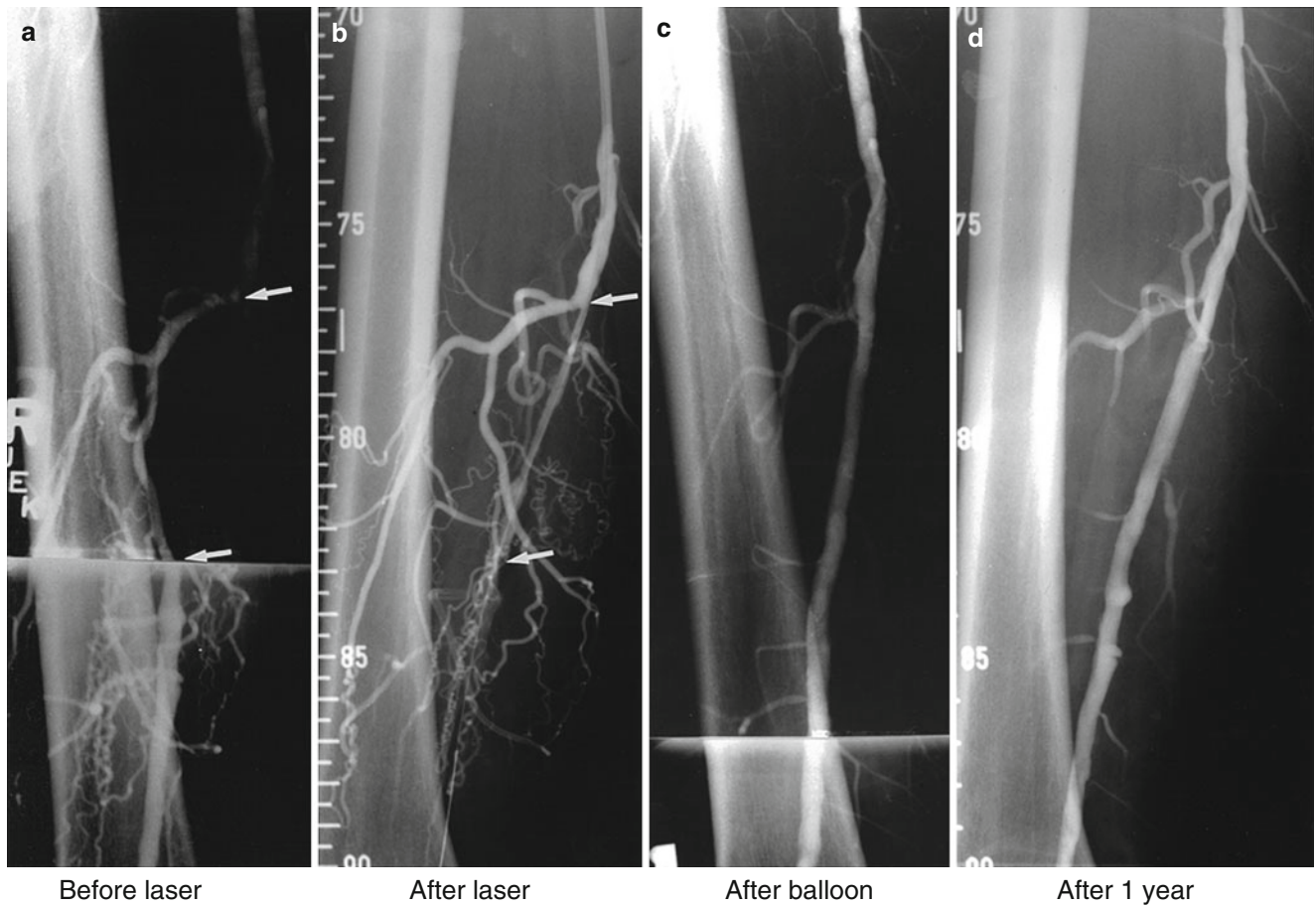


Fig. 27.9 Angiograms of a 61-year-old Caucasian man with <2 block right calf claudication of 7 months' duration (ABI=0.66). (a) Control angiogram. (b) angiogram after laser recanalization with hybrid probe

and guide wire still in the artery. (c) Further dilatation achieved following balloon angioplasty. (d) Angiogram at 1 year with widely patent artery (ABI >1) (Barbeau et al. [49], with permission)

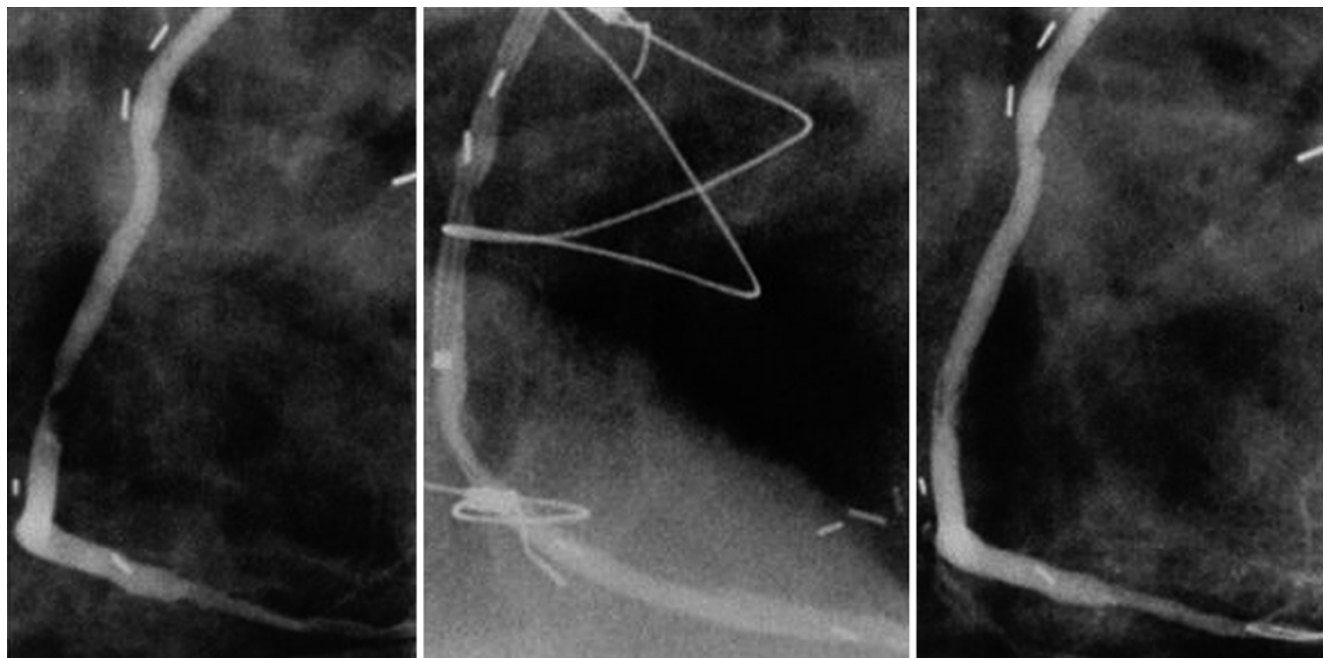


Fig. 27.10 Angiograms of saphenous bypass graft to the right coronary artery in a 51-year-old man who developed recurrent angina 5 years following coronary bypass surgery. *Left panel* shows a 90 % midgraft stenosis. *The middle panel* shows the stenosis after the first laser treatment using a

2.0-mm-diameter laser catheter as described. The catheter tip is seen above the lesion site. *The right panel* shows the final result following completion of laser angioplasty. Minimal residual stenosis (<20 %), and this was left as a laser stand-alone result (Abela et al. [77], with permission)

A sham controlled randomized trial by Leon et al. did not demonstrate a significant difference between a laser treated group and a sham group with respect to exercise duration, improved angina class or visual summed stress single-photon-emission computed tomography scores [64]. Currently, TMR is rarely used as a direct or adjunct treatment for non-bypassable regions of the myocardium.

Other Laser Applications

The excimer laser has been used effectively as a pacemaker lead wire extraction device and this continues to be an important and frequently used application [65–67]. Lasers have been very effective in treatment of varicose veins and this has become a very popular application [68]. Lasers have been used for arterial welding especially for small arteries [69, 70]. Lasers have also been used in electrophysiology as a method to ablate arrhythmia source in the heart including AV node ablation as well as for ventricular tachycardia foci and atrial fibrillation (Fig. 27.11) [71–74]. Photodynamic therapy of atherosclerotic plaque has also been tested with some potential for plaque stabilization [75, 76]. However, clinical applications have not been performed.

Summary

Laser applications in the cardiovascular field have generated much interest in both the cardiovascular community as well as the general public. Over the course of the last two decades clinical applications and basic research of the cardiovascular laser has transitioned to larger volume medical centers with cardiovascular subspecialties. The pulsed-wave, ultraviolet excimer laser that operates at the 308 nm wavelength of the light spectrum has become the primary system being utilized. Absorption of excimer laser energy within targeted biologic tissues creates unique effects on the non-aqueous components of the atherosclerotic plaque and on the accompanying thrombus resulting in vaporization and debulking of intravascular obstructions. Currently, the primary patient candidates for laser angioplasty are those with symptomatic coronary and peripheral arterial disease. These patients often present with complex atherosclerotic and thrombotic lesions which are considered non-amenable for standard technologies of percutaneous intervention or for surgical revascularization. The cardiovascular excimer laser system is approved in the US, Europe and Japan for treatment of symptomatic patients who require revascularization of diseased native coronary arteries, old saphenous vein grafts, chronic total occlusions and diseased peripheral arteries. This laser system is also used for extraction and removal of old and dysfunctional or abandoned pacemaker leads. As the technology continues to evolve the laser could be applied to the more challenging and complex arterial lesions. The most recent developments with laser

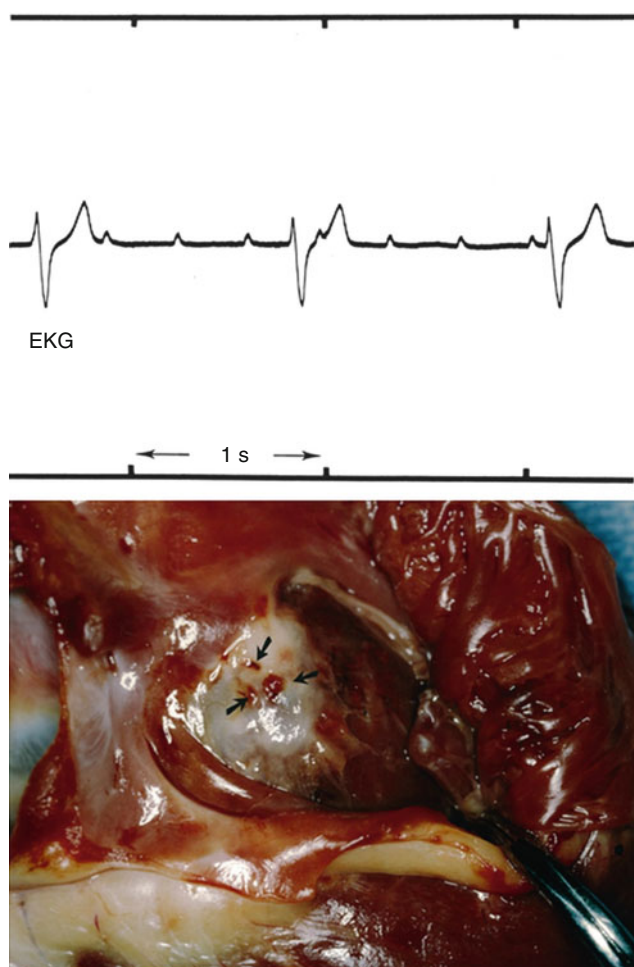


Fig. 27.11 Top, surface electrocardiogram (lead II) recorded following laser-induced complete heart block. There is a ventricular escape rhythm of 47 beats/min. Bottom, Superior portion of the septal leaflet of the tricuspid valve showing three thermal burns at lased sites. Curtis et al. [72], with permission

applications have focused on percutaneous treatment of venous vasculature conditions including removal of permanent embolic protection filters from the inferior vena cava as well as venous thrombolysis. Treatment of varicose veins has been very successful and future developments are anticipated for arrhythmia ablation.

References

1. Einstein A. Zur quantentheorie de strahlung. Phys Z. 1917;18: 121–8.
2. Schawlaow AL, Townes CI. Infrared and optical masers. Physiol Rev. 1958;112:1940.
3. Maiman TH. Stimulated optical radiation in ruby. Nature. 1960; 187:493–4.
4. Goldman L. Biomedical aspects of the laser. New York: Springer; 1967.
5. Koester CJ, Snitzer E, Campbell CJ, Rittler MC. Experimental laser retina coagulator. J Opt Soc Am. 1962;52:607.
6. McGuff PE, Bushnell D, Soroff HS, Deterling RA. Studies of the surgical application of laser light. Surg Forum. 1963;14:143–5.

7. Macruz R, Martins JRM, Tupinamba A, Lopes EA, Vargas H, Pena AF, et al. Therapeutic possibilities of laser beams in atheromas. *Ar Bras Cardiol (Port)*. 1980;34(1):9–12.
8. Abela GS, Conti CR, Geiser EA, Normann S, et al. The effect of laser radiation on atheromatous plaque: a preliminary report (abstr). *Am J Cardiol*. 1982;49:1008.
9. Abela GS, Normann S, Cohen D, Feldman RL, Geiser EA, Conti CR. Effects of carbon dioxide, ND-Yag and argon laser radiation on coronary atheromatous plaques. *Am J Cardiol*. 1982;50(6):1199–205.
10. Abela GS, Pepine CJ. Emerging applications of laser therapy of occlusive vascular disease. *Cardiovasc Rev Rep*. 1985;6(3):269–78.
11. Fenech A, Abela GS, Crea F, Smith W, Feldman R, Conti CR. A comparative study of laser beam characteristics in blood and saline media. *Am J Cardiol*. 1985;55(11):1389–92.
12. Choy DS, Stertz SH, Rotterdam HZ, Bruno MS. Laser coronary angioplasty: experience with 9 cadaver hearts. *Am J Cardiol*. 1982;50(6):1209–11.
13. Abela GS, Normann S, Cohen DM, Franzini D, Feldman RL, Crea F, et al. Laser recanalization of occluded atherosclerotic arteries: an in vivo and in vitro study. *Circulation*. 1985;71(2):403–11.
14. McAuley BJ, Oesterle S, Simpson JB. Advances in guidewire technology. *Am J Cardiol*. 1984;53(12):94C–6.
15. Anderson HV, Zaatari GS, Roubin GS, Leimgruber PP, Gruentzig AR. Coaxial laser energy delivery using a steerable catheter in canine coronary arteries. *Am Heart J*. 1987;113(1):37–48.
16. Bittl JA, Sanborn TA, Abela GS, Isner JM. Wire-guided excimer laser coronary angioplasty: instrument selection, lesion characterization, and operator technique. *J Interv Cardiol*. 1992;5:275–91.
17. Ishibashi F, Aziz K, Abela GS, Waxman S. Update on coronary angiography: review of a 20-year experience and potential application for detection of vulnerable plaque. *J Interv Cardiol*. 2006;19(1):1–9.
18. Deckelbaum LI, Lau JK, Cobin HS, Clubb KS. Discrimination of normal and atherosclerotic aorta by laser induced fluorescence. *Lasers Surg Med*. 1987;7(4):330–5.
19. Kittrell C, Willet RL, de Los Santos-Pacheo C, Ratliff NB, Kramer JR, Malk EG, Feld MS. Diagnosis of fibrous arterial atherosclerosis using fluorescence. *Appl Opt*. 1985;24(15):2280–1.
20. Sartori M, Sauerbrey R, Kobodero S, Tittle FK, Roberts R, Henry P. Auto fluorescence maps of atherosclerotic human arteries—a new technique in medical imaging. *IEEE J Quantum Electron*. 1987;10:1794–7.
21. Leon MB, Lu DY, Prevosti LG, Macy W, Smith PD, Granovsky M, et al. Human arterial surface fluorescence: atherosclerotic plaque identification and effects of laser thrombus ablation. *J Am Coll Cardiol*. 1988;12(1):94–102.
22. Friedl SE, Mathews ED, Miyamoto A, Abela GS. Intravascular ultrasound can be used to evaluate pulsed Ho:YAG laser ablation of arterial tissue. *Lasers Surg Med*. 1995;16(2):156–63.
23. Abela GS, Fenech A, Crea F, Conti CR. “Hot tip”: another method of laser vascular recanalization. *Lasers Surg Med*. 1985;5(3):327–35.
24. Ryan TJ, Sanborn TA, Cumberland DC, Faxon DP, Haudenschild CC. Laser thermal angioplasty: from the experimental model to early human experience. *Trans Am Clin Climatol Assoc*. 1987;98:36–42.
25. Abela GS, et al. Catheter systems for laser angioplasty in lasers. In: Abela GS, editor. *Cardiovascular medicine and surgery: fundamentals and Techniques*. Norwell: Kluwer Publishers; 1990. Published with permission.
26. Hoffman RG, Abela GS, Friedl SE, Hojjatie B, Barbeau GR. Dosimetry of plaque ablation using thermal-optical probe system. *Proc SPIE Optical Fibers Med*. 1989;IV(1067):120–6.
27. Abela GS, Seeger JM, Barbieri E, Franzini D, Fenech A, Pepine CJ, Conti CR. Laser angioplasty with angioscopic guidance in humans. *J Am Coll Cardiol*. 1986;8(1):182–94.
28. Barbeau GR, Abela GS, Seeger JM, Friedl SE, Tomaru T, Giacomino P. Temperature monitoring during peripheral thermo-optical laser recanalization in humans. *Clin Cardiol*. 1990;13:690–7.
29. Verdaasdonk RM, Borst C. Ray tracing of optically modified fiber tips. 1: spherical probes. *Appl Opt*. 1991;30(16):2159–71.
30. Jenkins RD, Spears JR. Laser balloon angioplasty. A new approach to abrupt coronary occlusion and chronic restenosis. *Circulation*. 1990;81(3 Suppl):IV101–8.
31. Spokojny AM, Serur JR, Skillman J, Spears JR. Uptake of hematoporphyrin derivative by atherosclerotic plaques: studies in human in vitro and rabbit in vivo. *J Am Coll Cardiol*. 1986;8(6):1387–92.
32. Deckelbaum LI, Isner JM, Donaldson RF, Laliberte SM, Clarke RH, Salem DN. Use of pulsed energy delivery to minimize tissue injury resulting from carbon dioxide laser irradiation of cardiovascular tissues. *J Am Coll Cardiol*. 1986;7(4):898–908.
33. Bowker TJ, Cross FW, Rumsby P, Gower MC, Rickards AF, Bown SG. Excimer laser angioplasty: quantitative comparison in vitro of three ultraviolet wavelengths on tissue ablation and haemolysis. *Lasers Med Sci*. 1986;1(2):91–100.
34. Isner JM, Donaldson RF, Deckelbaum LI, Clarke RH, Laliberte SM, Ucci AA, et al. The excimer laser: gross, light microscopic and ultrastructural analysis of potential advantages for use in laser therapy of cardiovascular disease. *J Am Coll Cardiol*. 1985;6(5):1102–9.
35. Grundfest WS, Litvack F, Forrester JS, Goldenberg T, Swan HJ, Morgenstern L, et al. Laser ablation of human atherosclerotic plaque without adjacent tissue injury. *J Am Coll Cardiol*. 1985;5(4):929–33.
36. Goldenberg, T. Patent # WO1986003598A1, Dec 5, 1985 Jun 19, 1986. Delivery system for high-energy pulsed ultraviolet laser light. 1986.
37. Tomaru T, Geschwind HJ, Boussignac G, Lange F, Tahk SJ. Characteristics of shock waves induced by pulsed lasers and their effects on arterial tissue: comparison of excimer, pulse dye, and holmium YAG lasers. *Am Heart J*. 1992;123(4 Pt 1):896–904.
38. Van Leeuwen TG, Van Erven L, Meertens JH, Motamedi M, Post MJ, Borst C. Origin of arterial wall dissections induced by pulsed excimer and mid-infrared laser ablation in the pig. *J Am Coll Cardiol*. 1992;19:1610–8.
39. Isner JM, Rosenfeld K, White CJ, Ramee S, Kearney M, Pieczek A, Langevin E, Razvi S. In vitro assessment of vascular pathology resulting from laser irradiation. *Circulation*. 1992;85:2185–96.
40. Gijssbers GHM, Sprangers RLH, Keijzer M, de Bakker JMT, van Leeuwen TG, Verdaasdonk RM, Borst C, van Gemert MJC. Some laser-tissue interactions in 308 nm excimer laser coronary angioplasty. *J Interv Cardiol*. 1990;3:231–41.
41. Abela GS. Abrupt closure after pulsed laser angioplasty: spasm or a “Mille-Feuilles” effect? *J Interv Cardiol*. 1992;5(4):259–62.
42. Tchong JE. Saline infusion in excimer laser coronary angioplasty. *Semin Interv Cardiol*. 1996;1(2):135–41.
43. Topaz O, Minisi AJ, Morris C, Mohanty PK, Carr Jr ME. Photoacoustic fibrinolysis: pulsed-wave, mid-infrared laser-clot interaction. *J Thromb Thrombolysis*. 1996;3(3):209–14.
44. Topaz O, Shah R, Mohanty PK, McQueen RA, Janin Y, Bernardo NL. Application of excimer laser angioplasty in acute myocardial infarction. *Lasers Surg Med*. 2001;29(2):185–92.
45. Topaz O, Ebersole D, Das T, Alderman EL, Madyoon H, Vora K, et al. Excimer laser angioplasty in acute myocardial infarction (the CARMEL multicenter trial). *Am J Cardiol*. 2004;93(6):694–701.
46. Cumberland DC, Sanborn TA, Taylor DI, et al. Percutaneous laser thermal angioplasty: initial clinical results with a laser probe in total peripheral artery occlusions. *Lancet*. 1986;1(8496):1457–9.
47. Sanborn TA, Cumberland DC, Greenfield AJ, Welsh CL, Guben JK. Percutaneous laser thermal angioplasty: initial results and 1-year follow-up in 129 femoropopliteal lesions. *Radiology*. 1988;168(1):121–5.
48. Walker C, Abben R, Chaisson G, Ladd W, Kowalski J, Pharo W, et al. Glide wire and laser in angioplasty of the superficial femoral

- artery initial outcomes and complications in 222 patients. *J Am Coll Cardiol.* 1992;19(Suppl A):314a
49. Barbeau GR, Seeger JM, Kaelin LD, Friedl S, Jablonski S, Abela GS. Peripheral artery recanalization in humans using balloon and laser angioplasty. *Clin Cardiol.* 1996;19(3):232–8.
 50. Laird JR. Peripheral excimer laser angioplasty (PELA) trial results. Presented at TCT annual meeting, Sept 2002, Washington, DC.
 51. Laird JR, Zeller T, Gray BH, Scheinert D, Vranic M, Reiser C, Biamino G, LACI Investigators, et al. Limb salvage following laser-assisted angioplasty for critical limb ischemia: results of the LACI multicenter trial. *J Endovasc Ther.* 2006;13(1):1–11.
 52. Litvack F, Eigler NL, Margolis JR, Grundfest WS, Rothbaum D, Linnemeier T, et al. Percutaneous excimer laser coronary angioplasty. *Am J Cardiol.* 1990;66(15):1027–32.
 53. Karsch KR, Haase KK, Voelker W, Baumbach A, Mauser M, Seipel L. Percutaneous coronary excimer laser angioplasty in patients with stable and unstable angina pectoris. Acute results and incidence of restenosis during 6-month follow-up. *Circulation.* 1990;81(6):1849–59.
 54. Sanborn TA, Bittl JA, Hershman RA, Siegel RM. Percutaneous coronary excimer laser-assisted angioplasty: initial multicenter experience in 141 patients. *J Am Coll Cardiol.* 1991;17(6 Suppl B):169B–73.
 55. Stone GW, de Marchena E, Dageforde D, Foschi A, Muhlestein JB, McIvor M, et al. Prospective, randomized, multicenter comparison of laser-facilitated balloon angioplasty versus stand-alone balloon angioplasty in patients with obstructive coronary artery disease. The Laser Angioplasty Versus Angioplasty (LAVA) Trial Investigators. *J Am Coll Cardiol.* 1997;30(7):1714–21.
 56. Appelman YE, Piek JJ, Strikwerda S, Tijssen JG, de Feyter PJ, David GK, et al. Randomized trial of excimer laser angioplasty versus balloon angioplasty for treatment of obstructive coronary artery disease. *Lancet.* 1996;347(8994):79–84.
 57. Reifart N, Vandormael M, Krajcar M, Göhring S, Preusler W, Schwarz F, et al. Randomized comparison of angioplasty of complex coronary lesions at a single center. Excimer laser, rotational atherectomy and balloon angioplasty comparison (ERBAC) Study. *Circulation.* 1997;96(1):91–8.
 58. Latib A, Takagi K, Chizzola G, Tobis J, Ambrosini V, Niccoli G, et al. Excimer Laser LESion modification to expand non-dilatatable stents: the ELLEMENT registry. *Cardiovasc Revasc Med.* 2014;15(1):8–12.
 59. Piquet P, Bournot P, Caminat JF, Pellissier C, Mercier C. Excimer laser irradiation of non-calcified and calcified human atheroma (248 and 308 nm wavelengths). *Lasers Med Sci.* 1992;7(1–4):393–9.
 60. Vineberg AM, Walker J. The surgical treatment of coronary artery disease by internal mammary artery implantation: report of 140 cases followed up to thirteen year. *Dis Chest.* 1964;45:190–206.
 61. Sen PK, Udwardia TE, Kinare SG, Parulkar G. Transmyocardial acupuncture: a new approach to myocardial revascularization. *J Thorac Cardiovasc Surg.* 1965;50:181–9.
 62. Mirhoseini M, Cayton MM. Revascularization of the heart by laser. *J Microsurg.* 1981;2(4):253–60.
 63. Mirhoseini M, Shelgikar S, Cayton MM. New concepts in revascularization of the myocardium. *Ann Thorac Surg.* 1988;45(4):415–20.
 64. Leon MB, Kornowski R, Downey WE, Weisz G, Baim DS, Bonow RO, et al. A blinded, randomized, placebo-controlled trial of percutaneous laser myocardial revascularization to improve angina symptoms in patients with severe coronary disease. *J Am Coll Cardiol.* 2005;46(10):1812–9.
 65. Levy T, Walker S, Paul V. Initial experience in the extraction of chronically implanted pacemaker leads using the Excimer laser sheath. *Heart.* 1999;82(1):101–4.
 66. Kennergren C. Excimer laser assisted extraction of permanent pacemaker and ICD leads: present experiences of a European Multi-Centre Study. *Eur J Cardiothorac Surg.* 1999;15(6):856–60.
 67. Byrd CL, Wilkoff BL, Love CJ, Sellers TD, Reiser C. Clinical study of the laser sheath for lead extraction: the total experience in the United States. *Pacing Clin Electrophysiol.* 2002;25(5):804–8.
 68. Apfelberg DB, Smith T, Maser MR, Lash H, White DN. Study of three laser systems for treatment of superficial varicosities of the lower extremity. *Lasers Surg Med.* 1987;7(3):219–23.
 69. Zelt DT, LaMuraglia GM, L'Italien GJ, Megerman J, Kung RT, Stewart RB, Abbott WM. Arterial laser welding with a 1.9 micrometer Raman-shifted laser. *J Vasc Surg.* 1992;15(6):1025–31.
 70. White RA, Abergel RP, Lyons R, Klein SR, Kopchok G, Dwyer RM, Uitto J. Biological effects of laser welding on vascular healing. *Lasers Surg Med.* 1986;6(2):137–41.
 71. Kimura T, Takatsuki S, Miyoshi S, Fukumoto K, Takahashi M, Ogawa E, et al. Nonthermal cardiac catheter ablation using photodynamic therapy. *Circ Arrhythm Electrophysiol.* 2013;6(5):1025–31.
 72. Curtis AB, Abela GS, Griffin J, Hill JA, Normann SJ. Transvascular Argon laser ablation of atrioventricular conduction in dogs: feasibility and morphologic results. *Pace.* 1989;12(2):347–57.
 73. Curtis AB, Barbeau GR, Friedl SE, Kunz WF, Mansour M, Abela GS. Modification of AV conduction using a percutaneous combined laser-electrode catheter. *Pace.* 1994;17(3 Pt 1):337–48.
 74. Wagshall A, Abela GS, Maheshwari A, Gupta A, Bowden R, Huang S. A novel catheter design for laser photocoagulation of the myocardium to ablate ventricular tachycardia. *J Interv Card Electrophysiol.* 2002;7(1):13–22.
 75. Litvack F, Grundfest WS, Forrester JS, Fishbein MC, Swan HJ, Corday E, Rider DM, McDermid IS, Pacala TJ, Laudenslager JB. Effects of hematoporphyrin derivative and photodynamic therapy on atherosclerotic rabbits. *Am J Cardiol.* 1985;56(10):667–71.
 76. Waksman R, McEwan P, Moore T, Pakala R, Kolodgie F, Hellinga D, et al. PhotoPoint photodynamic therapy promotes stabilization of atherosclerotic plaques and inhibits plaque progression. *J Am Coll Cardiol.* 2008;52(12):1024–32.
 77. Abela GS, Conti CR. The use of the laser in the treatment of coronary and peripheral arterial obstruction. In: Schlant RC, Alexander RW, O'Rourke RA, Roberts R, Sonnenblick EH, editors. *Hurst's the heart.* 8th ed. New York: McGraw-Hill Publisher; 1994.

Index

- A**
Acute myocardial infarction, 55–66, 73, 97, 114, 159, 305
Angiogenesis, 221, 273, 279, 298–299, 306, 308, 309, 313–314, 317, 355
Angioplasty balloon, 31, 161, 173–175, 192, 195, 353
Anterograde-dissection, 31, 34
Antioxidant, 308, 309
Aortic dissection, 193, 195
Aortic repair, 191–196
Atherectomy, 1, 19, 20, 27, 28, 31–52, 77–79, 84–86, 88, 94, 97, 99, 100, 103–122, 125, 127, 130, 133–135, 141–143, 145–151, 159, 163, 164, 167, 168, 171, 177, 178, 181–189, 354, 153154
Atherosclerosis, 15, 69, 70, 72, 75, 80, 86, 87, 103, 107, 141, 273, 308, 317, 349
Atherosclerotic plaque, 15, 27, 35, 56, 58, 75, 85, 106, 349–351, 353, 357
- B**
Balloon-resistant lesion, 11, 89, 97, 99, 100
Bubble, 3–6, 9, 10, 16–18, 20–28, 34, 86, 89, 93, 94, 121, 125, 159, 163, 167, 168, 174, 291, 292, 322, 353
Bypass graft, 31, 39, 55, 56, 62, 63, 69, 70, 72, 74, 77–80, 83, 125, 132, 136, 271, 278, 279, 287, 293, 295, 297, 316
- C**
CABG. *See* Coronary artery bypass graft
Calcified coronary lesion, 31
Calcified coronary stenosis, 83
Calcified lesions, 12, 34, 36, 83–94, 97, 99–101, 103, 168, 173
Calcified plaques, 10, 18, 21, 23, 25, 27–29, 35, 45, 84, 89, 168
Cardiac arrhythmias, 199–217, 234
Cardiac implantable electronic device (CIED), 245, 247–251, 256–258, 260
infection, 249, 256, 260
Cavitation, 3, 16–28, 222, 224, 225, 234, 291, 292
Chagas disease, 199, 240
Chromophore absorption, 321
Chronic total occlusions (CTO), 31–32, 34–37, 39–45, 47–49, 52, 55, 56, 73, 83, 84, 86–88, 92, 94, 97, 99–103, 110, 112, 122, 135, 143, 159, 162, 167, 169, 181, 357
Claudication, 15, 48, 126, 133–135, 142–144, 148, 149, 151, 181, 191, 196, 354, 356
CO₂, 2, 6, 104, 183, 252, 264, 272, 282, 288–299, 306, 311–317, 349, 355
CO₂ lasers, 2, 292, 311–317
Complex coronary lesions, 31, 97, 100
Continuous wave laser, 288, 353, 354
Coronary artery bypass graft (CABG), 31, 39, 45, 48, 70, 72, 74, 79, 80, 83, 86, 94, 114, 121, 278, 279, 281, 287, 288, 293–295, 297, 298, 305, 306, 311, 314–317, 355
Coronary artery disease, 72, 85, 97, 149, 199, 262, 271, 279, 281, 297, 299, 311, 316, 355
angina, 97, 271, 355
myocardial ischemia, 274, 276, 280, 316
transmyocardial laser, 316
Coronary intervention, 31–52, 55, 72, 75, 76, 97, 102–122, 271, 287, 306, 311, 353
Critical limb ischemia, 126, 141–154, 157, 160, 162, 174, 176, 181–183, 188, 354
CTO. *See* Chronic total occlusions
CTO PCI algorithm, 31
- D**
De novo lesions, 38, 182
Depolarization, 199–206, 210, 211, 213, 214, 239
Device infection, 248, 249, 251, 262
Distal embolization, 34, 57, 59, 60, 62, 64, 73, 75, 77, 88, 93, 94, 143, 144, 151, 157–164, 174, 176–178, 182, 188, 353, 354
Drug-eluting balloons, 98, 127, 171–178, 181–189
- E**
ECLA. *See* Excimer coronary laser angioplasty (ECLA)
ELCA. *See* Excimer laser coronary atherectomy
Electrophysiological communication, 199, 201
Endovenous laser ablation (EVLA), 337
Endovenous therapy, 321
EVLA. *See* Endovenous laser ablation
Excimer, 1, 15, 31–52, 56, 69, 83–94, 97, 103–122, 125–141, 157–164, 174, 184, 245, 255–269, 288, 307, 330, 345–347, 353
Excimer coronary laser angioplasty (ECLA), 69, 75–78, 80, 83, 86, 89
Excimer laser, 1, 15, 31, 56, 75, 83–94, 97, 103–122, 125–141, 157–164, 174, 186, 245, 255–269, 288, 307, 330, 345–347, 353,
Excimer laser atheroablation, 97–102
Excimer laser coronary atherectomy (ELCA), 1, 3, 5, 11, 31–52, 37, 76, 78–80, 83–86, 88, 89, 91, 94, 97–122, 354
Excimer laser lead extraction, 245–252
- F**
Femoropopliteal in-stent restenosis, 141, 148
Fiberoptic catheters, 1, 351
Fiber optics, 6–8, 10, 15, 19, 20, 22, 27, 125, 205, 206, 209–215, 349–350, 353

- Fluence, 2, 4, 10, 11, 19, 20, 28, 34, 36, 59, 65, 89, 90, 100, 101, 125, 159, 174, 191, 193, 205, 209, 216, 256, 307, 321, 322, 325, 331, 345, 353
- Free radicals, 306, 307, 314
- Function, 19, 20, 22–27, 38, 40, 41, 45–47, 50, 72, 116, 164, 183, 202, 205, 207, 208, 210, 214, 229, 230, 239, 246, 268, 274, 280, 287–299, 306, 314, 321
- G**
- Great saphenous vein (GSV), 323, 326–329, 337, 339–341
- H**
- Ho:YAG, 2, 288–293, 295–299, 312–314, 316, 317, 353
- Hypertrophic obstructive cardiomyopathy, 239
- I**
- Implantable cardioverter defibrillator (ICD), 199, 238, 240, 250
lead, 258, 260–262, 264–267
- Incompetent perforating veins (IPV), 337–342
- Infarction, 36, 42, 44, 49, 55–66, 72–74, 76–78, 97, 98, 110, 114, 159, 188, 199, 204, 214, 228, 232, 234, 240, 242, 279, 294, 297, 305–307, 315, 353, 354
- Infra-inguinal arteries, 141
- In-stent restenosis, 11, 12, 38, 55, 80, 83, 85–86, 90, 97–98, 110, 112, 121, 127, 133, 141, 142, 147–149, 171–178, 181–189, 355
- In-stent use of laser atherectomy, 142, 148
- Interventional cardiology, 75, 83, 271
- IPV. *See* Incompetent perforating veins
- Ischemia, 33, 38, 44, 47, 57, 62, 63, 66, 126, 127, 132, 133, 141–154, 157, 159, 160, 162, 164, 174, 176, 181–183, 188, 189, 191, 193, 199, 274, 276–278, 280, 296, 297, 305–308, 315, 316, 354
- L**
- Laser, 1–12, 15–29, 31–52, 55–66, 69–80, 83–94, 97–122, 125–154, 157–164, 167–178, 181–189, 191–196, 199–217, 221–242, 245–252, 255–269, 271–281, 287–299, 305, 311–317, 321–335, 337–342, 345–347, 349–357
- ablation, 4, 6, 15, 16, 18, 21, 22, 24, 159, 160, 162, 163, 211, 214, 215, 230, 234, 236–240, 247, 261, 292, 337–342
- angioplasty, 6, 55, 60, 69, 75, 76, 80, 89, 97, 98, 126, 144, 174, 350–352, 357
- catheter, 6–8, 11, 12, 34–36, 38, 40–45, 50, 51, 57, 58, 60–65, 75, 78, 84, 88, 89, 91–94, 97, 99–101, 103, 114, 125–127, 141–143, 161, 167, 174, 175, 186, 187, 191, 193–195, 199–216, 221, 223–225, 227, 229, 230, 232–234, 237, 240, 330, 350, 354, 356
- in clot, 4, 56, 164
- as crossing tool, 125, 126
- drug-eluting balloons, 178
- lead extraction, 251, 256, 261–264, 269
- light, 1, 2, 5, 7, 18–20, 75, 116, 125, 204–207, 211–213, 217, 221–223, 225, 229, 238–242, 255, 271, 288–290, 322, 325, 349, 353
- mapping, 222–225, 227, 237
- revascularisation, 69–80
- as therapy of in-stent stenosis, 127
- wavelength, 2, 22, 205, 214, 289, 321, 322, 353
- Laser atherectomy, 1, 31–52, 78, 84, 103, 106, 111, 120, 125, 127, 130, 133, 141–151, 153, 154, 164, 171, 178, 181–189
- infrapopliteal disease, 128, 160
- popliteal artery, 128, 138, 146, 149–151, 174, 176, 178, 186
- superficial femoral artery, 91–93, 126, 142, 149, 163, 167–171, 174–178, 181–189, 354, 355
- Lead fracture, 264, 267
- Limb ischemia, 126, 141–154, 157, 160, 162, 164, 174, 176, 181–183, 188, 354
- Limb salvage, 126, 141, 143–145, 148, 157, 162, 354
- M**
- Myocardial, 36, 55–66, 71, 97, 111, 159, 188, 199, 224, 246, 271, 287–299, 305–309, 311–317, 353
- Myocardial coagulation, 323
- O**
- Occlusion, 12, 15, 31–52, 55, 70, 83, 97, 103, 125, 141, 157–164, 167, 172, 181, 203, 241, 247, 257, 274, 299, 307, 326, 354
- Open irrigated laser catheter, 121, 129, 230, 233
- Optical fibers, 2, 3, 7, 9, 11, 12, 222, 223, 229, 242, 292, 299, 350, 351
- P**
- Pacemaker lead, 260, 262, 346, 357
- Percutaneous coronary intervention (PCI), 31–52, 55, 56, 59, 64, 65, 70, 72, 73, 75–80, 83, 88, 97, 103–121, 271, 281, 287, 294, 295, 299, 305, 306, 311, 353
- Peripheral arterial disease, 56, 85, 126, 157–158, 357
- Peripheral arteries, 84, 125, 157–164, 177, 354, 357
- Peripheral vessel stenosis, 83
- Photoablation, 1, 3, 162, 178, 290–292, 298
- Photocoagulation, 201, 203–206, 208–210, 212–215, 217
- Plasma formation, 18, 20, 22, 23, 292
- Platelets, 35, 56, 59, 62–66, 71, 73, 88, 107, 116, 117, 121, 159, 162, 164, 171, 172, 182, 183, 262, 263, 268, 273, 353
- PPCI. *See* Primary percutaneous coronary intervention
- Preconditioning, 280, 305–309
- Primary percutaneous coronary intervention (PPCI), 114, 116
- Pulsed laser, 16, 18, 20–24, 97, 288, 292, 322, 331, 353
- Pulse duration, 2, 7, 20, 22, 24, 56, 288, 290, 292, 293, 307, 308, 312, 321, 322, 324, 325, 337
- R**
- Relaxation time, 2, 21, 22, 321, 322
- Renal denervation, 241
- Reperfusion, 55, 77, 280, 294, 305–308, 311, 317
- Retrograde approach, 31
- Retrograde laser fenestration, 191, 193, 195, 196
- Revascularization, 31, 55, 74, 83–94, 97, 125, 141–154, 157, 175, 181, 191, 217, 271, 287–298, 305–309, 311–317, 321–335, 353
- S**
- Saphenous vein graft (SVG), 66, 69, 70, 72–80, 114, 122
- Severe dermal changes,
- SFA. *See* Superficial femoral artery

Small saphenous vein (SSV), 326–329, 337, 339
Spallation, 20–23, 26–28
Step by step, 91–93, 126, 128, 138, 139, 142–144, 151, 167–170, 239
Subacute and chronic thrombus, 163–164
Superficial femoral artery (SFA), 91–93, 126, 127, 134, 135, 139, 142–144, 146, 149, 150, 163, 167–171, 174–178, 181–189, 354, 355
occlusion, 126, 127, 134, 135, 167, 354

T

TEVAR. *See* Thoracic endovascular aneurysm repair (TEVAR)
Thermo-elastic expansion, 20–22
Thoracic aortic aneurysm, 195
Thoracic endovascular, 191–196
Thoracic endovascular aneurysm repair (TEVAR), 191–193, 195, 196
Thrombosis, 27, 31, 36, 57, 62, 64, 69, 72, 73, 114–120, 147, 157, 162, 164, 172, 176, 177, 181, 189, 250, 251, 256, 257, 260, 268, 313, 322, 327–331, 338, 341, 345, 353
Tissue interaction, 1–3, 19–20, 114, 115, 210, 217, 288, 291, 321
Transmyocardial, 271–281, 287–299, 305–309, 311–317

Transmyocardial laser revascularization, 271–281, 289–299, 311, 316
Transmyocardial revascularization, 294, 295, 305–309, 311–317
Transseptal laser puncture, 236, 241–242
Transvenous lead extraction, 245–252, 258, 259

U

Uncrossable total occlusions, 84, 86–88
Undilatable in-stent stenosis, 84

V

Vaporization, 3, 4, 15, 16, 18–21, 23, 25–28, 56, 66, 84, 207, 211, 214, 216, 217, 222, 224, 231, 234, 279, 289–293, 314, 349, 350, 357
Vascular calcification, 83, 106, 267
Vein graft, 34, 45, 56, 59, 62, 63, 69–80, 97, 109, 113–116, 354, 357
Venostenosis, 80
Venous ulcer, 326